

**FEB - FRESENIUS ENVIRONMENTAL BULLETIN**

Founded jointly by F. Korte and F. Coulston

Production by PSP - Vimy Str. 1e, 85354 Freising, Germany in  
cooperation with PRT-Parlar Research & Technology

Vimy Str 1e, 85354 Freising

Copyright© by PSP and PRT, Vimy Str. 1e, 85354 Freising, Germany

All rights are reserved, especially the right to translate into foreign language or other processes - or convert to a machine language, especially for data processing equipment - without written permission of the publisher. The rights of reproduction by lecture, radio and television transmission, magnetic sound recording or similar means are also reserved.

**Printed in Germany-ISSN 1018-4619**

**FEB-EDITORIAL BOARD****CHIEF EDITOR:****Prof. Dr. Dr. H. Parlar**Parlar Research & Technology-PRT  
Vimy Str.1e  
85354 Freising, Germany**MANAGING EDITOR:****Dr. P. Parlar**Parlar Research & Technology  
PRT, Vimy Str.1e  
85354 Freising, Germany**CO-EDITORS:****Environmental Spectroscopy****Prof. Dr. A. Piccolo**Universita di Napoli "Frederico II"  
Dipto. Di Scienze Chimica Agrarie  
Via Universita 100, 80055 Portici, Italy**Environmental Biology****Prof. Dr. G. Schuurmann**UFZ-Umweltzentrum  
Sektion Chemische Ökotoxikologie  
Leipzig-Halle GmbH,  
Permoserstr.15, 04318  
04318 Leipzig, Germany**Prof. Dr. I. Holoubek**Recetox-Tocoen  
Kamenice126/3, 62500 Brno, Czech Republic**Prof. Dr. M. Hakki Alma**Kahramanmaras Sutcu Imam University  
Avsar Kampusu, 46100 Kahramanmaras, Turkey**Environmental Analytical Chemistry****Prof. Dr. M. Bahadir**Lehrstuhl für Ökologische Chemie  
und Umweltanalytik  
TU Braunschweig  
Lehrstuhl für Ökologische Chemie  
Hagenring 30, 38106 Braunschweig, Germany**Dr. D. Kotzias**Via Germania29  
21027 Barza(Va), Italy**Environmental Management****Dr. K. I. Nikolaou**Env.Protection of Thessaloniki  
OMPEPT-54636 Thessaloniki  
Greece**Environmental Toxicology****Prof. Dr. H. Greim**Senatkommision – DFG / TUM  
85350 Freising, Germany**Environmental Proteomic****Dr. A. Fanous**Halal Control GmbH  
Kobaltstr. 2-4  
D-65428 Rüsselsheim, Germany**Environmental Education****Prof. Dr. C. Bayat**Esenyurt Üniversitesi  
34510 Esenyurt, Istanbul, Turkey**Advisory Board****K. Bester, K. Fischer, R. Kallenborn****DCG. Muir, R. Niessner, W. Vetter,****A. Reichlmayr-Lais, D. Steinberg,****J. P. Lay, J. Burhenne, L. O. Ruzo****Marketing Manager****Cansu Ekici, B. of B.A.**PRT-Research and Technology  
Vimy Str 1e  
85354 Freising, Germany**E-Mail: [parlar@wzw.tum.de](mailto:parlar@wzw.tum.de)****[parlar@prt-parlar.de](mailto:parlar@prt-parlar.de)****Phone: +49/8161887988**

**Fresenius Environmental Bulletin is abstracted/indexed in:**

**Biology & Environmental Sciences, BIOSIS, CAB International, Cambridge Scientific abstracts, Chemical Abstracts, Current Awareness, Current Contents/Agriculture, CSA Civil Engineering Abstracts, CSA Mechanical & Transportation Engineering, IBIDS database, Information Ventures, NISC, Research Alert, Science Citation Index (SCI), Scisearch, Selected Water Resources Abstracts**

---

## CONTENTS

### ORIGINAL PAPERS

- A BIBLIOMETRIC ANALYSIS FOR GLOBAL PM<sup>2.5</sup> RESEARCH 5080  
**Suli Zhao, Haobo Hou, Limin Jiao, Tianxue Yang**
- UPTAKE OF CHLORTETRACYCLINE BY YELLOW LUPIN (LUPINUS LUTEUS L.) GROWING UNDER PHOTOPERIOD OR AT CONSTANT DARKNESS 5096  
**Michał Baciak, Agnieszka I. Piotrowicz-Cieslak, Barbara Adomas**
- GIS MODELING AND SOCIAL-ORIENTED MULTI-CRITERIA EVALUATION IN LANDFILL SITE SELECTION IN RURAL AREAS – A CASE STUDY OF SERBIAN VILLAGES 5105  
**Marina Nenkovic-Riznic, Igor Maric, Mila Pucar**
- EFFICACY OF IN VITRO PROPAGATED COONTAIL (CERATOPHYLLUM DEMERSUM L.) ON QUALITY OF DIFFERENT WATER SAMPLES 5113  
**Mehmet Karatas, Muhammad Aasim, Muhammet Dogan**
- VARIATION IN COMMUNITY COMPOSITION OF NIRS-TYPE DENITRIFIERS IN SEDIMENT OF BASINS WITH DIFFERENT TROPHIC STATES WITHIN A SHALLOW LAKE 5120  
**Yao Zhang, Yuqian Liu, Zijun Zhou, Siyang Wang, Xiuyun Cao, Chunlei Song, Yiyong Zhou**
- DIVERSE AND DISTINCT BACTERIAL COMMUNITIES ASSOCIATED WITH COMPLEX CONSTITUTES OF COKING WASTEWATER IN ANAEROBIC PROCESS 5130  
**Shuang Zhu, Haizhen Wu, Yesheng Wang, Qiwei Li, Lin Zhou, Chaohai Wei**
- AN EXPERIMENTAL STUDY INTO DISCHARGE COEFFICIENT OF LABYRINTH WEIRS WITH RECTANGULAR-SHAPED PLANS 5138  
**Hadi Rostami, Mohammad Heidarnejad, Mohammad Hosein Purmohammadi, Amirabbas Kamanbedast, Amin Bordbr**
- ANALYSIS OF HCHS AND DDTS IN A TYPICAL PESTICIDE CONTAMINATED SITE 5145  
**Xuebin Chen, Wenxia Liu, Yingxia Zhou, Xinyue Qiao, Jiabao Zhao, Haifeng Li, Ying Han, Xiao Liao, Mengjing Wang, Wenbin Liu**
- FUNCTIONALIZATION OF CARBON NANOTUBES AND ITS APPLICATION IN ADSORPTION AND SOLID PHASE EXTRACTION 5151  
**Xiaoxing Zhang, Li Zhang, Hui Liu**
- CHARACTERIZATION OF PM<sub>2.5</sub> AND IT'S CHEMICAL COMPOSITIONS UNDER DIFFERENT AIR QUALITY GRADES IN HANDAN, CHINA 5162  
**Simeng Ma, Litao Wang, Zhe Wei, Fenfen Zhang, Chenchen Meng, Jing Yang**
- INNOVATIVE PRECONCENTRATION TECHNIQUE ON POLYMER SORBENT FOR SIMULTANEOUS DETERMINATION OF PLATINUM GROUP METALS IN THE WATERS AND LICHEN HYPOGYMNIA PHYSODES 5172  
**Renata Komendova, Jana Nevrla, Jan Kuta, Lumir Sommer**
- ISOLATION AND IDENTIFICATION OF ENTOMOPATHOGENIC FUNGI BEAUVERIA BASSIANA FROM TURKEY 5180  
**Alev Haliki Uztan, Ozlem Abaci Gunyar, Aysegul Yoltas, Nevin Keskin**
- CLASSIFICATION AND IDENTIFICATION OF ORGANIC COUPOUNDS BY PATTERN RECOGNITION BASED ON NEAR INFRARED SPECTROSCOPY 5186  
**Mingyue Liu, Jin Liu, Yanjun Yu, Peng Zhou, Rongxin Su, Wei Qi, Libing Wang, Zhimin He**
- A QUANTITATIVE ANALYSIS OF URBAN WATER LANDSCAPE PATTERN CHANGES AND THEIR IMPACTS ON SURFACE TEMPERATURES 5194  
**Lei Wang, Yunlong Yao, Shuwen Zhang**
- EVALUATING AND MAPPING TRAFFIC-INDUCED NOISE POLLUTION IN URBAN PARKS IN THE CITY OF KAHRAMANMARAŞ, TURKEY 5202  
**Neslihan Doygun, Hakan Doygun, Merve Gozcu**

RESEARCH ON THE VARIATIONS OF SNOW COVER OVER THE TIBETAN PLATEAU AND ITS RESPONSES TO CLIMATE CHANGE <b>Yuxue Guo, Guohua Fang, Lei Zhou, Xin Wen</b>	5208
A COMBINED WAVELET AND NEURAL NETWORK MODEL FOR FORECASTING STREAMFLOW DATA <b>Alpaslan Yarar, Mustafa Onucyildiz, Nadim K Copty</b>	5217
SORPTION OF CADMIUM BY BIOCHAR PRODUCED FROM PYROLYSIS OF CATTLE MANURE IN AQUEOUS SOLUTION <b>Fengfeng Ma, Baowei Zhao, Jingru Diao, Hongtao Qiao, Jinkui Zhong</b>	5226
USING DIATOMS IN WATER QUALITY ASSESSMENT IN THE ANDIK STREAM (ISPARTA-TURKEY) <b>Hasan Kalyoncu, Hatice Dayioglu, Fusun Kilcik</b>	5237
PRECONCENTRATION OF CADMIUM, LEAD, COPPER, ZINC AND MANGANESE WITH POLYSTYRENE DIVINYLBENZENE COPOLYMER CONTAINING DITHIOCARBAMATE GROUP, AND DETERMINATION WITH FAAS <b>Ali Alkan, Mehtap Yagan Asci, Bekir Bati</b>	5245
LEVELS OF HEAVY METALS IN FISHES (POLYSTEAGANUS COERULEOPUNCTATUS, ARGYROPS SPINIFER AND ARGYROPS FILAMENTOSUS) FROM THE GULF OF AQABA, JORDAN <b>Tariq Al-Najjar, Rashad Gassaymah, Maroof Khalaf, Mohammad Wahsha, NoomanKhalaf, Khalid Abu Khadra</b>	5253
ESTIMATION OF LEAF AREA INDEX(LAI) OF POYANG LAKE BASIN IN SUMMER USING GF-1 DATA <b>Hui Jiang, Xiaoling Chen, Yao Liu, Lian Feng, Xinxin Han</b>	5261
DIURNAL VARIATION IN THE SELECTED INDICATORS OF WATER CONTAMINATION IN THE BIAŁKA RIVER AFFECTED BY A SEWAGE TREATMENT PLANT DISCHARGE <b>Anna Lenart-Boron, Justyna Prajsnar, Kinga Krzesiwo, Anna Wolanin, Lukasz Jelonkiewicz, Ewelina Jelonkiewicz, Miroslaw Zelazny</b>	5271
TOXIC EFFECTS OF THE JOINT EXPOSURE OF CD AND DECA-BROMODIPHENYL ETHER ON SOIL MICROBIAL POPULATION <b>Zhaoxiang Han, Ning Wang, XingyuYang, Rui Zhou</b>	5280
UTILIZATION OF SHELLFISH WASTE: EFFECTS OF CHITOSAN FROM SHRIMP SHELL WASTE ON FATTY ACID PROFILES OF EUROPEAN EEL <b>Aygul Kucukgulmez, Yasemen Yanar, Ali Eslem Kadak, Gozde Gercek, Serap Gelibolu, Mehmet Celik</b>	5287
QUANTITATIVE EVALUATION SYSTEM OF HABITAT ENVIRONMENTAL QUALITY IN YELLOW RIVER DELTAS <b>Hou Kang, Li Xu-xiang</b>	5291
SCREENING AND OPTIMIZATION OF POLY-B-HYDROXYBUTYRATE (PHB) PRODUCTION BY CERTAIN BACTERIA ISOLATED FROM SOIL <b>Halil Biyik, Esin Poyrazoglu Coban, Betul Aktas</b>	5297
IMAGE PROCESSING BASED INTELLIGENT SPRAYING ROBOT FOR WEED CONTROL <b>Kadir Sabanci, Cevat Aydin</b>	5305
THE STUDY ON EXPLOITATION, UTILIZATION AND ENVIRONMENTAL EFFECTS OF WIND RESOURCES IN LIAONING PROVINCE, CHINA <b>Zhidong Li, Shushen Zhang, Shuming Ma</b>	5313
REMOVAL OF PB <sub>2</sub> <sup>+</sup> AND CD <sub>2</sub> <sup>+</sup> FROM AQUEOUS SOLUTIONS BY CHEMICALLY MODIFIED CELLULOSE OF CASSAVA WASTE <b>Zhang Luo, Shengxu Luo, Cheng Niu, Shanhu Hu, Linqian Chen, Chunlei Fan</b>	5326
MODIFICATION OF REUSED FURNACE IRON WASTE (FIW) WHICH HAD SURFACE REDUCED WITH ZERO-VALENT IRON/FIW (ZFIW) CATALYTIC FOR DYES WASTEWATER TREATMENT <b>Chih-Tsung Tsai, Jian-Zhi Lian, Yung-Hsu Hsieh</b>	5336
REUSED HAND-WARMER WASTES FOR DEGRADATION OF AR27 DYES IN WASTE WATER <b>Chih-Tsung Tsai, Jian-Zhi Lian, Yung-Hsu Hsieh</b>	5341

- PEDO-STRATIGRAPHICAL RECORDS OF AL-WU'AIRA CASTLE (PETRA, JORDAN) 5347  
**Mohammad Wahsha , Raid Al-Jawasreh, Marta Mariotti Lippi, Mohammad Al-Tawaha, Claudio Bini**
- HISTOPATHOLOGICAL EVALUATION OF EFFECTS OF LEAD HEAVY METAL APPLIED TO CALIFORNIAN RED WORM (EISENIA FOETIDA) ON SKIN TISSUE 5354  
**Nurgul Senol**
- GENOTOXIC ASSESSMENT OF AMOXICILLIN IN RAINBOW TROUT (ONCORHYNCHUS MYKISS) BY COMET ASSAY AND MICRONUCLEUS TEST 5358  
**Ceren Anlas, Oya Ustuner**
- MATERNAL AGE EFFECTS OF ASPIDIOTUS NERII BOUCHÉ BOUCHE (HEMIPTERA: DIASPIDIDAE) ON POTATO 5365  
**Alime Bayindir, Senay Ozger, Ismail Karaca, Mehmet Sedat Sevinc**
- ADSORPTION BEHAVIOR OF NATURAL AND THERMALLY MODIFIED DIATOMITE FOR 1-NAPHTHOL FROM AQUEOUS SOLUTION 5371  
**Song Chengjie, Liu Jingjing, Wang Liping, Xu Xia, Wang Shaomang**
- CHANGES IN MACROELEMENTS CONCENTRATIONS IN TUBERS OF THREE POTATO CULTIVARS DUE TO AN APPLICATION OF HERBICIDES 5381  
**Marek Gugala, Krystyna Zarzecka, Krzysztof Kapela, Anna Sikorska, Ewa Krasnodebska, Alicja Baranowska**
- DEVELOPMENT AND CHARACTERIZATION OF SSR MARKERS FROM FUSARIUM INFECTED BARLEY (HORDEUM VULGARE) CDNA DATA SETS 5388  
**Hulya Sipahi, Aysen Yumurtaci, Hakan Hekimhan**
- STUDIES ON DEGRADATION CHARACTERISTICS OF CHLORIMURON-ETHYL BY BACILLUS SUBTILIS STRAIN D-6 5394  
**Yingjie Dai, Binbin Zhang, Yan Ji, Xuezhao Li, Dianqiu Lv, Yanju Bai**
- AN INVESTIGATION INTO CHANGES IN PHOSPHORUS FORMS AND PHOSPHORUS LEACHING FROM DREDGED SEDIMENTS SOLIDIFICATION OF TAIHU LAKE 5399  
**Shengwei Wang, Wei Zhu, Yiyan Lv, Huiwen Zhang**
- PHOTOCHEMICAL FORMATION OF SINGLET OXYGEN IN ALGAE-LADEN WATER 5406  
**Junwei Zhang, Qianning Song, Panpan Jiang, Jin Gu**
- SYNTHESIS AND IN-VITRO ANTIMICROBIAL AND ANTI-MUTAGENIC ACTIVITIES OF SOME NOVEL 2-(2-HYDROXYBENZYLIDENEAMINO)-5,7-DIHYDRO-4H-THIENO[2,3-C]PYRAN-3-CARBONITRILE DERIVATIVES 5411  
**Aliye Altundas, Yasemin Erdogan, Hatice Ogutcu, Hamit Emre Kizil, Guleray Agar**
- EVALUATION OF ANTIBACTERIAL ACTIVITY OF SOME PLANT METHANOLIC EXTRACTS 5419  
**Fulya Tugba Artun, Ali Karagoz, Zuhail Zeybek, Miray Ustunturk-Onan, Gulay Melikoglu, Sezin Anil, Sukran Kultur**
- DISTRIBUTION CHARACTERISTICS AND ECOLOGICAL RISK ASSESSMENT OF NONYLPHENOL IN JIAOZHOU BAY IN QINGDAO, CHINA 5424  
**Peng Zhang, Chang-you Wang, Sheng-kang Liang, Xiao-yan Wang, Xiu-lin Wang**
- CARBON DIOXIDE EVOLUTION AND ENZYMATIC ACTIVITIES OF SOIL UNDER DIFFERENT LAND USE PRACTICES LOCATED NEAR BHAWANIPATNA TOWN IN ODISHA, INDIA 5432  
**Chandan Sahu, Sradhanjali Basti, Sanjat Kumar Sahu**
- ACCUMULATION AND POLLUTION TRENDS OF HEAVY METALS IN THE TOPSOIL FROM AN INDUSTRIAL PARK LOCATED IN A TYPICAL NEW CHINESE DEVELOPING AREA 5440  
**Xinyu Miao, Qixing Zhou**
- FARMERS' RISK PERCEPTION AND WILLINGNESS TO PAY FOR ENVIRONMENT: CASE STUDY OF GAP-SANLIURFA, TURKEY 5449  
**Mustafa Hakki Aydogdu**
- CO-OCCURRENCE AND DIVERSITY OF NITRITE-DEPENDENT ANAEROBIC METHANE OXIDIZING AND ANAEROBIC AMMONIUM OXIDIZING BACTERIA IN THE WATER-LEVEL FLUCTUATION ZONE OF THE THREE GORGES RESERVOIR, CHINA 5456  
**Ruifei Wang, Xinkuan Han, Peili Lu, Qingxiang Yang**

- PHYLOGENETIC RELATIONSHIPS OF GERANIUM SPECIES IN DIFFERENT REGIONS OF TURKEY 5467  
**Onur Koloren, Secil Eker**
- OPTIMIZATION OF MICROWAVE INDUCED ELECTRODELESS ULTRAVIOLET DISINFECTION REACTOR USING COMPUTATIONAL FLUID DYNAMICS 5473  
**Yue Zhang, Guangshan Zhang, Peng Wang, Qiao Wang**
- STUDY ON THE IMPACT OF ENVIRONMENTAL REGULATION ON FIRM SIZE DISTRIBUTION: A CASE STUDY OF GUANGDONG PROVINCE 5483  
**Yang Yuanhua, Niu Guohua, Tang Dengli**
- ENVIRONMENTAL CONTAMINATION OF HEAVY METALS IN THE YAĞLIDERE STREAM (GİRESUN), SOUTHEASTERN BLACK SEA 5492  
**Arzu Aydin Uncumusaoglu, Umit Sengul, Tamer Akkan**
- BIOLOGICAL RISK ANALYSIS OF GREEN LAND IN CHINA 5499  
**Tang Guimei, Liu Guibin, Huang Yao, Chen Chan, Zheng Huabin, Li Jingyi, Long Yuelin, Cheng Tianyin**
- THE RESPONSE OF COTTON (GOSSYPIUM HIRSUTUM L.) TO SOIL APPLIED ELEMENTAL SULPHUR UNDER BORON TOXICITY 5511  
**Firat Kurt, Mefhar Gültekin Temiz**
- CHARACTERISTICS OF PHOSPHORUS LOSSES DUE TO SURFACE RUNOFF IN A PEACH ORCHARD AND THE EFFECTS OF INTER-PLANTING WHITE CLOVER (TRIFOLIUM REPENS L.) ON FRUIT YIELD AND QUALITY 5516  
**Zhi Guo, Hong-jiang Liu, Wei Zhou, Liu-gen Chen, Jian-chu Zheng**
- DEVELOPMENT OF FUNGAL BIOFILM ON LUFFA CYLINDRICA FOR BIOSORPTION OF ZINC (II) FROM AQUEOUS SOLUTION 5528  
**Rukhsar Muzaffar, Arifa Tahir, Essam N Sholkamy, Ashraf A Mostafa, Abdullah A Al-arfaj, Tarad Abalkhail, Ahmed Abdel-Megeed**
- DEVELOPMENT OF A MICROBIAL PREPARATION BY USING A CHLORIMURON-ETHYL DEGRADING BACTERIUM, BACILLUS TEQUILENSIS JW18 5534  
**Zhu Jiang-wei, Zhao Yan, Wu Lei, Yang Ying**
- MULCHING AND ORGANIC-INORGANIC FERTILIZER APPLICATION REDUCE RUNOFF LOSSES OF NITROGEN FROM TOBACCO FIELDS 5542  
**Hou Maomao, Chen Danyan, Shao Xiaohou, Zhai Yaming**
- CHANGE IN ECOSYSTEM CARBON STORAGE OF THE MANGROVE FOREST ALONG THE CHINESE COAST BETWEEN 1990 AND 2010 5555  
**Gang Wang, Dongsheng Guan, M. R. Peart, Rongbo Xiao, Qiuping Zhang**
- USING NTA AND EDTA TO ENHANCE Cd PHYTOEXTRACTION BY AMARANTHUS HYBRIDUS L. 5565  
**Zhangwei Li, Boling Xu and Huimin Zhang**
- ORNITOFAUNA OF KORFEZ WETLANDS (KOCAELİ, TURKEY) 5575  
**Bilgenur Yasa, Ali Uzun**
- A STUDY ON THE DEVELOPMENT PERFORMANCES OF GOJI BERRY (LYCIUM BARBARUM L.) VARIETIES 5581  
**H Ibrahim Oguz, Oktay Erdogan**
- COMPARISON OF HEAVY METALS AND BENEFICIAL ELEMENTS IN NORTHEASTERN AND SOUTHERN RICE OF CHINA BY ICP-MS 5587  
**Zhang Hongxing, Liu Hui, Xie Yuanhong**
- AN EXPERIMENTAL STUDY INTO HYDRAULIC COEFFICIENT IN TRAPEZOIDAL LABYRINTH WEIR AND PIANO KEY WEIR 5590  
**Ramin Gharibvand, Mohammad Heidarnejad, HeidarAli Kashkouli, Houshang Hasoonizadeh, Amir Abbas Kamanbedast**
- EFFECT OF WATER FLOODING AND PLANTING DENSITY ON THE CHLOROPHYLL FLUORESCENCE RESPONSE IN COCULTIVATED CYNODON DACTYLON AND HEMARTHRIA ALTISSIMA 5599  
**Wenchao Ma, Hong Wei, Yuan Liu, Ting Wang, Cui Zhou, Zhenxia Wang, Yeyi Zhang**
- GENETIC IDENTIFICATION FOR SOME FUSARIUM SPP. USING RANDOM AMPLIFIED POLYMORPHIC DNA POLYMERASE CHAIN REACTION (RAPD-PCR) TECHNIQUE 5611  
**Ayten Celebi Keskin, Leyla Acik, Aydan Araz, Perihan Guler**

WATER AND SEDIMENT QUALITY IN THE NATIONAL MARINE PARK OF ALONISSOS AEGEAN SEA

5618

**Paraskevi Ovezikoglou, Manos Ladakis, Manos Dassenakis**





# A BIBLIOMETRIC ANALYSIS FOR GLOBAL PM<sub>2.5</sub> RESEARCH

Suli Zhao<sup>1,2</sup>, Haobo Hou<sup>1\*</sup>, Limin Jiao<sup>1</sup>, Tianxue Yang<sup>1</sup>

<sup>1</sup>School of Resource and Environmental Sciences, Wuhan University, Wuhan, P.R.China

<sup>2</sup>Central Southern China Electric Power Design Institute, Wuhan, P.R.China

## ABSTRACT

Ambient fine particulate matter with diameter less than 2.5  $\mu\text{m}$  (PM<sub>2.5</sub>) is a cause for concern largely due to its negative impact on human health. This study evaluated the research on PM<sub>2.5</sub> using a bibliometric analysis of published research from 1999 to 2014 based on the Science Citation Index (SCI) database. We presented the publication indicators in PM<sub>2.5</sub> research, evaluated the research performance of countries and institutes and analyzed the research trends and hot topics by statistics of keywords. The annual number of research outputs grew from 118 in 1999 to 1262 in 2014, although there was a decline from 2008 to 2010. The USA contributed the most publications (36.0%), with the US EPA, the Chinese Academy of Science and Harvard University being the most productive institutes. We also listed the top journals that published the most articles on PM<sub>2.5</sub> and the articles cited the most in top20. Keywords analyses showed that the chemical composition, source apportionment and health effects of PM<sub>2.5</sub> are the most popular topics in PM<sub>2.5</sub> research, followed by size distribution, pollutant diffusion and GIS techniques in the spatial simulation of PM<sub>2.5</sub> concentration. We also carried out national and temporal analyses of keywords. We further analyzed the emphasis and trends with respect to the popular topics and listed typical research results from across the world.

## KEYWORDS:

PM<sub>2.5</sub>; Bibliometric; Research performance; Research orientation

## INTRODUCTION

Fine particles with an aerodynamic diameter less than 2.5  $\mu\text{m}$  (PM<sub>2.5</sub>) are of concern largely due to their significant negative impacts on human health, which has been associated with human morbidity and mortality [1,2,3,4]. Fine particles are respirable, with the ability to penetrate the lungs and

reach the alveoli [5,6,7]. Compared to coarse particles, fine particles are smaller in size with a larger surface area. Many harmful substances can be adsorbed on the surface of fine particles, such as heavy metals, organic matters, bacteria and viruses, etc. [6,8]. Fine particles have natural origins, with a variety of anthropogenic sources. Anthropogenic fine particles can dominate the ambient air quality of urban and industrial areas. It is difficult to accurately identify the sources of PM<sub>2.5</sub> [5]. PM<sub>2.5</sub> can stay in the air for a long time and is likely to be transported over a long distance [9]. These characteristics of PM<sub>2.5</sub> have led to massive research, including concentration monitoring, composition analysis, source apportionment, health impacts, concentration prediction and simulation, etc. A bibliometric analysis of the global PM<sub>2.5</sub> research could reveal the trends of the development and progress in the research, which can significantly facilitate future studies.

Bibliometric analysis is a combination of quantitative and qualitative analysis methods that could help evaluate the performance of PM<sub>2.5</sub> research and could contribute to the understanding of and insight into this subject [10,11]. Bibliometric analysis has a long history and has been applied to evaluate research performance in various fields [12,13,14,15,16,17,18]. Xie et al. [19] provided a bibliometric analysis of world aerosol research, with focus on scientific output, research performances and trends by the frequency of keywords. According to their research, the frequency of PM<sub>2.5</sub> as a keyword generally increases with year and ranks the third in the 2003–2006 period. Li et al. [20,21] evaluated the research output of secondary organic aerosols (SOA) by bibliometric analysis and discussed the patterns, tendencies, methods and hot topics of SOA research. According to their study, the frequency of PM<sub>2.5</sub> ranks third among all keywords, indicating that research related to PM<sub>2.5</sub> has caught much more attention in recent years.

A bibliometric analysis of global PM<sub>2.5</sub> research performance will offer insights into this relevant topic. This study summarizes significant publication patterns in PM<sub>2.5</sub> related research and evaluates research performance from multiple

perspectives, including scientific output, nation, journal and keywords. This study also provides substantive discussion of research progress for some popular topics related to PM<sub>2.5</sub>.

## DATA AND METHODS

The data used in this study was based on the online Scientific Citation Index (SCI) database. We used “PM<sub>2.5</sub>” as the keyword to search titles, abstracts and keywords of the publications in the database over the past 15 years from 1999 to 2014. “PM<sub>2.5</sub>” is the most widely used term in studies on fine particulate matter pollution in ambient air environment. Although “fine particle/particles” and “fine particulate (particle) matter” are often used with “PM<sub>2.5</sub>” simultaneously, they were not included in our search because many studies with these keywords, excluding “PM<sub>2.5</sub>”, were not related to ambient air environment study. We then retrieved the document information, including title, keywords, author name(s), author affiliation(s), subject category(ies), journal name and year of publication. We eliminated duplicated records. Eventually, 7739 articles were identified as being related to PM<sub>2.5</sub>.

We then performed a bibliometric analysis on the preprocessed data, including literature types, language, scientific outputs, popular journals, popular articles, author affiliations and keywords. Based on these analyses, we determined the trends and hotspots of PM<sub>2.5</sub> related research.

## RESULTS AND DISCUSSIONS

**Document Type and Language of Publication.** Nine document types were found in the 7739 articles. The most frequent document type was journal article, with 6898 documents and accounting for 89.1% of the total publications. This was followed by proceeding paper (396 publications; 5.1%), meeting abstract (236 publications; 3.0%) and review (139 publications, 1.8%). The other five types of publications which are less common include editorial material (21 publications; 0.3%), letter (19 publications; 0.2%), correction (16 publications; 0.2%), news item (13 publications; 0.2%) and reprint (1 publication).

Languages of all of the PM<sub>2.5</sub> publications were grouped. Overall, eleven different languages were found. In summary, 7644 of the 7739 publications were written in English, accounting for 98.8%. The other ten languages were as follows: German (22 publications; 0.3%), Spanish (14 publications; 0.2%), French (14 publications; 0.2%), Chinese (12 publications; 0.2%), Italian (9 publications; 0.1%), Polish (7 publications; 0.1%), Portuguese (6 publications; 0.1%), Japanese (6 publications; 0.1%), Turkish (4 publications; 0.1%) and Hungarian (1 publication). English was found to be the prevalent academic language for PM<sub>2.5</sub> related research.

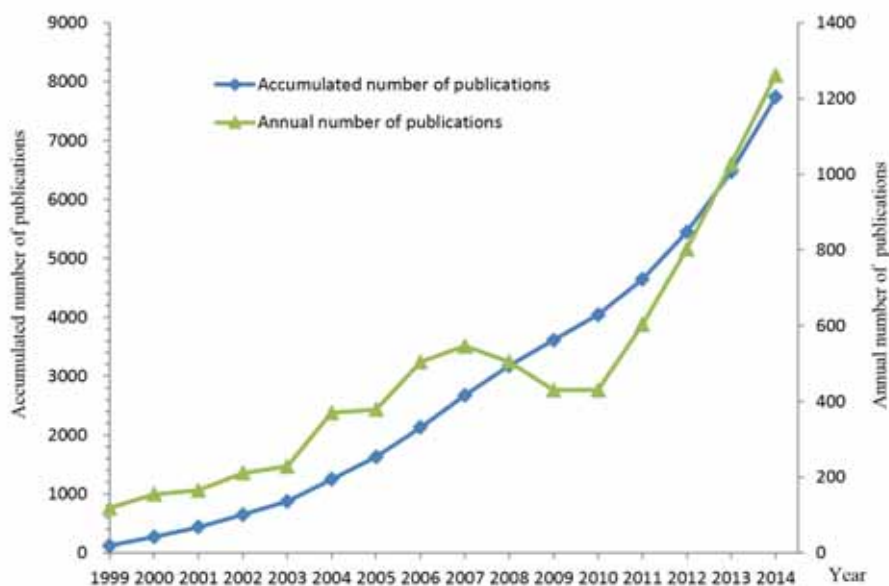


**FIGURE 1**  
PM<sub>2.5</sub>-related research production by year

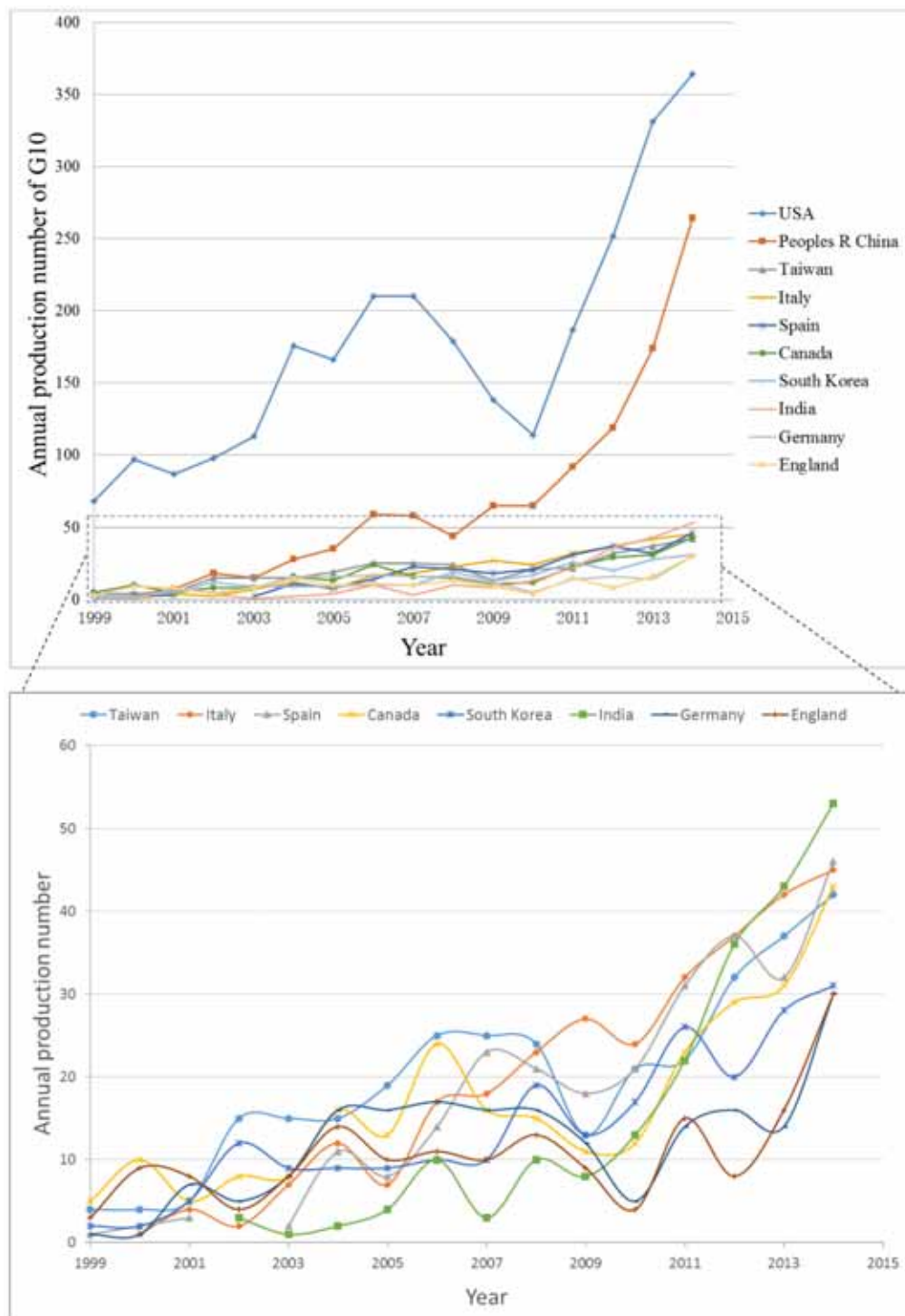


**FIGURE 2**

**Change of annual publications of the 10 most productive countries/territories**

**Publication outputs.** The output of publication on  $PM_{2.5}$  from 1999 to 2014 is summarized in Fig. 1. There has been an upward trend for the annual number of publications, which grew from 118 in 1999 to 1262 in 2014. The average of the number of authors per article gradually increased from 4.6 in 1999 to 7.0 in 2014, which suggested that the  $PM_{2.5}$  research has been becoming increasingly

collaborative. The number of cited references increased significantly, from 20.3 in 1999 to 44.1 in 2014.

The 10 most productive countries/territories (G10) with regard to  $PM_{2.5}$  research were USA, China mainland, Taiwan, Italy, Spain, Canada, South Korea, India, Germany and England (see Fig. 2). The publication output on  $PM_{2.5}$  research from

the G10 countries/territories accounts for 72.5% of the world total. USA topped the productivity ranking of countries/territories with 2789 publications, accounting for 36.0% of the total publication. China mainland ranked second, with a steep upward trend in publication output since 2004. The annual output of USA and China accounts for 49.8% of the total number in 2014.

There are over 1200 ground monitors to measure PM<sub>2.5</sub> concentration throughout the USA [22]. USA began to measure PM<sub>2.5</sub> nationally in the late 1990s. The National Ambient Air Quality Standards (NAAQS) have been revised several times to further restrict emissions. The PM<sub>2.5</sub> standards were tightened in 2005. At present, the daily maximum limit for PM<sub>2.5</sub> is 35  $\mu\text{g}/\text{m}^3$ , while the annual standard is 15  $\mu\text{g}/\text{m}^3$ . The available monitoring data and the strict standards have boosted PM<sub>2.5</sub> related research in recent years in this country.

PM<sub>2.5</sub> research has attracted greater attention in China mainland during the past decade due to the aggravated air pollution, especially in metropolitan areas [23]. China revised its ambient air quality standards in 2012, along with including PM<sub>2.5</sub> in

regular monitoring. 74 cities in China mainland publish the results of their monitoring of PM<sub>2.5</sub> online since January 1<sup>st</sup>, 2013. This number has increased to 161 at present. All of the cities in China will begin regular monitoring of PM<sub>2.5</sub> from Jan 1<sup>st</sup>, 2016. It is expected that PM<sub>2.5</sub> research in China will develop more rapidly than before.

**Popular journals and articles.** PM<sub>2.5</sub>-related articles were published in 673 journals. Of these, 579 journals (accounting for 86.0% of the total) published less than 10 PM<sub>2.5</sub>-related articles. In particular, 320 of these journals published only one PM<sub>2.5</sub>-related article. The top 20 journals that published the most PM<sub>2.5</sub>-related articles are listed in Table 1. The PM<sub>2.5</sub>-related articles from these 20 journals account for 61.6% of the total publication. Atmospheric Environment published the most number of PM<sub>2.5</sub>-related articles, accounting for 20.2%, which was much higher than the second, Journal of the Air & Waste Management Association (5.4%). Among the top 20 journals, there were 5 journals that were related to environment health and contributed 9.2% of the articles.

**TABLE 1**  
**The top 20 Journals that published most PM<sub>2.5</sub> articles**

No.	Journals	TP	TP%	TC	TC%	TC/TP	IF(2014)
1	Atmospheric Environment	1561	20.2	31341	28.8	20.1	3.281
2	Journal of the Air & Waste Management Association	416	5.4	5666	5.2	13.6	1.342
3	Science of the Total Environment	327	4.2	4077	3.7	12.5	4.099
4	Environmental Science & Technology	323	4.2	7199	6.6	22.3	5.330
5	Atmospheric Chemistry and Physics	289	3.7	3471	3.2	12.0	5.053
6	Environmental Health Perspectives	247	3.2	9099	8.4	36.8	7.977
7	Epidemiology	205	2.6	2274	2.1	11.1	6.196
8	Journal of Geophysical Research-Atmospheres	178	2.3	3342	3.1	18.8	3.426
9	Aerosol and Air Quality Research	164	2.1	482	0.4	2.9	2.094
10	Aerosol Science and Technology	152	2.0	3324	3.1	21.9	2.413
11	Atmospheric Research	140	1.8	1125	1.0	8.0	2.844
12	Environmental Monitoring and Assessment	105	1.4	474	0.4	4.5	1.679
13	Inhalation Toxicology	104	1.3	1666	1.5	16.0	2.260
14	Journal of Exposure Science and Environmental Epidemiology	94	1.2	959	0.9	10.2	3.185
15	Environmental Research	89	1.2	844	0.8	9.5	4.373
16	Atmospheric Pollution Research	88	1.1	148	0.1	1.7	1.371
17	Chemosphere	73	0.9	1804	1.7	24.7	3.340
18	Journal of Environmental Monitoring	70	0.9	533	0.5	7.6	2.179
19	Air Quality Atmosphere and Health	70	0.9	221	0.2	3.2	1.804
20	Environment International	70	0.9	739	0.7	10.6	5.559

Note: TP means total publication in the journal. TP% means TP accounts for the proportion of the total number of PM<sub>2.5</sub> publication. TC means total cited time in the journal. TC% means TC accounts for the proportion of the total cited times of PM<sub>2.5</sub> publication.

**TABLE 2.**  
**The top 20 most frequently cited productions**

No.	Article	Journal	Corresponding author	Year	TC
1	Species contributions to PM <sub>2.5</sub> mass concentrations: Revisiting common assumptions for estimating organic mass	Aerosol Science and Technology	Turpin, BJ (USA)	2001	656
2	Increased particulate air pollution and the triggering of myocardial infarction	Circulation	Peters, A (Germany)	2001	597
3	Association of fine particulate matter from different sources with daily mortality in six US cities	Environmental Health Perspectives	Laden, F (USA)	2000	543
4	Measuring and simulating particulate organics in the atmosphere: problems and prospects	Atmospheric Environment	Turpin, BJ (USA)	2000	483
5	Fine particulate air pollution and hospital admission for daily mortality	Jama-journal of the American Medical Association	Dominici, F (USA)	2006	434
6	Ambient pollution and heart rate variability	Circulation	Gold, DR (USA)	2000	414
7	Rethinking organic aerosols: Semivolatile emissions and photochemical aging	Science	Robinson, AL (USA)	2007	409
8	A review of carbon nanotube toxicity and assessment of potential occupational and environmental health risks	Critical Reviews in Toxicology	Lam, CW (USA)	2006	364
9	Chemical and microphysical characterization of ambient aerosols with the aerodyne aerosol mass spectrometer	Mass Spectrometry Reviews	Canagaratna, MR (USA)	2007	356
10	The effect of air pollution on lung development from 10 to 18 years of age	New England Journal of Medicine	Gauderman, WJ (USA)	2004	355
11	Particulate Matter Air Pollution and Cardiovascular Disease An Update to the Scientific Statement From the American Heart Association	Circulation		2010	349
12	European aerosol phenomenology-2: chemical characteristics of particulate matter at kerbside,urban,rural and background sites in Europe	Atmospheric Environment	Putaud, JP (Italy)	2004	330
13	The characteristics of PM <sub>2.5</sub> in Beijing,China	Atmospheric Environment	He, KB (Peoples R China)	2001	327
14	O/C and OM/OC ratios of primary,secondary,and ambient organic aerosols with high-resolution time-of-flight aerosol mass spectrometry	Environmental Science & Technology	Jimenez, J (USA)	2008	323
15	Reduction in fine particulate air pollution and mortality - Extended follow-up of the Harvard six cities study	American Journal of Respiratory and Critical Care Medicine	Laden, F (USA)	2006	313
16	Particulate matter in the atmosphere: which particle properties are important for its effects on health?	Science of the Total Environment	Harrison, RM (England)	2000	309
17	Spatial analysis of air pollution and mortality in Los Angeles	Epidemiology	Jerrett, M (USA)	2005	282
18	Source apportionment of PM <sub>2.5</sub> in the southeastern United States using solvent-extractable organic compounds as tracers	Environmental Science & Technology	Zheng, M (USA)	2002	275
19	Ambient air pollution and atherosclerosis in Los Angeles	Environmental Health Perspectives	Kunzli, N (USA)	2005	270
20	Daily variation of particulate air pollution and poor cardiac autonomic control in the elderly	Environmental Health Perspectives	Creason, J (USA)	1999	254

TC: times cited

**TABLE 3.**  
**Top 20 productive institutes on PM<sub>2.5</sub> research**

No	Institution of the first author	Count (%)	Institution of the corresponding author	Count (%)	Institutions for all authors	Count (%)
1	US EPA <sup>a</sup>	222(2.9)	US EPA	210(2.7)	Harvard Univ	596(7.7)
2	Harvard Univ	198(2.6)	Chinese Acad Sci	199(2.6)	US EPA	555(7.2)
3	Chinese Acad Sci	197(2.5)	Harvard Univ	156(2.0)	Chinese Acad Sci	528(6.8)
4	Peking Univ	98(1.3)	Peking Univ	93(1.2)	Univ Washington	309(4.0)
5	Clarkson Univ	86(1.1)	Clarkson Univ	88(1.1)	Peking Univ	235(3.0)
6	Univ Calif Davis	84(1.1)	Univ Calif Davis	84(1.1)	Univ Calif Davis	204(2.6)
7	Univ So Calif	76(1.0)	Desert Res Inst	78(1.0)	Univ So Calif	174(2.2)
8	Desert Res Inst	73(0.9)	Tsinghua Univ	72(0.9)	Clarkson Univ	171(2.2)
9	Tsinghua Univ	73(0.9)	CSIC	70(0.9)	Georgia Inst Technol	169(2.2)
10	CSIC <sup>b</sup>	72(0.9)	Univ So Calif	68(0.9)	Hong Kong Univ Sci & Technol	163(2.1)
11	Univ Washington	71(0.9)	Univ Washington	67(0.9)	Univ Calif Berkeley	163(2.1)
12	Georgia Inst Technol	70(0.9)	Fudan Univ	61(0.8)	Tsinghua Univ	145(1.9)
13	Fudan Univ	63(0.8)	Georgia Inst Technol	61(0.8)	Univ Utrecht	139(1.8)
14	Hong Kong Univ Sci & Technol	57(0.7)	Hong Kong Univ Sci & Technol	58(0.7)	Univ Wisconsin	138(1.8)
15	Hungkuang Univ	55(0.7)	Hungkuang Univ	56(0.7)	Univ Michigan	135(1.7)
16	Hong Kong Polytech Univ	52(0.7)	Hong Kong Polytech Univ	51(0.7)	Environm Canada	132(1.7)
17	Univ Calif Berkeley	52(0.7)	Brigham Young Univ	46(0.6)	Univ N Carolina	127(1.6)
18	NYU <sup>c</sup>	50(0.6)	N Carolina State Univ	44(0.6)	Carnegie Mellon Univ	123(1.6)
19	Brigham Young Univ	49(0.6)	NYU	44(0.6)	CSIC	120(1.6)
20	Hlth Canada	49(0.6)	Carnegie Mellon Univ	43(0.6)	Fudan Univ	117(1.5)

Note:

a: US Environmental Protection Agency

b: Consejo Superior de Investigaciones Científicas.

c: New York University

The top 20 most frequently cited publications are listed in Table 2. Moreover, 12 of the 20 top publications are about health. Topics related to health include daily mortality, asthma, myocardial infarction, cardiovascular disease, atherosclerosis, etc.

**Influential Institutions.** We analyzed the publishing institutes and found an uneven distribution. The 20 most productive institutes based on first author, corresponding author and all authors are shown in Table 3. As for institutes based on corresponding author, US EPA is the most productive institution with 210 papers, accounting for 2.7%. This was followed by the Chinese

Academy of Sciences with 199 papers (2.6%), Harvard University with 156 papers (2.0%) and Peking University with 93 papers (1.2%). As for the institutes based on all authors, Harvard University ranks first and University Washington ranks high. The distribution of institutes for the first author, corresponding author and all authors are similar in general.

**Analyses of Keywords. (1) The 20 most common keywords.** We analyzed the keywords to find the popular topics within PM<sub>2.5</sub> research. There were 9378 keywords used by the authors, with a total of 27915 occurrences. Overall, 6798 (72.5%) keywords appeared only once, while 9050 (96.5%)

keywords appeared less than ten times. The 20 most frequently used keywords are listed in Table 5 (see the first two columns). We grouped the keywords with similar meaning but with different spellings or forms (see the notes in Table 4.). It was not unexpected that the keywords referring to PM<sub>2.5</sub> and particulate matter (including “PM<sub>2.5</sub>”, “Particulate matter (PM)”, “PM<sub>10</sub>”, and “aerosol”) showed a high frequency of occurrence. The keywords referring to air (such as “air pollution” and “air quality”) also frequently appeared in PM<sub>2.5</sub>-related articles. It needs to be mentioned that indoor air appears to have attracted much attention in PM<sub>2.5</sub> research because the keyword “indoor air” ranked ninth in the list of keywords. As for the rest of the keywords, there were mainly three groups, namely, chemical composition, source apportionment and health effects. The keywords related to chemical composition include “Polycyclic Aromatic Hydrocarbons (PAHs)” that accounts for 0.8%, followed by “organic carbon (OC)” (0.7%), “metal” (0.7%), “elemental carbon (EC)” (0.6%) and “chemical composition” (0.6%). As for the keywords related to source apportionment, “source apportionment” accounts for 1.1%, while “positive matrix factorization (PMF)” (0.6%) was the mostly discussed model for source apportionment. “Traffic” (0.5%) and “biomass burning” (0.4%) were the source of PM<sub>2.5</sub> that were discussed the most. The keywords among the top 20 that related to health effects include “exposure” (1.0%) and “epidemiology” (0.4%).

We analyzed the keywords over different periods to find a change in the focus of PM<sub>2.5</sub> research. The annual number of articles changed in an unstable way from 1999 to 2014. It grew steadily from 1999 to 2003, followed by a rapid growth from 2004 to 2007. However, there was an unexpected sharp decline from 2008 to 2010, followed by a rapid growth from 2011 to 2014 (Fig. 1). Therefore, we analyzed the keywords over four periods. The 20 most common keywords during each period are shown in Table 5.

It can be observed that the distribution of keywords during the first period (1999–2003) apparently differs from the ones during the subsequent three periods that are similar. It seems that the PM<sub>2.5</sub> research in the first period almost equally covered basic and diverse topics in the area, including health effects (represented by the keywords such as “exposure”, “epidemiology”, “asthma”, “mortality”), chemical composition (“PAHs”, “OC”, “sulfate”, “metal”) and source apportionment (“source apportionment”, “traffic”). PM<sub>2.5</sub> and other related particles were also frequently discussed together in the first period because “total suspended particles (TSP)” and “coarse particles” were included in the top 20 keywords of the stage.

However, they were not included in the top 20 keywords for the subsequent periods. By comparing the four periods, we found some changes for the popular topics related to PM<sub>2.5</sub> research. Firstly, the topics related to health effects were not as popular during the last three periods as they were in the first period. Especially from 2008 to 2010, there was only one keyword about health. Secondly, PM<sub>2.5</sub> source apportionment is the most popular topic from 2004 because the related keywords rank high. Traffic sources were the major cause of concern in source apportionment research. Thirdly, chemical composition was always the most popular research topic during the four periods as “PAHs”, “OC” and “EC” appear in the top 20 keywords during every period. Fourthly, indoor air pollution was increasingly popular in PM<sub>2.5</sub> research.

**(2) Analysis of keywords by Country.** We analyzed the keywords of the articles from the 10 most productive countries to compare the research hotspots in different countries. The research production of the top 10 countries accounts for 75.6% of the total.

The results show that the top 20 keywords in research publications from USA, Germany, Canada, England and Spain include keywords related to health effects of PM<sub>2.5</sub>, while the top 20 keywords in research from China, Taiwan, South Korea and India do not. It implies that the research from American and European countries is more focused on the health effects of PM<sub>2.5</sub>. In addition, the top 20 keywords for the most productive countries include keywords related to composition and source apportionment, which indicates that research on the two aspects is popular in many countries.

In particular, we analyzed the keywords of articles from USA separately because USA is the most productive country and home of leading institutes with regard to PM<sub>2.5</sub> research (such as the US EPA and Harvard University). The statistics for the keywords are shown in Table 5 for the same four periods as in Table 4. It can be observed that the research on the health effects of PM<sub>2.5</sub> attracted much attention from 1999 to 2014. The most popular keywords related to health effects in this period include “exposure”, “epidemiology”, “mortality”, “asthma”, “cardiovascular disease”, “heart rate variability”, “inflammation” and “children”. Health-related keywords ranked the highest in general from 1999 to 2003, compared to keywords related to chemical composition and source apportionment. It seems that research on health effects was not very significant from 2004 to 2010, especially from 2008 to 2010, during which the number of health related keywords was the least. However, the rank of health related keywords increased over the next periods. The PM<sub>2.5</sub> source apportionment was much more

significant from 2004, with the keyword “source apportionment” ranking 4<sup>th</sup>. Keywords related to chemical composition have gradually decreased from the list of the top 20 keywords. The keywords from 2011 to 2014 were mainly related to source apportionment and health effects. We also noticed

that “Community Multi-scale Air Quality Model” (CMAQ) appeared in the list of top 20 keywords during the last two periods and ultimately ranked 9<sup>th</sup>. Its frequency increased from 0.5% to 0.9%. This suggests that air pollution simulation by the model has become increasingly popular.

**TABLE 4**  
**The top 20 most frequent keywords in different periods**

No	All (1999~2014)	%	1999~2003	%	2004~2007	%	2008~2010	%	2011~2014	%
1	PM <sub>2.5</sub>	6.0	PM <sub>2.5</sub>	8.1	PM <sub>2.5</sub>	7.0	PM <sub>2.5</sub>	6.3	PM <sub>2.5</sub>	5.4
2	PM	4.0	PM	4.8	PM	3.5	PM	4.0	PM	4.0
3	Air pollution	2.7	PM <sub>10</sub>	3.5	air pollution	2.5	PM <sub>10</sub>	3.0	Air pollution	2.8
4	PM <sub>10</sub>	2.1	air pollution	2.3	PM <sub>10</sub>	2.1	air pollution	2.6	PM <sub>10</sub>	1.5
5	Source apportionment	1.1	exposure	1.4	source apportionment	1.1	source apportionment	1.3	Source apportionment	1.2
6	exposure	1.0	PAHs	0.9	aerosol	1.0	PAHs	1.2	exposure	1.0
7	aerosol	0.9	Aerosol	0.9	EC	0.9	Exposure	1.1	Indoor air	0.9
8	PAHs	0.8	Indoor air	0.9	PAHs	0.8	Aerosol	1.5	PAHs	0.8
9	indoor air	0.7	OC	0.7	Exposure	0.8	Indoor air	0.8	PMF	0.7
10	OC	0.7	TSP	0.7	Indoor air	0.8	Air quality	0.8	Air quality	0.7
11	metal	0.7	Epidemiology	0.7	OC	0.8	OC	0.8	Metal	0.7
12	air quality	0.7	Chemical composition	0.7	Size distribution	0.7	Metal	0.8	Aerosol	0.6
13	PMF	0.6	Source apportionment	0.7	Metal	0.6	EC	0.7	Traffic	0.6
14	EC	0.6	Coarse particles	0.7	PMF	0.6	PMF	0.7	EC	0.6
15	Chemical composition	0.6	Asthma	0.7	Air quality	0.5	chemical mass balance (CMB)	0.5	OC	0.6
16	Traffic	0.6	Mortality	0.6	Sulfate	0.5	Traffic	0.5	Biomass	0.6
17	Size distribution	0.5	Air quality	0.6	Receptor model	0.5	Receptor model	0.5	Size distribution	0.5
18	ozone	0.4	Sulfate	0.6	Chemical composition	0.5	Ozone	0.4	Epidemiology	0.5
19	Epidemiology	0.4	Metal	0.6	Traffic	0.5	Size distribution	0.4	Ozone	0.5
20	Biomass burning	0.4	Traffic	0.5	Asthma	0.4	Trace element	0.4	Black carbon	0.5

Note: The keywords with the same meaning but in different spelling forms were grouped, and they are listed as follows.

PM<sub>2.5</sub>: PM<sub>2.5</sub>, PM (2.5), fine particle, fine particles, fine particle matter, fine particulate matter.

PM: PM, particulate matter(s), particulate(s), particle(s), air pollution particulate matter, and atmospheric particulate matter(s).

PM<sub>10</sub>: PM<sub>10</sub>, PM(10), and PM<sub>10</sub> dust.

Aerosol: aerosol, aerosols, ambient aerosol, and atmospheric aerosol.

Source apportionment: source apportionment, and aerosol source apportionment.

Exposure: exposure and personal exposure.

Size distribution: size distribution, size distributions, aerosol mass size distribution, and mass size distribution.

Sulfate: sulfate, sulfates, PM<sub>2.5</sub> sulfate, and PM<sub>2.5</sub> sulfates.

Chemical composition: chemical composition, chemical compositions, aerosol chemical compositions, and chemical constituents.

Traffic: traffic, traffic pollution, and road traffic.

Receptor model: receptor model, receptor models, and receptor modeling.

Metal: metal(s), metal element(s), metallic element(s), and heavy metal(s).



**TABLE 5**  
Most frequent keywords during the four periods in the publications from USA

No.	1999~2003		2004~2007		2008~2010		2011~2014	
	Top20	%	Top20	%	Top20	%	Top20	%
1	PM <sub>2.5</sub>	7.1	PM <sub>2.5</sub>	6.9	PM	5.5	PM <sub>2.5</sub>	5.5
2	PM	5.4	PM	4.4	PM <sub>2.5</sub>	5.1	PM	4.9
3	Air pollution	3.1	Air pollution	3.1	Air pollution	3.7	Air pollution	4.3
4	Exposure	2.1	Source	2.0	Source	2.1	Source	1.5
5	PM <sub>10</sub>	1.5	apportionment		apportionment		apportionment	
6	Asthma	1.1	PMF	1.4	Exposure	2.0	Exposure	1.3
7	PAHs	0.9	PM <sub>10</sub>	1.0	Ozone	1.2	Indoor air	1.2
8	Children	0.9	Sulfate	0.9	Diesel	1.1	Ozone	1.1
9	Epidemiology	0.8	EC	0.8	Asthma	1.0	air quality	0.9
10	OC	0.8	Receptor modeling	0.8	Air quality	0.9	CMAQ	0.9
11	Ozone	0.8	Ozone	0.8	OC	0.9	epidemiology	0.9
12	Mortality	0.7	OC	0.8	Traffic	0.9	Traffic	0.9
13	Source apportionment	0.7	Aerosol	0.8	PMF	0.8	environmental health	0.8
14	Carbon monoxide	0.7	Exposure	0.7	EC	0.7	Asthma	0.7
15	Receptor modeling	0.7	Asthma	0.7	Aerosol	0.6	Biomass burning	0.6
16	Nitrate	0.6	Mortality	0.6	Black carbon	0.6	PMF	0.6
17	Aerosol	0.6	Heart rate variability	0.6	Epidemiology	0.6	Exposure assessment	0.6
18	Air quality	0.5	Diesel	0.6	Carbon monoxide	0.5	PM <sub>10</sub>	0.6
19	Ammonia	0.5	Epidemiology	0.5	CMAQ	0.5	Black carbon	0.6
20	Health effects	0.5	Nitrogen dioxide	0.5	Children	0.4	inflammation	0.5
			Traffic	0.5	Coarse particulate matter	0.4	mortality	0.5

**TABLE 6**  
Most frequent keywords of China from 1999~2014

No.	Keywords	P%	No.	Keywords	P%
1	PM <sub>2.5</sub>	6.7	11	chemical composition	0.8
2	Source apportionment	2.3	12	China	0.8
3	PM <sub>10</sub>	1.8	13	Haze	0.8
4	PM	1.7	14	Size distribution	0.7
5	EC	1.6	15	dust storm	0.7
6	OC	1.4	16	Seasonal variation	0.6
7	aerosol	1.3	17	biomass burning	0.6
8	Air pollution	1.2	18	Water-soluble ions	0.6
9	Beijing	1.1	19	Pearl River Delta	0.6
10	PAHs	1.0	20	Shanghai	0.6

China is the second major productive country, with the number of publication increasing the fastest. PM<sub>2.5</sub> pollution in China has been drawing much attention globally, making the research on PM<sub>2.5</sub> from China important. There is no literature on PM<sub>2.5</sub> for 1999 from China, but the number of PM<sub>2.5</sub>

publications from China has increased rapidly from 3 in 2000 to 264 in 2014. We analyzed the keywords of PM<sub>2.5</sub> research from China to find the popular ones. The top 20 keywords are shown in Table 6. These keywords are related to PM<sub>2.5</sub> source studies, composition studies, and case areas. The keyword

“source apportionment” ranks second, which shows that source apportionment is the most popular topic of PM<sub>2.5</sub> studies from China. At present, most of the local governments of cities with heavy PM<sub>2.5</sub> pollution are promoting PM<sub>2.5</sub> source apportionment research, which is a background work for PM<sub>2.5</sub> pollution control. The three most significant case areas for PM<sub>2.5</sub> research in China are Beijing, Shanghai and the Pearl River Delta area.

## RESEARCH ORIENTATION ANALYSIS

We conducted a statistical analysis for main keywords to discover the most popular topics within PM<sub>2.5</sub> research. Because there were 9378 different keywords in total, it was difficult to examine each of them. We only chose the top 1000 keywords, based on frequency, out of the 9378 to conduct the statistical analysis. The frequency of each keyword in the set was less than 3. We examined each one of the 1000 keywords and classified them.

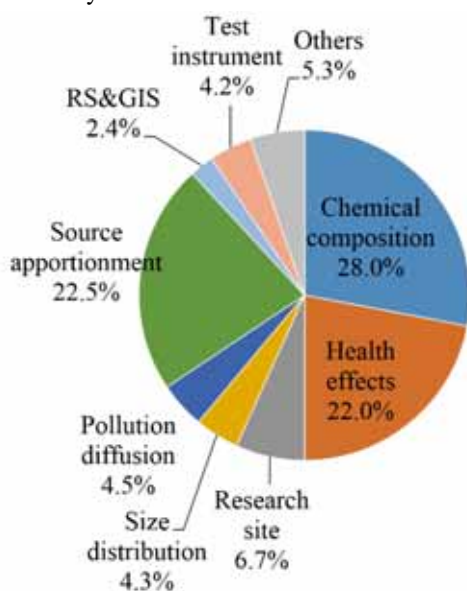


**FIGURE 3**  
Research fields of PM<sub>2.5</sub> publications

Except for the keywords generally describing particulate matter and air pollution, such as “PM<sub>2.5</sub>”, “fine particle(s)”, “PM<sub>10</sub>”, “particulate matter”, “coarse particle(s)”, “air quality” and “aerosol”, we classified the rest of the keywords into nine categories, namely, chemical composition, health effects, source apportionment, size distribution, pollutant transport, remote sensing (RS) and geographic information system (GIS), research site, test instrument and others (see Fig. 3). The RS&GIS category includes keywords related to RS data, image classification methods, GIS techniques and methods of spatial analysis and spatial simulation.

The “others” category includes analytic methods (such as “time series analysis”, “multiple linear regression”, “molecular marker”), air cleaning, environmental impact etc. The top three categories were chemical composition, source apportionment and health impact

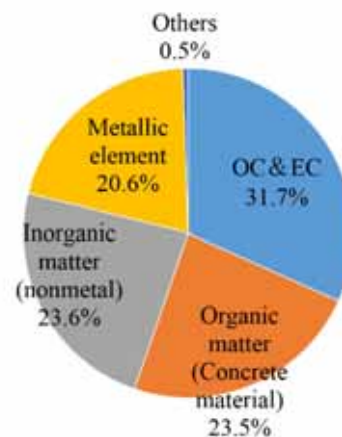


**FIGURE 4**  
Types of keywords in PM<sub>2.5</sub> composition research

of PM<sub>2.5</sub>, which occupied almost three quarters of all of the keywords. In addition, the keywords that include particle size distribution, pollution diffusion, RS and GIS, research site and test instrument are less than 10%. It can be observed that the chemical composition, source apportionment and health effects are the three main aspects of PM<sub>2.5</sub> research. There are some important studies on other aspects as well, such as prediction of PM<sub>2.5</sub> concentration [24], diffusion [25], particle size distribution [26,27], RS and GIS techniques [22,24,28] and test instrument [29,30,31].

We further examined the keywords related to chemical composition, source apportionment and health effects, separately.

As for the keywords related to the chemical composition of PM<sub>2.5</sub>, except for the keywords describing composition itself (such as “composition”, “chemical composition”, etc.), the rest were classified into five categories, namely, OC & EC (including “OC”, “EC”, “BC”, etc.), organic matter (including “PAHs”, “VOCs”, etc.), non-metallic inorganic matter (including “sulfate”, “ammonia”, “nitrates”, etc.), metallic inorganic matter (including “metals”, “trace elements”, “lead”, “arsenic”, etc.), and others (including the keywords with very low frequency, such as “pollen”, “fungi”, etc.). The corresponding statistics are shown in Fig. 4.

The chemical composition of PM<sub>2.5</sub> may include OC, EC, sulfate, nitrate, ammonium and geological material, etc. [32,33,34]. The composition and proportions of different matters often vary across regions or cities due to

environmental conditions, such as transportation, fuel consumption, industries and geographic features [33]. For example, airborne  $PM_{2.5}$  in seaside cities may contain sea-salt, while  $PM_{2.5}$  around industries may contain heavy metals or specific pollutants. The composition of  $PM_{2.5}$  and proportions of matters can also vary temporally, for example, depending on the season. We reviewed articles related to  $PM_{2.5}$  composition and have listed the typical research results in Table 7. According to these results, OC and EC are the main matters in the composition of  $PM_{2.5}$ , with a proportion from approximately 20% to 60%. The proportion of OC is usually larger than EC. Sulfate is also a common composition matter, with a proportion from approximately 10% to 35%. This is followed by nitrate and ammonium, which occupy less than 20%.

For research on source apportionment of  $PM_{2.5}$ , keywords were divided into source apportionment models and specific sources, which include industry emissions, biomass burning, traffic exhausts, soil and agriculture and others (such as dust storm, mineral dust, sea salt, tobacco smoke, cooking, incense, etc.). The statistics for keyword categories above is shown in Fig. 5. It can be observed that more than a quarter of keywords are related to source apportionment models. The models mainly include receptor model, principal component analysis (PCA), positive matrix factorization (PMF), chemical mass balance (CMB), UNMIX, etc. Zheng et al. [46] reviewed the receptor model based source apportionment methods. The other keywords describe specific sources of  $PM_{2.5}$ , of which industry emission, biomass burning and traffic are the most significant keywords. “Coal” occupies the highest proportion, at 22.4%, in industry emission related keywords.

Source apportionment of  $PM_{2.5}$  provides fundamental support for reduction in  $PM_{2.5}$ . Therefore, researchers studied the source apportionment of  $PM_{2.5}$  in different places around the world to support local policymaking. According to their results, we found that the sources of  $PM_{2.5}$  were diverse across the world. Table 8 lists some typical research results from different places in the world. According to [47], secondary sulfates are the main sources of  $PM_{2.5}$  and contribute almost a half of the  $PM_{2.5}$  in three cities in USA. Viana et al. [48] found that vehicular emissions are the largest source of  $PM_{2.5}$  in five cities in Spain, followed by industrial emissions and secondary sulfates and nitrates. Scheff and Valiozis [49] also found that vehicular and industrial emissions dominate the sources of  $PM_{2.5}$  in another European city—Athens, Greece. However,

the studies from developing countries in Asia suggest that coal combustion might be the main source of  $PM_{2.5}$  [50,51,52,53].

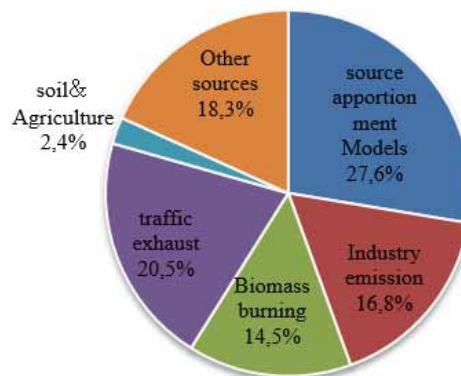


FIGURE 5

Types of keywords in  $PM_{2.5}$  source research

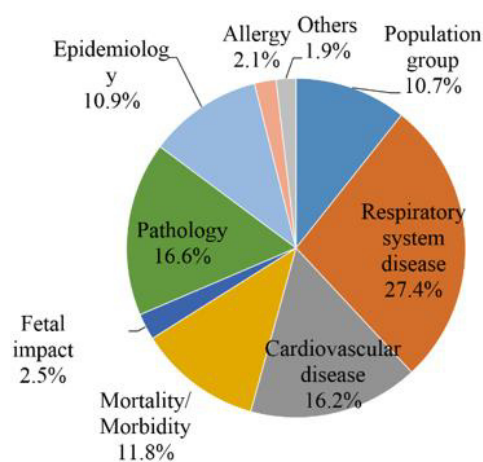


FIGURE 6

Types of keywords in  $PM_{2.5}$  health research

As for research regarding the health effects of  $PM_{2.5}$ , the statistics for the keywords are shown in Fig. 6. Specific population groups, such as children, seniors and pregnant women, were studied by many studies in relation to health effects from  $PM_{2.5}$ . Respiratory and cardiovascular diseases were the most discussed diseases related to  $PM_{2.5}$  exposure. Meanwhile, the impact of  $PM_{2.5}$  exposure on mortality was also a very popular topic in these studies, followed by the impact on fetal development and allergy. In addition, there were also many other keywords about health effects, such as cancer, mutagenicity, stroke, diabetes and obesity, which had low frequencies.

**TABLE 7**  
**Some typical results of studies on PM<sub>2.5</sub> composition**

Country/ territory	City or region	Reference	Composition matters and their percentages (%)							Geological material	Note
			OC	Inorganic matter					Else <sup>a</sup>		
				EC	Sulfate	Nitrate	Ammonium				
South Korea	Chong ju	[35]	11.3	10.0	18.6	8.2	6.4	-	-	Samples was collected over four seasons from 27 October 1995 to 25 August 1996	
China	Pearl river Delta region	[36]	42	3.7	19	12	8.4	-	-	24-hr PM <sub>2.5</sub> samples were collected during November- December 2010	
	Beijing	[37]	37.9	3.1	26.7	15.8	15.9	0.87(Cl)	-	Samples was collected during 24 July to 20 September 2008	
	Shanghai	[38]	30.2	11.2	23.4		18.2	2.7(K <sup>+</sup> )	9.6	Weekly PM <sub>2.5</sub> samples was collected at two sites for 1 year March 2002 to February 2008	
Taiwan	Taipei	[39]	15.9	5.4	21.1	5.8	-	-	-	Twenty-four samples from November 1991 to October 1992.	
Japan	Sapporo	[40]	17.8-35.1	13.8-34.2	10.0-28.8	0.6-6.9	1.6-9.2	-	-	14 intensive sampling days from 9 July to 31 August 1990	
USA	California	[41]	40-60			25-35		-	-	40-day period during November and December, 1978	
	Denver	[42]	21.6	15.3	33.6	-	-	-	-	Samples were collected at six sites within the urban area during February and March 2003	
Mexico	Salamanca	[43]	34	12.9	25.1	-	-	-	12.5	33 samples from December 19, 1989 through February 5, 1990	
	Mexico City	[44]	35.6	14.4	16.9	3.33	-	-	-	Samples were collected from 23 February to 22 March 1997	
	Mexico City	[45]	50			30			15		

a: "Else" includes inorganic matters (such as Na<sup>+</sup>, Ca<sup>+</sup>, Cl<sup>-</sup>, etc.) and water.

**TABLE 8**  
Some typical results of studies on PM<sub>2.5</sub> source apportionment

Country	City	References	Secondary source	Sources and their percentages (%)							Models	
				Fuel combustion			Industry	Vehicular emissions	Crustal sources	Sea salt		Else
				Coal combustion	Oil combustion	Biomass burning						
USA	WashingtonDC		67	10	3	-	5	9	3	3	-	PMF
	Brigantine NJ	[47]	63	8	2	8	5	6	1	8	-	
	Underhill VT		53	7	7	14	7	-	4	1	7	
India	Jorhat	[51]	8	26	-	9		19	38	-	-	EF,CA, PCA
China	Beijing	[50]	31	19	-	11	6	6	9	-	8	PMF
	Zhengzhou	[52]	24	23		13	4	10	26	-	-	PMF
	Jinan	[53]	55.15	20.98	-	4.55	2.87	6.06	9.30	-	-	PMF
South Korea	Incheon	[54]	44.4		6.1	6.1	8.5	23	6	5.9		PMF
Spain	Albacete*		34	-	-	-	31	39	-	3	0	
	Barcelona		15	-	-	-	20	53	-	5	7	
	Galdakao	[48]	14	-	-	-	13	44	-	3	26	PCA
	Huelva		24	-	-	-	24	35	-	7	10	
	Oviedo		16	-	-	-	24	41	-	4	15	
Greece	Athens	[49]	13.0	-	-	-	23.3	20.3	4.5	-	38.9	CMB
Italy	Milan	[55]	43.6			43.1			13.3			PCA APCA

**Note:**

EF: Enrichment Factor

CA: Correlation Analysis

PCA: Principal Component Analysis

APCA: Absolute Principal Components Analysis

The health effects of PM<sub>2.5</sub> were popular topics for many years. USA published the most papers related to health effects due to PM<sub>2.5</sub> from 1999 to 2014, but researchers from developing countries such as China started to pay more attention on this issue in recent years [56]. In 2004, the American Heart Association (AHA) suggested that exposure to PM<sub>2.5</sub> pollution could increase cardiovascular morbidity and mortality [57]. Brook et al. [6] reviewed numerous corresponding studies and believed these findings further confirmed the AHA's scientific statement published in 2004. Pope and Dockery [58] comprehensively evaluated the research related to PM<sub>2.5</sub> health effects and concluded that previous studies provided persuasive evidence that exposure to PM<sub>2.5</sub> has negative effects on cardiopulmonary health.

## CONCLUSION

We conducted a bibliometric analysis of global PM<sub>2.5</sub> research from 1999 to 2014, evaluated the research performance and provided perspectives on the research trends. Journal article is the most frequent document type, while English is the most prevalent language among these publications. The annual number of publications increased in general during this period, from 118 in 1999 to 1262 in 2014.

However, we did observe a clear decline from 2008 to 2010. USA occupied the leading position in the ranking list of research outputs on PM<sub>2.5</sub>, by contributing 36.0% of the total outputs. China ranked the second, with a steep upward trend since 2004. Atmospheric Environment published the most PM<sub>2.5</sub> articles, followed by The Air & Waste Management Association Journal, Science of The Total Environment, Environmental Science & Technology and Environmental Health Perspectives. The top 5 most productive institutes of RP-printer were US EPA, Chinese Academy of Science, Harvard University, Peking University and Clarkson University.

Analysis of keywords showed that there were three popular topics in PM<sub>2.5</sub> research, namely, chemical composition, source apportionment and health effects. Size distribution, pollutant diffusion, and RS & GIS techniques were also much discussed. Meanwhile, we also noticed that the PM<sub>2.5</sub> research covered a wide range of sub-topics because a large number of keywords appeared only once. In particular, 96.5% of the keywords appeared less than ten times. The most frequent keywords relating to composition included "PAHs", "OC" and "EC". PMF and receptor model were the most frequently mentioned methods in source apportionment research, while traffic was the most frequently discussed source. By analyzing the keywords during

different periods, we found that PM<sub>2.5</sub> source apportionment attracted more and more attention. Indoor air quality was also a cause of concern in recent years. We further found that the researchers from American and European countries were more concerned about health effects than the ones from Asian countries. However, developing countries such as China paid close attention to the research of PM<sub>2.5</sub> source apportionment and chemical composition.

We further conducted keywords analyses for each of the three popular topics mentioned above and listed some typical research results from around the world. The results showed that the composition of PM<sub>2.5</sub> varies around the world. Generally, PM<sub>2.5</sub> is composed of OC, EC, sulfates, nitrates, ammonium, etc. PM<sub>2.5</sub> has diverse sources due to different environment conditions. Chemical composition and source apportionment were popular topics across time and countries. The research on health effects of PM<sub>2.5</sub> covered a large range of sub-topics, including various human diseases. However, respiratory and cardiovascular diseases were the most common.

#### ACKNOWLEDGEMENTS

The research was funded by LIESMARS Special Research Funding and the National Natural Science Foundation of China (41571385).

#### REFERENCES

- [1] Dockery, D. W., Schwartz, J., Spengler, J. D., 1992. Air pollution and daily mortality: associations with particulates and acid aerosols. *Environmental Research*, 59, 362-373.
- [2] Dogkery, D. W., III, C. A. P., Xu, X., Spengler, J. D., Ware, J. H., Fay, M. E., et al., 1993. An association between air pollution and mortality in six U.S. cities. *The New England Journal of Medicine*, 329(24), 1753-1759.
- [3] Pope, C. A. I., Renlund, D. G., Kfoury, A. G., May, H. T., Horne, B., D., 2008. Relation of Heart Failure Hospitalization to Exposure to Fine Particulate Air Pollution. *American Journal of Cardiology*, 102, 123-1234.
- [4] Pope, C. A., 3rd, Burnett, R. T., Turner, M. C., Cohen, A., Krewski, D., Jerrett, M., et al., 2011. Lung cancer and cardiovascular disease mortality associated with ambient air pollution and cigarette smoke: shape of the exposure-response relationships. *Environment Health Perspective*, 119(11), 1616-1621.
- [5] Chen, M. L., Mao, I. F., Lin, I. K., 1999. The PM<sub>2.5</sub> and PM<sub>10</sub> particles in urban areas of Taiwan. *Science of the Total Environment*, 226, 227-235.
- [6] Brook, R. D., Rajagopalan, S., Pope, C. A., 3rd, Brook, J. R., Bhatnagar, A., Diez-Roux, A. V., et al., 2010. Particulate matter air pollution and cardiovascular disease: An update to the scientific statement from the American Heart Association. *Circulation*, 121(21), 2331-2378.
- [7] Makkonen, U., Hellen, H., Anttila, P., Ferm, M., 2010. Size distribution and chemical composition of airborne particles in south-eastern Finland during different seasons and wildfire episodes in 2006. *Science of the Total Environment*, 408(3), 644-651.
- [8] Rasmussen, P. E., Wheeler, A. J., Hassan, N. M., Filiatreault, A., Lanouette, M., 2007. Monitoring personal, indoor, and outdoor exposures to metals in airborne particulate matter: Risk of contamination during sampling, handling and analysis. *Atmospheric Environment*, 41(28), 5897-5907.
- [9] Wang, J., Hu, Z., Chen, Y., Chen, Z., Xu, S., 2013. Contamination characteristics and possible sources of PM<sub>10</sub> and PM<sub>2.5</sub> in different functional areas of Shanghai, China. *Atmospheric Environment*, 68, 221-229.
- [10] Saracevic, T., Perk, L. J., 1973. Ascertaining activities in a subject area through bibliometric analysis. *Journal of the American Society for Information Science*, (2), 120-134.
- [11] Liu, X., Zhan, F.B., Hong, S., Niu, B., Liu, Y., 2012. A bibliometric study of earthquake research: 1900–2010. *Scientometrics*, 92(3), 747-765.
- [12] Chiu, W.T., Ho, Y.S., 2007. Bibliometric analysis of tsunami research. *Scientometrics*, 73(1), 3-17.
- [13] Ho, Y.S., 2007. Bibliometric analysis of adsorption technology in environmental science. *Journal of Environmental Protection Science*, 1, 1-11.
- [14] Liu, X., Zhang, L., Hong, S., 2011. Global biodiversity research during 1900–2009: a bibliometric analysis. *Biodiversity and Conservation*, 20(4), 807-826.
- [15] Nederhof, A. J., Zwaan, R., De Bruin, R., Dekker, P., 2005. Assessing the usefulness of bibliometric indicators for the humanities and the social and behavioural sciences: A comparative study. *Scientometrics*, 15, 423–435.
- [16] Tian, Y., Wen, C., Hong, S., 2008. Global scientific production on GIS research by bibliometric analysis from 1997 to 2006. *Journal of Informetrics*, 2(1), 65-74.
- [17] Tsay, M.Y., 2011. A bibliometric analysis and comparison on three information science journals. *Scientometrics*, 89, 591-606.

- [18] Zhuang, Y., Hong, S., Lin, H., Niu, B., 2011. Global Environmental Impact Assessment Research Trends (1973-2009). *Procedia Environmental Sciences*, 11, 1499-1507.
- [19] Xie, S., Zhang, J., Ho, Y.-S., 2008. Assessment of world aerosol research trends by bibliometric analysis. *Scientometrics*, 77(1), 113-130.
- [20] Li, J.F., Zhang, Y.H., Veber, M., et al., 2013. Bibliometric analysis of research on secondary organic aerosols: A Science Citation Index Expanded-based analysis (IUPAC Technical Report). *Pure and Applied Chemistry*, 85(6): 1241-1255.
- [21] Li, J.F., Zhang, Y.H., Herjavec, G., Wine, P.H., Klasinc, L., 2014. Bibliometric analysis of research on secondary organic aerosols: Update. *Pure and Applied Chemistry*, 86(7): 1169-1175.
- [22] Superczynski, S. D., Christopher, S. A., 2011. Exploring Land Use and Land Cover Effects on Air Quality in Central Alabama Using GIS and Remote Sensing. *Remote Sensing*, 3(12), 2552-2567.
- [23] Shi, X. H., Xu, X. D., 2012. Progress in the study of regional impact of aerosol and related features of heavy fog in Beijing City. *Chinese Journal of Geophysics-Chinese Edition*, 55, 3230-3239.
- [24] Hochadel, M., Heinrich, J., Gehring, U., Morgenstern, V., Kuhlbusch, T., Link, E., et al., 2006. Predicting long-term average concentrations of traffic-related air pollutants using GIS-based information. *Atmospheric Environment*, 40(3), 542-553.
- [25] ApSimon, H. M., del Campo, M. T. G., Adams, H. S., 2001. Modelling long-range transport of primary particulate material over Europe. *Atmospheric Environment*(35), 343-352.
- [26] Solci, A. d. M. F. e. M. C., 2009. Characterization of PM10 and PM2.5 and Size Distribution of Chloride, Nitrate and Sulphate in Urban and Rural Atmospheres of Londrin. *Quimica Nova*, 32(7), 1750-1754.
- [27] Wang, Z., Chen, L., Tao, J., Zhang, Y., Su, L., 2010. Satellite-based estimation of regional particulate matter (PM) in Beijing using vertical-and-RH correcting method. *Remote Sensing of Environment*, 114(1), 50-63.
- [28] Sahu, S. K., Beig, G., Parkhi, N. S., 2011. Emissions inventory of anthropogenic PM2.5 and PM10 in Delhi during Commonwealth Games 2010. *Atmospheric Environment*, 45, 6180e6190.
- [29] Bogo, H., Otero, M., Castro, P., Ozafrán, M. J., Kreiner, A., Calvo, E. J., et al., 2003. Study of atmospheric particulate matter in Buenos Aires city. *Atmospheric Environment*, 37(8), 1135-1147.
- [30] Tian, J., Chen, D. M., 2007. Evaluating Satellite-Based Measurements for Mapping Air Quality in Ontario, Canada. *Journal of Environmental Informatics*, 10, 30-36.
- [31] Tiwary, A., Reff, A., Colls, J. J., 2008. Collection of ambient particulate matter by porous vegetation barriers Sampling and characterization methods. *Aerosol Science*, 37, 40-47.
- [32] Sillanpää, M., Hillamo, R., Saarikoski, S., Freya, A., Pennanen, A., Makkonen, U., 2006. Chemical composition and mass closure of particulate matter at six urban sites in Europe. *Atmospheric Environment*, 40, S212-S223.
- [33] Mu, C.C., Feng, Y.L., Zhai, J.Q., Xiong, B., Zou, T., 2010. Determination of Dicarbonyl Compounds in Ambient Fine Particles by High Performance Liquid Chromatography after 2,4-Dinitrophenylhydrazine Derivative. *Chinese Journal of Analytical Chemistry*, 38(11), 1573-1577.
- [34] Zhu, C.S., 2012. Indoor and Outdoor Chemical Components of PM2.5 in the Rural Areas of Northwestern China. *Aerosol and Air Quality Research*, 12(6), 1157-1165.
- [35] Lee, H. S., Kang, B.-W., 2001. chemical characteristics of principal PM2.5 species in Chongju, South Korea. *Atmospheric Environment*, 35, 739-746.
- [36] Wang, X., Ding, X., Fu, X., He, Q., Wang, S., Bernard, F., et al., 2012. Aerosol scattering coefficients and major chemical compositions of fine particles observed at a rural site in the central Pearl River Delta, South China. *Journal of Environmental Sciences*, 24(1), 72-77.
- [37] Huang, X. F., He, L. Y., Hu, M., Canagaratna, M. R., Sun, Y., 2010. Highly time-resolved chemical characterization of atmospheric submicron particles during 2008 Beijing Olympic Games using an Aerodyne High-Resolution Aerosol Mass Spectrometer. *Atmospheric Chemistry and Physics*, 10, 8933-8945.
- [38] Ye, B., Ji, X., Yang, H., Yao, X., Chan, C. K., Cadle, S. H., et al., 2003. Concentration and chemical composition of PM2.5 in Shanghai for a 1-year period. *Atmospheric Environment*, 37, 499-510.
- [39] Chang, S. C., Chou, C. C. K., Chan, C. C., Lee, C. T., 2010. Temporal characteristics from continuous measurements of PM2.5 and speciation at the Taipei Aerosol Supersite from 2002 to 2008. *Atmospheric Environment*, 44, 1088-1096.
- [40] Ohta, S., Hori, M., Yamagata, S., Murao, N., 1998. Chemical characterization of atmospheric fine particles in Sapporo with determination of



- water content. *Atmospheric Environment*, 32(6), 1021-1025.
- [41] Chow, J.C., Watson, J.G., Lu, Z., Lowenthal, D.H., Frazier, C. A., Solomon, P.A., et al., 1996. Descriptive analysis of PM<sub>2.5</sub> and PM<sub>10</sub> at regionally representative locations during SJVAQS/AUSPEX. *Atmospheric Environment*, 30(12), 2079-2112.
- [42] Countess, R. J., Wolff, G. T., Cadle, S. H., 1980. The Denver Winter Aerosol: A Comprehensive Chemical Characterization. *Journal of the Air Pollution Control Association*, 30(11), 1194-1200.
- [43] Vega, E., Ruiz, H., Martínez-Villa, G., Sosa, G., González-Ávalos, E., Reyes, E., et al., 2007. Fine and Coarse Particulate Matter Chemical Characterization in a Heavily Industrialized City in Central Mexico during Winter 2003. *Journal of the Air & Waste Management Association*, 57(5), 620-633.
- [44] Vega, E., Garcia, I., Apam, D., Ruiz, M. E., Barbiaux, M., 1997. Application of a chemical mass balance receptor model to respirable particulate matter in Mexico City. *Journal of Air and Waste Management Association*, 47, 524-529.
- [45] Chow, J. C., Watson, J. G., Edgerton, S. A., Vega, E., 2002. Chemical composition of PM<sub>2.5</sub> and PM<sub>10</sub> in Mexico City during winter 1997. *The Science of the Total Environment*, 287, 177-201.
- [46] Zheng, M., Zhang, Y., Yan, C., Zhu, X., Schauer, J.-J., Zhang, Y., 2013. Review of PM<sub>2.5</sub> source apportionment methods in China. *Acta Scientiarum Naturalium Universitatis Pekinensis*, 50(6), 1141-1154.
- [47] Song, X. H., Polissar, A. V., Hopke, P. K., 2001. Sources of fine particle composition in the northeastern US. *Atmospheric Environment*, 35, 5277-5286.
- [48] Viana, M., Querol, X., Götschi, T., Alastuey, A., Sunyer, J., Forsberg, B., et al., 2007. Source apportionment of ambient PM<sub>2.5</sub> at five Spanish centres of the European community respiratory health survey (ECRHS II). *Atmospheric Environment*, 41(7), 1395-1406.
- [49] Scheff, P. A., Valiozis, C., 1990. Characterization and source identification of respirable particulate matter in Athens, Greece. *Atmospheric Environment*, 24A(1), 203-211.
- [50] Song, Y., Zhang, Y., Xie, S., Zeng, L., Zheng, M., Salmon, L. G., et al., 2006. Source apportionment of PM<sub>2.5</sub> in Beijing by positive matrix factorization. *Atmospheric Environment*, 40(8), 1526-1537.
- [51] Khare, P., Baruah, B. P., 2010. Elemental characterization and source identification of PM<sub>2.5</sub> using multivariate analysis at the suburban site of North-East India. *Atmospheric Research*, 98, 148-162.
- [52] Geng, N.B., Wang, J., Xu, Y.F., Zhang, W.D., Chen, C., Zhang, R.Q., 2013. PM<sub>2.5</sub> in an industrial district of Zhengzhou, China: Chemical composition and source apportionment. *Particuology*, 11, 99-109.
- [53] Yang, L.X., Cheng, S.H., Wang, X.F., Nie, W., Xu, P.J., Gao, X.M., Yuan, C., Wang, W.X., 2013. Source identification and health impact of PM<sub>2.5</sub> in a heavily polluted urban atmosphere in China. *Atmospheric Environment*, 75, 265-269.
- [54] Choi, J.K., Heo, J.B., Ban, S.J., Yi, S.M., Zoh, K.D., 2013. Source apportionment of PM<sub>2.5</sub> at the coastal area in Korea. *Sci Total Environ*, 447, 370-380.
- [55] Marcazzan, G. M., Ceriani, M., Valli, G., Vecchi, R., 2003. Source apportionment of PM<sub>10</sub> and PM<sub>2.5</sub> in Milan (Italy) using receptor modelling. *Science of the Total Environment*, 317(1-3), 137-147.
- [56] Huang, W., Cao, J., Tao, Y., Dai, L., Lu, S. E., Hou, B., et al., 2012. Seasonal variation of chemical species associated with short-term mortality effects of PM(2.5) in Xi'an, a Central City in China. *Am J Epidemiol*, 175(6), 556-566.
- [57] Brook, R. D., Franklin, B., Cascio, W., Hong, Y., Howard, G., Lipsett, M., et al., 2004. Air pollution and cardiovascular disease: a statement for healthcare professionals from the Expert Panel on Population and Prevention Science of the American Heart Association. *Circulation*, 109(21), 2655-2671.
- [58] Pope, C. A. I., Dockery, D. W., 2006. Health Effects of Fine Particulate Air Pollution: Lines that Connect. *Journal of the Air & Waste Management Association*, 56, 709-742.

---

**Received: 15.05.2015**

**Accepted: 18.09.2016**

---

#### CORRESPONDING AUTHORS

---

##### Haobo Hou

School of Resource and Environment Science  
Wuhan University  
129 Luoyu Road  
430079 Wuhan – P.R. CHINA

E-Mail: hhb-bhh@163.com



# UPTAKE OF CHLORTETRACYCLINE BY YELLOW LUPIN (*LUPINUS LUTEUS* L.) GROWING UNDER PHOTOPERIOD OR AT CONSTANT DARKNESS

Michał Baciak<sup>1</sup>, Agnieszka I Piotrowicz-Cieslak<sup>2,\*</sup>, Barbara Adomas<sup>1</sup>

<sup>1</sup> Department of Environmental Toxicology, Faculty of Environmental Management and Agriculture, University of Warmia and Mazury in Olsztyn, Prawocheńskiego 17, 10-720 Olsztyn, Poland

<sup>2</sup> Department of Plant Physiology, Genetics and Biotechnology, Faculty of Biology and Biotechnology, University of Warmia and Mazury in Olsztyn, Oczapowskiego 1A, 10-718 Olsztyn, Poland

## ABSTRACT

Tetracyclines are a group of the most commonly-used antibiotics in the world. They are sensitive to light and are degraded by light and oxidative factors. The studies were conducted under photoperiodic conditions and constant darkness in order to establish whether solar light has an impact on the uptake of chlortetracycline by 8-day-old yellow lupin seedlings. In addition, it was investigated whether chlortetracycline in soil (under photoperiod or darkness) influences the activity of peroxidase and superoxide dismutase, i.e. the enzymes that neutralize free radicals, in yellow lupin roots and stems. Yellow lupin seedlings growing in darkness produced longer roots and stems in comparison to plants growing under photoperiodic conditions by 23% and 155%, respectively. The length of stems was affected by the tested concentrations of the drug and light conditions. There was an inhibition of the growth of stems on soil contaminated with the drug (at 100 mg · kg<sup>-1</sup> of soil) at constant darkness and photoperiod by 82% and 77%, respectively. The concentration of chlortetracycline in roots and stems growing in light was lower (370 and 10 ng · g<sup>-1</sup> of fresh weight, respectively) than in plants growing in darkness (643 and 34 ng · g<sup>-1</sup> of fresh weight, respectively). The content of chlortetracycline determined after eight days in roots and stems of yellow lupin seedlings growing in a photoperiod and at constant darkness clearly proves that roots, regardless of light conditions, contained more drug than stems. Moreover, the activity of superoxide dismutase in roots and stems growing in constant darkness doubled in comparison with photoperiodic plants. In roots it ranged from approximately 1 U (photoperiod) to about 2 U (darkness) while in stems it ranged between 2 (photoperiod) and 4 U (darkness).

## KEYWORDS:

chlortetracycline; *Lupinus luteus* L.; photoperiod; constant darkness

## INTRODUCTION

Veterinary antibiotics are important measures for the treatment of diseases in production animals [1]. However, the annual increase in their use in cattle and poultry production is disturbing. In Europe in 1996, the volume of antibiotics used in veterinary medicine was about 10,000 tons, of which 50% were medicaments and growth stimulators. In the USA in 2000, approximately 23,000 tons of antibiotics were used in animal production (of which growth stimulators constituted about 40%) [2]. Tetracyclines, including tetracycline, chlortetracycline and oxytetracycline, are among the most commonly used antibiotics worldwide [3, 4, 5]. Since they are poorly absorbed and excreted in substantial amounts in the digestive tract of animals (about 50 – 80%) with faeces and urine [6, 7], chlortetracycline, oxytetracycline and tetracycline are detected in manure and slurry. As reported by Martínez-Carballo et al. [8], the concentrations of chlortetracycline, oxytetracycline and tetracycline in pig manure are 46 mg · kg<sup>-1</sup>, 29 mg · kg<sup>-1</sup> and 23 mg · kg<sup>-1</sup>, respectively. In fresh chicken manure, the lowest detected limit of oxytetracycline, tetracycline and chlortetracycline were 0.029 mg · kg<sup>-1</sup>, 0.055 mg · kg<sup>-1</sup> and 0.073 mg · kg<sup>-1</sup>, respectively [9]. The presence of tetracyclines in manure and slurry result in their occurrence in soil. Tetracyclines tend to persist and may accumulate in sandy soils after repeated fertilizations with liquid manure [10]. High concentrations of tetracyclines have been detected in soil in Turkey and Spain (up to 0.5 mg · kg<sup>-1</sup> and 0.2 mg · kg<sup>-1</sup>, respectively) [11, 12], whereas in soil fertilized with manure, the content of oxytetracycline, tetracycline and chlortetracycline reaches levels as high as 5.17, 0.553 and 0.588 mg · kg<sup>-1</sup>, respectively [13]. The presence of antibiotics in soil influences the metabolism and physiology of plants. Chlortetracycline is phytotoxic to maize and pinto bean. An increase in the content of chlortetracycline in soil causes a significant increase in the activity of plant stress proteins, namely, glutathione S-transferases (GST)

and peroxidases (POX), in maize [14]. Physiological changes in plants growing on soil with tetracyclines have been repeatedly demonstrated [14, 15, 16]. An increase in the activity of stress proteins (glutathione S-transferases and peroxidase) in maize [14], a reduction in photosynthesis rate and in assimilative transport of electrons have been reported in *Salix fragilis* L. [17]. A phytotoxic effect of tetracycline on maize consists in the formation of free radicals, mainly the hydroxyl radical [16], whereas in *Saccharomyces cerevisiae*, superoxide dismutase (SOD1) is essential to reduce susceptibility to oxytetracycline [18]. While protecting against unfavorable environmental factors, including xenobiotics such as drugs, plants developed a range of enzymatic and non-enzymatic defensive mechanisms. The first line of defense against harmful environmental factors consists of peroxidase [POD, EC 1.11.1.7] and superoxide dismutase [SOD, EC 1.15.1.1] [19]. Peroxidases (POD, a donor: hydrogen peroxide oxydoreductase) are found in all terrestrial plants, except for unicellular algae [20, 21]. This is a widespread family of enzymes that can be found in many cellular organelles, including chloroplasts [22]. Peroxidases are secretory glycoproteins that take part in the process of cell elongation – construction of the cell wall. Their specific functions include oxidation of toxic compounds [20, 23, 24, 25]. Superoxide dismutase (SOD) is one of the more important antioxidative enzymes. It plays a significant role in disproportioning and degradation of reactive oxygen species [26], the disproportioning reaction of SOD results in the removal of more toxic superoxide anion  $O_2^-$  into less harmful hydrogen peroxide which can be further converted into molecular oxygen. This reaction occurs in all oxygen-metabolizing organisms and it is thus a very important element of the antioxidant defense system [27, 28, 29]. Tetracyclines are susceptible to light. Under the influence of light and oxidizing factors, tetracyclines are degraded [30]. This process forms the basic mechanism for removal of this group of antibiotics from aqueous solutions [31, 32]. A question arises: do photoperiod or constant darkness conditions impact the uptake of chlortetracycline by plants? Moreover, in view of the fact that the phytotoxic effect of oxytetracycline consists in the formation of free radicals (hydroxyl radicals): does chlortetracycline in soil influence the activity of peroxidase and superoxide dismutase in roots and stems of yellow lupin (under photoperiodic conditions and in constant darkness)?

## MATERIAL AND METHODS

### Plant material and growth conditions.

Seeds of yellow lupin (*Lupinus luteus* L.) cv. Mister were germinated for eight days in Phytotoxkit plates (MicroBio Test, Inc., Belgium). Germination was carried out under controlled climatic conditions with temperature set at 25° C and 90% relative humidity (RH), in a photoperiod (16/8 day/night, light intensity 3.4 klx) and in constant darkness. Ninety milliliters of soil (sand, vermiculite, peat 1:0.3:1, v/v/v) were placed in each plastic microbiotest plate. The soil was covered with Whatman No. 1 filter paper and watered with 27 ml distilled water supplemented with chlortetracyclines (Sigma-Aldrich) at final concentrations of 5, 12.5, 25, 50, 100 mg · kg<sup>-1</sup> of soil. The control plants were watered with pure distilled water. The root length was estimated after eight days of germination using Image Tool for Windows. Fresh weight of seedlings was determined according to standard seed testing recommendations [33]. The experiment was carried out with four replicates, each containing 40 seedlings.

**Chlortetracycline content in seedlings.** The extraction of chlortetracyclines from eight days-old seedlings which had previously been rinsed with distilled water was performed by a manual solid phase extraction (SPE) method. Plant sap was squeezed from fresh plant material with mortar and pestle. For all extractions SPE cartridges Chromabond®Easy, 3 ml/200 mg, Macherey-Nagel, Dairen, Germany were used. SPE cartridges were rinsed with methanol and after loading with plant saps were eluted with 250 µl methanol. Chlortetracycline content in seedlings was analysed by HPLC according to [34] with small modifications. Briefly, the chromatographic system consisted of a Water Alliance 2695 HPLC system (Waters Corp.) with a binary high-pressure gradient pump, an automatic injector and a column oven (tab). The chromatographic column was an Atlantis T3 column (150×3.0 mm, 3 µm) (Waters Corp.) at 40°C. The MS–MS analyser consisted of Quattro micro® API MS (Waters Corp.) using electrospray in the positive mode (ESI+). N<sub>2</sub> was used as nebuliser, drying, curtain and collision gas. A chromatographic gradient was applied for the separation of the analytes depending on the ionization mode employed, with a total chromatographic run of 18 min. Gradient elution was carried out with aqueous 0.1% formic acid : 0.1% formic acid in acetonitrile at a flow rate of 0.45 ml · min<sup>-1</sup>. Validation of the method included the assessment of selectivity, linearity (1 to 11 µg · ml<sup>-1</sup>), limits of detection (8 ng · ml<sup>-1</sup>) and quantification (26 ng · ml<sup>-1</sup>). Chromatographic system and data collection were controlled with a

MassLynx 4.1. chromatographic software interfaced to a personal computer.

**Guaiacol peroxidase activity.** Extracts used to determine peroxidase activity were prepared on ice. The roots and stems (500 mg) that grew in soil with water or with chlortetracycline were homogenized for 30 minutes in the extraction buffer (0.1 M Tris/HCl, 8.75% polyvinylpyrrolidone, 0.1 M KCl, 0.28% Triton X-100). Samples were centrifuged for 30 minutes at  $4000 \cdot g$  at  $4^{\circ}C$ . The supernatant was passed through membrane filters  $0.45 \mu m$  in diameter. The protein content in samples was determined with the Lowry et al., (1951) protein assay. Peroxidase activity was determined based on the spectrophotometric detection (Cecil, CE2021 2000 Series) in mixture containing  $100 \mu l$  1% guaiacol, 2 ml 0.1 M  $KH_2PO_4$ ,  $150 \mu l$  supernatant and  $20 \mu l$  0.18%  $H_2O_2$ . The absorption rate increase was measured at room temperature at the wavelength of 470 nm. One Unit of activity equals oxidation of  $1 \mu M H_2O_2$  during 1 minute. Each peroxidase activity analysis was carried out in four replications.

**Superoxide dismutase activity.** Extracts used to determine superoxide dismutase (SOD) activity were prepared on ice. The roots and stems material (200 mg) were homogenized in the extraction buffer (1 ml) consisting of 50 mM phosphate buffer [pH 7.0], 1% polyvinylpyrrolidone, 0.1 M KCl, 0.1% Triton X-100. Samples were centrifuged for 15 minutes at  $15\ 000 \cdot g$  at  $4^{\circ}C$ , and supernatants were used as crude extract for soluble protein quantification according to Lowry et al., [35] with bovine serum albumin as the standard. Total SOD activity was assayed by the inhibition of the photochemical reduction of nitroblue tetrazolium (NBT) according to modified method of Beyer and Fridovich, [36]. The reaction mixture (2.2 ml) contained, 0.05 M buffer  $Na_2CO_3/NaHCO_3$  (pH 10.2), 0.0001 M EDTA, 0.0001 M xantin,  $2.5 \cdot 10^{-5}$  M NBT and  $50 \mu l$  of plant extract. The reduction of NBT by superoxide radicals to blue coloured formazan was followed at 560 nm. One Unit of SOD activity is defined as that amount of enzyme required to inhibit the reduction of NBT by 50% under the specified conditions per 1 mg protein.

## RESULTS

**Plant material and growth conditions.** The impact of increasing chlortetracycline concentrations (0, 5, 12.5, 25, 50,  $100 \text{ mg} \cdot \text{kg}^{-1}$  of soil) on the growth of roots and stems of yellow lupin was investigated. Tests were carried out for eight days in a photoperiod or constant darkness. The length of roots and stems and their fresh weight

was determined at the end of the experiment. Chlortetracycline present in soil inhibited the growth of roots and stems proportionally to an increase in the concentration of the drug. Roots growing for eight days in soil with  $100 \text{ mg}$  of chlortetracycline  $\cdot \text{kg}^{-1}$  of soil without access of light and in a photoperiod were shorter by 65% and 72%, respectively (Fig. 1A). Similarly to roots, the length of stems depended on the drug concentration and light conditions during the experiment. The growth of stems on soil contaminated with  $100 \text{ mg}$  of chlortetracycline  $\cdot \text{kg}^{-1}$  of soil in darkness and a photoperiod was inhibited by 82 and 77%, respectively (Fig. 1B). The concentration of chlortetracycline at  $50 \text{ mg}$  chlortetracycline  $\cdot \text{kg}^{-1}$  of soil caused a minor stimulation of stem growth in darkness.

Longer plants growing in darkness had higher fresh weight of roots and stems compared to plants growing in a photoperiod. The fresh weight of roots growing on soil contaminated with the highest of the examined drug concentrations in darkness and a photoperiod was lower by 73% and 70%, respectively (Fig. 1C). The values of fresh weight were lower by 85% (darkness) and 84% (photoperiod). Similar to the length of stems, their fresh weight was stimulated with  $50 \text{ mg}$  of chlortetracycline  $\cdot \text{kg}^{-1}$  of soil (Fig. 1D).

**Chlortetracycline content in seedlings.** In lupin stems that were grown in a photoperiod, the content of drugs ranged from 10 to  $370 \text{ ng} \cdot \text{g}^{-1}$  of fresh weight and increased together with incremental doses of chlortetracycline in soil. The content of chlortetracycline in roots of lupine seedlings growing in darkness was on average two times higher than in seedlings growing in a photoperiod and ranged between 42 and  $643 \text{ ng} \cdot \text{g}^{-1}$  of fresh weight. The exception were roots grown on soil that contained two of the lowest tested concentrations:  $5 \text{ mg}$  of chlortetracycline  $\cdot \text{kg}^{-1}$  of soil generated a four-time increase in its content ( $42 \text{ ng} \cdot \text{g}^{-1}$  of fresh weight) and at  $12.5 \text{ mg}$  of chlortetracycline  $\cdot \text{kg}^{-1}$  of soil, the content of the antibiotic in stems was  $50 \text{ ng} \cdot \text{g}^{-1}$  of fresh weight (Fig. 2).

Yellow lupin stems growing in a photoperiod contained less drug (from  $4.5$  to  $10 \text{ ng} \cdot \text{g}^{-1}$  of fresh weight) than stems that were grown at constant darkness (from  $5.5$  to  $34 \text{ ng} \cdot \text{g}^{-1}$  of fresh weight). In stems growing in a photoperiod on soil that contained the lowest of the tested concentrations ( $5$  and  $12.5 \text{ mg} \cdot \text{kg}^{-1}$  of soil), chlortetracycline was not detected as opposed to stems grown at constant darkness on soil with the same concentrations of the drug. Stems growing in a photoperiod on soil with the highest tested concentration of chlortetracycline, namely  $50$  and  $100 \text{ mg} \cdot \text{kg}^{-1}$  of soil, contained on average three times less of the

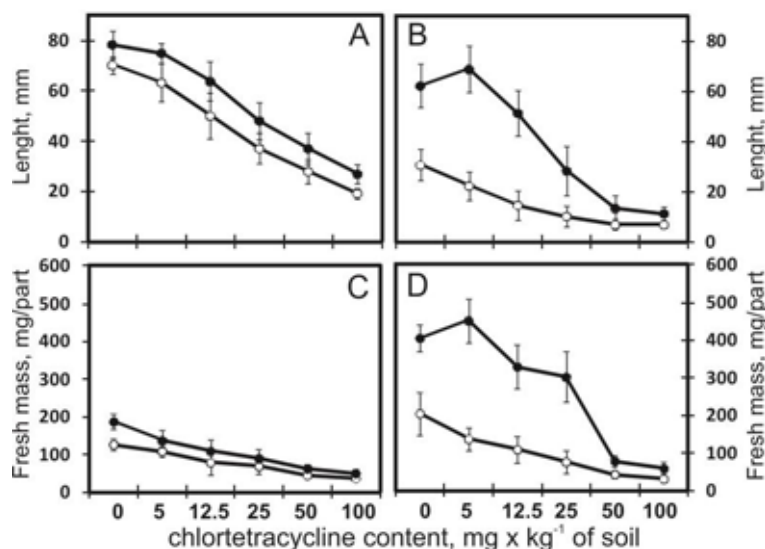


FIGURE 1

Root (A) and stem (B) length and fresh mass of root (C) and stem (D) growing under photoperiod (○) or at constant darkness (●) on soil supplemented with chlortetracycline concentrations (0, 5, 12.5, 25, 50, 100 mg · kg<sup>-1</sup> of soil). Bars are the average ± SD, where bars are not apparent, the SD was smaller than the height of the symbol.

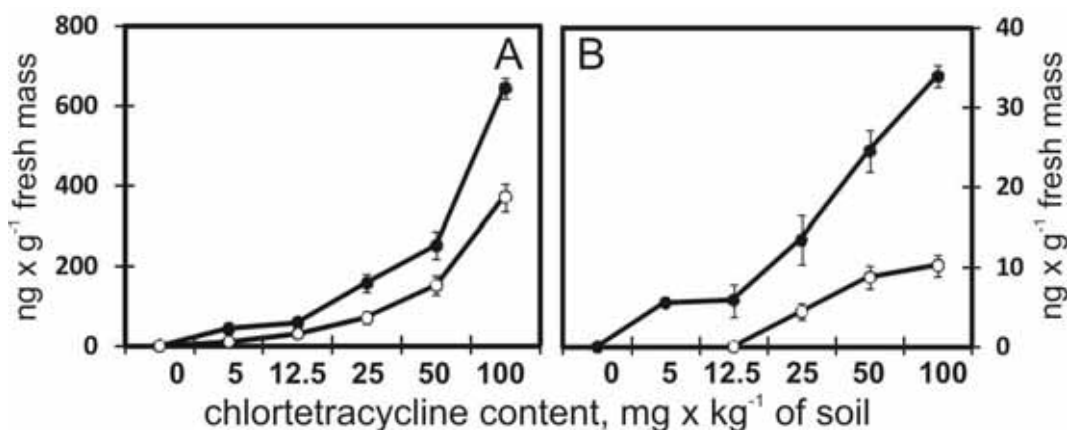


FIGURE 2

Chlortetracycline content in root (A) and stem (B) growing under photoperiod (○) or at constant darkness (●) on soil supplemented with chlortetracycline concentrations (0, 5, 12.5, 25, 50, 100 mg · kg<sup>-1</sup> of soil).

Bars are the average ± SD, where bars are not apparent, the SD was smaller than the symbol.

antibiotic in comparison with stems grown at constant darkness (Fig. 2).

**Enzymes activity.** The activity of peroxidase and superoxide dismutase was evaluated in the roots and stems of 8-day-old yellow lupin seedlings depending on the examined concentrations of chlortetracycline. The activity of peroxidase in both roots and stems of lupin rose, together with increasing chlortetracycline concentrations in soil. However, in a photoperiod, the increase in the activity of peroxidase was lower in roots and stems than in darkness (Fig. 3A, 3B). The absolute values

of peroxidase activity were higher in roots (the organs that are directly exposed to a drug) than in stems. In roots growing in a photoperiod, there was an increase in the activity of peroxidase by 35% in comparison with the control sample. In darkness, the increase in the activity of the enzyme up to 49% was recorded to the concentration of 50 mg · kg<sup>-1</sup> of soil, yet at the highest chlortetracycline concentration (100 mg · kg<sup>-1</sup> of soil), there was a rapid reduction of peroxidase activity in lupin roots (Fig. 3A).

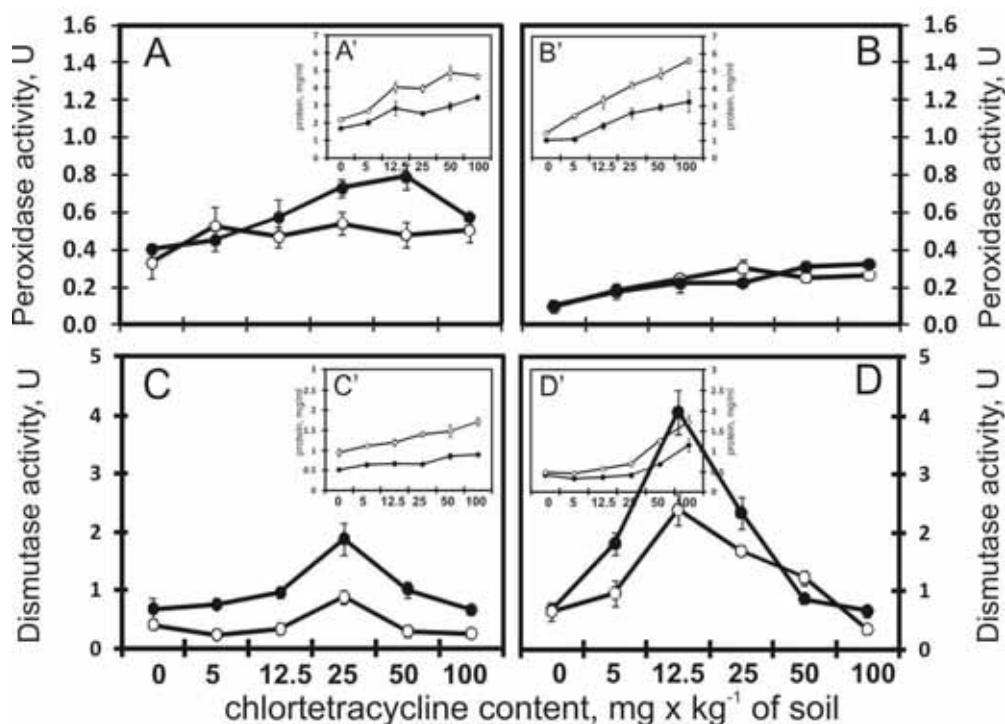


FIGURE 3

Guaiacol peroxidase activity in roots (A) and stems (B) and superoxide dismutase activity in roots (C) and stems (D) growing under photoperiod (○) or at constant darkness (●) on soil supplemented with chlortetracycline concentrations (0, 5, 12.5, 25, 50, 100 mg · kg<sup>-1</sup> of soil). Panel A', B', C', D' content the total protein using BSA as standard according to Lowry methods. Bars are the average ± SD, where bars are not apparent, the SD was smaller than the height of the symbol.

In stems, regardless of light conditions, there was an incremental tendency of peroxidase activity up to 64.4% and 68.5% in a photoperiod and complete darkness (Fig. 3B). The pattern of superoxide dismutase in roots and stems of yellow lupin seedlings was different. Regardless of the light conditions, the highest activity of superoxide dismutase was detected in roots and stems growing on soil contaminated with 25 and 12.5 mg chlortetracycline · kg<sup>-1</sup> of soil (Fig. 3C, 3D). The activity of this enzyme in roots increased up to the concentration of 25 mg chlortetracycline · kg<sup>-1</sup> of soil and rose up to 1.7 U (photoperiod) and 1.9 U (darkness) (Fig. 3C). The activity of this enzyme in stems increased up to the concentration of 12.5 mg chlortetracycline · kg<sup>-1</sup> of soil and reached the highest values: 2 U (photoperiod) and 4 U (darkness) in comparison with the control. A further increase in the concentration of the drug in soil resulted in a rapid reduction of superoxide dismutase activity in stems regardless of light conditions (Fig. 3D). While comparing the activity of the investigated enzyme, it may be concluded that the activity of superoxide dismutase doubled in roots and stems growing in darkness in comparison with a photoperiod. In roots, it ranged from approximately 1 (photoperiod) to about 2 U (darkness), whereas in stems it ranged between 2

(photoperiod) and 4 U at constant darkness (Fig. 3C, D).

## DISCUSSION

Studies on the impact of xenobiotics on plants destined for consumption are a very important component of the environmental evaluation. It has been found that chlortetracycline (CTC) in soil inhibits the growth of roots and above-ground parts in maize (*Zea mays* L.) and alfalfa (*Medicago sativa* L.) and thus reduces biomass yield [16, 37]. The concentration of oxytetracycline at 80 µmol · l<sup>-1</sup> reduces root mass in wheat by 73.23% and stem mass by 51.09% [38]. Among environmental factors, light plays an important role during growth and development of plants and may change the properties of many drugs and their phytochemical instability constantly increases [39]. Degradation of drugs during storage is determined by the drug's structure, pH of solution, humidity and temperature. Tetracycline is stable during storage at room temperature, in darkness and in humidity between 20% and 65% [40]. Degradation of tetracycline consists, among others, in hydroxylation of some active groups in the drug. During degradation in the presence of light (photolysis), intermediate compounds are formed that are more toxic than

parent drugs [41]. Light and UV radiation play an important role in removing tetracycline from water [42]. Only 15 minutes of irradiation with solar light are needed to completely remove tetracycline from an aqueous solution [32]. The proven impact of light on tetracyclines was the reason for undertaking studies in a photoperiod and in darkness.

In the studies reported here, chlortetracycline in soil inhibited the growth of roots and stems proportionally to the drug's concentrations (Fig. 1). The capacity to uptake drugs in such plants as *Arabidopsis thaliana*, tomato, Indian mustard and carrot was investigated by Bowman et al., [43] 2011 and Bansal, [44]. The uptake of chlortetracycline by plants is based on passive transport [45]. Our studies also demonstrated that yellow lupin seedlings growing for eight days on soil contaminated with chlortetracycline took up the drug (Fig. 2). The concentration of chlortetracycline in stems was lower than in roots (Fig. 2). This data indirectly indicates passive transport and deposition of the drug in the stem. Although the concentration of chlortetracycline in maize (*Zea mays* L.), green onion (*Allium cepa* L.), and cabbage (*Brassica oleracea* L. Capitata group) is low (2-17 ng · g<sup>-1</sup> fresh weight), it increases together with incremental amounts of the drug in slurry [46]. Similarly, chlortetracycline is taken up by vegetable crops [47]. The concentration of chlortetracycline in yellow lupin root and stem tissues was 10 ng · g<sup>-1</sup> of fresh weight and rose parallel to the increasing concentrations of the antibiotic in soil (Fig. 2). The concentration of CTC in lettuce and tomato is 3.4 ng · g<sup>-1</sup> and 0.7 ng · g<sup>-1</sup>, respectively [48]. Based on the conducted studies, it may be concluded that the determined content of chlortetracycline in roots and stems of lupin seedlings depended on the degree of soil contamination with the antibiotic and that roots, as the organs with a direct contact with soil, contained more drug than stems. The increase in soil contamination with chlortetracycline generated an increase in the content of the drug in roots and stems. The tested experimental conditions (photoperiod and content darkness) indicate that the presence of light (or lack thereof) during the growth of yellow lupin determined the amount of uptaken drug. Roots and stems that were grown in light contained less chlortetracycline than the plants grown in darkness (Fig. 2). The results proved that tetracyclines are degraded under the influence of light. A confirmation of our studies and studies by Jiao et al., [30] found reduced peroxide and superoxide dismutase activity in stems and roots of lupin growing in a photoperiod, which proves that light has an effect on the phytotoxicity of chlortetracycline.

The studies provided, for the first time, a comparison of the impact of photoperiod and darkness on the uptake of chlortetracycline, a drug

belonging to tetracyclines which, according to Jiao et al., [30], are thought to be degraded when influenced by light.

Light conditions affected the content of chlortetracycline in the examined organs of yellow lupin. A higher amount of the drug was detected in roots and stems growing in darkness 643 and 34 ng · g<sup>-1</sup> fresh weight, respectively (Fig. 2). Peroxidase and superoxide dismutase were investigated because they are the enzymes involved in antioxidative defense mechanisms (reduction of O<sub>2</sub><sup>-</sup> excess in vegetal tissues). The activity of peroxidase and superoxide dismutase rose together with increasing concentrations of chlortetracycline in soil up to 25 mg and 12.5 mg chlortetracycline · kg<sup>-1</sup> of soil in yellow lupin stems and roots, respectively (Fig. 3). Thereafter, this increase in the concentration of the drug in soil and in plants induced a rapid reduction in the activity of peroxidase and superoxide dismutase. The activity of these enzymes was higher in roots and in stems growing in darkness (Fig. 3). Chlortetracycline was found to be a stress factor to yellow lupin seedlings that contributed to an increase in the activity of the tested enzymes. Maize (*Zea mays* L.) reacted similarly to CTC in early growth stages and, influenced by the drug, generated free hydroxyl radicals, which increased the activity of antioxidative enzymes [16]. A reduction in the activity of superoxide dismutase and catalase was found in *Phragmites australis* (Cav.) Trin. ex Steud under the influence of oxytetracycline. The highest concentration of the drug (1000 mg · l<sup>-1</sup>) inhibits the activity of enzymes by over 50%. In contrast, the activity of peroxidase follows a different pattern, as it is dramatically increased at lower concentrations of antibiotics in a solution [49].

It has been shown that chlortetracycline also impacts the respiratory enzymes (NAD-malic enzyme) and alters calcium-dependent processes in vegetal tissues. The uptake of chlortetracycline by roots reduces the content of intracellular calcium due to chelation [43]. It was demonstrated that the content of chlortetracycline in yellow lupin tissues growing in a photoperiod was lower than in plants growing in darkness.

## CONCLUSION

The studies indicate that yellow lupin seedlings take up chlortetracycline from soil more intensely when the plants are grown in darkness than in a photoperiod. The content of the drug in the plant rises together with the increasing concentration of the antibiotic in soil. The activity of peroxidase and superoxide dismutase under photoperiod is lower than in plants growing in darkness. It is quite possible that light conditions may play a significant role also in other studies on

the effects of environmental toxins (not necessarily antibiotics) on plants.

## ACKNOWLEDGEMENTS

The present study was financially supported by project NCN Poland, UMO-2011/01/B/NZ9/02646

## REFERENCES

- [1] Kim, Y.K., Lim, S.J., Han, M.H. and Cho, J.Y. (2012) Sorption characteristics of oxytetracycline, amoxicillin, and sulfathiazole in two different soil types. *Geoderma* 185-186, 97-101.
- [2] Wang, Y.J., Sun, R.J., Xiao, A.Y., Wang S.Q. and Zhou, D.M. (2010) Phosphate affects the adsorption of tetracycline on two soils with different characteristics. *Geoderma* 156(3-4), 237-242.
- [3] Gu, Ch., Karthikeyan, K.G., Sibley, S.D. and Pedersen, J.A. (2007) Complexation of the antibiotic tetracycline with humic acid. *Chemosphere* 66(8), 1494-1501.
- [4] O'Connor, S. and Aga, D.S. (2007) Analysis of tetracycline antibiotics in soil: Advances in extraction, clean-up, and quantification. *Trends in Analytical Chemistry* 26 (6), 456-465.
- [5] Hao, R., Xiao, X., Zuo, X., Nan, J. and Zhang, W. (2012) Efficient adsorption and visible-light photocatalytic degradation of tetracycline hydrochloride using mesoporous BiOI microspheres. *Journal of Hazardous Materials*. 209-210, 137-145.
- [6] Wu, X., Wie, Y., Zheng, J., Zhao, X. and Zhong, W. (2011) The behavior of tetracyclines and their degradation products during swine manure composting. *Bioresource Technology* 102, 5924-5931.
- [7] Kong, W., Li, Ch., Dolhi, J.M., Li, S., He, J. and Qiao, M. (2012) Characteristics of oxytetracycline sorption and potential bioavailability in soils with various physical-chemical properties. *Chemosphere* 87, 542-548.
- [8] Martínez-Carballo, E., González-Barreiro, C., Scharf, S., Gans, O., 2007. Environmental monitoring study of selected veterinary antibiotics in animal manure and soils in Austria. *Environmental Pollution* 148, 1-10.
- [9] Sun, G., Yuan, S.J., Peng, S.C., Chen, F.Q. and Hu, Z.H. (2010) Determination of oxytetracycline, tetracycline and chlortetracycline in manure by SPE-HPLC method. *Environmental Chemistry* 29, 739-743 (in Chinese, abstract in English)
- [10] Hamscher, G., Pawelzick, H.T., Höper, H. and Nau, H. (2005) Different behavior of tetracyclines and sulfonamides in sandy soils after repeated fertilization with liquid manure. *Environmental Chemistry* 24 (4), 861-868.
- [11] Andreu, V., Vazquez-Roig, P., Blasco, C. and Pico, Y. (2009) Determination of tetracycline residues in soil by pressurized liquid extraction and liquid chromatography tandem mass spectrometry. *Analytical and Bioanalytical Chemistry* 394 (5), 1329-1339.
- [12] Karci, A. and Balcioglu, I.A. (2009) Investigation of the tetracycline, sulfonamide, and fluoroquinolone antimicrobial compounds in animal manure and agricultural soils in Turkey. *Science of The Total Environment* 407(16), 4652-4664.
- [13] Zhang, H.R., Zhang, M.H. and Gu, G.P. (2008) Residues of tetracyclines in livestock and poultry manures and agricultural soils from north Zhejiang Province. *Journal of Ecology Rural Environment* 24(3), 69-73.
- [14] Farkas, M.H., Berry, J.O. and Aga, D.S. (2007) Chlortetracycline detoxification in maize via induction of glutathione S-transferases after antibiotic exposure. *Environmental Science & Technology* 41(4), 1450-1456.
- [15] Liu, F., Ying, G., Tao, R., Zhao, J., Yang, J. and Zhao, L. (2009) Effects of six selected antibiotics on plant growth and soil microbial and enzymatic activities. *Environmental Pollution* 157(5), 1636-1642
- [16] Wen, B., Liu, Y., Wang, P., Wu, T., Zhang, S., Shan, X. and Lu, J. (2012) Toxic effects of chlortetracycline on maize growth, reactive oxygen species generation and the antioxidant response. *Journal Environmental Science (China)*, 24(6), 1099-1105.
- [17] Michelini, L., Meggio, F., La Rocca, N., Ferro, S. and Ghisi, R. (2012) Accumulation and effects of sulfadimethoxine in *Salix Fragilis* L. plants: A preliminary study to phytoremediation purposes. *International Journal of Phytoremediation* 14( 4), 388-402.
- [18] Angrave, F.E. and Avery, S.V. (2001) Antioxidant functions required for insusceptibility of *Saccharomyces cerevisiae* to tetracycline antibiotics. *Antimicrobial Agents and Chemotherapy* 45(10), 2939-42.
- [19] Van Breusegem, F., Vranová, E., Dat, J.F. and Inzé, D. (2001) The role of active oxygen species in plant signal transduction. *Plant Science* 161(3), 405-414.
- [20] Passardi, F., Longet, D., Penel, C. and Dunand, C. (2004) The class III peroxidase multigenic family in rice and its evolution in land plants. *Phytochemistry* 65(13), 1879-1893.
- [21] Cesarino I., Araújo P., Paes Leme A.F., Creste S. and Mazzafera P. (2013) Suspension cell culture as a tool for the characterization of

- class III peroxidases in sugarcane. *Plant Physiology Biochemistry* 62: 1-10.
- [22] Vergara-Domínguez, H., Roca, M. and Gandul-Rojas, B. (2013) Characterisation of chlorophyll oxidation mediated by peroxidative activity in olives (*Olea europaea* L.) cv. Hojiblanca. *Food Chemistry* 139(1-4), 786–795.
- [23] Bakalovic, N., Passardi, F., Ioannidis, V., Cosio, C., Penel, C., Falquet, L. and Dunand, C. (2006) PeroxiBase: A class III plant peroxidase database. *Phytochemistry* 67(6), 534-539.
- [24] Hynninen, P.H., Kaartinen, V. and Kolehmainen, E. (2010) Horseradish peroxidase-catalyzed oxidation of chlorophyll a with hydrogen peroxide. Characterization of the products and mechanism of the reaction. *Biochimica et Biophysica Acta (BBA) - Bioenergetics* 1797(5), 531-542.
- [25] Watanabe, L., Ribeiro de Moura, P., Bleicher, L., Nascimento, A.S., Zamorano, L.S., Calvete, J.J., Sanz, L., Pérez, A., Bursakov, S., Roig, M.G., Shnyrov, V.L. and Polikarpov, I. (2010) Crystal structure and statistical coupling analysis of highly glycosylated peroxidase from royal palm tree (*Roystonea regia*). *Journal of Structural Biology* 169(2), 226-242.
- [26] Miura, C., Sugawara, K., Neriya, Y., Minato, N., Keima, T., Himeno, M., Maejima, K., Komatsu, K., Yamaji, Y., Oshima, K. and Namba, S. (2012) Functional characterization and gene expression profiling of superoxide dismutase from plant pathogenic phytoplasma. *Gene* 510(2), 107-112.
- [27] Gill, T., Sreenivasulu, Y., Kumar, S. and Singh Ahuja, P. (2010) Over-expression of superoxide dismutase exhibits lignifications of vascular structures in *Arabidopsis thaliana*. *Journal of Plant Physiology* 167(9), 757-760.
- [28] Skyba, M., Petijová, L., Košuth, J., Koleva, D.P., Ganeva, T.G., Kapchina-Toteva, V.M. and Cellárová, E. (2012) Oxidative stress and antioxidant response in *Hypericum perforatum* L. plants subjected to low temperature treatment. *Journal of Plant Physiology* 169(10), 955-964.
- [29] Qin, X., Zhang, M., Qin, J., Yuan, S., Hou, Y. and Liu, J. (2012) Two-step purification of Cu,Zn-superoxide dismutase from pumpkin (*Cucurbita moschata*) pulp. *Separation and Purification Technology* 87, 79–83.
- [30] Jiao, S., Zheng, S., Yin, D., Wang, L. and Chen, L. (2008) Aqueous photolysis of tetracycline and toxicity of photolytic products to luminescent bacteria. *Chemosphere* 73(3), 377-382.
- [31] Reyes, C., Fernández J., Freer, J., Mondaca, M.A., Zaror, C., Malato, S. and Mansilla, H.D. (2006) Degradation and inactivation of tetracycline by TiO<sub>2</sub> photocatalysis. *Journal of Photochemistry and Photobiology A: Chemistry* 184, 141-146.
- [32] Di Paola, A., Addamo, M., Augugliaro, V., García-López, E., Loddo, V., Marci, G., Palmisano, L. (2004) Photolytic and TiO<sub>2</sub>-assisted photodegradation of aqueous solutions of tetracycline. *Fresen. Environ. Bull.*, 13(11 B), 1275-1280.
- [33] ISTA (2011) International Rules for Seed Testing Edition 2011. Basserdorf, Zurich The International Seed Testing Association 1-56.
- [34] Pailler, J., Krein, A., Pfister, L., Hoffmann, L. and Guignard, C. (2009) Solid phase extraction coupled to liquid chromatography-tandem mass spectrometry analysis of sulfonamides, tetracyclines, analgesics and hormones in surface water and wastewater in Luxembourg. *Science of The Total Environment* 407(16), 4736-4743.
- [35] Lowry, O.H., Rosebrough, N.J., Farr, A.L. and Randall, R.J. (1951) Protein measurement with the Folin phenol reagent. *Journal of Biological Chemistry* 193(1), 265-275.
- [36] Beyer, W.F., Jr, and Fridovich, I. (1987) Assaying for superoxide dismutase activity: some large consequences of minor changes in conditions. *Analytical Biochemistry* 161(2), 559-566.
- [37] Kong, W.D., Zhu, Y.G., Liang, Y.C., Zhang, J., Smith, F.A. and Yang, M. (2007) Uptake of oxytetracycline and its phytotoxicity to alfalfa (*Medicago sativa* L.). *Environmental Pollution* 147, 187-193.
- [38] Zhao-jun, Li, Xiao-yu, X., Shu-qing, Z. and Yong-chao, L. (2011) Negative effects of oxytetracycline on wheat (*Triticum aestivum* L.) growth, root activity, photosynthesis, and chlorophyll contents. *Agricultural Sciences in China* 10(10), 1545-1553.
- [39] Langner, M.D. and Maibach, H.I. (2009) Many common drugs in dermatology are light, temperature, or moisture-sensitive. *Skin Therapy Letter* 14(1), 3-5.
- [40] Wu, Y. and Fassihi, R. (2005) Stability of metronidazole, tetracycline HCl and famotidine alone and in combination. *International Journal of Pharmaceutics* 290(1-2), 1-13.
- [41] Niu, J., Li, Y. and Wang, W. (2013) Light-source-dependent role of nitrate and humic acid in tetracycline photolysis: kinetics and mechanism. *Chemosphere* 92(11), 1423-1429.
- [42] Verma, B., Headley, J.V. and Robarts, R.D. (2007) Behaviour and fate of tetracycline in river and wetland waters on the Canadian Northern Great Plains. *Journal of Environmental Science and Health. Part A, Toxic/hazardous Substances & Environmental Engineering* 42(2), 109-117.



- [43] Bowman, S.M., Drzewiecki, K.E., Mojica, E.R., Zieliński, A.M., Siegel, A., Aga, D.S. and Berry, J.O. (2011) Toxicity and reductions in intracellular calcium levels following uptake of a tetracycline antibiotic in *Arabidopsis*. *Environmental Science and Technology* 45(20), 8958-8964.
- [44] Bansal, O.P. (2013) Green remediation of tetracyclines in soil-water systems. *Health* 5(12), 2039-2044.
- [45] Boonsaner, M. and Hawker, D.W. (2012) Investigation of the mechanism of uptake and accumulation of zwitterionic tetracyclines by rice (*Oryza sativa* L.). *Ecotoxicology and Environmental Safety* 78, 142-147.
- [46] Kumar, K, Gupta, S.C., Baidoo, S.K., Chander, Y. and Rosen, C.J. (2005) Antibiotic uptake by plants from soil fertilized with animal manure. *Journal of Environmental Quality* 34(6), 2082-2085.
- [47] Kang, H.D., Gupta, S., Rosen, C., Fritz V., Singh, A., Chander, Y., Murray, H. and Rohwer, Ch. (2013) Antibiotic Uptake by Vegetable Crops from Manure-Applied Soils. 2013. *Journal of Agricultural and Food Chemistry* 61(42), 9992-10001
- [48] Seo, Y., Cho, B., Kang, A., Jeong, B. and Jung, Y.S. (2010) Antibiotic Uptake by Plants from Soil Applied with Antibiotic-Treated Animal Manure. *Korean Journal of Soil Science and Fertilizer* 43(4), 466-470.
- [49] Liu, L., Liu, Y., Liu, Ch., Wang, Z., Dong, J., Zhu, G. and Huang, X. 2012. Potential effect and accumulation of veterinary antibiotics in *Phragmites australis* under hydroponic conditions. *Ecological Engineering* 53, 138-143.

---

**Received: 10.12.2014**

**Accepted: 18.08.2016**

---

#### **CORRESPONDING AUTHOR**

---

**Agnieszka I Piotrowicz-Cieslak**

Department of Plant Physiology, Genetics and Biotechnology,

Faculty of Biology and Biotechnology,

University of Warmia and Mazury in Olsztyn,

Oczapowskiego 1A,

10-718 Olsztyn– POLAND

E-mail: [acieslak@uwm.edu.pl](mailto:acieslak@uwm.edu.pl)

# GIS MODELING AND SOCIAL-ORIENTED MULTI-CRITERIA EVALUATION IN LANDFILL SITE SELECTION IN RURAL AREAS – A CASE STUDY OF SERBIAN VILLAGES

Marina Nenkovic-Riznic\*, Igor Maric, Mila Pucar

Institute of architecture and urban and spatial planning of Serbia, Bulevar Kralja Aleksandra 73/II, 11000 Belgrade, Serbia

## ABSTRACT

GIS modeling is a new tool used in landfill site selection in urban and rural areas. Previously used deterministic methods and techno-economic criteria used within multi-criteria evaluation proved to be insufficient in any relevant and accurate theoretical considerations, since the choice of methods and criteria resulted in a subjective evaluation. In addition, the problem also lay within the fact that the planning evaluation did not include social criteria in the context of the landfill site selection. This paper will present a new, adapted, and socially adjusted methodology which will improve expert multi-criteria evaluation for the selection of landfill sites, with a clear emphasis placed on social considerations (preferences of the local population, behavioral models, etc.). This methodology was applied to the selection of landfill sites in the territory of villages in the Stara planina Nature Park, located in Eastern Serbia. The research was conducted using the ArcGIS Spatial Analyst software, with the aim of stressing the importance of using mathematical and geo-statistical analysis in planning practice.

The overall conclusion of this research is that the degree of success in solid waste management in rural settlements primarily depends on the degree of participation of local residents in the decision-making process (especially in landfill site selection). The GIS model used in this research could be adapted to offer multiple applications in different location studies in spatial planning.

## KEYWORDS:

GIS modeling, landfill site selection, social criteria, villages in Serbia

## INTRODUCTION

There have been an increasing number of theoretical studies in the domain of environmental planning and waste management planning [1], [2], [3], [4], [5] directed towards finding adequate solid

waste management systems and waste planning methods, primarily in urban centers and places with a high population density. These studies indicate the importance of the adequate treatment of waste by means of recycling and/or disposal at landfill areas outside of the city centres. On the other hand, in rural areas, the research activities that are carried out in the field of municipal solid waste management are considerably smaller in scope, or are, as in the case of Serbia, practically neglected. Structural differences in demographic and economic characteristics, in the behavioral patterns of the local residents, as well as in the environmental premises in towns and villages, also require different inputs in determining the methods and locations for disposing of municipal waste in rural areas. The smaller number of studies that have indirectly dealt with rural areas [14], [15] have used the so-called techno-economic criteria for landfill location (engineering and geological ground conditions, property-legal relations, economic efficiency, etc.) [11]. However, despite the use of these planning-based criteria, criteria for the selection of existing landfill sites have not been taken into account that originate directly from the local people, their behavioral patterns, affinities, etc. (the criteria of open landfills). These criteria have neither been the subject of contemporary research, nor have they been taken into account in landfill site selection.

However, considering that, due to the marginalization of the criteria for open landfills, certain theory-based selections of landfill sites have not been implemented, a new field of research has been opened with the aim of determining the correlations between criteria/conditions taken into account in creating open landfills and the location criteria/conditions that are a result of theoretical assessment and scientific foundations, as well as research with clearly predefined methodology (techno-economic criteria). This has been taken as the basis for the hypothesis of this research study. The main problem that has led to the formulation of the hypothesis of this research is the fact that the issue of waste management in rural areas has been raised by only a small number of authors in terms

of the latest theory. Therefore, the hypotheses which are tested in this study are based on decision theory, location theories, behavioral theory, the theory of rational planning, participatory planning and others. The main hypothesis that this study sought to test is whether there is a correlation between the criteria/conditions which occur with the spontaneous creation of landfills, (which are based on behaviour models of the local population, with their habits, affinities and visual assessments) and the local criteria/conditions that are a result of theoretical checks, scientific foundation and research with clear, pre-established methodology.

The entire methodology for this research and testing is primarily based on a comparative analysis of different case studies (examples) conducted by well-known researchers in the sphere of the GIS application for landfill site selection in rural settlements (Greece, Spain, China) [6], [7], [8], [9], [10], [11], [12], [13], [14], etc. It is also based on the establishment of joint location criteria which could be taken into account as the general techno-economic criteria, as well as on predefined multi-criteria analyses (through modified and adapted AHP (analytic hierarchy process) and SAW (Simple Additive Weighting Method) methods and methods of socially-based multi-criteria analysis), and techno-economic criteria for the landfill site selection in a pilot area in Serbia (villages of the Stara planina mountain Nature Park), as well as the multi-criteria analysis of open landfills based on spontaneously created criteria. Furthermore, the degree of concordance between locations obtained through the analysis of techno-economic and open landfill criteria has been determined through a comparative analysis, and conclusions have been drawn. All of the mentioned phases rely on the direct application of GIS technologies in the analysis, in which geospatial databases are created and used for detailed visualization of the results. In this way, a model has been created which, when adapted to local conditions, can be used for landfill site selection in rural settlements with different geographic, demographic and engineering-geological characteristics, etc. These methods were monitored in all phases, both through the survey method and through regression analysis of the data (in order to identify the attitudes of local people on the selection of methods and sites for solid waste management purposes, as well as to define specific open landfill criteria).

## **MATERIALS AND METHODS**

The methodology used within this research represents a consolidation of the existing methodological frameworks used for landfill site selection, also supplemented with the analysis

carried out using the geospatial databases (GIS methodology).

Through a comparative analysis of certain examples of European, but also world practice (Greek, Spain, China, etc.), it can be seen that authors [9], [14], [15] and [16] have also defined methods for structuring the model-based approach used in the landfill site analysis, as well as for the uniform location criteria used in them. The mentioned analyses and research activities have been taken into consideration, due not only to their specific methodology for selecting sites, but also, and primarily, due to a direct link between the social aspect and the aspect of decision-making related to the location conditions.

The analysis was performed by combining multi-criteria analyses and AHP methods. It was then visualized and mathematically modeled through a geographic information system. Based on representations of the abovementioned “successful scenarios”, i.e. principles of landfill site selection for waste management purposes that have already been implemented, it was also possible to establish a research framework by laying down a uniform methodological procedure for determining realistic location parameters for this type of activity in Serbia. Thus, not only was a clear methodological procedure in the form of recommendations for further implementation defined, but also a specific model for defining landfill sites in rural settlements.

After selecting the methodology for the location analysis, it was necessary to establish the evaluation criteria based on predefined methodologies. There are location-specific requirements, or factors, that depend on various parameters linked to site-specific natural conditions. These conditions are: hypsometry, slope, terrain exposition, presence of ground and surface waters, water accumulations, soil, flora, fauna, previous protection, geomorphology, geology, seismics, flood-proneness, soil engineering, geologic conditions, etc. They also depend on certain economic factors such as location availability, property/legal relations, costs of preparation, connection with surroundings/transport costs, the problem of parcel revitalization, etc. The research conducted by [3], [10], [14] and [16] only recognizes these criteria, but does not consider open landfill criteria which are directly associated with the behavioral patterns and affinities of local people. In this research, these criteria have been classified into: the free space criterion (ownership of the land, location availability); distance from housing groups in the village; terrain configuration (geomorphologic criterion); visual impression (aesthetic criterion); behavioral patterns (models) – habits; and consent of those living in rural settlements (public participation).

This set of criteria has also been supplemented with the opinions of local residents from several

villages on the territory of the Republic of Serbia who took part in various field surveys and interviews.

In the evaluation process, a large number of man-made and natural location factors were selected, and their ranking was performed by weighting their importance for each area. Criteria weighting is based on the analysis and opinions of experts. Thus, this evaluation can also be considered as a quantitative classification of location factors. After classification of the location factors, based on their theoretically and empirically predefined levels of importance for a specific problem, the suitability limit values were defined for each individual evaluation criterion (or location factor). Namely, the quantitatively and qualitatively checkable parameters for each of the location factors give the land capacity value (qualitative determinant of suitability) relative to the considered problem, thereby their suitability is given the value expression (1-5, 1-10 or classification into suitable, conditionally suitable and unsuitable) related to the land use.

Cartographic diversification of space depending on the degree of suitability of the location relative to the previously established location criteria was carried out using a geographic information system within the ArcGIS (Spatial Analyst) software package. This methodology contributed not only to the easier geospatial consideration of locations, but also enabled the creation of more accurate, mathematics-based waste disposal sites in rural settlements using mathematical procedures. The calculations were performed using the ArcGIS Spatial Analyst software package for performing not only the mathematical calculation of the most suitable location, but also its visualization. A raster of specific zones or line directions was created to show the distribution of constraints and their later reclassification relative to the suitability criteria which are commonly used in Serbia (suitable, unsuitable, conditionally suitable). Thus, a clear idea of the zoning of the location criteria was obtained. Through overlapping the degree of suitability of different location criteria and their recalculation using this software package, accurate mathematically calculated locations were created that are directly related to the previously established weights and location criteria. The results obtained in this way are graphically expressed as dots or zones according to the predefined weights.

The area of three villages located in the Stara planina Mt. National Park in Serbia was chosen as the pilot area in which the main hypothesis was tested.

**Case Study- 3 Villages Located In The Stara Planina Mt. National Park.** Three villages

located in the Stara planina Mt. National Park (the villages of Dojkinci, Gostuša and Senokos in the Serbian municipalities of Pirot and Dimitrovgrad) were chosen as a pilot area for testing the GIS model. The reason for choosing these villages lies not only in the availability of significant databases and expertise necessary for various plans and studies [17], [18], but also in the fact that the mentioned area is a protected natural area. Therefore, this elimination criterion was taken into consideration in addition to the other techno-economic parameters, thus increasing the relevance of this research. In order to define the method and system for municipal solid waste disposal in the territory of rural settlements in Serbia, as well as to use previously elaborated methodology, it was necessary to determine the main input parameters, including: data on spatial coverage of settlements (topographic features, development of traffic, water resources and energy infrastructure, existing waste management system, locations closest to the existing/planned landfills), population (demographic structure and projections of the resident population, disposition of settlements), data on the amount and structure of municipal solid waste in rural settlements and data on the existing methods of household generated solid waste and wastewater treatment.

After creating a database on the abovementioned parameters, it was necessary to carry out their mapping, through determining the exact locations of the rural settlements, existing waste disposal sites, existing and planned land use, existing and planned protection zones of natural and cultural heritage, possible geomorphologic/hydrogeological barriers in the terrain (water accumulation protection zones, infrastructure corridors, etc.) and the spatial distribution of the space users (based on the projected population) [19]. All of the mentioned multi-criteria analyses were conducted using the ArcGIS (Spatial Analyst) software package, and based on our own methodology, as well as on studies by authors [13], [16], [20], [21] and [23]. All of the mentioned parameters are necessary for defining the waste collection method in a given territory, and also to tentatively define the locations and outlines of the landfill capacity in villages. From the aspect of determining the potential landfill sites, it was necessary to conduct additional analyses [22]. The research encompassed the determination of techno-economic, deterministic criteria used in the landfill site selection (such as geological, hydro-geological, geo-morphological, seismic, climatic criteria, existing and planning methods of land use, ecological criteria, criteria for the protection of natural and cultural historical values, existing infrastructure, etc.).

Altogether 18 different criteria were determined, according to which the most suitable

locations for the newly planned landfill sites in villages were determined using AHP methodology.

However, based on previous research, and also on the authors' practical experience, it was revealed that not all criteria can be classified in the same rank. Therefore, it was necessary to carry out the ranking of their relevant importance to the problem. Three criteria were defined based on their rank of importance, as it follows:

- rank 3, weight 0.15,
- rank 2, weight 0.35 and
- rank 1, weight 0.5.

The lowest ranking criteria are related to the hypsometric, seismic, climate and infrastructure facilities. In fact, since there is a huge difference in elevation between the villages of Stara Planina Mt., elevation is given third place in the range of criteria. The situation is similar for the seismic criterion, which can be considered as an immutable category. Climatic characteristics (which serve as bonus criterion for elimination) and radial distance of point infrastructure (substations, etc.) are also in this rank.

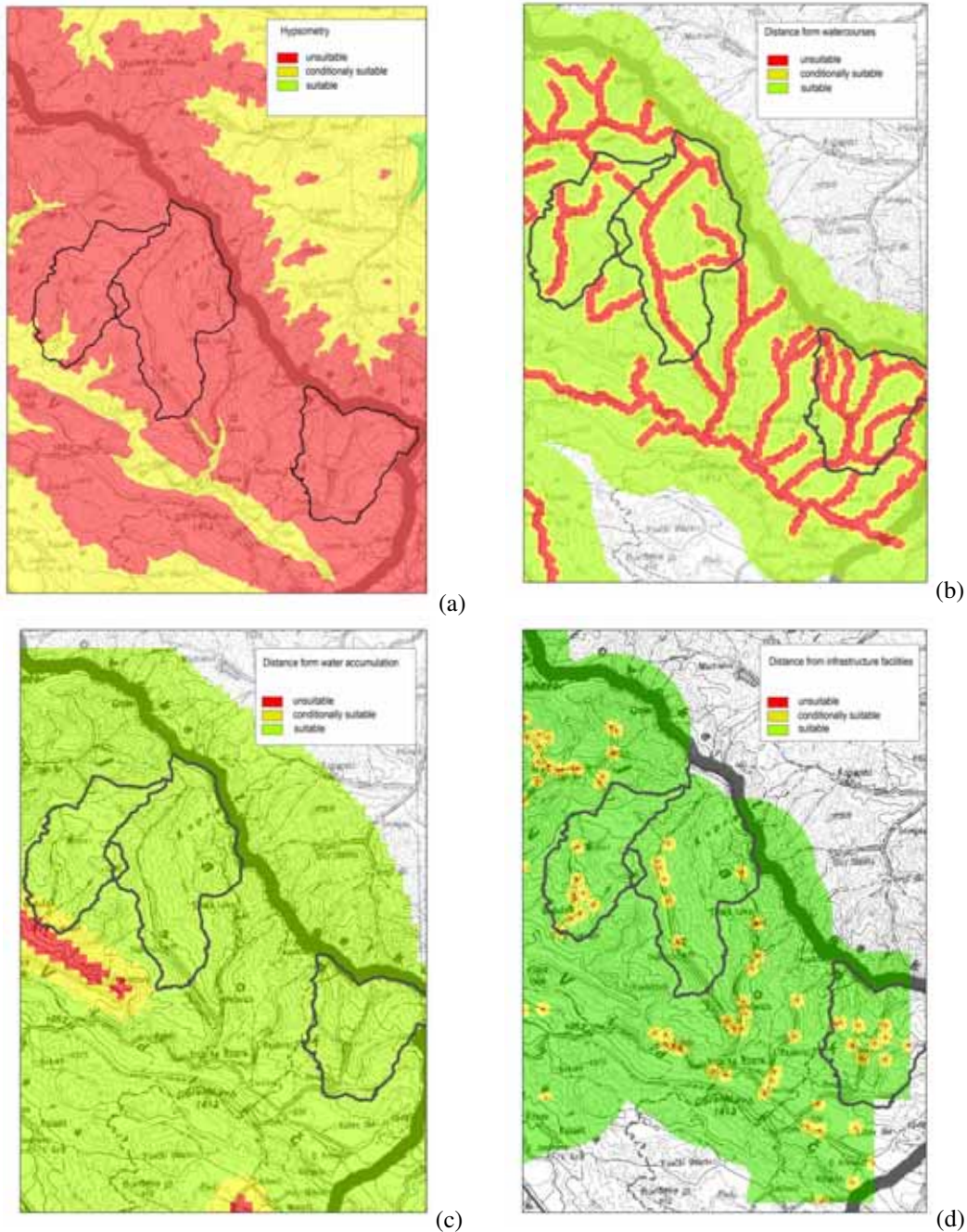


**FIGURE 1**

**Zones suitable for landfill construction relative to the aspect of area hypsometry (a), distance from watercourses (b), distance from water accumulations (c), distance from infrastructure facilities (d)**

Rank 2 includes the criteria in connection with slope, distance from objects of cultural heritage, distance from energetic and telecommunicational corridors etc.

Rank 1 includes the most important criteria in the area of municipal solid waste management: social acceptance (which is evaluated qualitatively), distance from the transport infrastructure, distance from the natural areas (the above mentioned villages are situated in the Nature park) and all the other criteria related to hydrogeological and geological characteristics.

## RESULTS AND DISCUSSION

After the weighting of criteria, their values were established, and based on them, the evaluation was conducted.

Serbian planning practice recognizes the classification of locations in relation to the criteria of three-level benefits (1-3) - suitable, conditionally suitable, unsuitable position. This categorization is maintained in the framework of the approach used for this model.

All the criteria were additionally evaluated using a geospatial database and then graphically presented. The most suitable locations have been denoted in green, the conditionally suitable ones are yellow, while the unsuitable sites according to these criteria are red. It is interesting to note that the research has been based only on three quantitative suitability ranks (suitable, conditionally suitable and unsuitable), since this is a common classification in Serbian planning practice. Figure 1 (a,b,c,d) depicts

the analyses of specific rural settlements which are situated in the pilot area located in the Stara planina Mt. Nature Park (which has three protection regimes of natural and cultural areas [24]). In Figure 1, zones suitable for landfill construction are presented relative to the aspect of area hypsometry (a), distance from watercourses (b), distance from water accumulations (c), and the suitability levels of locations depending on their distance from infrastructure facilities (d). Figure 1 shows only some of the analyses (out of a total of 18). Other analyses are suitability analyses relative to locations of existing settlements, climatic parameters, distance from state roads of the first and second category, etc. [25].

The locations obtained through the analysis are a direct reflection of the predefined techno-economic criteria, which can also be determined with a higher level of accuracy through an additional, more detailed, analysis (Figure 2a). Parallel to this analysis, an analysis for identifying the existing landfill sites was also conducted in the chosen pilot area of villages in the Stara planina mountain Nature Park (Figure 2b). In order to prove the initial assumptions on the significance of social criteria in selecting waste disposal sites in rural settlements, an additional criteria – social acceptance, was included in the originally realized techno-economic model, and a new set of locations, territorially considerably closer to open landfills, were determined through additional analyses (Figure 2c).

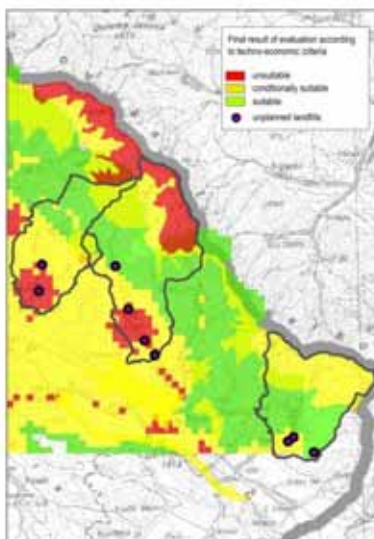


**FIGURE 2a)**  
Final result of evaluation according to techno-economic criteria in the ARCGIS software package

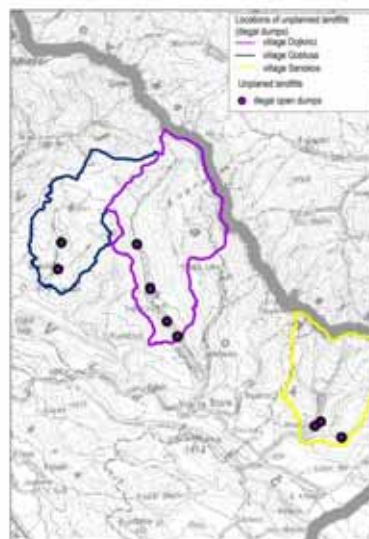


**FIGURE 2b)**  
Dotted distribution of open landfills in one of the analyzed localities (Stara planina Mt. Nature Park)

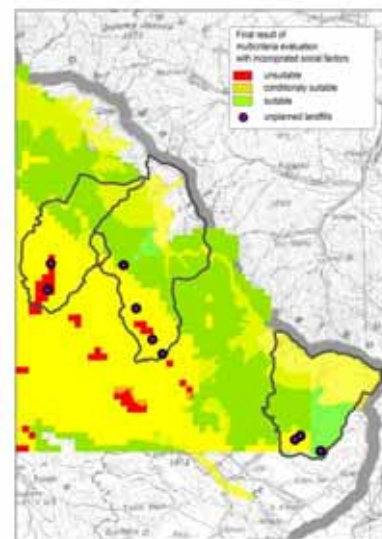


**FIGURE 2c)**  
Result of multi-criteria analysis with the additional rank of social acceptance for the site (with existing landfill sites)

Based on comparative representations of the existing open landfills, as well as locations obtained through the model-based approach, it may be concluded that the degree of success in solid waste management through the construction of landfills/transfer stations/recycling yards in rural settlements primarily depends on the degree of participation of the local population in the decision-making process in the sense of taking into account their attitudes in making decisions and, even more importantly, the degree to which their habits and behavior are taken into account in the multi-criteria analysis.

While surveying local residents for this research, it was determined that the landfill location was spontaneously formed based on the criteria of free space, i.e., on places for which property law relations are unknown (in cases of waste disposal in riverbeds, traffic corridors), or in places in which waste packaging was disposed of due to specific use (local stores). It is interesting to note that the local population continued to dispose of their waste at the same location, even after the shop had closed because of, in their own words, “habits, and it can be said a formed reflex to dispose of plastic bottles in this location”. Not one inhabitant could explain why they still, almost a year after the shop had closed, continued to dispose of their waste at this location. In addition to this, the survey results show that the locals who are currently disposing of waste at that location are prepared to sort their own waste, not only for an evident financial compensation, but also “for the possibility of doing something useful and entertaining in their free time”.

This clear cause-and-effect relation that exists in human behavior models, but also the demographic structure and habits and way of life, on the one hand, and waste disposal, on the other hand, indicate that the individual interests of the local population, their habits, as well as personal preferences, are a major factor in selecting waste disposal sites. In this sense, and due to a way of life that mainly does not include social engagement, it is possible to take action to stimulate villagers to collect waste within the village territory.

In the context of decision-making it can be concluded that although the model approach from the viewpoint of spatial planning is more relevant, given that it includes an evaluation of all the available factors of location – and behind the establishment of favorability criteria lies expert insight into the problem – in decision-making processes the social factor is most frequently defined as a decisive factor, i.e., the acceptability degree of the location/ local participation. Thereby, it was confirmed that for the precise determination of landfill location and/or transfer station it is necessary to include the habits, behavioral patterns and affinities of the locals in the decision-making processes.

The new combined methodology used in this research, with some small alterations, can be used for determining the locations for other potentially environmentally hazardous uses. By changing the number of criteria and their rank inside the model, the research can achieve an even greater level of detail.

Unlike the methodologies of the previously mentioned authors for finding locations for landfill sites [11], [13], [14], [15], [16], this method has shown significant success in terms of social acceptance, since, apart from the techno-economic criteria, it also takes into account criteria considered relevant by the local residents. Compared to the mentioned authors, this research has achieved a significant step forward in the quantification and weighting of social criteria, which has resulted in the convergence of locations by also including the modeling of locations where the local residents disposed of their waste. This emphasises the significance of respecting the social criteria in any relevant analysis of location.

## CONCLUSIONS

---

Research into the existing means of waste disposal in villages in Serbia, but also worldwide, has enabled the creation of a basis for more detailed consideration of the approach to this problem so far. Through specific research into the existing waste disposal sites in the area chosen as the research area (villages of the Stara planina Mountain), as well as through determining model and theory-based locations and their degree of “territorial convergence” depending on changes in the significance of social factors in the overall multi-criteria analysis of space for specific land-use (solid waste disposal), this paper presents the main suggestions regarding increasing the importance of social factors in multi-criteria analyses. The methodological procedure implemented was based precisely on the fact that previously used techno-economically generated models have introduced the social criterion but paid no special attention to it in the past. In current world research activities, the social criterion is rather marginalized, because of which the major constraint in finding locations for facilities according to the previously established model lies in the inability of local people to adapt to the new purpose of the site.

This GIS model, created for ranking the location suitability from the aspect of different criteria, may after further elaboration (by increasing or reducing the number of criteria, depending on the research), be used for diverse multi-criteria location analyses that are not directly associated with waste management. Thus, the model also finds multiple applications in different location studies in spatial planning.

More relevant research results have been achieved using GIS instruments in combination with standard AHP and SAW analyses than in previous studies, thus also achieving a higher degree of objectivity in research on locations. Thus, it may be concluded that, besides standard methods in spatial location analyses, it is also necessary to include the new GIS instruments which provide more accurate models that find multiple applications in environmental planning.

## ACKNOWLEDGEMENT

This work has resulted from research within the scientific project: “Sustainable Urban Development In The Serbian Danube Region” (TR 36036), which was financed within the program Technological development by the Ministry of Education and Science of the Republic of Serbia from 2011 to 2016.

## REFERENCES

- [1] Christensen, T.H., Cosso, R. and Stegmann, R. (1999) Waste management and treatment of Municipal solid waste (vol. V), CISA (Environmental sanitary engineering centre), Cagliari, Sardinia
- [2] Calvo, F., Moreno, B., Zamorano, M. and Szanto, M. (2005) Environmental diagnosis methodology for municipal waste landfills. *Waste management* Vol 25, 768-779.
- [3] Tchobanoglous, G., Theisen, H., Vigil, S. (1993) Integrated solid waste management, Engineering Principles and Management Issues. Editors: Tchobanoglous, G., McGraw-Hill International Editions, New York, USA
- [4] Tchobanoglous, G. and Kreith, F. (2002) Handbook of Solid Waste Management. Editors: Tchobanoglous, G. and Kreith, F. McGraw Hill, New York, USA
- [5] McDougall, F., White, P., Franke, M., Hindle, P. (2003) Integrated Solid Waste Management: a Life Cycle Inventory -second edition. Blackwell science library, Oxford, UK.
- [6] Al-Khatib, I., Arafat, H., Basheer, T., Shawahneh, H., Salahat, A., Eid, J. and Ali, W. (2007) Trends and problems of solid waste management in developing countries: A case study in seven Palestinian districts. *Waste Management* Vol. 27, 1910-1919.
- [7] Achankeng, E. (2003) Globalization, urbanization and municipal solid waste treatment in Africa. In African Studies Association of Australasia and the Pacific 2003 Conference Proceedings, University of Adelaide, Australia, 1-22.
- [8] Liu, C.N., Chen, R.H. and Chen K.S. (2006) Unsaturated consolidation theory for the prediction of long term municipal solid waste landfill settlement. *Waste management and Research* Vol.24, 80-91.
- [9] Mazzanti, M. and Zoboli, R. (2008) Waste Generation, Incineration and Landfill Diversion. De-coupling Trends, Socio-Economic Drivers and Policy Effectiveness in the EU, Working Papers 2008.94, Fondazione Eni Enrico Mattei, Italy
- [10] Rotich, K.H., Yongsheng, Z. and Jun, D. (2006) Municipal solid waste management challenges in developing countries – Kenyan case study. *Waste Management* Vol. 26, 92-100
- [11] Pereira, J. and Duckstein, L. (1993) A multiple criteria decision making approach to GIS based land suitability evaluation. *International journal of GIS* Vol.7 (5), 407-424.
- [12] Vidanaarachchi, C., Yuen, S. and Pilapitiya, S. (2006) Municipal solid waste management in the Southern Province of Sri Lanka: Problems, issues and challenges. *Waste Management* Vol. 26, 920-930.
- [13] Kontos, T., Komilis, D., and Halvadakis, C. (2005) Siting MSW landfills with a spatial multiple criteria analysis methodology. *Waste management*, No 25, 818-832.
- [14] Zamorano, M., Molero, M., Hurtado, A., Grindlay, A. and Ramos, A. (2008) Evaluation of a municipal landfill site in Southern Spain with GIS-aided methodology. *Journal of Hazardous Materials* Vol. 160, 473-481.
- [15] Kontos, T. and Halvadakis, C., (2002) Development of a Geographic Information System (GIS) for land evaluation for landfill siting: The Case of Lemnos Island. In: Editor Tsoulos L. Proceedings of 7th National Conference of Hellenic Cartographic Society, Mytilene, Lesbos, Greece
- [16] Guiquin, W., Li, Q., Guoxue, L. and Lijun, C. (2009) Landfill site selection using spatial information technologies and AHP: A case study in Beijing, China. *Journey of environmental Management* Vol 90., 2414-2421.
- [17] Milijić, S., Nikolić, M., Maric, I., Pucar, M., Dabić, D., Nenковиć, M. and Krunić, N. (2007) Rural infrastructure feasibility and costing study for the Stara planina Mt. Nature park – Study. Ministry of agriculture, Forestry and Water Management, World Bank, Belgrade, Serbia
- [18] Institute of Architecture and Urban & Spatial Planning of Serbia, (2009) Spatial Plan for the Special Purpose Area of the Stara planina Mt. Nature Park, Belgrade
- [19] Nenковиć-Riznić, M. (2007) Communal waste elimination problem and recycling possibilities





- in rural areas – example of villages on the Stara planina Mt. In: Editors M. Bogdanovic, M., Cvijanovic, R., Vosnakos, F.K. Proceedings of International conference: Multifunctional agriculture and rural development, Book II, Institute of Agricultural Economics, Beocin, Serbia, 826-836
- [20] Parisakis, G., Skordilis, A., Andrianopoulos, A., Lolos, T., Andrianopoulos, I., Tsompanidis, C. and Lolos, G. (1991) Qualitative and quantitative analysis of MSW in the island of Kos. Technical Report, National Technical University of Athens, Laboratory of Inorganic and Analytical Chemistry, Athens, Greece
- [21] Herrmann, S. and Osinski, E. (1999) Planning sustainable land use in rural areas at different spatial levels using GIS and modelling tools. *Landscape and Urban Planning* Vol. 46, 93-101.
- [22] Nenković-Riznić, M. and Pucar, M. (2009) Modern technologies and their application in waste elimination in Serbia's urban spa regions. In: Editors Kungulos, A., Aravossis, K., Karagiannidis A., Samaras P. Proceedings of the 2nd International Conference on Environmental Management, Engineering, Planning and Economics (CEMEPE 2009) and SECOTOX Conference, University of Thessaly, Mykonos, Greece, 2217-2223
- [23] Aivaliotis, V., Dokas, I., Hatzigiannakou, M. and Panagiotakopoulos, D. (2004) Functional relationships of landfill and land raise capacity with design and operation parameters. *Waste management Res* Vol 22, 283-290.
- [24] Maric, I. (2006) Traditional Moravska architecture and contemporary architecture (in Serbian), Editor Pucar M., Institute of architecture and urban & spatial planning, Belgrade, Serbia
- [25] Nenkovic-Riznic, M. (2011) Waste management in Serbian rural areas. Doctoral thesis, Faculty of Architecture, University of Belgrade, Belgrade, Serbia

---

**Received:** 09.01.2015

**Accepted:** 12.09.2016

---

#### **CORRESPONDING AUTHOR**

**Marina Nenkovic-Riznic**

Institute of Architecture and Urban & Spatial Planning of Serbia, Bulevar Kralja Aleksandra 73/II, 11000 Belgrade, Serbia,

Email : [marina@iaus.ac.rs](mailto:marina@iaus.ac.rs),  
[m.nenkovic.riznic@gmail.com](mailto:m.nenkovic.riznic@gmail.com)

# EFFICACY OF *IN VITRO* PROPAGATED COONTAIL (*CERATOPHYLLUM DEMERSUM* L.) ON QUALITY OF DIFFERENT WATER SAMPLES

Mehmet Karatas<sup>1</sup>, Muhammad Aasim<sup>1\*</sup>, Muhammet Dogan<sup>2</sup>

<sup>1</sup>Department of Biotechnology, Faculty of Science, Konya Necmettin Erbakan University, Konya, Turkey.

<sup>2</sup>Department of Biology, Kamil Ozdag Faculty of Science, Karamanoglu Mehmetbey University, Yunus Emre Campus, 70200, Karaman, Turkey.

## ABSTRACT

Coontail (*Ceratophyllum demersum* L.) is an important aquatic macrophyte used for phytoremediation of heavy metals. Shoot tip, 1<sup>st</sup> and 2<sup>nd</sup> nodal meristem explants were cultured on Murashige and Skoog (MS) medium containing 0.05-0.40 mg/L 6-benzylaminopurine (BA) + 0.10 mg/L  $\alpha$ -Naphthalene acetic acid (NAA). Shoot regeneration frequency ranged 83.33-91.67% and 58.33-83.33% and 50.00-91.67 % respectively for shoot tip, 1<sup>st</sup> and 2<sup>nd</sup> nodal meristem explant. Number of shoots per explant ranged 10.33-29.53, 16.25-26.89 and 12.42-24.66 for shoot tip, 1<sup>st</sup> and 2<sup>nd</sup> stem nodes respectively. Maximum number of 29.53 and 26.89 shoots per explant of shoot tip and 1<sup>st</sup> stem node were obtained from MS medium containing 0.10 mg/L BA+ 0.10 mg/L NAA. Whereas, maximum of (24.66) shoots per explant from 2<sup>nd</sup> stem node were scored on MS medium with 0.05 mg/L BA+0.10 mg/L NAA. Mean shoot length for shoot tip, 1<sup>st</sup> and 2<sup>nd</sup> stem node explants ranged 0.50-1.49 cm, 0.94-1.93 cm and 0.68-1.68 cm respectively. *In vitro* regenerated plants significantly affected the water quality of water samples. Water conductivity and hardness of dam water increased after 15 and 30 days. While water conductivity and hardness of tap water decreased after 15 and 30 days. Water conductivity of drinking water decreased after 15 and 30 days with no change in hardness. pH of all water samples increased after 15 and 30 days. Only drinking water had high Al, Fe and Cu concentrations and Al concentration decreased from 51.0  $\mu$ g/L to below 20  $\mu$ g/L, Fe concentration decreased from 372.0  $\mu$ g/L standard level of <50.0  $\mu$ g/L and Cu concentration in public water was very high (360  $\mu$ g/L) and decreased rapidly to below 0.02  $\mu$ g/L within 15 days (S2) after culture of *in vitro* grown plants. The study suggests the possible and efficient use of *in vitro* grown coontails plants for phytoremediation studies.

## KEYWORDS:

Heavy metals; *In vitro*; Stem node explants; Water quality

## INTRODUCTION

Phytoremediation that include phytoextraction, phytodegradation, rhizofiltration, phytostabilization and phytovolatilization is a process of cleaning water bodies or to render them harmless by introducing plants in their environment that have ability to absorb contaminants through leaves, roots or other body part [1]. Non-radioactive (Cd, Cu, Hg, Pb and Zn) or radioactive (Sr, Cs and U) toxic elements are introduced into environment through industrial, agricultural or domestic wastes. These metals cause DNA damage and have carcinogenic effects on humans and animals due to their ability to mutate [2, 3]. Heavy metals can stay in soil for centuries due to non-degradable and without intervention. These elements could be easily removed from water and soil environment by phytoremediation using plants [4, 5].

Aquatic plants are found in natural environment with ability of pytoremediation. Submergent aquatic macrophyte coontail or hornwort (*Ceratophyllum demersum* L. family Ceratophyllaceae) [6, 7] is an aquatic plant that provide many benefits to aquatic organisms like zooplankton, bacteria and fish [8, 9]. It is largely associated with phytoremediation of heavy metals [10-14] and as pollution biomonitor of water bodies [15]. Although, aquatic plants show wide distribution in water bodies all over the world and can grow and propagate by vegetative means. These plants are collected from water bodies for different purposes like medicinal or phytoremediation studies. Recent advances in plant tissue culture techniques enable to develop micropropagation protocols for environment friendly plants to cope with increasing pollution. Micropropagation could help in easy multiplication of phytoremediation plants; that could be introduced in large number thereafter to keep environment safe clean and healthy [16]. Depending on need and strategy,

plants could be transformed for phytoremediation purpose and these transgenes could accumulate toxic heavy metals in their body [17, 18]. There are reports that show over expression of specific genes in transgenes results in increased metal uptake, sequestration, translocation, and targeting of intracellulars. Tissue culture and genetic transformation are powerful tools that can be used to create or involved in transition metal transport [19].

In this study, we propagated coontail plants under *in vitro* conditions followed by checking the efficacy of these *in vitro* grown plantlets on cleaning water samples collected from different sources.

## MATERIALS AND METHODS

The coontails plants were purchased from a local ornamental aquarium seller of Karaman province in Turkey. Surface sterilization of the twigs was performed accordingly reported by Karatas et al. [20]. Thereafter, shoot tip, 1<sup>st</sup> and 2<sup>nd</sup> nodal meristem explants were isolated under aseptic conditions and they were cultured on MS [21] medium enriched with 3% sucrose and 0.05, 0.10, 0.20 and 0.40 mg/L BA + 0.10 mg/L NAA (Table 1) in Magenta GA<sup>7</sup> vessels and solidified with 0.65% agar. After 8 weeks of culture, multiple regenerated shoots were isolated under aseptic conditions for introduction in aquariums. The experiment was run in triplicate and the pH of all culture media was adjusted to 5.8±0.1 before autoclaving (103.4 kPa atmospheric pressure, 120 °C for 21 min). The cultures were incubated under 16-h light photoperiod (1500 lux) using white Light Emitting Diodes (LED) lights.

Water samples from Gödet Dam, public drinking water in Karaman and tap water of

Molecular Biology and Biotechnology Laboratory of Biology department, Karamanoglu Mehmetbey University were collected and analyzed (S1) before use in order to check the effects of *in vitro* propagated plants on water quality. Plants of similar length (~ 8-10 cm) were divided into sets of equal number (10 plants) and transferred to small aquariums (18×10×20 cm) containing 2000 cm<sup>3</sup> water. The aquariums were placed in growth room at 26±2°C in three replicates. Data regarding water conductivity (20°C), pH and hardness, Aluminum (Al), Iron (Fe), Copper (Cu), and Fluorine (F) were evaluated at Public Health Laboratory, Ministry of Health, Karaman, Turkey after 15 days (S2) and 30 days (S3) respectively. Water conductivity (µS/cm) and pH of all the samples were analyzed by using electrometric method. Hardness (°F) of the water samples were analyzed by titration method. Concentrations of Aluminum (Al) (µg/L), Iron (Fe) (µg/L) and Copper (Cu) (µg/L) were analyzed by Spectronic Unicam Spectrophotometer using respective kits by Merck (Germany). To analyze the results of water samples, they were compared with minimum value approved by Ministry of Health, Turkey.

Statistical analysis was performed as one-way ANOVA using IBM SPSS 20 for Windows. Means were compared using post hoc Duncan multiple range test. Data given in percentages were arcsine transformed [22] before subjecting them to statistical analysis.

## RESULTS

***In vitro* micropropagation:** All explants showed shoot initials on all culture mediums within two weeks followed by multiple shoot induction within 4 weeks. After 8 weeks of culture, data

**TABLE 1**  
Response of different nodal explants of Coontail to BA-NAA on multiple shoot regeneration

BA (mg/L)	NAA (mg/L)	Frequency of Shoot Regeneration (%)			Shoots Per Explants			Shoot Length (cm)		
		shoot meristem	1 <sup>st</sup> stem node	2 <sup>nd</sup> stem node	shoot meristem	1 <sup>st</sup> stem node	2 <sup>nd</sup> stem node	shoot meristem	1 <sup>st</sup> stem node	2 <sup>nd</sup> stem node
0.05	0.10	83.33	66.67	58.33 <sup>b</sup>	19.67 <sup>ab</sup>	18.55 <sup>b</sup>	24.66 <sup>a</sup>	1.49 <sup>b</sup>	1.33 <sup>c</sup>	1.23 <sup>bc</sup>
0.10	0.10	83.33	75.00	50.00 <sup>b</sup>	29.53 <sup>a</sup>	26.89 <sup>a</sup>	15.55 <sup>b</sup>	1.73 <sup>b</sup>	1.93 <sup>b</sup>	1.68 <sup>b</sup>
0.20	0.10	91.67	58.33	91.67 <sup>a</sup>	10.94 <sup>bc</sup>	17.44 <sup>b</sup>	14.94 <sup>b</sup>	0.66 <sup>c</sup>	1.04 <sup>c</sup>	0.79 <sup>c</sup>
0.40	0.10	91.67	83.33	58.33 <sup>b</sup>	10.33 <sup>bc</sup>	16.25 <sup>b</sup>	12.42 <sup>b</sup>	0.50 <sup>c</sup>	0.94 <sup>c</sup>	0.68 <sup>c</sup>
Control		91.67	91.67	100.00 <sup>a</sup>	1.19 <sup>c</sup>	1.72 <sup>c</sup>	1.58 <sup>c</sup>	4.02 <sup>a</sup>	2.45 <sup>a</sup>	2.78 <sup>a</sup>

Means followed by different small letters within columns are significantly different ( $p < 0.01$ )

regarding frequency of shoot regeneration (%), shoots per explant and mean shoot length were taken and subjected to statistical analysis. The results revealed that explants showed significantly different response ( $p < 0.01$ ) to variants of BA + NAA in terms of shoot regeneration frequency of shoot tip, 1<sup>st</sup> and 2<sup>nd</sup> stem nodes that ranged 83.33-91.67%, 58.33-83.33% and 50.00-91.67% respectively (Table 1). Comparing explants type, shoot regeneration frequency of shoot tip explant was relatively better compared to 1<sup>st</sup> and 2<sup>nd</sup> stem nodes on all concentrations of BA+NAA. Shoot regeneration on MS medium (Control) ranged 91.67-100.00%.

Results on number of shoots per explant of all explants showed significant differences ( $p < 0.01$ ) among them and ranged 10.33-29.53, 16.25-26.89 and 12.42-24.66 for shoot tip, 1<sup>st</sup> and 2<sup>nd</sup> stem nodes respectively. Whereas, 1.19-1.72 shoots per explants were recorded on MS medium (control). Maximum number of shoots per explant were noted on shoot tip (29.53) and 1<sup>st</sup> stem node (26.89) cultured on MS medium containing 0.10 mg/L BA+0.10 mg/L NAA. Contrarily, maximum of (24.66) shoots per explant of 2<sup>nd</sup> stem node were obtained on MS medium supplemented with 0.05 mg/L BA+0.10 mg/L NAA. Increasing concentrations of BA with 0.10 mg/L NAA were inhibitory with decreased number of shoots on all explants.

Mean shoot length of all explants showed significant variations ( $p < 0.01$ ) with range of 0.50-1.49 cm, 0.94-1.93 cm and 0.68-1.68 cm respectively for shoot tip, 1<sup>st</sup> and 2<sup>nd</sup> stem node explants. In general, longer shoots were recorded on 1<sup>st</sup> stem node explant compared to shoot tip and 2<sup>nd</sup> stem node explant on all variants of BA + NAA. Maximum shoot length on all explants was recorded on MS medium supplemented with 0.10 mg/L BA+0.10 mg/L NAA. However, comparatively longer shoots were recorded on all explants cultured on control (MS medium).

**Effects of *in vitro* propagated plants on water quality:** In order to check the efficacy of *in vitro* regenerated plants on water quality, regenerated plants were transferred to the aquariums containing different water samples collected from Karaman and analyzed after 15 (S2) and 30 days (S3). Water conductivity of dam, public and tap water prior to transfer of plants (S1) was recorded 324, 1088 and 508  $\mu\text{S}/\text{cm}$

respectively (Fig. 1a). *In vitro* regenerated plants increased the water conductivity of dam water up to 352.0  $\mu\text{S}/\text{cm}$  after 15 days (S2) and 397.0  $\mu\text{S}/\text{cm}$  after 30 days (S3). Contrarily, water conductivity of public water and tap water decreased gradually and recorded as 767  $\mu\text{S}/\text{cm}$  and 468  $\mu\text{S}/\text{cm}$  after 30 days respectively (Fig. a).

Water hardness of different samples changed variably after culturing *in vitro* regenerated plants. Hardness of dam water increased slightly from 18.0 to 20 °F in 30 days (Fig. 1b). Contrarily, hardness of tap water decreased continuously with passage of time and declined from 26.0 to 21.0 °F after 30 days of culture. Hardness of drinking water did not change and remained same after 15 (S2) and 30 days (S3) (Fig. 1b). pH of all water samples (S1) was almost similar and recorded 7.8 (dam water), 7.6 (public water) and 7.7 (tap water) (Fig. 1c). However, transfer of plants increased the pH level of all waters within 15 days that remained stable up to 30 days. Maximum change of pH level was recorded from public water that raised from 7.6 to 9.2 (S2) followed by minor change in pH of 9.3 after 30 days (S3). pH of water samples from Gödet dam increased up to 8.7 (S2) and 8.8 (S3) (Fig. 1c). On the other hand, pH of tap water raised up to 8.5 (S2) and remained same after 30 days (S3). The results showed that water inclined towards alkalinity after culture of *in vitro* cultured plantlets.

Aluminum (Al), Iron (Fe) and Copper (Cu) responded in similar way after 15 (S2) and 30 days (S3) in all water samples. Al, Fe and Cu concentrations of water samples taken from dam and tap were already below of minimum standard (S1). Results showed that concentrations of all metals remained well below minimum standard level after 15 (S2) and 30 days (S3) of culturing plants. Contrarily, concentrations of Al, Fe and Cu of public water were found relatively higher than standard values prior to the culture. After transferring the plants, Al concentration decreased from 51.0  $\mu\text{g}/\text{L}$  to below 20  $\mu\text{g}/\text{L}$  (S2) (Fig. 1d). Fe concentration in drinking water was recorded 372.0  $\mu\text{g}/\text{L}$  and decreased gradually to 122  $\mu\text{g}/\text{L}$  (S2) and recorded below standard level of <50.0  $\mu\text{g}/\text{L}$  (S3) (Fig. 1e). Cu concentration in public water was very high (360  $\mu\text{g}/\text{L}$ ) and decreased rapidly to below 20  $\mu\text{g}/\text{L}$  (S2) after culture (Fig. 1f). Whereas, Cu concentration in dam and tap water was already very low below standard and remained below in S2 and S3 samples.

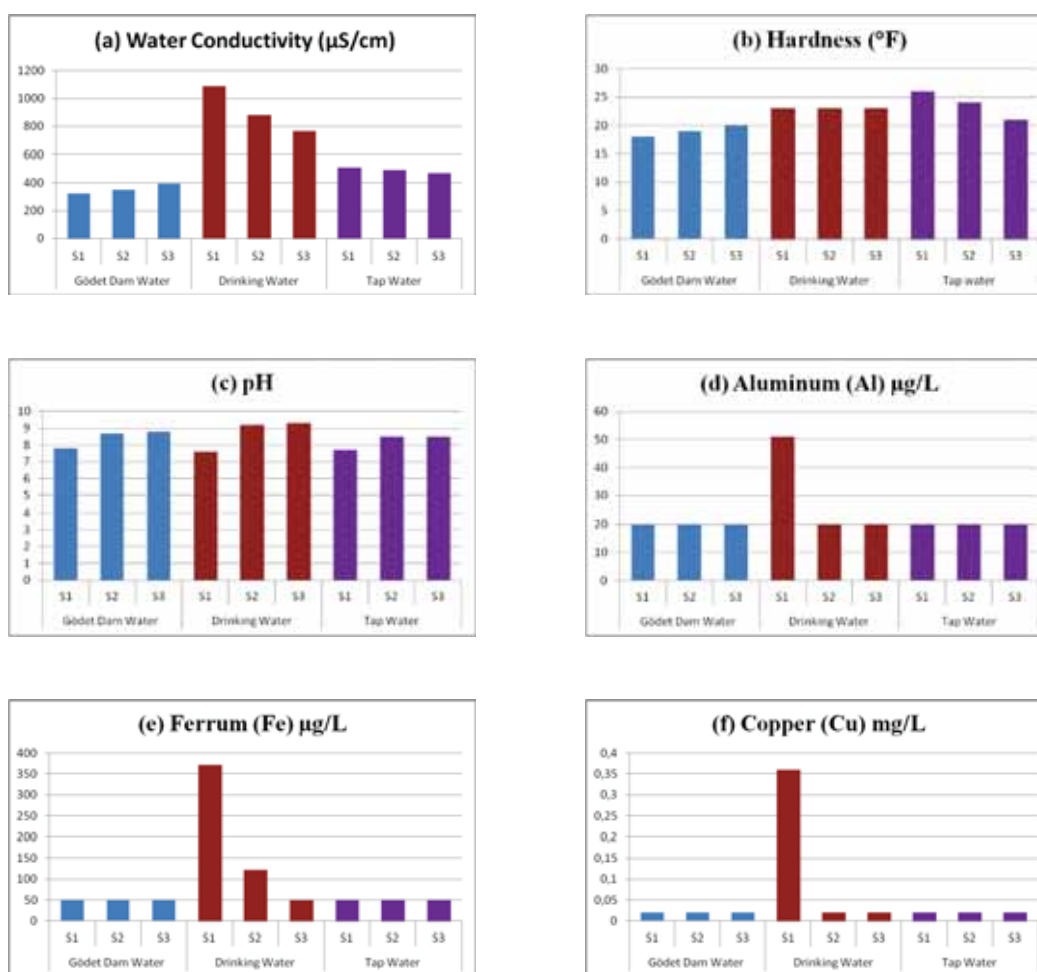


FIGURE 1

Efficiency of *in vitro* propagated plants of coontail on water quality parameters and heavy metals of different water samples

## DISCUSSION AND CONCLUSIONS

Shoot meristem and stem nodes are widely used explants for multiple shoot regeneration of aquatic plants [23-27]. Results illustrated that shoot regeneration started within two weeks of time without callus induction support the previous findings of Karatas et al. [20] in *C. demersum*. Contrarily, Results on shoot regeneration frequency showed variable response of explants to growth variants as shoot meristem explant was more responsive than other explants [20] irrespective of NAA in the culture medium. However, the results are contrarily to the findings of Karatas et al. [28] who achieved 100.0 % shoot regeneration on shoot tip, 1<sup>st</sup>, 2<sup>nd</sup> and 3<sup>rd</sup> internode and leaf explants of *B. monnieri* cultured on MS medium supplemented with different concentrations of BA+NAA.

Maximum number of shoots from shoot tip and 1<sup>st</sup> node were achieved at similar concentration of BA+NAA in the culture medium are in line with the findings of Karatas et al. [26] who also obtained maximum number of shoots from stem internodes

and leaf explant of *B. monnieri* at 0.25 mg/L BA-0.25 mg/L NAA. Results further illustrated that number of shoots decreased with increase of BA concentration in line with Sharma et al. [29] who also reported negative effects of increased BA concentration on shoots per explant of *B. monnieri*. However, the results are contrary to the findings of Jo et al. [30] in *Alocasia amazonica*. Results on mean shoot length also showed importance of growth regulator and explant type. 1<sup>st</sup> stem node was found to be more responsive to generate longer shoots compared to other explants. Previously, Karatas et al. [20] reported longer shoots of *C. demersum* from 2<sup>nd</sup> node explant compared to shoot tip and 1<sup>st</sup> stem node segment which might be due to presence of NAA in the culture medium or culture in liquid MS medium.

Aquatic plants are very important in plant water ecology due to providing oxygen, important part of food chain and providing nutrients in the water bodies. These aquatic plants interacts with their environment through different processes like chemical bio-concentration, excretion, shading,



organic matter production and decomposition [31, 32]; which, ultimately change the water quality [33, 34]. Water conductivity, hardness and pH of the water are some quality parameters of the water which are affected by number of plants. This study revealed variable effects of *in vitro* grown plants on water quality of water samples collected from different sources. Conductivity indicates the total concentration of dissolved ions in the water and water bodies. Higher conductivity shows water pollution from nutrients like nitrate, sodium and phosphate. Water conductivity of fresh water streams ranging 50-500  $\mu\text{S}/\text{cm}$  and water bodies with 150-500  $\mu\text{S}/\text{cm}$  is found to be safe for diverse aquatic life [35]. In our results, water conductivity of dam water showed increased conductivity pattern but remained within the safe range to support plant survival. On the other hand, decreased conductivity of public and tap water with time showed positive effects of the plants on respective water bodies. The results also revealed close relationship of pH and water hardness. Increase in pH of the water might be due to extraction of  $\text{CO}_2$  from the water for photosynthesis by plants [36]. Results further revealed the change in the water hardness by plants. However, water hardness still remained in soft category according to UN standards [36] after 30 days.

Contamination of drinking or irrigation water by heavy metal due to heavy industrialization is causing serious threat to plant growth, and humans all over the world. Quality of drinking water in public areas is heavily contaminated and needs to be tested and efforts must be employed to provide heavy metal free drinking water to the public. Aquatic plants have been used for improving water quality or water treatment [37] by biosorption [11]. Our results revealed the efficiency of *in vitro* grown *C. demersum* plants on decreasing heavy metals concentrations from different water samples used in the study. Results clearly showed that *in vitro* grown plants can be successfully used for phytoremediation studies. Although, Al and Fe in all water samples were in safe range, but Cu concentration was relatively high and plants successfully absorbed the Cu and reduced the Cu concentration. Accumulation of Cu by *C. demersum* support the findings of Matache et al. [38], who reported maximum accumulation of Cu by *C. demersum* compared to *Potamogeton pectinatus*, *Potamogeton lucens*, *Potamogeton perfoliatus*. Other reports also suggested the importance of *C. demersum* in order to clean water contaminated with different metals. Foroughi [39] reported that Mg concentration in *C. demersum* increased 96.29%, 100% and 73.52% respectively in treated municipal wastewater (TMW), raw municipal wastewater (RMW), diluted compost latex (DCL) after 18 days. Abdallah [40] investigated the phytoremediation of Cr and Pb from aqueous

solutions by *C. demersum* and reported that the highest removal percentages were as 84.3% and 95.0% in Cr and Pb respectively. Similarly, previous results on *C. demersum* revealed the successful use of *C. demersum* for cleaning of water (phytoremediation) against other heavy metals like Fe [11], Ni [37], Cu [41, 42], Zn [42] and Pb, Cd [43].

The study presents the first ever report on the use of *in vitro* propagated plants of coontails for adaptation in different waters and their efficacy on water quality and removal of heavy metals in the water samples. This study opens the new window for use of *in vitro* propagation protocols for the phytoremediation studies of coontail and other plants. Besides that, the protocol can be employed for genetic transformation studies in these plants by incorporating genes related to phytoremediation.

## ACKNOWLEDGEMENTS

Authors acknowledge Mr. Yusuf Serin for his help to ensure water analysis at Public Health Laboratory, Ministry of Health, Karaman, Turkey.

**Author's Contribution.** The whole project was designed by Prof. Dr. Mehmet Karataş and Assoc. Prof. Dr. Muhammad Aasim. All experiments were performed by Muhammet Dogan under the guidance of Prof. Dr. Mehmet Karataş and Assoc. Prof. Dr. Muhammad Aasim. Manuscript has been written by Assoc. Prof. Dr. Muhammad Aasim and controlled by all authors prior to submission.

## REFERENCES

- [1] Rugh, C.L., Wilde, D., Stack, N.M., Thompson, D.M., Summers, A.O. and Meagher, R.B. (1996) Mercuric ion reduction and resistance in transgenic Arabidopsis thaliana plants expressing a modified bacterial merA gene. Proceedings of the National Academy of Sciences of the United States of America 93, 3182-3187.
- [2] Baudouin, C., Charveron, M., Tarrouse, R. and Gall, Y. (2002) Environmental pollutants and skin cancer. Cell Biology and Toxicology 18, 341-348.
- [3] Hooda, V. (2007) Phytoremediation of toxic metals from soil and waste water. Journal of Environmental Biology 28, 367-376.
- [4] Raskin, I., Smith, R.D. and Salt, D.E. (1997) Phytoremediation of metals: using plants to remove pollutants from the environment. Current Opinion in Biotechnology 8, 221-226.

- [5] Han, Y., Huang, S., Yuan, H., Gu, J., Zhao, J., Wu, X. and Si, W. (2013) Effect of Pb and Zn combined stress on the growth and elements accumulation of two different ecotype species of *Iris* L. in artificial contaminated soils. *Fresen. Environ. Bull.*22, 1548-1555.
- [6] Seçmen, Ö. and Leblebici, E. (1997) Türkiye Sulak Alan Bitkileri ve Bitki Örtüsü. Ege University, Faculty of Science Publications, İzmir, Turkey.
- [7] Arber, A. (2010) Water plants. A study of aquatic angiosperms. Cambridge University Press, New York, U.S, p. 88.
- [8] Hao, Z.; Liu, Y., Wang, G., Li, G., Li, X. and An, Y. (2012) A two months test of an artificial closed aquatic ecosystem containing *Ceratophyllum demersum* L. and *Bulinus australianus*. *Fresen. Environ. Bull.*21, 426-432.
- [9] Dai, Y., Chang, J., Zhang, L., Wu, Z. and Liang, W. (2014) Effects of submerged macrophytes *Ceratophyllum demersum* L. on sediment microbial community. *Fresen. Environ. Bull.*23, 2474-2480.
- [10] Saygıdeğer, S. and Doğan, M. (2004) Lead and cadmium accumulation and toxicity in the presence of EDTA in *Lemna minor* L. and *Ceratophyllum demersum* L.. *Bulletin of Environmental Contamination and Toxicology* 73, 182-189.
- [11] Foroughi, M., Najafi, P. and Toghiani, S. (2011b) Trace elements removal from water water by *Ceratophyllum demersum*. *Journal of Applied Sciences and Environmental Management* 15, 197-201.
- [12] Park, S., Kang, D., Kim, Y., Lee, A.M., Chung, Y. and Sung, K. (2011) Biosorption and growth inhibition of wetland plants in water contaminated with a mixture of arsenic and heavy metals. *Engineering in Life Sciences* 11, 84-93.
- [13] Kamel, K.A. (2013) Phytoremediation potentiality of aquatic macrophytes in heavy metal contaminated water of El-Temsah Lake, Ismailia, Egypt. *Middle East Journal of Scientific Research* 14, 1555-1568.
- [14] Xing, W., Wu, H., Hao, B., Huang, W. and Liu, G. (2013) Bioaccumulation of heavy metals by submerged macrophytes: Looking for hyperaccumulators in eutrophic lakes. *Environmental Science & Technology* 47, 4695-470.
- [15] Krems, P., Rajfur, M., Waclawek, M. and Kłós, A. (2013) The use of water plants in biomonitoring and phytoremediation of waters polluted with heavy metals. *Ecological Chemistry and Engineering S* 20, 353-370.
- [16] Castiglione, S., Franchin, C., Fossati, T., Lingua, G., Torrigiani, P. and Biondi, S. (2007) High zinc concentrations reduce rooting capacity and alter metallothionein gene expression in white poplar (*Populus alba* L. cv. Villafranca). *Chemosphere* 67, 1117-1126.
- [17] Clemens, S., Palmgren, M.G. and Krämer, U. (2002) A long way ahead: understanding and engineering plant metal accumulation. *Trends in Plant Science* 7, 309-314.
- [18] Eapen, S. and D'Souza, S.F. (2005) Prospects of genetic engineering of plants for phytoremediation of toxic metals. *Biotechnology Advances* 23, 97-114.
- [19] Capuana, M. (2011) Heavy metals and woody plants - biotechnologies for phytoremediation. *Journal of Biogeosciences and Forestry* 4, 7-15.
- [20] Karatas, M., Aasim, M. and Dogan, M. (2014) Multiple shoot regeneration of *Ceratophyllum demersum* L. on agar solidified and liquid mediums. *Fresen. Environ. Bull.*23, 3-9.
- [21] Murashige, T. and Skoog, F. (1962) A revised medium for rapid growth and bioassays with tobacco tissue cultures. *Plant Physiology* 15, 473-497.
- [22] Snedecor, G.W. and Cochran, W.G. (1997) *Statistical methods*. The Iowa State University Press, Iowa, USA.
- [23] Karatas, M., Dogan, M., Emsen, B. and Aasim M. (2015) Determination of *in vitro* free radical scavenging activities of various extracts from *in vitro* propagated *Ceratophyllum demersum* L. *Fresen. Environ. Bull.*24, 2946-2952.
- [24] Raja, H.D. and Arockiasamy, D.I. (2008) *In vitro* propagation of *Mentha viridis* L. from nodal and shoot tip explants. *Plant Tissue Culture and Biotechnology* 18, 1-6.
- [25] Dogan, M., Karatas, M. and Aasim M. (2015). An efficient *in vitro* plantlet regeneration of *Ceratophyllum demersum* L., an important medicinal aquatic plant. *Fresen. Environ. Bull.*24, 3499-3504.
- [26] Janarthanam, B., Gopalakrishnan, M., Lakshmi Sai, G. and Sekar, T. (2009) Plant regeneration from leaf derived callus of *Stevia rebaudiana* Bertoni. *Plant Tissue Culture and Biotechnology* 19, 133-141.
- [27] Ugraiah, A., Karuppusamy, S. and Pullaiah, T. (2010) Micropropagation of *Marsdenia brunoniana* Wight & Arn. A rare antidiabetic plant. *Plant Tissue Culture and Biotechnology* 20: 7-12.
- [28] Karatas, M., Aasim, M., Dogan, M. and Khawar, K.M. (2013) Adventitious shoot regeneration of the medicinal aquatic plant water hyssop (*Bacopa monnieri* L. Pennell) using different internodes. *Archives of Biological Sciences* 65, 297-303.
- [29] Sharma, N., Satsangi, R., Pandey, R. and Devi, S.V. (2007) *In vitro* clonal propagation



- and medium term conservation of Brahmi [*Bacopa monnieri* (L) Wettst]. Journal of Plant Biochemistry and Biotechnology 16, 139-143.
- [30] Jo, U.A., Murthy, H.N., Hahn, E.J. and Paek, K.Y. (2008) Micropropagation of *Alocasia amazonica* using semisolid and liquid cultures. *In Vitro Cellular & Developmental Biology - Plant* 44, 26-32.
- [31] Honnell, D.R., Madsen, J.D. and Smart, R.M. (1993) Effects of selected exotic and native aquatic plant communities on water temperature and dissolved oxygen. Information Exchange Bulletin A932. U.S. Army Engineer Research and Development Center, Vicksburg, MS, USA.
- [32] Fleming, J.P., Madsen, J.D. and Dibble, E.D. (2011) Macrophyte re-establishment for fish habitat in Little Bear Creek Reservoir, Alabama, USA. *Journal of Freshwater Ecology* 26, 105-114.
- [33] Chambers, P. and Prepas, E. (1994) Nutrient dynamics in riverbeds: The impact of sewage effluent and aquatic macrophytes. *Water Research* 28, 453-464.
- [34] Schultz, M., Kozerski, H.P. Pluntke, T. and Rinke, K. (2002) The influence of macrophytes on sedimentation and nutrient retention in the lower River Spree (Germany), *Water Research* 37, 569-578.
- [35] Sharon, B. (1997) Testing the Waters: Chemical and Physical Vital Signs of a River. Montpelier, River Watch Network, Dubuque, Iowa, USA.
- [36] Carr, G.M. and Neary, J.P. (2008) Water quality for ecosystem and human health, united nations environment programme global environment monitoring system/water programme, Canada.
- [37] Chorom, M., Parnian, A. and Jaafarzadeh, N. (2012) Nickel removal by the aquatic plant (*Ceratophyllum demersum* L.). *International Journal of Environmental Science and Development* 3, 372-375.
- [38] Matache, M.L., Marin, C., Rozyłowicz, L. and Tudorache, A. (2013) Plants accumulating heavy metals in the Danube River wetlands. *Journal of Environmental Health Science and Engineering* 11, 39.
- [39] Foroughi, M. (2011a) Role of *Ceratophyllum demersum* in recycling macro elements from wastewater. *Journal of Applied Sciences and Environmental Management* 15, 401-405.
- [40] Abdallah, M.A.M. (2012) Phytoremediation of heavy metals from aqueous solutions by two aquatic macrophytes, *Ceratophyllum demersum* and *Lemna gibba* L. *Environmental Technology* 33, 1609-1614.
- [41] Keskinan, O., Goksu, M.Z., Basibuyuk, M. and Forster, C.F. (2004) Heavy metal adsorption properties of a submerged aquatic plant (*Ceratophyllum demersum*). *Bioresource Technology* 92, 197-200.
- [42] Pourkhabbaz, A.R., Pourkhabbaz, H.R., Khazaei, T., Behraves, S. and Ebrahimipour, M. (2011) Assessment of heavy metal accumulation in Anzali wetland, Iran, using a submerged aquatic plant, *Ceratophyllum demersum*. *African Journal of Aquatic Science* 36, 261-265.
- [43] VahdatiRaad, L. and Khara, H. (2012) Heavy metals phytoremediation by aquatic plants (*Hydrocotyle ranocloides*, *Ceratophyllum demersum*) of Anzali lagoon. *Journal of Marine Science and Engineering* 2, 249-254.

---

**Received:** 13.08.2015

**Accepted:** 10.04.2016

---

**CORRESPONDING AUTHOR**

**Muhammad Aasim**

Department of Biotechnology,  
Faculty of Science,  
Necmettin Erbakan University,  
Konya, Turkey.

e-mail: [mshazim@gmail.com](mailto:mshazim@gmail.com)



# VARIATION IN COMMUNITY COMPOSITION OF *NirS*-TYPE DENITRIFIERS IN SEDIMENT OF BASINS WITH DIFFERENT TROPHIC STATES WITHIN A SHALLOW LAKE

Yao Zhang<sup>1,2</sup>, Yuqian Liu<sup>1,2</sup>, Zijun Zhou<sup>1,2</sup>, Siyang Wang<sup>1,2</sup>, Xiuyun Cao<sup>1</sup>, Chunlei Song<sup>1</sup>, Yiyong Zhou<sup>1,\*</sup>

<sup>1</sup>The State Key Laboratory of Freshwater Ecology and Biotechnology, Institute of Hydrobiology, the Chinese Academy of Sciences, No. 7 Donghu South Road, Wuchang District, Wuhan, Hubei, People's Republic of China

<sup>2</sup>University of Chinese Academy of Sciences, No. 19 Yuquan Road, Beijing, 100039, People's Republic of China.

## ABSTRACT

Denitrification is of great concern as part of the global nitrogen cycle leading to nitrogen loss from lake. However key factors controlling this process still remain unclear. A shallow Chinese lake (Lake QingLing) is divided into aquaculture zone (QLN) and natural zone covered by macrophytes (QLS), providing an ideal model to identify environment factors, rather than geographical and hydrological ones, affecting community structure of denitrifiers. Targeting the *nirS* gene and using the terminal restriction fragment length polymorphism (T-RFLP) analysis and cloning composition structure of denitrifiers were studied in sediment of Lake QingLing. Trophic states were largely different between the two basins. In parallel, a few unique T-RFs appeared in QLN. Furthermore, most sequences were grouped into *Proteobacteria*, majority genes from QLN were found to be prevalent in *Alphaproteobacteria* and *Gammaproteobacteria* while most sequences from QLS were in *Betaproteobacteria* and *Gammaproteobacteria*. Canonical correspondence analysis (CCA) indicated that organic matter (OM) in sediment,  $\text{NH}_4^+$  and pH value in pore water were important environmental factors shaping these communities.

## KEYWORDS:

denitrification; *nirS*; sediment; alternative stable state; shallow lakes.

## INTRODUCTION

Denitrification is a major biological process to reduce nitrate to molecular nitrogen ( $\text{N}_2$ ). In shallow eutrophic lakes, this process can remove the largest portion of fixed nitrogen and plays an important role in self-purification of these ecosystems [1]. Denitrification consists of four enzymatic reaction steps which are catalysed by four metalloproteins:

nitrate reductase, nitrite reductase, nitric-oxide reductase and nitrous oxide reductase [2]. Nitrite reductase is the key enzyme in this process which is encoded by the copper-containing *nirK* and the cytochrome  $\text{cd}_1$  *nirS* gene [3]. It has been demonstrated that the two reductases are mutually exclusive in any given strain, though the *Nir* type may differ within the same genus and even within the same species [4]. The  $\text{cd}_1$ -*Nir* reductase is assumed to dominate in denitrification bacteria while the copper reductase show greater variation in molecular weight and present in more diverse taxa [3, 4]. Recent studies indicated that the water type [1], geomorphological [5, 6] and hydrological conditions [7], physical and chemical factors as well as biological factors [8] could have influence on community composition of denitrifiers. To be brief, it remains unknown which is the key environmental factor affecting denitrifying community, so it is helpful to choose certain circumstance where influences of geographical and hydrological factors are excluded and consequently environment factors can be highlighted.

Lake QingLing, locates in the western suburbs of Wuhan city, China. It is divided into two parts, one is used for aquaculture and the other, covered by macrophytes, has remained in natural conditions. The geomorphological and hydrological characteristics of the two parts are the same but trophic states are totally different between them. Thus, the lake provides an ideal model to identify the environmental factors that shape the community structure of denitrifiers. In this study, we focus on how environmental factors affect the community structure and the molecular diversity of denitrifying bacteria, using the *nirS*-type denitrifiers as an example.

## MATERIALS AND METHODS

**Study area and sample collection.** Lake QingLing (30°25'–30°27'N, 114°13'–114°14'E) is

an urban freshwater lake in Wuhan, it is about 9.7 km<sup>2</sup>. The southern part (QLS) with a mean depth of 1.6m was natural developed and was growing different kinds of water plants such as *Trapa natans* L., *Nelumbo nucifera*, *Potamogeton crispus* L., *Lemna minor* L. and so on, and the coverage of the former accounted for 90% [9]. In contrast, the northern part (QLN) with a mean depth of 2.3m was used for intensive fish farming and macrophytes were extinct [9]. Fish feed were thrown into the farming area by automatic feeding machine three times a day.

Sediment was collected (21 Sept, 2012) using a beaker-type sampler which takes surface sediment with depth of around 50mm. Sampling sites were shown in Fig.1. All the samples were stored in an ice cooler until they were brought back to the laboratory. About 15 g sediment were stored at -80 °C for DNA extraction, the rest of the sample were stored at 4 °C until chemical analysis.



**FIGURE 1**

**Map of Lake QingLing showing the location of sampling sites.**

#### **Analysis of chemical properties of sediment.**

Pore water was obtained by centrifugation of approximately 100g sediment at 3500r/min for 15 min. The pore water was decontaminated via glass microfiber filters (Whatman) filtration before chemical analysis. The obtained water samples were analyzed for pH value and concentrations of NO<sub>3</sub><sup>-</sup>, NO<sub>2</sub><sup>-</sup> and NH<sub>4</sub><sup>+</sup> [10]. Total nitrogen (TN) and total phosphorous (TP) of overlaying water were tested according to environmental quality standards for surface water (GB 3838-2002). The sediment organic matter (OM) was determined by loss-on-ignition in muffle furnace [11].

**Molecular microbiological work. DNA extraction.** DNA was extracted from approximately

0.3 g fresh sediment samples by UltraClean Soil DNA Isolation Kit (Mo Bio Laboratories, Carlsbad, CA) according to the manufacturer's instructions. The DNA was divided into three parts and stored at -80 °C.

**Polymerase chain reaction (PCR).** PCR of *nirS* genes were performed with primers *nirS1F-nirS6R* using conditions described previously [12]. Amplification products (890bp) were inspected by agarose gel electrophoresis on 2% (wt/vol) and visualized by UV excitation. PCR products were purified by elution from an agarose gel (2% wt/vol) using the Gel Extraction Kit (MoBio laboratories, CA).

**Terminal restriction fragment length polymorphism (T-RFLP).** The composition of the denitrifying communities was determined by T-RFLP. Twenty-five microliters of PCR reaction mixture consisted of about 10 to 20 ng of DNA, 0.4 μM of primer, 0.25 μL of 0.1% BSA, 0.32 mM of dNTP, 2.5 μL of 10 × PCR Buffer (Mg<sup>2+</sup> Plus), 1 U rTaq (TaKaRa). The forward primer was fluorescently labeled at the 5' end with 6-carboxyfluorescein (FAM) and the primers used were FAM-*nirS1F* and *nirS6R*. PCR products were purified by elution from an agarose gel (2% wt/vol) using the Gel Extraction Kit (MoBio laboratories, CA). After purification, approximately 10 ng of *nirS* PCR products were digested at 37 °C with the *Hha* I and *Rsa* I, at 65 °C with *Taq* I restriction enzyme (MBI Fermentas, Hanover, MD) separately, all the enzyme digestions run for 3 hours. After digestion, 2 μl of each sample was mixed with 12 μl of formamide and 0.3 μl of LIZ-labeled internal size standard. Fragment size analysis was carried out with ABIPRISM 3730xl genetic analyzer. The peak heights were automatically quantified by GENESCAN analysis software (Applied Biosystems). Given the differences in running time among all samples, we considered fragments from different profiles with less than 1 bp difference to be the same. Peaks of less than 50 bp were excluded.

**Cloning, sequencing and phylogenetic analyses.** PCR amplification was performed using the primers and conditions mentioned previously, mixed DNA samples of QLS (equal amounts of the three sites) as well as QLN (equal amounts of the three sites) were used for DNA template, then the clone libraries were constructed. The cloning was performed by using the pGEM T-Easy vector (Promega) system according to the instructions. The presence of the *nirS* gene was checked by PCR amplification using vector primers (M13F and M13R). Positive clones were randomly selected for sequencing by the Invitrogen Company (Shanghai,

China). Operational taxonomic unit (OTU) was performed using DOTUR [13] in order to bin sequences into clusters based on 97% sequence similarity. The obtained sequences were aligned by ClustalW and a phylogenetic tree was constructed using the neighbor-joining method in MEGA version 4.0 [14], gaps were complete deletion and the model was maximum composite likelihood.

*NirS* gene sequences from environmental samples were deposited in GenBank under accession numbers KR819924 to KR819980.

**Statistical methods.** Independent-Samples T test was performed using SPSS version 18.0 (SPSS, Inc., Illinois), with  $\alpha$  value of 0.05 or 0.01 selected for significance. Microbial community profiles were statistically analyzed for differences due to the T-RFLP results using analysis of similarity (ANOSIM) (Primer V 5.0 software, PRIMER-E, Plymouth, UK). A binary matrix was constructed by scoring based on the Bray-Curtis to do clustering analysis, similarity coefficients was used to analyze the relatedness of individual community profiles, similarity value ranges between 0 and 100; with 100 indicating no differences in community structure, and 0 indicating complete difference in community structure. A canonical correspondence analysis (CCA) with the Monte Carlo permutation test with 499 permutations was used with the software CANOCO for windows, version 4.5 [15] to determine which biogeochemical parameters contributed to the differences among studying areas. Presence (percentage of area) or absence of terminal-restriction fragments were used as species data whereas geochemical data were included in the analysis as environmental variables. Resulting ordination biplots approximated the weighted differences between the individual communities (T-RFLP patterns) with respect to each of the geochemical factors, which were represented as arrows. The length of the corresponding arrows indicated the relative importance of the geochemical factor in explaining variation in the microbial T-

RFLP profiles, whereas the angle between arrows indicated the degree to which they were correlated.

## RESULTS AND DISCUSSION

**Sediment properties.** As shown in table 1, QLN had significantly higher concentrations of TN ( $P<0.05$ ) and TP ( $P<0.01$ ), probably due to the intensive fish farming there. On the other hand, QLS with coverage of macrophytes showed significantly higher  $\text{NH}_4^+$  concentration ( $p<0.05$ ) and lower pH value ( $p<0.01$ ) in pore water and significantly higher OM content in sediment ( $p<0.01$ ). These differences could be mainly explained by the role of microphytes, firstly organic matter accumulation in wetlands is the net result of primary production and decomposition, decomposition of dead plant material is slowed significantly in wetlands due to anaerobic conditions. It was found that humic substances were the major proportion of OM in created wetlands [16]. Additionally in a large macrophyte-dominated shallow lake (Lake Baiyangdian) in the north China plain, the humification degree of natural organic matter was higher in the lake outlet area than at aquaculture areas [17]; Secondly, during habitats humification, some water and sediment characteristics, such as pH value is low and almost invariable in very acid lakes [18]. Thirdly, decomposition of organic matter facilitates ammonia production. For example, in a high productive polymictic lake system, it seems likely that release of ammoniacal nitrogen depend on decomposition of rich reserves of organic matter in superficial 10 cm bottom sediment layer [19]. Furthermore, in the sediments of a mesohaline lagoon,  $\text{NH}_4^+$  was produced in sediments by the decomposition of organic matter through aerobic pathways in the upper 1 cm and below this depth through anaerobic pathways mainly sulfate reduction [20]. In short,

**TABLE 1**  
**Biogeochemical characteristics of the sampling site of Lake QingLing**

Sampling sites	$[\text{NO}_3^-]\text{-N}$ in pore water ( $\mu\text{g/L}$ )	$[\text{NO}_2^-]\text{-N}$ in pore water ( $\mu\text{g/L}$ )	$[\text{NH}_4^+]\text{-N}$ in pore water ( $\mu\text{g/L}$ )	OM in sediment (%)	pH in pore water	TN in overlying water (mg/L)	TP in overlying water (mg/L)
QLS1	282.7	10.3	1064.0	17.18	6.75	2.62	0.17
QLS2	178.8	8.6	1167.9	20.93	6.84	2.19	0.22
QLS3	209.9	5.2	853.0	16.32	6.95	2.33	0.24
QLN4	282.7	3.4	446.1	8.29	7.98	3.21	1.88
QLN5	313.9	5.2	410.1	10.25	8.12	3.35	2.01
QLN6	303.5	6.9	443.6	8.49	7.94	3.32	2.03

Note: OM, organic matter; TN, total nitrogen; TP, total phosphorous.

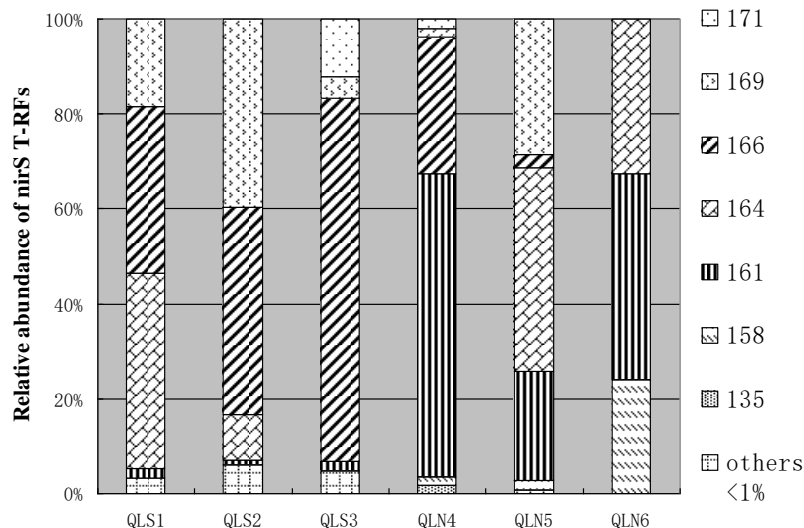


**FIGURE 2**

**Terminal restriction fragment length polymorphism analysis of amplified *nirS* genes hydrolysed with Hha I. Those T-RFs of less than 1% of the total peak height were grouped together as a single group denoted as others < 1%. x-axis, samples; y-axis, relative abundance of T-RFs in percentage of the total peak height.**

based on the processes and mechanisms mentioned above, sediment in the QLS gave significantly higher OM content, coupled with a significantly lower pH value and higher ammonia concentration in pore water. In conjunction with our results organic matter derived from a macrophyte (*Potamogeton crispus*) could induced black bloom, which was characterized by relatively low pH value and an increased ammonium nitrogen in overlying water in Lake Taihu, China [21].

**T-RFLP analysis of *nirS* genes.** Terminal restriction fragments (T-RFs) obtained from *Hha* I digests provide the highest level of resolution among the three enzymes used in this study. As shown in Fig.2, there were a few unique T-RFs in QLN without the coverage of macrophytes. In details, the 135 bp T-RF appeared only in QLN4. Additionally, the 158 bp T-RF occurred in all the sites of QLN. Consistently, in a created wetlands, the community structure and diversity of *nirS*-type denitrifiers based on T-RFLP analysis showed no significant change due to hydrologic pulsing, while the presence and absence of vegetation altered their community structure [22]. Statistical analysis of individual T-RF dominance suggested that the *nirS*-type denitrifier communities were related to chlorophyll-a in the Fitzroy river estuary [23]. In a coastal freshwater wetland on Lake Huron, The sediments in the zone invaded by an emergent exotic plant (*Typha x glauca*) showed dramatically higher concentrations of soluble nutrients, including greater than 10-fold higher soluble ammonium. T-RFLP analyses

revealed significant differences in the composition of denitrifier communities (based on *nirS* genes) between invaded and uninvaded zones [24]. Additionally T-RF 78 of *nirS* dominated in a tea soil of pH 3.71 [25]. All these data strengthened the role of key environmental factors such as organic matter, ammonia and pH value in shapping *nirS* denitrifying bacterial communities as occurred in Lake QingLing. Moreover, T-RF 161 and T-RF 166 co-occured in both QLS and QLN, consistently in the stratified water column of Lake Kinneret, Israel, according to the T-RFLP profiles and clone libraries of *nirS* products, 2 groups of denitrifiers were common to and dominant in all depths [26]. Further to these observations, the distribution patterns of these two fragments were market different between the two lake basins. For example the 161 bp T-RF showed high percentage in QLN (63.72% at QLN4, 22.92% at QLN5 and 43.42% at QLN6). On the other hand, the 166 bp T-RF exhibited a relatively high abundance in QLS (34.92% at QLS1, 43.82% at QLS2 and 76.28% at QLS3) (Fig.2). Some key environment factor partitioning the lake basins such as nitrogen status may contribute to this differentiation. In parallel, T-RFLP analysis of *nirS* genes revealed that the 100 bp T-RF substantially increased in the nitrate treatments in rice field soils [27].

T-RFLP profiles compared by presence/absence as well as relative abundance of T-RFs showed a clustering according to sampling sites (Fig.3). The first dichotomy separated QLS's T-RFs from QLN's, then, to the northern part, QLN4

separated from QLN5 and QLN6 at the similarity of about 40%, and QLN5 did so from QLN6 at the similarity of about 60%; to the southern part, QLS3 separated from QLS1 and QLS2 at the similarity of about 50%, and QLS1 did so from QLS2 at the similarity of about 70% (Fig.3). In conjunction with these observation, During the short-term N-transformation study in pastoral soil, communities of nitrogen cycling bacteria formed 3 distinct clusters corresponding to elevated levels of urine derived  $\text{NH}_4^+\text{-N}$  [24], what is more, T-RFLP analysis of *nirS* gene could group sediment samples according to the sampling location and thus clearly distinguish Puget Sound and the Washington margin populations [28]. In our results, these communities were distinguishable even within a small shallow lake between the two basins. In short, differences in the distribution of bacteria containing *nirS* indicating that this types of denitrifiers apparently occupy different ecological niches [29].

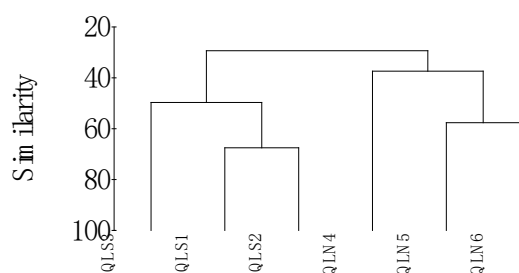


**FIGURE 3**  
Dendrogram of the hierarchical clustering analysis based on presence/absence as well as relative abundance of *nirS* T-RFs.

**Phylogenetic analysis.** A total of 57 clones (28 from QLS and 29 from QLN) were sequenced, and all of these clones were identified as *nirS* sequences by BLAST search. The clones were grouped into 43 OTUs by 97% sequence similarity. Phylogenetic analysis of *nirS* sequences showed that the *nirS* denitrifiers could be divided into four clusters (Fig.4). Most of the *nirS* gene sequences were grouped in cluster I and III, accounting for 82.46% of the total clones, with percentage of cluster I being 49.12% and that of cluster III being 33.33%. Cluster I contained mostly *Betaproteobacteria*, but was

interspersed with *Gammaproteobacteria*. Cluster III grouped strains belonging to *Roseobacter denitrificans*, a kind of *Alphaproteobacteria* and also *Pseudomonas aeruginosa*, which is *Gammaproteobacteria*. Sequences in cluster I (32.14% from QLN and 67.86% from QLS) and cluster III (57.89% from QLN and 42.11% from QLS) were related to reference sequences from a broad range of environments such as Pearl river Estuary, East lake, greenhouse soil, wetland soil, grassland soil, intertidal marshes of the Yangtze and intertidal marshes of the Yangtze Estuary. Among which the first was shared by the two clusters, so these two clusters had capability to adapt for broad range of habitats. Furthermore, accounting for 8.77% of the total sequence, cluster II contained all *Alphaproteobacteria*, with highly related sequences from representatives of *Azospirillum brasiliense*. What is more, this cluster was related to references from the Beiyun river and Hai river sediment, and most of it (80%) were from QLN with extensive aquaculture activity and significantly higher concentrations of TN and TP as a consequence (Table 1). Similarly the surface water in Beiyun river system was heavily polluted due to high pollution discharge [30]. Moreover, in the Zhangweinan Canal basin, one of the most highly stressed watercourses in the heavily developed Hai River basin, the spatial variations of COD and  $\text{NH}_3\text{-N}$  accumulations in the different sections indicated that the accumulation loads were closely related to pollutant inflows and environmental fluxes [31]. Thus pollution to some extents was responsible for the formation of these distinct clusters. Additionally, all clones of cluster IV (8.77% of the total) were from QLN, which was absent in QLS, this cluster was related to reference only from East lake sediment. Noticeably successful integrated measures were taken in an experiment for raising fish in this lake by way of (1) stocking the right kinds of fish; (2) producing a large number of sizeable fingerlings; (3) improving fish screens; (4) controlling predatory fish; and (5) applying the 'driving and concentrating' bulk harvesting fishing method [32]. Hence, similar environmental conditions are inhabited by similar denitrifier communities despite large geographic distances. Taken together, the inhabitants with a heavier nutrient input from either discharge or agriculture harboured some special community of *nirS*-type denitrifiers.

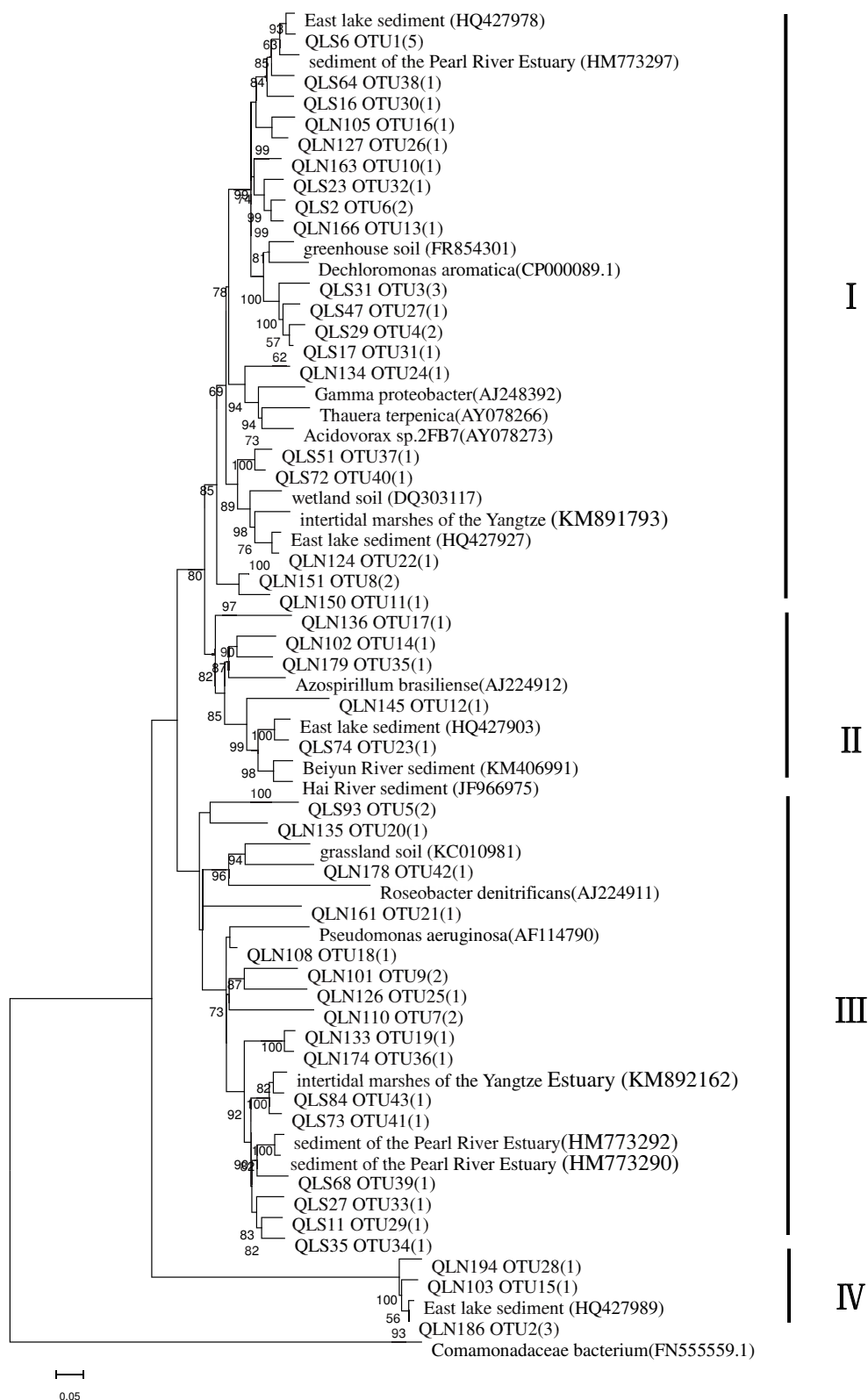


**FIGURE 4**

Phylogenetic analysis of *nirS* sequences. Neighbour joining tree based on partial *nirS* amplicons. Clones with > 97% sequence similarity were considered to be the same OTU. Bootstrap values were generated from 1000 replicates of neighbour joining. Bootstrap values below 50% were omitted. Sequences from the southern part of Lake QingLing are described as QLS; the northern part as QLN.

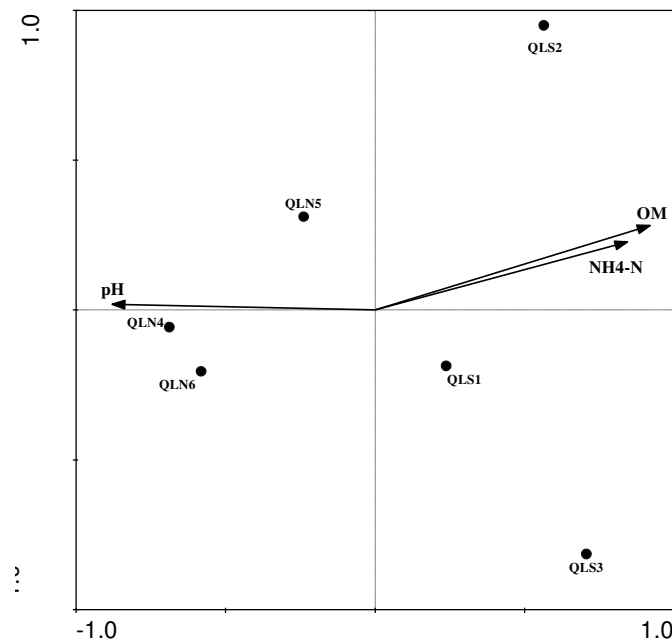


**FIGURE 5**  
**Canonical correspondence analysis (CCA) based on *nirS* T-RFLP patterns and biogeochemical parameters.**

In conjunction, the proportion of specialist taxa increased with increasing supply of nutrients, suggesting that addition of fertilizer may create conditions that expand the niche space for denitrifying organisms and may enhance the genetic capacity for denitrification [33]. Overall the *nirS*-type denitrifiers in Lake Qingling and those originated from broad inhabitants had some taxonomic overlapping on a phylogenetic tree. Hence, environment factors in microniche rather than geographic condition play key roles in regulating community structure of denitrifiers. Consistently similar environmental conditions are inhabited by similar denitrifier communities despite large geographic distances.

**Effects of environmental factors on the community of the *nirS*-type bacteria.** Canonical correspondence analysis (CCA) was used to analyse the influence of environmental factors on communities of *nirS*-type denitrifiers (Fig.5). The length of the arrow in the figure represents the effect of the environmental factors on the microbial community distribution, which increased along the arrow's direction. The bacterial communities were mainly influenced by OM,  $\text{NH}_4^+\text{-N}$  and pH value. The eigenvalues, the cumulative percentage variance of species data and the cumulative variance in the species–environment relationship along the first and the second axes of the CCA analysis were 0.492 and 0.168 respectively. The cumulative percentage

variance of species–environment relation of the first axes was 73.1%, and 98.0% for the second axes. These results were in conjunction with observations of recent other studies. For example, OM significantly altered *nirS*-denitrifier community structure in tidal freshwater wetlands soils [34]. Denitrifier community composition was also affected by pH values in surrounding environments [35, 36]. Besides, ammonium nitrogen had a significant effect on the community structures of bacterial including denitrifiers in sediment of Yellow river [37]. In additionally, in an eutrophic Lake (East lake) in the same city where Lake QingLing locates, total organic carbon and  $\text{NH}_4^+$  were important environmental factors affecting the dispersion of *NirS*-type denitrifier in the sediment among different basins [1]. Overall, within a shallow urban freshwater lake, community composition of *nirS*-type denitrifiers was distinguishable between turbid state dominated by algal and clean state dominated by macrophytes. Environmental factors, such as organic matter, pH value, and  $\text{NH}_4^+\text{-N}$  serve as the key factors shaping the community of denitrifiers.

## CONCLUSIONS

Within a shallow urban freshwater lake, QLN (the fish farming basin) had significantly higher concentrations of TN ( $P < 0.05$ ) and TP ( $P < 0.01$ ). On

the other hand, QLS with coverage of macrophytes showed significantly higher  $\text{NH}_4^+$  concentration ( $p < 0.05$ ) and lower pH value ( $p < 0.01$ ) in pore water and significantly higher OM content in sediment ( $p < 0.01$ ). Community composition of *nirS*-type denitrifiers was distinguishable between turbid state dominated by algal and clean state dominated by macrophytes. Phylogenetic analysis showed that most sequences were grouped into *Proteobacteria*, majority genes from QLN were found to be prevalent in *Alphaproteobacteria* and *Gammaproteobacteria* while most sequences from QLS were in *Betaproteobacteria* and *Gammaproteobacteria*. Environmental factors, such as organic matter, pH value and  $\text{NH}_4^+$  serve as the key factors shaping the community of denitrifiers. Echoing the observations made in another lake with different sub-lakes in the same city. Hence, in sediment of shallow lakes community composition of denitrifiers may be largely dependent on contents of organic carbon and inorganic nitrogen in general.

#### ACKNOWLEDGEMENTS

This work was supported by the grants from the National Natural Science Foundation of China (41230748; 41173081; 41273089), the State Key Laboratory of Freshwater Ecology and Biotechnology (2014FBZ01). We thank Xi Chen for his help with the statistical analysis, and Jie Hou for his guidance on experiments.

#### REFERENCES

- [1] Yang, J.K., Cheng, Z.B., Li, J. and Miao, L.H. (2013) Community Composition of NirS-Type Denitrifier in a Shallow Eutrophic Lake. *Microb. Ecol.* 66(4): 796-805.
- [2] Zumft, W.G. (1997) Cell biology and molecular basis of denitrification. *Microbiol. Microbiol. Mol. Biol. R.* 61(4): 533-616.
- [3] Braker, G., Fesefeldt, A., and Witzel, K.P. (1998) Development of PCR primer systems for amplification of nitrite reductase genes (*nirK* and *nirS*) to detect denitrifying bacteria in environmental samples. *Appl. Environ. Microb.* 64(10): 3769–3775.
- [4] Coyne, M.S., Arunakumari, A., Averill, B.A., and Tiedje, J.M. (1989) Immunological identification and distribution of dissimilatory heme cd1 and non-heme copper nitrite reductases in denitrifying bacteria. *Appl. Environ. Microb.* 55(11): 2924–2931.
- [5] Tatariw, C., Chapman, E. L., Sponseller, R. A., Mortazavi, B., Edmonds, J. W. (2013) Denitrification in a large river: consideration of geomorphic controls on microbial activity and community structure. *Ecology.* 94(10): 2249-62.
- [6] Rissanen, A. J., Tirola, M., Hietanen, S., and Ojala, A. (2013) Interlake variation and environmental controls of denitrification across different geographical scales. *Aquat. Microb. Ecol.* 69(1): 1-16.
- [7] Kjellin, J., Hallin, S., Worman, A. (2007) Spatial variations in denitrification activity in wetland sediments explained by hydrology and denitrifying community structure. *Water. Res.* 41(20): 4710-4720.
- [8] Poulsen, M., Kofoed, M. V. W., Larsen, L. H., Schramm, A., Stief, P. (2014) Chironomus plumosus larvae increase fluxes of denitrification products and diversity of nitrate-reducing bacteria in freshwater sediment. *Syst. Appl. Microbiol.* 37(1): 51-59.
- [9] Hu, C.Y. (1999) The density and diversity of zooplanktons in the succession of five lakes (in Chinese). *Acta hydrobiologica sinica.* 23(3): 217-226.
- [10] Eaton, A.D., and Franson, M.A.H. (Editors). (2005) Standard methods for the examination of water and wastewater. 21st ed. American Public Health Association, Washington, D.C., USA.
- [11] Luczak, C., Janquin, M.A., and Kupka, A. (1997) Simple standard procedure for the routine determination of organic matter in marine sediment. *Hydrobiologia.* 345(1): 87–94.
- [12] Braker, G., Zhou, J.Z., Wu, L.Y., Devol, A.H., and Tiedje, J.M. (2000) Nitrite reductase genes (*nirK* and *nirS*) as functional markers to investigate diversity of denitrifying bacteria in Pacific Northwest marine sediment communities. *Appl. Environ. Microb.* 66(5): 2096–2104.
- [13] Schloss, P.D., and Handelsman, J. (2006) Introducing SONS, a tool for operational taxonomic unit-based comparisons of microbial community memberships and structures. *Appl. Environ. Microbiol.* 72(10): 6773 – 6779.
- [14] Tamura, K., Dudley, J., Nei, M., and Kumar, S. (2007) MEGA4: Molecular evolutionary genetics analysis (MEGA) software version 4.0. *Mol. Biol. Evol.* 24(8): 1596-1599.
- [15] ter Braak, C.J.F., Smilauer, P. (2002) CANOCO Reference Manual and CanoDraw for Windows User's Guide: Software for Canonical Community Ordination (Version 4.5). Microcomputer Power, Ithaca, N.Y., USA.
- [16] Hernandez, M. E. and W. J. Mitsch. (2007) Denitrification potential and organic matter as affected by vegetation community, wetland age, and plant introduction in created wetlands. *J.*



- Environ. Qual. 36(1): 333-342.
- [17] Yuan, D. H., He, L. S., Xi, B. D., Yan, C. L., Zhang, L. Y., Huo, S. L., Liu, H. L. (2011) Characterization of Natural Organic Matter (Nom) in Waters and Sediment Pore Waters from Lake Baiyangdian, China. *Fresen. Environ. Bull.* 20(4A): 1027-35.
- [18] Banas, K. (2002) Impact of humic substances on *Sphagnum denticulatum* habitats. *Acta. Soc. Bot. Pol.* 71(1): 63-69.
- [19] Solim, S. U., and Wanganeo, A. (2009) Factors influencing release of phosphorus from sediments in a high productive polymictic lake system. *Water. Sci. Technol.* 60(4): 1013-23.
- [20] Lopez, P. (2004) Composition of porewater and benthic fluxes in the mesohaline Es Grau lagoon (Minorca, Spain) during spring and early summer. *Wetlands.* 24(4): 796-810.
- [21] Shen, Q. S., Zhou, Q. L., Shang, J. G., Shao, S. G., Zhang, L., Fan, C. X. (2014) Beyond hypoxia: Occurrence and characteristics of black blooms due to the decomposition of the submerged plant *Potamogeton crispus* in a shallow lake. *J. Environ. Sci-China.* 26(2): 281-8.
- [22] Song, K., Lee, S. H., Mitsch, W. J., Kang, H. (2010) Different responses of denitrification rates and denitrifying bacterial communities to hydrologic pulsing in created wetlands. *Soil. Biol. Biochem.* 42(10): 1721-1727.
- [23] Abell, G. C. J., Revill, A. T., Smith, C., Bissett, A. P., Volkman, J. K., Robert, S. S. (2010) Archaeal ammonia oxidizers and nirS-type denitrifiers dominate sediment nitrifying and denitrifying populations in a subtropical macrotidal estuary. *Isme. J.* 4(2): 286-300.
- [24] Anderson, C. R., Hamonts, K., Clough, T. J., Condron, L. M. (2014) Biochar does not affect soil N-transformations or microbial community structure under ruminant urine patches but does alter relative proportions of nitrogen cycling bacteria. *Agr. Ecosyst. Environ.* 191:63-72.
- [25] Huang, Y., Long, X. E., Chapman, S. J., Yao, H. Y. (2015) Acidophilic denitrifiers dominate the N<sub>2</sub>O production in a 100-year-old tea orchard soil. *Environ. Sci. Pollut. R.* 22(6): 4173-4182.
- [26] Junier, P., Kim, O. S., Witzel, K. P., Imhoff, J. F., Hadas, O. (2008) Habitat partitioning of denitrifying bacterial communities carrying nirS or nirK genes in the stratified water column of Lake Kinneret, Israel. *Aquat. Microb. Ecol.* 51(2): 129-140.
- [27] Yuan, Q., Liu, P. F., Lu, Y. H. (2012) Differential responses of nirK- and nirS-carrying bacteria to denitrifying conditions in the anoxic rice field soil. *Env. Microbiol. Rep.* 4(1): 113-122.
- [28] Braker, G., Ayala-del-Río, H.L., Devol, A.H., Fesefeldt, A., and Tiedje, J.M. (2001) Community structure of denitrifiers, Bacteria, and Archaea along redox gradients in Pacific Northwest marine sediments by terminal restriction fragment length polymorphism analysis of amplified nitrite reductase (nirS) and 16S rRNA genes. *Appl. Environ. Microb.* 67(4): 1893-1901.
- [29] Kim, O. S., Imhoff, J. F., Witzel, K. P., Junier, P. (2011) Distribution of denitrifying bacterial communities in the stratified water column and sediment-water interface in two freshwater lakes and the Baltic Sea. *Aquat. Ecol.* 45(1): 99-112.
- [30] Jing, H.W., Zhang, Z. G., Guo, J. (2013) Water pollution characteristics and pollution sources of Bei Canal river system in Beijing (in Chinese). *China environmental science.* 33(2):319-327.
- [31] Wang, X. Q., Zhang, Y., Zhang, M., Liu, C. M. (2011) Fate of COD and ammonia-nitrogen in a highly stressed watercourse in Northern China: the Zhangweinan Canal basin. *Water. Int.* 36(7): 937-947.
- [32] Liu, J. K., Cai, Q. H. (1998) Integrated aquaculture in Chinese lakes and paddy fields. *Ecol. Eng.* 11(1-4): 49-59.
- [33] Bowen, J. L., Byrnes, J. E. K., Weisman, D., Colaneri, C. (2013) Functional gene pyrosequencing and network analysis: an approach to examine the response of denitrifying bacteria to increased nitrogen supply in salt marsh sediments. *Front. Microbiol.* 4: 342.
- [34] Morrissey, E. M., and Franklin, R. B. (2015) Resource effects on denitrification are mediated by community composition in tidal freshwater wetlands soils. *Environ. Microbiol.* 17(5): 1520-1532.
- [35] Peralta, A. L., Matthews, J. W., Flanagan, D. N., Kent, A. D. (2012) Environmental Factors at Dissimilar Spatial Scales Influence Plant and Microbial Communities in Restored Wetlands [J]. *Wetlands.* 32(6): 1125-1134.
- [36] Oueriaghli, N., Gonzalez-Domenech, C.M., Martinez-Checa, F., Muyzer, G., Ventosa, A., Quesada, E., and Bejar, V. (2014) Diversity and distribution of *Halomonas* in Rambla Salada, a hypersaline environment in the southeast of Spain. *FEMS. Microbiol. Ecol.* 87(2): 460-474.
- [37] Xia, N., Xia, X.H., Zhu, B.T., Zheng, S.K., and Zhuang, J. (2013) Bacterial diversity and community structure in the sediment of the middle and lower reaches of the Yellow River, the largest turbid river in the world. *Aquat. Microb. Ecol.* 71(1): 43-U168.



---

**Received: 04.09.2015**

**Accepted: 08.10.2016**

---

**CORRESPONDING AUTHOR**

---

**Yiyong Zhou**

The State Key Laboratory of Freshwater Ecology and Biotechnology, Institute of Hydrobiology, the Chinese Academy of Sciences, No. 7 Donghu South Road, Wuchang District, Wuhan, Hubei, People's Republic of China

e-mail: [zhouyy@ihb.ac.cn](mailto:zhouyy@ihb.ac.cn)

# DIVERSE AND DISTINCT BACTERIAL COMMUNITIES ASSOCIATED WITH COMPLEX CONSTITUTES OF COKING WASTEWATER IN ANAEROBIC PROCESS

Shuang Zhu<sup>1</sup>, Haizhen Wu<sup>2</sup>, Yesheng Wang<sup>1</sup>, Qiwei Li<sup>1</sup>, Lin Zhou<sup>1</sup>, Chaohai Wei<sup>3,\*</sup>

<sup>1</sup> Guangdong Province Key Laboratory for Biotechnology Drug Candidates, School of Biosciences and Biopharmaceutics, Guangdong Pharmaceutical University, Guangzhou 510006, PR China

<sup>2</sup> College of Biological Science and Engineering, South China University of Technology, Guangzhou 510006, P.R. China

<sup>3</sup> School of Environment and Energy, South China University of Technology, Guangzhou 510006, PR China

## ABSTRACT

The anaerobic process of coking wastewater treatment is the key step for the subsequent aerobic biodegradation. Understanding the bacterial community involved in anaerobic bioreactor will facilitate coking wastewater treatment optimization. In this study, the phylogenetic composition of bacterial community in the sludge of anaerobic process of coking wastewater treatment was investigated using a culture-independent molecular approach. The physico-chemical characteristics of influent and effluent coking wastewater in anaerobic process were analyzed by GC/MS methods to examine their effects on the bacterial communities. Of the 103 clones analyzed, a total of 36 operational taxonomic units (OTUs) were found. Molecular phylogenetic analysis revealed that more than 80 % of the screened clones were affiliated with *Proteobacteria*. The other 20 % of the total clones were either affiliated with Low-G+C gram-positive bacteria, the *Cytophaga-Flexibacter-Bacteroides* (CFB) group and *Verrucomicrobia* or *Spirochaetes*, where the clone distribution was 12.9 %, 4 %, 2 % and 1 %, respectively. The most frequent OTUs represented more than 40 % of the total bacterial 16S rDNA sequences, and 78 % of the OTUs comprised a single clone. Some OTUs fell into genera or taxons that were classically identified within anaerobic treatment systems and expected with known functions. The high toxic compounds within anaerobic process of coking wastewater treatment may also select a diverse bacterial population. This indicated that the bacterial communities associated with the anaerobic process of coking wastewater treatment was far more complex and variable than expected and thus could be challenging to control.

## KEYWORDS:

Bacteria; Coking wastewater; Molecular diversity; 16S rDNA

## INTRODUCTION

Coal is the main energy resource in China which produces more than 60 % coke in the world. Coking wastewater is produced in the process of coking and coal liquefaction and is a typical industrial organic/hard-biodegradable wastewater with complicated components and large discharge amount. It is composed of complex inorganic and organic contaminants. Some of them are refractory, highly concentrated, toxic, mutative and carcinogenic, such as ammonia, phenolic compounds, cyanide, polynuclear aromatic hydrocarbons (PAHs), thiocyanide, polycyclic nitrogen-containing aromatics, oxygen- and sulfur-containing heterocyclics and acyclic compounds [1-3]. Biological treatments have been applied to pollutant degradation, and most of pollutant compounds have been removed during bioremediation with activated sludge containing a complex microbial community. However, the bacterial community involved in coking wastewater treatment system has not yet been precisely characterized and this process remains a 'black box' with limited efficiency [4-6].

The anaerobic process is often used in coking wastewater treatment [1,7]. It is the key step for partial degradation of some refractory and inhibitory organic compounds to lighten the load of subsequent anoxic and aerobic processes. Inefficient anaerobic process may lead to low degradation rates of coking wastewater and long hydraulic retention time (HRT) [8]. The anaerobic process is far from being optimized partially due to limited knowledge of microbiology. There has been considerable attempted to characterize the complex microbial community involved in coking wastewater biodegradation by the traditional cell culture method [9-10]. However, little is known about the bacterial profile involved in anaerobic process of coking wastewater treatment system [11].

In this study, we investigated the characteristics of coking wastewater and the diversity of bacterial community in the anaerobic processes of a full-scale coking wastewater treatment system using three-

phase fluidized bed bioreactor. The aim of this work is to identify the dominant members of bacterial community responsible for the anaerobic process, and predict the biodegradation potential of dominant bacterial genera in the anaerobic bioreactor. The results support that complex, distinct bacterial communities are associated with the anaerobic process of coking wastewater treatment. The major function of anaerobic bioreactor is predicted to reduce toxicity and to hydrolyze large molecular contaminants into biodegradable small molecular substances. Our work may help to develop new control strategies to practically improving coking wastewater treatment efficiency.

## MATERIALS AND METHODS

**Sample collection and DNA extraction.** Shaogang coking wastewater treatment project I (SG-I), an on-going Anaerobic-Oxic-Oxic (A/O/O) three-phase fluidized bed biological coking wastewater treatment system in Shaogang, Guangdong Province, P.R.China. The design of biological reactor directly influenced the reaction efficiency and microbial population. In order to deal with high COD load rate, one type of internal-loop multiphase airlift fluidized-bed reactor was developed by our research group [12], and it was applied in current system. This system has been undergoing stabilized for eight years with the national discharge standards, which treat coking wastewater with 70 m<sup>3</sup>/h and the total HRT was 42 h [1]. The sludge of anaerobic process was collected from the anaerobic fluidized bed of SG-I system in summer of 2014. Community nucleic acids were extracted from the sludge by using a lysozyme - freezing and thawing - proteinase K - sodium dodecyl sulfate (SDS) treatment followed by standard phenol / chloroform extractions [6].

**Physico-chemical analysis.** The Physico-chemical characteristics of the influent and effluent coking wastewater in anaerobic fluidized bed were analyzed by GC/MS methods and related procedures described by Greenberg et al. The volatile constituents of coking wastewater were identified and quantified by GC analysis using an Agilent 6890N gas chromatograph (Agilent, USA) equipped with a hydrogen flame detector (GC-FID) and a quartz capillary chromatograph column (DB5) (30 m × 0.25 mm i.d., film thickness 0.25 μm). The injector temperature was set to 280 °C and the oven program was as follows: 40 °C for 5 min, followed by a 10 °C/min temperature ramp to 150 °C with a 2-min hold and then another temperature ramp of 5 °C/min to 280 °C with a 3-min hold. The carrier gas was high-purity helium, which was applied at a constant flow rate of 10 mL/min. The volume of helium injected into the equipment was 0.1 μL. The GC

injection was conducted in split mode at a ratio of 10:1.

**PCR amplification and cloning.** Bacterial 16S rDNAs were amplified by PCR using the combination of universal primer 1492r (5' GGT TAC CTT GTT ACG ACT T 3') and bacterial primer 27f (5' AGA GTT TGA TCC TGG CTC AG 3'). The PCR reaction was performed with a thermal program which comprised 25 cycles at 94 °C for 1 min, 50 °C for 1 min, and 72 °C for 2 min. The amplified products were purified with a QIAquick PCR purification kit (Qiagen, Hilden, Germany). Bacterial 16S rDNA amplicon (ca. 1,500 bases) was then excised from a 1 % agarose gel and eluted with a Qiaex II gel extraction kit (Qiagen). Finally, the purified product was ligated into the T-vector (Takara) and the ligation product was transformed into *Escherichia coli* DH-5α competent cells with ampicillin and blue / white screening.

**RFLP screening of rDNA clones.** rDNA inserts from recombinant clones were reamplified by PCR with vector primers P47 and P48. The amplifications were subjected to separate enzymatic digestions with *Hae*III and *Msp*I (Takara) endonucleases following the manufacturer's instructions, and the digested DNA fragments were run in 2 % agarose gels. After stained with ethidium bromide, the gels were photographed using an image-capture system equipped with a Kodak DC-120 digital camera, and scanning image analyses were performed manually.

**DNA sequencing and phylogenetic analysis.** One to three representative clones from each unique RFLP type were selected for sequencing. The rDNA inserts were determined for orientation and then sequenced using M13/pUC universal sequencing primers P47 and P48. Sequencing was performed BGI Company. The resulting sequences (next to the primer 27f and at least 1000 bp) were compared with those available in GenBank by use of the BLAST network service to determine their approximate phylogenetic affiliation. Chimeric sequences were identified by use of the CHECK-CHIMERA program [13], and by independently comparing the alignments at the beginning and the end of each sequence and the alignments of the entire sequence. Rarefaction and diversity statistics were calculated using DOTUR software [14]. Operational taxonomic units (OTUs) were defined as groups in which sequences differed by ≤ 3 %. Each group was represented by a phylotype sequence. Phylogenetic trees were calculated by the Kimura two-parameter model [15] and the neighbor-joining algorithm [16] using the PAUP software (version 4.0 b8) [17]. One thousand bootstraps were performed to assign confidence levels to the nodes in the trees. The 69 partial 16S rRNA gene sequences obtained in this

study have been deposited in the GenBank under accession number KP238592- KP238660.

## RESULTS

Before we analyze the bacteria composition, we checked the efficiency of anaerobic process in the SG-I system. Physico-chemical characteristics of influent and effluent in anaerobic process were measured as the efficiency indicator (Table 1). The influent coking wastewater COD concentration was  $\sim 2200 \text{ mg L}^{-1}$  and COD removal rate can steadily

reach  $\sim 50 \%$ , which is also supported by the volatile phenol with 93 % removal efficiency. The influent and effluent concentration of ammonia nitrogen and cyanide are also listed in Table 1. The performance of nitrification ( $\text{NH}_3\text{-N}$  removal efficiency at  $-120 \%$ ) is poor. The pH values of anaerobic process was in a range of 7.3–7.8. Furthermore, the BOD/COD ratio of the effluent and influent of the anaerobic process were measured. The results indicated that the ratio of BOD/COD to the influent was 0.30, while the ratio of BOD/COD to the effluent was up to 0.45, which means that the biodegradability of the coking wastewater increased greatly after the anaerobic process.

**TABLE 1**  
Physico-chemical characteristics of influent and effluent in anaerobic process of coking wastewater. (Concentrations in  $\text{mg L}^{-1}$ )

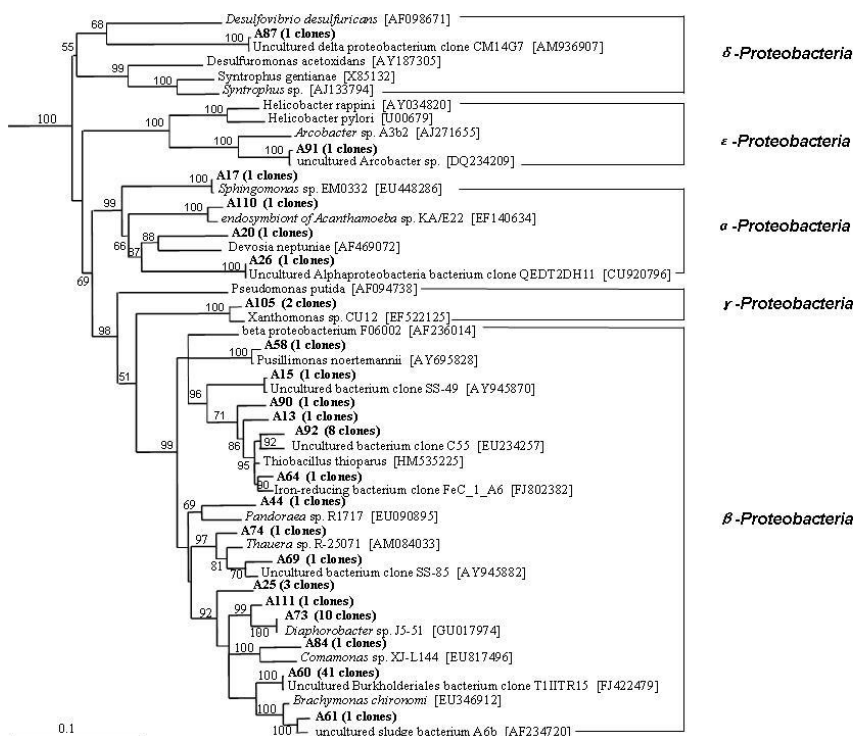
Parameter	Influent (mean $\pm$ S.D.)	Effluent (mean $\pm$ S.D.)
pH	9.3 $\pm$ 0.3	6.9 $\pm$ 0.1
Chemical oxygen demand (COD)	2200 $\pm$ 190	1100 $\pm$ 90
Volatile Phenol	420 $\pm$ 28	30 $\pm$ 8
Cyanide	25 $\pm$ 6	18 $\pm$ 5
$\text{NH}_4^+\text{-N}$	150 $\pm$ 17	180 $\pm$ 19

**TABLE 2**  
Distribution of bacterial sequence types from the 16S rDNA library

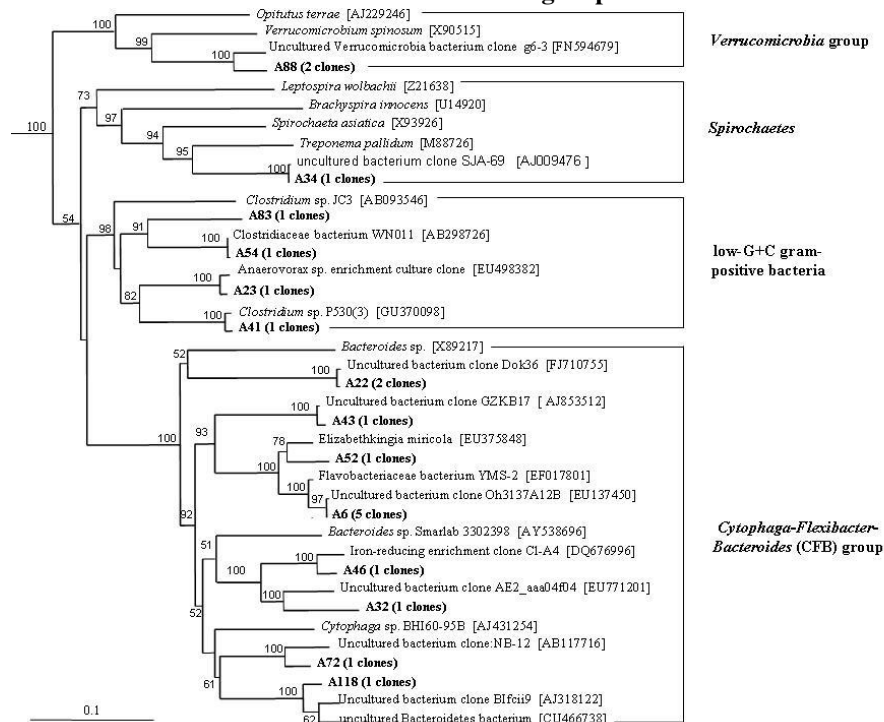
Putative division (% representation)	No. of Sequence types <sup>a</sup>	No. of RFLP patterns	No. of clones	Closest relatives <sup>b</sup>
<i>Cytophaga-Flexibacter- Bacteroides</i> (CFB)	8	12	13	Uncultured bacterium clone Oh3137A12B [EU137450]
Low-G+C gram-positive	4	4	4	<i>Clostridiaceae</i> bacterium WN011 [AB298726]
$\alpha$ -Proteobacteria	4	4	4	Uncultured <i>Alphaproteobacteria</i> clone QEDT2DH11 from anaerobic digestion of sludge [CU920796]
$\beta$ -Proteobacteria	15	41	73	Iron-reducing bacterium enrichment culture clone FeC_1_A6 from river sediment [FJ802382]
$\gamma$ -Proteobacteria	1	2	2	<i>Xanthomonas</i> sp. CU12 isolated from sugarcane plants grown in Cuba [EF522125]
$\delta$ -Proteobacteria	1	1	1	uncultured <i>delta proteobacterium</i> from a pilot-scale bioremediation process of a hydrocarbon-contaminated soil [AM936907]
$\epsilon$ -Proteobacteria	1	1	1	uncultured <i>Arcobacter</i> sp. from river estuary [DQ234209]
<i>Spirochaetales</i>	1	1	1	uncultured bacterium clone SJA-69 from an anaerobic, trichlorobenzene-transforming microbial consortium [AJ009476]
<i>Verrucomicrobia</i> group	1	2	2	uncultured <i>Verrucomicrobia</i> bacterium in rock biofilms from an ancient gold mine [FN594679]

<sup>a</sup> Groups of two or more highly similar sequences ( $\geq 97\%$  identity) are considered to belong to the same sequence type.

<sup>b</sup> Database match as determined by the BLAST method.

(A) The *Proteobacteria* group and relatives.

*Clostridium formicaceticum* (X77836) and *Clostridium aminobutyricum* (X76161) are used as outgroups.



(B) The *Cytophaga-Flexibacter-Bacteroides* (CFB) group, Low-G+C gram-positive bacteria, *Spirochaetales* and *Verrucomicrobia* group and relatives. *Synechococcus* sp. (X03538) and *Methanobacterium formicicum* (AF169245) are used as outgroups

FIGURE 1

16S rDNA-based dendrograms showing phylogenetic relationships of coking wastewater treatment bacterial sequence types (shown in bold) to closely related sequences from public database.

Bootstrap values ( $n = 1,000$  replicates) of  $\geq 50\%$  are reported as percentages.

The scale bar represents the number of changes per nucleotide position.

Total-community genomic DNAs were extracted from microbial assemblages in the sludge of anaerobic process by using a lysozyme - freezing and thawing - proteinase K - sodium dodecyl sulfate (SDS) treatment. Without any further purification, the bulk DNA sample was used successfully as a template in the PCR amplification employing a universally conserved primer and a *Bacteria*-16S rDNA targeted primer, and a bacterial 16S rRNA gene library was established subsequently. A total of 103 recombinant clones were randomly selected, and their rDNA inserts were subjected to restriction RFLP analysis, resulting in 70 different RFLP types. One to three representative clones in each unique RFLP type were partially sequenced. Two chimeric sequences were identified and excluded from subsequent analyses. Both of them belonged to unique RFLP types represented by a single clone. Sequencing and phylogenetic analysis of 101 randomly selected clones from the cloning library revealed 36 unique OTUs assigned to at least five distinct phyla (Table 2, Figure 1). Comparative analysis of the retrieved sequences showed that all the clones could be grouped into the *Bacteria* domain. It was determined that most bacterial sequences recovered from various anaerobic habitats, including a fluidized-bed anaerobic digester [18, 19] and had relatively low levels of similarity with their closest counterparts in the public databases. Since some sequences were not closely related to any cultivated organisms, neither their physiology nor their phylogeny placement was very clear at this point. 78 % of the OTUs comprised a single clone, indicating high levels of bacterial diversity. This was further supported by the steep rarefaction curves (data not show). Only a small fraction of the retrieved sequences represented by 20 % of the total OTUs was affiliated with 16S rRNA gene sequences of known bacterial species with  $\geq 97$  % identity. This indicated that the bacterial community associated with the anaerobic process of coking wastewater treatment was complex. The most frequently detected phyla were *Proteobacteria* and *Cytophaga-Flexibacter-Bacteroides*. Other minor lineages detected included *Firmicutes*, *Verrucomicrobia* and *Spirochaetes*. Our phylogenetic analyses placed the 36 OTUs (101 clones) in the following groups of the *Bacteria* domain: (i) the phylum *Proteobacteria*; (ii) the *Cytophaga-Flexibacter-Bacteroides* (CFB) group; (iii) the low-G+C gram-positive bacteria; (iv) the *Verrucomicrobia* group; (v) the phylum *Spirochaetes*.

**(i) The *Proteobacteria* phylum.** A total of 81 clones, represented by 22 OTUs and accounting for 80 % of the gene library, were phylogenetically associated with the *Proteobacteria* (Table 2; Fig. 1A). Most of the *Proteobacteria* clones were more closely to previously cultivated organisms or

environmental sequences in the GenBank. The  $\beta$ -*Proteobacteria* represented the most abundant *Proteobacterial* group. OTUs A60 representing a total of 41 clones, were closely related (99 % similarity) to T1IITR15, a bacterial clone recovered from tannery effluent common treatment plant in final aeration tank. OTUs A73 representing 10 clones, were closely related (98 to 99 % similarities) to *Diaphorobacter* sp. J5-51, a recently isolated bacterium from coking water capable of 4-chlorophenol degrading. OTUs A92 representing 8 clones, were closely related (97 to 99 % similarities) to C55, a bacterial clone recovered from penicillin G production wastewater. All of the remaining 12  $\beta$ -*Proteobacteria* OTUs included no more than three clones. Noteworthy, OTUs A74, A69 and A15 were closely related to *thauera*, which was known as functionally important genera in a denitrifying quinoline-removal bioreactor [20]. In the  $\alpha$ -*Proteobacteria*, all of them (OTUs A26, A110, A17 and A20) were closely related to cultivated organism or environmental sequences recovered from anaerobic digestion of sludge and this subgroup was functionally pyridine biodegradation. In the  $\gamma$ -*Proteobacteria*, OTUs A105 was closely related (96 % similarity) to *Xanthomonas* sp. CU12, a recently isolated bacterium from sugarcane plants in Cuba. In the  $\varepsilon$ -*Proteobacteria*, OTUs A91 was closely related (96 % similarity) to uncultured *Arcobacter* sp. clone DS126 which recovered from the Danshui river estuary of Northern Taiwan. *Arcobacter*-related organisms are mainly known as potential pathogens previously. Recent report suggested that *Arcobacter* also conducted the oxidation of acetate with Mn oxide (i.e., dissimilatory Mn reduction) in the Black Sea sediments. It is somewhat surprising that OTUs A87 in  $\delta$ -*Proteobacteria* was retrieved from the anaerobic process of coking wastewater treatment, since  $\delta$ -*Proteobacteria* is a group that are well known for anaerobic respiration. Absence of  $\delta$ -*Proteobacteria* clones was also reported in other molecular surveys of anaerobic treatment systems, e.g. a laboratory-scale anaerobic digester fed with glucose [21], and a thermophilic methanogenic granular sludge treating artificial wastewater [22].

**(ii) CFB group.** Eight OTUs, representing 13 bacterial clones and accounting for 12.9 % of the gene library, were grouped within the CFB phylum (Table 2; Fig. 1B). Most of the clone sequences in this group showed low levels of similarity with their closest counterparts in the databases. Most of them, except for those represented by OTUs A6 and A43, had less than 3 % divergence from 16S rDNA sequences available in GenBank. Five bacterial clones, represented by OTUs A6, which was the most abundant sequence type in this group, were closely related (99 % similarities) to Oh3137A12B, a bacterial clone recently recovered from Bartonella-positive fleas [23]. OTUs A43 was closely related

(98 % similarities) to GZKB, a bacterial clone recovered from anaerobic landfill. The OTUs A22 represented by two clones (the second most abundant OTUs in this group) was distantly related (93 % similarities) to Dok36, a bacterial clone obtained from a long-term operated anammox biofilm reactor. The other five OTUs, each representing a single clone, were distantly related (90 %-93 % similarities) to anaerobic environment, such as wastewater treatment plant anoxic basin and autotrophic nitrifying biofilms.

**(iii) Low-G+C gram-positive bacteria.** Four OTUs, each representing a single clone, were phylogenetically associated with the low-G+C gram-positive bacteria (Table 2; Fig. 1B). OTUs A83 and A54 were only remotely related (87 % to 88 % similarities) to *Clostridiaceae* bacterium WN011, a bacterial clone recently recovered from a methanogenic fermenter of cattle waste. The other two OTUs represented by A23 and A41 were found to be closely related (97 % to 98 % similarities) to *Anaerovorax* sp. enrichment culture clone D2CL, a bacterial clone recovered from a dechlorinating mixed culture anaerobic enrichment culture [24] and *Clostridium* sp. P530, respectively.

**(iv) *Verrucomicrobia* group.** None of these clones were closely related to known cultivated *Bacteria* members, and they were only distantly related to their closest environmental sequences in GenBank. Two clones were clustered with the *Verrucomicrobia* group (Table 2; Fig. 1B) which was distantly related (93 % to 94 % similarities) to uncultured *Verrucomicrobia* bacterium and recovered from the rock biofilms from an ancient gold mine.

**(v) *Spirochaetes*.** We also retrieved one OTUs (representing only one single clone) that was clustered with the the *Spirochaetes* group (Table 2; Fig. 1B) which was related to uncultured bacterium SJA-69 with highly identity of 99 % similarities, a bacterial clone retrieved from an anaerobic bioreactors in treating chloroaromatic-contaminated wastewater [25]. Most importantly, This OTUs was distantly related to cultivated *Spirochaetes* so far.

## DISCUSSION

This work documented the comprehensive profile of the bacterial populations associated with the anaerobic process of coking wastewater treatment. The representation of the bacteria domain was extremely diverse as more than 36 OTUs distributing among five well-established bacterial divisions. Most of the OTUs falling into genera or taxons that were classically identified within anaerobic treatment systems and expected with

known functions were retrieved, including *Clostridium*, *Bacteroides* and *Proteobacteria*. However, lots of the OTUs were not closely related to known cultivated species, indicating that parts of bacterial species associated with anaerobic process of coking wastewater treatment is still not characterized. Anaerobic digestion involves numerous interactions between various metabolic groups of microorganisms that are generally accepted as present in anaerobic treatment systems. They are believed to interact with each other in anaerobic treatment systems. It is known that bacteria play the primary role in the trophic web. The bacterial diversity, implying functions variety, may be a reflection of the substrate complexity. Based on this theory, the highly complex constitutes within anaerobic process of coking wastewater treatment may also select a diverse bacterial population.

The *Proteobacteria* represented the most abundant (80 % of the total clones examined) and the most diverse (61 % of the total OTUs detected) group in the anaerobic process of coking wastewater treatment community. Five subclasses ( $\alpha$ ,  $\beta$ ,  $\gamma$ ,  $\delta$  &  $\epsilon$ ) of the *Proteobacteria* were detected, where the clone distribution was 90.1 %, 4.9 %, 2.5 %, 1.2 % and 1.2 %, respectively. The *Thauera* genus of  $\beta$ -*Proteobacteria* has been described as important aromatic compound degraders. The coking wastewater biochemical-degradation analysis showed that the *Thauera* could degrade most of the main organic pollutants, phenol, methylphenol, and indole, but not quinoline under aerobic conditions. The characteristic of the *Thauera* could potentially be for aromatic pollutant-containing wastewater treatment [26]. *Thauera* and *Azoarcus* were functionally important genera in a denitrifying quinoline-removal bioreactor [20]. We also found members falling into difficult-to-cultivate groups that were previously detected in anaerobic treatment systems only by molecular inventory studies [18, 21, 27], including *Verrucomicrobia* and *Spirochaetes*. Although presenting at a very low frequency in our gene library, *Spirochaetes*-related bacteria were found to be metabolically highly active and were assumed to serve as the main polysaccharide consumer in the anaerobic digester studied by Delbes et al.

Anaerobic process has been proved to be enhanced the biological coking wastewater degradation in different technical flowchart. It is believed that anaerobic process contributes to the subsequent biodegradation unit which in turn can remove most of the organic pollutants. Previous study on the microbiology of anaerobic digestion ecosystems was investigated mainly by traditional culture-based methods [28]. Using comparative 16S rRNA sequencing, recently molecular surveys have revealed high microbial diversities in various anaerobic digesters. Numerous novel rDNA



sequences have been retrieved, indicating that our knowledge of the microbiology in these ecosystems is still severely limited. To date, molecular microbiological data from the anaerobic process of coking wastewater treatment are few, and none of the related studies has focused on identification of members from the whole bacteria domain (19, 22, 29, 30). In this research, we showed that the bacterial species in anaerobic process of coking wastewater treatment are rich and highly divergent. This study enhanced our understanding about the anaerobic processes of biological coking wastewater degradation. It will help to optimize the daily-operations condition and to shorten the coking-wastewater-processes biodegradation time. Further exploring and developing the functional microorganism from the anaerobic sludge would facilitate the coking wastewater treatment.

## CONCLUSIONS

The results obtained in this study revealed diverse and distinct bacterial communities involved in the anaerobic process of the industrial-scale coking wastewater treatment system. The dominant phyla in the anaerobic bioreactor are *Proteobacteria* and *Cytophaga-Flexibacter-Bacteroides*. This study also predicts the functional role of dominate genus in the anaerobic biological treatment process. The major function of anaerobic bioreactor is to reduce toxicity and improve the BOD/COD ratio. The diverse and distinct microbial community involved in the anaerobic biological processes of CWW indicates that water characteristics and operational parameters determine the microbial community composition.

## ACKNOWLEDGEMENTS

This works was supported by the National Natural Science Foundation of China (21207021 and 21377040), the State Key Program of the National Natural Science Foundation of China (21037001) and to the Program for Science & Technology of Guangdong Province, China (project No.2015A020215008, 2016A020221037 and 2015B020235005)

The authors declare that they have no conflict of interest.

## REFERENCES

- [1] Wei, C.H., He, M.H. and Wu, C.F. (2007) Engineering application of biological three-phase fluidized bed A/O<sup>2</sup> process in coking wastewater treatment. *Acta Scientiae Circumstantiae*. 27, 1107-12.
- [2] Zhang, W.H., Wei, C.H., Chai, X.S., He, J.Y., Cai, Y., Ren, M., Yan, B., Peng, P.A. and Fu, J.M. (2012) The behaviors and fate of polycyclic aromatic hydrocarbons (PAHs) in a coking wastewater treatment plant. *Chemosphere*. 88, 174-82.
- [3] Lu, Y., Yan, L., Wang, Y., Zhou, S., Fu, J. and Zhang, J. (2009) Biodegradation of phenolic compounds from coking wastewater by immobilized white rot fungus *Phanerochaete chrysosporium*. *J Hazard Mater*. 165, 1091-7.
- [4] L.W. Zhang; K. Sun; N. Hu and W.W Zhang. (2011) Study on treatment of coking wastewater by zeolite biofilm system. *Fresen. Environ. Bull.* 20(9A), 2357-64.
- [5] Leser, T.D., Amenuvor, J.Z., Jensen, T.K., Lindecrona, R.H., Boye, M. and Moller, K. Culture-independent analysis of gut bacteria: the pig gastrointestinal tract microbiota revisited. *Appl. Environ. Microbiol.* 68, 673-90.
- [6] K. Xie; J.X. Li; R.Y. Jia; H.X. Li; L. Duan; X.t. Xu and S.Q. Xia. (2011) Microbial diversity and composition in two full-scale wastewater treatment plants (WWTPs) in Shanghai. *Fresen. Environ. Bull.* 20(6A), 1525-34.
- [7] Li, Y.M., Gu, G.W., Zhao, J.F., Yu, H.Q., Qiu, Y.L. and Peng, Y.Z. (2003) Treatment of coke-plant wastewater by biofilm systems for removal of organic compounds and nitrogen. *Chemosphere*. 52, 997-1005.
- [8] Li, B., Sun, Y.L. and Li, Y.Y. (2005) Pretreatment of coking wastewater using anaerobic sequencing batch reactor (ASBR). *J Zhejiang Univ Sci B*. 6, 1115-23.
- [9] Ma, Q., Qu, Y.Y., Shen, W.L., Zhang, Z.J., Wang, J.W., Liu, Z.Y., Li, D.X., Li, H.J. and Zhou, J.T. (2015) Bacterial community compositions of coking wastewater treatment plants in steel industry revealed by Illumina high-throughput sequencing. *Bioresour Technol.* 179, 436-43.
- [10] Heylen, K., Vanparys, B., Wittebolle, L., Verstraete, W., Boon, N. and Vos, D. (2006) Cultivation of denitrifying bacteria: optimization of isolation conditions and diversity study. *Appl. Environ. Microbiol.* 72, 2637-43.
- [11] Wharfe, E.S., Jarvis, R.M., Winder, C.L., Whiteley, A.S. and Goodacre, R. (2010) Fourier transform infrared spectroscopy as a metabolite fingerprinting tool for monitoring the phenotypic changes in complex bacterial communities capable of degrading phenol. *Environ Microbiol.* 12, 3253-63.
- [12] Wei, C.H., Xie, B., Xiao, H. L. and Wang, D.S. (2000) Volumetric mass transfer coefficient of oxygen in an internal loop airlift reactor with a convergence-divergence draft tube. *Chem Eng Technol.* 23, 597-603.
- [13] Maidak, B.L., Olsen, G. J., Larsen, N.,



- Overbeek, R., McCaughey, M. J. and Woese, C.R. (1997) The RDP (Ribosomal Database Project). *Nucleic Acids Res.* 25, 109-10.
- [14] Schloss, P.D. and Handelsman, J. (2005) Introducing DOTUR, a computer program for defining operational taxonomic units and estimating species richness. *Appl. Environ. Microbiol.* 71, 1501-06.
- [15] Kimura, M. (1980) A simple method for estimating evolutionary rate of base substitutions through comparative studies of nucleotide sequences. *J. Mol. Evol.* 16,111-20.
- [16] Saitou, N. and Nei, M. (1987) The neighbor-joining method: a method for constructing phylogenetic trees. *Mol. Biol. Evol.* 4, 406-25.
- [17] Swofford, D.L. (1999) PAUP: Phylogenetic analysis using parsimony, version 4.0. Illinois Natural History Survey, Champaign, IL.
- [18] Fernandez, S., Huang, S., Xing, J., Hickey, R., Criddle, C. and Tiedje J. (1999) How Stable Is Stable? Function versus Community Composition. *Appl. Environ. Microbiol.* 65, 3697-704.
- [19] Huang, L.N., Zhou, H., Chen, Y.Q., Luo, S., Lan, C.Y. and Qu, L. H. (2002) Diversity and structure of the archaeal community in the leachate of a full-scale recirculating landfill as examined by direct 16S rRNA gene sequence retrieval. *FEMS Microbiol. Lett.* 214, 235-40.
- [20] Liu, B.B., Zhang, F., Feng, X., Liu, Y., Yan, X., Zhang, X., Wang, L. and Zhao, L.P. (2006) *Thauera* and *Azoarcus* as functionally important genera in a denitrifying quinoline-removal bioreactor as revealed by microbial community structure comparison. *FEMS Microbiol. Ecol.* 55, 274-86.
- [21] Delbes, C., Moletta, R. and Godon, J.J. (2000) Monitoring of activity dynamics of an anaerobic digester bacterial community using 16S rRNA polymerase chain reaction--single-strand conformation polymorphism analysis. *Environ. Microbiol.* 2, 506-15.
- [22] Dyke, V. and McCarthy, A.J. (2002) Molecular biological detection and characterization of *Clostridium* populations in municipal landfill sites. *Appl. Environ. Microbiol.* 68, 2049-53.
- [23] Ryan, T., Katherine, F. and McCormick, A.P. (2008) Bacterial Communities of Bartonella-Positive Fleas: Diversity and Community Assembly Patterns. *Appl. Environ. Microbiol.* 74, 1667-70.
- [24] Rowe, A.R., Lazar, B.J., Morris, R.M. and Ruth, E. (2008) Richardson Characterization of the Community Structure of a Dechlorinating Mixed Culture and Comparisons of Gene Expression in Planktonic and Biofloc-Associated "Dehalococcoides" and *Methanospirillum* Species. *Appl. Environ. Microbiol.* 74, 6709-19.
- [25] Wintzingerode, F., Selent, B., Hegemann, W. and Göbel, B. (1999) Phylogenetic Analysis of an Anaerobic, Trichlorobenzene-Transforming Microbial Consortium. *Appl. Environ. Microbiol.* 65, 283-6.
- [26] Mao, Y., Zhang, X., Xia, X., Zhong, H. and Zhao, L.P. (2010) Versatile aromatic compound-degrading capacity and microdiversity of *Thauera* strains isolated from a coking wastewater treatment bioreactor. *J. Ind. Microbiol. Biotechnol.* 37, 927-34.
- [27] Godon, J.J., Zumstein, E., Dabert, P., Habouzit, F. and Moletta, R. (1997) Molecular microbial diversity of an anaerobic digester as determined by small-subunit rDNA sequence analysis. *Appl. Environ. Microbiol.* 63, 2802-13.
- [28] Archer, D.B. and Kirsop, B.H. (1990) The microbiology and control of anaerobic digestion, In: A. Wheatley (Eds.), *Anaerobic digestion: a waste treatment technology*. Elsevier Science Publishing Ltd., London, England. pp. 43-89.
- [29] Larbi, B. and Djamel, E.A. (2013) Isolation, identification and antibacterial activity of lactic acid bacteria from traditional Algerian dairy products. *Fresen. Environ. Bull.* 6, 15.
- [30] Huang, L.N., Chen, Y.Q., Zhou, H., Luo, S., Lan, C.Y. and Qu, L.H. (2003) Characterization of methanogenic Archaea in the leachate of a closed municipal solid waste landfill. *FEMS Microbiol. Ecol.* 46, 171-77.

---

**Received:** 23.09.2015

**Accepted:** 05.05.2016

---

#### CORRESPONDING AUTHOR

---

**Chaohai Wei**

School of Environment and Energy  
South China University of Technology  
Guangzhou 510006 – PR CHINA

E-mail: [cechwei@scut.edu.cn](mailto:cechwei@scut.edu.cn)

# AN EXPERIMENTAL STUDY INTO DISCHARGE COEFFICIENT OF LABYRINTH WEIRS WITH RECTANGULAR-SHAPED PLANS

Hadi Rostami<sup>1</sup>, Mohammad Heidarnejad<sup>2,\*</sup>, Mohammad Hosein Purmohammadi<sup>3</sup>,  
Amirabbas Kamanbedast<sup>2</sup>, Amin Bordbr<sup>2</sup>

<sup>1</sup>Department of Water Science Engineering, khuzestan Science and Research Branch, Islamic Azad University, Ahvaz, Iran

<sup>2</sup>Department of Water Science Engineering, Ahvaz Branch, Islamic Azad University, Ahvaz, Iran

<sup>3</sup>Department of Water Science Engineering, Shoushtar Branch, Islamic Azad University, Shoushtar, Iran

## ABSTRACT

Due to the significantly lower cost and fewer construction problems associated with labyrinth weirs, designers often consider them as proper design solutions. The reason is that the effective length of the weir increases across the width of the of the weir channel. This study examines the discharge coefficient in one- and two-cycle labyrinth weirs with rectangular-shaped plans and different hydraulic loads. The results showed that increasing the weir hydraulic head ratio ( $H_d/P$ ) would decrease the discharge coefficient ( $C_d$ ). In addition, as compared with the single-cycle weir, the double-cycle weir exhibited a tangibly higher  $C_d$  for  $H_d/P < 0.3$ .

## KEYWORDS:

Labyrinth weir, weir with rectangular-shaped plan, discharge coefficient, cycle, discharge-scale curve

## INTRODUCTION

Water management and transfer have been important throughout the development of human civilization. Many different hydraulic structures have been designed and constructed to meet the

demands. Weirs are typical structures integrated in many dams and water transfer channels for the purpose of discharging water, measuring water flow rate, and controlling water level. During a flooding peak, the flow of water passes over the weir within a short time; hence, this structure must be designed in a way as to accommodate a high discharge coefficient. To this end, labyrinth weirs are used because their discharge coefficient is greater than that of linear weirs. Where labyrinth weirs are used, the reserve water in the dam reservoir also increases [1]. Whereas the discharge volume is a function of the weir crest length and form, a great number of studies have so far been conducted on the effect of hydraulic and geometric parameters on discharge coefficient and flow rate over different weirs. One of the effective ways of increasing the overflow length within a given width is using weirs with nonlinear plans such as triangular, trapezoidal, circular, parabolic, etc. (Figure 1), called polyhedral, castellated, or labyrinth weirs. These can be constructed as single- or multi-cycle structures. Building such weirs would increase the flow over and require a lower headway at the upstream as compared with linear weirs. This is of particular importance when the weir acts as a flood discharge structure because the flow over due to flooding is thus facilitated [2].

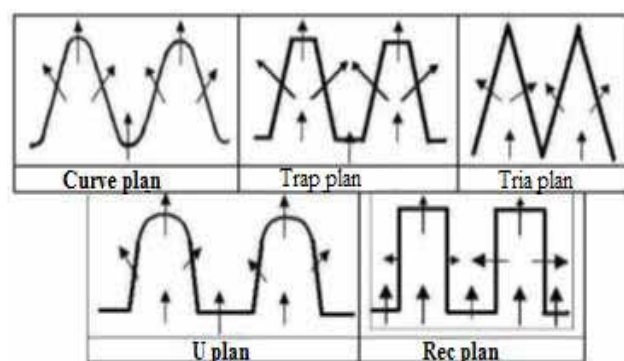


FIGURE 1  
Schematics of various labyrinth weirs

The collision of different stream layers at the downstream of labyrinth weirs leads to greater aeration as compared with linear weirs. This would not only improve water quality, but also reduce the probability of negative pressure and cavitation, thus leading to a substantial decrease in dam and weir maintenance costs [3].

Hay and Taylor compared the hydraulic efficiency of labyrinth weirs with triangular- and trapezoidal-shaped plans with that of sharp-edged linear weirs. They concluded that the labyrinth weirs with triangular-shaped plans produced a higher efficiency than those with trapezoidal-shaped plans [4, 5]. Darvas used the experimental results obtained from the physical models of Veranova and Owen weirs in Australia to present a set of curves for designing labyrinth weirs [6]. Studying the effect of the discharge coefficient on labyrinth weirs, Cassidy et al concluded that the value of this coefficient decreased at higher flow heads as compared with straight weirs [7].

Conducting experiments on the physical model of a labyrinth weir, Lux obtained the discharge coefficient of these weirs as a function of their total upstream head [8].

In their experimental studies, Tullis et al conducted tests on castellated weirs with trapezoidal-shaped plans and apex angles between 6 and 18 degrees, obtaining a relation for the discharge coefficient of these weirs as a function of total upstream head, weir height, weir edge length, and weir apex angle. They also conducted experiments for determining the effect of submersion conditions on the performance of these weirs and derived a relation for plotting the discharge-scale curve [9, 10].

Qodsian and Amanian studied discharge coefficient variations in labyrinth weirs with semicircular-shaped plans. Evaluating the parameters affecting  $C_d$  in castellated weirs with semicircular-shaped plans, they observed that increasing the weir radius would lead to a corresponding increase in  $C_d$ . The rate of  $C_d$  variations gradually decreased with increase in flow head, tending to a constant value for all the tested radii. They also recommended the use of labyrinth weirs with semicircular-shaped plans and, presenting appropriate relations for the discharge coefficient, proposed a method for designing this type of weir [11].

Shenavai and Qodsian showed in his research that, in triangular labyrinth weirs, the semicircular crest shape was hydraulically superior to the sharp-edged crest shape [12].

Conducting experiments on single-cycle labyrinth weirs with rectangular- and U-shaped plans, Heydarpour et al concluded that increasing weir head would lead to a corresponding increase in the discharge coefficient at a given  $HT/P$  (i.e., ratio of total upstream energy to weir head). By

comparing the corresponding values, they showed that increasing the length parallel to the flow direction in labyrinth weirs would reduce the discharge coefficient ( $C_d$ ), and increasing the length perpendicular to the flow direction would increase the discharge coefficient [13].

Yassi and Mohammadi studied the effect of changing the flood-level rim radius of curvature in two-cycle labyrinth weirs with triangular-, trapezoidal-, and rectangular-shaped plans. Their results showed that arched weir rims would increase the weir hydraulic efficiency [14].

Kumar et al conducted an experimental study on the discharge coefficient of a castellated weir with a triangular-shaped plan. A comparison of the results demonstrated that a decrease in the weir apex angle would increase the length of the interference area and considerably decrease the weir discharge coefficient. Furthermore, relations for calculating the discharge coefficient with different apex angles were put forward [15].

Crookston B.M., and Tullis studied experimentally the interference characteristics of the free-falling nappes and local submersion in castellated triangular weirs with two and four cycles and different apex angles. They showed that, due to less interference between free-falling nappes at lower flow rates, the discharge coefficient was greater than that of the linear weir, and that such interference increased gradually at higher flow rates. This caused the discharge coefficient to decrease towards the values obtained for broad-crested weirs [16, 17].

In line with the research by Houston on extending the labyrinth weirs into the dam reservoir, the same researchers (Crookston and Tullis) also examined different weir positions inside the reservoir. Through examining the superior performance of arched labyrinth weirs, they concluded that the increased discharge coefficient in this type of weir is due to the more favorable orientation of the inlet flows in different cycles [16, 18].

**Geometric and Hydraulic Parameters of Labyrinth Weirs.** With due consideration of the results obtained from previous research, it may be concluded that the following factors affect the performance of labyrinth weirs (Figure 2):

Geometric parameters including weir width, weir crest length, weir upstream crest elevation (measured from upstream floor), length of the inner rim, structural features including crest shape, weir aprons and wall thickness, operating conditions including the total hydraulic load, weir aeration and submersion stages, downstream conditions including crest elevation, water depth, downstream gradient, etc., upstream conditions including weir inlet conditions, and the shape of training walls, the presence of upstream gradient, etc [19].

The exact description of 3D flow over labyrinth weirs is a difficult task. The mathematical expression derived for this purpose must allow for energy, momentum, and continuity equations as well as such parameters as weir geometry, crest shape, local submersion, interference of stream layers passing over the weir, non-parallel streamlines, pressure under the stream nappes, existence/non-existence of air cavities behind stream nappes, surface tension effects, viscosity effects, etc [19].

The following general equation was used by Tullis et al for labyrinth weirs [9]:

$$Q = \frac{2}{3} C_d L \sqrt{2g} H_0^{1.5}$$

In this equation, Q is the flowrate passing over the weir, L is the characteristic length (e.g. weir crest length), g is the acceleration of gravity,  $H_0$  is the total hydraulic head, and  $C_d$  is the non-dimensional discharge coefficient (determined through experiment). Upon conducting dimensional analysis and eliminating constant parameters, the effect of the following two constants on  $C_d$  in labyrinth weirs was investigated (Q is flow rate and n the number of weir cycles):

$$C_d = F(Q, n)$$

## MATERIALS AND METHODS

The experiments were conducted on test models in a rectangular test flume (10m x 0.3m x

0.6m) at Hydraulic Laboratory, Training Complex, Khuzestan Water and Power Organization, Iran (Figure 4). The transparent flume walls were made of glass, making possible the observation of water profile and flow conditions during the tests. The flume was of the free-flow type. To obtain more exact results, it was ensured that all the sections of the flume had been properly sealed before commencing the experiments. The specifications of different flume sections and the laboratory apparatus used in this study are as follows (Figures 2 and 3):

- Flume supply water reservoir
- Digital flowmeter (measuring accuracy: 0.2 L/sec)
- Laminar flow stabilizer at flume inlet

Water submersible pump (pipe diameter: 3 inches; max. flowrate: 120 m<sup>3</sup>/s) The constant bed of the flume was horizontal without any slope (within the practical range of accuracy). Water was first drawn from the ground reservoir via the pump and guided to the settling (head) tank at the upstream inlet to the flume. The inlet flow to the channel and passing over the weir was laminar. Upon changing the flow rate, the hydraulic conditions of the flow passing over the weir were studied and recorded. Ultimately, the flow would enter (upon passing over the weir through the downstream channel) the pumping reservoir so that the cycle could be repeated.

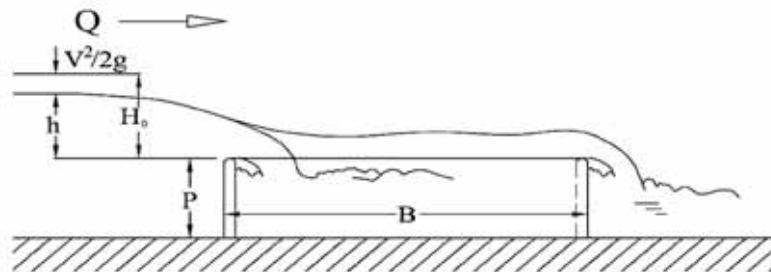


**FIGURE 2**  
Parameters affecting labyrinth weirs performance [19]



**FIGURE 3**  
Layout of the double-cycle rectangular weir inside the laboratory flume

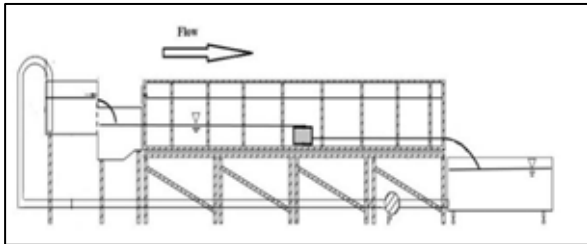
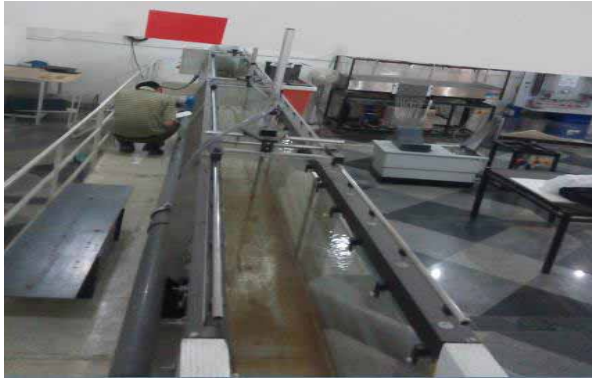


**FIGURE 4**  
Sample flume and laboratory equipment



**FIGURE 5**  
Single-cycle rectangular labyrinth weir



**FIGURE 6**

### Double-cycle rectangular labyrinth weir

Single- and double-cycle labyrinth weirs with rectangular-shaped plans were tested at different flow rates (Figures 5 and 6). The labyrinth weirs were made of Plexiglas. In all the tests, the upstream and downstream bed elevations were equal. The width of the discharge was 30cm and the ratio of cycle width to weir height was adjusted at 3, 2.5, and 2. Thickness  $t$  was 5mm and the inlet channel widths in the single and double cycle cases were 14.2 and 7.1, respectively. A thickness of 5mm was selected for the flat crest. Each weir geometry was subjected to 12 flows with different hydraulic loads so that the effect of parameter  $H_0/P$  on the performance of the studied weirs would be determined with greater precision. Tables 1 and 2 present the geometric and hydraulic specifications of the tested weirs.

## RESULTS AND DISCUSSION

**Effect of Weir Water Head (Hydraulic Load) on Discharge Coefficient.** Labyrinth weirs with geometric (rectangular, triangular, trapezoidal, arched, etc.) plan shapes are efficient structures for flow regulation and discharge along a limited width. The hydraulic performance of weirs with rectangular-shaped plans and different number of cycles was examined experimentally. Comparisons showed that upon increasing the hydraulic load in all the studied cases, the discharge coefficient underwent an initial increase followed by a decrease. Local submersion threshold occurred within the  $H_T/P > 0.48$  region.

According to Diagram 1, maximum  $C_d$  occurred at an approximate flow rate of 12 m<sup>3</sup>/h for the double-cycle weir with a width to head ratio of  $w/p=2$ . In both the single- and double-cycle weirs,  $C_d$  increased with increasing weir height ratio ( $P$ ). According to the diagrams,  $C_d$  sharply decreased with increasing flowrate. In single-cycle weirs, the slope of this decrease is less than the previous case (Diagram 2).

**Effect of Number of Cycles on  $C_d$  in Weirs with Arched-Shaped Plans.** Different submergence flow rates were obtained for different cases. However, in all cases, the submergence flow rate occurred in the range  $H_t/p > 0.33$ .

In general, values of  $C_d$  in the double-cycle weir were greater than those in the single-cycle weir for  $H_t/p < 0.35$ . At low hydraulic loads, this difference was large at first, but subsequently decreased as we approached the 0.35 limit. For  $H_t/p > 0.35$ , approximately equal values are obtained for  $C_d$  in both single- and double-cycle cases (Diagram 3).

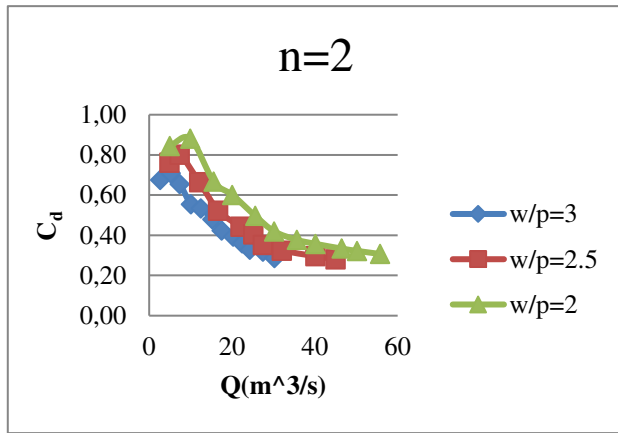


**DIAGRAM 1**

Effect of flow rate on  $C_d$  in double-cycle weirs with rectangular-shaped plans

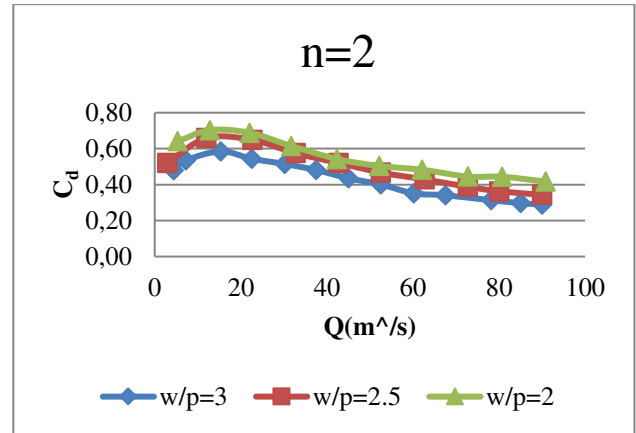


**DIAGRAM 2**

Effect of flow rate on  $C_d$  in single-cycle weirs with rectangular-shaped plans

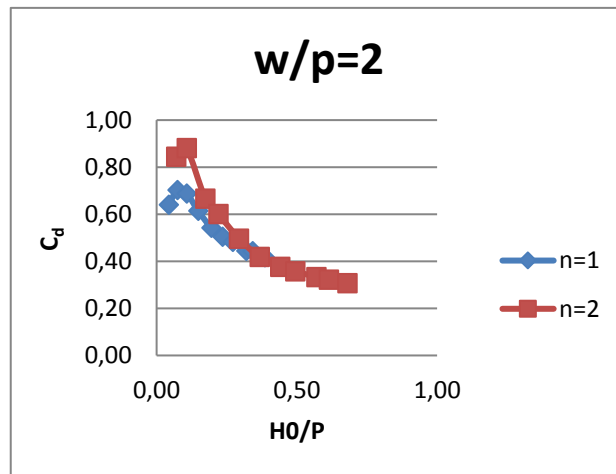
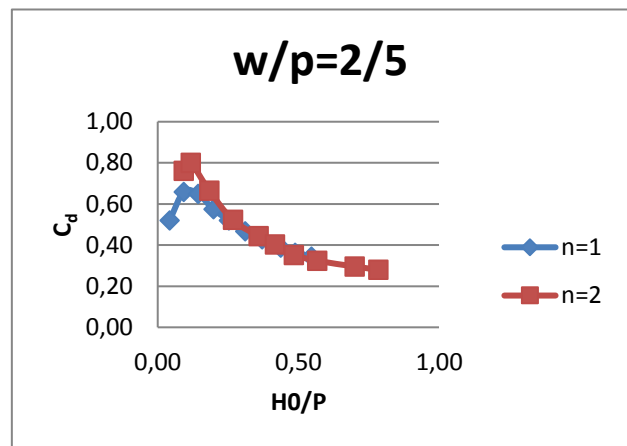
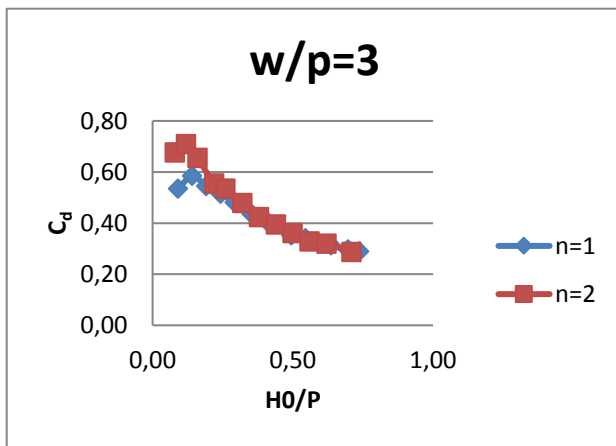


**DIAGRAM 3**

Effect of number of cycles on  $C_d$  in a labyrinth weir with a rectangular-shaped plan

**TABLE 1**

Geometric and hydraulic specifications of single-cycle rectangular labyrinth weirs

Model	W (cm)	w/p	L (mm)	T (mm)	N	Weir plan shape	No. of tests
Single-Cycle	30	2, 2.5, 3	148.5	5	1	Rectangular	36

**TABLE 2**  
**Geometric and hydraulic specifications of double-cycle rectangular labyrinth weirs**

Model	W (cm)	w/p	L (mm)	T (mm)	N	Weir plan shape	No. of tests
Double-Cycle	15	2, 2.5, 3	148.5	5	2	Rectangular	36

## CONCLUSION

Regarding the effect of hydraulic conditions on  $C_d$  in labyrinth weirs with rectangular-shaped plans, it was concluded that discharge coefficient initially increased with hydraulic load ( $H_0/P$ ) which varied between 0.05 and 0.74. However,  $C_d$  then underwent a sharp decrease, resulting in a maximum 65% decrease in the double-cycle weir at  $w/p=2$ . Moreover, for hydraulic head ratios less than 0.35, the discharge coefficient in the double-cycle weir with a rectangular-shaped plan was greater than that in the single-cycle weir. At higher hydraulic ratios, the discharge coefficients for both single- and double-cycle weirs with rectangular-shaped plans were almost equal.

## REFERENCES

- [1] Falvey, H.T. (2003). Hydraulic Design of Labyrinth Weirs. ASCE press, USA.
- [2] Crookston, B.M., Tullis, B.P. (2012). Discharge efficiency of reservoir application specific labyrinth weirs. *Journal of Irrigation and Drainage Engineering*. ASCE. 138(6), 773-776.
- [3] Wormleaton, P., Soufiani, E. (1998). Aeration performance of triangular planform labyrinth weirs. *American Society of Civil Engineering, Journal of Environmental Engineering*. 124(8), 709-719.
- [4] Taylor, G. (1968). The performance of labyrinth weirs. PhD thesis. University of Nottingham, Nottingham, England.
- [5] Hay, N., Taylor, G. (1970). Performance and design of labyrinth weirs. *American Society of Civil Engineering, Journal of Hydraulic Engineering*. 96(11), 2337-2357.
- [6] Darvas, L.A. (1971). Performance and design of labyrinth weirs. *Journal of The Hydraulics Division*. ASCE, 97(8), 1246-1251.
- [7] Cassidy, J.J., Cardner, C.A., Peacock, R.T. (1985). Bordman labyrinth crest. *Journal of Hydraulic Engineering*. ASCE. 3(3), 398-416.
- [8] Lux, F. (1993). Design methodologies for labyrinth weirs. *Proceeding of water power and dam construction*. Nashville Tennessee, USA. 1397-1407.
- [9] Tullis, P., Amanian, N., Waldron, D. (1995). Design of labyrinth weirs. *Journal of Hydraulic Engineering*. ASCE. 121(3), 247-255.
- [10] Tullis, B., Young J., Chandler, M. (2007). Head-Discharge Relationships for Submerged Labyrinth Weirs. *Journal of Hydraulic Engineering*. 133(3), 248-254.
- [11] Qodsian, M., Amanian, N. (2001). Discharge Coefficient of Castellated Weirs with Semicircular-Shaped Weirs. *Amirkabir University Scientific Journal*. 49(13), 76-83.
- [12] Shenavai, H., Qodsian, M. (2001). Effect of Crest Geometry on Discharge Coefficient in Labyrinth Weirs with Triangular-Shaped Plans. *International Conference on Hydraulic Structures*, Kerman, Iran.
- [13] Heydarpour, M., Mousavi, F., Roshanizarmehri, A.R. (2006). Multihedral Weirs with Rectangular- and U-Shaped Plans. *Journal of Agricultural Sciences and Natural Resources*. Isfahan University of Technology, Iran. 10(3), 1-11.
- [14] Yassi, M., Mohammadi, M. (2007). Labyrinth Weirs with Arched-Shaped Plans. *Journal of Agricultural Sciences and Natural Resources*, Isfahan University of Technology, Iran. 41(11) 1-12.
- [15] Kumar, S., Ahmada, Z., Mansoor, T. (2011). A new approach to improve the discharging capacity of sharp crested triangular plan form weirs. *Flow Measurement and instrumentation*. 22(3), 175-180.
- [16] Crookston, B.M., Tullis, B.P. (2012). Arced labyrinth weirs. *Journal of Hydraulic Engineering*. ASCE. 138(6), 555-562.
- [17] Crookston, B.M., Tullis, B.P. (2012). Labyrinth weirs: nappe interference and local submergence. *Journal of Irrigation and Drainage Engineering*. ASCE. 138(8), 757-765.
- [18] Houston, K. (1983). Hydraulic model study of Hyrum Dam auxiliary labyrinth weir. Report No. GR-82-13. U.S. Bureau of Reclamation. Denver. Colorado.
- [19] Crookston, B.M. (2010). Labyrinth weirs. PhD thesis. Utah State University, Logan, UT.

**Received: 29.09.2015**

**Accepted: 14.09.2016**



## **CORRESPONDING AUTHOR**

---

**Mohammad Heidarnejad**

Department of Water Science Engineering

Ahvaz Branch

Islamic Azad University

Ahvaz – IRAN

E-mail: [mo\\_he3197@yahoo.com](mailto:mo_he3197@yahoo.com)

# ANALYSIS OF HCHs AND DDTs IN A TYPICAL PESTICIDE CONTAMINATED SITE

Xuebin Chen<sup>1,2</sup>, Wenxia Liu<sup>1,\*</sup>, Yingxia Zhou<sup>1</sup>, Xinyue Qiao<sup>1</sup>, Jiabao Zhao<sup>1</sup>, Haifeng Li<sup>2</sup>, Ying Han<sup>2</sup>, Xiao Liao<sup>2</sup>, Mengjing Wang<sup>2</sup>, Wenbin Liu<sup>2</sup>

1. Department of Environmental Sciences, College of Forestry, Henan Agricultural University, Zhengzhou 450002, People's Republic of China

2. Research Center for Eco-Environmental Sciences, Chinese Academy of Sciences, Beijing 100085, People's Republic of China

## ABSTRACT

Seventeen soil samples were collected from a typical pesticide contaminated site in Henan Province, China. The concentrations and distribution of hexachlorocyclohexanes (HCHs) and dichlorodiphenyltrichloroethanes (DDTs) in the soils were investigated. The concentrations of HCHs ranged from 0.17 to 84.26 mg/kg (average 8.82 mg/kg) and that of DDTs ranged from 0.19 to 751.82 mg/kg (average 80.09 mg/kg). Vertical distribution of pollutants in soil samples indicated that the pollutants were mainly concentrated in top soils rather than deeper soils. The contribution of  $\beta$ -HCH was the highest among the four HCHs isomers, and the proportion of p,p'-DDT was the highest among DDTs isomers. The spatial distributions of HCHs and DDTs in top soils were calculated by a Kriging model, revealing that soils in the historical storage and production workshop were still seriously contaminated.

## KEYWORDS:

Soil • OCPs • Contaminated site • Distribution

## INTRODUCTION

Organochlorine pesticides (OCPs), such as dichlorodiphenyltrichloroethane (DDTs), and hexachlorocyclohexanes (HCHs), belong to the group of Persistent Organic Pollutants that are restricted or banned globally under the Stockholm Convention. With high toxicity, environmental persistence, bioaccumulation and long term transportation, OCPs have attracted global concern. OCPs have often been used in developing countries even after they had been banned in Europe, North America and Japan, presumably because of a lack of

effective and affordable alternatives and limited capacity for chemical regulation and enforcement [1, 2]. China is the largest developing country and DDTs and HCHs were widely used in China from the 1950s until their production was banned in May 1983. The total production of HCHs (4.9 million tons) and DDTs (0.4 million tons) in China accounted for 33 and 20 % of the global production, respectively [3].

OCPs have high n-octanol/water partition coefficients and low vapor pressures. Therefore, they readily accumulate in the environment, especially in organic carbon-rich media such as soil, sediment and biota [4, 5]. Among these media, soil has been demonstrated to act as a conservative matrix of OCPs in the environment and to reflect long-term exposure. Large amounts of OCPs residues exist in soil, which might be the result of their wide use and the strong adsorption ability of soil for hydrophobic organic contaminants. OCPs contaminations were widely found in soil in China and other countries [6, 7, 8] clouding the Polar Regions and the Tibetan Plateau that are distant from human activities. [9]

The distribution of pollutants, environmental risk and other factors at existing production sites indicate that the severity of pollution at OCPs production sites is much higher than that of agricultural soils and urban soils, despite the limited contamination area of the production sites [10, 11] For example, Zhao et al [12] studied the spatial distribution of DDTs residue in soils around an enterprise and found that the DDTs content near the plant was more than 10,000 mg/kg. Similarly, the HCHs and DDTs contamination status in surface soil of a pesticide plant was studied in Beijing [13]. The results showed that the soil in this plant was seriously contaminated and that the concentrations of most soil samples exceeded the Chinese soil environmental quality live standard (1 mg/kg) and commercial land (4 mg/kg) limits.

In this study, a pesticide plant in Henan

Province, China, was selected as a typical OCPs-contaminated site. With increasing urbanization, this site will be developed as commercial land. It is essential to investigate the environmental levels and distributions of HCHs and DDTs to evaluate the risk of pollutants on the environment and human health.

## MATERIALS AND METHODS

The pesticide factory, covering an area of 318 acres, was used for 40 years to produce DDTs, HCHs, chlordane, mirex and other pesticides. The production of HCHs was the largest and the cumulative production of HCHs was more than a million tons before 1982 when HCHs production ceased. 17 sampling points were selected based on the status of the production site in July 2014 (Fig. 1).

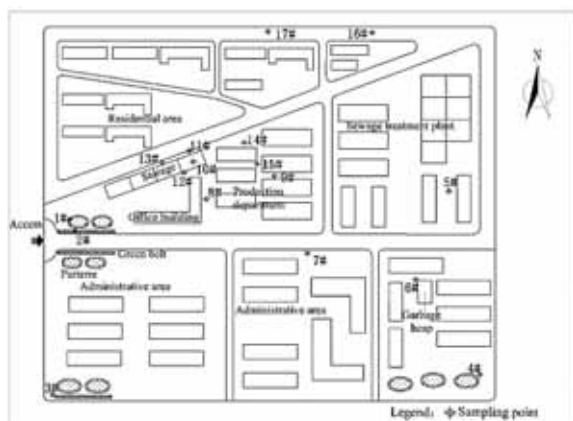


**FIGURE 1**  
Location of the sampling sites in the study area

Semi-circular groove drill set samplers were used to collect the soil samples. The surface soil (0–20 cm) and some deep soil samples at depths of 0–20, 20–40 and 40–60 cm were collected at sampling sites 2, 3 and 8. The soil samples were brown, mostly sandy loam and silt loam in texture. The samples were air dried at room temperature, and sieved to pass through a 35 mesh sieve, and then refrigerated at  $-4\text{ }^{\circ}\text{C}$  before analysis. The analysis of HCHs and DDTs in soil adopted the Chinese national standard method GB/T 14550-2003. The samples were extracted using ultrasonication method and then purified with Florisil column. Finally, the fraction was concentrated under nitrogen to 0.2 mL. Quantitative analysis of HCHs and DDTs was carried out using an Agilent 6890/5975 GC/MS (Agilent Technologies, Santa Clara, CA, USA). Method blanks were run using the same solvents as for real samples. HCHs and DDTs contaminants

were below the detection limits in the method blanks ( $n = 3$ ). The Geostatistical Interpolation Technique was used to create a continuous three-dimensional contour map of HCHs and DDTs concentrations in the soil samples with the widely used Ordinary Kriging algorithm. The map was produced using Golden Software Surfer 8.0 with cross-validations.

## RESULTS AND DISCUSSION

The concentrations of HCHs and DDTs in the soil samples are shown in Fig. 2.

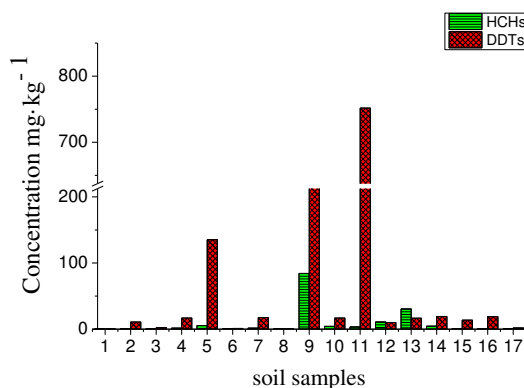


**FIGURE 2**  
Concentrations of HCHs and DDTs in soil samples

High concentrations of HCHs and DDTs were detected in some soil samples. The concentrations of HCHs were in the range of 0.17–84.26 mg/kg with an average of 8.82 mg/kg, while the concentrations of DDTs in soil samples were in the range of 0.19–751.82 mg/kg with an average of 80.09 mg/kg. The concentrations of HCHs in 59% of sites and DDTs concentrations in 88% of the sites exceeded the secondary residential land limit (1.0 mg/kg) of soil environmental quality standards in China. The concentrations of HCHs in 41% and DDTs in 71% of soil samples exceeded the secondary commercial land limit (4.0 mg/kg) of soil environmental quality standards. From these results, it was determined that the contaminated site still has a high health and environmental risk for residential and commercial use.

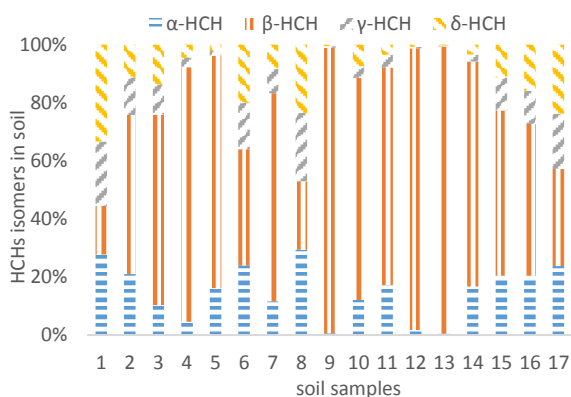


FIGURE 3

### Composition of HCHs isomers in soils

DDTs concentrations in the soil surface were generally higher than that of HCHs.

The proportions of four HCHs isomers in soil samples were significantly different (Fig. 3).

The proportions of  $\beta$ -HCH,  $\alpha$ -HCH,  $\delta$ -HCH and  $\gamma$ -HCH in different soil samples varied in the range of 17–99, 1–29, 1–33 and 1–23%, respectively, with the corresponding average proportions of 65, 15, 11 and 9%, respectively (Fig. 3). The different proportions and degradation rates of the four isomers might be influenced by their different stability and toxicity.

About 5–14% of  $\beta$ -HCH, 55–80% of  $\alpha$ -HCH, 2–10% of  $\delta$ -HCH, 12–14% of  $\gamma$ -HCH, and other small amounts of organic chlorine compounds exist in the HCHs of commodities. By comparing the HCHs compositions in commodities and the soil samples in this study, the ratio of  $\beta$ -HCH in soil was much higher than that in commodities. Studies showed that the process of microbial degradation is the main degradation pathway of HCHs. In the balanced stage of microbial growth, the rate of dechlorination of HCHs is in the following order:  $\gamma$ -HCH >  $\alpha$ -HCH >  $\delta$ -HCH >  $\beta$ -HCH [14]. If the environment is alkaline, the dechlorination of HCHs will be enhanced and  $\gamma$ -HCH is susceptible to attack by soil microbes and conversion to produce  $\alpha$ -HCH by photochemical reaction. In addition, large amounts of  $\alpha$ -HCH can be transformed into  $\beta$ -HCH [15].

Significant differences in HCHs isomer patterns in soil samples are closely related to their physicochemical properties. The content of  $\beta$ -HCH isomers in most of the soil samples was the highest among the four HCHs isomers, which mainly resulted from its high stability, low volatility and low solubility. The conversion of  $\alpha$ -HCH played an important role in determining the isomer proportions, which cannot be ignored.  $\beta$ -HCH usually had the

highest content among the four HCHs isomers in typical contaminated sites because of the difficulty in degrading or converting this isomer, similar to the findings in this study [16]. The results showed that the high level of HCHs in the contaminated site was the result of long term OCPs production and decomposition. The relatively similar isomer patterns and high percentages of  $\beta$ -HCH in all of the samples indicated that there was no new source of HCHs in the study area.

The proportions of DDTs isomers in soil are shown in Fig. 4.

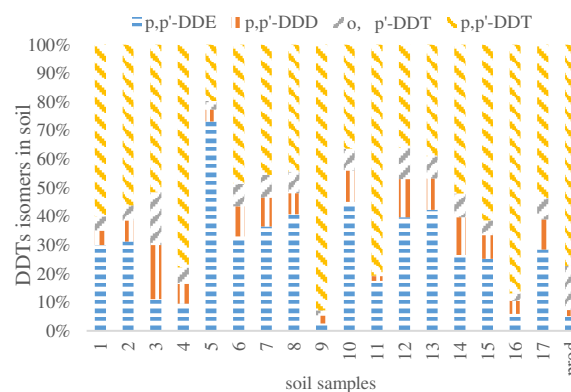


FIGURE 4

### Composition of DDTs isomers in soils

The proportions of p,p'-DDT, o,p'-DDT, p,p'-DDE, p,p'-DDD in different soil samples were in the range of 20–93, 2–18, 3–73 and 2–19%, respectively. Among the four DDTs isomers, the proportion of p,p'-DDT was the highest, with an average of 55%.

Previous studies found that DDTs would convert to DDEs under aerobic conditions, while under anaerobic conditions, DDTs would dechlorinate to DDDs [17]. Therefore, the ratio of DDEs/DDDs can be used to speculate on the redox conditions during the process of DDTs degradation. If the ratio of DDEs/DDDs is > 1, the degradation environment is likely aerobic. In this study, the ratio of p,p'-DDE/p,p'-DDD of 15 soil samples was > 1, indicating that the p,p'-DDE level was significantly higher than p,p'-DDD and the microbial degradation of DDTs in this contaminated site occurred mainly under aerobic conditions.

Generally, industrially-produced DDTs contains 75% p,p'-DDT, 15% o,p'-DDT, 5% p,p'-DDE and < 5% p,p'-DDD. When comparing the DDTs compositions in commodities and soil samples, the proportion of o,p'-DDT in commodities is 15%, slightly higher than the average proportion in soil samples of 7%. The average proportion of p,p'-DDE

in soil samples was 29%, while the proportion in commodities is only 5%. The decrease in *o,p'*-DDT and the increase in *p,p'*-DDE concentrations might result from the aerobic microbial degradation of DDTs. The proportion of *p,p'*-DDT in site 9 from near the workshop was 93%. The results showed that soil near the workshop might have a new source of DDTs contamination that has undergone only a short degradation time, leading to the high proportion of *p,p'*-DDT compared with the other three isomers and a high proportion of *p,p'*-DDT when compared with industrially-produced DDTs.

The spatial distribution of HCHs and DDTs concentrations in soil were analyzed using the Kriging interpolation method. This method is a common interpolation method that can simulate the contamination trend of HCHs and DDTs in the surface soil, as shown in Fig. 3.

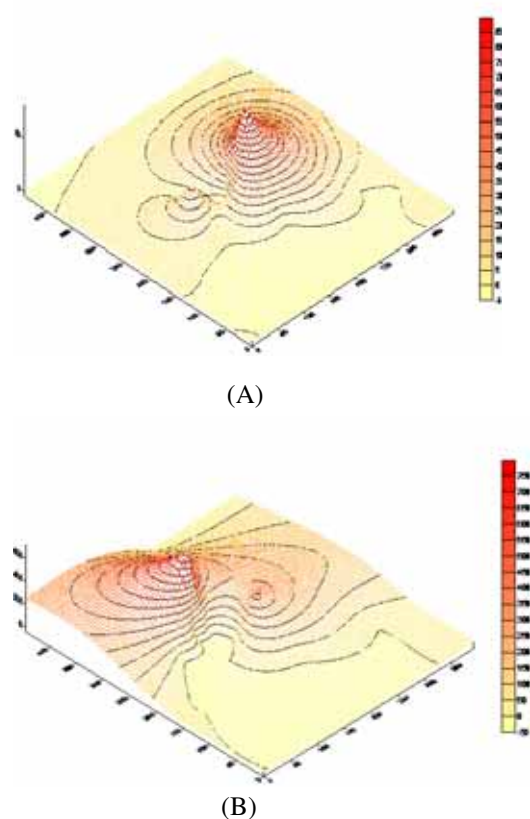


**FIGURE 5**  
Contour maps of HCHs (A) and DDTs (B) in soils of the study site

The color in the red zone deepens with increasing contaminant concentration. The highest concentration of HCHs was found in the central north of the site, which is in the vicinity of the workshop. The contamination tendency of this site was emanative. The dust generated during pesticide production would waft with the wind and pollutants

contained in the dust would be mixed into the soil, leading to HCHs contamination. As a result, the highest content of HCHs was observed in the soil around the workshop. From the contour map above, the HCHs-contaminated area was about 82,137 m<sup>2</sup>, accounting for 46% of the total area.

Similarly, the highest concentrations of DDTs were mainly concentrated in the northwest of the factory near the storehouse (site 11). The main reasons for this were that the raw materials and DDTs products were stacked on the northwest side of the road and outside the walls of the factory and that the storage conditions were very poor and simple. The open storage of pesticides and long-term accumulation enabled the transfer of pesticides into the soil from the gaps in damaged packaging. The DDTs-contaminated area was about 91,569 m<sup>2</sup>, accounting for 52% of the total site area.

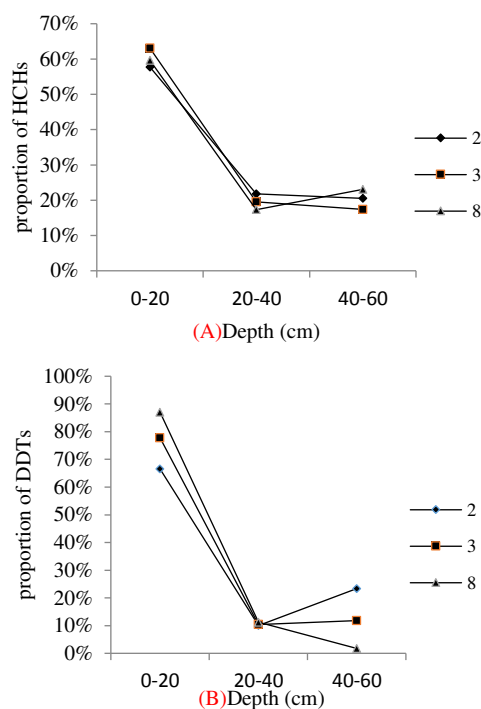


**FIGURE 6**  
Proportion of HCHs (A) and DDTs (B) at different soil depth

The concentrations of HCHs and DDTs in soil samples collected from 0–20, 20–40 and 40–60 cm depth at sites 2, 3, 8 were analyzed to explore whether pollution was mitigated with increasing depth. The proportions of HCHs and DDTs at different soil depths were shown in Fig. 6.

The concentrations of HCHs and DDTs significantly reduced with increasing depth. In deep soil, the  $\beta$ -HCH content was still the highest among the four HCHs isomers. The reason for this might be

that after the surface and sub-surface soil was contaminated by HCHs, all HCHs would migrate downward at a constant rate, leading to a stable proportion of each HCHs isomer at all soil depths. The average percentage of HCHs in surface soil was 60% of the total and that in deep soil samples was 20%, taking the three sampling sites into account.

DDTs concentrations were generally higher than HCHs in deep soil samples, and the dominant DDTs isomer was still p,p'-DDT, which was quite similar to the surface soil. DDTs content in surface soil contributed 87% of the total, and that in deep soil contributed only 2% at sampling point 8. The difference between the contribution of HCHs and DDTs to contamination at the surface and in deep soil might result from the difference in vertical migration of DDTs compared with HCHs.

On the basis of the secondary residential land limit of environmental quality of soil (1.0 mg/kg), the concentrations of HCHs and DDTs in soil to 50 cm depth reached the limit of the standards and the contaminated volume of this research site was about 45,785m<sup>3</sup>. The results of this study on the concentration and distribution of HCHs and DDTs in soils were revealed that this pesticide contaminated site is still seriously polluted, which will be helpful to dispose the historical pesticide contaminated sites.

#### ACKNOWLEDGEMENTS

This study was supported by the National 973 Program (2015CB453103), the National Natural Science Foundation of China (21477150, 21321004) and open fund project of State key laboratory (KF-2012-10).

#### REFERENCES

- [1] Barra, R. Colombo, JC. Eguren, G. Gamboa, N. Jardim, WF. Mendoza, G. (2006) Persistent organic pollutants (POPs) in eastern and western South American countries. *Reviews of environmental contamination and toxicology*, 185, 1-33.
- [2] Daly, GL. Lei, YD. Teixeira, C. Muir, DC. Castillo, LE. Jantunen, LM. Wania, F. (2007) Organochlorine pesticides in the soils and atmosphere of Costa Rica. *Environmental science & technology*, 41(4), 1124-1130.
- [3] Li, J. Zhang, G. Qi, S. Li, X. Peng, X. (2006) Concentrations, enantiomeric compositions, and sources of HCH, DDT and chlordane in soils from the Pearl River Delta, South China. *Science of the Total Environment*, 372(1), 215-224.
- [4] Meneses, M. Schuhmacher, M. Domingo, JL. (2002) A design of two simple models to predict PCDD/F concentrations in vegetation and soils. *Chemosphere*, 46(9-10), 1393-1402.
- [5] Polder, A. Gabrielsen, G. Odland, JØ. Savinova, T. Tkachev, A. Løken, K. Skaare, J. (2008) Spatial and temporal changes of chlorinated pesticides, PCBs, dioxins (PCDDs/PCDFs) and brominated flame retardants in human breast milk from Northern Russia. *Science of the Total Environment*, 391(1), 41-54.
- [6] Aigner, EJ. Leone, AD. Falconer, RL. (1998) Concentrations and enantiomeric ratios of organochlorine pesticides in soils from the US corn belt. *Environmental science & technology*, 32 (9), 1162-1168.
- [7] Meijer, SN. Halsall, CJ. Harner, T. Peters, A. Ockenden, W. Johnston, A. Jones, KC. (2001) Organochlorine pesticide residues in archived UK soil. *Environmental science & technology*, 35(10), 1989-1995.
- [8] Sun, K. Zhao, Y. Gao, B. Liu, X. Zhang, Z. Xing, B. (2009) Organochlorine pesticides and polybrominated diphenyl ethers in irrigated soils of Beijing, China: levels, inventory and fate. *Chemosphere*, 77(9), 1199-1205.
- [9] Wang, XP. GONG, P. YAO, TD. (2008) Progress about the Research of Atmospheric Persistent Organic Pollutants in Remote Areas. *Environmental Science*, 29(2), 273-82.
- [10] MA, Y. HUANG, QF. WANG, Q. YANG, ZL. (2009) Spatial Distribution of HCH in A Typical Contaminated Site Journal of Agro. *Environment Science*, 8, 005.
- [11] Pan, F. Wang, L. Zhao, H. You, Q. Liu, L. (2013) Residual characteristics of HCHs in soils of a former lindane production enterprise. *Environmental Science*, 34(2), 705-711.
- [12] Na-na, Z. Qi-fei, H. Qi, W. (2007) Spatial distribution of DDT in a typical contaminated site. *Acta Scientiae Circumstantiae*, 27, 1669-1674.
- [13] CONG, X. XUE, ND. LIANG, G. WANG, SJ., LI, FS. (2008) Residual characteristics of pollutants in topsoil of a former organochlorine pesticide manufacturing enterprise. *Journal of Agro-environment Science*, 850-854.
- [14] Willett, KL. Ulrich, EM. Hites, RA. (1998) Differential toxicity and environmental fates of



hexachlorocyclohexane isomers. *Environmental science & technology*, 32(15), 2197-2207.

- [15] Piao, X. Wang, X. Tao, S. Shen, W. Qin, B. Sun, R. (2004) Vertical distribution of organochlorine pesticides in farming soils in Tianjin area. *Research of Environmental Sciences*, 17(2), 26-29.
- [16] Li, C. Liu, W. Wang, L. Ba, T. Gao, L. Zhang, L. Zheng, M. (2008) Analysis of HCH in a typical waste contaminated site. *Environmental Science*, 29(3), 809-813.
- [17] You, G. Sayles, GD. Kupferle, MJ. Kim, IS. Bishop, PL. (1996) Anaerobic DDT biotransformation: enhancement by application of surfactants and low oxidation reduction potential. *Chemosphere*, 32(11), 2269-2284.

---

**Received:** 14.10.2015

**Accepted:** 25.02.2016

---

**CORRESPONDING AUTHOR**

---

**Wenxia Liu**

Department of Environmental Sciences, College of Forestry, Henan Agricultural University, Zhengzhou 450002, People's Republic of China

Email: [hjxliuwenxia@163.com](mailto:hjxliuwenxia@163.com)

# FUNCTIONALIZATION OF CARBON NANOTUBES AND ITS APPLICATION IN ADSORPTION AND SOLID PHASE EXTRACTION

Xiaoxing Zhang\*, Li Zhang, Hui Liu

College of Environmental Sciences and Engineering, Dalian Maritime University, Dalian 116026, China

## ABSTRACT

Compared with the conventional adsorption materials, carbon nanotubes have advantages of high adsorption capacity and rapid adsorption due to its unique structure and have been one of the most attractive adsorbents for solid phase extraction. However, in practical applications, carbon nanotubes tend to aggregate and thus dramatically deteriorate its adsorption ability. In addition, the bare carbon nanotubes generally exhibit non-specific adsorption for a wide range of targets, which restricts its sorption selectivity and analytical sensitivity of adsorptive substances. The application range of carbon nanotubes can be broadened via surface functionalization. In this paper, the structure and properties of carbon nanotubes are introduced briefly, and, the functionalization methods of carbon nanotubes and its application in the adsorption and solid phase extraction of inorganic metal ions, organic compounds and biomolecules are presented. The adsorption mechanisms of metal ions and organic compounds by carbon nanotubes are also discussed. Further, the promising application of carbon nanotubes in the fields of adsorption and solid phase extraction is prospected. Novel functionalization methods need to be developed to improve the sorption selectivity and analytical sensitivity of adsorbed substances, and, further research needs to be done on the adsorption mechanisms.

## KEYWORDS

Carbon nanotubes; Functionalization; Adsorption; Solid phase extraction

## INTRODUCTION

**Carbon nanotubes.** Since its discovery in 1991[1], carbon nanotubes (CNTs) have received tremendous interest of researchers because of its unique structure. CNTs can be viewed as a graphene

sheet (sp<sup>2</sup> carbon) rolled up into a tube with both ends capped by a half spherical structure of bucky balls. Carbon nanotubes have large length-diameter ratio with the diameter varying from several nanometers to tens of nanometers and the length from hundreds of nanometers to tens of micrometers even up to centimeter-level. CNTs can be classified into single-walled carbon nanotubes (SWNTs) and multi-walled carbon nanotubes (MWNTs) according to layer number. A single layer of graphene sheet is rolled up into the former, and the latter comprising 2-50 concentric cylindrical shells of graphene sheets with a fixed distance between layer and layer (ca. 0.34 nm).

As a one-dimensional nanomaterial, carbon nanotubes have unique surface effect, small size effect, quantum effect and macro quantum tunnel effect, meanwhile, its unique hollow tubular structure gives excellent mechanical, electrical, thermal properties. In addition, CNTs show the excellent performance on adsorbing gas and liquid due to its stable chemical properties and great specific surface area, expecting to be used as a new hydrogen storage material and adsorbent. CNTs have been applied in many fields such as composite material [2], hydrogen storage [3], catalyst support [4], anti-cancer drug carrier [5], battery [6], modified electrode [7], chemical sensor [8], microscope probe [9], separation[10-11-12], etc. because of the above mentioned excellent properties.

In practical applications, although CNTs have excellent performance, it is easy to aggregate into bundles and ropes due to van der Waals forces between tubes. In addition, it is almost insoluble in water and organic solvents because of its smooth surface with very few dangling bonds. This greatly restricts its applications in various aspects. Therefore, it is necessary to functionalize CNTs to improve its solubility. The novel functionalized composites may meet the demands of practical applications. With the improvement of the preparation technology for CNTs, the functionalization of CNTs has been a main research direction.



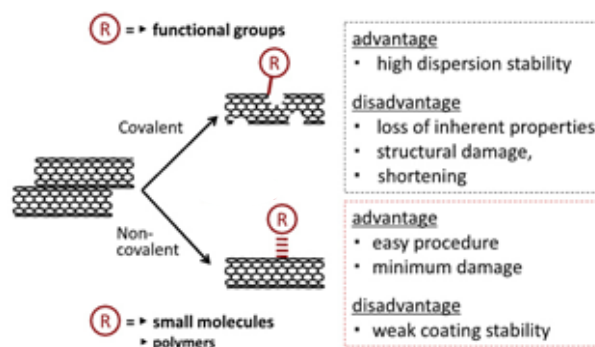


FIGURE 1

**Main CNTs functionalization methods. Reprinted with permission from ref 14. (This work is licensed under the Creative Commons Attribution 3.0 licence. To view a copy of this license, visit <https://creativecommons.org/licenses/by/3.0/>.)**

**Solid phase extraction.** Solid phase extraction (SPE), a separation technique put forward in the 1970s, is a sample pretreatment technique based on liquid-solid separation and extraction, developed from liquid-solid extraction technique combined with column liquid chromatography. The measurable substance is selectively adsorbed on the fine-grained porous solid adsorbent from the solution and then eluted by another solvent with smaller volume or thermal desorption method, thus, it can be separated and concentrated. It is an effective way to extract and concentrate target species simultaneously.

Compared with conventional liquid liquid extraction, SPE has the following advantages: no use large amount of organic solvents, no emulsification, high efficiency of sample treatment, effective separation, simple operation, high recovery, good reproducibility, easy to realize automation, etc. SPE has been one of the most commonly used sample pretreatment method presently.

The extraction efficiency of SPE is influenced by various factors, such as type and amount of adsorbent, type and property of eluent, volume of sample solution, sampling flow rate, sample matrix, etc. The property of adsorbent directly influences the reliability and accuracy of analytical method, thus, it is important to select proper adsorption materials.

Compared with conventional adsorbents, CNTs has large adsorption capacity and short equilibration time [13]. A large number of literatures have reported its application in the fields of adsorption and SPE.

This paper will summarize the functionalization methods of carbon nanotubes and its application in the adsorption and SPE, and prospect its further promising application.

## THE FUNCTIONALIZATION OF CARBON NANOTUBES

As shown in Fig. 1[14], the functionalization methods of CNTs can be divided into two major categories: covalent functionalization and non-covalent functionalization. For covalent functionalization, the chemical groups are covalently connected with the conjugate skeleton of CNTs through chemical reactions, which may occur on the tips or sidewall of CNTs. The chemical activity of the tips is the strongest. CNTs often need to be oxidized before functionalized to get oxygen-containing groups at sidewalls and tips that can be modified as active sites. The sidewall defects (e.g. vacancy, pentagon-heptagon) on CNTs may increase its chemical activity. The functionalization of the sidewall may produce sp<sup>3</sup> carbon and destruct the band to band transition of  $\pi$  electrons, resulting in the decrease of its excellent properties such as conductivity, mechanical performance, etc. Compared with covalent functionalization, for non-covalent functionalization with the advantage that the structure and electron system of CNTs itself may not be destructed, the supermolecular with functional groups (polyaromatic hydrocarbon, surfactant, polymer, biomolecule) is adsorbed or coated on CNTs surface through non-covalent interaction (Van der Waals force,  $\pi$ - $\pi$  interaction).

**Covalent functionalization. (1) Defect site chemistry - oxidation reactions.** Oxidation of CNTs is the most widely studied among various surface functionalization methods. Early treatment approaches used gas-phase oxidation mainly in air and oxidative plasmas. A report also mentions a method to introduce oxygen species on the sidewalls of CNTs using nitric acid vapor [15]. Liquid-phase oxidation mainly involved hot nitric acid or

sulfuric/nitric acid [16]. Sonication assisted oxidation treatment of CNTs in mixed acid increases the population density of surface oxide groups onto CNTs sidewalls [17]. Using piranha solutions may yield short, cut nanotubes [18].

#### (2) Esterification-amidation reactions.

Carboxylated CNTs is often used as precursors for further covalent functionalization. Carboxylic groups on the sidewalls and tips of CNTs are converted to acyl chloride groups via reaction with thionyl or oxalyl chloride, followed by the introduction of proper alcohol or amine. Other substituents, including organic substances, biomolecules, polymers, or photosensitive compounds, can be interacted with CNTs by this procedure [19]. Acyl chloride-modified MWNTs reacted with highly branched molecules like poly(amidoamine) (PAMAM) dendrons, resulting in dendrimer-MWNTs hybrid materials, employed as templates for the deposition of silver nanoparticles [20].

**(3) Halogenation.** Treatment of purified SWNTs with peroxytrifluoroacetic acid under ultrasonication generated not only oxygen based functional groups, but also trifluoroacetic groups covalently attached to the SWNT surface. Moreover, these functionalized SWNTs were shortened into ca. 300 nm length, easily dispersed in polar solvents such as DMF, water and ethanol [21]. Fluorinated SWNTs can be covalently functionalized with urea, guanidine, thiourea and aminosilane moieties, resulting in partial substitution of fluorine atoms [19]. The iodination of SWNTs via modified Hunsdiecker reactions can further introduce aryl halides or large aromatic moieties onto CNTs surface by metal-mediated coupling reactions [22].

**(4) Other covalent functionalization methods.** In addition to the abovementioned covalent approaches, there are other methods like complexation reactions, cycloaddition reactions, radical additions, nucleophilic additions, electrophilic additions, ionic liquids, electrochemical modifications, plasma-activation, mechanochemical functionalizations [19], and click chemistry developed in recent years [23].

**Non-covalent functionalization. (1) Polynuclear aromatic compounds.** Aromatic derivatives carrying a hydrophilic or hydrophobic moiety can dissolve CNTs in aqueous and organic media. Nakashima et al. [24] studied the solubilization of CNTs in aqueous solutions with phenyl, naphthalene, phenanthrene, and pyrene-ammonium amphiphiles, and stated the importance of  $\pi$ - $\pi$  interactions between the aromatic moieties

and CNTs sidewalls. Dai et al. [25] synthesized a variety of biomolecules modified CNTs using the  $\pi$ - $\pi$  interactions between pyrene derivatives and CNTs.

**(2) Surfactants.** Surfactants are amphiphilic, whose hydrophilic parts interact with the solvent and hydrophobic parts are adsorbed onto CNTs surface, thus preventing CNTs from the aggregation into bundles and ropes and dispersing them in the solvent. Cationic, anionic and nonionic surfactants can be used for non-covalent functionalization of CNTs. Typical examples include cetyltrimethyl ammonium bromide (CTAB), sodium dodecyl sulfate (SDS), Triton, etc. The literature [26] discussed the mechanism of dispersing CNTs in the surfactant solutions.

**(3) Polymers.** Polymer wrapping through non-covalent interactions may control the surface properties of CNTs and increase its stability and dispersity in the solvent. The wrapped polymers on CNTs surface have been utilized to support and/or reinforce the unique functionality of the CNTs, leading to the development of high-performance devices. Fujigaya et al. [14] reviewed various polymer wrapping approaches, together with the applications of the polymer-wrapped CNTs. Using  $\pi$ - $\pi$  interactions between conjugated luminescent polymers PmPV and SWNTs could give a stable suspension of SWNTs [27]. The hydrophobic interactions mostly with side chains ensure strong binding of the amphiphilic polycation to the CNTs surface, while the hydrophilic parts of the polymers provide solubility in polar solvents [28]. A new type of SWNTs doping polymers, as a replacement for indium tin oxide, a commodity transparent conductor, has the advantages like good mechanical properties, smooth, high temperature resilience, etc [29].

**(4) Biomolecules.** Various biomolecules, including natural proteins with high molecular weight like lysozyme [30], oligopeptides like cyclic peptide [31], polysaccharides like chitosan [32], nucleic acid like single-stranded DNA [33], can be spontaneously adsorbed onto the sidewalls of CNTs through hydrophobic interaction, improving the dispersity of CNTs in solutions. The non-covalent functionalized CNTs with bioactivities have opened up an entire new and exciting research direction in the field of chemical biology.

**Other functionalization methods.** Besides the abovementioned covalent and non-covalent functionalization approaches, fullerenes, organic substances, inorganic substances, etc. can be encapsulated in the cavity of CNTs. Metal nanoparticles also can be decorated on the surface of

CNTs through covalent linkage, electrodeposition, non-covalent interactions [19].

## THE APPLICATION OF CNTS IN ADSORPTION AND SPE

CNTs have rich porous structure with large specific area. Therefore, it has excellent adsorption capability. In addition, CNTs have stable chemical property and can be functionalized via multiple methods. In adsorbing harmful metal ions (e.g. Cr(VI), Cd(II), As(V), Hg(II), Pb(II), etc.) and organic pollutants in water, CNTs have high adsorption capacity and high adsorption speed, far better than conventional adsorption materials such as activated carbon. It has important applications in the fields of adsorption and SPE.

**Adsorption and SPE of metal ions.** Existing researches have shown that CNTs are a potential adsorption material for heavy metals in aqueous solutions. In 2010, Pyrzynska [10] overviewed the applications of CNTs for enrichment and separation of metal ions, and speciation. The sorption mechanism appears to be mainly attributable to chemical interactions between metal ions and the functional groups on the surface. The main mechanism is considered to be surface complexation with functional groups (Fig. 2) [10]. Thus, the sorption performance is mainly related to the properties and concentration of these groups. The effects of surface oxidation and chemical functionalization, sorption capacities and process parameters, are also discussed. Numerous studies explained the sorption mechanism mainly by oxygen-containing functional groups on CNTs surfaces but neglected the potential role of metal catalyst residues in CNTs. The literature [34] firstly reported the effect of residual metal impurities (Co and Mo) in one type of commercially available CNTs (P-CNTs) on the adsorption of Pb(II) from water.

The metal impurities released into the solutions during the sorption, and experiments demonstrated that PbMoO<sub>4</sub> formation between Pb(II) and CNT-released MoO<sub>4</sub><sup>2-</sup> and subsequent precipitation in the sorptive solutions is the main mechanism for the apparent sorption of Pb(II) by P-CNTs. Thus, sorption capacity of P-CNTs (27.3 mg g<sup>-1</sup>) for Pb(II) was much higher than that of the water-washed P-CNTs (4.7 mg g<sup>-1</sup>). Qiu et al. [35] studied the adsorption of Cr(VI) on MWNTs in aqueous solution. Effects of Cr(VI) concentration, solution pH, coexisting Cr(III) on the Cr(VI) adsorption were examined. Acid condition, low pH, is favorable for the adsorption. The maximum adsorption capacity is 532.215 mg g<sup>-1</sup>. Addition of Cr(III) into the solution could decrease the Cr(VI) removal capacities because of their competitive adsorption on CNTs. Under the same conditions, CNTs showed an adsorption capacity of Cr(VI) 2-6 times as large as the commercial activated carbon. The literature [36] studied competitive adsorption of heavy metal ions on CNTs and the desorption in simulated biofluids. Oxidized CNTs had meaningful adsorption capacities for Pb<sup>2+</sup>, Cu<sup>2+</sup>, Zn<sup>2+</sup> and Cd<sup>2+</sup>, while Pb<sup>2+</sup> showed the highest adsorption in the competitive adsorption evaluations. The desorption behaviors of heavy metal ions were completely different in various biofluids, where the desorption was significantly influenced by pH and the presence of proteins/other cations. The desorption was most effective in simulated stomach juice, and much less effective in other simulated biofluids. More Pb<sup>2+</sup> stuck to CNTs than others, resulting in less desorption. Interestingly, the competitive desorption behaviors of four ions were largely changed comparing to the individual desorption behaviors. This work also has a certain meaning to the biosafety evaluations of CNT.

The sorption mechanisms of metal ions on CNTs composites obtained via various functionalization methods are related to not only the properties of CNTs itself but also the introduced

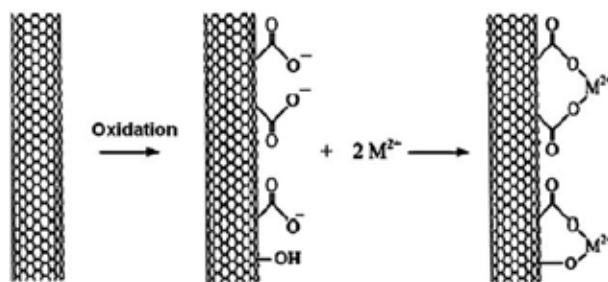


FIGURE 2

Major mechanism for sorption of metal ions onto the surface of a carbon nanotube. Reprinted with permission from ref 10. Copyright 2010 Elsevier.

molecules/groups in the functionalization process. The main purpose of functionalization is to effectively eliminate its non-specific adsorption toward target species, improve its sorption capacity, sorption selectivity and anti-interfering capability. According to the authors' work [37], modified MWNTs with noncovalent wrapping by a hydrophilic polyelectrolyte PDDA converts the surface charge property of MWNTs and provides a favorable adsorbent for the selective adsorption of Cr(VI) in the presence of a certain amount of Cr(III). When compared to bare MWNTs, the PDDA-MWNTs composites offers a much improved adsorption efficiency for Cr(VI). In another work [38], the incubation of MWNTs in Fe<sup>3+</sup> solution produces a layer of amorphous FePO<sub>4</sub> assembled on its surface. The functionalized MWNTs composites are found to exhibit excellent adsorption selectivity toward cadmium in comparison with bare carbon nanotubes. The composites also provide a much higher adsorption capacity to cadmium. Tan et al. [39] used anionic surfactant SDBS to enhance the adsorption of nickel on oxidized MWNTs. The adsorption mechanism was mainly attributed to

chemical interaction between nickel and the surface functional groups of MWNTs and surface adsorbed SDBS. The adsorbed SDBS on MWNTs could lead to the modification of the MWNTs surfaces and partial complexation of nickel with SDBS adsorbed on MWNTs. Hu et al. [40] synthesized the magnetic composite of  $\beta$ -cyclodextrin grafted onto MWNTs/iron oxides to remove Pb(II) from aqueous solutions. The adsorption capacity is 12.29 mg g<sup>-1</sup>, apparently higher than MWNTs/iron oxides, oxidized MWNTs and iron oxides. The grafted  $\beta$ -cyclodextrin on the MWNTs/iron oxides contributed to an enhancement of the adsorption capacity because of the strong abilities of the multiple hydroxyl groups and the inner cores of the hydrophobic cavity in  $\beta$ -cyclodextrin to form complexes with metal ions.

A large number of literatures have reported the SPE of metal ions by CNTs, as shown in Table 1. Soyak et al. [41] used MWNTs for on-line preconcentration of Cu(II) in natural waters. Zhao et al. [42] used oxidized MWNTs for on-line preconcentration of Cu, Zn, Mn, Pb. Chen et al. [43]

**TABLE 1**  
**Examples of carbon nanotubes in the solid phase extraction of metal ions**

Adsorbent	Metal	ACa (mg g <sup>-1</sup> )	PFb	Technique	Sample	LODc ( $\mu$ g L <sup>-1</sup> )	Ref.
MWNTs	Cu(II)		60	FAAS	Natural waters	1.46	41
Oxidized MWNTs	Cu Zn Mn Pb		20.3 14.2 20.6 15.4	FAAS	Vegetables	0.59 0.62 0.28 1.00	42
SWNTs	Mn(II) Mn(VII)	0.87 0.53		ICP-MS	Biological and environmental samples	0.031 0.054	43
Oxidized MWNTs	Ni Pb			ETAAS	Municipal sludge, Lake sediment	0.03 0.01	44
NBHAE-MWNTs	Au(III) Mn(II)	75 7.5	250	FAAS	Tap, well and waste waters	0.03 0.01	45
EDA modified MWNTs	Cr(III) Fe(III) Pb(II)	39.58 28.69 54.48	200	ICP-OES	Biological and natural water samples	Under 0.35	46
L-tyr-CNTs	Co	37.58 $\pm$ 3.06d	180	FAAS	Natural waters	0.05	47
CTAC hemimicellecapped MWNTs	As			HG-AFS	Environmental waters	0.02	48
PIDA-MWNTs	Fe(III) Cu(II) Pb(II)	64.5 30.5 17.0	100	ICP-OES	River and tap waters	0.26 0.15 0.18	49
MWNTs- D2EHPA-TOPO	Cu Ni Zn	4.90 4.78 4.82	25	FAAS	Natural water, electroplating waste waters	50 40 60	50
BSA modified MWNTs	Cd	21.98	10.8	TS-FF-AAS	Blood serum	0.24	51

ACa: Adsorption capacity; PFb: Preconcentration factor; LODc: Limit of detection  
d:  $\mu$ mol Co g<sup>-1</sup> of CNTs (Column capacity)

used SWNTs for simultaneous enrichment of Mn(II) and Mn(VII). Savio et al. [44] compared the adsorption performance of MWNTs, oxidized MWNTs and L-alanine modified MWNTs, and used oxidized MWNTs with the optimal adsorption performance for on-line enrichment of Ni and Pb. Shamspur et al. [45] used Schiff base modified MWNTs for on-line enrichment of trace Au(III) and Mn(II) in waters simultaneously. Zang et al. [46] used EDA modified MWNTs for simultaneous enrichment of Cr(III), Fe(III) and Pb(II) in biological and natural water samples. Pacheco et al. [47] used L-tyrosine modified MWNTs for the preconcentration of Co in natural waters. Li et al. [48] used surfactant CTAC hemimicellecapped MWNTs for on-line enrichment of As in environmental waters. Cui et al. [49] used MWNTs covalently grafted by phenyl-iminodiacetic acid groups for SPE of trace Fe(III), Cu(II) and Pb(II) in environmental waters. Vellaichamy et al. [50] used MWNTs-D2EHFA-TOPO for on-line enrichment of Cu, Ni and Zn, and analyzed electroplating waste water, tap water and well water. Barbosa et al. [51] functionalized bovine serum albumin (BSA) on MWNTs surface for direct extraction of cadmium from human serum samples.

**Adsorption and SPE of organic compounds and biomolecules.** The literatures [12,52] summarized the applications and mechanisms of organic chemical adsorption on CNTs, considering that different mechanisms may act simultaneously, mainly hydrophobic interactions,  $\pi$ - $\pi$  bonds, electrostatic interactions, and hydrogen bonds. In 2015, Apul et al. [53] reviewed the adsorption of synthetic organic contaminants from waters by carbon nanotubes in recent 10 years. Adsorption depends upon the physicochemical properties of the adsorbates and CNTs as well as the background water chemistry. Among all properties reported in the literature, no parameter was reported as solely controlling the adsorption. Besides the two major factors: specific surface area and pore volume, hydrophobic interaction is the primary driving force for the adsorption of organic compounds from water on CNTs surface. Other principle factors are,  $\pi$ - $\pi$  interactions between  $\pi$  electron density of organic compounds and rich  $\pi$  electrons on CNTs surface, and, polar moieties of organic compounds enhancing dipole-dipole attractions. In addition, molecular size of organic compounds, oxygen content on CNTs surface are also proposed influencing the adsorption. In general, pH and ionic strengths exhibited no significant difference on nonionic organic compounds. Some dependence to pH and ionic strength were observed for adsorption of ionizable organic compounds (e.g. phenolic compounds, anilines etc.), existing two counter-balancing forces

influencing adsorption: salting-out effect and squeezing-out effect. In terms of temperature effect, adsorption of organic compounds by CNTs was predominantly reported as an exothermic process; therefore, increase in temperature decreased adsorption capacity. As illustrated in the research of Chen et al. [54], the adsorption affinity of organic compounds with CNTs increased in the order of nonpolar aliphatic < nonpolar aromatics < nitroaromatics. The strong adsorptive interaction between CNTs and nitroaromatics was due to  $\pi$ - $\pi$  interactions. Dai et al. [25] developed a controlled method for immobilizing proteins onto SWNTs. The results showed that the highly aromatic compounds could interact with CNTs surface via  $\pi$  stacking.

Many references have reported SPE of organic compounds by CNTs. Cai et al. [55] developed a method for the enrichment of bisphenol A, 4-n-nonylphenol, and 4-tert-octylphenol by using a MWNTs-packed cartridge. The retained analytes are desorbed with methanol and determined by HPLC-FL, achieving LOD of 0.083, 0.024, and 0.018 ng mL<sup>-1</sup>, respectively. The developed method was applied to analyzing environmental water samples. Yu et al. [56] used MWNTs for simultaneous SPE of 11 triazine herbicides residues in Songhuajiang river water detected by LC-MS-MS with LOD lower than 0.1 ng L<sup>-1</sup>. Springer et al. [57] developed a method for chlorsulfuron and metsulfuron methyl determination in water samples using MWNTs and capillary electrophoresis, with LOD of 0.40 and 0.36  $\mu$ g L<sup>-1</sup>. Lu et al. [58] used MWNTs as SPE adsorbent for the determination of chloramphenicol in egg, honey, and milk by HPLC-MS-MS, with LOD of 0.003-0.004  $\mu$ g kg<sup>-1</sup>. Luo et al. [59] used magnetic MWNTs for extraction of 16 phthalate acid esters from beverage, environmental water and perfume samples by GC-MS, with LOD of 4.9-38 ng L<sup>-1</sup>. Chen et al. [60] used magnetic MWNTs for enrichment of linear alkylbenzene sulfonates in environmental water samples by HPLC-UV, with enrichment factor of 500 and LOD of 0.013-0.021  $\mu$ g L<sup>-1</sup>. Lee et al. [61] used magnetic MWNTs for extraction of volatile organic compounds including benzene, toluene, ethyl benzene, xylene, and styrene detected by GC-MS with LOD of 0.7-0.9 ppbv.

In 2007, Wang's research group in Northeastern University firstly used functionalized CNTs as SPE adsorbents for isolation and preconcentration of biomolecules. Using hemoglobin and cytochrome c as model proteins, MWNTs were employed as sorbents for the isolation and preconcentration of basic proteins from biological sample matrices, through oxidative modification of MWNTs surface [62]. It was considered that the protein adsorption onto carbon nanotubes might be attributable to electrostatic interaction and that an ion-exchange mechanism was

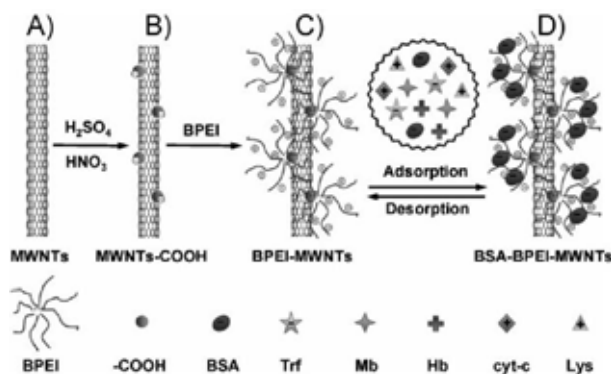


**FIGURE 3**

**Illustrations of the functionalization process of MWNTs with the hyperbranched polyethyleneimine (BPEI) and its adsorption of proteins. A: MWNTs; B: MWNTs oxidized with a sulfuric acid/nitric acid mixture; C: the immobilization of BPEI onto the sidewalls of MWNTs; D: selective adsorption of BSA by the functionalized BPEI-MWNTs. Reprinted with permission from ref 64. Copyright 2010 Wiley-VCH.**

involved in the elution/desorption process. In addition, through appropriate choice of the elution conditions, sequential elution of protein species with different isoelectric points from each other might be achieved. The practical applicability of this system was demonstrated by processing of human whole blood for isolation of hemoglobin. PDDA-MWNTs composites [63] were used for on-line enrichment of acidic proteins from human whole blood detected by UV-Vis, with sorption capacity of 26 mg g<sup>-1</sup>, enrichment factor of 14, and LOD of 1.0 µg mL<sup>-1</sup>. As shown in Fig.3, hyperbranched BPEI functionalized MWNTs composites, BPEI-MWNTs [64], were employed for on-line enrichment of human serum albumin from whole blood. The branched architecture of polyelectrolyte on the surface of carbon nanotubes significantly improved the adsorption capacity of proteins due to the fact that the branched polyelectrolyte provides a lot more positions for protein adsorption on its branches and effectively reduces the lateral repulsion of protein molecules within the adsorbed layer. A dynamic adsorption capacity of 167 mg g<sup>-1</sup> for BSA was achieved, along with enrichment factor of 10 and LOD of 0.74 µg mL<sup>-1</sup>. Chitosan/MWNTs composites [65] were applied for extraction of hemoglobin from human whole blood detected by UV-Vis, with sorption capacity of 15.41 mg g<sup>-1</sup>. Ding et al. [66] used magnetic carbon nanotubes for extraction of estrogens in milk by HPLC-FL, with LOD of 1.21-2.35 µg L<sup>-1</sup>. Vinas et al. [67] used MWNTs as SPE adsorbents for on-line speciation of 4 cobalamins in seafoods by HPLC-UV, with LOD of 0.35-30 ng mL<sup>-1</sup>. Huang et al. [68] described a method for SPE of biogenic thiols (glutathione, cysteine, acetylcysteine) in human urine and blood samples using MWNTs as adsorbent, and their

subsequent determination via HPLC-FL. The respective LOD were 20, 4, 80 pM.

## SUMMARY AND OUTLOOK

Carbon nanotubes have excellent adsorption capability due to its unique structure and potentially broad application in the fields of adsorption and SPE. Future work can focus on the following areas:

Its application range can be broadened through developing multiple functionalization methods, novel SPE methods and analytical techniques for trace analysis. Select the type of functional group for target substances and improve the functionalization methods to improve the sorption selectivity and analytical sensitivity.

At present there are only few commercialization applications of CNTs in the fields of adsorption and SPE, possibly because of relatively high cost of preparation/purification techniques of CNTs. Thus, it is necessary to develop cheap and fine preparation/purification techniques and functionalization methods to lower costs and open up a new path to its industrialization.

Studies on SWNTs in adsorption and SPE are relatively less, possibly because its market price is considerably higher than MWNTs. However, the specific area of SWNTs is higher than MWNTs (SWNTs: 373±146m<sup>2</sup>g<sup>-1</sup>; MWNTs: 216±159 m<sup>2</sup>g<sup>-1</sup>) [53]. So we should also promote the future study on SWNTs.

There are more studies on adsorption equilibrium of CNTs than its adsorption kinetics and desorption behavior in present literatures, which are equally important in understanding the adsorption process. We should strengthen this work in future research.

Although some work has been done on the exploration of adsorption mechanisms and the building of adsorption models for CNTs, it is still rather shallow, especially for the adsorption behavior and mechanism of CNTs in heterogeneity and complex system.

## ACKNOWLEDGEMENTS

This work was supported by the National Natural Science Foundation of China (21407018, 41206095), the Fundamental Research Funds for the Central Universities (3132014101, 3132015221) and Scientific Public Research Foundation of Liaoning Province (2013003007).

## REFERENCES

- [1] Iijima, S. (1991) Helical microtubules of graphite carbon. *Nature*, 354, 56-58.
- [2] Wang, J. L., Xiong, G. P., Gu, M., Zhang, X. and Liang, J. (2009) A study on the thermal conductivity of multiwalled carbon nanotube/polypropylene composite. *Acta Phys. Sin.*, 58, 4536-4541.
- [3] Orinakova, R. and Orinak, A. (2011) Recent applications of carbon nanotubes in hydrogen production and storage, *Fuel*, 90, 3123-3140.
- [4] Che, G. L., Lakshmi, B. B., Fisher, E. R. and Martin, C. R. (1998) Carbon nanotubule membranes for electrochemical energy storage and production, *Nature*, 393, 346-349.
- [5] Zhang, W. X., Zhang, Z. Z. and Zhang, Y. G. (2011) The application of carbon nanotubes in target drug delivery systems for cancer therapies, *Nanoscale Res. Lett.*, 6, 555.
- [6] Li, C. M., Zhao, L. Z., Liu, Z. P., Zhang, R. Y. and Li, W. S. (2009) Electrochemical performance of carbon nanotubes as anode materials for lithium ion battery. *New Chem. Mater.*, 37, 28-29.
- [7] Zhu, Y. P., Yuan, R., Chai, Y. Q., Qin, S. and Yuan, Y. L. (2012) An immunosensor for  $\alpha$ -fotoprotein antigen based on multi-walled nanotubes/L-cysteine and Au@Fe<sub>3</sub>O<sub>4</sub> nanocomposite. *Chinese J. Anal. Chem.*, 40: 359-364.
- [8] Kong, J., Franklin, N. R., Zhou, C. W., Chapline, M. G., Peng, S., Cho, K. J. and Dai, H. J. (2000) Nanotube molecular wires as chemical sensors. *Science*, 287, 622-625.
- [9] Natsuki, T., Ni, Q. Q. and Endo, M. (2011) Stability analysis of double-walled carbon nanotubes as AFM probes based on a continuum model. *Carbon*, 49, 2532-2537.
- [10] Pyrzynska, K. (2010) Carbon nanostructures for separation, preconcentration and speciation of metal ions. *TrAC, Trends Anal. Chem.*, 29, 718-727.
- [11] Valcarcel, M., Cardenas, S., Simonet, B. M., Moliner-Martinez, Y. and Lucena, R. (2008) Carbon nanostructures as sorbent materials in analytical processes. *TrAC, Trends Anal. Chem.*, 27, 34-43.
- [12] Yang, K. and Xing, B. S. (2010) Adsorption of organic compounds by carbon nanomaterials in aqueous phase: Polanyi theory and its application. *Chem. Rev.*, 110, 5989-6008.
- [13] Hu, X., Zhao, N. and Wei, J. (2009) Adsorption of triclosan on carbon nanotubes. *Chinese J. Environ. Eng.*, 8, 1462-1464.
- [14] Fujigaya, T. and Nakashima, N. (2015) Non-covalent polymer wrapping of carbon nanotubes and the role of wrapped polymers as functional dispersants. *Sci. Technol. Adv. Mater.*, 16, 024802 (21 pp).
- [15] Xia, W., Jin, C., Kundu, S. and Muhler, M. (2009) A highly efficient gas-phase route for the oxygen functionalization of carbon nanotubes based on nitric acid vapor, *Carbon*, 47, 919-922.
- [16] Datsyuk, V., Kalyva, M., Papagelis, K., Parthenios, J., Tasis, D., Siokou, A., Kallitsis, I. and Galiotis, C. Chemical oxidation of multiwalled carbon nanotubes, *Carbon*, 2008, 46, 833-840.
- [17] Xing, Y. C., Li, L., Chusuei, C. C. and Hull, R. V. (2005) Sonochemical oxidation of multiwalled carbon nanotubes, *Langmuir*, 21, 4185-4190.
- [18] Ziegler, K. J., Gu, Z. N., Peng, H. Q., Flor, E. L., Hauge, R. H. and Smalley, R. E. (2005) Controlled oxidative cutting of single-walled carbon nanotubes. *J. Am. Chem. Soc.*, 127, 1541-1547.
- [19] Karousis, N., Tagmatarchis, N. and Tasis, D. (2010) Current progress on the chemical modification of carbon nanotubes. *Chem. Rev.*, 110, 5366-5397.
- [20] Tao, L., Chen, G. J., Mantovani, G., York, S. and Haddleton, D. M. (2006) Modification of multi-wall carbon nanotube surfaces with poly(amidoamine) dendrons: Synthesis and metal templating. *Chem. Commun.*, 47: 4949-4951.
- [21] Liu M H, Yang Y L, Zhu T, et al. (2005) Chemical modification of single-walled carbon nanotubes with peroxytrifluoroacetic acid. *Carbon*, 43(7): 1470-1478.
- [22] Coleman, K. S., Chakraborty, A. K., Bailey, S. R., Sloan, J. and Alexander, M. (2007) Iodination of single-walled carbon nanotubes. *Chem. Mater.*, 19, 1076-1081.

- [23] Song, Y. J., Qu, K. G., Xu, C., Ren, J. S. and Qu, X. G. (2010) Visual and quantitative detection of copper ions using magnetic silica nanoparticles clicked on multiwalled carbon nanotubes. *Chem. Commun.*, 46, 6572-6574.
- [24] Tomonari, Y., Murakami, H. and Nakashima, N. (2006) Solubilization of single-walled carbon nanotubes by using polycyclic aromatic ammonium amphiphiles in water-Strategy for the design of high-performance solubilizers. *Chem. Eur. J.*, 12, 4027-4034.
- [25] Chen, R. J., Zhang, Y. G., Wang, D. W. and Dai, H. J. (2001) Noncovalent sidewall functionalization of single-walled carbon nanotubes for protein immobilization. *J. Am. Chem. Soc.*, 123, 3838-3839
- [26] Wang H. (2009) Dispersing carbon nanotubes using surfactants. *Curr. Opin. Colloid Interface Sci.*, 14(5): 364-371.
- [27] Star, A., Stoddart, J. F., Steuerman, D., Diehl, M., Boukai, A., Wong, E. W., Yang, X., Chung, S. W., Choi, H. and Heath, J. R. (2001) Preparation and properties of polymer-wrapped single-walled carbon nanotubes. *Angew. Chem. Int. Ed.*, 40, 1721-1725.
- [28] Sinani, V. A., Gheith, M. K., Yaroslavov, A. A., Rakhnyanskaya, A. A., Sun, K., Mamedov, A. A., Wicksted, J. P. and Kotov, N. A. (2005) Aqueous dispersions of single-wall and multiwall carbon nanotubes with designed amphiphilic polycations. *J. Am. Chem. Soc.*, 127, 3463-3472.
- [29] Zhu, J., Shim, B. S., Di.Prima, M. and Kotov, N. A. (2011) Transparent conductors from carbon nanotubes LBL-assembled with polymer dopant with pi-pi electron transfer. *J. Am. Chem. Soc.*, 133, 7450-7460.
- [30] Nepal, D. and Geckeler, K. E. (2006) pH-sensitive dispersion and debundling of single-walled carbon nanotubes: Lysozyme as a tool. *Small*, 2, 406-412.
- [31] Ortiz-Acevedo, A., Xie, H., Zorbas, V., Sampson, W. M., Dalton, A. B., Baughman, R. H., Draper, R. K., Musselman, I. H. and Dieckmann, G. R. (2005) Diameter-selective solubilization of single-walled carbon nanotubes by reversible cyclic peptides. *J. Am. Chem. Soc.*, 127, 9512-9517.
- [32] Gandra, N., Chiu, P. L., Li, W. B., Anderson, Y. R., Mitra, S., He, H. X. and Gao, R. M. (2009) Photosensitized singlet oxygen production upon two-photon excitation of single-walled carbon nanotubes and their functionalized analogues. *J. Phys. Chem. C*, 113, 5182-5185.
- [33] So, H. M., Won, K., Kim, Y. H., Kim, B. K., Ryu, B. H., Na, P. S., Kim, H. and Lee, J. O. (2005) Single-walled carbon nanotube biosensors using aptamers as molecular recognition elements. *J. Am. Chem. Soc.*, 127, 11906-11907.
- [34] Tian, X. L., Zhou, S., Zhang, Z. Y., He, X. A., Yu, M. J. and Lin, D. H. (2010) Metal impurities dominate the sorption of a commercially available carbon nanotube for Pb(II) from water. *Environ. Sci. Technol.*, 44, 8144-8149.
- [35] Qiu, K. D. and Li, W. B. (2006) Adsorption of hexavalent chromium ions on multi-wall carbon nanotubes in aqueous solution. *Acta Phys. - Chim. Sin.*, 22, 1542-1546.
- [36] Ma X, Yang S -T, Tang H, Liu, Y. F. and Wang, H. F. (2015) Competitive adsorption of heavy metal ions on carbon nanotubes and the desorption in simulated biofluids. *J. Colloid Interf. Sci.* 448: 347-355.
- [37] Zhang, X. X., Chen, M. L., Yu, Y. L., Yang, T. and Wang J. H. (2011) Polyelectrolyte-modified multi-walled carbon nanotubes for the adsorption of chromium(VI). *Anal. Methods*, 3, 457-462.
- [38] Zhang, X. X., Zhang, L. P., Yang, T., Shen, L. M., Chen, M. L. and Wang J. H. (2012) Improvement on the selectivity and sorption capacity of cadmium by iron loaded carbon nanotubes with detection by electrothermal atomic absorption spectrometry. *J. Anal. Atom. Spectrom.*, 27, 1680-1687.
- [39] Tan, X. L., Fang, M., Chen, C. L., Yu, S. M. and Wang, X. K. (2008) Counterion effects of nickel and sodium dodecylbenzene sulfonate adsorption to multiwalled carbon nanotubes in aqueous solution, *Carbon*, 46, 1741-1750.
- [40] Hu, J., Shao, D. D., Chen, C. L., Sheng, G. D., Li, J. X., Wang, X. K. and Nagatsu, M. (2010) Plasma-induced grafting of cyclodextrin onto multiwall carbon nanotube/iron oxides for adsorbent application. *J. Phys. Chem. B*, 114, 6779-6785.
- [41] Soylyak, M. and Ercan, O. (2009) Selective separation and preconcentration of copper(II) in environmental samples by the solid phase extraction on multi-walled carbon nanotubes. *J. Hazard. Mater.*, 168, 1527-1531.
- [42] Zhao, X. W., Song, N. Z., Jia, Q. and Zhou, W. H. (2009) Determination of Cu, Zn, Mn, and Pb by microcolumn packed with multiwalled carbon nanotubes on-line coupled with flame atomic absorption spectrometry. *Microchim. Acta*, 166, 329-335.
- [43] Chen, S. Z., Zhu, L., Chen, X. L., Wang, X. and Zhou, X. R. (2011) Simultaneous determination of Mn(II) and Mn(VII) by single-wall carbon nanotubes preconcentration hyphenated with ICP-MS. *At. Spectrosc.*, 32, 12-16.
- [44] Savio, M., Parodi, B., Martinez, L. D., Smichowski, P. and Gil, R. A. (2011) On-line



- solid phase extraction of Ni and Pb using carbon nanotubes and modified carbon nanotubes coupled to ETAAS. *Talanta*, 85, 245-251.
- [45] Shamspur, T., and Mostafavi, A. (2009) Application of modified multiwalled carbon nanotubes as a sorbent for simultaneous separation and preconcentration trace amounts of Au(III) and Mn(II). *J. Hazard. Mater.*, 168, 1548-1553.
- [46] Zang, Z. P., Hu, Z., Li, Z. H., He, Q. and Chang, X. J. (2009) Synthesis, characterization and application of ethylenediamine-modified multiwalled carbon nanotubes for selective solid-phase extraction and preconcentration of metal ions. *J. Hazard. Mater.*, 172, 958-963.
- [47] Pacheco, P. H., Smichowski, P., Polla, G. and Martinez, L. D. (2009) Solid phase extraction of Co ions using L-tyrosine immobilized on multiwall carbon nanotubes. *Talanta*, 79, 249-253.
- [48] Li, L., Huang, Y. M., Wang, Y. and Wang, W. D. (2009) Hemimicelle capped functionalized carbon nanotubes-based nanosized solid-phase extraction of arsenic from environmental water samples. *Anal. Chim. Acta*, 631, 182-188.
- [49] Cui, Y., Hu, Z. J., Yang, J. X. and Gao, H. W. (2012) Novel phenyl-iminodiacetic acid grafted multiwalled carbon nanotubes for solid phase extraction of iron, copper and lead ions from aqueous medium. *Microchim. Acta*, 176, 359-366.
- [50] Vellaichamy, S. and Palanivelu, K. (2011) Preconcentration and separation of copper, nickel and zinc in aqueous samples by flame atomic absorption spectrometry after column solid-phase extraction onto MWCNTs impregnated with D2EHPA-TOPO mixture. *J. Hazard. Mater.*, 185, 1131-1139.
- [51] Barbosa, A. F., Barbosa, V. M. P., Bettini, J., Luccas, P. O. and Figueiredo, E. C. (2015) Restricted access carbon nanotubes for direct extraction of cadmium from human serum samples followed by atomic absorption spectrometry analysis. *Talanta*, 131, 213-220.
- [52] Pan, B. and Xing, B. S. (2008) Adsorption mechanisms of organic chemicals on carbon nanotubes. *Environ. Sci. Technol.*, 42, 9005-9013.
- [53] Apul, O. G. and Karanfil, T. (2015) Adsorption of synthetic organic contaminants by carbon nanotubes: A critical review. *Water Res.*, 68, 34-55.
- [54] Chen, W., Duan, L. and Zhu, D. (2007) Adsorption of polar and nonpolar organic chemicals to carbon nanotubes. *Environ. Sci. Technol.*, 41, 8295-8300.
- [55] Cai, Y. Q., Jiang, G. B., Liu, J. F. and Zhou, Q. X. (2003) Multiwalled carbon nanotubes as a solid-phase extraction adsorbent for the determination of bisphenol a, 4-n-nonylphenol, and 4-tert-octylphenol. *Anal. Chem.*, 75, 2517-2521.
- [56] Yu, Z. G., Qin, Z., Ji, H. R., Du, X., Chen, Y. H., Pan, P., Wang, H. and Liu, Y. Y. (2010) Application of SPE using multi-walled carbon nanotubes as adsorbent and rapid resolution LC-MS-MS for the simultaneous determination of 11 triazine herbicides residues in river water. *Chromatographia*, 72, 1073-1081.
- [57] Springer, V. H. and Lista, A. G. (2010) A simple and fast method for chlorsulfuron and metsulfuron methyl determination in water samples using multiwalled carbon nanotubes (MWCNTs) and capillary electrophoresis. *Talanta*, 83, 126-129.
- [58] Lu, Y., Shen, Q., Dai, Z. and Zhang, H. (2010) Multi-walled carbon nanotubes as solid-phase extraction adsorbent for the ultra-fast determination of chloramphenicol in egg, honey, and milk by fused-core C18-based high-performance liquid chromatography-tandem mass spectrometry. *Anal. Bioanal. Chem.*, 398, 1819-1826.
- [59] Luo, Y. B., Yu, Q. W., Yuan, B. F. and Feng, Y. Q. (2012) Fast microextraction of phthalate acid esters from beverage, environmental water and perfume samples by magnetic multi-walled carbon nanotubes. *Talanta*, 90, 123-131.
- [60] Chen, B., Wang, S., Zhang, Q. M. and Huang, Y. M. (2012) Highly stable magnetic multiwalled carbon nanotube composites for solid-phase extraction of linear alkylbenzene sulfonates in environmental water samples prior to high-performance liquid chromatography analysis. *Analyst*, 137, 1232-1240.
- [61] Lee, P. L., Chiu, Y. K., Sun, Y. C. and Ling, Y. C. (2010) Synthesis of a hybrid material consisting of magnetic iron-oxide nanoparticles and carbon nanotubes as a gas adsorbent. *Carbon*, 48, 1397-1404.
- [62] Du, Z., Yu, Y. L., Chen, X. W. and Wang, J. H. (2007) The isolation of basic proteins by solid-phase extraction with multiwalled carbon nanotubes. *Chem. Eur. J.*, 13, 9679-9685.
- [63] Du, Z., Yu, Y. L. and Wang, J. H. (2009) Functionalization of multi-walled carbon nanotubes and their application for selective isolation of acidic proteins. *Macromol. Biosci.*, 9, 55-62.
- [64] Chen, M. L., Chen, M. L., Chen, X. W. and Wang, J. H. (2010) Functionalization of MWNTs with hyperbranched PEI for highly selective isolation of BSA. *Macromol. Biosci.*, 10, 906-915.
- [65] Chen, X. W., Wang, W. J., Song, Z. N. and Wang, J. H. (2011) Chitosan/carbon nanotube

composites for the isolation of hemoglobin in the presence of abundant proteins. *Anal. Methods*, 3, 1769-1773.

- [66] Ding, J., Gao, Q., Li, X. S., Huang, W., Shi, Z. G. and Feng, Y. Q. (2011) Magnetic solid-phase extraction based on magnetic carbon nanotube for the determination of estrogens in milk. *J. Sep. Sci.*, 34, 2498-2504.
- [67] Vinas, P., Lopez-Garcia, I., Bravo, M. B., Hernandez-Cordoba, M. (2011) Multi-walled carbon nanotubes as solid-phase extraction adsorbents for the speciation of cobalamins in seafoods by liquid chromatography. *Anal. Bioanal. Chem.*, 401, 1393-1399.
- [68] Huang, K. J., Han, C. H., Han, C. Q., Li, J., Wu, Z. W. and Liu, Y. M. (2011) Determination of thiol compounds by solid-phase extraction using multi-walled carbon nanotubes as adsorbent coupled with high-performance liquid chromatography-fluorescence detection. *Microchim. Acta*, 174(3-4): 421-427.

---

**Received: 10.10.2015**

**Accepted: 11.09.2016**

---

#### **CORRESPONDING AUTHOR**

---

**Xiaoxing Zhang**

College of Environmental Sciences and Engineering  
Dalian Maritime University  
Linghai Road No. 1  
Dalian, Liaoning 116026– P. R. CHINA

E-mail: xxcl126@126.com

# CHARACTERIZATION OF PM<sub>2.5</sub> AND IT'S CHEMICAL COMPOSITIONS UNDER DIFFERENT AIR QUALITY GRADES IN HANDAN, CHINA

Simeng Ma\*, Litao Wang, Zhe Wei, Fenfen Zhang, Chenchen Meng, Jing Yang

Department of Environmental Engineering, School of City Construction, Hebei University of Engineering, Handan, 056038

## ABSTRACT

The pollution characteristics of PM<sub>2.5</sub> and its chemical compositions under different air quality grades (HJ 633-2012) were analyzed from January 1 to December 31, 2013, by using the online monitoring data at four representative air quality monitoring sites, and the chemical compositions of sampled PM<sub>2.5</sub> in Handan. The results showed that the average annual concentration of PM<sub>2.5</sub> was 139  $\mu\text{g m}^{-3}$  in Handan city in 2013, which was about 4 times of the national Grade II standard (35  $\mu\text{g m}^{-3}$ ), and the percentages of the number of the days exceeding the national Grade II air quality standard (GB3095-2012) were 74.4%. There were no excellent days, and moderately to severely polluted days accounted for 50% throughout the year. With the deterioration of air quality grades, the mass concentrations of PM<sub>2.5</sub> and its chemical compositions were elevated, and the mass concentrations of most chemical compositions increased dramatically when severe pollution occurred except for a few elements. The mass concentrations of elemental carbon (EC) and organic matter (OM) on severely polluted days were approximately 5.9 and 5.5 times those of good days. NO<sub>3</sub><sup>-</sup>/SO<sub>4</sub><sup>2-</sup> and OC/EC ratio increase when air quality index (AQI) increased, and peaked in moderately and heavily polluted days, respectively, and slightly fall down under the severely polluted days. The enrichment factors (EF) of all elements had different degree of increase, and the EF of anthropogenic elements were elevated consistent with the increasing of the AQI, while the elements from crustal sources did not show the obvious change.

**KEYWORDS:** PM<sub>2.5</sub>; Air quality grades; Water-soluble inorganic ions; Carbonaceous components; Inorganic elements.

## INTRODUCTION

Frequent large scale and severe haze pollution occurred since 2013 over the regions of mid-eastern China, which causes wide attention of academic and public all over the world. The serious haze pollution has become the most urgent atmospheric environmental problems which need to solve. Hebei is the most polluted province in China. In the report by the Ministry of Environmental Protection of China, the most ten polluted cities in 2013 are Xingtai, Shijiazhuang, Handan, Tangshan, Baoding, Ji'nan, Hengshui, Xi'an, Langfang, and Zhengzhou, seven of which are located in Hebei province. Then the most ten polluted cities in 2014 are Baoding, Xingtai, Shijiazhuang, Tangshan, Handan, Hengshui, Ji'nan, Langfang, Zhengzhou and Tianjin.

The problem of air pollution in the southern Hebei was more serious than in the northern, which was related to the special geographical locations of the southern area [1]. Handan, located in the southern edge of Hebei and adjacent to Taihang Mountain, is the border of the four big industrial province (Shanxi, Henan, Shandong and Hebei). The air pollutants of Handan are industrial emissions, which are mainly caused by thermal power, steel, building materials and so on.

There are few related studies on the characteristics of PM<sub>2.5</sub> in Handan at present. The Mesoscale Modeling System Generation 5 (MM5) and the Models-3/Community Multi-Scale Air Quality (CMAQ) modeling system have been applied to simulate the severe regional hazes in East Asia and the northern China in winter in 2013 to quantify the space and sector sources [2, 3]. The pollution characteristics of particulate matter in summer and autumn in Handan city were analyzed, by using the online monitoring data of 4 months by Zhang *et al.* [4]. Wei *et al.* [5] used the online monitoring data to analyze the severe haze pollution process in January 2013 in Handan. The seasonal variation and possible source of water-soluble

inorganic ions were studied, by using the water-soluble inorganic ion of sampled PM<sub>2.5</sub> data in 2013 [6]. However, research on multiple components of PM<sub>2.5</sub> is relatively deficient. Therefore, in this study, the pollution characteristics of PM<sub>2.5</sub> and its chemical compositions under different air quality grades were analyzed from January 1 to December 31, 2013, by using the online monitoring data at four representative air quality monitoring sites, and the chemical compositions of sampled PM<sub>2.5</sub> in Handan to provide a scientific basis for the control of air pollutants in the future of Handan city.

## MATERIALS AND METHODS

### Sample collection and chemical analysis.

Samples were collected continuously from January 1 to December 31, 2013. PM<sub>2.5</sub> was sampled each day from 8:00 to 7:30 the next day in the non-heating period (from March 16 to November 14), and two samples were collected each day from 8:00 to 19:30 and from 20:00 to 7:30 the next day in the heating period (from November 15 to next March 15). Then the sampled filters were packed in aluminum foil to avoid light. The sampling site is located on the roof of the experimental building of School of City Construction in Hebei University of Engineering, using VFC-PM<sub>2.5</sub> high volume sampler produced by Thermo Fisher. The 24-hours flow accuracy of the sampler is less than 1%. Quartz fiber filters were used for sampling.

**Water-soluble inorganic ions.** A 2 cm diameter quartz fiber filter was cut off from the sampled filters, and then put into a weighing bottle (25mm × 40mm) after cut into fragments, and 10mL of ultrapure water (resistivity: 18.2MΩ cm) was added. After a 20 min ultrasonic bath with ice, the solution was drawn into a 5mL syringe, filtered by a syringe filter, and injected into a polymeric centrifugal tube with filter cap. Then 5 mL ultrapure water was added to the remainder sample. After a repeated 20 min ultrasonic bath, second filtration was proceed. Finally, two filtrate solutions were mixed to prepare for carrying on the analysis of the water soluble ion component.

The polymeric centrifugal tube were put into a Dionex AS-DV Autosampler and analyzed by ion chromatography (ICS-1000, DX-600) for water-soluble inorganic ions (NH<sub>4</sub><sup>+</sup>, Na<sup>+</sup>, K<sup>+</sup>, Mg<sup>2+</sup>, Ca<sup>2+</sup>, SO<sub>4</sub><sup>2-</sup>, Cl<sup>-</sup>, NO<sub>2</sub><sup>-</sup>, NO<sub>3</sub><sup>-</sup>). The test was completed in the center for analysis and testing of Beijing Normal University.

**Carbonaceous components.** A 0.526 cm<sup>2</sup> punch from each quartz fiber filter was analyzed for eight carbon fractions by a thermal optical carbon analyzer (DRI-2001A), following the IMPROVE\_A protocol [7, 8, 9]. The test was completed in Tsinghua University-Suez environmental science and engineering experiment practice teaching center.

**Inorganic elements.** ICP-MS was used to analyse the inorganic elements (i.e., Ti, V, Cr, Mn, Ni, Cu, Zn, As, Se, Sr, Cd, Ba, Pb, Br, Sb, Co, Rb, K, Fe and Ca). A 2cm diameter punch from each quartz fiber filter was put into PTFE digestion tube after being folded. Then 8 mL of HNO<sub>3</sub> (BV-III) and 0.5mL of H<sub>2</sub>O<sub>2</sub> solution (30%) were added into the digestion tube for 25 min microwave digestion at 190 °C. After cooling, the solution was filtered and decanted into a centrifugal tube, and diluted to 15mL with ultrapure water. The test work was completed in the institute of environment of the Chinese Academy of Sciences.

### Quality control. Sample collection process.

Quartz fiber filters used for sampling were all baked at 450 °C for 4h prior to sampling to remove adsorbed organic vapors and other impurities. The silicone oil was replaced every two weeks to ensure the effective sampling rate of PM<sub>2.5</sub>. Check the flow meter of the sampling pump everyday to avoid the error caused by the sampling flux. Filters were put in a chamber at 25°C and 40±5% of relatively humidity for 24h before and after sampling. The filters were sealed preserved in a refrigerator at -20 °C. Ensure the seal of the samples in the process of storage and transport, and ensure that the process from the sampling locations to the laboratory without missing and pollution outside.

**Chemical analysis process.** The containers used for experimental process such as beakers, plastic centrifuge tubes, pipettes, plastic dropper should clean by ultrasonic cleaning machine lasting 15 minutes every time. Then wash two times with high purity water to prevent the inaccuracy of experimental data caused by the external factors. In this study, the concentration measurement of water-soluble inorganic ions, carbonaceous components and inorganic elements of PM<sub>2.5</sub> were added three groups of blank filter experiments under the same conditions to calculate the background concentration of each ion, carbon component, inorganic element in the blank filter, and further revised the sample data. All processes were strict to ensure the accuracy and reliability of the resulting data.

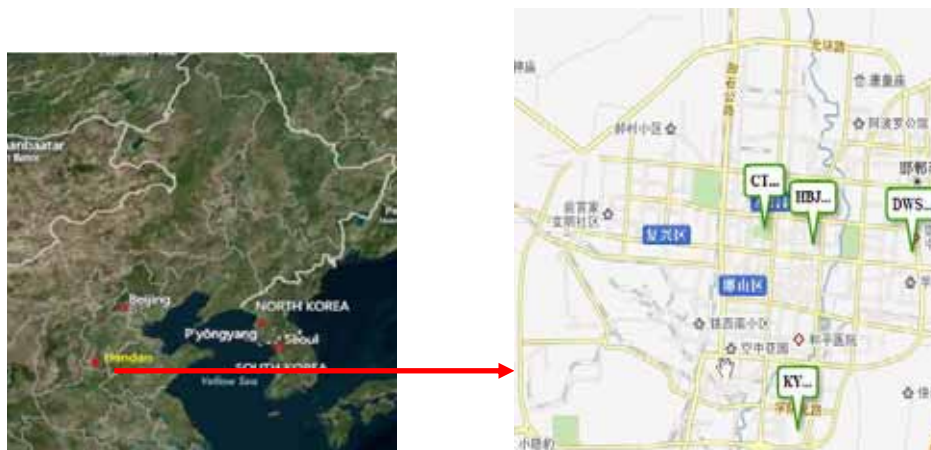


FIGURE 1

### Geographical locations of the monitoring sites in Handan

**Source of the monitoring data.** The online monitoring concentration data of  $PM_{2.5}$  was derived from four state-controlled sites, which provided by the Environmental Protection Bureau of Handan. Four state-controlled sites are located in the Environmental Protection Bureau of Handan (HBJ: residents commercial transportation mixed District), East sewage treatment plant (DWS: general industrial zone), Hebei University of Engineering (KY: typical educational ranking people mixing zone) and Congtai Park (CT: urban green space). The specific geographic location is shown in (Fig. 1).

## RESULTS AND DISCUSSIONS

**$PM_{2.5}$  concentrations and air quality grades.**  **$PM_{2.5}$  concentrations.** The average annual concentration of  $PM_{2.5}$  was  $139 \mu g m^{-3}$  in 2013 in Handan city, which was about 4 times of the national Grade II standard ( $35 \mu g m^{-3}$ ), and the percentages of

days exceeding the national secondary air quality standard were 74.4%. Moreover, the average daily concentrations of  $PM_{2.5}$  showed an intense episodic variations as shown in (Fig. 2). The most polluted months were January and December, the average monthly concentration of which were  $284 \mu g m^{-3}$  and  $233 \mu g m^{-3}$ , respectively. And the air pollution of August was the lightest, which had an average monthly concentration of  $67 \mu g m^{-3}$ . The  $PM_{2.5}$  mass concentration showed an overall trend of the rise after the fall. This was mainly due to Handan is a coal heating city in winter (January, February and December), which caused the increase of the pollutants emissions to  $PM_{2.5}$ , combined with the poor air convection, resulting in a rapid accumulation of particulate matter in a long time. However, the relatively abundant precipitation and the more conducive meteorological conditions, coupled with the relative less pollutant emissions than the heating period in summer (June, July and August) resulted in the lowest mass concentration of  $PM_{2.5}$  in August.

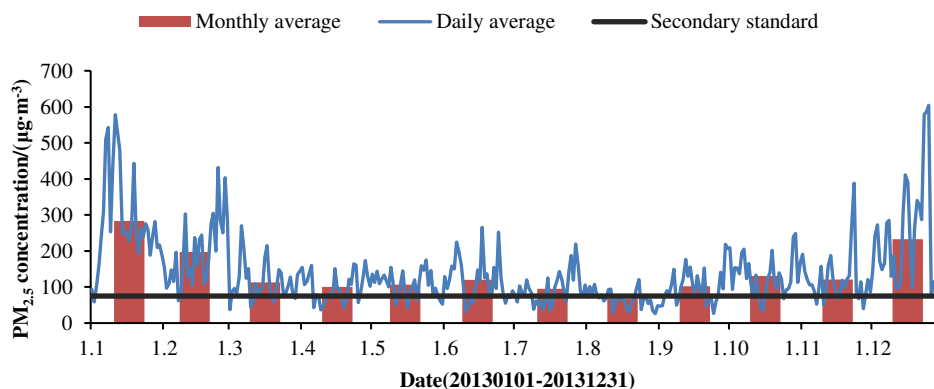
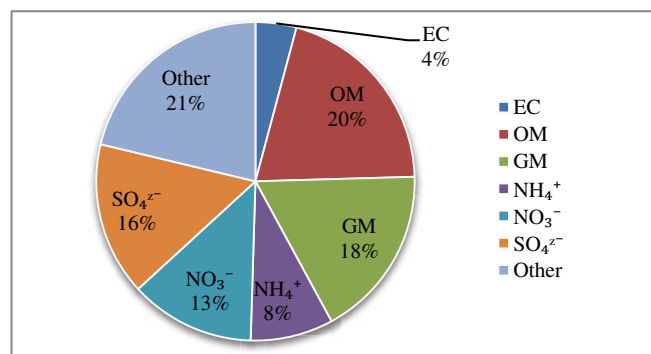


FIGURE 2

### Geographical locations of the monitoring sites in Handan



**FIGURE 3**  
**Material balance of PM<sub>2.5</sub> in Handan**

In order to further understand the contribution of each component to PM<sub>2.5</sub> mass concentration in Handan city, the mass balances of PM<sub>2.5</sub> in 2013 was calculated, as shown in Fig. 3. In this study, the calculation equality of OM was  $OM = k \times OC$ . Turpin [10] recommended that the urban areas should take K of  $1.6 \pm 0.2$ , so the value of K was selected of 1.6 in this study. There are many estimation methods of GM (Geological Material), but considering the integrity of the data, this study selected  $GM = [Fe]/0.04$ , which was consistent with the research methods of Zhang *et al.* [11].

As shown in (Fig. 3), the percentage components of each chemical composition of PM<sub>2.5</sub> in Handan in 2013 was ranking for  $OM > GM > SO_4^{2-} > NO_3^- > NH_4^+ > EC$ , consistent with the results of the research in Xi'an in 2011 [12]. Thus, it can be seen that the most components of PM<sub>2.5</sub> in Handan city was OM, accounting for 20% of the total PM<sub>2.5</sub> mass concentration. Followed by GM, accounted for 18% of the total PM<sub>2.5</sub> mass concentration. As for SNA, the proportion (16%) of  $SO_4^{2-}$  to PM<sub>2.5</sub> mass concentration was the highest, which had the direct connection of the large coal-fired emissions in heating period.  $NO_3^-$ , followed  $SO_4^{2-}$ , accounted for 13% of the total PM<sub>2.5</sub> mass concentration. Compared to  $SO_4^{2-}$  and  $NO_3^-$ , the ratio of  $NH_4^+$  to the total PM<sub>2.5</sub> mass concentration was slightly lower, accounting for 8%.

**Air quality grades.** According to the Technical Regulation on Ambient Air Quality Index (on trial) (HJ 633 - 2012) [13], the air quality index (AQI) are divided into six grades. When AQI is in the scope of 0~50, 51~100, 101~150, 151~200, 201~300, and more than 300, the air quality grades is regarded as grade I (Excellent), grade II (Fine), grade III (Slightly polluted), grade IV (Moderately polluted), grade V (Heavily polluted) and grade VI (Severely polluted), respectively. The larger AQI is, the higher grade is, which show the more serious pollution and more

obvious effects on human health. The distribution of air quality grades in Handan city in 2013 are in (Fig. 4), and the AQI of each pollutant was calculated by the concentration data provided by the Municipal Environmental Protection Bureau of Handan. From (Fig. 4) we can see, there were no excellent days, and the number of the fine days was 52, only accounting for 14% throughout the year. At the same time, slightly polluted days accounted for 36% (132 days) all through the year. Moreover, moderately polluted and the above days accounted for 50% throughout the year in 2013. In conclusion, the air pollution in Handan city was extremely severe.

**Characteristics of the components in PM<sub>2.5</sub> under different air quality grades. Characteristics of the concentration variation.** In order to understand the variation characteristics of PM<sub>2.5</sub> components under different air quality grades, the ambient air quality grades were divided into Excellent ( $0 \sim 35 \mu\text{g m}^{-3}$ ), Fine ( $35 \sim 75 \mu\text{g m}^{-3}$ ), Slightly polluted ( $75 \sim 115 \mu\text{g m}^{-3}$ ), Moderately polluted ( $115 \sim 150 \mu\text{g m}^{-3}$ ), Heavily polluted ( $150 \sim 250 \mu\text{g m}^{-3}$ ) and Severely polluted (more than  $250 \mu\text{g m}^{-3}$ ) respectively in accordance with the mass concentration of PM<sub>2.5</sub>, comparing to the contributions of each component to PM<sub>2.5</sub> mass concentration.

The variation characteristics of PM<sub>2.5</sub> and its main components mass concentration under different air quality grades are depicted in (Fig. 5). As shown in (Fig.5), with the deterioration of air quality grades, the mass concentrations of PM<sub>2.5</sub> and its chemical compositions were elevated, and increase dramatically when severe pollution occurs, especially for EC and OM. The mass concentrations of EC and OM on severely polluted days were approximately 5.9 and 5.5 times those of fine days, respectively. Following EC and OM, the mass concentrations of  $NH_4^+$ ,  $NO_3^-$  and  $SO_4^{2-}$  on severely polluted days were about 4.6, 3.2 and

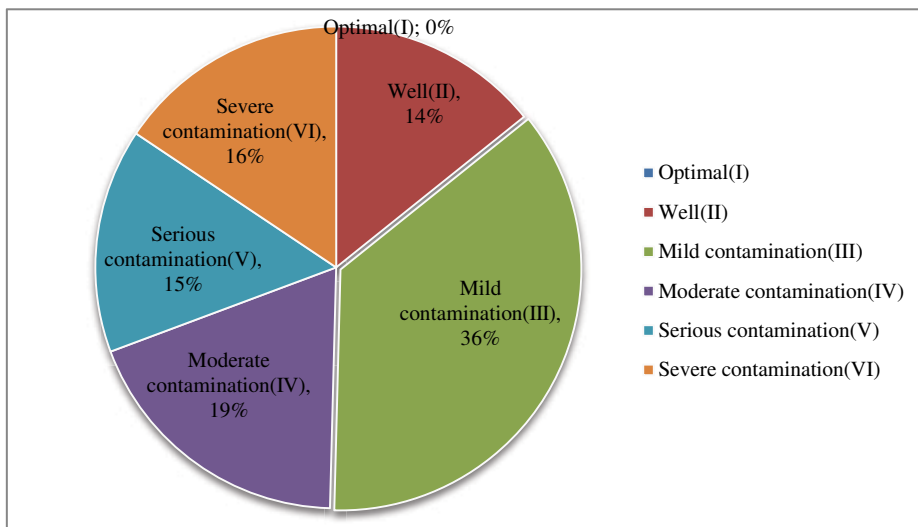


**FIGURE 4**  
Distribution of daily air quality grades

3.7 times those of the fine days, respectively. It is worth noting that the concentration variation of GM was the smallest, but it peaked when slightly polluted days, and fall down from the moderately polluted days to the severely polluted days. The percentage of each component in PM<sub>2.5</sub> are shown in (Fig. 6). The variation of the percentage of EC in PM<sub>2.5</sub> was consistent with the percentage of OM under different air quality grades, decreasing first and then increasing. However, the percentage of EC in PM<sub>2.5</sub> peaked under the severely polluted days, accounting for 6.2% of PM<sub>2.5</sub>, but the percentage of OM in PM<sub>2.5</sub> peaked while in the heavily polluted days and fall down when in the

severely polluted days, which mainly due to the increase of PM<sub>2.5</sub> mass concentration. The change trend of the percentage of NO<sub>3</sub><sup>-</sup> and SO<sub>4</sub><sup>2-</sup> in PM<sub>2.5</sub> was consistent, but the percentage of SO<sub>4</sub><sup>2-</sup> increased while the percentage of NO<sub>3</sub><sup>-</sup> decreased in severely polluted days. The percentage variation of NH<sub>4</sub><sup>+</sup> in PM<sub>2.5</sub> was similar to EC, showing a trend of decreasing first and then increasing with the deterioration of air quality grades. Large difference to other components in PM<sub>2.5</sub>, the percentage of GM in PM<sub>2.5</sub> increased first and then decreased. The percentage of GM in PM<sub>2.5</sub> peaked under the good days, accounting for 26.5% of the PM<sub>2.5</sub> mass concentration.

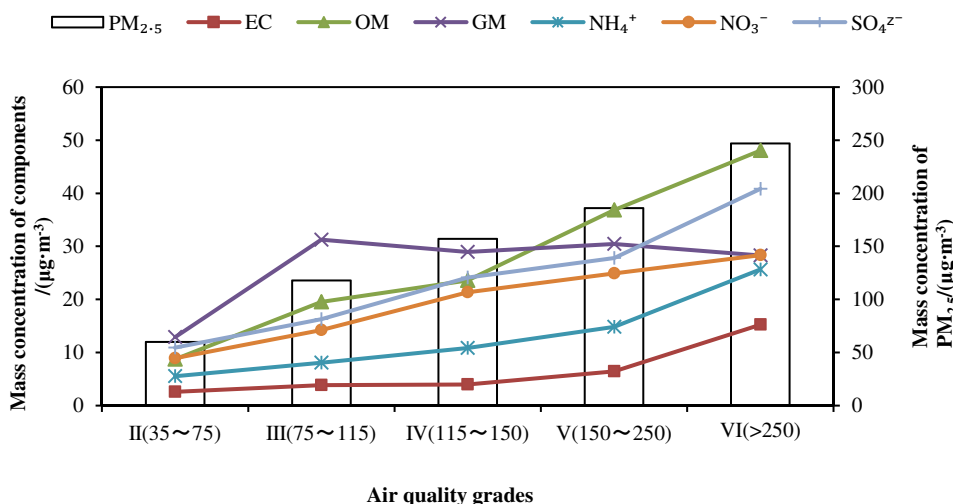


**FIGURE 5**  
Variation characteristics of PM<sub>2.5</sub> and its main components under different air quality grades

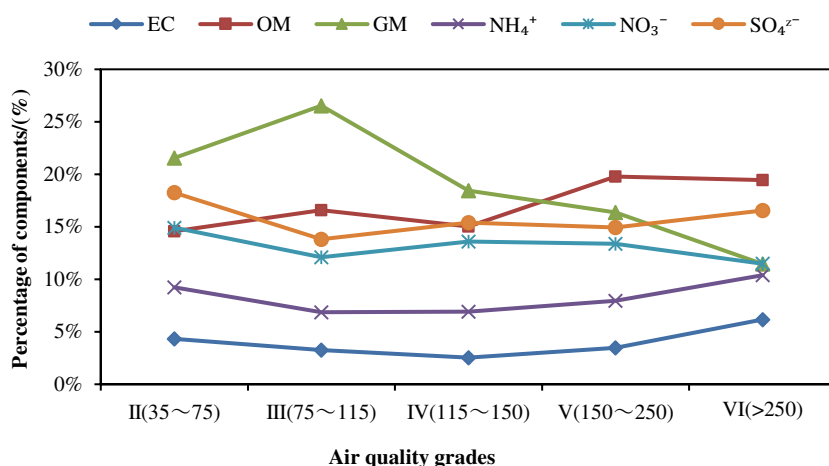


FIGURE 6

The percentage of each components in PM<sub>2.5</sub> under different air quality grades

The percentage of GM in PM<sub>2.5</sub> continued to decline from moderately polluted days to severely polluted days, and the minimum value occurred when in the severely polluted days, accounting for 11.5% of the PM<sub>2.5</sub> mass concentration with the rate of decline up to 57%. Little influence on GM by air quality, combined with the increase of PM<sub>2.5</sub> mass concentration with the degree of pollution, lead to the opposite trend of the percentage of GM in PM<sub>2.5</sub> with PM<sub>2.5</sub> mass concentrations.

**Characteristics of NO<sub>3</sub><sup>-</sup>/SO<sub>4</sub><sup>2-</sup> ratio.** The mobile source and stationary source contributions to PM<sub>2.5</sub> in the atmosphere can be reflected by the ratio of NO<sub>3</sub><sup>-</sup>/SO<sub>4</sub><sup>2-</sup>. When the ratio is greater than 1.0, the influence of mobile sources is stronger than the stationary source, indicating that the mobile source is the major pollution source at the sampling sites [14, 15, 16] and vice versa. The average annual NO<sub>3</sub><sup>-</sup>/SO<sub>4</sub><sup>2-</sup> ratio was 0.87 in Handan city in 2013, and 1.26 in winter, which was 1.2~1.4 times of other three seasons. It was mainly related to the coal-fired energy structure in Handan city in winter.

(Fig.7) shows the mass concentrations variation of NO<sub>3</sub><sup>-</sup>, SO<sub>4</sub><sup>2-</sup> and NO<sub>3</sub><sup>-</sup>/SO<sub>4</sub><sup>2-</sup> under different air quality grades in Handan city. As shown in (Fig.7), with the deterioration of air quality grades, the mass concentrations of NO<sub>3</sub><sup>-</sup> and SO<sub>4</sub><sup>2-</sup> increased, especially for the mass concentrations of SO<sub>4</sub><sup>2-</sup>, and the increase of maximal amplitude occurred in severely polluted days. NO<sub>3</sub><sup>-</sup>/SO<sub>4</sub><sup>2-</sup> ratio increased slowly and then decreased with the deterioration of air quality grades. The ratios were less than 1.0 and in the scope of 0.71~0.98. The maximum value appeared under the moderately polluted days and the minimum value

occurred under the severely polluted days, indicating that the influence of stationary source was more important than the mobile sources in Handan city, and the influence of stationary source increased from moderately polluted days to severely polluted days.

**Characteristics of OC/EC ratio.** OC/EC ratios can be used to express the emission and transformation characterization of carbonaceous aerosol [17, 18]. When the value is greater than 2.0, indicated that organic carbon occurred secondary transformation. Previous studies [19, 20, 21, 22] have shown that the ratio of OC/EC was in the scope of 1.0~4.2, indicating that the emissions were mainly derived from diesel and gasoline vehicles, and the ratio of 2.5~10.5 indicated the source of coal-fired emissions, and the ratio of 16.8~40.0 indicated the source of wood burning emissions, and the ratio about 7.7 indicated the source of biomass burning. The average annual OC/EC ratio was 3.4, and the ratio of most samples was between 2.0 to 4.0 in spring, summer and winter, but OC/EC ratio was as high as about 6.0 in autumn, indicating that secondary carbon pollution exist in Handan City throughout the year, and the most serious pollution occurred in autumn, which mainly due to the large amounts of biomass fuel burning combined with adverse weather conditions.

(Fig.8) shows the variation of the mass concentration of OC, EC and OC/EC in different air quality grades. As shown in (Fig.8), with the deterioration of air quality grades, the mass concentration of OC and EC increased under different degrees. The growth of OC mass concentration was more significant, showing a linear increase trend, and the OC mass concentration in heavily polluted days was 5.5 times than those under fine days.



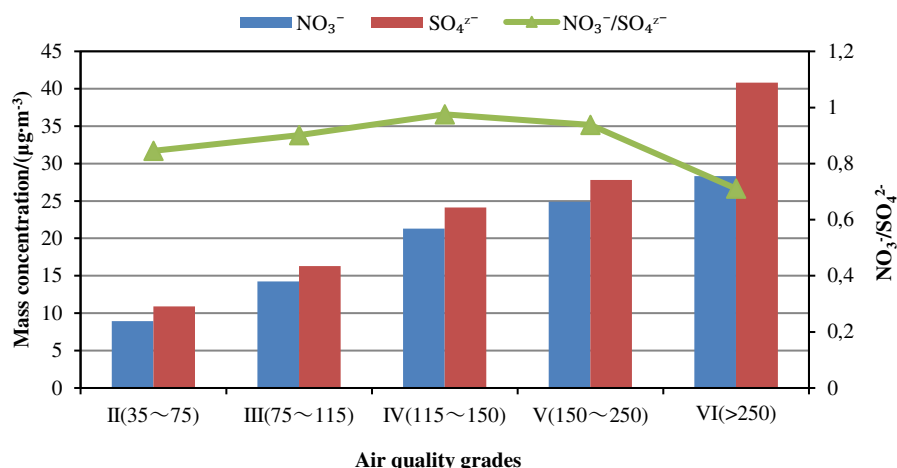


FIGURE 7

Mass concentrations variation of NO<sub>3</sub><sup>-</sup>, SO<sub>4</sub><sup>2-</sup> and NO<sub>3</sub><sup>-</sup>/SO<sub>4</sub><sup>2-</sup> under the different air quality grades

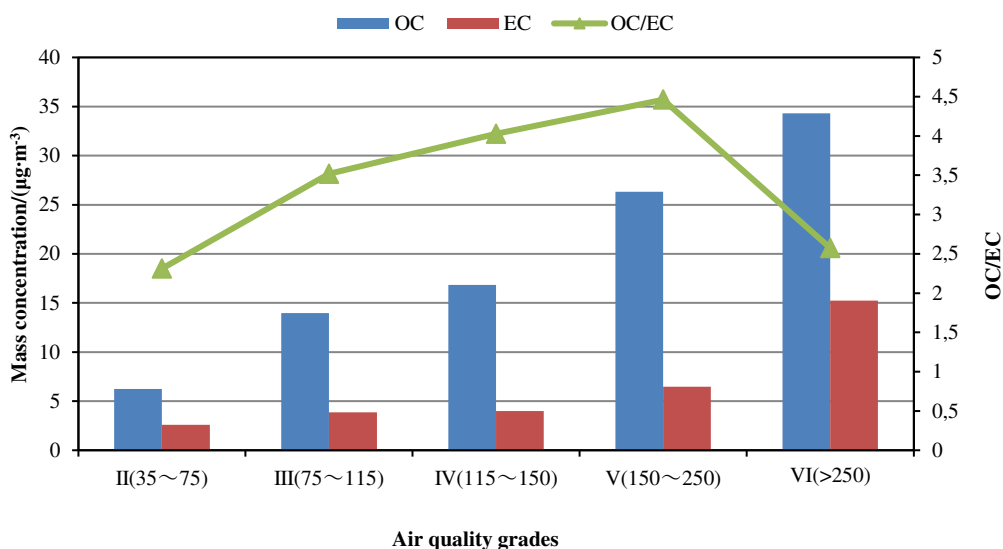


FIGURE 8

Variation of the mass concentration of OC, EC and OC/EC in different air quality grades

The mass concentration of EC increased slowly from the fine days to the heavily polluted days, and an obvious increase was shown in the severely polluted days. The ratio of OC/EC were greater than 2.3 under different air quality grades, showing an increase of lineation from 2.3 under the fine days to 4.5 under the heavily polluted days. After that, the ratio declined to 2.6 under the severely polluted days. It is indicated that there were secondary carbon pollution under different air quality grades in Handan city, and with the deterioration of air quality grades, the source of EC and OC in the atmosphere of Handan was mainly influenced by coal combustion and vehicle exhaust collectively.

**Characteristics of enrichment factor of inorganic elements.** In order to further understand the characteristics of pollution and sources variation of inorganic elements in PM<sub>2.5</sub>, enrichment factor method were used to study the process of enrichment of inorganic elements in PM<sub>2.5</sub> [23]. The man-made sources and natural sources of the pollution elements in atmospheric particulate matter were distinguished by the degree of enrichment of each element in PM<sub>2.5</sub>. This method eliminated the sampling effect in the process of wind speed, wind direction, distance from the pollution source and sample quantity variable factors, so it was more reliable than judging sources of various chemical elements in atmospheric particulates by the absolute concentration [24].

A stable crustal element, high abundance and less anthropogenic pollution in general, R, was selected as reference element when calculating the enrichment factor of each element in  $PM_{2.5}$ . Different reference elements result in different enrichment factors, and reflect the different pollution information. This study selected Ti as the reference element [25]. The formula of enrichment factor is as follows:

$$EF_i = \frac{(C_i/C_r)_P}{(C_i/C_r)_R} \quad (1)$$

where  $EF_i$  is the enrichment factor of the  $i$ th element;  $C_i$  is the concentration of the  $i$ th element;  $C_r$  is the concentration of the reference element selected; P is in aerosol and R is in reference material. When  $EF < 10$ , the main source of the element in  $PM_{2.5}$  is regarded as derived from the earth's crust or soil. While  $EF > 10$  indicates the elements in atmospheric samples enriched, the element is both influenced by crustal material and anthropogenic pollution sources [26]. At the same time, the larger EF is, the more serious anthropogenic pollution is.

The average background value of the main soil types (a layer soil) in Hebei province was regarded as the reference system [27] in this study to calculate the enrichment factors of each element in  $PM_{2.5}$  under different air quality grades in Handan city in 2013. The result is shown in (Fig. 9). The enrichment factors of each element in  $PM_{2.5}$  varied widely, which can be roughly divided into two classes: the first class include V, Cr, Mn, Sr, Ba, K, Ca, Fe, and Rb, and their average enrichment factors were 3.7, 7.4, 7.9, 3.3, 5.1, 3.6, 4.0, 2.5 and 3.2, which were all less than 10, suggesting that these elements were mainly derived from the soil and other natural source. The second class included Co, Cu,

As, Zn, Sb, Pb and Br, and their average enrichment factors were 26.2, 70.4, 237.5, 336.4, 443.5, 770.4, and 790.8, far greater than 10, even more than 100, suggesting that these elements are mainly influenced by anthropogenic emissions. As shown in (Fig. 9), with the deterioration of air quality grades, the two types of the elements enrichment factors showed the different variations. EF of the elements from crustal sources were not increased along with air quality grades except in severely polluted days. While EF of anthropogenic elements (except Sb) increasing with the deterioration of air quality degrees, especially in the severely polluted days. The enrichment factors of anthropogenic elements in severely polluted days were 4.0-11.9 times those of in fine days. Thus it demonstrated that the EF of all elements were rising obviously in severely days, and the EF of anthropogenic elements were elevated consistent with the increasing of AQI, while the elements from crustal sources were not observed the same growth. In addition, it is worth noting that the EF of most elements were not the lowest, while the minimum value appeared under the fine days. The result also showed that better air quality grades will not always lead to less pollutants by anthropogenic pollution.

## CONCLUSIONS

The average annual concentration of  $PM_{2.5}$  was  $139 \mu g m^{-3}$  in Handan city in 2013, which was about 4 times of the national Grade II standard, and the percentages of the number of the days exceeding the national Grade II air quality standard (GB3095-2012)

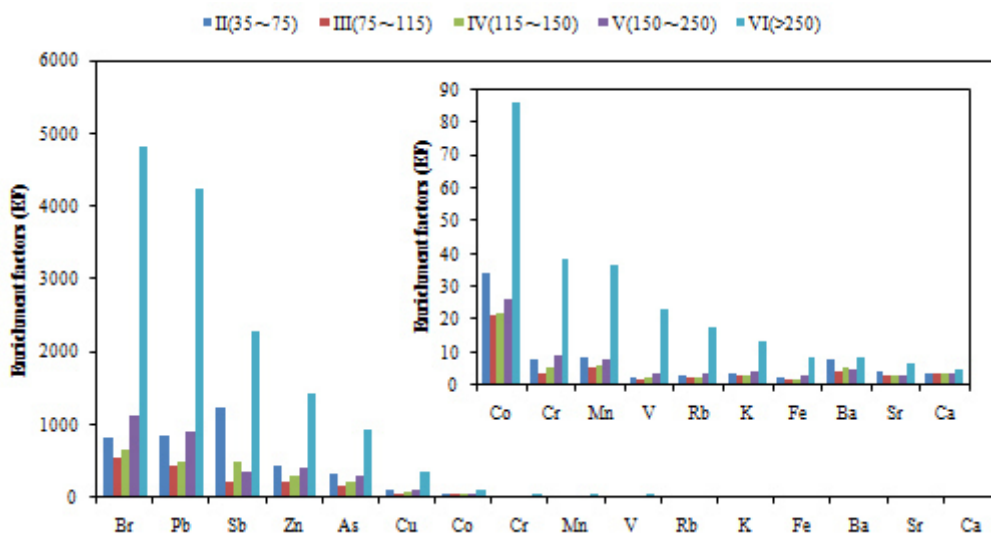


**FIGURE 9**  
Enrichment factors of each element in  $PM_{2.5}$  under different air quality grades

were 74.4%. The most polluted months were January and December, while the air pollution of August was the lightest. There were no excellent days, and moderate to severe polluted days accounted for 50% throughout the year.

With the increasing of air quality grades, the mass concentration of PM<sub>2.5</sub> was elevated to show a generally increasing trend of the AQI, and the mass concentration of most chemical composition were dramatically increased in the severely polluted days except for a few elements. The mass concentrations of EC and OM in severely polluted days were approximately 5.9 and 5.5 times those of fine days.

NO<sub>3</sub>/SO<sub>4</sub><sup>2-</sup> and OC/EC ratio increased with the deterioration of air quality, and peaked in moderately and heavily polluted days respectively, and slightly fall down under the severely polluted days.

The enrichment factors of all elements had different degree of increase when air quality deteriorate, and the EF of anthropogenic elements were elevated consistent with the increasing AQI, while the elements from crustal sources were relatively stable under different air quality grades.

## ACKNOWLEDGEMENTS

This study was sponsored by the National Natural Science Foundation of China (No. 41475131, No. 41105105), the State Environmental Protection Key Laboratory of Sources and Control of Air Pollution Complex (No. SCAPC201307), the Program for the Outstanding Young Scholars of Hebei Province, the Excellent Young Scientist Foundation of Hebei Education Department (No. YQ2013031), and the Environmental Protection Bureau of Handan, Hebei, China.

## REFERENCES

- [1] Wang, L. T., Wei, Z., Yang, J., Zhang, Y., Zhang, F. F., Su, J., Meng, C. C. and Zhang, Q. (2014) The 2013 severe haze over southern Hebei, China: model evaluation, source apportionment, and policy implications. *Atmospheric Chemistry and Physics*, 14(6), 3151-3173.
- [2] Wang, L., Xu, J., Yang, J., Zhao, X. J., Wei, W., Cheng, D. D., Pan, X. M. and Su, J. (2012) Understanding haze pollution over the southern Hebei area of China using the CMAQ model. *Atmospheric Environment*, 56, 69-79.
- [3] Wei, W., Wang, L. T., Pan, X. M., Cheng, D. D. and Su, J. (2013) Simulation study of haze pollution sources in cities of Hebei Province. *Environmental Science and Technology*, 2, 024.
- [4] Zhang, P., Tan, S. B., Wang, L. T., Zhao, X. J., Su, J., Zhang, F. F., Wei, Z., Wei, W. and Cheng, D. D. (2013) Characteristics of atmospheric particulate matter pollution in Handan City. *Acta Scientiae Circumstantiae*, 33(10), 2679-2685.
- [5] Wei, Z., Yang, J., Wang, L. T., Wei, W., Zhang, F. F. and Su, J. (2014) Characteristics of the severe haze episode in Handan City in January, 2013. *Acta Scientiae Circumstantiae*, 34, 1181-1124.
- [6] Meng, C. C., Wang, L. T., Zhang, F. F., Wei, Z., Ma, S. M., Yang, J., Zhang, H. L. and Shi, C. H. (2015) Pollution characteristics and source apportionment of water soluble inorganic ions in PM<sub>2.5</sub> in Handan City. *Acta Scientiae Circumstantiae*, 35(11), 3443-3451.
- [7] Chow, J. C., Watson, J. G., Chen, L. W. A., Chang, M. O., Robinson, N. F., Trimble, D. and Kohl, S. (2007) The IMPROVE\_A temperature protocol for thermal/optical carbon analysis: maintaining consistency with a long-term database. *Journal of the Air and Waste Management Association*, 57(9), 1014-1023.
- [8] Chow, J. C., Watson, J. G., Crow, D., Lowenthal, D. H. and Merrifield, T. (2001) Comparison of IMPROVE and NIOSH carbon measurements. *Aerosol Science and Technology*, 34(1), 23-34.
- [9] Chow, J. C., Watson, J. G., Pritchett, L. C., Pierson, W. R., Frazier, C. A. and Purcell, R. G. (1993) The DRI thermal/optical reflectance carbon analysis system: description, evaluation and applications in US air quality studies. *Atmospheric Environment. Part A. General Topics*, 27(8), 1185-1201.
- [10] Turpin, B. J. and Lim, H. J. (2001) Species contributions to PM<sub>2.5</sub> mass concentrations: Revisiting common assumptions for estimating organic mass. *Aerosol Science and Technology*, 35(1), 602-610.
- [11] Zhang, X. Y., Gong, S. L., Arimoto, R., Shen, Z. X., Mei, F. M., Wang, D. and Cheng, Y. (2003) Characterization and temporal variation of Asian dust aerosol from a site in the northern Chinese deserts. *Journal of Atmospheric Chemistry*, 44(3), 241-257.
- [12] Cao J. J. (2014) PM<sub>2.5</sub> and the environment, Science press, Beijing.
- [13] Ministry of Environmental Protection of the People's Republic of China. Technical Regulation on Ambient Air Quality Index (on trial). 2012-02-29.
- [14] Li, C. X. (2007) Pollution characteristics of water-soluble ions in atmospheric PM<sub>10</sub> and PM<sub>2.5</sub> in Changsha City in summer. *China Environmental Science-Chinese Edition*, 27(5), 599.

- [15] Wang, Y., Zhuang, G. S., Zhang, X. Y., Huang, K., Xu, C., Tang, A., Chen, J. M. and An, Z. S. (2006) The ion chemistry, seasonal cycle, and sources of PM<sub>2.5</sub> and TSP aerosol in Shanghai. *Atmospheric Environment*, 40(16), 2935-2952.
- [16] Arimoto, R., Duce, R. A., Savoie, D. L., Prospero, J. M., Talbot, R., Cullen, J. D., Tomza, U., Lewis, N. F. and Ray, B. J. (1996) Relationships among aerosol constituents from Asia and the North Pacific during PEM-West A. *Journal of Geophysical Research: Atmospheres*, 101(D1), 2011-2023.
- [17] Chow, J. C., Watson, J. G., Lu, Z., Lowenthal, D. H., Frazier, C. A., Solomon, P. A., Thuillier, R. H. and Magliano, K. (1996) Descriptive analysis of PM<sub>2.5</sub> and PM<sub>10</sub> at regionally representative locations during SJVAQS/AUSPEX. *Atmospheric Environment*, 30(12), 2079-2112.
- [18] Gianini, M. F. D., Piot, C., Herich, H., Besombes, J. L., Jaffrezo, J. L. and Hueglin, C. (2013) Source apportionment of PM<sub>10</sub>, organic carbon and elemental carbon at Swiss sites: An intercomparison of different approaches. *Science of the Total Environment*, 454, 99-108.
- [19] Schauer, J. J., Kleeman, M. J., Cass, G. R. and Simoneit, B. R. (1999) Measurement of emissions from air pollution sources. 2. C1 through C30 organic compounds from medium duty diesel trucks. *Environmental Science and Technology*, 33(10), 1578-1587.
- [20] Schauer, J. J., Kleeman, M. J., Cass, G. R. and Simoneit, B. R. (2002) Measurement of emissions from air pollution sources. 5. C1-C32 organic compounds from gasoline-powered motor vehicles. *Environmental science and technology*, 36(6), 1169-1180.
- [21] Chen, Y., Zhi, G., Feng, Y., Fu, J., Feng, J., Sheng, G. and Simoneit, B. R. (2006) Measurements of emission factors for primary carbonaceous particles from residential raw-coal combustion in China. *Geophysical Research Letters*, 33(20).
- [22] Schauer, J. J., Kleeman, M. J., Cass, G. R. and Simoneit, B. R. (2001) Measurement of emissions from air pollution sources. 3. C1-C29 organic compounds from fireplace combustion of wood. *Environmental Science and Technology*, 35(9), 1716-1728.
- [23] Liu, Y. S., Yang, B., Li, R. M., Wang, Y., Cao, F., Xu, H. Z. and Li, A. G. (2010) Preliminary study on source area and physical and chemical characteristics for Aeolian dust deposits in Beijing, China. *Geological Bulletin of China*, 29(8), 1220-1227.
- [24] He, K. B., Yang, F. M., Duan, F. K. and Ma, Y. L. (2011) Atmospheric particulate matter and regional compound pollution, Science press, Beijing.
- [25] Wang, Q. J., Cao, J. J., Gan, X. F., Tu, X. M., Shen, Z. X., Guo, X. and Tao, J. (2010) Characteristics of elements in PM<sub>2.5</sub> during normal and haze period in Chengdu. *Environmental Chemistry*, 29(4), 644-648.
- [26] Cao, J. J., Lee, S. C., Zhang, X. Y., Chow, J., An, Z. S., Ho, K. F., Watson, J., Fung, K., Wang, Y. Q. and Shen, Z. X. (2005) Characterization of airborne carbonate over a site near Asian Dust source regions during spring 2002 and its climatic and environmental significance. *Journal of geophysical research: atmospheres*, 110(D3), 1-8.
- [27] State Department of Environmental Conservation. (1990) Chinese soil elements background values, China Environmental Science Press, Beijing.

---

**Received:** 18.10.2015

**Accepted:** 14.02.2016

---

#### CORRESPONDING AUTHOR

---

**Simeng Ma**

Department of Environmental Engineering,  
School of City Construction, Hebei University of  
Engineering,  
Handan, 056038

e-mails: [wlt@tsinghua.edu.cn](mailto:wlt@tsinghua.edu.cn)

# INNOVATIVE PRECONCENTRATION TECHNIQUE ON POLYMER SORBENT FOR SIMULTANEOUS DETERMINATION OF PLATINUM GROUP METALS IN THE WATERS AND LICHEN *HYPOGYMNIA PHYSODES*

Renata Komendova<sup>1,\*</sup>, Jana Nevrla<sup>1</sup>, Jan Kuta<sup>2</sup>, Lumir Sommer<sup>1</sup>

<sup>1</sup> Institute of Chemistry and Technology of Environmental Protection, Faculty of Chemistry, Brno University of Technology, Purkyňova 464/118, 61200 Brno, Czech Republic

<sup>2</sup> Research Centre for Toxic Compounds in the Environment (RECETOX), Faculty of Science, Masaryk University, Kamenice 126/3, 625 00, Brno, Czech Republic

## ABSTRACT

This study is focused on optimization of preconcentration procedure of trace amounts of platinum group metals (PGMs) by solid phase extraction. Amberlite polystyrene-divinylbenzene based sorbent was used for this purpose. Under the optimizing process were optimized number of parameters such as pH value of sorption; type and concentration of complexing agent; concentration and type of cationic surfactant; type, pH, and volume of eluent mixture; acidity of final solution and various interfering influences (presence of various ions, matrix effects). Ammonium-pyrrolidindithiocarbamate, thiourea, 4-(2-pyridylazo) resorcinol and 8-hydroxyquinoline-5-sulfonic acid were used as complexing agents for PGMs. Sorbent was conditioned using cationic surfactant solution. Benzyltrimethylammonium chloride, N-( $\alpha$ -carbethoxypentadecyl)-trimethyl ammonium bromide and benzyltrimethylammonium bromide were tested. Mixture of acetonitrile and HCl was proved as eluent. The influences of various concentrations of hydrochloric acid during the complexation, elution and partial evaporation of the eluent prior to the determination were tested. Effects of various elements and ions were studied during the sorption and retention on the above mentioned sorbent. Simultaneous determination of PGMs was performed by ICP-MS spectrometer using helium collision cell and internal standard. Detection limits for individual elements at discussed conditions were evaluated. The optimized method of solid phase extraction was applied to spiked real water samples and lichens for testing influences of matrix and efficiency of sorption process. It was discovered that recovery ratio of sorption process is diverse for individual studied elements. Acceptable results were achieved for Platinum and Palladium which showed recovery ratio about 100 % and 95 % for Osmium.

## KEYWORDS:

Platinum group metals, preconcentration, separation, cationic surfactant, lichens, ICP-MS

## INTRODUCTION

The problems of determination of platinum group metals in environmental samples is very topical because of the concentration of PGMs in the environment currently constantly increasing as a result of increasing intensity of car transport. Especially, monitoring of platinum, rhodium and palladium is important because these metals are widely used as catalysts in many branches of industry and primarily as catalytic converters in cars [1]. In this way, the platinum metals get into all environmental media, such as air, airborne dust, water, soil and biological materials [2]. Elevated levels of platinum group metals in these samples were detected only near the busy roads, but also in remote areas with no car traffic [3-5].

Moreover, the use of a number of platinum (II) complexes in medicine against various kinds of cancer has to be mentioned [1, 6-8].

However, the concentrations of these elements in the environment are still very low and they are difficult to detect even using modern analytical methods such as atomic absorption spectrometry with electrothermal atomization (ET-AAS), atomic emission spectrometry with inductively coupled plasma (ICP-OES) or mass spectrometry with inductively coupled plasma (ICP-MS) [9].

The point of analytical determination of PGMs in samples originating from the environment lies mainly on enrichment and removal of interfering influences of matrix. For this purpose, preconcentration and separation process of trace elements prior to the analysis is necessary. Solid phase extraction (SPE) is currently one of the most widely used and effective methods of pre-analytical preparation of environmental samples [10, 11]. Low time and financial demands, regeneration of sorbent,

low consumption of organic solvents including lower production of waste, achieving of high preconcentration factor and removal of a large number of matrix belong between the major advantages of this method.

This paper is focused on optimizing of preconcentration procedure of PGMs using modified sorbent Amberlite XAD (Strata SDB-L, Phenomenex) and their determination by ICP-MS. Optimized preconcentration procedure was applied to real water samples and lichens.

## MATERIALS AND METHODS

**Instrumentation.** An ICP-MS spectrometer Agilent 7500ce (Tokyo, Japan) equipped with concentric silica nebulizer MicroMist with a double pass Scott-type spray chamber (cooled at +2 °C) was used for analysis. The ICP-MS spectrometer contains an octapole collision-reaction cell, quadrupole analyser and electron multiplier detector which worked in pulse/analogous mode. Other conditions and setting parameters of measurement (ICP-MS) are mentioned in Table 1. The tuning

solutions were adjusted to achieve optimal signal stability, low background and low signal of double charged ions, in normal mode. The ion lenses of the spectrometer were optimized prior to each analysis. Polyatomic interferences from the matrix of samples were removed using the octapole collision cell in the helium mode. For monitoring of matrix influence was used internal standard solution which contained mixture of In, Re and Bi in 1% HCl. The instrumental limits of detection (LOD) were based on the  $3\sigma$  definition [12] and were evaluated from 10 measurements of the blank solutions. These LOD values (in  $\mu\text{g L}^{-1}$ ) were observed for Ru-0.0184, Rh-0.0025, Pd-0.1177, Os-0.0387, Ir-0.0092 and Pt-0.0084.

**Reagent and solutions.** A multi element standard stock solution contained  $100 \pm 0.002 \text{ mg L}^{-1}$  platinum group metals in the form of chlorocomplexes in 15% HCl (Analytika, Prague, Czech Republic).

The tuning solutions for ICP-MS contains  $1 \mu\text{g L}^{-1}$  of  $\text{Ce}^{3+}$ ,  $\text{Li}^+$ ,  $\text{Y}^{3+}$  and  $\text{Tl}^+$  in 2%  $\text{HNO}_3$  originated by Agilent, HPST s.r.o., Prague, Czech Republic.

**TABLE 1**  
**Setting parameters on ICP-MS.**

Parameter	Value
<b>Acquisition parameters</b>	
Analytes	$^{99}\text{Ru}$ , $^{101}\text{Ru}$ , $^{103}\text{Rh}$ , $^{105}\text{Pd}$ , $^{188}\text{Os}$ , $^{189}\text{Os}$ , $^{191}\text{Ir}$ , $^{193}\text{Ir}$ , $^{194}\text{Pt}$ , $^{195}\text{Pt}$
Internal standards	$^{115}\text{In}$ , $^{185}\text{Re}$ , $^{209}\text{Bi}$
Integration times	0.5 s (analytes), 0.3 (ISTD 5x repetition/sample)
<b>Sample introduction</b>	
Nebulizer	MicroMist
Spray chamber	Scott double pass
Temperature in spray chamber	2 °C
Sample intake	0.4 mL $\text{min}^{-1}$ (sample), 0.125 mL $\text{min}^{-1}$ (internal standards)
<b>Inductively coupled plasma</b>	
RF power	1500 W
Plasma gas (Ar)	15 L $\text{min}^{-1}$
Sampling depth	8 mm
Carrier gas	0.75 mL $\text{min}^{-1}$
Make up gas	0.25 mL $\text{min}^{-1}$
<b>Ion optics</b>	
Extract 1	Typically 1 - 4 V
Extract 2	Typically (-130) – (-180) V
Omega bias-ce	Typically (-16) – (-30) V
Omega lens-ce	Typically 1 - 3 V
<b>Collision cell</b>	
Cell entrance	-30 V
Cell exit	-50 V
OctP RF	200 V
OctP Bias	-19 V
Collision gas flow (He)	5.5 mL $\text{min}^{-1}$
<b>Quadrupole</b>	
QP focus	-10 V
QP Bias	-15 V

Solutions of internal standard ( $100 \mu\text{g L}^{-1}$   $^{115}\text{In}$ ,  $^{185}\text{Re}$  and  $^{209}\text{Bi}$  in 1% HCl) were prepared from standard solution  $1 \text{ mg L}^{-1}$  (Analytika, Prague, Czech Republic) by dilution.

Acidity of all solutions was adjusted by anal pure HCl (Analytika, Prague, Czech Republic).

Solutions of cationic surfactants and complexing agents were prepared by weigh out and dissolving of accurate amount in deionized water. N-( $\alpha$ -carbethoxypentadecyl) trimethylammonium bromide  $\text{C}_{21}\text{H}_{44}\text{O}_2\text{NBr}$  (Septonex®) (GNB a.s., Czech Republic), benzyltrimethyltetradecylammonium chloride  $\text{C}_{23}\text{H}_{42}\text{NCl}$  (Zephyramine®) and benzyltrimethyl-dodecylammonium bromide  $\text{C}_{21}\text{H}_{38}\text{NBr}$  (Ajatin®) (both Sigma Aldrich, Steinheim, Germany) were tested as cationic surfactants. Ammonium-pyrrolidindithiocarbamate (APDC), thiourea (TU), 4-(2-pyridylazo) resorcinol (PAR) and 8-hydroxyquinoline-5-sulfonic acid (8-HQS) (all Sigma Aldrich, Steinheim, Germany) were used as complexing agents for PGMs.

The other used chemicals and solvents were all of analytical grade purity.

Modified sorbent Strata SDB-L in original columns (500 mg per 3 mL of column volume) by Phenomenex, Torrance, California, USA, has particle size 55  $\mu\text{m}$ .

**Environmental samples.** River and peat bog water samples and lichens (class *Hypogymnia physodes*) were collected in Šumava National Park, Czech Republic. Water samples were filtered through the membrane filter Pragozor 6 (Pragochema s.r.o., Czech Republic) with pore size 0.40  $\mu\text{m}$ , prior to the analysis.

Samples of lichens were dried, grinded and decomposed by microwave assisted digestion in presence of *aqua regia* (HCl:HNO<sub>3</sub> 3:1). Conditions of microwave digestion in Milestone Digestion/drying mls 1200 (Milestone) equipped with six Teflon™ cartridges consisted of five steps were 200W for 2 min, 400 W for 2 min, 0 W for 5 min and 600 W for 10 min. Finally, it was set to 20 min cooling. After digestion and cooling the residue was filtered with the paper filter No. 0.025, collected in a volumetric flask and made up to 50 mL.

**SPE arrangement.** During sorption process solution was simultaneously pumped through repeatedly used plastic cartridge columns placed in a water-pump-operated vacuum solid phase extraction column processor Baker SPE-12G (J.T. Baker).

A peristaltic pump PCD 82.4 K (Kouřil, Kyjov, Czech Republic) was equipped with four positions for 3 mm silicone tubing to connect the cartridges and operated with an optimized solution flow rate of  $1 \text{ mL min}^{-1}$ .

An electric hot plate (Altec s.r.o., Czech Republic) served for evaporation of the eluate with

organic solvent before ICP-MS determination.

**Sorption and elution procedures on Amberlite™ Strata SDB-L.** Cartridges with the sorbents were first washed with 10 mL of 96% ethanol and then conditioned with 10 mL of cationic surfactant solution or complexation agent with selected concentration. Optimization studies were tested with 50 mL of sorption solution containing  $10 \mu\text{g L}^{-1}$  of PGMs. After sorption followed elution of PGMs with 10 mL of organic solvent or organic solvent in the presence of  $1 \text{ mol L}^{-1}$  HCl. The organic solvent was then evaporated from elution solution on electric hot plate and residue was supplemented to a 10 mL volumetric flask by  $1 \text{ mol L}^{-1}$  HCl. The enrichment factor was 5. For optimization of preconcentration were simultaneously sorbed four parallel solutions under the same conditions. Resulting values of recoveries were averaged and relative standard deviation of recovery was calculated. All results of recoveries are given in % of recoveries and were compared to five times the signal of intensity of a reference sample (solution with  $10 \mu\text{g L}^{-1}$  of PGMs in  $0.1 \text{ mol L}^{-1}$  HCl).

## RESULTS AND DISCUSSION

**Optimization of sorption.** For the optimization purposes, the influences of pre-treatment of column (conditioning of sorbent) by complexing agents or surfactants, combination of complexing agents with surfactants, concentration of complexing agents in sorbed solutions, acidity of sorbed solutions and influence of surfactant concentration in conditioning solution were studied.

Pre-treatment of SDB-L sorbent was performed using conditioning by various complexing agents, such as ammoniumpyrrolidindithiocarbamate (APDC), thiourea (TU), 4-(2-pyridylazo)resorcinol (PAR) and 8-hydroxyquinoline-5-sulfonic acid (8-HQS) or by using various cationic surfactants: benzyltrimethyltetradecylammonium chloride (Zephyramine®), N-( $\alpha$ -carbethoxypentadecyl)trimethylammonium bromide (Septonex®) and benzyltrimethyl-dodecylammonium bromide (Ajatin®). The results are shown in Table number 2. Among them, it is evident that conditioning of the sorbent using complexing agents is not appropriate. In contrast conditioning by cationic surfactant can be advantageously used.

Because the sorbent conditioning by complexing agent prior to the sorption of platinum group metals was not successful, was tested by conditioning with cationic surfactant and in the presence of complexing agents in sorbed solution. They were all tested combinations of cationic surfactants and agents. Sorption was carried out under similar conditions as described below the

Table 2. All results are shown in Table 3. As is evident from the above results, it seems most appropriate combination Septonex® and 4-(2-pyridylazo)resorcinol (PAR). In this system, the recovery of sorption was about 100% both for platinum, palladium and osmium. This system was used for further optimization tests of sorption efficiency of platinum group metal sorbed on SDB-L.

The next step was to determine the optimal concentration of reagent PAR. Tested concentrations  $2.5 \cdot 10^{-6}$ ,  $5 \cdot 10^{-6}$ ,  $1 \cdot 10^{-5}$  and  $2.5 \cdot 10^{-5}$  mol L<sup>-1</sup> of PAR showed that the best results of sorption efficiency was achieved at  $1 \cdot 10^{-5}$  mol L<sup>-1</sup> concentration. This amount of agent was used in the next experiments.

One of the other tested parameters during optimization process was an acidity of sorbed solution. Sorption of 50 mL with 10 µg L<sup>-1</sup> of PGMs

and  $1 \cdot 10^{-5}$  mol L<sup>-1</sup> PAR in 0.1 mol L<sup>-1</sup> HCl was carried out under optimal sorbent pre-treatment by  $5 \cdot 10^{-3}$  mol L<sup>-1</sup> Septonex® and followed elution by acetonitrile with 1 mol L<sup>-1</sup> HCl (4:1). Average recoveries show that under high pH (5-7) occurred to increasing sorption efficiency only for Rh and Ir. For platinum, palladium and osmium seems to be the best lower pH. As optimal acidity was selected pH 1 (caused by the presence of 0.1 mol L<sup>-1</sup> HCl) in order to avoid adsorption of platinum group metal complexes on the volumetric flask wall at higher pH values. At pH 1 was achieved return sorption for Pt, Pd and Os, exceeding 95%. All other measurements are therefore carried out under conditions of pH 1.

To determine optimal concentration of surfactant were tested various concentrations of Septonex®, results are viewed in Table 4. The

**TABLE 2**  
Sorption efficiency (%) for various pre-treatment of the sorbent.

	Ru	Rh	Pd	Os	Ir	Pt
<b>Conditions 1</b>						
APDC <sup>a</sup>	2.7±0.8	0.6±0.04	25.8±1.6	83.6±2.8	6.9±0.7	65.2±1.3
TU <sup>b</sup>	2.5±0.2	0.2±0.01	96.8±1.8	85.6±1.3	6.1±0.8	48.8±1.7
PAR <sup>c</sup>	0.5±0.03	0.1±0.01	94.4±3.7	14.3±1.3	5.6±0.7	6.4±0.3
8-HQS <sup>d</sup>	0.6±0.09	0.2±0.02	58.1±2.5	24.9±2.8	6.5±0.9	9.4±0.7
<b>Conditions 2</b>						
Zephyramine®	44.5±1.99	2.2±0.2	98.6±2.1	57.1±0.6	60.5±1.2	70.2±0.8
Septonex®	43.5±0.6	1.7±0.02	58.3±2.8	89.8±3.9	82.0±1.4	86.9±1.9
Ajatin®	42.3±1.6	1.4±0.03	96.7±1.9	29.8±0.5	64.4±0.4	55.9±0.2

<sup>a</sup>-Ammoniumpyrrolidindithiocarbamate, <sup>b</sup>-thiourea, <sup>c</sup>-4-(2-pyridylazo) resorcinol, <sup>d</sup>-8-hydroxyquinoline-5-sulfonic acid. **Conditions 1** – conditioning of sorbent by 10 mL of  $5 \cdot 10^{-6}$  mol L<sup>-1</sup> of agent in 0.1 mol L<sup>-1</sup> HCl. **Conditions 2** - conditioning of sorbent by 10 mL of  $1 \cdot 10^{-3}$  mol L<sup>-1</sup> of cationic surfactant in 0.1 mol L<sup>-1</sup> HCl. Followed sorption of 10 µg L<sup>-1</sup> of PGMs in 0.1 mol L<sup>-1</sup> HCl, elution by 10 mL acetonitrile with 1 mol L<sup>-1</sup> HCl (4:1).

**TABLE 3**  
Sorption efficiency (%) for various pre-treatment of the sorbent by cationic surfactants and in the presence of complexing agents in sorbed solutions.

	Ru	Rh	Pd	Os	Ir	Pt
<b>Zephyramine®</b>						
APDC <sup>a</sup>	43.5±1.3	3.7±0.07	24.8±0.2	73.6±1.4	46.2±1.4	93.9±0.9
TU <sup>b</sup>	42.5±0.8	2.3±0.1	61.3±3.4	95.4±0.9	57.0±1.0	91.2±0.7
PAR <sup>c</sup>	41.6±1.2	1.9±0.1	88.0±4.6	71.0±0.6	48.5±0.7	86.5±0.9
8-HQS <sup>d</sup>	44.7±1.7	1.8±0.1	78.6±3.4	58.9±0.6	72.9±1.0	84.6±0.8
<b>Septonex®</b>						
APDC <sup>a</sup>	44.9±1.3	1.6±0.08	19.3±0.4	91.4±1.0	36.5±2.2	98.9±1.8
TU <sup>b</sup>	42.2±1.8	1.1±0.04	97.9±2.7	73.8±1.0	29.6±1.2	57.8±1.6
PAR <sup>c</sup>	<b>41.4±1.3</b>	<b>1.1±0.04</b>	<b>99.4±2.9</b>	<b>96.9±3.1</b>	<b>42.5±1.0</b>	<b>99.4±1.7</b>
8-HQS <sup>d</sup>	40.4±1.6	1.1±0.09	98.1±4.4	62.4±1.5	24.0±0.4	88.2±1.8
<b>Ajatin®</b>						
APDC <sup>a</sup>	40.8±0.7	1.8±0.04	7.8±1.2	52.1±4.8	40.9±0.6	77.3±0.7
TU <sup>b</sup>	39.8±0.3	1.6±0.05	31.9±3.9	10.2±1.7	51.6±0.6	25.6±0.7
PAR <sup>c</sup>	43.1±0.5	1.7±0.05	80.0±2.5	18.0±0.6	51.7±1.1	40.5±1.6
8-HQS <sup>d</sup>	37.1±2.0	1.4±0.2	36.0±2.4	8.8±2.4	62.0±3.6	33.7±1.4

<sup>a</sup>-Ammoniumpyrrolidindithiocarbamate, <sup>b</sup>-thiourea, <sup>c</sup>-4-(2-pyridylazo) resorcinol, <sup>d</sup>-8-hydroxyquinoline-5-sulfonic acid. See conditions of sorptions under Table 2.



sorption conditions were following: conditioning of SDB-L sorbent by 10 mL of  $1.10^{-4}$ ,  $5.10^{-4}$ ,  $1.10^{-3}$  or  $5.10^{-3}$  mol L<sup>-1</sup> Septonex® in the presence of 0.1 mol L<sup>-1</sup> HCl, sorption of 50 mL solution with 10 µg L<sup>-1</sup> of PGMs in 0.1 mol L<sup>-1</sup> HCl in the presence of  $5.10^{-6}$  mol L<sup>-1</sup> 4-(2-pyridylazo) resorcinol (PAR). Elution was performed using 10 mL of mixture with acetonitrile and 1 mol L<sup>-1</sup> HCl (4:1). The tested Septonex® concentrations showed that increasing concentrations increases the sorption efficiency. The concentration  $5.10^{-3}$  mol L<sup>-1</sup> this cationic surfactant Septonex® seems to be the best concentration. Higher concentrations were not tested because of possible contamination ICP-MS instrument.,

**Optimization of elution.** To determine the optimal elution efficiency were tested by series of eluents. The sorption was carried out under the following conditions: conditioning of sorbent by 10 mL of  $5.10^{-3}$  mol L<sup>-1</sup> Septonex® in 0.1 mol L<sup>-1</sup> HCl, sorption of 50 mL solution with 10 µg L<sup>-1</sup> of PGMs in 0.1 mol L<sup>-1</sup> HCl in the presence of  $5.10^{-6}$  mol L<sup>-1</sup> 4-(2-pyridylazo) resorcinol (PAR). For elution was always used 10 mL of solution, presented in Table 5.

The most suitable eluent was mixture of

acetonitrile and 1 mol L<sup>-1</sup> HCl in the ratio 4:1 because of almost 100% recoveries for platinum (IV) and palladium (II).

After finding the optimal eluent mixture was also examined in detail the elution volume for the quantitative elution of the adsorbed platinum group metal complexes. The conditions of sorption were: conditioning of sorbent by 10 mL of  $5.10^{-3}$  mol L<sup>-1</sup> Septonex® in 0.1 mol L<sup>-1</sup> HCl, sorption of 50 mL solution with 10 µg L<sup>-1</sup> of PGMs in 0.1 mol L<sup>-1</sup> HCl in the presence of  $1.10^{-5}$  mol L<sup>-1</sup> 4-(2-pyridylazo) resorcinol (PAR). For elution was used 10 mL of solution mixture of acetonitrile: 1 mol L<sup>-1</sup> HCl (4:1) (see Table 5). To determine the elution curve was collected a total of 10 mL of elution mixture for each milliliter of separately. Thereafter, the individual fractions of the eluate were prepared similarly as above (evaporated on a hot plate and transfer to the 10 mL volumetric flasks). From the elution curve shown in Figure 1 is seen that the quantitative elution for all intercepted platinum group metal complexes occurs during the first five milliliters. For quantitative elution is recommended twice the amount of eluate, meaning 10 mL. This elution volume was used during each sorption.

**TABLE 4**  
The effect of different Septonex® concentrations on average recoveries (%).

concentration <sup>a</sup>	Ru	Rh	Pd	Os	Ir	Pt
$1.10^{-4}$	8.0±0.5	0.2±0.03	63.8±1.7	51.4±1.6	13.2±0.5	52.5±1.9
$5.10^{-4}$	32.1±0.6	0.6±0.02	89.5±2.1	64.1±1.0	17.3±0.4	82.6±2.0
$1.10^{-3}$	38.1±1.7	0.7±0.08	98.6±3.0	71.3±0.8	18.5±0.4	97.4±0.5
<b><math>5.10^{-3}</math></b>	<b>43.2±0.8</b>	<b>2.5±0.6</b>	<b>99.9±1.5</b>	<b>73.5±0.2</b>	<b>46.6±4.1</b>	<b>101.7±1.8</b>

<sup>a</sup>–Concentration (mol L<sup>-1</sup>) of Septonex® in conditioning solution

**TABLE 5**  
Average recoveries (%) PGMs after elution by various solvents.

eluent	Ru	Rh	Pd	Os	Ir	Pt
ET <sup>a</sup>	39.0±0.8	0.8±0.1	44.7±0.7	87.0±1.9	24.4±0.4	66.9±1.9
AC <sup>b</sup>	43.0±0.7	0.9±0.09	95.5±2.7	76.4±1.2	19.5±1.2	80.2±1.3
ACN <sup>c</sup>	35.7±0.5	0.9±0.09	71.0±1.7	95.9±2.9	21.6±0.4	78.6±0.5
ET:AC (1:1)	36.2±0.2	0.6±0.07	77.4±1.3	55.6±0.7	16.2±0.2	73.2±1.3
ET:ACN (1:1)	38.8±0.6	0.9±0.1	76.0±2.8	43.7±1.5	12.3±0.8	72.5±0.8
AC:ACN (1:1)	41.7±0.9	0.8±0.08	93.9±2.6	71.1±2.5	13.5±1.4	89.0±1.4
ET:HCl <sup>d</sup> (4:1)	42.7±1.1	1.4±0.2	58.7±1.9	68.4±1.7	21.5±1.4	94.3±1.8
AC:HCl (4:1)	40.4±0.3	1.3±0.3	89.5±2.4	66.3±0.9	43.3±1.2	99.4±0.9
<b>ACN:HCl (4:1)</b>	<b>40.0±0.3</b>	<b>1.0±0.1</b>	<b>99.8±0.4</b>	<b>93.3±1.2</b>	<b>32.0±1.7</b>	<b>99.0±0.6</b>
ET:AC:HCl (2:2:1)	41.9±0.3	1.1±0.1	83.5±1.2	67.9±1.4	28.8±0.1	98.8±1.7
ET:ACN:HCl (2:2:1)	45.4±0.9	1.1±0.06	88.2±2.4	68.1±1.3	30.1±1.7	100.6±2.5
AC:ACN:HCl (2:2:1)	45.4±0.8	1.2±0.09	89.8±1.9	69.0±1.1	33.2±0.6	98.8±1.7

<sup>a</sup>–ET absolute ethanol, <sup>b</sup>–AC acetone (concentrated), <sup>c</sup>–ACN acetonitrile (concentrated), <sup>d</sup>–hydrochloric acid with concentration 1 mol L<sup>-1</sup>.

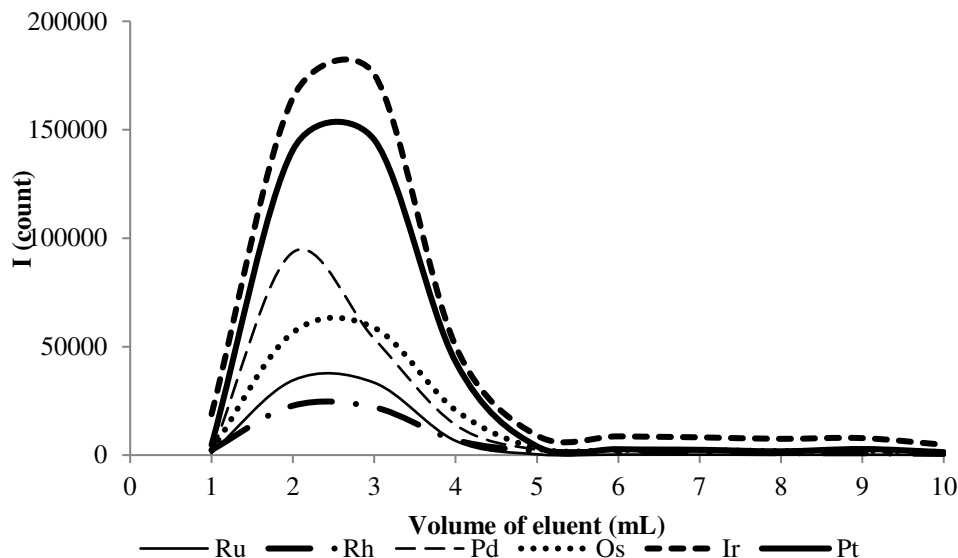


**FIGURE 1**  
Elution curves for all platinum group metals.

**Effect of foreign ions.** The effect of various concentrations of selected cations, anions and their mixtures to the sorption efficiency of the platinum group metals was studied. The sorption was carried out under optimal conditions. Selected individual ions were  $\text{Na}^+$ ,  $\text{K}^+$ ,  $\text{Ca}^{2+}$ ,  $\text{Mg}^{2+}$ ,  $\text{Al}^{3+}$ ,  $\text{Fe}^{3+}$ ,  $\text{Cl}^-$ ,  $\text{NO}_3^-$ ,  $\text{SO}_4^{2-}$ ,  $\text{PO}_4^{3-}$  and  $\text{CO}_3^{2-}$ . To the amount of platinum group metals in sorbed solution were calculated excess of interfering ions 1:100, 1:1000, 1:2500 and 1:10000, which corresponds to the range concentrations  $1.10^{-5}$ ,  $1.10^{-4}$ ,  $2.5.10^{-4}$  and  $1.10^{-3}$  mol  $\text{L}^{-1}$  of ions. Also tested were mixed standard solutions containing  $\text{Al}^{3+}$ ,  $\text{Ba}^{2+}$ ,  $\text{Ca}^{2+}$ ,  $\text{Cd}^{2+}$ ,  $\text{Co}^{2+}$ ,  $\text{Cr}^{3+}$ ,  $\text{Cu}^{2+}$ ,  $\text{Fe}^{2+}$ ,  $\text{Mg}^{2+}$ ,  $\text{Mn}^{2+}$ ,  $\text{Na}^+$ ,  $\text{Ni}^{2+}$ ,  $\text{Pb}^{2+}$ ,  $\text{Ti}^{4+}$ ,  $\text{Zn}^{2+}$  and mixture of anions, such as  $\text{Br}^-$ ,  $\text{Cl}^-$ ,  $\text{F}^-$ ,  $\text{NO}_3^-$ ,  $\text{SO}_4^{2-}$ ,  $\text{PO}_4^{3-}$  and  $\text{SO}_4^{2-}$  both in the excess 1:100 and 1:1000 against to platinum group metal concentrations.

No interference was observed for platinum and palladium in all tested conditions in the presence of various ions or their combinations. Only osmium showed reduce sorption efficiency to 60% and the other platinum group metals recoveries remained unchanged.

**Real samples of water and lichens.** This sorption system was developed for the analysis of real samples from the environment. There were tested three types of real samples – river water, peat

bog water and lichens (class *Hypogymnia physodes*). In these samples, we unexpected the presence of platinum group metals because of their origin from the Šumava National park in Czech Republic. They have been used as a real matrix for verifying the effectiveness of the sorption of platinum group metals for the analysis of real samples, under real conditions.

The samples of water and lichens were treated as described in section 2.3. After this, sorption under optimized conditions was applied conditioning of SDB-L in plastic cartridge sorbent by 10 mL of  $5.10^{-3}$  mol  $\text{L}^{-1}$  of Septonex® in 0.1 mol  $\text{L}^{-1}$  HCl, sorption of 50 mL real sample solution with 10  $\mu\text{g L}^{-1}$  of PGMs in 0.1 mol  $\text{L}^{-1}$  HCl in the presence of  $1.10^{-5}$  mol  $\text{L}^{-1}$  4-(2-pyridylazo) resorcinol (PAR). For elution was used 10 mL of solution mixture of acetonitrile : 1 mol  $\text{L}^{-1}$  HCl (4:1). The recovery results demonstrate that the matrix of real samples no affects the success of the SPE and the process may therefore be used for their analysis regard to the content of platinum metals.

After finding no matrix effect of lichens on recoveries of sorption for platinum group metals, the samples of lichens *Hypogymnia physodes* were exposed to the exhaust gases near the busy road in the city of Brno. Traffic frequency of this road is average about 16,000 vehicles per 24 hours.

**TABLE 6**  
The contents of platinum group metals ( $\mu\text{g kg}^{-1}$ ) in lichen samples.

Samples	Ru	Rh	Pd	Os	Ir	Pt
Exposed lichens <sup>1</sup>	< LOD	< LOD	< LOD	< LOD	721.4	187.9
Exposed lichens <sup>2</sup>	168.9	< LOD	397.1	1534.5	748.9	246.0

<sup>1</sup> Direct determination by ICP-MS, <sup>2</sup> ICP-MS determination after SPE on SDB-L sorbent.

Samples of lichens were installed in strainers (about 10 g) using the dry bag technique and placed on the crash barrier. The time exposure of these samples was three months. After this the samples were collected, weighted 0.25 g of lichens and pre-treated as described in section 2.3. Then followed the sorption on SDB-L sorbent under optimized conditions. The quantity of determined platinum group metals in sample of blank and in exposed samples were shown in Table 6. For comparison is shown the direct determination<sup>(1)</sup> of platinum group metals in pre-treated samples and determination which preceded the solid phase extraction<sup>(2)</sup> for separation of matrix effect and preconcentration of determined metals. This experiment, preceded by the determination of blanks, that was determination of uncontaminated samples of lichens by direct measurement and determination after the sorption procedure. All measured values of blanks lying below the detection limits for platinum group metals.

## CONCLUSIONS

The preconcentration technique SPE of platinum group metals on Amberlite polystyrene-divinylbenzene based sorbent (Strata SDB-L) was optimized. There were tested conditions for pre-treatment of sorbent, conditioning, conditions for the sorption process and was found optimal elution. The optimum for the sorption of platinum group metals appears following: conditioning of sorbent by 10 mL of  $5.10^{-3}$  mol L<sup>-1</sup> Septonex® in 0.1 mol L<sup>-1</sup> HCl, sorption of 50 mL solution with 10 µg L<sup>-1</sup> of PGMs in 0.1 mol L<sup>-1</sup> HCl in the presence of  $1.10^{-5}$  mol L<sup>-1</sup> 4-(2-pyridylazo) resorcinol (PAR). For elution with success was used 10 mL of solution mixture of acetonitrile: 1 mol L<sup>-1</sup> HCl (4:1). Under these conditions 100% recoveries has been achieved for platinum, palladium and osmium. The sorption efficiency for ruthenium and iridium were about 40% and rhodium is not possible preconcentrated by this method of SPE.

In the analysis of real samples the matrix effect has been detected for river and peat bog water and for decomposed samples of lichens *Hypogymnia physodes*. The samples of lichens *Hypogymnia physodes* were exposed to the exhaust gases near the busy road in the city of Brno, installed in strainers (about 10 g) using the dry bag technique and placed on the crash barrier. The time exposure of these samples was three months and following the application of optimized SPE method. During the direct determination only iridium and platinum were detected. After optimized SPE methods also the others platinum group metals were determined.

Thus, this procedure can successfully be used for evaluating the content of the platinum group metals, especially Platinum and Palladium, in environmental samples.

## ACKNOWLEDGEMENTS

This work was supported by the Ministry of Education, Youth and Sports of the Czech Republic under the research project, number FCH-S-16-3364.

## REFERENCES

- [1] Ravindra, K., Bencs, L., Van Grieken, R. (2004) Platinum group metals in the environment and their health risk. *The Science of the Total Environment* 318, 1-43.
- [2] Reith, F., Campbell, S.G., Ball, A.S., Pring, A., Southam, G. (2014) Platinum in Earth surface environments. *Earth-Science Reviews* 131, 1-21.
- [3] Jackson, M.T., Sampson, J., Prichard, H.M. (2007) Platinum and palladium variations through the urban environment: Evidence from 11 sample types from Sheffield, UK. *The Science of the Total Environment* 385, 117-131.
- [4] Lesniewska, B.A., Godlewska-Zylkiewicz, B., Bocca, B., Caimi, S., Caroli, S., Hulanicki, A. (2004) Platinum, palladium and rhodium content in road dust, tunnel dust and common grass in Bialystok area (Poland): a pilot study. *Science of the Total Environment* 321, 93-104.
- [5] Wang, J., Zhu, R., Shi, Y. (2007) Distribution of platinum group elements in road dust in the Beijing metropolitan area, China. *Journal of Environmental Sciences* 19, 29-34.
- [6] Pawlak, J., Lodyga-Chruscinska, E., Chrustowicz, J. (2014) Fate of platinum metals in the Environment. *Journal of Trace Elements in Medicine and Biology* 28, 247-254.
- [7] Bencs, L., Ravindra, K., Van Grieken, R. (2011) Platinum: Environmental Pollution and Health Effects. Reference Module in Earth Systems Sciences from Encyclopedia of Environmental Health, Elsevier, 580-595.
- [8] Platinum, Environmental Health Criteria 125 (1991) World Health Organization, Geneva, 1-139.
- [9] Bencs, L., Ravindra, K., Van Grieken, R. (2003) Methods for the determination of platinum group elements originating from the abrasion of automotive catalytic converters. *Spectrochimica Acta Part B* 58, 1723-1755.
- [10] Komendova-Vlasankova, R., Sommer, L. (2002) Separation and preconcentration of platinum group metals and gold on modified silica and XAD sorbents in the presence of cationic surfactants for their determination by ICP-AES. *Collect. Czech. Chem. Commun.* 67, 454-469.
- [11] Ljubomirova, V., Djingova, R. (2008) Speciation of inorganic platinum-chloride complexes in spiked environmental samples by



SPE and ICP-AES. Anal. Chim. Acta 614, 119-126.

[12] Guidelines for data acquisition and data quality evaluation in environmental chemistry (1980). Analytical Chemistry 52, 2242-2249.

---

**Received:** 15.10.2015

**Accepted:** 25.02.2016

---

#### **CORRESPONDING AUTHOR**

---

**Renata Komendova**

Brno University of Technology, Faculty of Chemistry, Institute of Chemistry and Technology of Environmental Protection, Purkynova 118  
612 00 Brno, CZECH REPUBLIC

e-mail: [komendova@fch.vutbr.cz](mailto:komendova@fch.vutbr.cz)

# ISOLATION AND IDENTIFICATION OF ENTOMOPATHOGENIC FUNGI *BEAUVERIA BASSIANA* FROM TURKEY

Alev Haliki Uztan<sup>1</sup>, Ozlem Abaci Gunyar<sup>1\*</sup>, Aysegul Yoltas<sup>1</sup>, Nevin Keskin<sup>2</sup>

<sup>1</sup>Ege University, Faculty of Science, Department of Biology, Basic and Industrial Microbiology Section, 35100, Bornova, Izmir, Turkey

<sup>2</sup>Hacettepe University, faculty of Science, department of Biology, Applied Biology Section, Ankara, Turkey

## ABSTRACT

The control of the agricultural pests is crucial for commercial products. There is a growing interest for biological control of these pests and one of the most effective and safe biocontrol agents is *Beauveria bassiana* (Balsamo-Crivelli) Vuillemin, which is an entomopathogenic fungus. The soil environment is a significant resource for entomopathogenic fungi. In this study the diversity and distribution of entomopathogenic fungus *Beauveria bassiana* (Bals.-Criv.) Vuill. was assessed throughout an extensive soil survey in Turkey carried out during 2013 and 2014. Soil samples from the seven regions of Turkey were taken and *Beauveria* spp. isolates were obtained from six of these regions, with 32 positive sites out of 150 sites sampled. The isolates were identified as *Beauveria bassiana* based on phenotypic and molecular data. *Beauveria bassiana* was isolated from the European (Marmara) as well as the Asiatic peninsula (Anatolia) of Turkey.

## KEYWORDS:

*Beauveria bassiana*, isolation, Galleria bait method, entomopathogenic fungus, data.

## INTRODUCTION

Since 1980 there is a growing interest for biological control of pest insects [1-4]. Fungi are important biological control agents and among all the biological control agents of entomopathogenic fungi species, *Beauveria bassiana* (Balsamo-Crivelli) Vuillemin which was firstly described about 178 years ago, has always been considered as a hotshot fungus that can be used for control of pest insects. The first review on the genus *Beauveria* was published by MacLeod, including a taxonomic revision of both *Beauveria* and *Tritirachium*. The study encompassed cultural and morphological characteristics of numerous *Beauveria* isolates and species [5]. This research was followed by the study of De Hoog, in 1972, in which the genus was restricted to three species: *B. bassiana*, *B.*

*brongniartii* and *B. alba*. Humber and Domsch et al. presented advanced descriptions of *Beauveria* spp. in 1997 and 1980 respectively [6 – 8]. The studies on phylogenetics of the genus *Beauveria* took place in 2005 by Rehner & Buckley [9, 10]. Among all the studies interested in *Beauveria* spp. there are only a few about the genus in Turkey, one them belonging to Sevim et al. (2010) [11]. The aim this study is to determine the abundance, distribution and identification of entomopathogenic fungus *Beauveria* spp.

## MATERIALS AND METHODS

### Sampling sites and collection of soil samples.

180 soil samples were collected from different sampling sites in Turkey during 2013-2014. Detailed information that is related to the soil sources for positive sites and isolates is given in Table 1. Within the given site, approximately three soil samples of 1 kg each were taken and placed in polyethylene bags, sealed with an adhesive tape and transported to the laboratory. Each subsample of soil was obtained with a hand trowel from the upper 15-20 cm after removing the surface litter and after collecting of each soil sample, the hand trowel was immediately sterilized with 70% ethyl alcohol.

**Isolation of *Beauveria bassiana*.** Isolates of *Beauveria* spp. were collected from soil samples using “Galleria bait method” [12]. The wax moth, *Galleria mellonella* L. came from a continuously reared colony maintained at 24±2 °C. Approximately 240 ml soil, dampened with distilled water was placed in 250 ml plastic container and five last instar larvae of *Galleria mellonella* (L.) were placed on the soil, and the container was covered with a perforated lid and inverted. According to a modified method used by Woodring and Kaya (1988), before the baiting procedure, wax mouth larvae were immersed in 55 °C water for 25-30 s to impede their ability to produce silk webbing in the soil [13]. During the fourteen days of baiting, the containers were daily stirred to ensure contact of spores to larvae. Soil samples were checked in every three days and dead larvae were removed and surface-sterilized in 1%

sodium hypochlorite for 2-3 min, then washed in sterile distilled water [14]. Then they were placed on damp filter paper within a sterile petri dish and incubated at  $26 \pm 2$  °C for 7–14 days [15]. After the incubation period, fungi were isolated from all larvae showing external mycelia growth on Sabouraud dextrose agar medium with 1% yeast extract (SDAY, Merck) to which 50 µg /ml chloramphenicol and 1 ml dodine ( 1 g dodine was dissolved in 10 ml distilled water ) were added to prevent bacterial and other fungal growth [16].

**Identification of *Beauveria bassiana*.**  
**Phenotypic Identification.** Pure cultures of fungi on Oat Meal Agar without antibiotic were used for morphological identification. Colony morphology and spore shape of isolated fungal strains were used in the first identification process with a light microscope and initially identified according to the key described by Humber (1997) [7].

**Molecular Studies.** DNA isolation was made

as previously described, with some modification (Liu et al, 2000) [17]. Genomic DNA was electrophoresed in an agarose gel and control of purity and concentrations were made as described by Olgun et al. [18].

ITS1- 5.8-ITS2 region (ITS) of the nuclear ribosomal DNA was amplified with ITS1 and ITS4 universal primers [19].

The determination of the base sequences of the ITS region in our study were fulfilled in Atlas Biotechnology Laboratory with Applied Biosystem Model 3130. The data obtained were evaluated with Finch TV (Blast) and Ap E programs. Type determination was performed by examining the similarities through the comparison of nucleotide sequences on the web page of Gene Bank (<http://www.ncbi.nlm.nih.gov/blast/Blast.cgi>) open to the access of researchers. Dendrograms were drawn with the MEGA 4.0 program.

**TABLE 1**  
**Isolate numbers, GenBank accession numbers for the ITS1- 5.8-ITS2 region (ITS) of the nuclear ribosomal DNA and isolation details of the *Beauveria bassiana* strains**

Isolate name	Accession numbers	Isolation source-Location
Ank1	KP862991	Grassland Soil-Ankara/Güdül
Ank2	KP862973	Herbage Soil-Ankara/Karacaören A
Ank3	KP862968	Grassland Soil-Ankara/Karacaören B
AnkH3	KP862969	Agricultural field-Ankara/Haymana
Ank4	KP862993	Undisturbed Soil-Ankara/Beyazarı
Ank5	KP862970	Agricultural field-Ankara/Gölbashi
Ank6	KP862994	Grassland Soil-Ankara/İncek
Ank11	KP862971	Agricultural field-Ankara/Tulumtaş
Ank13	KP862995	Agricultural field-Ankara/Ballıkuyumcu
Ank20	KP862977	Hayfield Soil-Ankara/Çubuk
Aydinakbuk	KP862966	Agricultural field-Aydın/Akbük
Aydinsoke	KP862967	Agricultural field-Aydın/Söke
Bb3	KP862992	Hayfield Soil-Kayseri
Bb5H6	KP862978	Agricultural Field-Kayseri/Hacılar
Bb12	KP862979	Undisturbed Soil-Niğde
Bb15	KP862974	Undisturbed Soil-Nevşehir
Bb19	KP862975	Forest Soil-Artvin
Bb20	KP862976	Hayfield Soil-Erzurum
Bb69/3	KP862996	Hayfield Soil-Bayburt
Den1	KP862984	Grassland Soil-Denizli
Den2	KP862985	Agricultural field-Denizli/Tavas
Istanbulcatalca	KP862981	Hayfield Soil-İstanbul/Çatalca
Istanbuldilbileyen	KP862980	Undisturbed Soil-İstanbul/Dilbileyen
Kizilder	KP862983	Undisturbed Soil-Tokat/Kızıldere
Lul1	KP862965	Forest Soil-Kırklareli/Lüleburgaz1
Lul2	KP862972	Sunflower Field-Kırklareli/Lüleburgaz2
Lul5	KP862990	Grassland Soil-Kırklareli/Lüleburgaz5
Mer019-20	KP862986	Pine Forest Soil-Mersin
Sb1B	KP862987	Poplar Planted Soil-Ankara/Beytepe1
Sb2	KP862988	Poplar Planted Soil-Ankara/Beytepe2
Sb4	KP862989	Undisturbed Soil-Ankara/Beytepe4
Ordu	KP862982	Hazelnut Orchard Soil-Ordu



**FIGURE 1**

Neighbour-joining tree generated by Mega 4.0 for ITS regions, including ITS1-5.8S-ITS2. The sequences of the isolates have been deposited in the GenBank, and their accession numbers are given in Table1. \**Beauveria bassiana* isolate EABb08\_04Ep was identified by Landa et al. (2013) [20] and its accession number is KC753384J.

## RESULTS

Isolates were obtained from six out of seven regions (except for southeast of Anatolia) of Turkey. A total of 32 soil isolates out of 150 soil samples was found positive for *Beauveria* spp (Table 1). Phenotypic examination was made according to Humber (1997) [7]. According to phenotypic identification, our isolates were defined as *Beauveria bassiana*.

For the molecular analyses, the ITS region was amplified and sequenced. Phenotypic identification of our isolates was confirmed to be *B. bassiana* by molecular identification (Figure 1).

## DISCUSSION

The aim of this study was to provide information about the diversity and abundance of entomopathogenic fungus *Beauveria* spp. Isolates were obtained from six out of seven regions (except for southeast of Anatolia) of Turkey, with 32 positive sites out of 150 sites sampled. *Beauveria bassiana* is found to be apparently one of the common occupants of soil and the isolates detected in this study were within the expected range based on previous studies performed using the Galleria bait method [16, 21, 22].

Among *Beauveria* sp., *B. bassiana* is the most widely distributed species. It is found both in temperate and tropical areas throughout the world [5,

8, 12]. According to Zimmerman (2007), habitats for *B. bassiana* range from an alpine soil, to heathland, peat bogs, soils with savannah type vegetation, forest and cultivated soils, sand blows and dunes and desert soil. Likewise, we found *B. bassiana* both agricultural and nonagricultural soils and in undisturbed soils of different region of Turkey (Table 1) [23].

Morphological criteria are generally used to identify and classify *Beauveria* spp. But identifying fungi in species level correctly has major importance before doing any further experiment and is very difficult and sometimes impossible depending on only macro- and micromorphological data. Distinction between *Beauveria* species is troublesome, since there is comparatively large heterogeneity in *B. bassiana* species. The main difference between the most common species, *B. bassiana* and *B. brogniartii*, is the shape and size of conidia. While *B. bassiana* has mainly spherical conidia, the spores of *B. brogniartii* are more cylindrical. But it is shown that spore shape could alter after culturing. Accounting these difficulties researchers face with morphological identification, a number of molecular techniques were developed to assist correct species identification of *Beauveria* [16, 24, 25]. It is stated that placing the fungi in separate phylogenetic clades or species based on molecular markers will provide much more information to their ecology in both managed and natural ecosystems than will traditional morphological characterization [26].

As for all the fungi, molecular genetic techniques have gain importance in solving the problems of taxonomy, identification, and genetic variation for entomopathogenic fungi in recent years. The discrimination of *Beauveria* species can be performed by the analysis of electrophoretically separated restriction enzyme-digested total genomic DNA. Combining these restriction fragment- length polymorphisms (RFLPs) with certain DNA probes can even determinate specimens at the strain level. In addition to that, random amplified polymorphic DNA (RAPD) analyses have been used to differentiate entomopathogenic fungal isolates [27]. These methods can distinguish accurately; however, for routine analyses, they are rather complex and time consuming, and require expensive materials and equipment. Moreover, these methods are difficult to apply routinely and require a lot of experience.

Basic DNA-based approaches such as Polymerase Chain Reaction (PCR), has transformed fungal taxonomy in species delimitation [25, 28]. Among all rapid methods in detecting microbial pathogens, PCR, which include steps such as, DNA extraction, PCR amplification and the detection of amplicons is one of the most sensitive. DNA extraction methods which were used in our study are rapid, easy-to-perform and do not require expensive chemicals such as zymolase. PCR assay we used is

also rapid and easy to interpret. Fragments containing the ITS1- 5.8-ITS2 region (ITS) of the nuclear ribosomal DNA that were amplified using primers ITS1 and ITS4 primers.

For addressing the phylogenetics and identification of fungi, the nuclear rRNA cistron has been used for more than 20 years. The eukaryotic rRNA cistron includes 18S, 5.8S, and 28S rRNA genes transcribed as a unit by RNA polymerase I. The cistron is split by posttranscriptional processes, ends up in removing two internal transcribed spacers. These two spacers, including the 5.8S gene, are usually referred to as the Internal Transcribed Spacers or the ITS region. In phylogenetics the 18S nuclear ribosomal small subunit rRNA gene (SSU) is commonly used. Species are occasionally discriminated by only 28S nuclear ribosomal large subunit rRNA gene (LSU) or a combination of ITS with this gene. Exhibiting the barcode gap between inter- and intraspecific variation that can be most clearly identified, the internal transcribed spacer region is the ribosomal cistron region, which can, most probably, be successfully identified to have the broadest range of fungi [29].

In some fungi ITS can also be used for providing an indication of delimitation by a measure of the genetic distances. In terms of the discrimination of fungi species, ITS was generally predominant over LSU, in addition to having a barcode gap that could be identified more clearly. Schoch et al. recommended ITS to be the standard barcode for fungi in consideration of all these arguments [29].

Even though the universal barcode for Fungi ITS is widely used in taxonomic analysis [29, 30], sequencing of regions in the DNA are also increasingly being used to separate species based for putting together phylogenetic data sets. In our study the determination of the base sequences of the ITS region of the 32 isolates which were identified phenotypically as *B. bassiana* were fulfilled. Sequence data sets were explicit and can be deposited in on-line databases GenBank. Their accession numbers are given in Table 1. Dendrograms were drawn with the MEGA 4.0 program.

Through this way, phenotypical identification was confirmed by molecular identification. *Beauveria bassiana* was isolated from the European (Marmara) as well as the Asiatic peninsula (Anatolia) of Turkey.

## REFERENCES

- [1] Austwick, PKC. (1980). The Pathogenic Aspects of the Use of Fungi: The Need For Risk Analysis and Registration of Fungi. *Ecological Bulletin (Stockholm)*, 31, 91-102.
- [2] Burges, HD. (1981). Safety, Safety Testing and



- Quality Control of Microbial Pesticides. In: *Burges HD, editor. Microbial control of pests and plant diseases 1970-1980. London: Academic Press, 737-767.*
- [3] Hall, R.A., Zimmermann, G., Vey, A. 1982. Guidelines for the registration of entomogenous fungi as insecticides. *Entomophaga*, 27: 121 – 127.
- [4] Laird, M., Lacey, LA., Davidson, EW. (1990). Safety of Microbial Insecticides. *CRC Press., Boca Raton, FL, 259.*
- [5] MacLeod, DM. (1954). Investigations on the Genera *Beauveria* Vuill. and *Tritirachium* Limber. *Canadian Journal of Botany* Laird M, Lacey LA, Davidson EW, editors. 1990. Safety of microbial insecticides. *Boca Raton, FL: CRC Press. 259.*
- [6] De Hoog, GS. (1972). The Genera *Beauveria*, *Isaria*, *Tritirachium* and *Acrodontium* gen. nov. *Studies in Mycology*, 1, 1-41.
- [7] Humber, RA. (1997). Fungi: Identification. In: *Lacey LA, editor. Manual of techniques in insect pathology. San Diego, CA: Academic Press, 153-185.*
- [8] Domsch, KH., Gams, W., Anderson, TH. (1980). Compendium of Soil Fungi. *London: Academic Press., 136-140.*
- [9] Rehner, SA., Buckley, E. (2005). *Beauveria* Phylogeny Inferred from Nuclear IST and EFI-Asequences: Evidence for Cryptic Diversification and Links to Cordyceps Teleomorphs. *Mycologia*, 97, 84-98.
- [10] Rehner, SA. (2005). Phylogenetics of the Insect Pathogenic Genus *Beauveria*. In: Vega FE, Blackwell M, editors. *Insect-fungal associations. Ecology and evolution. Oxford: University Press, 3-27.*
- [11] Demir, I., Sevim, A., Höfte, M., Humber, R.A., Demirbag, Z. 2010. Isolation and characterization of entomopathogenic fungi from hazelnut-growing region of Turkey. *BioControl*, 55: 279–297.
- [12] Zimmermann, G. (1986). The ‘Galleria bait method’ for Detection of Entomopathogenic Fungi in Soil. *Journal of Applied Entomology*, 102, 213-215.
- [13] Woodring, JL., Kaya, HK. (1988). Steinernematid and Heterorhabditid Nematodes: A Handbook of Biology and Techniques. *Arkansas Agricultural Experiment Station, Fayetteville*
- [14] Chase, A.R., Osborne, L.S., Ferguson, V.M. 1986. Selective isolation of the entomopathogenic fungi *Beauveria bassiana* and *Metarhizium anisopliae* from an artificial potting medium. *The Florida Entomologist* 69: 285 – 292.
- [15] De La Rosa, W., Segura, HR., Barrera, JF., Williams, T. (2000). Laboratory Evaluation of the Impact of Entomopathogenic Fungi on *Prorops Nasuta* (Hymenoptera: Bethyridae), A Parasitoid of the Coffee Berry Borer. *Environmental Entomology*, 29, 126-131.
- [16] Meyling, NV., Eilenberg, J. (2007). Methods for Isolation of Entomopathogenic Fungi from the Soil Environment. *Laboratory manual. http://orgprints.org/11200*, 32, 818-890.
- [17] Liu, D., Coloe, S., Baird, R., Pederson, J. 2000. Rapid Mini-Preparation of Fungal DNA for PCR, *Journal of Clinical Microbiology*, 38 (1): 471.
- [18] Olgun, A., Topal, A. 1998. . Methods Used in Molecular Biology. In: Temizkan, G., Yilmazer, S. Research and Application Center of Biotechnology and Genetic Engineering (BIYOGEM), Publication no 1. Hall, RA., Zimmermann, G., Vey, A. (1982). Guidelines for the Registration of Entomogenous Fungi as Insecticides. *Entomophaga*, 27. 121-127.
- [19] Samson, R.A., Visagie, C.M., Houbraken, J., Hong, S.B., Hubka, V., Klaassen, C.H.W., Perrone, G., Seifert, K.A., Susca, A., Tanney, J.B., Varga, J., Kocsube, S., Szigeti, G., Yaguchi, T., Frisvad J.C. 2014. Phylogeny, identification and nomenclature of the genus *Aspergillus*. *Studies In Mycology*. 78: 141–173. Keller, S., Kessler, P., Schweizer, C. (2003). Distribution of Insectpathogenic Fungi in Switzerland with Special Reference to *Beauveria brongniartii* and *Metarhizium anisopliae*. *BioControl*, 48, 307–319
- [20] Landa, BB., Lopez-Diaz, C., Jimenez-Fernandez, D., Montes-Borrego, M., Munoz-Ledesma, FJ., Ortiz-Urquiza, A., Quesada-Moraga, E. (2013). In-Planta Detection and Monitorization of Endophytic Colonization by a *Beauveria Bassiana* Strain Using a New-Developed Nested and Quantitative PCR-Based Assay and Confocal Laser Scanning Microscopy. *J. Invertebr. Pathol.*, 114 (2), 128-138.
- [21] Chandler, D., Hay, D., Reid, A.P. 1997. Sampling and occurrence of entomopathogenic fungi and nematodes in UK soils. *Appl Soil Ecol.*, 5: 133–141.
- [22] Keller, S., Kessler, P., Schweizer, C. 2003. Distribution of insectpathogenic fungi in Switzerland with special reference to *Beauveria brongniartii* and *Metarhizium anisopliae*. *BioControl*, 48: 307–319.
- [23] Zimmermann, G. (2007). Review on Safety of the Entomopathogenic Fungi *Beauveria bassiana* and *Beauveria brongniartii*. *Biocontrol Science and Technology*, 17(5/6), 553-596.
- [24] Safavi, S.A. 2010. Isolation, Identification and Pathogenicity Assessment of a new Isolate of Entomopathogenic Fungus, *Beauveria bassiana* in Iran. *Journal of Plant Protection Research*, 50 (2): 158 – 163. Tsedaley, B. (2015). A Review



- on Disease Detection, Pathogen Identification and Population Genetics in Fungi. *Journal of Biology, Agriculture and Healthcare*, 5 (1), 6-20.
- [25] Agrawal, Y., Mual, P., Shenoy, BD. (2014). Multi-gene Genealogies Reveal Cryptic Species *Beauveria rudraprayagi* sp. nov. from India. *Mycosphere*, 5 (6), 719–736.
- [26] Tsedaley, B. 2015. A Review on Disease Detection, Pathogen Identification and Population Genetics in Fungi. *Journal of Biology, Agriculture and Healthcare*, 5 (1): 6 – 20.
- [27] Sabbahi R., Lavallée, R., Merzouki A., Guertin C. 2009. Differentiation of entomopathogenic fungus *Beauveria bassiana* (Ascomycetes: Hypocreales) isolates by PCR-RFLP. *Phytoprotection*, 90 (2) : 49 – 56.
- [28] Shenoy, BD., Jeewon, R., Hyde, KD. (2007). Impact of DNA Sequence-data on the Taxonomy of Anamorphic Fungi. *Fungal Diversity*, 26, 1–54.
- [29] Schoch, C.L., Seifert, K.A., Huhndorf, S., Robert, V., Spouge, J.L., Levesque, C.A., Chen, W. 2012. Fungal Barcoding Consortium, Nuclear ribosomal internal transcribed spacer (ITS) region as a universal DNA barcode marker for Fungi. *Proceedings of National Academy of Sciences (PNAS)*, 109 (16): 6241–6246.
- [30] Seifert, K.A. 2009. Barcoding Fungi: Progress Towards DNA Barcoding of Fungi. *Molecular Ecology Resources*, 9 (1): 83 – 89.

---

**Received:** 10.11.2015

**Accepted:** 11.04.2016

---

**CORRESPONDING AUTHOR**

---

**Ozlem Abaci Gunyar**

Ege University, Faculty of Science, Department of Biology, Basic and Industrial Microbiology Section, 35100, Bornova, Izmir, Turkey

e-mail: [ozlemabaci@yahoo.com](mailto:ozlemabaci@yahoo.com)

# CLASSIFICATION AND IDENTIFICATION OF ORGANIC COMPOUNDS BY PATTERN RECOGNITION BASED ON NEAR INFRARED SPECTROSCOPY

Mingyue Liu<sup>1</sup>, Jin Liu<sup>2</sup>, Yanjun Yu<sup>3</sup>, Peng Zhou<sup>2</sup>, Rongxin Su<sup>1,4,\*</sup>, Wei Qi<sup>1,4</sup>, Libing Wang<sup>3</sup>, Zhimin He<sup>1</sup>

<sup>1</sup>State Key Laboratory of Chemical Engineering, Tianjin Key Laboratory of Membrane Science and Desalination Technology, School of Chemical Engineering and Technology, Tianjin University, Tianjin 300072, P. R. China.

<sup>2</sup>College of Precision Instrument and Optoelectronics Engineering, Tianjin University, Tianjin 300072, China

<sup>3</sup>Technical Center for Safety of Industrial Products, Tianjin Entry-Exit Inspection and Quarantine Bureau, Tianjin 300308, China;

<sup>4</sup>Collaborative Innovation Center of Chemical Science and Engineering (Tianjin), Tianjin 300072, China

## ABSTRACT

Near infrared spectroscopy (NIRS) combined with chemometrics has emerged as a prominent analytical technique for testing of food stuffs, agricultural products, pharmaceutical products, and a variety of other chemicals. In this paper, we have investigated the feasibility of using near infrared (NIR) absorption spectroscopy combined with pattern recognition to rapidly classify and identify a group of 101 liquid organic compounds, consisting of 25 alcohols, 14 carboxylic acids, 12 aldehydes, 15 ketones and 35 esters (including 11 phthalate esters). A strategy of combining linear discriminant analysis (LDA) classifiers and principal component analysis (PCA) classifiers in a cascade structure was used to build the classification and identification models. The built models had a correct classification rate of 99.01% (100/101) and a correct identification rate of 96.04% (97/101) for the spectra of 101 organic compounds in the test set. These results demonstrate that NIR spectroscopy combined with pattern recognition is a promising method for the fast classification and identification of organic compounds.

## KEYWORDS:

Near infrared spectroscopy, Organic compounds, Pattern recognition, LDA, PCA.

## INTRODUCTION

The NIR region spans the wavelength range of 780–2500 nm, in which absorption bands correspond mainly to overtones and combinations of fundamental vibrations [1]. The NIR spectrum of a sample provides information on the relative proportions of C-H, N-H, and O-H bonds, which are the primary structural components of organic molecules [2].

Combined with chemometrics, NIRS provides a powerful set of tools for quantitative and

qualitative modelling of foodstuffs [3], agricultural products [4], pharmaceutical products [5] and other chemicals. In recent years, the many advantages of NIRS such as its low cost, high speed of analysis, non-destructive nature [6] and non-requirement of pre-treatment have made it a popular analytical tool for a variety of testing applications. NIRS technique has been reported to find applications in the confirmation of origin and authenticity of European extra virgin olive oil samples and classification of Spanish extra virgin olive oils [3, 7], identification of edible oil and swill-cooked dirty oil [8], determination of fermentation process parameters of Chinese rice wine [9], classification of vinegar and lettuce [10, 11], determination the concentrations of lead and zinc in Chinese herbs [12], adulterant detection of milk powder [13], determination of the geographical origin of wheat [14], identification of pharmaceutical excipients [15], etc. Fundamentally, these applications are based on the combination of chemometrics and NIR spectra, which is produced by the organic compounds in these products.

Among the various applications of NIRS, only a few are directly related to organic compounds, such as determination of alcohol and extract concentration in beer [16], quantitative analysis of glucose [6], quantification of glucose, fructose and sucrose in bayberry juice [17], and determination of chemical composition of complex mixtures of alcohols, acetone, acetonitrile, hydrocarbons and water [18]. However, to the best of our knowledge, no study has been reported on the application of NIRS to classify or identify organic compounds.

The most popular modern tools for identification of organic compounds are mass spectrometry, nuclear magnetic resonance, chromatography, UV/Vis-spectroscopy, infrared spectroscopy, as well as certain combinations of these techniques. Compared with the traditional classical methods for identification of organic compounds, which depend on colour changes, solubility, and generation of by-products in some special reactions, these methods are accurate and

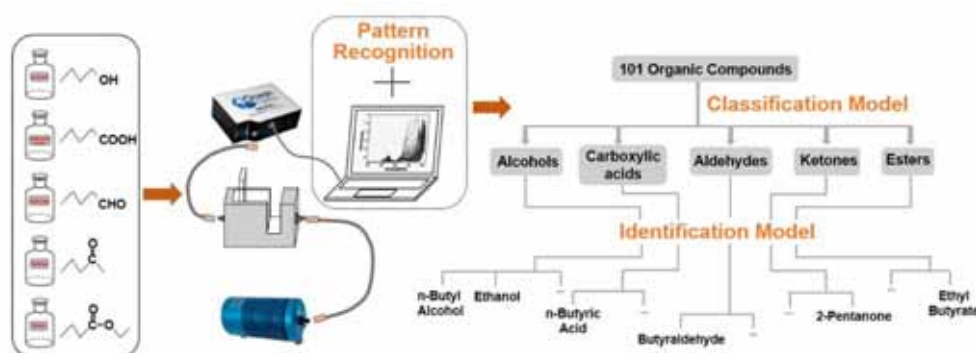


FIGURE 1

A schematic illustration of classification and identification of 101 organic chemicals

reliable. While these techniques are extremely effective in qualitative analysis, there are still a few drawbacks, such as lengthy analysis times, high cost and requirement for trained operator.

Therefore, there is a need for rapid and low-cost techniques for the qualitative analysis of organic compounds, and one such promising method involves the combination of spectroscopy and pattern recognition. In this field, Lavine et al. have used NIRS and pattern recognition to classify carboxylic acids and non-carboxylic acids [19]. Even though the bands in the near infrared region often overlap [20], NIRS can still exploit meaningful information from the spectrum for qualitative analysis with the help of chemometrics.

The object of this study is to develop a simple, fast, cost-effective and robust model to classify and identify liquid organic compounds. A group of 101 chemicals, including alcohols, carboxylic acids, aldehydes, ketones and esters was chosen for model building (Table S1, ESI†). The 101 chemicals were chosen without any special criteria, just because they are representative, common, and easy to find in laboratories. The strategy of successively combining classifiers in a cascade structure was applied for the model building. In this process, the two most common pattern recognition methods, principal component analysis (PCA) and linear discriminant analysis (LDA), were applied. As shown in figure 1, spectra of chemicals were measured by a NIRQuest spectrometer at the first step. Then the classification and identification model was built to classify and identify the 101 organic compounds with the help of pattern recognition.

## MATERIALS AND METHODS

**Materials.** A group of 101 organic chemicals, including 25 alcohols, 14 carboxylic acids, 12 aldehydes, 15 ketones and 35 esters (11 phthalate esters included) were used in this paper. Some of the organic compounds were purchased from

Aladdin Chemistry Co., Ltd. (Shanghai, China). The rest were obtained from Sinopharm Chemical Reagent Co., Ltd (Tianjin, China), Concord Technology Co., Ltd. (Tianjin, China) and Guangfu Technology Development Co., Ltd (Tianjin, China). All the chemicals were liquid and of analytical grade quality or higher.

**NIR spectral collecting.** The NIR transmission spectra were collected on a NIRQuest spectrometer (Ocean Optics Co., Ltd) over a wavelength range of 900 to 1720 nm at 1.55-1.64 nm intervals. Quartz cuvettes (Puxi optical instrument factory, Jiangsu, China) with a capacity of 0.7 mL and a path length of 2 mm were used. After testing each sample, the cuvette was washed using absolute ethyl alcohol and double-distilled water, and dried by an air compressor.

During the experimental period, there were some variations in the ambient conditions (temperature and moisture level), cuvettes and instrument status, which led to a slight difference among various measurements on the spectra of the same organic compound. So, one measurement was regarded as one sample. Samples in training set were randomly measured in one month (ambient room temperature: 19-26 °C). Each of the 101 organic compounds was measured once, and 3 replicates were obtained at each measurement. Thus, the training set has 101 samples and 303 spectra. The spectra of 101 organic compounds in training set are shown in figure 2.

To test the reliability and robustness of the model, the samples in test set were measured during a period of several months, during which the ambient room temperature varied from 18 to 31 °C. The test set contained 210 samples and 4733 spectra (Table S2, ESI†). In the test set, if any spectrum of a sample is misclassified or misidentified, that sample will be regarded as misclassified or misidentified and the corresponding chemical will not be counted in the correct rate.

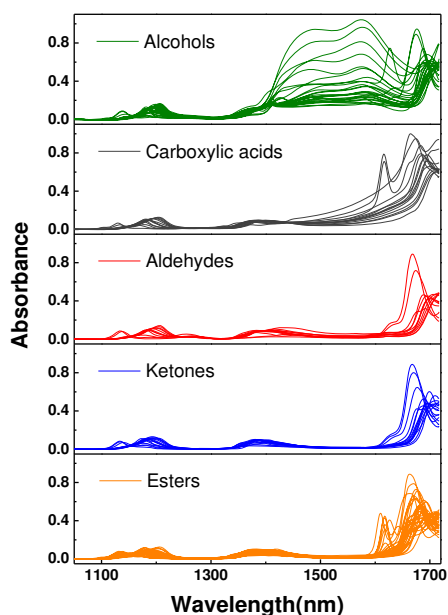


**FIGURE 2**  
Spectra of 101 organic compounds in training set (after offset correction)

enomic DNA was extracted with protocol and reagents followed by Sigma-Aldrich GenElute™ Plant genomic DNA Mini-prep Kit. Total amount of DNA was quantified through Qubit® 2.0 Fluorometer. Protocol fluorometer used 199  $\mu\text{L}$  Qubit buffer plus 1  $\mu\text{L}$  Qubit reagent to prepare reaction buffer then for standard 190  $\mu\text{L}$  of reaction buffer 10  $\mu\text{L}$  of standard from kit followed by 199  $\mu\text{L}$  of reaction buffer and 1  $\mu\text{L}$  of DNA sample quantified against standard. Nineteen primers table.1 (Thermo Scientific) were used for RAPD analysis; fourteen primers that produced clear and reproducible fragments were selected for further PCR reactions. The PCR reaction was performed with an initial denaturation steps one cycle of 15 min at 94°C, followed by 44 cycles of 94°C for 1 minute denaturation, 36°C for 1 minute annealing and 72°C for 2 minute extension followed by a final extension period of 5 minutes at 72°C PCR was allowed to ensure full extension of all implied products [24]. The amplifications were carried out in triplicate. PCR products and a 100-bp DNA ladder (Gene-On) were resolved electrophoretically in 1 % agarose gels containing 0.5  $\mu\text{L}$  ethidium bromide, and run at 100V for about 1 hr. RAPD banding patterns were visualized using UVP gel documentation system.

**Statistical Analysis.** Polymorphism was observed in RAPD profiles included disappearance of a normal band and appearance of a new band comparing all samples with RAPD profiles. Amplified bands were scored as 1 (presence) or 0 (absence). Only strong bands were scored for

analysis. The size and images of each amplification product were captured using the Vision Works LS Version 6.8 automatically estimated using a high resolution scan and digitalized images evaluated directly for RAPD analysis. The data was scored from the RAPD profiles through PAST version 3.08, were subjected to UPGMA cluster analysis to establish the relationship among the eight accessions selected from the different areas [32]. Genetic similarity coefficient among the different localities of *M. azedarach* was estimated through [41] coefficient matrix. The polymorphism percentage was estimated by dividing the number of polymorphic bands over the total number of amplified bands. **Data pre-processing:** Offset correction was firstly applied to correct for a parallel baseline shift [21], which may be caused by variations in ambient conditions during the measurements, slight differences of the path length and any contaminants in the cuvettes, etc. In this application, the average absorbance from the 26th to 92nd point in each spectrum was subtracted from every point in the spectrum independently (as defined by Eq. S1, ESI†).

A comparison between the spectra of ethanol which were measured on different dates, without any pre-processing and after offset correction showed that the baseline shift in the vertical direction was weakened, especially in the wavelength band of 900-1500 nm, resulting in a zero baseline at the beginning of the spectrum (Figure S1, ESI†).

To reduce the size of the spectral data and remove the insignificant information, only the wavelength band of 1050-1700 nm of spectrum (after offset correction) was selected for model building. Another pre-processing method, such as the first derivative (direct difference) method combined with moving window smoothing (Eq. S2, ESI†), with a window width of 5 variables, was further applied after offset correction, when any classification problem occurred.

**Algorithms:** The purpose of the classification model is to classify an unknown sample into one of the five categories, namely alcohols, carboxylic acids, aldehydes, ketones and esters. The identification model is also built to determine which category an unknown sample belongs to, and in this case there are 101 categories involved. Due to the large number of categories into which a sample may be classified, one single classifier is not enough, especially for the identification model. So a strategy of successively combining classifiers in a cascade structure was applied for the model building, in an approach called the cascade classifier [22]. In this framework, the unknown sample will be classified by a sequence of classifiers until it is classified into a category,

which is typically the correct category for the sample. Algorithms applied in the process of model building were LDA and PCA, both of which have been widely used in the field of pattern recognition, such as face recognition [23, 24], handwriting recognition [25], and object detection [26].

In the process of designing LDA and PCA classifiers, the training data (after pre-processing) is the input for the algorithms, and eigenvalues and eigenvectors are the outputs. As we want to perform the process of classification in 1-D space, only the eigenvector associated with the maximal eigenvalue of LDA is saved for classification, which will allow the classifier to achieve maximum separation among categories. In the case of PCA, depending on the actual results, the first principal component (PC1) or the second principal component (PC2) will be saved for classification. These vectors (eigenvector, PC1 or PC2) are called the optimal discriminant projection vector (ODPV) [24].

The training data will be compressed after projecting onto the ODPV, and each sample of the training set will be represented as a score, which is given by TRS (score of sample in training set). The classification threshold (CT) is then determined by these TRS scores. Serving as the boundary of two classes, CT directly affects the classification error [28], which makes it important to define CT properly. In this paper, CT is defined as the average of the maximum TRS of the class with lower score on the whole and the minimum TRS of the other class. This computational method of CT is described by Eq. S3 (ESI†).

For an unknown sample to be classified, the pre-processing will be firstly applied to the raw spectrum of the sample. Then a score will be obtained from the projection of the data vector of spectrum onto ODPV of the classifier. The score of the unknown sample will be marked as TES (score of sample in test set). Meanwhile, the TES will be used for the classification by comparing with the CT of this classifier. In two-class cases, the decision method is described by Eq. S4 (ESI†).

**Classification model:** The classification model consisted of a four-layer cascade structure of LDA classifiers (Figure S2a, ESI†). At the first stage of the cascade, a LDA classifier was trained to separate 25 kinds of alcohols from the 101 organic compounds. The subsequent three LDA classifiers were also trained to separate out carboxylic acids, aldehydes, ketones and esters successively in the last three stages of the cascade. Meanwhile, the ODPV and CT values of each classifier were also saved in this training set. Thus, the cascade classifier for classification was built.

The test set, which was sorted into a sequence of alcohols, carboxylic acids, aldehydes, ketones and esters, was used to test the classification model.

The TESs at each stage were calculated after the spectral data in the test set were projected onto ODPV. Fig. 3 depicts the classification process of all the samples in test set. As shown in Fig. 3a, all samples of alcohols (the first 1447 black dots) in test set are positioned above the line of decision threshold along with samples of alcohols in training set, which indicate that all these 1447 spectra (67 samples, see Table S2, ESI†) had a correct classification. The inset of Fig. 3a is the score plots of training set in the first stage of the cascade, which was actually a classifier of alcohols and non-alcohols. As they have already been classified, these samples are not shown in the next figures. Figure 3b-3d describe the classification process of the samples of carboxylic acids, aldehydes and ketones in test set.

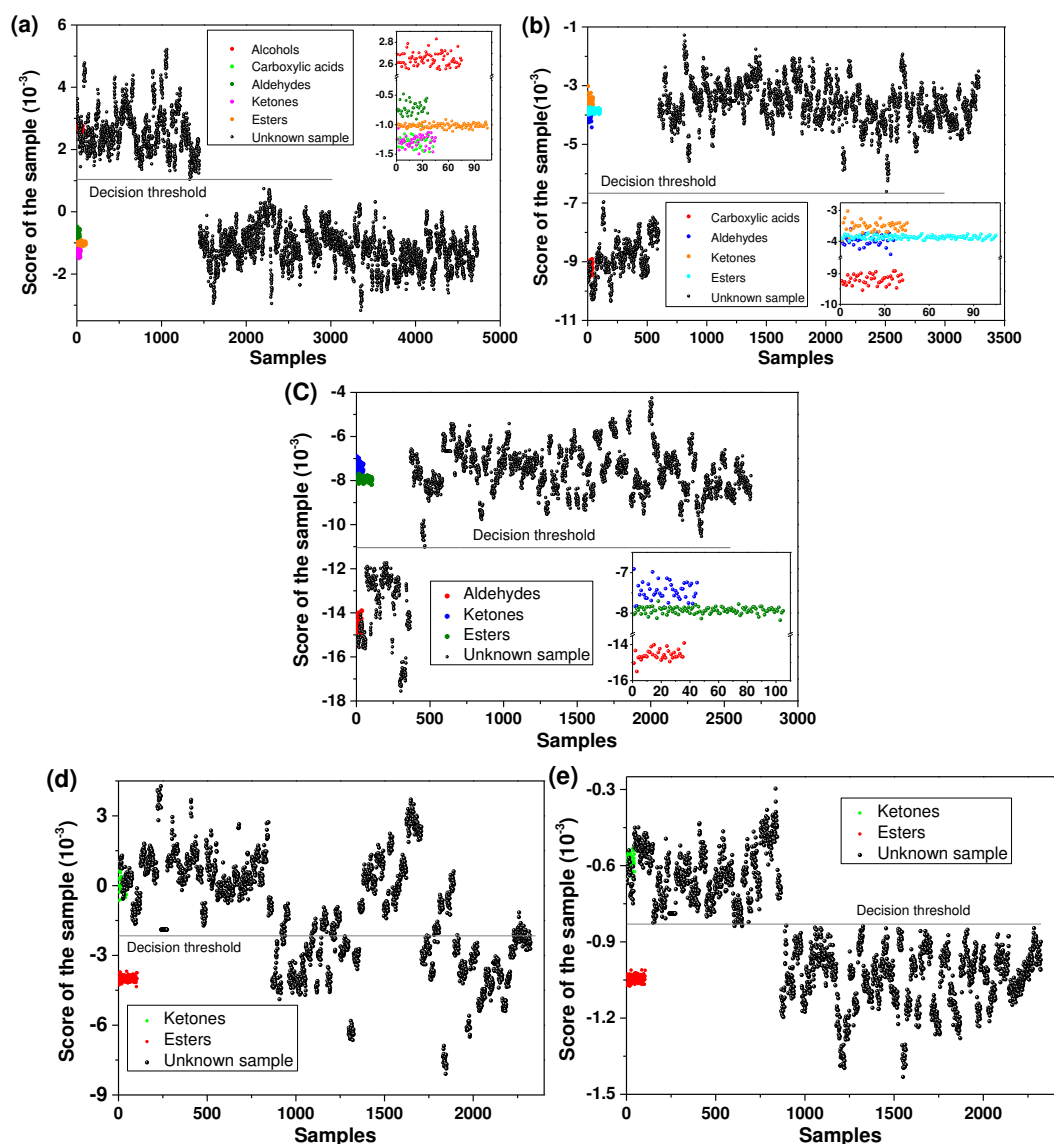
In all, samples of alcohols, carboxylic acids, aldehydes and ketones in the test set had a correct classification rate of 100%, while many samples of esters were incorrectly classified as ketones. This may be caused by similar spectra of ketones and esters and the fact that the second classifier faces a more difficult task than the first in the cascade classifier [22]. Therefore, the first derivative method was applied after offset correction and moving window smoothing to increase the differences in spectra between ketones and esters. Then, the fourth stage of the cascade classifier was rebuilt by LDA.

The correct classification rate of samples of ketones and esters in test set increased from 66% (33/50) to 98% (49/50) after part of the classification model was rebuilt as described above.

**Identification model:** Based on the classification model, we proceeded to build the identification model with LDA classifiers and PCA classifiers. The approach used contains both pre-classification and final classification steps.

Firstly, the classification model was embedded into the identification model. The samples in training set were initially classified into five categories. In the manual design procedure of cascade structure, cluster analysis was applied to divide each of the five categories into a few sub-categories, and these sub-categories were further divided into even smaller sub-categories until only one sample was contained in all the sub-categories. It should be noted that the esters were grouped into phthalate esters and non-phthalate esters at the second stage (Figure S2b, ESI†). Serving as a cluster analysis method, PCA played an important role in the pre-classification. PCA determined the number and members of classes that a sub-category will be divided into, which were important inputs for the supervised algorithm of LDA.

Finally, the PCA and LDA classifiers were trained by the samples in training set to get ODPV and CT of each classifier, and the cascade classifier



(a) Samples of alcohols in test set were separated out from the first classifier of the classification model  
 (b) Samples of carboxylic acids in test set were separated out from the second classifier of the classification model  
 (c) Samples of aldehydes in test set were separated out from the third classifier of the classification model  
 (d) Score plots of the first classification model for the remaining samples in training set and test set  
 (e) Score plots of the second classification model for the remaining samples in training set and test set

**FIGURE 3**  
**Score plots of samples in test set (black dots) and training set (colored dots)**

for identification of the 101 organic compounds was built. The test set was used again to validate the identification model.

## RESULTS

The models we built displayed a correct classification rate of 99.01% (100/101) and a correct identification rate of 96.04% (97/101).

The misidentification of the samples of 3-hexanone can be attributed to the misclassification of the 3-hexanone samples. If the samples were not misclassified, they could be correctly identified (Table S2, ESI<sup>†</sup>). Compared with the first classification model, the second one is able to distinguish clearly between the spectra of the esters and ketones, thus making the scores of samples of esters in test set closer to that of training set (Fig. 3d and Fig. 3e). At the same time, the scores of

samples of ketones in the test set became relatively closer to the line of decision threshold.

Besides the samples of 3-hexanone, samples of hexanoic acid, n-nonaldehyde and isovaleraldehyde were also partly or completely misidentified. As the classification and identification models were built on the absorbance of wavelength band of 1050-1700 nm, the misclassification and misidentification of the samples in test set can be attributed to the differences of spectra between samples in test set and training set for the same kind of organic compound. This is likely the reason for the samples of hexanoic acid to be misidentified as heptanoic acid and 2-ethylhexanoic acid. The spectra of hexanoic acid and heptanoic acid (or 2-ethylhexanoic acid) in training set are very different in the wavelength band of 1400-1700nm, but they overlap considerably in the wavelength band of 1680-1700 nm (Fig. S3a). As the classifier assigns different weights to the wavelength points of 1050-1700 nm, they can be potentially misclassified if their difference focus on the wavelength band with larger weights.

The misidentification of samples of n-nonaldehyde in test set may be caused by the similarity of spectra of n-nonaldehyde, undecylic aldehyde and n-heptaldehyde even in training set (Fig. S3b). In fact, any difference between the spectra of n-nonaldehyde in training and test sets will give rise to increase in spectral similarity of n-nonaldehyde with undecylic aldehyde or n-heptaldehyde, which will then increase the risk of misidentification. The misidentification of the first sample of isovaleraldehyde was not only caused by the similarity between the spectra of isovaleraldehyde and butyraldehyde in the training set (Fig. S3c), but also due to the principal of the model. Mathematically speaking, the model is a comparison of TRS and TES values, which depend on the absorbance of wavelength band of 1050-1700 nm and corresponding weights, and not on the portion of spectra or the waveform of spectra. That is why the spectrum (second measurement in test set) which had a large difference from the spectrum of isovaleraldehyde in the wavelength band of 1650-1700nm was correctly identified, while the spectrum (first measurement in test set) with less difference in the same wavelength band was incorrectly identified (Table S2, ESI†).

Briefly, it can be concluded that almost all the spectra in samples of an organic compound (marked as A) that were misidentified as another organic compound (marked as B) have at least one of the following characteristics: 1) the spectra of A and B are similar in part or even in the whole wavelength band of 1050-1700nm; 2) only the spectrum of A in test set is similar with the spectrum of B in training set. The misclassification and misidentification that originate from deviation

among spectra in test set and training set may be produced by a combined effect of temperature [29], ambient humidity [30], cuvettes, equipment noise, etc.

Although there was some misclassification and misidentification of samples in the test set, it must be noted that 17 samples of ethanol measured at different times and different ambient conditions were all classified and identified correctly (Table S2, ESI†), which indicates the robustness, reliability and temperature-stability of the models.

## DISCUSSION AND CONCLUSIONS

In summary, we have investigated the method of NIRS combined with pattern recognition to rapidly classify and identify a group of liquid organic compounds, and the results indicate that this method is feasible and reliable. Once the model is built, the spectral measurement takes just a minute or two, after which the classification and identification results will be exported from the model almost instantaneously. There are many potential applications of this method, such as rapid inspection of imported and exported goods, low-cost and fast detection of dangerous and forbidden organic compounds, etc. This promising technique can also provide a safe testing approach for unknown/unlabeled waste organic compounds generated in laboratories and factories. However, these models are only available for the organic compounds included in the training set. The identification of pure or mixed organic compounds that are not included in the training set will require further study.

## ACKNOWLEDGEMENTS

This work was supported by the Ministry of Science and Technology of China (No. 2012AA06A303), General Administration of Quality Supervision, Inspection and Quarantine of China (No. 2014IK072).

The first two authors contributed equally to the study.

## REFERENCES

- [1] M. Blanco and I. Villarroya. (2002) NIR spectroscopy: a rapid-response analytical tool. *TrAC, Trends Anal. Chem.*, 21, 240-250.
- [2] B. H. Stuart. (2005) *Infrared Spectroscopy: Fundamentals and Applications*. John Wiley & Sons, Ltd, p. 44.
- [3] T. Woodcock, G. Downey and C. P. O'Donnell. (2008) Confirmation of declared provenance of European extra virgin olive oil



- samples by NIR spectroscopy. *J. Agric. Food. Chem.*, 56, 11520-11525.
- [4] C. A. Watson. (1977) Near infrared reflectance spectrophotometric analysis of agricultural products. *Anal. Chem.*, 49, 835A-840A.
- [5] M. Blanco, J. Coello, H. Iturriaga, S. Maspocho and C. de la Pezuela. (1998) Near-infrared spectroscopy in the pharmaceutical industry. *Analyst*, 123, 135R-150R.
- [6] K. C. Patchava, M. Benaissa, B. Malik and H. Behairy. (2015) Local linear embedded regression in the quantitative analysis of glucose in near infrared spectra. *Anal. Methods*, 7, 1484-1492.
- [7] C. Pizarro, S. Rodriguez Tecedor, N. Perez-del Notario, I. Esteban Diez and J. M. Gonzalez Saiz. (2013) Classification of Spanish extra virgin olive oils by data fusion of visible spectroscopic fingerprints and chemical descriptors. *Food Chem.*, 138, 915-922.
- [8] Y. Zhou, T. Liu, J. Li and Z. Chen. (2015) Rapid identification of edible oil and swill-cooked dirty oil by using near-infrared spectroscopy and sparse representation classification. *Anal. Methods*, 7, 2367-2372.
- [9] Z. Wu, J. Long, E. Xu, C. Wu, F. Wang, X. Xu, Z. Jin and A. Jiao. (2015) Application of FT-NIR spectroscopy to Chinese rice wine for rapid determination of fermentation process parameters. *Anal. Methods*, 7, 2726-2737.
- [10] W. Fan, H. Li, Y. Shan, H. Lv, H. Zhang and Y. Liang. (2011) Classification of vinegar samples based on near infrared spectroscopy combined with wavelength selection. *Anal. Methods*, 3, 1872-1876.
- [11] A. L. B. Brito, D. A. Araujo, M. J. C. Pontes and L. F. B. L. Pontes. (2015) Near infrared reflectance spectrometry classification of lettuce using linear discriminant analysis. *Anal. Methods*, 7, 1890-1895.
- [12] A. Kolasani, H. Xu and M. Millikan. (2010) Analysis of metals in plant parts of selected Chinese herbs by near infrared spectroscopy. *Fresen. Environ. Bull.*, 19, 131-136.
- [13] L. L. Botros, J. Jablonski, C. Chang, M. M. Bergana, P. Wehling, J. M. Harnly, G. Downey, P. Harrington, A. R. Potts and J. C. Moore. (2013) Exploring authentic skim and nonfat dry milk powder variance for the development of nontargeted adulterant detection methods using near-infrared spectroscopy and chemometrics. *J. Agric. Food. Chem.*, 61, 9810-9818.
- [14] H. Zhao, B. Guo, Y. Wei and B. Zhang. (2013) Near infrared reflectance spectroscopy for determination of the geographical origin of wheat. *Food Chem.*, 138, 1902-1907.
- [15] A. Candolfi, R. De Maesschalck, D. L. Massart, P. A. Hailey and A. C. E. Harrington. (1999) Identification of pharmaceutical excipients using NIR spectroscopy and SIMCA. *J. Pharm. Biomed. Anal.*, 19, 923-935.
- [16] S. Castritius, A. Kron, T. Schafer, M. Radle and D. Harms. (2010) Determination of alcohol and extract concentration in beer samples using a combined method for near-infrared (NIR) spectroscopy and refractometry. *J. Agric. Food. Chem.*, 58, 12634-12641.
- [17] L. Xie, X. Ye, D. Liu and Y. Ying. (2009) Quantification of glucose, fructose and sucrose in bayberry juice by NIR and PLS. *Food Chem.*, 114, 1135-1140.
- [18] M. V. Reboucas, D. S. Brandão, A. Trindade, M. F. Pimentel and L. S. G. Teixeira. (2011) Chemical composition determination of complex organic-aqueous mixtures of alcohols, acetone, acetonitrile, hydrocarbons and water by near-infrared spectroscopy. *Vib. Spectrosc.*, 55, 172-182.
- [19] B. K. Lavine, K. Nuguru, N. Mirjankar and J. Workman, Jr.. (2012) Pattern recognition assisted infrared library searching. *Appl. Spectrosc.*, 66, 917-925.
- [20] B. H. Stuart. (2005) *Infrared Spectroscopy: Fundamentals and Applications*. John Wiley & Sons, Ltd, p. 47.
- [21] A. Candolfi, R. De Maesschalck, D. Jouan imbaud, P. A. Hailey and D. L. Massart. (1999) The influence of data pre-processing in the pattern recognition of excipients near-infrared spectra. *J. Pharm. Biomed. Anal.*, 21, 115-132.
- [22] P. Viola and M. J. Jones. (2004) Robust real-time face detection. *International Journal of Computer Vision*, 57, 137-154.23.
- [23] R. Gottumukkal and V. K. Asari. (2004) An improved face recognition technique based on modular PCA approach. *Pattern Recogn. Lett.*, 25, 429-436.
- [24] L. F. Chen, H. Y. M. Liao, M. T. Ko, J. C. Lin and G. J. Yu. (2000) A new LDA-based face recognition system which can solve the small sample size problem. *Pattern Recogn.*, 33, 1713-1726.
- [25] Y. Wen, Y. Lu and P. Shi. (2007) Handwritten Bangla numeral recognition system and its application to postal automation. *Pattern Recogn.*, 40, 99-107.
- [26] L. Malagón-Borja and O. Fuentes. (2009) Object detection using image reconstruction with PCA. *Image and Vision Computing*, 27, 2-9.
- [27] Y. Jian, D. Zhang, A. F. Frangi and Y. JingYu. (2004) Two-dimensional PCA: a new approach to appearance-based face



- representation and recognition. IEEE Transactions on Pattern Analysis and Machine Intelligence, 26, 131-137.
- [28] P. B. Garcia-Allende, O. M. Conde, J. Mirapeix, A. Cobo and J. M. Lopez-Higuera. (2008) Quality control of industrial processes by combining a hyperspectral sensor and Fisher's linear discriminant analysis. Sens. Actuators B, 129, 977-984.
- [29] W. S. Pegau, D. Gray and J. R. V. Zaneveld. (1997) Absorption and attenuation of visible and near-infrared light in water: dependence on temperature and salinity. Appl. Opt., 36, 6035-6046.
- [30] S. H. F. Scafi and C. Pasquini. (2001) Identification of counterfeit drugs using near-infrared spectroscopy. Analyst, 126, 2218-2224.

---

**Received: 03.12.2015**

**Accepted: 11.05.2016**

---

#### **CORRESPONDING AUTHOR**

---

**Rongxin Su**

State Key Laboratory of Chemical Engineering  
School of Chemical Engineering and Technology,  
Tianjin University  
Tianjin 300072, PR China

e-mail: surx@tju.edu.cn



# A QUANTITATIVE ANALYSIS OF URBAN WATER LANDSCAPE PATTERN CHANGES AND THEIR IMPACTS ON SURFACE TEMPERATURES

Lei Wang<sup>1,\*</sup>, Yunlong Yao<sup>2</sup>, Shuwen Zhang<sup>3</sup>

1. College of Architectural Engineering, Heilongjiang University of Science and Technology, 150022, Harbin, China;

2. College of Wildlife Resource, Northeast Forestry University, Harbin 150040, China

3. The Northeast Institute of Geography and Agroecology, Chinese Academy of Science, 130102, Changchun, China;

## ABSTRACT

The urban heat island effect is one of the most characteristic ecological and environmental problems during rapid urbanization. However, contemporaneous research on the mitigating factors of urban heat island effects is rare. Landsat TM images of Changchun city in 1993 and 2005 were used as data sources where information on urban water landscape changes was extracted and land surface temperatures were quantitatively estimated by a mono-window algorithm. Spatial relationships between water landscape density, water patch size, and land surface temperature was analyzed by geo-statistical analysis. Results show that the water landscape had substantial effects on temperature. Land surface temperature is greatly reduced when the area of water with the city reached 10 ha. There is a high correlation between shape index and the lowest water surface temperature; the correlation coefficient is 0.321 ( $P < 0.05$ ) and 0.321 ( $P < 0.01$ ) in 1993 and 2005, respectively. Water bodies had a high impact on the surrounding temperature within a buffer zone of a width of 720 m. In this buffer zone, the temperature increased by 1.440 °C from the water at 0-120 m and inland to 120-240 m, and then the temperature increased by 0.513°C from 120-240 m to 240-360 m in 1993, showing that the warming trend had a landward decrease. A landward increase continued by only 0.155°C from 480-600 m to 600-720 m. In 2005, the temperature increased by 1.336°C from 0-120 m to 120-240 m, by 0.640°C from 120-240 m to 240-360 m, and by only 0.011°C from 480-600 m to 600-720 m. The difference in temperature decreased gradually. The cooling effect was less substantial with an increase in the distance to water bodies. Therefore, if the area of water is too small, there will be little impact on the urban thermal environment. Also, increasing

the shape complexity of water patches appears to help promote heat exchange between water bodies and the surrounding landscape and could mitigate the urban heat island effect.

## KEYWORDS:

Water landscape, patch, land surface temperature, spatial analysis of GIS

## INTRODUCTION

Rapid urbanization increasingly exacerbates prominent environmental heat island problems and increases the frequency of extreme weather. With increasing urbanization, the regional climate and weather patterns can change and endanger the lives and safety of the urban residents [1, 2]. Of all the environmental effects of urbanization, the thermal environmental problem caused by the urban heat island effect has attracted recent attention from researchers [3-5]. Rapid urbanization has led to the change of the Earth's surface, causing the ground absorption and reflection of long-wave radiation energy to change. The reason for this long-wave radiation energy change is that vegetation, water, soil, and other natural land cover systems that have large heat capacity and thermal inertia are gradually replaced by artificial and impervious surfaces. At the same time, the artificial heat produced by human industry and life also changes such that these two processes come to jointly promote the emergence of an urban thermal environment problem [6, 7]. Those remaining natural landscape systems inside the city are of great significance toward mitigating the urban heat island effect [8]. However, human activities that result in the excessive development of water resources and land use/cover cause the water landscape patterns to

change, which accelerates water degradation [9].

Water is an important part of the urban landscape in terms of land-surface heat balance because it has a relatively large thermal inertia and thermal capacity as well as low heat conduction and thermal radiation rate [10]. Water is an inherent part of the underlying surface of the city and the regulating role that large bodies of water play in regulating role in the local thermal field cannot be overstated. To a certain extent, water bodies absorb and weaken the release of artificial heat sources so as to improve the local thermal environment of city. The size, boundary shape, and space distribution characteristics of urban water bodies comprise different landscape mosaics. The relationship between the landscape spatial pattern and ecological role of the mosaic is an important issue in landscape ecology research [11]. To study the issue, the spatial characteristics of landscape mosaics often need quantitative description, such as number, size, geometric shape, relative space position, etc., of the patches. The shape characteristics of landscape mosaics affect the movement of energy, materials, and biology, mainly by way of diffusion, mass flow, and locomotion [12]. This paper addresses the impacts of water landscape and patch features (patch size and boundary complexity) on urban land surface temperatures.

Changchun City is located in the middle latitudes of the northern hemisphere and is in the Great Plains hinterland of Northeast, China. The city's general geographic coordinates are 43° 46' to 43° 58'N and 125° 09' to 125° 48'E, which is in a temperate zone with semi-humid continental monsoon climate. There is a strong continental climate that causes a high annual temperature range. Changchun City is one of the economically important cities in Northeast Asia and is one of older industrial bases in the northeast, China. Urbanization has had a great impact on the climate of Changchun City and an environmental consequence of urbanization is the urban heat island effect. Thus, it appears that urban life could suffer from this serious threat to the ecological environment. In this case study, we selected a build-up area that has become urbanized over a decade (1993-2005) toward determining the influence of its evolving urban spatial structure on the natural ecological system. As a starting point, we used comprehensive classification principles for urban built-up areas from both the Chinese and international literature to establish a base map of

where the process of urbanization has converted land with natural surface cover to buildings and artificial cover, specifically both among the city's existing urban infrastructure and where its exterior urban fringes juxtapose outlying agricultural areas. To this end, remote sensing imagery and topographic maps were combined with field survey data, and from which geographic boundary lines establishing the urban-rural border around Changchun city were extracted.

## MATERIALS AND METHODS

**Data and image pre-processing.** Landsat Thematic Mapper (TM) images from September 8, 2005 and September 7, 1993 had very clear atmospheric conditions with no influence of clouds, and were used for extracting water landscape based on related geography analysis and expert knowledge. An image from the SPOT 5 satellite acquired on September 12, 2004 provided multispectral imagery of 10 meters spatial resolution and pan-sharpened imagery with a spatial resolution of 2.5 meters. Urban 1:500 topographic maps (n=33) were used to evaluate the classification accuracy of the urban water landscape; the results showed that the 91% success rate for correct interpretation. In addition, Landsat Thematic Mapper (TM) images were used to estimate land surface temperatures (LST).

**Analysis of water landscape pattern.** The density of landscape elements reflects the overall degree of fragmentation or differentiation. The landscape density index is the number landscape elements per unit area. Higher ratios correspond with greater proportions of certain types of landscape elements. The urban water landscape is a mosaic of water patches and corridors, which interact and are interconnected. Toward the study of urban water landscape mosaic pattern characteristics, that water landscape density index shows the distribution of water landscape elements and is thus chosen as a characterization parameter.

The spatial distribution of water landscape density was determined by grid methods in a geographic information system with spatial interpolation. First, we generated a 500 m by 500 m grid with Fishnet in ArcGIS and used the study area boundary grid for tailoring in order to avoid calculation errors along the edges [13]. Second, using a spatial query and index, the water landscape

was overlaid on the grid, so that the generated figure had a grid index ID with water landscape attributes [14]. The proportion of water landscape area in the whole grid is considered as the grid density of water landscape. The sampling points of spatial interpolation were obtained by information grid methods and gravity models in 1993 and 2005 of which were used in the spatial interpolation methods for geo-statistical analysis.

According to the study of Wiens (1993), the ratio of perimeter to area was one of the main indicators reflecting the patch shape; the greater the ratio of perimeter to area was, the more complex the shape. This complex shape could communicate more easily with the surrounding environment [15], therefore it is reasonable to take the shape index to reflect the thermal environment. Herein, we mainly analyze the impacts of patch characteristics (area and boundary complexity) on the urban heat island effect.

**Land surface temperature estimation.** In order to avoid the dependence on radiosounding in the RTE method, Qin *et al.* (2001) developed the following mono-window algorithm for obtaining LST from TM6 [16]:

$$T_s = \frac{1}{C} [a(1-C-D) + (b(1-C-D) + C+D)T_o - DT_a] \quad (1)$$

where  $T_s$  is land surface temperature (K);  $a = -67.355351$ , and  $b=0.458606$ ;  $C = \varepsilon\tau$ ,  $D = (1-\tau)[1 + (1-\varepsilon)\tau]$ ,  $\varepsilon$  is the land surface emissivity,  $\tau$  is the total atmospheric transmissivity;  $T_o$  is the effective at-sensor brightness temperature(K);  $T_a$  represents the mean atmospheric temperature given by

$$T_a = 16.011 + 0.92621T_o \quad (2)$$

$T_o$  being the near-surface air temperature. Qin *et al.* also estimated the atmospheric transmissivity from  $w$ , the atmospheric water vapor content, for the range 0.4-1.6 g/cm<sup>2</sup>, according to

$$\tau = 0.974290 - 0.08007 w \text{ (high } T_o) \quad (3a)$$

$$\tau = 0.982007 - 0.09611 w \text{ (low } T_o) \quad (3b)$$

More details about this algorithm and its sensitivity could be found in the work of Qin *et al.* (2001). Also, the computation of  $\varepsilon$  and  $T_o$  is explained by Xiao and Weng [17], and Jiménez-Munoz and Sobrino [18].

### Spatial buffer, overlay and statistic analysis.

The temperatures of the water patches are determined by the mean temperatures of the pixels. The LST\_MN (the mean LST) showed the potential of the cold island effect produced by water. Spatial overlay analyses were performed with the water patch and urban land surface temperatures [19], from which the relationships between water landscape and the LST were analyzed and regression models were constructed.

To further analyze the influence of local low temperatures created by water patches on surrounding environment a buffer analysis was made with respect to the water body. The TM images were selected to estimate the land surface temperature separately for the 0-120 m, 120-240 m and 240-360 m, and 600-720 m away from a given water patch with spatial resolution for the thermal infrared band of 120 m. Spatial overlay and statistical analyses were performed on the urban land surface temperatures and the buffer zones around the water patch. Correlation analyses were performed with SPSS statistics software [20].

## RESULTS AND DISCUSSION

### Analysis on the relationship between water landscape density and its surface temperature.

The urban water landscape provides a high ecological service function and makes a significant contribution in maintaining surface temperatures. We selected the water patch density as a characteristic parameter and analyzed its spatial relation with respect to surface temperature; the specific results are discussed in section 3.2 and shown in Fig. 1 and Fig. 2. The overlay analyses of the results and total factor map in Changchun city shows a high level of water density that mainly appears in the Yitong River system and the South Lake in 1993, with significantly lower surface temperatures in these regions that are herein termed "urban cold island" areas. With the expansion of the city, water patch density increased in 2005, and expanded to the south and to the north around Yitong River and South Lake. At the same time, the Yanming Lake and Crescent Reservoir in the northwest of the city showed another increased level of water patch density and the corresponding surface temperature were also low in these areas.

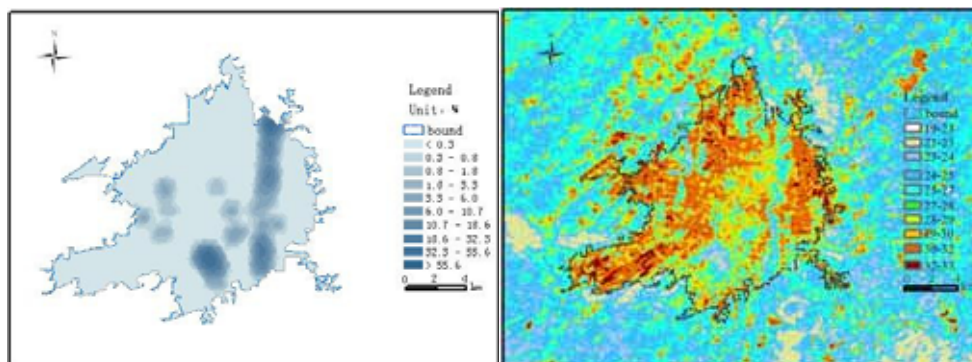


FIGURE 1

The density of water patches and land surface temperature of Changchun City in 1993

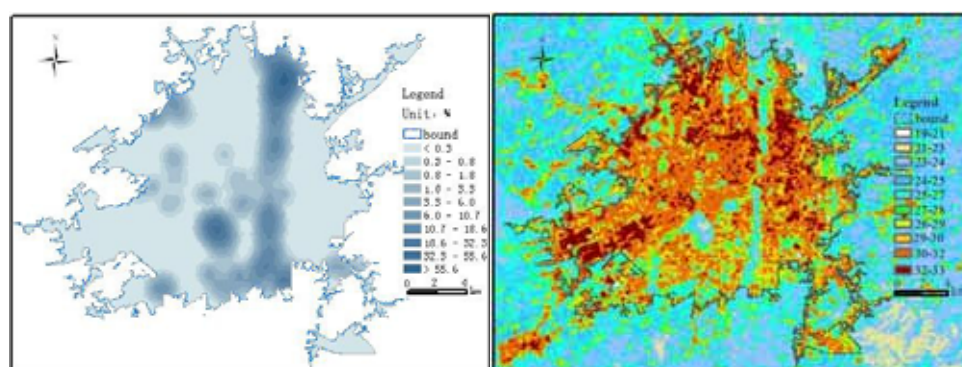


FIGURE 2

The density of water patches and land surface temperature of Changchun City in 2005

**Impacts of water patch characteristics on its surface temperature.** The relationship between the area of water bodies and surface temperatures was calculated by the Zone Statistic function in ArcGIS. The Pearson correlation analysis function in SPSS was used to determine the correlation between water body area and surface temperature. The results show that there was a high degree of correlation between water body area and the water body surface minimum temperature with two correlation coefficients of -0.415 and -0.443 ( $P < 0.01$ ); there was a low correlation between water body area and maximum and mean temperatures. These results show that the minimum temperature was greatly influenced by the area of the water body. Linear regression analysis was performed on the minimum temperature and the water body area as shown in Fig. 3a and 4a and shows that the goodness of fit was lower. However, when we removed the area that was less than 10 ha,

than the goodness of fit improved (Fig. 3b and 4b). It is therefore suggested that an increase area of water bodies would help to reduce the temperature of water body to some extent.

The results show that there is a high degree of correlation between the water body shape index and the minimum surface temperature of that same water body with a correlation coefficient of 0.321 ( $P < 0.05$ ) and 0.381 ( $P < 0.01$ ) in 1993 and 2005, respectively; there is a low degree of correlation between the water body shape index and the maximum and mean temperatures. Linear regression analyses were performed on the minimum temperature and the water body shape index (Fig. 5). We found that minimum temperatures were lower with increasing shape index. It is therefore concluded that increasing the shape complexity of the water body would help to reduce the water body temperature.

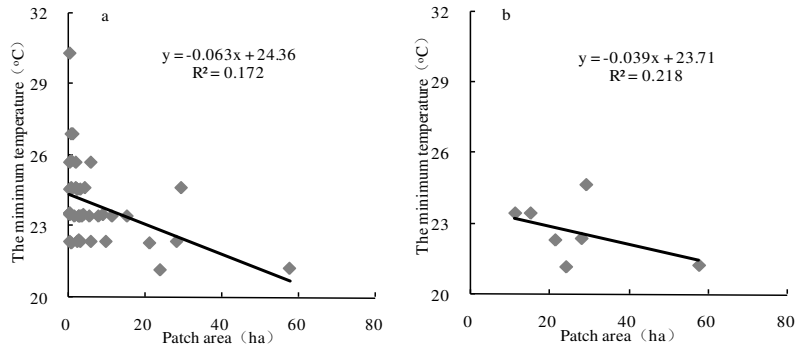


**FIGURE 3**

**The relationship between the water body area and surface minimum temperature in 1993**

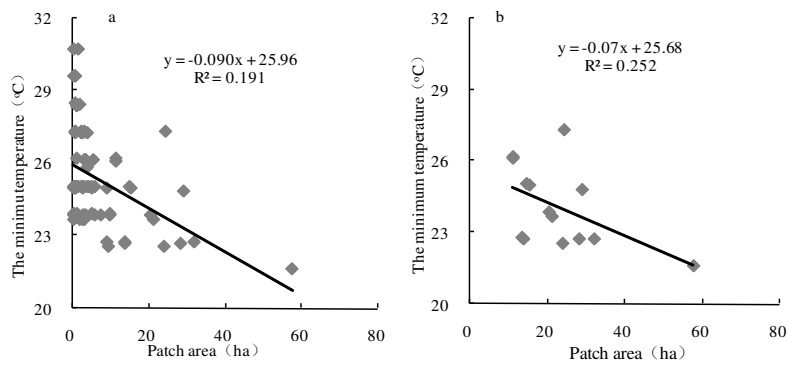


**FIGURE 4**

**The relationship between the water body area and surface minimum temperature in 2005**

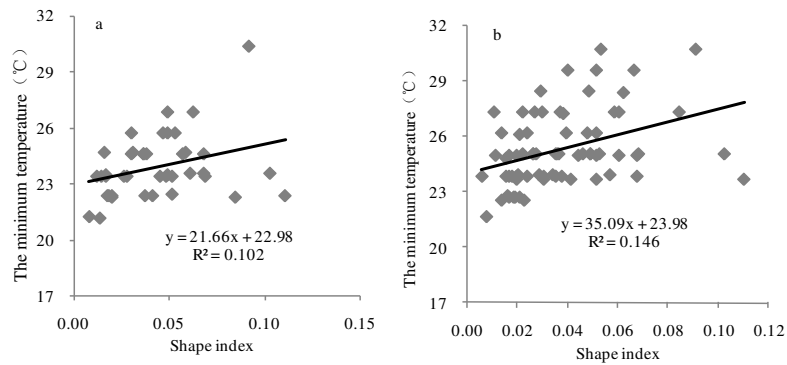


**FIGURE 5**

**Regression analysis of the shape index and the surface water temperature (a:1993 year , b : 2005 year)**

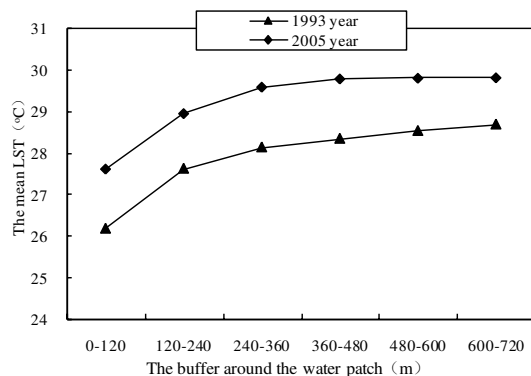


**FIGURE 6**

**The land surface temperature surrounding the urban water**

**The impacts of water patch on the land surface temperature around water.** It was found that the mean LST gradually increased with an increase in the distance from a given water body within a 720 m buffer zone. The degree of this temperature increase gradually declined (Fig. 6). It can be concluded that water bodies have an impact on land surface temperature at a distance of 0-720 m with a cooling trend that shows a gradual landward decrease.

The area around water bodies can be subdivided into several buffer zones on the basis of temperature trends. In 1993, the average buffer zone temperature increased by 1.440 °C and 0.513 °C in the 0-120 m to 120-240 m and 120-240 m to 240-360 m buffer zones, respectively, and shows that the warming trend was decreasing. The temperature increased by 0.155 °C in the 480-600 m to 600-720 m buffer zones. Likewise, the temperature increased by 1.336 °C from 0-120 m to 120-240 m buffer zone in 2005, 0.640 °C from 120-240 m to 240-360 m buffer zone, and only 0.011 °C from 480-600 m to 600-720 m buffer zone. The temperature differences gradually decreased and showed that the temperature mitigation effect is not obvious. The results also show that water bodies have a great influence on the surrounding land surface temperatures with a local low temperature effect that extends as far inland as 720 m. The cooling effect was not significant with increasing distance from the water body. The results also verified that there was a clear difference in the impacts of water bodies on different buffer zones. When there was active communication with the water body there was a greater influence on the areas nearer the water. The temperature of the

surrounding areas in these cases showed some uniformity with the surface water temperatures. The heat flow between the local urban system and the surrounding environment was not substantial in the areas farther from the water, therefore the mitigation capacity was relatively weak in these cases.

## CONCLUSION

In this paper, which builds upon the theories of the landscape mosaics in landscape ecology, we mainly analyzed the impacts of the water landscape patch characteristics (area and boundary complexity) on urban surface temperatures and their influence of local low temperature climate formed by water patches on the surrounding environment.

It can be concluded that there is a low degree of correlation between water body area and its maximum and mean temperatures in 1993 and 2005. There is a higher degree of correlation between water body area and the water body's minimum surface temperature. When the water body area is more than 10 ha, there is a corresponding great decrease in the LSTs. Thus, there is little impact on the urban local thermal environment when water area is too small.

Also, there is a low degree of correlation between the water body shape index and the maximum and mean surface temperatures. Conversely, there is a higher degree of correlation between the water body shape index and the water body minimum surface temperature. Minimum surface temperatures are greatly influenced by water body patch shape in that the minimum surface



temperature rise with increases in the complexity. This illustrates that the complexity of the water patch shape is influential on the heat exchange between water bodies and the surrounding landscape and is therefore an important factor in mitigating the urban heat island effect. This mitigation effect is substantial within 720 m of water bodies in Changchun city, but substantially decreases beyond this distance from water body.

The results of this study could have implications for environmental management and landscape planning with respect to the urban water landscape. The results revealed that LSTs are sensitive to the area and shape of water. As such, any planning and design that takes into account the complexity and size of water bodies, as outlined herein, would be expected to be highly useful toward mitigating an urban heat island effect.

#### ACKNOWLEDGEMENT

The authors would like to express gratitude to Benjamin Spaier for help with English editing and to the research grant support kindly provided by University Nursing Program for Young Scholars with Creative Talents in Heilongjiang Province (Ecological environmental vulnerability and land reclamation in Coal Mining Areas of Heilongjiang Province), the National Nature Science Foundation of China for Young Scholars (No.41101177, 41301081), Philosophy and social sciences research program of Heilongjiang Province (No.16GLC04), the University Strategic Reserve Personnel Abroad Research project funded by Heilongjiang Province, Scientific Research Fund of Heilongjiang Provincial Education Department (No.12511494), the Project for Young Talent of Heilongjiang University of Science and Technology (No.Q20110203), and The University Key Laboratory Program in Heilongjiang Province (HT2012-03).

#### REFERENCES

- [1] Lambin E.F., Turner B.I., Geist H.J. (2001) The causes of land use and land cover change: Moving beyond the myths. *Global Environment Change*, 11(4), 261-269.
- [2] Patz J.A., Campbell-Lendrum D., Holloway T. et al. (2005) Impact of regional climate change on human health. *Nature*, 438, 310-317.
- [3] Wilson J.S., Clay M., Martin E. et al. (2003) Evaluating environmental influences of zoning in urban ecosystems with remote sensing. *Remote Sensing of Environment*, 86(3), 303-321.
- [4] Lo C.P., Quattrochi D.A., Luvall J.C. (1997) Application of high-resolution thermal infrared remote sensing and GIS to assess the urban heat island effect. *International Journal of Remote Sensing*, 18(2), 287-304.
- [5] Carlson T.N., Gillies R.R., Perry E.M. (1994) A method to make use of thermal infrared temperature and NDVI measurements to infer surface soil water content and fractional vegetation cover. *Remote Sensing Reviews*, 9(1/2), 161-173.
- [6] Weng Q.H., Rajasekar U., Hu X.F. (2011) Modeling urban heat islands and their relationship with impervious surface and vegetation abundance by using ASTER images. *IEEE Transactions on Geoscience and Remote Sensing*, 49(10), 4080-4089.
- [7] Weng Q.H., Liu H., Liang B.Q., et al. (2008) The spatial variations of urban land surface temperatures: pertinent factors, zoning effect, and seasonal variability, *IEEE Journal of Topics in Applied Earth Observations and Remote Sensing*, 1(2), 154-166.
- [8] Yue W.Z., Xu L.H. (2013) Thermal environment effect of urban water landscape. *Acta Ecologica Sinica*, 33(6), 1852-1859.
- [9] Yao Y.L., Lv X.G., Wang L., et al. (2010) A quantitative analysis of climate change impacts on runoff in Naoli River. *Advances in Water Science*, 21(6), 765-770.
- [10] Wilson J.S., Clay M., Martin E., et al. (2003) Evaluating environmental influences of zoning in urban ecosystems with remote sensing. *Remote Sensing of Environment*, 86(3), 303-321.
- [11] Forman R.T.T., Godron M. (1986) *Landscape Ecology*. New York: John Wiley & Sons.
- [12] Wu J.G. (2000) *Landscape Ecology—pattern, process, scale and grade*, Beijing: China Higher Education Press.
- [13] Liu J.Y., Zhang Z.X., Zhang S.W., et al. (2005) Temporal-spatial information research on land use change based on remote sensing in China in 1990s. Beijing: China Higher Education Press.
- [14] Ning J., Zhang S.W., Li Y., et al. (2008) Analysis on Wetland shrinking characteristics and its cause in Heilongjiang Province for the



- last 50 Years. *Journal of Natural Resources*, 23(1), 79-86.
- [15] Wiens J.A., Stenseth N.C., Van Horne B., et al. (1993) Ecological mechanisms and landscape ecology. *Oikos*, 66(3), 369-380.
- [16] Qin Z., Karnieli A., Berliner P. (2001) A mono-window algorithm for retrieving land surface temperature from Landsat TM data and its application to the Israel-Egypt border region. *International Journal of Remote Sensing*, 22(18), 3719-3746.
- [17] Xiao H.L., Weng Q.H. (2007) The impact of land use and land cover changes on land surface temperature in a Karst Area of China. *Journal of Environmental Management*, 85(1): 245-257.
- [18] Jiménez-Munoz J.C., Sobrino J.A. (2003) A generalized single-channel method for retrieving land surface temperature from remote sensing data. *Journal of Geophysical Research*, 108(D22), 4688-4695.
- [19] Wang L. (2013) Thermal environment effect of land use change based on remote sensing and geographical information system. *Information Technology Journal*, 12(22), 6812-6816.
- [20] Wang L., Zhang S.W. (2015) Analysis on the relationship between the pattern of green spaces and land surface temperature based on normalized difference vegetation index: A case study in Changchun City, China. *Fresen. Environ. Bull.*, 24(8), 2444-2451.

---

**Received:** 03.12.2015

**Accepted:** 23.03.2016

---

#### **CORRESPONDING AUTHOR**

---

**Lei Wang**

College of Architectural Engineering  
Heilongjiang University of Science and Technology  
150022, Harbin, CHINA

E-mail: [wanglei\\_happiness@163.com](mailto:wanglei_happiness@163.com)

# EVALUATING AND MAPPING TRAFFIC-INDUCED NOISE POLLUTION IN URBAN PARKS IN THE CITY OF KAHRAMANMARAŞ, TURKEY

Neslihan Doygun<sup>1,\*</sup>, Hakan Doygun<sup>1</sup>, Merve Gozcu<sup>2</sup>

<sup>1</sup> University of Kahramanmaraş Sütçü İmam, Faculty of Forestry, Department of Landscape Architecture, Kahramanmaraş, Turkey

<sup>2</sup> University of Kahramanmaraş Sütçü İmam, Graduate School of Natural and Applied Sciences, Kahramanmaraş, Turkey

## ABSTRACT

The aim of this research was to analyze the traffic-induced noise in urban parks and to develop urban green space planning approaches. Forty-three measurements were collected in five parks that differed in their physical structures and environmental conditions. The measurements have been compared with the cut-off value proposed by the WHO (55 dBA). GIS-based maps were produced to evaluate the spatial distribution of noise. The findings indicated that the distance from urban areas and the size of the parks were the main determinants of the level of noise pollution, and building parks outside of urban areas can be the most convenient method to protect the visitors from noise pollution. However, building the parks in an urban area is an essential planning method that can facilitate the access to the parks. Therefore, it is crucial to design and build large noise free park zones, regardless of whether they are located in or out of the urbanized area. Finally, to effectively decrease the effects of noise on people in urban parks, well-textured evergreen perennial, shrub, and tree species should surround the roadsides of the parks.

## KEYWORDS:

Noise pollution, urban environmental protection, green space, Kahramanmaraş.

## INTRODUCTION

The world population living in urban areas is projected to increase to from 3.6 billion in 2011 to 6.3 billion 2050. Thus, the growing population is expected to be concentrated in urban areas over the next four decades [1]. These unprecedented developments had increased the demand for high quality green spaces in urban areas. Urban green spaces are viewed as the last remnants of nature [2], and rapid urbanization and increased leisure time increase people's awareness of urban green space. On the other hand, urban green spaces and their environmental and social benefits are becoming

inadequate due to urban environmental problems [3]. Cities and towns experience increasing signs of environmental stress, particularly in the form of poor air quality and excessive noise. Among them, environmental noise level is one of the key determinants of life quality in urban areas of modern cities [4, 5]. The European Environment Agency [6] estimated that more than 40% of citizens are exposed to road noise levels above 55 dB, which is high enough to cause annoyance, aggressive behavior, and sleep disturbance [7].

The aim of the research is to analyse the levels of traffic-induced noise pollution in urban parks in the city of Kahramanmaraş (K.Maraş), Turkey. The study consisted of three main phases: i) Measuring and mapping noise levels to quantify spatial distribution of noise pollution, ii) Comparing measurement results with international noise limits, and iii) Developing environmental protection and planning policies to increase the benefits of urban parks and the visitors' wellbeing.

## MATERIALS AND METHODS

**Study area.** The study compared five urban parks located throughout the city of K.Maraş, Turkey. Located in the Eastern Mediterranean Region of Turkey, the city of K.Maraş is among the most rapidly urbanizing cities in the country. The population was 326,198 in 2000 but increased by 40% during the past 13 years, reaching 450,000 in 2013 [8]. The built-up land also expanded in parallel with the population increase, with the amount of constructed area increasing from 1200 ha in 2000 to 2200 ha in 2006 [9, 10]. Because of rapid urbanization, the number of motor vehicles has risen almost three-fold during the past decade, from about 60,000 in 2000 to 170,000 in 2013 [11, 12]. Five urban parks were compared in terms of their physical structures and environmental conditions: location, areal coverage, plant coverage, types of buildings, traffic, and visitor density. Geographical locations and some features of the parks are indicated in Figure 1 and Table 1.



**FIGURE 1**  
Geographical location of the city of K.Maraş, and the parks

**TABLE 1**  
General characteristics of the parks

	Location	Area (m <sup>2</sup> )	Traffic density	Plant density	Visitor density
Kılavuzlu Park	Non-urbanized	48,500	Low	Low	Weekend
Muhsin Y. Park	Non-urbanized	10,500	Moderate	Low	Weekend
12 Subat Park	Urbanized	14,500	High	Low	All week
Atatürk Park	Urbanized	105,000	High	Moderate	Weekend
Selale Park	City core	4000	Very high	High	All week

#### Measurement procedure and evaluation.

Forty-three measurements have been collected from 43 points to analyze the traffic-induced noise in urban parks. A homogenous distribution was considered while locating the measurement points in the park areas. According to a real width of the parks, the number of measurement points ranged from 6 to 11.

The measurements have been carried out on the weekends, between 1:00 and 5:00 p.m., under ideal meteorological conditions when there was no rain or wind. The measurement schedule represents the most suitable activity period in terms of both the traffic and park visitors' density. The duration of each measurement was 3 min [13, 14] during which A-weighted continuous equivalent sound level  $L_{eq}$  was collected. The Delta OHM HD2010 sound level meter with tripod was fixed at 1.5 m above local ground level at a vertical angle of 45°.

The measurement results have been evaluated by considering the cut-off values established by the World Health Organization (WHO) [13, 15]. WHO's

limitations regarding environmental noise specify that recommended noise levels for outdoor living areas should be 55 dBA.

Geographic Information System (GIS) based maps were produced for each urban park to analyze the spatial distribution of noise pollution in the entire area. The maps enabled us to associate the measured noise levels with traffic density. In this study, noise maps were generated on a 1 × 1 m cell using Spatial Analyst extension in ArcGIS 9.3 software. The extension enabled us to create spatial distribution from point features. It means that it is possible to interpolate data values for the entire area based on pre-defined measurement locations.

#### RESULTS AND DISCUSSION

The measurements collected in five urban parks in the city of K. Maraş revealed mean noise level of 58 dBA, 3 dBA more than the cut-off value specified by the WHO (55 dBA) (Table 2). It means that traffic

**TABLE 2**  
**Number of measurement points according to WHO limit, and mean noise levels.**

	Number of measurements			Mean dBA
	<55 dBA	=55 dBA	>55 dBA	
Kilavuzlu Park	5	2	2	54
Muhsin Yazicioğlu Park	4	0	4	55
12 Subat Park	2	2	5	58
Atatürk Park	3	1	7	59
Selale Park	0	0	6	64
Total	14	5	24	58

induced noise does not pose a significant threat to park visitors' wellbeing throughout the city, from the viewpoint of mean noise level. On the other hand, 56% of the total 43 measurements exceeded the limit of 55 dBA, ranging from 56 to 71 dBA. While 12% of the measurement were equal to the limit, 32% of the measurements were smaller than it.

Each urban park in the city displayed different noise levels, depending on the variability of their physical or environmental conditions. Among urban parks, only the measurements in Selale Park exceeded the WHO limit of 55 dBA (Figure 2). Minimum and maximum noise levels were 63 and 66 dBA. The mean noise level was 64 dBA. Although the plant cover is well developed, high noise levels have been measured because the park is located in the city core and surrounded by roads with high traffic density. Furthermore, the size of the park is another important factor in noise levels. The areal coverage of the park is about 4000 square meter (40 x 100 m). Accordingly, traffic induced noise in the entire park area is being perceived as high.

Atatürk Park, located on a densely used inter-city road, displayed the second highest value, with the mean noise level of 59 dBA. The results of the 11 measurements ranged from 52 to 71 dbA, and 7 of them exceeded the WHO limit. On the other hand, Figure 3 clearly shows that the noise level measurements collected adjacent to inter-city road were high while the measurements collected further away were quite low. The distance from road to the back of the park was about 250m length, and the difference between the measurements collected in the front versus the back was about 15 dBA. Hence,

the size of the Atatürk Park played an important role in the spatial distribution of noise levels.

With the mean noise level of 58 dBA, 12 Subat Park is located in newly urbanized part of the city. The measurements collected close to densely used road had the highest values (61 – 65 dBA) while other parts of the park had relatively low values (52 – 60 dBA). Five of the total 9 measurements were higher than the WHO's cut-off value of 55 dBA, and the other four were equal to or smaller than this value.

Compared to other three parks, Muhsin Yazicioğlu and Kilavuzlu Parks, which are located outside the urban area of K.Maraş, had low values. Mean noise level in Muhsin Yazicioğlu Park was 55 dBA, and the 8 values ranged from 52 dBA to 58 dBA. Half of the values were higher compared to the WHO's recommended values. Moderate traffic density was the main reason for these results.

Kilavuzlu Park, with its mean noise level of 54 dBA, 1 dBA lower than the cut-off value established by the WHO (55 dBA), is unique among the five urban parks. The park is located far from both an urban area and high traffic density. The 9 values ranged from 47 to 62 dbA. Only two of them exceeded the WHO cut-off value. Two measurements had the same and five measurements had lower values compared to the WHO's cut-off.

GIS-based noise maps of the five urban parks displayed spatial distribution of traffic-induced noise pollution in the entire area. As shown in Figure 3, the type and the traffic density of the roads are the main factors in the distribution of noise. The noisiest regions are generally around the main roads while the noise decreases in areas with less traffic density.

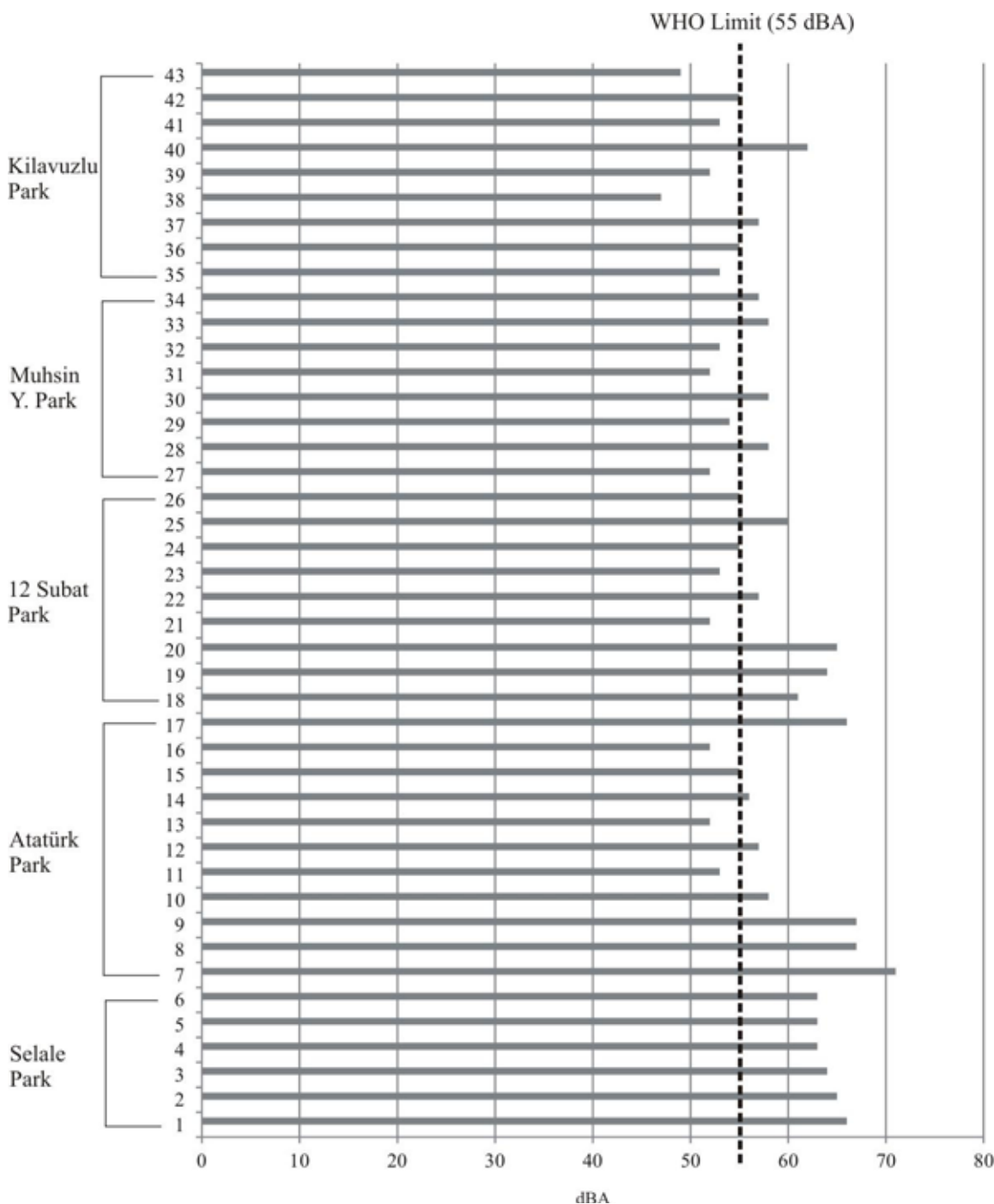


**FIGURE 2**  
Noise measurements according to WHO limit.

**CONCLUSIONS**

The aim of this study was to measure and map traffic-induced noise pollution in urban parks in the city of K.Maraş. Overall, 43 measurements were collected in five parks that differed in their physical structures and environmental conditions. The results were compared to the cut-off value established by the WHO (55 dBA), and GIS-based maps were produced to evaluate the spatial distribution of noise. The results of the measurements ranged from 47

dBA up to 71 dBA. Overall, 56% of the total 43 measurements exceeded the limit of 55 dBA. Among five urban parks, Selale Park, which is located at the city’s core, showed the highest mean noise level (64 dBA) while Kilavuzlu Park, located far from urbanized area, had the lowest mean level (54 dBA). The measurement indicated that the difference between mean noise levels of the parks located inside and outside of the urban area was about 10 dBA. On the other hand, the size of the parks also appeared to be an important factor in the spatial

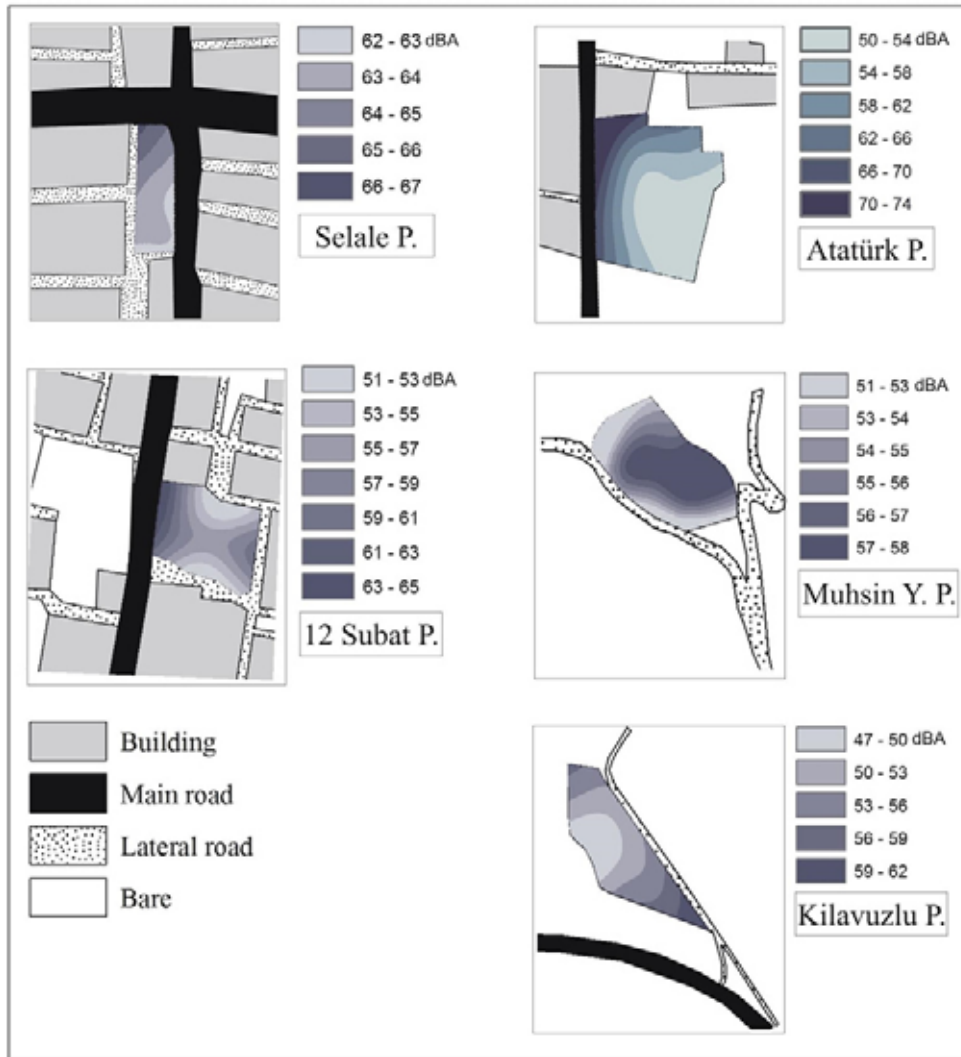


**FIGURE 3**  
Noise maps of the urban parks.

distribution of noise. Noise measurements within small size parks had similar values (65 – 63 dBA) while the measurements differed significantly within parks that cover larger areas (71 – 52 dBA).

Our findings indicated that environmental noise is one of the most important factor that should be considered in the planning of urban green areas and promoting public well-being. According to study conducted in the city of K.Maraş, building the parks outside of the urban area can protect the visitors from noise pollution. However, on the other hand, building the parks in urban areas can increase the access to the parks. Therefore, careful planning of the urban parks should generate noise free park zones, regardless of whether they are located inside or outside of the urban area. In addition to areal coverage, the lack of well-developed plant cover is another important problem in the prevention of noise pollution in urban parks. To decrease effectively the effects of noise on people, well-textured evergreen perennial, shrub, and tree species should be planted along the roadsides of the parks.

#### ACKNOWLEDGEMENTS

The authors acknowledge The University of Kahramanmaraş Sütçü Imam for financial support of this study (Project no. 2005/5-10), and to Mr. Gökay Külahlıoğlu for his valuable help during field studies.

#### REFERENCES

- [1] United Nations (2012). World Urbanization Prospects, The 2011 Revision, Highlights. Department of Economic and Social Affairs, Population Division, New York.
- [2] Beatley, T. (2000). Green urbanism: Learning from European cities. Island Press, Washington DC
- [3] Doygun, H., & Ilter, A. A. (2007). Kahramanmaraş kentinde mevcut ve öngörülen

- aktif yeşil alan yeterliğinin incelenmesi. *Ekoloji*, 16(65), 1-8.
- [4] Prascevic, M. R., Mihajlov, D. I., & Cvetkovic, D. S. (2014). Measurement and evaluation of the environmental noise levels in the urban areas of the city of Nis (Serbia). *Environmental Monitoring and Assessment*, 186, 1157-1165.
- [5] Popa, D., Corches, M. T., Buzgar, A. G. (2015) Evaluation of Environmental Noise Pollution Caused by Road Traffic in the City of Alba Iulia, Romania. *J of Environmental Protection and Ecology*, 16 (3), 824.
- [6] EEA (2009) Ensuring quality of life in Europe's cities and towns: Tackling the environmental challenges driven by European and global change. European Environment Agency, Report no: 5/2009 3(5), 1776-1784.
- [7] Stanners, D., Bourdeau, P. (Eds.) (1995) Europe's environment - the Dobris assessment. European Environment Agency, Earthscan Publications, London
- [8] TSI (2013) Kahramanmaraş urban population. Turkish Statistical Institute <http://www.tuik.gov.tr> Accessed 10 December 2013
- [9] Doygun, H., Alphan, H., & Gürün, D. K. (2008). Analysing urban expansion and land use suitability for the city of Kahramanmaraş, Turkey, and its surrounding region. *Environmental Monitoring and Assessment*, 145, 387-395.
- [10] Doygun, H. (2009). Effects of urban sprawl on agricultural land: a case study of Kahramanmaraş, Turkey. *Environmental Monitoring and Assessment*, 158, 471-478.
- [11] Doygun, H., & Gürün, D. K. (2008). Analysing and mapping spatial and temporal dynamics of urban traffic noise pollution: a case study in Kahramanmaraş, Turkey. *Environmental Monitoring and Assessment*, 142, 65-72.
- [12] TSI (2013) Number of motor vehicles in Kahramanmaras. Turkish Statistical Institute <http://www.tuik.gov.tr> Accessed 10 December 2013
- [13] Zannin, P. H. T., Ferreira, A. M. C., & Szemeretta, B. (2006). Evaluation of noise pollution in urban parks. *Environmental Monitoring and Assessment*, 118, 423-433.
- [14] Zannin, P. H. T., Engel, M. S., Fiedler, P. E. K., & Bunn, F. (2013). Characterization of environmental noise based on noise measurements, noise mapping and interviews: A case study at a university campus in Brazil. *Cities*, 31, 317-327.
- [15] WHO (1999) Guidelines for community noise. World Health Organization, B Berglund, T Lindvall, DH Schwela (Eds.)

---

**Received:** 30.11.2015

**Accepted:** 23.03.2016

---

#### CORRESPONDING AUTHOR

---

**Dr. Neslihan Doygun**

University of Kahramanmaraş Sütçü Imam

Faculty of Forestry

Department of Landscape Architecture

Kahramanmaraş – TURKEY

e-mail: nesdoy@mynet.com



# RESEARCH ON THE VARIATIONS OF SNOW COVER OVER THE TIBETAN PLATEAU AND ITS RESPONSES TO CLIMATE CHANGE

Yuxue Guo<sup>1</sup>, Guohua Fang<sup>1,\*</sup>, Lei Zhou<sup>2</sup>, Xin Wen<sup>1</sup>

<sup>1</sup>College of Water Conservancy and Hydropower Engineering, Hohai University, Nanjing 210098, China

<sup>2</sup>Power China Huadong Engineering Corporation Limited, Hangzhou, 311122, China

## ABSTRACT

Snow cover over Tibetan Plateau (TP) plays an important role in hydrological and energy circulation in many Asian river basins. The paper aims to assessing spatial-temporal changes of snow cover over TP and exploring its responses to the climate change during 2001-2011. As the result, statistical negative changes are indicated in the seasonal snow cover fraction variation for three seasons with the decreasing rate: -0.916%/a (spring), -0.005%/a (summer) and -0.050%/a (winter), while positive change is detected for autumn with the increasing rate 0.272%/a. The trend analysis shows 41.19% of TP exhibiting declining trend (1.42% with a significant decline) and 38% of TP indicating increasing trend (1.77% with a significant increase). Also, snow cover fraction shows significant negative correlation with temperature and precipitation in spring, summer and autumn months. In winter, snow cover fraction indicates significant positive correlation with precipitation and not significant negative correlation with temperature at the 0.01 level.

## KEYWORDS:

Snow cover, Spatial-temporal responses, Tibetan Plateau, Climate change, Correlation analysis

## INTRODUCTION

Snow cover over Tibetan Plateau (TP) is the main component of Eurasian snow cover. It plays an important role in regional hydrological and surface energy balance for its high reflectivity, high phase change latent heat and low thermal conductivity [1, 2]. As global warming intensifies, many previous studies proved that snow cover was quite sensitive to the climate change. Meanwhile, changes in snow cover would also affect hydrological processes at both regional and global level [3]. Therefore, researches on spatial-temporal distributions of snow cover are meaningful to understand the implications and mechanism of

climate and hydrological system [4-7].

Snow cover in Northern Hemisphere exhibit complex responses to increasing temperature and precipitation [8]. Snow cover areas have decreased significantly in the Northern Hemisphere, their variations are negatively correlated with winter temperatures [9]. Western China did not experience a continual decrease in snow cover during the great warming period of the 1980s and 1990s, no correlation was identified between temperature and precipitation in the snow cover seasons [5]. In 2000s, the inter-annual fluctuation of snow cover can be explained by the high negative correlations between the snow cover amount and the in situ temperature [10].

The satellite remote sensing technology provides a possible way to monitor the long-term changes in snow cover. Due to the launch of the first generation of the meteorological observation satellite TIROS in 1966, weekly snow cover maps of Northern Hemisphere have been finished by National Oceanic and Atmospheric Administration (NOAA) [11]. The Terra satellite was launched by NASA in 1998 with the first Moderate Resolution Imaging Spectroradiometer (MODIS) instrument which provides a new and improved capability for terrestrial satellite remote sensing [12, 13]. MODIS products (500m resolution) are capable to separate most snow and clouds [14]. MODIS snow cover fraction data have been used in terms of snow presence detection in Colorado and Washington states [15], snow cover variability in central Asia [16, 17] and snow cover characteristics of Europe [18]. The accuracy of the MODIS high-resolution snow cover data has been evaluated by comparing the data with in situ Chinese snow observations, the results showed that overall accuracy of is about 90% over the TP area and even higher under clear sky conditions [19].

The purpose of this paper is to provide a detailed analysis of variations in snow cover over the TP and to explore its spatial and temporal responses to the climate change. Specifically, we investigate the trends and variability of snow cover changes over TP at diverse temporal scales and different elevation bands. Correlation analysis is conducted between snow cover and climate factors

including daily surface temperature and precipitation. Finally, the statistical significance levels of snow cover changes have been calculated.

## DATA AND RESEARCH AREA

**Snow cover data.** Snow cover data used in this research are daily cloud-removed MODIS Fractional Snow Cover (FSC) products (2001-2011) provided by Environmental and Ecological Science Data Center for West China, National Natural Science Foundation of China (<http://westdc.westgis.ac.cn>). In particular, a cloud removal method based on cubic spline interpolation has been applied to fill in the gaps caused by clouds over the TP [10]. In order to be consistent with the spatial grid of meteorological data, regridding method was performed on snow cover data.

**Meteorological data.** Meteorological datasets used in this study include China Daily Surface Temperature  $0.5^{\circ} \times 0.5^{\circ}$  Gridded Dataset (V2.0) and China Daily Surface Precipitation  $0.5^{\circ} \times 0.5^{\circ}$  Gridded Dataset (V2.0). They can be obtained from China Meteorological Data Sharing Service System (<http://cdc.nmic.cn>). The datasets consist of daily surface air temperature and precipitation gridded data with  $0.5^{\circ} \times 0.5^{\circ}$  horizontal resolution in China. The meteorological observational datasets from

high-density stations compiled by National Meteorological Information Center were interpolated spatially by Thin Plate Spline (TPS) to generate the datasets.

**Study area.** TP, named as "the roof of the world" and "the third pole", is the highest region on Earth with the largest number of inland lakes. TP is located in central Asia with mean elevation of more than 4000 m and an area of about 2.3 million  $\text{km}^2$ . Surrounded by the Earth's highest mountains, TP is the highest and most extensive plateau in the world. It has the largest cryosphere extent outside the polar region. It is also the birthplace of many large rivers in Asia. The geographic location and elevation characteristics of the TP are shown in Figure 1.

There are many scopes and boundaries defining the TP [10, 19, 20], but no unified rule has been put forward. Here, TP's boundary is defined on the basis of geomorphic characters, while the integrity of the plateau is embraced also [21].

As exhibited in Figure 1, we divide TP into 4 elevation bands in which the first elevation band (below 3000 m) occupies 8.96% of the total area, the second elevation band (3000 m to 4000 m) occupies 18.50%, the third elevation band (4000 m to 5000 m) occupies 48.49%, and the fourth elevation band (5000 m to 8806 m) occupies 24.05% of TP area.

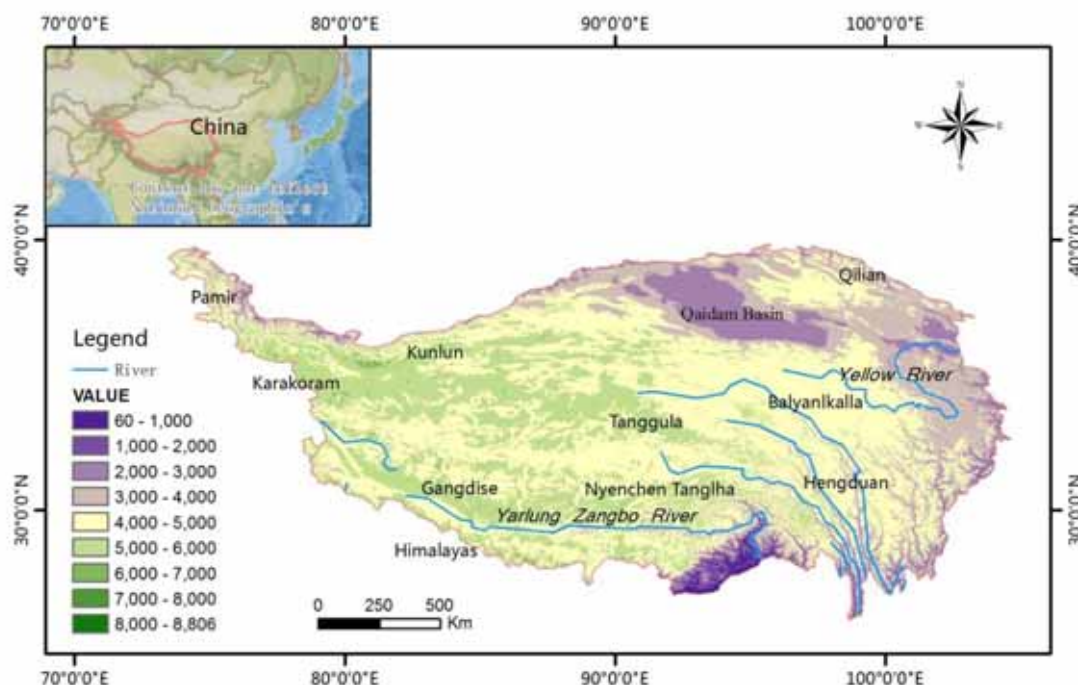
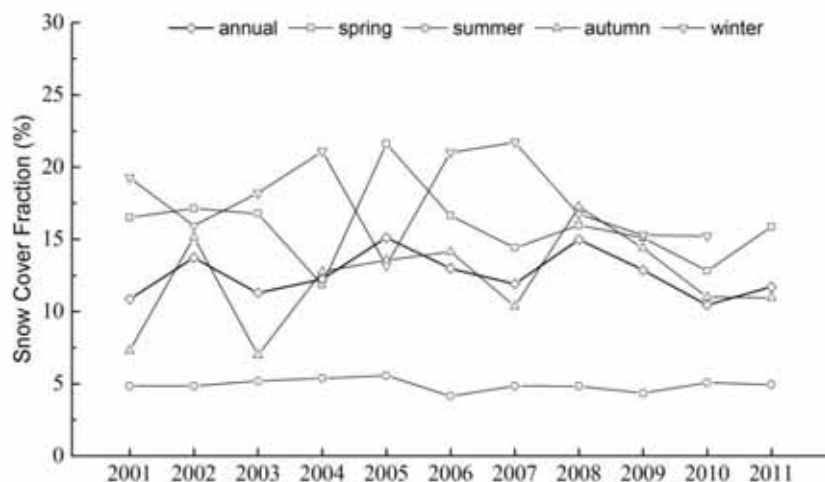
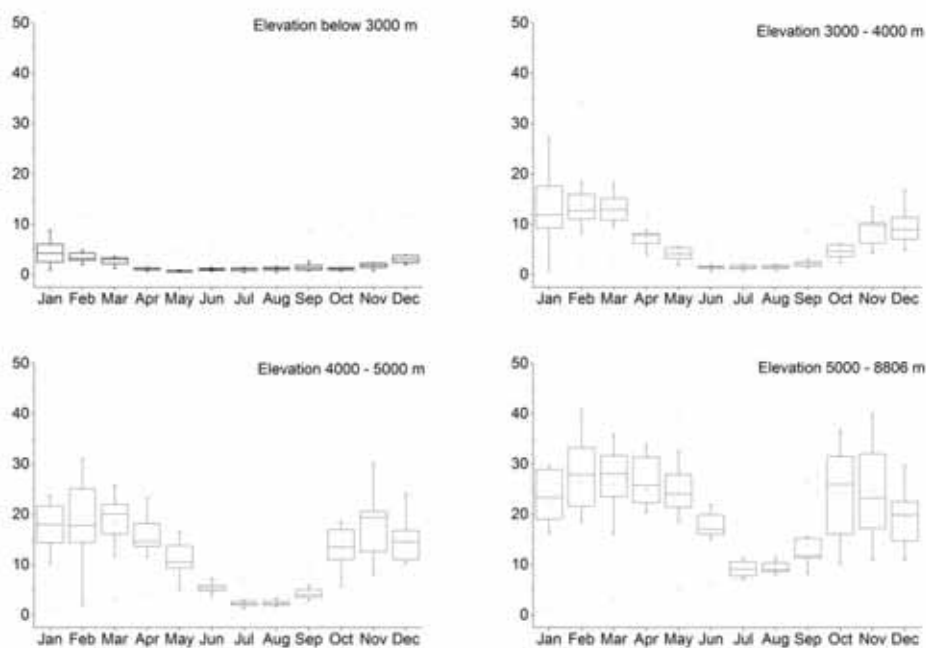


FIGURE 1  
Location and elevation characteristics over TP



**FIGURE 2**  
Time series of annual and seasonal snow cover fraction from 2001 to 2011



**FIGURE 3**  
Boxplots of Monthly mean variations of snow cover fraction in various elevation bands based on 11 years from 2001 to 2011

### SPATIAL AND TEMPORAL VARIATIONS OF SNOW COVER

Spatial-temporal variations of snow cover are explored initially. In terms of seasonal changes, March to next February is divided as a year's cycle. Spring, summer, autumn and winter are expressed as MAM, JJA SON and DJF, respectively.

**Annual variation.** Annual mean snow cover fraction over TP from 2001 to 2011 is 12.56%, showing downward variation trend at the rate of 1.69%/a, as presented in Figure 2. At the seasonal level, average snow cover fraction in spring, summer, autumn and winter are 15.93%, 4.87%, 12.03% and 17.52%, respectively. Statistical negative changes are indicated for three seasons with the decreasing rate: -0.916%/a (spring), -0.005%/a (summer) and -0.050%/a (winter), while

positive change is detected in autumn with the increasing rate: 0.272%/a. Compared with annual changes, seasonal snow cover changes show large variability, particularly in spring, autumn and winter.

**Inter-annual variation.** Figure 3 presents monthly mean variations of snow cover fraction in various bands from 2001 to 2011. In the summer months, the snow cover is lower than 5% for the regions below 5000 m and around 10% for the fourth elevation band. In comparison, the snow cover increases at similar level in spring and autumn months, and continues to grow in winter months. Not surprisingly, the upward variations in snow cover fraction are in consistent with the increase in elevation. The first elevation band shows the minimum annual snow cover coverage (2.08%), while 9.6% of the fourth elevation band is covered with snow through the year. For the seasonal snow cover over high regions above 3000m, there exists large variability among different years in the research period, particularly in winter and spring months.

**Spatial distributions and variation trends.** The seasonal snow cover distribution is further explored from 2001 to 2011. As shown in Figures 4 a-d, snow cover distributions maintain a high consistency with distributions of high mountains in spring, autumn and winter. Most of the high snow covered areas are among the Himalayas and Nyenchen Tanglha, their snow cover fraction are generally larger than 80%. By contrast, Qaidam

Basin and other regions of low elevation (below 2000 m) exhibit low snow cover fraction (below 10%). Figure 5 indicates the spatial pattern of annual snow cover from 2001 to 2011 and its statistical significance levels. The linear trend of snow cover change varies from -1.2%/a to 0.7%/a. Moreover, 41.19% of the study area maintains a declining trend, only 1.42% grids show statistically significant declining trend ( $p < 0.05$ ). Meanwhile, 38% of pixels of the area show the increasing trend, while 1.77% exhibits the significant increase. Snow cover reducing areas are mainly concentrated in the southwest of TP.

## TEMPERATURE AND PRECIPITATION CHANGES IN TP

**Temperature changes.** The regional mean temperature of TP exhibits an upward tendency at the rate of 0.493°C/10a from 2001 to 2011. The highest annual average temperature -0.58°C appeared in 2006, while the lowest -1.51°C was detected in 2008. Figure 6 presents the geographical pattern of linear trend and the corresponding statistical significance levels of annual mean temperature. Most areas of TP present increasing trend at the rate of 0.04-0.14°C/a. About 97.17% of the region exhibits an increasing trend, and 46.59% shows significant increase ( $p < 0.05$ ). By contrast, only 2.83% of the grids indicate declining trend and no statistically significant variation is detected.

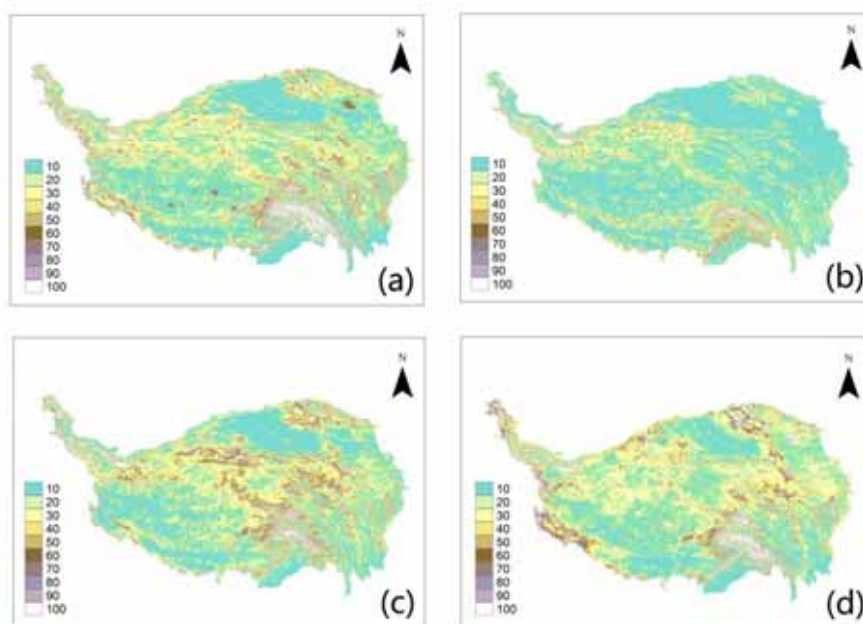


**FIGURE 4**  
Spatial distribution of seasonal mean snow cover fraction from 2001 to 2011: (a) spring (b) summer (c) autumn (d) winter

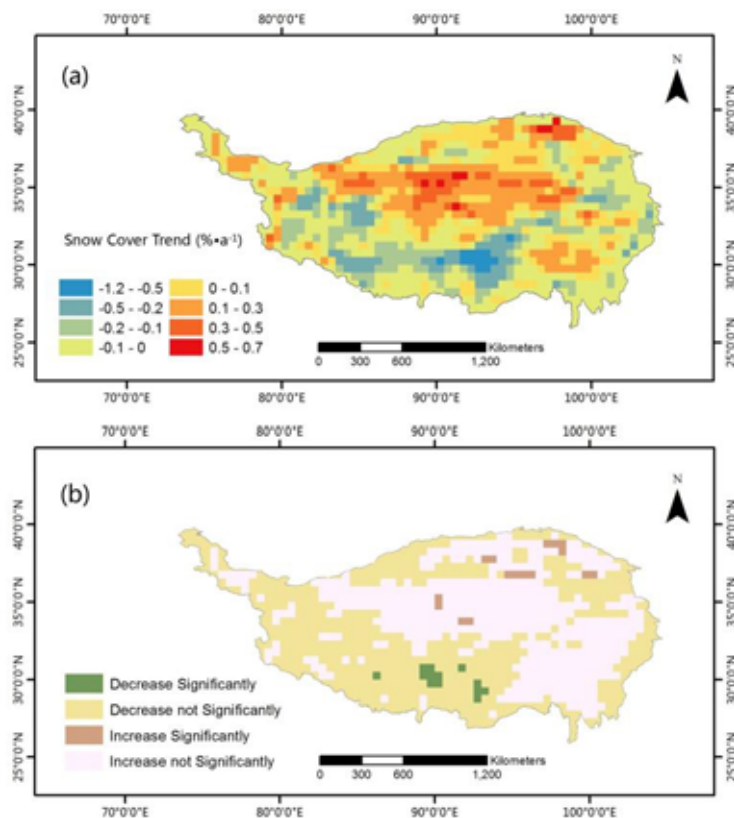


**FIGURE 5**

Distribution of monthly snow cover trend from 2001 to 2011: (a) trend and (b) significant of trend. ( $p < 0.05$ )

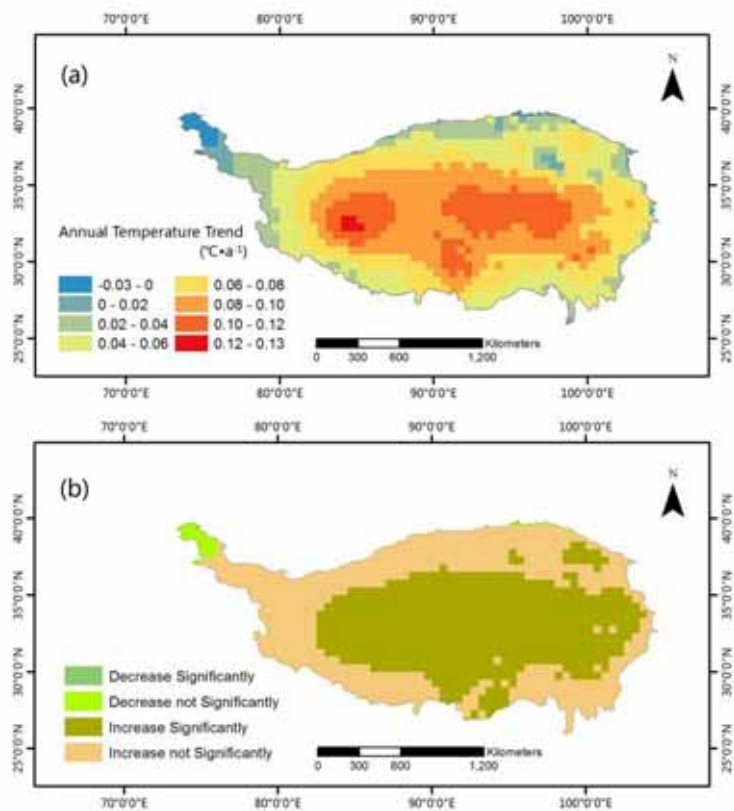


**FIGURE 6**

Spatial distribution of annual temperature trend from 2001 to 2011: (a) trend and (b) significant of trend. ( $p < 0.05$ )

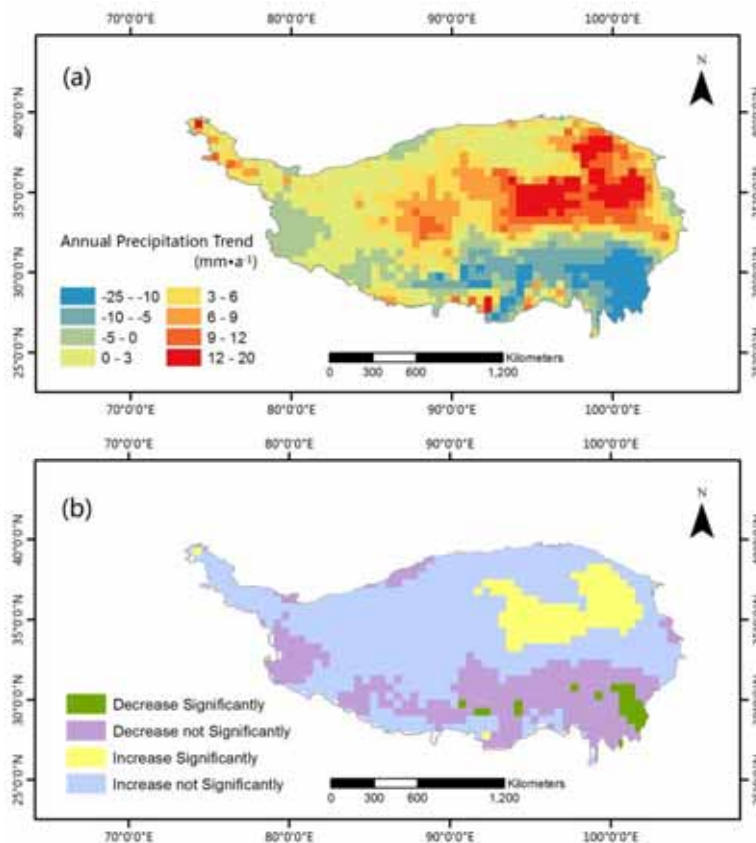


**FIGURE 7**

**Spatial distribution of annual precipitation trend from 2001 to 2011: (a) trend and (b) significant of trend. ( $p < 0.05$ )**

**Precipitation changes.** Annual precipitation over TP shows an upward tendency at the rate of about 21mm/10a during 2001-2011. The largest annual precipitation (504.65mm) appeared in 2008, while the least (434.51mm) was observed in 2001. Figure 7 exhibits the linear trend and the corresponding statistical significance levels of annual precipitation. Generally, the northern TP shows increasing trend while the southern part showing downward changes. About 66.78% of the study area exhibit an increasing trend, and 10.19% of TP experiences a significant increase ( $p < 0.05$ ). Only 28.52% of the grids show the declining trend, and 2.48% of the total grids indicates the statistically significant downward trend.

## RESPONSES OF SNOW COVER CHANGES TO TEMPERATURE AND PRECIPITATION VARIATIONS

Correlation analysis are employed to quantify the relations between monthly snow cover fraction and the corresponding temperature and precipitation. As listed in Tables 1 and 2, snow cover fraction shows significant negative correlation with temperature and precipitation in spring, summer and autumn months, passing the 0.01 significance tests

on both sides. While in winter months, snow over fraction shows significant positive correlation with precipitation and not significant negative correlation with temperature at the 0.01 level.

In spring months, snow cover below 5000 m shows significant negative correlation with temperature and precipitation. For the high regions above 5000 m covered with perennial snow and glaciers, snow cover has less significant negative correlation with temperature and no significant negative correlation with precipitation. The rise of temperature in spring weakens the ability of rain turning into snow. In summer months, snow cover below 4000 m presents no significant correlation, while the bands above 4000 m have a strong negative correlation, passing the 0.01 significance tests on both sides. In autumn months, snow cover between 3000 to 4000 m shows no significant positive correlation with precipitation and other elevation bands has shown significant negative correlations. In winter months, the influences of the temperature on the snow cover have been weakened, since no significant negative correlation is detected between them. However, the significant positive correlation has been proved between snow cover and precipitation, which indicate that precipitation contributes a lot to the increase of snow cover over TP in winter.

**TABLE 1**  
Correlation analysis results of seasonal snow cover fraction with temperature

Seasons	Elevation (m)				
	below 3000	3000 to 4000	4000 to 5000	5000 to 8806	Whole
MAM	-0.849**	-0.908**	-0.802**	-0.373*	-0.821**
JJA	-0.212	-0.224	-0.847**	-0.945**	-0.851**
SON	-0.354*	-0.849**	-0.829**	-0.579**	-0.829**
DJF	-0.410*	-0.289	-0.319	-0.257	-0.265

\* Means significantly correlated (bilateral) at the 0.05 level.

\*\* Means significantly correlated (bilateral) at the 0.01 level.

**TABLE 2**  
Correlation analysis results of seasonal snow cover fraction with precipitation

Seasons	Elevation (m)				
	below 3000	3000 to 4000	4000 to 5000	5000 to 8806	Whole
MAM	-0.607**	-0.783**	-0.658**	-0.090	-0.670**
JJA	0.466**	0.330	-0.610**	-0.632**	-0.557**
SON	-0.278	-0.771**	-0.751**	-0.414*	-0.607**
DJF	0.304	0.616**	0.646**	0.655**	0.649**

\* Means significantly correlated (bilateral) at the 0.05 level. \*\* Means significantly correlated (bilateral) at the 0.01 level.

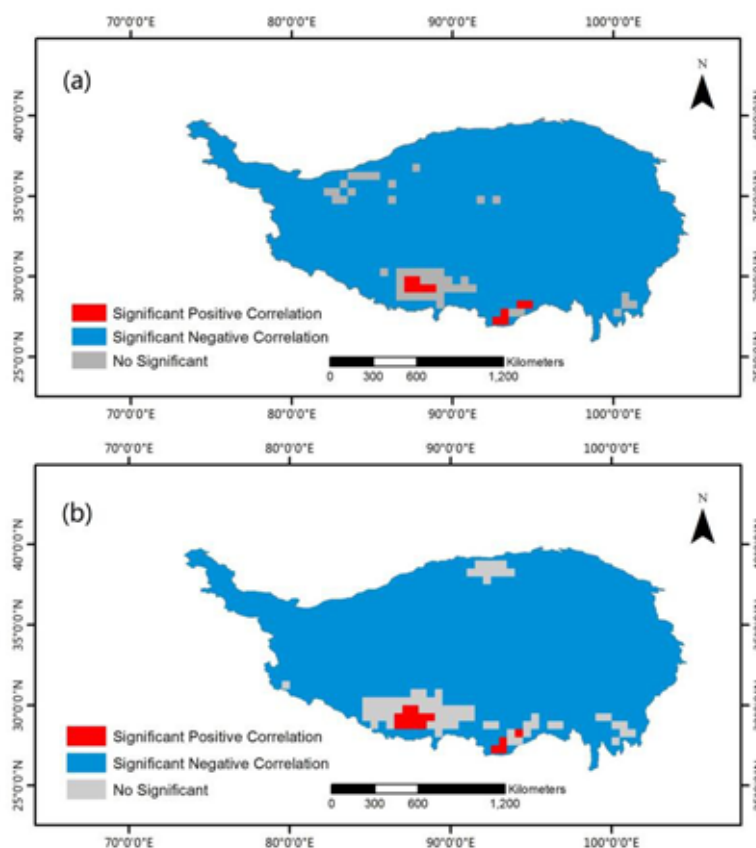


**FIGURE 8**  
Spatial correlation analysis results of snow cover with climate factors: (a) temperature and (b) precipitation

Significance level analysis is conducted based on the time sequence of spatial snow cover fraction dataset and the corresponding temperature and precipitation data during 2001-2011. Statistical significance was at the 0.05 level. As presented in Figure 8a, 94% area of TP shows obvious significant negative correlation between snow cover and temperature, only 0.97% of regions exhibit significant positive correlation. The significantly positive and no significant correlation areas are mainly concentrated along Himalaya and Hengduan Mountains. In Figure 8b, 92.38% of TP shows obvious significant negative correlation between snow cover and precipitation while 1.33% of the region presents significant positive correlation.

## CONCLUSIONS

This paper reviewed the spatial-temporal changes of snow cover over TP and explored its responses to temperature and precipitation variation during 2001-2011. The key conclusions are summarized as follows.

1) From the spatial perspective, the changes in snow cover distribution in different elevation bands are in consistent with the elevation change. High snow covered areas in the southwest of TP are among the Himalayas and Nyenchen Tanglha persisting for all the seasons. Qaidam Basin and other regions of relatively low elevation show lower snow cover fraction.

2) From the temporal perspective, there exists a large inter-annual variability in the monthly snow cover, particularly in winter and spring months. Seasonal snow cover changes occupy large variability, particularly in spring, autumn and summer months.

3) From 2001 to 2011, 41.19% of the grids indicate a declining trend (1.42% with a significant decline) and 38% showing the increasing trend (1.77% with a significant increase).

4) Correlation analysis indicates snow cover fraction shows significant negative correlation with temperature and precipitation in spring, summer and autumn months. In winter, snow over fraction shows significant positive correlation with precipitation and not significant negative correlation with temperature at the 0.01 level.

5) 94% of TP shows obvious significant negative correlation between snow cover and temperature, 92.38% regions exhibit obvious significant negative correlation.

## ACKNOWLEDGEMENTS

This research is funded by the CRSRI Open Research Program (CKWV2016370/KY), National Natural Science Foundation of China (51609061),

Fundamental Research Funds for the Central Universities (2015B28614) and the Priority Academic Program Development of Jiangsu Higher Education Institutions (PAPD). Also, we would like to thank Environmental and Ecological Science Data Center for West China for providing Snow Cover products over the Tibetan plateau area (2000-2011) and China Meteorological Data Sharing Service System for meteorological data.

## REFERENCES

- [1] Fierz C, Riber P, Adams EE, Curran AR, Fohn PMB, Lehning M, Pluss C. (2003) Evaluation of snow-surface energy balance models in alpine terrain. *Journal of Hydrology*, 282, 76-94.
- [2] Kelleners TJ, Chandler DG, McNamara JP, Gribb MM, Seyfried MS. (2009) Modeling the Water and Energy Balance of Vegetated Areas with Snow Accumulation. *Vadose Zone Journal*, 8, 1013-30.
- [3] Kang SC, Xu YW, You QL, Flugel WA, Pepin N, Yao TD. (2010) Review of climate and cryospheric change in the Tibetan Plateau. *Environmental Research Letters*, 5, 8.
- [4] Wu ZW, Li JP, Jiang ZH, Ma TT. (2012) Modulation of the Tibetan Plateau Snow Cover on the ENSO Teleconnections: From the East Asian Summer Monsoon Perspective. *Journal of Climate*, 25,2481-9.
- [5] Qin DH, Liu SY, Li PJ. (2006) Snow cover distribution, variability, and response to climate change in western China. *Journal of Climate*, 19,1820-33.
- [6] Liu XD, Chen BD. (2000) Climatic warming in the Tibetan Plateau during recent decades. *International Journal of Climatology*, 20, 1729-1742.
- [7] Bamzai AS, Shukla J. (1999) Relation between Eurasian snow cover, snow depth, and the Indian summer monsoon: An observational study. *Journal of Climate*,12, 3117-3132.
- [8] Brown RD, Mote PW. (2009) The Response of Northern Hemisphere Snow Cover to a Changing Climate. *Journal of Climate*, 22, 2124-2145.
- [9] Dye DG.(2002) Variability and trends in the annual snow-cover cycle in Northern Hemisphere land areas, 1972-2000. *Hydrological Processes*, 16, 3065-3077.
- [10] Tang ZG, Wang J, Li HY, Yan LL. (2013) Spatiotemporal changes of snow cover over the Tibetan plateau based on cloud-removed moderate resolution imaging spectroradiometer fractional snow cover product from 2001 to 2011. *Journal of Applied Remote Sensing*, 7, 14.



- [11] Matson M. (1991) NOAA SATELLITE SNOW COVER DATA. *Global and Planetary Change*, 90, 213-218.
- [12] Justice CO, Vermote E, Townshend JRG, Defries R, Roy DP, Hall DK, Salomonson VV, Privette JL, Riggs G, Strahler A, Lucht W, Myneni RB, Knyazikhin Y, Running SW, Nemani RR, Wan ZM, Huete AR, van Leeuwen W, Wolfe RE, Giglio L, Muller JP, Lewis P, Barnsley MJ. (1998) The Moderate Resolution Imaging Spectroradiometer (MODIS): Land remote sensing for global change research. *IEEE Trans Geosci Remote Sensing*, 36, 1228-1249.
- [13] Bergeron J, Royer A, Turcotte R, Roy A. (2014) Snow cover estimation using blended MODIS and AMSR-E data for improved watershed-scale spring streamflow simulation in Quebec, Canada. *Hydrological Processes*, 28, 4626-4639.
- [14] Hall DK, Riggs GA, Salomonson VV, DiGirolamo NE, Bayr KJ. (2002) MODIS snow-cover products. *Remote Sens Environ*, 83, 181-94.
- [15] Arsenault KR, Houser PR, De Lannoy GJM. (2014) Evaluation of the MODIS snow cover fraction product. *Hydrological Processes*, 28, 980-998.
- [16] Dietz AJ, Kuenzer C, Conrad C. (2013) Snow-cover variability in central Asia between 2000 and 2011 derived from improved MODIS daily snow-cover products. *International Journal of Remote Sensing*, 34, 3879-3902.
- [17] Xu L, Shi HC, Zhang HG, Wu SL, Ieee. (2005) Fractional snow cover estimation in Tibetan plateau using MODIS and ASTER. New York: IEEE, 3, 1940-1942.
- [18] Dietz AJ, Wohner C, Kuenzer C. (2012) European Snow Cover Characteristics between 2000 and 2011 Derived from Improved MODIS Daily Snow Cover Products. *Remote Sensing*, 4, 2432-2454.
- [19] Pu ZX, Xu L, Salomonson VV. (2007) MODIS/Terra observed seasonal variations of snow cover over the Tibetan Plateau. *Geophysical Research Letters*, 34, 6.
- [20] Gao J, Williams MW, Fu XD, Wang GQ, Gong TL. (2012) Spatiotemporal distribution of snow in eastern Tibet and the response to climate change. *Remote Sensing of Environment*, 121, 1-9.
- [21] Duo C, Xie HJ, Wang PX, Guo JP, La J, Qiu YB, Zheng ZJ. (2014) Snow cover variation over the Tibetan Plateau from MODIS and comparison with ground observations. *Journal of Applied Remote Sensing*, 8, 13.

---

**Received:** 30.11.2015

**Accepted:** 18.09.2016

---

**CORRESPONDING AUTHOR:**

**Guo-Hua Fang**

College of Water Conservancy and Hydropower Engineering  
Hohai University  
210098 Nanjing-CHINA

e-mail: 1506767081@qq.com

# A COMBINED WAVELET AND NEURAL NETWORK MODEL FOR FORECASTING STREAMFLOW DATA

Alpaslan Yazar<sup>1,\*</sup>, Mustafa Onucyildiz<sup>1</sup>, Nadim K Copt<sup>2</sup>

<sup>1</sup>Selcuk University, Engineering and Architecture Faculty, Civil Engineering Department Hydraulics Division, 42031 Konya, Turkey

<sup>2</sup>Bogazici University, Institute of Environmental Sciences, 34342 Bebek, Istanbul, Turkey

## ABSTRACT

The modeling of streamflow is often needed for the sustainable management of water resources and for the protection against flooding. Over the years numerous streamflow forecasting models have been developed, black-box models, like Artificial Neural Networks (ANN), have become quite popular in the field of hydrologic engineering, because of their rapidity and less data requirements compared to physics-based models. In this study, a hybrid model, Wavelet-Neural Network (WNN), for the prediction of streamflow is developed. The model incorporates ANN and wavelet transform for the analysis of variations in streamflow time series. For demonstration, the model is applied to streamflow data from four flow observation stations (FOS), located in the West Mediterranean Basin of Turkey. Monthly mean streamflow data from the four FOS were used in the model. Original series were decomposed sub-series by wavelet transform. These sub-series were used for ANN model. In order to evaluate the performance of the WNN model, a multi regression (MR) model was also developed based on the same data set. Results show that WNN model forecasts the streamflow more accurately than the MR model with correlations between estimated and observed streamflow data ranging from 0.84-0.88.

## KEYWORDS:

Streamflow modeling, wavelet transform, artificial neural network, multi regression.

## INTRODUCTION

Human settlements are often located near surface water bodies, such as rivers or lakes that serve as vital sources of freshwater and important contributors to economical, recreational and transportation activities. However, the proximity of populations to water bodies also involves some risks. Excessive precipitation can lead to flooding and extensive loss in property and livelihood and, in some cases, loss of life. Low precipitation on the

other hand, can cause draughts threatening water resources and leading to excessive losses in agricultural production and other economic sectors. These risks further highlight the need to develop predictive water quality and quantity models for the effective management of water resources both at the local and global scale.

Hydrological processes are influenced by numerous dynamic effects that are quite hard, if not impossible, to accurately consider in analytical studies. To overcome this limitation black-box type models have been shown as a viable tool in various fields including surface water modeling. In recent years, such data-driven models have become widely used for the analysis of hydrological problems because they are relatively easy to use, require less data and at the same time can provide accurate system predictions [1].

Many data-driven models, including those based on linear, nonparametric or nonlinear approaches, have been applied for hydrologic discharge time series prediction [2]. K-Nearest-Neighbors (KNN) algorithm, Artificial Neural Networks (ANN) and Support Vectors Machine (SVM) are among the more commonly used forecast methods for dynamic systems [3, 4, 5]. Prediction techniques for a dynamic system can be broadly divided into two approaches: local and global. Local approaches use only nearby states to make predictions whereas global approaches involve all the states. A detailed review of ANN applications for modelling water resource variables can be found in [6, 7]. Recent developments in ANN modeling that are relevant to the current study are briefly reviewed below.

Zhang et al. [8] summarized various potential applications of neural networks in system predictions. Deo et al. [9], Agrawal and Deo [10] and Tsai et al. [11] have used ANNs for predicting wave parameters. Kazeminezhad et al. [12] used an adaptive network-based fuzzy inference systems (ANFIS) model, which is a fuzzy inference system, whose rules parameters are tuned by ANNs, in prediction of wave parameters in fetch-limited condition. Zanganeh et al. [13] combined genetic algorithms (Gas) and ANFIS models for the prediction of wave parameters.

Hatzikos et al. [14] utilized neural networks with active neurons as a modeling tool for the prediction of seawater quality indicators like water temperature, pH, dissolved oxygen (DO) and turbidity. Palani et al. [15] demonstrated the application of ANNs to model selected seawater quality variables, with dynamic and complex processes influencing the monitored data itself. Feed-forward neural Networks (FNN) have been successfully applied for time series modeling in various hydrological contexts such as rainfall-runoff [16, 17], river flow [18, 19], flood forecasting [20] and water quality modelling [21, 22]. Coulibally et al. [23] used different types of ANNs for monthly predictions of groundwater levels in the Gondo Plain, Burkina Faso. Nayak et al. [24] employed ANN for forecasting monthly water levels in two different wells of an unconfined coastal aquifer in Godavari Delta System, India. Trichakis et al. [25] employed ANN for daily forecasting of the water stage of a karstic aquifer in the region of Attica, Greece. In spite of the robustness and flexibility of ANN in modeling hydrologic time series, ANN may exhibit some shortcomings particularly when signal fluctuations are highly non-stationary and the hydrologic process occurs over a large range of times scales varying from 1 day to several decades. In such a situation, ANNs may not be able to adequately cope with non-stationary data if pre-processing of the input and/or output data is not performed [26]. In recent years wavelet transform prior to ANN has been proposed. Wavelet transform allows for the segmentation of data into specific frequency components which are subsequently analyzed with an appropriate resolution. An ANN-wavelet conjunction model was first proposed by Aussem et al. [27] for financial time series forecasting. Zhang and Dong [28] proposed a short-term load forecast model based on ANN and multi-resolution wavelet decomposition. In hydrology, Wang and Ding [29] applied wavelet-network model to forecast shallow groundwater level and daily discharge.

In this study, we evaluate the ability of Wavelet-Neural Network (WNN) to model streamflow data. The streamflow data used in the study are from four stations, located in the West Mediterranean Basin, Turkey. To evaluate the WNN model's performance a Multi Regression (MR) model was also developed. Section 2 of the paper describes the model used to analyze the streamflow data. It includes the wavelet transform and how it was incorporated with ANN. Section 3 presents the application of the WNN to the streamflow data from the West Mediterranean Basin.

## MODEL DESCRIPTION

**Wavelet Analysis.** A wavelet transform (WT), like a short-time Fourier transform (STFT), can be used in applications involving signal analysis [30]. In contrast to the STFT, which uses a single analysis window, the WT uses short windows at high frequencies and long windows at low frequencies [31]. Continuous Wavelet Transform (CWT) and Discrete Wavelet Transform (DWT) are the main types of wavelet transform.

A wavelet series is a sampled version of a CWT. The computation of a wavelet series may consume significant amount of time and resources, depending on the resolution required. All the wavelet functions used in the transformation are derived from the mother wavelet through translation (shifting) and scaling (dilation or compression). Denoting  $\psi(t)$ , as the mother wavelet or the basis function successive wavelets can be mathematically expressed as:

$$\psi_{a,b}(t) = \frac{1}{\sqrt{|a|}} \psi\left(\frac{t-b}{a}\right) \quad (1)$$

Where  $\psi_{a,b}(t)$  is the successive wavelet,  $a$  is the frequency factor, and  $b$  is the time factor. A CWT can be written as:

$$X_{WT}(a,b) = \frac{1}{\sqrt{|a|}} \int f(t) \cdot \psi^*\left(\frac{t-b}{a}\right) dt \quad (2)$$

Where  $f(t)$  is the signal to be analyzed,  $\psi^*$  is the complex conjugate functions of  $\psi(t)$ .

A DWT, which is based on sub-band coding, is evaluated to yield fast computation of the wavelet transform. Discrete wavelet transform of  $f(t)$  can be written as:

$$X_{WT}(j,k) = \frac{1}{\sqrt{|a_0|^{-j}}} \int f(t) \cdot \psi^*\left(\frac{t}{a_0^{-j}} - kb_0\right) dt \quad (3)$$

The most common choice for the parameters  $a_0$  and  $b_0$  is 2 and 1 time steps, respectively. This power of two logarithmic scaling of the time and scale is known as dyadic grid arrangement and is the simplest and the most efficient case for practical purposes [32].

**Artificial Neural Networks.** The composition of ANN is inspired from biological neural networks. A neuron is one of the basic components of neural networks. It can vary in terms of size and shape, according to its function and mission in neural systems.

The network consists of layers of parallel processing elements, also called neurons. Each layer is fully connected to the backflow layer by interconnections which are characterized by interconnection strengths, or weights. Fig. 1 illustrates a three-layer neural network consisting of layers  $i$ ,  $j$ , and  $k$ , with the interconnection weights  $W_{ij}$  and  $W_{jk}$  between the layers of neurons.

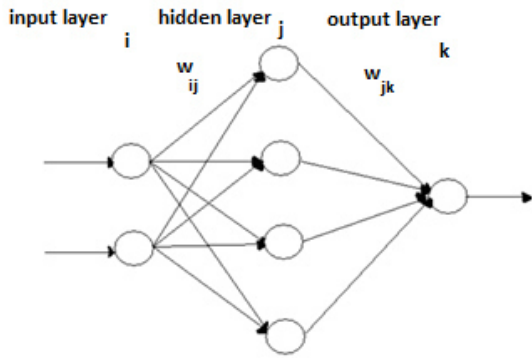


**FIGURE 1**  
An ANNs architecture.

The methodology used in this study for adjusting the weights is called “momentum back propagation”, and is based on the “generalized

delta rule”, as presented by Rumelhart et al. [33]. Throughout all ANN simulations, the adaptive learning rates were used for increasing the convergence velocity. For each epoch, if the performance decreases toward the goal, then the learning rate is increased by the factor of learning increment. If the performance increases, the learning rate is adjusted by the factor of learning decrement.

**STUDY AREA AND MODEL APPLICATION**

**Study Area.** Turkey can be divided into a total of 26 basins as shown in Figure 2. The West Mediterranean Basin (Figure 3) is the basin designated as number 08 in Figure 2.



**FIGURE 2**  
Basins of Turkey.

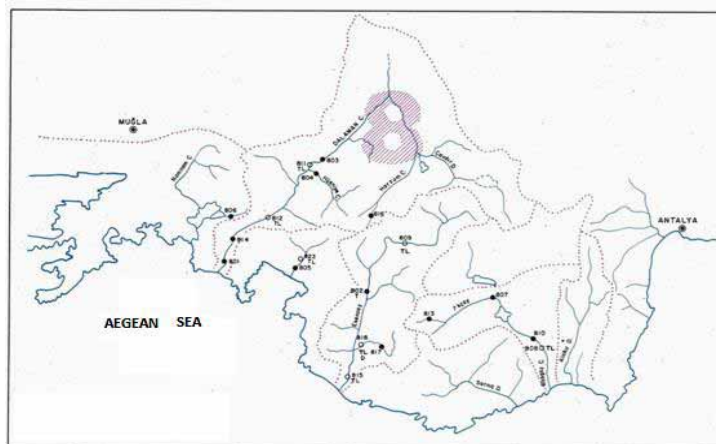


**FIGURE 3**  
West Mediterranean Basin.

The basin's area is 20953 km<sup>2</sup> with mean annual flow of 8.93 km<sup>3</sup>. The annual maximum and minimum temperatures are 21.3°C and 9.5°C respectively. Precipitation is most intensive in the months of March and November. The basin has three main river: the Dalaman River in the west, the Eşençay River in the middle and the Başgöz River in the east. The Dalaman River which is 190 km long has the highest streamflow, while snowmelt in

the Spring season is highest in the Eşençay River, which is 128 km long. The stations, which are used in this study, are Suçatı (811) and Akköprü (812) stations on the Dalaman River, Çatallar (808) station on the Başgöz River and Kavaklıdere (809) station on the Eşençay River.

Characteristic of the four stations are presented in Table 1.

**TABLE 1**  
Characteristics of the four stations used in this study.

Station Number	Station Name	Precipitation Area (km <sup>2</sup> )	Approximately Altitude (m)	Long Term Mean Streamflow (m <sup>3</sup> /s)
808	Başgöz Çayı-Çatallar	770	342	3,90
809	Eşençay-Kavaklıdere	547	1115	3,69
811	Dalaman Çayı-Suçatı	3820	589	14,70
812	Dalaman Çayı-Akköprü	4622,3	128	43,2

**TABLE 2**  
Correlation of Stream Flow with various parameters for each FOS.

Station	Flow Unit	Input Data	Correlations with Streamflow Data (Q <sub>t</sub> )
<b>808</b>	m <sup>3</sup>	D3 <sub>t-1</sub>	0.378
		A <sub>t-2</sub>	0.715
		A <sub>t-1</sub>	0.873
		Q <sub>t-12</sub>	0.726
		Q <sub>t-11</sub>	0.717
		Q <sub>t-2</sub>	0.684
		Q <sub>t-1</sub>	0.846
<b>809</b>	m <sup>3</sup>	D3 <sub>t-1</sub>	0.510
		D2 <sub>t-1</sub>	0.320
		A <sub>t-2</sub>	0.466
		A <sub>t-1</sub>	0.773
		Q <sub>t-12</sub>	0.663
		Q <sub>t-11</sub>	0.598
		Q <sub>t-2</sub>	0.438
<b>811</b>	m <sup>3</sup>	Q <sub>t-1</sub>	0.739
		D3 <sub>t-1</sub>	0.447
		D2 <sub>t-1</sub>	0.438
		A <sub>t-2</sub>	0.512
		A <sub>t-1</sub>	0.813
		Q <sub>t-12</sub>	0.708
		Q <sub>t-11</sub>	0.672
<b>812</b>	m <sup>3</sup>	Q <sub>t-2</sub>	0.483
		Q <sub>t-1</sub>	0.749
		D3 <sub>t-1</sub>	0.423
		D2 <sub>t-1</sub>	0.370
		A <sub>t-2</sub>	0.407
		A <sub>t-1</sub>	0.738
		Q <sub>t-12</sub>	0.670
Q <sub>t-11</sub>	0.606		
Q <sub>t-1</sub>	0.650		

**Model Applications.** Monthly mean streamflow data from the four flow observation stations (FOS) were used in the model. As the results will show, four FOS is sufficient for the accurate prediction of streamflow. The input layer data of the ANN modeling consist of (i) the decomposed sub-time series,  $D_1$ ,  $D_2$ , and  $D_3$  of the three-layer ANN, (ii) the approximation time series of the previous 2 months  $A$ , which were obtained from DWT, and (iii) the streamflow data, of the previous month. The output layer data is the monthly streamflow.

Table 2 shows the correlation between input and output data sets for each FOS. In this table  $Q_t$  denotes streamflow at time  $t$ ;  $D_1$ ,  $D_2$ , and  $D_3$  denote the decomposed sub-time series under each level (level 1, 2 and 3);  $A$  denotes approximation series, and the subscripts  $t-1$ ,  $t-2$  denote the two previous months' data, respectively. Table 2 shows that  $Q_{t-1}$  and  $A_{t-1}$  having the highest correlations but that all seven parameters exhibit high correlation with the streamflow data. Consequently, these parameters were used in the subsequent WNN and multi-regression models.

For WNN modeling, forward feed back-propagation ANN was selected along with the scaled conjugate gradient (SCG) algorithm. The SCG algorithm is a complex algorithm which was developed by Moller [34] for the purpose of deriving a profit in the period of direct searching. Its basic approach depends on the combination of safe areas and the reaching model-true approach which also used in the Levenberg-Marquart algorithm. The model was implemented using MATLAB computer programming.

A hybrid modeling approach was adopted with WNN. A hybrid modeling process consists of two parts: a training step followed by a testing one. In the application to the West Mediterranean Basin a total of 420 monthly data were used for modeling. 210 monthly data were selected for training process which consisted of sub-time series  $D$ , and approximation series  $A$  as input layer and monthly streamflow data  $Q$  as output layer.

Different layer, different confidential knot number and different epoch numbers were tried for every station in ANN modeling to obtain the best structure of the model.

In the testing procedure, the remaining 210 monthly data were utilized in the ANN models obtained from the training procedure. The best model depends on the epoch number which was determined by calculating the Root Mean Squared Errors (RMSE) of the models. The agreements between the observed streamflow values and the estimated values using the hybrid model WNN are shown in Figure 4. For all 4 FOS, the estimated monthly streamflows matched well with the observed data, with correlations ranging for 0.83 to 0.87. The WNN model was capable of capturing the seasonal variations as well as low and high streamflows which ranged from less than  $2 \text{ m}^3/\text{s}$  to about  $200 \text{ m}^3/\text{s}$  quite well.

MR models were also formed in order to compare the WNN model with traditional ones. The data used for the purpose of training in the ANN were used for the calibration of the MR models, while the data used for testing were used for validity control. The MR model equations are given in Table 3.

Fig. 5 compares the observed data to the MR model predictions for the testing streamflow data only. On the whole the MR model was able to capture the seasonal variations of the monthly streamflow data, but the predicted peak flow rates were generally lower than the peak observed flow. The correlations of the MR model ranged from 0.57 to 0.85 which are lower than the corresponding values of the WNN model. Another unfavorable aspect of the MR model is that in some instances slightly negative flow rates were predicted. The corresponding (RMSE) and  $R^2$  values for both the WNN and MR models are given in Table 4.

The RMSE and  $R^2$  values are consistently better for the WNN model for all FOS. Overall, this study shows the flexibility of WNN models and demonstrates that they are a powerful tool for the analysis of streamflow data.

**TABLE 3**  
**Regression model equations for each FOS using.**

Station	Regression Equation
808	$Q_t = 0.138D_{3,t-1} + 0.446A_{t-2} + 1.251A_{t-1} - 0.019Q_{t-12} + 0.225Q_{t-11} - 0.810Q_{t-2} - 0.140Q_{t-1} + 0.293$
809	$Q_t = 0.123D_{3,t-1} - 0.146D_{2,t-1} + 0.414A_{t-2} + 1.062A_{t-1} + 0.049Q_{t-12} + 0.241Q_{t-11} - 0.742Q_{t-2} - 0.075Q_{t-1} + 0.170$
811	$Q_t = 0.090D_{3,t-1} - 0.024D_{2,t-1} + 0.268A_{t-2} + 1.088A_{t-1} - 0.013Q_{t-12} + 0.334Q_{t-11} - 0.465Q_{t-2} - 0.233Q_{t-1} + 0.291$
812	$Q_t = 0.037D_{3,t-1} - 0.095D_{2,t-1} - 0.070A_{t-2} + 0.899A_{t-1} + 0.077Q_{t-12} + 0.359Q_{t-11} - 0.0166Q_{t-1} + 0.243$

**TABLE 4**  
Performance statistics of the WNN and regression models.

	RMSE		R <sup>2</sup>	
	WNN	WLR	WNN	WLR
<b>808</b>	1.00	1.11	0.88	0.85
<b>809</b>	1.37	1.82	0.84	0.70
<b>811</b>	4.68	5.26	0.85	0.77
<b>812</b>	11.66	19.21	0.84	0.57

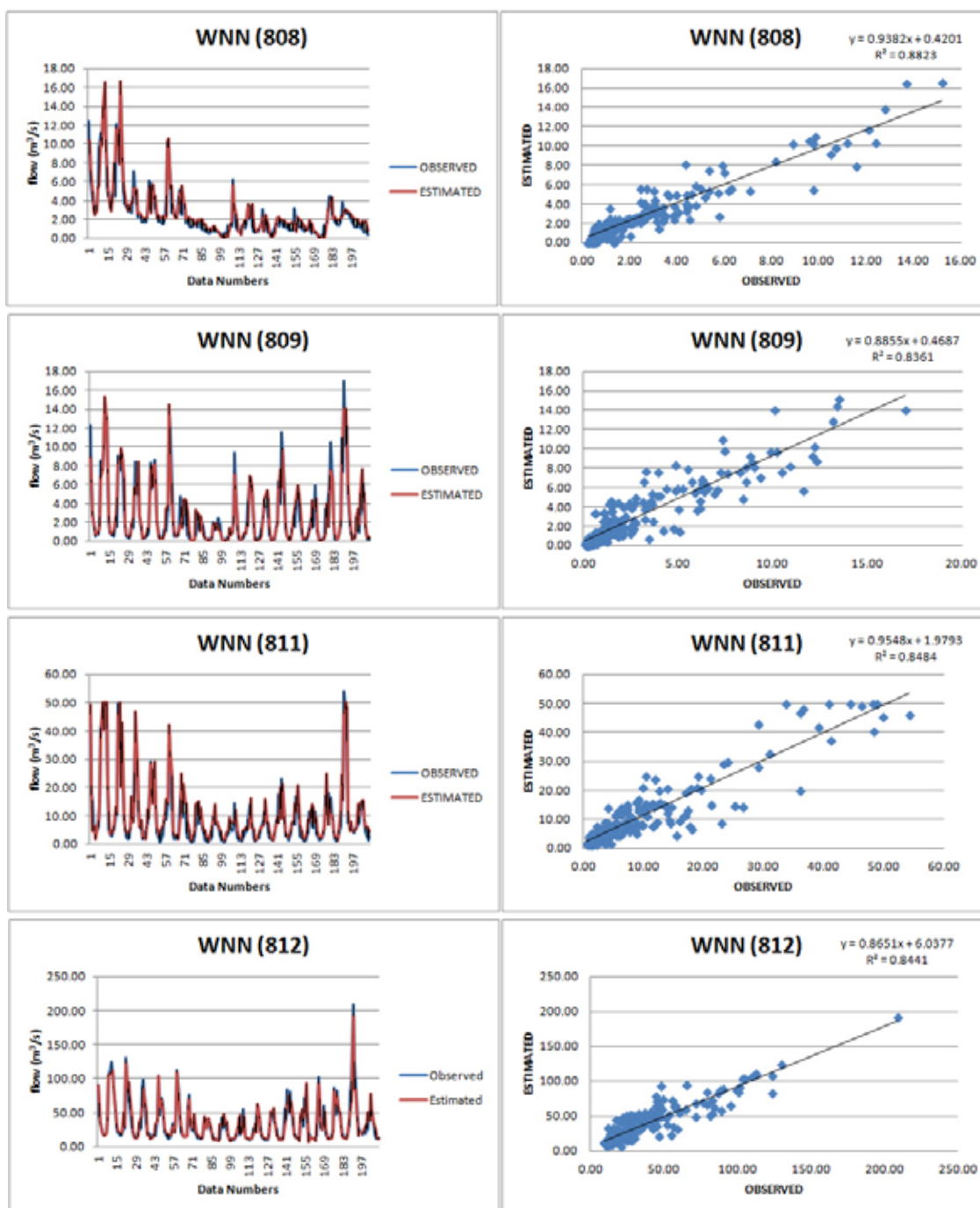


**FIGURE 4**  
Comparison of the observed streamflow data to the streamflow data estimated with the WNN model.

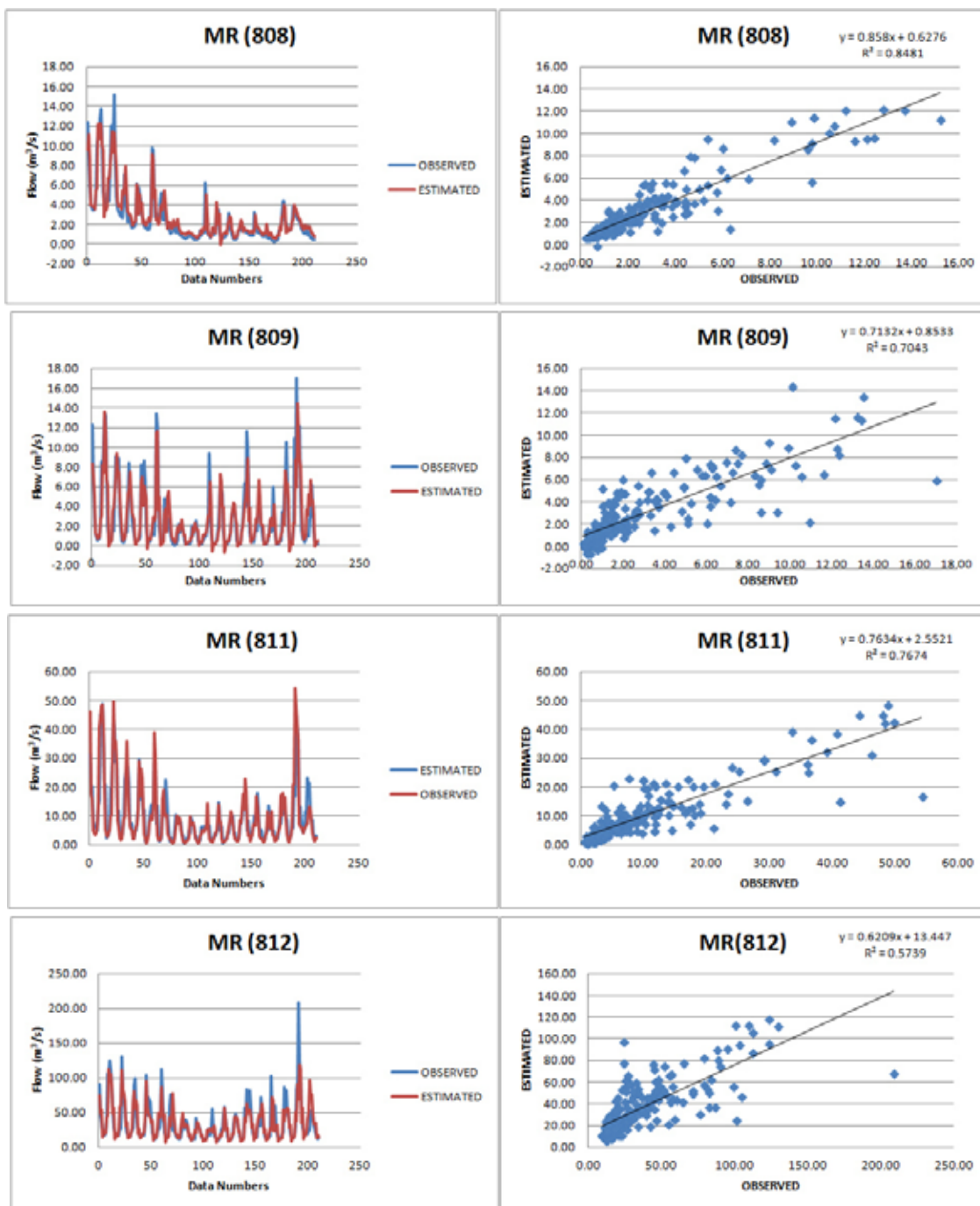


**FIGURE 5**  
**Comparison of the observed streamflow data to the streamflow data estimated with the MR model.**

**CONCLUSION**

In this study we investigate the use a Wavelet Neural Network model for estimating streamflow data. For this purpose, data from 4 flow observation stations located in the West Mediterranean Basin of Turkey which is susceptible to frequent flooding, were used. Monthly mean streamflow data were decomposed into subseries and their correlations

with the following months' data were analyzed. Subseries which have high correlations value were selected as the input data set for WNN model. Monthly streamflow data were used as the output data set. A hybrid modeling approach was adopted whereby half of the data were used for training and the other half for testing. The predicted monthly streamflow were then compared to the observed streamflow for the testing data at the 4 FOS, with





correlations values ranging between 0.84 and 0.88. To evaluate the performance of the WNN model, a MR model which utilized the same data was constructed. Results of this application showed that the RMSE and  $R^2$  values of the WNN were better for each of the four FOS. It was seen that the WNN model gave favorable results compared to the MR model. In summary this study demonstrates that the WNN model can provide reliable estimates of the streamflow data. This predictive tool can be further used to identify optimal policies for the protection from floods and the sustainable management of the available water resources.

## REFERENCES

- [1] Yarar, A., 2014. A hybrid wavelet and neuro-fuzzy model for forecasting the monthly streamflow data. *Water Resources Management*, 28, 553-565.
- [2] Marques, C.A.F., Ferreira, J. Rocha, A. Castanheira, J. P. Gonçalves, Vaz., N., Dias, J.M., 2006. Singular spectral analysis and forecasting of hydrological time series. *Physics and Chemistry of the Earth*, 31, 1172-1179.
- [3] Sivapragasam, C., Liong, S. Y., Pasha, M. F. K., 2001. Rainfall and runoff forecasting with SSA-SVM approach. *J. Hydroinformatics* 3(3), 141–152.
- [4] Laio, F., Porporato, A., Revelli, R., Ridolfi, L., 2003. A comparison of nonlinear flood forecasting methods. *Water Resources Research*, 39(5): 1129.
- [5] Wang, M. X., Liu, G. D., Wu, W. L., Bao, Y. H., Liu, W. N., 2006. Prediction of agriculture derived groundwater nitrate distribution in North China Plain with GIS-based BPNN. *Environment Geology*, 50 (5), 637–644.
- [6] Maier, H.R., Dandy, G.C., 2000. Neural networks for the prediction and forecasting of water resources variables: a review of modelling issues and applications. *Environmental Modelling and Software*, 15: 101-124.
- [7] Maier, H. R., Jain, A., Dandy, G. C., Sudheer, K. P., 2010. Methods used for the development of neural networks for the prediction of water resource variables in river systems: Current status and future directions. *Environmental Modelling & Software*, 25, (8), 891-909.
- [8] Zhang, G., Patuwo, B. E., Hu, M. Y., 1998. Forecasting with artificial neural networks: The state of the art. *International Journal of Forecasting*, 14, 35–62.
- [9] Deo, M.C., Jha, A., Chaphekar, A.S. and K. Ravikant, 2001. Neural networks for wave forecasting. *Ocean Engng.*, 28, 889-898.
- [10] Agrawal, J.D., M.C. Deo, 2002. On-line wave prediction. *Marine Structures*, 15, 57-74.
- [11] Tsai, C.P., Hsu, J.R.-C., Pan, K.L., 2000. Prediction of storm-built beach profile parameters using neural network. *Proc.27th Int. Conf. Coastal Engineering, ASCE, V.4, 3048-3061.*
- [12] Kazeminezhad, M.H., Etemad-Shahidi, A., Mousavi, S.J., 2005. Application of fuzzy inference system in the prediction wave parameters. *Ocean Engineering*. 32, 1709–1725.
- [13] Zanganeh, M., Mousavi, S., Etemad-Shahidi, A., 2006. A genetic algorithm-based fuzzy inference system in prediction of wave parameters, *computational intelligence. Theory and Applications (Part 25)*, 741–750.
- [14] Hatzikos E., Anastasakis L., Bassiliades N., Vlahavas I., 2005. Simultaneous prediction of multiple chemical parameters of river water quality with tide. *Proc. 2nd Int. Sci. Conf. Computer Sci., IEEE Computer Society, May 11-13, Varna, Bulgaria.*
- [15] Palani, S., Liong, S.Y., Tkalich, P., 2008. An ANN application for water quality forecasting. *Mar Pollut Bull*, 56, 1586–1597.
- [16] Dawson, C.W., Wilby, R.L., 1998. An artificial neural network approach to rainfall-runoff modeling. *Hydrol Sci.* 43 (1), 47–67.
- [17] Hsu, K.L., Gupta, H.V., Sorooshian, S., 1995. Artificial neural network modeling of the rainfall-runoff process. *Water Resour Res.* 31 (10), 2517–30.
- [18] Cheng, C.T., Chau, K.W., Sun, Y.G., Lin, J.Y., 2005. Long-term prediction of discharges in Manwan Reservoir using artificial neural network models. *Lecture Notes in Computer Science*, Vol. 3498, pp.1040–1045.
- [19] Joorabchi, A., Zhang, H., Blumenstein, M., 2007. Application of artificial neural networks in flow discharge prediction for the Fitzroy River. Australia. *Journal of Coastal Research*, 50: 287-291.
- [20] Chau, K. W., Wu, C. L., Li, Y. S., 2005. Comparison of several flood forecasting models in Yangtze River. *Journal of Hydrologic Engineering, ASCE*, 10(6), 485-491.
- [21] Muttil, N., Chau, K. W., 2006. Neural network and genetic programming for modelling coastal algal blooms; *International Journal of Environment and Pollution*, 28, 223–238.
- [22] May, D.B., Sivakumar, M., 2009. Prediction of urban stormwater quality using artificial neural networks. *Environmental Modeling and Software* 24 (2), 296–302.
- [23] Coulibaly, P., Anctil, F., Aravena, R., Bobée, B., 2001. Artificial neural network modeling of water table depth fluctuations. *Water*



- Resources Research, Vol. 37 No. 4, pp. 885 – 896.
- [24] Nayak, P. C., Rao, S. Y. R., Sudheer, K. P., 2006. Groundwater level forecasting in a shallow aquifer using artificial neural networks. *Water Res. Manage.* 20:77-90.
- [25] Trichakis, I.C., Nikolos, I.K., Karatzas, G.P., 2009. Optimal selection of artificial neural network parameters for the prediction of a karstic aquifer's response. *Hydrol. Processes* 23 (20), 2956–2969.
- [26] Cannas B., Fanni A., See L., Sias G., 2006. Data preprocessing for river flow forecasting using neural networks: wavelet transforms and data partitioning. *Phys Chem Earth A/B/C* 31(18):1164–1171.
- [27] Aussem, A., Campbell, J., Murtagh, F., 1998. Wavelet-based feature extraction and decomposition strategies for financial forecasting. *Journal of Computational Intelligence in Finance*, 6(2), 5-12.
- [28] Zhang, B. L., Dong, Z. Y., 2001. An adaptive neural-wavelet model for short term load forecasting. *Electer. Pow. Syst. Res.*, 59, 121–129.
- [29] Wang, D., Ding, J., 2003. Wavelet network model and its application to the prediction of hydrology. *Nat Sci* 1(1):67–71.
- [30] Daubechies, I., 1990. The wavelet transform, time–frequency localization and signal analysis. *IEEE Transactions on Information Theory* 36(5): 961–1005.
- [31] Rioul, O., Vetterli, M., 1991. Wavelets and signal processing. *IEEE Signal Process* 8: 14–38.
- [32] Mallat, S., 1989. A theory for multiresolution signal decomposition: the wavelet representation, *IEEE Trans. Pattern Anal. Mach. Intell.*, 11 (7), 674-693.
- [33] Rumelhart, D.E., Hinton, G.E., Williams, R.J., 1986. Learning internal representation by error propagation. In: Rumelhart, D.E., McClelland, J.L. (Eds.), *Parallel Distributed Processing. Foundations*, vol. 1. MIT Press, Cambridge, MA.
- [34] Moller, M., 1993. A scaled conjugate gradient algorithm for fast supervised learning. *Neural Networks*, 6(4):525–533.

---

**Received:** 12.01.2016

**Accepted:** 06.09.2016

---

#### **CORRESPONDING AUTHOR**

**Assist. Prof. Dr. Alpaslan Yayar**

Selcuk University

Engineering Faculty,

Civil Engineering Department Hydraulics Division,

42031 Konya - TURKEY

E-mail: [ayayar@selcuk.edu.tr](mailto:ayayar@selcuk.edu.tr)

# SORPTION OF CADMIUM BY BIOCHAR PRODUCED FROM PYROLYSIS OF CATTLE MANURE IN AQUEOUS SOLUTION

Fengfeng Ma, Baowei Zhao\*, Jingru Diao, Hongtao Qiao, Jinkui Zhong

School of Environmental and Municipal Engineering, Lanzhou Jiaotong University, Lanzhou 730070, P. R. China

## ABSTRACT

Biochar from waste product is considered to be an alternative adsorbent for the removal of aqueous heavy metals. In this work, experimental investigations were conducted to study the effect of biochar that was pyrolytically produced from cattle manure waste on the removal of aqueous cadmium (Cd). The results showed that the highest sorption capacity of cattle manure biochar was 18.12 mg/g. The sorption ability of Cd increased with increasing pH, and the sorption of Cd was favorable at a pH value of 8.0. The equilibrium data were well fitted by Freundlich model. The kinetic data were fitted well by the pseudo-second-order model. The fitting results from intra-particle diffusion model showed that the sorption process might be a complex natural process that consisted of both surface sorption and intra-particle diffusion. The thermodynamic studies indicated that the sorption was endothermic, and the randomness of the adsorbed species increased and was spontaneous at high temperatures. The sorption was attributed primarily to the oxygen-containing functional groups of biochar, which was confirmed by batch sorption experiments, mathematical modeling, and characterization of the Cd-laden biochar samples using SEM-EDS, XRD, FTIR and XPS.

## KEYWORDS:

biochar; cattle manure; sorption; heavy metal

## INTRODUCTION

The widespread contaminations of water and soil by heavy metals have become the particularly serious current environmental issues worldwide. Heavy metal ions are one sort of the most significant contaminants in water, causing potential threat to aquatic lives and humans because of their

accumulation in food chain [1]. Heavy metal contamination of water is a result of industrial activities, such as discharges from metal plating, tanneries, mining, refineries and paper industries [2]. Heavy metals such as cadmium (Cd) are widely distributed in water and soils, and can enter food chain through crops and threaten human health [3]. Long-term exposure to Cd can cause malfunctioning of kidneys and liver, cancer, and osteoporosis [4]. Additionally, heavy metals are prior toxic pollutants that severely limit the beneficial use of water for industrial or domestic applications [5]. Hence the removal of heavy metals from water and wastewater is of particular concern.

Conventional methods have been used for the removal of toxic metal ions from water and wastewater, including biological treatments [6], ionic liquids [7], chemical precipitation [8], membrane filtration [9], and electrolysis methods [10]. However, most of these methods have disadvantages, including the use of expensive equipment and higher energy consumption, which limit their application in Cd wastewater treatment. Sorption is an effective technology for heavy metal removal with the advantages of low cost and straightforward design [11]. However, large-scale application of this method is limited by the high costs for the regeneration and purchase of the commercial adsorbents, such as activated carbons. In order to overcome the limitations, there is a need to extensive research concerning the identification of relatively inexpensive and environmental friendly adsorbent with significant removal efficiency for heavy metals from wastewater. Biosorbents have been suggested as potential candidates to remove toxic metals from wastewater [2].

Biochar is pyrogenic black carbon that is derived from pyrolysis of biomass in the presence of N<sub>2</sub> or at oxygen limited conditions [12], and it is a potential cheaper adsorbent produced from the wastes of agriculture and industry [13]. Recently,

many studies have suggested that biochar can be a promising sorbent for the sorption of heavy metals [13, 14] and organic pollutants [15, 16] from wastewater. The structural characteristics and sorption properties of biochars have shown good sorption capacity to heavy metal ions in water [15]. The possible mechanisms of heavy metal sorption by biochars depend on the properties of heavy metals and biochar, including: (i) ion exchange; (ii) chemical precipitation; (iii) surface interactions with the free surface oxygen-containing functional groups; (iv) coordination of heavy metals with  $\pi$  electrons (C=C) of carbon; (v) electrostatic interaction [14,17,18]. However, to our knowledge, little information is available on the utilization of cattle manure biochar as a sorbent for sorption of Cd in aqueous solution and the sorption mechanisms.

The objective of the present study is to investigate the capacity of biochar derived from cattle manure to remove heavy metals with Cd as the model heavy metal. Batch sorption experiments were used to examine the sorption behaviors of Cd on the biochar, and the characterizations of the before and after sorption biochar were determined. Mathematical models assisted the data analysis and interpretation of the sorption mechanism. The specific objectives of the present research are to: (1) determine the sorption characteristics of Cd on the biochar, (2) assess the effects of biochar dosage, solution pH value, and ionic strength on Cd sorption, and (3) discuss the sorption mechanism of Cd interaction with the biochar.

## EXPERIMENTAL

**Preparation of biochar.** Cattle manure (CM0) was collected from a feeding farm in Wuwei, China. The cattle manure air-dried for 2 days, and then it was dried overnight in an oven at 70-80 °C. The manure was ground and then passed through a 0.18 mm sieve. The cattle manure-derived biochar was produced by pyrolyzing cattle manure at 300 °C in oxygen-limited conditions using a modified method [16]. Briefly, the cattle manure powder (170 g) was tightly packed into a ceramic pot, covered with a fitted lid, and then pyrolyzed at 300 °C in a muffle furnace (KSW 12-11, Shanghai Laboratory Equipment Company Limited, China) for 6 h. Then, the biochar was washed with 0.1 M HCl, which was followed by ionized water flushing until it reached a neutral pH. It was subsequently oven-dried at

80 °C, gently milled, and passed a 0.18 mm sieve (80 mesh) prior to further analysis. 0.1 M HCl was used to wash the biochar to decrease the pH of biochar and to remove dissolved organic matter (DOM), some nutrients and carbonates. The biochar sample is referred to as CM300, where the suffix number represents the pyrolytic temperature.

**Characterization of biochar.** The ash content of biochar was measured by heating the sample at 800 °C for 4 h. Elemental (C, H, N) analyses were performed on a varioELcube elemental analyzer (Heraeus, Germany). The oxygen content was determined using the mass balance method. The atomic (O+N)/C and H/C ratios were calculated to evaluate the polarity and aromaticity of the biochar, respectively. Fourier transform infrared (FTIR) spectra were performed in the 4000-400  $\text{cm}^{-1}$  region on a Nexus870 (Nicolte, USA) with a resolution of 4.0  $\text{cm}^{-1}$  to identify the surface functional groups. The specific surface areas were measured by  $\text{N}_2$  adsorption at liquid nitrogen temperature using an ASAP-2010 surface area analyzer (Micromeritics ASAP 2010, USA). Specific surface areas were analyzed using the Brunauer-Emmett-Teller (BET) sorption methods. The X-ray diffraction (XRD) patterns for CM300 before and after sorption of cadmium were obtained on a X'Celerator diffractometer (PAN-alytical, Netherland) using Cu  $K\alpha$  radiation. The surface morphologies of the biochars before and after sorption of cadmium were examined using scanning electron microscope (SEM) imaging analysis with a JSM-5600LV scanning microscope (Japan). The surface elemental sample composition analysis of CM300 before and after sorption of cadmium was also determined simultaneously with SEM at the same surface locations using energy dispersive X-ray spectroscopy (EDS, INCA, Oxford Instrument). The XPS analysis was performed with an ESCALAB 250 xi system (Thermo Fisher Scientific, USA).

**Batch sorption experiments.** The sorption kinetics of Cd on CM300 were performed on a shaker (CHA-S Shaker, Jintan Danyang Instrumental Company, China) at 298 K by placing 0.1 g of CM300 in a glass bottle with 20 mL of Cd solution, which had initial concentration of 50 and 100 mg/L. The samples were subjected to filtration through a 0.45  $\mu\text{m}$  nylon membrane filter at appropriate time intervals. The Cd concentrations were determined using an atomic absorption

spectrophotometer (AA110/220, Varian Co. Ltd., America).

Equilibrium isotherm experiments were performed at 298 K for initial Cd concentrations ranging from 10 to 500 mg/L. The glass bottles were shaken for 24 h, and the necessary time for shaking was previously determined by the kinetic experiments.

To examine the effect of solution pH values on the Cd sorption onto CM300, the Cd sorption experiments were conducted with different aqueous solutions (pH = 2, 3, 4, 5, 6, 7, 8 and 9), and the solution pH value was adjusted with a NaOH or a HNO<sub>3</sub> (0.1 M) solution. The Cd concentration and temperature of sorption were fixed at 50 mg/L and 298 K, respectively. The effect of CM300 dosage on sorption process was examined by adding different amounts (0.1, 0.2, 0.3, 0.4, and 0.5 g) of CM300 into different glass bottles of which each contained 20 mL of a fixed initial concentration of Cd (100 mg/L). The bottles were then placed in the shaker at 150 rpm for 24 h at 298 K. To examine the effect of temperature on the Cd sorption onto CM300, the Cd sorption was conducted for 24 h at 25, 35, and 45 °C.

The effect of common coexisting cations were investigated by adding concentrations ranging from 0.01 to 0.2 mol/L of NaNO<sub>3</sub> and Ca(NO<sub>3</sub>)<sub>2</sub> to 100 mg/L Cd solutions in the glass bottles and then placing them in the shaker at 150 rpm for 24 h at 298 K. The amount of Cd that was absorbed from the aqueous solution was expressed as removal capacity per unit mass of biochar ( $q$ ) as:

$$q = \frac{(c_0 - c_e)V}{m} \quad (1)$$

where,  $c_0$  is the initial concentration of Cd in aqueous solution (mg/L),  $c_e$  is the equilibrium concentration of Cd in solution (mg/L),  $V$  is the batch volume (L) and  $m$  is the biochar mass (g). The percent of Cd removal efficiency ( $R$ ) from aqueous solution was then calculated from:

$$R(\%) = \frac{(c_0 - c_e)}{c_0} \times 100\% \quad (2)$$

## RESULTS AND DISCUSSION

**Biochar characterization.** Table 1 presents the elemental compositions and surface area of CM0 and CM300. The biochar yield was determined by the final mass without washing after pyrolysis by the initial quality. The yield of CM300

was 40.46%. The elemental composition on a dry-ash-free basis was 46.89% C, 3.49% H, 3.39% N and 46.23% O. The carbon content was higher in CM300 than in CM0, but there were high H and O contents in CM0. The elemental ratios of H/C and O/C can be used to determine the degree of aromaticity and polarity of the biochar sample. As shown in Table 1, the H/C and O/C ratios of CM300 were much lower than those in CM0. The results showed that the carbon chains in CM300 were extremely unsaturated, indicating that an aromatic structure was formed in CM300 due to the carbonization of CM0 at high temperature. The specific surface area (SSA) and total pore volume (TPV) of CM300 were 3.35 m<sup>2</sup>/g and 0.0184 cm<sup>3</sup>/g, respectively.

**TABLE 1**  
The element compositions and atomic ratios, SSA, and TPV of CM0 and CM300

Sample	CM0	CM300
yield (%)	/	40.64
C (%)	29.42	46.89
H (%)	4.06	3.49
N (%)	2.04	3.39
O (%)	64.48	46.23
H/C	1.66	0.89
O/C	1.64	0.74
(O+N)/C	1.69	0.81
Ash (%)	35.86	32.11
pH	/	4.87
SSA (m <sup>2</sup> /g)	-	3.35
TPV (cm <sup>3</sup> /g)	-	0.0184

**Sorption studies. (1) Sorption Kinetics.** The effect of contact time on the sorption of Cd is shown in Figure 1. Figure 1 indicates that the sorption of Cd on CM300 increased consistently with time and reached equilibrium at approximately 6 h. Different mathematical models such as pseudo-first-order, pseudo-second-order, Elovich and intra-particle diffusion models were used to describe the sorption kinetics of Cd on CM300. The equations for these models are listed below [19]:

$$\frac{dq_t}{dt} = k_1(q_e - q_t) \quad \text{pseudo-first-order} \quad (3)$$

$$\frac{dq_t}{dt} = k_2(q_e - q_t)^2 \quad \text{pseudo-second-order} \quad (4)$$

$$\frac{dq_t}{dt} = \alpha \exp(-\beta q_t) \quad \text{Elovich} \quad (5)$$

$$q_t = k_d t^{1/2} + C_i \quad \text{intra-particle diffusion} \quad (6)$$

where,  $q_t$  (mg/g) and  $q_e$  (mg/g) are the adsorbed amount of Cd at time  $t$  (h) and at

equilibrium, respectively,  $k_1$  ( $\text{h}^{-1}$ ),  $k_2$  ( $\text{g}/\text{mg}/\text{h}$ ), and  $k_d$  ( $\text{mg}/\text{g}/\text{h}^{-1/2}$ ) are sorption rate constants of the pseudo-first-order, pseudo-second-order, and intra-particle diffusion, respectively,  $\alpha$  ( $\text{mg}/\text{g}/\text{h}$ ) is the initial sorption rate,  $\beta$  ( $\text{g}/\text{mg}$ ) is the desorption constant, and  $C_1$  is the intercept reflecting the boundary layer thickness.

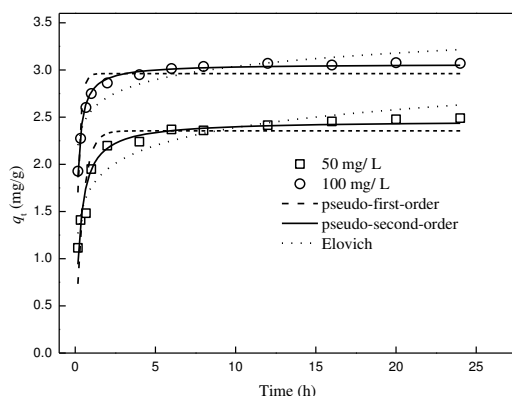


FIGURE 1

**Sorption kinetic data and modeling for Cd on CM300 with different initial concentrations**

Pseudo-first-order and pseudo-second-order models describe the kinetics of solid-solution system being based on mononuclear and binuclear sorption, respectively, with respect to adsorbent capacity. Elovich model is an empirical formula that considers the desorption [19]. The best fitting parameters of the sorption kinetics models are listed in Table 2. As shown, the coefficients  $R^2$  of the pseudo-second-order model were higher than those of the other two models, and the values of  $q_{\text{exp}}$  were closer to the theoretical values that were calculated by the pseudo-second-order model, indicating that the pseudo-second-order model was the most

suitable to describe the sorption kinetics of Cd on CM300. Hence, the present sorption process of Cd onto CM300 was chemisorptions involving rate determining step surface sorption.

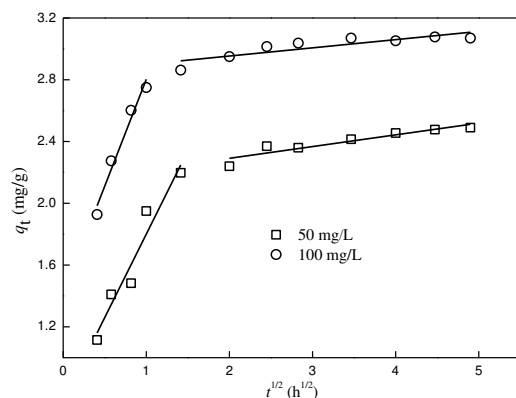
To understand the rate controlling process of Cd on CM300, the intra-particle diffusion model was used to fit the data (Table 3). The intra-particle diffusion model permits the determination of rate-limiting step in a sorption process [20]. The relationship between  $t^{1/2}$  and  $q_t$  is shown in Figure 2. The plots of  $q_t$  versus  $t^{1/2}$  should be linear if intra-particle diffusion is involved in the sorption process, and if the resulting straight line passes through the origin, then intra-particle diffusion is the rate-limiting step in the sorption process. Otherwise, the sorption process may involve some other sorption mechanisms along with intra-particle diffusion [21]. In this study, the resulting lines have a nonzero intercept in Figure 2, which indicates that the sorption process may be a complex natural process that includes both surface sorption and intra-particle diffusion [21]. The sorption data points were related by two straight lines for Cd during the sorption process. The first linear section of the data represents the occupation of readily-available sites on the biochar surface, and the second one may represent very slow diffusion of Cd from the surface sites into the inner pores. Similar results have been recorded for Cd sorption on different biochars [22]. The values of  $k_{d1}$  and  $C_1$  are show in Table 3. The values of  $k_{d1}$  are larger than those of  $k_{d2}$ , while values of  $C_1$  are less than those of  $C_2$ , which indicates that the whole sorption process is controlled by intra-particle diffusion of Cd in the inner pores of CM300.

TABLE 2  
Sorption kinetic parameters for Cd on CM300

$c_0$	pseudo-first-order			pseudo-second-order			Elovich		
	$q_m$	$k_1$	$R^2$	$q_m$	$k_2$	$R^2$	$\alpha$	$\beta$	$R^2$
50	2.3549	2.2398	0.8291	2.4628	1.5055	0.9485	1.7585	3.6483	0.9082
100	2.9617	5.1312	0.8204	3.0636	3.0369	0.9901	2.5681	4.9044	0.8471

TABLE 3  
The intra-particle diffusion kinetic parameters for Cd onto the CM300

$C_0$	$k_{d1}$	$C_1$	$R^2$	$k_{d2}$	$C_2$	$R^2$
50	1.0809	0.7195	0.9197	0.0759	2.1394	0.8572
100	1.3832	1.4198	0.9548	0.0531	2.8475	0.7144



**FIGURE 2**  
Intra-particle diffusion plots for Cd onto CM300 with different initial concentrations

(2) **Sorption isotherms.** Sorption isotherms play an important role in representing how the adsorbate molecules distribute between the solid and liquid phases under equilibrium state. In this study, four typical sorption isotherm models, the Langmuir, Freundlich, Langmuir-Freundlich, and Temkin equations [19] were used to measure the fitness of the experimental data:

Langmuir equation:

$$q_e = \frac{q_m K_L c_e}{1 + K_L c_e} \quad (7)$$

Freundlich equation:

$$q_e = K_F c_e^{1/n} \quad (8)$$

Langmuir-Freundlich equation:

$$q_e = \frac{q_m K_{LF} c_e^n}{1 + K_{LF} c_e^n} \quad (9)$$

Temkin equation:

$$q_e = A \ln K_t c_e \quad (10)$$

where  $q_e$  is the equilibrium sorption capacity of Cd on the adsorbent (mg/g),  $c_e$  is the equilibrium concentration of Cd in the aqueous solution (mg/L), and  $K_L$  is the Langmuir constant (L/mg).  $K_F$  (L/mg) and  $n$  (dimensionless) are the Freundlich isotherm constants,  $K_F$  is an indicator of the sorption capacity,  $n$  is the sorption intensity factor, and  $q_m$  is the maximum sorption capacity (mg/g).  $K_t$  is the equilibrium binding constant (L/mol) corresponding

to the maximum binding energy;  $A$  is a constant related to the adsorption heat and is equal to  $RT/B_t$ , and the constant  $B_t$  is the Temkin isotherm constant. The Langmuir model assumes monolayer sorption on the homogeneous surface with no interaction between the adsorbed molecules, while the other models are semi-empirical or empirical equations that are often used to represent heterogeneous sorption processes.

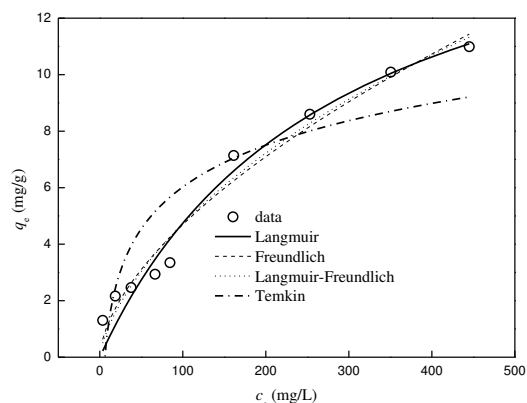


**FIGURE 3**  
Sorption isotherm data and modeling for Cd onto CM300

The sorption isotherms are shown in Figure 3 and all the parameter coefficients for the Langmuir, Freundlich, Langmuir-Freundlich, and Temkin models are presented in Table 4. Based on the  $R^2$  values, the sorption of Cd on CM300 at 298 K was well described by the Freundlich model. This suggests that the sorption of Cd on CM300 occurred via heterogeneous process. It can be calculated that the maximum theoretical sorption capacity of Cd on CM300 was approximately 18.12 mg/g from the Langmuir isotherm equation. Although the BET surface area of CM300 was very small (3.35 m<sup>2</sup>/g), its sorption capacity for Cd was much higher, indicating that physical sorption did not dominate the sorption of Cd on CM300. According to the Freundlich isotherm model, the  $n$  value (1.6768) of Cd sorption on CM300 was between 1 and 10, indicating that the sorption was favorable under the selected conditions [23].

**TABLE 4**  
Isotherm constants for Cd sorption on CM300

model	parameter 1	parameter 2	parameter 3	$R^2$
Langmuir	$K_L=0.0036$	$q_m=18.1189$	$R_L=0.3571-0.9653$	0.9631
Freundlich	$K_F=0.3011$	$n=1.6768$		0.9671
Langmuir-Freundlich	$K_{LF}=0.0045$	$q_m=46.7396$	$n=1.4301$	0.9624
Temkin	$A=2.1339$	$K_t=0.1684$		0.5670

**TABLE 5**  
**Thermodynamic parameters for Cd sorption on CM300**

$T$ (K)	$K_L$ (L/mol)	$\Delta G^0$ (kJ/mol)	$\Delta H^0$ (kJ/mol)	$\Delta S^0$ (J/mol/K)
298	399.51	-14.8413		
308	360.25	-15.0744	3.1669	60.0371
318	434.33	-16.0582		

To determine whether the sorption is favorable or not with the Langmuir type sorption process, “ $R_L$ ” is defined in Eq. (11):

$$R_L = \frac{1}{1 + K_L c_0} \quad (11)$$

The  $K_L$  denotes the Langmuir constant and  $c_0$  is the initial concentration. The  $R_L$  parameter is a separation factor and is indicator of the sorption [24]. There are four possibilities for the  $R_L$  value: (1) favorable sorption,  $0 < R_L < 1$ , (2) unfavorable sorption,  $R_L > 1$ , (3) linear sorption,  $R_L = 1$ , and (4) irreversible sorption,  $R_L = 0$ . The values of  $K_L$  and  $R_L$  for sorption of Cd on CM300 are listed in Table 4. In this study, the  $R_L$  values remain from 0.3571 to 0.9653 for Cd sorption on CM300, suggesting that the sorption process was favorable for CM300.

**(3) Thermodynamics of sorption.** The sorption capacity of Cd increased with increasing temperature (results are not shown), which indicates that the sorption process was endothermic and high temperature favors the sorption. The sorption isotherms of Cd that were obtained at 298, 308, and 318 K were used to determine the thermodynamic parameters. The standard Gibbs free energy change ( $\Delta G^0$ ), standard enthalpy change ( $\Delta H^0$ ), and standard entropy change ( $\Delta S^0$ ) were calculated from the following equations:

$$\Delta G^0 = -RT \ln K_L \quad (12)$$

$$\Delta G^0 = \Delta H^0 - T\Delta S^0 \quad (13)$$

$$\ln K_L = -\frac{\Delta H^0}{RT} + \frac{\Delta S^0}{R} \quad (14)$$

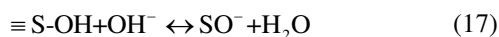
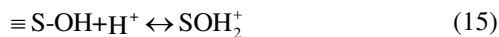
where  $K_L$  is the Langmuir constant when the concentration term is expressed in L/mol,  $R$  (8.314J/mol/K) is the universal gas constant and  $T$  (K) is the absolute temperature.  $\Delta H^0$  and  $\Delta S^0$  are obtained from the slope and intercept of the linear plots of  $\ln K_L$  versus  $1/T$ .

The thermodynamic parameters are shown in Table 5. The negative values for  $\Delta G^0$  indicate that the sorption performance of Cd on CM300 was spontaneous. Moreover, the decrease in the  $\Delta G^0$  values with increasing temperature shows that the sorption performance was favorable at higher

temperatures. Additionally, the values of  $\Delta G^0$  in the present study are within the ranges of -14.8313 to -16.0582 kJ/mol, indicating that the mechanism of Cd sorption onto CM300 was primarily physical sorption [25]. The positive values of  $\Delta H^0$  indicate that the sorption was endothermic, which revealed that the sorption process was more favorable at higher temperatures. The positive values of  $\Delta S^0$  indicate that the randomness at the solid and solution interface increased during the sorption process.

**(4) Effect of pH value of solution.** In the sorption process, the solution pH value is generally a vital parameter that affects the dissociation of functional groups and the surface charge on the adsorbent. Additionally, the solution pH value also influences the degree of speciation and ionization of metal ions in solution [26]. Thus, it is necessary to evaluate the optimum pH for the sorption process of Cd onto CM300. As shown in Figure 4, a higher solution pH (in the pH range from 2 to 8) is more favorable for the sorption of Cd onto CM300. Specifically, at pH 2-3, the removal efficiency was minimum and increased rapidly between pH 3 and 5. Under strongly acidic conditions, due to the existence of a high concentration of  $H^+$  ions in solution, the surface of CM300 was protonated and positively charged; hence the Cd ions cannot move toward the positively charged surface of CM300 due to the electrostatic repulsion. Therefore, less removal efficiency was observed at low solution pH values. When the solution pH value increased, the available sorption sites on CM300 become negatively charged. Thus, more Cd ions were removed with the increase in solution pH. The FTIR spectroscopic analysis shows that CM300 consists of surface hydroxyl groups (S-OH)<sub>n</sub> and these surface sorption sites are Lewis-acid type functional groups that are effective for Cd ions sorption. The S-OH groups on the surface of CM300 will attain negative or positive charges by the dissociation or association of protons [26]. The deprotonation and protonation reactions of the S-OH groups can be written as:





The result was further explained by the Cd speciation, which is pH dependent in aqueous solution. The dominant Cd species below a pH of 8 are  $\text{Cd}^{2+}$ ,  $\text{Cd}(\text{OH})^+$  and  $\text{Cd}(\text{OH})_2$ , one of which is the predominant ions ( $\text{M}^{2+}$ ) in aqueous solution, may undergo solvation, hydrolysis, and polymerization, as shown below [27]:

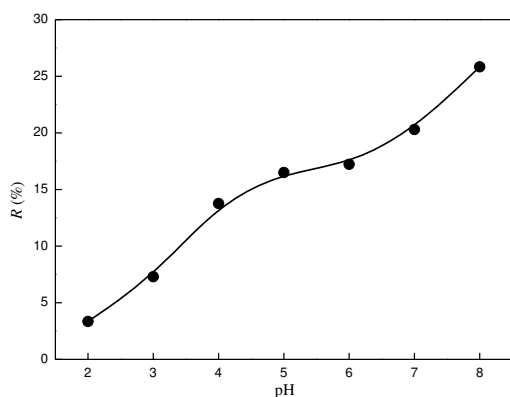
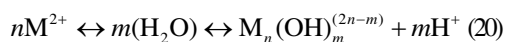
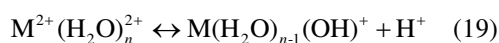
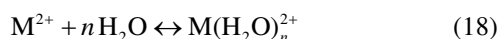


**FIGURE 4**  
Effect of solution pH values on sorption of Cd onto CM300

**(5) Effect of adsorbent dosage.** Adsorbent dosage is one of the parameters that significantly affect the sorption process in an aqueous solution, determining the adsorbate-adsorbent equilibrium of a system. This is an important parameter, because adsorbent dosage decides the capacity of an adsorbent for a given initial concentration of the adsorbate [28]. The effect of adsorbent dosage on the sorption Cd is shown in Figure 5. As the dosage of CM300 increased from 5.0 to 25.0 g/L, the amount of Cd adsorbed was doubled (1.53-3.25 mg/g) before the equilibrium was attained. The removal efficiency of Cd decreased from 38.15% to 16.26%. The number of available sites for the sorption of Cd is directly proportional to the amount of CM300 used in the measurement. Thus,

increasing the amount of CM300 could provide more number of active sites and, therefore, resulted in a linear increase in the number of Cd ions adsorbed by CM300 [29].

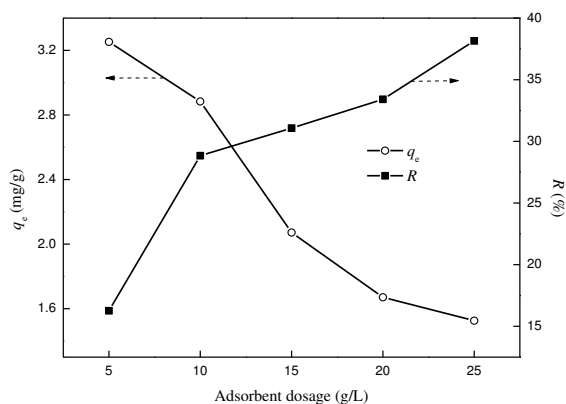


**FIGURE 5**  
Effect of adsorbent dosage on sorption of Cd onto CM300

**(6) Effect of ionic strength.** Electrolytes in solution play an important role in solute sorption because they can affect the electrostatic interactions between the adsorbent and the solute and the surface charges on the adsorbent. Moreover, the salt ions may compete with the solute for sorption on the adsorbent [30]. Thus, the effect of ionic strength was investigated by adding  $\text{NaNO}_3$  and  $\text{Ca}(\text{NO}_3)_2$  in the range of 0.01 to 0.2 mol/L at a 100 mg/L Cd concentration. The results are shown in Figure 6. The presence of electrolytes has a negative correlation with the sorption of Cd onto CM300. As the electrolytes concentration increased from 0 to 0.2 mol/L, the amount of Cd adsorbed decreased from 5.09 mg/g to 3.13 mg/g and 5.09 to 1.51 mg/g for  $\text{NaNO}_3$  and  $\text{Ca}(\text{NO}_3)_2$ , respectively. The negative influence of the ionic strength on the Cd sorption suggests the possibility of ion exchange mechanisms in the sorption process. As the ion exchange increases, the active sites on the surface of CM300 and the active concentration of Cd decrease, causing the interaction between the positive charge and the negative charge to become weak. Therefore, the sorption capacity for Cd decreases. It is theoretically expected that the effect of  $\text{Ca}^{2+}$  on the sorption would be more evident than the effect of  $\text{Na}^+$  at the same concentration. This is may be attributed to the larger positive charge number of  $\text{Ca}^{2+}$ , which inhibits the sorption of  $\text{Cd}^{2+}$  on the surface of CM300 particles due to the competitive sorption between the cationic  $\text{Cd}^{2+}$  and  $\text{Ca}^{2+}$  [31].

**Sorption mechanisms.** Scanning electron microscopy is generally used to investigate the morphological features and pore shapes of adsorbent materials. SEM (magnification 2000 $\times$ ) and EDS of the surface structures of the CM300 before and after sorption of cadmium are shown in Figure 7. A few pores can be found on the thin surface of CM300. The data indicate the presence of C, O, Si, Mg, Al, and Na on the surface of CM300, but Cd was not detected (Figure 7(a)). After sorption, Cd was present on the surface (Figure 7(b)).

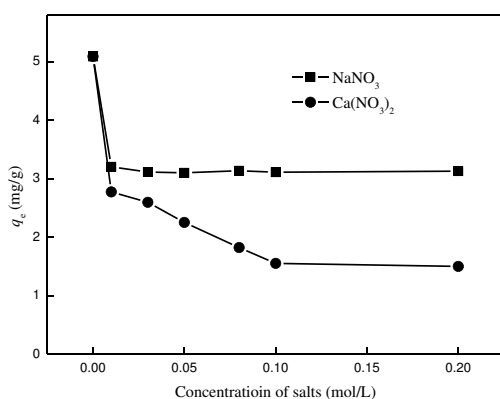


**FIGURE 6**  
Effect of ionic strength on sorption of Cd onto CM300

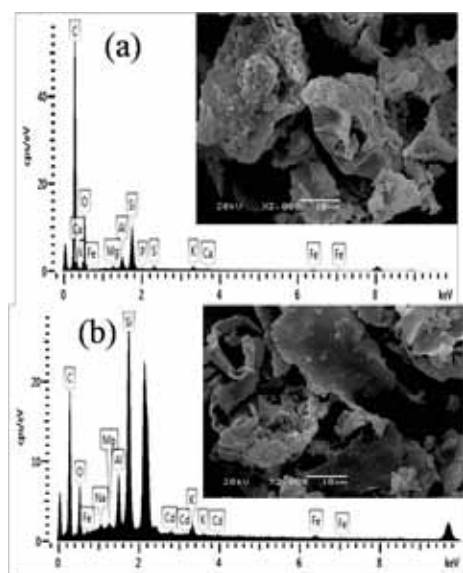


**FIGURE 7**  
SEM image and EDS spectra of before sorption CM300 (a) and after sorption CM300 (b) at 2000 $\times$

The corresponding EDS spectra of the focused SEM area shows large peaks for cadmium (Figure 7(b)), which demonstrates the presence of cadmium on the surfaces of the CM300 after sorption. This

strongly suggests that cadmium from the aqueous solution absorbed onto CM300 surfaces because the SEM-EDS analysis of the CM300 before sorption exhibited no cadmium or crystals of this type in the original biochar.

To determine the contribution of chemical precipitation for Cd sorption, the original and Cd-loaded CM300 were scanned by X-ray diffraction. The X-ray diffraction analyses of CM300 before and after sorption of cadmium are provided in Figure 8(a). The sharp strong peaks for CM300 indicated that CM300 was primarily composed of quartz. These large CM300 peaks are consistent with the highest Si and ash contents in CM300 (Table 1 and Figure 7). In this study, XRD analysis did not detect any crystalline structures in either the pre- or post-sorption biochar. This indicated that the surface precipitation may not be the primary mechanism for Cd sorption by CM300.

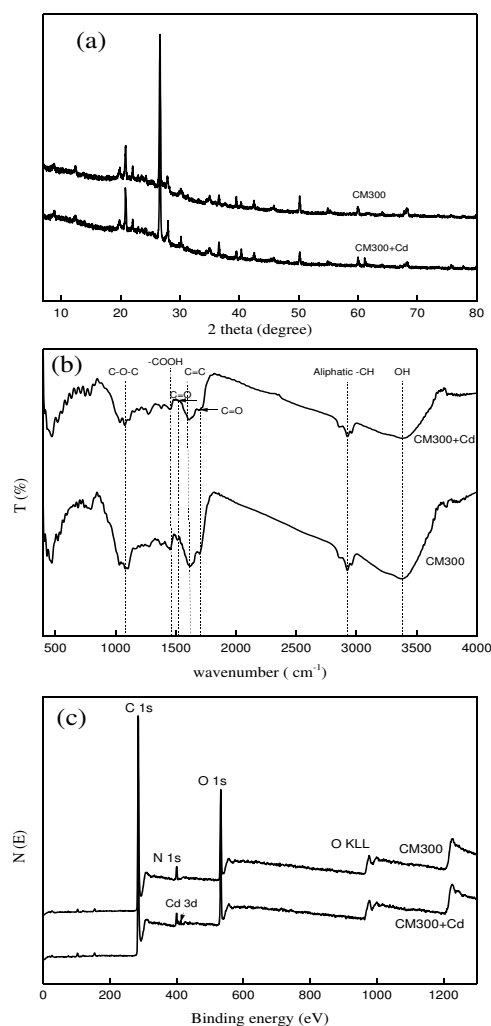


**FIGURE 8**  
(a) XRD spectra, (b) FTIR spectra, and (c) XPS analysis of pre- and post-sorption CM300

The CM300 FTIR spectra displayed a number of peaks that indicate its complex nature (Figure 8(b)). The broad peak at  $3394\text{ cm}^{-1}$  represents the bonded hydroxyl of the phenol group. The peak at approximately  $2923\text{ cm}^{-1}$  is indicative of aliphatic  $-\text{CH}$  stretching. The peaks at  $1702$  and  $1515\text{ cm}^{-1}$  are related to the  $\text{C}=\text{O}$  stretching of the carboxylic group [32]. The peaks at  $1618$  and  $1103\text{ cm}^{-1}$  corresponded to the  $\text{C}=\text{C}$  stretch and the  $\text{C}-\text{O}-\text{C}$  bonds associated with cellulose, hemicelluloses and lignin in biomass, respectively.

The FTIR spectra of CM300 before and after sorption of cadmium show some significant differences, indicating that physical and/or chemical changes occur due to the Cd sorption. Cd sorption changed the peaks of the functional groups in CM300. The disappearance of the carboxyl stretching bands at  $1515\text{ cm}^{-1}$  and  $1702\text{ cm}^{-1}$  was noted in the Cd-loaded CM300 (Figure 8(b)), which is typical of the interaction of a carboxyl group with metal ions [32]. Furthermore, the peak at  $3394\text{ cm}^{-1}$  that is due to bonded a hydroxyl group decreased, indicating the involvement of hydroxyl groups in the Cd sorption. Other studies have shown that the sorption of heavy metals by biochars is directly correlated with the amount of oxygen-containing functional groups [33, 34]. In the present study, the Cd sorption by CM300 was attributed mainly to the oxygen-containing functional groups.

The XPS analysis of Cd-loaded CM300 provided better understanding of the Cd sorption mechanism. Compared with the CM300 spectra, the XPS spectra of CM300+Cd included the Cd peaks, indicating the immobilization of Cd on the biochar surface (Figure 8(c)). The XPS and FTIR data indicated that functional groups, such as carbonyl groups and hydroxyl, were responsible for the Cd sorption by CM300.

## CONCLUSIONS

The sorption of Cd using the biochar that was pyrolytically produced from cattle manure was investigated. The solution pH value significantly affected the sorption characteristics of Cd on the biochar. The sorption experiments indicated that the pseudo-second-order model fit the kinetic data well, while the intra-particle diffusion was not the only rate controlling step of the sorption process. The sorption equilibrium data were better simulated by the Freundlich model. The sorption is more spontaneous at higher temperatures, and it tends to

be endothermic and indicates that randomness at the solid/solution interface increased in the internal structure of sorption. The sorption of cadmium can be attributed to the complexation of Cd with oxygen-containing functional group. Utilization of the biochar derived from biomass waste can benefit the overall process of waste thermal processing. Thus, biochar that is pyrolytically produced from cattle manure waste is a green cost-effective sorbent for the sorption of Cd from aqueous solutions.

## ACKNOWLEDGEMENTS

This study was supported by the National Natural Science Foundation of China (21167007, 21467013), Young Scholars Science Foundation of Lanzhou Jiaotong University (2013015) and Specialized Research Fund for the Doctoral Program of Higher Education of China (20136204110003).

## REFERENCES

- [1] Wang N.-X., Zhang X.-Y., Wu J., Xiao L., Yin Y., Miao A.-J., Ji R., Yang L.-Y. (2012) Effects of microcystin-LR on the metal bioaccumulation and toxicity in *Chlamydomonas reinhardtii*, *Water Res.* 46, 369-377.
- [2] Inyang M., Gao B., Yao Y., Xue Y., Zimmerman A.R., Pullammanappallil P., Cao X. (2012) Removal of heavy metals from aqueous solution by biochars derived from anaerobically digested biomass, *Bioresource Technol.* 110, 50-56.
- [3] Muehe E.M., Adaktylou I.J., Obst M., Zeitvogel F., Behrens S., Planer-Friedrich B., Kraemer U., Kappler A. (2013) Organic Carbon and Reducing Conditions Lead to Cadmium Immobilization by Secondary Fe Mineral Formation in a pH-Neutral Soil, *Environ Sci Technol.* 47, 13430-13439.
- [4] Mohan D., Singh K.P. (2002) Single-and multi-component adsorption of cadmium and zinc using activated carbon derived from bagasse—an agricultural waste, *Water Res.* 36, 2304-2318.
- [5] Li C., Zhong H., Wang S., Xue J., Zhang Z. (2015) A novel conversion process for waste residue: Synthesis of zeolite from electrolytic

- manganese residue and its application to the removal of heavy metals, *Colloids & Surfaces A Physicochemical & Engineering Aspects*. 470, 258–267.
- [6] Zuo Y., Chen G., Zeng G., Li Z., Yan M., Chen A., Guo Z., Huang Z., Tan Q. (2015) Transport, fate, and stimulating impact of silver nanoparticles on the removal of Cd(II) by *Phanerochaete chrysosporium* in aqueous solutions, *J Hazard Mater*. 285, 236-244.
- [7] de los Ríos A.P., Hernández-Fernández F.J., Alguacil F.J., Lozano L.J., Ginestá A., García-Díaz I., Sánchez-Segado S., López F.A., Godínez C. (2012) On the use of imidazolium and ammonium-based ionic liquids as green solvents for the selective recovery of Zn(II), Cd(II), Cu(II) and Fe(III) from hydrochloride aqueous solutions, *Sep Purif Technol*. 97, 150-157.
- [8] Ennaassia E., El Kacemi K., Kossir A., Cote G. (2002) Study of the removal of Cd(II) from phosphoric acid solutions by precipitation of CdS with Na<sub>2</sub>S, *Hydrometallurgy*. 64, 101-109.
- [9] Bessbousse H., Rhlalou T., Verchère J.F., Lebrun L. (2008) Removal of heavy metal ions from aqueous solutions by filtration with a novel complexing membrane containing poly(ethyleneimine) in a poly(vinyl alcohol) matrix, *J Membrane Sci*. 307, 249-259.
- [10] Butter T.J., Evison L.M., Hancock I.C., Holland F.S., Matis K.A., Philipson A., Sheikh A.I., Zouboulis A.I. (1998) The removal and recovery of cadmium from dilute aqueous solutions by biosorption and electrolysis at laboratory scale, *Water Res*. 32, 400-406.
- [11] Mi L., Qiang L., Guo L., Zhang Y., Lou Z., Yang W., Qian G. (2012) Cu(II) removal from aqueous solution by *Spartina alterniflora* derived biochar, *Bioresource Technol*. 141, 83–88.
- [12] Zhao B., Shi X., Ma F. (2016) Adsorption of Cr(VI) onto biochars derived from typical vegetable oil crop biomasses originating in loess areas, *Fresen. Environ. Bull*. 25, 588-601.
- [13] Uchimiya M., Lima I.M., Thomas Klasson K., Chang S., Wartelle L.H., Rodgers J.E. (2010) Immobilization of heavy metal ions (CuII, CdII, NiII, and PbII) by broiler litter-derived biochars in water and soil, *J Agr Food Chem*. 58, 5538-5544.
- [14] Cao X., Ma L., Gao B., Harris W. (2009) Dairy-manure derived biochar effectively sorbs lead and atrazine, *Environ Sci Technol*. 43, 3285-3291.
- [15] Mohan D., Sarswat A., Ok Y.S., Pittman Jr C.U. (2014) Organic and inorganic contaminants removal from water with biochar, a renewable, low cost and sustainable adsorbent—a critical review, *Bioresource Technol*. 160, 191-202.
- [16] Chen B., Zhou D., Zhu L. (2008) Transitional adsorption and partition of nonpolar and polar aromatic contaminants by biochars of pine needles with different pyrolytic temperatures, *Environ Sci Technol*. 42, 5137-5143.
- [17] Jiang S., Huang L., Nguyen T.A.H., Yong S.O., Rudolph V., Yang H., Zhang D. (2015) Copper and zinc adsorption by softwood and hardwood biochars under elevated sulphate-induced salinity and acidic pH conditions, *Chemosphere*. 142, 64–71.
- [18] Tan C., Zhou Z., Rong H., Meng R., Wang H., Lu W. (2015) Adsorption of cadmium by biochar derived from municipal sewage sludge: Impact factors and adsorption mechanism, *Chemosphere*. 134, 286–293.
- [19] Yao Y., Gao B., Chen J., Yang L. (2013) Engineered biochar reclaiming phosphate from aqueous solutions: mechanisms and potential application as a slow-release fertilizer, *Environ Sci Technol*. 47, 8700-8708.
- [20] Cobas M., Ferreira L., Sanromán M., Pazos M. (2014) Assessment of sepiolite as a low-cost adsorbent for phenanthrene and pyrene removal: Kinetic and equilibrium studies, *Ecol Eng*. 70, 287-294.
- [21] Kolodynska D., Wnetrzak R., Leahy J., Hayes M., Kwapinski W., Hubicki Z. (2012) Kinetic and adsorptive characterization of biochar in metal ions removal, *Chem Eng J*. 197, 295-305.
- [22] Cui X., Hao H., Zhang C., He Z., Yang X. (2016) Capacity and mechanisms of ammonium and cadmium sorption on different wetland-plant derived biochars, *Sci Total Environ*. 539, 566-575.
- [23] Pan N., Deng J., Guan D., Jin Y., Xia C. (2013) Adsorption characteristics of Th(IV) ions on reduced graphene oxide from aqueous solutions, *Appl Surf Sci*. 287, 478-483.
- [24] Gupta V.K., Mittal A., Malviya A., Mittal J. (2009) Adsorption of carmoisine A from wastewater using waste materials—bottom ash and deoiled soya, *J Colloid Interface Sci*. 335, 24-33.
- [25] Zhu X., Liu Y., Qian F., Zhou C., Zhang S., Chen J. (2014) Preparation of magnetic porous



- carbon from waste hydrochar by simultaneous activation and magnetization for tetracycline removal, *Bioresource Technol.* 154, 209-214.
- [26] Reddy D.H.K., Lee S.-M. (2014) Magnetic biochar composite: Facile synthesis, characterization, and application for heavy metal removal, *Colloids and Surfaces A: Physicochemical and Engineering Aspects.* 454, 96-103.
- [27] Mohan D., Kumar H., Sarswat A., Alexandre-Franco M., Pittman C.U. (2014) Cadmium and lead remediation using magnetic oak wood and oak bark fast pyrolysis bio-chars, *Chem Eng J.* 236, 513-528.
- [28] Pelleria F.-M., Giannis A., Kalderis D., Anastasiadou K., Stegmann R., Wang J.-Y., Gidarakos E. (2012) Adsorption of Cu (II) ions from aqueous solutions on biochars prepared from agricultural by-products, *J Environ Manage.* 96, 35-42.
- [29] Anwar J., Shafique U., Salman M., Dar A., Anwar S. (2010) Removal of Pb (II) and Cd (II) from water by adsorption on peels of banana, *Bioresource Technol.* 101, 1752-1755.
- [30] Karimaian K.A., Amrane A., Kazemian H., Panahi R., Zarrabi M. (2013) Retention of phosphorous ions on natural and engineered waste pumice: Characterization, equilibrium, competing ions, regeneration, kinetic, equilibrium and thermodynamic study, *Appl Surf Sci.* 284, 419-431.
- [31] Sharma A., Lee B.-K. (2014) Cd (II) removal and recovery enhancement by using acrylamide-titanium nanocomposite as an adsorbent, *Appl Surf Sci.* 313, 624-632.
- [32] Elangovan R., Philip L., Chandraraj K. (2008) Biosorption of hexavalent and trivalent chromium by palm flower (*Borassus aethiopum*), *Chem Eng J.* 141, 99-111.
- [33] Uchimiya M., Chang S., Klasson K.T. (2011) Screening biochars for heavy metal retention in soil: Role of oxygen functional groups, *J Hazard Mater.* 190, 432-441.
- [34] Uchimiya M., Wartelle L.H., Klasson K.T., Fortier C.A., Lima I.M. (2011) Influence of pyrolysis temperature on biochar property and function as a heavy metal sorbent in soil, *J Agr Food Chem.* 59, 2501-2510.

---

**Received:** 12.01.2016

**Accepted:** 26.09.2016

---

#### **CORRESPONDING AUTHOR**

---

**Baowei Zhao**

School of Environmental and Municipal Engineering  
Lanzhou Jiaotong University  
88 West Anning Rd.  
Lanzhou 730070 - P. R. CHINA

e-mail: zhbw2001@sina.com  
baowei.zhao@yahoo.com

# USING DIATOMS IN WATER QUALITY ASSESSMENT IN THE ANDIK STREAM (ISPARTA-TURKEY)

Hasan Kalyoncu<sup>1,\*</sup>, Hatice Dayioglu<sup>1</sup>, Fusun Kilcik<sup>2</sup>

<sup>1</sup> Süleyman Demirel University, Faculty of Science and Art, Department of Biology, Isparta, Turkey

<sup>2</sup> Süleyman Demirel University, Water Institute, Isparta, Turkey

## ABSTRACT

In this study, water and epilithic diatom samples were collected from 6 stations selected between July 2010- June 2011 along the Andik Stream. The most dominant genus in station 1 was *Navicula* (36,42%), in station 2 *Navicula* (26,86%), in station 3 *Ulnaria* (24,98%), in station 4 *Navicula* (32,6%), in station 5 *Cocconeis* (15,41%), in station 6 *Nitzschia* (55,51%) at the Andik Stream. At the first three stations and station 5, the most dominant species was *Ulnaria ulna* (in station 1 26,21%, station 2 25,93%, station 3 24,98%, station 5 13,73%), in station 4 *Achnanthes minutissima* Brebisson (22,87%) and in station 6 *Nitzschia palea* (Kützing) W.Smith (48,63%). According to Physicochemical parameters, the first five stations were determined as oligosaprop and station six as betamesosaprop. Also, the water quality of Andik stream was determined according to diatom taxa by using OMNIDIA Software Program. Results show that the indices have quite low correlation with the chemical variables and that GDI seems to be the best while IDAP seems to be the worst for our study. Besides, the pollution in station 6 has increased according to all indices applied. Although GDI yields good results, more work is needed to support this.

## KEYWORDS:

Diatom Indices, Water Quality, Andik Stream, OMNIDIA, Turkey.

## INTRODUCTION

The use of biological data on water quality assessments has been increasing in recent years and in these studies; fishes [1], macrophytes [2], algae [3, 4] and macro-invertebrates [5] have been used. However, frequently used organisms are particularly macro-invertebrates [6] and diatoms [4,7]. Diatom indices have been used both in Europe and the remaining of the world. In South America [8, 9], Africa [10] and Asia [11], these indices still have been used. Most of the countries, use these developed indices on their streams; as the

others modified the indices according to their own ecological status. These indices are based on Saprobic Index that suggested by Kolkwitz and Marsson [12] in 1900s. Saprobic index was developed by many researchers [13-15] in time; and variations were occurred [16, 17] due to calculations within the indices and quality class differentials. In Turkey; the first study that Saprobic index applied, was in Isparta and Ağlasun Streams [18]. As in 2000s; the indices using in Europe and the world, were applied in Turkey to various streams [19-22]. Despite all these applications; in Turkey, indices are still a new study area. In recent years, indices included in OMNIDIA program, have been started to use [23, 24]. There are limited numbers of studies in Turkey; and limited numbers of researchers have been studying on the subject. In this study; the indices included in OMNIDIA were applied on Andik Stream and the results were evaluated.

## MATERIALS AND METHODS

**Study Area.** Andik Stream which takes place in Aksu Stream basin and forms Aksu Stream; is one of the tributaries of Isparta Stream that feeds dam lakes of Karacaören I and II. It stems from the basin around Gölcük Lake; that is 1300 m high from sea level and approximately 5 km southwest of Isparta and originates from a crater filled with water; and it passes above Dere Street and flow into Isparta Stream. Significant part of the tap water of Isparta is ensured from springs of Andik Stream.

Andik Stream originates from two different springs. On the streams, there are two waterfalls formed by geological structure. One of the waterfalls is named as Bezirgan Waterfall and takes place on Dere Street. Following of the waterfall, the stream flows on artificially formed stream bed and flows along Isparta City which this part named as Çay Boyu and then it joins Isparta Stream. Andik Stream originates by joining of two different springs. 1<sup>st</sup> and 2<sup>nd</sup> stations are on this two different springs, 3<sup>rd</sup> station is on main branch to detect differences after the mixture of these springs. 4<sup>th</sup> station is on following of the first waterfall and 5<sup>th</sup> station is on a site right before the second waterfall.

**TABLE 1**  
Quality classes and mean values of physicochemical parameters according to stations

Parameters	1.station	2.station	3.station	4.station	5.station	6.station
DO mg/L	6,78	6,38	8,06	8,15	7,05	7,1
Temperature C <sup>0</sup>	15,16	15,36	11,45	11,1	14,3	18,95
pH	8,12	8,04	8,6	8,6	8,19	7,2
EC $\mu$ S/cm	298	301	306	388	277	326
NO <sub>3</sub> -N mg/L	1,7	1,05	BDL	BDL	BDL	BDL
NO <sub>2</sub> -N mg/L	BDL	BDL	BDL	BDL	BDL	BDL
NH <sub>4</sub> - N mg/L	0,09	0,06	0,09	0,05	0,05	0,06
PO <sub>4</sub> - P mg/L	0,12	0,09	0,2	0,09	0,05	0,13
Cl mg/L	4,71	3,07	3,23	3,6	2,6	2,6
BOD <sub>5</sub> mg/L	2,18	2,19	1,26	1,9	2,93	3,58

6<sup>th</sup> station is on a branch where Andık Stream joins Isparta Stream. Locations of the stations were mapped in arcGIS 10, CBS program (Figure 1).

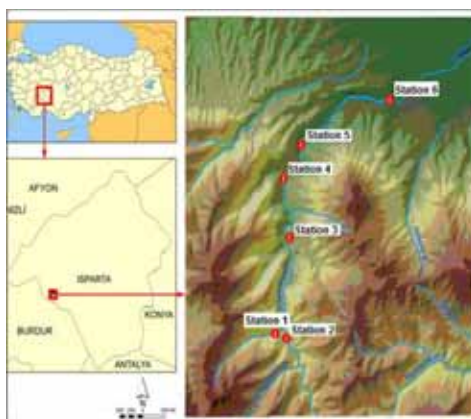


**FIGURE 1**

Map of the stations and Andık Stream that mapped in ArcGIS 3D Analysis software

**Environmental Variables.** Water samples were taken monthly between July 2010 – June 2011 from determined stations to make physicochemical evaluations every month. Samples from all stations were taken between in 15<sup>th</sup>-20<sup>th</sup> of every month. Samples were taken to 1 Lt plastic bottles from the points which represent water quality at the best level. Water temperature (°C): with Testo 915-1 brand oxygen-meter, pH values: with WTW pH 330i brand pH-meter, Dissolved oxygen (mg O<sub>2</sub> L<sup>-1</sup>) : with WTW oxi 340 brand oximeter, Electrical conductivity ( $\mu$ S cm<sup>-1</sup>): with WTW cond.330 brand; were measured on site. The amount of Chloride ion (Cl<sup>-</sup> mg L<sup>-1</sup>): with Spectrophotometric method and Merck Nova 60-14897, Nitrite Nitrogen (NO<sub>2</sub>-N mg L<sup>-1</sup>): with Spectrophotometric method and Merck Nova 60-14776, Nitrate Nitrogen (NO<sub>3</sub>-N mg L<sup>-1</sup>) : with Spectrophotometric method and Merck Nova 60-09713, Ammonium Nitrogen (NH<sub>4</sub>-N mg L<sup>-1</sup>): with Spectrophotometric method and Merck Nova 60-14752, Orthophosphate ions (PO<sub>4</sub>-P mg L<sup>-1</sup>): with Spectrophotometric method and Merck

Nova 60-14543 kits were used for measuring. Biochemical Oxygen Demand (BOI<sub>5</sub> mgO<sub>2</sub> L<sup>-1</sup>): was measured with oxygen-meter during the time on site, by incubating the samples at 20°C in the dark for 5 days; by using glass bottles with sockets. All of the laboratory measurements were performed at Süleyman Demirel University, Research and Application Center for Geothermal Energy, Groundwater and Mineral Resources.

**Biological Elements.** Epilithic diatom samples were taken from the surface of stones in different sizes which generates an area of approximately 25 cm<sup>2</sup> in total; by scratching with a box cutter or brushing with a toothbrush [25]. Samples, that collected into 100 ml glass jars and brought back to the laboratory and fixated in formaldehyde, were kept for later examination. For identifications of diatoms, equal volumes of sulfuric acid and nitric acid were added in a part of the collected diatom samples and boiled for 15 minutes at 120<sup>0</sup> C in fume cupboard. Frustules (diatom shells), that separated from organic matter by this method, were neutralized by washing with distilled water. 10x100 magnification binocular research microscope was used for examination of the samples and Krammer and Lange-Bertalot [26-29] and Cox [30] were used for identification.

Neutralized frustules were put into small glass bottles for examination. A drop from this suspension that put onto a slide, was left to dry. A drop of canada balsam was dripped onto dried frustules and covered with coverglass and left to dry, after borders of the slide cleaned with alcohol. Prepared slides were examined by 10x100 magnification binocular research microscope. Diatom samples, both after the washing procedure and in alive prepareate, were counted. In every prepareate, there were at least 300 diatom frustules and countings were avaraged after the counting repeated 3 times.

Indices were calculated by entering the counted diatom species to OMNIDIA 5.3 [31]. Calculated indices were: The Eutrophication/Pollution Index-Diatom based (EPI-

**TABLE 2**  
**Identified organisms and distribution according to stations**

Diatom Taxa	STATIONS					
	1	2	3	4	5	6
<i>Melosira varians</i> C.Agardh	+	+	+		+	+
<i>Diatoma hyemalis</i> (Roth) Heiberg	+	+	+		+	
<i>D. mesodon</i> (Ehrenberg) Kützing	+	+	+	+	+	
<i>D. moniliformis</i> Kützing						+
<i>D. vulgaris</i> Bory	+	+		+		+
<i>Ulnaria ulna</i> (Nitzsch) P.Compère	+	+	+	+	+	+
<i>Ulnaria ulna</i> var. <i>acus</i> (Kützing) Lange-Bertalot					+	
<i>Meridion circulare</i> (Greville) C.Agardh	+	+	+	+	+	+
<i>Achnanthes lanceolata</i> Brebisson	+	+			+	+
<i>A. minutissima</i> Kützing	+	+	+	+	+	+
<i>Cocconeis pediculus</i> Ehrenberg	+	+	+	+	+	+
<i>C. placentula</i> Ehrenberg	+	+	+	+	+	+
<i>C. placentula</i> var. <i>lineata</i> (Ehrenberg) Cleve	+				+	+
<i>Anomoeoneis</i> sp.		+				
<i>Cymbella affinis</i> Kützing	+	+				+
<i>C. cymbiformis</i> C.Agardh	+	+				
<i>C. delicatula</i> Kützing				+		+
<i>C. helvetica</i> Kützing		+				
<i>C. microcephala</i> Grunow	+		+			+
<i>C. minuta</i> Hilse	+	+	+	+	+	+
<i>Gomphonema angustum</i> C. A. Agardh	+	+				
<i>G. hastatum</i> (Wislouch) Lange-Bertalot & Reichardt						+
<i>G. minutum</i> C. A. Agardh				+	+	+
<i>G. micropus</i> Kützing	+	+	+		+	
<i>G. olivaceum</i> (Hornemann) Brebisson	+		+	+	+	+
<i>G. olivaceum</i> var. <i>minutissimum</i> Hustedt		+		+		+
<i>G. parvulum</i> Kützing	+	+		+	+	+
<i>G. truncatum</i> Ehrenberg	+	+		+	+	+
<i>Navicula accomoda</i> Hustedt		+			+	
<i>N. angusta</i> Grunow	+			+		
<i>N. cincta</i> (Ehrenberg) Rolfs in Pritchard	+	+			+	
<i>N. cryptocephala</i> Kützing	+	+	+	+	+	
<i>N. cryptotenella</i> Lange-Bertalot				+		
<i>N. gregaria</i> Dankin					+	+
<i>N. lanceolata</i> (C.Agardh) Kützing	+		+	+	+	
<i>N. longicephala</i> Hustedt	+	+				
<i>N. menisculus</i> Schumann	+	+	+	+	+	+
<i>N. protracta</i> Kützing						+
<i>N. radiosa</i> Kützing	+	+	+	+	+	+
<i>N. rhyncocephala</i> Kützing	+	+	+	+	+	+
<i>N. reinhardtii</i> Grunow	+	+	+	+	+	+
<i>N. subminuscula</i> Manguin	+	+	+	+	+	+
<i>N. subrhyncocephala</i> Hustedt				+		+
<i>N. subtilissima</i> Cleve			+			
<i>N. tripunctata</i> (O. F. Müller) Bory	+				+	
<i>N. veneta</i> Kützing	+	+	+	+	+	+
<i>Pinnularia gibba</i> var. <i>parva</i> (Ehrenberg) Grunow	+			+		+
<i>P. microstauron</i> (Ehrenberg) Cleve	+					
<i>P. viridis</i> (Nitzsch) Ehrenberg	+		+	+	+	
<i>Amphora ovalis</i> (Kützing) Kützing	+	+	+	+	+	+
<i>A. veneta</i> Kützing						+
<i>Nitzschia acicularis</i> (Kützing) W. Smith			+	+	+	
<i>N. amphibia</i> Grunow		+	+			
<i>N. brevissima</i> Grunow in van Heurck					+	
<i>N. dissipata</i> (Kützing) Grunow	+			+		
<i>N. gracilis</i> Hantzsch		+				
<i>N. frustulum</i> (Kützing) Grunow in Cleve & Grunow	+		+	+	+	+
<i>N. hantzschiana</i> Robenhorst		+				
<i>N. palea</i> (Kützing) W.Smith	+	+	+	+	+	+
<i>N. recta</i> Hantzsch ex Rabenhorst		+	+	+		+
<i>N. sigmoidea</i> (Nitzsch) Ehrenberg		+			+	+
<i>N. sociabilis</i> Hustedt			+			
<i>N. solita</i> Hustedt	+		+	+		+
<i>N. vermicularis</i> (Kützing) Hantzsch			+			
<i>Epithemia adnata</i> (Kützing) Robenhorst					+	+
<i>E. argus</i> Kützing	+	+	+	+	+	+
<i>Rhopalodia gibba</i> (Ehrenberg) O. Müller	+	+		+	+	+
<i>Surirella brebissonii</i> Krammer ve Lange-Bertalot	+	+	+	+	+	
<i>Surirella rabusta</i> Ehrenberg	+	+	+	+	+	
<i>S. ovalis</i> Brebisson		+		+	+	



D), Biological Diatom Index (BDI), Schiefele & Schreiner Index (SHE), The Saprobic Index (SID), Trophic Index (TID), Watanabe Index (WAT), Specific Pollution Sensitivity Index (SPI), Sladeczek Index (SLA), Descy's Pollution Index (DESCY), Leclercq (IDSE), Generic Diatom Index (GDI), European Economic Community Index (CEC), Trophic Diatom Index (TDI), Pampean Diatom Index (IDP), Artois – Picardie Diatom Index (IDAP), LOBO Index (LOBO), Hurlimann Suisse Index (DI-CH). Indices except CEC, SHE, TDI and WAT; are using the formula developed by Zelinka and Marvan [17] SPSS 13.0 [32] was used for Pearson Correlation and Multivariate Regression analysis.

## RESULTS

In this study on Andık Stream, increasing or decreasing of physicochemical values between stations on a regular basis could not be identified. Only among pH values; 6<sup>th</sup> station, according to mean value, approaches to neutral while other stations are at alkaline condition. The highest average temperature was determined at 6<sup>th</sup> station, while temperature values were changing by depending on seasonal conditions. Nitrate nitrogen at 3<sup>rd</sup>, 4<sup>th</sup>, 5<sup>th</sup> and 6<sup>th</sup> stations and Nitrite nitrogen at all stations were determined as a value below detection limit (BDL). The amount of Cl<sup>-</sup> was low at all stations and the highest average value of both BOD<sub>5</sub> and PO<sub>4</sub>-P, were determined at 6<sup>th</sup> station (Table 1).

Epilithic diatoms of Andık stream were studied by monthly taken specimens between July 2010 - June 2011. As a result; 17 genus of epilithic diatoms and 70 taxa under these genus were identified. *Navicula* (18) which had the highest number of taxa, was respectively followed by *Nitzschia* (13), *Gomphonema* (8), *Cymbella* (6), *Diatoma* (4), *Cocconeis* (3), *Surirella* (3), *Pinnularia* (3), *Ulnaria* (2), *Achnanthes* (2), *Amphora* (2), *Epithemia* (2), *Melosiria* (1), *Meridion* (1), *Anomoeoneis* (1) and *Rhopalodia* (1) (Table 2).

With dissolved oxygen between DESCY, IDSE, GDI, CEE, IPS, IBD, EPI-D and IPD at level of  $p < 0,05$ ; with NH<sub>4</sub>-N, between DESCY and LOBO at level of  $p < 0,01$ , between IPS, SID and TID at level of 0,05 and with Cl<sup>-</sup> between DESCY, GDI (negative), IPS, LOBO, SID and TID (positive) at level of  $p < 0,05$ ; significant correlation was determined. The highest significant correlation was determined with EPI-D, while there were no correlation with temperature between SLA, LOBO, SID and TDI. With pH and between IDAP, SLA and TID there were not a correlation at significant level while the highest correlation level was determined with GDI (Table 4). While there were not a determined correlation with electrical conductivity between SLA, DESCY, WAT, CEE, IDAP, IDP, LOBO and TID; the highest significant correlation was with GDI. With all indices and between NO<sub>3</sub>-N, PO<sub>4</sub>-P and BOD<sub>5</sub> there were no correlation at significant level was determined (Table 3).

**TABLE 3**  
Relation between diatom indices and physicochemical parameters according to Pearson correlation analysis (n=66)

	DO	°C	pH	Conductivity	NO <sub>3</sub> -N	NH <sub>4</sub> -N	PO <sub>4</sub> -P	Cl	BOI <sub>5</sub>
SLA	-0,055	0,089	0,224	0,239	-0,026	-0,101	0,13	-0,028	0,074
DESCY	,255*	-,304*	-,606**	-0,188	-0,055	-,368**	-0,059	-,296*	0,082
IDSE	,257*	-,357**	-,490**	-,244*	-0,049	-0,161	-0,107	-0,148	-0,019
SHE	0,219	-,281*	-,680**	-,290*	0,065	-0,046	0,078	-0,118	-0,179
WAT	0,241	-,284*	-,556**	-0,225	-0,043	-0,17	-0,007	-0,135	-0,067
TDI	-0,199	,361**	,341**	,264*	0,108	0,022	-0,089	-0,012	0,199
GDI	,306*	-,328**	-,759**	-,377**	-0,002	-0,183	0,103	-,299*	-0,07
CEE	,289*	-0,157	-,393**	-0,24	-0,111	-0,182	-0,005	-0,21	0,154
IPS	,272*	-,331**	-,715**	-,292*	-0,027	-,270*	-0,003	-,297*	-0,056
IBD	,249*	-,327**	-,578**	-,327**	-0,055	-0,216	-0,069	-0,239	-0,043
IDAP	0,03	-0,047	0,144	-0,056	-0,081	0,108	-0,242	0,045	0,01
EPI-D	-,301*	,358**	,335**	,283*	0,18	0,231	0,162	0,169	-0,038
DI-CH	-0,228	,265*	,572**	,268*	-0,016	0,142	0,065	0,239	0,003
IDP	-,291*	,324**	,557**	0,235	0,049	0,184	-0,037	0,21	0,031
LOBO	-0,147	0,213	,389**	0,063	0,12	,390**	-0,028	,265*	-0,122
SID	-0,052	0,208	,525**	,245*	-0,088	,296*	0,109	,278*	-0,025
TID	-0,059	-0,003	0,149	0,093	0,165	,283*	0,133	,266*	-0,152

\*\*correlation is significant at level of 0,01 \*correlation is significant at level of 0,05

**TABLE 4**  
**Relation between diatom indices and physicochemical parameters according to Multivariate regression analysis (n=66)**

	R	R Square	Adjusted R <sup>2</sup>	Std. Error of the Estimate	F	Sig.
<b>GDI</b>	0,771	0,595	0,53	0,42102	9,142	0
<b>IPS</b>	0,733	0,537	0,463	0,51919	7,225	0
<b>SHE</b>	0,719	0,517	0,439	0,59091	6,648	0
<b>DESCY</b>	0,672	0,452	0,364	0,59128	5,132	0
<b>IBD</b>	0,62	0,384	0,285	0,3285	3,879	0,001
<b>SID</b>	0,596	0,355	0,252	0,28679	3,427	0,002
<b>DI-CH</b>	0,594	0,353	0,249	0,71587	3,395	0,002
<b>WAT</b>	0,58	0,336	0,229	13,60555	3,147	0,004
<b>IDP</b>	0,578	0,334	0,227	0,43888	3,122	0,004
<b>LOBO</b>	0,574	0,33	0,222	0,6024	3,064	0,005
<b>IDSE</b>	0,557	0,31	0,199	0,34899	2,799	0,009
<b>EPI-D</b>	0,555	0,308	0,197	0,32822	2,771	0,009
<b>TDI</b>	0,494	0,244	0,122	11,41832	2,005	0,056
<b>CEE</b>	0,483	0,233	0,11	1,76623	1,894	0,072
<b>TID</b>	0,419	0,175	0,043	0,35991	1,321	0,247
<b>SLA</b>	0,397	0,158	0,022	0,25874	1,164	0,336
<b>IDAP</b>	0,395	0,156	0,021	0,50703	1,152	0,343

**TABLE 5**  
**Physicochemical quality levels and alterations of Evennes and Diversity values**

	1. Station	2. Station	3. Station	4. Station	5. Station	6. Station
<b>Klee (1991)</b>	I-II	I-II	I-II	I-II	I-II	II
<b>Evennes</b>	0,78	0,86	0,84	0,86	0,88	0,67
<b>Shannon-Waever</b>	3,08	2,95	2,75	3,08	3,16	2,32

As a result of physicochemical parameters and multivariate regression analysis between indices, the highest Adjusted R<sup>2</sup> value was determined (0,53) in GDI. R<sup>2</sup> values of the other indices were not exceed 0,5. IDAP was the index that has the lowest R<sup>2</sup> value, followed by SLA (Table 4).

According to all indices used on determination of the water quality, increasing pollution was determined at station VI. However, most of the diatom indices were determined different levels from quality classes that were specified based on physicochemical parameters. The majority of indices, identified station 6 as polluted or exceedingly polluted and first 5 stations as moderately polluted. In terms of water quality levels provided by physicochemical parameters; the most compatible indices were TDI and SLA. All stations were identified as oligotrophic to TDI; as well as betamezosaprob to SLA. On the other hand; in multivariate regression analysis that was evaluated based on physicochemical parameters, considerably low Adjusted R<sup>2</sup> values were determined for the both two indices (Table 4).

## DISCUSSION

As the result of these studies on Andık Stream,

according to physicochemical parameters, first 5 stations were determined as less polluted (Oligo-betamesosaprob) while 6<sup>th</sup> station determined as slightly polluted betamesosaprobic stream. It was determined that alteration was also supported by Diversity and Evennes values. The highest value of diversity was determined at 5<sup>th</sup> station and it was respectively followed by the stations 1,4,2 and 3. 6<sup>th</sup> station was determined lowest diversity value (Table 5). This part of the river is considered to be under the effects of urban areas. Moreover, diatom index values also indicate increasing of pollution at 6<sup>th</sup> station. However, it was detected that increasing pollution was at half saprobic level according to the assessment of saprobic index.

When dominance at the stations are evaluated in genus level, the dominant species were; %36,42 *Navicula* at 1<sup>st</sup> station, %26,86 *Navicula* at 2<sup>nd</sup> station, at 3<sup>rd</sup> station it was %24,98 *Ulnaria* and %32,6 *Navicula* at 4<sup>th</sup> station, %15,41 *Cocconeis* at 5<sup>th</sup> station and at 6<sup>th</sup> station, it was *Nitzschia* with a rate of %55,51. The taxa under *Navicula* have an extensive ecological area [33]. *Nitzschia* genus which was found in sites, where there are microbiological recycled materials or abundance of nutrients, is common in oxygen-poor and nutrient-enriched organically polluted waters; in addition, as a result of increased pollution, decreasing of the taxa which belong to *Cocconeis* genus was observed[34].

At first 3 stations and 5<sup>th</sup> station; the dominant taxon was *U. ulna* and had abundance rate as; 1<sup>st</sup> station %26,21, 2<sup>nd</sup> station %25,93, 3<sup>rd</sup> station %24,98 and 5<sup>th</sup> station %13,73. This species was frequently observed at all stations. At stations 4 and 6, *U. ulna* was not the dominant species, but still it was one of the abundant species. This taxon which is not only highly tolerant to pollution but also is largely distributed, is a very common species; and it can be found in areas from mezotrophic to polytrophic [35]. At station 4, the dominant taxa was *A. minutissima* with a rate of %22,87. According to Harding et al. [36]; *A. minutissima* represents the slightly polluted sites on a stream. To Lange-Bertalot [37-39], *A. minutissima* is the organism that included to quality class I. Also Barlas [40] expressed the similar findings. Therewithal, these species are tolerant to organic pollution and eutrophication [34]. At station 6, the dominant taxon was %48,63 *N. palea*. Pursuant to Cox [30]; *N. palea* which shows tolerance from alpha mezosaprobic to polysaprobic conditions, is very widespread organism and it was expressed that it can be found in regions which have low nutrient content but it will not be in the dominant situation. Lange-Bertalot [37]; defined *N. palea* as a tolerant species against intense toxic effects and determined that it thrives better in the stream parts which included to water quality class II-III and III. But all of the diatom species thrive in areas from oligosaprobic to mezosaprobic, therefore these taxa can be seen in these quality classes.

When evaluated in terms of relationship with physicochemical parameters, the determined highest relation was with GDI and lowest with IDAP. GDI is easy to use and a simple index that evaluates diatoms in genus level, uses 174 taxa [41]. By the genus based evaluation of organisms, GDI gives ease of application in different regions. It was reported by Prygiel and Coste [42] for slow-flowing rivers of France and by Kelly et al. [43] for fast-flowing rivers of England that it gave similar results; as to Bere and Tundisi [9] all indices were applicable in the region of São Carlos. Kwandras et al. [44] remarked that in the rivers of Poland, IPS and GDI gave optimal results; and [45] stated that EPI-D, TDI, %PT, IPS and IDG gave optimal results for Central Italy. In studies on Akçay; Solak et al. [20] mentioned that the DESCY index gave optimal result. In study on Isparta and Darıören streams; Kalyoncu et al. [21] stated that DI-CH and TID indices complied more with physicochemical parameters. In study on Aksu stream; both SID and SLA indices, reflected the water quality alterations more accurate [22]. Besides this, according to all indices that applied; there were increasing pollution at station 6. However, diatom indices show deviation as indicated by relation levels with physicochemical parameters. According to multivariate regression analysis; GDI has the

highest Adjusted R<sup>2</sup> value, but the value (0,53) is relatively low. Therewithal water quality levels differ according to indices. Pursuant to results of physicochemical parameters, both TDI and SLA indices seem like the most compatible indices to water quality class. All stations are identified as oligotrophic to TDI; as well as betamezosaprobic to SLA. Yet the correlations between physicochemical parameters and both TDI and SLA indices are low. Between physicochemical parameters and SLA there is not a significant relation (Table 4). According to GDI; 1<sup>st</sup> station is classified as quality class IV; 2<sup>nd</sup>, 3<sup>rd</sup>, 4<sup>th</sup> and 5<sup>th</sup> stations are classified as quality class III and finally 6<sup>th</sup> station is classified as quality class V. However GDI quality values show deviation pursuant to physicochemical classification. As mentioned in this study; GDI, according to multivariate regression analysis, has the best Adjusted R<sup>2</sup> value; but to support this conclusion, more study is needed. Because; saprobic and trophic values were determined by the region where the indices were developed and it is known that indication weight is calculated according to both geographical and ecological conditions of the region.

#### ACKNOWLEDGEMENT

This research has been supported by Unit Scientific Research Projects, University of Süleyman Demirel (Project No: 2340-YL-10). We are deeply grateful to them for their financial support.

#### REFERENCES

- [1] Angermeier, P.L. and Karr, R.J. (1986) Applying an Index of Biotic Integrity Based on Stream-Fish Communities: Considerations in Sampling and Interpretation. North American Journal of Fisheries Management Oceanological and Hydrobiological Studies 6 (3): 418-429.
- [2] Kargioğlu, M., Serteser, A., Kıvrak, E., İçağa, Y. and Konuk, M. (2012) Relationships between epipellic diatoms, aquatic macrophytes, and water quality in Akarçay Stream, Afyonkarahisar, Turkey. Oceanological and Hydrobiological Studies 41 (1): 74-84.
- [3] Sladeček, V. (1973). System of water quality from the biological point of view. Ergebnisse der Limnologie 7: 1-128.
- [4] Rott, E., Hofmann, G., Pall, K., Pfister, P. and Pipp, E. (1997) Indikationslisten für Aufwuchsalgen. Teil 1. Saprobien Indikation. Bundesministerium für Land- und Forstwirtschaft, Wien: 1-73.
- [5] DIN 38410-2. (1990) Biological-ecological

- Analysis of water (group M); determination of the saprobic index (M2), German Standard Methods for the Examination of Water. Waste Water and Sludge, 10.
- [6] Plafkin, J.L., Barbour, M.T., Porter, K.D., Gross, S.K. and Hughes, R.M. (1989) Rapid Bioassessment Protocols for use in Streams and Rivers: Benthic Macroinvertebrates and Fish. U.S. Environmental Protection Agency. EPA 440/4-89/001. 8 chapters, Appendices A-D.
- [7] Kelly, M.G. (1998) Use of the trophic diatom index to monitor eutrophication in rivers, *Water Research* 32(1): 236-242.
- [8] Gómez, N. and Licursi, M. (2001) The Pampean Diatom Index (IDP) for assessment of rivers and streams in Argentina. *Aquatic Ecology* 35: 173-181.
- [9] Bere, T. and Tundisi, J.G. (2011) Applicability of borrowed diatom-based water quality assessment indices in streams around São Carlos-SP, Brazil. *Hydrobiologia* 673:79-192.
- [10] Harding, W.R., Archibald, C.G.M., Taylor, J.C. and Mundree, S. (2004) The South African Diatom Collection: An Appraisal And Overview Of Needs And Opportunities. WRC Report Number: TT 242/04.
- [11] Watanabe, T., Asai, K. and Houki, A. (1986) Numerical estimation of organic pollution of flowing waters by using the epilithic diatom assemblage – Diatom Assemblage Index (DIApo). *Science of the Total Environment* 55: 209-218.
- [12] Kolkwitz, R. and Marsson, M. (1902) Grundsätze für die biologische Beurteilung des Wassers nach seiner Flora und Fauna. *Mitt. Aus d. Kgl. Prüfungsanstalt für Wasserversorgung u. Abwasserbeseitigung Berlin* 1: 33-72.
- [13] Liebmann, H. (1947) Die Notwendigkeit Einer Revision Des Saprobien - Systems Und Deren Bedeutung Für Die Wasserbeurteilung. *Ges. Ing.* 68: 33 – 37.
- [14] Sladeček, V. (1986) Diatoms as indicators of organic pollution. *Acta Hydrochimica et Hydrobiologica* 14: 555-566.
- [15] Walley W.J, Grbovic, J. and Eroski, S. (2001) A Reappraisal Of Saprobic Values And Indicator Weights Based On Slovenian River Quality Data. *Wat. Res.* 35 (18): 4285-4292.
- [16] Pantle, R., and Buck, H. (1955) Die biologische Überwachung der Gewässer und die Darstellung der Ergebnisse. *Gas - und Wasserfach* 96 (18): 604.
- [17] Zelinka, M. and Marvan, P. (1961) Zur praxisierung der biologischen klassifikation der reinheit fliessender gewässer. *Archive Hydrobiologica* 57: 389-407.
- [18] Kalyoncu, H. and Barlas, M. (1997) Isparta Deresi'nde yoğun olarak belirlenen epilithic diatomların su kalitesine bağlı olarak mevsimsel değişimleri. In: IX. Ulusal Su Ürünleri Sempozyumu, 17-19 Eylül 1997, Eğirdir/Isparta, 310-324.
- [19] Gürbüz, H. and Kıvrak, E. (2002) Use of epilithic diatoms to evaluate water quality in the Karasu River of Turkey. *Journal of Environmental Biology* 23 (3): 239-246.
- [20] Solak, C.N., Fehér, G., Barlas, M. and Pabuçcu, K. (2007) Use of epilithic diatoms to evaluate water quality of Akçay Stream (Büyük Menderes River) in Mugla/Turkey. *Archiv Für Hydrobiologie Suppl.*, 161 (3-4), Large Rivers, 17(3-4): 327-338.
- [21] Kalyoncu, H., Çiçek, N.L., Akköz, C. and Özçelik, R. (2009a) Epilithic Diatoms from the Darıören Stream (Isparta/Turkey): Biotic indices and multivariate analysis. *Fresen. Environ. Bull.* 18(7b): 1236-1242.
- [22] Kalyoncu, H., Barlas, M. and Ertan, Ö.O. (2009b) Aksu Çayı'nın Su Kalitesinin Biotik İndekslere (Diyatomlara ve Omurgasızlara Göre) ve Fizikokimyasal Parametrelere Göre İncelenmesi, Organizmaların Su Kalitesi ile İlişkileri. *Türk Bilim Dergisi* 2(1): 46-57.
- [23] Kalyoncu, H., Barlas, M., Şerbetçi, B., Gün, B., Dayıoğlu, H., Yorulmaz, B. and Zeybek, M. (2010) Aksu Çayı'nın Su Kalitesinin OMNIDIA Programına Göre Belirlenmesi, Karşılaştırılması ve İndekslerin Fizikokimyasal Parametrelerle İlişkisi. 4. Ulusal Limnoloji Sempozyumu, 4-6 Ağustos 2010, Bolu, 32.
- [24] Solak, C.N. (2011) The application of diatom indices in the Upper Porsuk River, Kütahya-Turkey. *Turk J Fish Aquat Sci* 11: 31-36.
- [25] Sonneman, J.A., Walsh, C.J., Bren, P.F. and Sharpe, A.K. (2001) Effects of urbanization on streams of the Melbourne region, Victoria, Australia. II. Benthic diatom communities. *Freshwater Biology* 46: 553-565.
- [26] Krammer, K. and Lange-Bertalot, H. (1986) Bacillariophyceae. 1. Teil: Naviculaceae. Süßwasser von mitteleuropa. Gustav Fischer Verlag, Band 2-1, Stuttgart.
- [27] Krammer, K. and Lange-Bertalot, H. (1988) Bacillariophyceae. 2. Teil: Bacillariophyceae, Epithemiaceae, Surirellaceae. Süßwasser von mitteleuropa. Gustav Fischer Verlag, Band 2-2, Stuttgart.
- [28] Krammer, K. and Lange-Bertalot, H. (1991a) Bacillariophyceae. 3. Teil: Centrales, Fragilariaceae, Eunotiaceae. Süßwasser von mitteleuropa. Gustav Fischer Verlag, Band 2-3, Stuttgart.
- [29] Krammer, K. and Lange-Bertalot, H. (1991b) Bacillariophyceae. 4. Teil: Achnantheceae, Kritische Ergänzungen zu Navicula (Lincolatae) und Gomphonema. Cesamptliteraturverzeichnis. Süßwasser von mitteleuropa. Gustav Fischer Verlag, Band 2-4, Stuttgart.

- [30] Cox, E.J. (1996) Identification of Freshwater Diatoms From Live Material. Chapman and Hall, London.
- [31] Lecointe, C., Coste, M. and Prygiel, J. (1993) "Omnidia": software for taxonomy, calculation of diatom indices and inventories management. *Hydrobiologia* 269 (270): 509–513.
- [32] SPSS INC. (2004) SPSS Professional Statistics 13.0 SPSSINC, Chicago.
- [33] Potapova, M. and Charles, D.F. (2003) Distribution of benthic diatoms in U.S. rivers in relation to conductivity and ionic composition. *Freshwater Biology* 48: 1311–1328.
- [34] Van Dam, H., Mertens, A. and Sinkeldam, J. (1994) A coded checklist and ecological indicator values of freshwater diatoms from the Netherlands. *Aquatic Ecology* 28: 117–133.
- [35] Kupe, L. and Miho, A. (2006) Considerations about environmental state of important aquatic habitats in Albania based in algal assessment – A Review. To be printed in the Proceedings of RiverNet Conference, Tirana 15-16 May 2006.
- [36] Harding, W.R., Archibald, C.G.M. and Taylor, J.C. (2005) The relevance of diatoms for water quality assessment in South Africa: a position paper. *Water SA* 31: 41–46.
- [37] Lange-Bertalot, H. (1978) Diatomeen-Differentialartenanstellung von Leitformen: ein geeigneteres Kriterium der Gewässerbelastung. *Arch. Hydrobiol. Suppl.* 51. *Algological Studies* 21: 393-427.
- [38] Lange-Bertalot, H. (1979a) Pollution tolerance of diatoms as a criterion for water quality estimation. *Nova Hedwigia Beiheft* 64: 285–304.
- [39] Lange-Bertalot, H. (1979b) Toleranzgrenzen und Pollutionsdynamik benthischer diatomeen bei unterschiedlich starker abwasserbelastung. *Arch. Hydrobiol. Algological Studies* 23: 184-219.
- [40] Barlas, M. (1988) Limnologische untersuchungen an der Fulda unter besonderer berücksichtigung der fischparasiten, ihrer Wirtsspektren und der Wassergüte. Dissertation. PhD Thesis. Universität Kassel.
- [41] Taylor, J.C. (2004) The application of diatom-based pollution indices in the Vaal catchment. Unpublished Msc. Thesis. North-West University, Potchefstroom Campus, Potchefstroom, South Africa.
- [42] Prygiel, J. and Coste, M. (1993) The assessment of water quality in the Artois-Picardie water basin (France) by the use of diatom indices. *Hydrobiol.* 269 (279): 343-349.
- [43] Kelly, M.G., Penny, C.J. and Whitton, B.A. (1995). Comparative performance of benthic diatom indices used to assess river water quality. *Hydrobiol.* 302: 179-188.
- [44] Kwadrans, J., Eloranta, P., Kawecka, B. and Kryzysztow, W. (1998) Use of benthic diatom communities to evaluate water quality in rivers of southern Poland. *Journal of Applied Phycology* 10: 193–201.
- [45] Bela, D.V., Puccinelli, C., Marcheggiani, S. and Mancini, L. (2007) Benthic diatom communities and their relationship to water chemistry in wetlands of central Italy. *Ann. Limnol. - Int. J. Lim.* 43 (2): 89-99.

---

**Received:** 13.01.2016

**Accepted:** 07.09.2016

---

#### CORRESPONDING AUTHOR

---

**Hasan Kalyoncu**

Süleyman Demirel University, Faculty of Science and Art, Department of Biology, Isparta, Turkey

e-mail: [hasankalyoncu@sdu.edu.tr](mailto:hasankalyoncu@sdu.edu.tr)

# PRECONCENTRATION OF CADMIUM, LEAD, COPPER, ZINC AND MANGANESE WITH POLYSTYRENE DIVINYLBENZENE COPOLYMER CONTAINING DITHIOCARBAMATE GROUP, AND DETERMINATION WITH FAAS

Ali Alkan<sup>1,\*</sup>, Mehtap Yagan Asci<sup>2</sup>, Bekir Bati<sup>2</sup>

<sup>1</sup> Karadeniz Technical University, Institute of Marine Sciences and Technology, Trabzon, Turkey

<sup>2</sup> Ondokuz Mayıs University, Faculty of Science, Department of Chemistry, Samsun, Turkey

## ABSTRACT

This study aimed to synthesize a new dithiocarbamate derivative resin with Amberlite XAD-4, which is a polystyrene divinylbenzene copolymer. The applicability of this new resin was investigated for the preconcentration of Cd(II), Pb(II), Cu(II), Zn(II) and Mn(II). Metal ions sorbed on functionalized Amberlite XAD-4 resin were eluted with 1 mol L<sup>-1</sup> HNO<sub>3</sub>, and were determined with flame atomic absorption spectrometer (FAAS). The effects of parameters such as pH, sample flow rate, sample volume, type and the concentration of the elution solution and foreign ions were examined and optimum conditions were outlined. The recovery of the metal ions from aqueous solutions was determined to be higher than 95% in the range pH 4-5. The limit of detection was determined as 0.0032; 0.0055; 0.0069; 0.0075; 0.0043 µg mL<sup>-1</sup> for Cd(II), Pb(II), Cu(II), Zn(II) and Mn(II) ions, and the limit of quantification was 0.0079, 0.0159, 0.0188, 0.0254 and 0.0160 µg mL<sup>-1</sup> for these ions respectively. The accuracy of the method was tested with a variety of certified reference materials (SLRS4, MESS-3, DOLT-4). The method was successfully applied to river and sea water samples.

## KEYWORDS:

Amberlite XAD-4, dithiocarbamate, trace metals, flame atomic absorption spectroscopy, 2-ethylamino ethylamine dithiocarbamate (EADTC)

## INTRODUCTION

Heavy metals are important hazardous chemicals in terms of biological and ecological aspects. They cause environmental pollution due to their toxic effects and durability when they are accumulated on living tissues. Because of the heavy metal pollution, which is of the urgent problems to

be solved today, micro and macro levels of metal analysis in such environmental samples as biota and sediment, particularly in water, has been of great interest [1].

Due to its low cost, the most widely used technique for the determination of heavy metal ions is flame atomic absorption spectrometry (FAAS). However, there are two major problems in the determination of trace heavy metal ions with FAAS. These are low concentrations of metal ions in the sample and interference effect of the basic components of the sample. Therefore, FAAS is alone not satisfactory enough in terms of sensitivity for very low trace metal concentrations in environmental samples [2]. The direct determination of the heavy metals by FAAS and electrothermal atomic absorption spectrometry (ETAAS) in the samples with very low concentrations of analytes requires preconcentration and matrix elimination processes in order to increase the selectivity and improve the detection limit in the analyses of trace elements [3-5].

The most commonly used preconcentration techniques are co-precipitation, ion exchange, solvent extraction, solid-phase extraction, and biosorption [6]. The solid-phase extraction is widely used in the separation and preconcentration of the target analyte of the complex matrices containing trace amounts of inorganic and organic species [7-9]. It has many advantages over other enrichment techniques. A good separation as well as high concentration factors is achieved with solid-phase extraction. Thus, both lower detection limits and more reliable results are obtained in the determination of inorganic and organic components [10].

Various solid-phase sorbents such as activated carbon, Amberlite XAD resins, polymeric fibers, Ambersorb, naphthalene, alumina, and silica gel are used in the preconcentration of trace metals from various media [8, 9, 11, 12]. The development of chelating resins in solid-phase extraction has

attracted special attention due to its advantages including pH control, high selectivity, durability and high metal capacity for trace metal enrichment [9, 13]. The most widely used solid-phase sorbents are styrene-divinylbenzene copolymers with hydrophobic surface [14]. Dithiocarbamate type ligands are frequently used for preconcentration as they form a durable complex with transition metals. The metal complexes of dithiocarbamate ligands are interesting because of their various structural alternatives and biological activities [15].

In this study, Amberlite XAD-4 resin was modified and a resin of dithiocarbamate derivative was synthesized, and the availability of this new resin was investigated for the purpose of separation and preconcentration in the determination of cadmium, lead, copper, zinc, and manganese. The applicability of the developed method on synthetic samples and environmental samples was tested as well.

## MATERIALS AND METHODS

**Instruments.** Metal determinations were carried out with AAS (GBC 905, Australia) using air-acetylene flame after preconcentration. Single-element hollow cathode lamps were used as the light source. The recommended instrument parameter values by the manufacturer were used for the elements measured. pH measurements were performed with a Mettler Toledo Multi pH meter. The study also used a shaker (IKA KS250 model) and a centrifuge (Hettich EBA 3S). Deionized water  $18.2 \text{ MOhm cm}^{-1}$  was used from Barnstead Easy Pure RF. IR spectra were taken with Perkin-Elmer Spectrum One FTIR spectrophotometer. For the digestion of SRM, a microwave digestion system (Milestone Ethos D, Italy) was used.

**Reagents and solutions.**  $1000 \mu\text{g mL}^{-1}$  Cd(II) (Sigma 51994), Pb(II) (Sigma 16595), Cu(II) (Sigma 38996), Zn(II) (Sigma 18827) and Mn(II) (Sigma 119789) in 1%  $\text{HNO}_3$  were used as metal stock solutions. Working standards were prepared by diluting the standard solutions with the necessary proportions of deionized water. A buffer solution (pH 4.5), a mixture of  $0.1 \text{ mol L}^{-1}$  sodium acetate (67.8 mL) and  $0.1 \text{ mol L}^{-1}$  acetic acid (32.2 mL), were used to buffer the solutions.  $1 \text{ mol L}^{-1}$   $\text{HNO}_3$  solution was used for sorbed metal ions elution from resin.

Amberlite XAD-4 resin (Sigma), Acetyl chloride (Merck, %>99), 2-ethylamino ethylamine (Aldrich, 98%), Aluminum chloride (Merck, %>98), 1,2 Dichloromethane (Merck, %>99), and carbon disulfide (Merck, %>99.9) were utilized in the synthesis of the modified resin. SLRS-4 (river water reference material), MESS-3 (marine

sediment reference material), and DOLT-4 (fish liver reference material) were used to test the suitability of the method for different matrices.

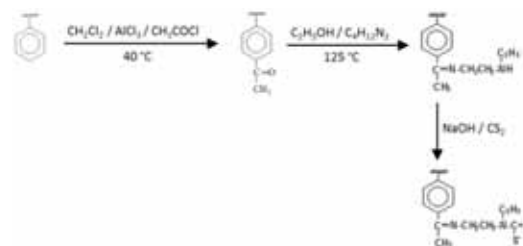


**FIGURE 1**  
Synthesis and chemical structure of Amberlite XAD-4-EADTC resin

**Synthesis of chelating resin (XAD-4-EADTC).** The synthesis of 2-ethylamino ethyl amine dithiocarbamate (XAD-4-EADTC) derivative of Amberlite XAD-4 was carried out as shown in Figure 1. XAD-4 resin was washed with deionized water and methanol before modification. Afterwards, it was shaken with methanol on a shaker for 24 hours and dried in an oven at  $60 \text{ }^\circ\text{C}$  for 48 hours [16]. In the acetylation of XAD-4 resin, 5.00 g of XAD-4 resin was put into 20 mL of 1,2-dichloromethane and stirred and 5.62 g (42 mmol) of anhydrous aluminum chloride. Then, 2.75 mL (35 mmol) of acetyl chloride was added and it was subjected to reaction at  $40 \text{ }^\circ\text{C}$  for 16 hours. The product obtained was washed with concentrated hydrochloric acid, water, and methanol respectively [16]. The product dried under vacuum was made into a KBr disk and its FTIR spectrum was recorded.

2.00 g of acetylated XAD-4 resin was stirred for 15 min in 25 mL of ethanol, and 5 drops of concentrated  $\text{H}_2\text{SO}_4$  were added and continued to stirring. Ethanol phase was separated with decantation. 16 mL of 2-ethylamino ethylamine was added in drops to the reaction mixture at room temperature [17]. It was refluxed at  $125 \text{ }^\circ\text{C}$  for 7 days and cooled down to room temperature at the end of the reaction. The product was washed first with water and then with methanol. After it was dried, its IR spectrum was taken.

2.50 g of XAD-4 imine derivative was stirred in 20 mL of  $1.0 \text{ mol L}^{-1}$  NaOH for 30 minutes. 5 mL of  $\text{CS}_2$  was added, stirred at room temperature for 24 hours, and then filtered. It was washed first with water and then methanol, and finally, with  $0.10 \text{ mol L}^{-1}$  sodium acetate solution of pH 8.0. Then, it was dried in the open air [17].

**Preparation of disc.** The filtration apparatus of Nalgen trademark with polyethersulphonate of  $0.2 \mu\text{m}$  pore diameter and 50 mm of membrane diameter, and 150 mL of reservoir volume were

**TABLE 1**  
Effect of type and concentration of elution agents on the recoveries of Cd(II), Pb(II), Cu(II), Zn(II) and Mn(II) ions

Elution agent	Concentration (mol L <sup>-1</sup> )	Recovery (%)*				
		Pb	Cd	Cu	Zn	Mn
HNO <sub>3</sub>	0.1	96±1	99±1	89±1	99±1	99±1
	0.5	97±1	98±1	99±2	100±1	100±1
	1.0	99±1	100±2	100±1	99±2	100±1
	2.0	99±1	99±1	97±1	100±1	99±1
	4.0	98±1	96±1	96±1	98±2	99±1
HCl	0.1	94±3	100±1	94±2	99±2	98±1
	0.5	99±3	99±1	97±1	100±1	100±1
	1.0	99±1	99±1	99±3	99±2	99±1
	2.0	100±1	97±1	94±1	99±2	100±2
	4.0	97±1	98±1	88±1	93±1	89±1

\* Results are mean ± standard deviation of three replicate analyses (Elution flow rate: 2 mL min<sup>-1</sup>)

used in the preparation of the separation disc. The synthesized modified resin was placed on the disc to fill about 0.2 g of filter surface and analytical tests were performed on three parallel extraction disc. The extraction disc was conditioned with 10mL of buffer solution of pH 4.5, because the highest recovery for the investigated metal was between pH 4 and 5 prior to each separation and preconcentration process.

**Separation and general preconcentration procedure.** Disc technique was used for the separation and enrichment of metal ions. Adjusted to pH 4.5, analyte solutions of 100 mL (0.100 µg mL<sup>-1</sup> for Cd(II) and Zn(II), 0.200 µg mL<sup>-1</sup> for Cu(II) and Mn(II), and 0.500 µg mL<sup>-1</sup> for Pb(II)) were passed through the disc with 2 mL min<sup>-1</sup> flow rate. Then, 10 mL of 1.0 mol L<sup>-1</sup> HNO<sub>3</sub> solution were passed through the disc with 2 mL min<sup>-1</sup> flow rate; the metal ions attached to the disc were eluted, and the absorbance of the eluate was measured with FAAS. The disc was washed with 100 mL of deionized water and made available for re-use.

## RESULTS AND DISCUSSION

**Characterization of (XAD-4-EADTC).** FTIR spectra of the products in each step of the XAD-4-EADTC resin synthesis were taken and their synthesis reactions were observed. In the FTIR spectrum of acetylated XAD-4, the peaks of CH<sub>3</sub> vibrational frequencies at 1262 and 1171 cm<sup>-1</sup> and deformation peaks at 1352 and 1369 cm<sup>-1</sup> as well as the peak of C=O group at 1687 cm<sup>-1</sup> were observed. In the IR spectrum of imine derivative, the peak of C=O at 1687 cm<sup>-1</sup> of the acetyl derivative synthesized in the previous step disappeared and the peak of C=N at 1642 cm<sup>-1</sup> appeared. A vibration of C=N bond was observed at 1637 cm<sup>-1</sup> in the FTIR

spectrum of the product obtained during the synthesis of dithiocarbamate derivative. The peak at 1506 cm<sup>-1</sup> belonged to C-N bond in CS<sub>2</sub>-NR group and the peaks observed at 1116 and 1083 cm<sup>-1</sup> belonged to C=S bond in CS<sub>2</sub> group.

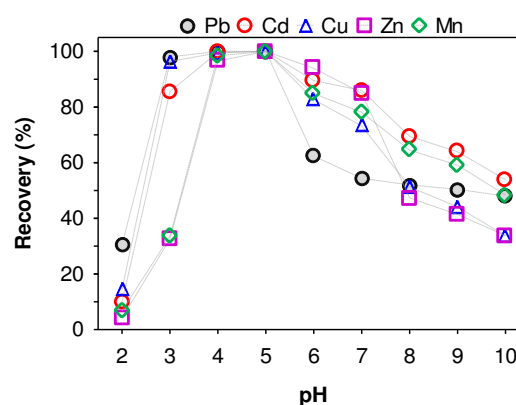


**FIGURE 2**  
Effect of pH (Experimental conditions: 100 mL metal solution of Cd, Zn: 0.100 µg mL<sup>-1</sup>, Cu, Mn: 0.200 µg mL<sup>-1</sup>, Pb: 0.500 µg mL<sup>-1</sup>, 0.2 g resin, elution flow rate: 2 mL min<sup>-1</sup>)

**Effect of pH on the recovery.** As the ligands used in chelating resins have weak acidic-basic properties, pH is an extremely important parameter in the sorption of metal ions. This effect also depends on the type of the sorbent used. As shown in Figure 2, metal sorption took place in all the pH levels tested, but the highest recovery of the metal ions occurred within the range pH 4-5.

**Choice of elution agents.** In this study, different concentrations of nitric acid and hydrochloric acid were tested as elution solutions. High recoveries were obtained in different concentrations of both nitric acid and hydrochloric acid in the elution of many metals (Table 1).



However, 1.0 mol L<sup>-1</sup> HNO<sub>3</sub> was preferred as the elution solution because it is more useful than other acids.

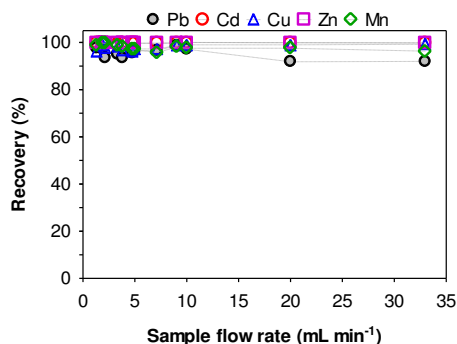


FIGURE 3

**Effect of sample flow rate (Experimental conditions: 100 mL metal solution of Cd, Zn: 0.100 µg mL<sup>-1</sup>, Cu, Mn: 0.200 µg mL<sup>-1</sup>, Pb: 0.500 µg mL<sup>-1</sup>, 0.2 g resin, elution flow rate: 2 mL min<sup>-1</sup>)**

**Effect of sample flow rate.** The recovery values from the experiments at different flow rates were given in Figure 3. The larger diameter of the extraction disc and the smaller mesh size of the resin used in the practice increased the contact surface, and higher metal sorptions were observed at very high filtration rates upper 30 mL min<sup>-1</sup>.

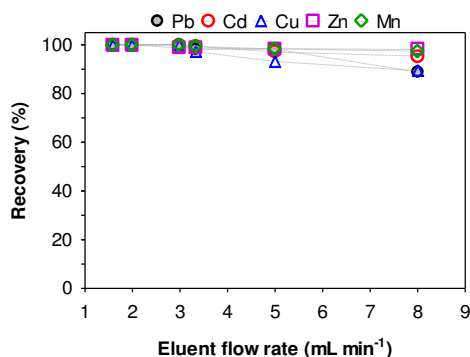


FIGURE 4

**Effect of elution flow rate (Experimental conditions: 100 mL metal solution of Cd, Zn: 0.100 µg mL<sup>-1</sup>, Cu, Mn: 0.200 µg mL<sup>-1</sup>, Pb: 0.500 µg mL<sup>-1</sup>, 0.2 g resin)**

**Effect of elution solution flow rate and volume.** The flow rate of the elution solution needs to be fast enough to be time efficient and slow enough to allow the quantitative recovery of the target species. Generally, higher flow rate requires large volumes of elution solution to complete the elution. Faster elution causes losses, especially, for lead and copper (Figure 4). For this reason, elution solution flow rate must be below 5 mL min<sup>-1</sup>.

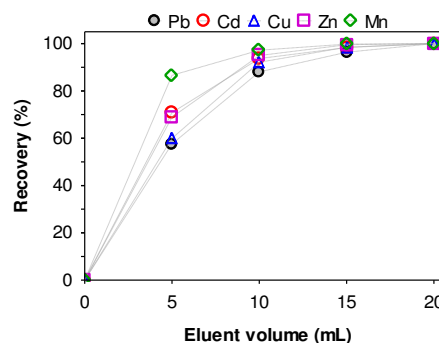


FIGURE 5

**Effect of elution volume of solution (Experimental conditions: 100 mL metal solution of Cd, Zn: 0.100 µg mL<sup>-1</sup>, Cu, Mn: 0.200 µg mL<sup>-1</sup>, Pb: 0.500 µg mL<sup>-1</sup>, 0.2 g resin, elution flow rate: 2 mL min<sup>-1</sup>)**

The volumes of 5, 10, 15, and 20 mL of 1.0 mol L<sup>-1</sup> HNO<sub>3</sub> solution were used for the elution of Cd(II), Pb(II), Cu(II), Zn(II) and Mn(II) ions sorbed on the disc, and the results of the recovery values obtained were given in Figure 5. The volume of the elution solution is very important in terms of enrichment. The study observed that more than 95% of the metals sorbed in the resin were eluted with 10 mL of 1.0 mol L<sup>-1</sup> HNO<sub>3</sub> solution (Figure 5). The lead was eluted later than other metals which might be due to stronger interaction of the sulfur in functional group with Pb(II) of a soft character and to its sorption in a wide pH range below the optimum pH value compared to other metal ions.

**Sorption capacity of resin.** Total sorption capacity of resin was determined by the interaction of 100 mL solutions of Pb(II), Cd(II), Cu(II), Zn(II) and Mn(II) ions at 50 µg mL<sup>-1</sup> concentration with 0.200 g of resin. The solution was separated by filtration from the resin saturated with excessive amounts of metal, and the metals sorbed were eluted with 1.0 mol L<sup>-1</sup> HNO<sub>3</sub> solution. Both filtration and elution solution absorbance were measured with FAAS after necessary dilutions and the sorption capacity was calculated for each metal. The sorption capacities of XAD-4-EADTC resin for Pb(II), Cd(II), Cu(II), Zn(II) and Mn(II) ions were found as 0.29; 0.20; 0.26; 0.17 and 0.15 mmol g<sup>-1</sup> respectively.

**Resin re-usability test.** Resin stability and re-usability are very important in practice. The stability of XAD-4-EADTC resin was determined by examining the change in resin sorption capacity after the re-use of the same resin. For this reason the resin was stored in room conditions for more than six months and its durability and stability were tested by filtrating more than 100 liters of metal solution in total.

It was observed that metal sorption capacity of the resin didn't change more than %5 in this application period. The stable results of the resin in a long time practice proved that it had re-usability advantages.

**Influence of diverse ions.** The presence of diverse ions in high amounts in natural samples can implement a problem by interfering in solid-phase extraction applications. The developed method was applied to 0.250  $\mu\text{g mL}^{-1}$  of Cd(II), Cu(II), Zn(II) and Mn(II) solutions and 0.500  $\mu\text{g mL}^{-1}$  of Pb(II) solution by adding diverse ions,  $\text{Na}^+$ ,  $\text{K}^+$ ,  $\text{Ca}^{2+}$  and  $\text{Mg}^{2+}$ ,  $\text{Cl}^-$  and  $\text{SO}_4^{2-}$  each with 50, 100, 250, 500, 1000, 5000 and 10000  $\mu\text{g mL}^{-1}$ , and diverse ion concentrations, which change the analyte ion concentration as  $\pm 5\%$ , were determined. The results obtained in the presence of these ions were given in Table 2. When the obtained values were evaluated, it was observed that the tolerance limits detected for the method were higher than the concentrations of anions and cations in water samples. Therefore, the study concluded that the method could be used for real samples.

**Sorption kinetics and loading half-time.** Equilibrium time is defined as the time required for metal sorption to reach 99-100%. The time required for sorption to reach 50% of the total sorption capacity is known as loading half-time ( $t_{1/2}$ ). In order to determine the effect of contact time on metal sorption, 50 mL metal solutions with 30  $\mu\text{g/mL}$  of concentration were adjusted to pH 4.5 and buffered with 1.0 ml of buffer solution. Then, they were put into a capped tube, shaken for 1, 3, 5, 10, 20 and 40 min, passed through the disc at a speed of 30  $\text{mL min}^{-1}$ , and the metals sorbed by the resin were eluted with 50 mL of 1.0  $\text{mol L}^{-1}$   $\text{HNO}_3$ . The absorbance of the samples was measured with FAAS after necessary dilutions. The study concluded that the equilibrium time for the metals examined was 20 min. However, the results revealed that the time required for the sorption of 50 % of the metals was less than 2 min (Figure 6).

Short equilibrium time shows that the interaction of the chelating groups of the modified resin with Cu(II), Cd(II), Zn(II), Mn(II) and Pb(II) ions is fast.

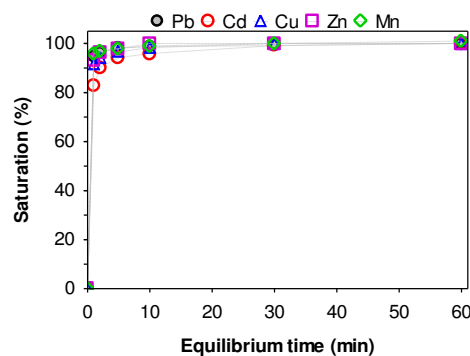


FIGURE 6

**Effect of contact time on metal sorption**  
(Experimental conditions: 50 mL metal solution, 30  $\mu\text{g mL}^{-1}$  metal ion, 0.2 g resin)

**Preconcentration factor and break-through capacity.** High preconcentration factor is one of the major advantages for analytical methods. The highest sample volume that can be used in environmental samples containing very low concentrations of metal ions is an important parameter to be examined in order to obtain high preconcentration factor. In order to determine metal sorption changes related to sample volume, several experiments were made up to 2000 mL and over 95% of metal recovery were found.

**Analytical features and applications of method.** The limit of detections (LOD) were determined as the concentration corresponding to the absorbance value taken by adding 3 times of the standard deviation to the mean absorbance value of 20 blank samples. Additionally, the limit of quantification (LOQ) were determined as the concentration corresponding to the absorbance value taken by adding 10 times of the standard

TABLE 3  
The analysis results of standard reference materials

SRM		Cu	Mn	Zn	Pb	Cd
MESS-3 ( $\mu\text{g g}^{-1}$ )	Value of Certification	33.9 $\pm$ 1.6	324 $\pm$ 12	159 $\pm$ 8	21.1 $\pm$ 0.7	-
	Value obtained	32.8 $\pm$ 1.2	320 $\pm$ 10	161 $\pm$ 8	20.8 $\pm$ 1.1	-
	Recovery (%)	97.8 $\pm$ 3.4	98.8 $\pm$ 3.3	101 $\pm$ 5	98.6 $\pm$ 5.4	-
DOLT-4 ( $\mu\text{g g}^{-1}$ )	Value of Certification	31.2 $\pm$ 1.1	-	116 $\pm$ 6	-	24.3 $\pm$ 0.8
	Value obtained	30.5 $\pm$ 1.2	-	119 $\pm$ 7	-	23.8 $\pm$ 1.0
	Recovery (%)	96.3 $\pm$ 3.7	-	103 $\pm$ 6	-	97.9 $\pm$ 3.9
SLRS-4 ( $\mu\text{g L}^{-1}$ )	Value of Certification	1.81 $\pm$ 0.08	3.37 $\pm$ 0.18	-	-	-
	Value obtained	1.75 $\pm$ 0.12	3.23 $\pm$ 0.19	-	-	-
	Recovery (%)	96.8 $\pm$ 6.6	95.9 $\pm$ 5.9	-	-	-

**TABLE 4**  
The values obtained for spiked water samples

Analytes	Added amount ( $\mu\text{g}$ )	Obtained value*	Recovery (%)
<b>Cd</b>	0	< LOQ	-
	10	10.18 $\pm$ 0.25	98.8 $\pm$ 2.5
	20	20.68 $\pm$ 0.27	98.9 $\pm$ 1.3
<b>Pb</b>	0	< LOQ	-
	10	10.51 $\pm$ 0.53	102.1 $\pm$ 3.2
	20	20.68 $\pm$ 0.55	101.3 $\pm$ 2.8
<b>Cu</b>	0	2.52 $\pm$ 0.16	-
	10	12.45 $\pm$ 0.54	99.3 $\pm$ 5.4
	20	22.26 $\pm$ 0.63	98.7 $\pm$ 3.1
<b>Zn</b>	0	20.61 $\pm$ 0.91	-
	10	30.35 $\pm$ 1.02	97.0 $\pm$ 10
	20	40.64 $\pm$ 0.86	99.9 $\pm$ 4.2
<b>Mn</b>	0	9.33 $\pm$ 0.27	-
	10	20.28 $\pm$ 0.33	109.5 $\pm$ 3.2
	20	29.68 $\pm$ 0.34	101.7 $\pm$ 1.7

\* N:3 ( $\bar{X} \pm s$ ) (Experimental condition: Sample volume 100 mL, eluent volume 10 mL).

**TABLE 5**  
The values of the Cd, Pb, Cu, Zn, and Mn in some river waters and the sea water (Black Sea)

Sampling Location	Concentrations ( $\mu\text{g L}^{-1}$ )				
	Cd	Pb	Cu	Zn	Mn
Çoruh River	< LOQ	< LOQ	1.94 $\pm$ 0.15	3.01 $\pm$ 0.10	6.17 $\pm$ 0.22
Beyazsu Stream	< LOQ	< LOQ	2.85 $\pm$ 0.16	21.83 $\pm$ 0.57	12.98 $\pm$ 0.36
The Yeşilirmak River	< LOQ	< LOQ	1.32 $\pm$ 0.12	12.06 $\pm$ 0.58	6.95 $\pm$ 0.23
The Kızılırmak River	< LOQ	< LOQ	1.19 $\pm$ 0.13	15.72 $\pm$ 0.63	11.47 $\pm$ 0.24
Black Sea Water (Surface)	1.11 $\pm$ 0.12	2.10 $\pm$ 0.21	3.91 $\pm$ 0.18	8.41 $\pm$ 0.15	1.81 $\pm$ 0.27
Black Sea Water (200 m)	1.23 $\pm$ 0.14	1.96 $\pm$ 0.22	3.77 $\pm$ 0.14	7.72 $\pm$ 0.32	252 $\pm$ 9

(Experimental condition: Sample volume 1000 mL, eluent volume 10 mL, preconcentration factor: 100).

deviation to the mean absorbance value of 20 blank samples. LOD and LOQ were 0.0032, 0.0055, 0.0069, 0.0075 and 0.0043  $\mu\text{g mL}^{-1}$  and 0.0079, 0.0159, 0.0188, 0.0254 and 0.0160  $\mu\text{g mL}^{-1}$  for Cd(II), Pb(II), Cu(II), Zn(II) and Mn(II), respectively.

Through the method applied with the synthesized dithiocarbamate derivative of resin, a linear relationship was observed in the range of 0-1, 0-5, 0-2, 0-1, 0-2  $\mu\text{g mL}^{-1}$  concentration for Cd, Pb, Cu, Zn and Mn and  $R^2$  values were found as 0.9980, 0.9994, 0.9991, 0.9992, and 0.9996 respectively.

The method was applied to MESS-3, DOLT-4 and SLRS-4 standard reference materials in order to test its accuracy. MESS-3 and DOLT-4 were digested under pressure in microwave system before preconcentration. The results obtained were given in Table 3. The results were found to be consistent with the certificate values ( $p < 0.05$ ) and the accuracy of the method was found to be analytically acceptable. In order to determine the accuracy and the validity, the method developed

was applied to the water samples with metal spiked, and the results obtained are given in Table 4.

Water samples taken from Çoruh (Artvin-Turkey), Kızılırmak and Yeşilirmak (Samsun-Turkey) rivers and Beyazsu stream (Rize-Turkey) were filtered through 0.45  $\mu\text{m}$  porous cellulose ester filters. The separation and preconcentration processes in water samples were carried out by applying the method developed. The same procedure was applied to the samples of sea water taken with Nansen bottles from the surface and a depth of 200 m at 40°58.662' N - 39°51.275' E of the Black Sea (Table 5).

## CONCLUSIONS

Compounds of sulfur-containing functional groups act as selective ligands forming stable complexes with transition metals. Therefore, resins of dithiocarbamate groups are used effectively to keep a lot of heavy metal ions. Another advantage

is that dithiocarbamate resins show very little affinity to the alkali and alkaline earth materials [18]. As a result, new synthesized XAD-4-EADTC resin could be used in the preconcentration and separation of Cd(II), Pb(II), Cu(II), Zn(II) and Mn(II) ions in natural and synthetic samples. In addition, since the method developed in this study was applied to environmental samples, it could contribute to other studies on analysis of trace elements as an alternative treatment in terms of routine work.

#### ACKNOWLEDGEMENT

The authors of this study are grateful to Dr. Beytullah Ertem for helping during the process of synthesis and Muammer Erdöl for his assistance FTIR spectrophotometer.

#### REFERENCES

- [1] Babu, S.H., Kumar, K.S., Suvadhan, K., Kiran, K., Rekha, D., Krishnaiah, L., Janardhanam, K. and Chiranjeevi, P. (2007) Preconcentration technique for the determination of trace elements in natural water samples by ICP-AES. *Environmental monitoring and assessment* 128, 241-249.
- [2] Uzun, A., Soylak, M. and Elçi, L. (2001) Preconcentration and separation with Amberlite XAD-4 resin; determination of Cu, Fe, Pb, Ni, Cd and Bi at trace levels in waste water samples by flame atomic absorption spectrometry. *Talanta* 54, 197-202.
- [3] Dogru, M., Gul-Guven, R. and Erdogan, S. (2007) The use of *Bacillus subtilis* immobilized on Amberlite XAD-4 as a new biosorbent in trace metal determination. *Journal of hazardous materials* 149, 166-173.
- [4] Hosseini, M.S., Raissi, H. and Madarshahian, S. (2006) Synthesis and application of a new chelating resin functionalized with 2,3-dihydroxy benzoic acid for Fe(III) determination in water samples by flame atomic absorption spectrometry. *Reactive and Functional Polymers* 66, 1539-1545.
- [5] Tokman, N., Akman, S. and Ozcan, M. (2003) Solid-phase extraction of bismuth, lead and nickel from seawater using silica gel modified with 3-aminopropyltriethoxysilan filled in a syringe prior to their determination by graphite furnace atomic absorption spectrometry. *Talanta* 59, 201-205.
- [6] Wen, B., Shan, X.Q., Liu, R.X. and Tang, H.X. (1999) Preconcentration of trace elements in sea water with poly (acrylamino phosphonic-dithiocarbamate) chelating fiber for their determination by inductively coupled plasma mass spectrometry. *Fresenius Journal of Analytical Chemistry* 363, 251-255.
- [7] Keil, O., Dahmen, J. and Volmer, D.A. (1999) Automated matrix separation and preconcentration for the trace level determination of metal impurities in ultrapure inorganic salts by high-resolution ICP-MS. *Fresenius Journal of Analytical Chemistry* 364, 694-699.
- [8] Türker, A.R. (2007) New Sorbents for Solid-Phase Extraction for Metal Enrichment. *CLEAN – Soil, Air, Water* 35, 548-557.
- [9] Türker, A.R. (2012) Separation, Preconcentration and Speciation of Metal Ions by Solid Phase Extraction. *Separation & Purification Reviews* 41, 169-206.
- [10] Young-Sang, K., Gyo, I., Cheol-Woo, H. and Jong-Moon, C. (2005) Studies on synthesis and application of XAD-4-salen chelate resin for separation and determination of trace elements by solid phase extraction. *Microchemical Journal* 80, 151-157.
- [11] Camel, V. (2003) Solid phase extraction of trace elements. *Spectrochimica Acta Part B* 58, 1177-1233.
- [12] Vanloot, P., Boudenne, J.L., Brach-Papa, C., Sergent, M. and Coulomb, B. (2007) An experimental design to optimize the flow extraction parameters for the selective removal of Fe(III) and Al(III) in aqueous samples using salicylic acid grafted on Amberlite XAD-4 and final determination by GF-AAS. *Journal of hazardous materials* 147, 463-70.
- [13] Sturgeon, R.E., Berman, S.S., Willie, S.N. and Desauiniers, A.H. (1981) Preconcentration of Trace Elements from Seawater with Silica-Immobilized 8-Hydroxyquinoline. *Anal. Chem.* 53, 2337-2340.
- [14] Lee, C.H., Kim, J.S., Suha, M.S. and Leeb, W. (1997) A chelating resin containing 4-(2-thiazolylazo) resorcinol as the functional group Synthesis and sorption behaviour for trace metal ions. *Analytica Chimica Acta* 339, 303-312.
- [15] Venkatesan, K.A., Srinivasan, T.G. and Rao, P.R.V. (2001) Cobalt-extraction studies on dithiocarbamate grafted on silica gel surface. *Colloids and Surfaces A: Physicochemical and Engineering Aspects* 180, 277-284.
- [16] Boudenne, J.L., Boussetta, S., C., B.P., Branger, C., Margailan, A. and Theraulaz, F. (2002) Modification of poly(styrene-co-divinylbenzene) resin by grafting on an aluminium selective ligand. *Polymer International* 51, 1050-1057.
- [17] McClain, A. and Hsieh, Y.L. (2004) Synthesis of Polystyrene-Supported Dithiocarbamates and Their Complexation with Metal Ions.



Journal of Applied Polymer Science 92, 218-225.

- [18] Roy, P.K., Rawat, A.S. and Rai, P.K. (2003) Synthesis, characterisation and evaluation of polydithiocarbamate resin supported on macroreticular styrene-divinylbenzene copolymer for the removal of trace and heavy metal ions. *Talanta* 59, 239-246.

---

**Received: 07.01.2016**

**Accepted: 21.08.2016**

---

#### **CORRESPONDING AUTHOR**

---

**Dr. Ali Alkan**

Karadeniz Technical University, Institute of Marine  
Sciences and Technology, 61080, Trabzon,  
TURKEY

e-mail : [aalkan@ktu.edu.tr](mailto:aalkan@ktu.edu.tr)

# LEVELS OF HEAVY METALS IN FISHES (*POLYSTEGANUS COERULEOPUNCTATUS*, *ARGYROPS SPINIFER* AND *ARGYROPS FILAMENTOSUS*) FROM THE GULF OF AQABA, JORDAN

Tariq Al-Najjar<sup>1,\*</sup>, Rashad Gassaymah<sup>1</sup>, Maroof Khalaf<sup>1</sup>, Mohammad Wahsha<sup>2</sup>, NoomanKhalaf<sup>3</sup>, Khalid Abu Khadra<sup>4</sup>

<sup>1</sup>Department of Marine Biology, The University of Jordan, Aqaba Branch, Jordan

<sup>2</sup>Marine Science Station, The University of Jordan, Aqaba Branch, Jordan

<sup>3</sup>Al-Ahliyya Amman University, Faculty of Pharmacy and Medical Sciences, Amman

<sup>4</sup>Department of Biological Sciences, Yarmouk University, Irbid, Jordan

## ABSTRACT

Heavy metal concentrations of Zn, Cr, Cd and Cu were investigated using flame Atomic Absorption Spectrophotometer (AAS) in liver, gills and muscles of three mesopelagic fish species from the northern Gulf of Aqaba (*Argyrops filamentosus*, *Argyrops spinifer* and *Polysteganus coeruleopunctatus*) collected during the period from 21/6/2014 to 15/1/2015. The results did not show any significant difference between different fish species, yet liver was found to be the major organ of bioaccumulation of Zn, Cr, Cd and Cu followed by gills, whereas muscles were found to have the lowest level of bioaccumulation. The levels of metal concentration of the present study were generally lower or within the ranges of those found in the fish of the Red Sea. After all, fish of this study were found to be safe for consumption and do not pose a significant threat to the health of human consumers.

## KEYWORDS:

Heavy metals, Fishes, Levels, Concentrations, Aqaba, Red Sea

## INTRODUCTION

Heavy metals constitute one of the most insidious and dangerous pollutants known to human. They are now considered to be among the most effective environmental contaminants, and their release into the environment has increased since the last decades, threatening all creatures and the environment. Heavy metals are not readily converted into harmless components; they are often accumulated in the tissues of organisms, which can't excrete them [1].

Bioindicators are species that can be used to

monitor the health of an environment or ecosystem. They are any biological species or group of species whose function, population, or status can reveal the qualitative status of the environment. Recently, biological organisms such as fish, molluscs, and echinoderms have been used as indicators for quantitative heavy metal concentrations in their different tissues or organs.

There are many reports about fish contamination by chemicals in the marine environment [2]. Fish may concentrate large amounts of metals from water and they might be toxic for human consumption [3]. According to [4] heavy metals may enter fish bodies by three possible routes, through the body surface, gills and the digestive tract. However, fish are the major part of the human diet, fishes are situated at the top of the aquatic food chain therefore they accumulate heavy metals from food, water and sediment which is one of the most dangerous aspects of pollution [5, 6].

Several studies reveal a susceptibility of the Gulf of Aqaba to metal pollution [7, 8, 9, 10, 11, 12, 13, 14, 15, 16], these studies stated that the Gulf of Aqaba is surrounded mostly by dry desert lands, thus, it has a great chance to get polluted with metals carried by air winds[17], in addition to that, the development of Aqaba city after the declaration from the Jordanian authority that Aqaba city is special economic zone authority in the year 2000, and the large human activity that affected the landscape and marine ecosystem increased the probability to raise the level of heavy metals in the marine biota. This study aims to provide knowledge and establish data base of the levels of heavy metals in three species of the family Sparidae: *Polysteganus coeruleopunctatus*, *Argyrops spinifer* and *Argyrops filamentosus* that live in mesopelagic water and are consumed by local's community.



**FIGURE 1**

**Gulf of Aqaba, with its semi-enclosed nature**

## MATERIALS AND METHOD

**Study Area.** The Gulf of Aqaba is located at the east fork of the Red Sea (Figure 1). Its coasts are shared by Jordan, Palestine, Egypt and Saudi Arabia. The Gulf contains the only port for Jordan, Aqaba port, which the Gulf is named after. The Gulf biodiversity is unique, and some species are endemic to the area. It gained a high and unique biodiversity due to its semi enclosed nature, which also makes it more susceptible to pollution with these metals. After the year 2000, Aqaba was declared as a special economic zone. The chance for pollution to occur has increased in the Jordanian sector of the Gulf of Aqaba, especially the chance for metal pollution due to the developments that were made along the coastline of the Gulf, represented by the projects carried out in different fields such as industry and tourism [16].

**Sample collection.** Fifteen fish from each species were collected by professional fishermen using fish traps, long line with about 120 hooks and short long line with about 20 hooks from areas along the Jordanian coast of the Gulf of Aqaba (located at the most northern corner of the Gulf (latitude N29° 30' 137" and longitude E 34° 59' 200") (Fig. 1). Fish samples were placed in clean plastic bags and carried to the laboratory of the Marine Science Station., each fish was washed by distilled water, to get rid of any remnants of trace metals on the outer surface of the fish. After that, the samples were dissected using a stainless steel knife. Samples of each of the following organs were taken: liver, muscle, and gills then placed in clean plastic bags and kept under -20°C for further analysis [13].

## Sample treatment and digestion.

Samples of liver, muscle and gills were dried using oven for 24hrs to obtain a constant weight. Sub sample from each organ (0.1-0.5 mg/ dry. wt.) were burned using muffle furnace at 550°C, after that samples were cooled to room temperature and then digested in acid cleaned jars with hot concentrated nitric acid to release heavy metals. The organic materials in each sample were completely digested. The digests were allowed to cool, filtered through a 0.45µm Millipore membrane filter, The filtrate was transferred to 25 ml volumetric flasks and made up to mark with 1% nitric acid and diluted with double distilled water to 25 ml. The digests were kept in plastic bottles, heavy elements, Cu, Cr, Cd and Zn concentrations were determined using Atomic Absorption Spectrophotometer (AAS) (modified form [18] available in Marine Science Station. Metal contents were expressed as µg g<sup>-1</sup> dry weight [18].

## RESULTS

Table (1) show the mean concentration ± Standard Deviation (S.D) of the four elements, Cu, Cr, Cd and Zn in the selected organs, (liver, muscle and gills) of the three mesopelagic fish *A. filamentosus*, *A. spinifer* and *P. coeruleopunctatus*.

Figure 2 shows the mean concentration of Cu, Cr, Cd and Zn in all sampled organs ± Standard Deviation. Liver was found to be the major organ of copper bioaccumulation ( $p < 0.05$ ), with mean concentration of 15.21 µg/g, followed by the Gills, with mean concentration of 4.35 µg/g, and Muscles with mean concentration of 0.99 µg/g. Liver was found to be the major site of Chromium bioaccumulation, with mean of 30.59 µg/g ( $p < 0.05$ ), followed by the Muscles, with mean concentration of 16.8 µg/g, and Gills with mean concentration of 16.57 µg/g ( $p < 0.05$ ). Liver was found to be the major site of Cadmium accumulation with mean of 6.66 µg/g ( $p < 0.03$ ), followed by the Gills, with mean concentration of 6.22 µg/g, and Muscles with mean concentration of 4.17 µg/g ( $p < 0.05$ ). Liver was also found to be the major site of Zinc bioaccumulation, with mean of 281.2 µg/g, followed by the Gills, with mean concentration of 205.42 µg/g, and Muscles with mean concentration of 94.7 µg/g.

Figures (3-6) summarize the results of the investigated metals (Cu, Cr, Cd and Zn) with the fish species (*A. filamentosus*, *A. spinifer* and *P. coeruleopunctatus*). The results showed that the fish species had no statistical significant effect on all of the metal concentrations.

**TABLE 1**  
**Mean concentration ( $\mu\text{g/g}$ )  $\pm$  S.D of Cu, Cr, Cd and Zn in, Liver, Muscle and Gills of *A. filamentosus*,  
*A. spinifer* and *P. coeruleopunctatus*.**

Fish species	Element Organ	<i>Cu</i>	<i>Cr</i>	<i>Cd</i>	<i>Zn</i>
		<i>A. filamentosus</i>	Liver	26.36 $\pm$ 32.15	34.01 $\pm$ 22.10
	Muscle	0.39 $\pm$ 0.20	17.97 $\pm$ 8.19	4.34 $\pm$ 0.17	200.74 $\pm$ 116.66
	Gills	7.38 $\pm$ 3.80	14.98 $\pm$ 2.98	6.57 $\pm$ 0.28	230.80 $\pm$ 49.77
	Mean $\pm$ S.D	11.38 $\pm$ 12.05	22.32 $\pm$ 11.09	6.06 $\pm$ 1.24	222.09 $\pm$ 95.11
<i>A. spinifer</i>	Liver	10.31 $\pm$ 7.69	21.92 $\pm$ 12.35	6.33 $\pm$ 2.85	286.69 $\pm$ 171.72
	Muscle	1.32 $\pm$ 0.83	13.49 $\pm$ 0.81	4.17 $\pm$ 0.23	123.62 $\pm$ 18.18
	Gills	3.22 $\pm$ 1.23	11.99 $\pm$ 6.72	6.21 $\pm$ 0.32	204.74 $\pm$ 48.18
	Mean $\pm$ S.D	4.95 $\pm$ 3.25	15.8 $\pm$ 6.63	5.57 $\pm$ 1.13	205.02 $\pm$ 79.36
<i>P. coeruleopunctatus</i>	Liver	8.96 $\pm$ 3.90	35.83 $\pm$ 30.53	6.07 $\pm$ 2.71	322.18 $\pm$ 124.94
	Muscle	1.24 $\pm$ 0.53	18.93 $\pm$ 7.19	3.99 $\pm$ 0.21	80.06 $\pm$ 20.15
	Gills	2.44 $\pm$ 0.65	22.74 $\pm$ 16.21	5.87 $\pm$ 0.25	180.73 $\pm$ 29.65
	Mean $\pm$ S.D	4.21 $\pm$ 1.69	25.83 $\pm$ 17.98	5.31 $\pm$ 1.06	194.32 $\pm$ 58.25
	Permissible Limit	37500*	100**	1250*	125000*

\* [19]

\*\*[20]

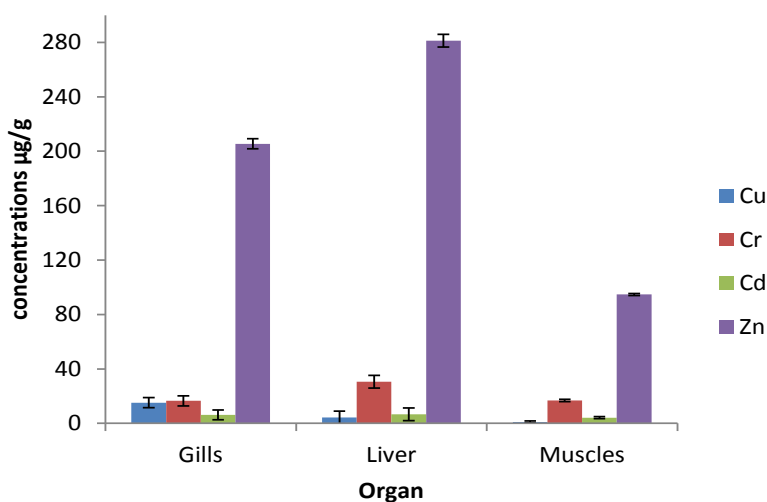


**FIGURE 2**  
**Mean concentration ( $\mu\text{g/g}$ )  $\pm$  S.D of Cu, Cr, Cd and Zn in Gills, Livers and Muscles of the three fish species.**



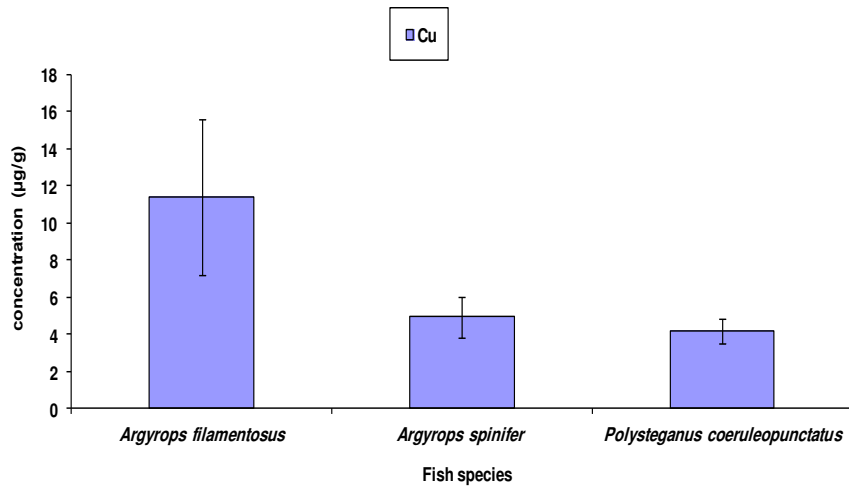


**FIGURE 3**  
Mean concentration (µg/g) ± S.D of Cu in different fish species

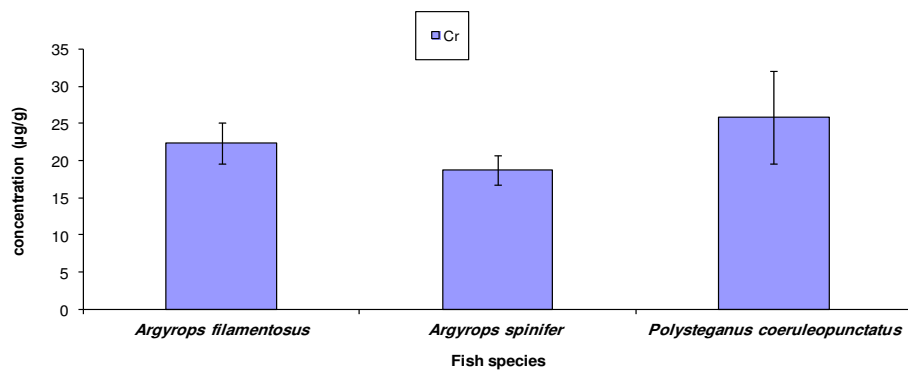


**FIGURE 4**  
Mean concentration (µg/g) ± S.D of Cr indifferent fish species

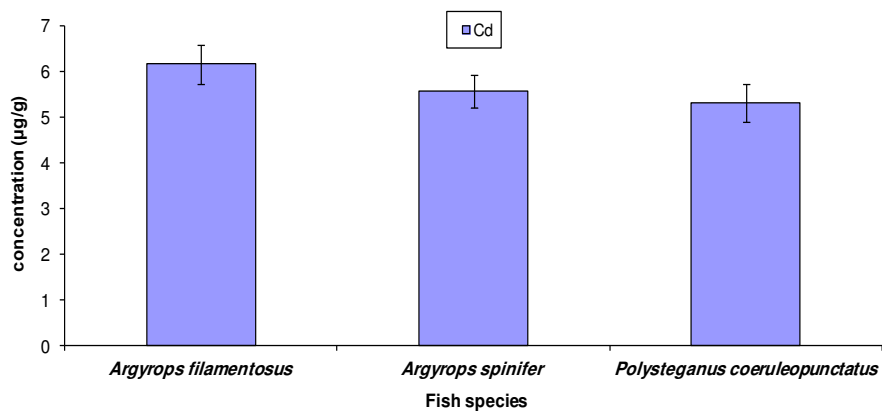


**FIGURE 5**  
Mean concentration (µg/g) ± S.D of Cd indifferent fish species

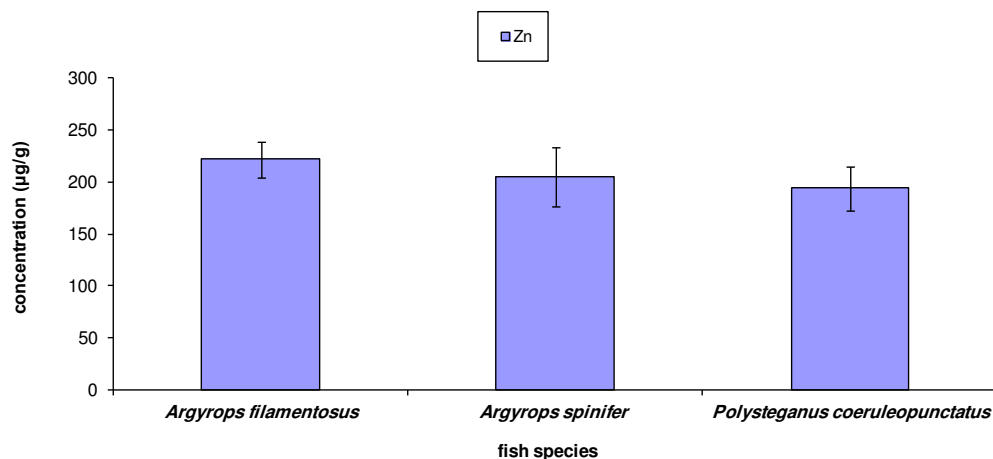


**FIGURE 6**  
**Mean concentration (µg/g) ± S.D of Zn in different fish species**

## DISCUSSION

The assessment and determination of the levels of heavy metals in commercial fish species have reached a considerable level of attention in different countries and organizations around the world because of the toxicity of heavy metals and their accumulation in biota. This interest aimed to insure the safety of the food supply, to minimize the potential hazard effect on human health and to evaluate ecosystem situation.

Our results revealed that, there is no significant difference between heavy metal concentration and different fish species of this study; this could be due to the same feeding habits of the three demersal mesopelagic fish species. Several studies showed that the feeding habits play an important role in the final metal concentrations of different fish species. [8], found significant differences in heavy metal concentrations in six coral reef fish species from the same area of different feeding habits, from piscivorous species such as the lizardfish (*Synodus variegates*) to those feed on invertebrates, such as the goatfish (*Parupeneus barberinus*), or on algae, such as the Sergeant Major fish (*Abudefduf saxatilis*). In a study on three species, *Oreochromis mossambicus*; an omnivore fish, *Ophiocephalus striatus*; a piscivore fish and *Heteropneustes fossilis*; a detritivore fish, it was found that the piscivore had the highest bioaccumulation for all metals that were measured because of the bio-magnification factor, except for Fe and Mn, which were the highest in the detritivore species, which might be due to very high levels in the sediments [21].

Our results indicated that, metal concentration vary among different fish organs. It was found that the livers of a three commercially important fish

species studied had higher levels of Cu, Cr, Zn and Cd compared to muscle tissues and gills. The lowest concentrations were measured in muscles. The high accumulation of heavy metals in the livers of the three species of this study has likewise been reported in numerous studies [14, 15, 22, 23]; these studies suggested that the liver plays an important role in the metabolic processes of heavy metals in fishes. According to [24], muscles are primary part of metal intake, the liver is an organ that specializes in metal storage and detoxification, and the gills are directly exposed to the surrounding environment. Our results are in accordance with the study of [13], where the researchers reported that muscles have the lowest concentration of metals in most of the nine species that were studied, while stomach and liver had the highest. Also, our results are in accordance with the study by [14], they indicated significant differences for most of the heavy metal elements among different organs of the same species, particularly the presence of low concentrations of Cu, Pb, Zn, Cd and Fe in the muscles of *D. macarelleus* and low concentrations of Ni, Pb, Zn and Fe in the muscles of *D. macrosoma*. Similarly, in *D. russelli* the lowest concentration of Cu, Pb, Zn, Cd and Fe were found in muscles. In contrast, [15], found that, Cu, Pb, Cd and Fe were mainly concentrated in the liver and kidney, he found that there are no significant differences in the concentrations of metals between the two fish species *Caesio varilineata* and *Caesio lunaris*, but it was found that different organs have concentrated different metals. [23], studied trace element concentrations in the livers and muscles of *E. affinis* collected from Malaysia, and found that almost all elements have higher concentrations in the liver than those in the muscles, especially Zn, were they found that *E. affinis* had extremely high level of

**TABLE 2**  
**Heavy metals in muscles (mg/g) of fish from the Red Sea and other regions.**

Fish Species	Site	Cu	Zn	Cr	Cd	Reference
<i>Acanthopagurus bifaclatus</i>	Red Sea	0.51	4.34	0.72	0.26	[32]
<i>Ctenochaetus striatus</i>	Gulf of Aqaba Red Sea	0.87	21.38	1.36	0.83	[12]
<i>Lethrinus sp.</i>	Red Sea	0.40	8.00	0.34	0.45	[29]
<i>Scomberomrus commerson</i>	Yemen Gulf Aden	1.3	8.00	0.9	0.39	[33]
<i>Boops boops</i>	Black Sea	3.08	6.81	0.22	0.10	[34]
<i>Thunnus thynnus</i>	Mediterranean Sea	1.01	16.54	0.74	0.05	[35]
<i>Nemipterus japonicas</i>	Hurghada Red Sea	0.28	2.13	0.82	0.02	[36]
<i>Caranxsex faciatus</i>	Jeddah coast Red Sea	0.91	5.33	0	0.9	[31]

Zn in liver compared to the muscles. Liver had the highest level of Mg, this could be related to the role of Mg in the detoxification reactions in the liver, as a cofactor for enzymes that catalyze phase II detoxification reactions.

According to [25], muscles are not an active site for metal biotransformation and accumulation, but in polluted aquatic habitats the concentration of metals in fish muscles may exceed the permissible limits for human consumption and imply severe health threats. To assess public health risk of fish consumption in the Gulf of Aqaba, we compared metal levels in muscles of the current study with the maximum permissible limits for human consumption reported by [26]. The metal concentrations in the examined fish species from the Gulf of Aqaba were below the permissible limits for human consumption. The results from previous literatures (Table 2) were somewhat closer to or lower than our obtained concentrations for other fish species. For instance, [27], recorded the concentrations of Cd, Pb, Cu and Zn in the muscles of *Sardinella aurita*, *Sardinella rivulatus* and *Synodus saurus* from two main harbors in Alexandria, Egypt, who reported metal levels much higher than those recorded in the same species of the current work. In addition, metal levels in the present study were generally lower or within the ranges of those found in the fish of the Red Sea recorded by [28, 29, 30, 31]. After all, fishes of this study were found to be safe for consumption and do not pose a significant threat to the health of human consumers.

## CONCLUSIONS

Heavy metals concentrations in the three studied fish species were within the same range or lower than other species from previous studies in the

Jordanian water or elsewhere.

The results showed that metal accumulation varied between organs, the highest concentrations was for livers and the lowest concentrations for muscles, which agrees with the previous studies for the other fishes of the Gulf of Aqaba in which liver is the sink of these heavy metals, and the detoxification site. The results showed that the studied heavy metals accumulation did not vary between species. The heavy metals concentrations in the examined fish species from the Gulf of Aqaba were below the permissible limits for human consumption reported by WHO, (1989).

## ACKNOWLEDGEMENTS

The authors would like to thank the efforts of Aqaba marine Park staff Khaldoun AlKhudari, Mohammad Abu- Ghrigane and Hareth Abu Miatiq for their great help in collecting samples from the fishermen. A special thanks for all the staff of the Marine Science Station in Aqaba, mainly Shadia Al-Riyati, for all the help she provided during the digestion, reading of the samples using Atomic Absorption Spectrophotometer. The Authors would like to thank the financial support and logistic cooperation with UNDP.

## REFERENCES

- [1] Phillips, D.J.H. (1977) The use of biological indicator organism to monitor trace metal pollution in marine and 154 estuaries environment - A review. *Knvirnn. Pollution International*. 13: 281-317.
- [2] Hajeb, P., Jinap, S., Ismail, A., Fatimah, A.B., Jamilah J., and Rahim, M.A. (2009) Assessment

- of mercury level in commonly consumed marine fishes in Malaysia. *Food Control* 20(1): 79-84.
- [3] Rasheed, R.O. (2012) Assessment of some Heavy Metals in Muscle Tissue of *Silurus triostegus* from Derbendikhan Reservoir, Kurdistan Region –Iraq. *Raf. J. Sci.* 23(1): 11-18.
- [4] Javed, M. (2005) Heavy metal contamination of freshwater fish and bed sediments in the river Ravi stretch and related tributaries. *Pakistan Journal of Biological Sciences.* 8: 1337-1341.
- [5] Rayment, G.E. and Barry, G.A. (2000) Indicator tissues for heavy metal monitoring-additional attributes. *Marine Pollu. Bull.* 7: 353-358.
- [6] Turkmen, A., Turkmen M., Tepe, Y. and Akyurt, I. (2005) Heavy metals in three commercially valuable fish species from Iskenderun bay, Northern East Mediterranean Sea, Turkey. *Food Chem.* 91: 167-172.
- [7] Wahbeh, M.I., (1985) Levels of zinc, iron, magnesium and cadmium in the tissue of fish from Aqaba, Jordan. *Dirasat.* 12: 35-42.
- [8] Wahbeh, M.I., and Mahasneh, D.M., (1987) Concentrations of metals in the tissues of six species of fish from Aqaba, Jordan. *Dirasat.* 14: 119-129.
- [9] Al-Sayed, M. (2008) Levels of trace metals in some Carnivorous fish of Gulf of Aqaba, Red Sea. Master's Thesis, Hashemite University, Zarka.
- [10] Al-Zgool, A. (2008) Levels of trace metals in food chain of some carnivores fishes (Family: Carangidae) collected from the Gulf of Aqaba, Red Sea. Master's Thesis, Hashemite University, Zarka.
- [11] Batayneh, M. (2010) Levels of trace metals in some Herbivorous fish of Gulf of Aqaba, Red Sea. Master's Thesis, Hashemite University, Zarka.
- [12] Ismail, N.S. and Abu-Hilal, A.H. (2008) Heavy metals in three commonly available coral reef fish species from the Jordan Gulf of Aqaba, Red Sea. *Jordan Journal of Biological Sciences.* 2: 61-66.
- [13] Abu-Hilal, A.H. and Ismael, N.S. (2008) Heavy metals in eleven common species of fish from the Gulf of Aqaba, Red Sea. *Jordan Journal of Biological Sciences.* 1:13-18.
- [14] Khalaf, M. A., Al-Najjar, T., Alawi, M., Disi, A. M. (2012) Levels of Trace Metals in Three Fish Species *Decapterus macrellus*, *Decapterus macrosoms* and *Decapterus russelli* of the Family Carangidae from the Gulf of Aqaba, Red Sea, Jordan. *Natural Science.* 4: 362-367.
- [15] Al-Najjar T., Khalaf, N., Allawi, M., Disi, A. (2012) Levels of Trace Metals in Two Fish Species *Caesio varilineata* and *Caesio lunaris* of the Family Caesionidae from the Gulf of Aqaba, Red Sea. *Fresen. Environ. Bull.* 21(5): 1152-1157.
- [16] Al-Najjar, T., Abu Khadra, K., Rawashdeh, O.Y., Khalaf, M., Wahsha, M. (2015) Levels of Trace Metals in (*Euthynnus affinis*) Fish from the Gulf of Aqaba, Jordan. *Fresen. Environ. Bull.* 24(9a): 2995-3000.
- [17] Chen, Y., Paytan, A., Chase Z., Measures C., Aaron, J., Sergio, B., San, A., Wilhelmy, U., and Anton F. P. (2008) Sources and fluxes of atmospheric trace elements to the Gulf of Aqaba, Red Sea. *Journal of Geophysical Research.* 1-13.
- [18] Bernhard, M. (1976) *Manual of Methods in the Aquatic Environment Research*, FAO Fisheries Technical Paper, Food and Agriculture Organisation, no.158
- [19] Mokhtar, M. (2009) Assessment level of heavy metals in *Penaeus monodon* and *Oreochromis spp.* in selected aquaculture ponds of high densities development area. *Eur J Sci Res.* 30: 348-60.
- [20] Katz, S.A., Salem, H. (1992) The toxicology of chromium with respect to its chemical speciation: A review. *Journal of Applied Toxicology.* 13 (3): 217–224.
- [21] Wijesinghe, M.R., Wijeratne, Y.N.A., and Hewamanna, R. (1999) Bio-accumulation of heavy metals in *Oreochromis mossambicus* (extended abstract).
- [22] Honda, K., Sahrul, M., Hidaka, H. and Tatsukawa, R. (1983), Organ and tissue distribution of heavy metals and their growth-related changes in Antarctic fish, *Pagothenia borchgrevinki*. *Agricultural and Biological Chemistry.* 47: 2521–2532.
- [23] Agusa, T., Kunito, T., Kubota, R., Tanabe, R. and Iwata, H. (2012) Exposure, metabolism, and effects of arsenic in residents from arsenic-contaminated Groundwater Areas of Southeast Asia. *Interdisciplinary Studies on Environmental Chemistry Environmental Pollution and Ecotoxicology.* 125-132.
- [24] Kotze, P.H., Preez, H.H. and VanVuren J.H.J. (1999) Bioaccumulation of copper and zinc in *Oreochromis mossambicus* and *Clarias garipinus*, from the Olifants River, Mpumalanga, South Africa. *Water SA.* 25: 99-110.
- [25] Elnabris, K.J., Muzyed S.K., El-Ashgar, N.M. (2013) Heavy metal concentrations in some commercially important fishes and their contribution to heavy metals exposure in Palestinian people of Gaza Strip (Palestine). *Journal of Association of Arab Universities for Basic and Applied Sciences.* 13: 44-51.
- [26] WHO. (1996) *Guidelines for Drinking Water Quality Volume 2, Health Criteria and Other*



- Supporting Information, World Health Organization, Geneva, Switzerland.
- [27] Abdallah, M.A.M. (2008) Trace element levels in some commercially valuable fish species from coastal waters of Mediterranean Sea. Egypt. Journal of Marine System. 73: 114-22.
- [28] Hanna, R.G.M. (1989) Levels of heavy metals in some Red Sea fish before Hot Brine pools' mining. Marine Pollution Bulletin, 20, 631–635.
- [29] Abdelmoneim, M.A., El-Deek, M.S. (1992) Lethrinus family: a model of edible Red Sea fish with low heavy metals accumulation. National Institute of Oceanography and Fisheries. 19: 589-596.
- [30] Emara, H.I., El-Deek, M.S., Ahmed, N.S. (1993) A comparative study on the levels of trace metals in some Mediterranean and Red Sea fishes. Chemistry and Ecology. 8: 119-127.
- [31] Ali, A.A., Elazein, E.M., Alian, M.A. (2011) Investigation of heavy metals pollution in water, sediment and fish at Red Sea- Jeddah Coast-KSA at two different locations. Journal of Applied Environmental Biological Sciences, 1(12): 630-637.
- [32] Abdelmoneim, M. Khaled, A. and Iskander, M. (1994) A study on the levels of some heavy metals in EL-mex, west of Alexandria, Egypt .The 4th conf. of the Environ. Prot. 10-12 May, 155-174.
- [33] Al-Adrise, M.A.M. (2002) Concentration of some heavy metals in Khor-Kutheb Area (Al-Hodiedah) as a result of the sewage effluent impacts. M.Sc Thesis. Faculty of Science, Sana'a University, Yemen.
- [34] Gorur, F.K., Keser, R., Akcay, N., Dizman, S. (2012) Radioactivity and heavy metal concentrations of some commercial fish species consumed in the Black Sea Region of Turkey. Chemosphere. 87, 356-361.
- [35] Hussein, A., and Khalid, A. (2014) Determination of metals in tuna species and bivalves from Alexandria, Egypt. Egyptian Journal of Aquatic Research. 40(1): 9-17.
- [36] El-Moselhy, K.H.M., Othman, .A.I., Abd El-Azem, B. H. and El-Metwally M.E.A. (2014) Bioaccumulation of heavy metals in some tissues of fish in the Red Sea, Egypt. Egyptian Journal of Basic and Applied Sciences. 1: 97 -

105.

---

**Received:** 17.01.2016  
**Accepted:** 21.08.2016

---

#### **CORRESPONDING AUTHOR**

---

**Tariq Al-Najjar**

Department of Marine Biology, The University of Jordan, Aqaba Branch, Jordan

Email: m.wahsha@ju.edu.jo

# ESTIMATION OF LEAF AREA INDEX(LAI) OF POYANG LAKE BASIN IN SUMMER USING GF-1 DATA

Hui Jiang<sup>1,2</sup>, Xiaoling Chen<sup>1,\*</sup>, Yao Liu<sup>2</sup>, Lian Feng<sup>1</sup>, Xinxin Han<sup>1</sup>

<sup>1</sup> State Key Laboratory of Information Engineering in Surveying, Mapping and Remote Sensing, Wuhan University, Wuhan 430079, China;

<sup>2</sup> JiangXi Engineering Research Center of Water Engineering Safety and Resources Efficient Utilization, Nanchang Institute of Technology, Nanchang, 330099, China

## ABSTRACT

GF-1 is a China's new high-resolution remote sensing satellite, which is characterized by high temporal and spatial resolutions as well as wide coverage. It provides new satellite resource to accurately and effectively monitor leaf area index (LAI). In this study, the monitoring of LAI was conducted with different land cover types during two times (July 26th ~July 30th, 2014, and July 28th~August 5th, 2015), with the adoption of the Poyang Lake basin as the study area. Then the linear and nonlinear correlation analyses were conducted on the measured LAI data and the corresponding single-band data of GF-1 as well as 8 vegetation indexes (VIs). By constructing the LAI remote sensing inversion model, the high-accuracy LAI data were extracted. The research results indicate that, the data in the BLUE, GREEN, RED bands of GF-1 have high correlations with each other ( $R > 0.89$ ), but the data in near-infrared (NIR) band of GF-1 have poor correlations with the data in other three bands ( $R < 0.3$ ). The NIR and RED bands has strong reflection and absorption capacities separately, which is connected with the plant's spectral characteristics. LAI is negatively correlated with the reflectivity data in the BLUE, GREEN, RED bands of GF-1 but is positively correlated with VIs and the reflectivity data in the NIR band of GF-1. Most VIs are superior to single-band models in terms of the inversion of LAI. However, using the exponential model, the correlation between NDVI and the measured LAI is largest ( $R^2 = 0.744$  and  $RMSE = 0.303$ ). The results satisfy F test and have significant correlations. Accordingly, GF-1 satellite data is applicable to the monitoring of LAI with a high resolution over large areas.

## KEYWORDS:

Leaf area index (LAI); GF-1; Remote Sensing; Vegetation indexes; Poyang Lake

## INTRODUCTION

Vegetation is a key component of the earth's ecological system, which temporal and spatial variations are quite crucial for global or regional climate changes as well as environmental management. Leaf area index (LAI) is a main variable parameter for the monitoring of vegetation, which controls the plants' many processes such as photosynthesis, respiration, transpiration and precipitation interception. Furthermore, LAI is an important input parameter in ecology, hydrology, meteorology and biogeochemical models. Leaf area index (LAI) is defined as one half of the total green leaf area per unit horizontal ground surface area [1]. How to accurately and effectively gain LAI has become a key question in many studies, and therefore, the monitoring of LAI over a large area based on the remote sensing data is very significant. Currently, it is an efficient way to extract LAI information based on satellite remote sensing data, and many global LAI products using the data collected by MODIS, SPOT, GLASS, AVHRR and IRC-TIP satellites have been developed [2-6]. Most of LAI data were acquired using the medium-resolution or high-resolution remote sensing data with the spatial resolution above 30 m, such as Landsat TM and ETM+ [7], HJ-1A/1B [8] and ASTER [9]. Owing to their easy accessibility, these data have been widely applied in the LAI studies. Nevertheless, these satellite data cannot satisfy the requirements in the studies of LAI on a small scale. For the small regions with great spatial heterogeneity, the data with a high spatial resolution are required for accurately extracting LAI data from the ecological environmental parameters, so that the acquired data can accurately reflect the temporal and spatial variations. With the development of satellite technology, the spatial resolution of satellite image becomes increasingly higher and the spectral characteristics also become more targeted. For example, China plans to launch 9 high-resolution satellites, in which the first Gaofen Satellite (GF-1) has been launched in 2013. This study aims at deriving high-spatial-resolution (16m) of GF-1

Satellite data to monitor LAI through the statistical regressions between vegetation indexes and field samplings. So far, few literatures on the analysis of LAI using the data collected by GF Satellite have been reported, and more in-depth studies should be performed on the exploration and analysis of the data collected by China's new satellites so as to derive the high-resolution vegetation indexes (VIs) which are closely related to LAI. In this study, 8 VIs, namely, normalized difference vegetation index (NDVI), renormalized difference vegetation index (RDVI), enhanced vegetation index (EVI), simple ratio vegetation index (SR), soil adjustment vegetation index (SAVI), modified soil adjustment vegetation index (MSAVI), modified simple ratio index (MSR) and atmospherically resistant vegetation index (ARVI), were selected for analysis, all of which are located from BLUE band to near-infrared (NIR) band. These VIs are suitable for the applications of GF-1 satellite multi-spectrum data and can favorably reflect the vegetation growth characteristics.

## MATERIALS AND METHODS

**Study area.** Poyang Lake basin is located on the South Bank in the middle and lower reaches of Yangtze River (24°33'–30°07'N, 113°50'–118°30'E)(Fig.1). It covers an area of 162200 km<sup>2</sup>, which occupies 9% of the total area of the Yangtze River basin and 93.9% of the area of Jiangxi Province. The Poyang Lake basin is surrounded by the mountains,

in which water from Ganjiang, Fuhe, Raohe, Xinjiang and Xiuhe flows into the Poyang Lake, the largest freshwater lake in China, and then feeds into the Yangtze River. The study area is characterized by a subtropical humid monsoon climate, with four distinctive seasons. It is abundant in rainfall and has an annual average temperature of 17°C. According to the classification of vegetation coverage by GLOBCOVER CLASSIFY, the study area includes woodland, farmland, grassland and water area, in which the area of woodland occupies 54.0% of the total area. To make a further classification, the woodland includes the mixed forest, evergreen broad-leaf forest, evergreen coniferous forest and *etc.*, in which the area of mixed forest occupies 95.4% of the total area of woodland. For the farmland which occupies 23.5% of the total area, the main soil types include mountainous yellow soil, yellow brown soil, red soil, purple soil and paddy soil. To be specific, yellow soil and yellow brown soil are mainly distributed in the area with the elevation over 800 m, red soil is widely distributed in the hilly downland with the elevation below 800 m. Purple soil is mainly distributed in the Poyang Lake basin, paddy soil is mainly distributed in valleys among mountains, valley plain and terrace. Additionally, mountain meadow soil is distributed in the area with the elevation over 1,400m.

**Data acquisition and measurement. LAI collection.** Using the Plant Canopy Analyzer (PCA, LAI-2000), the field analyses and measurements of

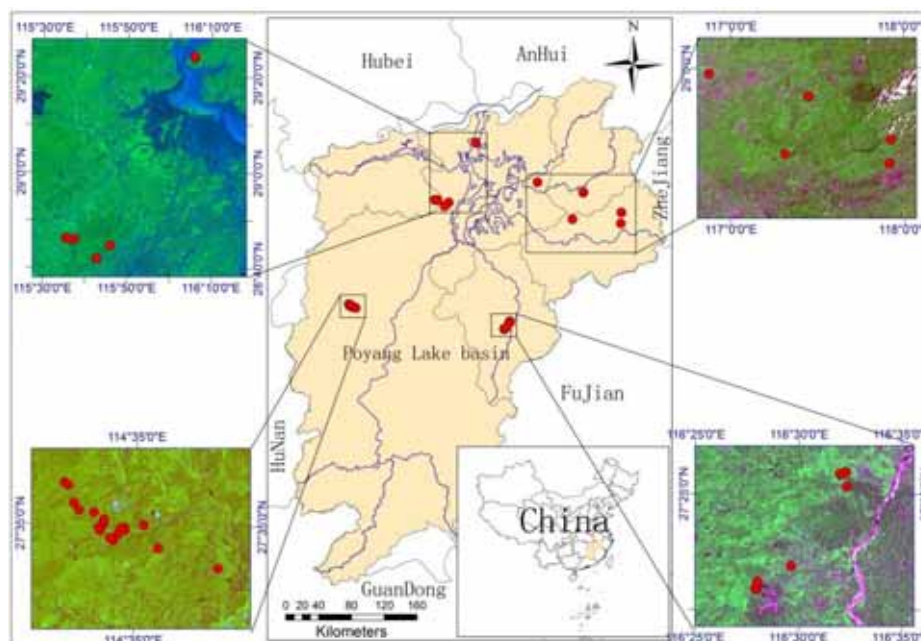


FIGURE 1

The location of the Poyang Lake basin in JiangXi Province, China

plant canopies were conducted on different types of vegetation coverage in the Poyang Lake basin. Assuming a random leaf angle distribution, the impact of clumping has been assessed only partially using the PCA and its corresponding LI-COR software. Hence, the LAI measurement taken by the PCA, has been termed 'effective' LAI because of the contamination of this measure by self-shading at the leaf-to-shoot level, branch and canopy levels and stand level [10]. The PCA is based on the amount of canopy light transmittance measured across a hemispherical field by five concentrically nested sensors [11]. Since the effective LAI is less variable and easier to measure than LAI, and is also an intrinsic attribute of plant canopies [12]. The LAI-2000 has been successfully used and compared to other techniques in numerous studies [13-15] used the LAI-2000 in various land cover types such as grassland, forests or agricultural crops, thus the impact of the instrument's handling of measurements has not been discussed in detail. The measurements were conducted on 8 sample plots in Dagangshan Nature Reserve from July 26th, 2014 to July 30th, 2014, and 37 sample plots in Dagangshan Nature Reserve, Meiling Scenic Spot, Nanfeng County, Shangrao City, Leping County, Poyang County and Duchang Country from July 28th, 2015 to August 5th, 2015 (Fig. 1). Totally 45 LAI data were acquired. These sample plots have a same area of 30 m\*30 m. We should choose the samples plots which are surrounded by the uniform vegetations so as to avoid the mixed pixels in satellite images. When the measurements were conducted on the mountainous woodland, the actual side length of sample plot should be adjusted in accordance with the mountain's slope; additionally, the slope facing the sun should be selected so as to avoid the interference induced by the mountain's shadow. Each set of LAI values include the averages values at five points in the sample plot (i.e., four corner points and one central point). The coordinates of five points were recorded using GPS. The land cover types in the present LAI monitoring mainly include woodland, farmland and grassland.

**GF-1 data preprocessing.** GF-1 satellite was launched on April 26th, 2013, which carries two different types of cameras for optical observations. Specifically, two multispectral cameras with the panchromatic band resolution of 2 m and four multispectral cameras with the resolution of 16 m were installed. GF-1 has a kind of optical remote sensing technology which combines high temporal resolution, high spatial resolution and multispectral technique. It travels in the sun synchronization repeating orbit, with the orbit altitude and repeat period of 645 km and 41 days, respectively. The carried multispectral camera include four bands, i.e.,

450nm~520nm, 520nm~590nm, 630nm~690nm and 770nm~890nm, corresponding to the first band (BLUE), second band (GREEN), third band (RED) and fourth band (NIR), respectively. The multispectral camera, with the high spatial resolution and spectral width of 16 m and 800 km, combines four wide-field-of-view (WFV) cameras. The revisit time was set as 4 days, and the data were downloaded from China Center for Resource Satellite Data and Application (<http://www.cresda.com/site1/index.shtml>). GF-1 has been significantly improved in temporal resolution. GF-1 also has the largest spectral width, and therefore a large amount of work on data processing can be saved, which is conducive to data analysis over a large area. The data collected by the multi-spectral camera of GF-1 were used in the present study, which includes 12 scenes on 30 July 2014 and 3 August 2015.

In order to achieve a ground space consistency, geometric correction is crucial for the processing of image data, especially the high-resolution image data. To conduct geometric correction on the image data in ENVI 5.1 Classic, the ortho-rectification is performed using the command RPC or RSM. However, the correction on the image can only be regarded as the rough correction, with the correction accuracy ranging from 3~5 pixels. Fine correction using the other corrected high-resolution images should be further conducted. For example, Landsat 8 satellite data after fine correction can be used. Additionally, manual correction can also be used, i.e., the image correction by searching the characteristic point with the use of GPS. In the present study, the panchromatic data of Landsat 8 OLI with the resolution of 15 m were used. All data should use the unified coordinates, the projection type of UTM Zone 50 was used while WGS84 was selected as the datum. Then, the radiation correction should be conducted, FLAASH was used in the present study, FLAASH is a first-principles atmospheric correction modelling tool for retrieving spectral reflectance from hyperspectral radiance images. FLAASH is also appropriate for multispectral imagery [16]. The FLAASH module (based on the modified MODTRAN4+ model) provided by ENVI5.1 software. Any of the standard MODTRAN model atmospheres and aerosol types may be chosen to represent the scene, and a unique MODTRAN solution is computed for each image. In this study, input parameters for the FLAASH module were tropical atmosphere model, mid-latitude summer model, the initial visibility of 40 km and the average latitude was 400m. However, the visibility values were determined by trial and error until a typical spectral pattern of plants was obtained. As a result, all bands were converted to surface reflectance in this study area.



**Method. Extraction of spectral Vis.** In the present study, totally 45 sample plots were monitored. The data collected from 2 sample plots are abnormal due to climate changes, and therefore, the data of 43 sample plots were used for modeling. The ground reflectivity data collected by GF-1 after atmospheric correction were used for the calculation of VIs. According to the four bands set of GF-1, 8 VIs related to BLUE, GREEN, RED and NIR bands were selected, namely, NDVI, RDVI, EVI, SR, MSAVI, SAVI, MSR and ARVI. Due to their high correlations with LAI observation data on the ground, these VIs were selected [17-20]. Tab.1 describes the definition of VIs and their relationships with canopy parameters, which were verified by the related literatures (the formulas of VIs and the corresponding references are also listed in Tab.1). The close correlation between LAI and VIs was also discussed in the literatures. The reason why these 8 VIs were selected are described briefly as follows.

The ratio-based NDVI [21] and SR[17] are the most frequently used to correlate with LAI and other canopy structure parameters[22,23,24]; NDVI and SR indices are not fit for vegetation which efficiently combine the characteristics of vegetation with high absorption in the RED band for photosynthesis and high reflectivity in the NIR region due to cell structure's multiscattering phenomenon[22,25]. The RDVI tends to saturate at a higher vegetation density than NDVI and might therefore be suitable for high LAI values [26]. MSAVI can decrease the influence of different soil types on spectral reflectance, while ARVI can reduce the changes in vegetation indices caused by different atmospheric conditions[27], both variables are used as satellite-derived parameters for calculating surface photosynthesis, evapotranspiration, and net primary production, which in turn are used to calculate terrestrial energy, carbon, water cycle processes, and biogeochemistry of vegetation.

SAVI is a soil-adjusted vegetation index, but an adjustment factor L was introduced in order to minimize the influence of soil brightness and to produce vegetation isolines more independent of the soil background, L ranges from 0 for very high vegetation cover to 1 for very low vegetation cover[4]. Due to possible non-linear relationship, MSR attempt to linearize relationships with surface parameters that tend to be non-linear[12].

**Accuracy assessment criteria.** The linear, quadratic, logarithmic, power, exponential and logistic fitting were conducted on the calculated VIs and the measured LAI data, respectively. The remote sensing estimation model of LAI can then be determined with the adoption of the correlation coefficient between VIs and LAI as the indexes. In the present study, the pearson correlation coefficient (R) and the coefficient of determination ( $R^2$ ) and root mean square error (RMSE) were used as the evaluation indexes of the constructed model. Besides, F-test and two-tailed significance test were performed on the model. RMSE can be calculated by:

$$RMSE = \sqrt{\frac{\sum_{i=1}^N (Y_i - \hat{Y}_i)^2}{N}} \quad (1)$$

in which  $Y_i$  and  $\hat{Y}_i$  denote the measured and predicted values, respectively, and N denotes the number of samples.

## RESULTS AND DISCUSSION

**Correlation analysis.** Linear and nonlinear univariate analysis were then conducted on the observed LAI data of 43 sample plots and the bands or the composite functions of bands of the corresponding satellite data.

Based on linear correlation analysis results

**TABLE 1**  
**Summary of 8 VIs using in this study**

Vegetation index	Formula	Reference
NDVI	$NDVI = (NIR - RED) / (NIR + RED)$	Rouse et al.1974[21]
RDVI	$RDVI = (NIR - RED) / (NIR - RED)^2$	Haboudane.2004[26]
EVI	$EVI = (NIR - RED) / (GREEN + 6 * RED - 7.5 * BLUE + 1)$	Huete, A.R.1988[27]
SR	$SR = NIR / RED$	Jordan C F.1969[17]
MSAVI	$MSAVI = 0.5 * ((2 * NIR + 1) - (2 * NIR + 1)^2 - 8 * (NIR - RED)^{0.5})$	Huete, A.R.2015[18]
SAVI	$SAVI = (NIR - RED) / (NIR + RED + L) * (1 + 0.5)$	Huete A R.1988[27]
MSR	$MSR = (NIR / RED - 1) / ((NIR / RED + 1)^{0.5})$	Soudani et al. 2006[7]
ARVI	$ARVI = (NIR - 2 * RED + BLUE) / (NIR + 2 * RED - BLUE)$	Kaufman Y J.1992[20]

Note: BLUE (the first band of GF-1) denotes the spectral reflectivity data in blue band; GREEN (the second band of GF-1) denotes the spectral reflectivity data in green band; RED (the third band of GF-1) denotes the spectral reflectivity data in infrared band; and NIR (the fourth band of GF-1) denotes the spectral reflectivity data in near-infrared band.

(Tab.2), one can observe that the Pearson correlation coefficients of the fourth band and the other bands of GF-1 are smaller than 0.3, i.e., the NIR band and the other bands are not significantly correlated; the Pearson correlation coefficients between the BLUE, GREEN and NIR bands of GF-1 (except the NIR band) exceed 0.89, i.e., the spectral correlations among the BLUE, GREEN and NIR bands of GF-1 are favorable. The NIR band has favorable correlations with EVI, SR, MSAVI and SAVI, but poor correlations with NDVI, RDVI, MSR and ARVI. LAI is positively correlated with VIs and the reflectivity in the NIR band while is negatively correlated with the reflectivity values in the BLUE, GREEN and NIR bands of GF-1.

In which the formula of line model is denoted as  $Y = aX + b$ ; the formula of logarithmic model is denoted as  $Y = a \log(X) + b$ ; the formula of two polynomial model is denoted as  $Y = aX^2 + bX + c$ ; the formula of power model is denoted as  $Y = aX^b$ ; the formula of exponential model is denoted as  $Y = ae^{bX}$ ;  $a$ ,  $b$  and  $c$  are the constants;  $X$  and  $Y$  denote the

variable and dependent variable of sample plot, respectively.

These indices are subsequently correlated to field data of a variable of interest, e.g. LAI [28], in this paper we restricted the fitting method to ordinary least-squares linear regression. All data are used to fit the model to validate see Tab.3, one can observe from the linear and nonlinear analysis results that the linear correlation between the reflectivity in the GREEN band of GF-1 and the measured LAI data is highest, with the correlation coefficient  $R^2$  of 0.496. Among these VIs, MSR has a highest linear correlation with the measured LAI, with the  $R^2$  of 0.591. According to the non-linear model fitting results, NDVI has a largest correlation with LAI using exponential model (Fig.2).  $R^2$  can reach up to 0.744 and RMSE is smallest, being 0.303. The results can pass F tests, i.e., the correlation is of significance. Therefore, the following exponential model can be adopted as the regression model of the inversion of LAI.

TABLE 2

The linear correlation coefficient (R) analysis among 4 bands reflectivity of GF-1, Vis and LAI

		$\rho_1$	$\rho_2$	$\rho_3$	$\rho_4$	NDVI	RDVI	EVI	SR	MSAVI	SAVI	MSR	ARVI	LAI
$\rho_1$	Pearso	1	0.969*	0.959*	-	-	-	-	-	-	-	-	-	-
	sig.		0	0	0.531	0	0	0	0	0	0	0	0	0
$\rho_2$	Pearso		1	0.965*	0.035	-	-	-	-	-	-	-	-	-
	sig.			0	0.824	0	0	0	0	0	0	0	0	0
$\rho_3$	Pearso			1	-	-	-	-	-	-	-	-	-	-
	sig.				0.498	0	0	0	0	0	0	0	0	0
$\rho_4$	Pearso				1	0.036*	0.335*	0.7	0.504**	0.745**	0.71	0.469**	0.24	0.227
	sig.					0.017	0.028	0	0.001	0	0	0.002	0.121	0.143
NDVI	Pearso					1	0.997**	0.8	0.882**	0.886**	0.90	0.946**	0.983**	0.746**
	sig.						0	0	0	0	0	0	0	0
RDVI	Pearso						1	0.8	0.845**	0.867**	0.89	0.919**	0.983**	0.726**
	sig.							0	0	0	0	0	0	0
EVI	Pearso							1	0.832**	0.976**	0.97	0.857**	0.778**	0.583**
	sig.								0	0	0	0	0	0
SR	Pearso								1	0.898**	0.88	0.987**	0.831**	0.746**
	sig.									0	0	0	0	0
MSAVI	Pearso									1	0.99	0.918**	0.809**	0.650**
	sig.										0	0	0	0
SAVI	Pearso										1	0.912**	0.838**	0.651**
	sig.											0	0	0
MSR	Pearso											1	0.906**	0.769**
	sig.												0	0
ARVI	Pearso												1	0.736**
	sig.													0
LAI	Pearso													1
	sig.													

Note: \*\*. denotes that VIs and the reflectivity are significantly correlated through two-tailed tests at the level of 0.01; \*. denotes that VIs and the reflectivity are significantly correlated through two-tailed tests at the level of 0.05;  $\rho_1$ ,  $\rho_2$ ,  $\rho_3$  and  $\rho_4$  denote the spectral reflectivity values in the first, second, third and fourth bands of GF-1, respectively.

TABLE 3

Accuracy assessment of LAI retrieval models between measured LAI and reflectivity ( $\rho_i$ ) of GF-1 or VIs

Param eters	Line model				Logarithmic model				Two polynomial model			
	R <sup>2</sup>	RMSE	F	Sig.	R <sup>2</sup>	E	F	Sig.	R <sup>2</sup>	E	F	Sig.
$\rho_1$	0.50	0.84	41.85	0	0.539	0.81	47.91	0	0.54	0.82	24.28	0
$\rho_2$	0.49	0.85	40.35	0	0.556	0.80	51.30	0	0.56	0.80	26.41	0
$\rho_3$	0.47	0.87	37.74	0	0.585	0.77	57.72	0	0.59	0.78	28.74	0
$\rho_4$	0.05	1.17	2.231	0.14	0.06	1.17	2.602	0.11	0.09	1.16	1.967	0.15
NDVI	0.55	0.80	51.32	0	0.491	0.86	39.52	0	0.60	0.77	30.31	0
RDVI	0.52	0.83	45.63	0	0.491	0.86	39.52	0	0.60	0.77	30.33	0
EVI	0.33	0.98	21.07	0	0.404	0.93	27.78	0	0.46	0.89	17.46	0
SR	0.55	0.80	51.52	0	0.594	0.76	60.08	0	0.60	0.77	30.21	0
MSAV	0.42	0.91	29.97	0	0.446	0.89	32.99	0	0.45	0.9	16.84	0
SAVI	0.42	0.91	30.14	0	0.435	0.90	31.57	0	0.44	0.91	15.93	0
MSR	0.59	0.77	59.27	0	0.565	0.79	53.20	0	0.59	0.77	29.56	0
ARVI	0.54	0.81	48.35	0	0.44	0.90	32.19	0	0.60	0.76	30.67	0

Param eters	Power model				Exponential model				Logistic regression model			
	R <sup>2</sup>	RMSE	F	Sig.	R <sup>2</sup>	E	F	Sig.	R <sup>2</sup>	E	F	Sig.
$\rho_1$	0.64	0.35	74.989	0	0.665	0.34	81.42	0	0.66	0.34	81.42	0
$\rho_2$	0.66	0.34	79.885	0	0.656	0.35	78.23	0	0.65	0.35	78.23	0
$\rho_3$	0.70	0.32	96.528	0	0.676	0.34	85.67	0	0.67	0.34	85.67	0
$\rho_4$	0.06	0.57	3.046	0.0	0.064	0.57	2.795	0.10	0.06	0.57	2.795	0.10
NDVI	0.71	0.31	104.83	0	0.744	0.30	119.1	0	0.74	0.30	119.1	0
RDVI	0.71	0.31	104.83	0	0.737	0.30	114.7	0	0.73	0.30	114.7	0
EVI	0.58	0.38	56.72	0	0.45	0.44	33.60	0	0.45	0.44	33.60	0
SR	0.71	0.32	100.83	0	0.575	0.39	55.37	0	0.57	0.39	55.37	0
MSAV	0.61	0.37	65.018	0	0.534	0.40	46.96	0	0.53	0.40	46.96	0
SAVI	0.62	0.36	67.685	0	0.563	0.39	52.86	0	0.56	0.39	52.86	0
MSR	0.73	0.30	115.95	0	0.665	0.34	81.30	0	0.66	0.34	81.30	0
ARVI	0.67	0.34	85.619	0	0.732	0.31	111.7	0	0.73	0.31	111.7	0

$$LAI = 0.1158e^{4.066NDVI} (R^2 = 0.744, RMSE = 0.303) (2)$$

**Relations between LAI and GF-1 data.** As shown in Fig.3, the reflectivity data in the NIR band of GF-1 is positively correlated with LAI, but the correlation is not significant. LAI is negatively correlation with the reflectivity data in the BLUE, GREEN and RED bands of GF-1, and the  $R^2$  all exceeds 0.479, i.e., the correlations are significant. The results agree well with the research results by Wu *et al* [29]. NIR and RED bands have strong reflection and absorption capacities, which

are connected with the plant's spectral characteristics. 8 VIs are positively correlated with LAI. In terms of linear relationship, most VIs are more suitable for the inversion of LAI than the single-band models.

NDVI, RDVI, SR, MSR and ARVI have favorable correlations with LAI using both linear and nonlinear models; in particular, the model using the exponential function of NDVI is best. However, the model can reach saturation at high values of NDVI, which cannot reflect the variation of actual LAI values.

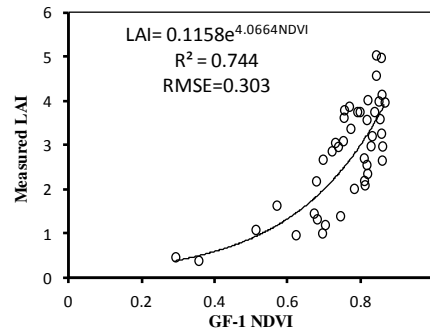


FIGURE 2

Plot showing the optimum regression method for estimating LAI in Poyang Lake basin with NDVI

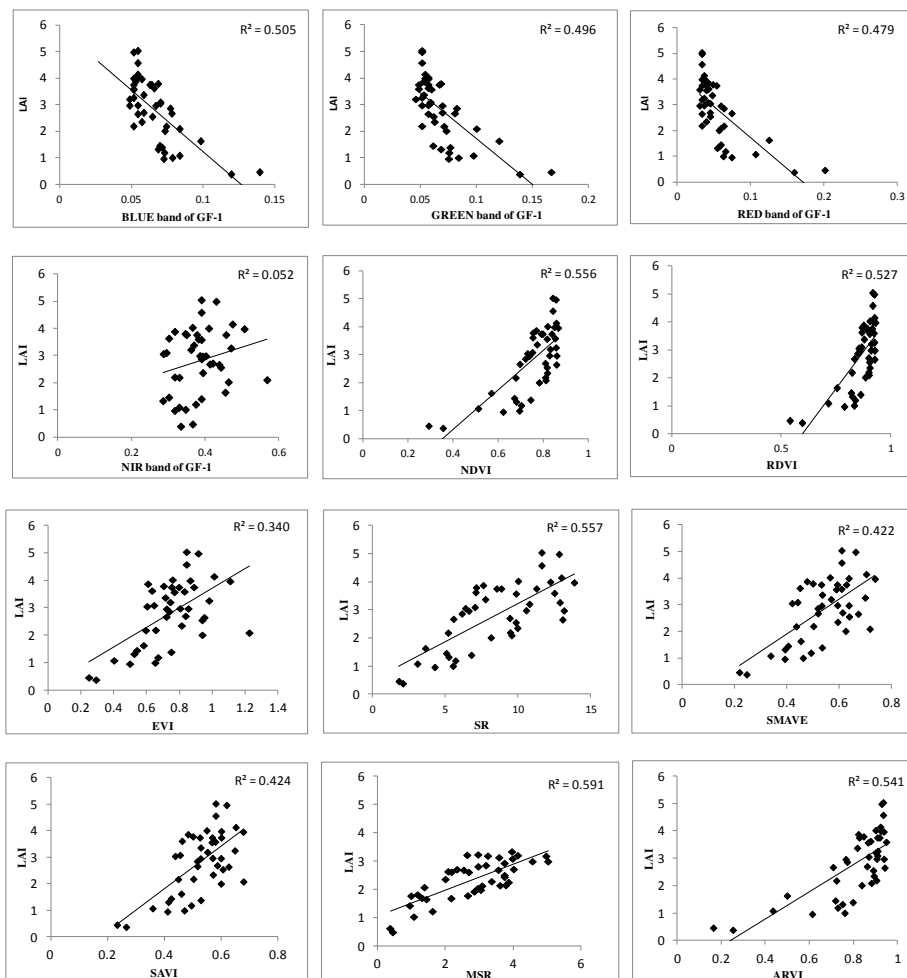
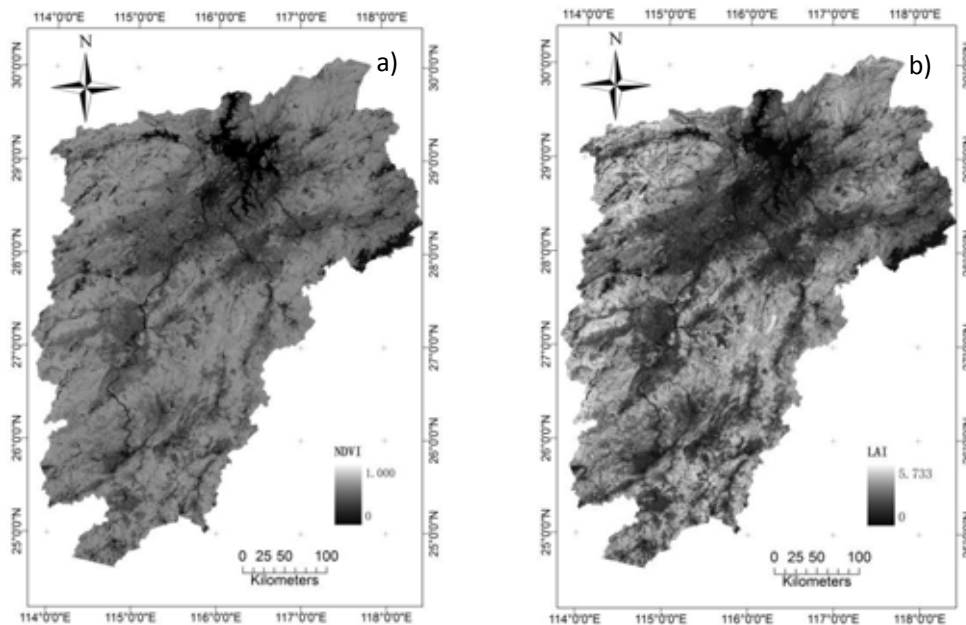


FIGURE 3

Scatter diagram between measured LAI and reflectivity ( $\rho_i$ ) of GF-1 or Vis

**Modelling and mapping LAI.** The GF-1 data in the Poyang Lake basin collected on April 3rd, 2015, were preprocessed and the NDVI values were acquired. Then image mosaic and boundary trimming were conducted for acquiring the NDVI value of the whole basin (see Fig.4 (a)). Using the obtained regression model, the pixel data of each image were calculated and finally the LAI values of the whole basin with the high spatial resolution of 16 m were acquired (see Fig.4 (b)). The collected

images can quite clearly display the spatial distribution of LAI in this region. The maximum LAI value in this basin is 7.246 and the average LAI value is 2.293. LAI values in eastern, western and southern regions are relatively high (with the average LAI of 3.5), where are mostly the woodland. The average LAI value of farmland is 2.2 and the LAI value is relatively low in middle part of the basin.



**FIGURE 4**

- (a) NDVI value of the Poyang Lake basin based on GF-1 data in 3 August 2015;  
 (b) LAI value of the Poyang Lake basin based on GF-1 data in 3 August 2015

## CONCLUSIONS

In this article, based on remote sensing data collected by GF-1 satellite in four bands, the relationship between the data in different bands and LAI as well as the relationship between various VIs and LAI were analyzed. With the adoption of the Poyang Lake basin as the study area, the LAI data of some major land coverage types were monitored in two summers. Then, linear and nonlinear correlation analyses were conducted on LAI and the data in each single bands of GF-1 as well as 8 VIs. The remote sensing inversion model of LAI of the Poyang Lake basin in summer was constructed and the LAI data with the resolution of 16 m were extracted.

In terms of bands of GF-1, the correlations between any two bands among BLUE, GREEN and RED bands are relatively high, and the data in the fourth band of GF-1 exhibit no significant correlations with the data in the three other bands. LAI in the Poyang Lake basin is positively correlated with VIs, and LAI is negatively correlation with the reflectivity data in the BLUE, GREEN and RED bands of GF-1. Most VIs are superior to single-band models in terms of the inversion of LAI, however, NDVI has the highest correlation with the measured LAI. The results can pass F-test, which is connected with the strong reflection and absorption capabilities in NIR and RED bands. On the whole, favorable inversion results of LAI can be achieved using NDVI data; however, the correlation of the exponential model between NDVI and the measured LAI

decreases in the regions with densely distributed woodland, i.e., the LAI data may be underestimated. The data collected by GF-1 WFV have relatively high spatial resolution, which can clearly present the spatial distribution of LAI in this region and can contribute to reflecting LAI data in the region with great spatial variations. It means that GF-1 satellite data can be used for the monitoring of LAI over large areas. In future studies, we will focus on the application research of GF-1 satellite data in accordance with their advantages, increase the measurements of LAI in different seasons for different ground surface features and investigate the inversion of LAI in the Poyang Lake basin under various phenologic condition yearly. Moreover, the GF-1 data (including the PMS data with the resolutions of 2 m and 8 m, respectively, and WFV data with the resolution of 16 m) should be fused with the LAI production data of MODIS and SPOT so as to improve the temporal and spatial resolution of the data. All of these studies can contribute to the development of LAI products with high temporal and spatial resolutions.

## ACKNOWLEDGMENTS

This work was supported by the Natural Science Foundation of China under Grant [number 41461080, 41331174, 51269020] and Special Fund by Surveying & Mapping and Geoinformation Research in the Public Interest (201512026), and

Jiangxi key Research and Development Program (20161BBG70052).

## REFERENCES

- [1] Chen, J. M. and Black, T. A. (1992) Defining Leaf Area Index for Non-Flat Leaves. *Plant Cell Environment*, 15 (4):421-429.
- [2] Myneni, R. B., Hoffman, S., Knyazikhin, Y. et al. (2002) Global products of vegetation leaf area and fraction absorbed PAR from year one of MODIS data. *Remote Sensing of Environment*, 83(1-2):14-231.
- [3] Knyazikhin, Y., Aronchik, M. J., Myneni, R., Diner, D., Running, S. (1998) Synergistic algorithm for estimating vegetation canopy leaf area index and fraction of absorbed photosynthetically active radiation from MODIS and MISR data. *Journal of Geophysical Research Atmospheres*, 103:32257 -32275.
- [4] Camacho, F., Cernicharo, J., Lacaze, R., Baret, F. and Weiss, M. (2013) Geov1: lai, fapar essential climate variables and fcover global time series capitalizing over existing products. part 2: validation and intercomparison with reference products. *Remote Sensing of Environment*, 137(10):310-329.
- [5] Xiao, Z., Liang, S., Wang, J., Chen, P., Yin, X. and Zhang, L. et al. (2014) Use of general regression neural networks for generating the glass leaf area index product from time-series modis surface reflectance. *IEEE Transactions on Geoscience & Remote Sensing*, 52(1):209-223.
- [6] Pinty, B., Andredakis, I., Clerici, M., Kaminski, T., Taberner, M., Verstraete, M., Gobron, N., Plummer, S. and Widlowski, J.L. (2011) Exploiting the MODIS albedos with the two-stream inversion package (JRC-TIP): 1. Effective leaf area index, vegetation, and soil properties. *Journal of Geophysical Research Atmospheres*, 116(D9):1-20.
- [7] Soudani, K., François, C., Lemaire, G., Dantec, V.L. and Dufrêne, E. (2006) Comparative analysis of IKONOS, SPOT, and ETM+ data for leaf area index estimation in temperate coniferous and deciduous forest stands. *Remote Sensing of Environment*, 102:161-175.
- [8] Wu, Q., Jin, Y., Bao, Y., Hai, Q., Yan, R. and Chen, B. et al. (2015) Comparison of two inversion methods for leaf area index using hj-1 satellite data in a temperate meadow steppe. *International Journal of Remote Sensing*, 36(19):1-16.
- [9] Qu, Y., Han, W., Ma, M. (2015) Retrieval of a Temporal High-Resolution Leaf Area Index (LAI) by Combining MODIS LAI and ASTER Reflectance Data. *Remote Sensing*, 7(1):195-210.
- [10] White, J.D., Running, S.W., Nemani, R., Keane, R.E. and Ryan, K.C. (1997) Measurement and remote sensing of LAI in rocky mountain Montane ecosystems. *Canadian Journal of Forest Research*, 27:1714-1727.
- [11] Welles, J.M. and Norman, J.M. (1991) Instrument for indirect measurement of canopy architecture. *Agronomy Journal*, 83:818-825.
- [12] Chen, J. M. and Cihlar, J. (1996) Retrieving Leaf Area Index of Boreal Conifer Forests Using Landsat TM Images. *Remote Sensing of Environment*, 55:153-162.
- [13] Breda, N.J.J. (2003) Ground-Based Measurements of Leaf Area Index: A Review of Methods, Instruments and Current Controversies. *Journal of Experimental Botany*, 54:2403-2417.
- [14] Vuolo, F., Atzberger, C., Richter, K., Urso, G. D. and Dash, J. (2010) Retrieval of biophysical vegetation products from rapid eye imagery. *Isprs Tc VII Symposium-100 Years Isprs*, 38, Part 7A, Vienna, July 5-7.
- [15] Asam, S., Fabritius, H., Klein, D., Conrad, C. and Dech, S. (2013) Derivation of leaf area index for grassland within alpine upland using multi-temporal rapid eye data. *International Journal of Remote Sensing*, 34(34):8628-8652.
- [16] Flaash User's Guide. (2004) *Envi Flaash Version 4.1*, September, 2004 Edition, pp. 1-80 (Boulder, CO: Research Systems, Inc.).
- [17] Jordan, C.F. (1969) Derivation of leaf-area index from quality of light on the forest floor. *Ecology*, 50(4):663-666.
- [18] Huete, A.R., Justice, C. and van Leeuwen, W. (2015) MODIS Vegetation Index (MOD 13)-Algorithm Theoretical Basis Document (Version 3). Available online: [http://modis.gsfc.nasa.gov/data/atbd/atbd\\_mod13.pdf](http://modis.gsfc.nasa.gov/data/atbd/atbd_mod13.pdf).
- [19] Soudani, K., François, C., Maire, G., L. Dantec, V. and Dufrêne, E. (2006) Comparative analysis of ikonos, spot, and etm+ data for leaf area index estimation in temperate coniferous and deciduous forest stands. *Remote Sensing of Environment*, 102(1-2):161-175.
- [20] Kaufman, Y.J., Tanre, D. (1992) Atmospherically resistant vegetation index (ARVI) for EOS-MODIS. *IEEE Transactions on Geoscience and Remote Sensing*, 30(2):261-270.
- [21] Rouse, J. W., Haas, R. H., Schell, J. A. and Deering, D. W. (1974) *Monitoring Vegetation Systems in the Great Plains with ERTS*. Nasa Special Publication, 351, 309-317.
- [22] Fassnacht, K.S., Gower, S.T., Mackenzie, M.D., Nordheim, E.V. and Lillesand, T.M. (1997) Estimating the leaf area index of north central Wisconsin forests using the Landsat Thematic

- Mapper. Remote Sensing of Environment, 61: 229-245.
- [23] Treitz, P.W. and Howarth, P.J. (1999) Hyperspectral remote sensing for estimating biophysical parameters of forest ecosystems. Progress in Physical Geography, 23: 359-390.
- [24] Turner, D. P. Cohen, W. B. Kennedy, R. E. Fassnacht, K. S. and Briggs, J. M. (1999) Relationships between leaf area index and landsat tm spectral vegetation indices across three temperate zone sites. Remote Sensing of Environment, 70(1): 52-68.
- [25] Gate, D. Keegan, J.J. Chleter, S. J.C. and Weidner, V.R. (1965) Spectral properties of plant. Applied Optics, 4: 11-20.
- [26] Haboudane, D. (2004) Hyperspectral Vegetation Indices and Novel Algorithms for Predicting Green LAI of Crop Canopies: Modeling and Validation in the Context of Precision Agriculture. Remote Sensing of Environment, 90: 337-352.
- [27] Huete, A. (1988) A Soil-Adjusted Vegetation Index (SAVI). Remote Sensing of Environment, 25: 295-309.
- [28] Rivera Caicedo, J. Verrelst, J. Delegido, J. Veroustraete, F. Moreno, J. (2014) On the semi-automatic retrieval of biophysical parameters based on spectral index optimization. Remote Sensing, 6 (6), 2866-2889.
- [29] Wu, Q. Yun, X.J. Bao, Y.H. Yan, R.R. Chen, B.R. Zhang, H.B. Zhang, B.H. Li, Z.W. Li, X.Y. and Xin, X.P. (2015) Comparison of two inversion methods for leaf area index using HJ-1 satellite data in a temperate meadow steppe. International Journal of Remote Sensing, 1-16.

---

**Received: 14.01.2016**

**Accepted: 21.09.2016**

---

#### **CORRESPONDING AUTHOR**

##### **Xiaoling Chen**

State Key Laboratory of Information Engineering in Surveying, Mapping and Remote Sensing, Wuhan University, Wuhan 430079, China

e-mail: xiaoling\_chen@whu.edu.cn

# DIURNAL VARIATION IN THE SELECTED INDICATORS OF WATER CONTAMINATION IN THE BIAŁKA RIVER AFFECTED BY A SEWAGE TREATMENT PLANT DISCHARGE

Anna Lenart-Boron<sup>1,\*</sup>, Justyna Prajsnar<sup>2</sup>, Kinga Krzesiwo<sup>3</sup>, Anna Wolanin<sup>4</sup>, Łukasz Jelonkiewicz<sup>4</sup>, Ewelina Jelonkiewicz<sup>4</sup>, Mirosław Zelazny<sup>4</sup>

<sup>1</sup> Department of Microbiology, University of Agriculture in Cracow; Mickiewicza Ave. 24/28, 30-059 Cracow, Poland

<sup>2</sup> Faculty of Biotechnology and Horticulture, University of Agriculture in Cracow, 29 listopada Ave. 54, 31-425 Cracow, Poland

<sup>3</sup> Department of Entrepreneurship and Spatial Management, Institute of Geography, Pedagogical University of Cracow, Podchorążych str. 2, 30-084 Cracow, Poland

<sup>4</sup> Department of Hydrology, Institute of Geography and Spatial Management, Jagiellonian University in Cracow; Gronostajowa 7, 30-387 Cracow, Poland

## ABSTRACT

This study was aimed to assess the diurnal variability in the number of microbial indicators of water quality and the content of the selected main ions at 3 sites located on the Białka river, Podhale. The examined sites included the stream being a receiver of sewage from the treatment plant, before the treatment plant and few kilometers downstream of the sewage discharge - at the water intake for artificial snowing of the largest ski station in the region. Twelve series of samples were collected over 36 hours period. Temperature, pH, electrical conductivity and dissolved oxygen were measured onsite, microbiological analyses included the numbers of mesophilic bacteria, fecal *Escherichia coli* and *Enterococcus faecalis*, chemical analyses determined the concentration of main ions. *E. faecalis* was not detected in this study, while the concentration of mesophilic bacteria and *E. coli* varied largely between sites and hours of sampling. The smallest content of microorganisms was observed before the treatment plant and significantly increased at the sewage discharge. It was found that the cycle of the sewage treatment plant operation affects microbial contamination of water both in the stream which receives effluent from the treatment plant and in the downstream part of the river.

## KEYWORDS:

Białka river, *Escherichia coli*, mesophilic bacteria, nutrients, sewage treatment plant

## INTRODUCTION

From 1992 the European Union has been implementing the "Natura 2000" system, which is aimed for the protection of the European biological

diversity, preserving natural habitats, plants and animal species [1]. One of the sites covered by this program includes the valley of the Białka river, starting from the Leśnicki Stream's mouth to the Białka until the Białka river's mouth to the Czorsztyńskie Lake. Moreover, waters of the Białka river are considered as ones of the most pure in Poland. It is among the class I (the best) rivers in terms of biological, hydromorphological and water indexes quality [2]. Many animal species, characteristic of mountain streams with small degree of conversion and high class of water purity have been found to dwell in this river [3].

However, it has appeared recently that the natural characteristics of the Białka river have been strongly reduced by human activity. There are several reasons for such situation including, among others, anthropogenic transformations of the riverbed, both conducted under the supervision of hydrotechnical companies and by local tenants as a prevention measure against flooding [4]. Another aspect is the exploitation of the riverbed material, in the form of pebbles and wood rubble – the first one being used for building e.g. house foundations and hardening roads, while the latter one being used as firewood [4]. Another two aspects of anthropogenic disturbance of the Białka river are directly related to the issue analyzed and discussed in this paper. The first one is related to increasing water uptake from the Białka river – for drinking water as well as for artificial snowing of several ski stations operating in the neighborhood of the Białka valley, which results in the total consumption of more than 1,350 m<sup>3</sup>/h of water [5]. The last and the most severe problem is related to the fact that the river acts a sewage receiver from households of the municipality – Bukowina Tatrzańska, in which only 49.8% of the population uses sewerage system [6]. Studies conducted previously in the catchment of the Białka river [7], indicate that the sewage treatment plant, operating in



the Bukowina Tatrzańska municipality is insufficient, which results in large loads of pollutants being discharged into the river. Moreover, there are numerous discharge sites of untreated sewage, which during winter increase the amount of sewage inflow and may degrade the quality of water in this region [8].

There are studies, reporting that some microbial genera and species are able to survive the process of freezing, required for the production of artificial snow [9, 10], thus causing the threat of microbial contaminants being transferred to snow cannons and then to artificial snow deposited over numerous slopes in the vicinity of the Białka river catchment.

Białka Tatrzańska is the resort, located in the Bukowina Tatrzańska municipality, by the Białka river. This locality is specialized in ski tourism, whose role is dominant in the structure of their overall tourism function. It is one of the largest and the best ski stations in Poland [11]. In the winter season 2014/2015 the ski base in this territory comprised 23 ski lifts, including 8 cableways with a total transportation capacity of 28,400 people/hour and 27 ski runs with a total length of 17.2 km. As many as 88.9% of them allows skiing after dark, and 81.5% is equipped with snow cannons. The ski runs are located in the eastern, north-eastern and south-eastern slopes of Kotelnica (918 m a.s.l.), Jankulakowski Wierch (934 m a.s.l.) and Horników Wierch (926 m a.s.l.). The largest ski resorts in Białka Tatrzańska are: Kotelnica Białczańska, Bania and Kaniówka [11]. In this area tourist traffic in winter significantly predominates the one in summer [11]. In recent years there was a significant increase in the number of tourists visiting Białka Tatrzańska in the period of winter holidays, starting from mid-January and ending in late March. People skiing or snowboarding usually use long-term stays in Białka Tatrzańska or in the Bukowina Tatrzańska municipality, which causes shortages in accommodation places in this area [11]. For instance, in the winter season 2014/2015 Kotelnica Białczańska ski resort (the largest ski resort in Białka Tatrzańska) was visited by between 320 and 340 thousand tourists [12]. Such situation resulted in a deterioration of the efficiency of the sewage treatment plant operating in the Bukowina Tatrzańska municipality and therefore a significant decrease in water quality from the section of Bukowina Tatrzańska until the river mouth to the Czorszyńskie Lake [7].

Water quality monitoring programs vary widely with different numbers of samples being collected for the analysis and possible decisions [13] as sampling design is rarely based on empirical and/or anticipated variation. According to Whitman & Nevers [13] these limitations in monitoring protocols cause that the efforts should be made to provide accurate and reliable results. Understanding

the processes affecting the water quality requires sound scientific data on the variability of the concentration, sources and faith of fecal contaminants [14].

Having this in mind, a study was undertaken in order to assess a diurnal variability in the abundance of microbial indicators of water quality and the content of the selected main ions in three sites located on the Białka river – by the mouth of a stream being a direct receiver of sewage from the treatment plant in Bukowina Tatrzańska, before the treatment plant and in the neighboring village - Białka Tatrzańska at the water intake for artificial snowing of the slopes of the largest ski station in the region.

The selection of the sampling sites was a direct effect of a 2-year study conducted throughout the Białka river [7], which indicated that even though large proportion of the municipality is not sewered, resulting in numerous households discharging their effluent directly into the river, still the insufficiently operating treatment plant is the most important factor which affects dramatically decreased quality of the Białka waters.

The studies will allow for more detailed assessment of the operation and efficiency of the sewage treatment plant and its direct effect on the quality of water in the river, which has been widely considered as pure, as well as on the quality of water being deposited over the mountain slopes in the form of artificial snow.

## **METHODS**

**Sampling strategy.** Three measuring points were selected for the study, two of which were located on the river Białka. The first one is situated before the municipal sewage treatment plant (1), the second one – by the sewage discharge from the treatment plant (2) – both located in Bukowina Tatrzańska. The third measuring point was situated at the site of water intake (3) for artificial snowing of the slopes of the biggest ski station in the region, located in Białka Tatrzańska – the village neighboring Bukowina (Fig. 1.). The study was conducted over a weekend in mid-February, which is the middle of the “high ski season” in Poland, when the considered area is visited by the greatest number of tourists throughout the year [8]. Water samples were collected during 36 hours at 2 to 4-hour interval. The samples were collected into 1,000 ml and 500 ml autoclaved polypropylene bottles. During sampling, measurements of temperature (T), pH, electrical conductivity (EC<sub>25°C</sub>) and dissolved oxygen (DO) were conducted by a digital multimeter Multi 3430 (WTW) with a combined glass electrode type SenTix 940 (WTW), a conductometric sensor TetraCon 925 (WTW) with a constant k=0.475 and optical dissolved oxygen sensors FDO 925 (WTW).

Each sensor had a built-in temperature sensor.

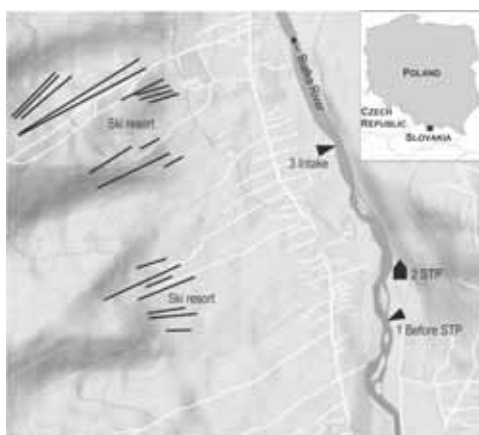


**FIGURE 1**  
Study area

**Laboratory analyses.** *Escherichia coli* (Blue-green colonies on TBX agar, incubated at 44°C, 48 h) and *Enterococcus faecalis* (small dark red to light brown colonies on Slanetz-Bartley agar, 37°C, 72 h) were enumerated using the membrane filtration method, while the number of mesophilic bacteria (trypticase soy agar, 37°C, 48 h) was determined using the serial dilutions method. After incubation, grown colonies were counted and expressed as colony forming units per 100 ml of water for the membrane filtration method and per 1 ml for the serial dilutions method (CFU/100 ml and CFU/ml, respectively).

In order to determine the chemical composition, water samples were collected to 500 ml polyethylene bottles. Chemical composition of water was determined in the laboratory of the Institute of Geography and Spatial Management, Jagiellonian University in Kraków. After filtration of water with a 0.45 µm PTFE syringe filter, the chemical composition of water was determined by ion chromatography using two chromatographs DIONEX ICS-2000 and an autosampler AS-40. The chromatographic system composed of anionic and cationic modules allows the simultaneous separation and determination of the following ions in water: Ca<sup>2+</sup>, Mg<sup>2+</sup>, Na<sup>+</sup>, K<sup>+</sup>, NH<sub>4</sub><sup>+</sup>, SO<sub>4</sub><sup>2-</sup>, Cl<sup>-</sup>, NO<sub>3</sub><sup>-</sup>, NO<sub>2</sub><sup>-</sup>, PO<sub>4</sub><sup>3-</sup>, F<sup>-</sup>. HCO<sub>3</sub><sup>-</sup> was determined by titration using 855 Robotnic Titrosampler (Metrohm). Mineralization of water (total dissolved solids – TDS) was also calculated as a sum of individual ions concentrations.

**Statistical analysis.** Statistical analysis was performed using Statistica v. 10 (StatSoft) software, by calculating basic descriptive statistics and a one-way T-test [15] was used to verify the significance of differences in the number of microbial indicators between the sampling sites and different times of sampling. In order to verify the differences in the

investigated physical and chemical parameters between the sampling sites, the analysis of variance (ANOVA) and post-hoc Scheffe test were applied for p=0.95. On the other hand, a one-sample T test was applied to verify the significance of differences in physical and chemical characteristics of water over the study period. The confidence interval was 0.05. Spearman's correlation coefficient was used to determine the relationship between the tested parameters for each of the sampling sites.

Multivariate statistical analysis, particularly Principal Component Analysis, has been successfully applied in a number of hydrochemical studies [16, 17]. On the other hand, Thyne et al. [18] believe that this method can be applied in order to extract key information from large sets of data on water quality. Principal Component Analysis (PCA) was used to identify factors affecting the microbiological and hydrochemical parameters in the investigated points. In the case of points STP (No. 2) and Intake (No. 3) the analysis included data on mesophilic bacteria, *E. coli* and T, EC<sub>25°C</sub>, DO, Na<sup>+</sup>, K<sup>+</sup>, NH<sub>4</sub><sup>+</sup>, Cl<sup>-</sup>, NO<sub>3</sub><sup>-</sup> and PO<sub>4</sub><sup>3-</sup>. On the other hand, in the case of the point Before STP (No. 1) only data on mesophilic bacteria, *E. coli*, NH<sub>4</sub><sup>+</sup> and NO<sub>3</sub><sup>-</sup> were included due to the small amount of water samples collected during the experiment and also small variation of the obtained results. Before conducting the analysis, data were standardized and normalized. The factors for the analysis were selected based on the Kaiser criterion (eigenvalue >1 and when the value of the explained variance was greater than 10%).

## RESULTS AND DISCUSSION

Table 1 presents the results of varying concentrations of microorganisms over the 36-hour period of the study. *E. faecalis* was not detected in the examined samples, which may indicate that the origin of the microbial contamination is of anthropogenic character, as there have been studies showing that the number of fecal coliforms in human feces significantly outnumbers fecal streptococci [19]. Also, ratios between fecal coliforms and fecal streptococci greater than 4 have been suggested to indicate a human source of water pollution, while ratios less than 0.7 would indicate animal source [20].

The concentration of another indicator of fecal contamination, *E. coli* varied significantly, both between the examined sites and within individual sites – between different hours of sampling. At the site located before the treatment plant the concentration of *E. coli* ranged from 17 to 164 CFU/100 ml of water (with a mean of 87 CFU/100 ml) and it increased severely at the site located by the STP, where it ranged from 71 thousand CFU/100 ml

of water in series No. 4 and 9 to even 1.5 million CFU/100 ml of water in series 1 and 8 with the mean

**TABLE 1**  
**The number of microbial indicators of fecal contamination recorded during the diurnal study.**

Location	Sample No.	<i>E. coli</i> (CFU/100 ml)	<i>E. faecalis</i> (CFU/100 ml)	Mesophilic bacteria (CFU/ml)
Before STP	1	17	0	50
Before STP	2	120	0	42
Before STP	3	164	0	105
Before STP	4	47	0	70
Mean	-	87	0	67
Std. deviation	-	67	0	28
STP	1	1,450,600	0	159,800
STP	2	788,800	0	102,100
STP	3	1,156,000	0	93,950
STP	4	71,540	0	36,400
STP	5	1,142,000	0	79,450
STP	6	952,000	0	79,200
STP	7	1,224,200	0	416,000
STP	8	1,496,000	0	136,700
STP	9	71,120	0	64,000
STP	10	816,100	0	261,300
STP	11	140,080	0	5,650
STP	12	680,000	0	32,500
Mean	-	832,370	0	122,254
Std. deviation	-	509,373	0	114,633
Intake	1	18	0	95
Intake	2	14	0	58
Intake	3	23	0	50
Intake	4	51	0	97
Intake	5	816	0	7,480
Intake	6	571	0	480
Intake	7	470	0	4,510
Intake	8	512	0	765
Intake	9	115	0	210
Intake	10	1,870	0	2,340
Intake	11	2,320	0	1,175
Intake	12	860	0	340
Mean	-	637	0	1,467
Std. deviation	-	754	0	2,303

of c.a. 832 thousand CFU/100 ml. Also at the Intake the number of these indicator bacteria varied significantly depending on the hour of sampling and

it ranged from only 14 CFU/100 ml (series. 2) to as much as nearly 2500 CFU/100 ml (series 11) with a mean of 637 CFU/100 ml. The number of *E. coli* at the water intake for artificial snowing allowed to classify these waters either to class A1 or to A2. This means that they require typical physical and chemical treatment, including disinfection by chlorination [21]. This is one of the most important observations resulting from this study, as on one hand the waters of the Białka river have been considered exceptionally clean, while on the other hand they are being constantly contaminated with undertreated sewage. Fecal pollution of surface waters is of particular concern, as the most dangerous bacterial gastrointestinal human infections, such as cholera, salmonellosis or shigellosis are primarily transmitted by water polluted with feces of infected people [22].

The number of mesophilic bacteria may be also used to determine the extent of microbiological contamination of water, as this group of microorganisms consists of most species related to sewage contamination [23]. Most of these bacteria are incapable of proliferating in water environment, therefore their presence may indicate relatively fresh contamination with sewage [23]. The number of mesophilic bacteria at the site No. 1 (before the treatment plant) ranged from 42 to 105 CFU/ml of water. According to the Regulation of the Minister of Environment on the requirements for surface water used for supplying people in drinking water [21], water at this site can be classified to A1 or A2 category. However, the prevalence of these microorganisms increased significantly by the sewage discharge from the treatment plant - No. 2 (range between 5,650 CFU/ml and 416 thousand CFU/ml), which then affected the quality of water at the intake for artificial snowing (No. 3), where the number of mesophilic bacteria ranged from 50 CFU/ml (series 3) to almost 7,500 CFU/ml (series 5).

The diurnal variation in the microbial indicators' concentration in both of the sites, i.e. STP and Intake, located downstream of the discharge from the treatment plant, are consistent with the observations of Meays et al. [14] and confirm the conclusions drawn from their study, as well as the remarks given by Whitman & Nevers [13] concerning the main limitations related to bacterial monitoring protocols. As also shown in our study, if a monitoring was designed to obtain a single sample per site per day, the results of the *E. coli* concentrations at the intake for artificial snowing could range from only 14 or 18 CFU/100 ml to even 2,320 CFU/100 ml. The situation is similar by the discharge from the STP – even though the *E. coli* concentrations are huge, they still could vary from 71 thousand CFU/100 ml to as many as 1.5 million CFU/100 ml (Table 1). The assessment of the fecal contamination based on these outermost results will

be very different and can lead to incorrect conclusions.

Given the fact that the examined three sampling sites are located within a few kilometer distance from each other, it appears that also designing a reliable network of sampling sites and selecting the most representative ones is not only a very significant matter, but it can be also very difficult task. The location of a sampling site within a catchment can affect the concentrations of *E. coli* and other microbial indicators of fecal contamination of water [14]. The concentrations and sources of *E. coli* can be also affected if a sampling site is located below a highly used area versus a more remote one [14].

Statistical analysis showed that the differences in the numbers of *E. coli* between the sampling sites, i.e. STP/before-STP and STP/Intake, are statistically significant (T-values 3.19 and 5.66, respectively). There were also statistically significant differences in the number of mesophilic bacteria between the sampling sites (T-values of 2.08 and 3.65, respectively). Moreover, there were statistically significant differences in the concentrations of *E. coli* and mesophilic bacteria over the study period in each of the measuring points.

Determination of the Spearman's correlation coefficient revealed no significant correlation between the microbial indicators (*E. coli* and mesophilic bacteria) and physico-chemical characteristics of water at the measuring point Before STP (Tab. 2). At the measuring point No. 3 (Intake) a significant positive relationship between the concentrations of *E. coli* and mesophilic bacteria, and EC<sub>25°C</sub>, Na<sup>+</sup>, NH<sub>4</sub><sup>+</sup>, Cl<sup>-</sup>, PO<sub>4</sub><sup>3-</sup> was found. Similarly, in the case of mesophilic bacteria, there was no significant correlation only with phosphate ions. At the measuring point STP there was a

significant positive correlation between *E. coli* and EC<sub>25°C</sub>, Na<sup>+</sup>, K<sup>+</sup>, NH<sub>4</sub><sup>+</sup>, Cl<sup>-</sup> and PO<sub>4</sub><sup>3-</sup>, and significant negative correlation with DO and NO<sub>3</sub><sup>-</sup>. On the other hand, there is a significant relationship with mesophilic bacteria only in the case of DO and K<sup>+</sup>. There was no significant correlation with the water temperature in any of the measuring points, although other Authors report such relationship in their papers [24, 25].

Table 3 shows mean, minimum and maximum values, as well as coefficient of variation (Cv) for physical and chemical parameters at the examined sites. In the Bialka river, both before the treatment plant and at the intake, water was characterized by high oxygen content, low temperature and alkaline pH (pH~8). Water conductivity was around 270 μS/cm and TDS around 230 mg/l. The concentration of nutrients (NH<sub>4</sub><sup>+</sup>, NO<sub>3</sub><sup>-</sup>, NO<sub>2</sub><sup>-</sup>, PO<sub>4</sub><sup>3-</sup>) was low or their values were below limit of detection. On the other hand, the outflow from the sewage treatment plant was characterized by far higher values of TDS, EC<sub>25°C</sub>, temperature and the concentration of ions, as well as by significantly lower content of dissolved oxygen. Very high values of NH<sub>4</sub><sup>+</sup> and at the same time low values of NO<sub>3</sub><sup>-</sup> and NO<sub>2</sub><sup>-</sup> evidence very poor efficiency of biological treatment of sewage in the examined treatment plant.

The outflow from the sewage treatment plant differs significantly (ANOVA) in terms of all examined physical and chemical parameters from the values of these parameters at the points Before STP and Intake. On the other hand, the site Before STP differs significantly from the Intake only in terms of EC<sub>25°C</sub>, TDS, Na<sup>+</sup>, NH<sub>4</sub><sup>+</sup>, Cl<sup>-</sup>. The outflow from the treatment plant adversely affects the chemical composition of water in the Bialka river

**TABLE 2**  
Significant Spearman's correlation coefficients (p<0.05) between microbiological indicators and physico-chemical characteristics of water at each of the sampling sites.

Parameter	Before STP		STP		Intake	
	<i>E. coli</i>	mesophilic bacteria	<i>E. coli</i>	mesophilic bacteria	<i>E. coli</i>	mesophilic bacteria
<i>E. coli</i>	1.00	-	1.00	0.66	1.00	0.85
mesophilic bacteria	-	1.00	0.66	1.00	0.85	1.00
DO	-	-	-0.62	-0.78	-	-
T	-	-	-	-	-	-
EC <sub>25°C</sub>	-	-	0.77	-	0.65	0.64
Na <sup>+</sup>	-	-	0.81	-	0.91	0.77
K <sup>+</sup>	-	-	0.72	0.64	-	-
NH <sub>4</sub> <sup>+</sup>	-	-	0.80	-	0.96	0.77
Cl <sup>-</sup>	-	-	0.80	-	0.88	0.78
NO <sub>3</sub> <sup>-</sup>	-	-	-0.82	-	-	-
PO <sub>4</sub> <sup>3-</sup>	-	-	0.76	-	0.67	-

**TABLE 3**  
**Physical and chemical water parameters during the diurnal study.**

Parameter	Unit	Before STP				STP				Intake			
		Mean	Min	Max	Cv [%]	Mean	Min	Max	Cv [%]	Mean	Min	Max	Cv [%]
DO	mg/L	13.9	13.6	14.3	1.7	5.0	3.0	8.0	35.1	13.5	11.4	14.2	5.3
T	°C	0.2	-0.2	1.0	179.4	6.8	3.7	9.1	26.1	0.4	-0.1	1.0	121.6
pH		8.07	8.00	8.13	0.5	7.40	7.25	7.60	1.4	8.02	7.91	8.11	0.8
EC <sub>25°C</sub>	µS/cm	264.0	257.4	270.5	1.8	1,031.7	616.4	1,436.3	30.0	272.4	263.2	283.2	2.4
TDS		231.2	227.1	236.5	1.4	808.0	529.2	1,069.1	25.1	236.3	229.0	246.2	2.2
Na <sup>+</sup>		3.49	3.35	3.67	2.8	68.3	18.9	116.7	53.4	3.9	3.46	4.7	10.0
K <sup>+</sup>		0.89	0.72	1.74	34.4	15.3	5.1	22.5	42.2	1.1	0.72	1.9	38.0
NH <sub>4</sub> <sup>+</sup>	mg/L	0.02	0.01	0.03	30.7	35.8	6.7	68.2	62.6	0.14	0.01	0.51	109.1
Cl <sup>-</sup>		4.86	4.51	5.11	3.7	70.3	19.0	117.5	53.9	5.2	4.70	5.9	8.2
NO <sub>3</sub> <sup>-</sup>		3.56	3.44	3.69	2.3	4.11	3.70	4.89	13.4	3.64	3.48	3.97	3.9
NO <sub>2</sub> <sup>-</sup>		below limit of detection				0.2	0.1	0.3	47.4	below limit of detection			
PO <sub>4</sub> <sup>3-</sup>		below limit of detection				7.1	0.7	17.7	83.9	0.007	0.003	0.015	76.7

(point Intake). Inflow of insufficiently treated sewage causes a decrease in the dissolved oxygen content and water pH, as well as an increase in the concentration of ions in the water of Białka. This is most evident in the case of NH<sub>4</sub><sup>+</sup>, whose average increase between the points Before STP and Intake was about 60%. The average increase in the concentration of Na<sup>+</sup>, K<sup>+</sup> and Cl<sup>-</sup> ions is also evident and reaches 9.9%, 7.0% and 6.7%, respectively.

The differences in physical and chemical parameters during the day were statistically significant in each of the measuring points. The greatest diurnal changes were related to ions, whose occurrence in water can be associated with anthropogenic pressure (i.e. NH<sub>4</sub><sup>+</sup>, NO<sub>3</sub><sup>-</sup>, PO<sub>4</sub><sup>3-</sup>, K<sup>+</sup>, Na<sup>+</sup>, Cl<sup>-</sup> – Fig. 2). For example, at the point Before STP the maximum daily value of NH<sub>4</sub><sup>+</sup> was 3.5 times greater than the smallest one measured throughout the day. Much larger diurnal fluctuations were observed at the point Intake. There was a 35-fold increase in the concentration of NH<sub>4</sub><sup>+</sup> during the day. 10-fold diurnal variation in the concentration of NH<sub>4</sub><sup>+</sup> was observed at the STP, but the variation in the concentrations of PO<sub>4</sub><sup>3-</sup> was even more evident (25-fold difference in the concentration values throughout the day).

The inflow of sewage from an ineffectively operating sewage treatment plant together with numerous unregistered discharge points of untreated sewage in the Bukowina Tatrzńska municipality result in the deterioration of water quality in the Białka river. However, the mountainous nature of the river, characterized by turbulent water flow, low temperature of water and very good oxygenation causes that in terms of physical and chemical parameters it can be classified as the highest, first

class of water quality [26].

The Principal Component Analysis (PCA, Fig. 3.) allowed to determine the main factors affecting the concentration of microbial indicators of fecal contamination, as well as hydrochemical characteristics of water at the examined sampling points in the diurnal cycle. At the site No. 1 (Before STP), PCA allowed to distinguish one factor that explains 72.7% of variance. Based on the factor coordinates, a strong correlation between *E. coli*, mesophilic bacteria and NH<sub>4</sub><sup>+</sup> and NO<sub>3</sub><sup>-</sup> ions can be observed. This factor can be explained by the anthropogenic influence, as the higher nutrient concentrations, whose origin is mainly related to human activity, the higher the prevalence of bacteria.

By the discharge from the sewage treatment plant (site No. 2 – STP), PCA also allowed to recognize one factor that explains 74.5% of variance. It is characterized by a strong positive relationship between the number of bacterial indicators and T, EC<sub>25°C</sub>, Na<sup>+</sup>, K<sup>+</sup>, NH<sub>4</sub><sup>+</sup>, Cl<sup>-</sup> and PO<sub>4</sub><sup>3-</sup> and negative relationship with pH, DO and NO<sub>3</sub><sup>-</sup>. This factor may evidence the discharge of fresh, untreated sewage from the treatment plant, where the nitrification process did not occur. This is particularly apparent in the negative relationship between NO<sub>3</sub><sup>-</sup> and NH<sub>4</sub><sup>+</sup>, i.e. the occurrence of large concentrations of ammonium ions with very low concentrations of nitrate ions [27]. Usually, untreated sewage contains nitrogen in the form of NH<sub>4</sub><sup>+</sup>, while the amount of nitrates and nitrites is small.

Principal Component Analysis carried out for the sampling site No. 3 (Intake) showed that there are two factors affecting the quality of water throughout the day. Factor 1 explains 56.2% of variance and represents positive relationship between the content

of bacteria in water and the values of  $EC_{25^{\circ}C}$ , TDS,  $Na^+$ ,  $NH_4^+$ ,  $Cl^-$ ,  $NO_3^-$ ,  $PO_4^{3-}$ . In contrast, factor 2 explains 21.4% of variance and represents negative relationship showing that the higher the values of  $EC_{25^{\circ}C}$  and  $NO_3^-$  the lower the values of T,  $K^+$  and  $PO_4^{3-}$ . In the case of factor 1 we can consider the anthropogenic effect and deterioration of water quality through the sewage discharge to the Bialka

river. This is evidenced by the increase in the number of bacteria and  $NH_4^+$ ,  $NO_3^-$ ,  $PO_4^{3-}$  ions, which are of anthropogenic origin. Factor 2 is related to the diurnal activity of people, resulting in the production of smaller amount of sewage during night. Therefore, the efficiency of sewage treatment is greater and the process of nitrification is more effective which results in higher  $NO_3^-$  values in

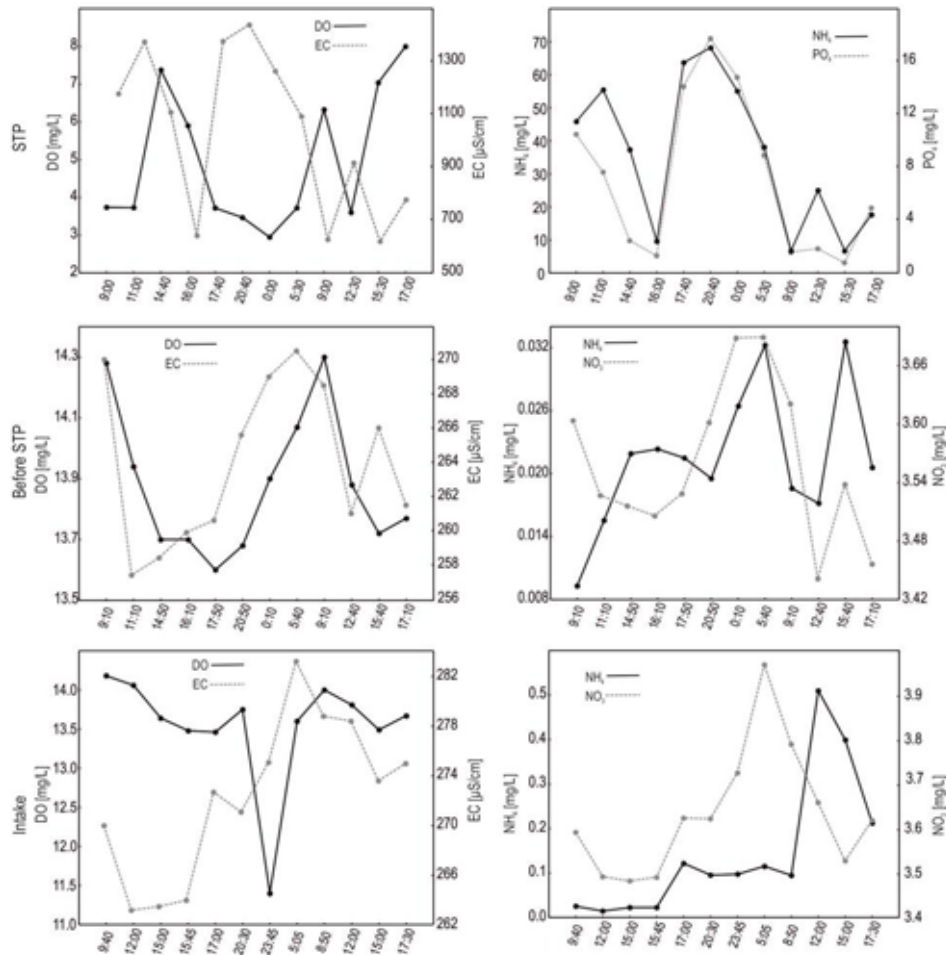


**FIGURE 2**  
Changes in the selected physico-chemical parameters at the measuring points throughout the study period.

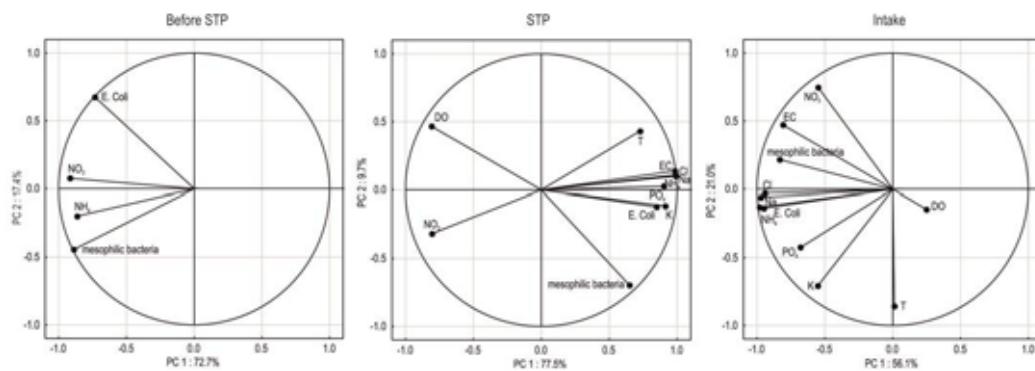


**FIGURE 3**  
Principal Component Analysis of microbiological and physicochemical parameters determined for the sampling sites.

sewage discharged to the river. At the same time, low temperature of water at night causes that snow does not melt, thus not causing dilution of water and therefore the water conductivity being higher.

## CONCLUSIONS

The number of microbial indicators of fecal contamination depends on the location of the sampling sites and their location towards the main source of water contamination, i.e. the sewage treatment plant. A variation in a diurnal cycle of the concentration of the tested microbial parameters of water quality, as well as the physico-chemical characteristics of water was also evident. The cycle of the sewage treatment plant operation affects the number of microbial contaminants of water both in the stream which receives the effluent from the treatment plant and in the part of the river downstream of the treatment plant.

The conducted analyses revealed that in terms of chemical parameters water in the Białka river can be assessed as good quality, while the detected microbiological contamination indicates that without very thorough treatment, those waters cannot be used neither for consumption or for the technological use. It is important to carefully select sampling sites, as their location within catchments may affect the concentrations of microbial indicators of fecal contamination.

## ACKNOWLEDGEMENTS

This study was funded by statutory measures of the University of Agriculture in Kraków, within a grant No. BM 4149/2014 and a grant No. DS 3102/KM/2014, as well as by the Jagiellonian University grant No. K/KDU/000153 - Hydrochemical and hydrological monitoring of the Białka subcatchments in the neighborhood of Kotelnica (2013-2015).

## REFERENCES

- [1] [http://ec.europa.eu/environment/nature/natura2000/index\\_en.htm](http://ec.europa.eu/environment/nature/natura2000/index_en.htm), Accessed September 20<sup>th</sup> 2015.
- [2] Pająk B. (2014). Report on the condition of the environment in the Lesser Poland voivodeship in 2013, Provincial Environmental Protection Inspectorate WIOŚ in Kraków Poland.
- [3] Heldak M. 2010 The Białka River in the Rural Landscape of Podhale. *Landscape Architecture*, 2, 39-46.
- [4] Krąż P. (2012). Anthropogenic hazards to the Białka Valley natural environment. *Geographical Papers*, 128, pp. 45-54 (in Polish).
- [5] [www.supersnow.pl](http://www.supersnow.pl), Accessed July 7<sup>th</sup> 2015.
- [6] Central Statistical Office. (2013). [http://stat.gov.pl/bdl/app/strona.html?p\\_name=indeks](http://stat.gov.pl/bdl/app/strona.html?p_name=indeks)
- [7] Lenart-Boroń A., Wolanin A., Jelonkiewicz Ł., Chmielewska-Błotnicka D., Żelazny M. (2016) Spatiotemporal Variability in Microbiological Water Quality of the Białka River and Its Relation to the Selected Physicochemical Parameters of Water. *Water Air & Soil Pollution* 227(1): 10.1007/s11270-015-2725-7
- [8] Smoroń S., Twardy S. & Kowalczyk A. (2007). Surface water quality in tourist areas of the Western Carpathians. Part 1. The dynamics of chemical substances load in domestic wastewaters. *Water-Environment-Rural Areas*, 21, 155-166 (in Polish).
- [9] Parker L.V., Yushak M.L., Martel J. & Reynolds C.M. (2000). Bacterial Survival in Snow Made from Wastewater. Technical Report ERDC/CRREL TR-00-9. US Army Corps of Engineers, Cold Regions Research & Engineering Laboratory, New Hampshire, USA.
- [10] Walker V.K., Palmer G.R. & Voordouw G. (2006). Freeze-thaw tolerance and clues to the winter survival of a soil community. *Applied and Environmental Microbiology*, 72(3), 1784-1792.
- [11] Krzesiwo K. (2014). Development and functioning of ski stations in the Polish Carpathians. Kraków: Institute of Geography and Spatial Management, Jagiellonian University.
- [12] Krzesiwo K. (2015). Tourist traffic in the Kotelnica Białczańska Ski Station in the winter season 2014/2015, research report, Kinga Krzesiwo Research & Consulting, Pisarzowice, Poland.
- [13] Whitman R.L. & Nevers M.B. (2004). *Escherichia coli* sampling reliability at a frequently closed Chicago beach: monitoring and management implications. *Environmental Science and Technology*, 38, 4241-4246.
- [14] Meays C.L., Broersma K., Nordin R., Mazumder A. & Samadpour M. (2006). Diurnal variability in concentrations and sources of *Escherichia coli* in three streams. *Canadian Journal of Microbiology*, 52, 1130-1135.
- [15] <http://www.socscistatistics.com/tests/studentttest/Default.aspx>, Accessed September 18<sup>th</sup> 2015.
- [16] Wakelin S.A., Colloff M.J. & KooKana R.S. (2008). Effect of wastewater treatment plant effluent on microbial function and community structure in the sediment of a freshwater stream with variable seasonal flow. *Applied and Environmental Microbiology*, 74(9), 2659-2668.

- [17] Mishra A. (2010) Assessment of water quality using principal component analysis: A case study of the river Ganges. *Journal of Water Chemistry and Technology*, 32(4), 227-234.
- [18] Thyne G., Guler C. & Poeter E. (2004). Sequential analysis of hydrochemical data for watershed characterization. *Ground Water*, 42(5), 711-723.
- [19] Sinton L.W., Finlay R.K. & Hannah D.J. (1998). Distinguishing human from faecal contamination in water: a review. *New Zealand Journal of Marine Freshwater Research*, 32, 323-348
- [20] Cabral J.P.S. (2010) Water Microbiology. Bacterial Pathogens and Water. *International Journal of Environmental Research and Public Health*, 7(10), 3657-3703.
- [21] Regulation of the Minister of the Environment of 27<sup>th</sup> November 2002 on the requirements to be met by surface water used to supply people with drinking water. *Journal of Laws of the Republic of Poland No. 204, item 1728.*
- [22] Grabow W.O.K. (1996). Waterborne diseases: update on water quality assessment and control. *Water SA*, 22, 193-202.
- [23] Kukuła E. (2006). Assessment of microbiological quality of waters of the San river. *Proceedings of the 2<sup>nd</sup> Scientific and Technical Conferences "Blue San"*, Rzeszów University, 121 – 125.
- [24] Kolarevic S., Knezevic-Vukcevic J., Paunovic M., Vasiljevic B., Kracun M., Gacic Z. & Vukovic-Gacic B. (2012). Seasonal variations of microbiological parameters of water quality of the Velika Morava River Serbia. *Archives of Biological Sciences, Belgrade*, 64(3), 1017-1027.
- [25] North R.L., Khan N.H., Ahsan M., Prestie C., Korber D.R., Lawrence J.R. & Hudson I.J. (2014). Relationship between quality parameters and bacterial indicators in a large prairie reservoir: Lake Diefenbaker, Saskatchewan, Canada. *Canadian Journal of Microbiology*, 60(4), 243-249.
- [26] Regulation of the Minister of Environment of 22<sup>nd</sup> October 2014 on the classification status of surface waters and environmental quality standards for priority substances. *Journal of Laws of the Republic of Poland No. 2014, item. 1482.*
- [27] Bothe H., Jost G., Schloter M., Ward B.B. & Witzel K-P. (2000). Molecular analysis of ammonia oxidation and denitrification in natural environments. *FEMS Microbiology Reviews*, 24, 673-690.

---

**Received:** 07.01.2016  
**Accepted:** 17.08.2016

---

#### CORRESPONDING AUTHOR

---

**Anna Lenart-Boron**

Department of Microbiology, University of Agriculture in Cracow Mickiewicza Ave. 24/28, 30-059 Cracow, Poland

e-mail: [a.lenart-boron@ur.krakow.pl](mailto:a.lenart-boron@ur.krakow.pl)



# TOXIC EFFECTS OF THE JOINT EXPOSURE OF Cd AND DECABROMODIPHENYL ETHER ON SOIL MICROBIAL POPULATION

Zhaoxiang Han<sup>1,2,\*</sup>, Ning Wang<sup>3</sup>, Xingyu Yang<sup>1</sup>, Rui Zhou<sup>4</sup>

<sup>1</sup> School of Chemical Engineering, Huaihai Institute of Technology, Lianyungang, Jiangsu, 222005, China

<sup>2</sup> Jiangsu Provincial Key Laboratory of Coastal Wetland Bioresources and Environmental Protection, Yancheng, Jiangsu, 224002, China

<sup>3</sup> School of Environment and safety Engineering, Jiangsu University, Zhenjiang, Jiangsu, 212000, China

<sup>4</sup> College of environment, Hohai University, Jiangsu, 210098, China

## ABSTRACT

In order to make clear the toxic effects of the joint exposure of Cd and decabromodiphenyl ether (BDE-29) on soil microbial population. During the 35 days after exposure to moderate Cd concentration resulted in a significant increase in *pseudomonas aeruginosa*, the high Cd concentrations exerts a significantly inhibiting effect on the *pseudomonas aeruginosa* populations, similar trends were also observed in *Actinomyces* at lower and moderate Cd concentration. The inhibition rate of *fungi* in Cd treatments did not have significant differences at all treatments. The order of inhibiting rate of culturable soil microbial populations under Cd pollution was proved to be: *pseudomonas aeruginosa* > *actinomycetes* > *fungi*. BDE-209 inhibited the growth of soil *pseudomonas aeruginosa*, *fungin* and *Actinomyces* populations, even at a low concentration. The population of the three soil microbes generally declined with increasing BDE-209 concentration following certain dose-response relationships during the entire incubation period. The inhibition ratios were dependent on incubation time, indicating a notable time-effect trend. The inhibition of joint Cd and BDE-209 exposure on soil microbial population was stronger than that of either of the two chemicals at moderate level Cd and BDE-209. The inhibition ratios of three microbial populations increased with increasing Cd + BDE-209 concentration and incubation time following certain dose-response relationships and time-effect trends during the entire incubation period, respectively. The sensitivity of soil microbial population followed the order: *pseudomonas aeruginosa* > *fungi* > *actinomycete*.

## KEYWORDS:

Cd, BDE-209, joint exposure, microbial population.

## INTRODUCTION

With the rapid development of electric technology, waste electrical and electronic equipment, also known as e-waste, refers to end-of-life products including computer, cellular phone and television is rather striking. It has been estimated that 20-50 million tonnes of e-waste are produced annually in the world and increases rapidly at a rate of 3-5% per year [1]. Taking advantage of inexpensive cost of labor and weak enforcement of environmental laws, much more e-waste is being exported to developing countries. However, the recycling techniques in these countries are often crude and do not have the appropriate facilities [2], waste processing operations such as uncontrolled dismantling, acid stripping and open burning in Chinese e-waste recycling sites have resulted in severe environmental contamination [3,4]. The hazard of e-waste lies in the high content of many toxic substances. As a result of the unprotected recycling techniques, various high toxic pollutants such as heavy metals (e.g. Cd and Cu) and persistent organic pollutants (POPs) (e.g. PBDEs), were released into the environment [3-6]. Some studies have been focused on the environment pollution caused by e-wastes in China since the last decade. The accumulation of heavy metals and PBDEs in soil has been reported in some sites of e-waste recycling locations [7-10]. However, since these data do not take into account the possible combined effects of different contaminants, as well as their bioavailability. Soil microflora plays a major role in the decomposition of organic matter and the mineralization of nitrogen, phosphorus, and sulfur in the agro-ecosystem, they also play significant roles in maintenance of soil structure, detoxification of noxious chemicals, and the control of plant pests and plant growth [11,12]. Since soil microorganisms can respond rapidly, they reflect a hazardous environment and are, therefore, considered when monitoring soil status. A number of soil microbiological parameters, notably such as

microbial community structure, microbial biomass, have been suggested as possible indicators of soil environmental quality, and have been employed in national and international monitoring programs [13,14]. Heavy metal not only produce adverse effects on plant quality and yield but also cause changes in the size, composition, and activity of soil microbial community [15,16]. BDE-209 was dominant PBDEs congener. It is reported that BDE-209 can reach toxic concentrations that are detrimental to the environment as well as to human health [17,18]. Although heavy metals and PBDEs are both present in many e-waste recycling sites, there has been no report about their joint toxicity on soil microbes. This study was conducted primarily to explore the toxicological effects of Cd and BDE-209 contamination on soil culturable microbial population. The observations and related findings will establish some useful scientific basis for soil ecological risk assessment in e-waste recycling sites.

## MATERIALS AND METHODS

**Chemicals.** BDE-209 (purity>98.0%) was obtained from Dongguan Boye Instrument Machinery Co. Ltd., Guangdong, China. Cadmium chloride ( $\text{CdCl}_2$ ) and other reagents were analytical grade and obtained from Sinopharm Chemical Reagent Beijing Co., Ltd., China.

**Experimental design of the incubation test.** The soil used in this experiment (silty clay loam, 5.8% organic matter, pH 6.9) was collected from around the e-waste of Changzhou in Jiangsu province, China. A composite soil sample was prepared by collecting soil samples from six separate locations across the field. At the laboratory, the soil was fully mixed, pebbles and large plant residues were removed, and then the soil was sieved using a 2 mm sieve. Cadmium stock solution was prepared by dissolving  $\text{CdCl}_2$  in deionized water, and BDE-209 stock solution was prepared by dissolving the BDE-209 powder in DMSO 5 g of the soil sample each was added to several 10 mL tissue culture flasks, the flasks were then filled with the BDE-209 and Cd stock

solutions to expose the sample to the contaminants (Table1). Each treatment was conducted in three replicated runs. The control received the same amounts of distilled water instead of the contaminant solution. All treatments were incubated at room temperature, and were kept in complete darkness. Soil samples were collected for further analysis at 0, 7, 14, 21, 28 and 35d after incubation.

**Microbial enumeration.** All the following measurements were made in triplicate soil samples and the results are expressed as oven-dry mass. Enumeration of soil microorganisms was performed using the spread plate counting method [10,16].

**Evaluation of data and modeling.** The inhibition ratios (IR) of microbial population exposed to Cd, BDE-209 or Cd+BDE-209 were calculated as Eq. (1):  $\text{IR}=(Y-X)/Y$  (1), where Y is the value of the control soil and X is the value of the contaminated soil. The results were expressed as the average of three paralleled determinations of the mixture of three duplicates soil samples.

In order to account for combined effect of different important independent variables, second-order polynomial models are preferred [10,19]. Therefore, it was thought of interest to develop a model describing the effects of two selected independent variables (Cd and BDE-209 concentrations) on the inhibition ratios of soil microbial population. The model was expressed as (2):

$Y=X_i+X_j+X_iX_j+\epsilon$  (2), where Y is the predicted value of the inhibition ratio of microbial populations, X is the independent variables corresponding to the concentration of Cd and BDE-209 [10,17];  $\epsilon$  is the erratic error; is the constant and also called intercept;  $j$  and  $i$  is the regression coefficient estimated by the stepwise regression method at a confidence level of 95%, and  $j$  represents the interaction properties and strength of these contaminants. If the value of  $j$  is positive, the interactive effect is synergistic, and a negative value represents antagonistic, while zero stands for additive toxicity.

**TABLE 1**  
**Cd and BDE-209 contamination levels of different treatment designs (mg/kg)**

Contaminant	Control	Low treatments	Moderate treatments	High treatments
Cd	0	1.0,2.0	4.0, 6.0	8.0,10.0
BDE-29	0	1.0	10.0	50.0
Cd +BDE-29	0	1.0+1.0	4.0+10.0	8.0+50.0

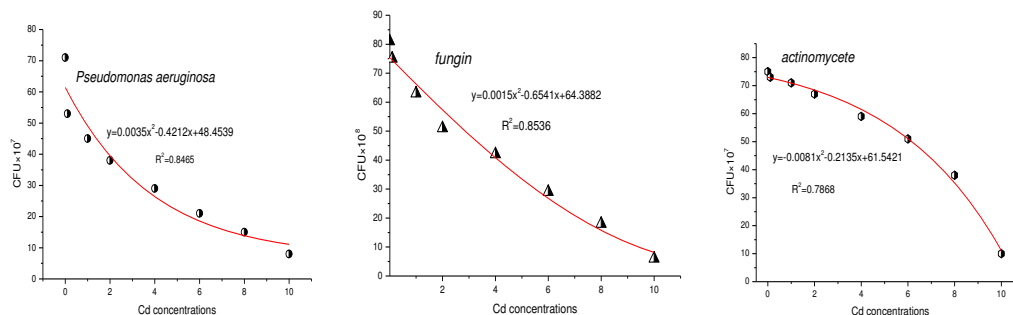


**FIGURE 1**  
Correlation between Cd concentrations versus number of microorganisms.

## RESULTS

**Effect of Cd single exposure on number of microorganisms.** Soil contamination with 1.0, 2.0, 4.0, 6.0, 8.0 and 10.0 mg Cd/kg of soil significantly inhibited the growth of *pseudomonas aeruginosa*, *fungin* and *Actinomycete* in soil on either assay date, respectively. Higher concentrations of cadmium caused decrease in the number of these microorganisms in all series of experiments, and especially in the series with 10.0 mg/kg of soil. The results of polynomial regression equations (Figure1) and Pearson's simple correlation coefficients seem indicative of a significant, negative correlation between the number of soil microorganisms and cadmium contamination concentrations, which reaffirms the research of [20].

**Effect of Cd single exposure on soil microbial population.** In order to explain further the reason of number of microorganisms in 3.1, we try to illustrate of inhibitory effects for Cd single exposure on soil microbes. Figure 2 illustrated the inhibitory effects of contaminant Cd on the growth of soil *pseudomonas aeruginosa*, *fungin* and *Actinomycete*. In all the soil treatments, as the exposure concentration and incubation time increased, the inhibition ratios increased for *pseudomonas aeruginosa*. During the 35 days after exposure to low Cd concentrations (1.0 and 2.0 mg/kg), soil culturable microbial population of the treated samples were the same or only slightly different to the control. The application of moderate (4.0 and 6.0 mg/kg) Cd concentration resulted in a significant increase in *pseudomonas aeruginosa* from 7 to 35 days of incubation time, the high Cd concentrations exerts an significantly inhibiting effect on the *pseudomonas aeruginosa* populations, the inhibitory rate increased with the increased Cd concentration from 8.0 to 10.0 mg/kg and the incubation time. Similar trends were also observed in *Actinomycete* at lower and moderate Cd concentration, but the extent of inhibition was larger than the lower Cd treated soils in most time.

When the concentrations of Cd were larger than 4.0 mg/kg, the inhibition rate increased slowly in the later time, but the inhibition rate in soils added with Cd at higher level (8.0 mg/kg) began to decrease. The inhibition rate of *fungi* in Cd treatments did not have significant differences at all treatments, the inhibition rate of *fungi* increased slightly though all the incubation time in soils treated with Cd concentration from moderate treatments (4.0-6.0 mg/kg) to higher treatments (8.0-10.0 mg/kg). The order of inhibiting rate of culturable soil microbial populations under Cd pollution was proved to be: *pseudomonas aeruginosa* > *actinomycetes* > *fungi*.

**Effect of BDE-209 single exposure on soil microbial population.** Contaminant BDE-209 inhibited the growth of soil *pseudomonas aeruginosa*, *fungin* and *Actinomycete* populations, even at a low concentration (1.0 mg/kg), as shown in Figure 3. The population of the three soil microbes generally declined with increasing BDE-209 concentration following certain dose–response relationships. The inhibition ratios were dependent on incubation time, indicating a notable time-effect trend. As for soil *pseudomonas aeruginosa*, 1.0 mg/kg dose of BDE-209 did not produce the significant population inhibition as caused by the higher dose of 50 mg/kg. Also, both treatments inhibited the growth of *Actinomycete* and *fung in* populations in the following days. The treatments of BDE-29 decreased the total *actinomycetes* counts during the entire experiment, and 10.0 mg/kg and 50.0 mg/kg BDE-29 inhibited the total *pseudomonas aeruginosa* counts by 81.8% and 89.5%, respectively, in 35 days, as well as *actinomycetes* inhibited the total cell counts by 68.4% and 73.2%, respectively, in whole period of incubation time. The total *fung in* cell counts of the middle and high concentration BDE-29 treatments were increased by 1.68 and 2.02 fold on the 35th day, respectively. The microbial biomass increased but the increase was smaller than in control samples, the result indicated that the BDE-29 had an inhibition effect first and then could be used as

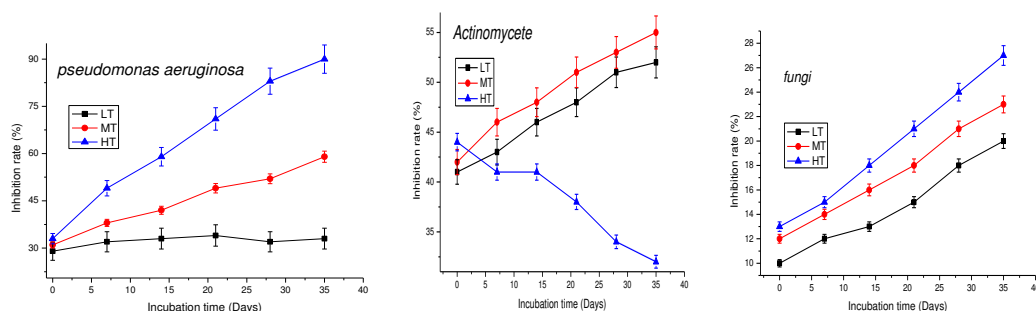


FIGURE 2

Inhibition rate of microbial populations in tested soils with different Cd concentrations.

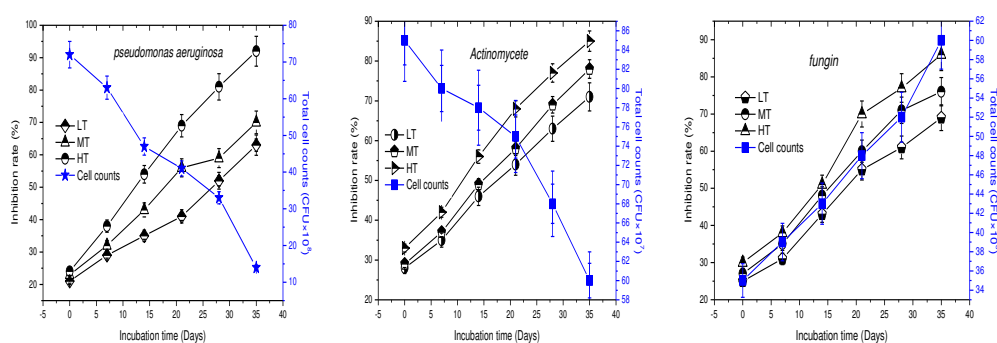


FIGURE 3

The influence of BDE-209 on inhibition rate and total cell counts (mean±standard deviation) of soil microbes ( $P < 0.01$ )

the carbon source by the *fungin* [21]. However, in the soil microcosms spiked with BDE-209, significant suppression ( $P < 0.01$ ) was observed and the suppression effect increased with the higher BDE-209 concentration.

**Joint exposure of Cd and BDE-209 on soil microbial population.** The microbes population quantity decreased with the increasing Cd and BDE-209 concentration and incubation time. Table 2 summarizes the second-order polynomial model representation of the observed inhibitory effects of Cd and BDE-209 on microbial population, the  $\beta_{ij}$  values were negative in almost all treated groups. And the regression coefficients of Cd-BDE-209 on the growth inhibition were negative during most incubation periods except for *fungi* exposed to 14 d and *actinomycete* exposed to 28 d, indicating the interactive effects of the two contaminants were antagonistic effect. On the contrary, after *fungi* or *actinomycete* exposed to 35 d, the joint toxicity exhibited synergistic effect, the combined effect showed additive role to *pseudomonas aeruginosa* after 35 d incubation time. The inhibition ratios of *fungi* growth were relatively stable in the combined treatment runs of low and moderate levels of Cd

and BDE-209 during the first 14 day and then increased sharply. Lower concentrations (1.0 mg/kg) of Cd and the lower levels of BDE-209 (1.0 mg/kg) combination inhibited the *pseudomonas aeruginosa* growth, *actinomycete* also displayed the inhibitory effects exposed to 1.0 mg/kg of BDE-209 and its combination with 1.0 mg/kg of Cd, 35 d exposure later the *pseudomonas aeruginosa* was clearly inhibited by all levels of both chemicals, whereas only high doses of Cd and BDE-209 combination reduced the population of *fungi* and *actinomycete*. At relatively moderate level (Cd:4.0 mg/kg and BDE-209:10.0 mg/kg), the inhibition of joint Cd and BDE-209 exposure on soil microbial population was stronger than that of either of the two chemicals. Cd was more toxic to the soil microbes than BDE-209. Generally, during the entire incubation period, the inhibition ratios of three microbial populations increased with increasing Cd+BDE-209 concentration and incubation time following certain dose-response relationships and time-effect trends, respectively. Data analysis suggested the sensitivity of soil microbial population followed the order: *pseudomonas aeruginosa* > *fungi* > *actinomycete*.

TABLE 2

A summary of the second order model representations of the observed soil microbial growth inhibition ratios (R) and exposure concentrations of Cd (C<sub>1</sub>) and BDE209 (C<sub>2</sub>).

Soil strain	Incubation time (d)	Multiple regression model	R <sup>2</sup>	Sig.
pseudomonas aeruginosa	14	R=0.012 C <sub>1</sub> +0.002 C <sub>2</sub> -4.263×10 <sup>-6</sup> C <sub>1</sub> C <sub>2</sub> +0.046	0.859	<0.01
	21	R=0.006 C <sub>1</sub> +0.018 C <sub>2</sub> -2.186×10 <sup>-5</sup> C <sub>1</sub> C <sub>2</sub> +0.058	0.914	<0.01
	28	R=0.018 C <sub>1</sub> +0.035 C <sub>2</sub> +3.594×10 <sup>-5</sup> C <sub>1</sub> C <sub>2</sub> +0.167	0.925	<0.01
	35	R=0.035 C <sub>1</sub> +0.002 C <sub>2</sub> +6.152×10 <sup>-4</sup> C <sub>1</sub> C <sub>2</sub> +0.255	0.889	<0.01
actinomycete	14	R=0.015 C <sub>1</sub> +0.029 C <sub>2</sub> -1.385×10 <sup>-6</sup> C <sub>1</sub> C <sub>2</sub> +0.172	0.961	<0.01
	21	R=0.038 C <sub>1</sub> +0.0195 C <sub>2</sub> -5.967×10 <sup>-5</sup> C <sub>1</sub> C <sub>2</sub> +0.239	0.895	<0.01
	28	R=0.056 C <sub>1</sub> +0.007 C <sub>2</sub> -4.853×10 <sup>-5</sup> C <sub>1</sub> C <sub>2</sub> +0.452	0.943	<0.01
	35	R=0.067 C <sub>1</sub> +0.019 C <sub>2</sub> +4.769×10 <sup>-4</sup> C <sub>1</sub> C <sub>2</sub> +0.581	0.836	<0.01
fungi	14	R=0.113 C <sub>1</sub> +0.117 C <sub>2</sub> -6.206×10 <sup>-6</sup> C <sub>1</sub> C <sub>2</sub> +0.133	0.917	<0.01
	21	R=0.257 C <sub>1</sub> +0.009 C <sub>2</sub> -3.471×10 <sup>-5</sup> C <sub>1</sub> C <sub>2</sub> +0.0553	0.882	<0.01
	28	R=0.025C <sub>1</sub> +0.036 C <sub>2</sub> -1.397×10 <sup>-5</sup> C <sub>1</sub> C <sub>2</sub> +0.128	0.976	<0.01
	35	R=0.035 C <sub>1</sub> +0.061 C <sub>2</sub> +3.258×10 <sup>-4</sup> C <sub>1</sub> C <sub>2</sub> +0.016	0.885	<0.01

## DISCUSSION AND CONCLUSIONS

We employed microorganisms to examine the single and jointed effects of Cd and BDE-209 exposure to allow direct comparison. During the 35 days after exposure to low Cd concentrations, soil culturable microbial population of the treated samples were the same or only slightly different to the control. The application of moderate Cd concentration resulted in a significant increase in *pseudomonas aeruginosa* from 7 to 35 days of incubation time, the high Cd concentrations exerts an significantly inhibiting effect on the *pseudomonas aeruginosa* populations, similar trends were also observed in *Actinomycete* at lower and moderate Cd concentration. The inhibition rate of *fungi* in Cd treatments did not have significant differences at all treatments, the inhibition rate of *fungi* increased slightly though all the incubation time in soils treated with Cd concentration from moderate treatments to higher treatments. The order of inhibiting rate of culturable soil microbial populations under Cd pollution was proved to be: *pseudomonas aeruginosa*>*actinomycetes*>*fungi*. BDE-209 inhibited the growth of soil *pseudomonas*

*aeruginosa*, *fungin* and *Actinomycete* populations, even at a low concentration. During the entire incubation period, the population of the three soil microbes generally declined with increasing BDE-209 concentration following certain dose–response relationships. The inhibition ratios were dependent on incubation time, indicating a notable time-effect trend. Lower concentrations of Cd and the lower levels of BDE-209 combination inhibited the *pseudomonas aeruginosa* growth, *actinomycete* also displayed the inhibitory effects exposed to 1.0 mg/kg of BDE-209 and its combination with 1.0 mg/kg of Cd, 35 d exposure later the *pseudomonas aeruginosa* was clearly inhibited by all levels of both chemicals. At relatively moderate level Cd and BDE-209, the inhibition of joint Cd and BDE209 exposure on soil microbial population was stronger than that of either of the two chemicals. Generally, during the entire incubation period, the inhibition ratios of three microbial populations increased with increasing Cd+BDE-209 concentration and incubation time following certain dose-response relationships and time-effect trends, respectively. The sensitivity of soil microbial population



followed the order: *pseudomonas aeruginosa*>*fungi*>*actinomycete*.

## ACKNOWLEDGEMENTS

This research was supported by innovation foundation of Huaihai Institute of Technology (No.Z2014014), Jiangsu Provincial Key Laboratory of Coastal Wetland Bioresources and Environmental Protection (No.JLCBE11004), and the Center for Studies of Marine Economy and Sustainable Development of Jiangsu province (No. HJ12007). The Priority Academic Program Development of Jiangsu Higher Education Institutions.

## REFERENCES

- [1] Robinson, B.H.,(2009)E-waste: An assessment of global production and environmental impacts. *Science of The Total Environment* 408(2): p. 183-191.
- [2] Tang, X., et al.,(2010) Inorganic and organic pollution in agricultural soil from an emerging e-waste recycling town in Taizhou area, China. *Journal of Soils and Sediments* 10(5): p. 895-906.
- [3] Wong, C.S.C., et al.,(2007) Evidence of excessive releases of metals from primitive e-waste processing in Guiyu, China. *Environmental Pollution* 148(1): p. 62-72.
- [4] Zhang, W., et al., (2012)The combined effect of decabromodiphenyl ether (BDE-209) and copper (Cu) on soil enzyme activities and microbial community structure. *Environmental Toxicology and Pharmacology* 34(2): p. 358-369.
- [5] Wong, M.H., et al.,(2007) Export of toxic chemicals – A review of the case of uncontrolled electronic-waste recycling. *Environmental Pollution* 149(2): p. 131-140.
- [6] Ni, H.-G., et al., (2010)Environmental and human exposure to persistent halogenated compounds derived from e-waste in China. *Environmental Toxicology and Chemistry* 29(6): p. 1237-1247.
- [7] Cai, Z. and G. Jiang, (2006)Determination of polybrominated diphenyl ethers in soil from e-waste recycling site. *Talanta* 70(1): p. 88-90.
- [8] Yu, X.Z., et al., (2006)Distribution of polycyclic aromatic hydrocarbons in soils at Guiyu area of China, affected by recycling of electronic waste using primitive technologies. *Chemosphere* 65(9): p. 1500-1509.
- [9] Hu, X., D. Hu, and Y. Xu, (2009)Effects of tetrabrominated diphenyl ether and hexabromocyclododecanes in single and complex exposure to hepatoma HepG2 cells. *Environmental Toxicology and Pharmacology* 27(3): p. 327-337.
- [10]Zhang, W., et al., (2012)Ecotoxicological effects of decabromodiphenyl ether and cadmium contamination on soil microbes and enzymes. *Ecotoxicology and Environmental Safety* 82: p. 71-79.
- [11]Elsgaard, L., S.O. (2001)Petersen, and K. Debosz, Effects and risk assessment of linear alkylbenzene sulfonates in agricultural soil. 1. Short-term effects on soil microbiology. *Environmental Toxicology and Chemistry* 20(8): p. 1656-1663.
- [12]Filip, Z., (2002)International approach to assessing soil quality by ecologically-related biological parameters. *Agriculture, Ecosystems & Environment* 88(2): p. 169-174.
- [13]Dick, R.P., (1994)Soil enzyme activities as indicators of soil quality. *Soil Science Society of America Journal* 58: p. 107-124.
- [14]Yao, H. and C.D. (2000)Campbell, Microbial Biomass and Community Structure in a Sequence of Soils with Increasing Fertility and Changing Land Use. *Microbial Ecology* 40(3): p. 223-237.
- [15]Guangyu, S., et al., (2013)Aerobic biotransformation of decabromodiphenyl ether (PBDE-209) by *Pseudomonas aeruginosa*. *Chemosphere* 93(8): p. 1487-1493.
- [16]Mallavarapu, M., et al., (1998)Genetic requirements for the expression of benzylamine dehydrogenase activity in *Pseudomonas putida*. *Fems Microbiology Letters* 166(166): p. 109-114.
- [17]Covaci, A., et al., (2008)Polybrominated diphenyl ethers (PBDEs) and polychlorinated biphenyls (PCBs) in human liver and adipose tissue samples from Belgium. *Chemosphere* 73(2): p. 170-5.
- [18]Hernández-León, R., et al.,(2015) Characterization of the antifungal and plant growth-promoting effects of diffusible and volatile organic compounds produced by *Pseudomonas fluorescens* strains. *Biological Control* 81: p. 83-92.
- [19]Korthals, G.W., et al., (1996)Long-term effects of copper and ph on the nematode community in an agroecosystem. *Environmental Toxicology & Chemistry* 15(6): p. 979-985.
- [20]Hiroki, M., (2012)Effects of heavy metal contamination on soil microbial population. *Soil Science & Plant Nutrition* 38(1): p. 141-147.
- [21]Lu, L., et al.,(2011) Effect of decabromodiphenyl ether (BDE 209) and dibromodiphenyl ether (BDE 15) on soil microbial activity and bacterial community composition. *Journal of Hazardous Materials* 186(1): p. 883-90.



---

**Received:** 20.01.2016  
**Accepted:** 20.08.2016

---

**CORRESPONDING AUTHOR**

---

**Zhaoxiang Han**

School of Chemical Engineering,  
Huaihai Institute of Technology,  
59# Cangwu Road,  
Lianyungang city,  
Jiangsu 222005, PRC, China.

e-mail: [hjyyzx@sina.com](mailto:hjyyzx@sina.com)

# UTILIZATION OF SHELLFISH WASTE: EFFECTS OF CHITOSAN FROM SHRIMP SHELL WASTE ON FATTY ACID PROFILES OF EUROPEAN EEL

Aygul Kucukgulmez\*, Yasemen Yanar, Ali Eslem Kadak, Gozde Gercek, Serap Gelibolu, Mehmet Celik

Department of Fishing and Fish Processing Technology, Faculty of Fisheries, Cukurova University, Adana, Turkey

## ABSTRACT

The effects of chitosan extracted from shrimp (*Metapenaeus stebbingi*) shell waste and commercial chitosan on fatty acid profile of European eel (*Anguilla anguilla*) fillet pieces during refrigerated storage were investigated. Fish pieces samples were treated with aqueous solution of 0.1 and 1% extracted and commercial chitosan, and then stored at 4°C for 18 days. The fillet pieces samples were analyzed periodically for fatty acid analysis. No statistically significant change was detected in the total saturated fatty acid (SFA) contents of eel fillet pieces in the all groups at the end of storage ( $p>0.05$ ). There were no significant difference in monounsaturated fatty acid (MUFA) and polyunsaturated fatty acid (PUFA) contents of the groups added 1% extracted and commercial chitosan ( $p>0.05$ ), while a percentage decrease was determined in MUFA and PUFA contents of groups control, added 0.1% extracted and commercial chitosan at the end of storage ( $p<0.05$ ). It was concluded appropriate to use chitosan obtained from shrimp shells not evaluated and discarded as waste products in Turkey during the storage of fatty fish like eel.

## KEYWORDS:

Shellfish waste, Shrimp, Chitosan, European eel, Fatty acids

## INTRODUCTION

Eel is one of the most important fatty fish species. In Turkey, the European eel is especially present in the rivers flowing into the Aegean and Mediterranean Sea, natural lakes and dams [1]. They are consumed fresh general, and the great majority of them are exported to Europe as fresh, frozen or smoked. It is quite susceptible to oxidation, especially due to its high fat content. Oxidation of fats causes unwanted changes in taste and flavor, deterioration in the structure of essential fatty acids, and loss in nutritional value. These changes occurring during the storage period could

be delayed by synthetic antioxidants such as butylated hydroxyanisole (BHA) and butylated hydroxytoluene (BHT) and propyl gallate (PG). However, due to concern for the reliability of synthetic antioxidants used food industry, the interest in natural antioxidant has increased in recent years. At present, consumers prefer natural foods as much as possible, and therefore, studies to obtain natural antioxidants from different materials have been accelerated.

Chitosan ( $\beta$ -(1, 4)-2-amino-2-deoxy-D-glucopyranose), is mainly made from crustacean shells, is the second most abundant natural and non-toxic polymer in nature after cellulose [2]. Due to its non-toxic nature, antibacterial and anti-oxidative activity, film forming property, biocompatibility and biodegradability, chitosan has attracted much attention as a natural food additive [3]. Solubility and activity of chitosan having a polycationic characteristic are much higher than chitin and it is widely used in food practices. Being antioxidant and antimicrobial, chitosan is of great importance for the storage of foods. In addition, it has various other usage means such as clarifier for juice, edible films for the storage of fruit and vegetables, emulsifying, thickener and stabilizer substance and mordant [4]. There are plenty of studies on the quality of chitosan and its derivatives during the cold storage [5-11] and freeze storage [3, 12] of various fish species in the literature. On the other hand, there is very limited information about the effect of chitosan on fatty acid composition of fish.

## MATERIALS AND METHODS

**Materials.** Chitosan was extracted from shrimp (*Metapenaeus stebbingi*) shells, using a chemical method [13]. The eels (*Anguilla anguilla*) were caught from Akyatan lagoon (Northeastern Mediterranean Sea). They were transferred in an insulated box with ice to the laboratory. The head, viscera, bone and skin were removed. The average weight of eel was 500-650 g (40 individuals; 10 individuals for each group) and the fillets were cut into approximately 5 x 4 cm pieces.



**Chitosan treatment.** Chitosan was dissolved in acetic acid (1%) at two concentrations (1 and 0.1%). Eel fillet pieces were dipped into the following solutions as different treatments for 5 min: Control without any solutions, 0.1 and 1% (w/v) extracted chitosan (EC), 0.1 and 1% (w/v) commercial chitosan (CC). Then, samples were removed from the treatment solution, placed in sterile vacuum bags (Baglight, 20 x 25 cm, 400 mL, Interscience, Nom la Bretèche, France) and then vacuumed by Reepack equipment (Reepack, RV-50, Seriate [BG], Milan, Italy). Samples were stored in the refrigerator for 18 days. All analyses were performed in triplicate on days 0, 3, 6, 9, 12 and 18.

**Fatty acid analysis.** Lipids were extracted by the method of Bligh and Dyer [14]. Extracted lipids were used to prepare the methyl ester by transmethylation using 2 M KOH in methanol and n-heptane. Lipid was dissolved in 2 mL of heptane followed by 4 mL of 2 M methanolic KOH. The mixture was centrifuged at 4,000 rpm for 10 min, and the heptane layer was taken for gas chromatography (GC) analysis [15].

**Statistical analysis.** The SPSS (Chicago, IL) software was used for the statistical analysis. Comparisons among groups were made using one way analysis of variance, and significant differences were determined by Duncan's multiple range tests at 5% confidence level.

## RESULTS AND DISCUSSION

Changes in fatty acid composition of the European eel fillet pieces treated with chitosan at different concentrations are given in Table 1. Within these groups, the major fatty acids were palmitic acid (16:0), stearic acid (18:0), oleic acid (18:1), eicosapentaenoic acid (EPA, 20:5) and docosahexaenoic acid (DHA, 22:6). These fatty acids were found to be dominant by other studies on the fatty acid profiles of eel [16-18]. No statistically significant difference was determined in the total SFA content of the control group during the cold storage of eel fillet pieces ( $p>0.05$ ), while a percentage decrease was observed in MUFA and PUFA contents (especially 15. and 18. days of storage) ( $p<0.05$ ). Similarly, significant decrease in PUFA content of various fish species were reported by related studies [19-20]. The highly unsaturated fatty acids mostly found in seafood are especially sensible to oxidative changes taking place throughout the storage period [6]. Such changes which can be observed in PUFA value throughout the storage period result from effortless oxidation of these fatty acids and enzymatic hydrolysis of lipids [6, 19, 21]. No significant changes occurred

at the beginning and end of the storage in the rates of n3/n6 and EPA/DHA in control group ( $p>0.05$ ).

Considering the fatty acid profiles of the groups treated with both 0.1% extracted chitosan and 0.1% commercial chitosan, it can be seen that no change occurred in total SFA; a decrease was observed in total MUFA and PUFA at the end of the storage compared to the beginning (except for MUFA content of 0.1% CC group). During the storage of these groups in refrigerator, some changes were observed in the rates of n3/n6 and EPA/DHA; however, no significant difference observed between the first and last days of storage ( $p>0.05$ ).

No change was observed between the beginning and end of the storage despite percentile falls and rises in SFA, MUFA and PUFA values of the 0.1% extracted and commercial chitosan groups for some days during the storage. These results indicate the positive effect of chitosan, which not only we obtained individually but also we supplied commercially, on oxidation of fatty acids. Hence, various functional substances like nutraceuticals, antioxidants and antimicrobial agents might be carried efficiently by chitosan which is owing to the fact that there is a great density of amino groups and hydroxyl groups in polymer structure of the chitosan [22]. In parallel with this study, the effect of chitosan on fatty acid composition was researched. The n-3 fatty acid rate of chitosan uncoated fish samples was found between 0.45-0.74%, while that of chitosan coated samples was detected between 1.11- 2.27% [22]. In addition to the studies conducted on the effect of chitosan on fatty acid composition, positive effects of various natural and commercial antioxidant practices on fatty acid composition of fish were reported [20, 23].

To conclude, this study detected that fillet pieces of eel treated with 1% concentrations of both commercial and extracted chitosan have positive effects on MUFA and PUFA fatty acid profiles. The present study suggested that PUFA, highly susceptible to environmental conditions, could be saved as an alternative to commercial antioxidants with the chitosan from shrimp. To conclude, this study detected that fillet pieces of eel treated with 1% concentrations of both commercial and extracted chitosan have positive effects on MUFA and PUFA fatty acid profiles. In general, shellfish wastes which are not utilized in aquaculture processing plants offer a great potential. When these wastes are transferred into sea without being used, they lead to significant problems such as environmental pollution and adversely affect human health. The use of wastes is a highly important issue in terms of both aquaculture industry and public health. This study is of importance in terms of not only obtaining food-preservative substances which are safe for human

**TABLE 1**  
**Fatty acid profiles of eel fillet pieces treated with chitosan during refrigerated storage**

Days/	0.1% EC	1% EC	0.1% CC	1% CC	Control
<b>SFA</b>					
0	28.05±0.10 <sup>a,1</sup>	28.32±0.52 <sup>ab,12</sup>	29.28±0.12 <sup>b,2</sup>	28.53±0.59 <sup>ab,12</sup>	28.24±0.50 <sup>a,1</sup>
3	28.00±0.05 <sup>a,1</sup>	28.01±0.07 <sup>ab,1</sup>	28.37±0.41 <sup>ab,1</sup>	28.98±0.11 <sup>b,2</sup>	28.19±0.05 <sup>a,1</sup>
6	28.23±0.10 <sup>a,12,3</sup>	27.67±0.03 <sup>a,1</sup>	27.83±0.20 <sup>ab,12</sup>	28.31±0.37 <sup>ab,2,3</sup>	28.72±0.25 <sup>a,3</sup>
9	28.41±0.02 <sup>a,1</sup>	28.10±0.36 <sup>ab,1</sup>	28.24±0.59 <sup>ab,1</sup>	28.32±0.15 <sup>ab,1</sup>	28.29±0.33 <sup>a,1</sup>
12	28.68±0.04 <sup>a,1</sup>	28.05±0.48 <sup>ab,1</sup>	28.20±0.80 <sup>ab,1</sup>	28.55±0.52 <sup>ab,1</sup>	28.16±0.21 <sup>a,1</sup>
15	28.69±0.06 <sup>a,1</sup>	28.52±0.06 <sup>b,1</sup>	29.11±0.03 <sup>b,1</sup>	28.57±0.04 <sup>ab,1</sup>	28.82±0.67 <sup>a,1</sup>
18	27.46±0.00 <sup>a,1</sup>	28.05±0.10 <sup>ab,12</sup>	29.08±0.39 <sup>b,3</sup>	28.40±0.02 <sup>ab,2</sup>	28.46±0.34 <sup>a,2</sup>
<b>MUFA</b>					
0	51.30±0.36 <sup>ab,1</sup>	52.94±0.55 <sup>ab,1</sup>	52.24±0.32 <sup>a,1</sup>	54.79±1.17 <sup>b,2</sup>	54.99±0.00 <sup>ab,2</sup>
3	51.26±0.41 <sup>ab,1</sup>	53.36±0.36 <sup>ab,2,3</sup>	53.63±0.05 <sup>b,2,3</sup>	52.09±0.80 <sup>a,12</sup>	54.43±0.86 <sup>a,4</sup>
6	53.78±0.08 <sup>c,1</sup>	54.28±0.74 <sup>ab,1</sup>	53.37±0.53 <sup>ab,1</sup>	53.67±0.63 <sup>ab,1</sup>	53.55±1.35 <sup>a,1</sup>
9	52.68±1.31 <sup>bc,1</sup>	52.97±1.75 <sup>ab,1</sup>	53.57±0.48 <sup>b,1</sup>	53.54±0.14 <sup>ab,1</sup>	54.28±0.09 <sup>a,1</sup>
12	53.02±0.73 <sup>bc,1</sup>	54.53±0.78 <sup>b,1</sup>	53.36±1.06 <sup>ab,1</sup>	53.61±1.72 <sup>ab,1</sup>	54.81±0.84 <sup>ab,1</sup>
15	52.16±1.55 <sup>abc,1</sup>	52.05±0.87 <sup>a,1</sup>	52.90±0.07 <sup>ab,12</sup>	54.39±0.04 <sup>ab,2,3</sup>	53.30±0.15 <sup>a,2</sup>
18	50.07±0.33 <sup>a,1</sup>	53.41±0.79 <sup>ab,2</sup>	53.34±0.05 <sup>ab,2</sup>	54.96±0.78 <sup>b,3</sup>	53.84±0.03 <sup>a,3</sup>
<b>PUFA</b>					
0	18.00±0.41 <sup>b,4</sup>	16.94±0.32 <sup>c,3</sup>	16.56±0.15 <sup>c,2,3</sup>	16.09±0.21 <sup>ab,12</sup>	15.69±0.07 <sup>ab,1</sup>
3	18.16±0.09 <sup>b,2</sup>	16.59±0.03 <sup>bc,1</sup>	15.74±0.19 <sup>a,1</sup>	16.85±0.76 <sup>b,1</sup>	15.80±0.52 <sup>b,2</sup>
6	15.84±0.04 <sup>a,1</sup>	15.68±0.48 <sup>ab,1</sup>	15.91±0.14 <sup>a,1</sup>	16.00±0.80 <sup>ab,1</sup>	16.01±0.75 <sup>b,1</sup>
9	16.33±1.29 <sup>a,1</sup>	16.54±1.05 <sup>bc,1</sup>	15.99±0.19 <sup>a,1</sup>	15.96±0.42 <sup>ab,1</sup>	16.18±0.17 <sup>b,1</sup>
12	16.30±0.03 <sup>a,1</sup>	15.59±0.03 <sup>ab,1</sup>	16.13±0.29 <sup>ab,1</sup>	16.32±0.09 <sup>ab,1</sup>	15.43±0.78 <sup>ab,1</sup>
15	16.57±0.09 <sup>a,3,4</sup>	17.10±0.50 <sup>c,4</sup>	15.70±0.04 <sup>a,2</sup>	15.84±0.36 <sup>ab,2,3</sup>	14.51±0.25 <sup>a,1</sup>
18	16.95±0.05 <sup>ab,2</sup>	17.11±0.04 <sup>c,3</sup>	15.83±0.21 <sup>a,1</sup>	15.89±0.02 <sup>ab,1</sup>	14.05±0.36 <sup>a,1</sup>
<b>n3/n6</b>					
0	1.61±0.07 <sup>ab,1</sup>	2.37±0.06 <sup>b,3</sup>	2.09±0.02 <sup>a,2</sup>	2.08±0.01 <sup>a,2</sup>	1.99±0.01 <sup>a,2</sup>
3	1.49±0.01 <sup>a,1</sup>	2.30±0.03 <sup>b,3</sup>	2.04±0.05 <sup>a,2</sup>	2.25±0.04 <sup>b,3</sup>	2.12±0.02 <sup>a,2</sup>
6	1.74±0.00 <sup>ab,1</sup>	2.00±0.08 <sup>a,2</sup>	2.06±0.00 <sup>a,2</sup>	2.12±0.15 <sup>a,2</sup>	2.06±0.11 <sup>a,2</sup>
9	2.23±0.17 <sup>c,1</sup>	2.22±0.16 <sup>ab,1</sup>	2.07±0.10 <sup>a,1</sup>	2.00±0.01 <sup>ab,1</sup>	2.02±0.01 <sup>a,1</sup>
12	2.17±0.00 <sup>c,1</sup>	2.05±0.06 <sup>a,1</sup>	2.12±0.05 <sup>a,1</sup>	2.10±0.03 <sup>ab,1</sup>	2.09±0.05 <sup>a,1</sup>
15	2.14±0.26 <sup>c,1</sup>	2.42±0.13 <sup>b,1</sup>	2.00±0.01 <sup>a,1</sup>	2.06±0.02 <sup>a,1</sup>	2.20±0.17 <sup>a,1</sup>
18	1.82±0.00 <sup>ab,1</sup>	2.06±0.01 <sup>a,2</sup>	2.07±0.04 <sup>a,2</sup>	1.98±0.01 <sup>a,2</sup>	2.07±0.06 <sup>a,2</sup>
<b>EPA/DHA</b>					
0	0.82±0.05 <sup>a,4</sup>	0.62±0.03 <sup>ab,2,3</sup>	0.54±0.00 <sup>a,12</sup>	0.53±0.02 <sup>ab,1</sup>	0.63±0.00 <sup>ab,3</sup>
3	0.68±0.03 <sup>a,2,3</sup>	0.76±0.03 <sup>b,3</sup>	0.58±0.00 <sup>a,2</sup>	0.41±0.06 <sup>a,1</sup>	0.62±0.07 <sup>ab,2</sup>
6	0.70±0.00 <sup>a,1</sup>	0.51±0.00 <sup>ab,1</sup>	0.60±0.12 <sup>a,1</sup>	0.55±0.18 <sup>ab,1</sup>	0.46±0.08 <sup>a,1</sup>
9	0.71±0.16 <sup>a,1</sup>	0.71±0.18 <sup>ab,1</sup>	0.60±0.02 <sup>a,1</sup>	0.61±0.03 <sup>b,1</sup>	0.55±0.03 <sup>ab,1</sup>
12	0.69±0.18 <sup>a,1</sup>	0.72±0.05 <sup>b,2,3</sup>	0.61±0.03 <sup>a,1</sup>	0.58±0.01 <sup>ab,1</sup>	0.60±0.16 <sup>ab,1</sup>
15	0.80±0.10 <sup>a,3</sup>	0.73±0.07 <sup>b,2</sup>	0.62±0.00 <sup>a,12</sup>	0.49±0.02 <sup>ab,1</sup>	0.72±0.02 <sup>b,2,3</sup>
18	0.87±0.01 <sup>a,4</sup>	0.66±0.00 <sup>ab,3</sup>	0.53±0.00 <sup>a,1</sup>	0.63±0.01 <sup>b,2</sup>	0.53±0.00 <sup>ab,1</sup>

Data are expressed as means ± standard deviation. Different letters within the column denote significant differences ( $p < 0.05$ ). Different number within the row denote significant differences ( $p < 0.05$ ). CC, commercial chitosan; EC, extracted chitosan.

health and making them revenue for economy but also preventing the damage of unutilized wastes to the environment. Also study findings are considered to be useful for the economic use of shrimp wastes in Turkey and light the way for future studies on crustacean species.

#### ACKNOWLEDGEMENTS

This work was supported by Scientific Research Fund of Cukurova University in Turkey.

#### REFERENCES

- [1] Tekelioglu, N. (1998). Deniz Balıkları Yetiştiriciliği, Çukurova Üniversitesi Su Ürünleri Fakültesi, Adana, Turkey.
- [2] Charoenvuttitham, P., Shi, J. and Mittal, G. (2006). Chitin Extraction from Black Tiger Shrimp (*Penaeus monodon*) Waste using Organic Acids. Sep. Sci. Technol., 41, 1135–1153.
- [3] Fan, W., Sun, J., Chen, Y., Qiu, J., Zhang, Y. and Chi, Y. (2009). Effects of Chitosan Coating on Quality and Shelf Life of Silver

- Carp during Frozen Storage. *Food Chem.*, 115, 66-70.
- [4] Shahidi, F., Arachchi, J.K.V. and Jeon, Y.J. (1999). Food Applications of Chitin and Chitosan. *Trends. Food Sci.Tech.*, 10, 37-51.
- [5] Jeon, Y.J., Kamil, J.Y.V.A. and Shahidi, F. (2002). Chitosan as an Edible Invisible Film for Quality Preservation of Herring and Atlantic Cod. *J. Agric. Food Chem.* 50, 5167-5178.
- [6] Kamil, J.Y.V.A., Jeon, Y.J. and Shahidi, F. (2002). Antioxidative Activity of Chitosans of Different Viscosity in Cooked Comminuted Flesh of Herring (*Clupea harengus*). *Food Chem.*, 79(1), 69-77.
- [7] Tsai, G.J., Su, W.H., Chen, H.C. and Pan, C.L. (2002). Antimicrobial Activity of Shrimp Chitin and Chitosan from Different Treatments and Applications of Fish Preservation. *Fisheries Sci.*, 68, 170-177.
- [8] Kim, K.W. and Thomas, R.L. (2007). Antioxidative Activity of Chitosans with Varying Molecular Weights. *Food Chem.*, 101, 308-313.
- [9] Ojagh, S.M., Rezaei, M., Razavi, S.H. and Hosseini, S.M.H. (2010). Effect of Chitosan Coatings Enriched with Cinnamon Oil on the Quality of Refrigerated Rainbow Trout. *Food Chem.*, 120, 193-198.
- [10] Souza, B.W.S., Cerqueira, M., Ruiz, H.A., Martins, J.T., Casariego, A., Teixeira, J.A. and Vicente, A.A. (2010). Effect of Chitosan-Based Coatings on the Shelf Life of Salmon (*Salmo salar*). *J. Agric. Food Chem.*, 58, 11456-11462.
- [11] Cao, R., Liu, Q., Yin, B. and Wu, B. (2012). Chitosan Extends the Shelf-life of Filleted Tilapia (*Oreochromis niloticus*) during Refrigerated Storage. *J. Ocean Univ. China.*, 11(3), 408-412.
- [12] Sathivel, S., Liu, Q., Huang, J. and Prinyawiwatkul, W. (2007). The Influence of Chitosan Glazing on the Quality of Skinless Pink Salmon (*Oncorhynchus gorbuscha*) Fillets during Frozen Storage. *J. Food Eng.*, 83(3), 366-373.
- [13] Kucukgulmez, A., Celik, M., Yanar, Y., Sen, D., Polat, H. and Kadak, A. E. (2011). Physicochemical Characterization of Chitosan Extracted from *Metapenaeus stebbingi* Shells. *Food Chem.*, 126, 1144-1148.
- [14] Bligh, E.G. and Dyer, W.J. (1959). A Rapid Method of Total Lipid Extraction and Purification. *Can. J. Biochem. Phys.*, 37, 911-917.
- [15] Ichihara, K., Shibahara, A., Yamamoto, K., Nakayama, T. (1996). An Improved Method for Rapid Analysis of the Fatty Acids of Glycerolipids. *Lipids*, 31, 535-539.
- [16] Oku, T., Sugawara, A., Choudhury, M., Komatsu, M., Yamada, S. and Ando, S. (2009). Lipid and Fatty Acid Compositions Differentiate between Wild and Cultured Japanese Eel (*Anguilla japonica*). *Food Chem.*, 115, 436-440.
- [17] Polak-Juszczak, L. and Komar-Szymczak, K. (2009). Fatty Acid Profiles and Fat Contents of Commercially Important Fish from Vistula Lagoon. *Pol. J. Food Nutr. Sci.*, 59(3), 225-229.
- [18] Ersoy, B. (2011). Effects of Cooking Methods on the Proximate, Mineral and Fatty Acid Composition of European Eel (*Anguilla anguilla*). *International J. Food Sci. Tech.*, 46, 522-527.
- [19] Turhan, S., Sagir, I. and Temiz, H. (2009). Oxidative Stability of Brined Anchovies (*Engraulis encrasicolus*) with Plant Extracts. *Int. J. Food Sci. & Tech.*, 44, 386-393.
- [20] Kucukgulmez, A. and Celik, M. (2013). The Effects of Natural Antioxidant Extract Isolated from Giant Red Shrimp (*Aristaeomorpha foliacea*) Shells on Fatty Acid Profiles of Anchovy (*Engraulis encrasicolus*) during Refrigerated Storage. *J. Aquat. Food Product Tech.*, 22, 66-76
- [21] Varelziz, K., Koufidis, D., Gavriilidou, E., Papavergou, E. and Vasiliadou S. (1997). Effectiveness of a Natural Rosemary (*Rosmarinus officinalis*) Extract on the Stability of Filleted and Minced Fish during Frozen Storage. *Z. Lebensm. Unters. Forsch. A.*, 205, 93-96.
- [22] Duan, J., Cherian, G. and Zhao, Y. (2010). Quality Enhancement in Fresh and Frozen Lingcod (*Ophiodon elongates*) Fillets by Employment of Fish Oil Incorporated Chitosan Coatings. *Food Chem.*, 119, 524- 532
- [23] Selmi, S. and Sadok, S. (2008). The Effect of Natural Antioxidant (*Thymus vulgaris* Linnaeus) on Flesh Quality of Tuna (*Thunnus thynnus* Linnaeus) during Chilled Storage. *Pan-Am. J. Aquat. Sci.*, 3(1), 36-45.

---

**Received:** 22.01.2016

**Accepted:** 31.08.2016

---

#### CORRESPONDING AUTHOR

---

**Aygul Kucukgulmez**

Cukurova University, Faculty of Fisheries,  
Department of Fishing and Fish Processing  
Technology,  
Adana- TURKEY

E-mail address: [akucukgulmez@cu.edu.tr](mailto:akucukgulmez@cu.edu.tr)

# QUANTITATIVE EVALUATION SYSTEM OF HABITAT ENVIRONMENTAL QUALITY IN YELLOW RIVER DELTAS

Hou Kang, Li Xu-xiang\*

School of Human Settlements and Civil Engineering, Xi'an Jiaotong University, Xi'an, 710049, China

## ABSTRACT

Habitat environmental quality is directly related to the socio-economic development in the rapid development regions. Analyzing quality of habitat environment can provide an effective basis for regional planning in Yellow River Deltas, including 18 counties. This evaluation system involves three aspects: resource carrying capacity, natural environment and socio-economic factors. And habitat environmental quality is quantitatively analyzed with the application of geographic information systems (GIS) software and principal component analysis (PCA) model. The results show that there is an obvious zonal distribution of habitat environmental quality index (HEQI) descending from east to west in Yellow River Delta. And distribution of the natural environmental index (NEI) and socio-economic index (SI) are consistent with distribution of HEQI. The medium inhabitable zone with the largest area proportion accounts for 35.11%, the inhabitable zone accounts for 23.34%, the low inhabitable zone accounts for 18.08%, the high inhabitable zone accounts for 16.70%, and the uninhabitable zone only accounts for 6.76%.

## KEYWORDS:

Quantitative evaluation system, Habitat environmental quality index, Principal component analysis, Geographic information systems (GIS)

## INTRODUCTION

Yellow River Delta economic zone is China's largest delta. It adjoins Beijing and Tianjin in the north and Shandong Peninsula in the south, belonging to the National Nature Reserve of China. Due to the acceleration of urbanization, habitat environmental quality has attracted more and more attention in Yellow River Delta. Because of the limit of natural resources, population and energy, the quality of habitat environment directly affect development of the society and economy [1,2]. Many aspects can affect the condition of habitat environmental quality, such as the natural environment and socio-economic factors [3,4]. The

assessment of habitat environmental quality has been an indispensable part in city planning [5-8]. Most of the research focused on the limit scale, and lacked large-scale regional research. Then, they were short of the quantitative studies on spatial distribution of regional suitability of the habitat environment [9-13]. So it is important to build a quantitative evaluation system of habitat environment in Yellow River Delta.

Because spatial analysis techniques are widely used in environmental evaluation, habitat environmental quality can be analyzed with using geographic information system (GIS) [14, 15]. Meanwhile, combining PCA model with GIS can objectively evaluate complex large-scale regions [16-18], and the habitat environmental quality index (HEQI) model was developed. Then this research quantitatively analyzed the spatial distribution of HEQI in the Yellow River Delta economic zone.

## MATERIALS AND METHODS

**Study area and data.** Yellow River Delta is mainly distributed in the territory of Dongying and Binzhou in Shandong Province (Fig. 1). The study area is confined by the latitudes 36°55'-38°16'N and longitudes 117°31'-119°18'E. Topography and vegetation coverage data was derived from interpretation of remote sensing data, which the serial numbers are (131 34), (130, 34), (129, 34), (128, 34), (130, 35) and (129, 35). Meteorological data was obtained from meteorological departments in Dongying and Binzhou. Socio-economic data was also obtained from Statistical Yearbooks of these counties in 2011.

**Assessment index.** Because habitat environment involves many factors, how to select the representative factors is the key to this research. Generally, natural environmental factors and socio-economic factors should be reasonably selected [19]. The evaluation system includes three aspects: resource carrying capacity, natural environmental and socio-economic factors. Resource carrying capacity factors include population (population density, natural people growth rate), land resource (per capita wetland area,



**FIGURE 1**  
Location of the research area

per capita farmland area), per capita water area and energy (unit energy consumption, energy consumption per unit of GDP). Natural environment factors include climate (annual sunshine time, annual precipitation, relative humidity, annual average temperature) and geography (vegetation coverage and elevation). Socio-economic factors include public service (number of cultural and artistic venues, postal traffic per capita, number of doctors/ten thousand individuals, road density, per capita library collection, urban medical insurance coverage and passenger turnover, economy (rate/income ratio, GDP growth, GDP per capita, household consumption, per capita disposable income and per capita retail sales), life and settlement (per capita housing area, internet households rate, urban population density, family entertainment, education and cultural services spending, drinking water quality compliance rate, and sewage harmless).

**Evaluation system model.** In the multifactorial evaluation system, all evaluation factors will be effectively converted into a comprehensive evaluation factor that is the key to environmental assessment [20, 21]. The essence of the principal component analysis (PCA) is to explain a large number of the variables in the original data with a small number of variables. And it is an objective method to account the comprehensive evaluation index as concisely as possible [22]. Assessment system of the habitat environmental quality contains a large number of different aspects of the factors. Using principal component analysis method can be a good rational analysis of

multi-factor evaluation system, so habitat environmental quality index can be obtained by this method. The Habitat environmental quality index (HEQI) is defined as the sum of several weighted principal components as shown below:

$$HEQI(x) = m_1 n_1 + m_2 n_2 + \dots + m_i n_i \quad (1)$$

Where,  $HEQI(x)$  is the habitat environmental quality index;  $m_i$  is the principal component weight;  $n_i$  is the standardized value.

$$m_i = \frac{x_i}{\sum_{i=1}^p x_i} \quad (2)$$

Where  $x_i$  is the contribution ratio of the  $i$  th principal component, and,  $i$  is the eigenvalue of the  $i$  th principal component.

**Classification of the habitat environmental quality.** The classification of HEQI can clearly reflect changes in the habitat environmental quality. The natural breaks classification (NBC) method can effectively identify and classifies the interval. And then it can be appropriately grouped similar values and maximized the differences between the various classes [23]. NBC method was used to divide HEQI into five grades—uninhabitable (0.0043 ~ 5.2962), low inhabitable (5.2962 ~ 7.6247), inhabitable (7.6247 ~ 10.0943), medium inhabitable (10.0943 ~ 13.1939) and high inhabitable (13.1939 ~ 17.8558) in this study.

## RESULTS AND DISCUSSION

**Extracting the habitat environmental quality index.** On the basis of 31 evaluation factors, each component's weight is worked out by SPSS 18.0 software. According to the cumulative contribution of principal components, the number of components is affirmed to be eight. The corresponding results are shown in Table 1.

The higher HEQI value is, the more suitable habitat environmental quality is. According to formula (1) and Table 1, the habitat environmental

**TABLE 1**  
The results of principal component analysis (PCA)

Principal Component	Eigenvalue ( $\lambda_i$ )	Percentage of variance (%)
1	7.820	25.227
2	5.895	19.016
3	3.816	12.311
4	3.411	11.002
5	2.676	8.631
6	2.227	7.184
7	1.669	5.383
8	1.268	4.089

quality index (HEQI) can be calculated as follows:

$$HEQI = 0.2717N_1 + 0.2048N_2 + 0.1326N_3 + 0.1185N_4 + 0.0930N_5 + 0.0774N_6 + 0.0580N_7 + 0.0441N_8 \quad (3)$$

In this formula, HEQI is habitat environmental quality index,  $N_1 \sim N_8$  are eight principal components from 31 initial spatial variables.

**Analysis of the HEQI grade.** On the basis of the habitat environmental quality standard, map of the HEQI is classified as shown in Fig. 7. The medium inhabitable zone with the largest area proportion accounts for 35.11%, the inhabitable zone accounts for 23.34%, the low inhabitable zone accounts for 18.08%, the high inhabitable zone accounts for 16.70%, and the uninhabitable zone only accounts for 6.76%. Most of the study area presents that habitat environmental quality is at inhabitable, medium inhabitable, and high inhabitable levels, accounting for 75.15%, and it also reflects the quality of most regions is in a relatively good condition.

**Correlation analysis of main evaluation indexes and HEQI.** The difference between natural environmental index (NEI) and habitat environmental quality index (HEQI) can be shown in Fig.3. HEQI of Laizhou is greater than other counties. The curve of HEQI has relatively large fluctuations, which also reflects that the development of habitat environment in this region is uneven. The NEI is an important factor to affect the HEQI in a certain degree. Although the NEI of Laizhou is in the relatively moderate level, it has better socio-economic conditions to make up for weaknesses of the natural environment. On the contrary, the backwardness of socio-economic

conditions in Boxing and Changyi leads to the lower HEQI. Zhanhua County has the lowest NEI, so it leads to affect the habitat environment and has a lower HEQI than others.

It has a great difference between habitat environmental quality index (HEQI) and resource carrying capacity index (RCCI). Some counties have the small RCCI value, and it reflects that the pressure of environmental resources is small, such as Laoling and Qingyun (Fig.3). However their habitat environmental quality indexes are lower than others. When the RCCI in these counties is higher, HEQI is at the lower level, which shows that the developing industrial cities have heavier load in the aspect of resources carrying capacity, including Zhanhua and Wudi.

The socio-economic indexes (SI) of Laizhou and Shouguang are higher than other counties. In economically developed regions, HEQI increases with the increase of SI (Fig.3). Some counties with lower SI are distributed in Qingyun, Wudi and Zhanhua. Also these counties have the lower HEQI value. Therefore, it can be seen that the economy factors are one of the main factors to affect the quality of habitat environment.

**Analysis maps of the main evaluation indexes.** The regions of the high RCCI are mainly distributed in the energy cities of Yellow River Delta, such as Zhanhua and Dongying (Fig.4), and its distribution is related to the distribution of energy consumption and development. It reflects that the regional economic growth is dependent on traditional energy consuming. Due to the limit of technological innovation, development of Yellow River Delta has the problem of product structure and extensive growth modes, which leads to the excessive use of resources.

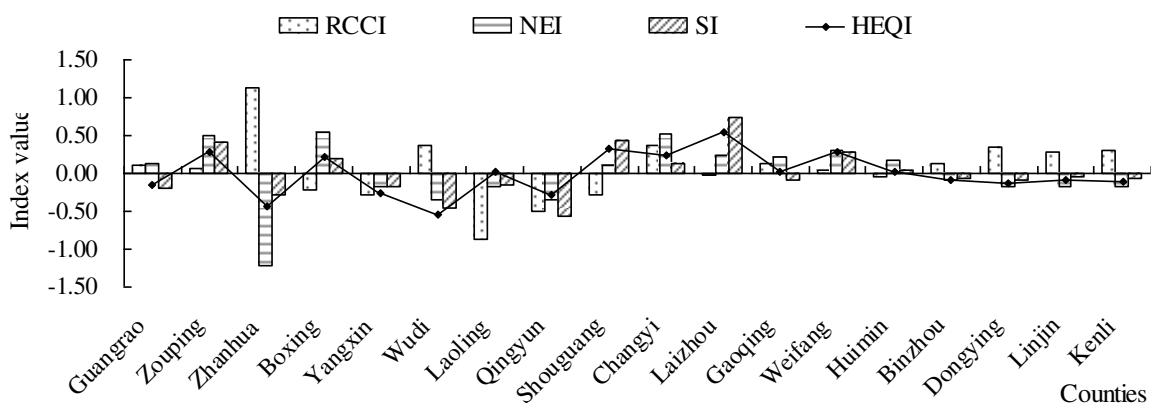
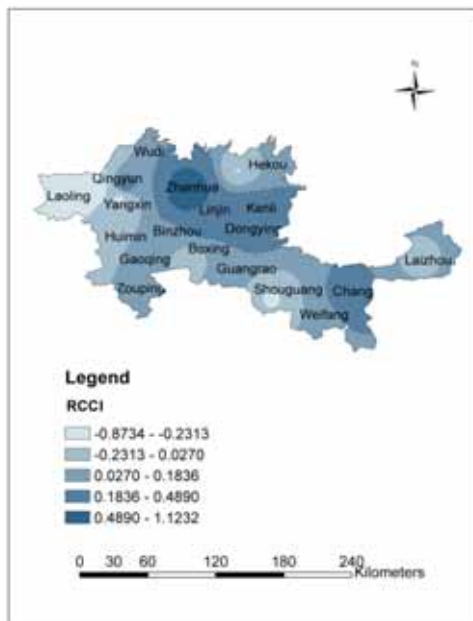
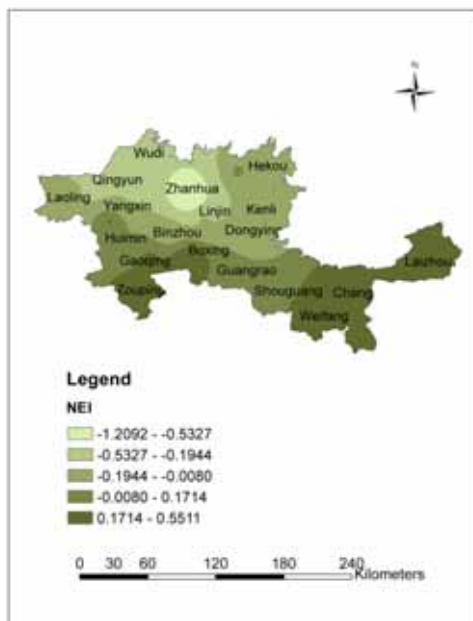


FIGURE 3

The contrast between habitat environmental quality index (HEQI) and natural environmental index (NEI), resource carrying capacity index (RCCI) and socio-economic index (SI)



**FIGURE 4**  
Distribution of resources carrying capacity index (RCCI)



**FIGURE 5**  
Distribution of natural environmental index (NEI)

The natural environmental index (NEI) is mainly distributed in descending order from east to west, which is consistent with the distribution of HEQI (Fig.5 and Fig.7). Laizhou, Changyi and Weifang are rich in natural resources. The western regions have the relatively low NEI, such as Zhanhua, Qingyun and Wudi. Influenced by marine soil and infiltration of seawater side, shallow underground fresh water reserves are small. Buried in 300-500 meters deep underground fresh water

contains high iodine and fluorine content. Maybe it is the reason that NEI is relatively low in these places. Coupled with the backward of economic development, the HEQI index in these counties is much lower than other counties.

The distribution of the higher socio-economic evaluation index is mainly in eastern areas, such as Laizhou, Shouguang and Weifang. This distribution is similar to distribution of HEQI (Fig.6 and Fig.7). The development of economy, transportation and municipal in Laizhou, Shouguang and Weifang is highest in this region, which leads to the higher HEQI. Because economic structure is not reasonable, the economic growth of some counties, such as Laoling, Qingyun, Wudi and Zhanhua, are less than the previous areas.

**Difference analysis of the habitat environmental quality index.** The habitat environmental quality index of Yellow River Delta can be shown as Fig.7. There is an obvious zonal distribution in study area. The HEQI of Laizhou is higher than other counties, and habitat environmental quality indexes of eastern counties are better than western regions.

Laizhou, Weifang and Shouguang are ranked in the forefront in the aspects of economic and transport, so it leads that their habitat environmental quality indexes are relatively higher than others. Although Dongying is the important industrial city in Shandong province, focusing on energy development and high resources carrying capacity make it a lower HEQI value. Dongying is the industrial base, and now is still the resource-consuming cities. Because the most counties in Yellow River Delta have the advantage of water resources and geographic position, the development in quality of human settlement environment is relatively favorable.

## CONCLUSION

This study developed the habitat environmental quality model and quantitatively analyzed the habitat environmental quality in a typical zone—Yellow River Delta. In this study, there is an obvious zonal distribution of HEQI. The HEQI of Laizhou is higher than other counties, and habitat environmental quality indexes of eastern counties are better than western regions. By comparison the relationship between HEQI and main evaluation indexes, the distribution of NEI and SI are consistent with distribution of HEQI.

The medium inhabitable zone with the largest area proportion accounts for 35.11%, the inhabitable zone accounts for 23.34%, the low inhabitable zone accounts for 18.08%, the high inhabitable zone

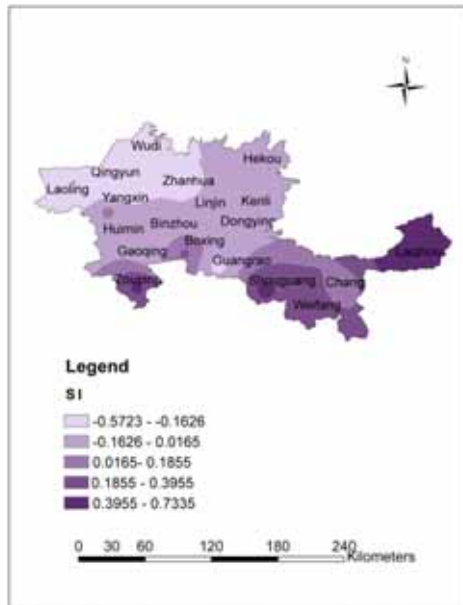


**FIGURE 6**  
Distribution of socio-economic evaluation index (SI)



**FIGURE 7**  
Distribution of habitat environmental quality index (HEQI)

accounts for 16.70%, and the uninhabitable zone only accounts for 6.76%. Most of the study area shows that the range of the habitat environmental quality index is at inhabitable, medium inhabitable, and high inhabitable levels, accounting for 75.15%, which also illustrates the quality of most regions is in relatively good condition.

Because of using GIS software and PCA model, the multiple factors model for assessing the system of habitat environmental quality was built. The results closely reflected the real situation of Yellow River Delta. But the evaluation factors are

based on counties, the system requires a more detailed evaluation unit and spatial pattern.

## ACKNOWLEDGEMENTS

We are grateful for constructive comments of the anonymous reviewers. Then we would like to thank Professor Jing Zhou for the modification of the language of the paper.

## REFERENCES

- [1] Pascual, M. A., Cussac, V., Dyer, B., Soto, D., Vigliano, P., Ortubay, S., & Macchi, P. (2007). Freshwater fishes of Patagonia in the 21st century after a hundred years of human settlement, species introductions, and environmental change. *Aquatic Ecosystem Health & Management*, 10(2): 212-227.
- [2] Vernet R. (2002). Climate during the late Holocene in the Sahara and the Sahel: Evolution and consequences on human settlement. *Droughts, food and culture*. Springer US: 47-63.
- [3] Gustafson, E. J., Hammer, R. B., Radloff, V. C., & Potts, R. S. (2005). The relationship between environmental amenities and changing human settlement patterns between 1980 and 2000 in the Midwestern USA. *Landscape Ecology*, 20(7): 773-789.
- [4] Dunin-Wasowicz T. (1990). *Natural Environment and Human Settlement over the Central European Lowland in the 13th Century. The Silent COUNTDOWN*. Springer Berlin Heidelberg: 92-105.
- [5] Gilbert A. (1998). An urbanizing world: Global report on human settlement. *Habitat International*, 22(1): 75-77.
- [6] Henderson F M, Xia Z G. (1997). SAR applications in human settlement detection, population estimation and urban land use pattern analysis: A status report. *Geoscience and Remote Sensing, IEEE Transactions on*, 35(1): 79-85
- [7] Jenerette, G. D., Harlan, S. L., Brazel, A., Jones, N., Larsen, L., & Stefanov, W. L. (2007). Regional relationships between surface temperature, vegetation, and human settlement in a rapidly urbanizing ecosystem. *Landscape Ecology*, 22(3): 353-365.
- [8] Pickett STA, Burch WR, Dalton SE, Foresman TW, Grove JM, Rowntree R. (1997). A conceptual framework for the study of human ecosystems in urban areas. *Urban Ecosyst* 1:185-199.
- [9] Deshpande, O., Batzoglou, S., Feldman, M. W., & Cavalli-Sforza, L. L. (2009). A serial founder effect model for human settlement out





- of Africa. Proceedings of the Royal Society of London B: Biological Sciences, 276(1655): 291-300.
- [10] Luck MA, Jenerette GD, Wu JG, Grimm NB. (2001). The urban funnel model and the spatially heterogeneous ecological footprint. *Ecosystems* 4:782–796.
- [11] Li, Y., Liu, C., Zhang, H., & Gao, X. (2011). Evaluation on the human settlement environment suitability in the Three Gorges Reservoir Area of Chongqing based on RS and GIS. *Journal of Geographical Sciences*, 21(2): 346-358.
- [12] Alberti M, Marzluff JM, Shulenberg E, Bradley G, Ryan C, Zumbrunnen C. (2003). Integrating humans into ecology: opportunities and challenges for studying urban ecosystems. *Bioscience* 53:1169–1179.
- [13] Emmanuel R. (2005). Thermal comfort implications of urbanization in a warm-humid city: The Colombo metro-politan region (CMR), Sri Lanka. *Building and Environment*, 40(12): 1591–1601.
- [14] Wilson JS, Clay M, Martin E, Stuckey D, Vedder-Risch K. (2003). Evaluating environmental influences of zoning in urban ecosystems with remote sensing. *Remote Sens Environ* 86:303–321.
- [15] Rong Z W W. (2007). Analyses on the Current Situation of Urban Human Settlement Environment in China. *Urban Studies*, 2: 021.
- [16] Parker, D. C., Manson, S. M., Janssen, M. A., Hoffmann, M. J., & Deadman, P. (2003). Multi-agent systems for the simulation of land-use and land-cover change: a review. *Annals of the Association of American Geographers*, 93(2), 314-337.
- [17] Hao H, Ren Z. (2009). Evaluation of Nature Suitability for Human Settlement in Shaanxi Province Based on Grid Data. *Acta Geographical Sinica*, 4: 014.
- [18] Plummer S.E. (2000). Perspectives on combining ecological process models and remotely sensed data. *Ecological modelling*, 129,169-186.
- [19] Pickett STA, Cadenasso ML, Grove JM, Nilon CH, Pouyat RV, Zipperer WC, Costanza R. (2001). Urban ecological systems: Linking terrestrial ecological, physical, and socioeconomic components of metropolitan areas. *Annu Rev Ecol Syst* 32:127–157.
- [20] Munda, G., Nijkamp, P. and Rietveld, P. (1994). Qualitative multicriteria evaluation for environment management. *Ecol.Econ.* 10(2): 97-112.
- [21] Mertens, B., & Lambin, E. F. (1997). Spatial modeling of deforestation in Southern Cameroon. *Applied Geography*, 17,143—162.
- [22] Shaw, G. and Wheeler, D. (1985). *Statistical Techniques in Geographical Analysis*. Wiley, New York. 199pp.
- [23] Li, A.N., Wang, A.S. and Liang, S.L. (2006). Ecological vulnerability evaluation in mountainous region using remote sensing and GIS—A case study in the upper reaches of Minjiang River, China. *Ecological Modelling*, 192,175-187.

---

**Received: 26.01.2016**

**Accepted: 28.07.2016**

---

#### CORRESPONDING AUTHOR

---

**Xuxiang Li**

School of Human Settlement and Civil Engineering,  
Xi'an Jiao tong University, No. 99, Yanxiang Road,  
Xi'an, 710049, P.R.CHINA

e-mail: [hupo0311@hotmail.com](mailto:hupo0311@hotmail.com)



# SCREENING AND OPTIMIZATION OF POLY- $\beta$ -HYDROXYBUTYRATE (PHB) PRODUCTION BY CERTAIN BACTERIA ISOLATED FROM SOIL

Halil Biyik\*, Esin Poyrazoglu Coban, Betul Aktas

Adnan Menderes University, Faculty of Science and Art, Department of Biology, Aydin, Turkey

## ABSTRACT

Polyhydroxybutyrates (PHB) are bacterial plastic that can replace the petroleum-based plastic. Many bacteria have the ability to synthesize PHB as intracellular granules. PHB granules are water-insoluble, relatively resistant to hydrolytic degradation biocompatible and nontoxic. It has a good oxygen permeability and ultra-violet resistance. Therefore, PHB have many useful applications in the manufacture of packaging containers, bottles, wrapping films, bags and so forth. The aim of this study is to evaluate the PHB yield of *Bacillus* sp., *Pseudomonas* sp. and *Azotobacter* sp. isolated from different garden soils. Besides, PHB productivity was optimized using various carbon, nitrogen sources, temperature and pH. Among total 121 isolates, 42 isolates have synthesized PHB. The results showed that the highest PHB production was with glucose (0.219 gL<sup>-1</sup>) as carbon source, glycine (0.212 gL<sup>-1</sup>) and peptone (0.206 gL<sup>-1</sup>) as nitrogen source, with a temperature of 30 °C (0.215 gL<sup>-1</sup>) and at 7.0 of pH (0.206 gL<sup>-1</sup>) by *Azotobacter* sp. A18.

## KEYWORDS:

Poly- $\beta$ -Hydroxybutyrate, Bacteria, Isolation, Extraction, Optimization

## INTRODUCTION

Plastics products are indispensable from automobiles to medicine in our lives. We used plastics and synthetic polymers are produced from petrochemicals. As synthetic plastics are persistent in the environment, plastic materials are a substantial source of environmental pollution and damage natural habitats. Several 100,000 tons of plastic are disposed in marine environments every year and accumulated in certain oceanic regions. In this case, approximately 1.000.000 sea creatures are dies every year [1]. With the advancement of biotechnological research, the production of environmentally friendly plastic produced by microorganisms has been the focus of researchers. Although,

polyhydroxyalkanoates (PHA's) are bacterial plastics, they could also be synthesized by many prokaryotic and eukaryotic microorganisms in the appropriate growth conditions. Polyhydroxybutyrates (PHB's) are the most significant member of polyhydroxyalkanoates first described by Lemoigne in *Bacillus megaterium* [2].

PHB is an energy and carbon reserve material in microorganisms that is accumulated as intracellular granules by *Bacillus* spp., *Azotobacter* spp., *Pseudomonas* spp. PHB are synthesized under the condition of limiting nutritional elements such as N, P, S, O or Mg in the presence excess carbon source [3].

PHB granules are water-insoluble, relatively resistant to hydrolytic degradation biocompatible and nontoxic. It has a high oxygen permeability and ultra-violet resistance. Therefore, PHB have many obvious applications in the manufacture of packaging containers, bottles, wrapping films, bags and the like. They also important medical uses as well, serving a surgical pins, stables, wound dressing, bone replacements and plates, and biodegradable carriers for the long-term release of medicines [4].

In this study, *Azotobacter*, *Pseudomonas* and *Bacillus* sp. in the soils taken from various fruit gardens were isolated and identified. Then, PHB productions by these bacteria were screened and then the amount of PHB production under different carbon, nitrogen sources, temperature and pH were determined.

## MATERIALS AND METHODS

**Isolation and identification of microorganisms.** Various soil samples were taken from different nine fruit gardens and lawn soil of Aydin in Turkey. The garden soil samples used in this study were collected from 0-15 cm layer. Each one gram of the sample was suspended in 99 mL of sterile distilled water and shaken. The samples were heated at 80 °C for 5 min in water bath for *Bacillus* sp. isolation from soil. Mannitol Agar Medium (10 g mannitol, 0.5 g K<sub>2</sub>HPO<sub>4</sub>, 0.2 g MgSO<sub>4</sub>·7H<sub>2</sub>O, 0.2 g NaCl, 0.2 g FeCl<sub>3</sub>·6 H<sub>2</sub>O, 0.005 g), *Pseudomonas*

Selective Agar (Difco) and Nutrient Agar (Sigma) were used for isolation of *Azotobacter sp.*, *Pseudomonas sp.* and *Bacillus sp.* respectively. Later, the liquid media were serially diluted in sterile 0.85% FTS (NaCl) solution and the dilutions from  $10^{-1}$  to  $10^{-6}$  were placed on Agar Medium. Plates were incubated at 28-37 °C for 24-48 h. For identification of isolated bacteria the bacterial strains were examined by Gram staining, morphological and biochemical characteristics using standard methods. The following biochemical tests were used: utilization of glucose, sucrose, mannitol, citrate, VP test, nitrate reduction, starch and gelatine hydrolysis, catalase [5].

**Identification of PHB by Sudan Black method.** Sudan Black stain was used to determine the PHB production of isolates. Sudan Black solution was added to the heat fixed bacterium culture samples and kept for 10 min. Decolorization process was performed by xylene end time. Later, safranin was added on slide and dried for 10 seconds. The inclusion bodies were visualized at 100x magnification using immersion oil under light microscope [6].

**PHB production and extraction.** Nutrient Broth containing 6% NaCl at pH 7.0 was used as basic medium for PHB production [7]. The isolates were inoculated to 100 mL of the production medium in a 250 mL Erlenmeyer flask and kept for incubation at 37 °C for 7 days.

PHB extraction was carried out by using sodium hypochlorite and chloroform [8- 10]. For PHB essays, stock cultures were inoculated into 100 mL of Nutrient Broth medium containing 6% NaCl in a 250 mL Erlenmeyer flask and measured the absorbance at 600 nm (OD 0.3-0.5). The new cultures were started by inoculating 2% of the culture supernatant and incubated at 30-37 °C for 48 h at 120 rpm in a shaker. At the end of incubation,

cells were collected by centrifugation at 8,000 rpm for 30 min at +4 °C and washed in phosphate buffered saline (PBS). The supernatant was removed and pellets were dried at 50 °C overnight and their weights determined. Chloroform and 6% sodium hypochlorite were added to the cell pellets and kept at +4°C overnight. 2N HCl solution (1:1) was added to the samples and kept for 2 h at 100 °C in water-bath and centrifuged at 5000 rpm for 20 min at +4 °C. Later, 5 mL chloroform was added to pellet and incubated at 30 °C overnight at 120 rpm. The precipitate was again centrifuged at 5000 rpm for 20 min at +4 °C. Chloroform was evaporated for 20 min. at 40 °C and 5 mL H<sub>2</sub>SO<sub>4</sub> was added to the pellet tube and kept for 20 min. at 100 °C in water-bath. PHB content in this mixture was quantified by measuring the absorbance at 235 nm.

**Effects of carbon, nitrogen sources, pH and temperature on PHB production.** To determine the effects of different carbon and nitrogen sources, we used glucose, sucrose, maltose, lactose (2 gmL<sup>-1</sup>), L-glycine, potassium nitrate, ammonium sulphate and peptone (0.2 gmL<sup>-1</sup>) as carbon and nitrogen sources, respectively. In addition, PHB production was tested at different pH (5.0-9.0) and temperature (25-40 °C).

## RESULTS AND DISCUSSION

**Isolation and identification of microorganisms.** A total of 121 bacterial colonies were isolated from ten different soil samples. We identified 47 of them as *Bacillus sp.*, 35 of them as *Pseudomonas sp.* and 39 of them *Azotobacter sp.* according to used morphological and biochemical tests (Fig. 1).

Morphological and biochemical characteristics of *Bacillus sp.*, *Pseudomonas sp.* and *Azotobacter sp.* are given in Table 1, 2 and 3, respectively.



**FIGURE 1**  
Image of *Azotobacter sp.*, *Bacillus sp.* and *Pseudomonas sp.* colonies on isolation medium.



**TABLE 3**  
**Morphological and biochemical characteristics of *Azotobacter* sp. from different soil samples.**

Number of isolates	Site of collection	Gram characteristic	Shape of cell	G	F	NR	U	I	H <sub>2</sub> S	C	CA	Identification
A1	6	-	Bacil	+	+	+	+	+	+	+	+	<i>Azotobacter</i> sp
A2	6	-	Bacil	+	+	+	+	+	+	+	+	<i>Azotobacter</i> sp
A3	6	-	Bacil	+	+	+	+	+	+	+	+	<i>Azotobacter</i> sp
A4	6	-	Bacil	+	+	+	+	+	+	+	+	<i>Azotobacter</i> sp
A5	6	-	Bacil	+	+	+	+	+	+	+	+	<i>Azotobacter</i> sp
A6	6	-	Bacil	+	+	+	+	+	+	+	+	<i>Azotobacter</i> sp
A7	6	-	Bacil	+	+	+	+	+	+	+	+	<i>Azotobacter</i> sp
A8	6	-	Bacil	+	+	+	+	+	+	+	+	<i>Azotobacter</i> sp
A9	6	-	Bacil	+	+	+	+	+	+	+	+	<i>Azotobacter</i> sp
A10	6	-	Bacil	+	+	+	+	+	+	+	+	<i>Azotobacter</i> sp
A11	6	-	Bacil	+	+	+	+	+	+	+	+	<i>Azotobacter</i> sp
A12	8	-	Bacil	+	+	+	+	+	+	+	+	<i>Azotobacter</i> sp
A13	8	-	Bacil	+	+	+	+	+	+	+	+	<i>Azotobacter</i> sp
A14	8	-	Bacil	+	+	+	+	+	+	+	+	<i>Azotobacter</i> sp
A15	8	-	Bacil	+	+	+	+	+	+	+	+	<i>Azotobacter</i> sp
A16	8	-	Bacil	+	+	+	+	+	+	+	+	<i>Azotobacter</i> sp
A17	8	-	Bacil	+	+	+	+	+	+	+	+	<i>Azotobacter</i> sp
A18	8	-	Bacil	+	+	+	+	+	+	+	+	<i>Azotobacter</i> sp
A19	8	-	Bacil	+	+	+	+	+	+	+	+	<i>Azotobacter</i> sp
A20	8	-	Bacil	+	+	+	+	+	+	+	+	<i>Azotobacter</i> sp
A21	8	-	Bacil	+	+	+	+	+	+	+	+	<i>Azotobacter</i> sp
A22	8	-	Bacil	+	+	+	+	+	+	+	+	<i>Azotobacter</i> sp
A23	8	-	Bacil	+	+	+	+	+	+	+	+	<i>Azotobacter</i> sp
A24	8	-	Bacil	+	+	+	+	+	+	+	+	<i>Azotobacter</i> sp
A26	8	-	Bacil	+	+	+	+	+	+	+	+	<i>Azotobacter</i> sp
A27	8	-	Bacil	+	+	+	+	+	+	+	+	<i>Azotobacter</i> sp
A27	7	-	Bacil	+	+	+	+	+	+	+	+	<i>Azotobacter</i> sp
A28	7	-	Bacil	+	+	+	+	+	+	+	+	<i>Azotobacter</i> sp
A29	7	-	Bacil	+	+	+	+	+	+	+	+	<i>Azotobacter</i> sp
A30	7	-	Bacil	+	+	+	+	+	+	+	+	<i>Azotobacter</i> sp
A31	7	-	Bacil	+	+	+	+	+	+	+	+	<i>Azotobacter</i> sp
A32	7	-	Bacil	+	+	+	+	+	+	+	+	<i>Azotobacter</i> sp
A33	7	-	Bacil	+	+	+	+	+	+	+	+	<i>Azotobacter</i> sp
A34	7	-	Bacil	+	+	+	+	+	+	+	+	<i>Azotobacter</i> sp
A35	7	-	Bacil	+	+	+	+	+	+	+	+	<i>Azotobacter</i> sp
A36	7	-	Bacil	+	+	+	+	+	+	+	+	<i>Azotobacter</i> sp
A37	7	-	Bacil	+	+	+	+	+	+	+	+	<i>Azotobacter</i> sp
A38	7	-	Bacil	+	+	+	+	+	+	+	+	<i>Azotobacter</i> sp
A39	7	-	Bacil	+	+	+	+	+	+	+	+	<i>Azotobacter</i> sp

1:Onion garden soil, 2:Vineyard land, 3:Olive garden soil, 4: Mulberry garden soil, 5:Plum garden soil, 6:Fig garden soil, 7:Lemon garden soil, 8:Lawn soil, 9: Quince garden soil, 10: Pomegranate garden soil

G:Glucose, F:Fructose, NR: Nitrate Reduction, U:Ureaze, I:Indole, H<sub>2</sub>S:H<sub>2</sub>S production, C:Citrate, CA:Catalase

Note: Onion garden soil (1), vineyard land (2), olive garden soil (3), mulberry garden soil (4), plum garden soil (5), quince garden soil (9) and pomegranate garden soil (10) were used for *Azotobacter* sp. but, it was not isolated.

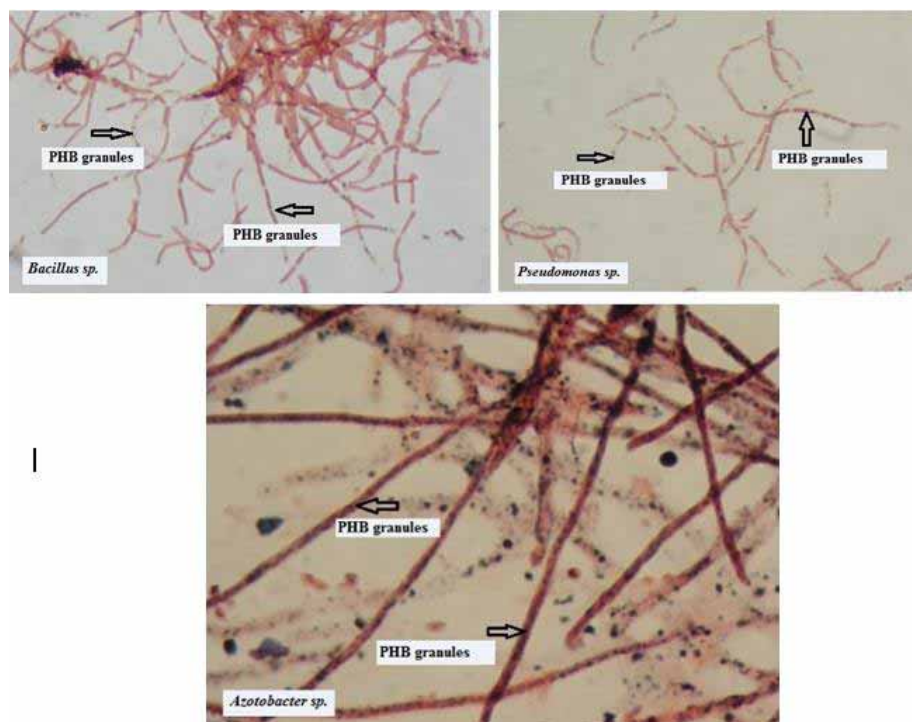


**FIGURE 2**  
**Identification of PHB by Sudan Black staining method (100x magnification).**

**Identification of PHB.** PHB productions of *Bacillus* sp., *Pseudomonas* sp. and *Azotobacter* sp. were tested with Sudan Black staining method. According to the method, PHB was the black granules inside pink cell walls (Fig. 2).

**PHB production and extraction.** A total of 121 isolates of bacteria were screened for identification of PHB by Sudan Black staining method at 100x magnification. PHB granules were found 42 of bacterial isolates under microscope. Quantification of PHB was determined from these bacterial isolates (Table 4).

A18 isolate (*Azotobacter* sp.) displayed the highest output of PHB among the screened isolates, thus it has been used in the remainder of the study.

**Effects of carbon, nitrogen sources, pH and temperature on PHB production.** To determine the effects of different carbon and nitrogen sources, we have used glucose, sucrose, maltose, lactose (2 g mL<sup>-1</sup>), L-glycine, potassium nitrate, ammonium sulphate and peptone (0.2 g mL<sup>-1</sup>) respectively as carbon and nitrogen sources. In addition, PHB production was also tested at a wide range of pH (5.0-9.0) and temperature (25-40 °C).

**TABLE 4**  
Isolates producing PHB and PHB production quantity.

Number of isolates	Identification	Dry weight of cell (g L <sup>-1</sup> )	PHB (g L <sup>-1</sup> )	Output of PHB (%)
B1	<i>Bacillus</i> sp.	0.45	0.082	18
B8	<i>Bacillus</i> sp.	0.26	0.071	28
B10	<i>Bacillus</i> sp.	0.31	0.052	17
B12	<i>Bacillus</i> sp.	0.54	0.125	23
B15	<i>Bacillus</i> sp.	0.40	0.065	16
B20	<i>Bacillus</i> sp.	0.37	0.075	20
B23	<i>Bacillus</i> sp.	0.48	0.094	20
B27	<i>Bacillus</i> sp.	0.51	0.105	21
B30	<i>Bacillus</i> sp.	0.73	0.095	13
B33	<i>Bacillus</i> sp.	0.41	0.075	18
B35	<i>Bacillus</i> sp.	0.55	0.120	22
B37	<i>Bacillus</i> sp.	0.48	0.115	25
B40	<i>Bacillus</i> sp.	0.65	0.096	15
B42	<i>Bacillus</i> sp.	0.52	0.100	19
B44	<i>Bacillus</i> sp.	0.35	0.086	25
B45	<i>Bacillus</i> sp.	0.20	0.042	21
B47	<i>Bacillus</i> sp.	0.62	0.124	20
P4	<i>Pseudomonas</i> sp.	0.50	0.092	18
P7	<i>Pseudomonas</i> sp.	0.33	0.085	25
P11	<i>Pseudomonas</i> sp.	0.29	0.063	22
P16	<i>Pseudomonas</i> sp.	0.76	0.135	17
P19	<i>Pseudomonas</i> sp.	0.32	0.084	26
P22	<i>Pseudomonas</i> sp.	0.60	0.105	18
P27	<i>Pseudomonas</i> sp.	0.55	0.098	18
P30	<i>Pseudomonas</i> sp.	0.32	0.060	19
P33	<i>Pseudomonas</i> sp.	0.64	0.132	21
P35	<i>Pseudomonas</i> sp.	0.52	0.075	14
A3	<i>Azotobacter</i> sp.	0.41	0.063	15
A5	<i>Azotobacter</i> sp.	0.32	0.076	24
A7	<i>Azotobacter</i> sp.	0.45	0.080	18
A10	<i>Azotobacter</i> sp.	0.51	0.095	19
A12	<i>Azotobacter</i> sp.	0.35	0.072	21
A15	<i>Azotobacter</i> sp.	0.47	0.094	20
A18	<i>Azotobacter</i> sp.	0.34	0.145	42
A21	<i>Azotobacter</i> sp.	0.38	0.095	25
A24	<i>Azotobacter</i> sp.	0.61	0.104	17
A26	<i>Azotobacter</i> sp.	0.43	0.092	21
A29	<i>Azotobacter</i> sp.	0.30	0.082	27
A32	<i>Azotobacter</i> sp.	0.59	0.100	17
A35	<i>Azotobacter</i> sp.	0.35	0.098	28
A38	<i>Azotobacter</i> sp.	0.53	0.102	19
A39	<i>Azotobacter</i> sp.	0.42	0.085	20

**TABLE 5**  
PHB production on different carbon and nitrogen sources by *Azotobacter* sp. A18.

Carbon and Nitrogen Sources	Dry weight of cell (g L <sup>-1</sup> )	PHB (g L <sup>-1</sup> )	Output of PHB (%)
Glucose	0.36	0.219	61
Sucrose	0.38	0.210	55
Maltose	0.40	0.165	41
Lactose	0.42	0.194	46
Glycine	0.37	0.212	57
Potassium nitrate	0.42	0.175	42
Ammonium sulfate	0.40	0.164	41
Peptone	0.35	0.206	59

**TABLE 6**  
**PHB production on different temperature and pH by *Azotobacter* sp. A18.**

Temperature and pH	Dry weight of cell (gL <sup>-1</sup> )	PHB (gL <sup>-1</sup> )	Output of PHB (%)
25 °C	0.38	0.205	54
30 °C	0.35	0.215	61
35 °C	0.38	0.194	51
40 °C	0.33	0.101	31
pH 5.0	0.30	0.125	42
pH 6.0	0.35	0.169	48
pH 7.0	0.36	0.206	57
pH 9.0	0.34	0.155	46

The PHB production of A18 isolate for the various carbon, nitrogen sources, pH and temperature were shown in Table 5 and 6.

Four different carbon sources as glucose, sucrose, maltose and lactose were used for PHB production by *Azotobacter* sp. A18. Among these carbon sources, glucose was found to be the most effective (0.219 gL<sup>-1</sup>) one. In sucrose and lactose containing medium, the PHB production was 0.210 gL<sup>-1</sup> and 0.194 gL<sup>-1</sup>, respectively. However, the PHB production was found to be the lowest (0.165 gL<sup>-1</sup>) in maltose-containing medium, (Table 5).

In this study, glycine, potassium nitrate, ammonium sulphate and peptone were used as nitrogen sources. Among nitrogen sources applied, glycine and peptone was found to be the best ones as a nitrogen source (0.212 gL<sup>-1</sup>-0.206 gL<sup>-1</sup>). The PHB yield was 0.175 gL<sup>-1</sup> in potassium nitrate-containing medium,. However, the PHB yield obtained in ammonium sulphate- containing medium was the lowest (0.164 gL<sup>-1</sup>) (Table 5).

In addition to the carbon and nitrogen sources, the effect of temperature and pH on the PHB production were also tested. The PHB yields in basic medium at different temperatures for *Azotobacter* sp. A18 were in the range 0.101 to 0.215 gL<sup>-1</sup>. However, the PHB yields in basic medium at different pH were found in the range of 0.155 to 0.206 gL<sup>-1</sup>. According to the results of this assay, optimum temperature was found to be 30 °C (0.215 gL<sup>-1</sup>) and optimum pH was determined as 7.0 (0.206 gL<sup>-1</sup>) for PHB production (Table 6).

PHB is synthesized by many bacteria such as *Bacillus* sp., *Pseudomonas* sp., *Azotobacter* sp. The yield of the biosynthesis process depends on many factors such as carbon and nitrogen source, C/N ratio, temperature, pH and time [9-17].

Yuksekdag et al. [11] carried out PHB production using *Bacillus subtilis* 25 and *Bacillus megaterium* 12 using different carbon and nitrogen sources. Their results showed that the best PHB productivity was on glucose (0.240-0.310 gL<sup>-1</sup>) and proteaz peptone (1.023-0.069 gL<sup>-1</sup>) as carbon and nitrogen sources, respectively.

Tamdogan and Sidal [12] investigated PHB production by *Bacillus subtilis* ATCC 6633 at different carbon and nitrogen sources, temperatures and pH. According to the study, the highest PHB

production was found in mannitol (23.6623 µg mL<sup>-1</sup>) and glycine (14.6217 µg mL<sup>-1</sup>) as carbon and nitrogen sources. Besides, optimum temperature and pH were found to be 30 °C and pH 7.0 (10.4981 µg mL<sup>-1</sup>), respectively.

Lasemi et al. [13] explored the effects of temperature, carbon and nitrogen source concentrations on PHB production of *Azotobacter beijerinckii* DSMZ 1041. The highest PHB production (5.84 gL<sup>-1</sup>) was obtained in concentration of glucose (50 gL<sup>-1</sup>) and ammonium chloride (1.5 gL<sup>-1</sup>) for carbon and nitrogen sources, respectively. In addition the optimum temperature for PHB production was at 30 °C.

Muralidharan et al. [9] researched PHB production of *Pseudomonas aeruginosa* MTCC 4673 different carbon and nitrogen sources. They found out that medium which contains glucose (8.5 mgL<sup>-1</sup>) and peptone (8.9 mgL<sup>-1</sup>) is more effective than sucrose, lactose, maltose, ammonium sulphate and tryptone.

Zhang et al., [14] reported that *Bacillus megaterium* R11 accumulated maximum PHB in medium containing glucose and xylose as carbon sources. Besides, tryptone was found as its best nitrogen source. PHB production (51.3%) was obtained from *Bacillus megaterium* R11.

Bora [15] demonstrated that *Bacillus megaterium* OU303A synthesized the best amount of PHB in medium containing glucose, mannitol, maltose, lactose and Na succinate. However *Bacillus* sp. yielded lower PHB when lactose or Na-succinate was used as carbon source.

Chandani et al., [16] optimized PHB production at different carbon and nitrogen sources, temperature and pH of *Bacillus tequilensis* NCS-3. The isolate output the most PHB (1.75 gL<sup>-1</sup>) using fructose and tryptone as carbon and nitrogen sources at 30 °C and pH 6.

Bhagowati et al., [17] used dextrose, lactose, sucrose, maltose, fructose, and galactose as carbon sources for PHB production by *Bacillus* spp. According to the study, maltose (5.63 gL<sup>-1</sup>) was found to be the most suitable carbon source for the accumulation of PHB in *Bacillus* spp.

Considering the articles above, it can be understood that best PHB production of *Bacillus* sp., *Pseudomonas* sp. and *Azotobacter* sp. were on



glucose, mannitol, glycine, proteaz peptone, peptone and ammonium chloride as carbon and nitrogen sources. Other tested carbon and nitrogen sources (arabinose, sucrose, maltose, lactose, ammonium sulphate and tryptone) displays relatively lower level of PHB production. Based on the carbon and nitrogen sources tested, change in PHB production amount become dissimilar in metabolic PHB synthesis pathways.

Results of this research were in accord with the results of previous studies. Our study showed that PHB production was depend on various carbon, nitrogen sources, temperature and pH. As a result, PHB synthesized by some bacteria is a substantial material and its use is widespread as industrial. Therefore, optimization studies carried out on maximum PHB production for industrial use are appreciable. The data obtained from this study would lead the future work.

## CONCLUSIONS

In this study, a total 121 bacteria were isolated from different ten soil samples as *Bacillus* sp., *Pseudomonas* sp. and *Azotobacter* sp. and strains these bacteria were screened in terms of PHB production in order to make optimization to increase the yield of PHB. According to result of these screening, maximum PHB yield was found in *Azotobacter* sp. A18. Therefore, the isolate was used for PHB optimization. Different carbon and nitrogen sources, temperature and pH were assayed for PHB efficiency by *Azotobacter* sp. A18. The highest PHB production was obtained from glucose, sucrose and peptone as a carbon and glycine as a nitrogen sources at 30 °C for pH 7.0. As a result of the optimization, output of PHB reached from 42% to 61%.

## ACKNOWLEDGEMENTS

This work was supported by the TUBITAK-BIDEP 1919B011401614. The authors are thankful to Microbiology Laboratory, Department of Biology, Adnan Menderes University which were used in this work. We also thanks Dr. Fevzi Bardakci to controlled English.

*The authors have declared no conflict of interest.*

## REFERENCES

- [1] Reddy, C.S., Ghai, R., Rashmi, K. and Kalai V.C. (2003) Polyhydroxyalkanoates: an overview. *Bioresource Technology*, 87, 137-146.
- [2] Lee, S.Y. (1996) Bacterial polyhydroxyalkanoates. *Biotechnology and Bioengineering*, 49, 1-14.
- [3] Verlinden, R.A.J., Hill, D.J., Kenward, M.A., Williams C.D. and Radecka, I. (2007) Bacterial synthesis of biodegradable polyhydroxyalkanoates. *Journal of Applied Microbiology*, 2, 1437-1449.
- [4] Anderson, A.J. and Dawes, E.A. (1990) Occurrence metabolism, metabolic role and industrial uses of bacteria polyhydroxyalkanoates. *Microbiological Reviews*, 54, 450-472.
- [5] Krieg, N.R. and Holt, J.G. (1984) *Bergey's Manual of Systematic Bacteriology*. Williams and Wilkins, Baltimore, MD.
- [6] Smibert, R.M. and Krieg, N.R. (1981) General characterization. In *Manual of methods for general bacteriology*. eds Gerhardt P., Murray R.G.E., Costilow R. N., Nester E.W., Wood W.A., Krieg N.R. and Phillips G.B. American Society for Microbiology, Washington, D.C., pp.409-443.
- [7] Prasanna, T., Ajay, B.P., Dhanavara, L.P., Chakrapani, R. and Ramachandra R.C.S.V. (2011) Production of poly (3-hydroxybutyrate) by *Bacillus* species isolated from soil. *International Journal Pharma Research & Review*, 1, 15-18.
- [8] Chang, Y., Hahn, S., Kim, B. and Chang, H. (1994) Optimization of microbial poly (3-hydroxybutyrate) recovery using dispersions of sodium hypochlorite solution and chloroform. *Biotechnology and Bioengineering*, 44, 256-261.
- [10] Muralidharan, R., Sindhuja, P.B., Sudalai, A. and Radha, K.V. (2013) Polyhydroxybutyrate production accompanied by the effective reduction of chemical oxygen demand (COD) and biological oxygen demand (BOD) from industrial effluent. *Korean Journal of Chemical Engineering*, 30, 2191-2196.
- [11] Singh, G., Kumari, A., Mittal, A., Yadav, A. and Aggarwal, N.K. (2013) Poly  $\beta$ -hydroxybutyrate production by *Bacillus subtilis* NG220 using sugar industry waste water. *BioMed Research International*, 2013, 1-10.
- [12] Yuksekdog, Z.N., Aslim, B., Beyatli, Y. and Mercan N. (2004) Effect of carbon and nitrogen sources and incubation times on polybeta-hydroxybutyrate (PHB) synthesis by *Bacillus subtilis* 25 and *Bacillus megaterium* 12. *African Journal of Biotechnology*, 3, 63-66.
- [13] Tamdogan, N. and Sidal U. (2011) Investigation of poly- $\beta$ -hydroxybutyrate (PHB) production by *Bacillus subtilis* ATCC 6633 under different conditions. *Kafkas Universitesi, Veteriner Fakultesi Dergisi*, 17, 173-176.
- [14] Lasemi, Z., Darzi, G.N. and Baei, M.S. (2012) Media optimization for poly ( $\beta$ -





- hydroxybutyrate) production using *Azotobacter beijerinckii*. *International Journal of Polymeric Materials*, 62, 265–269.
- [15] Zhang, Y., Sun, W., Wang, H. and Geng, A. (2013) Polyhydroxybutyrate production from oil palm empty fruit bunch using *Bacillus megaterium* R11. *Bioresource Technology*, 147, 307–314.
- [16] Bora, L. (2013) Polyhydroxybutyrate accumulation in *Bacillus megaterium* and optimization of process parameters using response surface methodology. *Journal of Polymer Environment*, 21, 415–420.
- [17] Chandani, N., Mazumder, P.B. and Bhattacharjee, A. (2014) Production of polyhydroxybutyrate (biopolymer) by *Bacillus tequilensis* NCS-3 isolated from municipal waste areas of Silchar, Assam. *International Journal of Science and Research*, 3, 198-203.
- [18] Bhagowati, P., Pradhan, S., Dash, H.R. and Das, S. (2015) Production, optimization and characterization of polyhydroxybutyrate, a biodegradable plastic by *Bacillus* spp. *Bioscience, Biotechnology, and Biochemistry*, 79, 1454–1463.

---

**Received:** 27.01.2016  
**Accepted:** 08.09.2016

---

#### **CORRESPONDING AUTHOR**

**Halil Biyik**  
Adnan Menderes University  
Faculty of Science and Art  
Department of Biology  
09100 Aydin Turkey

e-mail: [hbiyik@adu.edu.tr](mailto:hbiyik@adu.edu.tr)

# IMAGE PROCESSING BASED INTELLIGENT SPRAYING ROBOT FOR WEED CONTROL

Kadir Sabanci<sup>1,\*</sup>, Cevat Aydin<sup>2</sup>

<sup>1</sup>Department of Electrical and Electronics Engineering, Faculty of Engineering, Karamanoglu Mehmetbey University, Karaman, Turkey

<sup>2</sup>Department of Agricultural Machinery, Faculty of Agriculture, Selcuk University, Konya, Turkey

## ABSTRACT

At weed control, physico-mechanical is the most commonly used method in chemical weeding in the world and in our country despite genetic, biological and biotechnical methods. Pesticide use in agriculture has increased in recent years. Because of the difficulty in finding farm workers and damage to sugar beets caused by farm workers due to their carelessness during hoeing, the use of chemicals has increased. However, because the pesticide used in chemical weeding affect human health, the environment and the natural balance negatively and because of increased production costs pesticides should be applied precisely, cautiously and with the minimum agricultural pesticide loss. In this study, image processing based intelligent spraying robot was developed. Variable levelled herbicide was applied on weed by using image processing techniques. The covering rate of the spraying liquid applied on the weeds was determined for 8 different speed values of robot when nozzle height of the spraying robot is 50 and 30 cm. A reduction of 40% led to a decrease of 9.42% for 4 weed averagely in the covering value of the spraying liquid to the weed.

## KEYWORDS:

Image processing, precision agriculture, robotic weeding, weed control.

## INTRODUCTION

The most important issue for agricultural crop production is a weed control. The harmful effects, like crop yield and crop quality decrease, have influence on weed moisture and crop nutrients under sunlight impact. These effects are hardly managerial and harmful without control [1].

The most effective method for combating weeds on sugar beet agriculture is chemical combat. But pesticides must be applied sensitively and carefully and causing a minimum of drug loss due to drugs used in chemical control affecting human health, the environment and the natural balance in a negative way and rising production costs [2]. As a result of intense and unconscious use of agricultural

pesticides, used pesticide itself or its conversion products can remain in food, soil, water and air. Its negative effects on non-target other organisms and humans is seen and the natural balance is disturbed [3].

As a result of investigations, it is revealed that the pancreas, skin, lymphoma, kidney, breast, rain, prostate, liver, leukemia and lung cancers have a relation with the volume of pesticide exposure of the patient [4]. The leukemia in children have been associated with the coincidence of children to insecticides and herbicides [5]. The Parkinson's disease risk grows up tragically, like 70%, in highly pesticides exposed ones than others [6]. About 3 million people are employed in agriculture. It is claimed that 18.000 of them will be die because of pesticide poisoning in each year by the World Health Organization and the UN Environment Programme [7].

The herbicide usage generally has an unfavorable effect on bird population [8]. But the effect of herbicide use is so unstable on bird populations. Field studies are required to relieve it. But herbicide use in silviculture may pose serious effects on bird population. Due to the effect of herbicides on vegetation diversity, the low toxic herbicides also have effects on bird populations [9]. A relationship between herbicide use in agriculture and seed-eating bird that always depend on weeds which are affected by herbicides have been detected in Britain [10]. The herbicide granules that are eaten inadvertently as food grains by small birds, may cause death of them [11]. The aquatic flora may be affected from polluted water by herbicides. That may kill fish directly or indirectly by affecting the plants in the lakes or sea which are the habitat of them [12].

Modern agro-technologies of weed quality parameters control are based on reduced chemicals use, and it have reduced impacts on crop production quality, environmental protection and sustainable components for implementing precise agriculture as the main aim for any framework in any safe technology [13, 14].

The robotic technology are autonomous vehicles in unique systems reveal the opportunities to develop bio-technology for production new generation agro-production, and this tech-systems serve for optimization in complex agricultural

operations and precision weed management. Robotic weeding helps to construct autonomous platform [15], precision spraying system is suggested to be included to this platform as main element [16-19], automatic pest device for non-chemical control [20-23]. Nowadays the automatic weed classification and computed term plant control is available as an innovative technology [24, 25].

Jafari et al. [26] have used discriminant analysis to obtain the relation between red, green and blue components of the images. At different lighting conditions 300 images of seven types of sugar beet plants have been taken to provide information for discriminant analysis procedure. Discriminant functions and their success rate in weed detection and segmentation of different plant species have been evaluated. Burgos-Artizzu et al. [27] have proposed a real-time computer vision system that determines crop rows under daylight. The system consists of a fast response system for real time and a slow but more accurate system. Tests have been done under different condition, different illumination, soil humidity and weed/crop growth conditions. The success rates have been determined as 95% of weed detection and 80% of crop detection. These results were final as the preconditions of test were the beet field size, distance between rows in weeding, used processing technics and application of herbicide spray by using robot precise spraying [3]. Some different preconditions were applied – robot's precise spraying nozzle height 30 cm; the speed of robot –  $8.928 \text{ cm.s}^{-1}$  comparing with herbicide application on the same area  $1.6 \text{ m}^2$ . The economic effect was defined – drugs of 55.22 % were saved comparing with conventional one. The liquid was applied by robot precise spraying on weeds with at 8 speeds. There was measured the interaction between

increase of speed of spraying and use of robot with the decrease of spraying liquid.

The spraying robot designed in our study detects and sprays the weeds which are both between the rows and on the rows simultaneously by using 2 cameras and spraying nozzle. By using image processing algorithm between rows, only colour information of weed is examined. However, at the mode of on row, weeds are sprayed by classifying according to shape and colour information of weed and sugar beet by using image processing algorithm and artificial neural networks. Any studies that control between rows and on rows simultaneously are not found out in other studies at the literature.

In this study, weeds found in sugar beet with developed intelligent spraying robot were identified by using image processing techniques and the spraying liquid was applied on them. Tests for 8 different speed values of robot were made while nozzle height of the spraying robot is 50 and 30 cm to the ground. For these values, the covering rate of the spraying liquid applied on the weeds were determined.

## MATERIALS AND METHODS

In the study, an intelligent spraying robot, composed of spraying unit, control unit, cameras and laptop, was developed (Figure 1). 4- four wheels (6 cm diameter) are used for movement of the spraying robot. Spraying robot was moved back and forth by means of steel rope of 0.4 mm on a rail of 5 m in length.

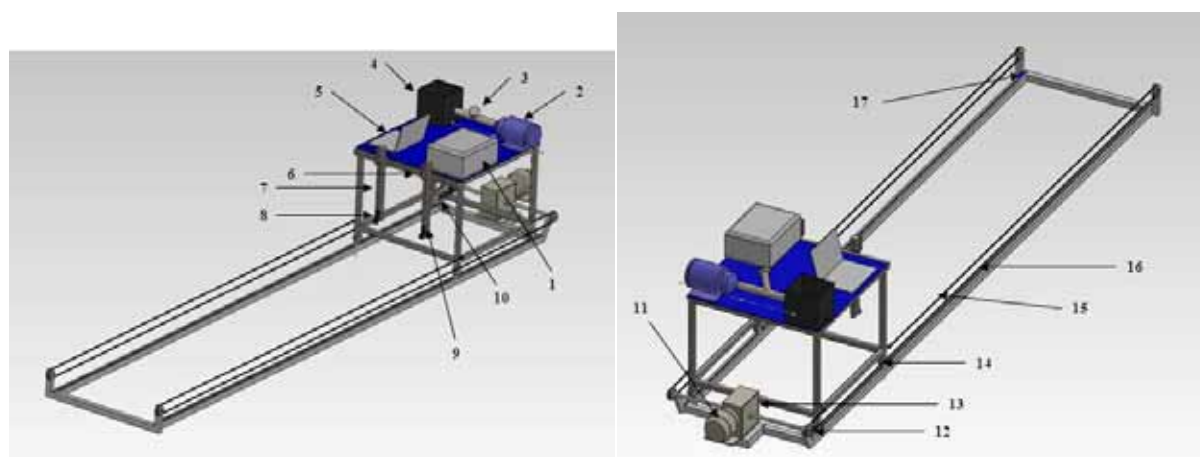


**FIGURE 1**

### Testing apparatus

1. Control unit 2. Pressure pump 3. Filter 4. Spraying tank, 5. Computer 6. Horizontal position profile, 7. Vertical position profile, 8. Webcam 9. Spraying nozzle, 10. Lighting system, 11. Induction motor, 12. Pulley, 13. Gear, 14. Tires, 15. Steel cables, 16. Ray, 17. Switches

Movement of intelligent spraying robot on rail was provided with 3-phase asynchronous motor of 0.75 kW. Inverter that controls engine speed, Delta brand, EL series, VFD015EL21 models, in a power of 1.5 kW was used.

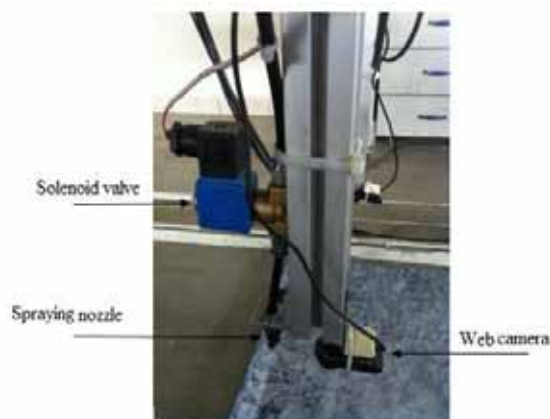


**FIGURE 2**  
Solenoid valve, spraying nozzle and web camera

In spraying unit, a 0.75 kW, 8 bar pressure pump is used to spray disinfection liquid applied on weeds from spraying nozzle. 80 microns jet rodding

check valve nozzle was used as the spraying nozzle (Figure 2).

System was controlled with a PLC which changes the status of the valves according to the signals coming from the laptop, enables the control the speed of spraying robot, controls the information coming from the limit switches, Delta brand DVP-14SS2 series, has relay outputs. Logitech C905 webcam which takes the images of sugar beet plants and weeds real-time and transfers to software *Matlab* was used (Figure 2). The pictures of sugar beet (*Beta vulgaris L.*) in a sugar beet field (38° 9' 24.78" N 31° 40' 32.74" E) at Doganhisar district of Konya in Turkey.

The lamb's quarters (*Chenopodium album*), musk thistle (*Carduus nutans*), prickly lettuce (*Lactuca serriola*), and cockspur grass (*Echinochloa crus-galli*) in the sugar beet fields were selected as weeds that will be used in our study. Black inky water (spraying liquid) was used to spray on weed.

This experimental work was conducted at Selcuk University, Agriculture Faculty, and Department of Agricultural Machinery Laboratory in 2013.

To choose the plant on the image taken by the webcam on precision disinfection robot, it is separated in to RGB channels and green colour value is obtained using 1 equation [28].

$$F=G-0.5*R-0.5*B \quad (1)$$

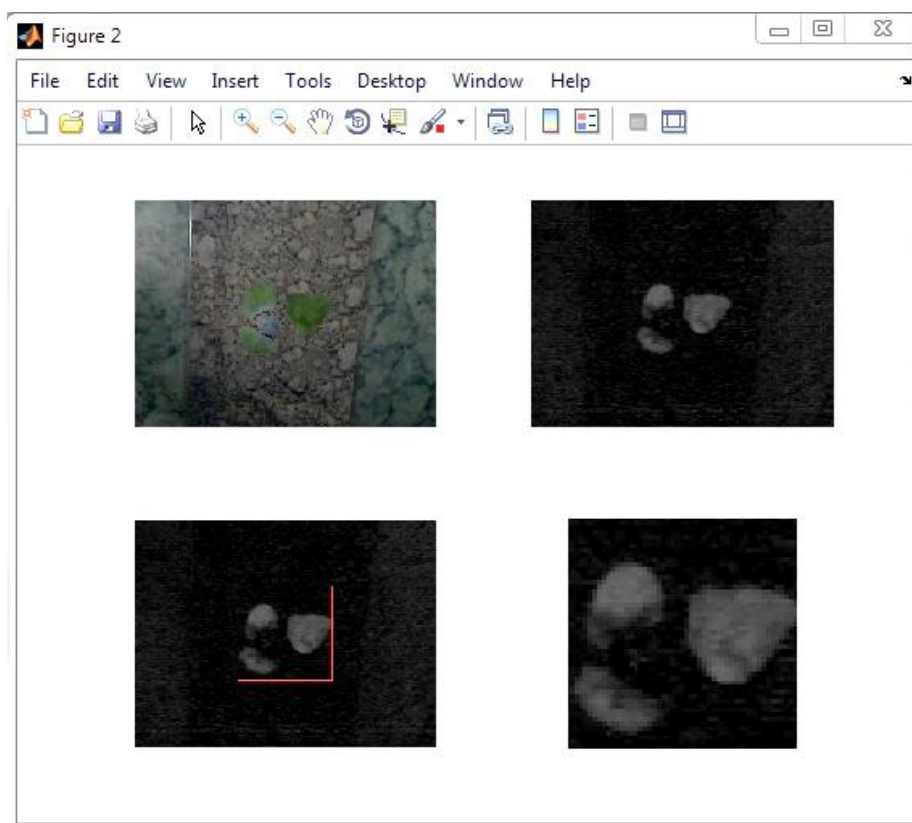


**FIGURE 3**  
Matlab screenshot of spraying between rows

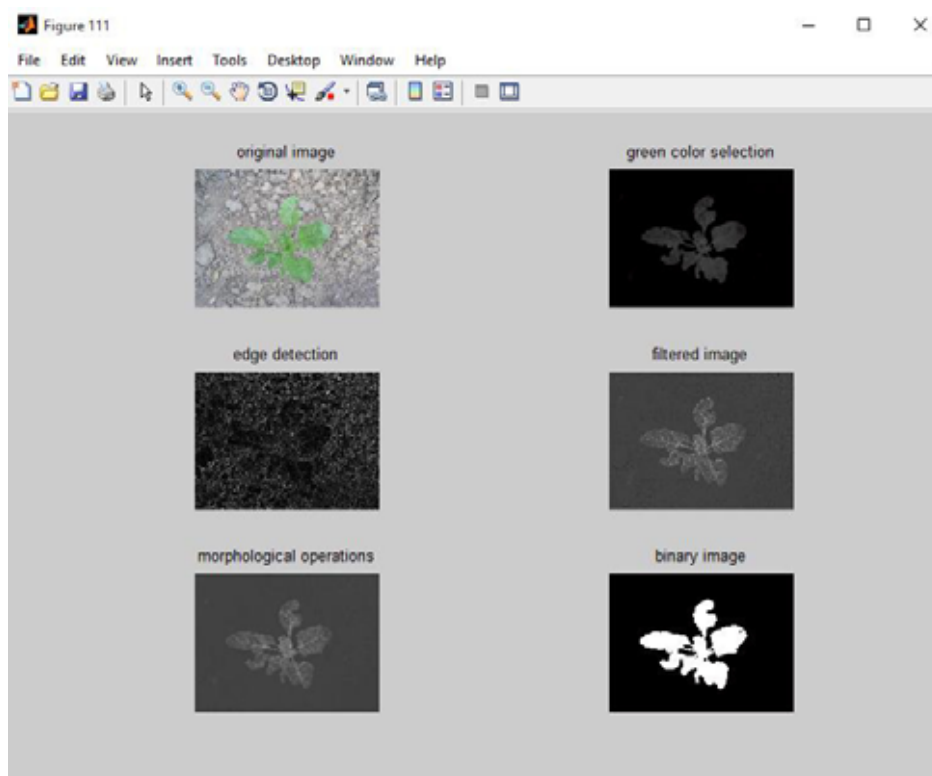


**FIGURE 4**  
**Image processing steps for the selection of plant**

To get green colour data red (R) and blue (B) colour values are multiplied with 0.5 and are subtracted from green (G) value. In this function (F), the aim is to get the closeness of the colour to green. This procedure is made in the field that has 100x100 pixel value instead of the whole image taken from the webcam. The spraying is made exactly when the plant is under the nozzle to implement the spraying liquid by sensitive way. In this field, the spraying liquid is implemented on the weed, if green colour level is above the specific threshold value (Figure 3).

While the spraying robot's speed increases, the frame amount taken from the webcam is decreased. The spraying liquid is implemented to the weed by evaluating the images taken from webcam with image processing techniques. The fastening target performance is tested because of the speed of the spraying robot. The spraying liquid which implementing to the weeds is evaluated on the scope of coverage of the weed area while the spraying robot's working on the inter row. To choose the plant, received image is separated into RGB channels first and green colour selection is made using equality 8. Then, filtering was determined by applying 3-channel edge determination to the obtained image. Morphological processing's are applied to filtered image knowledge and then converted to black and white image by using Otsu method [29] (Figure 4). Firstly, the nozzle height is

set as 50 cm with the help of the height profile on the precision spraying robot. The spraying liquid is implemented to the weeds by determining them while the spraying robot working on the line method. The spraying liquid implemented weeds are photographed (Figure 5). Same transactions is repeated by setting the spraying robot's nozzle height as 30 cm.

The percentage of the spraying liquids coverage on the plants is evaluated by using the image processing techniques of these photos. The borders of the weeds are marked on the photos. Same transaction is also made for the spraying liquid's space on the photos. While we are calculating the rates of covering as percentage, selected picture information is converted into gray level picture information firstly, and then it is converted into binary image information by using the Otsu method (Figure 6).

The painted weed area is found by multiplied the pixel value of the weed areas and the inked areas of the pixel values (Figure 7a). The unpainted weed area is found by multiplied the pixel value of the weed areas and the inked areas of the pixel values by taking the opposite (Figure 7b). Then the areas on the spraying liquid are determined as has spraying liquid or not (Figure 7c). The pixel area of the weed which is on the spraying liquid is evaluated to the



**FIGURE 5**  
Images on which spraying liquid was applied

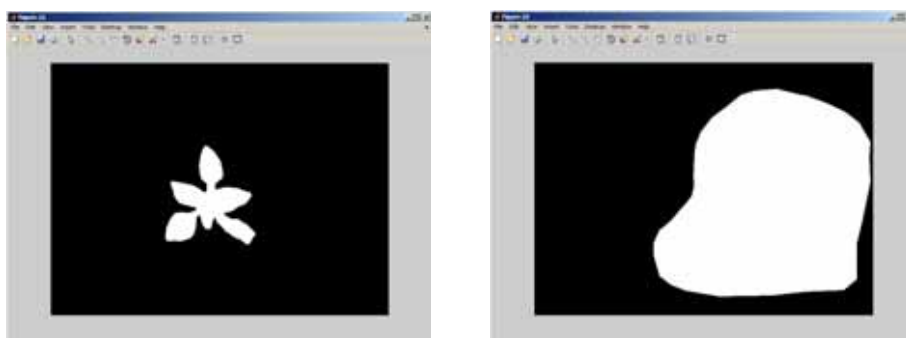


**FIGURE 6**  
Binary image data belonging to area of weeds and spraying liquid

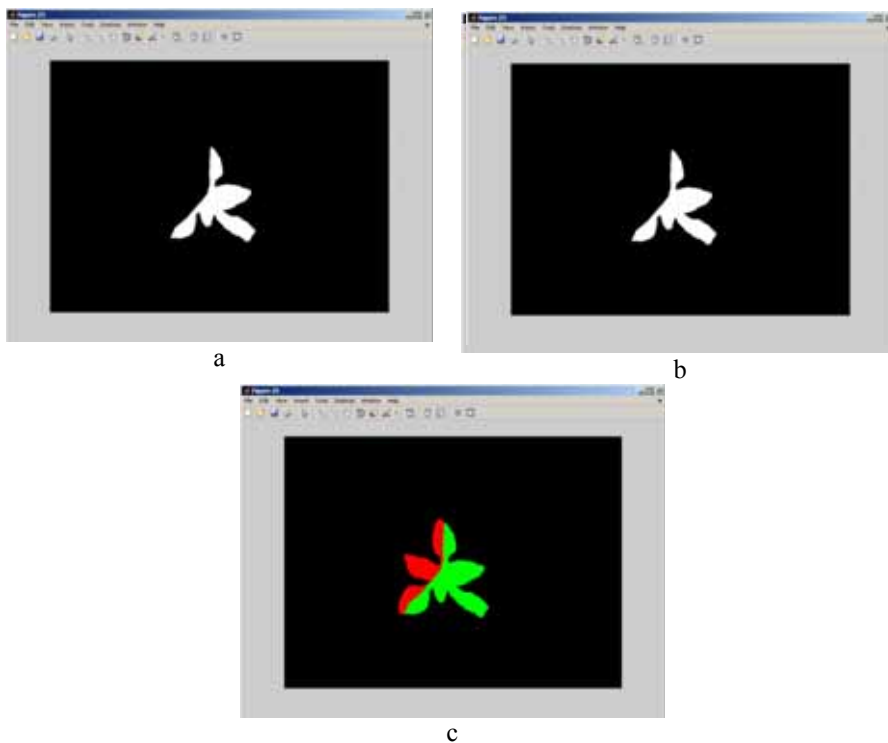


**FIGURE 7**  
a) The area of the weed on which there is spraying liquid  
b) The area of the weed on which there is not spraying liquid  
c) The area on which there is spraying liquid and there is not spraying liquid

rate of the weed's pixel areas. The coverage percentage of the spraying liquid is determined.

## RESULTS AND DISCUSSION

The precision spraying robot's rate of the covering the weed as percentage is evaluated on the spraying liquid on the weeds. The covering rate of the spraying liquid to the weeds is determined at 8 different speed values (2.232, 4.469, 6.329, 6.711, 8.928, 12.944, 19.607, 25.806  $\text{cm}\cdot\text{s}^{-1}$ ) of spraying liquid with the *Matlab* software while it is on the 50 and 30 cm nozzle height of the spraying robot.

The speed of spraying robot and the covering area were inversely proportional. When the speed of the spraying robot increase, the number of frames got from webcam decreases. Weeds were determined using image processing algorithms. When the system detected weed, *Matlab* transferred information to PLC. PLC triggered solenoid valve and applied inky water on lamb's quarters (*Chenopodium album*). Because the number of frames captured by webcam decrease, the shooting time of solenoid valve gets shorter. Because the application time of spraying liquid was shortened, the covering area decreased. Flow chart of inter row weed spraying is given in Figure 8.

When intelligent spraying robot nozzle height is 50 cm the speed raises from 8.928  $\text{cm}\cdot\text{s}^{-1}$  to 12.944  $\text{cm}\cdot\text{s}^{-1}$  (means there is 44.98% percent increase on the value), it causes a reduction as the 43.50% for lamb's quarters, 45.23% for musk thistle, 35.53% for prickly lettuce, 47.32% for cockspur grass on the percentage of the plant coverage.

When spraying robot speed value is raises from 12.944  $\text{cm}\cdot\text{s}^{-1}$  to 25,806  $\text{cm}\cdot\text{s}^{-1}$  (means there is 99.36% percent increase on the value), it causes reduction as the 63.33% for lamb's quarters, 61.35% for musk thistle, 64.49% for prickly lettuce, 63.04% for cockspur grass on the percentage of the plant coverage (Figure 9).

When spraying robot nozzle height is 30 cm the speed raises from 8.928  $\text{cm}\cdot\text{s}^{-1}$  to 12.944  $\text{cm}\cdot\text{s}^{-1}$  (means there is 44.98% percent increase on the value), it causes a reduction as the 42.97% for lamb's quarters, 43.09% for musk thistle, 37.22% for prickly lettuce, 48.51% for cockspur grass on the percentage of the plant coverage.

When spraying robot speed value is raises from 12.944  $\text{cm}\cdot\text{s}^{-1}$  to 25,806  $\text{cm}\cdot\text{s}^{-1}$  (means there is 99.36% percent increase on the value), it causes reduction as the 62.59% for lamb's quarters, 61.56% for musk thistle, 65.55% for prickly lettuce, 64.86% for cockspur grass on the percentage of the plant coverage (Figure 9).

When intelligent spraying robot speed is 8.928  $\text{cm}\cdot\text{s}^{-1}$ , the nozzle height is turned to 30 from 50 cm (means there is 40% percent decrease on the value) it causes reduction as the 11.10% for lamb's quarters,

10.09% for musk thistle, 7.87% for prickly lettuce, 8.63% for cockspur grass on the percentage of the plant coverage (Figure 9).

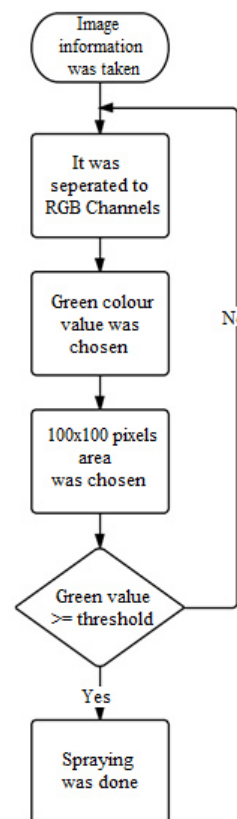


**FIGURE 8**  
Flow diagram of spraying weeds between rows

## CONCLUSIONS

The protection of the human, animal and environment health will be achieved by implementing the spraying liquid on the just weeds instead of the whole farm by determining the weeds with the improved system.

The percentage of the coverage on the weeds implemented by spraying liquid is switched as inversely proportional with the precision spraying robot. When precision spraying robot speed raises from 8.928  $\text{cm}\cdot\text{s}^{-1}$  to 12.944  $\text{cm}\cdot\text{s}^{-1}$  (means there is 44.98% percent increase on the value), it causes reduction as 42.28% for 4 weed averagely on the percentage of the plant coverage areas of the spraying liquid.

There is observed reduction on the precision spraying robot's nozzle height with the 40% percent and on the plant coverage percentage of the spraying liquid, there is reduction with the percent of the for 4 weed averagely 9.42%.

At the studies made at 8 different speed values of spraying liquid and while nozzle height is 50 cm,

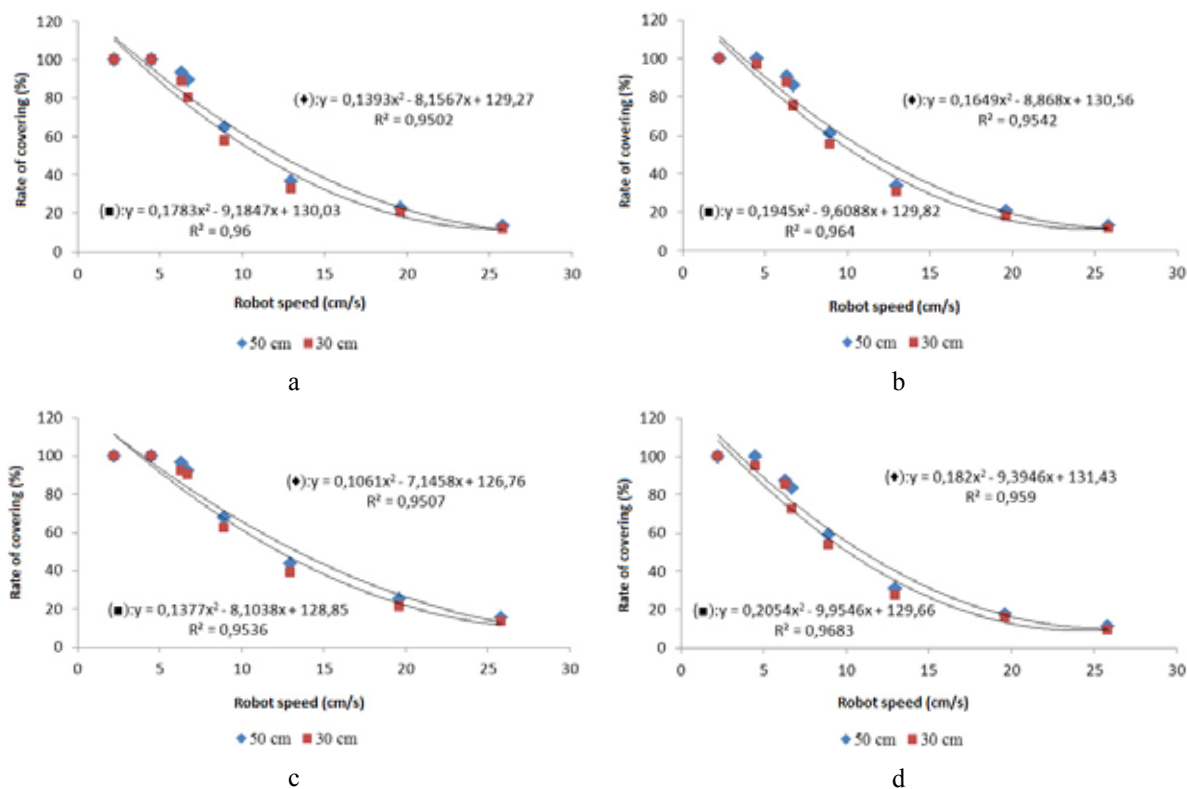


FIGURE 9

Percentages rate change of the precision spraying robot's rate of covering according to different speed values

a) lamb's quarters    b) musk thistle    c) prickly lettuce    d) cockspur grass

the average rates of covering rates of the spraying liquid, applied on weeds, to the weeds are 65.05% for lamb's quarters, 63.09% for musk thistle, 67.7% prickly lettuce, 61.26% cockspur grass. Developing the intelligent spraying system model, variable level herbicide application can be achieved at sugar beet fields. The same system can be used on plants grown at greenhouses and fluid fertilizer application. By this way, the input cost will be lessened.

This robot move on a rail with its 4 wheels with the aid of an engine. It is designed to be suitable to laboratory conditions. There are self-propelled robot works in the literature. However, tests will be made again by developing the system at our further studies to work more efficiently and regularly in field conditions and by adapting this system to the tractor three-point linkage system.

#### ACKNOWLEDGEMENTS

The authors acknowledge the support of this study by the Scientific Research Projects Coordination Office of Selcuk University.

#### REFERENCES

- [1] Slaughter, D.C., Giles D.K. and Downey D. (2008) Autonomous robotic weed control systems: A review. *Computers and Electronics in Agriculture*, 61(1): 63-78.
- [2] Dursun, E. (2000) Meme aşınmasının pülverizasyon karakteristiklerine etkileri. *Ekin Dergisi* 6(21): 62-66
- [3] Sabancı, K. and Aydın, C. (2014) Görüntü işleme tabanlı hassas ilaçlama robotu, *Tarım Bilimleri Dergisi - Journal of Agricultural Sciences*, 20(4): 406-414.
- [4] Gilden, R.C., Huffling K. and Sattler B. (2010) Pesticides and health risks. *Journal of Obstetric, Gynecologic, & Neonatal Nursing*, 39(1): 103-110.
- [5] Chen, M., Chang, C.H., Tao, L. and Lu, C. (2015) Residential exposure to pesticide during childhood and childhood cancers: A meta-analysis. *Pediatrics*, 136(4): 719-729.
- [6] Ascherio, A., Chen, H., Weisskopf, M.G., O'Reilly, E., McCullough, M.L., Calle, E.E., ... & Thun, M.J. (2006) Pesticide exposure and risk for Parkinson's disease. *Annals of neurology*, 60(2):197-203.
- [7] Miller, G.T. (2004) *Sustaining the Earth*, 6th edition. Thompson Learning, Inc. Pacific Grove, California. Chapter 9, Pages 211-216.





- [8] Blus, L.J. and Henny, C.J. (1997) Field studies on pesticides and birds: unexpected and unique relations. *Ecological Applications*, 7(4): 1125-1132.
- [9] MacKinnon, D.S. and Freedman, B. (1993) Effects of silvicultural use of the herbicide glyphosate on breeding birds of regenerating clearcuts in Nova Scotia, Canada. *Journal of Applied Ecology*, 395-406.
- [10] Newton, I. (2004) The recent declines of farmland bird populations in Britain: an appraisal of causal factors and conservation actions. *Ibis*, 146(4): 579-600.
- [11] Palmer, W.E., Bromley, P.T. and Brandenburg, R.L. (2007) *Wildlife & pesticides-Peanuts*. North Carolina Cooperative Extension Service, 21-28.
- [12] Helfrich, L.A., Weigmann, D.L., Hipkins, P.A. and Stinson, E.R. (2009) Pesticides and aquatic animals: a guide to reducing impacts on aquatic systems.
- [13] Stafford, J.V. (2006) The role of the technology in the emergence and current status of precision agriculture. In: Srinivasan, A. (Ed.), *Handbook of Precision Agriculture*. Food Products Press, New York, pp. 19–56.
- [14] Tellaache, A., Burgos-Artizzu, X.P., Pajares, G., and Ribeiro, A. (2008) A vision-based method for weeds identification through the Bayesian decision theory. *Pattern Recognition*, 41(2): 521-530.
- [15] Bakker, T., Van Asselt, K., Bontsema, J., Muller, J. and Van Straten G., (2010) Systematic design of an autonomous platform for robotic weeding. *J. Terramech*. 47: 63–73.
- [16] Sogaard, H.T. and Lund, I. (2007) Application accuracy of a machine vision-controlled robotic micro-dosing system. *Biosyst. Eng.* 96 (3): 315–322.
- [17] Gil, E., Lorens, J., Llop, J., Fábregas, X., Escolá, A. and Rosell-Polo, J.R. (2013) Variable rate sprayer. Part 2 – Vineyard prototype: design, implementation, and validation. *Comput. Electron. Agric.* 95: 136–150.
- [18] Sabanci, K. and Aydin, C. (2013) Real-time precise spraying robot for weed control. *International Conference of Ecosystems (ICE)*, 1-5 June, 2013 Tirana, Albania, pp: 356-359.
- [19] Tewari, V.K., Kumar, A.A., Nare, B., Prakash, S. and Tyagi A. (2014) Microcontroller based roller contact type herbicide applicator for weed control under row crops. *Comput. Electron. Agric.* 104: 40–45.
- [20] Tillet, N.D., Hague, T., Grundy, A.C. and Dedousis A.P. (2008) Mechanical within-row weed control for transplanted crops using computer vision. *Biosyst. Eng.* 99: 171–178.
- [21] Perez-Ruiz, M., Slaughter, D.C., Gliever, C.J. and Upadhyaya, S.K. (2012) Automatic GPSbased intra-row weed knife control system for transplanted row crops. *Comput. Electron. Agric.* 80: 41–49.
- [22] Perez-Ruiz, M., Slaughter, D.C., Fathallah, F.A., Gliever, C.J. and Miller B.J. (2014) Corobotic intra-row weed control system. *Biosyst. Eng.* 126: 45–55.
- [23] Nan, L., Chunlong, Z., Ziwen, C., Zenghong, M., Zhe, S., Ting, Y. and Junxiong, Z. (2015) Crop positioning for robotic intra-row weeding based on machine vision. *International Journal of Agricultural and Biological Engineering*, 8(6): 2029.
- [24] Arribas, J.I., Sanchez-Ferrero, G.V., Ruiz-Ruiz, G. and Gomez-Gil, J. (2011) Leaf classification in sunflower crops by computer vision and neural networks. *Computers and Electronics in Agriculture*, 78: 9–18.
- [25] Siddiqi, M.H., Lee, S.W. and Khan, A.M. (2014) Weed image classification using wavelet transform, stepwise linear discriminant analysis, and support vector machines for an automatic spray control system. *J. Inf. Sci. Eng.*, 30(4): 1227-1244.
- [26] Jafari, A., Mohtasebi, S.S., Jahromi, H.E. and Omid M. (2006) Weed detection in sugar beet fields using machine vision. *Int. J. Agric. Biol.* 8(5): 602-605.
- [27] Burgos-Artizzu, X.P., Ribeiro, A., Guijarro, M. and Pajares, G. (2011) Real-time image processing for crop/weed discrimination in maize fields. *Computers and Electronics in Agriculture*, 75(2): 337-346.
- [28] Ramaraju, S.S.V.S. and Kumar, N.U. (2014) Saliency detection algorithm for locating perceptible objects. *International Journal of Electronics & Communication Technology* 5(3): 97-100.
- [29] Otsu, N. (1979) A threshold selection method from gray-level histograms. *IEEE Trans. Sys., Man., Cyber.* 9 (1): 62–66.

---

**Received: 25.01.2016**

**Accepted: 20.09.2016**

---

#### **CORRESPONDING AUTHOR**

**Kadir Sabanci**

Department of Electrical and Electronics Engineering

Faculty of Engineering

Karamanoglu Mehmetbey University

70100, Karaman- TURKEY

E-mail: kadirsabanci@gmail.com



# THE STUDY ON EXPLOITATION, UTILIZATION AND ENVIRONMENTAL EFFECTS OF WIND RESOURCES IN LIAONING PROVINCE, CHINA

Zhidong Li, Shushen Zhang\*, Shuming Ma

Key Laboratory of Industrial Ecology and Environmental Engineering (MOE), School of Environmental Science and Technology, Dalian University of Technology, Linggong Road 2, 116024 Dalian, People's Republic of China

## ABSTRACT

Wind energy as a kind of renewable clean energy is considered to be one of the new energies with a bright prospect for development. The development and utilization of the rich wind energy resource in the Liaoning province has and would continue to have bright further. We used WAsP model to calculate wind resource distribution in Liaoning province, which will provide a basis for wind farm's site selections. Meanwhile, this article also introduces current situation of wind farm-built in Liaoning province. Wind farms-built replace coal consumption which will reduce pollutants emission, greenhouse gas (GHG), SO<sub>2</sub> and NO<sub>x</sub> and so on. These are one of the most significant factors in promoting the development of wind power in China. The calculation of environmental benefits is one of the important contents of environmental impact analysis of wind farm. In the paper, we propose a simplified calculation method only related to comprehensive coal consumption and pollutant discharge rate, so as to effectively standardize and quickly calculate the environmental benefits of wind farm.

## KEYWORDS:

Wind Energy Resources; WAsP Climate Analyst; Numerical Simulation; Environmental benefits; Clean Development Mechanism; Pollutants emission reductions

## INTRODUCTION

Wind can be defined as air in motion. The source of wind is the energy available from the sun. Daytime heating of the earth and night

time cooling gives rise to a temperature differential which triggers the pressure gradient. It is this horizontal gradient of pressure which causes the air to flow from one place to another in the form of wind. The pressure gradient in the vertical is usually balanced by gravitational force, and thus, the vertical velocity of air is minimal in magnitude when compared to horizontal velocity.

Wind is a renewable energy source, freely available in nature. Therefore, it is a potential energy source, which when harvested, enables the generation of electricity by implementing wind turbines. The main characteristics of wind are wind speed and wind direction. Wind direction can be divided into 12 or 16 sectors each of 30 or 22.5 degrees, respectively. Wind speed and wind direction are measured by anemometers at meteorological stations. Wind turbines start working at wind speeds greater than 5 m/s and wind power density increases as wind speed increases ([www.bwea.com](http://www.bwea.com)).

China is an important producer of coal. Its rapid socio-economic growth has been characterized by increasing population, high rates of urbanization, and substantial industrialization, which is transforming it into a large big energy consumer as well. In addition to urbanization, climatic conditions have played an important function in increasing demand for electricity in China. Wind Energy is a renewable energy which is produced by the uneven heating up of the earth surface by the sun. During the day time air on the land surface gets heated up faster than air on the water. The heated air expands and raises to the atmosphere the cold air over the water surface tries to replace it due to the low pressure on the land as a result wind is produced. At night time winds are reversed as the air on land gets cooled faster than the air on water and the same principle is applied for the

atmospheric winds. The development and utilization of wind energy is the most grown technique among renewable energy. In order to improve the energy structure and accelerate the utilization of wind energy, wind resource assessment has been intensified in China in recent years. By 2014, China has the world biggest installed capacity for wind turbines, but wind resource assessment is relatively backwards which will lead to build in wind resource-poor zone for many Wind farm. It caused serious waste of resources. A fast and efficient method of wind energy resource assessment and Wind farm site selection gets more attention in china, which becomes a hit issue for many scholars at present. By the end of 2014, the state-owned the Wind farm power capacity is 114609MW, 6615.15MW come from Liaoning. The first Wind farm have been built in 1993, its power capacity is 22.45MW, and 23 wind turbines have been installed, located in Dalian, Liaoning. From 1993 to 2014, the power capacity increased by 293.66%, has grown at an annual rate of 26.7%. (Bing Xue et al., 2015)

The aim of this research is to help identify the potential role of wind energy sources in Liaoning. In order to reduce the costs of wind resource assessment and improve the scientificness of the wind farm development, wind resource assessment of Liaoning have been studied by wind resource assessment Software-Wasp. It also forecasts mainly pollutants SO<sub>2</sub>, NO<sub>x</sub> and GHG emission reductions which from electricity generation in fossil fuel fired power plants that are displaced by wind farm-built in Liaoning province. These are one of the most significant factors in promoting the development of wind power in China.

## MATERIALS AND METHODS

### Study Area: Liaoning Province.

**Location:** Liaoning lies in the Northeast part of China, between latitudes 38.72 and 43.48 north, and longitudes 118.83 and 125.78 east. Its northeast borders are with Jilin province, its northwest borders are Nei Monggol province, and its west borders are Hebei province, and its southeast borders are North Korea. Its shores of the Bohai Gulf lie on the south. This special location provided Liaoning with a commercial

importance. As it is a natural outlet for the Northeast part of the China. The total area of Liaoning is 145900 square Kilometers, 18 percent of the total land area of Chinese land. The population up until December 2013 reached approximately 43,900,000. Liaoning geographic location is as shown in Figure 1.



**FIGURE 1**  
**Topography map of Liaoning, China**

**Topography:** Liaoning is mountains and hills topography in the eastern and western. The middle area of Liaoning is flat. The topography is north is higher than south, land slopes gradually to sea (Figure 2). The height of the eastern corner reaches 1347meters above sea level. The Gangshan is the Liaoning's highest place which it is located in Fushun of Liaoning. Mountains are spread in Liaoning, such as Changbaishan, Nuhuerhushan, and Yiwulvsan. The Liaoning Rivers are spread in different places. The most significant of the Liaoning Rivers are liaohe, hunhe and Yalu River, which are located in the middle and south area.

Liaoning topography is as shown in Figure 2.

**Climate:** Liaoning has a temperate continental monsoon climate, four distinct seasons, abundant sunshine, annual average temperature varies from 7 to 11 °C, annual average frost-free period varies from 130 to

200 days, sunshine duration varies from 2100 to 2600 hours. Rainfall varies from 400 to 1100 millimeters a year across the region. The rainy season often occurs during the summer months. The highest temperature sometimes reaches 40 °C during summer. During winter, the lowest temperature occasionally reaches minus 18 °C. Winter rainfall is irregular and varies in quantity from one year to another. Autumn and spring seasons are distinguished by their short periods.

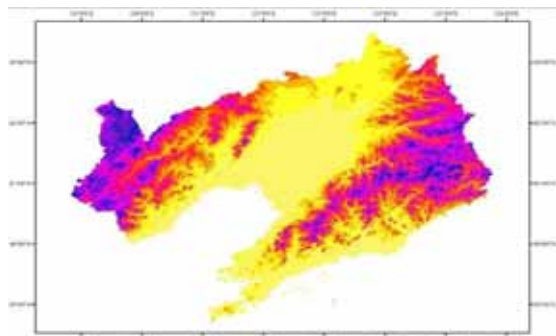


**FIGURE 2**  
**Topographic Map of Liaoning**

The dominant wind direction in Liaoning is north and south with winds blowing from this direction approximately 60 percent of the time.

**Models. What's new in Wasp?** One of the most widely used wind resource assessment models is the Wind Atlas Analysis and Application Program (WAsP). WAsP is the industry-standard software package for siting of wind turbines and Wind farms (Ayotte, K 2008). Many companies use WAsP worldwide for all steps from wind resource and energy yield assessments, to wind conditions and site suitability characterization; from single turbines in complex terrain to large Wind farms offshore. A widely popular software WAsP was chosen to perform the study. In 1987 the Wind Energy and Atmospheric Physics Department at Risø National Laboratory introduced WAsP – a powerful tool for wind data analysis, wind atlas generation, wind climate estimation, Wind farm production calculations and siting of wind turbines. Over the years, the program has become the industry standard for wind resource assessment and siting of wind turbines and Wind farms and it has been employed in more than 100 countries around the world.

Wind Atlas Analysis and Application Program (WAsP) is a linear numerical Microscale Model used to estimate the wind energy resources at any location (Troen, Petersen 1988; Landberg, L. et al., 2003). There are two main parts - wind atlas analysis and wind atlas application. Wind data, recorded through any meteorological station, gives information specific to that region. In order to apply this data to any other location, the data must be interpolated or extrapolated by some means so as to utilize it. WAsP is an integrated computer model which makes use of physical models such as Surface Layer Similarity Laws, the Geostrophic Drag Law, the Stability Model, the Roughness Change Model, the Shelter Model and the Orographic Model (Troen and Petersen 1989). It has been reported by Mortensen et al. (2004) that it is possible to obtain stable wind speed estimates which are close to the measured values with maps of 8 × 8 km<sup>2</sup>. They have also reported the influence of contour interval on the accuracy of wind speed prediction (Mortensen and Peterson 1997). Large prediction errors are associated with large contour intervals and the prediction error reduces with decreasing contour intervals. It is reported that a contour interval of 20 m or less is expected to provide fairly accurate predictions. WAsP application has many case studies in China, such as Zhejiang, Shandong, Ningxia, Shanghai, Guizhou, and so on.

**WAsP models:** WAsP is a PC-program for the vertical and horizontal extrapolation of wind climate statistics. It contains several models to describe the wind flow over different terrains and close to sheltering obstacles. Conceptually, WAsP consists of five main calculation blocks (Niels G. Mortensen et al., 2007).

**Analysis of raw data:** This option enables an analysis of any time-series of wind measurements to provide a statistical summary of the observed, site-specific wind climate. This part is implemented in separate software tools: The Observed Wind Climate (OWC) Wizard and the WAsP Climate Analyst. Generation of wind atlas data: Analyzed wind data can be converted into a regional wind climate or wind atlas data set. In a wind atlas data set the wind observations have been 'cleaned' with respect to site-specific conditions. The wind atlas data sets are site-independent and the wind distributions have been reduced to some standard conditions.

**Wind climate estimation.** Using a wind atlas data set calculated by WAsP or one obtained from another source – e.g. the European Wind Atlas – the program can estimate the wind climate at any specific point by performing the inverse calculation as is used to generate a wind atlas. By introducing descriptions of the terrain around the predicted site, the models can predict the actual, expected wind climate at this site.

#### Estimation of wind power potential:

The total energy content of the mean wind is calculated by WAsP. Furthermore, an estimate of the actual, annual mean energy production of a wind turbine can be obtained by providing WAsP with the power curve of the wind turbine in question.

The Figure 3 to the right is a schematic presentation of the wind atlas methodology of WAsP.

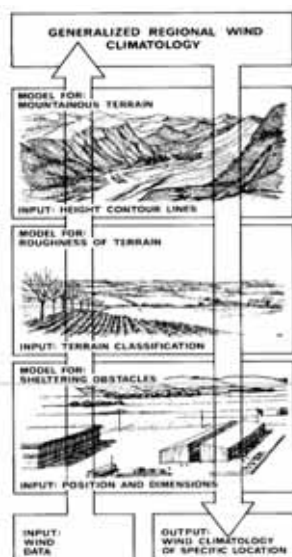


**FIGURE 3**

**The WAsP models and the wind atlas methodology (European Wind Atlas)**

In the analysis part (up arrow), the meteorological models are used to calculate the regional wind climatology from the raw or observed wind data.

In the reverse process - the application of wind atlas data (down arrow)-the wind climate at any specific site may be calculated from the regional climatology (Troen and Petersen 1989).

In general terms, accurate predictions using the WAsP program may be obtained (Bowen and Mortensen 1996) provided:

- 1) the reference site (meteorological station) and predicted site (wind turbine site or met. station) are subject to the same overall weather regime,
- 2) the prevailing weather conditions are close to being neutrally stable,
- 3) the reference wind data are reliable,
- 4) the surrounding terrain (of both sites) is sufficiently gentle and smooth to ensure mostly attached flows, and the topographical model inputs are adequate and reliable.

#### The required conditions for WAsP run.

**The wind data from the meteorological stations.** The data for this study are collected from NOAA National Climatic Data Center (NCDC.<http://www.noaa.gov/>). For this study, twenty-seven state-stations (Figure 4) monitored by the meteorological department have produced 15 years' worth of hourly and daily wind data. Each of the meteorological stations of the NCDC is based on a 10m tower and has the following components: five wind speed cup-type sensors at 2, 4, 6, 8 and 10m heights to derive the wind speed profile; one wind direction vane-type sensor at 10m height; one solar radiation sensor (pyrometer) with uncertainty  $\pm 5\%$ .

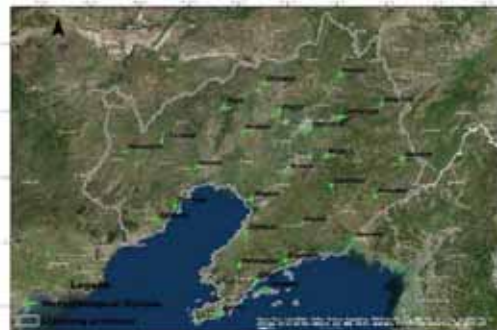


**FIGURE 4**

**A map of Meteorological station locations  
A contour map of the area**

The detailed surface features based on aerial photography conducted by the National Remote Sensing Agency in the year 2015 were available as 2x2 km<sup>2</sup> tiles in the AutoCAD dwg format. These files provide contours at 5m intervals, trees, buildings, temples, tombs, electricity and telegraph poles, waterways, marshy areas, roads, footpaths etc., in different layers. Information relevant to WAsP, namely

**TABLE 1**  
**Data from long-term observations in Liaoning**

Number	Station Name	Longitude	Latitude	Height above sea level, m
210922	Zhangwu	122.5333	42.4167	79
210901	Fuxin	121.7167	42.0833	167
211282	Kaiyuan	124.05	42.5333	98
210423	Qingyuan	124.9167	42.1	237
211301	Chaoyang	120.45	41.55	170
211322	Yemaishou	119.7	41.3833	422
210181	Xinmin	122.8333	41.9833	31
210726	Heishan	122.0833	41.6833	38
210701	Jinzhou	121.1167	41.1333	66
210301	Anshan	123	41.0833	77
210101	Shenyang	123.45	41.7333	45
210501	Benxi	123.7833	41.3167	185
210421	Zhangdang	124.0833	41.9167	119
210522	Huanren	125.35	41.2667	240
211481	Suizhong	120.35	40.35	15
211481	Xincheng	120.7	40.5833	9
210801	Yingkou	122.2667	40.6667	3
210881	Xiongyue	122.15	40.1667	20
210521	Caohekou	123.9	40.8833	233
210323	Xiuyan	123.2833	40.2833	80
210624	Kuandian	124.7833	40.7167	260
210601	Dandong	124.3333	40.05	14
210281	Wafangdian	122.0167	39.6333	119
210282	Pikou	122.3667	39.4167	43
210224	Changhai	122.5833	39.2667	36
210283	Zhuanghe	122.95	39.7167	35
210201	Dalian	121.6333	38.9	92

contours, open areas, farmlands, water bodies and urban and semi-urban areas, was retained by switching off the unwanted layers. Such tiles were joined together in the AutoCAD software and saved as dxf files (drawing exchange format), which could be imported into the Wasp Map Editor. In this study, contour intervals at 5m were retained and imported into the Wasp Map Editor for calculating the wind energy density throughout the area. The map was transformed to the Universal Transverse Mercator (UTM) projection with the datum of WGS 1984. The reasonably smooth contour lines as shown in Figure5.

**A simple description of the land use in the area.** Areas representing water bodies, forest land, cultivated land and semi-urban areas were marked and assigned roughness values as defined by WASP and given in Table 2. The wind monitoring station was marked on the vector map using its WGS 1984 coordinates. With reference to the wind monitoring station, nearby buildings and other obstructions were plotted using the utility

available for that purpose in WASP.



**FIGURE 5**  
**Digitized vector map of the area with 5 m contour intervals**

**The zooming grid.** WASP utilizes the 'BZ-model' of Troen (1989) to calculate the wind velocity perturbations induced by orographic features such as single hills or more complex terrain. The BZ-model belongs to a family of models related to the Jackson and Hunt theory for flow over hills (Jackson and Hunt 1975; Taylor, P.A and Teunissen, H.W 1987). The model was developed with the specific purpose of detailed wind energy siting in mind and has the following general features:

**TABLE 2**  
**Roughness class and terrain surface characteristics**

z0 (m)	Terrain surface characteristics	Roughness Class
1	city	
0.8	forest	
0.5	suburbs	
0.4		3 (0.40 m)
0.3	shelter belts	
0.2	many trees and/or bushes	
0.1	farmland with closed appearance	2 (0.10 m)
0.05	farmland with open appearance	
0.03	farmland with very few buildings/trees	1 (0.03 m)
0.02	airport areas with buildings and trees	
0.01	airport runway areas	
0.008	mown grass	
0.005	bare soil (smooth)	
0.001	snow surfaces (smooth)	
0.0003	sand surfaces (smooth)	
0.0002		0(0.0002 m)
0.0001	water areas (lakes, fjords, open sea)	

1)It employs a high-resolution, zooming, polar grid. This is coupled with a map analysis routine in order to calculate the potential flow perturbation profile at the central point of the model.

2)It integrates the roughness conditions of the terrain surface into the spectral or scale decomposition. The 'inner-layer' structure is calculated using a balance condition between surface stress, advection and the pressure gradient.

3)It uses an atmospheric boundary layer thickness of approx. 1 km to force the large scale (say, more than a few kilometers) flow around high-elevation areas.

The zooming grid of the BZ-model is illustrated in the Figure 6 below. A 25 by 25 sq. km section of Waspdale is shown in the upper left-hand corner of the Figure. The grid is centered at the WECS site on Beeverly Hill and has a radius of about 27 km. The BZ-model examines all the grid points shown when estimating the wind conditions at the hill site. In the upper right-hand corner, a closer view of the same site and grid is shown, covering an area of 5 by 5 sq. km. Still closer, the drawing in the lower left-hand corner covers an area of about 1 sq. km. Finally, the center of the grid is shown in the lower right-hand corner of the Figure; this covers

approximately 200 by 200 sq. m. The grid resolution at the center of the model is 4 m.

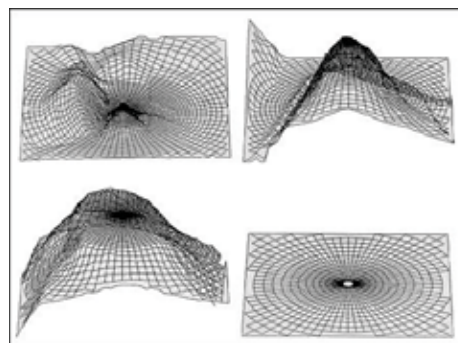


**FIGURE 6**

**A map of the zooming grid of the BZ-model**

**Obstacle model.** Shelter is defined as the relative decrease in wind speed caused by an obstacle in the terrain. Whether an obstacle provides shelter at the specific site depends upon:

- 1) the distance from the obstacle to the site ( $x$ )
- 2) the height of the obstacle ( $h$ )
- 3) the height of the point of interest at the site ( $H$ )
- 4) the length of the obstacle ( $L$ )
- 5) the porosity of the obstacle ( $P$ )

The reduction of wind speed due to shelter from an infinitely long two-dimensional obstacle of zero porosity is shown below. The

Figure 7 is based on the expressions given by Perera (1981).

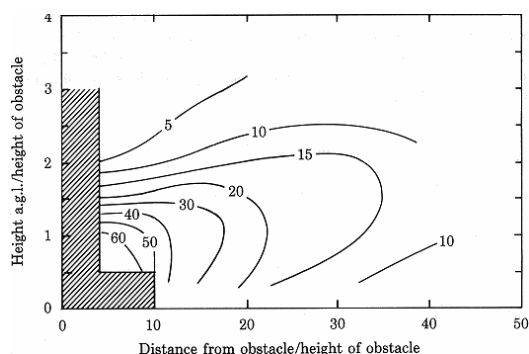


**FIGURE 7**  
A map of wind speed reduction due to the obstacles

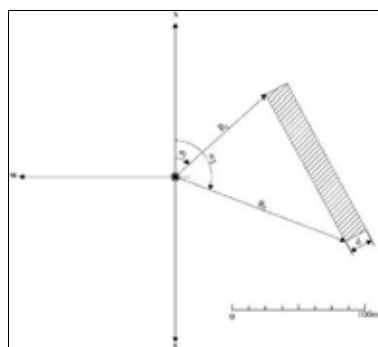


**FIGURE 8**  
Parameters for specifying an obstacle in WASP

**TABLE 3**  
Notations used for specifying the position of obstacles

Symbol	Angles
$\alpha_1$	angle from N to first corner [°]
$R_1$	radial distance to first corner [m]
$\alpha_2$	angle from N to second corner [°]
$R_2$	radial distance to second corner [m]
$h$	height of obstacle [m]
$d$	depth of obstacle [m]
$P$	estimated porosity (fraction 0-1)

**Specifying obstacles.** Obstacles are considered by WASP as 'boxes' with a rectangular cross-section and footprint. Each obstacle must be specified by its position relative to the site, its dimensions and must be assigned a porosity. The Figure below defines

the quantities that specify a single obstacle and that must be input to WASP; the '\*' marks the position of the site. Obstacles are thus specified relative to a specific site and are not linked directly to the topographic map. Angles are measured from 0° (north) to 360° clockwise, corresponding to bearings taken with a compass. Distances are measured in meters.

**Energy extraction from wind.** A column of wind upstream of the turbine with cross-sectional area  $A_1$  of turbine disc, has kinetic energy passing per unit time given by

$$P_0 = 1/2(\rho \times A_1 \times u_0^3) \quad (1)$$

Where  $\rho$  is the air density in kg/m<sup>3</sup>, and  $u_0$  the unperturbed wind speed in m/s. Air density  $\rho$  is a function of height above mean sea level and the prevailing meteorological conditions. Wind speed generally increases with height and is affected by local topography and varies greatly with time. However, only about half the power available in the wind can be extracted because it has to have sufficient energy to leave the turbine region. Therefore, the power extracted by the turbine  $P_T$  is given by

$$P_T = C_p P_0 \quad (2)$$

Where  $P_0$  is the power in the unperturbed wind and  $C_p$  is the fraction of power extracted or the power coefficient. The criterion for maximum power extraction is called the Betz criterion and is applicable to all turbines in an extended fluid stream.

Standard meteorological wind data are regularly collected by the India Meteorological Department at the standard height of 10 m near airports and towns for weather prediction and civil aviation requirements. Meteorological aspects of utilization of wind for the extraction of power have been well documented (World Meteorological Organization 1981). The usefulness of such data is limited to provide first-order estimates of wind power but is inadequate to carry out detailed planning for the installation of wind turbines for power generation. Careful and detailed measurements around a prospective site are needed at several locations and at different heights for several months to a year to carry out analysis and estimate the wind power availability at the hub height of the proposed wind turbine. It is



generally accepted that sites with an average wind speed of 8 m/s or more could be considered prospective. It is also necessary with match the machine characteristics to the prevailing wind regime for optimum power generation.

## RESULTS

**Wind Speed and Wind Power Density Estimations.** This study uses the software WAsP to estimate the land wind energy potential in Liaoning. The simulation areas include the whole domain in Liaoning. The WAsP simulation focuses on wind speed at 10m. The wind direction is mainly south, north and light northerly in whole domain Liaoning. The most frequent wind direction is mainly south and south by southwest in the central region, north in southern and southwest Liaoning.

In terms of wind speed, the annual mean wind speed at 10 m is greater than 3.5m/s in the coastal areas, Liaodong peninsula, midland, and northern plain areas in Liaoning. Some areas have higher speeds of approximately 4.0 m/s such as Panjin, Lushun, Dalian, and so on. The annual mean wind speed at 10 m is approximately 2.0 m/s in the eastern mountain area and the western foothills in Liaoning, and some areas are lower than 2.0 m/s. The results are shown in Figure 9.



**FIGURE 9**  
Distribution of yearly mean wind speed for 2000~2015 in Liaoning province

Wind power density is one of the important indices for evaluating a regional wind energy resources. Wind power density at 10 m in the Liaoning is approximately 9.9–130.7 W/m<sup>2</sup>, Wind power density is higher

than 100W/m<sup>2</sup> in the northern, central, Liaodong peninsula south end, on the island of Liaoning province. Wind power density is lower than 50W/m<sup>2</sup> in the eastern and western parts of Liaoning province. The results are shown in Figure 10.

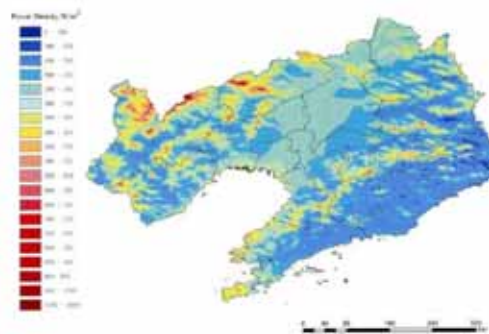


**FIGURE 10**  
Power Density in Liaoning province

**Available mean wind hours.** Available mean wind hours are 1368~ 6400 h when wind speed is in the range from 3.0 to 25.0 m/s in Liaoning, central and Liaodong peninsula is more than 4000, the eastern coast of northern liaodong bay, and a central narrow strip – stretching from north of liaodong bay available mean wind hours is more than 4500. Dalian, Chinghai, Lushun is more than 6000 h, the wind resource available close to the time of a year's 70%. Available mean wind hours are shown in Figure 11.



**FIGURE 11**  
Available mean wind hours in Liaoning province

**Wind energy reserves.** The district covers a land area of 148100 km<sup>2</sup> in Liaoning province. According to the existing data of provincial annual average, wind power density

is greater than 150 W/m<sup>2</sup> areas are about 2100 km<sup>2</sup>, which is mainly distributed in the hills of northern and close to the coast in Liaoning province; 100 ~ 150 W/m<sup>2</sup> areas are about 5900 km<sup>2</sup>, which is mainly distributed in the coastal plain and median plain; 50 ~ 100 W/m<sup>2</sup> areas are about 77100 km<sup>2</sup>, which is mainly distributed in the coastal areas and the central plains; annual average wind power density are under 50 W/m<sup>2</sup> in the eastern and western of Liaoning, and covers areas are about 63000 km<sup>2</sup>. Total wind energy reserves in the land area are 89206.3MW at 10m height. According to the entire province average wind power density, exploitation areas and capacity, with all the technology ingredients and wind power density is greater than 150 W/m<sup>2</sup>, are respectively 2100 km<sup>2</sup> and 2515.1 MW. Wind energy resources in Liaoning province's total detailed in table 3.

**TABLE 3**  
**Wind energy reserves in Liaoning**

Power Density, W/m <sup>2</sup>	Area, km <sup>2</sup>	Reserves, MW
< 50	63000	22096.5
50 ~100	77100	56590.3
100 ~150	5900	7315.5
150 ~200	2100	3204.0
> 200	0.00	0.00
Total	148100	89206.3

**The status of development of wind energy in Liaoning.** Began in the 1980s, Liaoning province had carried out up-front work on exploitation, utilization, census and the corresponding measurement of wind resources. The first Wind farm has been built in changing island town, wafangdian city in 1992. By the end of September 2015, the province has built 144 Wind farms, with a total installed capacity of 8042.85 MW, 5362 wind turbines. Total generating capacity is 1916.2 million kW·h/yr.

**Analysis of CDM (Clean Development Mechanism).** The Wind farms will not only supply renewable electricity to grid, but also contribute to sustainable development of the local community, the host country and the world by means of:

1)The operation of the proposed project will increase local revenues and promote local economy;

2)The proposed project will not only reduce GHG emission but also mitigate local environment pollution caused by pollutant emission from coal-fired power plants;

3)Creation of permanent and temporary employment opportunity for the local residents;

4)The operation of the proposed project will regulate local energy source composition by increasing renewable energy.

By the end of September 2015, fifty-eight Wind farms have got the Clean Development Mechanism (CDM) certification in Liaoning (<http://cdm.unfccc.int/>).

Emission reductions from all Wind farms in Liaoning can be calculated based on the ACM0002“Consolidated baseline methodology for grid-connected electricity generation from renewable sources” (Version 12.2.0.

<http://cdm.ccchina.gov.cn/list.aspx?clmId=20>) and the methodological tool “Tool to calculate the emission factor for an electricity system” (Version 02.2). According to ACM0002 (Version 12.2.0), it is required to estimate the Operating Margin (OM) and Build Margin (BM) emission factor ex-ante, and through weighted average of OM and BM, the Combined Margin baseline emission factor of NECPG can be obtained and then the emission reductions from CDM project activity can be estimated. For more information regarding the methodology and the tools as well as their consideration by the Executive Board, please refer

to:<http://cdm.unfccc.int/methodologies/PAmethodologies/approved.html>.

The details are shown below:

Baseline emissions include only CO<sub>2</sub> emissions from electricity generation in fossil fuel fired power plants that are displaced due to the project activity, calculated as follows:

$$BE_y = EG_{pj, y} \times EF_{Grid, CM, y} \quad (3)$$

Where:

$BE_y$ : Baseline emissions in year  $y$  (tCO<sub>2</sub>/yr);

$EG_{pj, y}$ : Quantity of net electricity generation that is produced and fed into the grid as a result of the implementation of the

CDM project activity in year  $y$  (MWh/yr);

$EF_{grid, CM, y}$ : Combined Margin CO<sub>2</sub> emission factor for NECPG in year  $y$  calculated using the latest version of the “Tool to calculate the emission factor for an electricity system” (Version 02.2) (tCO<sub>2</sub>/MWh);

The following is the process of calculating the baseline CO<sub>2</sub> emission of the grid, according to the steps provided by the approved baseline methodology ACM002 (Version 12.2.0).

$$EG_{PI, y} = EG_{facility, y} \quad (4)$$

$EG_{PI, y}$ : Quantity of net electricity generation that is produced and fed into the grid as a result of the implementation of the CDM project activity in year  $y$  (MWh/yr);

$EG_{facility, y}$ : The methodological tool “Tool to calculate the emission factor for an electricity system” (Version 02.2) determines the CO<sub>2</sub> emission factor for the displacement of electricity generated by power plants in NECPG, by calculating the “operating margin” (OM) and “build margin” (BM) as well as the “combined margin” (CM). The operating margin refers to a cohort of power plants that reflect the existing power plants whose electricity generation would be affected by the proposed CDM project activity. The build margin refers to a cohort of power units that reflect the type of power units whose construction would be affected by the proposed CDM project activity.

The proposed project uses method (a): Weighted average CM to calculate the combined margin emission factor, as follows:

$$EF_{grid, CM, y} = EF_{grid, OM, y} \times w_{OM} + EF_{grid, BM, y} \times w_{BM} \quad (5)$$

Where:

$EF_{grid, CM, y}$ : Baseline emission factor (tCO<sub>2</sub>e / MWh);

$EF_{grid, OM, y}$ : Operational Margin emission factor (tCO<sub>2</sub>/MWh);

$EF_{grid, BM, y}$ : Build margin CO<sub>2</sub> emission factor in year  $y$  (t CO<sub>2</sub>/MWh);

$w_{OM}$ : Weighting of operating margin emissions factor (%);

$w_{BM}$ : Weighting of build margin emissions factor (%).

The baseline emission factor  $EF_{grid, CM, y}$  should be calculated as the weighted average of the Operating Margin emission factor ( $EF_{grid,$

$OM, y$ ) and the Build Margin emission factor ( $EF_{grid, BM, y}$ ), where the weight of Operating Margin,  $w_{OM}$  is 0.75 and Build Margin,  $w_{BM}$  is 0.25 by default.

The combined baseline emission factor of the NECPG is:

$$EF_{grid, CM, y} = 1.1293 \text{ tCO}_2/\text{MWh} \times 0.75 + 0.7242 \text{ tCO}_2/\text{MWh} \times 0.25 = 1.028025 \text{ tCO}_2\text{e}/\text{MWh}.$$

$$BE_y (\text{all Wind farms in Liaoning}) = 19161659.4 \times 1.028025 = 19698664.9 \text{ tCO}_2\text{e}.$$

The all Wind farms in Liaoning will help reduce greenhouse gas (GHG) emissions generated from the high-growth, coal-dominated electricity generation in Northeast China Power Grid (NECPG). When all Wind farms is operated, the electricity generated by electricity will displace part of the electricity from the NECPG, and thus GHG (CO<sub>2</sub>) generated by coal-fired power plants could be reduced. The annual power generation is estimated to be 19161659.4MWh. The estimated annual GHG emission reductions are 19698664.9tCO<sub>2</sub>.

**Analysis of air pollutants emission reductions.** Wind farms are known to contribute to zero air pollutants as no fuel combustion is involved during any stage of the operation. The sources of air pollution are mainly due to the construction activities including the transportation of construction material, road construction and improvement etc. The impacts on air environment will be ended when the construction is completed. Several measures shall be taken into account, such as prohibiting the construction under strong wind weather, reducing as much as possible the area of construction, spraying water when undertaking construction, and reducing the speed of vehicles in the field. Hence, air pollution caused by the proposed project is not significant to the surrounding environment.

The calculation of environmental benefits is one of the important contents of environmental impact for wind farm. Due to lack of definite technical specification, the common calculation method of taking thermal power as comparative object is adopted. However, it is difficult to judge and compare identically because of large number of calculation parameters and wide value range,

and some differences exist among different results. Therefore, we propose a simplified calculation method only related to comprehensive coal consumption and pollutant discharge rate, so as to effectively standardize and quickly calculate the environmental benefits of wind power project.

Thermal power creates mainly pollutants, SO<sub>2</sub> and NO<sub>x</sub>, wind farms are known to contribute to zero atmospheric pollution as no fuel combustion is involved during any stage of the operation. Wind farms replace coal consumption which will reduce pollutants emission. Pollutants emission to calculate is as follows:

**SO<sub>2</sub> emission reduction.** SO<sub>2</sub> emission reduction is calculated according to coal consumption used in electricity production electricity. Computing method is from “Detailed rules for checking and accounting total emission reduction during twelfth five-year plan” ([http://www.zhb.gov.cn/gkml/hbb/bwj/201206/t20120605\\_230944.htm](http://www.zhb.gov.cn/gkml/hbb/bwj/201206/t20120605_230944.htm)). Calculation formulas is as follows:

$$E_{SO_2} = M \times S \times A \times (1 - \eta_{SO_2}) \times 10^4 \quad (6)$$

Where:

$E_{SO_2}$ : SO<sub>2</sub> emission (t)

$M$ : coal consumption (t)

$S$ : average sulfur content by weight, 0.6%

$A$ : convert ratio into air, 0.8%

$\eta_{SO_2}$ : desulfurization efficiency, 90%

Relationship between coal consumption and power generation is:

$$M_i = \beta \times P \quad (7)$$

Where:

$B$ : a coefficient of relationship between coal consumption and power generation, 300g/kWh

$P$ : power generation, kWh.

The annual power generation is estimated to be 19161659.4 MWh. The estimated annual SO<sub>2</sub> emission reductions are:

$$E_{SO_2} = 2 \times 19161659.4 \times 1000 \times 300 \times 80\% \times 0.6\% \times (1 - 90\%) = 5513.3 \text{ tSO}_2$$

The estimated annual SO<sub>2</sub> emission reductions are 5513.3tSO<sub>2</sub>.

**NO<sub>x</sub> emission reduction.** NO<sub>x</sub> emission reduction is calculated according to coal consumption used in electricity production electricity. Computing method is from “Detailed rules for checking and accounting

total emission reduction during twelfth five-year plan” ([http://www.zhb.gov.cn/gkml/hbb/bwj/201206/t20120605\\_230944.htm](http://www.zhb.gov.cn/gkml/hbb/bwj/201206/t20120605_230944.htm)). Calculation formulas is as follows:

$$E_{NOX} = M \times P_f \times (1 - \eta_{NOX}) \times 10 \quad (8)$$

Where:

$E_{NOX}$ : NO<sub>x</sub> emission (t)

$M$ : coal consumption (t)

$P_f$ : source intensity of NO<sub>x</sub> emission, 2.7kg (NO<sub>x</sub>) / t (coal)

$\eta_{NOX}$ : denitration efficiency, 90%

$$E_{NOX} = 19161659.4 \times 1000 \times 300 / 1000 \times 2.7 \times (1 - 60\%) / 1000 = 6053.3 \text{ t NO}_x$$

The estimated annual NO<sub>x</sub> emission reductions are 6053.3t.

### Impact on Ecosystem Environment.

The impact on ecosystem environment mainly caused during construction period, so the attention should be given regarding the landscape resource protection and recovery (Ilhami Kiziroglu and Ali Erdogan 2015). Damage to the vegetation caused by permanent land occupation of the wind turbine will be compensated correspondingly. In other words, vegetation with equal area and quality to the damaged will be recovered in another place. (Li, et al., 2016)

## DISCUSSION

In this work, mean wind speeds from several wind flow modeling methodologies were examined and compared to observational mean wind speed measurements from several 10 m met towers distributed across the study area.

The present article describes WASP for quantifying the wind conditions and energy potential of large areas based on several years of high resolution in-site measurements (in multiple points), adjusted for long-term reliability using meteorological stations. After quality assessment, the in-situ measured data were analyzed and adjusted to long-term reference using a mathematical process (Wind Atlas Method) which is able to transfer long-term data from a reference station nearby into the characteristic conditions at the study site, taking into consideration the orography, roughness and obstacles which are influencing

the wind flows in the area. The newly obtained long-term wind statistics, comprising sector wise Weibull distribution, mean wind speed, frequency of wind direction and wind energy distribution, were transformed into wind speed and energy maps, which were further used for the characterization of the wind energy potential within the location of interest.

Meanwhile, we introduce the situation of wind farm construction in Liaoning province. The first Wind farm has been built in changing island town, wafangdian city in 1992. By the end of September 2015, the province has built 144 Wind farms, with a total installed capacity of 8042.85 MW, 5362 wind turbines. Total generating capacity is 1916.2 million kW•h/yr.

By the end of September 2015, fifty-eight wind farms have got the Clean Development Mechanism (CDM) certification in Liaoning. The all wind farms in Liaoning will help reduce greenhouse gas (GHG) emissions generated from the high-growth, coal-dominated electricity generation in Northeast China Power Grid (NECPG). When all Wind farms is operated, the electricity generated by electricity will displace part of the electricity from the NECPG, and thus GHG (CO<sub>2</sub>) generated by coal-fired power plants could be reduced. The annual power generation is estimated to be 19161659. 4MWh. Wind farm are known to contribute to zero air pollutants as no fuel combustion is involved during any stage of the operation. Thermal power creates mainly pollutants is SO<sub>2</sub> and NO<sub>x</sub>. Wind farms are known to contribute to zero atmospheric pollution as no fuel combustion is involved during any stage of the operation. Wind farms replace coal consumption which will reduce pollutants emission. The estimated annual SO<sub>2</sub> emission reductions are 5513.3 t. The estimated annual NO<sub>x</sub> emission reductions are 6053.3t.

The impact on ecosystem environment mainly caused during construction period, so the attention should be given regarding the landscape resource protection and recovery. Damage to the vegetation caused by permanent land occupation of the wind turbine will be compensated correspondingly. In other words, vegetation with equal area and quality to the damaged will be recovered in another place.

## REFERENCES

- [1] Ayotte, K. (2008) Computational modelling for wind energy assessment. *J. Wind Eng. Ind. Aerodyn*, 96, 1571–1590
- [2] Bing Xue, Zhixiao Ma, Yong Geng, Peter Heck, Wanxia Ren, Mario Tobias, Achim Maas, Ping Jiang, Jose A. Puppim de Oliveira, Tsuyoshi Fujita. (2015) A life cycle co-benefits assessment of wind power in China. *Renewable and Sustainable Energy Reviews*, 1, 338–346
- [3] Troen, I., & Petersen, E.L. (1988). *European Wind Atlas*, Risø National Laboratory, Denmark.
- [4] Landberg, L.; Myllerup, L. Rathmann, O.; Petersen, E.L.; Jørgensen, B.H.; Badger, J.; Mortensen, N.G. (2003) Wind resource estimation—An overview. *Wind Energy*, 6, 261–271.
- [5] Troen, I.; Petersen, E.L. (1989). *European Wind Atlas*; Risø National Laboratory, Roskilde, Denmark.
- [6] Mortensen, N.G. (2004) *Wind atlas analysis and application programme (WASP)*. 2nd ed. Roskilde, Denmark, Riso National Laboratory, Riso-1-1950
- [7] Mortensen, N.G. and Peterson, E.L. (1997) *Wind energy and atmospheric physics*. European Wind Energy Conference and Exhibition, Dublin, Ireland.
- [8] Niels G. Mortensen, Duncan N., Heathfield, Lisbeth Myllerup, Lars Landberg and Ole Rathmann. (2007) *Getting Started with WASP 9*. Risø National Laboratory: Roskilde, Denmark.
- [9] Jackson, P.S.; Hunt, J.C.R. (1975) turbulent wind flow over a low hill. *Q. J. R. Meteorol. Soc.*, 101, 929–955.
- [10] Taylor, P.A.; Teunissen, H.W. (1987). *The Askervein Hill project: Overview and background data*. *Bound. Layer Meteorol.*, 39, 15–39.
- [11] Bowen, A. J. and Mortensen, N. G. (1996) *Exploring the Limits of WASP: The Wind Atlas Analysis and Application Program*. European Union Wind Energy Conference, 20–24, Goteborg, Sweden.
- [12] Zhidong Li, Fan Zhang, Guobao Song. (2016) *The Evaluative Study of Ecological Suitability of Wind Power Development Planning*. *Fresen. Environ. Bull.*, 25(6): 2063-2070



---

**Received: 02.02.2016**

**Accepted: 07.08.2016**

---

**CORRESPONDING AUTHOR**

---

**Shushen Zhang**

Key Laboratory of Industrial Ecology and Environmental Engineering (MOE), School of Environmental Science and Technology, Dalian University of Technology, Linggong Road 2, 116024 Dalian, People's Republic of China

Email: laephd@163.com

# REMOVAL OF Pb<sup>2+</sup> AND Cd<sup>2+</sup> FROM AQUEOUS SOLUTIONS BY CHEMICALLY MODIFIED CELLULOSE OF CASSAVA WASTE

Zhang Luo, Shengxu Luo\*, Cheng Niu, Shanhu Hu, Linqian Chen, Chunlei Fan

Key Laboratory of Tropical Biological Resources for Ministry of Education, College of Materials and Chemical Engineering, Hainan University, Haikou 570228, China

## ABSTRACT

This study investigated a novel cellulose-based heavy metals chelating material derived from cassava waste. The first part describes how the cellulose of cassava waste was extracted by the orthogonal experiment and optimization, followed by chemical modifications with succinic anhydride and polyamine to introduce carboxylic and amide functions, respectively. The obtained materials were characterized by FTIR and SEM. In the second part, the adsorption capacity of three different types of modified cellulose of cassava waste (MCCW) was evaluated by kinetic study, effect of pH, adsorption isotherms and regeneration studies. The adsorption equilibrium of MCCW 2, regarded as a promising adsorbent, was reached within 20 min for Pb<sup>2+</sup> and 30 min for Cd<sup>2+</sup>, and the calculated maximum adsorption capacity was 476.19 mg g<sup>-1</sup> for Pb<sup>2+</sup> and 289.02 mg g<sup>-1</sup> for Cd<sup>2+</sup> on MCCW 2. The adsorption process was described well by Pseudo-second-order and Langmuir model. Regeneration studies indicated that the adsorption efficiencies of MCCW 2 could still be maintained at 97.40% level for Pb<sup>2+</sup> and 93.16% level for Cd<sup>2+</sup> even after three cycles.

## KEYWORDS:

modified cellulose of cassava waste; chelating material; heavy metals; adsorption; regeneration

## INTRODUCTION

With the development of the modern industry, water contamination of heavy metal ions has become a serious global environmental problem. Lead (Pb) causes kidney and liver diseases, brain damage and toxicity to the reproductive system [1, 2]. Cadmium (Cd) causes lung failure, hypertension, bone lesions, renal dysfunction and cancer [3, 4]. Therefore, it is important to reduce or eliminate these heavy metals from industrial effluent in order to protect public health. In recent years, various techniques and methods were employed to remove the heavy metal ions from waste-water, such as ion exchange, chemical precipitation, membrane separation,

coagulation, electrolytic reduction and adsorption [5, 6]. Among these, adsorption has been proved as a very flexible, effective and economical method to remove heavy metal ions from waste-water [7]. Some artificial and natural materials, such as metal oxides, copolymer hydrogel, nanomaterials [8], biosorbents [9, 10], clay minerals [11] and surficial sediments [12], are reviewed as adsorbents to remove heavy metal ions from waste-water [13].

Cellulose, a natural polymer, is a renewable, cheap and biodegradable natural resource [14, 15]. Notably, cellulose can bind heavy metal ions because of the existence of abundant –OH groups [16]. And it has outstanding adsorption efficiency with appropriate chemical modification [17]. Cassava waste is abundant agricultural waste worldwide and it contains high levels of cellulose [18], which can reach 60%-70% by a series of extraction and optimization. Chemical modification has been successfully used to modify some agricultural wastes such as corn stalks [19], loofah fibers [20], corn-cob [21], sunflower stalks [22], sugarcane bagasse [23], rice husk [24], wheat Straw [25] and banana [26]. However, only a few have reported on the modification of cassava waste. Horsfall et al [27] have reported that modified cassava peelings waste with mercaptoacetic acid (MAA) shows maximum adsorption capacity of 127.3 mg g<sup>-1</sup> Cu<sup>2+</sup> and 119.6 mg g<sup>-1</sup> Cd<sup>2+</sup>.

To the best of our knowledge, high content cellulose of cassava waste was modified with succinic anhydride and polyamine to adsorb heavy metals in aqueous solution, which has rarely reported. Then, saturated sodium hydrogen carbonate was rarely reported as a detergent in regeneration studies, and detergent reported in the literatures and patents was usually distilled water [28] and sodium hydroxide [13].

In this study, we describe how the cellulose of cassava waste was extracted by the orthogonal experiment and optimization, followed by chemical modifications with succinic anhydride and polyamine to introduce carboxylic and amide functions, respectively. The adsorption capacity of three different types of modified cellulose of cassava waste (MCCW) was subsequently evaluated by kinetic study, effect of pH, adsorption isotherms and

regeneration studies. Finally, the mechanism of adsorption was analyzed by the pseudo-second-order kinetic model, Langmuir model and Freundlich model.

## MATERIALS AND METHODS

**Materials.** The cassava waste was provided by Hainan province of China. Succinic anhydride, 1,3-diisopropylcarbodiimide (DIC), sodium hydroxide (NaOH), sodium hydrogen carbonate (NaHCO<sub>3</sub>), Pb(NO<sub>3</sub>)<sub>2</sub>, Cd(NO<sub>3</sub>)<sub>2</sub>·4H<sub>2</sub>O and nitric acid, from local chemical suppliers, were used without further purification. Ethylenediamine, triethylenetetramine, N,N-dimethylformamide (DMF) and pyridine was added to activated molecular sieves overnight to remove water.

### Extraction of Cellulose from Cassava Waste.

Pretreatment of raw material: the cassava waste was washed in ultrapure water several times to remove the impurity and soluble substances, and then dried in an oven at 80 °C for 8 h. After that, the resulting material was sieved with 40 meshes and kept in a desiccator overnight.

The main extraction process: 10.00 g pretreated cassava waste was suspended in 60 mL ultrapure water and boiled for 5 min to completely gelatinize starch of cassava waste. Then 100 mL alpha-amylase with a certain concentration was added, and the enzymatic process was carried out under a certain power of ultrasound generator (XO-5200DTS, Nanjing Ultrasound Instrument Co., Ltd.) at 60 °C. Afterwards, the clear liquid above was discarded after enzyme deactivation (100 °C, 5 min) and centrifugation (4000 r/min, 20 min). 100 mL NaOH solution with a certain concentration was added into the remaining solid, and the alkaline hydrolysis process was implemented at 70 °C. Finally, the purified cellulose was filtered, washed, dried (65 °C, 8 h) and sieved with 40 meshes.

**Synthesis of MCCW 1 and MCCW 2.** Dried and grated cellulose of cassava waste (5.02 g) and succinic anhydride (12.56 g) were suspended in 120 mL anhydrous pyridine reflux for 18 h. After filtration, the obtained new celluloses (MCCW 1) were washed with 1 mol L<sup>-1</sup> solution of acetic acid (CH<sub>3</sub>COOH) in CH<sub>2</sub>Cl<sub>2</sub>, 0.1 mol L<sup>-1</sup> solution of hydrochloric acid (HCl), ethanol 95%, ultrapure water, and at last with ethanol 95%, sequentially [29]. And then it was dried at 80 °C for 3 h and left in a desiccator overnight. MCCW 1 (9.4446 g) with a mass increment of 88.14% was obtained. MCCW 2 was synthesized by treatment of MCCW 1 (2.8 g) with 250 mL saturated NaHCO<sub>3</sub> solution for 30 min under stirring. Afterwards, the modified product (MCCW 2) was filtered and washed with ultrapure

water and ethanol. Then, it was dried at 80 °C for 3 h and left in a desiccator overnight. MCCW 2 (3.0970 g) with a mass increment of 10.61% was obtained.

### Synthesis of MCCW 3 and MCCW 4.

MCCW 3 was synthesized by treatment of MCCW 1 (2.8 g) with 4.05 mL ethylenediamine and 7.85 mL 1,3-diisopropylcarbodiimide (DIC) in 60 mL anhydrous DMF under constant stirring and a nitrogen atmosphere for 22 h at room temperature. After the reaction, the solid materials (MCCW 3) were filtered and washed with DMF, saturated sodium bicarbonate solution, ultrapure water, and at last with ethanol 95%, sequentially. Finally, it was dried at 80 °C for 3 h and left in a desiccator overnight, MCCW 3 (3.1246 g) with a mass gain of 11.59% was obtained.

MCCW 4 was synthesized by treatment of MCCW 1 (2.8 g) with 12.75 mL triethylenetetramine and 7.85 mL 1,3-diisopropylcarbodiimide (DIC) in 60 mL anhydrous DMF under constant stirring and a nitrogen atmosphere for 22 h at room temperature. After the reaction, the solid materials (MCCW 4) were filtered and washed with DMF, saturated sodium bicarbonate solution, ultrapure water, and at last with ethanol 95%, sequentially. Finally, it was dried at 80 °C for 3 h and left in a desiccator overnight, MCCW 4 (3.1821 g) with a mass gain of 13.64% was obtained.

### Kinetic Study of Metal Ion Adsorption of MCCW 2, MCCW 3 and MCCW 4.

50.0 mg of adsorbent was put into the Erlenmeyer flask with a capacity of 150 mL which contained 50.0 mL of metal ion solution in specific concentrations, 200 mg L<sup>-1</sup> (Actual measurement 231.03 mg L<sup>-1</sup>) for Pb<sup>2+</sup> and 200 mg L<sup>-1</sup> (Actual measurement 217.12 mg L<sup>-1</sup>) for Cd<sup>2+</sup>. The experiments were respectively carried out at pH 5.0 for Pb<sup>2+</sup> and 5.5 for Cd<sup>2+</sup>. HCl or NaOH solutions (0.1–1.0 mol L<sup>-1</sup>) were used to adjust the pH. The adsorption studies were for different time intervals (5, 10, 20, 30, 40, 50, 70 min) at a constant shock speed (150 rpm) at 30 °C. Finally, the samples were separated by centrifugation at 4000 rpm for 20 min. And the concentrations of the metal ion were determined by an atomic absorption spectrophotometer (TAS-990, Purkinje General, China). The adsorption capacity q<sub>t</sub> (mg g<sup>-1</sup>) was calculated as follow: [30]

$$q_t = \frac{(C_0 - C_e) \times V_m}{m}$$

where V<sub>m</sub> (mL) represents the volume of metal ion solution. C<sub>0</sub> and C<sub>e</sub> (mg L<sup>-1</sup>) respectively represent the concentrations of initial and equilibrium metal ion. And m (mg) represents the mass of adsorbent.



**pH Study of Metal Ion Adsorption of MCCW 2, MCCW 3 and MCCW 4.** 50.0 mg of adsorbent was put into the Erlenmeyer flask with a capacity of 150 mL which contained 50.0 mL of metal ion solution in specific concentrations, 200 mg L<sup>-1</sup> (Actual measurement 231.43 mg L<sup>-1</sup>) for Pb<sup>2+</sup> and 200 mg L<sup>-1</sup> (Actual measurement 230.20 mg L<sup>-1</sup>) for Cd<sup>2+</sup>. The pH range studied for MCCW 2, MCCW 3 and MCCW 4 was from 1.5 to 6.5 for Pb<sup>2+</sup> and 2.5 to 7.5 for Cd<sup>2+</sup>, respectively. HCl or NaOH solutions (0.1–5.0 mol L<sup>-1</sup>) were used to adjust the pH. Each experiment was carried out during the times which were obtained from the kinetic study. The adsorption studies were at a constant shock speed (150 rpm) at 30 °C. Finally, the samples were separated by centrifugation at 4000 rpm for 20 min. And the concentrations of the metal ion were determined as described above.

**Adsorption Isotherms of MCCW 2, MCCW 3 and MCCW 4.** 50.0 mg of adsorbent was put into the Erlenmeyer flask with a capacity of 150 mL which contained 50.0 mL of metal ion solution in specific concentrations (between 100 mg L<sup>-1</sup> and 700 mg L<sup>-1</sup>). HCl or NaOH solutions (0.1–1.0 mol L<sup>-1</sup>) were used to adjust the pH. Each experiment was implemented during the time obtained from kinetic study and at the pH obtained pH study, respectively. The adsorption studies were at a constant shock speed (150 rpm) at 30 °C. Finally, the samples were separated by centrifugation at 4000 rpm for 20 min. And the concentrations of the metal ion were determined as described above.

**Regeneration Studies of MCCW 2.** To evaluate the reusability of material, the regeneration studies were implemented. 100.0 mg MCCW 2 was put into the Erlenmeyer flask with a capacity of 150 mL which contained 100.0 mL of metal ion solution in specific concentrations, 200 mg L<sup>-1</sup> (Actual measurement 229.06 mg L<sup>-1</sup>) for Pb<sup>2+</sup> and 200 mg L<sup>-1</sup> (Actual measurement 219.12 mg L<sup>-1</sup>) for Cd<sup>2+</sup>. The experiment was implemented at the pH obtained from the pH study. The adsorption times were 80 min for Pb<sup>2+</sup> and 90 min for Cd<sup>2+</sup>. The adsorption studies were at a constant shock speed (150 rpm) at 30 °C. After reaching equilibrium, the used adsorbent was separated by centrifugation. Then, the used adsorbent was eluted by 100.0 mL HCl (0.5 mol L<sup>-1</sup>). The desorption studies were also at a constant shock speed (150 rpm) at 30 °C. The desorption times were 80 min for Pb<sup>2+</sup> and 90 min for Cd<sup>2+</sup>. After centrifugation, 100.0 mL of ultrapure water or saturated NaHCO<sub>3</sub> solution was respectively put into two 150 mL Erlenmeyer flasks with the eluted adsorbent. Then, the two flasks were transferred in an ultrasound generator (XO-5200DTS, Nanjing Ultrasound Instrument Co., Ltd.) which operated with a power of 150 W (25 °C) at 45 kHz for 40 s. Finally, the mixtures were filtered and washed with ultrapure water until neutral. After each adsorption-

desorption cycle, adsorbent was reused in the succeeding cycle. The cycles were repeated continuously three times to evaluate the reusability of adsorbent.

## RESULTS

**Extraction of Cellulose from Cassava Waste.** Based on single factor experiments, the dosage of alpha-amylase, enzymolysis time, concentration of the NaOH solution and alkaline hydrolysis time were chosen as the main influence factors, and orthogonal experiments with four factors and three levels were carried out under the 105 W condition of optimal ultrasound power. The optimal conditions of extraction of cellulose from cassava waste were determined to be 0.8% alpha-amylase, 60 min enzymolysis time, 6% NaOH solution and 90 min alkaline hydrolysis time. Finally, the cellulose of cassava waste was extracted three times under the optimal conditions and in average the extracted cellulose of cassava waste (ECCW) was obtained with a content of 63.84%.

**Synthesis of MCCW 1, MCCW 2, MCCW 3 and MCCW 4.** The synthesis route of MCCW 1, MCCW 2, MCCW 3 and MCCW 4 are shown in Fig 1. Hydroxyl groups of materials made it possible to allow carboxylic and amine functional groups to be introduced into the materials through formation of ester bond and amide bond [31]. According to reaction, carboxylic functions were introduced into MCCW 1 which with a mass increment of 88.14% was obtained. Next, MCCW 2, which with a mass increment of 10.61% was obtained, was synthesized by treatment of MCCW 1 with saturated NaHCO<sub>3</sub> solution. Polyamines ethylenediamine was introduced into MCCW 3 which with a mass increment of 11.59% was obtained. Polyamines triethylenetetramine was introduced into MCCW 4 which with a mass increment of 13.64% was obtained.

**FTIR Analysis of MCCW 1, MCCW 3, and MCCW 4.** The spectrum of ECCW and MCCW 1 are shown in Fig 2. Comparing MCCW 1 with ECCW, significant change was noticed in the FTIR spectrum of MCCW 1 with a strong band at 1739 cm<sup>-1</sup>, which corresponded to its carbonyl functions. The presence of carbonyl functional groups demonstrates that succinic anhydride acylated the hydroxy group of ECCW to form an ester bond and a carboxylic acid functional group.

The spectrum of MCCW 3 is presented in Fig 3. The peak at 1740 cm<sup>-1</sup> corresponded to the stretching vibration of the carbonyl of the amide functions. Then, the absorption band at 1577 cm<sup>-1</sup> was assigned to deformation vibration of the N-H bond of the amide function. The new absorption

peaks at  $1158\text{ cm}^{-1}$  and  $1256\text{ cm}^{-1}$  corresponded to stretching vibration of the C-N bond of the secondary amide functional group. Finally, the absorption band at  $1056\text{ cm}^{-1}$  was assigned to stretching vibration of the C-N bond of the fatty amine.

The spectrum of MCCW 4 is shown in Fig 4. The absorption band at  $1740\text{ cm}^{-1}$  was assigned to the stretching vibration of the carbonyl of the amide functions. Then, the peak at  $1575\text{ cm}^{-1}$  and  $1621\text{ cm}^{-1}$  corresponded to deformation vibration of the N-H bond of the amide function and inner-plane deformation vibration of the N-H bond of the amine function. The new absorption band at  $1161\text{ cm}^{-1}$  was assigned to stretching vibration of the C-N bond of the secondary amide functional group. At last, the absorption band at  $1056\text{ cm}^{-1}$  corresponded to stretching vibration of the C-N bond of the fatty amine.

**SEM Characterization.** The surface morphologies of raw cassava waste (RCW), ECCW and MCCW 2 are presented in Fig 5, as the adsorption effect of MCCW 2 is better than MCCW 3 and MCCW 4. The RCW (Fig 5a and b) had a relatively smooth surface and a lot of particle matter which represented starch. The ECCW (Fig 5c and d) had a little particle matter, which implied that most of the starches of cassava waste were removed. However, the picture of Fig 5d showed that some starches were packaged by cellulose, which explained that the starch could not be removed completely. The MCCW 2 showed an obvious bundle of cellulose structure (Fig 5e) and appeared a rough surface and high porosity (Fig 5f), indicating increased specific surface area, which was considered beneficial to the adsorption of heavy metals.

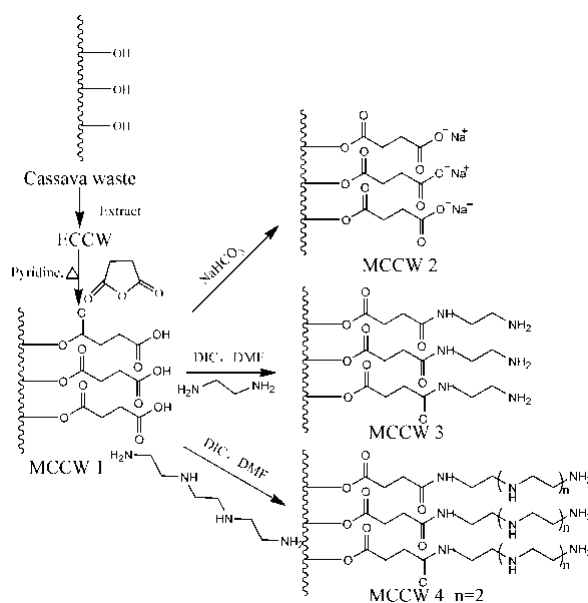


**FIGURE 1**  
The synthesis route to MCCW 1, MCCW 2, MCCW 3 and MCCW 4

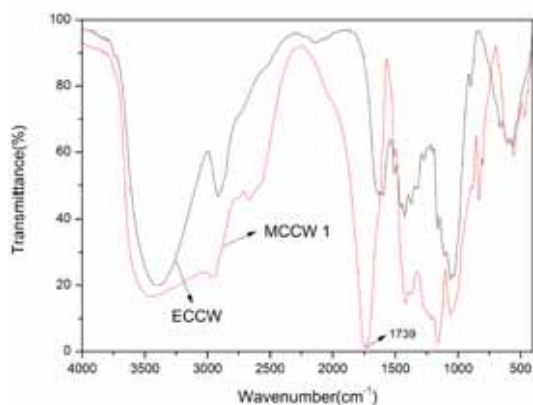


**FIGURE 2**  
FTIR spectra of ECCW and MCCW 1

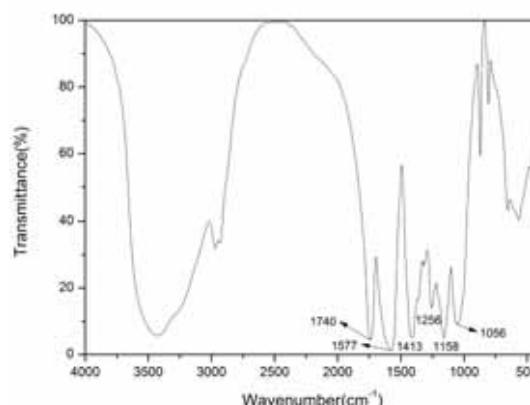


**FIGURE 3**  
FTIR spectra of MCCW 3

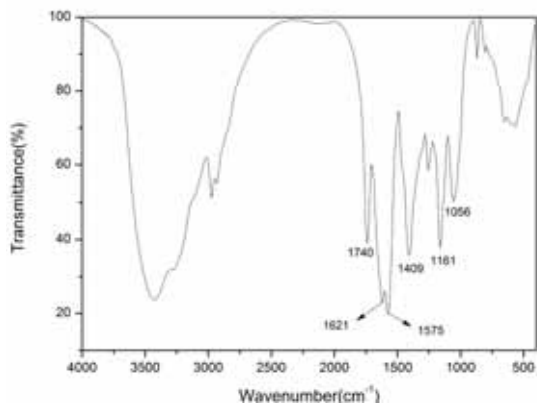


**FIGURE 4**  
FTIR spectra of MCCW 4

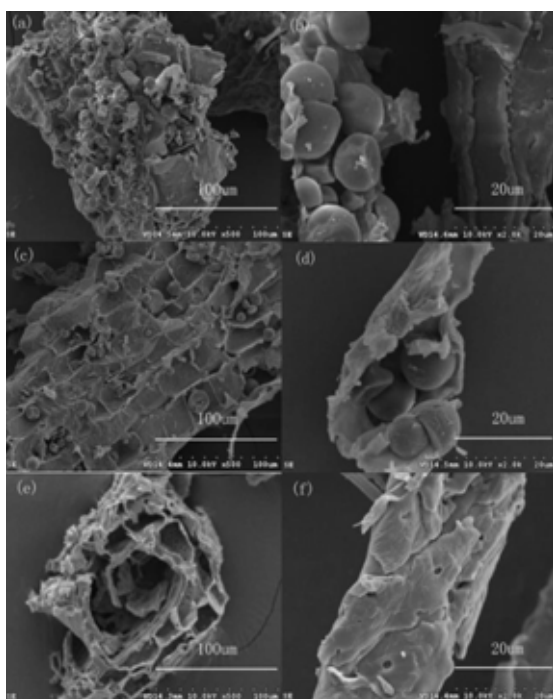


**FIGURE 5**  
SEM images of RCW (a and b), ECCW (c and d)  
and MCCW 2 (e and f)

**Adsorption Studies of Pb<sup>2+</sup> and Cd<sup>2+</sup> on MCCW 2, MCCW 3 and MCCW 4. kinetic Studies.** As a function of contact time, Pb<sup>2+</sup> and Cd<sup>2+</sup> adsorption by MCCW 2 is presented in Fig 6. The adsorption of Pb<sup>2+</sup> rapidly increased during the first 10 min, with more than 96% of Pb<sup>2+</sup> being adsorbed by the MCCW 2. And the adsorption of Cd<sup>2+</sup> rapidly increased during the first 20 min, with more than 94% of Cd<sup>2+</sup> being adsorbed by the MCCW 2. It indicated that these metal ions were absorbed by numerous active sites which existed on the adsorbent surface [30]. Then, adsorption equilibrium was reached within 20 min for Pb<sup>2+</sup> and 30 min for Cd<sup>2+</sup>. The phenomenon be explained by the fact that plenty of

active surface sites were occupied by Pb<sup>2+</sup> and Cd<sup>2+</sup>, and the rest of active surface sites were hard to be occupied because of the repulsive forces between molecules [32].

In order to investigate adsorption process, pseudo-second-order kinetic model was introduced to identify the rate and the rate-controlling step of the adsorption.

$$\frac{t}{q_t} = \frac{t}{q_e} + \frac{1}{k_2 q_e^2}$$

$$h = k_2 q_e^2$$

where  $k_2$  (g mg<sup>-1</sup> min<sup>-1</sup>) represents the rate constant of adsorption of the pseudo-second-order.  $q_e$  (mg g<sup>-1</sup>) is the equilibrium adsorption capacity which is calculated by the pseudo-second-order kinetic model.  $q_t$  is the amount of adsorption at time  $t$  (min).  $h$  (mg g<sup>-1</sup> min<sup>-1</sup>) represents the initial adsorption rate.

According to Fig 7 and Table 1, the values of the R<sup>2</sup> of both Pb<sup>2+</sup> and Cd<sup>2+</sup> were more than 0.9997, and the  $q_e$  values which is calculated by the pseudo-second-order kinetic model were closer to the experimental data. These results indicate that the utilization of pseudo-second-order kinetic model is feasible to clarify the adsorption process of Pb<sup>2+</sup> and Cd<sup>2+</sup> on the MCCW 2, which suggests that chemical adsorption which involved surface chelation reaction or ion exchange was as the rate-controlling step of the adsorption mechanism [33]. The initial adsorption rate ( $h$ ) of Pb<sup>2+</sup> and Cd<sup>2+</sup> are 341.30 and 184.84 mg g<sup>-1</sup> min<sup>-1</sup>, respectively, which implies that the initial adsorption was a rapid adsorption process.

As shown in Table 1 and Table 2, similar adsorption studies were conducted for Pb<sup>2+</sup> and Cd<sup>2+</sup> on MCCW 3 and MCCW 4 with similar results.

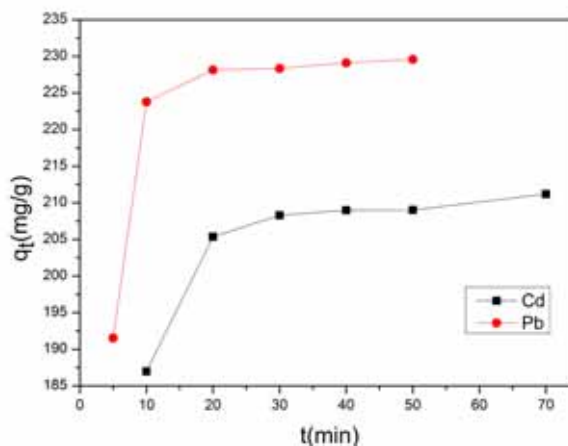


**FIGURE 6**  
Effects of contact time for Pb<sup>2+</sup> and Cd<sup>2+</sup>  
adsorption capacity onto MCCW 2

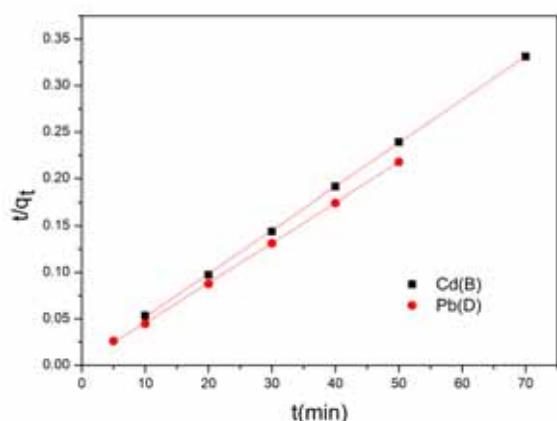


**FIGURE 7**  
The Pseudo-second-order adsorption kinetic model of MCCW 2

**Effect of pH** The adsorption process can be influenced by one of the key parameters which is the pH values of solution. The pH effect on  $\text{Pb}^{2+}$  and  $\text{Cd}^{2+}$  adsorption by MCCW 2 is shown in Fig 8. The adsorption capacity increased sharply from pH 1.5-3.5 for  $\text{Pb}^{2+}$  and 2.5-5.5 for  $\text{Cd}^{2+}$ , and reached the maximum values at pH approximately 4.5 for  $\text{Pb}^{2+}$  and 5.5 for  $\text{Cd}^{2+}$ , respectively. When the pH values was low, the carbonyl functions of MCCW 2 were readily associated with hydronium ions ( $\text{H}_3\text{O}^+$ ) rather than the metals of  $\text{Pb}^{2+}$  and  $\text{Cd}^{2+}$ , which formed a repulsive force for  $\text{Pb}^{2+}$  and  $\text{Cd}^{2+}$ . As the pH was increased, the surface of MCCW 2 was

deprotonated, which led to the increasing of the adsorption capacity of  $\text{Pb}^{2+}$  and  $\text{Cd}^{2+}$  [34]. It is the key effect of pH to the competition between  $\text{H}^+$  ions and metals ions for active adsorption sites [35]. The maximal adsorption capacities of  $\text{Pb}^{2+}$  and  $\text{Cd}^{2+}$  on MCCW 2 are  $227.41 \text{ mg g}^{-1}$  and  $222.58 \text{ mg g}^{-1}$ , respectively. And the maximal removal percentages of  $\text{Pb}^{2+}$  and  $\text{Cd}^{2+}$  on MCCW 2 are 98.26% and 96.69%, which suggests that almost all of the heavy metal ions are removed. Then the adsorption capacity decreased at pH above 4.5 for  $\text{Pb}^{2+}$  and 5.5 for  $\text{Cd}^{2+}$ , which was possibly because of the formation of metallic precipitation. As shown in Fig 8, the adsorption Capacity of MCCW 2 changed only slightly at the pH values from 2.5 to 6.5 for  $\text{Pb}^{2+}$  and 3.5 to 7.5 for  $\text{Cd}^{2+}$ , which indicates that the adsorbent material can be applied to the pH values of solution with a wide range.

As shown in Table 3, similar adsorption studies were conducted for  $\text{Pb}^{2+}$  and  $\text{Cd}^{2+}$  on MCCW 3 and MCCW 4 with similar results.

**Adsorption Isotherm.** The adsorption isotherms describe the interaction between the adsorbates and adsorbents. The adsorption isotherms of  $\text{Pb}^{2+}$  and  $\text{Cd}^{2+}$  for MCCW 2, MCCW 3 and MCCW 4 are shown in Fig 9. The adsorption capacity of  $\text{Pb}^{2+}$  and  $\text{Cd}^{2+}$  for MCCW 2, MCCW 3 and MCCW 4 constantly increased with the growth of the concentration of adsorption solution in the beginning, and gradually decreased after reaching the maximum adsorption. The reason may be as follows: when the concentration of adsorption solution was lower, the amount of metal ions in the

**TABLE 1**  
Pseudo-second-order kinetics constants for  $\text{Pb}^{2+}$  and  $\text{Cd}^{2+}$  on MCCW 2, MCCW 3 and MCCW 4

Metal	Adsorbents	Pseudo-second-order kinetics constants				$R^2$
		$q_{e,exp}$ ( $\text{mg g}^{-1}$ )	$q_e$ ( $\text{mg g}^{-1}$ )	$k$ ( $\text{g mg}^{-1}$ $\text{min}^{-1}$ )	$h$ ( $\text{mg g}^{-1}$ $\text{min}^{-1}$ )	
$\text{Pb}^{2+}$	MCCW 2	229.58	233.10	0.00628	341.30	0.99975
	MCCW 3	226.81	227.27	0.05178	2674.61	1
	MCCW 4	227.63	227.79	0.06853	3556.16	1
$\text{Cd}^{2+}$	MCCW 2	211.20	214.59	0.00401	184.84	0.99986
	MCCW 3	211.88	212.77	0.00909	411.52	0.99989
	MCCW 4	196.86	198.41	0.00847	333.33	0.99987

**TABLE 2**  
Adsorption equilibrium times of MCCW 2, MCCW 3 and MCCW 4

Adsorbents	Equilibrium time (min)	
	$\text{Pb}^{2+}$	$\text{Cd}^{2+}$
MCCW 2	20	30
MCCW 3	10	30
MCCW 4	10	20

solution was far below the saturated adsorption capacity. The metal ions were easy to spread into the interior of adsorption materials, and the adsorption was relatively sufficient. Therefore, adsorption capacity of materials constantly increased with the growth of the concentration of adsorption solution. When the concentration of adsorption solution was higher, the concentration of metal ions in the solution is relatively high and the adsorption rate was fast. Thus, the metal ions with chelation groups of adsorption materials on the surface together formed a rigorous network system before the metal ions diffused into the interior of adsorption materials, which hindered the entry of other metal ions, reducing the adsorption capacity of materials. Besides, adsorption solution with high concentration lowered the swelling property of adsorption materials to a certain extent so as to decrease adsorption capacity. Two typical isotherm models were used to evaluate the experimental data.

The Langmuir isotherm model assumes that a homogeneous surface of adsorbent is covered by adsorbate of monolayer, and there is no interaction between the adsorbate molecules [36]. The Langmuir equation is given as follows:

$$\frac{C_e}{q_e} = \frac{C_e}{q_m} + \frac{1}{bq_m}$$

$$R_L = \frac{1}{1 + bC_0}$$

where  $q_m$  ( $\text{mg g}^{-1}$ ) represents the maximum adsorption capacity.  $b$  ( $\text{L mg}^{-1}$ ) is a Langmuir constant which is related to the energy of adsorption.  $C_e$  ( $\text{mg L}^{-1}$ ) represents the concentration of equilibrium solution.  $q_e$  ( $\text{mg g}^{-1}$ ) represents the adsorption capacity at equilibrium.  $R_L$  is the equilibrium parameter used to reflect whether the adsorption is favorable.

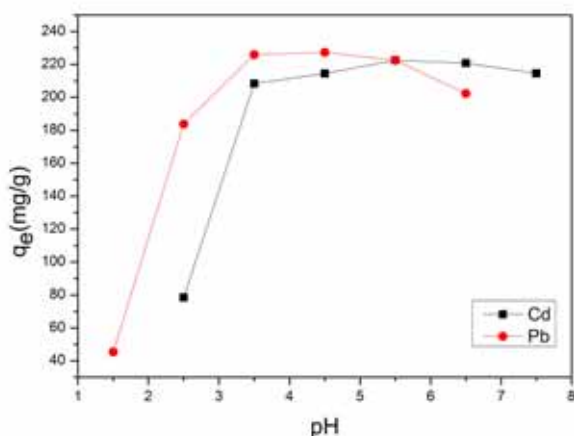


FIGURE 8

Effects of pH on  $\text{Pb}^{2+}$  and  $\text{Cd}^{2+}$  adsorption by MCCW 2

The Freundlich isotherm model is an empirical equation, which is more suitable for heterogeneous

adsorption and not restricted to form a monolayer [37]. The Freundlich equation is represented as follows:

$$\ln q_e = \ln K_F + \frac{1}{n} \ln C_e$$

where  $q_e$  ( $\text{mg g}^{-1}$ ) represents the adsorption capacity at equilibrium.  $C_e$  ( $\text{mg L}^{-1}$ ) represents the concentration of equilibrium solution.  $K_F$  and  $n$  represent the adsorption constants of Freundlich.

According to table 4, the Langmuir isotherm model was more appropriate than Freundlich isotherm model due to the higher correlation coefficient  $R^2$ . In addition, the maximum adsorption capacity, which was calculated by Langmuir model, of  $\text{Pb}^{2+}$  and  $\text{Cd}^{2+}$  for MCCW 2, MCCW 3 and MCCW 4 were extremely close to the corresponding experimental data. And the calculated maximum adsorption capacity was  $476.19 \text{ mg g}^{-1}$  for  $\text{Pb}^{2+}$  and  $289.02 \text{ mg g}^{-1}$  for  $\text{Cd}^{2+}$  on MCCW 2, respectively. The values of  $R_L$ , which was obtained from Langmuir model, ranged from 0.00065 to 0.02578, indicating that the adsorption of  $\text{Pb}^{2+}$  and  $\text{Cd}^{2+}$  for MCCW 2, MCCW 3 and MCCW 4 was a favorable ( $0 < R_L < 1$ ) and useful process [38].

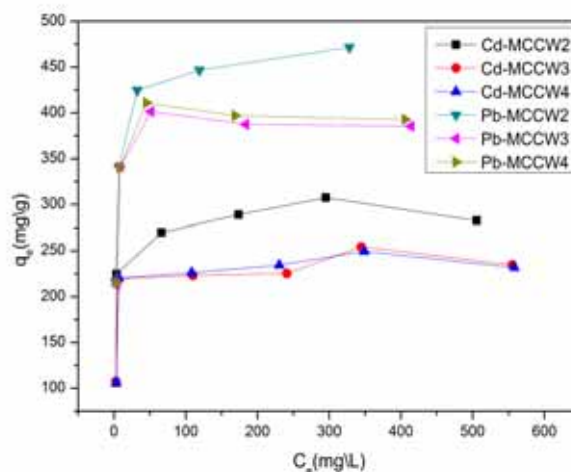


FIGURE 9

Adsorption isotherms for  $\text{Pb}^{2+}$  and  $\text{Cd}^{2+}$  on MCCW 2, MCCW 3 and MCCW 4

**Regeneration Studies.** The character of regeneration was one of the key parameters to evaluate the potential application value of the adsorbents [39]. In this study, the regeneration of MCCW 2 was eluted with ultrapure water or saturated  $\text{NaHCO}_3$  solution. From Table 5, the adsorption capacity of MCCW 2, which was eluted with ultrapure water, decreased from 227.13 to  $81.30 \text{ mg g}^{-1}$  for  $\text{Pb}^{2+}$  and from 206.29 to  $26.26 \text{ mg g}^{-1}$  for  $\text{Cd}^{2+}$ , respectively, after three cycles of adsorption-desorption. However, the adsorption efficiencies of MCCW 2, which was eluted with saturated  $\text{NaHCO}_3$  solution, could still be maintained at 97.40% level for  $\text{Pb}^{2+}$  and 93.16% level for  $\text{Cd}^{2+}$  even after three

**TABLE 3**  
**pH of largest adsorption of MCCW 2, MCCW 3 and MCCW 4**

Adsorbents	pH of largest adsorption	
	Pb <sup>2+</sup>	Cd <sup>2+</sup>
MCCW 2	4.5	5.5
MCCW 3	4.5	5.5
MCCW 4	4.5	6.5

**TABLE 4**  
**Isotherm constants of MCCW 2, MCCW 3 and MCCW 4**

Metal	Adsorbent s	q <sub>e,exp</sub> (mg g <sup>-1</sup> )	Langmuir model				Freundlich model		
			q <sub>m,cal</sub> (mg g <sup>-1</sup> )	b (L mg <sup>-1</sup> )	R <sub>L</sub>	R <sup>2</sup>	K <sub>F</sub>	n	R <sup>2</sup>
Pb <sup>2+</sup>	MCCW 2	471.61	476.19	0.261	0.00478-0.01716	0.99967	228.07	7.049	0.77918
	MCCW 3	401.38	386.10	1.472	0.00085-0.00309	0.99984	229.60	9.713	0.46990
	MCCW 4	411.04	393.70	1.939	0.00065-0.00234	0.99982	231.71	9.376	0.50018
Cd <sup>2+</sup>	MCCW 2	307.39	289.02	1.721	0.00073-0.00525	0.99687	134.52	7.118	0.53574
	MCCW 3	254.53	239.81	0.343	0.00367-0.02578	0.99582	130.99	9.446	0.47652
	MCCW 4	249.53	236.41	1.410	0.00090-0.00640	0.99739	127.56	8.996	0.45666

**TABLE 5**  
**Adsorption–desorption cycles of MCCW 2 for Pb<sup>2+</sup> and Cd<sup>2+</sup>**

Cycle	Pb <sup>2+</sup> adsorption (%)		Cd <sup>2+</sup> adsorption (%)	
	NaHCO <sub>3</sub>	H <sub>2</sub> O	NaHCO <sub>3</sub>	H <sub>2</sub> O
1	98.65	98.72	94.51	94.14
2	98.00	40.47	93.83	15.25
3	97.40	35.49	93.16	11.98

cycles. The probable reason was that saturated NaHCO<sub>3</sub> solution elution made the adsorbent surface become deprotonated, which enables the adsorbent to recover better adsorption capacity. Therefore, the regeneration studies showed that MCCW 2 could be successfully regenerated by saturated NaHCO<sub>3</sub> solution elution.

## DISCUSSION AND CONCLUSIONS

The chelating functions (carboxylic acid and amine) were introduced to cellulose of cassava waste by a fast, effective and cheap methodology. The adsorption equilibrium of MCCW 2 was reached within 20 min for Pb<sup>2+</sup> and 30 min for Cd<sup>2+</sup>, and the calculated maximum adsorption capacity was 476.19 mg g<sup>-1</sup> for Pb<sup>2+</sup> and 289.02 mg g<sup>-1</sup> for Cd<sup>2+</sup> on MCCW 2, which was better than the MCCW 3 and MCCW 4. The adsorption process was described well by Pseudo-second-order and Langmuir model, which implied that the process might be a monolayer chemical adsorption process. The adsorption capacity of MCCW 2 changed only slightly at the pH values from 2.5 to 6.5 for Pb<sup>2+</sup> and 3.5 to 7.5 for Cd<sup>2+</sup>. Regeneration studies indicated that the adsorption efficiencies of MCCW 2, which was eluted with saturated NaHCO<sub>3</sub> solution, could still be

maintained at 97.40% level for Pb<sup>2+</sup> and 93.16% level for Cd<sup>2+</sup> even after three cycles. All in all, MCCW 2 could be regarded as a promising adsorbent to remove Pb<sup>2+</sup> and Cd<sup>2+</sup> from polluted water.

## ACKNOWLEDGEMENTS

This work was financially supported by Scientific Research Special Foundation of the Higher Education Institutions of Hainan Province (Hnkyzx2014-01), and the Natural Science Foundation of Hainan Province (214016), China.

## REFERENCES

- [1] Repo, E.; Warchol, J. K.; Bhatnagar, A.; Sillanpaa, M., (2011) Heavy metals adsorption by novel EDTA-modified chitosan-silica hybrid materials. *Journal of Colloid and Interface Science*, 358, 261-267.
- [2] Shao, W. J.; Chen, L. H.; Lu, L. L.; Luo, F., (2011) Removal of lead (II) from aqueous solution by a new biosorption material by immobilizing Cyanex272 in cornstalks. *Desalination*, 265, 177-183.

- [3] Miretzky, P.; Munoz, C.; Carrillo-Chavez, A., (2010) Cd (II) removal from aqueous solution by *Eleocharis acicularis* biomass, equilibrium and kinetic studies. *Bioresource Technology*, 101, 2637-2642.
- [4] Li, Q.; Chai, L.; Qin, W., (2012) Cadmium(II) adsorption on esterified spent grain: Equilibrium modeling and possible mechanisms. *Chemical Engineering Journal*, 197, 173-180.
- [5] Hokkanen, S.; Repo, E.; Sillanpaa, M., (2013) Removal of heavy metals from aqueous solutions by succinic anhydride modified mercerized nanocellulose. *Chemical Engineering Journal*, 223, 40-47.
- [6] Repo, E.; Koivula, R.; Harjula, R.; Sillanpaa, M., (2013) Effect of EDTA and some other interfering species on the adsorption of Co(II) by EDTA-modified chitosan. *Desalination*, 321, 93-102.
- [7] Ismail, F. A.; Aris, A. Z.; Latif, P. A., (2014) Dynamic behaviour of Cd<sup>2+</sup> adsorption in equilibrium batch studies by CaCO<sub>3</sub>-rich *Corbicula fluminea* shell. *Environmental Science and Pollution Research*, 21, 344-354.
- [8] Firouzi, A. F.; Babaei, A. A.; Hosseini, S.; Heidarzadeh, F., (2015) Adsorption of copper(II) by modified magnetite nanoparticles: adsorption efficacy, equilibrium, kinetic and reusability. *Fresenius Environmental Bulletin*, 24, 2815-2823.
- [9] Kamari, A.; Putra, W. P.; Abd Wahid, N. S.; Yusoff, S. N. M., (2015) *Cerithidea obtusa* (mud creeper snail) shell as a green biosorbent for adsorption of Cu(II), Ni(II) and Pb(II) ions from aqueous solutions. *Fresenius Environmental Bulletin*, 24, 575-586.
- [10] Kamari, A.; Nazri, N. H., (2014) Soya dregs residue as a biosorbent for Cu(II), Ni(II) and Pb(II) removal from aqueous solutions: adsorption and characterisation studies. *Fresenius Environmental Bulletin*, 23, 1942-1952.
- [11] Lim, S.-F.; Lee, A. Y. W., (2015) Kinetic study on removal of heavy metal ions from aqueous solution by using soil. *Environmental Science and Pollution Research*, 22, 10144-10158.
- [12] Jeon, C., (2014) Adsorption characteristics of waste crab shells for silver ions in industrial wastewater. *Korean Journal of Chemical Engineering*, 31, 446-451.
- [13] Zhu, H.-X.; Cao, X.-J.; He, Y.-C.; Kong, Q.-P.; He, H.; Wang, J., (2015) Removal of Cu<sup>2+</sup> from aqueous solutions by the novel modified bagasse pulp cellulose: Kinetics, isotherm and mechanism. *Carbohydrate Polymers*, 129, 115-126.
- [14] Qing, Q.; Hu, R.; He, Y.; Zhang, Y.; Wang, L., (2014) Investigation of a novel acid-catalyzed ionic liquid pretreatment method to improve biomass enzymatic hydrolysis conversion. *Applied Microbiology and Biotechnology*, 98, 5275-5286.
- [15] Li, M.-C.; Wu, Q.; Song, K.; Lee, S.; Qing, Y.; Wu, Y., (2015) Cellulose Nanoparticles: Structure–Morphology–Rheology Relationships. *ACS Sustainable Chemistry & Engineering*, 3, 821-832.
- [16] Iqbal, M.; Saeed, A.; Zafar, S. I., (2009) FTIR spectrophotometry, kinetics and adsorption isotherms modeling, ion exchange, and EDX analysis for understanding the mechanism of Cd<sup>2+</sup> and Pb<sup>2+</sup> removal by mango peel waste. *Journal of Hazardous Materials*, 164, 161-171.
- [17] O'Connell, D. W.; Birkinshaw, C.; O'Dwyer, T. F., (2008) Heavy metal adsorbents prepared from the modification of cellulose: a review. *Bioresource technology*, 99, 6709-24.
- [18] Shi, J.; Luo, H.; Xiao, D.; Hu, J.; Zhang, G.; Li, Y.; Lin, B.; Liang, X.; Tu, Y., (2014) Bio-Sorbents from Cassava Waste Biomass and Its Performance in Removal of Pb<sup>2+</sup> from Aqueous Solution. *Journal of Applied Polymer Science*, 131.
- [19] Zheng, L.; Dang, Z.; Zhu, C.; Yi, X.; Zhang, H.; Liu, C., (2010) Removal of cadmium(II) from aqueous solution by corn stalk graft copolymers. *Bioresource Technology*, 101, 5820-5826.
- [20] Tang, X.; Li, Y.; Chen, R.; Min, F.; Yang, J.; Dong, Y., (2015) Evaluation and modeling of methyl green adsorption from aqueous solutions using loofah fibers. *Korean Journal of Chemical Engineering*, 32, 125-131.
- [21] Rahman, M. L.; Mustapa, N. R. N.; Yusoff, M. M., (2014) Synthesis of Polyamidoxime Chelating Ligand from Polymer-Grafted Corn-Cob Cellulose for Metal Extraction. *Journal of Applied Polymer Science*, 131.
- [22] Hashem, A., (2006) Amidoximated sunflower stalks (ASFS) as a new adsorbent for removal of Cu (II) from aqueous solution. *Polymer-plastics technology and engineering*, 45, 35-42.
- [23] Niu, X.; Zheng, L.; Zhou, J.; Dang, Z.; Li, Z., (2014) Synthesis of an adsorbent from sugarcane bagass by graft copolymerization and its utilization to remove Cd (II) ions from aqueous solution. *Journal of the Taiwan Institute of Chemical Engineers*, 45, 2557-2564.
- [24] Kumar, B.; Kumar, U., (2015) Adsorption of malachite green in aqueous solution onto sodium carbonate treated rice husk. *Korean Journal of Chemical Engineering*, 1655-1666.
- [25] Wang, D. J.; Chen, H.; Xu, H.; Sun, J. M.; Xu, Y. Y., (2014) Preparation of Wheat Straw Matrix-g-Polyacrylonitrile-Based Adsorbent by SET-LRP and Its Applications for Heavy Metal Ion Removal. *ACS Sustainable Chemistry & Engineering*, 2, 1843-1848.



- [26] Shibi, I.; Anirudhan, T.,( 2002) Synthesis, characterization, and application as a mercury (II) sorbent of banana stalk (*Musa paradisiaca*)-polyacrylamide grafted copolymer bearing carboxyl groups. *Industrial & engineering chemistry research*, 41, 5341-5352.
- [27] Horsfall, M.; SPIFF, A. I.; Abia, A.,( 2004) Studies on the influence of mercaptoacetic acid (MAA) modification of cassava (*Manihot sculenta* cranz) waste Biomass on the adsorption of  $\text{Cu}^{2+}$  and  $\text{Cd}^{2+}$  from aqueous solution. *Bulletin of the Korean Chemical Society*, 25, 969-976.
- [28] Simate, G. S.; Ndlovu, S.,( 2015) The removal of heavy metals in a packed bed column using immobilized cassava peel waste biomass. *Journal of Industrial and Engineering Chemistry*, 21, 635-643.
- [29] Karnitz, O., Jr.; Alves Gurgel, L. V.; Perin de Melo, J. C.; Botaro, V. R.,( 2007) Sacramento Melo, T. M.; de Freitas Gil, R. P.; Gil, L. F., Adsorption of heavy metal ion from aqueous single metal solution by chemically modified sugarcane bagasse. *Bioresource Technology*, 98, 1291-1297.
- [30] Sun, Z.; Liu, Y.; Huang, Y.; Tan, X.; Zeng, G.; Hu, X.; Yang, Z.,( 2014) Fast adsorption of  $\text{Cd}^{2+}$  and  $\text{Pb}^{2+}$  by EGTA dianhydride (EGTAD) modified ramie fiber. *Journal of Colloid and Interface Science*, 434, 152-158.
- [31] Yu, J.; Tong, M.; Sun, X.; Li, B.,( 2008) Enhanced and selective adsorption of  $\text{Pb}^{2+}$  and  $\text{Cu}^{2+}$  by EDTAD-modified biomass of baker's yeast. *Bioresource technology*, 99, 2588-2593.
- [32] Mall, I.; Srivastava, V.; Kumar, G.; Mishra, I.,( 2006) Characterization and utilization of mesoporous fertilizer plant waste carbon for adsorptive removal of dyes from aqueous solution. *Colloids and Surfaces A: Physicochemical and Engineering Aspects*, 278, 175-187.
- [33] Zhao, F. P.; Repo, E.; Yin, D. L.; Sillanpaa, M. E. T.,( 2013) Adsorption of  $\text{Cd}(\text{II})$  and  $\text{Pb}(\text{II})$  by a novel EGTA-modified chitosan material: Kinetics and isotherms. *Journal of Colloid and Interface Science*, 409, 174-182.
- [34] Alves Gurgel, L. V.; Gil, L. F.,( 2009) Adsorption of  $\text{Cu}(\text{II})$ ,  $\text{Cd}(\text{II})$  and  $\text{Pb}(\text{II})$  from aqueous single metal solutions by succinylated twice-mercerized sugarcane bagasse functionalized with triethylenetetramine. *Water Research*, 43, 4479-4488.
- [35] Li, F. T.; Yang, H.; Zhao, Y.; Xu, R.,( 2007) Novel modified pectin for heavy metal adsorption. *Chinese Chemical Letters*, 18, 325-328.
- [36] Langmuir, I.,( 1918) The adsorption of gases on plane surfaces of glass, mica and platinum. *Journal of the American Chemical society*, 40, 1361-1403.
- [37] Gusmão, K. A. G.; Gurgel, L. V. A.; Melo, T. M. S.; Gil, L. F.,( 2012) Application of succinylated sugarcane bagasse as adsorbent to remove methylene blue and gentian violet from aqueous solutions—Kinetic and equilibrium studies. *Dyes and Pigments*, 92, 967-974.
- [38] Yan, H.; Yang, L.; Yang, Z.; Yang, H.; Li, A.; Cheng, R.,( 2012) Preparation of chitosan/poly (acrylic acid) magnetic composite microspheres and applications in the removal of copper (II) ions from aqueous solutions. *Journal of hazardous materials*, 229, 371-380.
- [39] Lv, L.; Tsoi, G.; Zhao, X.,( 2004) Uptake equilibria and mechanisms of heavy metal ions on microporous titanosilicate ETS-10. *Industrial & engineering chemistry research*, 43, 7900-7906.

---

**Received: 03.02.2016**

**Accepted: 13.08.2016**

---

#### CORRESPONDING AUTHOR

---

##### Shengxu Luo

Key Laboratory of Tropical Biological Resources for Ministry of Education,  
College of Materials and Chemical Engineering,  
Hainan University,  
Haikou 570228, China

e-mail: shxluo@hainu.edu.cn



# MODIFICATION OF REUSED FURNACE IRON WASTE (FIW) WHICH HAD SURFACE REDUCED WITH ZERO-VALENT IRON/FIW (ZFIW) CATALYTIC FOR DYES WASTEWATER TREATMENT

Chih-Tsung Tsai\*, Jian-Zhi Lian, Yung-Hsu Hsieh

Physicochemical Treatment Lab of Department of Environmental Engineering, National Chung-Hsing University, Taichung, Taiwan

## ABSTRACT

This study investigates the recovery of furnace iron waste (FIW) prepared by a zero-valent iron/FIW (ZFIW) catalytic process for reducing surface via a chemical reducing method applied to the degradation of dye wastewater. The modification of the catalyst is attested by X-ray diffraction (XRD) measurements. The experimental tests are run at pH 3, pH 11 and the neutral pH 5.5 of the suspension. The results show that for obtaining 5 g FIW catalytic and 5 g ZFIW catalytic at pH 3, pH 11 and the neutral pH condition, the treatments are 0%, 6.4%, 15.5% and 10.5%, 17.1%, 82.9% efficient, respectively. Under the modified catalyst, the removal efficiency increases and the wastewater treatment process is shown to be successful.

## KEYWORDS:

Methylene blue, furnace iron waste, decolorization, zero-valent iron

## INTRODUCTION

Human activity has resulted in increased waste from industrial processes and every day articles; these wastes comprise more kinds of components [1]. However, waste materials can also be seen as resources, and more research is being done on methods to reuse, recycle and recover certain waste products. For example, one study focused on the recovery of iron oxides from acid mine drainage and how they can be reused [2]; also, adsorption studies of basic dye on activated carbon derived from agricultural waste [3] have been conducted which focus on the efficiency of pollutant treatment.

Iron is the most abundant element in the earth, and the oxidation-reduction of iron plays a leading

part in natural ecosystems, and the iron acts as catalyst to catalyze the hydroxyl radical in the environment to oxidize other substances [9]. Iron is a substance indispensable to human life, and it is used in the making of many commodities [4]. However, manufacturing processes produce large amounts of iron-bearing waste, with the residues from the casting and calcination processes including cementite, hematite and magnetite.

The iron-based material can be used to treat pollutants [6], and is used on its own or mixed with activated carbon as adsorbing material to enhance the electrification and adsorption capacity [5]. It can also be used as a catalyst in  $H_2O_2$  to generate a hydroxyl radical to oxidize pollutants [8], or prepared in a zero-valent iron-based material as a reducer to treat pollutants [7]. There are few studies on the recycling of forge iron slag waste to treat dye wastewater.

This study investigated the feasibility of recycling forge iron slag to treat dye wastewater. The surface of the recovered forge iron slag was reduced to zero-valent iron by chemical reduction, so as to enhance the treatment effect.

## MATERIALS AND METHODS

**Materials.** The furnace iron waste came from a furnace iron manufacturing company in New Taipei City, Taiwan. Methylene blue (MB) dye and  $HNO_3$  and NaOH were purchased from Aldrich Sigma in analytical purity and used in experiments directly without further purification.

**Preparation of  $Fe^0$ /FIW catalyst** Wrought iron slag was washed with deionized water first, dried process was conducted for two hours after the washing process at a temperature of 105 °C for two hours. FIW substrate was thus formed. FIW

substrate was then placed in side the base with 1N solution of sodium borohydride, iron surface of the substrate was then reduced to zero valent iron which is Fe<sup>0</sup>/FIW substrate after the backup system process.

**Experimental process.** Batch experiments were conducted in a 1000 ml glass beaker. Methylene blue dye with concentration of 20 ppm was put into a 1000 ml glass beaker in the beginning. 300 rpm stirring rate combined with the experimental time parameter. The base dose, different pH conditions were conducted in this experiment process and then compare with the treatment effect change for before and after modification of the substrate precursors.

**Analytical methods.** The MB concentration was determined using a spectrophotometer UV/Vis (Jasco V-650) and measured by recording its absorbance at 664 nm. The pH values were determined by means of a pH meter. All samples were centrifuged prior to analysis.

## RESULTS AND DISCUSSION

### Characterization of methylene blue (MB).

The phenothiazinium compound of methylene blue (MB) presents a planar heterocyclic aromatic structure, as shown in Fig. 1. The spectroscopic characterization showed an intense electronic absorption band in the red spectral region (~664 nm) [10]. A comparison with Fig. 2 showed the same, which under room light had not changed at 120 min. As Fig. 3 shows, the MB also remained unchanged under different pH conditions.

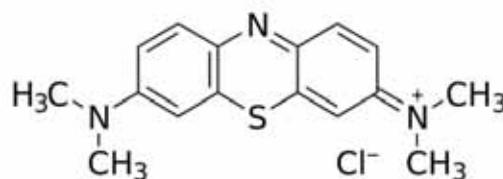


FIGURE 1

Characterization of methylene blue.

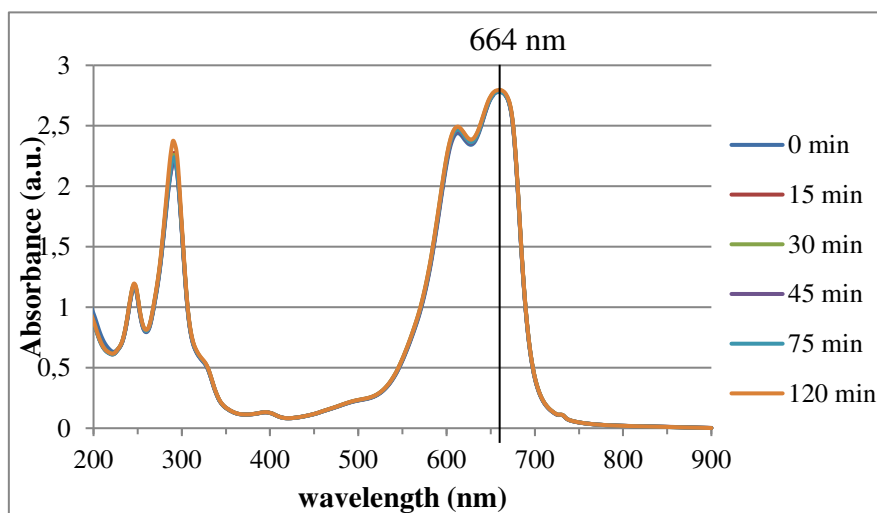
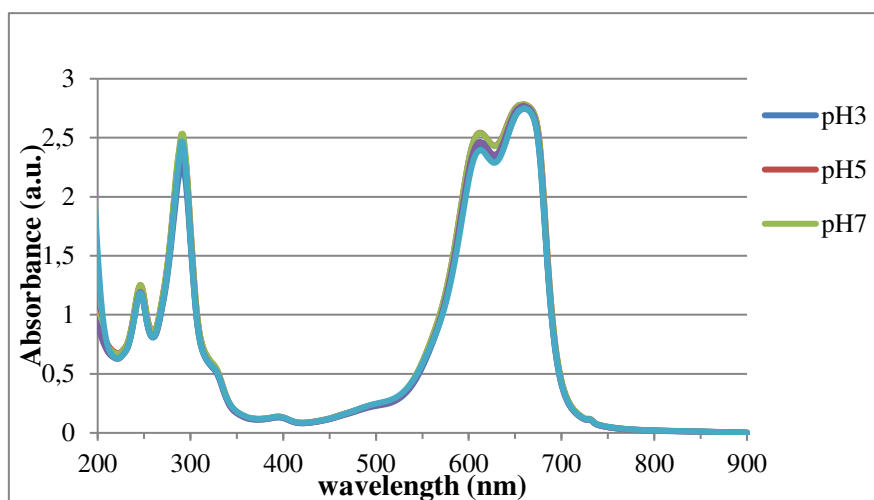
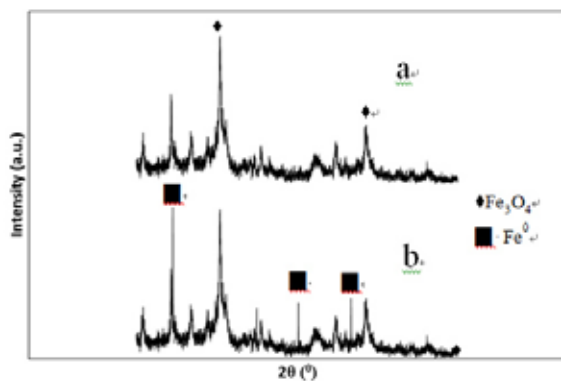


FIGURE 2

Photocatalysis of MB under room light condition.



**FIGURE 3**  
Photocatalysis of MB under different pH conditions.



**FIGURE 4**  
XRD profiles of (a) FIW, and (b) ZFIW.

**Characterization of FIW and ZFIW. XRD of FIW and ZFIW.** The XRD patterns of the non-exchanged and exchanged FIW are shown in Fig. 4 (profiles a and b, respectively). The experimental XRD profile of the non-exchanged FIW present two distinctive peaks at  $35.6^\circ$  and  $62.9^\circ$ ; the profile of the exchanged ZFIW present three distinctive peaks at  $21.0^\circ$ ,  $42.5^\circ$  and  $60.1^\circ$ . The observed diffraction peaks agree well with the structure of zero-valent iron (JCPDS card No. 65-4899).

**Treatment efficiency. Treatment efficiency of FIW.** The FIW adsorption efficiency of the MB dye solution at difference dosages was investigated. As Fig. 5 shows, when the dosage increased, the removal efficiency increased, with the results showing 55.6% removal efficiency at a 20 g dosage

of FIW. Fig. 6 shows the effect of different pH conditions on the removal of MB, with the results showing that at pH 3 and pH 11 conditions. Since under acidic (pH 3) conditions, the substrate surface is positively charged and positive dye was adsorbed against repulsion, and under this condition the free iron ions easily, so that the substrate surface to reduce the adhesive force, However, particularly under alkaline (pH 11) conditions, the adsorption capacity is also smaller natural water pH (pH 5.5) under the conditions in effect, Sodium hydroxide was added inference may not be formed on the substrate surface functional groups, affect adsorption space.

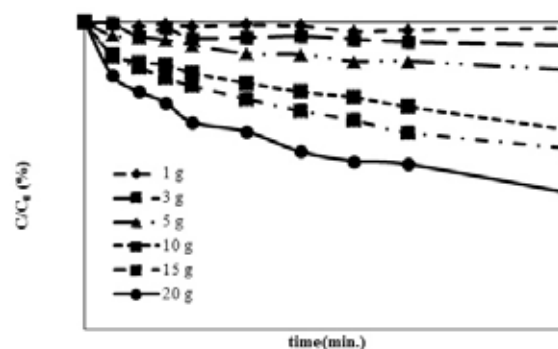


**FIGURE 5**  
Removal efficiency under different dosages of 20 ppm MB dye solution by FIW.

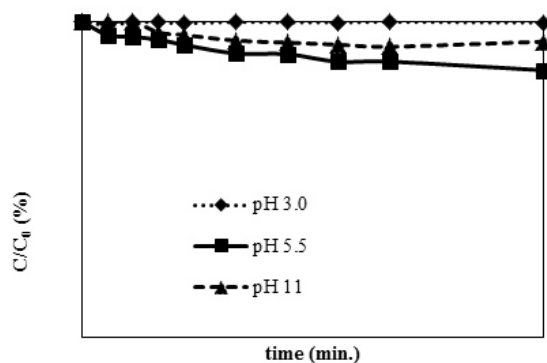


**FIGURE 6**  
Removal efficiency under different pH conditions of 20 ppm MB dye solution by 5 g FIW.

**Treatment efficiency of ZFIW.** The adsorption efficiency of the MB dye solution at different ZFIW dosages is shown in Fig. 7. The result showed that the removal efficiency increased when the dosage increased. It further showed that with an 82.9% removal efficiency obtained at a 5 g dosage of ZFIW. The results proved that the modification of FIW by using the chemical reduction method to prepare ZFIW increased the removal efficiency of the MB dye. Fig. 8 shows the effect of the different pH conditions on the removal of MB, with the pH 3 and pH 11 conditions which decreasing the adsorption efficiency. This result is the same as the results shown in Fig. 6.

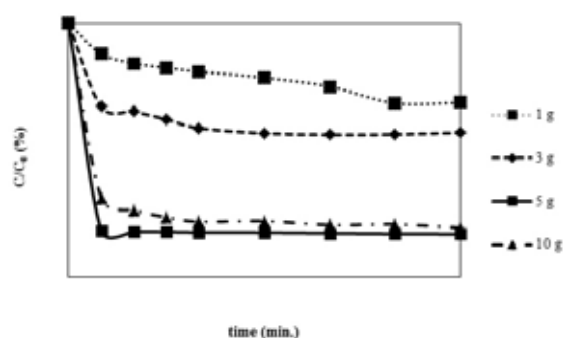


**FIGURE 7**  
Removal efficiency under different dosages of 20 ppm MB dye solution by ZFIW.

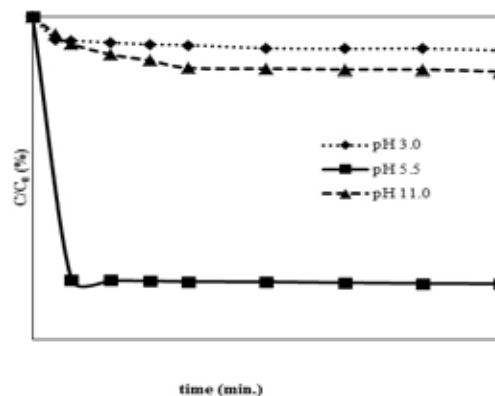


**FIGURE 8**  
Removal efficiency under different pH conditions of 20 ppm MB dye solution by 5 g of ZFIW.

## CONCLUSION

This paper has reported on the recovery of furnace iron waste (FIW) using the chemical reduction method to reduce surface prepared zero-iron/ FIW (ZFIW) for removing MB dye wastewater.

The experimental results showed that the modified FIW increased the removal efficiency of a 20 ppm concentration of MB dye solution, obtaining 82.9% at a neutral pH condition for 5 g of ZFIW.

The results show that the results are not conducive to the degradation of the dye under acid conditions. In other words, substrate surface potential impact was influenced by acidic conditions while substrate surface functional groups were relevant under alkaline conditions.

This study was shown that the surface modification of the iron-containing waste will increase the treatment effect of methylene blue. This finding will be used for the future treatment of dyeing wastewater.

## REFERENCES

- [1] Ajayi, S. O., Oyedele, L. O., Akinade, O. O., Bilal, M., Owolabi, H. A., Alaka, H. A. and Kadiri, K. O. (2016) Reducing waste to landfill: A need for cultural change in the UK construction industry. *Journal of Building Engineering*, 5, 185-193.
- [2] Flores, R. G., Andersen, S. L. F., Maia, L. K. K., José, H. J. and Moreira, R. F. P. M. (2012)



- Recovery of iron oxides from acid mine drainage and their application as adsorbent or catalyst. *Journal of Environmental Management*, 111, 53-60
- [3] Hameed, B. H. and Daud, F. B. M. (2008) Adsorption studies of basic dye on activated carbon derived from agricultural waste: Hevea brasiliensis seed coat. *Chemical Engineering Journal*, 139(1), 48-55.
- [4] Kathe, M. V., Empfield, A., Na, J., Blair, E. and Fan, L. S. (2016) Hydrogen production from natural gas using an iron-based chemical looping technology: Thermodynamic simulations and process system analysis. *Applied Energy*, 165, 183-201.
- [5] Liao, Q., Sun, J. and Gao, L. (2009) Degradation of phenol by heterogeneous Fenton reaction using multi-walled carbon nanotube supported Fe(2)O(3) catalysts. *Colloids and Surfaces A: Physicochemical and Engineering Aspects*, 345, 95-100.
- [6] Lim, H., Lee, J., Jin, S., Kim, J., Yoon, J. and Hyeon, T. (2006) Highly active heterogeneous Fenton catalyst using iron oxide nanoparticles immobilized in alumina coated mesoporous silica. *Chemical Communications*, 463-465.
- [7] Nie, Y., Hu, C., Qu, J., Zhou, L. and Hu, X., (2007) Photo assisted degradation of azo dyes over FeOxH<sub>2x-3</sub>/Fe<sup>0</sup> in the presence of H<sub>2</sub>O<sub>2</sub> at neutral pH values. *Environmental Science & Technology*, 41, 4715-4719.
- [8] Seyed Dorraji, M.S., Mirmohseni, A., Carraro, M., Gross, S., Simone, S., Tasselli, F. and Figoli, A. (2015) Fenton-like catalytic activity of wet-spun chitosan hollow fibers loaded with Fe<sub>3</sub>O<sub>4</sub> nanoparticles: batch and continuous flow investigations. *Journal of Molecular Catalysis A: Chemical*, 398, 353-357.
- [9] Svodoba, K., Slowinski, G., Rogut, J. and Baxter, D. (2007) Thermodynamic possibilities and constraints for pure hydrogen production by iron based chemical looping process at lower temperatures. *Energy Conversion and Management*; 48(12), 3063-3073.
- [10] Tardivo J.P., Del Giglio A., de Oliveira C.S., Gabrielli D.S., Junqueira H.C., Tada D.B., Severino D., de Fátima Turchiello R., Baptista M.S. (2005) Methylene blue in photodynamic therapy: From basic mechanisms to clinical applications. *Photodiagnosis and Photodynamic Therapy*, 2(3), 175-191.

---

**Received: 04.02.2016**

**Accepted: 20.08.2016**

---

#### **CORRESPONDING AUTHOR**

---

**Chih-Tsung Tsai**

Department of Environmental Engineering

National Chung-Hsing University

145 Xingda Rd., South Dist., Taichung - TAIWAN

E-mail: [only5341@yahoo.com.tw](mailto:only5341@yahoo.com.tw)

# REUSED HAND-WARMER WASTES FOR DEGRADATION OF AR27 DYES IN WASTE WATER

Chih-Tsung Tsai\*, Jian-Zhi Lian, Yung-Hsu Hsieh

Physicochemical Treatment Lab of Department of Environmental Engineering, National Chung-Hsing University, Taichung, Taiwan

## ABSTRACT

The present study aimed to investigate the degradation effect of AR27 dye in waste water by using reused hand-warmer waste (HWW).  $H_2O_2$  was also added to study the decolorization and the total organic carbon (TOC) removal effect. Experimental results obtained for a solution of pH 3 with 10 g of 40 ppm dye added showed a 98.69% decolorization effect. Adding  $H_2O_2$  resulted in a 94.54% decolorization effect and a 94.01% TOC removal effect. 67.87%, 42.25% and 40.57% decolorization effects were produced when in solutions with pH 5, pH 7 and pH 11, respectively. In addition, when adding  $H_2O_2$  obtained 83.22%, 49.72% and 88.46% decolorization effects and 61.67%, 15.82% and 11.36% TOC removal effects, respectively. Therefore, decolorization had good representation when in pH 3 and pH11 conditions. There was no TOC removal effect when solutions pH was 11. Moreover, further experimental results obtained by adding  $H_2O_2$ . The results showed that the remaining dye concentrations were decreased to 8.36 mg/L. Although the results principally exhibit the adsorption effect by adding  $H_2O_2$  to increase the decolorization effect, hand-warmer waste (HWW) may still be a low-cost and good adsorbent for removing AR27 dye.

## KEYWORDS:

AR27, hand-warmer, decolorization, TOC removal.

## INTRODUCTION

In winter when cold air comes many people in Asia use hand-warmers for comfort, but these become waste after use and are arbitrarily abandoned. This adds to the rising amount of waste [1]. Hand-warmer waste (HWW) contains iron oxide, active carbon, zeolites, NaCl and absorbent

polymers. In order to achieve both sound environmental protection and sustainable development, which is strongly associated with resource reuse, it is of great importance to maximize the recovery and recycling of iron oxide metals economically from HWW.

Iron is the fourth most abundant element in the Earth's crust, and reactions involving iron play a major role in the environmental cycling of a range of important contaminants [2]. Iron exists in the environment dominantly in two valence states: the relatively water-soluble Fe(II) (ferrous iron) and the highly water-insoluble Fe(III) (ferric iron), with the latter being the stable form in oxygen-rich environments under neutral to alkaline pH conditions. Zero-valent (or elemental/native) iron (Fe(0)) is also found under some specific environmental and geological conditions [3].

Iron oxides exist in many forms in nature and magnetite ( $Fe_3O_4$ ), maghemite ( $\gamma-Fe_2O_3$ ), and hematite ( $\alpha-Fe_2O_3$ ) are the most common forms [4]. In recent years, the synthesis and utilization of iron oxide with novel properties and functions have been widely studied, due to their size in a nano-range, high surface area to volume ratios and super paramagnetism [5]. In pollutant treatment iron oxide has been investigated for dye removal with great success [6] as well as for heavy metal removal [7] and so on. In an aqueous environment of wastewater treatment the advanced oxidation processes (AOPs) have attracted more attention because of the formation of hydroxyl radicals ( $HO^\bullet$ ) during degradation, which are the most powerful oxidizing species besides fluorine [8]. In the AOPs technologies, the Fenton-like reaction has been proven to be one of the most effective ways to degrade organic pollutants and this is based on solid-liquid interface reactions. Fenton-like reaction has more advantages than homogeneous Fenton reaction with regard to less generation of ferric sludge and mild reaction conditions [9]. Consequently, reuse and recovery of HWW is a feasible and cost saving technique for remediation

of dyes in wastewater and to provide other pollutant remediation. The main purpose of this study was to 1) investigate the degradation effect of AR27 dye in waste water by using reused hand-warmer waste (HWW) under different pH and hydrogen peroxide dose conditions. 2) to study the decolorization and the TOC (total organic carbon) removal effect by adding hydrogen peroxide dose. 3) find an applicable method for the waste disposal treatment in the future treatment of dye wastewater.

## MATERIALS AND METHODS

### Hand-warmer waste (HWW) preparation.

Hand-warmer waste (HWW) was purchased from supermarkets and recovered after normal use and from the Kobayashi Co. This experiment used clean materials to open the hand-warmer sand put them in air for 24 hours until they did not feel warm. Others were recovered from normally used materials for comparison of the different TOC residue. Each experiment dried the materials at 105°C after being weighed and well mixed.

**Materials.** AR27 dye, and H<sub>2</sub>O<sub>2</sub> (30%, w/w) were used in this study. HNO<sub>3</sub> and NaOH were purchased directly from Aldrich Sigma Inc., And HNO<sub>3</sub> and NaOH were in analytical grade and they can be used in experiments directly without any further purification.

**Experimental process.** Batch experiments were conducted in 1000 ml glass beakers. AR27 1000ml pigment was added into the reaction vessel by using a stirrer with 300 rpm stirring speed to conduct this experiment. In addition, substrate dosage as the experimental parameter accompanied with various dye concentrations and different pH conditions varied with time interval were also involved in this reaction process. Moreover, Fenton-like reaction effect by adding of hydrogen peroxide into this process was also discussed.

**Analytical methods.** AR27 concentrations were measured using a spectrophotometer UV-vis (JASCO V-530) and recording its absorbance at 520 nm. The pH values were recorded by a pH meter. BET surface area was determined from the nitrogen adsorption isotherms obtained at -196°C in a Quanta chrome Coulter apparatus with analyzed by BET-201-AC(Germany). The characterization analyzed by high resolution X-ray diffractometer

(D8 Discover SSS, Germany). All samples were centrifuged prior to analysis.

## RESULTS AND DISCUSSION

**The characterization of hand-warmer waste. N<sub>2</sub> adsorption Specific Brunauer–Emmett–Teller (BET).** A N<sub>2</sub> adsorption isotherm at 77 K of HHW sample (see Fig. 1) indicates that this material has a combination of micropores and mesopores. However, after the ion exchange the volume of N<sub>2</sub> adsorbed at low values of P/P<sub>0</sub> decreased, suggesting a reduction in the available microporosity. The determined pore volume, BET surface area and advantage pore diameter (4V/S) were 0.16 cm<sup>3</sup>/g, 125.18 m<sup>2</sup>/g and 52.7710 Å, respectively.

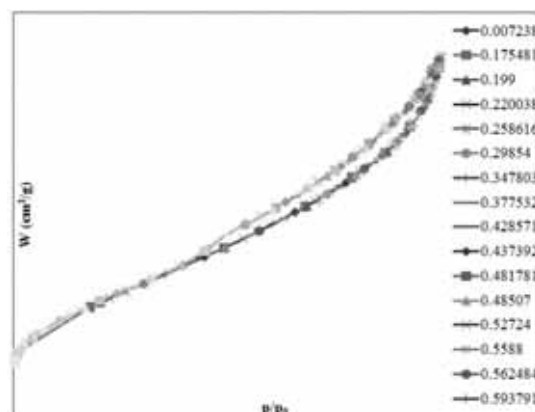


FIGURE 1  
N<sub>2</sub> adsorption isotherm of hand-warmer waste.

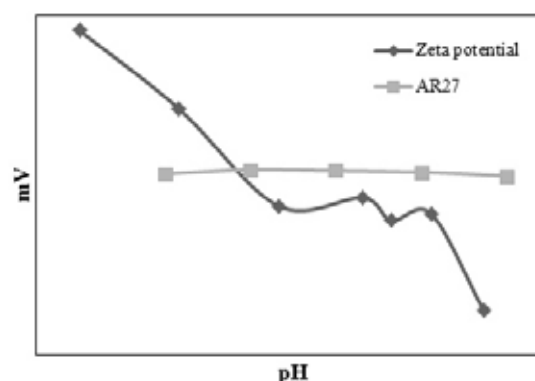


FIGURE 2  
Point of zero charge (PZC) of HHW and AR27.

**ZPC analyses of hand-warmer waste.** Figure 2 displayed the results of the point of zero charge (PZC) of the HHW sample. It showed that the PZC

value was 4.6, suggesting that at pH 4.6–11 the HHW particles are negatively charged, which cannot facilitate the anionic AR27 adsorption on their surface.

#### XRD analyses of hand-warmer waste.

Figure 3 shows that there were peaks appeared at the angle  $2\theta$  of  $20.8^\circ$ ,  $35.3^\circ$ ,  $50.03^\circ$ ,  $62.4^\circ$ , respectively. The above results further identified that the material should belong to  $\gamma\text{-Fe}_2\text{O}_3$  maghemite according to the JCPDS card (No. 13-0534).

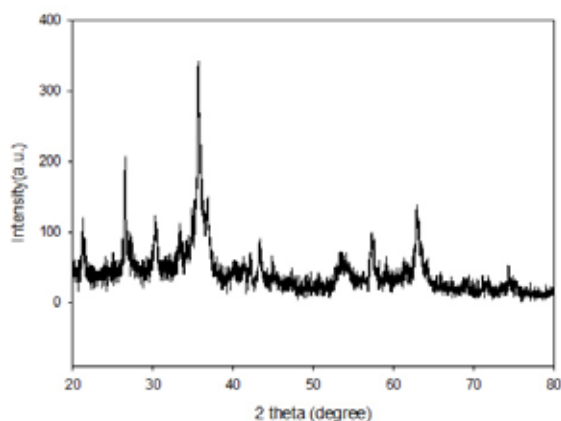


FIGURE 3

X-ray diffraction analysis results.

**Hand-warmer waste for dye adsorption effect. Different hand-warmer waste dosages for dye adsorption effect.** Fig. 4 shows the adsorption reaction in a non-controlled pH for dye concentrations of 40 ppm AR27 by HHW amounts in 3 g, 10 g, 30 g and 50 g with a reaction time of 150 min for decolorization of 4.05%, 16.78%, 63.78% and 92.33%, respectively. The results indicated that the adsorption capacity rises because larger amounts of space provide more adsorptive sites. Consequently, greater amounts of HHW may affect the adsorption of AR27 dye.

**Different pH conditions for dye's adsorption effect.** The results of a 40 ppm AR27 solution with the HHW of 30 g in pH 3, pH 5, pH 7, pH 11 and non-controlled pH levels are shown in Fig. 5. At a reaction time of 120 min, the decolorization efficiency of AR27 achieved 98.69% in a solution of pH 3; other results for pH 5, pH 7, pH 11 and non-controlled pH levels were 67.87%, 42.25%, 40.57% and 16.78%, respectively. Solutions with pH 3 or pH 5 definitely had significant adsorption effects.

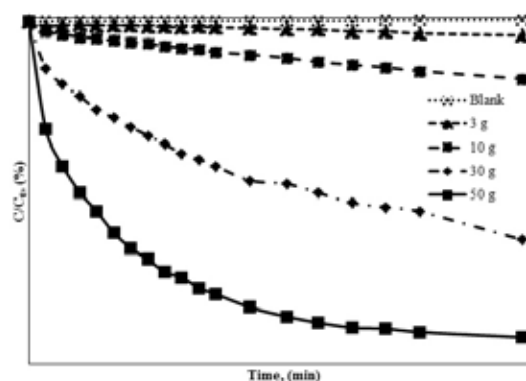


FIGURE 4

Decolorization effect of different HHW amounts for AR27 40 ppm and non-controlled pH levels.

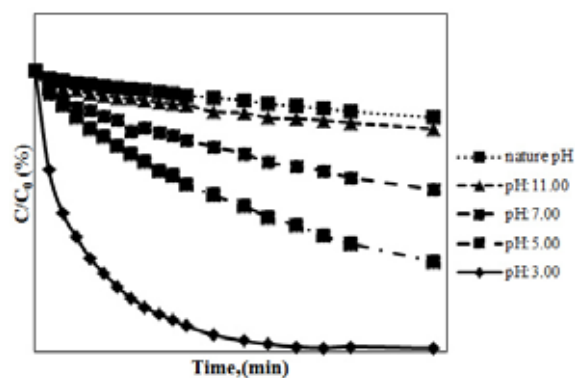


FIGURE 5

Decolorization effect of solutions with different pH levels for HHW of 10 g and AR27 of 40 ppm.

**Different dye concentrations adsorption effects.** The results of different AR27 concentrated solutions with the HHW of 10 g in a solution with pH 3 are shown in Fig. 6. The results indicated that the obtained values were 98.69%, 87.35% and 75.32% for 40 ppm, 80 ppm and 120 ppm, respectively. The results further indicated that a solution with pH 3 has a great decolorization effect.

**Added  $\text{H}_2\text{O}_2$  for reaction. Added  $\text{H}_2\text{O}_2$  for dye decolorization removal effect.** The reactor added to  $\text{H}_2\text{O}_2$  for decolorization removal effect, shown in Fig. 7.

The results show the decolorization rate was increased from 42.05% to 61.37% (0.0128 mmol) which indicated that decolorization effect was obtained by adding hydrogen peroxide to produce hydroxyl radicals in the reaction vessel. However, hydroxyl radical interaction was decreased by adding too much hydrogen hydroxide into the reaction vessel. And, thus, the decolorization effect



was also decreased.

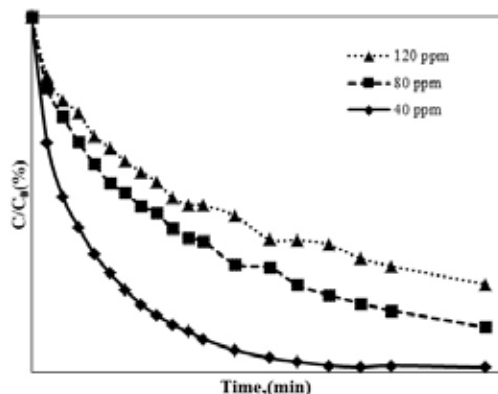


**FIGURE 6**  
Decolorization of different concentrations of HWW 10 g in pH 3 solution.

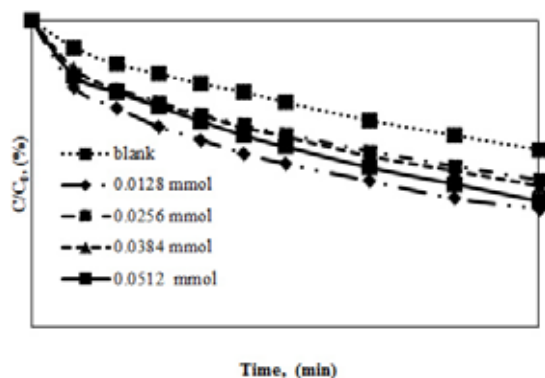


**FIGURE 7**  
Decolorization removal effect of 10 g HWW in a solution with pH 5 (dye concentration 40 ppm).

**Added H<sub>2</sub>O<sub>2</sub> for removal of dye in different pH conditions.** Hydrogen peroxide is an efficient metal ion sorbent and it can also create Fenton's reaction. Figure 8 showed the decolorization removal efficiency under different pH conditions after adding 0.0128 mmol hydrogen peroxide (purity of 30%) and 10 g HHW for 40 ppm AR27 dye. A low pH creates a Fenton reaction with a good effect, but a high pH 11 also has better effect.

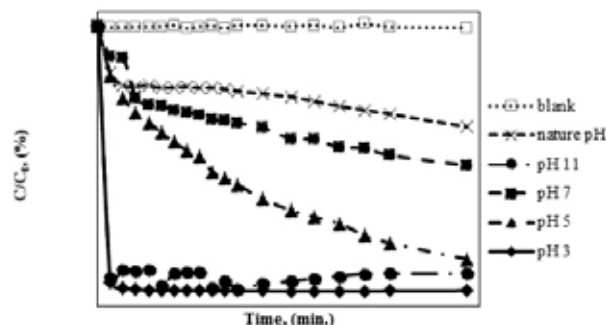


**FIGURE 8**  
Decolorization with 10 g HWW dosage at different pH levels (H<sub>2</sub>O<sub>2</sub> concentration 0.0128 mmol).

**Continue running experiment of decolorization removal effect.** Four-cyclic reaction was designed for the substrate (material) in order to obtain the repetitive recycling efficiency in this study. The first cycle reaction was processed by adding 30 g. substrate (material) dosage with dye of 40 mg/L concentrations. After that, the absorption reaction was then processed for 60 minutes. 40 mg of dye was then adding into this reaction vessel to make the concentrations back to about 40 mg/L. Peroxide hydrogen with concentrations of 0.0128 mmol dosage were then added into this vessel for 60 min. to complete the second recycle process. The third recycle process was continued the above cycle for another 60 min. After that, 40 mg/L of dye combined with

0.0128 mmol dosage of peroxide hydrogen were then added into this reaction vessel to complete the fourth cycle process. The sampling time interval was set at 5 min., 15 min., 30 min. and 60 min., respectively in this study.

As shown in Fig. 9, when substrate is treated with the ratio of substrate 30 g. with the dye concentration 40 mg/L, accompany with by addition of hydrogen peroxide to produce hydroxyl radicals oxidizing the substrate surface dye, the adsorption capacity of the substrate can be maintain. Moreover, decolorization rate with more than 80 % can be achieved for four cycle reactions process.

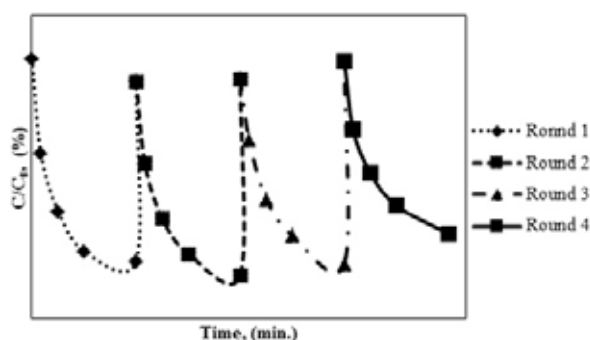


**FIGURE 9**

**Continue running experiment of decolorization removal effect (dosage 30 g, dye concentration 40 mg/L, H<sub>2</sub>O<sub>2</sub> 0.0128 mmol).**

## CONCLUSIONS

The earth resources will be used up due to the over developments for human beings with limit amounts of resources on earth. Therefore, how to recycle the discarded waste on earth has become the most important issue for people.

This study investigated the use of recycled hand-warmer wastes, which is used in dyeing wastewater treatment, the results are shown in natural water pH value in the substrate concentration 50 g dose of 40 ppm of AR27 dye wastewater obtained 92.33 % of decolorization efficiency by experimental analysis. The results can be obtained as followed by controlling different pH values in this study. It was shown as followed: Substrate with concentrations of 10 g dose of AR27 40 ppm of dye wastewater with pH 3 can have the best decolorization efficiency. The decolorization efficiency can also achieved 75.32% when AR27 concentrations increased to 120 ppm.

This study discussed the treatment of decolorization efficiency by adding the hydrogen peroxide in the dye wastewater. The results indicated that the decolorization efficiency was increased by adding hydrogen peroxide at 10 g, substrate dose with 40 ppm AR27 under pH 5 with reaction time of 60 min. Optimus results can be obtained by adding 0.0128 mmol dosage of hydrogen peroxide in the dye wastewater for this study. However, the results further indicated that the decolorization efficiency decrease as the amounts of hydrogen peroxide dose increase in the dye wastewater. The proposed reason is that excess of hydroxyl radicals to produce a chemical reaction with each other, so that hydroxyl radical number

decrease in the oxidation of dye in the wastewater. This study further showed that the optimum decolorization efficiency can be obtained by adding hydrogen peroxide at 10 g, substrate dose with 40 ppm AR27 under pH 3. This finding is the same as the previous study achieved by Fenton reactions. This research also found that the decolorization efficiency can be obtained at pH 11. This result is just opposite to the result conducted by adsorption experiment at the same pH 11 which revealed that less decolorization efficiency was found. Thus, Fenton reaction under heterogeneous base under conditions can also produce colorization effect.

This experiment confirmed that the use of recycled waste Nuan nuan Bao for the dye wastewater treatment is a feasible and efficient method. It can not only recycle waste and further reduce environmental pollutants. This study, In fact, provided an applicable method for the waste disposal treatment and can be further applied in the treatment of dye wastewater.

## REFERENCES

- [1] Andrew Porteous, (1997) Energy from Waste: A Wholly Acceptable Waste-management Solution Original Research Article Applied Energy, Volume 58, Issue 4, p 177-208
- [2] Andrew B. Cundy, Laurence Hopkinson, Raymond L.D. Whitby. (2008) Use of iron-based technologies in contaminated land and groundwater remediation: A review, Original Research Article Science of The Total Environment, Volume 400, Issues 1–3, p42-51
- [3] D.M. Cwiertny, S.J. Bransfield, K.J.T. Livi, D.H. Fairbrother, A.L. Roberts. (2006) Exploring the influence of granular iron additives on 1,1,1-trichloroethane reduction, Environ. Sci. Technol. Volume 40, p6837–6843.
- [4] U. Schwertmann, J. Friedl, G. Pfab (1996) A New Iron(III) Oxyhydroxynitrate Journal of Solid State Chemistry, Volume 126, Issue 2, p 336
- [5] M.E. McHenry, D.E. Laughlin, (2000) Nano-scale materials development for future magnetic applications, Original Research Article Acta Materialia, Volume 48, Issue 1, p 223-238



- [6] Yan Dong, Huiming Lin, Fengyu Qu, (2012) Synthesis of ferromagnetic ordered mesoporous carbons for bulky dye molecules adsorption, Original Research Article Chemical Engineering Journal, Volumes 193–194, p 169-177
- [7] Nicola Moraci, Paolo S. Calabrò, (2010) Heavy metals removal and hydraulic performance in zero-valent iron/pumice permeable reactive barriers, Original Research Article Journal of Environmental Management, Volume 91, Issue 11, p 2336-2341
- [8] L. Gu, F.Y. Song, N.W. Zhu,(2011) An innovative electrochemical degradation of 1-diazo-2-naphthol-4-sulfonic acid in the presence of Bi<sub>2</sub>Fe<sub>4</sub>O<sub>9</sub>, Appl. Catal. B: Environ. 110, p 186–194.
- [9] V. Camel, A. Ventura, G. Jacquet, A. Bermond, (2002) Electrochemical generation

of the Fenton's reagent: application to atrazine degradation, Water Res. 36,p3517–3522.

---

**Received: 06.02.2016**

**Accepted: 20.08.2016**

---

**CORRESPONDING AUTHOR**

---

**Chih-Tsung Tsai**

Department of Environmental Engineering

National Chung-Hsing University

145 Xingda Rd., South Dist., Taichung - TAIWAN

E-mail: [only5341@yahoo.com.tw](mailto:only5341@yahoo.com.tw)

# PEDO-STRATIGRAPHICAL RECORDS OF AL-WU' AIRA CASTLE (PETRA, JORDAN)

Mohammad Wahsha<sup>1,\*</sup>, Raid Al-Jawasreh<sup>1</sup>, Marta Mariotti Lippi<sup>2</sup>, Mohammad Al-Tawaha<sup>3</sup>, Claudio Bini<sup>4</sup>

<sup>1</sup> Marine Science Station, The University of Jordan, Aqaba branch, Jordan

<sup>2</sup> Department of Plant Biology, University of Florence, Italy

<sup>3</sup> The Royal Marine Conservation Society of Jordan (JREDS), Aqaba, Jordan

<sup>4</sup> Department of Environmental Sciences, Informatics and Statistics, Ca' Foscari University of Venice, Italy

## ABSTRACT

Al-Wu'Ayra castle is a Crusader fortified settlement located near Petra in the southern Jordanian governorate of Ma'an. Five stratigraphic sections were excavated in the archaeological area at al-Wu'Ayra to better understand the environmental conditions prevailing during the Crusader settlement and the reasons for the rapid abandonment of the site. Geopedological investigations indicate a limited evolution of the site over the last thousand years, with arenosols characterising limited stages of pedogenesis.

## KEYWORDS:

Pedostratigraphy, Petra, Archaeology.

## INTRODUCTION

Petra is an archaeological site about 250 kilometres south of Amman, Jordan, in a basin among the mountains east of Wadi Araba valley that extends from the Dead Sea to the Gulf of Aqaba. Petra is half-carved into the rock, with an altitude between 800 and 1396 m above the sea level and is surrounded by mountains riddled with passages and gorges. The site is accessible only from the north-west, a narrow mountain path, and from the east through a canyon about 1.5 kilometres long and up to 200 meters deep, the Siq, which housed the main access road. Petra is one of the world's most well-known archaeological sites, where ancient Eastern traditions blend with Hellenistic architecture [1].

Petra is part of a network of fortified sites located along the way from North to South of Jordan (Aqaba, Fig. 1), that constituted the strategic defence system of that land.

The al-Wu'Ayra Crusade castle, one of the fortified sites, is located on the summit of a rocky hill (Jabel Wu'Aira), close to Petra, on the road from el-Bared to Wadi Mousa. Geologically, the entire area is composed of coarse, whitish arenaceous limestone

with typical, rounded "inselberg" structures derived from the strong erosion processes that affected all the jebels of the region, especially during the Quaternary [2]. Indeed, several aggradational and erosional phases, caused by climatic fluctuations, are known in the area for the Late Pleistocene and Early Holocene [3-4]. Holocene geomorphic changes in the area are prevalently represented by alternating sequences of wadi alluviation during winter rains and erosion during dry periods [5]. In chronological terms, important deposition/erosion phases occurred in the early Neolithic, probably during the 6<sup>th</sup> and perhaps the 5<sup>th</sup> millennia Before Christ (BC). The 4<sup>th</sup> millennium BC (Bronze Age) saw the greatest human impact on the environment, e.g. increased deforestation and overgrazing. Afterwards, during the Iron Age (1200-580 BC) deposition re-occurred, evidenced by angular, poorly sorted gravels and sands elevated from abandoned hill slopes [3]. Finally, during the late Roman, Byzantine and early Arabic periods, the climate appears to have improved [5], although much of the alluvial accumulation may have resulted from agricultural activities [2-6].



**FIGURE 1**  
General map of the Crusader settlements in Transjordan and the Petra archaeological area.

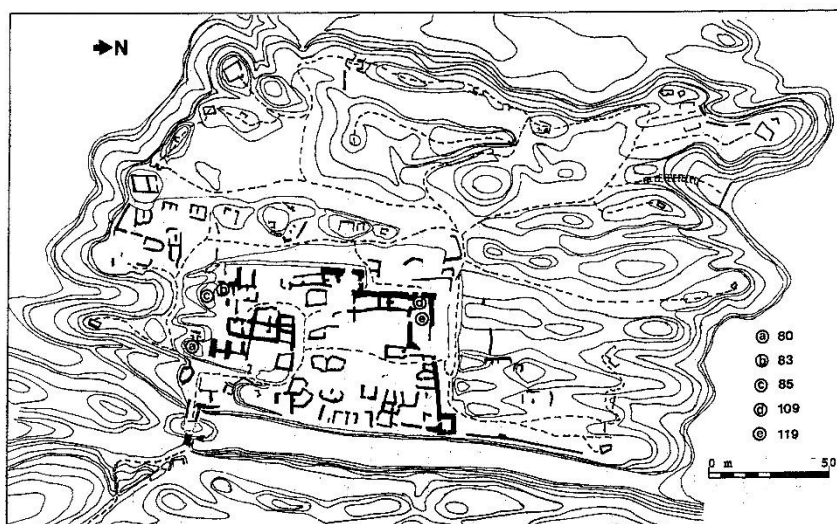


**FIGURE 2**

**Topographical sketch of the investigated area at Al-Wu'aira, with an indication of the stratigraphic sections examined (a=section 80; b=83; c=85; d=109; e=119). Thick black lines represent archaeological ruins.**

A period of aggradation period with remarkable sedimentation began around AD 1200 (Late Crusade Period), when progressive filling raised the wadi bed several meters. Down cutting and stream channel erosion occurred again in about AD 1700, and is still in progress until today [7]. Correspondingly, the vegetation cover changed several times; the original Mediterranean forest gradually degraded to forest-steppe and then to the present steppe-desert conditions [8].

The present-day climate is characterised by semi-desert conditions (maT = 25°C, maP = 150mm: data from the Meteorological Department, Amman), with episodic rainfall in winter [9]. Typical soils are sandy, shallow, grey in colour and rich in lime. The vegetation cover is scarce, with mostly Irano-Turanian steppe elements [7-10].

## **MATERIALS AND METHODS**

During the archaeological survey, five stratigraphic sections were excavated at different sites within the al-Wu'Aira area (approx 600 mq, Fig.2) in order to establish the main environmental conditions preceding or connected with human occupancy.

Each stratigraphic section was described in the field following the Soil Survey Manual [11]. Depth, colour, texture, structure, stones and reaction were chosen as the most important characters to identify the different stratigraphic levels. Representative samples of each layer were collected, air dried to a constant weight, and sieved through a 2 mm stainless sieve to separate skeleton from fine earth for standard laboratory analyses [12]. On the fine earth, routine analyses were: particle size distribution following the method recommended by

Wahsha et al. [13] and Zilioli et al. [14]; pH in water (1: 2.5 soil-water suspension) was measured potentiometrically following the protocol of Violante and Adamo [15]; organic carbon based on the method described by Walkley and Black [16]; available phosphorous (Olsen); total carbonates (gas-volumetric) was carried out according to the manual of the Italian Ministry of Agriculture and Forestry [15]. Undisturbed samples from selected horizons were embedded in epoxy resin to obtain thin sections for micromorphological investigations by light microscopy, following Bullock et al. [17].

## **RESULTS AND DISCUSSION**

The field description and physical and chemical characteristics of the investigated sections are reported in Table 1.

**Section n° 109.** This site is located in an open area near the Crusade cemetery, close to the church (Fig. 2). The entire sequence consists of five horizons. The parent material is a whitish arenaceous limestone, the same that constitutes most of the geology of the entire Al-Wu'Aira area. A shallow (60 cm) soil profile developed over this rock. The colour is yellowish (10YR 6/4 – 2.5 Y 6/2). The overall texture is a coarse loamy sand on the surface, with a finer texture (sandy loam) at the bottom. The structure is weak blocky, with the exception of level 1 (A horizon) where plant roots render the structure crumbly. Stoniness varies irregularly throughout the layers, suggesting some disturbance over time, The HCl-test reaction is strong to very strong in the overall section. The pH is alkaline, and carbonates occur down the whole section, with little increase in the subsoil.

**TABLE 1**  
Selected properties of the different stratigraphic units.

Section number	Layer	Depth cm	Colour	Texture	Structure	Stoniness %	Reaction
109	1	0-10	10YR6/3	loamy sands	crumb	15	strong
	2	10-25	10YR6/4	loamy sands	loose	50	strong
	3	25-35	10YR6/2	loamy sands	loose	25	strong
	4	35-45	2.5Y6/2	loamy sands	blocky	No	moderate
	5	45-60	2.5Y6/2	sandy loam	blocky	5	strong
119	1	0-140	7.5YR4/4	colluvium	loose	70	strong
	2	140-180	5YR5/1.5	loamy sands	blocky	No	strong
	3	180-190	5YR2.5/2	loamy sands	blocky	No	strong
	4	190-200	7.5YR5/4	sand	loose	No	strong
	5	>200	grey	limestone	rocky	90	strong
83	1	0-35	7.5YR4/4	loamy sands	sub blocky	70	strong
	2	35-40	7.5YR3/3	loamy sands	sub blocky	No	strong
	3	40-50	10YR4/3	loamy sands	sub blocky	No	strong
	4	50-78	10YR3/4	sandy loam	massive	10	strong
	5	78-90	10YR5/4	loamy sands	loose	10	strong
85	1	0-5	2.5Y4/2	sand	massive	5	moderate
	2	5-10	2.5Y7/3	sand	massive	No	strong
	R	>10	greyish	sandstone	rocky	90	moderate
80	1	0-30	10YR7/6	loamy sands	blocky	15	strong
	2	30-43/50	10YR7/4	sandy loam	blocky	25	strong
	3	43/50-65	10YR6/4	loamy sands	massive	15	strong
	4	65-80	10YR6/6	loamy sands	loose	5	strong
	5	80-90	10YR5/5	loamy sands	loose	No	moderate

Organic C and P decrease regularly with depth. The high P concentration, however, suggests that intense human frequentation occurred at this site.

Micromorphological examination of the thin sections from three horizons, corresponding to field descriptions n° 109/3, 109/4 and 109/5 (see Table 1), revealed the following features. The coarse fraction (>10  $\mu$ m, according to Bullock et al. [17]) consists mostly of fine quartzose sand with lesser amounts of fine calcite silt. The fine fraction (<10  $\mu$ m) consists of finely divided and dispersed quartz grains mixed with a dark brown plasmic material, which has an undifferentiated b-fabric (Fig. 3a). In sample 109/3, well preserved coatings occur in the form of non-laminated, limpid yellow-brown clay and dusty dark yellow-brown clay (Fig. 3b). Sample 109/4 shows a higher degree of aggregation in the matrix, with brown clay papules bordering mineral grains. Sample 109/5 exhibits a subangular blocky structure with a scarcely birefringent groundmass characterised by some brownish, opaque Fe-Mn nodules. Field and laboratory data: structure, organic carbon and phosphorus content suggest that this section represents a “*sensu stricto*” soil profile (Haplic Arenosol), developed from aeolian

depositional

events of approximately a thousand years ago, then briefly cultivated in the upper portion during the Crusader settlement.

**Section n°119.** This section was excavated at the site corresponding to the Crusade church, and therefore the time-span stretches from the establishment of the church (AD 1165) to its collapse and abandonment (AD 1185).

This sequence consists of 4 layers developed over the basal level consisting of large calcareous stones. The deepest (layer 4) is brown, sandy, loose, subalkaline and calcareous. Over this is a loamy sand, subalkaline, calcareous blackish level (layer 3). Although organic C and P occur in a rather low percentage, the dark colour (5YR2.5/2) and the weak blocky structure point to the occurrence of a fire. The next level upwards (layer 2) is a greyish-brown (5YR 5/1.5) loamy sand, weakly structured, alkaline, calcareous, and rich in fresh vegetal remnants and fecal pellets. Over this organic-rich layer is a deep deposit of colluvial, stone-rich material (layer 1), which accumulated after the collapse of the church, possibly as a consequence of the above mentioned

fire. As shown in Table 1, with the exception of layer 1, pH, carbonates, organic C and P decrease with depth along the whole section, while sand increases. Microscopic observations showed that the deepest layer (4°) is composed of a mosaic of fine calcite crystals (silt size), with little plasmic material (Fig. 3c). Layer 3 exhibits a spongy structure with large pores and interconnected chambers. Abundant charcoal fragments, plant remnants and burnt soil matrix constitute the solid phase and indicate that a natural or man-induced fire occurred during the Crusader settlement. Mineral components are scarce quartz grains embedded in a brown apedal groundmass (Fig. 3d). The mineral components in layer 2 prevail over the organic. Plant residues are unburnt, light brown, elongated fibres or spherical fragments. The latter are probably fecal pellets transported by gravity and are composed of yellow vegetal fibres, aggregated and intimately mixed with small mineral grains. A concentration of these pellets was found in the uppermost part of this layer.

Charred and uncharred wood was collected from layers 3 and 2 at this site. Morphological characteristics by scanning electron microscope (SEM) observations of these remnants suggest they belong to *Retama raetam* (Forssk.) Webb. The samples from layer 2 in particular show a peculiar state of preservation: in transverse sections, clusters of cells, very different in size, show a small cylindrical process in the middle of the lumen. This cylindrical process proved to be hollow and is connected to the outer wall by tiny threads. There cells are likely to be deteriorated non-storied fibres. The external wall corresponds to the middle lamella (with or without the primary wall), and the cylindrical process to the innermost layer of the wall. The data recorded indicate that the whole section consists of soil sediments displaced by gravity *in situ*, as a result of the structural collapse of the site.

**Section n°83.** This was excavated close to the site of an Arab smelter established after the Crusaders departed (AD 1189). It consists of five levels (for a total of 90 cm) of a loamy sand to sandy loam deposit with very weak alteration (see Table 1). The bottom level is light brown (10YR 5/4), loose, alkaline and calcareous. Unidentified charcoal and ceramic fragments are frequent and a stone line occurs at the bottom. Organic matter and P levels (Table 1) point to human settlement related to the first archaeological phase, early 12° century [18]. Above this level, a yellowish (10YR 3/4) compact, thick layer formed the base of a castle pavement (II archaeological phase, AD 1165-1185) during the Crusader settlement. Abundant charcoal fragments, massive structure, organic C and P support this suggestion.

A 10 cm thick layer overlies the former and represents the last Crusader settlement before their departure (III archaeological phase, AD 1189). It is

yellowish brown (10YR 4/3), sandy loamy, subalkaline, calcareous, weakly structured and with abundant charcoal fragments. An Arab smelter was established here at the end of 12° century, and was abandoned in the middle 13° century [18]. The uppermost layers are quite different from the previous, as can be seen from the physical characteristics and chemical data (Table 1). In particular, there is much less organic C and P than in the previous levels. This suggests the cessation of human activity, as indicated by archaeological records. Microscopically, the entire section is very homogeneous: it consists of loose quartz and (minor) calcite grains embedded in a brownish, apedal groundmass, with clay papules bordering mineral grains (Fig. 3e). The whole section appears composed of strongly disturbed and reworked archaeological horizons, as indicated by macro and micro morphological features.

**Section n° 85.** This section was excavated under a partially destroyed Eneolithic shelter (4,800 BP). Two levels were identified. The lowermost is sandy in texture; structure is massive to coarse angular blocky, hard when dry, alkaline and weakly calcareous. Organic matter and P are very low (see Table 1). The uppermost layer is windblown calcareous sand with a weak layered structure and alkaline reaction.

The origin of these two levels is clearly attributable to aeolian deposition under arid conditions. Two kinds of features may be distinguished:

- Sediments consisting essentially of sub-round, etched sand grains (upper layer, Fig. 3f), well sorted (150-200 µm);
- Non sorted sand grains (lower layer), consisting of a mixture of sub-round grains, as above, bordered or simply capped by plasmic material.

The former is the result of reworked aeolian sedimentation (recent depositional phase), the latter corresponds to runoff phases, which reworked sediments from the nearby rocks and soils. Our data and field evidence suggest that the whole section represents a recent aeolian deposit, formed in a short time after the shelter collapsed, with weak reworking, as indicated by sand grain etching and capping.

**Section n° 80.** This section was excavated close to the site of a prehistoric shelter, subsequently used by the Crusaders as a site guarding access to the castle.

It consists of 5 levels, all archaeologically sterile and weakly differentiated. Texture is sandy loam to loamy sand, reaction sub-alkaline with very high carbonates. The characteristics that render the levels different are structure, stoniness and the irregular distribution of organic C and P, as shown in

Table 1. Level 80/2 has a coarse angular blocky structure, frequent stones, alkaline reaction and high carbonates. The decrease in the amount of sand, organic C and P points to pedogenic reworking, in comparison with the subsequent levels. The top layer (80/1) is yellowish (10YR 7/6 dry), sandy loam with fine angular blocky structure and a surface crust (3 cm deep), suggesting the level is weakly pedogenised. The fine fraction (<10 m) is dominated

by brown silt and moderately oriented, speckled clay with weakly reticulate striated b-fabric.

The whole deposit, in our opinion, consists of post-depositional (colluvial) material carried in place by gravity and water or wind, with some pedogenic reworking, after the castle was abandoned (AD 1189). It is therefore likely to be about 800 years old.

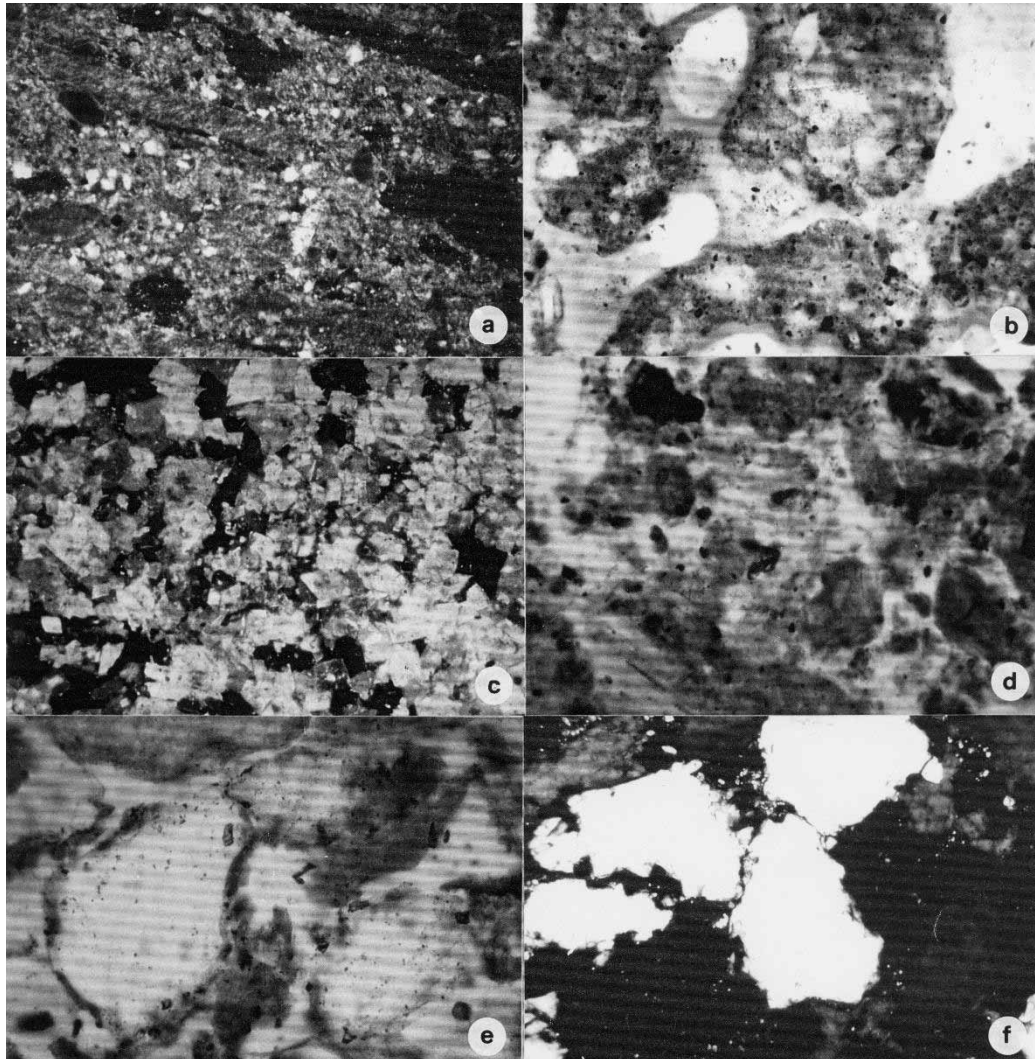


**FIGURE 3**

**Micrograph of thin sections from undisturbed samples collected at different sites in the investigated area.**

- Fine quartz crystals embedded in dark brown plasmic material with undifferentiated b-fabric (32x) from sample 109/3.
- Limpid yellow-brown clay coatings bridging and bordering dusty dark brown plasmic material (64x) from sample 109/3.
- Mosaic of fine calcite crystals, with very reduced pore space and a little plasmic material bordering the mineral fragments (32x) from sample 119/4.
- Apedal groundmass with dark brown clay papules (32x) from sample 119/3.
- Loose quartz grains (q) bordered by pale brown, limpid clay films (c) and papules (64x) from sample 83/3.
- Loose etched quartz grains, well sorted. Groundmass is almost absent (64x). Sample 85/1.



## SUMMARY AND CONCLUSIONS

The stratigraphic sections were excavated at different sites corresponding to different archaeological units of the castle area. These units conform to a limited time-span, ranging from about 1000 AD to the present day.

All the profiles showed generally uniform physico-chemical characteristics, derived from the parent rocks in the surrounding uplands. They are characterised by weak pedogenic alteration, have a single grain structure with very weak consistency in the sandy layers and a subangular blocky structure in the loamy layers, sub-alkaline reaction, little organic C and P. The data recorded are consistent with disturbed, archaeologically related deposits that have undergone some pedogenic reworking, particularly recognisable in thin sections. Pedogenic features such as corrosion, aggregation, caps and coatings point to short-term pedogenesis (one thousand years) of reworked soil material, with the formation of weakly developed Arenosols.

With regard to plant history, the highest number of Mediterranean trees and shrubby plants occurs in the most ancient levels (samples 109/5, 109/4, 85/2). This suggests that the dominant vegetation in the area was previously of Mediterranean type; it later became highly impoverished and degraded into steppe vegetation [2]. The decrease in Mediterranean flora elements coincides with the introduction of cultivated Cerealia. This cultivation lasted over a brief interval and can be referred to the Crusader settlement in the area (AD 1165-1189).

The landscape surrounding the castle appears to have remained quite similar in its global delineation since the Medieval Age up to today, and is consistent with the steppe vegetation of the Mediterranean region.

## REFERENCES

- [1] Seeger, J., Gus, W. and Beek, V. (1996) Retrieving the Past: Essays on Archaeological Research and Methodology. Eisenbrauns. p. 56.
- [2] Mariotti Lippi, M., Mori Secci, M., Bini, C. (2008) Archaeobotany in the Crusader castle of al-Wu'Aira (Petra, Jordan). *Journal of Plant Taxonomy and Geography*. 63: (1), 69-79.
- [3] Pringle, D. (1993) *The Churches of the Crusader Kingdom of Jerusalem: A Corpus: Volume 2, L-Z*. Cambridge University Press, P. 480.
- [4] Goldberg, P. (1986) Late Quaternary environmental history of the southern Levant. *Geoarchaeology*. 1: 224-244.
- [5] Goldberg, P., Bar-Yosef, O. (1990) The effect of man on geomorphological processes based upon evidence from the Levant and adjacent areas. In *Man's role in the shaping of the eastern mediterranean landscape*. Bottema, Entjes-Nieborg and Van Zeist (eds), 71-86.
- [6] Bruins, H.J. (1990) The impact of man and climate on the Central Negev and NE Sinai desert during the late Holocene. In *Man's role in the shaping of the eastern mediterranean landscape*. Bottema, Entjes-Nieborg and Van Zeist (eds), 87-99.
- [7] Nicolle, D. (2004) *Crusader Castles in the Holy Land 1097-1192*. Osprey Publishing Volume 21: P.
- [8] Horowitz, A. (1992) *Palinology of arid lands*. Elsevier, N.Y., 341-389.
- [9] Jenny, M., Smettan, U. and Facklam-Moniak, M., 1990. Soil-vegetation relationship at several arid microsites in the Wadi Araba (Jordan). *Vegetatio*. 89: 149-164.
- [10] Al-Eisawi, D. (1985) *Vegetation of Jordan*. In: Hadidi A. *Studies in the history and archaeology of Jordan*. II. Ministry of Archaeology. Amman: 45-57.
- [11] Soil Survey division staff. (1990) *Soil Survey Manual*. United States Department of Agriculture, Handbook N° 18, Washington DC.
- [12] Wahsha, M., Bini, C., Zilioli, D., Spiandorello, M., Gallo, M. (2014a) Potentially harmful elements in terraced agroecosystems of NE Italy: Geogenic vs anthropogenic enrichment. *Journal of Geochemical Exploration*. 144: 355-362.
- [13] Wahsha, M., Fontana, S., Nadimi-Goki, M., Bini, C. (2014b) Potentially toxic elements in foodcrops (*Triticum aestivum* L., *Zea mays* L.) grown on contaminated soils. *Journal of Geochemical Exploration*. 147: 189-199.
- [14] Zilioli, DM., Bini, C., Wahsha, M., Ciotoli, G. (2011) The pedological heritage of the Dolomites (Northern Italy): Features, distribution and evolution of the soils, with some implications for land management. *Geomorphology*. 135 (3): 232-247.
- [15] Violante, P., Adamo, P. (2000) III. Reazione. In: Violante, P. (Ed.), *Metodi di analisi chimica del suolo*. Ministero per le Politiche Agricole e Forestali, Osservatorio Nazionale Pedologico e per la Qualità del Suolo. Franco Angeli Editore, Milano.
- [16] Walkley, A. and Black, I.A. (1934) An examination of the Degtjareff method for determining soil organic matter, and proposed modification of the chromic acid titration method. *Soil Sci*. 37: 29-38.
- [17] Bullock, P., Fedoroff, N., Jongerius, A., Stoops, G., Tursina, T., (1985) *Handbook for soil thin sections description*. Waine Research Publ., Wolverhampton.
- [18] Vannini, G. and Vanni Desideri, A. (1995) Archaeological research on medieval Petra: a preliminary report. *Ann. Department of Antiquities, Jordan*. 39: 509-540.



---

**Received:** 09.02.2016  
**Accepted:** 28.09.2016

---

**CORRESPONDING AUTHOR**

---

**Mohammad Wahsha**  
Marine Science Station  
P.O. Box: 195  
Aqaba 77110- Jordan

e.mail: [m.wahsha@ju.edu.jo](mailto:m.wahsha@ju.edu.jo)

# HISTOPATHOLOGICAL EVALUATION OF EFFECTS OF LEAD HEAVY METAL APPLIED TO CALIFORNIAN RED WORM (*EISENIA FOETIDA*) ON SKIN TISSUE

Nurgul Senol\*

Süleyman Demirel University, Faculty of Health Sciences, Isparta, TURKEY

## ABSTRACT

In this study, lead of heavy metal was applied one month to California red worm (*Eisenia foetida*) in order to identify damage of lead accumulation in the soil. 36 adult California red worms (*Eisenia foetida*) were used. The first group was control group, the second group was applicated the daily 200 ppm lead standard and the third group was applicated lead standard and broccoli in the medium. Histopathological estimation of control group in skin tissue was not observed degeneration. The daily 200 ppm lead standard applicated the second group histopathological evaluation was observed cellular atrophy which shrinking the volume of epidermis cells and necrotic cells which losing the nuclei. Lymphocytic infiltration was detected at the dermis densely. Broccoli+lead applicated in group 3, where in the epidermal cells were detected swollen and vacuolated unlike the group 2. Especially, accretion and hypertrophy in goblet cell was greater. Cellular degeneration or injury was not observed in the dermis layer.

## KEYWORDS:

*Eisenia foetida*, Heavy metal; Histopathological; Lead; Skin

## INTRODUCTION

In the last century, rapidly growing industry and industrialization in the world brought a number of conveniences, but also certain problems as well. Environmental pollution has become one of the problems threatening our world as a result of the industrialization efforts. Rapidly increasing environmental pollution is topic that many countries are working on carefully [1, 2, 3].

Heavy metals are found in nature as mineral ores; these spread around the environment as a result of human activities and industrial uses. The rapid development of the industry, high chemicals production and consumption, lack of attention to decontamination are factors increasing the dimensions of environmental pollution. Heavy metals intensively spread through the environment

and enter into the food chain, accumulate in humans and cause various health issues [4, 5]. Problems with determination of the status of these toxic pollutants in the ecological process, characterization of sources and appropriate control criteria are among the most important and challenging issues that international decision makers face [6] “The Black List” compiled by the European Commission taking into account persistence, toxicity and bioaccumulative potential and containing most dangerous toxic compounds also involves cadmium, mercury and compounds of these heavy metals. “The Grey List” containing relatively less dangerous compounds primarily involves copper, nickel, lead, chromium and many more metal metalloids [7].

Toxic effects of heavy metals are generally concentrated on cell organelles, enzymes and cell membranes. The toxicity of metals involves the interaction between toxicological target and released metal ions. There are many factors involved in toxic effects of heavy metals. For example, the metabolism of main elements required for the tissue might be the same element causing the toxicity. Also, cells playing an active role during metal transfer (renal tubular, gastrointestinal, liver) are the most sensitive cells against the toxic effect [8].

Each year, communities are increasingly exposed to Pb contamination due to industrialization. Today, approximately 3 million tons of Pb is consumed around the world. This amount is 1 million tons more than the Pb consumption of 50 years ago [9].

Human body takes 15% of lead through air, 20% through water and 65% through food. Lead is absorbed through respiration and digestion. Lead absorption through intestines is very slow. In general, 10% of the lead taken through mouth by adults and 40% of the lead taken through mouth by children is absorbed by intestines. The excretion rate of lead is very slow and therefore, it accumulates in the body for life. At young and middle ages, lead mostly accumulates in soft tissues. Absorbed lead may spread to various organs (aorta, pancreas, lung, liver, cartilage, kidney,

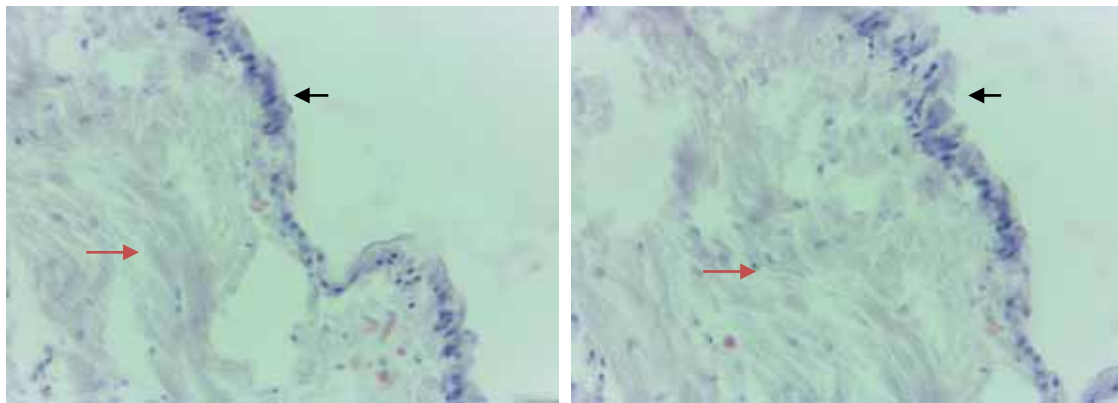


**FIGURE 1**  
Control group skin tissue, single-layer cubic-prismatic epithelium (←) tight, irregular connective tissue (→), 40' lens.

spleen and muscles) through blood circulation. In addition, the rate at which lead accumulates in bones increases with older age (50-60) and 90% of the lead in body accumulates in bones. Other than bones, lead accumulation in kidneys and liver is also important. Lead is a typical cumulative toxin and its excretion through feces and urine is very slow. 16% of excretion is through gall, 76% is through urine and the remaining is through other ways such as hair and epithelial tissue loss [10].

The length of worms used in this study ranges between 5-15 cm, while length of Giant Australia Worms (*Megascolides australis*) varies between 50-100 cm. Earth worms have long bodies and terrestrial rings. They mostly have a cylindrical structure, but their last parts may be rectangular, octagonal or trapezoidal in cross-section. In some individuals, the last part is flattened in back-abdomen direction and paler than back [11]. Worms do not have a skeleton. They have a segmented, colored body with seta and thin outer cuticle tissue. They usually have a red, brown color or a combination of these two colors. It has been reported that the reason why these worms have a reddish and pink color is due to hemoglobin content of capillary blood veins close to body walls [12].

The aim of this study is to investigate the effects of lead accumulation in soil and water on living organisms. It is known that heavy metals lead to toxic effects on living organisms in soil and water. In order to identify damages caused by lead accumulation in soil to living organisms, lead heavy metal was applied to Californian red worm (*Eisenia foetida*) for a month. After this application, histopathological examination of skin tissue was carried out using hematoxylin eosin staining method [13].

## **MATERIALS AND METHODS**

36 adult Californian red worms (*Eisenia foetida*) were used in this study. Californian red

worm were divided into 3 groups, each consisting of 12 worms. The first group was the control group, 200 ppm of lead standard was applied to the second group and the third group had broccoli in the feed area in addition to lead. A feed area containing tea residue, coffee ground, banana peel and egg shell was created for each group. However, broccoli cut into very small pieces was added to the feed area of the third group.

1. Group = Control Group (tea residue, coffee ground, banana peel and egg shell)
2. Group = 200 ppm lead per day (tea residue, coffee ground, banana peel and egg shell)
3. Group = broccoli + 200 ppm lead per day (tea residue, coffee ground, banana peel, egg shell and broccoli)

Heavy metal was applied for a month. At the end of the month, worms were killed and specimens were taken from anterior and posterior regions for histological examination of the skin tissue. Specimens were fixed in 10% formaldehyde solution for 48 hours. Tissues were washed under tap water for a night in order to remove the fixative. 70%-80%-96% and 100% alcohol were applied to the specimens to perform routine histological tissue tracking procedure. Xylol was used for more transparency and then the specimens were taken into paraffin. Tissues were buried into paraffin and sections with a thickness of 5 microns were taken. Hematoxylin eosin staining method was used on sections in order to evaluate the skin tissue in terms of histology. Examinations were performed using Leica DM 500 light microscope and photos were taken when deemed necessary.

## **RESULTS**

In observations, which continued for a month, it was seen that the worms in the second group grew even larger compared to the control group. On the other hand, the worms in the third group, which were given broccoli+lead, remained weaker

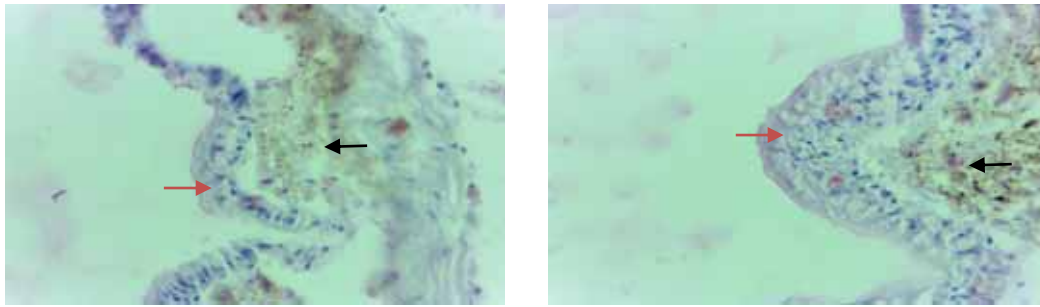


**FIGURE 2**  
Lead application of the second group, cellular atrophy in epidermis (→), lymphocyte infiltrations in dermis (←), 40' lens.

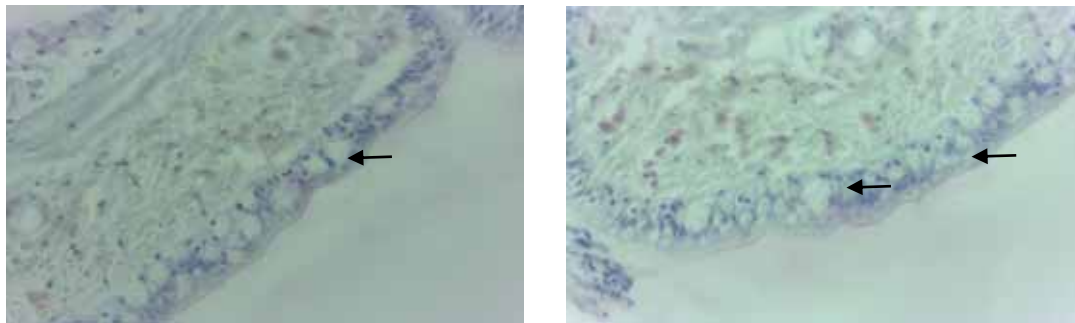


**FIGURE 3**  
Lead + Broccoli application of the third group, swollen, vacuolar and hypertrophic epithelium and goblet cells (←), 40' lens.

compared to the control group. Some of them couldn't even maintain their vital activities until end of the experiment.

It was observed in light microscope examinations that the skin constituted 2 layers, epidermis and dermis. It was found that the connective tissue of dermis formed papillae by projecting amongst the epithelium. It was identified that epidermis consisted of a single cubic-prismatic cell layer and these cells had sills on their apical surfaces. A large number of mucus-secreting goblet cells were observed between epithelium cells with sills.

No degenerations were found as a result of the histopathological evaluation of the skin tissue of the worms raised under normal conditions, the control group. It was determined that single-layer cubic-prismatic cells displayed an orderly arrangement. No pathological findings were obtained from the tight, irregular connective tissue in the dermis. Collagen fibers were found to be quite dense (Figure 1).

In the histopathological evaluation of the second group, given 200 ppm of lead per day, it was observed that epidermis cells shrank in terms of volume, i.e. cellular atrophy occurred, and some cells lost their nuclei and necroses. Dense lymphocyte infiltrations were found in dermis (Figure 2).

Unlike the second group, worms in the third group, given broccoli + lead, had a swollen and vacuolated appearance. The growth in volume, i.e.

hypertrophy, was observed in goblet cells in particular. No degeneration or cellular damage was observed in the dermis layer (Figure 3).

## DISCUSSION AND CONCLUSION

Body wall of worms is made up of cuticle, epidermis, nervous tissue, longitudinal and ring-shaped muscle layer and coelomic epithelium [12]. This longitudinal and transverse muscle system with the upper skin is called "skin-muscle sheath". Coelomic epithelium is very thin on the muscle sheath and septum. On the intestinal veins and veins, coelomic epithelium consists of "chloragogen cells" containing yellow, Brown, greenish grains. Coelomic cavity is filled with a colorless liquid containing different shaped lymphocytes, fragmented chloragogen cells and sexual glands. Some of the segments carry a puncture along the middle line of the back. These punctures connecting coelomic cavities to outside are called dorsal pores. It was found that, in case of a risk of drying, a certain portion of the body fluid is excreted from these punctures so that the skin humidity can be maintained [11].

In a study, specific concentrations of cadmium, copper, lead and zinc were given to artificial soil containing *Eisenia foetida* (Annelida: Oligochaeta) and mortality, growth and cocoon production were observed for 56 days. In addition,

the number of living cocoons and percentage of juveniles per cocoon were recorded. It was reported that heavy metals reduced cocoon production, breeding values, increased mortality and susceptibility to death. However, it was also reported that heavy metals did not have a significant effect on cocoon viability [14, 15].

In a study conducted by Helling et.al., [16] a certain ppm of copper was applied to *Eisenia foetida* species in a substrate under laboratory conditions. As the copper concentration increased, the accumulation in worms' tissues increased as well and growth, development and cocoon production were affected adversely.

It was observed in this study that application of 200 ppm of lead caused significant degenerations on the skin tissue of Californian redworm (*Eisenia foetida*). It was seen that the addition of broccoli, which is known for its antioxidant activity, to the feed area of the third group did not prevent the effects of lead and pathological issues were seen on the skin tissue for this group as well. Also, it was also found that broccoli acidified the environment and Californian red worm (*Eisenia foetida*) had a low tolerance for these conditions, and as a result, some of the worms could only live until the third week of the experiment. In conclusion, it was validated with this study that lead accumulation in soil caused severe damages on tissues of living organisms. We need to protect the environment and take necessary measures.

#### ACKNOWLEDGEMENTS

The authors would like to thank the Professor Dr. Ali COŞKAN, Department of Soil Science and Plant Nutrition, Suleyman Demirel University for providing Californian red worm (*Eisenia foetida*) in this work.

#### REFERENCES

- [1] Dağlı H (2005) Effects of drinking water quality and human health. Monthly Journal City Bank 3:16–21.
- [2] Atalık A (2006) Global warming effects on water resources and agriculture. Science Utopia 139:18–21.
- [3] Duruibe JO, Ogwuegbu MOC, Egwurugwu JN (2007) Heavy metal pollution and human bio toxic effects. International Journal of Physical Sciences 2(5):112–118.
- [4] Yılmaz O (1995) Heavy metal levels in human liver and kidney residue obtained from the Bursa region: I. Cıva. Yüzüncü Yıl University Journal of Health Sciences 1:6–11.
- [5] Yılmaz O (2002) Cadmium and lead levels in human liver and kidney samples obtained from

Bursa Province. International Journal of Environmental Health Research 12:181–185.

- [6] Thomas SL and Swain WR (1988) Session summary: sources, fate and controls of toxic contaminants. in: schmidtke, N.W. (Ed.) toxic contamination in large lakes, Vol III. sources, fate and controls of toxic contaminants, Lewis Publisher, Chelsea, Michigan. pp. 1–6.
- [7] Mason CF (1991) Biology of freshwater pollution. John Wiley and sons, Inc., New York.
- [8] Özdamar K (2001) Biostatistics using SPSS. Kaan Bookstore, Ankara, pp. 452.
- [9] Kaya S, Pirinççi I, Bilgili A (2002) Toxicology in veterinary medicine. Second edition, Medisan Publisher, Ankara, pp. 203–776.
- [10] Vural N (2005) Toxicology. Ankara University Faculty of Pharmacy Publications, No: 73.
- [11] Mısırlıoğlu M (2011) Earth worm biology, ecology and species Turkey. Nobel Publisher, Ankara, pp. 92.
- [12] Edwards CA, Bohlen PJ (1996) Biology and ecology of earthworms. 3rd. Ed. Chapman and Hall, New York, pp. 39–40.
- [13] Bancroft JD, Stevens A, Turner DR (1996) Theory and practice of histological techniques. London: Churchill Livingstone, pp.129.
- [14] Spurgeon DJ, Hopkin SP, Jones DT (1994) Effects of cadmium, copper, lead and zinc on growth, reproduction and survival of the earth worm *Eisenia foetida* (Savigny): Assessing the environmental impact of point-source metal contamination in terrestrial ecosystems. Environmental Pollution 84 (2):123–130.
- [15] Philips DH, Rainbow PS (1994) Bio monitoring of trace aquatic contaminants, Fenviron. London, pp.87.
- [16] Helling B, Reinecke SA, Reinecke AJ (2000) Effects of the fungicide copper oxychloride on the growth and reproduction of *Eisenia foetida* (Oligochaeta). Ecotoxicology Environmetal Safety. 46:108–116.

**Received: 11.02.2016**

**Accepted: 27.09.2016**

#### CORRESPONDING AUTHOR

**Nurgul Senol**

Süleyman Demirel University, Faculty of Health Sciences, Isparta – TURKEY

e-mail: [nurgulsenol@sdu.edu.tr](mailto:nurgulsenol@sdu.edu.tr)



# GENOTOXIC ASSESSMENT OF AMOXICILLIN IN RAINBOW TROUT (*ONCORHYNCHUS MYKISS*) BY COMET ASSAY AND MICRONUCLEUS TEST

Ceren Anlas\*, Oya Ustuner

Department of Pharmacology and Toxicology, Faculty of Veterinary Medicine, Istanbul University, Avcılar, 34320 Istanbul, Turkey

## ABSTRACT

The present study was undertaken to investigate the genotoxicity of amoxicillin in rainbow trout (*Oncorhynchus mykiss*) erythrocytes. The DNA damage was measured as the percentage of DNA in comet tails and micronucleus formation in erythrocytes of fish exposed to different concentrations of amoxicillin (80, 160 and 320 mg/kg bw). Cyclophosphamide was used as a positive control (4 mg/L). Blood erythrocytes were sampled on day 3, 6 and 10 of exposure. It was obtained that, amoxicillin induced a significant increase ( $p < 0.001$ ) in the percentage of DNA in comet tails as well as micronucleus frequency at 320 mg/kg bw treatment group when compared with negative control group at all exposure times. The highest DNA damage was found on day 6 of exposure with both micronucleus test and comet assay. The results of the study indicated that, amoxicillin has genotoxic effects on fish at high concentrations.

## KEYWORDS:

Amoxicillin, *Oncorhynchus mykiss*, genotoxicity, comet assay, micronucleus

## INTRODUCTION

Currently, various chemotherapeutic agents are intensely used in aquaculture to treat or prevent disease outbreaks [1-3]. Genotoxic effects of several antibiotics and antiparasitic agents have been reported in previous studies [4,5]. Due to fish are the alternative food source for human, genotoxic contamination of aquatic ecosystem also pose threat to human health as well as aquatic organisms. The relationship between the genotoxic concern of aquatic ecosystems and carcinogenic effects in human have been detected in previous epidemiological studies. Also, fish species act as a sentinel organism in genetic toxicology assessments and play significant role in early determining of potential risk for aquatic environment, due to they are directly exposed to environmental chemicals

[1,6].

Amoxicillin is a penicillin derivative antibiotic, frequently used in human and veterinary medicine due to its broad spectrum of activity. Also it is considered the most important penicillin derivative antibiotic applied in aquaculture [7] and used to treat or control of several important bacterial infections [8,9]. In food-producing animals, amoxicillin is approved for use as amoxicillin trihydrate [10]. Genotoxic effect of amoxicillin have been investigated by several genotoxicity test systems on mammalian species and controversial results have been reported. On the other hand, extremely limited data have been reported on genotoxic effect of amoxicillin on fish species.

A number of methods are applied to assess genotoxic damage in aquatic species. Comet assay and micronucleus (MN) test are currently the most widely methods to detect genotoxic damage in aquatic species. Several authors have suggested that both assays should be employed due to their abilities to detect different aspects of genotoxicity [11].

Amoxicillin or similar antibiotics that was usually considered non-genotoxic may injure genomic DNA via the induction of reactive oxygen species (ROS) [12]. Considering the lack of published data on genotoxic effect of amoxicillin on target aquatic species, the present study was conducted to investigate the *in vivo* genotoxic potential of amoxicillin in *Oncorhynchus mykiss*.

## MATERIAL AND METHODS

**Animals.** The experimental protocol was approved by Istanbul University Animal Experiments Native Ethical Committee (Protocol number 136). The tests were carried out on 150 adult rainbow trout (*Oncorhynchus mykiss*). Healthy specimens of *Oncorhynchus mykiss* with average body weight of 40-60 g., were obtained from Sapanca Inland Waters Research Center of the Fisheries Faculty of Istanbul University, Turkey. Fish were divided into 5 groups of 30 fish each and they were placed in fiberglass tanks with a 12h light-dark photoperiod. The tanks were supplied with 500 L of freshwater with an average temperature of 12-

18 °C, dissolved oxygen was maintained around 8-9 mg/ L and the pH amounted to 7.4-7.8. Fish were acclimated to laboratory conditions for 30 days before the experiments.

**Chemicals.** Amoxicillin trihydrate (CAS 61336-70-7) and cyclophosphamide (CAS 6055-19-2) were purchased from Sigma- Aldrich (St. Louis, MO). Giemsa stain was obtained from Carlo Erba, (Milan, Italy). All other chemicals were obtained from Merck (Germany).

**Experimental design.** The doses were selected based on the therapeutic protocol in fish species. Amoxicillin is used in medicated feed at a dose of 80-160 mg/kg of body weight (bw) for 10 days for treatment of fish diseases [13]. In this regard, treatment groups were exposed to amoxicillin both in therapeutic interval (80-160 mg/kg bw) and higher dose (320 mg/kg bw) for 10 days. Fish were fed daily (2% body weight) with rainbow trout pellets containing different concentrations of amoxicillin trihydrate. Commercial rainbow trout pellets were moistened with cornflower oil to ensure attachment of powdered drug to the pellets, then amoxicillin trihydrate was added and carefully mixed with the pellets [14]. Cyclophosphamide was used at concentration of 4 mg/L in a single dose as a positive control [1]. Another group of fish were maintained in dechlorinated tap water as a negative control. The food for the control groups was moistened with cornflower oil, without drug. Peripheral blood samples were obtained from the caudal vein of fish on the 3<sup>rd</sup>, 6<sup>th</sup>, and 10<sup>th</sup> days of the exposure period and processed for comet assay and MN test. For each sampling interval, ten fish were sampled from each groups.

**Single cell gel electrophoresis assay (Comet Assay).** The comet assay and the diffusion assay were carried out according to Frenzilli et al. (1999, 2004).

The comet assay was performed according to Cavas and Konen [15] with slight modifications. A few microliters of blood sample were diluted with 1 ml of cold phosphate- buffered saline (PBS). Sixty microliters of diluted sample were mixed with 200 µl of 0.65 % low melting point (LMP) agarose. Seventy- five microliters of the mixture were spread onto slides previously coated with 1 % normal melting point (NMP) agarose. The slides were immediately covered with a coverslip and kept in 4°C for 10-15 minutes to solidify agarose. Then, coverslips were carefully removed and the slides were immersed in cold lysing solution (2.5 M NaCl, 100 mM Na<sub>2</sub>EDTA, 10 mM Tris, pH 10 with 10 % dimethyl sulfoxide and 1% Triton- X- 100) for at least 1 hour, at 4°C. Afterwards, the slides were

placed on a horizontal electrophoresis tank filled with fresh electrophoresis solution (1mM Na EDTA, 300 mM NaOH, pH 13.5) and left in the solution for 20 minutes to allow the unwinding. Then, electrophoresis was performed at 25 V and 300 mA for 30 minutes. After the electrophoresis, the slides were rinsed three times with a neutralization solution (0.4 M Tris buffer at pH 7.5) for 5 minutes and stained with 75 µl etidium bromide. Slides were viewed under a fluorescence microscope (Olympus BX51, Olympus Optical Co. Ltd, Japan) and comet tails were analysed using a specific software (Bs 200 Pro, BAB Imaging System, Ankara, Turkey). At least 100 cells were counted in three replicated slides per sample to characterize DNA damage. The percentage of DNA in the tail of comets (% tail DNA) was used as the parameter of DNA damage.

**Micronucleus Test.** The MN test was performed according to Al-Sabti and Metcalfe [16]. Blood samples were obtained from caudal vein and immediately smeared onto precleaned slides. After fixation in pure ethanol for 20 minutes, slides were left to air- dry and stained with 10 % Giemsa solution for 25 minutes. Three slides were prepared for each fish and 2000 erythrocytes were scored from each slide under an Olympus CX31 microscope with x100 magnification. Small, non-refractive, circular or ovoid chromatin bodies displaying the same staining and focusing pattern as the main nucleus were scored as micronuclei.

**Statistical Analysis.** Statistical differences within groups at different exposure times were determined by repeated measurement of ANOVA, whereas differences between groups at each exposure times were compared by one- way ANOVA and Duncan's test in both the experiments. All the data were expressed as the mean ± standart error (SE) for each experiments. Three levels were considered statistically significant: \*p > 0.05, \*\*p < 0.05 and \*\*\*p < 0.001.

## RESULTS

Three levels were considered significant: \*p < 0.05, \*\*p < 0.01, and \*\*\*p < 0.001.

**Micronucleus Test.** The results on MN induction in erythrocytes of *Oncorhynchus mykiss* are presented in Table 1. As shown in the table, treatment with the highest dose of amoxicillin (320 mg/kg bw) caused a significant increase (p<0.001) in the MN frequency with respect to the negative control and other treated groups at all the exposure



**TABLE 1**  
**Micronucleus frequencies (MN/2000) in peripheral blood erythrocytes of *O. mykiss* (mean ± SE)**

Sampling time	Negative Control	CYP 4 mg/ L	AMX 80 mg/kg	AMX 160 mg/kg	AMX 320 mg/kg	Significance
3. day	5.07 ± 0.77 <sub>c, x</sub>	27.73 ± 1.01 <sub>a, x</sub>	4.77 ± 1.0 <sub>c, x</sub>	5.97 ± 0.83 <sub>c, x</sub>	15.80 ± 0.49 <sub>b, x</sub>	***
6. day	4.46 ± 0.80 <sub>c, x</sub>	28.26 ± 1.24 <sub>a, x</sub>	5.83 ± 1.12 <sub>c, x</sub>	6.97 ± 1.13 <sub>c, x</sub>	16.33 ± 0.53 <sub>b, x</sub>	***
10. day	4.63 ± 0.73 <sub>c, x</sub>	25.90 ± 1.13 <sub>a, x</sub>	5.33 ± 0.96 <sub>c, x</sub>	6.33 ± 0.65 <sub>c, x</sub>	15.90 ± 0.48 <sub>b, x</sub>	***
Significance	NS	NS	NS	NS	NS	

<sup>a,b,c</sup> : Differences between the mean values carrying different letters in the same line are significant.

<sup>x</sup> : Differences between the mean values carrying different letters in the same column are significant.

CYP : Cyclophosphamide, AMX: Amoxicillin, MN: Micronucleus

NS: Not significant (p>0.05); \*\*\* p< 0.001

**TABLE 2**  
**Percentage of DNA tail in peripheral blood erythrocytes of *O. mykiss* (mean ± SE)**

Sampling time	Negative Control	CYP 4 mg/ L	AMX 80 mg/kg	AMX 160 mg/kg	AMX 320 mg/kg	Significance
3. day	18.35 ± 2.09 <sub>c, x</sub>	65.40 ± 3.45 <sub>a, y</sub>	20.54 ± 3.89 <sub>c, x</sub>	23.05 ± 5.11 <sub>c, x</sub>	37.80 ± 1.67 <sub>b, y</sub>	***
6. day	17.87 ± 3.38 <sub>c, x</sub>	68.70 ± 2.93 <sub>a, xy</sub>	23.92 ± 2.73 <sub>c, x</sub>	22.06 ± 2.21 <sub>c, x</sub>	47.78 ± 2.93 <sub>b, x</sub>	***
10. day	18.23 ± 3.92 <sub>c, x</sub>	71.30 ± 2.61 <sub>a, x</sub>	19.97 ± 3.62 <sub>c, x</sub>	21.67 ± 3.35 <sub>c, x</sub>	35.31 ± 3.06 <sub>b, y</sub>	***
Significance	NS	*	NS	NS	**	

<sup>a,b,c</sup> : Differences between the mean values carrying different letters in the same line are significant.

<sup>x</sup> : Differences between the mean values carrying different letters in the same column are significant.

CYP : Cyclophosphamide, AMX: Amoxicillin NS: Not significant (p>0.05); \*\*\* p< 0.001; \*\* p<0.05

times. The damage started to increase from day 3 to day 6 and decrease from day 6 to day 10, but the differences were not found significant (p>0.5). The highest frequency of MN was observed at 6<sup>th</sup> day in the 320 mg/kg group. In the other treatment groups (80 and 160 mg/kg bw), no significant difference was found with respect to the negative control group.

**Single cell gel electrophoresis assay (Comet Assay).** The damage was measured by using the % tail DNA as the parameter of assessment. The results of comet assay are presented in Table 2 and typical comet images are shown in Fig. 1. When compared to control group, a clear and statistically significant increase (p<0.001) in the % tail DNA values was found in the group treated with the highest dose of amoxicillin (320 mg/kg bw) in all exposure times. Nevertheless no significant increase was observed in the groups exposed to 80 and 160 mg/kg bw of amoxicillin with respect to the negative control group (p>0.5). In the 320 mg/kg group, the highest DNA damage was observed at 6<sup>th</sup> day and the increase was found to be statistically significant

(p<0.05) compared to other exposure days. The damage showed a statistically significant decrease from day 6 to day 10.

## DISCUSSION

Currently, contamination of aquatic ecosystem by pharmaceutical compounds is the major environmental concern. Amoxicillin is considered as one of the primary contaminant for aquatic environment due to its pharmaceutical properties and it has the high risk for aquatic organisms [17, 18]. Various toxic effects of amoxicillin have been investigated on aquatic species previously. Amoxicillin (400 mg/kg) caused no abnormality of appetite, movement, external and internal views also haematological parameters excepting increased erythrophagocytosis of splenic macrophages in young yellowtail [19]. Otherwise, El-Nahhal and Dahdouh [20] investigated the single and mixture toxicities of amoxicillin, erythromycin and

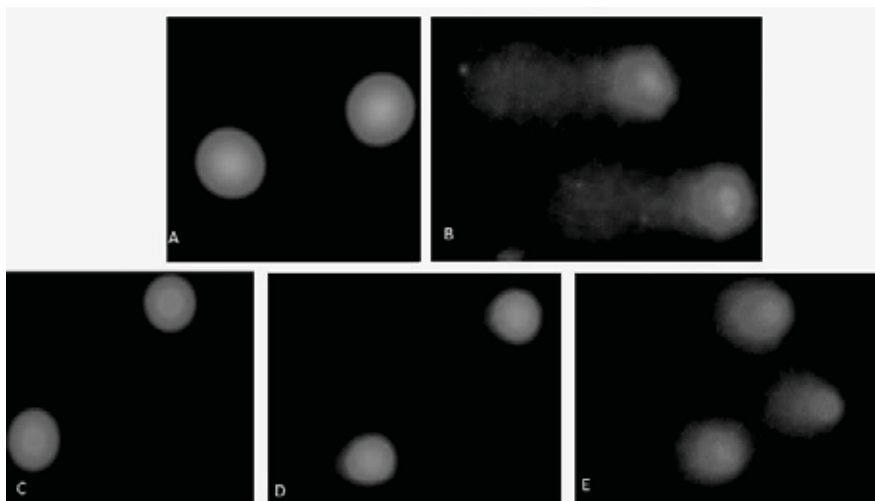


**FIGURE 1**

**Comet images in fish erythrocytes.**

- (A) Control cells. (B) Cells were treated with cyclophosphamide (4mg/L). (C) Cells were treated with 80 mg/kg bw of amoxicillin. (D) Cells were treated with 160 mg/kg bw of amoxicillin. (E) Cells were treated with 320 mg/kg bw of amoxicillin.

endosulfan on *Tilapia nilotica* and reported that, amoxicillin is the most toxic antibiotic to fish with respect to erythromycin and endosulfan. Reports on the genotoxic potential of amoxicillin on aquatic species are extremely limited. Vitture et al. [21], reported that amoxicillin derivatives have genotoxic and cytotoxic potentials on *Rutilus rubilio* chromosomes. On the other hand, controversial results have been reported regarding the genotoxic potential of amoxicillin on mammalian species. Amoxicillin induced DNA strand breaks and base modifications via free oxygen radical production in healthy and *Helicobacter pylori* infected gastric mucosa cells as well as in peripheral blood lymphocytes at high concentration (5 mmol/L) [22]. Free oxygen radicals are quite reactive molecules, they can cause oxidative base modifications and DNA strand breaks via interaction with DNA. Oxidative DNA damage may be the consequence of normal cellular metabolism and generated by endogenous physiological compounds as well as the damage may be induced by exogenous chemicals [23]. However amoxicillin-induced DNA damage has been repaired completely within 60 minutes [22]. Similarly, amoxicillin induced DNA lesions in human gastric adenocarcinoma (AGS) cells via the induction of ROS at 5mM concentrations. The damage obtained at 1 hour of treatment, then steadily declined and reached the basal level within 4 hour [12]. These findings indicate that, amoxicillin does not directly affect DNA, however induces DNA damage indirectly by increasing production of free radicals caused oxidative stress in mammalian species [12]. The damage induced by amoxicillin repaired by DNA repair mechanisms in a short time in mammalian cells. Previous *in vitro* studies have suggested that other  $\beta$ -lactam antibiotics may also

lead to DNA damage at high concentrations, again possibly through induction of ROS [24]. Otherwise it is reported that, amoxicillin most probably does not exert genotoxic effects in human blood lymphocytes in both the presence and the absence of a metabolic activator [25].

It is well known that, high dosage of drugs and chemicals can be frequently used in fish farms to treat or control of disease outbreaks [26]. As a consequence, aquatic species are exposed to higher concentration of antibiotics than recommended doses. In this context, when investigating the genotoxic potential of drugs used to treat fish diseases, high doses of these compounds should be evaluated. In the present study, we assessed the genotoxic potential of amoxicillin on peripheral blood erythrocytes of *Oncorhynchus mykiss* at high concentration (320 mg/kg bw) as well as therapeutic interval. On the other hand, Park et al. [27] reported that the dose of 400 mg/kg bw is the recommended therapeutic dose for fish species. Our present results obtained from both comet assay and MN test demonstrated that amoxicillin has no genotoxic potential at 80 and 160 mg/kg bw in *Oncorhynchus mykiss* erythrocytes. Otherwise, the highest concentration of amoxicillin (320 mg/kg bw) induces micronuclei frequency and comet formation for all sampling time points. Amoxicillin leads to oxidative stress in fish species as mammals via inhibit intracellular antioxidant enzyme catalase, which protect cells against oxidative stress and induce glutathione-S-transferases at high concentration [28]. ROS and oxidative stress have been demonstrated to be triggers of apoptosis [29]. In the present study, the increase of MN frequency and % tail DNA in cells at the highest concentration may probably be due to high production of ROS resulting

to cell apoptosis. In mammals, amoxicillin-induced DNA damage is completely repaired in a short time via repair mechanisms. However, fish cells have a low DNA repair activity compared to mammalian cells and therefore may be more susceptible to genotoxic agents [30]. In agreement with these results, in the present study, amoxicillin leads to long term consequences on DNA when compared to mammals. In the high-dose group, MN frequency and % tail DNA in cells started to decrease from day 6 to day 10, although the damage was not repaired completely. This may be the consequence of low repair capacity in fish species therefore inadequate repair of DNA damage by induced high concentration of amoxicillin. Furthermore, long-term exposure studies in fish species indicated that micronucleus frequencies in fish erythrocytes gradually decreased after 15-21 days of exposure period [31, 32].

MN test and comet assay are considered to be one of the most useful methods to detect genotoxicity in cells exposed to chemicals or physical agents under field and laboratory conditions. Both of assays, originally developed with mammalian species then successfully adapted to fish and other aquatic organisms. Several studies have been carried out using both comet assay and MN test to assess the genotoxic consequences of various compounds in aquatic environment [4, 15, 33]. % tail DNA is the most commonly used parameter for comet assay and it is considered more meaningful to determine DNA damage with respect to other parameters [34]. In the present study considering the obtained results from comet assay, the DNA damage level tended to increase with exposure time from day 3 to day 6 and the increase was found statistically significant in the highest concentration group. However, there was no significant difference in the number of micronuclei at the same sampling period. The difference can be explained by comet assay and MN test reflects different types of DNA damage and specific considerations need to be taken into account when assessing the performances of these two tests [33]. For instance, comet assay can detect directly DNA strand breaks that induced early after exposure to genotoxins. Otherwise, micronuclei are the result of chromosome breaks or mitotic anomalies that require necessarily a passage through mitosis to be recognisable [35]. Also it is known that, the mitotic activity of fish erythrocytes is quite low [36]. This may be the reason for the difference between our results obtained from comet assay and MN test.

## CONCLUSIONS

The present results suggest that amoxicillin has not genotoxic potential at therapeutic doses, however induces DNA damage at high concentrations in *Oncorhynchus mykiss* erythrocytes compared with

negative control. According to the results of previous studies on the genotoxicity of amoxicillin and DNA repair studies in fish, the formation of comet and MN at high concentrations may be the reason of ROS production and deficient DNA repair activity. The study confirmed that the MN test and comet assay are useful methods for determining genotoxic substances in aquatic environment. Further, long-term exposure studies should be performed to assess the DNA repair capacity in fish species.

## ACKNOWLEDGMENTS

The present study was supported by the Research Fund of Istanbul University, Project No: 10947. We would like to express our thanks to Prof. Bulent Ekiz (Istanbul University, Turkey) for statistical analyses.

## REFERENCES

- [1] Cavas, T. and Ergene- Gozukara, S. (2005) Genotoxicity evaluation of metronidazole using the piscine micronucleus test by acridine orange fluorescent staining. *Environ Toxicol Pharmacol* 19, 107-111.
- [2] Jerbi, M.A., Ouanes, Z., Besbes, R., Achour, L. and Kacem, A. (2011) Single and combined genotoxic and cytotoxic effects of two xenobiotics widely used in intensive aquaculture. *Mutat Res* 724, 22-27.
- [3] Zounkova, R., Klimesova, Z., Nepejchalova, L., Hilscherova, K., and Blaha, L. (2011) Complex evaluation of ecotoxicity and genotoxicity of antimicrobials oxytetracycline and flumequine used in aquaculture. *Environ Toxicol Chem* 30, 1184- 1189.
- [4] Rocco, L., Peluso, C. and Stingo, V. (2011) Micronucleus test and comet assay for the evaluation of zebrafish genomic damage induced by erythromycin and lincomycin. *Environ Toxicol* 27, 598-604.
- [5] Ustun Alkan, F. and Şener, S. (2009) Lack of the antimutagenic effect of ascorbic acid on the genotoxicity of albendazole in mouse bone marrow cells. *Bull Vet Inst Pulawy* 53, 493-497.
- [6] Lakra, W.S. and Nagpure, N.S. (2009) Genotoxicological studies in fishes: a review. *Indian J Anim Sci* 79, 93-98.
- [7] Langin, A., Alexy, R., König, A. and Kümmerer, K. (2009) Deactivation and transformation products in biodegradability testing of beta-lactams amoxicillin and piperacillin. *Chemosphere* 75, 347-354.
- [8] Branson, E. (1995) Rainbow trout fry syndrome. *Fish Vet J* 1, 1-7.
- [9] Ozturk, T., Didinen, B.I., Dogan, G., Ozer, A.

- and Bircan R. (2013) Lactococcosis in rainbow trout (*Oncorhynchus mykiss*, Walbaum, 1792) in the middle Black Sea Region in Turkey and antimicrobial susceptibility of the aetiological agent, *Lactococcus garvieae*. *Etlik Vet Mikrobiyol Derg* 24, 7-12.
- [10] WHO (2012) Toxicological evaluation of certain veterinary drug residues in food. Food additives series 66.
- [11] Frenzilli, G., Nigro, M. and Lyons, B.P. (2009) The comet assay for the evaluation of genotoxic impact in aquatic environments. *Mutat Res* 681, 80-92.
- [12] Li, P.Y., Chang, Y.C., Tzang, B.S., Chen, C.C. and Liu, Y.C. (2007) Antibiotic amoxicillin induces DNA lesions in mammalian cells possibly via the reactive oxygen species. *Mutat Res* 629, 133-139.
- [13] Armstrong, S.M., Hargrave, B.T. and Haya, K. (2005) Antibiotic use in finfish aquaculture: Modes of action, environmental fate and microbial resistance. *Hdb Env Chem* 5, 341-357.
- [14] Lunden, T., Lilius, E.M. and Bylund, G. (2002) Respiratory burst activity of rainbow trout (*Oncorhynchus mykiss*) phagocytes is modulated by antimicrobial drugs. *Aquaculture* 207, 203-212.
- [15] Cavas, T. and Konen, S. (2008) In vivo genotoxicity testing of the amnesic shellfish poison (domoic acid) in piscine erythrocytes using the micronucleus test and the comet assay. *Aqua Toxicol* 90, 154-159.
- [16] Al- Sabti, K. and Metcalfe, C.D. (1995) Fish micronuclei for assessing genotoxicity in water. *Mutat Res* 343, 121-135.
- [17] Alighardashi, A., Rashidi, A., Neshat, A.A. and Golsefatan, H.R. (2014) Environmental Risk Assessment of Selected Antibiotics in Iran. *Iranian Journal of Health, Safety & Environment* 1, 132-137.
- [18] Baghapour, M.A., Shirdarreh, M.R., Derakhshan, Z. and Faramarzi, M. (2014) Modeling Amoxicillin Removal From Aquatic Environments in Biofilters. *Health Scope* 3, 1-8.
- [19] Nakauchi, R. and Miyazaki, T. (1988) Toxicity of amoxicillin to yellowtail. *Fish Pathol* 23, 251-255.
- [20] El- Nahhal, Y. and El- Dahdouh, N.E. (2015) Toxicity of amoxicillin and erythromycin to fish and mosquito. *Ecotoxicol Environ Contam* 10, 13-21.
- [21] Vitturi, R., Zava, B., Colomba, S.M., Pellerito, A., Maggio, F. and Pellerito, L. (1995) Organometallic complexes with biological molecules: V. In vivo cytotoxicity of diorganotin (IV)- amoxicillin derivatives in mitotic chromosomes of *rutilus rubilio* (pisces, cyprinidae). *App Organomet Chem* 9, 561-566.
- [22] Arabski, M., Kazmierczak, P., Wisniewska-Jarosinska, M., Poplawski, T., Klupinska, G., Chojnacki, J., Drzewoski, J. and Blasiak, J. (2015) Interaction of amoxicillin with DNA in human lymphocytes and *H. Pylori*- infected gastric mucosa cells. *Chemico- Biol Inter* 152, 13-24.
- [23] Cooke, M.S., Evansi, M.D., Dizdaroglu, M. and Lunec, J. (2003) Oxidative DNA damage: mechanisms, mutation and disease. *Faseb J* 17, 1195-1214.
- [24] Quinlan, G.J. and Gutteridge, J.M. (1988) Oxidative damage to DNA and deoxyribose by beta-lactam antibiotics in the presence of iron and copper salts. *Free Radic Res Commun* 5, 149-158.
- [25] Istifli, E.S. and Topaktas, M. (2010) Cytogenetic genotoxicity of amoxicillin. *Environ Mol Mutagen* 51, 222-228.
- [26] Khoi, L.N.D. (2011) Quality Management in the Pangasius Export Supply Chain in Vietnam. *Fish Disease Prevention and Treatment Practices at the Farm Level*. University of Groningen Groningen The Netherlands, 141-156.
- [27] Park, E.K., Jung, W.C. and Lee, H.J. (2010) Application of a solid- phase fluorescence immunoassay to determine amoxicillin residues in fish tissue. *Acta Vet Hung* 58, 83- 89.
- [28] Oliveira, R., McDonough, S., Ladewig, J.C., Soares, A.M., Nogueira, A.J. and Domingues, I. (2013) Effects of oxytetracycline and amoxicillin on development and biomarkers activities of zebrafish (*Danio rerio*). *Environ Toxicol Pharmacol* 36, 903-912.
- [29] Shen, H.M. and Liu, Z.G. (2006) JNK signaling pathway is a key modification in cell death mediated by reactive oxygen and nitrogen species. *Free Radic Biol Med* 40, 928-939.
- [30] Castano, A., Becerril, C. and Llorente, M.T. (2003) Fish cells used to detect aquatic carcinogens and genotoxic agents, in: Mothersill, C. and Austin, B. *In vitro methods in aquatic toxicology*. Springer- Praxis Publishing, Chichester, UK, 241-275.
- [31] Campana, M.A., Panzeri, A.M., Moreno, V.J. and Dulout, F. (1995) Genotoxic evaluation of the pyrethroid lambda-cyhalothrin using the micronucleus test in erythrocytes of the fish *Cheirodon interruptus interruptus*. *Mutat Res* 438, 155-161.
- [32] Torres de Lemos, C., Rdel, M.P., Terra, N.R. and Erdtmann, B. (2001) Evaluation of basal micronucleus frequency and hexavalent chromium effects in fish erythrocytes. *Environ Toxicol Chem* 20, 1320-1324.
- [33] Bücker, A., Carvalhol, M.S., Conceição, M.B. and Alves-Gomes, J.A. (2012) Micronucleus test and comet assay in erythrocytes of the Amazonian electric fish *Apteronotus bonapartii* exposed to benzene. *J Braz Soc Ecotoxicol* 7,



65-73.

- [34] Kumaravel, T.S. and Awadhesh, N.J. (2006) Reliable comet assay measurements for detecting DNA damage induced by ionising radiation and chemicals. *Mutat Res* 605, 7-16.
- [35] Buschin, A., Martino, A., Gustavino, B., Monfrinotti, M., Poli, P., Rossi, C., Santoro, M., Dörr, A.J.M. and Rizzoni, M. (2004) Comet assay and micronucleus test in circulating erythrocytes of *Cyprinus carpio* specimens exposed in situ to lake waters treated with disinfectants for potabilization. *Mutat Res* 557, 119-129.
- [36] Bolognesi, C. and Hayashi, M. (2011) Micronucleus assay in aquatic animals. *Mutagenesis* 26, 205-213.

---

**Received: 10.02.2016**

**Accepted: 17.10.2016**

---

#### **CORRESPONDING AUTHOR**

---

**Ceren Anlas**

Istanbul University Faculty of Veterinary Medicine  
Department of Pharmacology and Toxicology,  
34320 Avcilar/ Istanbul, Turkey

e-mail: [cerenis@istanbul.edu.tr](mailto:cerenis@istanbul.edu.tr)

# MATERNAL AGE EFFECTS OF *ASPIDIOTUS NERII* BOUCHÉ BOUCHE (HEMIPTERA: DIASPIDIDAE) ON POTATO

Alime Bayindir<sup>\*1</sup>, Senay Ozger<sup>2</sup>, Ismail Karaca<sup>2</sup>, Mehmet Sedat Sevinc<sup>2</sup>

<sup>\*1</sup>Pamukkale University, School of Applied Sciences, Organic Farming Business Management Department, 20600, Çivril-Denizli, Turkey

<sup>2</sup>Süleyman Demirel University, Agricultural Faculty, Plant Protection Department, 32260, Isparta, Turkey

## ABSTRACT

*Aspidiotus nerii* Bouché (Hemiptera: Diaspididae) is an excellent host for rearing biological control agents for the control of scale insects. In this study, we investigated the maternal effect on the reproduction and development of *A. nerii* crawlers transferred to separate clean potato tubers at the 1<sup>st</sup>, 15<sup>th</sup> and 30<sup>th</sup> days. After the crawlers settled, each potato was divided into 4 cm<sup>2</sup> cells surface area surrounded by 'stickem special' to prevent their escape. When all crawlers in the cell became adults, one female and all the males were left in the cells, and the rest of the females were removed. Experiments were done at 25°C, 16:8 hours and 65% relative humidity in a climate chamber. Cells were observed daily and crawlers were removed after counting. Variance analysis and Tukey's multiple range tests were applied for statistical analysis. Life table parameters were also calculated. Intrinsic rate of increase ( $r_m$ ), net reproductive rate ( $R_o$ ), and mean generation time ( $T_o$ ) were 0.073, 0.072 and 0.034 females/female/day, 83.42, 27.95 and 5.47 females/female, 60.56, 46.11 and 49.56 days, respectively. The total crawler numbers were the 1<sup>st</sup>, 15<sup>th</sup> and 30<sup>th</sup> days age females were 208.57, 81.32 and 20.07 crawlers, respectively. These results clearly show that age does have a significant effect on crawler of females *A. nerii*.

## KEYWORDS:

*Aspidiotus nerii*, age dependent life table, maternal age effect, potato

## INTRODUCTION

As it is well known that most of the characters of the offspring in all living organisms were determined

by the parents. Morphological and biological differences of offspring are realized environmentally and genetically conditions which have effect on maternal effects [1,2,3,4,5,6]. In researches, it was determined that offspring from older mother has longer life spans, higher death rate and lower reproductive performance according to offspring from young mother [1,7,8,9,10,11,12,13]. This subject is also very important for natural enemies are used in biological control studies [14,15,16]. The declining parasitoid fecundity as an age of mother may be due to the decreasing related to age, number of eggs laid and parasitization ability of females [17,18]. Female age dependent fecundity of *A. nerii* one of the best prey for the production of biological control agents of scale insects [19], was investigated in this study.

## MATERIALS AND METHODS

Biparantel *Aspidiotus nerii* population grown on potato tubers in the insectarium of Plant Protection Department, Süleyman Demirel University, was used in this study. The potato tubers, containing *A. nerii* individuals in the same age, were placed on the top of the new clean potatoes when *A. nerii* individuals started to give new generations and kept 24 hours for the new generations passing to the clean potatoes. In this way, the 1<sup>st</sup> day crawlers of *A. nerii* were obtained. Fifteen days later, same method was used to transfer new generations from the potato tubers to the clean potatoes. Consequently, the 15<sup>th</sup> day crawlers of same aged *A. nerii* were obtained. The thirtieth day, again clean new potatoes were contacted to the potato tubers containing same aged *A. nerii* and kept for 24 hours to obtain the 30<sup>th</sup> day crawlers. Eventually, three different populations were constituted from same aged *A. nerii* giving birth at the 1<sup>st</sup> day, 15<sup>th</sup> day, and 30<sup>th</sup> day.

After the crawlers settled, each potato was divided into 4 cm<sup>2</sup> cells surface area surrounded by 'stickem special' to prevent their escape. When all crawlers in the cell became adults, one female and all the males were left in the cell and the rest of the females were removed. All males were removed after all of them become adult and mate with breeding female. Thus only one female left in each cells. Daily observations were made for each cell and crawlers were removed after counting. Experiments were done at 25°C, 16:8 hours and 65% relative humidity in a climate chamber (model KB 8400 F, Termax). Variance analysis and Tukey's multiple range tests were applied for statistical analysis [20]. Analysis were done by using CurveExpert pro (ver.1.6.7), SPSS, (ver.20.3), MS Excel (2010) softwares. Life table parameters were also calculated by using RmStat-3.2 [21]. These parameters;

- Age-specific survivor rate ( $l_x$ ) and fecundity rate ( $m_x$ ), [22],
- Net reproductive rate,  $R_0 = l_x \cdot m_x$  [22],
- Intrinsic rate of increase ( $r_m$ ),  $e^{r_m \cdot x} \cdot l_x \cdot m_x = 1$  [22],
- Mean generation time (day),  $T_0 = \frac{\ln R_0}{r_m}$  [22],
- Gross reproduction rate,  $GRR = m_x$  [22],
- Finite rate of increase,  $\lambda = e^{r_m}$  [22],
- Doubling time (day),  $T_2 = \frac{\ln 2}{r_m}$  [23],
- Reproductive value,  $V_x = \frac{\sum_{y=x}^{\infty} (e^{r_m \cdot y} \cdot l_y \cdot m_y)}{l_x \cdot e^{-r_m \cdot x}}$  [24],

- Life expectancy,  $E_x = \frac{\sum_{y=x}^{\infty} \frac{l_y + l_{y+1}}{2}}{l_x}$  [25,26],

- Stable age distribution,  $C_x = \frac{l_x \cdot e^{-r_m \cdot x}}{\sum_{x=0}^{\infty} (l_x \cdot e^{-r_m \cdot x})}$  [22],

- Age-dependent reproduction was calculated with the equation of Enkegaard [27,28].

$$F(x) = a \cdot x \cdot e^{(-b \cdot x)} \quad [27,28],$$

Where; F(x), daily age specific fecundity rate (egg/female/day); x, female adult age (day), a and b empirical constant. In the equation, first day is the female's first day as adult. The model was fitted to the data by nonlinear square technique; JMP (version 5.0.1), MS Excel 2010 and SPSS, (ver. 20.3) softwares.

## RESULTS AND DISCUSSION

Effect of mother age on growth and reproduction of *Aspidiotus nerii* was determined and life table parameters were given in Table 1. Total development periods of crawlers in the 1<sup>st</sup>, 15<sup>th</sup> and 30<sup>th</sup> days age females were observed 47.00, 37.00 and 45.00 days, oviposition periods 29.93, 22.14 and 7.87 days, respectively ( $P < 0.05$ ). Preoviposition period, life span and total life time decreased depending on age of mother. Omkar and Mishra [29] determined as 0- and 10-day-old females of *Propylea dissecta* (Mulsant) (Coleoptera: Coccinellidae) preoviposition period were found statistically different. Priest et al., [30] reported that *Drosophila melanogaster* Meigen (Diptera: Drosophilidae) offspring from older mother shorter life than did offspring from young mother.

**TABLE 1**  
Development and fecundity of in the 1<sup>st</sup>, 15<sup>th</sup> and 30<sup>th</sup> days age females of *Aspidiotus nerii* (\*)

	n	1 <sup>st</sup> Age	n	15 <sup>th</sup> Age	n	30 <sup>th</sup> Age
<b>Total development time</b>	28	47.00±0.00	22	37.00±0.00	30	45.00±0.00
<b>Preoviposition</b>	28	1.00±0.00	22	0.73±0.12	30	0.00±0.00
<b>Oviposition</b>	28	29.93±0.73 a	22	22.14±1.71 b	30	7.87±0.98 c
<b>Postoviposition</b>	28	1.00±0.00	22	0.55±0.21	30	1.27±0.19
<b>Generation time</b>	28	49.00±0.00	22	38.73±0.12	30	46.00±0.00
<b>Life span</b>	28	31.93±0.70	22	23.41±1.76	30	8.70±0.74
<b>Total life time</b>	35	69.14±3.40	32	44.66±4.46	55	40.96±2.88
<b>Daily number of crawlers</b>	28	6.50±0.15	22	3.64±0.36	30	1.70±0.21
<b>Total number of crawlers</b>	28	208.57±7.84 a	22	81.32±8.19 b	30	20.07±2.45 c

\*Means within a same row followed by the same letter do not differ significantly in Tukey test ( $P < 0.05$ ).

**TABLE 2**  
Life table parameters of in the 1<sup>st</sup>, 15<sup>th</sup> and 30<sup>th</sup> days age females of *Aspidiotus nerii* (\*)

Life Table parameters	1 <sup>st</sup> Age	15 <sup>th</sup> Age	30 <sup>th</sup> Age
Intrinsic rate of increase, $r_m^*$	0.073 a	0.072 a	0.034 b
Net reproduction rate, $R_o$	83.42	27.95	5.47
Mean generation time, $T_o$	60.56	46.11	49.56
Gross reproductive rate, $GRR$	110.39	51.28	12.84
Doubling time, $T_2$	9.48	9.59	20.21
Finite rate of increase, $\lambda$	1.08	1.07	1.03
n	35	32	55

\*Means within a same row followed by the same letter do not differ significantly in Tukey test ( $P < 0.05$ ).

It was recorded that generation times were 49.00, 38.73 and 46.00 days, crawlers number laid daily were 6.50, 3.64 and 1.70 crawlers and total crawlers number were 208.57, 81.32 and 20.07 crawlers, respectively. Yuztas et al., [13] determined in a study investigated the survival rate of bean aphid, *Aphis fabae* (Hemiptera: Aphididae) four different populations generated at the 1<sup>st</sup>, 6<sup>th</sup>, 11<sup>th</sup> and 16<sup>th</sup> days old mother, the highest nymph number was recorded 19.59 nymph in 6 day-old-mother, while in other groups as 7.25-14.14 nymph. Gunduz and Gulel [11] found that the mean numbers of total progeny per female *Bracon hebetor* (Hymenoptera: Braconidae) changed with the females age, between 1 day old and 5 day old females were not statistically significant; however, in the 10 day old females offspring production significantly decreased.

According to the life table, intrinsic rate of increase ( $r_m$ ) of in the 1<sup>st</sup> and 15<sup>th</sup> day age females were statistically in the same group while in the 30<sup>th</sup> day age females were in the different group ( $P < 0.05$ ). The mean generation time ( $T_o$ ), calculated from the time during which crawlers were constituted 24.50% (60.56 days), 26.55% (46.11 days) and 27.07% (49.56 days), respectively. At the end of the oviposition period, in the 1<sup>st</sup>, 15<sup>th</sup> and 30<sup>th</sup> day age females, gross reproductive rate ( $GRR$ ) were 110.39, 51.28 and 12.84 females/female, net reproductive rate ( $R_o$ ) were 83.42, 27.95 and 5.47 females/female, respectively (Table 2).

Nymphal mortalities were 0.20, 0.28 and 0.27 in the 1<sup>st</sup>, 15<sup>th</sup> and 30<sup>th</sup> day age females, respectively. Yüztaş et al., [13] identified that death rate increased depend on age of mother in survival rate of bean aphid, *A. fabae* four different populations generated by 1, 6, 11 and 16 days old mother. Fox et al., [9] reported that offspring from older parents often had shorter adult lifespan than offspring of younger parents in the seed

beetle, *Callosobruchus maculatus* (Coleoptera:Chrysomelidae).

At the beginning of oviposition period, the reproductive rate ( $m_x$ ) in the 1<sup>st</sup>, 15<sup>th</sup> and 30<sup>th</sup> days age females increased and at the 11<sup>th</sup> days (5.29 crawlers), at the 9<sup>th</sup> days (2.86 crawlers) and at the 2<sup>th</sup> days (1.30 crawlers) with reached maximum value, respectively. The oviposition period ended at the 36<sup>th</sup>, 37<sup>th</sup> day and 18<sup>th</sup> day in the 1<sup>st</sup>, 15<sup>th</sup> and 30<sup>th</sup> days age females, respectively (Figure 1).

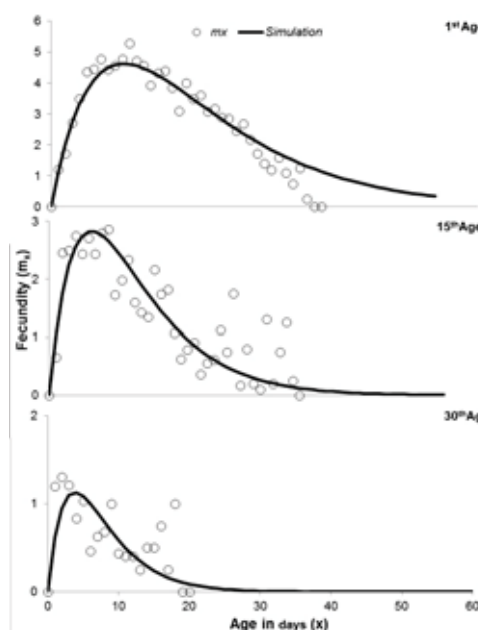


**FIGURE 1**  
Effect of female age on fecundity ( $m_x$ ) of *A. nerii* in the 1<sup>st</sup> day age females (Parameters:  $a=1.391\pm 0.058$ ,  $b=0.106\pm 0.002$ ,  $R^2=0.934$ ), in the 15<sup>th</sup> day age females ( $a=0.192\pm 0.128$ ,  $b=0.155\pm 0.009$ ,  $R^2=0.712$ ) and in the 30<sup>th</sup> day age females ( $a=0.798\pm 0.186$ ,  $b=0.261\pm 0.035$ ,  $R^2=0.313$ ).



The numbers of crawlers increased on the first days of the oviposition period and decreased regularly. Crawlers of young patterns were reflected in an increase in the daily number of crawlers laid per female. Another important indicator was to high numbers of crawlers produced by their first days of young females. Also oviposition period of females of young parents took longer than occurs in the elderly parents. This relation was determined with the Enkegaard equation and calculated parameters. Parameters were attained; in the 1<sup>st</sup> day age females  $a=1.391\pm 0.058$ ,  $b=0.106\pm 0.002$ ,  $R^2=0.934$ , in the 15<sup>th</sup> day age females  $a=0.192\pm 0.128$ ,  $b=0.155\pm 0.009$ ,  $R^2=0.712$  and in the 30<sup>th</sup> day age females  $a=0.798\pm 0.186$ ,  $b=0.261\pm 0.035$ ,  $R^2=0.313$ .

Female longevity was shorter in the 30<sup>th</sup> day age individuals. Daily fecundity was affected by maternal age. The fecundity was the highest for *A. nerii* reared from 1<sup>st</sup> day age females. They reproduce at the same time but decrease in daily fecundity as maternal age increases was observed. Similarly, reproductive value ( $V_x$ ) reached the highest level in the 1<sup>st</sup> day age females at 52<sup>th</sup> day, in the 15<sup>th</sup> day age females at 39<sup>th</sup> day and in the 30<sup>th</sup> day age females at 46<sup>th</sup> day, respectively. This value decreased quickly in following days with increasing death rate (Figure 2).

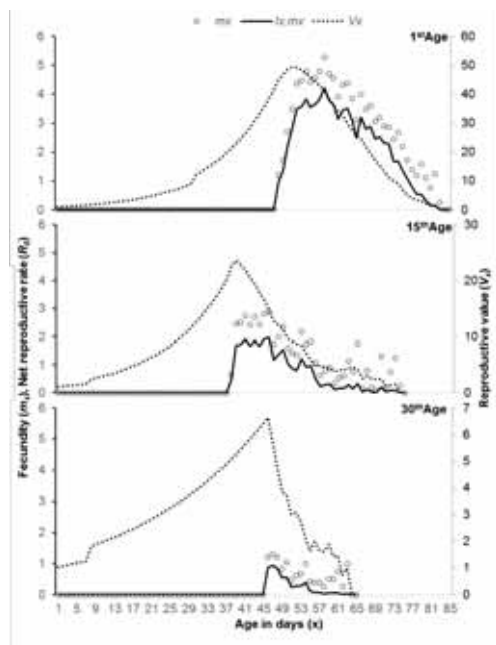


**FIGURE 2**  
Fecundity ( $m_x$ ), Net reproductive rate ( $R_0$ ) and Reproductive value ( $V_x$ ) of in the 1<sup>st</sup>, 15<sup>th</sup> and 30<sup>th</sup> days age females of *Aspidiotus nerii*.

Life expectancy ( $E_x$ ) in the beginning of nymph stage in the 1<sup>st</sup>, 15<sup>th</sup> and 30<sup>th</sup> days age females were calculated as 68.64, 44.16 and 40.46 days, but survival days 85, 75 and 64 days, respectively. Stable age distribution ( $C_x$ ) reached to 0.1 value in the 1<sup>st</sup> day age females at 63<sup>th</sup> day, in the 15<sup>th</sup> and in the 30<sup>th</sup> day age females at 43<sup>th</sup> day. It was reached to value of 1 depend on survival rate ( $l_x$ ) at the 85<sup>th</sup>, 75<sup>th</sup> and 64<sup>th</sup> days respectively (Figure 3).

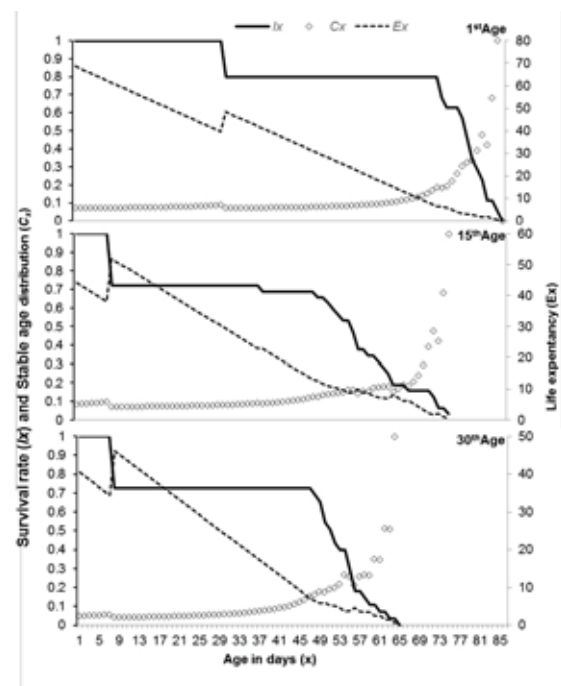


**FIGURE 3**  
Survival rate ( $l_x$ ), Stable age distribution ( $C_x$ ) and Life expectancy ( $E_x$ ) of in the 1<sup>st</sup>, 15<sup>th</sup> and 30<sup>th</sup> days age females of *Aspidiotus nerii*.

## CONCLUSIONS

The use of biological control agents has been increasing worldwide for the control of insect pests. However, quality control is required for the production and use of these natural enemies. In our study, we showed importance of using crawler of young females to produce the organisms used in biological control agents. These results clearly show that age of mother has a significant effect on the bioecology of crawlers. Reproduction was found to be dependent on adult age and decreased with maternal age.

## ACKNOWLEDGEMENTS

This study was presented as a poster presentation on the IV. Plant Protection Congress, which was held on 28-30 June 2011 in Kahramanmaraş, Turkey.

## REFERENCES

- [1] Mousseau, T.A. and Dingle, H. (1991). Maternal effects in insect life histories. *Annual Review of Entomology*, 36: 511-534.
- [2] Fox, C.W. (2000) *Maternal Effects in Insect-Plant Interactions: Lessons from a Desert Seed Beetle*. Department of Entomology, S-225 Agricultural Science Center North University of Kentucky Lexington, KY 40546-0091.
- [3] Bonduriansky, R. and Head, M. (2007) Maternal and paternal condition effects on offspring phenotype in *Telostylinus angusticollis* (Diptera: Neriidae). *Journal of Evolutionary Biology*, 20 (6): 2379-2388.
- [4] McLean, A.H.C., Ferrari J. and Godfray, H.C.J. (2009) Effects of the maternal and pre-adult host plant on adult performance and preference in the pea aphid, *Acyrtosiphon pisum*. *Ecological Entomology*, 34 (3): 330-338.
- [5] Lind, M.I., Berg, E. C., Alavioon, G. and Maklakov, A.A. (2015). Evolution of differential maternal age effects on male and female offspring development and longevity. *Functional Ecology* 29 (1): 104-110.
- [6] Birgucu, A.K., Turanlı, F., Gumus, E., Guzel., B. and Karsavuran, Y. (2015) The effect of grape cultivars on oviposition preference and larval survival of *Lobesia botrana* Den. & Schiff. (Lepidoptera: Tortricidae). *Fresenius Environmental Bulletin*, 24 (1): 33-38.
- [7] Fox C.W. (1993) Maternal and genetic influences on egg size and larval performance in a seed beetle (*Callosobruchus maculatus*): multigenerational transmission of a maternal effect. *Heredity* 73:509-517.
- [8] McIntyre, G.S. and Gooding, R.H. (2000). Effects of maternal age on larval competitiveness in house flies. *Heredity*, 85 (5): 480-489.
- [9] Fox, C.W., Bush, M.L. and Wallin, W.G. (2003) Maternal age affects offspring lifespan of the seed beetle, *Callosobruchus maculatus*. *Functional Ecology*, 17 (6): 811-820.
- [10] Opi, G.P. and Throne J.E. (2007) Influence of maternal age on the fitness of progeny in the rice weevil, *Sitophilus oryzae* (Coleoptera: Curculionidae). *Environmental Entomology*, 36(1): 83-89.
- [11] Gunduz, E.A. and Gulel, A. (2005) Investigation of fecundity and sex ratio in the parasitoid *Bracon hebetor* Say (Hymenoptera: Braconidae) in relation to parasitoid age. *Turkish Journal of Zoology*, 29: 291-294.
- [12] Al-Lawati, H. and Bienefeld, K. (2009) Maternal age effects on embryo mortality and juvenile development of offspring in the honeybee (Hymenoptera: Apidae). *Annals of Entomological Society America*, 102 (5): 881-888.
- [13] Yuztaş, G, Ozgokçe, M.S. and Karaca, I. (2015) Maternal age effects on fecundity and survival of *Aphis fabae* Scopoli (Hemiptera: Aphididae) on bean. *Turkish Journal of Entomology*, 39 (1): 67-77.
- [14] Kansu, I. A. and Uygun, N. (1980) Dogu Akdeniz Bölgesi'nde Turuncgöl Zararlilari ile Tum Savas Olanaklarinin Arastirilmesi. Ç.Ü. Ziraat Fakultesi Yayinlari 141, Bilimsel Arastirma ve Incelemeler 33: 63s. (in Turkish).
- [15] Karaca, I. and Uygun, N. (1990). Dogu Akdeniz Bolgesi Turuncgöllerinde Zararli Olan Aonidiella aurantii (Maskell) (Homoptera, Diaspididae)'nin Dogal Dusmanlari ve Bunlari Degisik Turuncgöl Tür ve Cesitlerinde Populasyon Gelismesinin Saptanmasi. Türkiye 2. Biyolojik Mucadele Kongresi Bildirileri, Entomoloji Derneği Yayinlari, No: 4: 97-108. (in Turkish).
- [16] Senal, D. (2006) Avcı Böcek *Chilocorus nigritus* (Fabricius) (Coleoptera: Coccinellidae)'un Bazı Biyolojik ve Ekolojik Özellikleri İle Doğaya Adaptasyonu Üzerinde Araştırmalar. Çukurova Üniversitesi, Fen Bilimleri Enstitüsü, Bitki Koruma Anabilim Dalı, Doktora Tezi, 127s. (in Turkish).
- [17] Melton, C.W. and Browning, H.W. (1986) Life history and reproductive biology of *Allorhogas pyralophagus* (Hymenoptera: Braconidae), a parasite imported for release against *Eoreuma loftini* (Lepidoptera: Pyralidae). *Annals of the Entomological Society of America*, 79: 402-406.
- [18] Orr, D.B., and Boethel, D.J. (1990) Reproductive potential of *Telenomus cristatus* and *T. podisi* (Hymenoptera: Scelionidae), two egg parasitoids of pentatomids (Heteroptera). *Annals of the Entomological Society of America*, 83 (5): 902-905.
- [19] Karaca, I. and Uygun, N. (1993) Zakkum kabuklubiti, *Aspidiotus nerii* Bouché (Hemiptera: Diaspididae)'nin degisik konukcular üzerindeki yasam cizelgeleri. *Türkiye Entomoloji Dergisi*, 17(4): 217-224 (in Turkish).
- [20] Sokal, R.R. and Rohlf., F.J. (1995) *Biometry: the principles and practice of statistics in biological research*, 3rd ed. W.H. Freeman: New York. 887 pp.

- [21] Ozgokçe, M.S. and Karaca, I. (2010) Yaşam Çizelgesi: Temel Prensipler ve Uygulamalar. Türkiye Entomoloji Derneği 1. Çalıştayı, Ekoloji Çalışma Grubu, 11-12 Haziran, Isparta (in Turkish).
- [22] Birch, L.C. (1948) The intrinsic rate of natural increase of an insect population. *Journal of Animal Ecology* 17: 15-26.
- [23] Kairo, M.T.K. and Murphy S.T (1995) The life history of *Rodolia iceryae* Janson (Coleoptera: Coccinellidae) and the potential for use in innoculative releases against *Icerya pattersoni* Newstead (Homoptera: Margarodidae) on coffee. *Journal of Applied Entomology*, 119: 487-491.
- [24] Imura, O. (1987) Demographic attributes of *Tribolium freemani* Hinton (Coleoptera: Tenebrionidae). *The Journal Applied Entomology and Zoology*, 22(4): 449-455.
- [25] Southwood, T. R. E. (1978) *Ecological methods*. Halsted Press, Chapman and Hall. London, 524 pp.
- [26] Carey, J. R. (1993) *Applied Demography for Biologists with Special Emphasis on Insects*. Oxford University Press, Oxford, UK, 206 pp.
- [27] Enkegaard, A. (1993) The poinsettia strain of the cotton whitefly, *Bemisia tabaci* (Hom.; Aleyrodidae), biological and demographic parameters on poinsettia (*Euphorbia pulcherrima*) in relation to temperature. *Bulletin of Entomological Research*, 83: 535-546.
- [28] Hansen, D.L., Brodsgaard, H.F. and Enkegaard, A. (1999) Life table characteristics of *Macrolophus caliginosus* preying upon *Tetranychus urticae*. *Entomologia Experimentalis et Applicata* 93: 269-275.
- [29] Omkar and Mishra, G. (2004) Influence of parental age on reproductive performance of an aphidophagous ladybird, *Propylea dissecta* (Mulsant). *Journal of Applied Entomology*, 128 (9-10): 605-609.
- [30] Priest, N.K., Mackowiak, B. and Promislow, D.E. (2002) The role of parental age effects on the evolution of aging. *Evolution*, 56 (5): 927-935.

---

**Received:** 16.02.2016

**Accepted:** 18.09.2016

---

**CORRESPONDING AUTHOR**

---

**Alime Bayindir**

Pamukkale University

School of Applied Sciences

Organic Farming Business Management Department

20600 Civril, Denizli – TURKEY

E-mail: abayindir@pau.edu.tr



# ADSORPTION BEHAVIOR OF NATURAL AND THERMALLY MODIFIED DIATOMITE FOR 1-NAPHTHOL FROM AQUEOUS SOLUTION

Song Chengjie, Liu Jingjing, Wang Liping\*, Xu Xia, Wang Shaomang

School of Environmental and Safety Engineering, Changzhou University, Changzhou, 213164, P. R. China.

## ABSTRACT

The adsorption of 1-naphthol from aqueous solution was investigated using unmodified and thermally modified diatomite at different temperature, pH, adsorbent mass and contact time. It can be observed that the modified diatomite improve the adsorption capacity rather than natural diatomite. The Langmuir, Freundlich and Dubinin-Radushkevich (D-R) isotherm models were applied to simulate the adsorption isotherms. The result showed that the Langmuir adsorption model fitted better in the temperature range. In addition, the experimental data were analyzed through the pseudo first-order model, the pseudo second-order model and the intraparticle diffusion model, respectively. The results displayed that the adsorption of 1-NAP on natural and modified diatomite could be explained by the pseudo second-order model. The thermodynamic parameters, such as Gibbs' free energy ( $\Delta G$ ), enthalpy ( $\Delta H$ ) and entropy changes ( $\Delta S$ ), were calculated. It may be observed that  $\Delta H$  values (less than 40 kJ/mol) was positive, which indicated that the adsorption process is the endothermic process of adsorption and belongs to physical adsorption.  $\Delta G$  values were negative. It indicated that the adsorption of 1-NAP onto natural and modified adsorbent were feasible and spontaneous.

## KEYWORDS:

1-naphthol; diatomite; kinetic; adsorption; thermodynamics

## INTRODUCTION

Contamination of surface water and groundwater with naphthalene compounds is one of the most serious environmental problems today, as they are potentially toxic to humans and aquatic life[1]. Among them, 1-naphthol (1-NAP) is of top priority contaminants and it is also the most important substructures of potentially carcinogenic

pollutants derived from pharmaceutical, dyestuff, photographic, and agrochemical industries, particularly in developing countries such as China[2]. However, the removal of 1-NAP cannot be accomplished in the natural environment or biological treatment plants [2-5]. 1-NAP has been detected in different types in water bodies and even in certain solid matrices. Therefore, the efficient elimination of 1-NAP has increasingly become a significant environmental issue.

Up to now, many methods have been widely used to remove naphthalene compounds, such as membrane technology [6, 7], biological degradation [8], ozonation [9, 10], photocatalytic degradation [11-15], coagulation [16] and ion exchange [17, 18]. Most of these methods suffer from disadvantages such as poor treatment efficiency, inconvenience of foster microbe, expensive analysis settings, labor-intensive sample preparation or generation of secondary pollutants, which limit their application and need further improvement [19, 20]. However, adsorption technique has been found to be an effective and attractive process for the treatment of these wastewaters because of the advantages of low operation temperature, short analysis time and high efficiency in the preconcentration of several pollutants [21, 22].

Various adsorbents have received much attention for naphthalene compounds removal. For instance, adsorbents for 1-NAP on sulfonated graphene nanosheets were produced by Zhao et al [23]. Zhang et al. have studied the removal of 1-NAP by a hydrophilic hyper-cross-linked polymer resin [24]. Wei et al. have studied the adsorption of naphthalene from aqueous solution on coal-based activated carbon modified by microwave induction [25]. The use of low cost materials as alternative and potential sorbents for the removal of the pollutant has been highlighted recently. To the best of our knowledge, there is little study regarding the adsorption of 1-NAP using diatomite in previous literatures.

Diatomite ( $\text{SiO}_2 \cdot n\text{H}_2\text{O}$ ), a sedimentary rock formed from accumulation of siliceous crusts of

diatomite, possesses unique physical-chemical properties [26-28]. It is applied as filtration media for various beverages, inorganic and organic chemicals in many industrial areas, since it has outstanding porous structure, low density, high surface area, chemical inertness and being sterile [29, 30]. Diatomite is one of low-cost and commercially available adsorbents for the adsorption of different heavy metal ions from water and wastewaters in recent report [31, 32].

This work investigated the feasibility of 1-NAP adsorption by thermal modification of raw diatomite. Surface properties of diatomite before and after modification were characterized by means of scanning electron micrograph (SEM), Fourier-transform infrared (FT-IR) spectra, XRD and BET. A number of experimental parameters are usually considered, including the effect of solution temperature, pH, adsorbent mass, as well as contact time. The experimental data were analyzed through Langmuir, Freundlich and D-R adsorption models. The kinetic adsorption results have been analyzed using pseudo-first-order, pseudo-second-order reactions and intraparticle diffusion model. The adsorption mechanism was also investigated in terms of thermodynamics and kinetics.

## MATERIALS AND METHODS

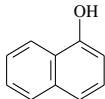
**Materials.** 1-NAP, analytical purity, obtained from Sinopharm Chemical Reagent Co., Ltd (Shanghai, China) (purity >99.5%). The relevant information of physical and chemical properties of 1-NAP were shown in Table 1. Sodium hydroxide (NaOH), sulfanilic acid, sodium nitrite (NaNO<sub>2</sub>), ethanol, sulfuric acid were obtained from Sinopharm Chemical Reagent Co., Ltd. (Shanghai, China). All chemicals in this work were analytically pure and used without further purification.

The natural diatomite used in this study was taken from Venture Chemical Co., Ltd. (Jiangsu, China). Before use, the diatomite sample was powdered by pounding in a porcelain mortar and washed several times by distilled water and then dried overnight in an oven at 100 °C. For making thermally modified diatomite, natural diatomite sample was heated and held at 450 °C for 2 h, and then it was cooled in a desiccator. It was put into polyethylene bags with “450-diatomite” label and stored to use in the future.

**Instruments.** The scanning electron microscope (SEM) images of natural diatomite and thermal modified diatomite were observed using JSM-7001F (Japan). Fourier-transform infrared (FT-IR) spectra were recorded on a Nicolet NEXUS-470 FT-IR apparatus (America) from 400 cm<sup>-1</sup> to 4000

cm<sup>-1</sup>, in order to investigate the surface characteristic of modified diatomite and adsorbed diatomite. The 1-NAP concentration was determined by a UV-visible spectrophotometer (UV-2450, Shimadzu, Japan). The solution pH was controlled by a precision pH/mV meter (PHB-9901, Shanghai, China). Batch adsorption experiments were performed by a constant temperature oscillator (THZ-C, Taicang, China). All chemicals and materials were weighed by electronic analytical balance (MS205DU, Shanghai, China). The supernatant was separated from the mixed solution using the centrifuge (TDL-5-A, Shanghai, China) in the Adsorption experimental procedure.

**TABLE 1**  
**Chemical and physical characteristic of 1-NAP**

Parameters	Value
CAS number	90-15-3
Molecular weight (g/mol)	144
Molecular formula	C <sub>10</sub> H <sub>8</sub> O
Chemical structure	

**Adsorption experiments.** The adsorption capability of natural diatomite and modified diatomite towards 1-NAP was investigated as a function of contact time, pH, temperature and the dosage of diatomite. In the work, all the adsorption experiments were performed by the batch technique using simulated water samples (10mg/L) for the adsorption studies. The adsorption characteristics were examined by mixing 0.1g, 0.2g, 0.3g, 0.4g, 0.5g and 0.6g of natural diatomite sample and modified sample with 100mL simulated water samples, respectively. pH = 1, 3, 5, 7, 9 and 11 of the solution was adjusted by using 0.1mol/L HCl or NaOH without adding any buffer. The resulting mixtures were shaken in a constant thermostatic oscillator at 150rpm at different temperatures of 15 °C, 25 °C, 35 °C, 45 °C until equilibrium condition had been attained. After a time period of mixing, the supernatant were centrifuged at 1000rpm for 10 min and then collected and analyzed by UV-vis spectrophotometer to determine the concentration of 1-NAP.

**Adsorption equilibrium isotherm.** Various models of adsorption equilibrium have been reported in the literatures to describe the adsorption process[33-35]. Each model has its limitation and is derived according to certain conditions. Langmuir, Freundlich and D-R isotherm models were applied to

describe the isotherm models, which were used to express the surface properties and affinity of the adsorbent.

A basic assumption of the Langmuir theory is monolayer sorption onto surface containing a finite number of identical sorption sites. The model can be written in a linear form by the literatures. [36, 37]:

$$\frac{1}{q_e} = \frac{1}{K_L Q_m} + \frac{1}{C_e} + \frac{1}{Q_m} \quad (1)$$

where  $q_e$  is the concentration of 1-NAP on sorbent at equilibrium (mg/g),  $C_e$  is the concentration of 1-NAP in the solution at equilibrium (mg/L),  $K_L$  is the Langmuir adsorption constant (L/mg) and  $Q_m$  (mg/g) is the theoretical maximum adsorption capacity (mg/g).

The Freundlich isotherm assumes a heterogeneous adsorption surface and active sites with different energy [38]. Its equation is given as follows:

$$\log q_e = \log K + \frac{1}{n} \log C_e \quad (2)$$

where the constant  $K$  (mg/g) is an approximate indicator of adsorption capacity and  $n$  is the empirical parameter related to the intensity of adsorption.

The equilibrium data were also applied to the D-R isotherm model to determine the nature of adsorption process. The D-R equation is [39]:

$$\ln q_e = \ln V_m - K_F e^{\varepsilon} \quad (3)$$

where  $V_m$  is D-R adsorption capacity (mg/g), the constant  $K_F$  related to adsorption energy ( $\text{mol}^2/\text{kJ}^2$ ),  $\varepsilon$  is Polanyi potential (kJ/mol), which is calculated as following:

$$e = RT \ln \left( 1 + \frac{1}{C_e} \right) \quad (4)$$

where  $R$  is gas constant (kJ /K mol) and  $T$  is temperature (K).

**Kinetic equation.** In order to explore reaction mechanism and pathways between the adsorbate and the adsorbent, the kinetic batch experimental data were analyzed using pseudo first-order model, pseudo second-order model and intraparticle diffusion model [40, 41], respectively.

The pseudo-first kinetic order equation is:

$$\ln(q_e - q_t) = \ln q_e - k_1 t \quad (5)$$

where  $q_e$  and  $q_t$  ( $\text{mg g}^{-1}$ ) are the adsorption capacity at equilibrium and at time  $t$ , respectively.  $k_1$  ( $\text{min}^{-1}$ ) is the rate constant of the pseudo-first order model.

The pseudo second-order adsorption equation is expressed as follows:

$$\frac{t}{q_t} = \frac{1}{k_2 q_e^2} + \frac{t}{q_e} \quad (6)$$

where  $k_2$  is the second-order rate constant ( $\text{g/mg} \cdot \text{min}$ )

The intraparticle diffusion model is expressed as following:

$$q_t = k_{id} \sqrt{t} + C \quad (7)$$

where  $k_{id}$  is the intraparticle diffusion rate constant ( $\text{mg/g h}^{1/2}$ ).  $C$  is the intercept (mg/g).

**Thermodynamic parameters.** The thermodynamic parameters such as Gibbs' free energy ( $\Delta G$ ), enthalpy ( $\Delta H$ ) and entropy changes ( $\Delta S$ ), for 1-NAP adsorption on raw diatomite and modified diatomite can be calculated from the temperature dependence of adsorption as follows [33]:

$$K_D = \frac{C_0 - C_e}{C_e} \cdot \frac{V}{m} \quad (8)$$

$$\Delta G^\circ = -RT \ln K_D \quad (9)$$

$$\ln K_D = \frac{\Delta S^\circ}{R} - \frac{\Delta H^\circ}{RT} \quad (10)$$

$R$  is the universal gas constant ( $8.314 \text{ J mol}^{-1} \text{ K}^{-1}$ ).  $K_D$  is the thermodynamic equilibrium constant.  $T$  is the absolute temperature in Kelvin (K).  $C_0$  is the initial concentration (mg/L).  $C_e$  is the equilibration concentration after centrifugation (mg/L).  $V$  is the volume (mL) and  $m$  is the mass of diatomite (g).

**Regenerability.** Regenerability was an important factor for an effective adsorbent. The diatomite samples, which were pre-adsorbed with 100 mL of solution containing 10 mg/L 1-NAP for 330 min at 25 °C, were washed with ethanol and stirred by magnetic stirring until no 1-NAP can be detected. Afterwards, the powder was dried overnight at 50 °C and reused for the next adsorption run.

## RESULTS AND DISCUSSION

**Characterization of Diatomite.** The morphological structures of diatomaceous earth and modified diatomite are investigated by SEM. As shown in Fig. 1a and b, diatomite frustules are mainly divided into two main categories: centric (discoïd) and pinnate (elongated). Compared with raw diatomite, thermally modified diatomite are shortened, and the particles are relatively more

evenly distributed. Moreover, it can be seen that modified diatomite has reduced particle sizes and decreased the agglomeration of diatomite, indicating that the calcination process increases the specific surface area of diatomite.

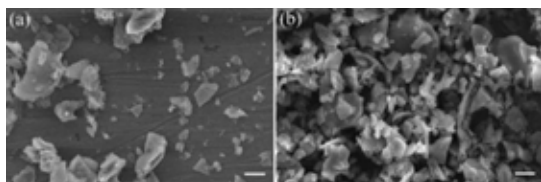


**FIGURE 1**  
SEM of the (a) raw diatomite and (b) 450-Diatomite. The scalebar is 10  $\mu\text{m}$ .

X-ray diffraction (XRD) analysis exhibits the lattice information, such as phase composition, purity and crystallinity. The XRD patterns for natural diatomite and 450-diatomite are illustrated in Fig. 2 (a). No other phases are found in 450-diatomite, suggesting that there is no appreciable chemical reaction occurs at thermally modification. The FT-IR spectra of natural diatomite together with 450-diatomite are given in Fig. 2 (b). Compared the spectra of natural diatomite and 450-diatomite, there are no new functional groups produced. From the spectrum, peaks at 1106 and 812  $\text{cm}^{-1}$  is caused by Si-O-Si asymmetry stretching vibration and the Si-O-Si symmetric stretching vibration peak, respectively [42, 43]. The peak at 478  $\text{cm}^{-1}$  is associated with the Si-O-Si bending vibration peak. Moreover, the stretching vibration and the bending vibration of OH functional group are found at the wave number of 3449 and 1657  $\text{cm}^{-1}$ , respectively. The pore size distributions of adsorbents are shown in Fig. 2 (c). It can be seen that the peak position of 450-diatomite shifted slightly toward the smaller pore diameter in comparison with natural dolomite that indicates the pore size of 450-diatomite is smaller than that of natural diatomite. Although, the pore volume of 450-diatomite is larger than that of natural diatomite.

**Effect of diatomite dosage, contact time and pH.** The dosage of diatomite is an important parameter governing adsorption on different adsorbents. As shown in Fig. 3 (a), with the diatomite dosage increased from 0.1 to 0.5g, the adsorption capacity increases from 0.28 to 1.48 mg/g. As the dosage approached to a certain value (0.5g), the adsorption capacity decreases slightly.

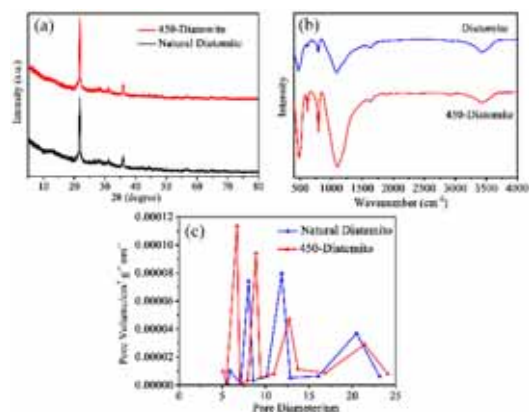


**FIGURE 2**  
(a) XRD patterns for natural diatomite and 450-diatomite; (b) FT-IR patterns for natural diatomite and 450-diatomite; (c) BET patterns for natural diatomite and 450-diatomite.

Therefore, the dosage of 0.5g diatomite is selected as optimum dosage for further experiments. The increasing process is ascribed to more active adsorption sites on the diatomite surface with increasing the dosage of the adsorbent [23]. The decreasing process could be due to aggregation of the adsorbent particles. In addition, it can be observed that the modified diatomite dramatically improve the adsorption capacity.

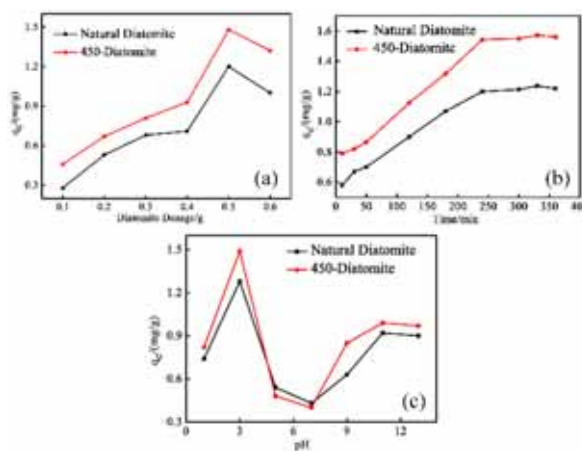


**FIGURE 3**  
(a) Diatomite adsorption 1-naphthol diatomite consumption versus adsorption capacity; (b) Diatomite adsorption 1-naphthol time versus adsorption capacity; (c) Diatomite adsorption 1-naphthol pH versus adsorption capacity

In order to ensure the sufficient adsorption equilibrium time, 0-400min are chosen as measurements. The effect of the contact time on the adsorption of 1-NAP onto the natural and thermally treated diatomite is illustrated in Fig. 3 (b). Initial adsorption of 1-NAP is rapid on both modified and unmodified diatomite, which is due to two reasons. On the one hand, at the initial stage, the amount of

adsorption sites are more, the 1-NAP could interact easily with diatomite. On the other hand, the concentration gradient between the bulk solution and the solid-liquid interface is higher in the initial period, so a higher adsorption rate is obtained. Besides, adsorption rate becomes slow and stagnate after contact time of 330min, which is due to less adsorption sites and slower diffusion. Thus, the contact time of 330min is the optimum contact time and used in the subsequent experiments. In addition, compared to the adsorption capability of natural diatomite towards 1-NAP, the adsorption capability of thermally treated diatomite significantly enhanced, indicating that the adsorption sites on modified diatomite could increase through thermal modification.

pH value is also an important parameter in the adsorption process, as it directly affects the surface charge of diatomite, the species of 1-NAP and the degree of ionization in solution. Hence, the effect of pH on the adsorption of 1-NAP on diatomite is studied at pH 1-13, 1-NAP initial concentration 10mg/L, adsorbent concentration 5 g/L, and temperature 45 °C. As shown in Fig. 3 (c), the adsorption capacity of diatomite shows a dramatic increase at pH value less than 3.0 and then decreased at 3 < pH < 7. When pH values increased from 7.0 to 13.0, the adsorption capacity of natural diatomite and modified diatomite increased gradually and then with small fluctuations to keep a stable value. The phenomenon can be explained that with the increase of pH, the concentration of hydroxide ion increased. Hydrogen bond may be formed by chemical reaction of hydroxide ion and hydroxyl group of 1-NAP, but the force of hydrogen bond is relatively weak. 1-Naphthol is an acid with a pKa of 9.34, therefore it would mainly exist as molecule form in an acidic solution and naphthalen-1-olate anion in an alkaline solution. At low pH, hydroxyl groups on the surface of diatomite gained proton and the diatomite surface had a positive charge. In addition, at higher pH values, the concentration of hydroxide ion increased. Hydrogen bond may be formed by chemical reaction of hydroxide ion and hydroxyl group of 1-NAP. But the force of hydrogen bond is relatively weak. Therefore, the best pH value of the system to remove 1-NAP from the solution using diatomite is 3.

**Adsorption isotherms.** Adsorption isotherms are essential to reveal the surface properties and affinity of the adsorbent so as to explore the reaction pathways and mechanism of the reaction. In this study, the Langmuir, Freundlich and D-R models are applied to fit the experimental data.

The Langmuir plots of  $1/q_e$  versus  $1/C_e$  have been given in Fig. 4 (a). The Freundlich plots supplied the graphic of  $C_e$  versus  $\log q_e$  have been given in Fig. 4 (b). And the lines supplied from the

graphics of  $e^2/10^5$  versus  $\ln q_e$  have been given in Fig. 4 (c).

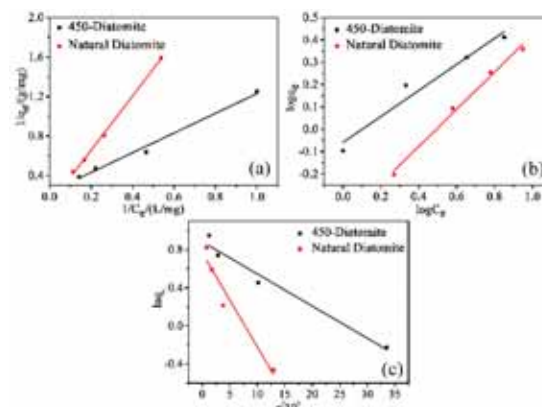


**FIGURE 4**  
**Diatomite adsorption 1-naphthol of Langmuir isotherm plots; (b) Diatomite adsorption 1-naphthol of Freundlich isotherm plots; (c) Diatomite adsorption 1-naphthol of D-R isotherm plots.**

From Fig. 4, when Langmuir, Freundlich, D-R mode are used to describe the adsorption of 1-NAP onto modified and unmodified diatomite, the linear plot with correlation coefficients  $R^2 = 0.98466, 0.99771; 0.9408, 0.98738; 0.9583, 0.91902$  are obtained. It is observed that data from both adsorbents fitted well to the Langmuir isotherm. Moreover, Fig. 4 (b) indicates the linear Freundlich isotherm plot and the standard error of parameter determination. In the event of  $n < 1$ , it shows that marginal adsorption energy decreases with increasing surface concentration. In case of  $n = 1$ , it indicates linear adsorption and equal adsorption energies for all sites. As for  $n > 1$ , it shows the favorable nature of adsorption and good adsorption. As seen from Fig. 4 (b), while  $n$  value is 1.199 on raw diatomite, the value of  $n$  is calculated 1.718 on thermal modified diatomite. The result suggested that 1-NAP is favorably adsorbed by diatomite.

**Kinetics of adsorption.** The pseudo-first kinetic order plots of  $\ln(q_e - q_t)$  versus  $t$  have been given in Fig. 5. The pseudo-second order plots of  $t/q_t$  versus  $t$  have been given in Fig. 6. The intraparticle diffusion model plots of  $q_t$  versus  $t^{0.5}$  have been given in Fig. 7. The parameters belonging to the all kinetic adsorption order plots of 1-NAP for original and modified diatomite are given in Table 2.

Fig. 5 shows that the pseudo-first order adsorption kinetics plots are not linear over the whole time range. Fig. 7 shows that the intraparticle diffusion adsorption kinetics plots are also not linear over the whole time range. For both adsorbents, the values of correlation coefficients are found to be



0.807~0.944. It indicated that the pseudo-first-order model did not fitted the experimental date very well. As Table 1, the values of  $q_e$  calculated from the pseudo-second-order model matched experimental results. The  $R^2$  values had been determined between 0.954 and 0.996 intervals. It is observed that the adsorption of 1-NAP on raw and modified diatomite could be explained by the pseudo second-order model better.

**Thermodynamic parameters.** The plots of  $\ln K_D$  against  $1/T$  are shown in Fig. 8. The  $R^2$  values are found to be 0.99483 and 0.9913, respectively. It is evident from  $R^2$  value that the data are well fitted. Then, the thermodynamic parameters are shown in Table 3.  $\Delta H$  and  $\Delta S$  can be calculated from the slope and intercept from the plot.

The values of  $\Delta H$  for raw and modified diatomite are determined as 25.70 and 37.04 kJ/mol, respectively.  $\Delta H$  values is positive, which belonged to the endothermic process of adsorption.  $\Delta H$  values is less than 40 kJ/mol which showed that the adsorption process is of a physical adsorption.

$\Delta S$  values, for modified and unmodified diatomite are 170 and 124 J/k/mol, respectively. The values have positive sign. It is realized that, some structural changes had happened in the adsorbate and adsorbents during the adsorption process. It also indicates the increasing randomness at the solid-liquid interface during the adsorption of 1-NAP on the adsorbents.

$\Delta G$  values are negative, which indicated that the adsorption of 1-NAP onto natural and modified adsorbent are feasible and spontaneous. In addition, the decrease in  $\Delta G$  with increasing temperature showed that better adsorption is obtained at higher

temperature.

**Regenerability.** The regeneration ability of thermally modified diatomite was studied by 1-naphthol adsorption-desorption cycles. The result of the cycling experiments was depicted in Figure 9.

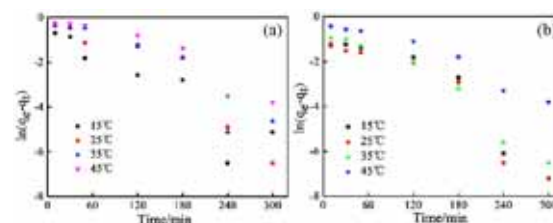


FIGURE 5

(a) Different temperatures of natural diatomite adsorption 1-naphthol of pseudo-first order adsorption kinetics plots; (b) Different temperatures of 450-diatomite adsorption 1-naphthol of pseudo-first order adsorption kinetics plots.

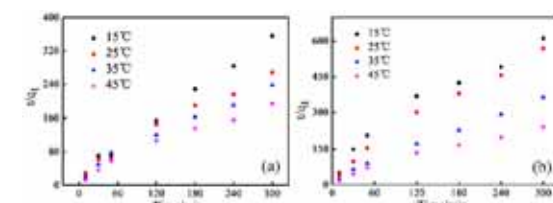


FIGURE 6

(a) Different temperatures of natural diatomite adsorption 1-naphthol of pseudo-second order adsorption kinetics plots; (b) Different temperatures of 450-diatomite adsorption 1-naphthol of pseudo-second order adsorption kinetics plots

TABLE 2

Different temperatures of diatomite adsorption 1-naphthol of intraparticle diffusion, pseudo-first, pseudo-second order kinetics parameters

Adsorbent	T/°C	$q_{e, \text{experimental}}$ (mg/g)	pseudo-first-order constants			pseudo-second-order constants			intraparticle diffusion constants	
			$k_1/(\text{min}^{-1})$	$q_e$ calculated/ (mg/g)	$R^2$	$k_2/(\text{g/mg/min})$	$q_e$ calculated/ (mg/g)	$R^2$	$k_{id}$	$R^2$
Natural diatomite	15	0.49	$2.11 \times 10^{-2}$	0.75	0.857	$5.90 \times 10^{-2}$	0.57	0.954	$2.30 \times 10^{-2}$	0.960
	25	0.53	$2.10 \times 10^{-2}$	0.61	0.858	$3.32 \times 10^{-2}$	0.57	0.984	$2.91 \times 10^{-2}$	0.975
	35	0.83	$2.00 \times 10^{-2}$	0.75	0.944	$4.70 \times 10^{-2}$	0.89	0.994	$3.20 \times 10^{-2}$	0.947
	45	1.24	$1.21 \times 10^{-2}$	0.95	0.940	$2.15 \times 10^{-2}$	1.34	0.978	$4.72 \times 10^{-2}$	0.981
Modified diatomite	15	0.85	$2.01 \times 10^{-2}$	0.58	0.807	$4.97 \times 10^{-2}$	0.91	0.996	$3.20 \times 10^{-2}$	0.807
	25	1.12	$1.79 \times 10^{-2}$	1.39	0.849	$2.25 \times 10^{-2}$	1.22	0.978	$4.73 \times 10^{-2}$	0.917
	35	1.27	$1.70 \times 10^{-2}$	1.28	0.845	$1.77 \times 10^{-2}$	1.31	0.977	$5.42 \times 10^{-2}$	0.953
	45	1.57	$1.32 \times 10^{-2}$	1.30	0.885	$1.42 \times 10^{-2}$	1.69	0.971	$6.00 \times 10^{-2}$	0.963

**TABLE 3**  
Thermodynamic parameters of 1-naphthol adsorption by Diatomite

Adsorbent	$\Delta H$ (kJ/mol)	$\Delta S$ (J/k/mol)	$\Delta G$ (kJ/mol)			
			288K	298K	308K	318K
Natural Diatomite	25.70	124	-10.06	-11.15	-12.55	-13.75
450-Diatomite	37.04	170	-11.97	-13.63	-15.11	-17.19

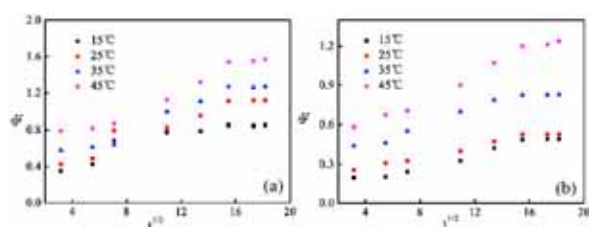


**FIGURE 7**

(a) Different temperatures of natural diatomite adsorption 1-naphthol of intraparticle diffusion adsorption kinetics plots; (b) Different temperatures of 450-diatomite adsorption 1-naphthol of intraparticle diffusion adsorption kinetics plots

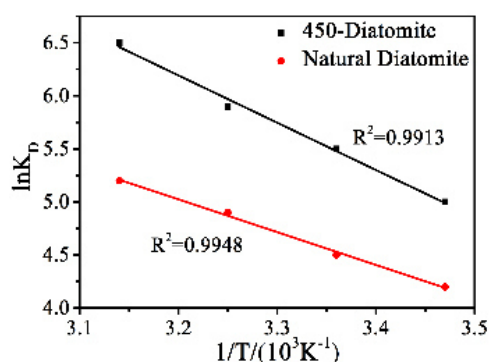


**FIGURE 8**

Natural diatomite and 450-diatomite adsorption on 1-naphthol of  $\ln KD$  versus  $1/T$  ( $\text{pH}=3$ ,  $[\text{1-naphthol}] = 10 \text{ mg/L}$ , Diatomite consumption  $0.5\text{g}$  and adsorption time  $30 \text{ min}$ )

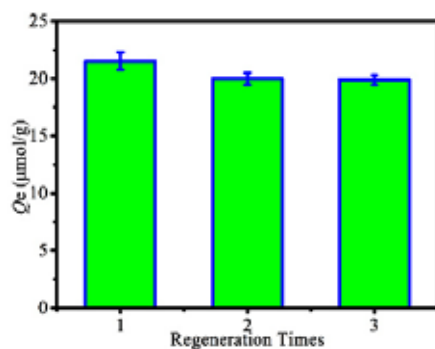


**FIGURE 9**

Regeneration of 450-diatomite for three cycles.

At the second recycle time, the adsorption capacity decreased by less than 4.93% and then showed an excellent capacity for regeneration. Until the third regeneration, the adsorption efficiency loss of thermally modified diatomite to 1-naphthol decreased by 7.14% but still remained at a high value. Therefore, the diatomite can be reused at least three times without significantly decreasing their adsorption capacities.

## CONCLUSION

(1) The adsorption of 1-NAP on raw and thermal modified diatomite was endothermic and spontaneous processes, controlled by physical mechanisms.

(2) The experimental datum are applied on the pseudo-first-order model, the pseudo-second-order model and the intraparticle diffusion model. It is found that, the adsorption of 1-NAP on natural and thermal modified diatomite could be explained by the pseudo-second-order model.

(3) For natural and thermal modified diatomite, the experimental data have been applied on Langmuir, Freundlich and D-R isotherm models. The Langmuir adsorption isotherm model fitted better in the temperature.

(4) The sorption of 1-NAP is strongly affected by pH, temperature and diatomite dosage. Compared with natural diatomite, it can be observed that the modified diatomite significantly improve the adsorption capacity.

## ACKNOWLEDGEMENTS

This work was supported by National Natural Science Foundation of China (N0.51308078); Natural Science Foundation of Jiangsu Province, China (N0. BK20130252); Project of Jiangsu Natural Science Foundation (N0. 14KJB10002); International Scientific and Technological Cooperation in Changzhou (CZ20140017).

## REFERENCES

- [1] Li JN, Fan RF, Lu SY, Zhang DR, Zhou YX, Lv YS. (2015) Exposure to polycyclic aromatic hydrocarbons could cause their oxidative DNA damage: a case study for college students in Guangzhou, China. *Environmental Science and Pollution Research*, 22(3), 1770-1777.
- [2] Gu L, Song FY, Zhu NW. (2011) An innovative electrochemical degradation of 1-diazo-2-naphthol-4-sulfonic acid in the presence of  $\text{Bi}_2\text{Fe}_4\text{O}_9$ . *Appl Catal B-Environ*, 110, 186-194.
- [3] Gu L, Guo HQ, Zhou P, Zhu NW, Zhang DF, Yuan HP, Lou ZY. (2014) Enhanced adsorptive removal of naphthalene intermediates from aqueous solution by introducing reed straw into sewage sludge-based activated carbon. *Environmental Science and Pollution Research*, 21(3), 2043-2053.
- [4] Hu J, Shao DD, Chen CL, Sheng GD, Li JX, Wang XK, Nagatsu M. (2010) Plasma-Induced Grafting of Cyclodextrin onto Multiwall Carbon Nanotube/Iron Oxides for Adsorbent Application. *J Phys Chem B*, 114(20), 6779-6785.
- [5] Huber MM, Ternes TA, von Gunten U. (2004) Removal of estrogenic activity and formation of oxidation products during ozonation of 17  $\alpha$ -ethinylestradiol. *Environ Sci Technol*, 38(19), 5177-5186.
- [6] Mu Y, Rabaey K, Rozendal RA, Yuan ZG, Keller J. (2009) Decolorization of Azo Dyes in Bioelectrochemical Systems. *Environ Sci Technol*, 43(13), 5137-5143.
- [7] Domingos FXV, Ribeiro CAO, Pelletier E, Rouleau C. [2011] Tissue Distribution and Depuration Kinetics of Waterborne C-14-labeled Light PAHs in Mummichog (*Fundulus heteroclitus*). *Environ Sci Technol*, 45(7), 2684-2690.
- [8] Mohanty S, Rao NN, Khare P, Kaul SN. [2005] A coupled photocatalytic-biological process for degradation of 1-amino-8-naphthol-3, 6-disulfonic acid (H-acid). *Water Research*, 39(20), 5064-5070.
- [9] Papic S, Peternel I, Krevzelj Z, Kusic H, Koprivanac N. (2014) Advanced Oxidation Of An Azo Dye And Its Synthesis Intermediates In Aqueous Solution: Effect Of Fenton Treatment On Mineralization, Biodegradability And Toxicity. *Environmental Engineering and Management Journal*, 13(10), 2561-2571.
- [10] Santiago-Morales J, Aguera A, Gomez MD, Fernandez-Alba AR, Gimenez J, Esplugas S, Rosal R. (2013) Transformation products and reaction kinetics in simulated solar light photocatalytic degradation of propranolol using Ce-doped  $\text{TiO}_2$ . *Appl Catal B-Environ*, 129, 13-29.
- [11] Du ED, Zhang YX, Zheng L, Li Z, Ieee. (2009) Optimization of Photocatalytic Degradation of Endocrine Disrupting Chemical Bisphenol A by Using Response Surface Methodology.
- [12] Du ED, Zhang YX, Zheng L. (2009) Photocatalytic degradation of dimethyl phthalate in aqueous  $\text{TiO}_2$  suspension: a modified Langmuir-Hinshelwood model. *React Kinet Catal Lett*, 97(1), 83-90.
- [13] Bokare AD, Chikate RC, Rode CV, Paknikar KM. (2008) Iron-nickel bimetallic nanoparticles for reductive degradation of azo dye Orange G in aqueous solution. *Appl Catal B-Environ*, 79(3), 270-278.
- [14] Debnath S, Ballav N, Nyoni H, Maity A, Pillay K (2015) Optimization and mechanism elucidation of the catalytic photo-degradation of the dyes Eosin Yellow (EY) and Naphthol blue black (NBB) by a polyaniline-coated titanium dioxide nanocomposite. *Appl Catal B-Environ*, 163, 330-342.
- [15] Muramatsu Y, Jin QL, Fujishima M, Tada H. (2012) Visible-light-activation of  $\text{TiO}_2$  nanotube array by the molecular iron oxide surface modification. *Appl Catal B-Environ*, 119, 74-80.
- [16] Merzouk B, Yakoubi M, Zongo I, Leclerc JP, Paternotte G, Pontvianne S, Lapique F. (2011) Effect of modification of textile wastewater composition on electrocoagulation efficiency. *Desalination*, 275(1-3), 181-186.
- [17] Wang CC, Juang LC, Lee CK, Hsu TC, Lee JF, Chao HP. (2004) Effects of exchanged surfactant cations on the pore structure and adsorption characteristics of montmorillonite. *J Colloid Interface Sci*, 280(1), 27-35.
- [18] Figueiredo H, Silva B, Quintelas C, Raposo MMM, Parpot P, Fonseca AM, Lewandowska AE, Banares MA, Neves IC, Tavares T. (2010) Immobilization of chromium complexes in zeolite Y obtained from biosorbents: Synthesis, characterization and catalytic behaviour. *Appl Catal B-Environ*, 94(1-2), 1-7.
- [19] Lou F, Yang D, Chen ZL, Megharaj M, Naidu R. (2015) The mechanism for degrading Orange II based on adsorption and reduction by ion-based nanoparticles synthesized by grape leaf extract. *J Hazard Mater*, 296, 37-45.
- [20] Stock HT, Kellogg RM. (1996) Synthesis of enantiomerically pure thiocrown ethers derived from 1,1'-binaphthalene-2,2'-diol. *Journal of Organic Chemistry*, 61(9), 3093-3105.
- [21] Lin DH, Xing BS. (2008) Adsorption of phenolic compounds by carbon nanotubes: Role of aromaticity and substitution of hydroxyl groups. *Environ Sci Technol* 2008, 42(19), 7254-7259.
- [22] Majzik A, Hornok V, Varga N, Tabajdi R, Dekany I. (2015) Functionalized gold nanoparticles for 2-naphthol binding and their fluorescence properties.

- Colloids and Surfaces a-Physicochemical and Engineering Aspects*, 481, 244-251.
- [23] Zhao GX, Li JX, Wang XK. (2011) Kinetic and thermodynamic study of 1-naphthol adsorption from aqueous solution to sulfonated graphene nanosheets. *Chem Eng J*, 173(1), 185-190.
- [24] Zhang WM, Hong CH, Pan BC, Zhang QJ, Jiang PJ, Jia K. (2009) Sorption enhancement of 1-naphthol onto a hydrophilic hyper-cross-linked polymer resin. *J Hazard Mater*, 163(1), 53-57.
- [25] Wei JM, Zhu RL, Zhu JX, Ge F, Yuan P, He HP, Ming C. (2009) Simultaneous sorption of crystal violet and 2-naphthol to bentonite with different CECs. *J Hazard Mater*, 166(1), 195-199.
- [26] Pan YF, Chiou CT, Lin TF. (2010) Adsorption of arsenic(V) by iron-oxide-coated diatomite (IOCD). *Environmental Science and Pollution Research*, 17(8), 1401-1410.
- [27] Khraishah MAM, Al-Ghouti MA, Allen SJ, Ahmad MN. (2005) Effect of OH and silanol groups in the removal of dyes from aqueous solution using diatomite. *Water Research*, 39(5), 922-932.
- [28] Yuan P, Liu D, Fan MD, Yang D, Zhu RL, Ge F, Zhu JX, He HP. (2010) Removal of hexavalent chromium Cr(VI) from aqueous solutions by the diatomite-supported/unsupported magnetite nanoparticles. *J Hazard Mater*, 173(1-3), 614-621.
- [29] Pantoja ML, Jones H, Garelick H, Mohamedbaker HG, Burkitbayev M. (2014) The removal of arsenate from water using iron-modified diatomite (D-Fe): isotherm and column experiments. *Environmental Science and Pollution Research*, 21(1), 495-506.
- [30] Xie FZ, Wu FC, Liu GJ, Mu YS, Feng CL, Wang HH, Giesy JP. (2014) Removal of Phosphate from Eutrophic Lakes through Adsorption by in Situ Formation of Magnesium Hydroxide from Diatomite. *Environ Sci Technol*, 48(1), 582-590.
- [31] Sheng GD, Wang SW, Hu J, Lu Y, Li JX, Dong YH, Wang XK. (2009) Adsorption of Pb(II) on diatomite as affected via aqueous solution chemistry and temperature. *Colloids and Surfaces a-Physicochemical and Engineering Aspects*, 339(1-3), 159-166.
- [32] Li E, Zeng XY, Fan YH. (2009) Removal of chromium ion (III) from aqueous solution by manganese oxide and microemulsion modified diatomite. *Desalination*, 238(1-3), 158-165.
- [33] Wang LG. (2012) Application of activated carbon derived from 'waste' bamboo culms for the adsorption of azo disperse dye: Kinetic, equilibrium and thermodynamic studies. *Journal of Environmental Management*, 102, 79-87.
- [34] Al-Othman ZA, Ali R, Naushad M. Hexavalent chromium removal from aqueous medium by activated carbon prepared from peanut shell: Adsorption kinetics, equilibrium and thermodynamic studies. *Chem Eng J*, 184, 238-247.
- [35] Li WG, Gong XJ, Li X, Zhang DY, Gong HN. (2012) Removal of Cr(VI) from low-temperature micro-polluted surface water by tannic acid immobilized powdered activated carbon. *Bioresource Technology*, 113, 106-113.
- [36] Aivalioti M, Vamvasakis I, Gidaracos E. (2010) BTEX and MTBE adsorption onto raw and thermally modified diatomite. *J Hazard Mater*, 178(1-3), 136-143.
- [37] Ghaedi M, Sadeghian B, Pebdani AA, Sahraei R, Daneshfar A, Duran C. (2012) Kinetics, thermodynamics and equilibrium evaluation of direct yellow 12 removal by adsorption onto silver nanoparticles loaded activated carbon. *Chem Eng J*, 187, 133-141.
- [38] Kacan E, Kutahyalı C. (2012) Adsorption of strontium from aqueous solution using activated carbon produced from textile sewage sludges. *Journal of Analytical and Applied Pyrolysis*, 97, 149-157.
- [39] Caliskan N, Kul AR, Alkan S, Sogut EG, Alacabey I. (2011) Adsorption of Zinc(II) on diatomite and manganese-oxide-modified diatomite: A kinetic and equilibrium study. *J Hazard Mater*, 193, 27-36.
- [40] Al-Aoh HA, Yahya R, Maah MJ, Bin Abas MR. (2014) Adsorption of methylene blue on activated carbon fiber prepared from coconut husk: isotherm, kinetics and thermodynamics studies. *Desalination and Water Treatment*, 52(34-36), 6720-6732.
- [41] Dural MU, Cavas L, Papageorgiou SK, Katsaros FK. (2011) Methylene blue adsorption on activated carbon prepared from *Posidonia oceanica* (L.) dead leaves: Kinetics and equilibrium studies. *Chem Eng J*, 168(1), 77-85.
- [42] Sun ZM, Zhang YZ, Zheng SL, Park Y, Frost RL. (2013) Preparation and thermal energy storage properties of paraffin/calcined diatomite composites as form-stable phase change materials. *Thermochimica Acta*, 558, 16-21.
- [43] Zhao XF, Zhang HJ, Fan JF, Guan DM, Zhao HD, Ni YW, Li Y, Chen JP. (2011) Dioxin-like compounds in sediments from the Daliao River Estuary of Bohai Sea: Distribution and their influencing factors. *Marine Pollution Bulletin*, 62(5), 918-925.



---

**Received: 17.02.2016**

**Accepted: 07.10.2016**

---

**CORRESPONDING AUTHOR**

---

**Wang Liping**

School of Environmental and Safety Engineering,  
Changzhou University, Changzhou, 213164, P. R.  
China.

e-mail: [wlp@cczu.edu.cn](mailto:wlp@cczu.edu.cn)

# CHANGES IN MACROELEMENTS CONCENTRATIONS IN TUBERS OF THREE POTATO CULTIVARS DUE TO AN APPLICATION OF HERBICIDES

Marek Gugala<sup>1,\*</sup>, Krystyna Zarzecka<sup>1</sup>, Krzysztof Kapela<sup>2</sup>, Anna Sikorska<sup>1</sup>,  
Ewa Krasnodebska<sup>1</sup>, Alicja Baranowska<sup>3</sup>

<sup>1</sup>Department Agrotechnology, University of Natural Sciences and Humanities in Siedlce, Poland

<sup>2</sup>Department of Agrometeorology and Agricultural Engineering, University of Natural Sciences and Humanities in Siedlce, Poland

<sup>3</sup>Institute of Agriculture, Pope John II State School of Higher Education in Biala Podlaska, Poland

## ABSTRACT

Tubers for laboratory analyses were obtained in a field experiment conducted at the Zawady Experimental Farm owned by the Siedlce University of Natural Sciences and Humanities in 2008-2010. The experiment was a two-factor split-plot arrangement with three replicates. The following factors were examined: three cultivars: Cekin, Satina, Tajfun, and four weed control methods based on an application of herbicides or their mixtures: Command 480 EC 0.2 dm<sup>3</sup>·ha<sup>-1</sup>, Dispersive Afalon 450 SC 1.0 dm<sup>3</sup>·ha<sup>-1</sup>, Stomp 400 SC 3.5 dm<sup>3</sup>·ha<sup>-1</sup> and no herbicide control. The aim of the study was to determine the effect of cultivars and herbicides mixtures on edible potato tuber contents of magnesium and potassium. Analysis demonstrated that genetic characteristics of the cultivars significantly affected magnesium content. The highest amount of magnesium was accumulated by Tajfun, on average 1.832 g kg<sup>-1</sup>, and the lowest by Cekin, on average 1.601 g kg<sup>-1</sup>. Also, variance analysis demonstrated a significant effect of weed control methods on magnesium content in potato tubers. Results of the study revealed that Tajfun and Cekin had, respectively, the highest and lowest potassium concentrations, on average 20.62 and 16.41 g kg<sup>-1</sup>. The herbicides and their mixtures applied in the experiment were found to significantly affect potato tuber dry matter content of potassium. A combination of mechanical and chemical weed control contributed to a decline in potassium content from 0.740 to 1.270 g kg<sup>-1</sup>, on average. Statistical analysis demonstrated that edible potato tuber content of potassium was significantly influenced by meteorological conditions in the study years.

## KEYWORDS:

herbicides, weed control methods, macroelements, potato

## INTRODUCTION

Potato is one of the most important plants in human nutrition. Potato tubers are a splendid source of carbohydrates, vitamins and minerals. White et al. [1] and Leszczyński [2] have reported that consumption of one average-sized potato weighing 200g provides the body with 18 to 30% daily intake of potassium, 5 to 15% intake of magnesium and 12% phosphorus.

Many authors [3-6] have claimed that agrotechnological factors and environmental conditions affect potato tuber contents of nutrients. Moreover, Grzebisz [7] has claimed that insufficient supply of macroelements is due to the fact that modern high-yielding cultivars are poorer in minerals than old low-yielding ones.

The aim of the study was to determine the effect of cultivars as well as herbicides and their mixtures on magnesium and potassium contents in edible potato tubers.

## MATERIALS AND METHODS

Tubers for laboratory analysis were obtained from a field experiment carried out from 2008 to 2010 at the Zawady Experimental Farm (52°03'N and 22°33'E) owned by the Siedlce University of Natural Sciences and Humanities. The experiment was arranged as a two-factor split-plot design with three replicates. The following factors were studied:

factor 1 - three cultivars: Cekin, Satina and Tajfun,

factor 2 - five weed control methods:

1. mechanical control: pre-emergence hilling followed by harrowing and one post-emergence hilling - control,

2. mechanic and chemical control: pre-emergence hilling followed by harrowing and spraying with Command 480 EC (chlomazon) 0.2 dm<sup>3</sup>·ha<sup>-1</sup> about 7 days before emergence,

3. mechanic and chemical control: pre-emergence hilling followed by harrowing and spraying with a mixture of Command 480 EC

(chlomazon) 0.2 dm<sup>3</sup>·ha<sup>-1</sup>+ Dispersive Afalon 450 SC (linuron) 1.0 dm<sup>3</sup>·ha<sup>-1</sup>,

4. mechanic and chemical control: pre-emergence hilling followed by harrowing and spraying with the herbicide Stomp 400 SC (pendimetalina) 3.5 dm<sup>3</sup>·ha<sup>-1</sup> about 7 days before emergence,

5. mechanic and chemical control: pre-emergence hilling followed by harrowing and spraying with a mixture of Stomp 400 SC (pendimetalina) 3.5 dm<sup>3</sup>·ha<sup>-1</sup>+ Dispersive Afalon 450 SC (linuron) 1.0 dm<sup>3</sup>·ha<sup>-1</sup> about 7 days before emergence.

The field experiment was set up on the the soil classified as the category - brown earth soils, type - eutrophic brown soil, formed from loamy sand, containing granulometric fraction with diameter <0.02 mm from 11.86 to 14.45% [8]. It was set up on soil classified as quality class IVa and very good rye complex in respect of agricultural usefulness, with a pH of 4.99 to 5.91 (1 mol KCl dm<sup>-3</sup>) as slightly acids soil pH and acid. Selected chemical soil properties prior to the experiment set-up are presented in Table 1. The soil contained a high and very high concentration of phosphorus, low and medium concentration potassium, very low and medium concentration of magnesium.

Potato was cultivated after winter cereals. The

same organic manuring and mineral fertilisation were applied, that is 25 t·ha<sup>-1</sup> FYM and 90 kg·ha<sup>-1</sup> N, 32.9 kg·ha<sup>-1</sup> P and 112.1 kg·ha<sup>-1</sup> K. Potatoes were harvested at the technological maturity stage, in early September. Magnesium potassium and calcium contents were determined in tuber dry matter after wet mineralisation of plant material using the Atomic Absorption Spectrophotometry (AAS). In contrast, the phosphorus was determined photometrically.

The results of the study were statistically analysed by variance analysis. Significance of sources of variation were checked by means of F Fisher-Snedecor test and significance of differences between means was determined by Tukey test at the significance level of P=0.05 [9].

Climatic conditions during the study period are presented in Table 2. The highest precipitation was recorded during the growing season of 2010 (459.7 mm) and the average air temperature was 15.6°C. The lowest precipitation (354.4 mm) was noted in 2009 when the average temperature was 15.1°C. The precipitation and average air temperature in the 2008 growing season were 371.4 mm and 14.9°C, respectively, the temperature not differing much from the long-term mean.

**TABLE 1**  
Chemical properties of the soil

Specification	Years		
	2008	2009	2010
Soil pH (1 M KCl)	4.99	5.15	5.91
Organic matter (g kg <sup>-1</sup> )	15.4	17.8	18.1
Content of available nutrients (mg kg <sup>-1</sup> )			
P	90.6	95.9	73.5
K	124.5	74.7	112.1
Mg	41.0	28.0	45.0

**TABLE 2**  
Characteristic of weather conditions of the period of potato vegetation (RSD Zawady)

Years	Months						IV-IX
	IV	V	VI	VII	VIII	IX	
	Rainfalls (mm)						Sum
2008	28.2	85.6	49.0	69.8	75.4	63.4	371.4
2009	8.1	68.9	145.2	26.4	80.9	24.9	354.4
2010	10.7	93.2	62.6	77.0	106.3	109.9	459.7
Multiyear sum (1987-2000)	38.6	44.1	52.4	49.8	43.0	47.3	275.2
	Air temperature (°C)						Mean
2008	9.1	12.7	17.4	18.4	18.5	12.2	14.7
2009	10.3	12.9	15.7	19.4	17.7	14.6	15.1
2010	8.9	14.0	17.4	21.6	19.8	11.8	15.6
Multiyear mean (1987-2000)	7.8	12.5	17.2	19.2	18.5	13.1	14.7

## RESULTS AND DISCUSSION

According to Westennann [10] and Martinez-Ballesta et al. [11] magnesium is an important component of potato tubers as it is a determinant behind basic processes of metabolism and energy conversion and plays a key role in preserving human health. Analysis of the effect of experimental factors on magnesium content demonstrated that the content was significantly affected by genetic characteristics of cultivars (Tab. 2). The highest amount of magnesium was accumulated by Tajfun, on average  $1.832 \text{ g}\cdot\text{kg}^{-1}$ , and the lowest by Cekin, on average  $1.601 \text{ g}\cdot\text{kg}^{-1}$ . Similar results were reported by many authors [1, 12-14] who found that potato tuber chemical composition is predominantly affected by the genotype.

Variance analysis revealed a significant impact of weed control methods on magnesium content in potato tubers (Tab. 3). The herbicides and their mixtures applied in the experiment increased magnesium content compared with control, the highest content being determined in plots where Stomp 400 SC + Dispersive Afalon 450 SC had been applied as a mixture at the respective rates of  $1.0$  and  $3.5 \text{ dm}^3\cdot\text{ha}^{-1}$  (on average  $1.773 \text{ g}\cdot\text{kg}^{-1}$ ) and plots where Command 480 EC + Dispersive Afalon 450 SC had been sprayed as a mixture at the respective rates of  $0.2$  and  $1.0 \text{ dm}^3\cdot\text{ha}^{-1}$  (on average  $1.753 \text{ g}\cdot\text{kg}^{-1}$ ). Similar results were reported in a previous work by Gugala et al. [13] who found that herbicides and their mixtures used to control weeds in potatoes significantly increased magnesium content, by  $2.7\%$  on average, compared with control. By contrast, Borowczak and Rębarz [5] concluded that a high input technology with full herbicide-based weed control led to a

decline in magnesium content in edible potato tubers.

Plant-derived food is characterised by a high potassium content [11]. According to Miles et al. [15], White et al. [1] and Wierzbička and Trawczynski [12], potato tuber content of potassium is influenced by genetic characteristics of cultivars. Results of the present study (Tab. 4) showed that the highest concentration of potassium was determined in Tajfun (on average  $20.62 \text{ g}\cdot\text{kg}^{-1}$ ), Cekin containing significantly less ( $16.41 \text{ g}\cdot\text{kg}^{-1}$ ). On the contrary, Wadas et al. [16], who cultivated early potato cultivars, found similar potassium contents and insignificant differences. Analysis of the results revealed that potassium content in potato tuber dry matter was significantly affected by herbicides and their mixtures applied in the experiment (Tab. 4). A combination of mechanical and chemical control contributed to a decline in potassium content ranging from  $0.740$  to  $1.270 \text{ g}\cdot\text{kg}^{-1}$ , on average. Significantly the lowest content of potassium compared to control - average  $17.84 \text{ g}\cdot\text{kg}^{-1}$ , found on the object 5., (mechanic and chemical control: pre-emergence hilling followed by harrowing and spraying with a mixture of Stomp 400 SC + Dispersive Afalon 450 SC about 7 days before emergence) and on the 4., (mechanic and chemical control: pre-emergence hilling followed by harrowing and spraying with the herbicide Stomp 400 SC about 7 days before emergence), average potassium content on this object was  $18.00 \text{ g}\cdot\text{kg}^{-1}$ . Also Klikocka [17] observed a tendency for potassium content to decline in potato tubers following an application of herbicides. However, Dobozi et al. [18] reported an increase in potato tuber content of potassium due to an application of herbicides.

**TABLE 3**  
Content of magnesium in the dry matter in potato tubers ( $\text{g kg}^{-1}$ )

Weed control methods	Years			Cultivars			Mean
	2008	2009	2010	Cekin	Satina	Tajfun	
1. Control object	1.302	1.821	1.908	1.568	1.700	1.763	1.677
2. Command 480 EC - $0.2 \text{ dm}^3\cdot\text{ha}^{-1}$	1.320	1.874	1.911	1.583	1.732	1.790	1.702
3. Command 480 EC $0.2 \text{ dm}^3\cdot\text{ha}^{-1}$ + Dispersive Afalon 450 SC - $1.0 \text{ dm}^3\cdot\text{ha}^{-1}$	1.343	1.923	1.993	1.603	1.781	1.876	1.753
4. Stomp 400 SC - $3.5 \text{ dm}^3\cdot\text{ha}^{-1}$	1.350	1.914	1.986	1.620	1.782	1.848	1.750
5. Stomp 400 SC - $3.5 \text{ dm}^3\cdot\text{ha}^{-1}$ + Dispersive Afalon 450 SC - $1.0 \text{ dm}^3\cdot\text{ha}^{-1}$	1.359	1.940	2.019	1.629	1.807	1.882	1.772
Mean	1.335	1.895	1.963	1.601	1.760	1.832	-

LSD<sub>0.05</sub> for: years -  $0.019$ , cultivars -  $0.019$ , weed control methods -  $0.040$ ;

interaction: weed control methods x cultivars - n.s.; weed control methods x years - n.s.

n.s. - not significant



**TABLE 4**  
**Content of potassium in the dry matter in potato tubers (g kg<sup>-1</sup>)**

Weed control methods	Years			Cultivars			Mean
	2008	2009	2010	Cekin	Satina	Tajfun	
1. Control object	21.22	17.44	18.68	17.12	18.85	21.37	19.11
2. Command 480 EC - 0.2 dm <sup>3</sup> ha <sup>-1</sup>	20.84	16.59	17.67	16.48	17.99	20.63	18.37
3. Command 480 EC - 0.2 dm <sup>3</sup> ha <sup>-1</sup> + Dispersive Afalon 450 SC - 1.0 dm <sup>3</sup> ha <sup>-1</sup>	20.70	16.24	17.60	16.43	17.58	20.53	18.18
4. Stomp 400 SC 3,5 dm <sup>3</sup> ha <sup>-1</sup>	20.64	15.77	17.59	16.04	17.60	20.36	18.00
5. Stomp 400 SC - 3.5 dm <sup>3</sup> ha <sup>-1</sup> + Dispersive Afalon 450 SC - 1.0 dm <sup>3</sup> ha <sup>-1</sup>	20.53	15.63	17.36	15.96	17.37	20.20	17.84
Mean	20.80	16,34	17.78	16.41	17.87	20.62	-

LSD<sub>0.05</sub> for: years - 0.29, cultivars - 0.29, weed control methods - 0.40; interaction: weed control methods x cultivars - n.s; weed control methods x years - 0.69; n.s. - not significant

Kolodziejczyk and Szmigiel [19], Szteke et al. [20], as well as Wierzbicka and Trawczynski [12] found in their studies that both magnesium and potassium contents were affected by weather conditions over individual growing seasons.

Analysis of the impact of weather conditions on the concentration of magnesium in potato tubers demonstrated that magnesium content was the highest (1.963 g·kg<sup>-1</sup>) in 2010 when both the precipitation and average air temperature during the growing season were the highest (Tab. 3).

In the present study, statistical calculations showed that potassium content in edible potato tubers was significantly affected by meteorological conditions in the study years (Tab. 4). The greatest amount of potassium was determined in tubers harvested in 2008 which had average precipitation and the lowest temperature compared with the remaining study years.

The results were confirmed in the study by Klikocka [17] who demonstrated that potato content was by 2% lower in a dryer year compared with a wet growing season. Unlike this author, Wierzbicka and Trawczynski [12] found the highest potassium content in a high precipitation year compared with the years with precipitation shortages.

In the study discussed here, an interaction of the experimental factors was observed for potassium content. Study years interacted with weed control methods, too, which means that potassium accumulation in potato tubers was different for herbicides examined in individual study years. No such interactions between the experimental factors were found for magnesium content.

The statistical analysis showed significant differences of the phosphorus content in potato

tubers (Tab. 5). The greatest concentration of phosphorus characterised the Satina variety - on average 2.326 g·kg<sup>-1</sup>, while the smallest the Tajfun variety - on average 2.293, these results were confirmed in studies of Zarzecka and Gąsiorowska [21], Wierzbicka and Trawczynski [12], who stated the significant impact of the variety factor on the phosphorus content in potato tubers. While Wadas et al. [22] did not report any significant impact of varieties on the phosphorus content in potato tubers.

Care treatments using herbicides contributed to the reduction of this macro element concentration (on average from 0.024 to 0.064 g·kg<sup>-1</sup>) compared to potatoes collected from the control object (Tab. 5). These results were confirmed in the previous studies by Zarzecka and Gąsiorowska [21] and Zarzecka and Gugala [23], who have demonstrated that the herbicides used in the care affected the reduction of the phosphorus content compared to tubers of the control object. While Dobozi et al. [18] showed a significant increase of the phosphorus content in potato tubers after using herbicides.

Genetic features of the cultivated varieties significantly determined the calcium content (Tab.6). Most of this component was accumulated by the Tajfun variety - on average 0.653 g kg<sup>-1</sup> while the least by the Cekin variety - on average 0.636 g·kg<sup>-1</sup>. These results were confirmed in studies by Tekalign and Hammes [24], Miles et al. [15] and Wadas et al. [22], who stated that the chemical composition of potato tubers is most of all shaped by the genotype.

The analysis of variance showed a significant impact of the care treatments on the calcium content in potato tubers (Tab. 6). Herbicides applied in the experiment and their mixtures caused the increase of the discussed component compared

to the control object. The largest calcium content characterised potato tubers collected in the objects, 5., on which the herbicide mixture Stomp 400 SC + Afalon Dispersive 450 SC was used - on average  $0.660 \text{ g kg}^{-1}$  and 3., where Command 480 EC + Afalon Dispersive 450 SC was used - on average  $0.649 \text{ g kg}^{-1}$ .

Weather conditions in the study years diversified the phosphorus and calcium content in the dry mass of potato tubers (Tab. 5, 6). The greatest amount of phosphorus was accumulated by tubers in 2008 ( $2.646 \text{ g kg}^{-1}$ ), which was damp and

cold, and significantly the least ( $2.145 \text{ g kg}^{-1}$ ) in 2009, in which temperatures were moderate and the rainfall quite evenly distributed. In contrast, analysing the impact of meteorological conditions on the calcium content in potato tubers it was stated that the largest amount was noted in 2009, while the smallest in 2010 - on average  $0.622 \text{ g kg}^{-1}$ , which was characterised by high rainfall and air temperature. The impact of weather conditions on these features are confirmed by Wierzbicka and Trawczynski [12], Wadas et al. [22], Klikocka and Glowacka [6] in their studies.

**TABLE 5**  
Content of phosphorus in the dry matter in potato tubers ( $\text{g kg}^{-1}$ )

Weed control methods	Years			Cultivars			Mean
	2008	2009	2010	Cekin	Satina	Tajfun	
1. Control object	2.678	2.179	2.179	2.339	2.374	2.323	2.345
2. Command 480 EC - 0.2 $\text{dm}^3 \text{ha}^{-1}$	2.652	2.160	2.151	2.328	2.331	2.304	2.321
3. Command 480 EC 0.2 $\text{L ha}^{-1}$ + Dispersive Afalon 450 SC - 1.0 $\text{dm}^3 \text{ha}^{-1}$	2.644	2.150	2.145	2.319	2.326	2.294	2.313
4. Stomp 400 SC 3,5 $\text{dm}^3 \text{ha}^{-1}$	2.639	2.139	2.138	2.316	2.310	2.290	2.305
5. Stomp 400 SC - 3.5 $\text{dm}^3 \text{ha}^{-1}$ + Dispersive Afalon 450 SC - 1.0 $\text{dm}^3 \text{ha}^{-1}$	2.618	2.099	2.129	2.303	2.290	2.252	2.282
Mean	2.646	2.145	2.148	2.321	2.326	2.293	2.313

LSD<sub>0.05</sub> for: years - 0.022, cultivars - 0.022, weed control methods - 0.024; interaction: weed control methods x cultivars - n.s.; weed control methods x years - n.s.  
n.s. - not significant

**TABLE 6**  
Content of calcium in the dry matter in potato tubers ( $\text{g kg}^{-1}$ )

Weed control methods	Years			Cultivars			Mean
	2008	2009	2010	Cekin	Satina	Tajfun	
1. Control object	0.623	0.629	0.599	0.604	0.618	0.629	0.617
2. Command 480 EC - 0.2 $\text{dm}^3 \text{ha}^{-1}$	0.644	0.651	0.617	0.623	0.634	0.654	0.637
3. Command 480 EC 0.2 $\text{dm}^3 \text{ha}^{-1}$ + Dispersive Afalon 450 SC - 1.0 $\text{dm}^3 \text{ha}^{-1}$	0.657	0.666	0.623	0.647	0.639	0.660	0.649
4. Stomp 400 SC 3,5 $\text{dm}^3 \text{ha}^{-1}$	0.652	0.659	0.631	0.647	0.641	0.654	0.647
5. Stomp 400 SC - 3.5 $\text{dm}^3 \text{ha}^{-1}$ + Dispersive Afalon 450 SC - 1.0 $\text{dm}^3 \text{ha}^{-1}$	0.661	0.678	0.641	0.657	0.657	0.666	0.660
Mean	0.647	0.656	0.622	0.636	0.638	0.653	0.642

LSD<sub>0.05</sub> for: years - 0.012, cultivars - 0.012, weed control methods - 0.014; interaction: weed control methods x cultivars - n.s.; weed control methods x years - n.s.;  
n.s. - not significant

## CONCLUSIONS

1. Studied cultivars differed significantly in terms of the content of macroelements. The highest content of magnesium, potassium and calcium was characterized by a variety Tajfun, while phosphorus Satina.

2. Herbicides and their mixtures applied in the experiment increased magnesium and calcium content and reduced potassium and phosphorus content in potato tubers compared with control where only mechanical control had been used.

3. Changeable weather conditions in individual study years had a significant effect on macroelements contents in the tubers of three edible potato cultivars.

## REFERENCES

- [1] White, P.J., Bradshaw, J.E., Finaly, M., Dale, B., Ramsay, G., Hammond, J.P., Broadley, M.R. (2009) Relationships Between Yield and Mineral concentrations in Potato Tubers. *Hort. Sci.*, 44(1), 6-11.
- [2] Leszczynski, W. (2012) Nutrition value of potato and potato products (Review of literature). *Biul. IHAR*, 266, 5-20. (In Polish)
- [3] Plaza, A. (2004) The chemical composition of table potato tubers in the conditions of varied organic fertilization. *Annales UMCS, Sec. E*, 59(3), 1327-1334. (In Polish)
- [4] Lachman, J., Hamouz, K., Dvorak, P., Orsak, M. (2005) The effect of selected factors on the content of protein and nitrates in potato tubers. *Plant Soil Environ.*, 51(10), 431-438.
- [5] Borowczak, F., Rębarz, K. (2006) The effects of different cultivation intensity an size and chemical composition of tubers in potato cv. Ania. *Biul. IHAR*, 242, 185-193. (In Polish)
- [6] Klikocka, H., Glowacka, A. (2013) Does the sulphur fertilization modify magnesium and calcium content in potato tubers. (*Solanum tuberosum* L.) *Acta Sci. Pol., Hortorum Cultus.*, 12(5), 41-53.
- [7] Grzebisz, W. (2011) Magnesium - food and human health. *J. Elem.*, 16(2), 299-323. DOI: 10.5601/jelem.2011.16.2.13
- [8] Marcinek, M., Komisarek, J. (red.) (2011) Polish soil systematics. *Wyd. 5. Rocz. Glebozn.*, 62(3), 1-179. (in Polish)
- [9] Trętowski, J., Wojcik, R. (1991) Methodology of agricultural experiments. *Wyd. WSRP Siedlce*: 1-500. (In Polish)
- [10] Westennann, D.T. (2005) Nutritional Requirements of Potatoes. *Amer. J. of Potato Res.*, 82, 301-307.
- [11] Martinez-Ballesta, M.C., Dominguez-Perles, R., Moreno D.A., Muries, B., Alcarza-Lopez, C., Bastías, E., Garcia-Viguera, C., Carwajal, M. (2010) Minerals in plant food: effect of agricultural practices and role in human health. A review. *Agron. Sustain. Dev.* 30: 295-309. DOI: 10.1051/agro/2009022
- [12] Wierzbicka, A., Trawczynski, C. (2011) Effect of irrigation and soil's microorganisms on the macro and micronutrient contents in organic potato tubers. *Fragm. Agron.*, 28(4), 139-148. (In Polish)
- [13] Gugala, M., Zarzecka, K., Mystkowska, I. (2012) Potato tuber content of magnesium and calcium depending on weed control methods. *J. Elem.*, 17(2), 247-254. DOI: 10.5601/jelem.2012.17.2.07
- [14] Flis, B., Zimnoch-Guzowska, E., Mankowski, D. (2012) Correlations among Yield, Taste, Tuber Characteristics and mineral Contents of Potato Cultivars Grown at Different Growing Conditions. *J. Agri. Sci.*, 4(7), 197-207. DOI: 10.5539/jas.v4n7p197
- [15] Miles, G.P., Buchman, J.L., Munyaneza, J.E. (2009) Impact of zebra chip disease on the mineral content of potato tubers. *Am. J. Potato Res.*, 86(6), 481-489. DOI: 10.1007/s12230-009-9104-0
- [16] Wadas, W., Jablonska-Ceglarek, R., Kosterna, E., Łęczycka, T. (2007) The potassium content in early potato tubers depending on cultivation metod. *Roczn. AR w Poznaniu, Ogrodn.*, 41, 643-647. (In Polish)
- [17] Klikocka, H. (2001) The influence of soil tillage systems and crop cultivation on content of macroelements in potato tubers. *Biul. IHAR*, 217, 197-203. (In Polish)
- [18] Dobozi, M., Lehoczky, E., Horváth, S. (2003) Investigation of the effect of soil herbicides on the growth and nutrient uptake of potato. *Commun. Agric. Appl. Biol. Sci.*, 68(4), 441-447.
- [19] Kolodziejczyk, M., Szmigiel, A. (2005) Content of macroelements in potato tubers depending on soil complex, cultivars and fertilization. *Fragm. Agron.*, 1(85), 436-445. (In Polish)
- [20] Szteke, B., Jędrzejczak, R., Reczajska, W. (2006) Relationships between macroelement and microelement content in potatoes. *Bromat. Chem. Toksykol.*, 39(3), 243-250. (In Polish)
- [21] Zarzecka, K., Gasiorowska B. (2000) Impact of some herbicides on the chemical composition of potato tubers. *EJPAU* 3(1). #04. <http://www.ejpau.media.pl/volume3/agronomy/art-04.html>
- [22] Wadas, W., Łęczycka, T., Borysiak-Marciniak, I. (2012) Effect of fertilization with multnutrient complex fertilizers on tuber quality of very early potato cultivars. *Acta Sci. Pol., Hortorum Cultus*, 11(3), 27-41.
- [23] Zarzecka, K., Gugala, M. (2004). Phosphor and potassium contents in edible potato bulbs



depending on the ways of weeds control.  
Hortic. Vegetable Growing, 23 (3), 128-135.  
[24] Tekalign, T., Hammes, P.S. (2005) Growth and  
productivity of potato as influenced by cultivar  
and reproductive growth. Growth analysis,  
tuber yield and quality. Sci. Hort., 105, 29-44.

---

**Received: 18.02.2016**

**Accepted: 08.09.2016**

---

#### **CORRESPONDING AUTHOR**

---

**Marek Gugala,**  
Department Agrotechnology  
University of Natural Sciences and Humanities in  
Siedlce Prusa 14, 08-110 Siedlce – POLAND

e-mail: [gugala@uph.edu.pl](mailto:gugala@uph.edu.pl)

# DEVELOPMENT AND CHARACTERIZATION OF SSR MARKERS FROM *FUSARIUM* INFECTED BARLEY (*HORDEUM VULGARE*) CDNA DATA SETS

Hulya Sipahi<sup>1,\*</sup>, Aysen Yumurtaci<sup>2</sup>, Hakan Hekimhan<sup>3</sup>

<sup>1</sup>Department of Biology, Faculty of Sciences and Arts, Sinop University, 57000, Sinop, Turkey

<sup>2</sup>Department of Biology, Faculty of Science and Letters, Marmara University, 34722, Istanbul, Turkey.

<sup>3</sup>Aegean Agricultural Research Institute, Menemen, İzmir, Turkey.

## ABSTRACT

In this study, a collection of 6666 expressed sequence tags (ESTs) deriving from two cDNA libraries (9841 and 24112) constructed under *Fusarium* infected conditions in *Hordeum vulgare* were screened to detect and characterize simple sequence repeat (SSR) motifs. Ninety-seven SSRs were identified in ESTs. Trinucleotides were the most frequent repeat (51%), followed by dinucleotides (38%) and tetranucleotides (8%), whereas motif size of pentanucleotides and hexanucleotides was only 1% and 4%, respectively, which is rarely found. Forty-nine SSR-containing EST unigenes were matched with *Hordeum vulgare* known protein with putative conserved domain via BLASTX. Out of 49 EST-SSRs, 33 of them were successfully used to design primer pairs and further confirmed in seven cultivated barley with significant differences in responses to *Fusarium* related root rot and head blight diseases. Nineteen of them gave amplification products. A total of 26 alleles were generated from 19 loci. The polymorphic information content (PIC) ranged from 0.28 to 0.60 and the expected heterozygosity (He) varied from 0.22 to 0.61. The seven cultivars were divided into three groups based on 19 SSR markers. These novel EST-SSR markers can be applied for genetic analysis, including marker-assisted selection for fusarium related diseases in barley breeding and genetic diversity analysis.

## KEYWORDS:

Barley, microsatellites, EST, *Fusarium*

## INTRODUCTION

The development and use of molecular markers for a variety of purposes, such as DNA functional gene tagging, map-based gene cloning, parental identification, genetic diversity analysis and molecular evolutionary studies, have gained momentum since the 1990s. Molecular markers allow the detection of sequence differences between

individuals. There are several kinds of molecular markers that analyse different aspects of DNA sequence variation. Simple sequence repeats detect variation in the number of short repeat sequences. The variability of SSR sequences in a genome is based on point mutations and the number of short repetitive motifs owed to slippage during replication or unequal crossing over. Because of their random distribution in genomes, abundance, multi-allelic nature, and co-dominant inheritance, SSRs are the best-suited marker system for sequence variation analysis. A large set of SSR markers is publicly available for the most agriculturally important crops [1, 2, 3, 4, 5, 6, 7].

In conventionally, SSR markers are developed as probes consisting of di-, tri-, tetra-, penta-, and hexanucleotide motifs to screen numerous clones in genomic DNA libraries. PCR primers are designed to identify SSRs that may be dispersed throughout the genome. These PCR primers can discriminate DNA sequences that share the same motifs, but contain a different number of repeats. Such development of SSRs is laborious, time-consuming and expensive. At the same time, increasing and copious amounts of data for expressed sequence tags (ESTs) are publicly available. ESTs have become landmarks of transcribed genome parts and deserve further investigation. Therefore, EST libraries offer an opportunity for the rapid and inexpensive development of SSRs. Furthermore, several software tools have been developed for screening SSR motifs [8]. Flanking regions of SSR at sufficient length is important in order to exclude reliable SSR sites. They provide suitable contexts for designing high-quality primers [9].

Barley (*Hordeum vulgare* L.) is one of the major cereal species grown in temperate areas and produced for feed and food consumption. It is under pressure from serial infection by fungi, agents for the most widely distributed plant diseases. Because of the harmful toxin biosynthesis, the *Fusarium* pathogen has caused serious yield loss in barley [10, 11]. In barley, as many as 501.838 ESTs are already available in the public domain ([http://www.ncbi.nlm.nih.gov/genbank/dbest/dbest\\_summary/](http://www.ncbi.nlm.nih.gov/genbank/dbest/dbest_summary/)). This study concentrated on exploring

SSRs from cDNA libraries of *Fusarium* infected barley, designing primers for their amplification and detecting allelic variance in cultivars resistant and sensitive to *Fusarium* related diseases.

## MATERIAL AND METHODS

**Plant materials.** A set of seven barley (*Hordeum vulgare* L.) cultivars were used to test SSR markers. Three of them were resistant (Hilal, Aydanhanım, Bolayır) and one susceptible (Bayrak) to *Fusarium* root rot; two of them were resistant (Hilal, Clarice) and two susceptible (Stander and Chevron) to *Fusarium* head blight. Genomic DNA was extracted as per Song and Henry [12].

**Bioinformatic analysis SSR identification.** After trimming of vector-contaminated sites in ESTs, a DNADragon (<http://www.sequentix.de/download/dnadragon.zip>) software 'sequence assemble' module was used to cluster all ESTs into condensed non-redundant groups. Non-clustered ESTs (singletons) were dissected and further analysed on eTRA 1.0 software developed by [13] Karaca et al. (2005) for extracting SSR-containing sequences. Consensus assemblies were processed to reveal the nucleotide-protein similarities by means of a Blastx (<http://www.ncbi.nlm.nih.gov/BLAST>) search. In addition, the barley-specific SSR-containing sites were used to map (<http://webblast.ipk-gatersleben.de/barley/viroblast.php>).

**PCR amplification and detection.** PCR reactions were carried out in a 20 µl reaction volume containing 10 µl of 2X master mix (120 µl of 25mM MgCl<sub>2</sub>, 40 µl of 10mM dNTP, 10 µl of Taq polymerase (5U/ µl), 200 µl of 10x PCR buffer, 630 µl of water), 1.5 µl of 10 µM of each primer, 3 µl of water and 30 ng template DNA. After initial denaturation at 94°C for 3 min, the following cycling parameters were applied: denaturation of 1 min at 94°C, annealing of 1 min at the respective temperatures (Table 2), extension of 2 min at 72°C. After 40 cycles of amplification, a final extension step was performed at 72°C for 7 min.

**Validation and diversity analysis.** The informativeness of a given DNA marker was measured by the PIC values described by Bostein et al. [14] and modified by Anderson et al. [15] 1993) and these were calculated according to the formula:

$$PIC = 1 - \sum_{i=1}^k p_i^2$$

where k is the total number of alleles detected for a given marker locus and p<sub>i</sub> is the frequency of

the i<sup>th</sup> allele.

EST-SSR alleles were scored for the presence (1) and absence (0) for seven cultivars. Genetic similarity was estimated according to Dice [16], and the unweighted pair-group method with the arithmetic means (UPGMA); a dendrogram was constructed using the NTSYSPC 2.0 software package [17].

## RESULTS

Assembly of the ESTs from two libraries (library numbers 9841 and 24112) produced 1 095 assembled contigs and 3 062 singletons, containing a total of 6 666 bp sequence lengths. The mining for SSR sequences revealed 97 SSRs in ESTs containing 6666 sequences. Ninety-seven SSRs included 14 different duplet, 24 triplet, 6 quadruplet, 1 quintuplet and 2 sextuplet motifs. The longest repeat present in the data set was a GA[24] di-nucleotide repeat. The longest polymorphic repeat detected was a (TTC)<sub>7</sub> trinucleotide repeat. Of 97 EST-SSRs, 49 SSR-containing EST unigenes showed significant similarities to known barley genes.

Only 33 primer pairs could be designed, which annotated to known barley genes (Table 1). These candidate EST-SSRs were validated in cultivars resistant and susceptible to *Fusarium* head blight and root rot diseases. Of the 33 primer pairs, 19 successfully amplified and produced clear band patterns of the expected size, whereas the remaining pair yielded an amplicon which was larger than expected (Tables 1 and 2). Of the 19 candidate SSRs, five were shown to be polymorphic, whereas the remaining SSR was monomorphic (Table 1). The five EST-SSRs revealed a total of 24 polymorphic alleles. The number of polymorphic alleles per primer pairs varied from one to three. When the informativeness of EST-SSR markers was measured, the polymorphic information content (PIC value) ranged from 0.28 to 0.60. Five of the 19 EST-SSR markers could function as useful markers.

As regards the values of genetic similarity of the cultivars based on EST-SSR markers, similarity coefficients ranged from 0.63 to 0.92. 'Hilal' and 'Clarice' had the largest genetic similarity (0.92) to 'Bayrak' and 'Stander', respectively, and the 'Chevron' cultivar was furthest from the 'Bolayır' cultivar with a genetic similarity of 0.63. The phenogram obtained on the basis of 19 EST-SSR markers differentiated the genotypes in three major groups (Fig. 1). The resulting UPGMA dendrogram could not manage to differentiate resistant cultivars from susceptible cultivars with regard to *Fusarium* related diseases.

**TABLE 1**  
**The putative proteins identified by BLASTX of 19 unigen sequences containing EST-SSRs.**

Sequence ID	Matched protein	Conserved region	Blast score	Genome	Repeat	Forward primer(5-3) Reverse primer (5-3)	Ta°C	Expected size (bp)
contig 624	predicted protein	RRM superfamily	RF 4E-40	2HL	(CATC)6	GCCAGACCAACCAATACC GGAGCAGCAACAATAGCA	51.9	110
contig 369	predicted protein	Gp-dh-N superfamily	1,00E-63	6HS	(CT)7	CGTGATAAGTATGAGGTGAGA AGCAGATATTGAGCGGAAG	54.1C	237
Contig 110	predicted protein	RabGTPase	7E-76	1H	(ATAA)5	CGGCAATGAGATGAAGGC TTATATCAGTCAGTCACG	52.9	408
Hv#S48849571 HVSMEI0016A02f2	predicted protein	Phosphate binding motif	5E-50	2HL	(TC)10	ATTGCTCATCTCATCCATACA GAGGGGAAGGAAGGAAG		153
Contig 642	predicted protein	Glyco hydro-3- superfamily	4E-149	4HL	(CCT)6	AGATGACCTCCTCCTCT CTCCTCGGCAAGAAGAAG	56	196
contig 35	gamma-3- hordein	Alpha-Amylase Inhibitors (AAIs) and Seed Storage (SS) Protein subfamily	6,00E-72	1H	(TTG)6	GGCTGTTGTTGAAGTTGGAT CGTTCCTCCGACCACATAT	54C	238
contig 381	gamma-3- hordein	Alpha-Amylase Inhibitors (AAIs) and Seed Storage (SS) Protein subfamily	1,00E-54	1H	(TTG)6	TGAGCAATAAGGTGGAACAT GCAACAACAACAACAAG	53.8C	218
contig 608	predicted protein	2-oxoacid dehydrogenases acyltransferase (catalytic domain)	5,00E-74	7HS	(TA)6	GCGGAGTGAGGTGTAA CCTGCGAAGAAGAGAAGAG	51.2	138
Hv#S12622295 HVSMEI0002A13f	UDP-D- glucose epimerase 1	UDP-glucose 4- epimerase	4- 1,00E-46	1H	(ATGG)7	ACCATCTTCCTTCCTTCCT CCTTCCTCCATCCATCCA	51.2C	117
Hv#S12624235 HVSMEI0010G24f	barwin=wound- induced protein homolog	Barwin family; this family is also named pathogenesis- related proteins PR-4. Members of this family are from barley seeds.	4,00E-22	3HL	(TG)10	CCAGGTCCCAGTTGTTCT TCCAGTTTCAGCCACCAA	51.7C	223
Hv#S12624944 HVSMEI0013J13f	predicted protein	DUF538; this family consists of several plant proteins of unknown function	4,00E-58	1H	(CAC)7	AACACTCACCACCACCAC CAGGAGGAGGCACAAGAAG	57.7C	111
Hv#S12625602 HVSMEI0017O10f	predicted protein	Condensing enzymes; Family of enzymes that catalyse a (decarboxylating or non-decarboxylating) Sm proteins; small nuclear ribonucleoprotein particles (snRNPs)	5,00E-41	1H	(TGC)7	GCTGTGGGTCTGTCTTTG CAAGGATGCTGCGAAGTA	52.1C	101
Hv#S12626423 HVSMEI0023G22f	predicted protein	involved in pre-mRNA splicing	2,00E-35	2HL	(CAT)7	GGAGCATTCACATCATCATC AGCAGGCAATATAGCAGAC	51.5C	135
Contig 305	predicted protein	ABC-2 type transporter	2E-107	4HS	(TTC)7	GGACTGACTGACGAAGGT CGATTAGAGGAGAGGAATAACA	55.8C	122
Contig 269	predicted protein	Nodulin MtN21 family protein	1,00E-40	7HS	(CAACGG)4	ATCATCACCCCGTCTCT TTGGAGCCGTTGCCGTT	59.1C	227
Hv#S48848420 HVSMEI0003G02r2	FT-like protein	Phosphatidyl Ethanolamine- Binding Protein (PEBP) domain regulation of flowering	2,00E-45	3HS	(ATC)12	AATGTGCGACGCATAGTTA GTGACCACACAAGAAGAAGAA		152
Hv#S48849653 HVSMEI0017O10f2	predicted protein	Condensing enzymes; Family of enzymes that catalyse (decarboxylating or non-decarboxylating)	4,00E-42	6HL	(AGC)7	GTCGCACAACCTCCTGTC TACTTCAAACCTCTTGCCCTG		155
Hv#S48848649 HVSMEI0006F02f2	predicted protein	Rubredoxin; nonheme iron binding domains	9,00E-55	5HS	(CT)15	AGACAGCAAAGGAAAAGTG GACAGGAGGGGTGGAGAC		128
Contig 114	predicted protein	The WRKY domain is a DNA binding domain	6E-72	3HL	(GCCGAT)4	GAAGACGACGGTGAGAGT ACGGACATCAGATTGAGAAC	59.5	407

**TABLE 2**  
**Characterization of 19 EST-SSR makers in barley cultivars.**

Locus	Repeat motif	Allele size (bp)	Number of alleles	Expected heterozygosity	Polymorphic information content (PIC)
contig 624	(CATC)6	117	1	-	-
contig 369	(CT)7	240-246	3	0.53	0.57
contig 110	(ATAA)5	408	1	-	-
Hv#S48849571 HVSMEI0016A02f2	(TC)10	155-157	2	0.22	0.43
contig 642	(TTG)6	296	1	-	-
contig 35	(TTG)6	252	1	-	-
contig 381	(TTG)6	218	1	-	-
contig 608	(TA)6	138	1	-	-
Hv#S12622295 HVSMEI0002A13f	(ATGG)7	117-121	2	0.28	0.28
Hv#S12624235 HVSMEI0010G24f	(TG)10	223-240	2	0.34	0.32
Hv#S12624944 HVSMEI0013J13f	(CAC)7	111	1	-	-
Hv#S12625602 HVSMEI0017O10f	(TGC)7	101	1	-	-
Hv#S12626423 HVSMEI0023G22f	(CAT)7	135	1	-	-
contig 305	(TTC)7	122-134	3	0.61	0.60
contig 269	(CAACGG)4	320	1	-	-
Hv#S48848420 HVSMEI0003G02r2	(ATC)12	152	1	-	-
Hv#S48849653 HVSMEI0017O10f2	(AGC)7	166	1	-	-
Hv#S48848649 HVSMEI0006F02f2	(CT)15	136	1	-	-
contig 114	(GCCGAT)4	407	1	-	-

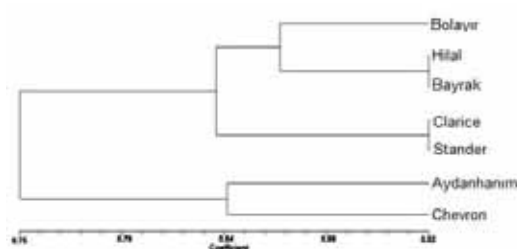


**FIGURE 1**  
**UPGMA phenogram showing the genetic similarity among the seven barley cultivars using EST-SSR**

## DISCUSSION

Polymorphic EST-SSR markers have been employed for several applications including tagging and mapping of genes related to agronomic and stress-resistant traits of interest, evolution, linkage mapping, and comparative analysis. Because of their genic function, EST-SSR markers have some advantages in terms of identifying the functional diversity of unique adaptive germplasm. In the

present study, the data sets from EST libraries consisting of 6666 sequences were surveyed to detect unique SSRs and design primers for them. Finally, 97 EST-SSRs were found. EST-SSRs with perfect SSRs were the most common, with a frequency of 31 and 50 for contig and singleton, respectively.

Among the repeat motifs, trinucleotide repeats were found to be the most abundant (51%), followed by dinucleotide (38%), tetranucleotide (8%), pentanucleotide (1%), and hexanucleotide (2%) repeats (Table 2). The highest frequency of trinucleotide motifs in our data is consistent with the frequencies reported for other cereals [8, 18, 19, 20, 21, 22, 23]. The suppression of non-trimeric SSRs in exons due to the risk of frameshift mutations may cause the dominance of triplet SSRs in the coding region [24].

Fourteen dinucleotide, twenty-four trinucleotide, six tetranucleotide, one pentanucleotide and two hexanucleotide different repeat motif types were identified in this data set. In contrast with other works [8, 23, 25, 26] which identified [AAG]*n*, [CCG]*n* and [AAT]*n* as the most and the least common motif, respectively, no



clear bias was observed in the abundance or scarcity of specific SSR motif types.

In the present study, even though only two libraries were used, the EST data cover a major part of the known barley genes. Forty-nine SSR-containing EST unigenes showed significant similarities to the known genes (Table 1). All the annotated proteins were from *Hordeum vulgare* L.

Only 58% of the designed primer pairs proved to be functional. The remaining 42% primer pairs failed to produce amplicons, possibly because of the presence of large introns, primers designed across exon/intron splice sites or primers that were derived from chimeric cDNA clones [8, 27].

Nineteen EST-SSR markers gave amplification products and five of them were found to be polymorphic. Of 19 functional primer pairs, two primer pairs gave amplicons larger than expected. The formation of products of unexpected size may be mainly owed to the insertion-deletion (indel) polymorphism within sequences or partly to the repeat length variability within SSRs.

In this study, chromosomes 1,2,3,4 and 6 were found to have a polymorphic EST-SSR region. A previous study indicated the importance of some QTL regions related to *Fusarium* resistance in barley which were predominantly found on chromosomes 2 and 6 [28]. Also, Li et al. [29] found a single QTL carrying two polymorphic SSRs, Bmac0209 and HMW33, located on chromosome 3HL in Chinese landrace 'TX9425', which was declared as moderately resistant to *Fusarium* crown rot infection. The discriminative activity of the Bmac0209 microsatellite marker was also confirmed by Sipahi and Yumurtacı [30] during the screening of diverse barley landraces. According our data, one polymorphic EST-SSR containing the repeat motif (TG)<sub>10</sub> on chromosome 3HL was matched with the 'Barwin wound induced protein'. This protein contains a conserved region known as pathogenesis-related protein PR-4, which was one of the members of barwin from barley seeds. Thus, these results showed the importance of barley chromosome 3H on both phylogenetic and *Fusarium* resistance testing in barley screening. Consequently, the newly developed markers in this study can also be used for construction of genetic linkage maps to perform gene-based association analysis especially for *Fusarium* related diseases.

In conclusion, the newly developed 33 EST-SSR markers can be used for construction of genetic linkage maps to perform gene-based association analysis especially for *Fusarium* related diseases and evaluated for genetic diversity analysis for barley.

#### ACKNOWLEDGEMENTS

This work was financially supported by a

Scientific Research Projects (BAP project no. FEF-1901.13-02) sponsored by University of Sinop, Turkey.

#### REFERENCES

- [1] Cregan, P.B., T. Jarvik, A.L. Bush, R.C. Shoemaker, K.G. Lark, A.L. Kahler, N. Kaya, T.T. VanToai, D.G. Lohnes, J. Chung, J.E. Henry. (1999) An Integrated Genetic Linkage Map of the Soybean Genome. *Crop Sci.* 39:1464–1490.
- [2] Milbourne, D., R. Meyer, A. Collins, L. Ramsay, C. Gebhardt and R. Waugh. (1998) Isolation, characterization and mapping of simple sequence repeat loci in potato. *Mol Gen Genet.* 259:233–246.
- [3] Ramsay, L., M. Macaulay, S. degli Ivanissevich, K. MacLean, L. Cardle, J. Fuller, K.J. Edwards, S. Tuveesson, M. Morgante, A. Massari, E. Maestri, N. Marmioli, T. Sjakste, M. Ganal, W. Powell, R. Waugh. (2000) A simple sequence repeat-based linkage map of barley. *Genetics.* 156:1997–2005.
- [4] Röder, M.S., V. Korzun, K. Wendehake, J. Plaschke, M.H. Tixier, P. Leroy and M.W. Ganal. (1998) A microsatellite map of wheat. *Genetics.* 149: 2007–2023.
- [5] Sharopova, N., M.D. McMullen, L. Schultz, S. Schroeder, H. Sanchez-Villeda, J. Gardiner, D. Bergstrom, K. Houchins, S. Melia-Hancock, T. Musket, N. Duru, M. Polacco, K. Edwards, T. Ruff, J.C. Register, C. Brouwer, R. Thompson, R. Velasco, E. Chin, M. Lee, W. Woodman-Cliekeman, M.J. Long, E. Liscum, K. Cone, G. Davis, E.H. Coe. (2002) Development and mapping of SSR markers for maize. *Plant Mol Biol.* 48:463-81.
- [6] Song, Q.J., E.W. Fickus and P.B. Cregan. (2002) Characterization of trinucleotide SSR motifs in wheat. *Theor Appl Genet.* 104:286–293.
- [7] Temnykh, S., W.D. Park, N. Ayers, S. Cartinhour, N. Hauck, L. Lipovich, Y.G. Cho, T. Ishii and S.R. McCouch. (2000) Mapping and genome organization of microsatellite sequences in rice (*Oryza sativa* L.). *Theor Appl Genet.* 100:697–712.
- [8] Varshney, R.K., T. Thiel, N. Stein, P. Langridge and A. Graner. (2002) In silico analysis on frequency and distribution of microsatellites in ESTs of some cereal species. *Cell Mol Biol Lett.* 7:537–546.
- [9] Tang, J., S.J. Baldwin, J.M.E. Jacobs, Van der Linden C.G., R.E. Voorrips, J.A.M. Leunissen, H. Van Eck and B. Vosman. (2008) Large-scale identification of polymorphic microsatellites using an in silico approach. *BMC Bioinformatics.* 9:374.



- [10] Buerstmayr, H., L. Legzdina, B. Steiner and M. Lemmen. (2004) Variation for resistance to Fusarium head blight in spring barley. *Euphytica*. 137:279-290.
- [11] Linkmeyer, A., M. Götz, L. Hu, S. Asam, M. Rychlik, H. Hausladen, M. Hess and R. Hüchelhoven. (2013) Assessment and introduction of quantitative resistance to Fusarium head blight in elite spring barley. *Phytopathology*. 103:1252-1259.
- [12] Song, W. and R.J. Henry. (1995) Molecular analysis of the DNA polymorphism of wild barley (*Hordeum spontaneum*) germplasm using the polymerase chain reaction. *Gen Res Crop Evol*. 42: 273–280.
- [13] Karaca M, Bilgen M, Onus A N, Ince AG, Elmasulu SY (2005) Exact tandem repeats analyzer (E-TRA): A new program for DNA sequence mining *Journal of Genetics* , 84(1): 49-54.
- [14] Bostein, D., R.L. White, M. Skolnick and R.W. Davis. (1980) Construction of genetic linkage map in man using restriction fragment length polymorphism. *Am J Hum Genet*. 32:314-331.
- [15] Anderson, J.A., G.A. Churchill, J.E. Sutriquet, S.D. Tanksley and M.E. Sorrel. (1993) Optimizing parental selection for genetic linkage maps. *Genome* 36:181-186.
- [16] Dice, L.R. (1945) Measures of the amount ecologic association between species. *Ecology*. 26:297-302.
- [17] Rohlf, F.J. (1998) NTSYS-pc. Numerical Taxonomy and Multivariate Analysis System, Version 2.02. Applied Biostatistics, New York.
- [18] Duran, C., R. Singhanian, H. Raman, J. Batley and D. Edwards. (2013) Predicting polymorphic EST-SSRs in silico. *Mol Ecol Resour*. 13:538–545.
- [19] Gao, L., J. Tang, H. Li and J. Jia. (2003) The analysis of microsatellites in major crops assessed by computational and experimental approaches. *Mol Breed*. 12:245–261.
- [20] Kantety, R.V., M. La Rota, D.E. Matthews and M.E. Sorrells. (2002) Data mining for simple sequence repeats in expressed sequence tags from barley, maize, rice, sorghum and wheat. *Plant Mol Biol*. 48:501–510.
- [21] Kota, R., R.K. Varshney, T. Thiel, K.J. Dehmer and A. Graner. (2001) Generation and comparison of EST-derived SSRs and SNPs in barley (*Hordeum vulgare* L.). *Hereditas*. 135:145-151.
- [22] Morgante, M., M. Hanafey and W. Powell. (2002) Microsatellites are preferentially associated with nonrepetitive DNA in plant genomes. *Nature Genetics*. 30:194–200.
- [23] Thiel, T., W. Michalek, R.K. Varshney and A. Graner. (2003) Exploiting EST databases for the development and characterization of gene-derived SSR-markers in barley (*Hordeum vulgare* L.). *Theor Appl Genet* 106:411–422.
- [24] Metzgar, D., J. Bytof and C. Wills. (2000) selection against frameshift mutations limits microsatellite expansion in coding DNA. *Genome Res*. 10:72-80.
- [25] Cuadrado, A., M. Cardoso and N. Jouve. (2008) Physical organization of simple sequence repeats (SSRs) in Triticeae: structural, functional and evolutionary implications. *Cytogenet. Genome Res*. 120:210–219.
- [26] Victoria, F.C., L.C. da Maia and A.C. de Oliveira. (2011) In silico comparative analysis of SSR markers in plants. *BMC Plant Biology*. 11:15.
- [27] Cordeiro, G. M., R. Casu, C.L. McIntyre, J.M. Manners and R.J. Henry. (2001) Microsatellite markers from sugarcane (*Saccharum* spp.) ESTs cross transferable to erianthus and sorghum. *Plant Sci*. 160:1115-1123.
- [28] Kosova, K., J. Chrpova and V. Šip. (2009) Cereal Resistance to Fusarium Head Blight and Possibilities of its Improvement through breeding. *Czech J Genet Plant Breed*. 45:87-105.
- [29] Li, H.B., M.X. Zhou and C.J. Liu. (2009) A major QTL conferring crown rot resistance in barley and its association with plant height. *Theor Appl Genet*. 118:903-910.
- [30] Sipahi, H and A. Yumurtacı. (2015) Dissection of Barley Landraces Originated From Twelve Different. *Tarım Bilimleri Dergisi* 21(3): 420-430.

---

**Received:** 16.02.2016

**Accepted:** 18.09.2016

---

#### CORRESPONDING AUTHOR

**Hulya Sipahi**

Department of Biology, Faculty of Sciences and Arts, Sinop University, 57000, Sinop, Turkey,

e-mail: [hulyasipahi@gmail.com](mailto:hulyasipahi@gmail.com)



# STUDIES ON DEGRADATION CHARACTERISTICS OF CHLORIMURON-ETHYL BY *BACILLUS SUBTILIS* STRAIN D-6

Yingjie Dai<sup>1</sup>, Binbin Zhang<sup>2\*</sup>, Yan Ji<sup>3</sup>, Xuezhao Li<sup>4</sup>, Dianqiu Lv<sup>4</sup> and Yanju Bai<sup>4</sup>

<sup>1</sup>College of Resources and Environment, Northeast Agricultural University, Harbin 150030, China

<sup>2</sup>Key Laboratory of Soybean Biology in Chinese Ministry of Education, Northeast Agricultural University, Harbin, 150030, China

<sup>3</sup>College of Environmental Science and Engineering, Nankai University, Tianjin, 300350, China

<sup>4</sup>Virus-free Seeding Research Institute, Heilongjiang Academy of Agricultural Sciences, Harbin 150010, China

## ABSTRACT

The chlorimuron-ethyl-degrading strain D-6 was isolated from contaminated soil and identified by 16S rRNA gene sequencing as *Bacillus subtilis* under laboratory conditions. When chlorimuron-ethyl was provided as the sole nitrogen source, the degradation efficiency in liquid medium was about 90.5% after 3 days of inoculation with strain D-6. The effects of chlorimuron-ethyl concentration, degradation time, and temperature on biodegradation were examined. The optimal conditions of chlorimuron-ethyl degradation by D-6 were chlorimuron-ethyl 300 mg/L, NH<sub>4</sub>NO<sub>3</sub> 1 g/L, at 30 °C, pH7.0 and 3 days.

## KEYWORDS:

Chlorimuron-ethyl; *Bacillus subtilis* strain; Isolation and screening; Degradation

## INTRODUCTION

Sulfonylurea is a family of herbicides that can control weeds in wheat, rice, soybean, barley, cotton, potato and corn [1, 2]. Chlorimuron-ethyl is one of the sulfonylureas used for pre- and postemergence broadleaf weed control, characterized by very low application rates, high herbicidal activity, good crop selectivity and low mammalian toxicity. The use of chlorimuron-ethyl to control weeds in soybean production in northeast of China has steadily increased over the past few years. In Heilongjiang Province of China, a total of 400 tons of chlorimuron-ethyl is used, and covers more than  $1.33 \times 10^6$  ha of soybean field each year [3]. Chlorimuron-ethyl can persist in soil for a long time (over 100 days), has raised increasing concerns about the damage of the rotation crops

and the risk of contaminating nearby aquatic systems [2, 4]. Moreover, chlorimuron-ethyl have high water solubility, it is prone to leach through soil to groundwater, easily causing groundwater pollution via precipitation and irrigation [5]. Consequently, there is a need to find a way to rapidly detoxify the residua of chlorimuron-ethyl in the environment.

There is very little information about the degradation of chlorimuron-ethyl. Ma et al. [6] studied that chlorimuron-ethyl was provided as the sole nitrogen source, the degradation efficiency of chlorimuron-ethyl in liquid medium was about 81.0% after 7 days of inoculation with LW3 (this is the bacterium of *Pseudomonas sp.* which is able to degrade chlorimuron-ethyl). Zhang et al. [7] study showed that when the initial concentration of chlorimuron-ethyl in culture was 5 mg/L, LF1 (this is the only yeast strain of *Sporobolomyces sp.* which is able to degrade chlorimuron-ethyl) could degrade more than 77% of the herbicide after incubation for 4 d at 30°C. The possible mechanism of chlorimuron-ethyl degradation by LF1 could be the acidic hydrolysis caused by the acids from the metabolism of the yeast strain. However, there has been no report on the chlorimuron-ethyl-degrading *Bacillus subtilis* strain.

The objectives of this study were to isolate and characterize the microbes for degrading chlorimuron-ethyl under laboratory conditions, and to determine the rate of chlorimuron-ethyl degradation in liquid culture with different conditions such as: identification and characterization of D-6, degradation time, different concentrations of chlorimuron-ethyl, and temperature.

## MATERIALS AND METHODS

**Chemicals and soil.** Chlorimuron-ethyl



(97% purity) is purchased from Shanghai Anpel Instrument Co., Ltd., China. Dichloromethane is of analytical reagent grade and redistilled before use. Methanol and acetic acid glacial are of chromatographic pure grade and filtrated before use. Other chemicals used in this study are all of analytical grade. The test soil is a chlorimuron-ethyl contaminated chernozem soil in Nenjiang County of Heilongjiang province of China.

**Enrichment and isolation of chlorimuron-ethyl degrading strains.** Twenty grams of 0–25 cm soil samples was added to 200 mL of nitrogen-limited minimal salts medium (NaCl 20.0 g, CaCl<sub>2</sub> 0.4 g, NH<sub>4</sub>Cl 1.0 g, KCl 0.2 g, KH<sub>2</sub>PO<sub>4</sub> 1.0 g, FeCl<sub>2</sub>·4H<sub>2</sub>O 0.04 g, K<sub>2</sub>HPO<sub>4</sub> 2.0 g, MgSO<sub>4</sub> 1.0 g, glucose 10.0 g, distilled water 2 L, pH 7.0) in 500 mL flask, and 10 mg of chlorimuron-ethyl as the sole nitrogen source for microbes was added to the mixture at 4-d intervals. After three additions of chlorimuron-ethyl, 10 mL of the soil suspension was transferred to a sterile mineral salts medium containing 100 mg/L chlorimuron-ethyl. When the mineral solution turned turbid, 1 mL of the suspension was transferred to a fresh sterile mineral salt medium containing 200 mg/L chlorimuron-ethyl. The procedure was repeated three times to increase the level of chlorimuronethyl to 500 mg/L. The final enriched culture was spread on the culture agar plates containing 100 mg/L chlorimuronethyl, and the medium comprised (per 1000 mL distilled water). Beef extract peptone semi solid culture medium: beef extract 1.0 g, peptone 1.0 g, NaCl 1.0 g, agar 1.6 g, pH 7.0. Actinomycetes culture medium: glucose 4.0 g, peptone 4.0 g, KH<sub>2</sub>PO<sub>4</sub> 0.1 g, MgSO<sub>4</sub>·7H<sub>2</sub>O 0.1g, KNO<sub>3</sub> 0.2g, NaCl 0.1 g, FeSO<sub>4</sub> 0.002 g, soluble starch 4.0 g, agar 4.0 g, distilled water 200mL. Enrichment medium: peptone 1.0 g, K<sub>2</sub>HPO<sub>4</sub> 0.2 g, MgSO<sub>4</sub> 0.1 g, distilled water 200mL, agar 30.0 g, and pH 7.2. before incubation. Different colonies were picked up, and further purified by using streak plating method. No bacteria and actinomycetes capable of degrading chlorimuron-ethyl were obtained from the enrichment culture, but a total of 6 *Bacillus subtilis* strains were found to possess the ability of degrading chlorimuron-ethyl, among which, strain D-6 had the highest degradation efficiency, and was selected for further studies.

**Identification and characterization of D-6 strain.** The identification of D-6 was based on its colony morphology and cultural and biochemical characteristics following with reference to *Bacillus subtilis* strain. The 16S rRNA gene was

amplified by using polymerase chain reaction (PCR) with the universal primer pair [8] of F<sub>27</sub> (5'-AGAGTTTGATCCTGGCTCAG-3') and R<sub>1541</sub> (5'-AAGGAGGTGATCCAGCCGCA-3'). The conditions for PCR were: denaturation at 95 °C for 5 min, followed by 35 cycles of denaturation at 94 °C for 30 s, at 52 °C for 30 s, and 72 °C for 60 s, and a final extension at 72 °C for 10 min. PCR fragments were purified by agarose gel electrophoresis. The 16S rRNA gene sequence was determined at Sangon Biotechnology Co., Ltd., Shanghai, China and compared with the most similar sequence in the Genbank nucleotide sequence database based on the percentage similarities. Sequences with the greatest similarity to the isolate D-6 sequence were extracted from the database and aligned. Software ClustalX was used for sequence analysis and contrast [9]. The tree was generated by Mega5.0.

**Inoculum preparation for degradation study.** The strain D-6 was cultured in 250 mL flask containing 100 mL of medium (peptone 5.0 g, malt extract 5.0 g, distilled water 1000 mL) supplemented with 100 mg/L chlorimuron-ethyl. At its exponential phase, D-6 was collected by centrifugation. The pellets were washed two times with 0.02 mol/L Na<sub>2</sub>HPO<sub>4</sub>-KH<sub>2</sub>PO<sub>4</sub> buffer, resuspended in the same buffer, and used for inoculation.

**Degradation of chlorimuron-ethyl by D-6.** D-6 was isolated from the minimal salts medium (MSM) supplemented with chlorimuron-ethyl as the sole nitrogen source. To have a better growth of D-6, the degradation test of chlorimuron-ethyl by D-6 was performed in MSM supplemented with nitrogen sources NH<sub>4</sub>NO<sub>3</sub> (MSNM) and chlorimuron-ethyl. An inoculum (1%, V/V) of D-6 was inoculated into MSNM, and all cultures were incubated in a rotary shaker at 165 rpm. The degradation efficiency was determined and estimated by the removal percentage of chlorimuron-ethyl from the liquid culture.

**Determination of optimum degradation conditions of chlorimuron-ethyl by D-6.** The effects of degradation conditions of chlorimuron-ethyl by D-6 strain with degradation time (12 h, 24 h, 48 h, 72 h and 96 h), initial concentration of chlorimuron-ethyl (100 mg/L, 200 mg/L, 300 mg/L, 400 mg/L, 600 mg/L and 800 mg/L), and temperature (10 °C, 20 °C, 30 °C and 40 °C) were carried out. Each treatment was triplicated, with uninoculation as the control.

## RESULTS AND DISCUSSION

### Identification and characterization of D-6.

The 16S rRNA gene sequence of D-6 was obtained, and a phylogenetic tree based on the partial 16S rRNA gene sequence of D-6 was constructed (Figure 1) with the sequence similarity score of 99%. The result of this phylogenetic analysis was consistent with that of morphological characterization and biochemical tests, and thus, the isolate D-6 was finally identified as *Bacillus subtilis*.

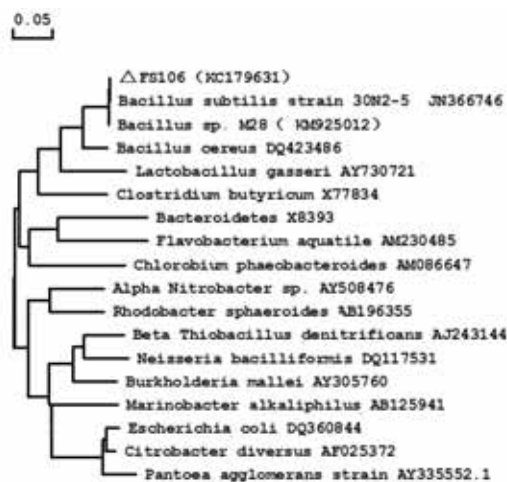


FIGURE 1

Phylogenetic tree based on the 16S rRNA gene sequences of D-6 strain and related species.

The GenBank accession number for each microorganism used in the analysis is shown after the species name. The scale bar indicates 0.001 substitutions per nucleotide position.

Bootstrap values obtained with 1000 resamplings were indicated as percentages at all branches.

**Effect of degradation time of chlorimuron-ethyl.** The effects of degradation time of chlorimuron-ethyl by strain D-6 were discussed with different degradation time (12-96 h). The degradation rates of chlorimuronethyl were increased with the increase of the degradation time from 12 to 72 h, and its values were 90.5% at between 72 and 96 h (see Figure 2).

**Effect of different concentrations of chlorimuron-ethyl.** The effects of initial concentrations of chlorimuron-ethyl by strain D-6 were analyzed with different initial concentrations (100-800 mg/L). Figure 3 shows that the degradation rates of chlorimuronethyl were increased from 25.1 to 90.5% with the increase of the initial concentrations from 100 to 300 mg/L, afterward it was decreased to 27.2%

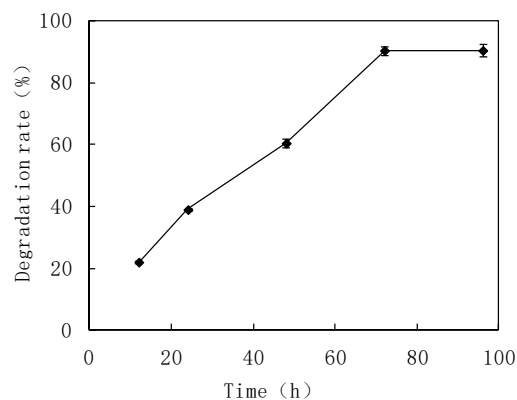


FIGURE 2

Effect of degradation time on its degradation. The initial chlorimuron-ethyl concentration of 300 mg/L, at 30°C and pH7.0.

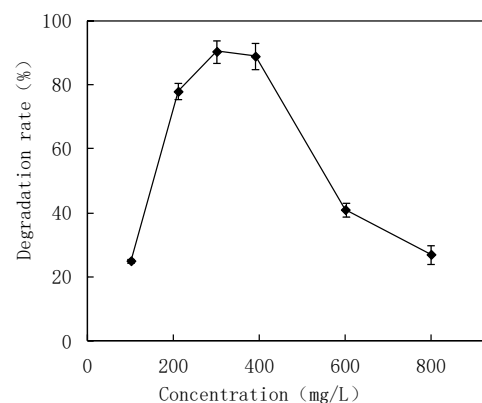
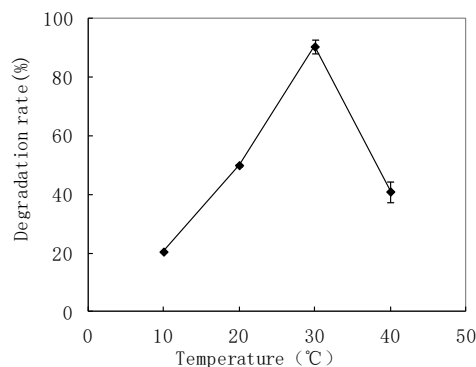


FIGURE 3

Effect of initial chlorimuron-ethyl concentration on its degradation.  $\text{NH}_4\text{NO}_3$ : 1 g/L, at 30°C, pH7.0 and 3 days.

at the initial concentrations of chlorimuron-ethyl was 800 mg/L. The optimum concentrations of chlorimuron-ethyl for degradation by strain D-6 is found to be 300 mg/L. Therefore, all the later experiments were carried out at chlorimuron-ethyl concentrations of 300 mg/L.

**Effect of temperature.** The effects of temperature by strain D-6 were tested with different temperature (10-40 °C). Figure 4 shows that the degradation rates of chlorimuron-ethyl were increased from 21.2% to 90.5% with the increase of the temperature from 10 to 30 °C, afterward it was decrease to 43.2% at the temperature 40 °C. The optimum temperature for degradation chlorimuron-ethyl by strain D-6 is found to be 30 °C. Therefore, all the later experiments were carried out at temperature 30 °C.



**FIGURE 4**

**Effect of temperature on its degradation. The initial chlorimuron-ethyl concentration of 300 mg/L, at pH7.0 and 3 days.**

## CONCLUSIONS

The strain D-6 isolated from a chlorimuron-ethyl polluted soil could be the *Bacillus subtilis* strain capable of degrading chlorimuron-ethyl. Incubation tests showed that when the initial concentration of chlorimuron-ethyl in culture was 300 mg/L, D-6 could degrade more than 90.5% of the herbicide after incubation for 3 d. The optimal conditions of chlorimuron-ethyl degradation by D-6 were chlorimuron-ethyl 300 mg/L,  $\text{NH}_4\text{NO}_3$  1 g/L, at 30 °C, pH7.0 and 3 d. Further study should be conducted to investigate the degradation pathways of chlorimuron-ethyl by D-6, and to approach the feasibility of using D-6 to degrade the chlorimuron-ethyl in soil system.

## ACKNOWLEDGEMENTS

Yingjie Dai and Binbin Zhang contributed equally to the work. The many precious and helpful comments provided by the reviewers of this manuscript are gratefully acknowledged. This work was supported by National Science and Technology Research Program of China (2012BAD06B02-01D2), Scientific Research Starting Foundation for Postdoctoral Scientists of Heilongjiang Province of China (LBH-Q13027) and Scientific Research Foundation for Postdoctoral Scientists of Heilongjiang Province of China (LBH-Z12047).

## REFERENCES

- [1] Zhou, Q., Liu, W., Zhang, Y., Liu, K., (2008) Action mechanisms of acetolactate synthase-inhibiting herbicides, *Pestic. Biochem. Phys.*, 89, 89–96
- [2] Nemat, A.M M, Badawi, A. M., Hassan, N. M., El-Bastawisy, Z. M., Badran, E. G., (2008) Effect of metribuzin, butachlor and chlorimuron-ethyl on amino acid and protein formation in wheat and maize seedlings, *Pestic. Biochem. Phys.*, 90, 8–18
- [3] Zhao, C. S., He, F. L., (2007) Effects of long residue herbicides on agricultural development of Heilongjiang Province, *J. Northeast Agricultural University*, 38(1), 136–139
- [4] Zawoznik, M.S., Tomaro, M.L., (2005) Effect of chlorimuron-ethyl on *Bradyrhizobium japonicum* and its symbiosis with soybean, *Pest Manag. Sci.*, 61, 1003–1008
- [5] Afyuni, M. M., Waggar, M. G., Leidy, R. B., (1997) Runoff of two sulfonylurea herbicides in relation to tillage system and rainfall intensity, *J. Environ. Qual.*, 26, 1318–1326
- [6] Ma, J., Wang, Z., Lu, P., Wang, H., Ali, S-W., Li, S., Huang, X., (2009) Biodegradation of the sulfonylurea herbicide chlorimuron-ethyl by the strain *Pseudomonas* sp. LW3, *FEMS Microbiol. Lett.*, 296, 203–209
- [7] Zhang, X., Zhang, H., Li, X., Su, Z., Wang, J., Zhang, C., (2009) Isolation and characterization of *Sporobolomyces* sp. LF1 capable of degrading chlorimuron-ethyl, *J. Environ. Sci.*, 21, 1253–1260
- [8] Hang, A., Pritsch, K., Ludwig, W., Schloter, M., (2003) Theoretical and practical approaches to evaluate suitable primer sets for the analysis of soil fungal communities, *Acta Biotechnol.*, 23(4), 373–381
- [9] Tamura, K., Dudley, J., Nei, M., (2007) MEGA4: molecular evolutionary genetics analysis (MEGA) software version 4.0, *Mol. Biol. Evol.* 24, 1596–1599



---

**Received: 23.02.2016**

**Accepted: 22.08.2016**

#### **CORRESPONDING AUTHOR**

---

**Binbin Zhang**

Key Laboratory of Soybean Biology in Chinese  
Ministry of Education, Northeast Agricultural  
University, Harbin, 150030, China

E-mail: [dai5188@hotmail.com](mailto:dai5188@hotmail.com)

# AN INVESTIGATION INTO CHANGES IN PHOSPHORUS FORMS AND PHOSPHORUS LEACHING FROM DREDGED SEDIMENTS SOLIDIFICATION OF TAIHU LAKE

Shengwei Wang<sup>1,2</sup>, Wei Zhu<sup>1,2,3,\*</sup>, Yiyang Lv<sup>1,2</sup>, Huiwen Zhang<sup>3</sup>

<sup>1</sup> Key Laboratory of Ministry of Education for Geomechanics and Embankment Engineering, Hohai University, Nanjing, China

<sup>2</sup> Jiangsu Research Center for Geotechnical Engineering Technology, Hohai University, Nanjing, China

<sup>3</sup> College of Environment, Hohai University, Nanjing, China

## ABSTRACT

Nutrients accumulate in eutrophic lakes, and some of them deposit into the lake sediment. As a water quality management method to control internal source pollution, sediment dredging is becoming more and more popular. There is now widespread concern that once the dredged sediments have been removed and disposed of, nutrients could be dissolved and become mobile, causing secondary pollutions. Meiliang Bay is one of the most eutrophied bays in the northern part of Taihu Lake in China. In this study, the authors analyzed the dredged sediments solidification from Meiliang Bay for their phosphorus content. We also investigated changes in phosphorus forms and phosphorus leaching before and after dredged sediments solidification. The total phosphorus content of the dredged sediment from Meiliang Bay was 5.15 g/kg. Org-P was the dominant fraction and made up 67.82 % of Total phosphorus (TP). Other forms were found in decreasing amounts as follows: occluded phosphorus (O-P), lime type phosphorus (Ca<sub>10</sub>-P), dicalcium phosphate (Ca<sub>2</sub>-P), octacalcium phosphate (Ca<sub>8</sub>-P), aluminum bound phosphorus (Al-P), iron bound phosphorus (Fe-P). It is found that Org-P is the most important factor in the acid extraction process, when pH is 2.64. The Phosphorus leaching risk is evaluated before and after dredged sediments solidification, and results confirmed that solidification effectively reduces the risk of phosphorus leaching from dredged sediments.

## KEYWORDS:

Taihu Lake, dredged sediments, solidification, phosphorus, leaching, forms

## INTRODUCTION

Taihu Lake is the third largest freshwater lake in China with a surface area of 2 338 km<sup>2</sup> and an average depth of about 2 m [1]. Meiliang Bay is one of the most eutrophied bays in the northern part of Taihu Lake. Over recent years, pollution from

external sources has decreased in Lake Taihu. Total nitrogen and total phosphorus concentrations are, however, decreasing very slowly, as a result of the internal source pollution. Phosphorus (P) is one of the limiting nutrients and its adequate supply to biota is very important in regulating primary productivity and regarded as a key factor responsible for the eutrophication of freshwater [2]. Dredging is carried out to control internal source pollution in Lake Taihu, and large amounts of dredged contaminated sediment are removed from the lake. Sediment dredging is a lake restoration technique to remove rich in pollutants and to control their release or nutrient bioavailability. Many studies have conducted to investigate sediment dredging and its environmental effects [3, 4]. This dredged sediment requires much storage space, and may cause secondary pollution, so it needs to be disposed of carefully. Various methods have been proposed to manage this sediment [5-9]. For example, solidification is a common treatment method for hazardous waste. This method stabilizes the contaminants in the treated material, and prevent the spread of pollutants that might be hazardous to humans and to the natural environment. The Environmental Protection Agency considers that solidification is the best method for dealing with the hazardous waste, and this technology has now been applied to dredged sediments [10].

Phosphorus in soil may be transformed into mobile forms and transported from surface water to groundwater, thereby causing pollution of the water environment [11, 12]. Therefore, the phosphorus stability and secondary contamination risks after dredged sediment solidification deserve some attention.

Zhang and Fan investigated the phosphorus forms in Lake Taihu. They found that the main phosphorus forms found in Taihu were, in reducing concentration order, organic phosphorus (Org-P) > calcium bound phosphorus (Ca-P) > aluminum bound phosphorus (Al-P) > iron bound phosphorus (Fe-P). Fractionation of sediment phosphorus from the north of Taihu showed that it had more organic phosphorus, which is closely related to the eutrophication and blue algae outbreaks [13].



Michael K. Stenstrom studied phosphorus release in the Han River and found that the pH of the leaching solution had a significant effect on phosphorus release rates [14]. According to previous studies, the pH of the leaching solution has an effect on Fe-P, Al-P and Ca-P, and can cause phosphorus release from sediments [15-17]. Yuan X-Y suggested that Al-P and Fe-P were not readily released under acidic conditions. He found that, when pH decreased or when CO<sub>2</sub> was produced by biodegradation, Ca-P solubility increased, resulting in increased release of phosphorus from the sediments [18]. Few research has been carried out on secondary phosphorus pollution from treated dredged sediments. However, the release of phosphorus from such sediments may have important influence on the eutrophication in the future; therefore it is necessary to investigate secondary phosphorus pollution after solidification of dredged sediments.

Solidification is a suitable method for solving the problems of sediment phosphorus release to water from dredged sediments. However, it is not clear how the phosphorus forms will change when the solidified dredged sediment is disposed of around the lake or reused for, e.g. paving and embankments. In this study, dredged sediments were treated with ordinary portland cement (OPC), sulfoaluminate cement (SAC) and quicklime (QL). It is important to investigate how phosphorus forms and phosphorus leachability change after solidification of dredged sediments. The changes in phosphorus forms, and phosphorus leachability in

Lake Taihu solidified dredged sediments are analysed, with the aim of (1) developing guidelines for treating contaminated sediments, and (2) providing insights into the secondary pollution from treated sediments.

## MATERIALS AND METHODS

**Tested Materials.** In this study, dredged sediments (DM) were taken from Meiliang Bay in northern Taihu. Basic physical index tests were conducted in accordance with the procedures given in GB/T 50123-1999 [19], and the basic physical properties of the DM are summarized in Table 1. The particle distributions were mainly tested with Malvern 2000 laser particle analyzer, which is shown in Fig. 1.

OPC, SAC and QL were used as the solidification materials. DO, DS and DQ were used to represent dredged sediments solidification, respectively. All the solidification materials content  $a_c = 100 \text{ kg/m}^3$  and they all had a curing time (t) of 7 days. Because the total phosphorus content of the treatment agents was very small relative to that of the DM, it was considered negligible in this study. The chemical composition of the OPC is given by Zhu et al. [20] and is summarized in Table 2. The SAC used was Portland cement, and its clinker contained 3 to 13 % C<sub>4</sub>A<sub>3</sub>S. The main component of QL was CaO.

**TABLE 1**  
Basic physical properties of the tested dredged material

Water content (%)	Specific Gravity	Clay content < 5 $\mu\text{m}$ (%)	Liquid limit (%)	Plastic Limit (%)	Organic Content (%)
105.00	2.36	24.00	62.00	27.00	3.50

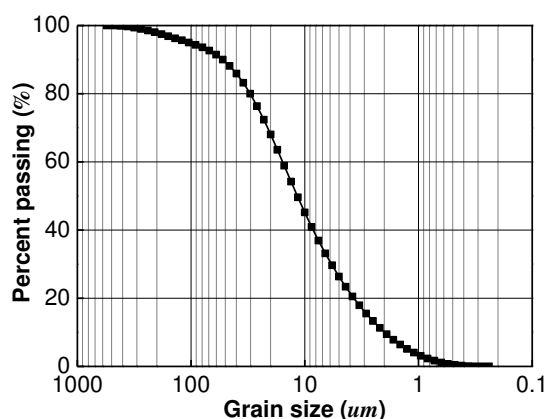


**FIGURE 1**  
Grain size distribution curve

**Tested Methods. 1) Total phosphorus.** Total phosphorus (TP) content was determined after digestion with strong acids [21]. In this method, mineral phosphate and organic phosphorus compounds in the soil particles are broken down by sulfuric acid and perchloric acid at a high temperature. All of the phosphorus is converted to phosphate. The phosphate is then determined by molybdenum dysprosium colorimetry.

**2) Phosphorus leaching experiments.** A solid waste-extraction procedure developed to determine the toxicity of leachate was used for the phosphorus leaching experiments using an acetic acid buffer solution [22].

**3) Analysis of phosphorus forms.** The authors used Yichu Gu's [23] modification method of

Jackson's [24] sequential phosphorus extraction in this study. The procedure successively extracts phosphorus from DM using different solvents and conditions. The resultant forms are aluminum bound phosphorus (Al-P, extractable by  $\text{NH}_4\text{F}$ ), iron bound phosphorus (Fe-P, extractable by  $\text{NaOH}$  and  $\text{Na}_2\text{CO}_3$  after Al-P extraction), occluded phosphorus (O-P, extractable by  $\text{Na}_3\text{C}_6\text{H}_5\text{O}_7$  and  $\text{Na}_2\text{S}_2\text{O}_4$  after Fe-P extraction), lime type phosphorus ( $\text{Ca}_{10}$ -P, extractable by  $\text{H}_2\text{SO}_4$  after O-P extraction). The resultant forms are dicalcium phosphate ( $\text{Ca}_2$ -P, extractable by  $\text{NaHCO}_3$ ), octacalcium phosphate ( $\text{Ca}_8$ -P, extractable by  $\text{CH}_3\text{COO-NH}_4$  after  $\text{Ca}_2$ -P extraction). Organic phosphorus is determined after burning of high temperature with  $\text{H}_2\text{SO}_4$  [21]. The procedures of the continuous chemical extracting method is shown in Fig. 2.

**TABLE 2**  
Chemical composition of ordinary Portland cement (OPC).

$\text{SiO}_2$ (%)	$\text{Al}_2\text{O}_3$ (%)	$\text{Fe}_2\text{O}_3$ (%)	$\text{CaO}$ (%)	$\text{MgO}$ (%)
21.43–22.17	4.75–5.83	3.31–3.91	64.39–66.23	1.12–2.08

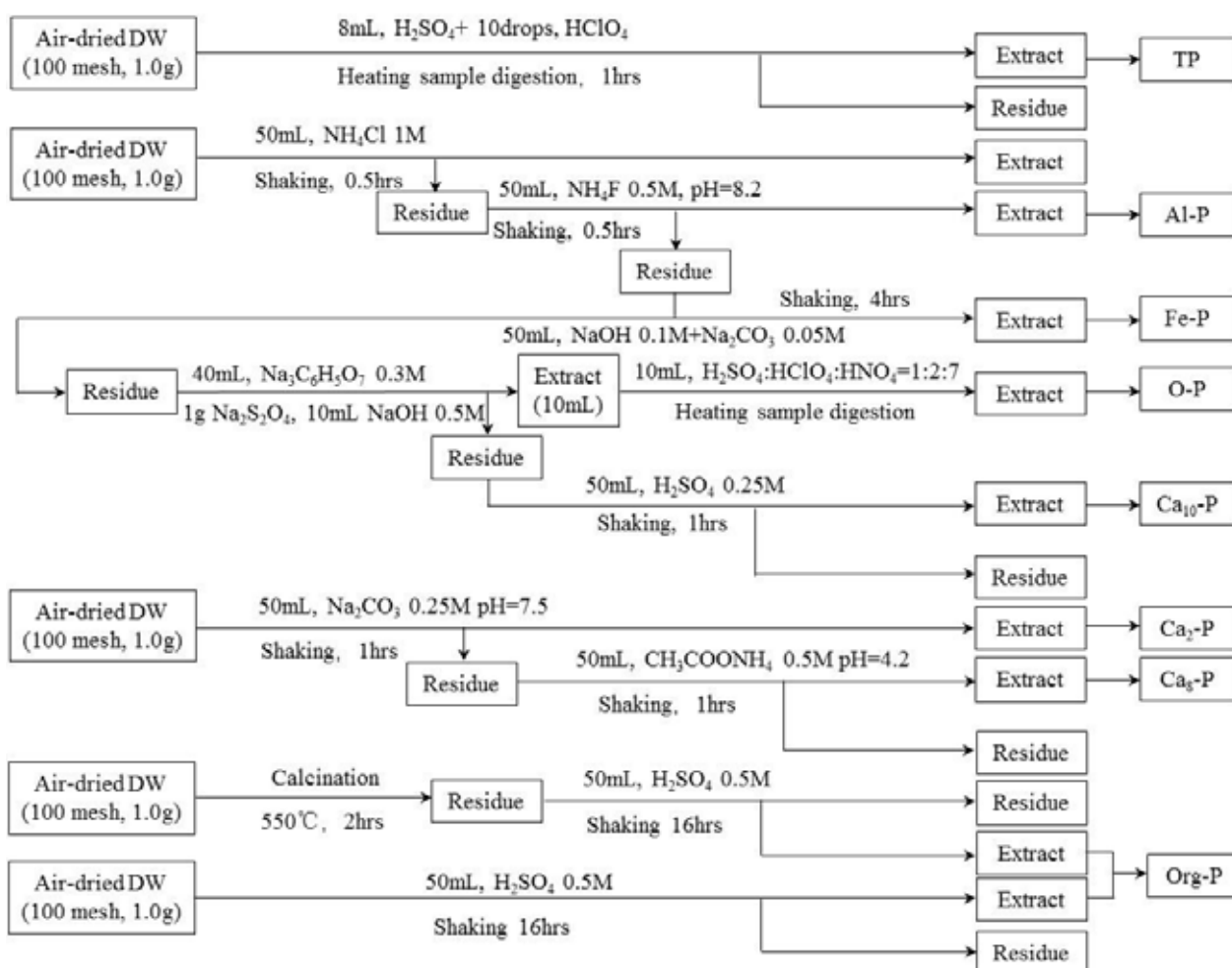


**FIGURE 2**  
The procedures of the continuous chemical extracting method

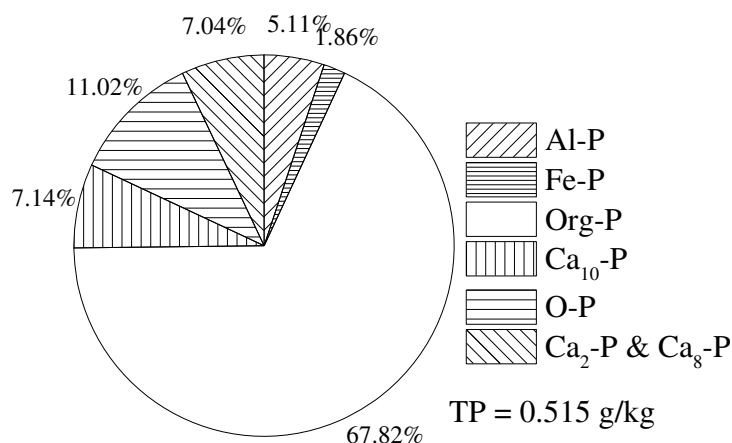


**FIGURE 3**  
TP and phosphorus forms of dredged sediments

**TABLE 3**  
Phosphorus forms concentrations before and after dredged sediments leaching (g/kg).

Phosphorus forms	Al-P	Fe-P	Ca <sub>2</sub> -P & Ca <sub>8</sub> -P	Org-P	Ca <sub>10</sub> -P	O-P
Before leaching	0.02633	0.00958	0.03625	0.34921	0.03673	0.05675
After leaching	0.02495	0.00890	0.04998	0.31891	0.03501	0.06251

## RESULTS

**Total phosphorus and phosphorus forms in dredged sediments.** Fig. 3 shows the contributions of the different phosphorus forms and TP content in the dredged sediments from Meiliang Bay. The TP content was 0.515 g/kg. Org-P was the dominant fraction and made up 67.82 % of TP. Other forms were found in decreasing amounts as follows:

O-P, Ca<sub>10</sub>-P, Ca<sub>2</sub>-P and Ca<sub>8</sub>-P, Al-P, Fe-P.

**Phosphorus forms before and after dredged sediments leaching.** The distribution of phosphorus forms was significantly different before and after dredged sediments leaching, as shown in Table 3. The content of Org-P, Al-P and Ca<sub>10</sub>-P all decreased after leaching of dredged sediments with the greatest decrease in Org-P, followed by Ca<sub>10</sub>-P.

**Change in phosphorus forms before and after dredged sediments solidification.** Phosphorus forms changed significantly in the solidification process as follows: Org-P decreased significantly, while all forms of inorganic phosphorus increased. Ca<sub>10</sub>-P and O-P increased significantly (Fig.4). The greatest decrease was in Org-P, while the Ca<sub>10</sub>-P fraction increased the most for dredged sediment treated with QL.

**Effect of solidification materials on phosphorus leaching.** The authors carried out phosphorus leaching experiments using an acetic acid solution with a pH of 2.64 as the extraction solvent at 20°C. The amount of phosphorus leached from solidified dredged sediments was significantly lower than that from dredged untreated sediments (Fig.5). The amount of phosphorus leached was lowest from dredged sediments treated with QL.

## DISCUSSION

**Leaching and forms relationships.** It can be seen from Table 3 that Org-P showed the greatest reduction after leaching of dredged sediments, followed by Ca<sub>10</sub>-P. This suggests that Org-P and Ca<sub>10</sub>-P are important in the acid extraction process. It can also be seen from Fig. 3 that the inorganic phosphorus increased significantly overall, but the amount of phosphorus leaching generally decreased after dredged sediment solidification under acidic conditions (pH = 2.64). This indicates that Ca<sub>10</sub>-P is not an important fraction in acidic conditions, when the pH = 2.64. So Org-P is the most important factor in the acid leaching process.

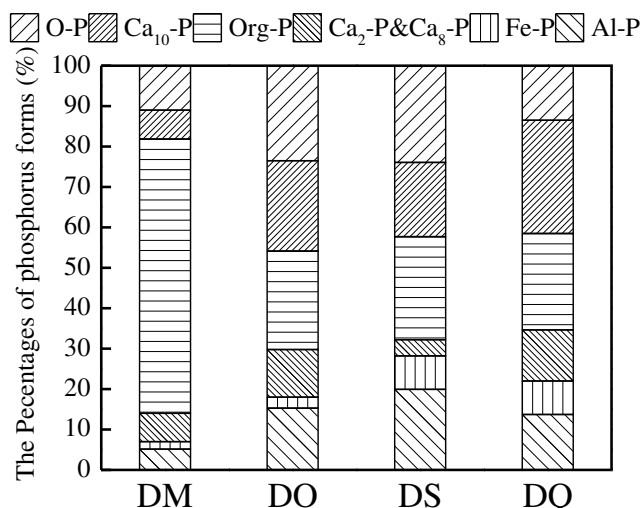


FIGURE 4

Comparison of phosphorus forms before and after dredged sediments solidification

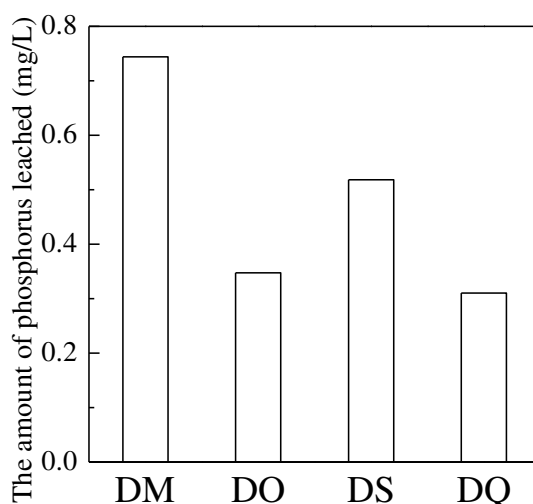


FIGURE 5

Comparison of phosphorus leached before and after dredged sediments solidification

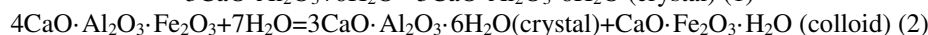
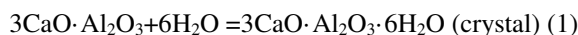
TABLE 4

Lake TP standard limits of the Environmental Quality Standards for Surface Water.

Type	I	II	III	IV	V
Lake TP (mg/L) ≤	0.01	0.025	0.05	0.1	0.2

**Transformations in phosphorus forms after solidification.** Phosphorus forms in dredged sediments changed significantly after solidification (Fig.3). This could be the result of the following processes occurred when solidification. First, the three solidification materials had alkaline properties and they neutralized acidic substances such as humic acid. As a result, Org-P was released, and the decrease in Org-P was related to the degree of alkalinity of the solidification material. Second, OPC, QL and SAC each contained a large amount of

Ca<sup>2+</sup>, and Ca-P was formed from the combination of Ca<sup>2+</sup> and the phosphate released from the Org-P. The greatest increases in Ca-P was observed when dredged sediments were solidified with QL. Third, OPC and SAC both contained large amounts of Fe<sup>3+</sup> and Al<sup>3+</sup>. Fe-P was formed from the combination of Fe<sup>3+</sup> and phosphate released from the Org-P, while Al-P was formed from Al<sup>3+</sup> combining with phosphate released from the Org-P. Four, the OPC hydration process can be explained by the chemical reactions shown Eq. (1) and Eq. (2).



Large amounts of  $\text{Fe}_2\text{O}_3$  and  $\text{Al}_2\text{O}_3$  were generated by the above reaction. Colloidal particles adsorbed phosphate released from the Org-P, leading to a large increase in O-P.

**Long-term effects of solidification of dredged sediments of Meiliang Bay.** Phosphorus leaching decreased significantly following dredged sediments solidification (Fig.4). According to 'The feasibility study of the Taihu ecological dredging project, Jiangsu Province, 2011 to 2012', the Meiliang Bay covers an area of 121.80 km<sup>2</sup>. The volume of dredged sediments was  $4.22 \times 10^6$  m<sup>3</sup> in 2012. The average density of dredged sediments is 1.44 g/cm<sup>3</sup>, and the average depth of Meiliang Bay lake is about 2 m. The total water volume in Meiliang Bay can be calculated using the following equation:

$$V_w = \rho_w \times S \times h = 2.436 \times 10^8 \text{ m}^3 \text{ (3)}$$

where  $V_w$  is the total water volume of Meiliang Bay (m<sup>3</sup>),  $\rho_w$  is lake water density (g/cm<sup>3</sup>),  $S$  is the area of Meiliang Bay (km<sup>2</sup>),  $h$  is average depth of Meiliang Bay (m).

Using an acetic acid solution (pH = 2.64) as the extraction solvent, the amount of phosphorus leaching is 0.0145 g/kg. The mass of phosphorus leaching from the total dredged sediments of Meiliang Bay is calculated by the following equation:

$$Q_{DM} = L_{DM} \times V \times \rho_{DM} = 8.8 \times 10^7 \text{ g (4)}$$

where  $Q_{DM}$  is the mass of phosphorus leaching from the total dredged sediments of Meiliang Bay (g),  $L_{DM}$  is the amount of phosphorus leached from dredged sediments (g/kg),  $V$  is total volume of dredged sediments in 2012 (m<sup>3</sup>),  $\rho_{DM}$  is average density of dredged sediments file://localhost/app/ds/density(g/cm<sup>3</sup>).

Assuming that the total mass of phosphorus leached will return to Meiliang Bay in groundwater or surface water, the phosphorus concentration in Meiliang Bay can be calculated using the following equation:

$$C_{DM} = Q_{DM} / V_w = 0.3617 \text{ mg/L (5)}$$

where  $C_{DM}$  is the phosphorus calculated concentration in Meiliang Bay.

When the total dredged sediments are treated by OPC, SAC and QL, the TP concentrations in Meiliang Bay are  $C_O = 0.1790$  mg/L,  $C_S = 0.2567$  mg/L and  $C_Q = 0.1535$  mg/L respectively. Comparison of the TP concentrations with the Environmental Quality Standards for Surface Water (GB3838-2002) suggests that, in the long term, the TP concentration of Meiliang Bay could fall within

Class V if dredged sediments are treated with OPC and QL (Table 4).

## CONCLUSIONS

(1) The TP content of the Meiliang Bay dredged sediments is 0.52 g/kg, of which 66.82% is Org-P. Other forms of phosphorus, in decreasing concentration order, are O-P, Ca<sub>10</sub>-P, Ca<sub>2</sub>-P and Ca<sub>8</sub>-P, Al-P, Fe-P.

(2) Phosphorus forms showed significant changes after dredged sediment solidification. The content of Org-P decreased significantly, and those of all inorganic phosphorus forms increased. The content of Ca<sub>10</sub>-P and O-P increased significantly. Under acidic conditions (pH = 2.64), Org-P is the leading factor controlling phosphorus leaching.

(3) Phosphorus leaching was significantly reduced after dredged sediment solidification in  $a_e = 100$  kg/m<sup>3</sup>, and a treatment time of 7 days. Better results were obtained after treatment with OPC and QL. If sediments are treated with OPC and QL, TP concentrations in Meiliang Bay may fall within Class V of the Environmental Quality Standards for Surface Water in the future.

## ACKNOWLEDGEMENTS

The authors would like to thank National Science and Technology Major Project (no. 2012ZX07103-005), the National Basic Research Program of China ('973' program, no. 2012CB719804), and Nurturing Project of National Engineering Research Center for Dredging and Mud Treatment (Jiangsu Province, China, No. BM2013013) for supporting this research.

## REFERENCES

- [1] Chen, W., Chen, X., Gao, X. and Yoshida, I. (1997) Eutrophication of Taihu and its control. *Agri. Engin. J* 6, 109–120.
- [2] Pant H K, Reddy K R. (2001) Phosphorus sorption characteristics of estuarine sediments under different redox conditions. *Journal of Environmental Quality* 30(4), 1474-80.
- [3] Voie, O. A., Johnsen, A. and Rosslund, H. K. (2002) Why biota still accumulate high levels of PCB after removal of PCB contaminated sediments in a Norwegian fjord. *Chemosphere* 46(9-10), 1367–1372.
- [4] Weston, D. P., Jarman, W. M., Cabana, G., Bacon, C. E. and Jacobson, L. A. (2002) An evaluation of the success of dredging as

- remediation at a DDT-contaminated site in San Francisco Bay, California, USA. *Environmental Toxicology & Chemistry* 21(10), 2216–2224.
- [5] Liang Zhanga, Song Hongb, Jing Heb, Fuxing Ganb, YuhShan Ho. (2011) Adsorption characteristic studies of phosphorus onto laterite. *Desalination & Water Treatment* 25(1-3), 98-105.
- [6] M.A. Camargo Valero, M. Johnson, T. Mather, D.D. Mara. (2009) Enhanced phosphorus removal in a waste stabilization pond system with blast furnace slag filters. *Desalination & Water Treatment* 4(1), 122-127.
- [7] J. Vymazal. (2007) Removal of nutrients in various types of constructed wetlands. *Science of the Total Environment* 380(1-3), 48–65.
- [8] C.J. Penn and J.G. Warren. (2009) Investigating phosphorus sorption onto kaolinite using isothermal titration calorimetry. *Soil Science Society of America Journal* 73(2), 560–568.
- [9] E.J. Dunne, N. Culleton, G. O'Donovan, R. Harrington, K. Daly. (2005) Harrington and K. Daly, Phosphorus retention and sorption by constructed wetland soils in Southeast Ireland. *Water Research* 39(18), 4355–4362.
- [10] EPA/540/S-92/105. *Engineering Bulletin-Solidification/Stabilization of Organics and Inorganics*.
- [11] Li Y-Y, Shao M-A. (2002) Effects of phosphorus application methods on phosphorus loss on sloping land under simulated rainfall. *Chinese Journal of Applied Ecology* 13(11), 1421–1424 (In Chinese).
- [12] Zhang Z-J, Zhu Y-M, Wang K, Wang G, Dong L. (2001) Phosphorus behavior in soil-water system of paddy field and its environment impact. *Chinese Journal of Applied Ecology* 12(2), 229–232 (in Chinese).
- [13] Zhang Lu, Fan Cheng-xin, Chi Qiao-qiao, Wang Jian-jun, Qin Bo-qiang. (2004) Phosphorus species distribution of sediments in Lake Taihu and its main inflow rivers. *Geochimica* 33(3), 423–433 (in Chinese).
- [14] Lee-Hyung Kim, Euiso Choi, Kyung-Ik Gil, Michael K. Stenstrom. (2004) Phosphorus release rates from sediments and pollutant characteristics in Han River, Seoul, Korea. *Science of the Total Environment* 321(1-3), 115–125.
- [15] Anderson J M. (1974) Nitrogen and Phosphorus budgets and the role of sediments in six shallow Danish lakes. *Arch. Hydrobiol* 74, 528–550.
- [16] Lee-Hyung Kim, Euiso Choi, Michael K. Stenstrom. (2003) Sediment characteristics, phosphorus types and phosphorus release rates between river and lake sediments. *Chemosphere* 50(1), 53–61.
- [17] JIN Xiang-can, WANG Sheng-rui, PANG Yan. (2004) The influence of phosphorus forms and pH on release of phosphorus from Sediments in Taihu Lake. *China Environmental Science* 24, 707–711 (in Chinese).
- [18] Li Bing, Yuan Xu-yin, Deng Xu. (2008) Phosphorus release of sediments in in-flowing rivers of the Tai hu as affected by pH. *Journal of Ecology and Rural Environment* 24, 57-62 (in Chinese).
- [19] Ministry of Construction P.R. China, GB/T 50123, 1999. Standard for soil test method, Beijing (in Chinese).
- [20] Zhu, W., Zhang, C.L., Chiu, A.C.F. (2007) Soil-water transfer mechanism for solidified dredged material, *Journal of geotechnical and geoenvironmental engineering* 133, 588–598.
- [21] Lu Ru-kun. (1999) Soil Science Society of China. *Soil Agrochemistry Analysis Method*, China Agriculture Science and Technique Press, Beijing.
- [22] H. T. (2007) Solid waste leaching toxicity of acetic acid buffer solution method (in Chinese).
- [23] Gu Yi-chu, Jiang Bo-qiang. (1990) Inorganic phosphorus measure method for calcareous soil. *Soils* 22, 101–102 (in Chinese).
- [24] Chang S C, Jackson M L. (1957) Fractionation of soil phosphorus. *Soil Science* 84, 133–144.

---

**Received:** 24.02.2016  
**Accepted:** 08.09.2016

---

#### CORRESPONDING AUTHOR

##### Wei Zhu

Key laboratory of Ministry of Education for Geomechanics and Embankment Engineering Hohai University  
 Nanjing 210098 – CHINA

E-mail: dvlove2007@126.com  
 zhuweiteam.hhu@gmail.com

# PHOTOCHEMICAL FORMATION OF SINGLET OXYGEN IN ALGAE-LADEN WATER

Junwei Zhang\*, Qianning Song, Panpan Jiang, Jin Gu

The Key Laboratory of Food Colloids and Biotechnology, Ministry of Education, School of Chemical and Material Engineering, Jiangnan University, Wuxi 214122, China

## ABSTRACT

Photochemical formation of singlet oxygen ( $^1\text{O}_2$ ) in algae-laden water was studied in order to further analyze transformation behavior of organic pollutant. Formation amount of  $^1\text{O}_2$  induced by algae was larger under UV irradiation, whereas formation amount of  $^1\text{O}_2$  was very less under the other conditions. Enhance of light intensity, suitable pH (pH 7) and suitable temperature (25 °C) were prone to formation of  $^1\text{O}_2$ , and ultrasonic pretreatment was of favorableness as well. Model of exponential growth and two-parameter exponential function could describe formation of  $^1\text{O}_2$  and the relationship between initial rate and algae concentration well. Main formation pathway of  $^1\text{O}_2$  probably derived from excited state of intermediate and pigment as well as participation of  $\text{O}_2$  and  $\text{H}^+$  via dismutation or intersystem crossing.

## KEYWORDS:

Algae-laden water;  $^1\text{O}_2$ ; photochemical formation; characteristic

## INTRODUCTION

Water, a kind of indispensable resource, is directly related to the survival of mankind and the development of society. Brutish behavior of human leads to the serious shortage of freshwater and the growing water pollution, especially for organic pollutant which poses a serious threat to the aquatic environment [1,2]. Photochemical behavior of algae can play the positive role in the transformation of organic pollutant in the aquatic environment [3,4]. Algae can give rise to the production of hydrated electron ( $e^-_{\text{aq}}$ ) via a series of photochemical reactions [5], and  $e^-_{\text{aq}}$  result in the production of hydroxyl radical ( $\cdot\text{OH}$ ) under UV irradiation due to the formation of hydrogen peroxide ( $\text{H}_2\text{O}_2$ ) with participation of  $\text{O}_2$  and  $\text{H}^+$  [6-7].

Singlet oxygen ( $^1\text{O}_2$ ), similar oxidation activity to  $\cdot\text{OH}$ , has been proven to form in plant [8], thus the

formation of  $^1\text{O}_2$  may be one of reasons for transformation of organic pollutant in the aquatic environment. Unfortunately,  $^1\text{O}_2$  has not yet been addressed to date for the transformation of organic pollutant in algae-laden water.  $^1\text{O}_2$  could be produced by photosensitizer via promoting ground state oxygen to excited singlet state [9]. Many organic substances (such as dissolved organic matter (DOM)) have been shown to act as sensitizers and lead to the formation of  $^1\text{O}_2$  under illumination [10]. Researchers have detected different concentrations of  $^1\text{O}_2$  in waters with trapping agent method [11,12]. To the best of our knowledge, formation characteristic and kinetics of  $^1\text{O}_2$  in algae-laden water has not been addressed.

Objectives of study were as follows: 1) analyzing initial formation rate of  $^1\text{O}_2$ ; 2) exploring effects of factors as well as possible formation mechanism of  $^1\text{O}_2$ .

## EXPERIMENTAL

**Materials.** Algae used in experiments were *Chlorella vulgaris* (CV) and *Microcystis aeruginosa* (MA) and obtained from Wuhan Hydrobiology Institute (China). All reagents were obtained from Shanghai Chemical Co. (China). Photochemical reactor (self-made, capacity 250 mL, diameter 8 cm, length 25 cm, built-in quartz cooling jacket, light source ( $\lambda_{\text{max}} = 360 \text{ nm}$ )).

**Preparation of algae.** Algae were grown in the axenic culture medium at 25 °C in the culturing room equipped with constant temperature air-conditioner [3,4]. Logarithmic growth phase of algae were taken for use in experiment after being washed. Different concentrations of algae were obtained by diluting the washed algae with the deionized water.

**Photochemical experiments.** All experiments were carried out in the photochemical reactor, algae and furfuryl alcohol (FFA, 0.1 mmol/L) were added into the reactor. Solution containing algae and FFA was continually mixed with magnetic stirrer as well as bubbling air. At intervals, sample was withdrawn

and centrifuged at 4000 rpm for 30 min, and the supernatant was determined with HPLC.

**Analysis.** FFA was used as the probe to detect formation of  $^1\text{O}_2$  in algae-laden water.  $^1\text{O}_2$ -mediated oxidation of FFA was nearly 90% yield [4,13]. Concentration change of FFA with reaction time was detected by HPLC (Pgrandsil STC C18, 4.6 mm  $\times$  250 mm) with methanol/water (50/50, v/v) as a mobile phase (1 mL/min) at 230 nm.

## RESULTS AND DISCUSSION

**Photochemical formation of  $^1\text{O}_2$ .** Algae could induce formation of large amount of  $^1\text{O}_2$  within short time under UV irradiation, and formation amount of  $^1\text{O}_2$  gradually increased with prolonging time. Thus,  $^1\text{O}_2$  is an important reason for transformation of organic pollutant except for  $\cdot\text{OH}$  in the aquatic environment, and degradation of organic pollutant should be a positive correlation with formation of reactive oxygen species from algae. Moreover, effect of light intensity on the formation of  $^1\text{O}_2$  was investigated with different UV lamps. Obviously, increase of light intensity was beneficial to formation of  $^1\text{O}_2$  (Fig.1B). This can be explained by more photos available in algae-laden water, which initiates intracellular photosensitizer to an excited singlet state from singlet ground electronic state.

Generally, viability of algae is stronger at suitable pH and suitable temperature, whereas algae should show low physiological activity which influences formation of  $^1\text{O}_2$ . We therefore analyze effects of pH and temperature on formation of  $^1\text{O}_2$ .

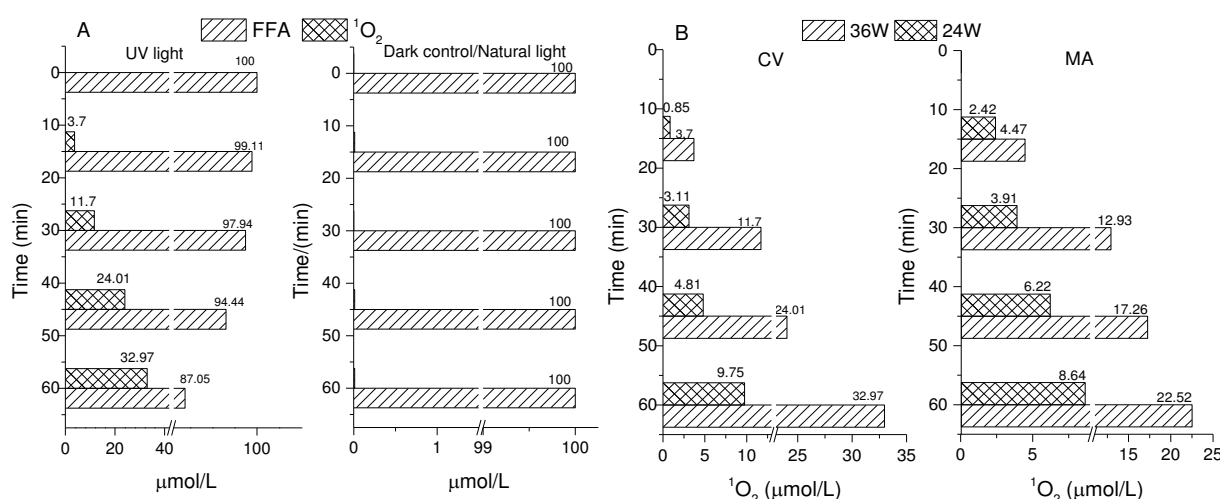


**FIGURE 1**  
Photochemical formation of  $^1\text{O}_2$  in algae-laden water where CV  $5 \times 10^8$  cell/L, MA  $5 \times 10^8$  cell/L, pH 7 and temperature 25 °C.

Results showed that algae-laden water at pH 7 was beneficial to formation of  $^1\text{O}_2$  (experimental range from pH 5 to pH 8), the formation amount of  $^1\text{O}_2$  was larger (CV 32.97  $\mu\text{mol/L}$ , MA 22.52  $\mu\text{mol/L}$ ) (see supplementary data).

Additionally, formation amount of  $^1\text{O}_2$  gradually increased with increasing temperature from 15 °C to 35 °C, but formation amount of  $^1\text{O}_2$  at 25 °C was closed to that at 35 °C (see supplementary data). Thus, bioactivity of algae will be inhibited due to unsuitable temperature. Moreover, formation amount of  $^1\text{O}_2$  in alga-laden water was very less at 50 °C (Fig.2). From this point of view, formation of  $^1\text{O}_2$  should be mainly derived from algae cell inside.

As seen in Fig.2, heat pretreatment (50 °C) significantly influenced formation amount of  $^1\text{O}_2$  and obviously destroyed the structure of intracellular photosensitizer.

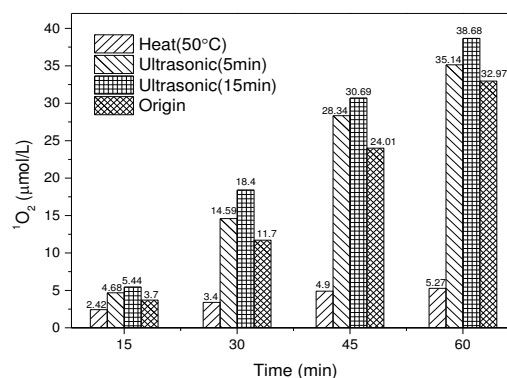


**FIGURE 2**  
Effect of pretreatment on formation of  $^1\text{O}_2$  where CV  $5 \times 10^8$  cell/L, light source 36 W and pH 7.



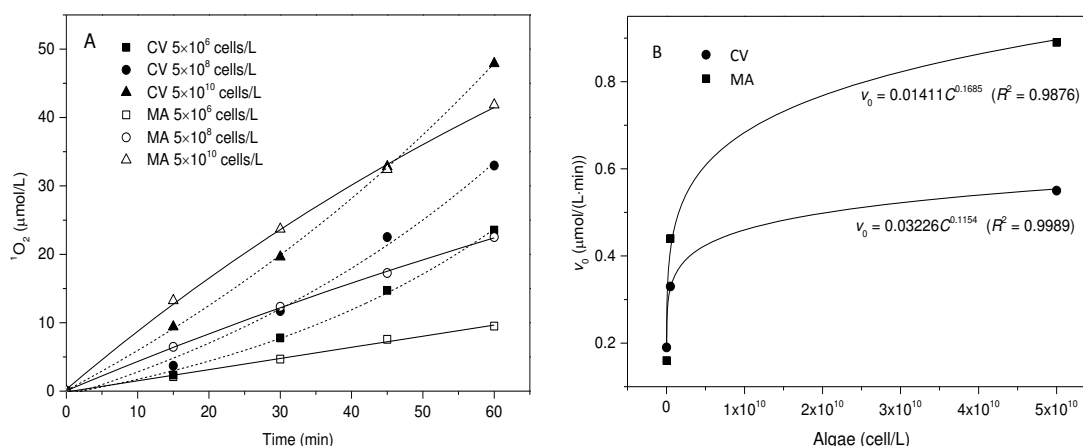


FIGURE 3

Fitted curves of formation amount of  $^1\text{O}_2$  (A) and fitted curves of initial rate of  $^1\text{O}_2$  formation (B).

TABLE 1  
Fitted equation of formation yield of  $^1\text{O}_2$ .

Algae (cells/L)	Fitted equation	$R^2$	$v_0 = a/b$
CV, $5 \times 10^6$	$y = 8.36 e^{t/44.26} - 8.74$	0.9962	0.19
CV, $5 \times 10^8$	$y = 18.88 e^{t/58.09} - 19.62$	0.9906	0.33
CV, $5 \times 10^{10}$	$y = 47.77 e^{t/86.49} - 47.67$	0.9998	0.55
MA, $5 \times 10^6$	$y = -1120.67 e^{-t/6845.28} - 1120.55$	0.9927	0.16
MA, $5 \times 10^8$	$y = -75.91 e^{-t/172.02} - 75.96$	0.9993	0.44
MA, $5 \times 10^{10}$	$y = -98.87 e^{-t/111.22} + 99.12$	0.9981	0.89

Ultrasonic pretreatment (80 W, 25 °C) was beneficial to formation of  $^1\text{O}_2$  and probably lead to release of active substance into water, and formation amount of  $^1\text{O}_2$  increased with prolonging treatment time. Indicating that ultrasonic pretreatment did not destroy the structure of photosensitive substance and only break the cell wall of algae.

**Initial formation rate of  $^1\text{O}_2$ .** Formation of  $^1\text{O}_2$  should be a function of photosensitive substance inside algae cell under condition of constant illumination without biological effect. For different algae concentrations, initial formation rate of  $^1\text{O}_2$  should also be different due to different contents of photosensitive substances.

Formation yield of  $^1\text{O}_2$  was closely dependent on algae concentration and gradually increased with prolonging illumination time (Fig.3A). Trend of formation amount of  $^1\text{O}_2$  should be expressed with model of exponential growth (Eq.(1)), and the coefficients obtained from the model were presented Table 1.

$$y = y_0 + ae^{t/b} \quad (1)$$

where  $y$  ( $\mu\text{mol/L}$ ) is formation yield of  $^1\text{O}_2$ ;  $y_0$ ,  $a$  and  $b$  are coefficients of model. Initial formation

rate of  $^1\text{O}_2$  ( $v_0$ ,  $\mu\text{mol}/(\text{L} \cdot \text{min})$ ) can be expressed with Eq. (2) via derivative of exponential growth function.

$$\frac{dy}{dt} \Big|_{t \rightarrow 0} = v_0 \Big|_{t \rightarrow 0} = \frac{a}{b} e^{t/b} \Big|_{t \rightarrow 0} = \frac{a}{b} \quad (2)$$

As listed in Table 1, formation yield of  $^1\text{O}_2$  could be described with the speculated model well, and correlation coefficients  $R^2$  were above 0.99. The power function could basically express relationship between initial formation rate of  $^1\text{O}_2$  and algae concentration. Moreover, initial formation rate of  $^1\text{O}_2$  should be an apparent initial rate since there have different formation pathways and complicated biochemical process. However, the macroscopic analysis of initial formation rate of  $^1\text{O}_2$  is necessary and essentially reveal formation characteristic of  $^1\text{O}_2$  with concentration change of alga.

#### Preliminary discussion of pathway.

Formation of  $^1\text{O}_2$  in algae-laden water mainly relies on photosensitive substance via dismutation reaction or intersystem crossing effect, and the photosensitivities of chlorophyll and carotenoids have been acknowledged. In fact, algae cell also contain phycoerythrobilin, phycocyanobilin and

allophycocyanin etc., which can play the roles of light adsorption and energy transduction, thus these substance inside algae cell should be one of source for  $^1\text{O}_2$  (other pigments for short). Meanwhile, algae cell should release DOM with a huge variety of functional group (e.g., carboxylic, phenolic hydroxyl) [10]. Zepp et al. [14] indicated that the superoxide anion radical ( $\text{O}_2^-$ ) deriving from interaction  $e_{\text{aq}}^-$  and  $\text{O}_2$  could lead to the formation  $^1\text{O}_2$  via participation of  $\text{H}^+$ .

Possible formation mechanism of  $^1\text{O}_2$  in algae-laden water was summarized on the basis of aforementioned discussion, the main pathway of  $^1\text{O}_2$  are shown in Fig. 4. Since the photosensitive substance inside algae cell, e.g., chlorophyll, carotenoids and phycoerythrobilin, can absorb light energy and further transfer, and the excited state of intermediates and/or pigments with energy subsequently occur,  $^1\text{O}_2$  could be finally produced by participation of  $\text{O}_2$  and/or  $\text{H}^+$  via dismutation or intersystem crossing. Especially, some photosensitive substances, e.g., carotenoids, phycoerythrobilin and phycocyanobilin, could indirectly interact with  $\text{O}_2$  and only absorb the light energy [15], and it then transfer excited energy to excited triplet state of substance, which still play an important role in absorption of photo during formation process of  $^1\text{O}_2$ .

Overall, oxidative activity of  $^1\text{O}_2$  formed in algae-laden water under illumination is similar to that of  $\cdot\text{OH}$  and can result in the degradation of organic pollutant, thus photochemical behavior of algae has an important influence to the natural water. So far, the explicit pathway for  $^1\text{O}_2$  except for the above main pathways is unclear via the analysis of photochemical model, further study is needed to explore participant inside algae cell and

photochemical mechanism, and we continuously focus on this aspect and plan to dig for more information.

## CONCLUSION

Algae could induce formation of large amount of  $^1\text{O}_2$  within short time under UV irradiation, and enhance of light intensity as well as suitable pH (pH 7) and suitable temperature ( $25\text{ }^\circ\text{C}$ ) were prone to formation of  $^1\text{O}_2$ . Meanwhile, Heat pretreatment for algae-laden water was unbeneficial to formation of  $^1\text{O}_2$ , whereas ultrasonic pretreatment was favorable. Model of exponential growth described formation process of  $^1\text{O}_2$  well, and relationship between initial formation rate and alga concentration could be expressed with the two-parameter exponential function. Possible main pathway of  $^1\text{O}_2$  formation was summarized, excited state of intermediate and/or pigments with energy subsequently resulted in formation of  $^1\text{O}_2$  with participation of  $\text{O}_2$  and/or  $\text{H}^+$ .

## ACKNOWLEDGEMENTS

This study was supported by the National Natural Science Foundation of China (21307042), the Natural Science Foundation of Jiangsu Province (BK20130124) and the Postdoctoral Research Foundation of Jiangsu Province (1601073B).

*The authors have declared no conflict of interest.*

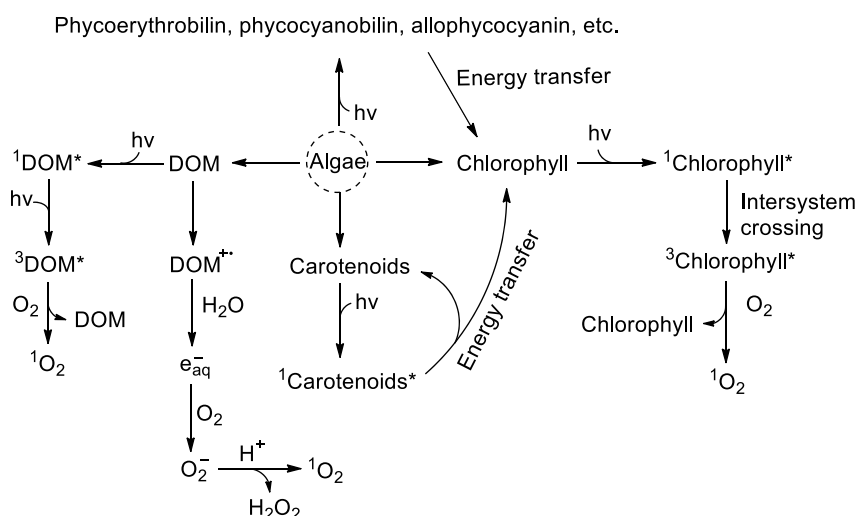


**FIGURE 4**  
Main formation pathway of  $^1\text{O}_2$  in algae-laden water.



## REFERENCES

---

- [1] Fernández-Rodríguez, M., Arrebola, J. P., Artacho-Cordón, F., Amaya, E., Aragones, N., Llorca, J., Perez-Gomez, B., Ardanaz, E., Kogevinas, M., Castano-Vinyals, G., Pollan, M., Olea, N. (2015) Levels and predictors of persistent organic pollutants in an adult population from four Spanish regions. *Sci. Total Environ.* 538, 152-61.
- [2] Liu, G., Zheng, M., Jiang, X., Jin, R., Zhao, Y., Zhan, J. (2016) Insight into the emission reduction of multiple unintentional persistent organic pollutants from industrial activities. *Chemosphere* 144, 420-424.
- [3] Liu, X., Wu, F., Deng, N. (2003) Photodegradation of 17 $\alpha$ -Ethinylestradiol exposed to a high pressure mercury lamp (250W). *Environ. Pollut.* 126, 393-398.
- [4] Peng, Z., Wu, F., Deng, N. (2006) Photodegradation of bisphenol A in simulated lake water containing algae, humic acid and ferric ions. *Environ. Pollut.* 144, 840-846.
- [5] Zhang, J., Ma, L. (2013) Photodegradation mechanism of sulfadiazine catalyzed by Fe(III), oxalate and algae under UV irradiation. *Environ. Technol.* 34, 1617-1623.
- [6] Wang, L., Zhang, C., Wu, F., Deng, N. (2007) Photodegradation of aniline in aqueous suspension of microalgae. *J. Photoch. Photobio. B* 87, 49-57.
- [7] Tai, C., Li, Y., Yin, Y., Cai, Y., Jiang, G. (2012) Free radical photochemistry of dissolved organic matter in natural water. *Prog. in Chem.* 24, 1388-1395.
- [8] Liu, X., Teng, L., Li, S. (2007) Advance of the research on the generation mechanisms of reactive oxygen species induced by algae. *J. Huangshi Inst. Technol.* 23, 44-47.
- [9] Bi, G., Tian, S., Feng, Z., Cheng, J. (2000) Studies on the sensitized photolysis of cypermethrin as singlet oxygen mechanism. *J. Anal. Sci.* 16, 450-455.
- [10] Deng, L., Wu, F., Deng, N., Zuo, Y. (2008) Photoreduction of mercury (II) in the presence of algae, *Anabaena cylindrical*. *J. Photoch. Photobio. B* 91, 117-124.
- [11] Zepp, R. G., Wolfe, N. L., Baughman, G. L., Hollis, R. C. (1997) Singlet oxygen in natural waters. *Nature* 267, 421-423.
- [12] Housari, F., Vione, D., Chiron, S., Barbati, S. (2000) Reactive photoinduced species in estuarine waters. Characterization of hydroxyl radical, singlet oxygen and dissolved organic matter triplet state in natural oxidation processes. *Photochem. Photobiolo. Sci.* 9, 78-86.
- [13] Haag, W.R., Hoigne, J., Gassman, E., Braun, A.M. (1984) Singlet oxygen in surface waters – Part I: Furfuryl alcohol as a trapping agent. *Chemosphere* 13, 631-640.
- [14] Zepp, R. G., Wolfe, N. L., Baughman, G. L., Hollis, R. C. (1997) Singlet oxygen in natural waters. *Nature* 267, 421-423.
- [15] Liu, X., Fan, X., Han, L. (1999) Reviews of research on seaweed carotenoids. *Stud. Mar. Sin.* 41, 92-101.

---

**Received:** 03.03.2016

**Accepted:** 10.09.2016

---

## CORRESPONDING AUTHOR

**Junwei Zhang**

School of Chemical and Material Engineering,  
Jiangnan University, Wuxi 214122, China

e-mail: [zjwseu@126.com](mailto:zjwseu@126.com)

# SYNTHESIS AND *IN-VITRO* ANTIMICROBIAL AND ANTI-MUTAGENIC ACTIVITIES OF SOME NOVEL 2-(2-HYDROXYBENZYLIDENEAMINO)-5,7-DIHYDRO-4H-THIENO[2,3-C]PYRAN-3-CARBONITRILE DERIVATIVES

Aliye Altundas<sup>1</sup>, Yasemin Erdogan<sup>1</sup>, Hatice Ogutcu<sup>2,\*</sup>, Hamit Emre Kizil<sup>3</sup>, Guleray Agar<sup>3</sup>

<sup>1</sup>Department of Chemistry, Gazi University, 06500, Ankara, Türkiye

<sup>2</sup>Department of Biology, Ahi Evran University, 40100, Kırşehir, Türkiye

<sup>3</sup>Department of Biology, Atatürk University, 25100, Erzurum, Türkiye

## ABSTRACT

In this investigation, a series of some novel 2-(2-hydroxybenzylideneamino)-5,7-dihydro-4H-thieno[2,3-c]pyran-3-carbonitriles (4a-f) have been synthesized. These substances have all been examined for antibacterial activities against pathogenic strains *Listeria monocytogenes* 4b, *Staphylococcus aureus*, *Escherichia coli*, *Salmonella typhi* H, *Pseudomonas putida*, *Brucella abortus*, *Shigella dysenteriae*, type 7, *Staphylococcus epidermis*, *Micrococcus luteus*, *Bacillus cereus*, *Enterobacter aerogenes* and antifungal activity against *Candida albicans*. Most of the studied compounds were found effective against bacteria and yeast. Compound 4f exhibited activity against *Pseudomonas putida*, *Brucella abortus*, *Staphylococcus aureus*, *Candida albicans* and 4c *Brucella abortus*, *Staphylococcus epidermis* comparable to standard antibiotics. In addition, the anti-genotoxic activity of these substances was evaluated by a micronucleus (MN) test. Among the synthesized compounds, 4c was found to have the most anti-mutagenic effect against AFB<sub>1</sub>. It was also found that different concentrations of these substances suppressed the mutagenic effects of Aflatoxin B<sub>1</sub> (AFB<sub>1</sub>) in the MN test (however 10 μM is the most effective dose). It seems that the antimutagenic effects of these substances may originate from their antioxidant potency or reaction of the aflatoxine lactone carbonyl functional group.

## KEYWORDS:

Cycloalkylaminocyanothiophenes, Imines, Antimicrobial Activity, Antimutagenic effect, Aflatoxine B<sub>1</sub>

## INTRODUCTION

Thiophene is a sulfur containing five-membered aromatic heterocyclic ring which is

widely distributed in nature and often plays an important role in various biochemical processes [1]. Thiophene derivatives are also an important structural fragment in many pharmaceutical and chemical compounds [2]. Furthermore, thiophenes in particular constitute an important class of compounds that attract medicinal chemists because of their wide applications in drug developments. For instance substituted 2-aminothiophenes can serve as anti tumor [3], anti-inflammatory [4], anti-microbial [5-6], antitubercular [7], antifungal [8] and antioxidant [9] agents. Aminothiophene carboxyamides have the potential to combat phytopathogenic diseases of plants and harvest food crops [10]. Substituted 2-aminothiophenes have also been found in wide applications in agrochemicals [11] and dyes [12]. The toxicity and the genotoxic activities of six thiophenes such as [benzo(b)] thiophene, dibenzothiophene, benzo(b)naphtha(2,1-d) thiophene, 6-methylbenzo(b)naphtha(2,1-d)thiophene, dinaphtho(2,1-b;1,2-d)thiophene, and diphenanthro(9,10-b;9,10-d)thiophene in the liver human cell line (HepG2) were evaluated by DNA adduct detection. However the correlation between cytotoxicity and genotoxicity depending on the structure in HepG2 cell was not able to be established. The only result that has been reached is that only high doses of dibenzothiophene act as a genotoxic agent [13].

So far various new thiophenes have been synthesized and screened biological properties in our laboratories.

2-[(Arylidene)amino]-cycloalkyl[b]thiophene-3-carbonitriles and its metal complexes have been evaluated for their *in vitro* antifungal and antimicrobial properties. The antifungal activity of cyclohexyl ring fused to the thiophene ring of 2-[(arylidene)amino]-cycloalkyl[b]thiophene-3-carbonitrile derivatives ranged from moderate to excellent [6,14]. The enthusiastic results and a few studies regarding the determination of genotoxic effects of thiophene or its derivatives promoted us to continue the

investigation.

The above prompted us to synthesize and a new series of 2-[(arylidene)amino]-cycloalkyl [b]thiophene-3-carbonitrile derived from aminothiophenes fused heteroatom containing cyloalkyl moiety with hydroxybenzaldehyde derivatives, thereby affording Schiff bases.

## MATERIALS AND METHODS

**Chemistry.** All reagents for syntheses were commercially available and used without further purification or purified by standard methods prior to use. The melting points were determined using an Electrothermal 9100 apparatus (Thermo Fisher Scientific Inc. in Great Britain), uncorrected. All NMR spectra were recorded on a Bruker 400 ( $^1\text{H}$ : 400 MHz,  $^{13}\text{C}$ : 100 MHz) NMR spectrometer (Bruker Corporation, in Germany), in  $\text{CDCl}_3$  or  $\text{DMSO}-d_6$ . Chemical shifts were reported in ppm relative to TMS as an internal standard;  $J$  in Hz. MS was obtained from Waters LCT Premier XE LTOF (TOF MS) instruments (Waters Corporation, Milford MA, USA). FTIR spectra were recorded on a Mattson 1000 spectrometer (Mattson Instruments, Baton Rouge, Louisiana, United States) using KBr pellets. The progresses of reactions were monitored by TLC using Silufol UV-254 plates from Merck CO (Germany).

**General procedure for the synthesis of 2-Amino-5,7-dihydro-4H-thieno[2,3-c]pyran-carbonitrile.** 2-Aminothiophene-3-carbonitrile 2 was prepared with respect to the procedure described by Gewalt and co-workers. A mixture of 1g (10.0 mmol) of tetrahydro-4H-pyran-4-one, 0.67 g (10 mmol) malononitrile, 0.32 g, (10 mmol) of sulfur, 0.87 g (10 mmol) of morpholine and 10 mL of ethanol were mixed at room temperature. At first an exothermic reaction was observed, the reaction mixture was heated to 50-60 °C for two hours then this mixture was poured into water. The resulting solid was collected and recrystallized from ethanol (yield 86% m.p.: 253-255 °C). IR ( $\nu$ ,  $\text{cm}^{-1}$ ): 3382 - 3326 ( $-\text{NH}_2$ ), 2191 ( $-\text{CN}$ );  $^1\text{H}$  NMR ( $\text{DMSO}-d_6$ ,  $\delta$ /ppm): 7.08 (2H,  $-\text{NH}_2$ ), 4.40 (2H,  $t$ ,  $J$ : 1.7 Hz,  $-\text{OCH}_2\text{-Ar}$ ), 3.80 (2H,  $t$ ,  $J$ : 5.5 Hz,  $-\text{OCH}_2$ ), 2.42 (2H,  $tt$ ,  $J$ : 5.5, 1.7 Hz,  $-\text{CH}_2$ ).  $^{13}\text{C}$  NMR ( $\text{DMSO}-d_6$ ,  $\delta$ /ppm): 163.5, 129.1, 115.7, 114.4, 82.8, 63.7, 63.3, 24.5.

**General procedure for the synthesis of 2-[(Arylidene)amino]-cycloalkyl[b]thiophene-3-carbonitriles 4a-f.** A mixture of hydroxybenzaldehyde (salicylaldehyde) derivatives 3a-f (1.0 mmol) and amine 2 (1.0 mmol) in 20 mL ethanol was refluxed for eight hours and then cooled to room temperature. The precipitated solid was

collected, washed with cold ethanol and recrystallized. All imine compounds were prepared by using the same procedure.

**2-(2-Hydroxybenzylideneamino)-5,7-dihydro-4H-thieno[2,3-c]pyran-3-carbonitrile 4a:** Yield 58%, m.p.: 205-208 °C; IR ( $\nu$ ,  $\text{cm}^{-1}$ ): 3396 ( $-\text{OH}$ ), 2192 ( $-\text{CN}$ ), 1610 ( $-\text{C}=\text{N}$ );  $^1\text{H}$  NMR ( $\text{CDCl}_3$ ,  $\delta$ /ppm): 11.88 (1H,  $s$ ,  $-\text{OH}$ ), 8.54 (1H,  $s$ ,  $\text{N}=\text{CH}-$ ), 7.41-6.98 (4H,  $m$ ,  $\text{Ar-H}$ ), 4.74 (2H,  $t$ ,  $J$ : 1.7 Hz,  $-\text{OCH}_2\text{-Ar}$ ), 4.03 (2H,  $t$ ,  $J$ : 5.5 Hz,  $-\text{OCH}_2-$ ), 2.81 (2H,  $tt$ ,  $J$ : 5.5; 1.7Hz,  $-\text{CH}_2$ ),  $^{13}\text{C}$  NMR ( $\text{CDCl}_3$ ,  $\delta$ /ppm): 161.8, 161.3, 158.4, 134.9, 133.0, 132.8, 129.8, 119.7, 118.3, 117.8, 113.3, 105.9, 64.8, 64.5, 24.8.  $m/z$  calcd for  $\text{C}_{15}\text{H}_{13}\text{N}_2\text{O}_2\text{S}$ : 285.0698; found 285.0681. Elemental Anal. Calcd for  $\text{C}_{15}\text{H}_{12}\text{N}_2\text{O}_2\text{S}\cdot 0.4\text{H}_2\text{O}$ : C, 61.80; H, 4.43; N, 9.63; S, 10.99. Found: C, 61.93; H, 4.06; N, 10.19; S, 10.63.

**2-(2-Hydroxy-5-methylbenzylideneamino)-5,7-dihydro-4H-thieno[2,3-c]pyran-3-carbonitrile 4b:** Yield 62%, m.p.: 182-184 °C; IR ( $\nu$ ,  $\text{cm}^{-1}$ ): 3456 ( $-\text{OH}$ ), 2215 ( $-\text{CN}$ ), 1622 ( $-\text{C}=\text{N}$ );  $^1\text{H}$  NMR ( $\text{CDCl}_3$ ,  $\delta$ /ppm): 11.67 (1H,  $s$ ,  $-\text{OH}$ ), 8.46 (1H,  $s$ ,  $\text{N}=\text{CH}-$ ), 7.26-6.92 (3H,  $m$ ,  $\text{Ar-H}$ ), 4.71 (2H,  $s$ ,  $-\text{OCH}_2\text{-Ar}$ ), 4.00 (2H,  $t$ ,  $J$ : 5.5 Hz,  $-\text{OCH}_2-$ ), 2.77 (2H,  $t$ ,  $J$ : 5.5 Hz,  $-\text{CH}_2-$ ), 2.30 (3H,  $s$ ,  $-\text{CH}_3$ ).  $^{13}\text{C}$  NMR ( $\text{CDCl}_3$ ,  $\delta$ /ppm): 161.8, 159.3, 158.6, 135.9, 132.7, 129.6, 128.9, 117.9, 117.6, 117.5, 113.3, 105.7, 64.8, 64.5, 24.8, 20.3.  $m/z$  calcd for  $\text{C}_{16}\text{H}_{15}\text{N}_2\text{O}_2\text{S}$ : 299.0854; found 299.0830. Elemental Anal. Calcd for  $\text{C}_{16}\text{H}_{14}\text{N}_2\text{O}_2\text{S}$ : C, 64.41; H, 4.73; N, 9.39; S, 10.75. Found: C, 64.13; H, 4.55; N, 9.48; S, 10.14.

**2-(5-Chloro-2-hydroxybenzylideneamino)-5,7-dihydro-4H-thieno[2,3-c]pyran-3-carbonitrile 4c:** Yield 51%, m.p.: 230-232 °C; IR ( $\nu$ ,  $\text{cm}^{-1}$ ): 3461 ( $-\text{OH}$ ), 2223 ( $-\text{CN}$ ), 1600 ( $-\text{C}=\text{N}$ );  $^1\text{H}$  NMR ( $\text{CDCl}_3$ ,  $\delta$ /ppm): 11.94 (1H,  $s$ ,  $-\text{OH}$ ), 8.47 (1H,  $s$ ,  $\text{N}=\text{CH}-$ ), 7.27 (2H,  $m$ ,  $\text{Ar-H}$ ), 6.95 (1H,  $d$ ,  $J$ : 8.4 Hz,  $\text{Ar-H}$ ), 4.73 (2H,  $s$ ,  $-\text{OCH}_2\text{-Ar}$ ), 4.02 (2H,  $t$ ,  $J$ : 5.5 Hz,  $-\text{OCH}_2-$ ), 2.83 (2H,  $t$ ,  $J$ : 5.5 Hz,  $-\text{CH}_2-$ ).  $^{13}\text{C}$  NMR ( $\text{CDCl}_3$ ,  $\delta$ /ppm): 161.8, 159.3, 157.6, 134.5, 133.1, 131.6, 130.6, 124.4, 119.4, 119.1, 113.1, 106.7, 64.8, 64.6, 24.8.  $m/z$  calcd for  $\text{C}_{15}\text{H}_{12}\text{ClN}_2\text{O}_2\text{S}$ : 319.0308; found 319.0293. Elemental Anal. Calcd for  $\text{C}_{15}\text{H}_{11}\text{ClN}_2\text{O}_2\text{S}\cdot 0.5\text{H}_2\text{O}$ : C, 54.96; H, 3.69; N, 8.55; S, 9.78. Found: C, 54.58; H, 3.58; N, 9.19; S, 10.10.

**2-(5-Bromo-2-hydroxybenzylideneamino)-5,7-dihydro-4H-thieno[2,3-c]pyran-3-carbonitrile 4d:** Yield 86%, m.p.: 258-260 °C; IR ( $\nu$ ,  $\text{cm}^{-1}$ ): 3434 ( $-\text{OH}$ ), 2219 ( $-\text{CN}$ ), 1616 ( $-\text{C}=\text{N}$ );  $^1\text{H}$  NMR ( $\text{CDCl}_3$ ,  $\delta$ /ppm): 11.90 (1H,  $s$ ,  $-\text{OH}$ ), 8.47 (1H,  $s$ ,  $\text{N}=\text{CH}-$ ), 7.54 (1H,  $s$ ,  $\text{Ar-H}$ ), 7.52 (1H,  $d$ ,  $J$ : 8.1 Hz,  $\text{Ar-H}$ ), 6.98 (1H,  $d$ ,  $J$ : 8.1 Hz,  $\text{Ar-H}$ ), 4.75

(2H, *t*, *J*: 1.7 Hz, -OCH<sub>2</sub>-Ar), 4.04 (2H, *t*, *J*: 5.6 Hz, -OCH<sub>2</sub>-), 2.83 (2H, *m*, -CH<sub>2</sub>-). <sup>13</sup>C NMR (CDCl<sub>3</sub>, δ/ppm): 160.3, 160.2, 157.6, 137.3, 134.6, 133.1, 130.6, 119.8, 119.7, 113.1, 111.2, 107.8, 64.8, 64.5, 24.8. *m/z* calcd for C<sub>15</sub>H<sub>12</sub>BrN<sub>2</sub>O<sub>2</sub>S: 362.9803; found 362.9807. Elemental Anal. Calcd for C<sub>15</sub>H<sub>11</sub>BrN<sub>2</sub>O<sub>2</sub>S·0.5H<sub>2</sub>O: C, 48.40; H, 3.25; N, 7.53; S, 8.61. Found: C, 47.98; H, 2.84; N, 7.64; S, 8.48.

#### 2-(3-Chloro-5-fluoro-2-hydroxybenzylidene amino)-5,7-dihydro-4H-thieno[2,3-c]pyran-3-carbonitrile 4e:

Yield 38%, m.p.: 244-246 °C; IR (ν, cm<sup>-1</sup>): 3444 (-OH), 2220 (-CN), 1569 (-C=N); <sup>1</sup>H NMR (CDCl<sub>3</sub>, δ/ppm): 12.21 (1H, *s*, -OH), 8.47 (1H, *s*, N=CH-), 7.32 (1H, *dd*, *J*: 2.8, 7.8 Hz, Ar-H), 7.06 (1H, *dd*, *J*: 2.9, 7.8 Hz, Ar-H), 4.75 (2H, *bs*, -OCH<sub>2</sub>-Ar), 4.03 (2H, *t*, *J*: 5.5 Hz, -OCH<sub>2</sub>-), 2.81 (2H, *t*, *J*: 5.5 Hz, -CH<sub>2</sub>-). <sup>13</sup>C NMR (CDCl<sub>3</sub>, δ/ppm): 160.5, 157.7, 152.2, 132.3, 131.9, 121.8, 121.5, 120.2, 116.4, 116.1, 113.2, 106.3, 64.3, 63.7, 24.1. *m/z* calcd for C<sub>15</sub>H<sub>11</sub>ClFN<sub>2</sub>O<sub>2</sub>S: 337.0214; found 337.0191. Elemental Anal. Calcd for C<sub>15</sub>H<sub>10</sub>ClFN<sub>2</sub>O<sub>2</sub>S: C, 53.50; H, 2.99; N, 8.32; S, 9.52. Found: C, 53.08; H, 2.86; N, 8.62; S, 8.93.

#### 2-(5-Fluoro-2-hydroxy-3-methylbenzylideneamino)-5,7-dihydro-4H-thieno[2,3-c]pyran-3-carbonitrile 4f:

Yield 39%, m.p.: 212-214 °C; IR (ν, cm<sup>-1</sup>): 3434 (-OH), 2221 (-CN), 1579 (-C=N); <sup>1</sup>H NMR (CDCl<sub>3</sub>, δ/ppm): 11.91 (1H, *s*, -OH), 8.44 (1H, *s*, N=CH-), 7.07 (1H, *dd*, *J*: 2.9, 8.7 Hz, Ar-H), 6.91 (1H, *dd*, *J*: 3.0, 8.2 Hz, Ar-H), 4.74 (2H, *t*, *J*: 1.5 Hz, -OCH<sub>2</sub>-Ar), 4.03 (2H, *t*, *J*: 5.5 Hz, -OCH<sub>2</sub>-), 2.83 (2H, *m*, -CH<sub>2</sub>-), 2.32 (3H, *s*, -CH<sub>3</sub>). <sup>13</sup>C NMR (CDCl<sub>3</sub>, δ/ppm): 160.8 (*J*<sup>4</sup><sub>CF</sub>: 5 Hz), 157.9-156.02 (*J*<sup>1</sup><sub>CF</sub>: 194 Hz), 156.8, 153.7, 132.9, 130.2, 129.1 (*J*<sup>3</sup><sub>CF</sub>: 10 Hz), 123.0 (*J*<sup>2</sup><sub>CF</sub>: 31 Hz), 117.0 (*J*<sup>3</sup><sub>CF</sub>: 11 Hz), 114.6 (*J*<sup>2</sup><sub>CF</sub>: 31 Hz), 113.2, 106.3, 64.8, 64.5, 24.8, 15.8. *m/z* calcd for C<sub>16</sub>H<sub>14</sub>FN<sub>2</sub>O<sub>2</sub>S: 317.0760; found 317.0754. Elemental Anal. Calcd for C<sub>16</sub>H<sub>13</sub>FN<sub>2</sub>O<sub>2</sub>S: C, 60.75; H, 4.124; N, 8.86; S, 10.14. Found: C, 60.35; H, 3.88; N, 8.81; S, 9.72.

**Pharmacological screening. Test Microorganisms and Medium.** The bacterial subcultures chosen were *Listeria monocytogenes* 4b ATCC19115, *Staphylococcus aureus* ATCC25923, *Escherichia coli* ATCC1280, *Salmonella typhi* H NCTC901.8394, *Pseudomonas putida* sp., *Brucella abortus* RSKK03026, *Staphylococcus epidermis* sp., *Micrococcus luteus* ATCC9341, *Shigella dysenteriae* type 7 NCTC9363, *Bacillus cereus* RSKK-863, *Enterobacter aerogenes* sp. an antifungal susceptibility test was used by *Candida albicans* Y-1200-NIH, Tokyo.

**Detection of antimicrobial activity.** The synthesized compounds were examined for their antimicrobial activity by the well-diffusion method [15]. The seven samples were kept dry at room temperature and dissolved (0.1 μg/μL) in DMSO. DMSO was used as both solvent and control. It was found to have no antimicrobial activity against any of the tested organisms 1% (v/v) of a 24 h broth culture containing 10<sup>6</sup> CFU/mL was placed in the sterile Petri dishes. Mueller-Hinton Agar (MHA) (15 mL) kept at 45 °C was then poured in to the Petri-dishes and allowed to solidify. Then wells of 6 mm diameter were punched carefully by using a sterile cork borer and were entirely filled with the test solutions. The plates were incubated for 24 h at 37 °C. On completion of the incubation period, the mean value obtained for the two holes was used to calculate the zone of growth inhibition of each sample. Bacterial subcultures and yeast were tested for resistance to five antibiotics produced by Oxoid Lt., Basingstoke, UK. These were: Ampicillin (prevents the growth of Gram-negative bacteria), Nystatin (binds to sterols in the fungal cellular membrane and alters the permeability allowing leakage of the cellular contents), Kanamycin (used in molecular biology as an agent in isolating bacteria), Sulphamethoxazol (a bacteriostatic antibacterial agent that interferes with folic acid synthesis in susceptible bacteria), Amoxycillin (a β-lactam antibiotic used to treat bacterial infections caused by sensitive microorganisms).

**Antimutagenic analysis.** Peripheral blood lymphocytes were taken from four nonsmoking healthy donors between the ages of 26 and 28. Lymphocyte cultures were set up by adding 0.5 mL of heparinized whole blood to RPMI-1640 chromosome medium supplemented with 15% heat inactivated fetal calf serum, 100 IU/mL streptomycin, 100 IU/mL penicillin and 1% L-glutamine. Lymphocytes were stimulated to separate by 1% phytohemagglutinin. Aflatoxin B<sub>1</sub> (AFB<sub>1</sub>; in concentration of 5 μM), 2 and 4a-f; in concentrations of 2.5, 5 and 10 μg/mL were added to the cultures just before incubation. The experiments were performed on 30 groups as listed (Table 1).

For MN analysis, cytochalasin B was added 44 h after PHA stimulation to a final concentration of 3 g/mL. Twenty-eight hours later (after 72 h of culture), the cells were collected by centrifugation (900 x g, 10 min). The supernatant was removed, the cells were mixed thoroughly and 5 mL of cold hypotonic solution (0.05 M KCl) was added. The cells were subsequently incubated at 37 °C for 20 min and centrifuged again (900 g, 10 min).

**TABLE 1**  
Experimental groups.

<b>Group 1:</b> Control	<b>Group 7: 4a</b> 20 μM	<b>Group 19: 4d</b> 20 μM
<b>Group 2:</b> 5 μM AFB <sub>1</sub>	<b>Group 8:</b> 5 Mm AFB <sub>1</sub> + <b>4a</b> (2.5 μg/mL)	<b>Group 20:</b> 5 μM AFB <sub>1</sub> + <b>4d</b> (2.5 μg/mL)
<b>Group 3:</b> 2 20 μM	<b>Group 9:</b> 5 μM AFB <sub>1</sub> + <b>4a</b> (5 μg/mL)	<b>Group 21:</b> 5 μM AFB <sub>1</sub> + <b>4d</b> (5 μg/mL)
<b>Group 4:</b> 5 μM AFB <sub>1</sub> + 2 (2.5 μg/mL)	<b>Group 10:</b> 5 μM AFB <sub>1</sub> + <b>4a</b> (10 μg/mL)	<b>Group 22:</b> 5 μM AFB <sub>1</sub> + <b>4d</b> (10 μg/mL)
<b>Group 5:</b> 5 μM AFB <sub>1</sub> + 2 (5 μg/mL)	<b>Group 11:</b> <b>4b</b> 20 μM	<b>Group 23:</b> <b>4e</b> 20 μM
<b>Group 6:</b> 5 μM AFB <sub>1</sub> + 2 (10 μg/mL)	<b>Group 12:</b> 5 μM AFB <sub>1</sub> + <b>4b</b> (2.5 μg/mL)	<b>Group 24:</b> 5 μM AFB <sub>1</sub> + <b>4e</b> (2.5 μg/mL)
	<b>Group 13:</b> 5 μM AFB <sub>1</sub> + <b>4b</b> (5 μg/mL)	<b>Group 25:</b> 5 μM AFB <sub>1</sub> + <b>4e</b> (5 μg/mL)
	<b>Group 14:</b> 5 μM AFB <sub>1</sub> + <b>4b</b> (10 μg/mL)	<b>Group 26:</b> 5 μM AFB <sub>1</sub> + <b>4e</b> (10 μg/mL)
	<b>Group 15:</b> <b>4c</b> 20 μM;	<b>Group 27:</b> <b>4f</b> 20 μM
	<b>Group 16:</b> 5 μM AFB <sub>1</sub> + <b>4c</b> (2.5 μg/mL)	<b>Group 28:</b> 5 μM AFB <sub>1</sub> + <b>4f</b> (2.5 μg/mL)
	<b>Group 17:</b> 5 μM AFB <sub>1</sub> + <b>4c</b> (5 μg/mL)	<b>Group 29:</b> 5 μM AFB <sub>1</sub> + <b>4f</b> (5 μg/mL)
	<b>Group 18:</b> 5 μM AFB <sub>1</sub> + <b>4c</b> (10 μg/mL)	<b>Group 30:</b> 5 μM AFB <sub>1</sub> + <b>4f</b> (10 μg/mL)

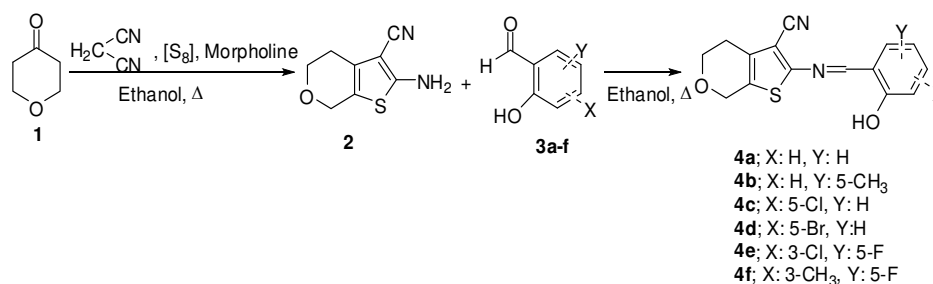


**FIGURE 1**  
Synthesis of 2-[(Arylidene)amino]-cycloalkyl[b]thiophene-3-carbonitriles **4a-f** derivatives.

The pellet was mixed thoroughly and 5 mL fresh fixative (1: 3 acetic acid: methanol) was added dropwise. This fixation procedure was repeated three times and the tube was centrifuged again. The cell pellet was resuspended in 1 mL of fresh fixative, dropped on to a clean microscope slide, incubated at 37 °C or at room temperature overnight and stained with Giemsa dye. Coded slides were scored blind by two independent individuals. Only binucleated cells were scored for MN analysis. For each subject, at least 2000 binucleated cells were analyzed for the presence of MN. For the MN scoring, the micronucleus criteria were used: a diameter less than 1/3 of the main nucleus, non-refractility, not touching, and with the same color as the nucleus or lighter [16].

The statistical analysis of MN frequencies was performed by use of the chi-square test.  $P < 0.05$  was accepted as statistically significant. For these procedures, SPSS 11.5 for Windows (SPSS Inc.,

Chicago, Illinois, USA) was used.

## RESULTS AND DISCUSSION

**Chemistry.** To improve the biological activities of the imines 2-(2-hydroxybenzylideneamino)-5,7-dihydro-4H-thieno[2,3-c]pyran-3-carbonitrile, we have outlined the synthesis of a series of oxygen heteroatom containing cyclohexyl fused thiophene N-arylideneimine derivatives. In fact, therapeutic agents containing thiophene have attracted the attention of researchers because these hetero aromatic compounds show various biological activities.

Following Gewald's procedure we synthesized 2-amino-5,7-dihydro-4H-thieno[2,3-c]pyran-3-carbonitrile (**2**) in high yield [17]. The latter 2-amino-3-cyanothiophene **2** was condensed with the

substituted 2-hydroxybenzaldehyde derivatives 3 which contain a phenolic unit. Under reflux in an ethanol solution the corresponding 2-(2-hydroxybenzylideneamino)-5,7-dihydro-4*H*-thieno[2,3-*c*]piran-3-carbonitrile (4a-f) derivatives 4a-f were obtained (Scheme 1). Structural assignment of compounds 2 and 4a-f were based on the IR, <sup>1</sup>H NMR, <sup>13</sup>C NMR and Mass spectral data and CHN analysis.

#### Biological activity and anti-mutagenic effect.

The synthesized compounds (2 and 4a-f) were screened for *in vitro* antibacterial and antifungal activity in DMSO solvent as a control substance. The compounds were tested with the same concentrations in DMSO solution (0.1 µg/µL). All the synthesized compounds and antibiotics exhibited varying degrees of inhibitory effects on the growth of different tested strains (Table 2).

The results of antibacterial screening indicated that 2-amino-5,7-dihydro-4*H*-thieno[2,3-*c*]pyran-carbonitrile (2) having the free amino group showed activity against most of the strains especially *E. coli* (23 mm). Compounds 2, 4a, 4c and especially 4f were the most potent growth inhibitors against *Br. abortus* with a zone value of 26 mm. *Br. abortus* is a gram-negative bacterium that causes premature abortion of cattle fetus [18], in addition it is a human pathogen which is a very serious, debilitating and sometimes chronic disease that may affect a variety

of organs [19].

Methyl substituted *N*-hydroxybenzylidene thienopyrancarboxitrile 4b showed the most inhibitor activity against *B. cereus* and *E. aerogenes*. Compound 4c (chloro-substituted at C-5 position on the aryl- ring) showed activity against *S. epidermis* (gram-). The bromo derivative, 4d, was the most active against *Sh.dys. .typ 7* which can cause shigellosis (bacillary dysentery). Compound 4e having a fluoro- and chloro- substituents on the aryl-ring was found to be the most active against *S. typhi H* and *M. luteus*. Furthermore, Salmonella serovars cause very diverse clinical symptoms, from asymptomatic infection to serious typhoid-like syndromes in infants or certain highly susceptible animals. All synthesized compounds show antifungal activity against *C. albicans*.

The azole antifungals are a group of fungistatic agents with broad-spectrum activity. The inhibition mechanism of azoles is found reversible inhibition of lanosterol 14- $\alpha$  demethylase (cytochrome P450 51) which converts lanosterol to ergosterol. Decreasing of ergosterol in yeast and fungi damages the cell membrane resulting in cell death. CYP51 is found in all biological kingdoms and the CYP51 active site consists of a large hydrophobic binding subsite above heme and two hydrophilic H-bond binding subsites with several polar positively charged amino acid residues (Ly and His). The core scaffold of lanosterol

**TABLE 2**  
Biological activity of compounds (2, 4a-f) (0.1 µg/mL) and standard reagents (diameter of zone inhibition (mm)).

Microorganisms	2	4a	4b	4c	4d	4e	4f	Control
<i>Sh.dys. typ 7</i>	15	16	12	-	18	14	13	-
<i>P.putida</i>	13	12	11	12	-	-	18	-
<i>S.typhi H</i>	14	12	-	13	12	16	14	-
<i>Br. abortus</i>	22	21	16	21	15	17	26	-
<b>Gram (-)</b> <i>E.coli</i>	23	16	12	13	11	16	14	-
<i>E. aerogenes</i>	15	11	20	15	-	13	15	-
<i>S.aureus</i>	13	17	15	-	-	14	18	-
<b>Gram (+)</b> <i>S.epidermis</i>	20	15	11	20	12	17	14	-
<i>L.monocytogenes4b</i>	12	11	11	12	-	-	11	-
<i>M.luteus</i>	12	-	-	15	13	17	-	-
<i>B.cereus</i>	16	13	19	14	12	16	17	-
<b>Yeast</b> <i>C. albicans</i>	28	21	22	25	21	25	24	-
<b>Positive control</b> <i>S.aureus</i>								
<b>K30</b>	25	14	25	20	-	-	-	-
<b>SXT25</b>	24	18	18	17	-	-	-	-
<b>AMP10</b>	30	8	10	11	-	-	-	-
<b>AMC30</b>	30	15	14	19	-	-	-	-
<b>NYS100</b>	-	-	-	-	-	-	20	-

SXT25, Sulphamethoxazol 25µg; AMP10, Ampicillin 10µg; NYS100, Nystatin 100µg ; K30, Kanamycin 30µg; AMC30, Amoxycillin 30µg.



subsite above the porphyrin ring heme. Nitrile, thiophene and furan reactive functional groups causing irreversible binding to CYPs behaved similar to lanosterol [20-21]. While compound 2, which has an amine functional group, is the most active *C. albicans* inhibitor with a zone value of 28 mm (positive control Nystatin 100 value is 20 mm), compounds 4c, 4e and 4f are also active inhibitors against *C. albicans* as non-azole compounds with zone values of 25, 25 and 24 mm, respectively. is the most active *C. albicans* inhibitor with a zone value of 28 mm (positive control Nystatin 100 value is 20 mm), compounds 4c, 4e and 4f are also active inhibitors against *C. albicans* as non-azole

compounds with zone values of 25, 25 and 24 mm, respectively. The hydrophobic parts of compounds 2, 4c, 4e and 4f, which consist of nitrile at C-3 of the thiophene ring and thiophene functional groups, were located above the active site of the heme porphyrin ring of CYP51 and interacted with Tyr118, Thr122, Phe126, Met306, Leu376, Phe380, Met508 and Val 509 through van der Waals interactions. Amino group in compound 2 and the hydroxyl- and electronegative halogen atom(s) (chlorine, bromine and/ or fluorine atom) substituents on the aryl- ring of compounds 4c, 4e and 4f were orientated towards a hydrophilic pocket.

**TABLE 3**  
**Comparison the effects on the number of MN different concentrations of 2 and 4a- f together with AFB<sub>1</sub> in human peripheral lymphocytes (<sup>a</sup>*P* < 0.05 compared with control, <sup>f</sup>*P* < 0.05 compared with AFB<sub>1</sub> (5μM) group).**

	Counted of MN	Sight of MN	MN/Cell		Counted of MN	Sight of MN	MN/Cell
<b>Control</b>	1012	30	2.99±0.18 <sup>a</sup>	<b>Control</b>	1002	32	3.19±0.18 <sup>a</sup>
<b>AFB<sub>1</sub> 5 μM</b>	1004	51	5.07±0.18 <sup>ef</sup>	<b>AFB<sub>1</sub> 5 μM</b>	1002	55	5.49±0.18 <sup>f</sup>
<b>2 (20μM)</b>	1012	49	4.88±0.18 <sup>de</sup>	<b>4a (20μM)</b>	1004	50	4.98±0.21 <sup>de</sup>
<b>AFB<sub>1</sub>(5μM)+2 (2.5μM)</b>	1013	48	4.78±0.18 <sup>d</sup>	<b>AFB<sub>1</sub>(5μM)+4a (2.5μM)</b>	1007	49	4.87±0.20 <sup>d</sup>
<b>AFB<sub>1</sub>(5μM)+2 (5μM)</b>	1009	42	4.28±0.18 <sup>c</sup>	<b>AFB<sub>1</sub>(5μM)+4a (5μM)</b>	1008	44	4.37±0.19 <sup>c</sup>
<b>AFB<sub>1</sub>(5μM)+2 (10μM)</b>	1011	39	3.88±0.18 <sup>b</sup>	<b>AFB<sub>1</sub>(5μM)+4a (10μM)</b>	1008	40	3.97±0.19 <sup>b</sup>
<b>Control</b>	1000	24	2.4±0.2 <sup>a</sup>	<b>Control</b>	1000	21	2.10±0.15 <sup>a</sup>
<b>AFB<sub>1</sub> 5 μM</b>	1000	44	4.4±0.2 <sup>f</sup>	<b>AFB<sub>1</sub> 5 μM</b>	1000	40	4.0±0.21 <sup>f</sup>
<b>4b (20μM)</b>	1000	34	3.4±0.2 <sup>cd</sup>	<b>4c (20μM)</b>	1000	32	3.2±0.15 <sup>cd</sup>
<b>AFB<sub>1</sub>(5μM)+4b (2.5μM)</b>	1000	38	3.8±0.2 <sup>e</sup>	<b>AFB<sub>1</sub>(5μM)+4c (2.5 μM)</b>	1000	35	3.5±0.15 <sup>de</sup>
<b>AFB<sub>1</sub>(5μM)+4b (5μM)</b>	1000	33	3.3±0.2 <sup>bc</sup>	<b>AFB<sub>1</sub>(5μM)+4c (5μM)</b>	1000	30	3.0±0.15 <sup>c</sup>
<b>AFB<sub>1</sub>(5μM)+4b (10μM)</b>	1000	30	3.0±0.2 <sup>b</sup>	<b>AFB<sub>1</sub>(5μM)+4c (10μM)</b>	1000	26	2.6±0.15 <sup>b</sup>
<b>Control</b>	1008	26	2.57±0.25 <sup>a</sup>	<b>Control</b>	1010	28	2.77±0.21 <sup>a</sup>
<b>AFB<sub>1</sub> 5 μM</b>	1008	43	4.27±0.25 <sup>ef</sup>	<b>AFB<sub>1</sub> 5 μM</b>	1010	49	4.85±0.21 <sup>ef</sup>
<b>4d (20μM)</b>	1008	40	3.97±0.25 <sup>cd</sup>	<b>4e (20μM)</b>	1010	39	3.86±0.21 <sup>cd</sup>
<b>AFB<sub>1</sub>(5μM)+4d (2.5μM)</b>	1008	40	3.99±0.25 <sup>de</sup>	<b>AFB<sub>1</sub>(5μM)+4e (2.5μM)</b>	1010	42	4.5±0.21 <sup>e</sup>
<b>AFB<sub>1</sub>(5μM)+4d (5μM)</b>	1008	36	3.57±0.25 <sup>bc</sup>	<b>AFB<sub>1</sub>(5μM)+4e (5μM)</b>	1010	36	3.56±0.21 <sup>bc</sup>
<b>AFB<sub>1</sub>(5μM)+4d (10μM)</b>	1008	33	3.27±0.25 <sup>b</sup>	<b>AFB<sub>1</sub>(5μM)+4e (10μM)</b>	1010	31	3.06±0.21 <sup>ab</sup>
<b>Control</b>	1012	27	2.67±0.12 <sup>a</sup>				
<b>AFB<sub>1</sub> 5 μM</b>	1012	49	4.84±0.12 <sup>f</sup>				
<b>4f (20μM)</b>	1012	44	4.35±0.12 <sup>de</sup>				
<b>AFB<sub>1</sub>(5μM)+4f (2.5μM)</b>	1012	42	4.15±0.12 <sup>d</sup>				
<b>AFB<sub>1</sub>(5μM)+4f (5μM)</b>	1012	38	3.75±0.12 <sup>c</sup>				
<b>AFB<sub>1</sub>(5μM)+4f (10μM)</b>	1012	35	3.46±0.12 <sup>b</sup>				



Because of these features, the amino group and electronegative atoms can form interactions between the positive Lys residues. The results obtained in our study were similar to those found in Tani et al.'s work [22].

MN test systems, AFB<sub>1</sub> was used as a positive control. Aflatoxine B<sub>1</sub> (AFB<sub>1</sub>) caused considerable MN formations on peripherally lymphocytes. It was determined that AFB<sub>1</sub> is a robust genotoxic agent and carcinogen which cause chromosomal aberrations (CA), micronucleus (MN) and sister chromatid exchange (SCE) in human cells [23]. On the other hand, these effects of AFB<sub>1</sub> on MN were diminished after treatment with 2 and 4a-f ( $P < 0.001$  and  $< 0.05$ ). Our study shows that all concentrations of substances effects MN frequency but it was also determined that 10  $\mu\text{M}$  is the most effective dose. In addition, it was also observed that 20  $\mu\text{M}$  and 40  $\mu\text{M}$  doses of substances possess genotoxic effects (Table 3).

The mechanism of protective action of these compounds against AFB<sub>1</sub> can be related to the detoxification methods of aflatoxin or antioxidant activity. One of the detoxification methods of aflatoxin in the literature is treatment with ammonia in the gaseous phase or in solution. The first step of this reaction is the opening of the aflatoxine lactone ring with ammonium hydroxide, so that the aflatoxine lactone ring converts into its carboxylic acid salt. Then the second step takes place and thus AFB<sub>1</sub> is converted into potentially much less mutagenic compounds [24]. Similarly, the reaction of the phenolic hydroxyl groups in our synthesized compounds with the aflatoxine lactone carbonyl may produce ester aflatoxine derivatives and reduce the effects of aflatoxine. The antimutagenic effects of these substances may be related to their role in enzymatic activation systems. In addition, it is probably related to the antioxidant property of substances which is known to protect against the damage caused by oxygen radicals. Phenolic compounds thereby have significant antioxidant activity [25].

## CONCLUSIONS

In this study, 2-(2-hydroxybenzylideneamino)5,7-dihydro-4H-thieno[2,3-c]piran-3-carbonitrile (4a-f) derivatives were synthesized by reaction of 2-aminothiophene-3-carbonitrile 2 and hydroxybenzaldehyde derivatives 3a-f, and there *in vitro* antimicrobial properties were evaluated against several pathogenic bacteria, *C. albicans* as a fungi. We have also studied the inhibitory effects of these substances against the mutagenicity of AFB<sub>1</sub>. Both electron donating and electron withdrawing groups on the aryl- ring of the compounds, influenced AFB<sub>1</sub>

activity. However the compounds possessing electronegative substituents such as fluorine and/or chlorine on the aryl- ring have shown the best anti-mutagenic and antibacterial properties.

## ACKNOWLEDGEMENTS

The authors would like to thank the Gazi University Research Fund (Project number: 05/2010-79) for their financial support, Elif Aynacı for elemental analysis, Nazlıgül Tolu for antibacterial studies and especially Bilal Altundas for his help in linguistic corrections.

## REFERENCES

- [1] Dalvie D K, Kalgutkar A S, Khojasteh-Bakht S C, Obach R S, O'Donnell J P (2002) Biotransformation reactions of five membered aromatic heterocyclic rings. *Chem. Res. Toxicol.* *Chem. Res. Toxicol* 15: 269-299.
- [2] Kagan J, Arora S K, Prakesh I, Üstünel A (1983) The synthesis of 2,2'-5',3''-terthiophene. *Heterocycles* 20(7): 1341-1345.
- [3] Abu-Hashem A A, El-Shehry M F, Badria F A (2010) Design and synthesis of novel thiophenecarbohydrazide, thienopyrazole and thienopyrimidine derivatives as antioxidant and antitumor agents. *Acta Pharm* 60: 311-323.
- [4] Fakhr I M I, Radwan M A, El-Batran S T, Omar M, El-Salam A, El-Shenawy S M (2009) Synthesis and pharmacological evaluation of 2-substituted benzo[b]thiophenes as anti-inflammatory and analgesic agents. *Eur J Med Chem* 44:1718-1725.
- [5] Kumar P S, Junapudi S, Gurrala S, Bathini R (2011) Synthesis of 2-substitued amino-3-carboxamido-4,5,6,7-tetramethylene thiophene derivatives and their anti-microbial. *International Journal of Pharmacy and Pharmaceutical Sci* 3(5):273-277.
- [6] Altundas A, Sari N, Colak N, Oğutçü H (2010) Synthesis and biological activity of new cycloalkylthiophene-Schiff bases ad their Cr(III) and Zn(II) complexes. *Med Chem Res* 19(6):576-588.
- [7] Balamurugan K, Perumal S, Reddy A S K, Yogeewari P, Sriram D (2009) A facile domino protocol for the regioselective and discovery of novel 2-amino-5-arylthieno- [2,3b]thiophenes as antimycobacterial agents. *Tetrahedron Lett* 50(6): 6191-6195.
- [8] Srivastava S, Das B (2011) Synthesis and evaluation of some novel thiophenes as potential antibacterial and mycolytic agents. *Der Pharma Chemica* 3(6): 103-111.
- [9] Ferreira I C F R, Queiroz M R P, Vilas-Boas M,



- Estevinho L M, Begouin A, Kirsch G (2006) Evaluation of the antioxidant properties of diarylamines in the benzo[b]thiophene series by free radical scavenging activity and reducing power. *Bioorg&Med Chem Lett* 16:1384–1387.
- [10] Selles P, Wailes J S, Whittingham W Gclarke (ed) (2005) 2-Aminothiophene compounds as fungicides. WO/044008 A2.
- [11] Nawwar G A M, Shafik N A (1995) Synthesis of 2-substituted benzothiazoles containing amino acid, imino or heteroaryl moieties with anticipated fungicidal activity. *Collect Czech Chem Comm* 60: 2200-2208.
- [12] Puterová Z, Krutosikova A, Végh D (2010) Gewalg reactions: synthesis, properties and applications of substituted 2-aminothiophenes. *Arkivoc* 1: 209–246.
- [13] Amat A, Pfohl-Leszkowicz A, Castegnaro M (2010) Genotoxic activity of thiophenes on liver human cell line (Hepg2). *Polycyclic Aromatic Compounds* 24:733-742.
- [14] Nartop D, Sari N, Altundas, A, Ogutcu, H (2012) Synthesis, Characterization, and Antimicrobial Properties of New Polystyrene-Bound Schiff Bases and Their Some Complexes *J Appl Polymer Sci.* 125 (3), 1796-1803.
- [15] Schillinger U, Lucke F K (1989) Antibacterial activity of *Lactobacillus sake* isolated from meat. *Applied and Environmental Microbiology* 55(8): 1901-1906.
- [16] Countryman P I, Heddle J A (1976) The production of micronuclei from chromosome aberrations in irradiated cultures of human lymphocytes. *Mutat Res* .41: 321–332.
- [17] Gewald K, Schinke E, Böttcher H (1966) Heterocyclen aus CH-aciden nitrilen, VIII. 2-amino-thiophene aus methylenaktiven Nitrilen. *Chemische Berichte* 99: 94–100.
- [18] Halling SM, Peterson Burch BD, Bricker BJ, Zuerner RL, Qing Z, L Li, Kapur V, Alt DP, Olsen SC (2005) Completion of the genome sequence of *Brucella abortus* and comparison to the highly similar genomes of *Brucella melitensis* and *Brucella suis* *Journal of Bacteriology* 187: 2715-2726.
- [19] [Sauret, JM, Vilissova N (2002) Human brucellosis. *J Am Board Fam Pract* 15: 401-406.
- [20] Rapp R P (2004) Changing strategies for the management of invasive fungal infections. *Pharmacotherapy* 24: 4-28.
- [21] Aoyama Y, Yoshida Y, Sato R (1984) Yeast cytochrome-p-450 catalyzing lanosterol 14 alpha-demethylation II. Lanosterol metabolism by purified P-450(14)DM and by intact microsomes. *J Biol Chem* 259:1661-1666.
- [22] Tani N, Rilla M R, Wittekindt C, Salminen K A, Ritvanen A, Ollakka R, Koskiranta J, Raunio H, Juvonen R O (2012) Antifungal activities of novel non-azol molecules against *S. cerevisiae* and *C.albicans*. *Eur J Med Chem* 47: 270-277.
- [23] Alpsoy L, Yildirim A, Agar G (2009) The antioxidant effects of vitamin a, c and e on aflatoxin b1-induced oxidative stress in human lymphocytes. *Toxicology and Industrial Health* 25: 121-127.
- [24] Piva G, Galvano F, Pietri A, Piva A (1995) Detoxification methods of aflatoxins. *A review. Nutrition Research* 15(5): 767-776.
- [25] Gulcin I, Bursal E, Sehitoglu MH, Bilsel M, Goren AC (2010) Polyphenol contents and antioxidant activity of lyophilized aqueous extract of propolis from Erzurum, Turkey. *Food and Chem Toxicol* 48: 2227–2238.

---

**Received: 03.03.2016**

**Accepted: 20.08.2016**

---

#### CORRESPONDING AUTHOR

##### Hatice Ogutcu

Faculty Arts and Science, Department of Biology,  
Ahi Evran University, 40100, Kırşehir, Turkey

e-mail: hogutcu@gmail.com

# EVALUATION OF ANTIBACTERIAL ACTIVITY OF SOME PLANT METHANOLIC EXTRACTS

Fulya Tugba Artun<sup>1</sup>, Ali Karagoz<sup>2\*</sup>, Zuhale Zeybek<sup>3</sup>, Miray Ustunturk-Onan<sup>3</sup>, Gulay Melikoglu<sup>4</sup>, Sezin Anil<sup>4</sup>, Sukran Kultur<sup>5</sup>

<sup>1</sup> Istanbul University, Institute of Science, Vezneciler, 34118, Istanbul, Turkey

<sup>2</sup> Istanbul University, Faculty of Science, Department of Molecular Biology and Genetics, Vezneciler, 34118, Istanbul, Turkey

<sup>3</sup> Istanbul University, Faculty of Science, Department of Biology, Vezneciler, 34118, Istanbul, Turkey

<sup>4</sup> Istanbul University, Faculty of Pharmacy, Department of Pharmacognosy, Beyazit, 34116, Istanbul, Turkey

<sup>5</sup> Istanbul University, Faculty of Pharmacy, Department of Pharmaceutical Botany, Beyazit, 34116, Istanbul, Turkey

## ABSTRACT

The purpose of our study is to evaluate antibacterial activity of the methanolic extracts of 14 medicinal plants 8 of which are endemic species to Anatolia using the Disc diffusion assay. By disk diffusion assay, the antibacterial activity of plant extracts was evaluated by using the noncytotoxic concentrations for Vero cell line determined by MTT assay. The methanolic extracts were evaluated for antibacterial activity against 9 standard strains (*Escherichia coli* ATCC 25922, *Pseudomonas aeruginosa* ATCC 27853, *Bacillus subtilis* ATCC 6633, *Klebsiella pneumoniae* ATCC 4352, *Staphylococcus aureus* ATCC 25923, *Staphylococcus marcescens* ATCC 13880, *Escherichia faecalis* ATCC 29212, *Staphylococcus enteritidis* ATCC 13076 and *Proteus mirabilis* ATCC 14153) and 11 environmental strains (*S.aureus* F1, F2, F3, *Serratia marcescens* F4, F5, F6, F7, *P. aeruginosa* F8, F9, *P. spp.* and *Salmonella spp.*). It was found that three plant extracts from the 14 plants studied had antibacterial activity. *Olea europaea* L. plant inhibited the growth of *Staphylococcus aureus* F1 environmental strain, *Cotinus coggygia* plant inhibited the growth of *Staphylococcus aureus*, *Escherichia coli*, *Bacillus subtilis*, *Enterococcus faecalis*, *Salmonella enteritidis*, *Proteus mirabilis* standard strains and *Staphylococcus aureus* F1, *Staphylococcus aureus* F2, *Staphylococcus aureus* F3 environmental strains and *Rosa damascena* plant inhibited the growth of *Staphylococcus aureus* F3 environmental strain.

## KEYWORDS:

Antibacterial activity, methanolic extracts, disk diffusion assay, MTT method

## INTRODUCTION

Plants form an integral part in traditional medicinal practices in all cultures worldwide and a

sizeable portion of the world population uses plant for prevention and management of different kinds of ailments. A complete storehouse of remedies has been provided by nature to cure ailment of mankind (1). The use of plants and plant products as medicines could be traced as far back as the beginning of human civilization. The earliest mention of medicinal use of plants are found in "Rigveda", which is said to have been written between 4500-1600 B.C. and is supposed to be the oldest repository of human knowledge. From over 300.000 species of higher plants to occur in nature, only about 2 percent have been screened so far (2).

The medicinal value of plants lies in some chemical substances that produce a definite physiological action on the human body. The most important of these bioactive compounds of plants are alkaloids, flavonoids, tannins and phenolic compounds (3). According to World Health Organization (WHO) medicinal plants would be the best source to obtain a variety of drugs. There is a continuous and urgent need to discover new antimicrobial compounds with diverse chemical structures and novel mechanisms of action for new and re-emerging infectious diseases. Therefore, researchers are increasingly turning their attention to folk medicine, looking for new leads to develop better drugs against microbial infections (2).

Medicinal plants are rich sources of antimicrobial agents. Many infectious diseases have been known to be treated with herbal extracts. The clinical efficacy of many existing antibiotics is being threatened by the emergence of multidrug resistant pathogens. Although, many plant species have been tested for antimicrobial properties, the majority of them have not been sufficiently evaluated. As an alternate source to the existing antibiotics, there is an urgent need to discover new antimicrobial compounds from various medicinal plants which can be used to treat many infectious diseases (4).

**TABLE 1**  
**List of plants used in the current study.**

Botanical name	Family	Specimen number (ISTE)	Plant part used	Districts of collection
<i>Crataegus microphylla</i> C. Koch	Rosaceae	76223	Leaves	Gölcük-Bolu
<i>Teucrium sandrasicum</i> O. Schwarz (Endemic)	Lamiaceae	87526	Aerial parts	Köyceğiz-Muğla
<i>Centaurea nerimaniae</i> Ş. Kültür (Endemic)	Asteraceae	98163	Aerial parts	Mersin
<i>Olea europaea</i> L.	Oleaceae	106286	Leaves	Şarköy-Tekirdağ
<i>Salvia hypargeia</i> Fisch.& Mey. (Endemic)	Lamiaceae	98205	Aerial parts	Mersin
<i>Cotinus coggygia</i> Scop.	Anacardiaceae	80926	Leaves	Kırklareli
<i>Hypericum kotschyanum</i> Boiss. (Endemic)	Hypericaceae	98173	Aerial parts	Mersin
<i>Nepeta italica</i> L.	Lamiaceae	98192	Aerial parts	Mersin
<i>Stachys cretica</i> L. subsp. <i>vacillans</i> Rech. Fil	Lamiaceae	98166	Aerial parts	Mersin
<i>Scorzonera tomentosa</i> L. (Endemic)	Asteraceae	98954	Aerial parts	Malatya
<i>Origanum sipyleum</i> L. (Endemic)	Lamiaceae	86060	Aerial parts	Mersin
<i>Rosa damascena</i> Miller	Rosaceae	106285	Flowers	Isparta
<i>Colchicum sanguicolle</i> K.M. Perss (Endemic)	Colchicaceae	48868	Cormus	Antalya
<i>Centaurea antiochia</i> Boiss. var. <i>praealta</i> (Boiss. & Bal) Wagenitz (Endemic)	Asteraceae	98247	Aerial parts	Mersin

## **MATERIALS AND METHODS**

**Plant selection and collection.** 14 medicinal plants were chosen for *in vitro* cytotoxicity and antibacterial activity testing by considering previous literature reviews and ethnobotanical information. The selected plants, which some of them are endemic, belong to different family groups were collected from different districts of Turkey ( Table 1).

**Preparation of extracts.** The dried plant material (*Crataegus microphylla*, *Teucrium sandrasicum*, *Centaurea nerimaniae*, *Olea europaea*, *Salvia hypargeia*, *Cotinus coggygia*, *Hypericum kotschyanum*, *Nepeta italica*, *Stachys cretica* subsp. *vacillans*, *Scorzonera tomentosa*, *Origanum sipyleum*, *Rosa damascena*, *Centaurea antiochia* var. *praealta*) were percolated with methanol (95%) in a room temperature. The methanolic extracts (ME) were evaporated to dryness under pressure and controlled temperature (40 to 50° C) in a rotary evaporator. The dried cormus of *Colchicum sanguicolle* were extracted with methanol (95%) in a Soxhlet apparatus. The ME was evaporated to dryness under pressure and controlled temperature (40 to 50 ° C) in a rotary evaporator. All the extracts were kept at -20° C and then were lyophilized. By this way, crude methanolic extracts were obtained. The ME's were

dissolved in distilled water, afterwards diluted in the medium (Eagle's minimum essential medium).

**Cell culture.** The normal African green monkey kidney epithelial (Vero) cell lines were grown and maintained in Eagle's minimum essential medium (EMEM) with Earle's saline, supplemented with an antibiotic-antimycotic mixture [penicillin (100 U/mL), streptomycin (100 µg/mL), amphotericin B (0,25 µg/mL)], and 10% fetal bovine serum. Vero cells were maintained in a humidified atmosphere containing 5 % CO<sub>2</sub> at 37°C.

**In vitro cytotoxicity assay.** The cytotoxicity assays were performed according to the microculture MTT method (5). The cells were harvested (2,0– 2,8 x 10<sup>5</sup> cells/well) and inoculated in 24 well plates. The cells were washed with phosphate buffered saline and the cultured cells were then inoculated with and without the extract (final extract concentrations are ranged 5-1000 µg/mL). After 72 h incubation, the medium is aspirated. 150 µL of MTT solution (5 mg/mL in PBS, pH 7,2) is added to each well and the plates incubated for 4 h at 37 °C. After incubation, 750 µL of dimethyl sulfoxide was added to each well of plates, followed by gentle shaking to solubilize the formazan dye for 15 min. Absorbance was read at

540 nm using a photometer and surviving fraction calculated. The cell viability was calculated by means of the formula:

$$\% \text{ viability} = (\text{Absorbancy of extracts treated cells} / \text{Absorbancy of control cells}) \times 100.$$

**TABLE 2**  
**Noncytotoxic concentrations of plant extracts used in disc diffusion assay.**

Plants	Concentration (µg/mL)
<i>Crataegus microphylla</i> C. Koch	500
<i>Teucrium sandrasicum</i> O. Schwarz (Endemic)	50
<i>Centaurea nerimaniae</i> Ş. Kültür (Endemic)	500
<i>Olea europaea</i> L.	500
<i>Salvia hypargeia</i> Fisch.& Mey. (Endemic)	500
<i>Cotinus coggygria</i> Scop.	500
<i>Hypericum kotschyianum</i> Boiss. (Endemic)	50
<i>Nepeta italica</i> L.	250
<i>Stachys cretica</i> L. subsp. <i>vacillans</i> Rech. fil	50
<i>Scorzonera tomentosa</i> L. (Endemic)	50
<i>Origanum sipyleum</i> L. (Endemic)	500
<i>Rosa damascena</i> Miller	500
<i>Colchicum sanguicolle</i> K.M. Perss (Endemic)	250
<i>Centaurea antiiochia</i> Boiss. var. <i>praealta</i> (Boiss. & Bal) Wagenitz (Endemic)	500

All experiments were performed in triplicate and mean values were used for calculation. Spectrophotometric determinations were performed using µ Quant Universal Microplate Spectrophotometer (Bio-Tek) and data was statistically processed by KCJunior Data Program.

**Bacterial strains.** In this study, it has been used 9 standart strains (*Escherichia coli* ATCC 25922, *Pseudomonas aeruginosa* ATCC 27853, *Bacillus subtilis* ATCC 6633, *Klebsiella pneumoniae* ATCC 4352, *Staphylococcus aureus* ATCC 25923, *Staphylococcus marcescens* ATCC 13880, *Escherichia faecalis* ATCC 29212, *Staphylococcus enteritidis* ATCC 13076 and *Pseudomonas smirabilis* ATCC 14153) and 11 environmental strains (*S.aureus* F1, F2, F3, *Serratia marcescens* F4, F5, F6, F7, *P. aeruginosa* F8, F9, *P. spp.* and *Salmonella spp.*).

**Evaluation of Antibacterial Activity by Disc Diffusion Assay.** Antibacterial activity was based on the disc diffusion assay using a cell suspension of microorganisms (6,7,8). The concentration of the cell suspension was equilibrated to a 0.5 McFarland standard and 100 µL of each microorganism's suspension was spread on a Mueller-Hinton agar plate. In addition, noncytotoxic concentration of methanolic extracts were pipetted onto sterile paper discs (6 mm diameter), which were allowed to dry in an open sterile Petri dish in a biological laminar flow bench. Control disc was prepared with sterile water. Standard antibiotic discs (Ampicillin 10µg, Cefotaxime 30µg, Erythromycin 15µg, Gentamicin 10µg, Methicillin 10µg, Penicillin G 10 units, Polymyxin B 300 units, Vancomycin 30 µg) were obtained commercially. All discs were placed on the surface of inoculated plates and incubated at 37 °C for 24 h. The diameters of the zones of bacterial inhibition were measured to the nearest millimeter. All experiments were performed in triplicate.

## RESULTS AND DISCUSSION

According to World Health Organization (WHO), the increase of resistance to antibiotics by bacterial pathogens is a growing problem in both developed and developing countries. The problem of microbial resistance is growing and the outlook of the use of antimicrobial drugs in future is uncertain. Therefore, action must be taken to reduce this problem, for example, to control the use of antibiotics, to develop research to better understanding of the genetic mechanism of resistance and to continue study to develop new drugs either synthetic or natural (9).

In recent years, further concerns about the possible spread of bacterial resistance in bacteria isolated from food and the environment has been proposed. Antibiotics are used widely in animal products during the past centuries. Excessive and uncontrolled use of antibiotics as routine supplements could lead to an increase in the number of antibiotic resistant bacteria. Although due to awareness of antibacterial resistance in humans with the use of antibiotics in animal feed may have suggested that ultimately limits their use in European countries but today these ideas are being used via acceleration of much attention worldwide to evaluate natural alternatives to antibiotics (7). Most of the current antibiotics have considerable limitations in terms of antimicrobial spectrum, side effects and their widespread overuse has led to increasing clinical resistance of previously sensitive microorganisms and to the occurrence of uncommon infections (10). Hence, there is need to look for alternative strategies for the management of resistant bacteria and one of the possible strategies towards this objective involves rational

localization of bioactive phytochemicals which have antibacterial activity and this may be one of the important approaches for the containment of antibiotics resistance (11).

A renewed interest in plant based antimicrobials has arisen during the last twenty years, but still plant based antimicrobials are poorly explored. Screening of plants extracts for antimicrobial activity has shown that higher plants represent a potential source of new anti-infective compounds. The antimicrobial compounds from plants may inhibit bacteria through different mechanism than the conventional antibiotics, and could therefore be of clinical value in the treatment of microbial infection. Plants are important source of potentially useful structures for the development of new chemotherapeutic agents. The first step towards this goal is the *in vitro* antibacterial activity assay. Crude plant extracts are generally a mixture of active and non-active compounds. The herbal based phytomedicine have large therapeutic applications since they can have less side effects when compared with synthetic antimicrobials (9). The cytotoxic effect of each extract was examined with the cell viability of Vero cells. Some plant extracts have cytotoxic activity in different degrees (data not shown). The concentrations selected for antimicrobial activity tests were noncytotoxic concentration (Table 2).

According to our results, only 3 of 14 medicinal plant extracts showed antibacterial activity in noncytotoxic concentrations. The antibacterial activities were produced to different extents by the methanolic extracts of *Olea europaea* L., *Cotinus coggygia* Scop. and *Rosa damascena*. Although *Cotinus coggygia* Scop. inhibited the growth of nine bacteria, *Olea europaea* L. and *Rosa damascena* inhibited one bacteria (Table 3). It was found that the inhibition zone of tested bacteria against plant extracts have changed between 7-11 mm. However, the inhibition zone of same bacteria against standard antibiotics was found between 11-40 mm.

Antimicrobial substances are desirable tools in the control of undesirable microorganisms especially in the treatment of infections and in preservation of food. The active components usually interfere with the growth or metabolism of microorganisms in a negative manner (10). The effects produced by *Olea europaea* L., *Cotinus coggygia* Scop. and *Rosa damascena* are however lower than the antibiotics used in the study; but this suggests that higher concentrations of these plant extracts could produce comparable antibacterial results since the noncytotoxic concentrations are only used. Our findings suggest that the antibacterial activity is not due to the cytotoxic activity of extracts.

**TABLE 3**  
**Antibacterial activity of the methanolic extracts.**

Bacteria	Bacteria inhibition zone (mm)											
	<i>Olea europaea</i> L.	<i>Cotinus coggygia</i> Scop.	<i>Rosa damascena</i> Miller	Ampicillin	Cefotaxime	Erythromycin	Gentamicin	Methicillin	Penicillin G	Polymyxin B	Vancomycin	Control
<i>Staphylococcus aureus</i>	-	11	-	34	33	28	24	29	41	11	20	-
<i>Bacillus subtilis</i>	-	9	-	37	40	35	33	37	37	15	28	-
<i>Enterococcus faecalis</i>	-	8	-	28	15	20	16	10	16	-	20	-
<i>Escherichia coli</i>	-	9	-	22	35	-	25	-	-	17	-	-
<i>Proteus mirabilis</i>	-	11	-	28	39	-	24	-	22	-	-	-
<i>Klebsiella pneumoniae</i>	-	-	-	-	-	-	-	-	-	-	-	-
<i>Pseudomonas aeruginosa</i>	-	-	-	-	-	-	-	-	-	-	-	-
<i>Serratia marcescens</i>	-	-	-	-	-	-	-	-	-	-	-	-
<i>Salmonella enteritidis</i>	-	11	-	27	30	12	24	-	13	15	-	-
<i>Staphylococcus aureus</i> F1	7	11	-	23	40	35	29	25	21	14	20	-
<i>Staphylococcus aureus</i> F2	-	9	-	38	32	28	22	26	16	-	20	-
<i>Staphylococcus aureus</i> F3	-	11	9	16	29	30	22	26	16	-	19	-
<i>Serratia marcescens</i> F5	-	-	-	-	-	-	-	-	-	-	-	-
<i>Serratia marcescens</i> F6	-	-	-	-	-	-	-	-	-	-	-	-
<i>Serratia marcescens</i> F7	-	-	-	-	-	-	-	-	-	-	-	-
<i>Pseudomonas aeruginosa</i> F8	-	-	-	-	-	-	-	-	-	-	-	-
<i>Pseudomonas aeruginosa</i> F9	-	-	-	-	-	-	-	-	-	-	-	-
<i>Pseudomonas</i> spp. F10	-	-	-	-	-	-	-	-	-	-	-	-
<i>Salmonella</i> spp. F11	-	-	-	-	-	-	-	-	-	-	-	-

“-”: no inhibition.

## CONCLUSION

Many medicinal plants may be used as a reponse to specific health problems. As can be seen in this study three plants extracts showed different levels of potency against all the tested microorganisms. The methanolic extracts of these three plants may help in the cure of diseases caused by these organisms (12). The methanolic extract of *Cotinus coggygia* Scop. showed antibacterial potency against *Escherichia coli*, *Bacillus subtilis*, *Enterococcus faecalis*, *Salmonella enteritidis*, *Proteus mirabilis*, *Staphylococcus aureus* and its environmental strains. *Staphylococcus aureus* is an important cause of human skin and soft tissue infections (SSTIs) worldwide (13,14). Therefore, the extract of *Cotinus coggygia* Scop. may be used as an agent for the treatment of these diseases. *Escherichia coli*, *Bacillus subtilis*, *Enterococcus faecalis*, *Salmonella enteritidis*, *Proteus mirabilis* can be controlled by the extract of *Cotinus coggygia* Scop., as well.

## ACKNOWLEDGEMENTS

This work was supported by the Research Fund of Istanbul University, Project number: ÖNAP-41488.

## REFERENCES

- [1] Kannaiyan, M., Thambidurai, P., Raja, V., Suresh, M., Abraham, S., Zewdneh, T. and Nooruddin, T. (2015). Efficacy of different solvent extracts of *Aristolochia krisagathra* and *Thottea pomnudianna* for potential antimicrobial activity. *J Pharm Res*, 9(1), 35,40
- [2] R. N. Gupta, K. Viswas, M. Pathak, S. S. Parihar, A. Gupta, Antibacterial Activities of Ethanolic Extracts of Plants Used in Folk Medicine. *Int J Res Ayurveda Pharm*, 1 (2), 529,535(2010).
- [3] A. Hassan, S. Rahman, F. Deeba, S. Mahmud, Antimicrobial activity of some plant extracts having hepatoprotective effects. *J. Med. Plants Res.*, 3 (1), 20,23(2009).
- [4] S. W. Goveas, A. Abraham, Evaluation of antimicrobial and antioxidant activity of stem and leaf extracts of *Coscinium fenestratum*. *Asian J Pharm Clin Res*, 6 (3),218,221(2013).
- [5] T. Mosmann, Rapid colorimetric assay for cellular grow and survival: application to Proliferation and cytotoxicity assays. *J Immunol Method*, 65, 55,63(1983).
- [6] CLSI (Clinical and Laboratory Standards Institute), Performance Standards for Antimicrobial Disk Susceptibility Tests; Approved Standard—Eleventh Edition, Vol. 32 No. 1(January 2012).
- [7] A. Miri, J. S. Rad, S. M. H. Alfatemı, M. S. Rad, A study of Antibacterial potentiality of some plants extracts against multi-drug resistant human pathogens. *Ann Biol Res*, 4(8), 35,41(2013).
- [8] S. S. Tek, G. C. L. Ee, S. H. Mah, Y. K. Yong, Y. M. Lim, M. Rahmanı, Z. Ahmad, *In vitro* Cytotoxic, Antioxidant and Antimicrobial Activities of *Mesua beccariana* (Baill.) Kosterm., *Mesua ferrea* Linn., and *Mesua congestiflora* Extracts. *BioMed Res. Int.*, Article ID 517072, 1,9(2013).
- [9] F. Ahmad, I. Hasan, D. K. ChIstI, H. Ahmad, Antibacterial Activity of *Raphanus sativus* Linn. Seed Extract. *GJMR*, 12 (11), 25,34 (2012).
- [10] K. C. Ofokansı, A. A. Attama, P. F. Uzor, M. O. Ovrı, Evaluation of the combined antimicrobial activity of the leaf extract of *Phyllanthus muellerianus* with ciprofloxacin. *ijpsdr*, 2, 2,6(2013).
- [11] F. C. M. Robertson, C.I. Onyeka, S. C. K. Tay, W. Walana, *In vitro* antimicrobial activity of “Antibact”, an herbal medicinal product against standard and clinical bacterial isolates. *JMPR*, 9(11), 370,378(2015).
- [12] I. C. Okwulehie, F. E. Akanwa, Antimicrobial Activity of Ethanol Extract of Four Indegenous Plants from South Eastern Nigeria. *ARPN J Sci. Tech.*, 3 (4), 350,355(2013).
- [13] V. Hemmige, M. McNulty, E. Silverman, M. Z. David, Predictors of skin and soft tissue infections in HIV-infected outpatients in the community-associated methicillin-resistant *Staphylococcus aureus* era. *Eur J Clin Microbiol Infect Dis*, 34(2), 339,347(2015).
- [14] N. Malachowa, S. D. Kobayashi, D. E. Sturdevant, D. P. Scott, F. R. DeLeo, Insights into the *Staphylococcus aureus*-Host Interface: Global Changes in Host and Pathogen Gene Expression in a Rabbit Skin Infection Model. *PloS one*, 10(2), 1,15(2015).

Received: 03.03.2016

Accepted: 16.09.2016

## CORRESPONDING AUTHOR

**Ali Karagoz**

Istanbul University, Faculty of Science, Department of Molecular Biology and Genetics, 34459, Vezneciler-Istanbul, Turkey

e-mail: [sanicula@istanbul.edu.tr](mailto:sanicula@istanbul.edu.tr)





# DISTRIBUTION CHARACTERISTICS AND ECOLOGICAL RISK ASSESSMENT OF NONYLPHENOL IN JIAOZHOU BAY IN QINGDAO, CHINA

Peng Zhang<sup>1,2</sup>, Chang-you Wang<sup>3</sup>, Sheng-kang Liang<sup>1,2,\*</sup>, Xiao-yan Wang<sup>1,2</sup>, Xiu-lin Wang<sup>1,2</sup>

<sup>1</sup> Key Laboratory of Marine Chemistry Theory and Technology, Ministry of Education, Qingdao 266100, (China)

<sup>2</sup> College of Chemistry and Chemical Engineering, Ocean University of China, Qingdao 266100, (China)

<sup>3</sup> School of Marine Sciences, Nanjing University of Information Science and Technology, Nanjing 210044, (China)

## ABSTRACT

Nonylphenol (NP) is an endocrine disruptor, and its environmental distribution and ecological risks have drawn widespread concerns. In this study, the distribution of NP was investigated in the waters of Jiaozhou Bay (JZB) in Qingdao, China in April 2007 and August 2009. The predicted no-effect concentration (PNEC) was calculated as the criterion for ecological risk assessment of NP based on the toxic experiments of NP on five dominant phytoplankton species in JZB (*Skeletonema macostatum*, *Chaetoceres curvisetus*, *Pseudo-nitzschia pungens*, *Dunaliella salina*, and *Platymonas helgolandica*). Results showed that the concentrations of NP in JZB ranged from 23.6 ng/l to 192.9 ng/l in April 2007 and from 18.5 ng/l to 179.3 ng/l in August 2009. High NP levels were observed in northeast and northwest JZB. The PNEC for NP in seawater was 79.0 ng/l, which was calculated using the EC<sub>50</sub> value of *C. curvisetus* because of its higher sensitivity compared with the other algae species. The risk quotients of NP in the waters of JZB ranged from 0.23 to 2.44, with an average of 0.76, thereby implying a significant risk for aquatic ecosystems in some areas of JZB.

## KEYWORDS:

Nonylphenol, Jiaozhou Bay, distribution, ecological risk assessment

## INTRODUCTION

In the environment, nonylphenol (NP) mainly originates from the degradation of nonylphenol polyethoxylates (NPnEO), a class of non-ionic surfactants that is widely used in industrial and household applications, such as detergents, pesticides, plastic additives, and wetting agents [1,

2]. Compared with its parent compounds, NP is more lipophilic and toxic. Numerous studies have indicated that NP can have harmful effects to humans and wildlife by interfering with the endocrine system [3–10]. NP is listed as one of the priority persistent toxic substances that should be controlled by the United Nations Environment Program. In China, the annual production of NP reaches 31,434 tons, which approximately accounts for 10% of the total world production [11]. NP enters into water bodies through the discharge of effluents from sewage treatment plants. Investigating the distribution characteristics and ecological risks of NP in aquatic ecosystems is important considering the harmful effects of NP on humans and wildlife.

The risk quotient (RQ), which is defined as the ratio of predicted environmental concentration (PEC) to predicted no-effect concentration (PNEC), is generally used in ecological risk assessment [12]. PEC values can be obtained through model prediction or environmental monitoring. PNEC values can be determined using the assessment factor (AF) method, the statistical extrapolation method based on species sensitivity distributions (SSD) [13], and other models [14]. The AF method is simple to use and feasible when toxicity data are limited. However, PNEC estimation with minimum toxicity value and a certain factor exhibits considerable uncertainty. PNEC values obtained using the SSD method are more reliable and reasonable since the estimates are based on a full of toxicity data set. To date, several reports on the PNEC or water quality criteria of NP worldwide have been presented [15, 16]. However, no water quality criterion or PNEC for NP has been established in China, which inevitably hinders the ecological risk assessment of this pollutant in the country. Gao et al. built an SSD model for estimating the PNEC of NP and assessed the ecological risks of the pollutant in the coastal waters of China using PNEC as the water quality criterion [11]. However, different ecosystems have varying dominant species and the acceptable effect levels of NP for different species, even those

belonging to the same category, vary significantly. Therefore, the PNEC calculated using SSD model built with the toxicity data of NP on aquatic organisms screened from the ECOTOX database of the US Environmental Protection Agency (EPA) does not possess the regional features of China. Wang et al. presented a 3D model and applied it to estimate the no detected toxic effect concentration (NDEC) with a percentile confidence interval [14]. In this model, the PNEC (referred to as NDEC) can be directly estimated using the measured toxicity data of the pollutant on local dominant species used in the experiment. This approach avoided the considerable uncertainties of the AF method and enabled PNEC estimation using the toxicity data of the pollutant on local dominant species. Hence, it is regarded as a promising method for determining the PNEC value of a specific aquatic ecosystem in China.

Jiaozhou Bay (JZB) is located in the southern part of the Shandong Peninsula; it has an average depth of 7 m and a surface area of 360 km<sup>2</sup> [17]. JZB is a typical semi-enclosed bay. It is surrounded by Qingdao City and connected to the Yellow Sea through a narrow channel that is seriously affected by anthropogenic activities. The water quality of JZB has deteriorated with the rapid economic development and the fast increasing population of Qingdao during the past two decades. Numerous studies have been conducted to determine the pollution status of JZB, and some of these studies have focused on the contamination level and ecological risk of NP [18, 19]. However, reports on PNEC based on toxicity experiments of NP conducted on local dominant species in JZB remain lacking [20]. In the present study, we investigate the distribution characteristics of NP in JZB and assess its ecological risks. For this purpose, surface water samples from JZB were collected and analyzed in April 2007 and August 2009. Five dominant microalgae in JZB were selected to test the toxic effects of NP on their growth rates and to obtain the PNEC value for ecological risk assessment using the model developed in [14].

## MATERIALS AND METHODS

**Materials.** Five species of algae (*Skeletonema macostatum*, *Chaetoceres curvisetus*, *Pseudonitzschia pungens*, *Dunaliella salina*, and *Platymonas helgolanidica*) were obtained from the college of Marine Life Science of the Ocean University of China. Seawater was collected from JZB to cultivate the algae.

**Chemicals and Standards.** NP, a mixture of compounds with different side chains, and 4-tert-

butylphenol (recovery standard), both of technical grade, were purchased from Tokyo Kasei Kogyo Co., Ltd., Japan. Dichloromethane, methanol, acetone, and hexane, at high-precision liquid chromatography grade, were purchased from Fisher Chemical, USA. C<sub>18</sub>-solid phase extraction (SPE) cartridges were obtained from Agilent Technologies, USA.

### Sampling Sites and Sample Collection.

Surface water samples from JZB were collected from 7 stations in April 2007 and from 22 stations in August 2009 (Fig. 1). Subsequently, 2 l filtered (GF/F, 0.45 μm) water sample was placed in an amber glass bottle with a Teflon-lined cap. Then, HCl solution (6 M) was added to achieve a pH of 2 to inhibit microbiological activities. The samples were stored at 4 °C until pretreatment. Detailed information on the sampling sites is listed in Table 1.

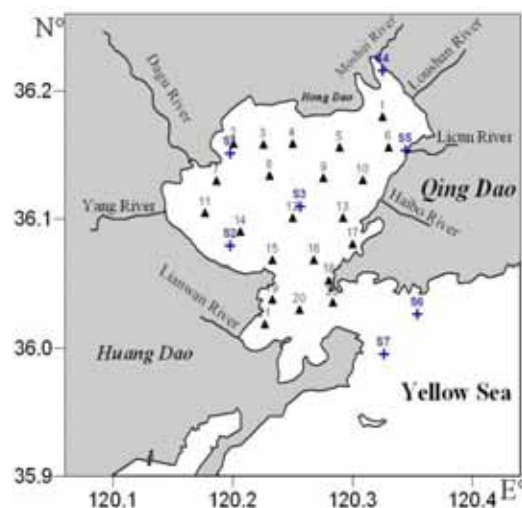


FIGURE 1

Locations of the sampling sites

**Extraction.** The extraction procedure for the target compounds is as follows. First, the C<sub>18</sub>-SPE cartridges were consecutively conditioned under vacuum with hexane (10 ml), dichloromethane (10 ml), methanol (10 ml), and nanopure water (10 ml). Then, the acidized water samples were spiked with a surrogate standard (4-tert-butyl phenol) and passed through the C<sub>18</sub>-SPE cartridges under vacuum at a flow rate of 10–15 ml/min. Finally, the C<sub>18</sub>-SPE cartridges were eluted with 10 ml dichloromethane/methanol (8:2, v/v). The extracts were concentrated to 1 ml under a gentle nitrogen stream before gas chromatography (GC)–mass spectrometry (MS) analysis.

**TABLE 1**  
Detailed information of the sampling sites.

Station	Longitude	Latitude	NP/ng/l	RQ	Sampling time
S1	120°10'48"	36°10'27"	40.49	0.51	2007.4
S2	120°10'44"	36°06'18"	36.06	0.46	2007.4
S3	120°14'24"	36°08'10"	23.62	0.30	2007.4
S4	120°18'32"	36°14'11"	165.9	2.10	2007.4
S5	120°19'48"	36°10'39"	192.9	2.44	2007.4
S6	120°20'28"	36°03'32"	34.25	0.43	2007.4
S7	120°18'32"	36°01'43"	35.84	0.45	2007.4
1	120°19'29"	36°10'44"	98.3	1.24	2009.8
2	120°12'03"	36°09'29"	69.8	0.88	2009.8
3	120°13'32"	36°09'28"	45.2	0.57	2009.8
4	120°15'00"	36°09'29"	37.9	0.48	2009.8
5	120°17'20"	36°09'19"	47.3	0.60	2009.8
6	120°19'48"	36°09'18"	179.3	2.27	2009.8
7	120°11'12"	36°07'44"	103.5	1.31	2009.8
8	120°13'50"	36°07'58"	24.3	0.31	2009.8
9	120°16'33"	36°07'52"	31.7	0.40	2009.8
10	120°18'30"	36°07'48"	72.3	0.92	2009.8
11	120°10'37"	36°06'14"	36.7	0.46	2009.8
12	120°15'00"	36°06'00"	18.5	0.23	2009.8
13	120°17'31"	36°06'00"	71.9	0.91	2009.8
14	120°12'24"	36°05'22"	40.5	0.51	2009.8
15	120°13'59"	36°04'01"	33.3	0.42	2009.8
16	120°16'04"	36°04'02"	40.2	0.51	2009.8
17	120°18'01"	36°04'48"	43.5	0.55	2009.8
18	120°16'49"	36°03'07"	41.2	0.52	2009.8
19	120°13'59"	36°02'13"	39.3	0.50	2009.8
20	120°15'20"	36°01'46"	44.5	0.56	2009.8
21	120°13'37"	36°01'05"	45.7	0.58	2009.8
22	120°17'00"	36°02'06"	42.5	0.54	2009.8

**Quantification via GC–MS.** GC–MS analysis was performed using a Hewlett-Packard 6890 gas chromatograph connected to a 5973 mass spectrometer. The target compounds were separated via GC with an HP-5MS (30 m × 0.32 mm i.d. × 0.25 µm film thickness) quartz capillary column. Helium gas was used as the carrier gas at a flow rate of 1 ml/min. The temperature program was initialized at 50 °C and subsequently increased to 180 °C at 20 °C/min. Then, it was increased to 200 °C at 2 °C/min (2 min), and finally increased to 280 °C at 30 °C/min (2 min). Afterward, 1 µl of the sample was injected in splitless mode at 280 °C. The selected ion monitoring mode was used for quantitative analysis.

**Quality Assurance and Quality Control.** The surrogate standard (4-tert-butyl phenol) was added

into each sample before extraction. The recoveries of NP and the surrogates were 87%–95% and 74%–108%, respectively, both within the range of 70%–120%. Good reproducibility of determination was obtained with a relative standard deviation of less than 9%. The method detection limit for NP was 0.8 ng/l.

**Algae Growth Inhibition Experiment and NPEC Calculation.** The testing toxicity effect of chemical pollutants on organisms, including fish, invertebrates, and algae, is a universal method to determine the safety effect concentration in an ecosystem. Chronic and acute toxicities of NP on aquatic organisms have been reviewed in [21, 22]. Algae appear to be more sensitive to NP than invertebrates and fish. Thus, five dominant algae

species in JZB, namely, *S. macostatum*, *C. curvisetus*, *P. pungens*, *P. helgolandica*, and *D. salina*, were selected as test species for the algae growth inhibition experiment by NP. The marine algae were cultivated in *f/2* medium with filtered seawater at a temperature of  $20 \pm 2$  °C [23], a light intensity of 3000 Lux, and a light/dark cycle of 12:12. The algae were then inoculated in 500 mL Erlenmeyer flasks with a starting cell density of  $10^5$  cells/ml. Each culture had two replicates. The NP dissolved in acetone was diluted with acetone to provide the desired concentrations of NP in the growth media. The series concentrations of NP for the five algae were fixed based on the preliminary results. Two contrast tests for blank control and acetone control were also performed. The measurement of algae density was repeated thrice per replicate using a hemacytometer every 24 hours. The  $EC_{50}$  value was calculated from the concentration–inhibition curve fitted via probit analysis [24]. The PNEC value was calculated using the 3D model constructed in [14] based on the minimum  $EC_{50}$ .

**Statistical Analysis.** Statistical significance was established at  $P \leq 0.05$  via one-way ANOVA. All statistical analyses were performed on MATLAB 7.0.

## RESULTS AND DISCUSSION

**NP Concentrations in JZB Seawater.** The NP concentrations in the surface water of JZB ranged from 23.6 ng/l to 192.9 ng/l in April 2007 and from 18.5 ng/l to 179.3 ng/l in August 2009. These results are close to the values ranging from 20.2 ng/l to 268.7 ng/l reported in [18] and higher than those in the South China Sea ( $<20$ – $40$  ng/l) [25], the Lingdingyang ( $<10$ – $14$  ng/l) [26], Bohai Bay (33–132 ng/l) [27], the German Bight of the North Sea (0.7–4.4 ng/l) [28], and Ariake Sea (11–49 ng/l) [29], but considerably lower than those observed in the coastal waters of Spain ( $<0.15$ – $4.1$   $\mu\text{g/l}$ ) [30], Singapore (320–2760 ng/l), [31] and Morro Bay ( $<0.9$   $\mu\text{g/l}$ ) [32].

In terms of spatial distribution, the NP concentrations in the northeastern area of JZB were generally higher than those in the northwestern area of the bay. Meanwhile, the NP concentrations in the central area and at the mouth of JZB were lower than those in the other areas of the bay (Fig. 2). On the one hand, the stations in the northeastern area of JZB are closer to the river mouths of Moshui River, Baisha River, Licun River, and Haibo River. These rivers pass through the main industrial area of

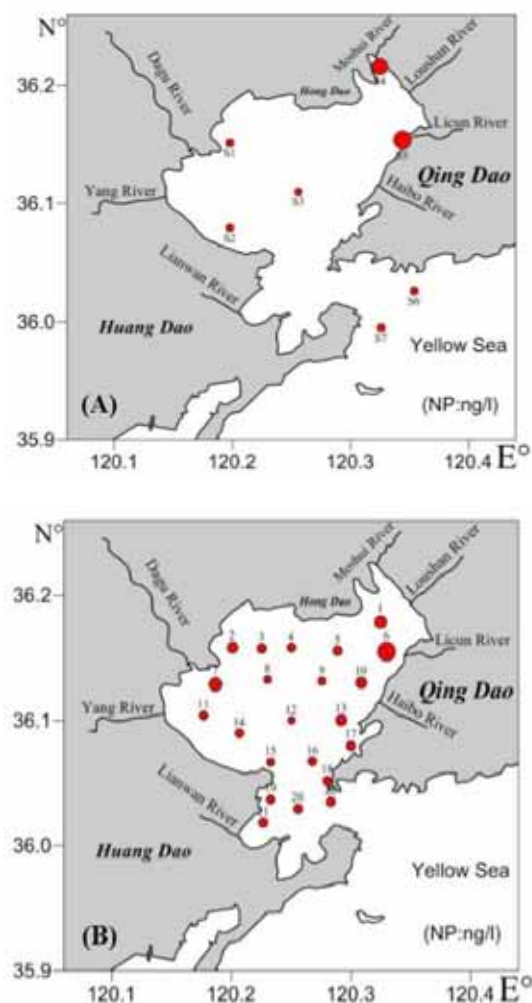


**FIGURE 2**  
The distribution of NP in the surface water of the Jiaozhou Bay in April 2007 (A) and in August 2009 (B)

Qingdao and receive large amounts of industrial effluents and domestic sewage [33]. On the other hand, the relatively lower NP levels in the northwestern area of JZB may be attributed to less pollutant sources and the clockwise tidal current in JZB. The capacity of transporting pollutants to the west is relatively weak because of the clockwise tidal current [19]. Thus, the northwestern area of the bay was less polluted. The NP concentrations at the mouth of the JZB were considerably lower because of the rapid exchange with the open ocean [19]. The NP levels in the central bay were also low because of the distance from the pollutant sources. However, the NP levels in the northwestern area of JZB were considerably higher than those in the central bay. This result is mainly caused by inputs from Dagu River, which is located in the northwestern coast of JZB and accounts for 84% of the total freshwater input to JZB [34].

**PNEC Estimation Based on the Toxicity Data of NP on the Dominant Algae in JZB.** Figure 3 presents the growth characteristics of five dominant algae in JZB under different NP concentrations. In general, the growth rate of the five algae decreased and some even became negative with increasing NP concentrations. The inhibitory effects increased with NP concentrations. In the exposure test, the growth rate of *S. macostatum* became negative after 24 h at a low NP concentration of 0.15 mg/l and increased gradually in the following 48 h. When NP concentration was higher than 1.2 mg/l, growth was completely inhibited. The growth pattern of *P. pungens* was similar to that of *S. macostatum*. When NP concentration was above 0.15 mg/l, the growth rate of *P. pungens* became negative after 24 h. However, complete inhibition was observed only at an NP concentration of 0.60 mg/l. The growth of *P. pungens* was completely inhibited when NP concentration was 2.5 mg/l. The growth of *D. salina* exhibited an obvious reduction after 24 h at any tested NP concentration. Its complete inhibition was observed at a concentration of 5.0 mg/l. *P. helgolandica* was more tolerant to NP than the other four algae. It only exhibited a negative growth after 24 h at concentrations of 5 mg/l and 10 mg/l. Complete inhibition was not observed at the tested concentrations.

The 96h-EC<sub>50</sub> values were calculated from the concentration–inhibition curves fitted via probit analysis. The 96h-EC<sub>50</sub> values of *S. costatum* and *C. curvisetus* were close to each other, i.e., 0.37 mg/L and 0.32 mg/L, respectively, which were both higher than the 96h-EC<sub>50</sub> values of *S. costatum* and *C. curvisetus* provided in [35] (0.13 mg/l and 0.22 mg/l for *S. costatum* and *C. curvisetus*, respectively). The 96h-EC<sub>50</sub> value of *P. Pungens* was 0.86 mg/l. However, the 96h-EC<sub>50</sub> values of *D. salina* and *P. helgolandica* were evidently higher than those of the other three algae, i.e., 1.03 mg/l and 2.60 mg/l, respectively. The 96h-EC<sub>50</sub> of *D. salina* in this study was lower than the result from [36] (1.47 mg/l). Thus, the inhibition effect decreased in the order of *C. curvisetus* > *S. costatum* > *P. Pungens* > *D. salina* > *P. helgolandica*. This result indicated that *C. curvisetus* is more sensitive to NP than the other four tested algae. Compared with the other reported 96h-EC<sub>50</sub> values of NP on common algae in China, such as *Chlorella vulgaris* (14.86 mg/l) [37], *Phaeocystis globosa* (0.42 mg/l) [38], and *Selenastrum capricornutum* (1.05 mg/l) [39], *C. curvisetus* is relatively sensitive to NP than the other tested algae species in the coastal water of China.

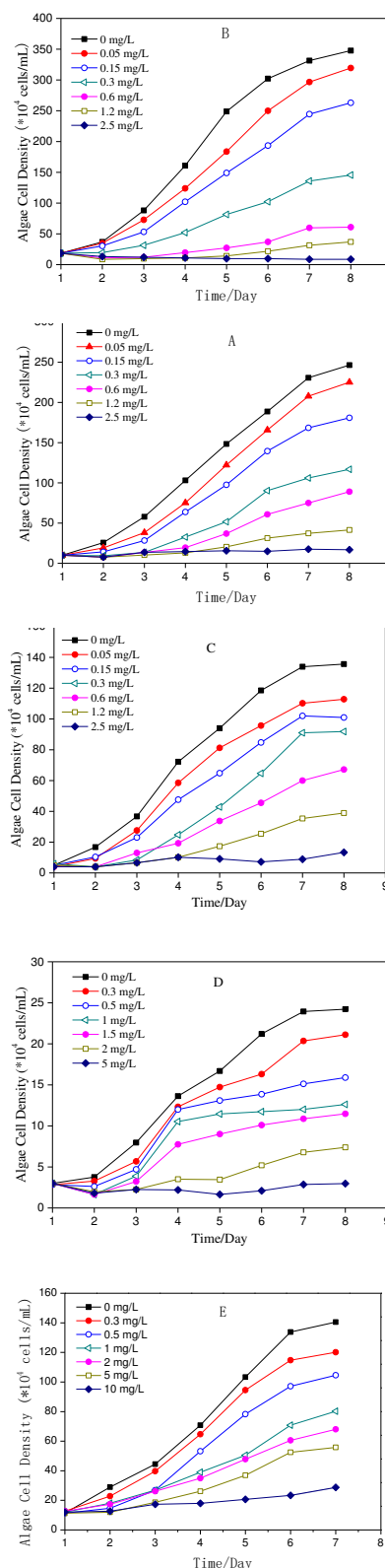


**FIGURE 3**  
**Growth curves of five marine microalgae under different NP concentrations.**  
**A: *Skeletone macostatum*; B: *Chaetoceres curvisetus*; C: *Pseudo-nitzschia pungens*; D: *Dunaliella salina*; E: *Platymonas helgolandica***

On the basis of the minimum 96h-EC<sub>50</sub> data of *C. curvisetus*, which was more sensitive to NP toxicity, the PNEC value (79.0 ng/l) was calculated using the model constructed in [14]. This result is higher than the PNEC value estimated in [35] (56.0 ng/l) and nearly one-third of the PNEC value estimated using the SSD model in [11] (0.28 µg/l), which is based on the toxicity data of NP on aquatic organisms screened from the ECOTOX database of the US EPA.

**Ecological Risk Assessment.** As mentioned earlier, RQ was used for ecological risk assessment of NP. If the RQ value is higher than one in a region, then implementing certain actions to reduce ecological risks is necessary. The results indicate that the RQs in the seawater of JZB ranged from 0.23 to 2.44, with an average value of 0.76. Among the stations with RQs higher than one, four were located in the northeastern bay and one was located in the northwestern bay, thereby implying a significant ecological risk of NP in these areas.

## CONCLUSIONS

This study investigated the distribution of NP in the waters of JZB in April 2007 and August 2009. It assessed the ecological risk of NP by using PNEC, which was calculated from the toxicity data of NP on five dominant species of microalgae in JZB, as the criterion. The results showed that the NP concentrations in JZB ranged from 23.6 ng/l to 192.9 ng/l in April 2007 and from 18.5 ng/l to 179.3 ng/l in August 2009. Meanwhile, the PNEC for NP, which was calculated via the EC<sub>50</sub> value of *C. curvisetus* because of its higher sensitivity compared with the other algae, was 79.0 ng/l. The RQs of NP in the waters of JZB ranged from 0.23 to 2.44, with an average of 0.76. Low NP levels were detected in the central bay and at the mouth of JZB, thereby indicating no significant ecological risks in these areas. By contrast, high NP levels were observed in the northeastern bay and the northwestern bay adjacent to a river mouth, thereby implying a significant ecological risk for aquatic ecosystems in these areas. Therefore, NP should be monitored further to prevent it from inducing additional biological effects on JZB.

## ACKNOWLEDGEMENT

The research was funded by the Natural Science Foundation of China (Project No. 41371314) and the Ocean Public Welfare Scientific Research

Project of the State Oceanic Administration, China (Grant No. 201205018).

## REFERENCES

- [1] Ying, G.G., Williams, B. and Kookana, R. (2002) Environmental fate of alkylphenols and alkylphenol ethoxylates—a review. *Environment International*, 28(3), 215-226.
- [2] Soares, A., Guieysse, B., Jefferson, B., Cartmell, E. and Lester, J.N. (2008) Nonylphenol in the environment: A critical review on occurrence, fate, toxicity and treatment in wastewaters. *Environment International*, 34(7), 1033-1049.
- [3] Soto, A.M., Justicia, H., Wray, J.W. and Sonnenschein, C. (1991) p-Nonylphenol: an estrogenic xenobiotic released from 'modified' polystyrene. *Environmental Health Perspectives*, 92, 167-173.
- [4] Harries, J.E., Sheahan, D.A., Jobling, S., Matthiessen, P., Neall, P., Sumpter, J.P., Tylor, T. and Zaman, N. (1997). Estrogenic activity in five United Kingdom rivers detected by measurement of vitellogenesis in caged male trout. *Environmental Toxicology and Chemistry*, 16(3) 534-542.
- [5] Hashimoto, S., Bessho, H., Hara, A., Nakamura, M., Iguchi, T. and Fujita, K. (2000) Elevated serum vitellogenin levels and gonadal abnormalities in wild male flounder (*Pleuronectes yokohamae*) from Tokyo Bay, Japan. *Marine Environmental Research*, 49(1) 37-53.
- [6] Ackermann, G.E., Schwaiger, J., Negele, R.D. and Fent, K. (2002) Effects of long-term nonylphenol exposure on gonadal development and biomarkers of estrogenicity in juvenile rainbow trout (*Oncorhynchus mykiss*). *Aquatic Toxicology*, 60(3-4) 203-221.
- [7] Kwack, S.J., Kwon, O., Kim, H.S., Kim, S.S., Kim, S.H., Sohn, K.H., Leea, R.D., Parka C.H., Jeungb, E.B., Anb, B.S. and Park, K.L. (2002) Comparative evaluation of alkylphenolic compounds on estrogenic activity in vitro and in vivo. *Journal of Toxicology and Environmental Health Part A*, 65(5-6), 419-431.
- [8] Kudo, C., Wada, K., Masuda, T., Yonemura, T., Shibuya, A., Fujimoto, Y., Nakajima, A., Niwa, H. and Kamisaki, Y. (2004) Nonylphenol induces the death of neural stem cells due to activation of the caspase cascade and regulation of the cell cycle. *Journal of Neurochemistry*, 88, 1416-1423.
- [9] Zhang, X., Yang, F., Cai, Y.Q. and Xu, Y. (2008) Oxidative damage in unfertilized eggs of Chinese rare minnow (*Gobiocypris rarus*)

- exposed to nonylphenol. *Environmental Toxicology and Chemistry*, 27(1), 213-219.
- [10] Chen, B.S. and Yen, J.H. (2013) Effect of endocrine disruptor nonylphenol on physiologic features and proteome during growth in *Arabidopsis thaliana*. *Chemosphere*, 91, 468-474.
- [11] Gao, P., Li, Z.Y., Gibson, M. and Gao H.W. (2013) Ecological risk assessment of nonylphenol in coastal waters of China based on species sensitivity distribution model. *Chemosphere*, 104, 113 – 119.
- [12] USEPA. (1998) Guidelines for ecological risk assessment. Risk Assessment Forum, USEPA. EPA/630/R095//002F. Washington, DC.
- [13] ECB (European Chemicals Bureau). (2003) Technical guidance document on risk assessment -Part II. Institute for Health and Consumer Protection, Italy, Ispra.
- [14] Wang, C.Y., Wang, X.L., Su, R.G., Liang, S.K. and Yang, S.P. (2011) No detected toxic concentrations in in situ algal growth inhibition tests—A convenient approach to aquatic ecotoxicology. *Ecotoxicology and Environmental Safety*, 74, 225-229.
- [15] ECB (European Chemicals Bureau). (2001) European Union risk-assessment report for 4-nonylphenol (branched) and nonylphenol, European Chemicals Bureau, Joint Research Centre, European Commission, Italy, Ispra.
- [16] Brooke, L. and Thursby, G. (2005) Ambient aquatic life water quality criteria for nonylphenol. Washington DC, USA: Report for the United States EPA, Office of Water, Office of Science and Technology.
- [17] Shi, J.H., Li, G.X. and Wang, P. (2011) Anthropogenic influences on the tidal prism and water exchanges in Jiaozhou Bay, Qingdao, China. *Journal of Coastal Research*, 27(1), 57-72.
- [18] Fu, M.Z., Li, Z.Y. and Gao, H.W. (2007) Distribution characteristics of nonylphenol in Jiaozhou Bay of Qingdao and its adjacent rivers. *Chemosphere*, 69, 1009-1016.
- [19] Liu, Z. (2004) Research on modelling water exchange and nutrient budget in Jiaozhou Bay. Ocean University of China, Qingdao.
- [20] Dan, L.X. (2010) Distribution characteristics and the flux of land-based into the sea of nonylphenols in Jiaozhou Bay and the ecological risk assessment. Ocean University of China, Qingdao.
- [21] Servos, M.R. (1999) Review of the aquatic toxicity, estrogenic responses and bioaccumulation of alkylphenols and alkylphenol polyethoxylates. *Water Quality Research Journal of Canada*, 34(1), 123-177.
- [22] Soares, A., Guieysse, B., Jefferson, B., Cartmell, E. and Lester, J.N. (2008) Nonylphenol in the environment: A critical review on occurrence, fate, toxicity and treatment in wastewaters. *Environment International*, 34(7) 1033-1049.
- [23] Guillard, R.R. and Ryther, J.H. (1962) Studies of marine planktonic diatoms. I. *Cyclotella nana* ustedt, and *Detonula confervacea* (cleve) Gran. *Canadian Journal of Microbiology*, 8, 229-239.
- [24] Vanewijk, P.H. and Hoekstra, J.A. (1993) Calculation of the EC50 and its confidence interval when subtoxic stimulus is present. *Ecotoxicology and Environmental Safety*, 25(1), 25-32.
- [25] Chen, B., Duan, J.C., Mai, B.X., Luo, X.J., Yang, Q.S., Sheng, G.Y. and Fu, J.M. (2006) Distribution of alkylphenols in the Pearl River Delta and adjacent northern South China Sea, China. *Chemosphere*, 63, 652-661.
- [26] Duan, J.C., Chen, B. and Mai, B.X. (2004) Survey of alkylphenols in aquatic environment of Zhujiang. *Environmental Science*, 25 (3): 48-52.
- [27] Shen, G., Zhang, Z., Yu, G., Li, X., Hu, H. and Li, F. (2005) Dissolved neutral nonylphenol ethoxylates metabolites in the Haihe River and Bohai Bay, People's Republic of China. *Bulletin of Environmental Contamination and Toxicology*, 75, 827-834.
- [28] Bester K., Theobald N. and Schrfder H.F. (2001) Nonylphenols, nonylphenol~ethoxylates, linear alkylbenzene sulfonates (LAS) and bis (4~chLorophenyl)~sulfone in the German Bight of the North Sea. *Chemosphere*, 45, 817-826.
- [29] Kim, Y.S., Katase, T., Horii, Y., Yamashita, N., Makino, M., Uchiyama, T., Fujimoto, Y. and Inoue, T. (2005) Estrogen equivalent concentration of individual isomer-specific 4-nonylphenol in Ariake sea water, Japan. *Marine Pollution Bulletin*, 2005, 51, 850-856.
- [30] González S., Petrovic M. and Barceló D. (2004) Simultaneous extraction and fate of linear alkylbenzene sulfonates, coconut diethanol amides, nonylphenol ethoxylates and their degradation products in wastewater treatment plants, receiving coastal waters and sediments in the Catalanian area (NE Spain). *Journal of Chromatography A*, 1052, 111-120.
- [31] Basheer, C., Lee, H.K. and Tan, K.S. (2004) Endocrine disrupting alkylphenols and bisphenol-A in coastal waters and supermarket seafood from Singapore. *Marine Pollution Bulletin*, 48(11) 1161-1167.
- [32] Diehl, J., Johnson, S.E., Xia, K., West, A. and Tomanek, L. (2012) The distribution of 4-nonylphenol in marine organisms of North American Pacific coast estuaries. *Chemosphere*, 87, 490-497.
- [33] Wang, X.L., Li, K.Q. and Shi, X.Y. (2006) The



- marine environmental carrying capacity of major pollutants in Jiaozhou Bay. Science Press, Beijing, 3-20.
- [34] Shen, Z.L., Dong, J.H. and Jiao, N.Z. (1995) The ecology research in Jiaozhou Bay. Science Press, Beijing, 13-17.
- [35] Liu, X., Zhao, J., Dan, L.X., Shi, X.Y. and Liang, S.K. (2012). Toxic effects of nonylphenol on dominant microalgae species in Jiaozhou Bay. *Marine Environmental Science*, 31(5), 667- 673.
- [36] Wang, J.J., Qian, X.J., An, M. and Duan, S.S. (2012) Effect of combined exposure of diethylphthalate and nonylphenol on growth of *Dunaliella salina*. *Ecological Science*, 31(4), 370-376.
- [37] Jiang, M., Peng, Z., An, S., Cai, Y. and Xue, L. (2006) Toxic effects of 4-nonylphenol on three aquatic organisms. *Acta Hydrobiologica Sinica*, 30(4), 489.
- [38] Guan, C., Sun, Z. W., Min, A. and Duan, S.S. (2011) The ecological toxic effects of nonylphenol on *Phaeocystis globosa*. *Ecology and Environmental Sciences*, 20(4), 640-645.
- [39] Gao, Q.T. and Tam, N.F.Y. (2011) Growth, photosynthesis and antioxidant responses of two microalgal species, *Chlorella vulgaris* and *Selenastrum capricornutum*, to nonylphenol stress. *Chemosphere*, 82, 346-354.

---

**Received: 04.03.2016**

**Accepted: 16.09.2016**

#### **CORRESPONDING AUTHOR**

---

**Sheng-kang Liang**

Key Laboratory of Marine Chemistry Theory and Technology, Ministry of Education, Qingdao 266100, China

e-mail: [liangsk@ouc.edu.cn](mailto:liangsk@ouc.edu.cn)



# CARBON DIOXIDE EVOLUTION AND ENZYMATIC ACTIVITIES OF SOIL UNDER DIFFERENT LAND USE PRACTICES LOCATED NEAR BHAWANIPATNA TOWN IN ODISHA, INDIA

Chandan Sahu\*, Sradhanjali Basti, Sanjat Kumar Sahu

P.G. Department of Environmental Sciences, Sambalpur University, Odisha, India

## ABSTRACT

Soil respiration and enzyme activities reflect the biochemical functioning and nutrient cycling in soil. Knowledge regarding them can be useful in describing changes due to land use, land cover system and defining management strategies for restoring soil ecosystem functioning. In the present study, carbon dioxide evolution and enzymatic activities in soil were studied in four land use systems viz. sugarcane field, rice field, forest land and pasture land from Sujapur village near Bhawanipatna town of Kalahandi, Odisha, India during April 2013 to November 2013. The study showed that carbon dioxide evolution and protease activity is decreasing in the order: Forest land > Rice field > Pasture land > Sugarcane field. Invertase activity was found to be highest in rice field (8.93  $\mu\text{g}$  glucose/g dry wt./h) with the lowest value in pasture land (6.71  $\mu\text{g}$  glucose/g dry wt./h) while, urease activity was found to be highest in agricultural land i.e. rice and sugarcane field (0.63 and 0.60  $\mu\text{g}$  urea/g dry wt./h respectively) than in pasture (0.49  $\mu\text{g}$  urea/g dry wt./h) and forest land (0.39  $\mu\text{g}$  urea/g dry wt./h). Phosphatase (acid and alkali) and dehydrogenase activity was maximum in forest (1.04, 0.83 mg PNP/g dry wt./h and 57.53  $\mu\text{g}$  TPF/g dry wt./h respectively) and minimum in pasture land (0.61, 0.38 mg PNP/g dry wt./h and 48.68  $\mu\text{g}$  TPF/g dry wt./h respectively). The result however, showed insignificant variation in carbon dioxide evolution and enzyme activities with respect to different land use practices and hence confirm a very slow degradation of soil quality till today from the course of transformation to agricultural land.

## KEYWORDS:

Land use, Soil ecosystem functioning, carbon dioxide evolution, enzyme activities

## INTRODUCTION

Soil sustains life on earth by providing a base

for agriculture and plant growth. It also helps in sustenance of forest by providing it with raw materials for its life by recycling the leaf litters, wood debris and dead animals [1]. Plant litter decomposition is accompanied by stimulation of a succession of soil enzymes [2, 3, 4]. However, land use changes like forest clearing and conversion of forest into cultivable land may result in changes of soil physical, chemical and biological characteristics [5].

Soil is a complex system with the physical, chemical and biological properties of it being in dynamic equilibrium. Studies of soil respiration and its enzymatic activities provide valuable information regarding the biochemical processes in soil. Enzymatic processes are a part of respiration pathways of soil micro-organisms and are closely related to the type of soil and soil air-water conditions [6, 7, 8]. Enzymes also play a critical role on various biogeochemical cycles [9, 10, 11]. Soil biochemical parameters indicate the ecological stress or restoration [12] and management induced changes in soil quality [13].

Carbon is stored in the soil organic matter and is respired by plants, bacteria, fungi and animals [14]. Soil enzyme activities are sensors of soil degradation since they integrate information about microbial status and physicochemical conditions [15, 16]. Measurements of enzymatic activities have also been used to test the soil biological fertility [17]. Therefore, it is necessary to assess the carbon dioxide evolution and enzymatic activities of soil under natural and artificial conversion to reason the change in soil quality.

## MATERIALS AND METHODS

**Geographical Location Of Study Area.** The study area belongs to the Sujapur village near headquarter town of Bhawanipatna in the district of Kalahandi, Odisha, India. The study includes four land use systems viz. Pasture land site (19°54'28.89" N, 83°11'33.83" E) which is 2 km away from the Bhawanipatna town towards Sujapur village, whereas, the rest three sites viz.

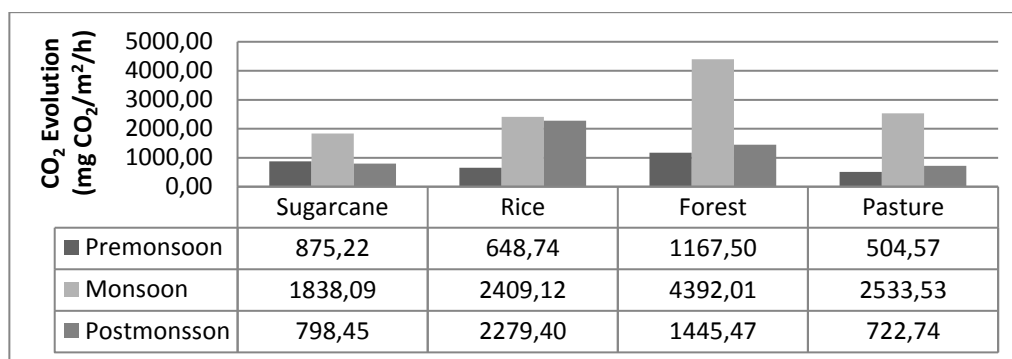


**FIGURE 1**  
Seasonal variation in CO<sub>2</sub> Evolution (mg CO<sub>2</sub>/m<sup>2</sup>/h) of soil in different land use systems during 2013

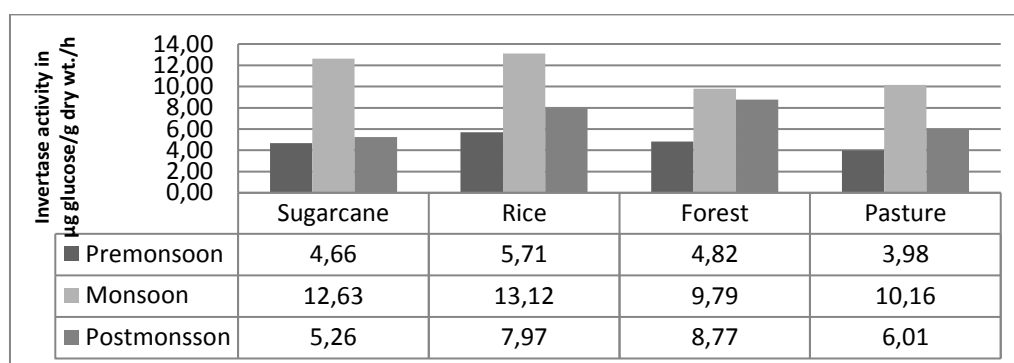


**FIGURE 2**  
Seasonal Variation in Invertase activity (µg glucose/g dry wt./h) of soil in different land use systems during 2013

Sugarcane field (19°54'27.10" N, 83°12'50.24" E), Rice field (19°54'27.23" N, 83°12'52.16" E) and Forest land (19°54'28.52" N, 83°12'50.04" E) is in the village area of Sujapur which is 5 km away from Bhawanipatna town.

**Sampling And Soil Analysis.** The sampling was done thrice during the year 2013 i.e. during Pre-monsoon (April), Monsoon (August) and Post-monsoon (November). The soil samples were taken using a cylindrical soil sampler. The sampler was inserted into the soil and samples were taken from the surface layer (0 – 10 cm) at 5 different locations (replicas) from each field (land use) by random sampling method. The soil samples were then packed in air-tight zip lock bags and kept inside the ice bucket. The ice buckets containing the samples were quickly transported to the laboratory and the analysis of requisite amount of fresh soil was used for enzyme analysis.

Carbon dioxide evolution was measured under field condition by inverted box method [18]. The upper vegetation of the soil was carefully cleared without disturbing the underground vegetation. 25 ml of 0.1 N KOH was taken in a beaker and a glass jar was placed over it in an inverted position in the pre cleaned area. The setup was left as such for 1 hour. Then the jar was removed and 10 ml of saturated barium chloride (BaCl<sub>2</sub>) was added to the

beaker to fix the sample. The sample was then titrated against 0.1 N HCl using phenolphthalein indicator. Simultaneously another setup was run as control without any soil in it. The carbon dioxide evolution in soil was expressed in mg CO<sub>2</sub>/m<sup>2</sup>/h.

Invertase activity was measured according to [19]. 0.2 ml of toluene, 6 ml of Sorenson's buffer (pH 5.5) and 6 ml of 5% (w/v) Sucrose solution was added to 2 grams of fresh sieved soil sample. The contents were mixed properly and were incubated at 37° C for 24 hours followed by the addition of 2 ml of 3,5 dinitrosalicylic acid to 1 ml of the supernatant solution. The yellow orange color intensity was measured by the spectrophotometer at 540 nm. The activity of invertase was expressed in µg glucose/g dry wt./h.

Protease activity was measured according to [20]. As per the method, 0.2 ml of toluene and 10 ml of tris buffer with sodium caesinate were added to 2 grams of fresh sieved soil sample. The contents of both the flasks were swirled for few seconds and then incubated at 37° C for 2 hours followed by addition of 4 ml of TCA, 3 ml of sodium carbonate and 1 ml of follin's reagent. The color intensity of the supernatant was measured by the spectrophotometer at 700 nm. The activity of protease was expressed in mg tyrosine/g dry wt./h.

Phosphatase (acid and alkaline) activity was measured according to [21]. 0.2 ml toluene, 4 ml of

Modified Universal Buffer((MUB), pH 6.5 for acid phosphatase and pH 11 for alkaline phosphatase and 1 ml of p-nitro phenyl phosphate solution was added to 1 gram of fresh sieved soil. The flask was then incubated at 37° C for 1 hour followed by the addition of 1 ml of 0.5 M CaCl<sub>2</sub> and 4 ml of 0.5 M NaOH. The yellow color intensity of the filtrate was measured by the spectrophotometer at 420 nm. The activity of the phosphatase (acid and alkaline) was expressed in mg PNP/g dry wt./h.

Urease activity was measured according to [21]. 5 ml of urea solution was added to 5 grams of wet soil sample and incubated for 5 hours at 37° C followed by the addition of 50 ml of 2M KCl + phenyl mercuric acetate (PMA) solution, 10 ml of KCl + PMA solution and 30 ml of the freshly prepared color reagent (Diacetyl monoxime (DAM) + Thiosemicarbazide (TSC) + Acid reagent). The reddish color intensity was measured by the spectrophotometer at 527 nm. The urease activity was expressed in µg urea/g dry wt./h.

Dehydrogenase activity was measured by triphenyl formazone (TPF) method [22]. 0.1 gram of CaCO<sub>3</sub>, 1 ml of 3% 2,3,5 triphenyl tetrazolium chloride (TTC) was added to 3 grams of fresh soil sample and incubated at 37° C for 24 hours followed by the addition of 10 ml of methanol. The reddish color intensity was measured by the spectrophotometer at 485 nm taking methanol as blank. The activity of dehydrogenase was expressed in µg TPF/g dry wt./h.

## RESULTS AND DISCUSSION

**Results.** Table 1 shows the range and mean values of different parameters of the soil samples in various land use practices. The highest CO<sub>2</sub> evolution was observed in forest land (4392.01 mg CO<sub>2</sub>/m<sup>2</sup>/h) during the monsoon and minimum in pasture land (504.57 mg CO<sub>2</sub>/m<sup>2</sup>/h) during the pre-monsoon (Fig. 1). Irrespective of seasons the lowest level of carbon dioxide evolution was observed in sugarcane field (1170.59 mg CO<sub>2</sub>/m<sup>2</sup>/h) and the highest level of it was observed in the forest land (2334.99 mg CO<sub>2</sub>/m<sup>2</sup>/h). This confirms to the fact that in natural condition the microbial activity is also high.

Maximum invertase activity was found in rice field (13.12 µg glucose/g dry wt./h) during monsoon season and the minimum activity was found in the pasture land (3.98 µg glucose/g dry wt./h) during the pre-monsoon (Fig. 2). Irrespective of seasons, the least activity of invertase was observed in pasture land (6.71 µg glucose/g dry wt./h) whereas, the highest activity was found to be in rice field (8.93 µg glucose/g dry wt./h). This may be due to the fact that the moisture content in the rice field was more as compared to forest land.

Protease activity was at its peak in forest land (2.60 mg tyrosine/g dry wt./h) during post monsoon season while its lowest activity was found in

**TABLE 1**  
**Range and Mean ± SD values of different parameters in various land use practices**

	Sugarcane		Rice		Forest		Pasture	
	Range	Mean ± SD	Range	Mean ± SD	Range	Mean ± SD	Range	Mean ± SD
CO <sub>2</sub> Evolution (mg CO <sub>2</sub> /m <sup>2</sup> /h)	798.45	1170.59	648.74	1779.09	1167.50	2334.99	504.57	1253.61
	-	±	-	±	-	±	-	±
	1838.09	473.04	2409.12	801.03	4392.01	1458.95	2533.53	909.41
Invertase (µg glucose/g dry wt./h)	4.66	7.52 ± 3.62	5.71	8.93 ± 3.10	4.82	7.79 ± 2.14	3.98	6.71 ± 2.57
Protease (mg tyrosine/g dry wt./h)	0.94	1.27 ± 0.24	1.22	1.47 ± 0.18	1.59	1.98 ± 0.44	1.30	1.48 ± 0.13
Acid Phosphatase (mg PNP/g dry wt./h)	0.38	0.76 ± 0.32	0.28	0.73 ± 0.34	0.60	1.04 ± 0.61	0.46	0.61 ± 0.13
Alkaline Phosphatase (mg PNP/g dry wt./h)	0.10	0.44 ± 0.24	0.11	0.47 ± 0.26	0.27	0.83 ± 0.71	0.33	0.38 ± 0.05
Urease (µg urea/g dry wt./h)	0.34	0.60 ± 0.23	0.17	0.63 ± 0.32	0.15	0.39 ± 0.28	0.20	0.49 ± 0.27
Dehydrogenase (µg TPF/g dry wt./h)	43.38	56.87 ± 10.03	42.46	51.26 ± 11.20	46.48	57.53 ± 11.65	40.15	48.68 ± 9.74

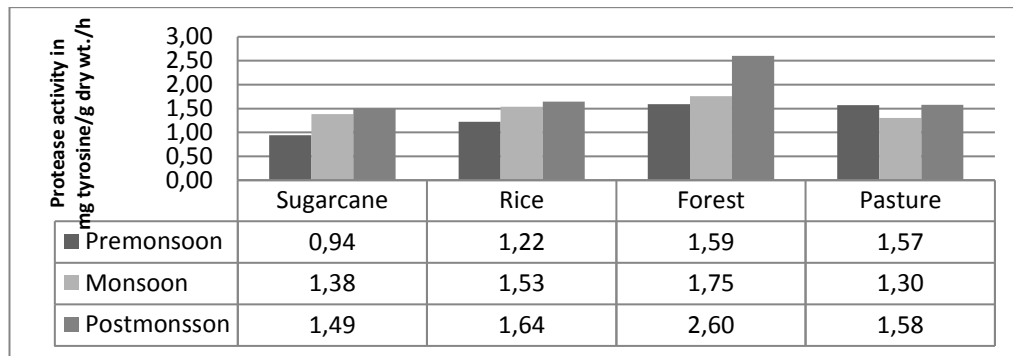


FIGURE 3

Seasonal variation in Protease activity (mg tyrosine/g dry wt./h) of soil in different land use systems during 2013

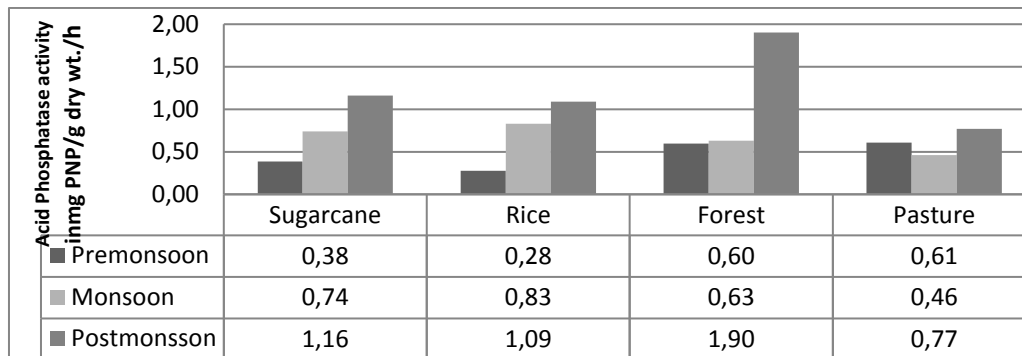


FIGURE 4

Seasonal variation in Acid Phosphatase activity (mg PNP/g dry wt./h) of soils in different land use systems during 2013

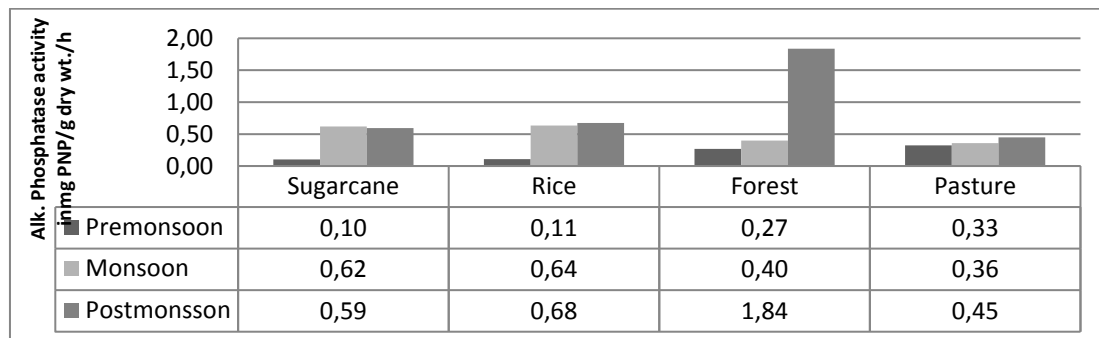


FIGURE 5

Seasonal variation in Alkaline Phosphatase activity (mg PNP/g dry wt./h) of soils in different land use systems during 2013

sugarcane field (0.94 mg tyrosine/g dry wt./h) during the pre monsoon (Fig. 3). Irrespective of seasons, the highest protease activity was observed in forest land (1.98 mg tyrosine/g dry wt./h) which justifies the fact that high level of organic matter might be present in this land use system whereas, least activity was observed in sugarcane field (1.27 mg tyrosine/g dry wt./h). This might have been due to low microbial activity in sugarcane field.

Maximum phosphatase (both acid and alkali) activity were found in forest land (1.90 and 1.84 mg PNP/g dry wt./h for acid and alkaline phosphatase respectively) during the post monsoon and minimum activities were found in rice field (0.28

and 0.11 mg PNP/g dry wt./h for acid and alkaline phosphatase respectively) during the pre monsoon (Fig. 4 and 5). The highest phosphatase activity was found in forest land (1.04 and 0.83 mg PNP/g dry wt./h for acid and alkaline phosphatase respectively) whereas, the lowest levels were found in pasture land (0.61 and 0.38 mg PNP/g dry wt./h for acid and alkaline phosphatase respectively) irrespective of seasons. This might have resulted from the high organic matter content in the forest land as compared to the pasture land.

Urease showed highest activity in rice field (0.92  $\mu$ g urea/g dry wt./h) during post monsoon and its lowest activity was found in forest land (0.15  $\mu$ g

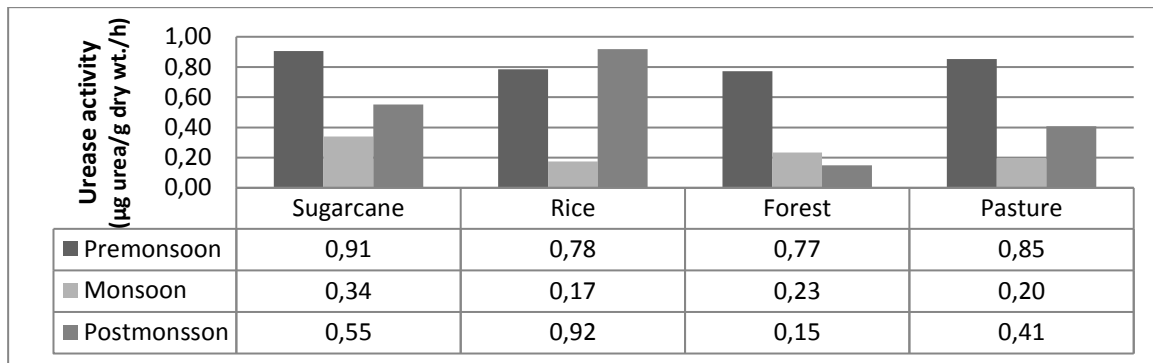


FIGURE 6

Seasonal variation in Urease activity ( $\mu\text{g urea/g dry wt./h}$ ) of soils in different land use systems during 2013

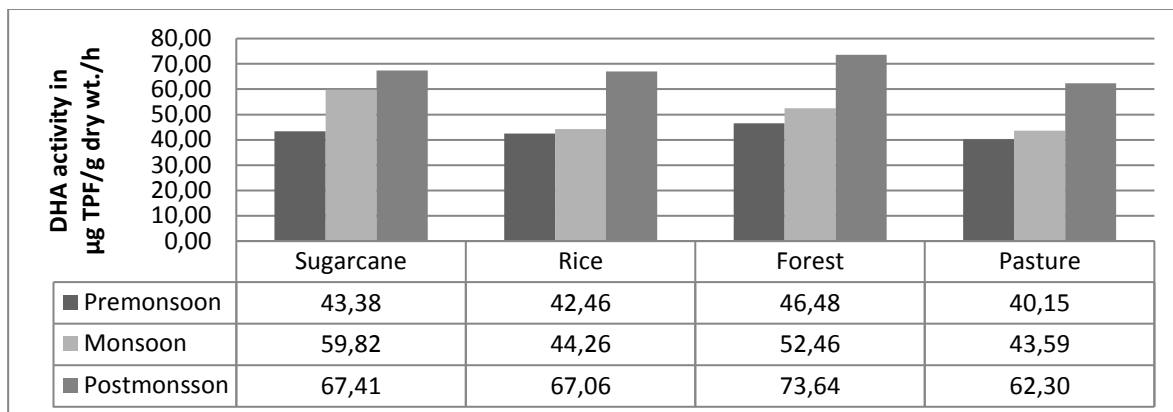


FIGURE 7

Seasonal variation in Dehydrogenase activity ( $\mu\text{g TPF/g dry wt./h}$ ) of soils in different land use systems during 2013

urea/g dry wt./h) during post monsoon (Fig. 6). In the study area, the highest activity was determined in rice field whereas ( $0.63 \mu\text{g urea/g dry wt./h}$ ), the lowest level of it was found in forest land ( $0.39 \mu\text{g urea/g dry wt./h}$ ) irrespective of the seasons. Although organic matter content is lower in pasture land than that of forest land, this enzyme activity was found high in pasture land than the forest land. This case can be explained that pasture lands in the study area have been used for grazing and hence, animal liquid and solid manure including urea contaminate might have accumulated in the soil.

Dehydrogenase activity declined from natural condition i.e. forest land ( $73.64 \mu\text{g TPF/g dry wt./h}$ ) during the post monsoon to that in the pasture land ( $40.15 \mu\text{g TPF/g dry wt./h}$ ) during the pre monsoon (Fig. 7). The present study showed that irrespective of seasons, the high level of dehydrogenase activity was found in the forest land ( $57.53 \mu\text{g TPF/g dry wt./h}$ ) and lowest level of it was observed in the pasture land ( $48.68 \mu\text{g TPF/g dry wt./h}$ ). This may be due to the fact that the forest land might have been rich with organic matter.

The data for each parameter was subjected to two-way ANOVA to see whether significant difference exist with respect to different land use

and seasons at 0.05 confidence limit and is given in Table - 2. From the table it is evident that protease and alkaline phosphatase activities do not show significant difference with respect to both land use practice and seasons ( $F_1 \leq 4.76$ ,  $F_2 \leq 5.14$ ,  $p > 0.05$ ) while, carbon dioxide evolution, invertase, acid phosphatase, urease and dehydrogenase activities show significant difference with respect to seasons only ( $F_2 \geq 5.14$ ,  $p < 0.05$ ).

A correlation matrix is also worked out and given in Table - 3 considering all the parameters irrespective of land use practices. The value of "r" marked with an asterisk (\*) represents strong positive or negative correlation at 0.05 level of significance. Carbon dioxide evolution was found to show positive correlation with protease, acid and alkaline phosphatase ( $r \geq 0.815$ ,  $p < 0.05$ ) and alkaline phosphatase showed a positive correlation with protease and acid phosphatase ( $r \geq 0.815$ ,  $p < 0.05$ ). On the contrary protease showed a negative correlation with the urease activity of the soil ( $r \geq -0.815$ ,  $p < 0.05$ ).

**Discussion.** Carbon dioxide evolution is a measure of soil fertility and is governed by the presence of microbial population in soil.

**TABLE 2**  
Two way ANOVA for different parameters between various land use practices and seasons

Parameters	Source of Variation	SS	df	MS	$F_{Cal}$	$F_{tab at 0.05}$	S or NS
<b>CO<sub>2</sub> Evolution</b>	Between Land use	2615659.29	3	871886.43	1.81	4.76	NS
	Between Seasons	8579694.94	2	4289847.47	8.93	5.14	S
<b>Invertase</b>	Between Land use	7.56	3	2.52	1.42	4.76	NS
	Between Seasons	91.19	2	45.59	25.70	5.14	S
<b>Protease</b>	Between Land use	0.83	3	0.28	4.27	4.76	NS
	Between Seasons	0.51	2	0.26	3.95	5.14	NS
<b>Phosphatase (Acid)</b>	Between Land use	0.30	3	0.10	1.10	4.76	NS
	Between Seasons	1.26	2	0.63	6.96	5.14	S
<b>Phosphatase (Alkali)</b>	Between Land use	0.38	3	0.13	0.81	4.76	NS
	Between Seasons	0.95	2	0.47	3.01	5.14	NS
<b>Urease</b>	Between Land use	0.11	3	0.04	0.97	4.76	NS
	Between Seasons	0.70	2	0.35	9.32	5.14	S
<b>Dehydrogenase</b>	Between Land use	167.38	3	55.79	3.54	4.76	NS
	Between Seasons	1275.04	2	637.52	40.43	5.14	S

**TABLE 3**  
Correlation matrix among different parameters in various land use practices

	CO <sub>2</sub> Evolution	Invert.	Prot.	Phosph. (Acid)	Phosph. (Alkali)	Urease	DHA
<b>CO<sub>2</sub> Evolution</b>	1.000						
<b>Invert.</b>	0.472	1.000					
<b>Prot.</b>	0.908*	0.063	1.000				
<b>Phosph. (Acid)</b>	0.845*	0.261	0.809	1.000			
<b>Phosph. (Alkali)</b>	0.915*	0.218	0.917*	0.976*	1.000		
<b>Urease</b>	-0.574	0.450	-0.862*	-0.601	-0.716	1.000	
<b>DHA</b>	0.397	0.145	0.337	0.811	0.669	-0.243	1.000

\*' p < 0.05

In the present study, the forest land shows highest carbon dioxide evolution (2334.99 mg CO<sub>2</sub>/m<sup>2</sup>/h), that confirms that under natural condition the microbial activity is optimum and this result supports the findings of [23].

Invertase plays an essential role in the carbon transformation and carbon cycle in soil, which hydrolyses soil carbohydrates to provide nutrients for plants and microorganisms. In the present study, the least activity of invertase was observed in pasture land (6.71 µg glucose/g dry wt./h) whereas the highest activity was observed in rice field (8.93 µg glucose/g dry wt./h). This may be due to the high moisture content with strong root nexus in rice field due to mulching activity. Our findings are in agreement with the findings of [24] who reported that invertase activity is low in soils containing low moisture and having less underground biomass.

Protease activity characterizes the nitrogen mineralization in soil and in the present study was found to be optimum in the natural forest (1.98 mg tyrosine/g dry wt./h) which might have been due to high microbial biomass in natural condition. High microbial biomass results in high turnover which is

accompanied by the release of protease [25].

Phosphatase is an enzyme of great agronomic value as it is associated with the hydrolysis of organic phosphorus thereby converting them to inorganic phosphorus. In the present study, high phosphatase activity was determined in natural forest (1.04 and 0.83 mg PNP/g dry wt./h for acid and alkaline phosphatase respectively) with that of the lowest value found in the pasture land (0.61 and 0.38 mg PNP/g dry wt./h for acid and alkaline phosphatase respectively) which is in accordance with the results reported by [26]. This may have been due to the high organic matter content in the forest land sourcing from the thick vegetation cover which has a significant influence on soil extracellular enzyme activities [27, 28].

Urease is involved in the hydrolysis of urea and hence directs the nitrogen mineralization in soil. A high urease activity found in the cultivated land (0.63 and 0.60 µg urea/g dry wt./h for rice and sugarcane field respectively) in the present study might be due to high application of urea. This supports the findings of [29].

Dehydrogenase is an endo-enzyme and its

activity is associated with the carbon cycling in soil and is influenced by the soil moisture content and the organic matter present. In the present study, lowest level of dehydrogenase activity was seen in the pre-monsoon which may have been due to the low moisture content and highest activity was found in the post-monsoon in all the land use practices which may have been due to the suitable environment for bacterial activity with respect to soil moisture, temperature and organic matter content. This result corroborates the findings of [30]. Further the dehydrogenase activity in forest (57.53  $\mu\text{g TPF/g dry wt./h}$ ) was found to be the maximal which might have been due to sufficient soil moisture and organic matter content [31].

## CONCLUSION

It is expected that when the natural forest gets converted to pasture land or to cultivable land, the soil quality and fertility diminishes, but our results shows that, the degradation is insignificant as of now and if proper steps are taken and modern sustainable agricultural practice like organic farming is adopted then the health of the soil can be restored quickly.

## REFERENCES

- [1] Barreto, R., Tsegaye, T. and Coleman, L. (2000) Land use effect on the distribution of soil physical and chemical properties under tropical rain forests of Puerto Rico. International Geosciences and Remote Sensing Symposium (IGARSS) – Honolulu, Hawaii, 605.
- [2] Panchoy, S.K. and Rice, E.L. (1973) Carbohydases in soil as affected by successional stages of revegetation. Soil Science Society of America Journal., 37, 227 - 229.
- [3] Sinsabaugh, R.L., Antibus, R.K. and Linkins, A.E. (1991) An enzymatic approach to the analysis of microbial activity during plant litter decomposition. Agriculture, Ecosystems and Environment, 34, 43 - 54.
- [4] Moorhead, D.L., Sinsabaugh, R.L., Linkins, A.E. and Reynolds, J.F. (1996) Decomposition processes: modelling approaches and applications. The Science of the Total Environment. 183, 137 - 149.
- [5] Houghton, R.A., Hacher, J.K. and Lawrence, K.T. (1999) The U.S. Carbon budget: Contributions from land use change. Science. 285, 574 – 578.
- [6] Doelman, P. and Haanstra, L. (1979) Effect of lead on soil respiration and dehydrogenase activity. Soil Biol. Biochem., 11, 475-479.
- [7] Kandeler, E. (1996) Nitrate. In: Schinner F, Öhlinger R, Kandeler E, Margesin R (eds). Methods in soil biology. Springer, Berlin Heidelberg New York, 408-410.
- [8] Gliniski, J. and Stepniewski, W. (1985) Soil Aeration and its Role for Plants. CRC Press, Boca Raton, Florida.
- [9] Speir, T.W. and Ross, D.J. (1978) Soil phosphatase and sulphatase. In: Burns RG (Ed.). Soil Enzymes. Academic Press, London, UK, 380, 197-250.
- [10] Andrews, R.K., Blakeley, R.L. and Zerner, B. (1989) Urease: A Ni (II) metalloenzyme. In The Bioinorganic Chemistry of Nickel, ed. J. R. Lancaster. VCH Publishers, New York, 141-166.
- [11] Byrnes, B.H. and Amberger, A. (1989) Fate of broadcast urea in a flooded soil when treated with N-(n-butyl) thiophosphoric triamide, a urease inhibitor. Fertil. Res., 18, 221-231.
- [12] Kizilkaya, R. and Bayrakli, B. (2005) Effects of N-enriched sewage sludge on soil enzyme activities. Applied Soil Ecology, 30, 192 – 202.
- [13] Kennedy, A.C. and Papendick, R.I. (1995) Microbial characteristics of soil quality. Journal of Soil and Water conservation, 50, 243 – 428.
- [14] Mishra, P.C., Mohanty, R.K. and Dash, M.C. (1979) Enzyme activities in subtropical surface soils under pasture. Ind. J. Agri. Chem., 12, 19-24.
- [15] Wick, B., Kühne, R.F. and Vlek, P.L.G. (1998) Soil microbiological parameters as indicators of soil quality under improved fallow management systems in southwestern Nigeria. Plant Soil, 202, 97-107.
- [16] Aon, M.A. and Colaneri, A.C. (2001) Temporal and spatial evolution of enzymatic activities and physico-chemical properties in an agricultural soil. Appl. Soil Ecol., 18, 255–270.
- [17] Dick, W.A. and Tabatabai, M.A. (1992) Potential uses of soil enzymes. In: Metting FB Jr. (Ed.), Soil Microbial Ecology: Applications in Agricultural and Environmental Management. Marcel Dekker, New York, 95-127.
- [18] Witkamp, M. (1966) Rates of carbon dioxide evolution from the forest floor. Ecology, 47, 492 – 494.
- [19] Ross, D.J. (1983) Invertase and amylase activities as influenced by clay minerals, soil-clay fractions and topsoils under grassland. Soil Biology & Biochemistry, 15, 287 - 293.
- [20] Ladd, J.N. and Jackson, R.B. (1982) In: Stevenson FJ (Ed.). Nitrogen in Agricultural Soils. Am. Soc. Agron., WI. 173-228.
- [21] Eivazi, F. and Tabatabai, M.A. (1977) Phosphates in soils. Soil Biol. Biochem. 9, 167-172.
- [22] Baruah, M. and Mishra, R.R. (1984)



Dehydrogenase and urease activities in rice field soils. *Soil Biol. Biochem.*, 16, 423-424.

- [23] Lipson, D., Wilson, R. and Oechel, W. (2005) Effects of Elevated Atmospheric CO<sub>2</sub> on Soil Microbial Biomass, Activity and Diversity in a Chaparral Ecosystem. *Applied and Environmental Microbiology*, 71, 12, 8573 – 8580.
- [24] Frankenberger Jr, W.T. and Johanson, J.B. (1983) Factors affecting invertase activity in soils. *Plant and Soil*, 74, 313 – 323.
- [25] Danneberg, O.H., Kandeler, E. and Wenzl, W. (1989) Zusammenhänge zwischen der Mikroflora, dem Mineralstickstoff und Fraktionen des 'heiBwasserlöslichen' Stickstoff im Boden. *VDLUFA – Schriftenreihe*, 28, 539 – 550.
- [26] Kizilkaya, R. and Dengiz, O. (2010) Variation of land use and land cover effects on some soil physicochemical characteristics and soil enzyme activity. *Zendirbyste – Agriculture*, 97(2), 15 – 24.
- [27] Hadas, A., Kautsky, L., Goek, M. and Kara E.E. (2004) Rates of decomposition of plant residues and available nitrogen in soil related to residue composition through simulation of carbon and nitrogen turnover. *Soil biology and biochemistry*, 36, 255 – 266.
- [28] Jezierska – Tys, S. and Frac, M. (2005) Changes in enzymatic activity and the number of proteolytic microorganisms in brown soil under the influence of organic fertilization and cultivation of spring wheat. *Polish Journal of Soil Science*, 38, 81 – 86.
- [29] Kizilkaya, R. and Ekberli, I. (2008) Determination of the effects of hazelnut husk and tea waste treatments on urease enzyme activity and its kinetics in soil. *Turkish Journal of Agriculture and Forestry*, 32, 299 – 310.
- [30] Quilchano, C. and Maranon, T. (2002) Dehydrogenase activity in Mediterranean forest soil. *Biol. Fertil. Soils*, 35, 102 – 107.
- [31] Banerjee, M.R., Burton, D.L., McCaughery, W.P.P. and Grant, C.A. (2000) Influence of pasture management on soil biological quality. *J. Range Manage*, 53, 127 – 133.

---

**Received: 04.03.2016**

**Accepted: 12.09.2016**

---

#### **CORRESPONDING AUTHOR**

---

**Chandan Sahu**

P.G. Department of Environmental Sciences,  
Sambalpur University, Jyoti Vihar, Burla, Odisha,  
India

e-mail: [cks.env@gmail.com](mailto:cks.env@gmail.com)





# ACCUMULATION AND POLLUTION TRENDS OF HEAVY METALS IN THE TOPSOIL FROM AN INDUSTRIAL PARK LOCATED IN A TYPICAL NEW CHINESE DEVELOPING AREA

Xinyu Miao<sup>1,2</sup>, Qixing Zhou<sup>1,2,\*</sup>

<sup>1</sup> Key Laboratory of Pollution Processes and Environmental Criteria (Ministry of Education), Tianjin, China

<sup>2</sup> Key Laboratory of Environmental Remediation and Pollution Control, College of Environmental Science and Engineering, Nankai University, Tianjin, China

## ABSTRACT

The levels of heavy metals in the Binhai New Area Dagang industrial park were investigated by analyzing 10 metals (Mn, As, Cu, Pb, Sr, Cr, Cd, Ni, Hg and Zn) in a series of ultraclean samples collected from 30 sites in the DaGang industrial park. Analysis of the pollution conditions and possible pollution causes and trends using comparative methods provides a basis for pollution control. The results showed that the mean concentrations of several heavy metals in the industrial areas were 473.5 (Mn), 38.1 (Pb), 93.4 (Sr), 25.5 (Cr), 17.2 (Ni), 8.3 (Hg), 10.7 (As), and 0.42(Cd) mg·kg<sup>-1</sup>. Zinc and Cu are necessary nutritional elements; however, their mean concentrations were only 64.4 and 17.6 mg·kg<sup>-1</sup>, respectively. The concentrations of Hg and Pb were higher than the values reported in a previous study of this area. The concentrations of As and Cd could not be detected in most territories. The soil properties, particularly the organic matter content, were found to be important factors in the distribution of the heavy metals. The heavy metal concentrations in the Dagang industrial park can provide data references for China to curb the environmental pollution of soil in the Binhai New Area.

## KEYWORDS:

heavy metal; topsoil; industrial park; pollution trends; distribution

## INTRODUCTION

The 'minamata' and 'itai-itai' diseases have been occurring since the 1950s in Japan. Scientists showed that these human diseases are caused by

mercury pollution and cadmium contamination. Much attention has been paid to the environmental pollution caused by heavy metals and preventive methods and measures have been applied. The soil pollution in China continues to deteriorate, along with industrialization and in-depth urbanization [1, 2]. The accelerating industrialization in North China over the last few decades has been accompanied by environmental pollution because of the human activity in heavy industrial areas [3-6], such as the southern industrial zone and the heavy chemical industrial zone in Southern Liaoning, which are contaminated. Thus, the new industrial park in China may have similar problems. Soils are generally regarded as being continuous recipients of heavy metals and other pollutants. The main sources of such pollutants are industrial discharges, coal, fuel combustion, vehicle emissions, and petroleum pollution [7]. Heavy metals, such as Cu, Pb, Cd and Zn, are essential elements in the human body, but the excess of heavy metals in soils may lead to the deterioration of the ecological environment, changes in the soil physicochemical properties, and other environmental problems [8]. It has been reported that the accelerating economic development can lead to increased concentrations of heavy metals, such as Cd, Ni, Cr, Mn, Cu, Hg, Sr, Pb, and Zn, which were discharged into the environment from atmospheric emissions, sewage products, and oil exploitation [9-11]. Moreover, the lack of essential elements, such as Zn and Cu, may cause crop diseases. It is important to know, whether heavy metal soil pollution is a problem in the new Chinese industrial park. Furthermore, future development trends need to be determined.

The Dagang industrial park in the Tianjin Binhai New Area is a very important industrial area in North China and was rapidly industrialized in recent years. It is a triangle zone located to the west



of Jinqi Road, south of South Circular Road, and north of the Duliujian River. The central part of the study area is characterized by a high concentration of chemical industrial activity, with several large state-owned chemical enterprises [1]. This area includes more than 600 villages and industrial enterprises of which nearly 800 are collectively owned urban enterprises and more than 700 are private enterprises or state-owned cooperatives. The collective commercial enterprises and individual businesses proliferate the city and countryside. An integrated vertical system, including petroleum exploration, processing, petrochemical and project construction, and equipment installation, has been created. The Chinese government gives great importance to the development of this region. Therefore, the selection of this area as the research object has a strong demonstrative effect. Is the heavy metal pollution in the Dagang industrial park more or less serious compared to the old industrial park? Are there new characteristics? How can one control the development of the pollution in the new industrial park, especially the heavy metal pollution in soils? The aim of this study is to address all these questions.

## MATERIAL AND METHODS

**Materials.** Yellow soil covering the Dagang industrial park; hydrochloric acid (CP); hydrogen nitrate (CP); Electro-Thermostatic Water Bath; ICP-OES (Varian 700-ES, USA).

**Sampling methods.** A total of 30 yellow soil samples (0–20 cm deep) was collected from the DaGang industrial park in December 2015. The sampling site locations are shown in Fig. 1. The study area covers approximately 55 km<sup>2</sup> between 117.3709° E and 117.5263° E and 38.6521° N and 38.7339° N. Three parallel samples were collected at each sample site, about 1 m<sup>2</sup>. The top 20-cm layer of the soil profile was removed using stainless steel trowels, leading to a total sample size of 5–6 kg. The soil samples were stored in valve bags and frozen for subsequent sample preparation and analysis.

**Analytical procedures.** Approximately 500 g of each sample was air-dried. The remainder of each sample was air-dried at room temperature (20°C)

and sieved through a 2-mm nylon mesh to remove stones and plant material in preparation for the determination of soil pH, organic matter, moisture content, permeability coefficient, available phosphorus, and particle density. The sieved soil was then passed through 0.2-mm nylon mesh sieves for the determination of heavy metals.

Because high temperature can lead to the volatilization of mercury and arsenic, each soil sample (0.2 g) was mixed with a solution (5 mL) containing 75% concentrated HNO<sub>3</sub> and 25% concentrated HCl (V/V) in a colorimetric tube. After settling overnight, the colorimetric tubes were placed into a stainless steel water bath for digestion at 95°C for 6 hours. The soil organic matter content was determined by potassium dichromate oxidation–ferrous sulfate titrimetry. The pH of each soil sample was determined using a glass electrode in a suspension of the soil in H<sub>2</sub>O, with a soil/solution ratio of 1:2.5 [12]. The soil moisture content was measured as the percentage of the difference between the air-dried weight and the drying weight. The soil particle density was determined using a pycnometer. The saturated soil hydraulic conductivity was obtained using a permeating bucket. A summary of the soil properties, including basic statistical data of the samples, is given in Table 1.

**Statistical analyses.** All measurements were performed in triplicate in independent experiments and the heavy metal concentration was determined on 2 parallel samples for all samples. The heavy metal concentrations were measured using ICP-OES and certified reference materials. The detection limit for the heavy metals was 0.01 mg·kg<sup>-1</sup>. Standard reference materials obtained from the Resource Technology Corporation (RTC, Laramie, WY 82073, USA) were used for the analysis of each sample batch of 3 samples for quality assurance purposes. The data were processed with Microsoft Excel 2007, OriginPro 8.5, and SPSS 19.0 software, including the calculation of average values and standard deviation. The values were expressed as the mean ± the standard deviation (SD) of the three replicates.

**Methods of comparison.** The main comparative methods include the subsoil comparison, the comparison with the soil background, and the comparison with old industrial areas.

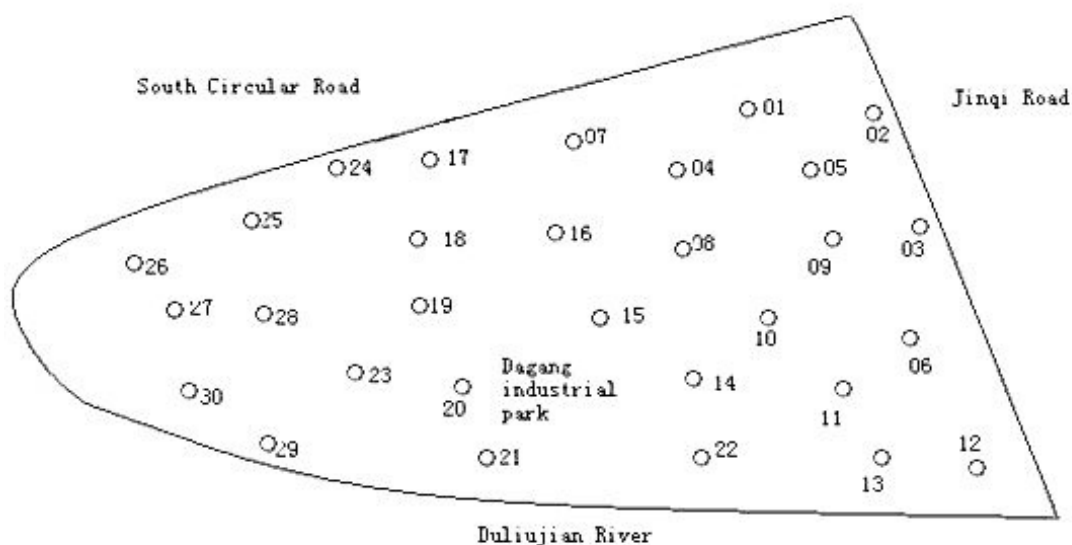


**FIGURE 1**  
Locations of the soil sampling sites around the Dagang industrial park in Tianjin, China.

**TABLE 1**  
Summary of soil properties, with basic statistical parameters, for the soils collected from the Dagang industrial area in Binhai New Area.

Sample site	pH	organic matter	soil	soil particle density	saturated soil hydraulic	total phosphorus
1	8.57	2.12	5.27	3.14	-	55.20
2	7.40	1.86	5.12	3.38	-	54.44
3	8.95	5.69	8.10	3.20	-	57.88
4	8.24	2.55	2.62	3.89	-	52.07
5	8.16	2.27	2.41	2.82	27.0	45.98
6	8.22	7.87	2.02	3.61	-	53.72
7	8.62	2.74	4.15	3.44	-	43.13
8	8.49	3.17	1.57	3.86	-	53.02
9	9.73	4.00	7.50	3.34	-	47.59
10	9.95	2.76	8.09	3.78	-	45.35
11	8.50	2.12	4.61	3.71	-	47.52
12	7.42	2.91	3.23	3.71	-	50.24
13	8.21	1.33	2.49	3.66	-	50.79
14	7.26	5.14	6.91	2.42	-	49.43
15	8.65	2.13	1.34	3.70	-	52.14
16	8.09	8.90	2.96	2.38	45.5	16.24
17	7.66	6.31	7.23	3.67	-	44.96
18	8.30	11.54	1.59	2.78	-	57.05
19	7.49	3.04	7.16	2.77	20.2	47.76
20	7.81	2.12	4.89	3.70	-	46.26
21	7.99	2.61	4.53	3.98	-	45.78
22	8.04	1.55	1.76	2.62	-	57.39
23	8.27	2.20	1.42	3.02	-	58.41
24	8.16	2.05	3.94	3.23	11.0	57.57
25	7.93	1.56	2.88	3.60	-	48.30
26	8.04	3.02	6.13	3.54	-	45.48
27	8.13	2.98	1.49	3.28	-	54.82
28	7.35	3.59	2.37	3.46	-	49.08
29	8.35	2.64	2.78	2.90	-	49.00
30	7.57	2.56	1.54	2.43	-	50.46

“-”: not detected

## RESULTS AND DISCUSSION

### Accumulation and distribution of heavy metals in the topsoil.

The metal distribution in the soils of the Dagang industrial park is shown in Fig. 2. As is shown in Table 2, the mean concentrations of As, Sr, Mn, Cd, Pb, Cr, Hg, Cu, Ni, and Zn were 10.7, 93.4, 473.5, 0.42, 38.1, 25.5, 8.3, 17.6, 17.2 and 64.4 mg·kg<sup>-1</sup>, respectively. The highest concentrations of these metals were 49.0, 151.5, 876.3, 0.98, 31.1, 51.9, 22.4, 286.6, and 128.1 mg·kg<sup>-1</sup>, respectively. The highest Hg and Pb concentrations were found in the west, northwest, and center of the Dagang industrial park, reaching up to 22.4 and 286.6 mg·kg<sup>-1</sup> in sites 10 and 21, respectively. However, the concentrations of these two metals in the east and northeast of the study area were generally lower. The concentration of Pb ranged from 5.7 to 20.6 mg·kg<sup>-1</sup> in 19 sites. No Pb was detected in site 3. The Hg levels in the northeast of the study area were lower than 3.7 mg·kg<sup>-1</sup>. Although the concentration of As was low in some sites, As could be detected in sites 21 and 29, reaching extremely high values up to 49.0 mg·kg<sup>-1</sup>. Analogously, the highest concentration of Cd was detected in site 16, with up to 0.98 mg·kg<sup>-1</sup>. In addition, the concentrations of Cu in most of the collected samples were low and the concentration trends were generally similar, except for site 16. The concentration of Cu in site 16 was quite high, reaching up to 51.9 mg·kg<sup>-1</sup>. The concentration of Mn surpassed 325.8 mg·kg<sup>-1</sup> in all of the 30 sites. The lowest concentration was determined at site 16; however, the concentration of several heavy metals peaked at site 16. It is worth mentioning that two of the highest Mn concentrations were detected at sites

21 and 29, similar to Pb. The Sr contents reached up to 80 mg·kg<sup>-1</sup> at 25 sites. The Sr concentrations were similar but extremely high in most sites. The highest concentration was measured for site 16, similar to several other metals, reaching up to 151.5 mg·kg<sup>-1</sup>. The Ni concentrations were similar at 28 sites and ranged from 14.5 to 22.4 mg·kg<sup>-1</sup>. However, those of sites 16 and 22 were notably lower than at other sites. In total, 22 out of the 30 sample sites showed similar levels of Zn, ranging from 43.8 to 59.4 mg·kg<sup>-1</sup>. The highest concentrations were determined for sites 21 and 29, reaching up to 128.1 mg·kg<sup>-1</sup>. The concentrations of Cr in the Dagang industrial park were lower in most sites, between 17.3 to 33.7 mg·kg<sup>-1</sup>, except for site 28.

### Pollution trends of heavy metals in the topsoil.

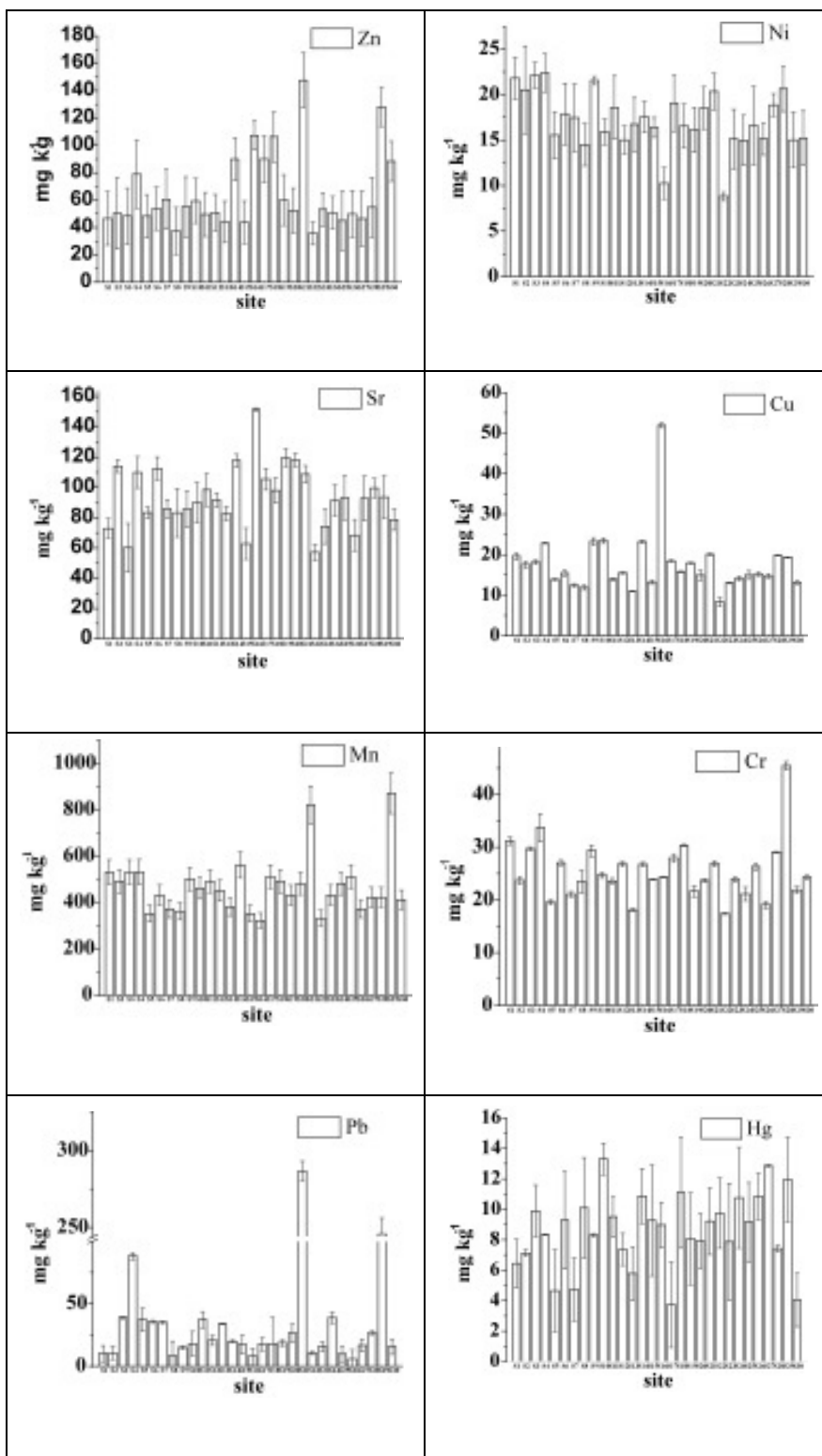
The concentrations of Hg, Cd, Pb and Mn in this study are higher than the background value (Table 2). The concentrations of As, Zn and Sr are similar to the background values of Tianjin. The remaining heavy metal concentrations are smaller than the background value. It can be inferred that part of the pollution is under control, but some of the heavy metal pollutants, such as Hg and Pb, indicate the trend of increasing pollution compared to a previous study on soils in Tianjin [13].

The soil background values of heavy metals in Tianjin are generally higher than in all of China. Compared to the background value in China, the pollution is similar to that of Tianjin. The only differences are that Arsenic in this study is lower than the average concentration in China and the concentrations of Cu and Zn are closer to the background value. Mercury and lead still reflect the pollution trend.

**TABLE 2**  
The background heavy metal concentrations (mg/kg found in Tianjin, Beijing, China, old industrial zone and this study [19])

	As	Cd	Cr	Cu	Hg	Ni	Pb	Zn	Mn	Sr
Tianjin, China	9.6	0.18	84.2	29	2.1	33	21	79	580	100
Beijing, China	NA	0.19	60	34	NA	26	40	90	660	112
China	11.2	0.097	61	22.6	0.065	26.9	26	74.2	583	NA
shenyang Tiexi old industrial	9.26	0.42	0.71	58.9	0.13	52.45	84.5	190.4	NA	NA
Mandoli industrial area, India	12.9	1.14	34.8	77.0	0.07	44.7	40.3	90.2	NA	NA
Palermo, Italy	NA	0.68	34	63	0.68	4.7	202	138	519	NA
In this study	10.7	0.42	25.5	17.6	8.3	17.2	38.1	64.4	876	93.4

NA: not available.



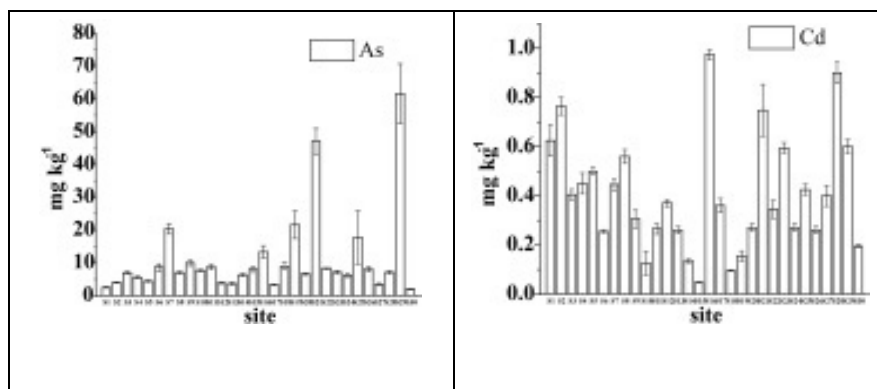


FIGURE 2

Heavy metal concentrations (mg/kg) measured in soils collected at various sites

The comparison of the data with that of the old industrial park of the Shenyang Tiexi old industrial zone shows that the concentrations of Cr and Hg in this study are much higher. The concentrations of As and Cd are similar and the concentrations of other heavy metals are much smaller than the values for the Tiexi old industrial zone. However, compared with the Mandoli industrial area in India, all of the metal concentrations are lower, except for Hg. Compared with the data of the city of Palermo, Italy, all heavy metal contents in this study were lower. Thus, the contamination control for heavy metals in the topsoil of the Dagang industrial park is satisfactory, but the concentration of Hg, which is much higher than in most other regions, needs to be considered.

#### Influences of industrial production.

Industrial activities are one of the main reasons behind the increasing concentrations of heavy metals in the atmosphere [14, 15]. The particles of the aerosol with heavy metals are suspended in the atmosphere because of long-term industrial activities [16]. Nevertheless, heavy metals generated from industrial activities often remain in the soil. The Ni, Sr, Mn and Cr distribution trends are generally similar in this zone, although their concentrations are different, indicating that these heavy metals may have had the same source. Zinc and Cu are necessary nutritional elements, but their mean concentrations are only 64.4 and 17.6 mg/kg, which is lower than the background level. One reason for this is the high organic content of the soils. The organic matter can adsorb Zinc and Cu and reduce their effectiveness. Another reason is the high phosphorus level, which leads to zinc deficiency. According to the summary of soil properties in this study, the sites with a high organic matter content generally also have high concentrations of heavy metals. The content and composition of soil organic matter can not only affect the accumulation of heavy metals in the soil

but also form complexes with heavy metals and influence the transportation and transformation, bioavailability, and other environmental processes of heavy metals in soil [17, 19]. The organic matter content in the soil samples near oil wells was generally high. Thus, the heavy metal content was relatively high at these sites. For example, site 16 has a high organic matter content and the concentration of most of the heavy metals peaked at this site. Some scholars concluded that the oil recovery operation omissions caused the soil pollution at this site. In this experiment, the northeast and center of the study area host many oil wells and the results of this work verify this point of view. The concentration of Hg was extremely low in the previous study. However, Hg was detected in many sites in this study and almost the whole area showed high Hg concentrations, especially near the wells and oil extraction factories. Therefore, it can be concluded that long-term industrial activities certainly affected the environment. Noticeably, the concentration of Pb at sites 29 and 21, close to the Dagang oilfield's electric power supply company and the Tianjin petrochemical company, reaches up to 286.6 mg·kg<sup>-1</sup>. This indicates that the primary environmental sources of Pb are the industrial activities of these two companies. Sites 21 and 29 also show high concentrations of As, Mn and Zn; however, the highest concentration of Cd can be detected at site 16. Although the cadmium pollution is not very serious compared to other industrial areas, it can be observed that there is a certain relationship between the heavy metal content and the hot-spot areas of As, Cd, Zn, Mn and Pb, which are mainly associated with heavy industrial activities. The highest concentration of As was detected at site 30, next to the Duliujian River. There are several oil wells near the road. Thus, this further illuminates that the oil is polluted by heavy metals during oil production. The concentrations of Zn and Mn were



similar in all sites, except for sites 21 and 29. One important reason for this phenomenon is that more soil granules contaminated with the heavy metals were blown into the atmosphere by wind and uniformly dropped by the rain in this area. Compared with the investigation of heavy metals in Tianjin in 1990, the heavy metal concentrations, including Cu, Cr, Ni and Zn, have decreased to some extent but still greatly exceed the national standard. The Zn content is strongly related with the south of this area next to South Circular Road and some oil wells, likely indicating the same source [20-25]. The concentrations of Cr and Ni are higher in the northeastern part than in other parts. The Dagang oilfield refinery, oil wells, the Dagang oilfield mud company, and the first drilling company of the Bohai Sea are in the northeastern area next to Jinqi Road. This implies that the contamination may originate from oil sludge omissions. Approximately 100 mg·kg<sup>-1</sup> of strontium is detected in most of the soil samples around the world. Strontium is one of the essential trace minerals in the human body. However, nuclear experts believe that radioactive strontium can have an impact on human health with time and can cause leukemia and lymphoma [26, 27]. As expected, all of the samples in this study showed high concentrations of Sr, whereby the concentrations in the northeastern and south central area are higher than in other parts. The highest content was detected at site 16, similar to Cu. There are many oil wells and the Dagang oilfield group limited company in the central part near site 16. Thus, the samples of this site contain a high quantity of organic substances. This fact once again reinforces that the oil extraction can cause heavy metal pollution in soils. It is a universal phenomenon that the concentrations of heavy metals in the northeastern, southern, southwestern, and center parts of the Dagang industrial park are higher than that of the northern, northwestern, and southeastern parts. The results demonstrate that the Technology Services Company of the Bohai Sea Drilling Engineering Company, the Dagang oilfield well logging company, and the fourth petroleum and chemical construction company of China provide good pollution control.

**Influence of traffic activities.** Rapid economic development has occurred in the Binhai New Area in the past ten years. The population increased rapidly, the business activity flourished, and the vehicle quantity multiplied. The heavy metal concentrations discharged into the atmosphere by

the gas combustion of automobile exhausts are immense, which has been recognized as pollution globally [28, 29]. All this led to the severe deterioration of the local environment.

In this study, the concentration of Pb is extremely high. The traffic activities are an important factor influencing the Pb pollution of soil. The Lead content of gasoline ranges from 0.08% to 0.13% and most of the Pb emissions from automobile exhausts are derived from the internal combustion engine. Lead contained in the exhausted gas is emitted into the atmosphere and pollutes the surrounding soil. Lead accumulation in human organs may cause harm to the heart and lungs and lead to anemia and mental decline. It can also cause infertility and high blood pressure [30].

Jinqi Road and South Circle Road are the two main traffic arteries in Dagang. The sites close to the sides of the road suffer a certain level of pollution. For instance, many diesel vehicles pass this road throughout the year. Thus, the Pb concentration at these four sites was high. Therefore, Pb is likely to have mainly originated from anthropogenic sources, such as vehicular traffic, which is in good agreement with previous studies in other areas.

## CONCLUSIONS

---

The statistical analysis of the concentrations of pollutants and metals can be used to identify the sources of metal pollution in industrial areas. We can conclude that the soil samples in the industrial park contained high concentrations of heavy metals due to long-term industrial and traffic activities. The majority of total heavy metals in the Dagang industrial park result from oil extraction. Thus, we should adjust the transport policy of the city, reduce the number of private cars, develop the public transport priority, and advocate using bicycles. Meanwhile, energy-efficient and environment-friendly cars should be developed to reduce the national dependency on fossil fuels. The pollution from enterprises needs to be controlled and ecological and health implications need to be further investigated. In summary, human activities are the main environmental sources of heavy metals, such as the traffic activities, long-term industrial activities, such as oil extraction, and industrial radiological processes. Furthermore, the levels of heavy metals in the Dagang industrial park in Tianjin can reflect and indicate the level of environmental pollution in the Chinese industrial zone.

## ACKNOWLEDGEMENTS

This work was financially supported by the National High Technology Research and Development Program ('863' Program) of China (grant No. 2013AA06A205) and the Key Laboratory of Pollution Processes and Environmental Criteria (Ministry of Education), College of Environmental Science and Engineering, Nankai University. The authors are also thankful for joint funds of the National Natural Science Foundation of Guangdong, China (grant No. U1133006).

## REFERENCES

- [1] Kelly, J., Thornton, I., Simpson, P.R., (1996). Urban geochemistry: a study of the influence of anthropogenic activity on the heavy metal content of soils in traditionally industrial and non-industrial areas of Britain. *Applied Geochemistry* 11, 1-2.
- [2] Mielke, H.W., Gonzales, C.R., Smith, M.K., Mielke, P.W., (1999). The urban environment and children's health: soils as an integrator of lead, zinc, and cadmium in New Orleans, Louisiana, U.S.A. *Environmental Research* 81, 117-129.
- [3] Zhao, L., Xu, Y.F., Hou, H., Shangguan, Y.X., Li, F.S., (2014). Source identification and health risk assessment of metals in urban soils around the Tanggu chemical industrial district, Tianjin, China. *Science of the Total Environment* 468, 654-662.
- [4] Guo, P., (2005). Study on Heavy Metal Contamination Mechanism and Countermeasure in Urban Soil of Changchun. Jilin university, Changchun. (In chinese).
- [5] Yang, Z.P., Lu, W.X., Xin, X., Li, J., Li, P., (2008). Lead isotope signatures and source identification in urban soil of Changchun City. *Journal of Jilin University (Earth Science Edition)* 38, 663-669 (In Chinese).
- [6] Yang, Z.P., Lu, W.X., Long, Y.Q., (2009) Atmospheric dry and wet deposition of heavy metals in Changchun city, China. *Research of Environmental Sciences* 22, 28-34 (In Chinese).
- [7] Wei, B., Yang, L., 2010. A review of heavy metal contaminations in urban soils, urban road dusts and agricultural soils from China. *Microchemical Journal* 94, 99-107.
- [8] Papa, S., Bartoli, G., Pellegrino, A., Fioretto, A., (2010). Microbial activities and trace element contents in an urban soil. *Environmental monitoring and assessment* 165, 193-203.
- [9] Feng H., Jiang H., Gao W., Weinstein MP., Zhang Q., Zhang W., (2011). Metal contamination in sediments of the western Bohai Bay and adjacent estuaries, China. *J Environ Manage* 92, 1185-97.
- [10] GuoW., Liu X., Liu Z., Li G., (2010). Pollution and potential ecological risk evaluation of heavymetals in the sediments around Dongjiang Harbor, Tianjin. *Procedia Environ Sci* 2, 729-36.
- [11] Wu, G., Su, R., Li, W., Zheng, H., (2008). Source and enrichment of heavy metals in sewage-irrigated area soil of Dagu Sewage Discharge Channel. *Environ Sci* 29, 1693-1698
- [12] ISO-10390., (2005). Soil quality-determination of pH. Geneva, Switzerland: International Standard Organization.
- [13] China National Environmental Monitoring Center (CNEMC)., (1990). The Backgrounds of Soil Environment in China. Environment Science Press of China.
- [14] Manta, D.S., Angelone, M., Bellanca, A., Neri, R., Sprovieri, M., (2002). Heavy metals in urban soils: a case study from the city of Palermo (Sicily), Italy. *Science of the Total Environment* 300, 229-243.
- [15] Kavouras, I.G., Koutrakis, P., Cereceda-Balic, F., Oyola, P., (2001). Source Apportionment of PM10 and PM25 in Five Chilean Cities Using Factor Analysis. *Journal of the Air & Waste Management Association* 51, 451-464.
- [16] An, J., Zhou, Q., Liu, W., Ren, L., (2008). Horizontal distribution and levels of heavy metals in the biggest snowstorm in a century in Shenyang, China. *Journal of Environmental Sciences* 20, 846-851.
- [17] Sun, Y., Zhou, Q., Xie, X., Liu, R., (2010). Spatial, sources and risk assessment of heavy metal contamination of urban soils in typical regions of Shenyang, China. *Journal of hazardous materials* 174, 455-462.
- [18] Lindsay, W., Norvell, W.A., (1978). Development of a DTPA soil test for zinc, iron, manganese, and copper. *Soil Science Society of America Journal* 42, 421-428.
- [19] Williams, D., Vlamis, J., Pukite, A., Corey, J., (1980). Trace element accumulation, movement, and distribution in the soil profile from massive applications of sewage sludge. *Soil Science* 129, 119.





- [20] Chen, T.-B., Zheng, Y.-M., Lei, M., Huang, Z.-C., Wu, H.-T., Chen, H., Fan, K.-K., Yu, K., Wu, X., Tian, Q.-Z., (2005). Assessment of heavy metal pollution in surface soils of urban parks in Beijing, China. *Chemosphere* 60, 542-551.
- [21] Kadi, M.W., (2009). "Soil Pollution Hazardous to Environment": A case study on the chemical composition and correlation to automobile traffic of the roadside soil of Jeddah city, Saudi Arabia. *Journal of hazardous materials* 168, 1280-1283.
- [22] Li, B., Cao, J., Liu, W., Shen, W., Wang, X., Tao, S., (2006). Geostatistical analysis and kriging of hexachlorocyclohexane residues in topsoil from Tianjin, China. *Environmental Pollution* 142, 567-575.
- [23] Shi, G., Chen, Z., Xu, S., Zhang, J., Wang, L., Bi, C., Teng, J., (2008). Potentially toxic metal contamination of urban soils and roadside dust in Shanghai, China. *Environmental Pollution* 156, 251-260.
- [24] Sun, Y., Zhou, Q., Xie, X., Liu, R., (2010). Spatial, sources and risk assessment of heavy metal contamination of urban soils in typical regions of Shenyang, China. *Journal of hazardous materials* 174, 455-462.
- [25] Yang, Z., Lu, W., Long, Y., Bao, X., Yang, Q., (2011). Assessment of heavy metals contamination in urban topsoil from Changchun City, China. *Journal of Geochemical Exploration* 108, 27-38.
- [26] Li, Z., Chen, Y., Yang, X., Wei, S., (2006). Assessment of potential ecological hazard of heavy metals in urban soils in Chongqing City. *Journal of Southwest Agricultural University Natural Science* 28, 227-230.
- [27] Shi, Z., Tao, S., Pan, B., Liu, W., Shen, W., (2007). Partitioning and source diagnostics of polycyclic aromatic hydrocarbons in rivers in Tianjin, China. *Environmental Pollution* 146, 492-500.
- [28] Colville, R., Hutchinson, E., Mindell, J., Warren, R., (2001). The transport sector as a source of air pollution. *Atmospheric Environment* 35, 1537-1565.
- [29] Lonati, G., Giugliano, M., Cernuschi, S., (2006). The role of traffic emissions from weekends' and weekdays' fine PM data in Milan. *Atmospheric Environment* 40, 5998-6011.
- [30] Pradhan, J.K., Kumar, S., (2014). Informal e-waste recycling: environmental risk assessment

of heavy metal contamination in Mandoli industrial area, Delhi, India. *Environmental Science and Pollution Research*, 1-16.

---

**Received:** 06.03.2016

**Accepted:** 20.09.2016

---

#### CORRESPONDING AUTHOR

---

##### **Qixing Zhou**

Key Laboratory of Environmental Remediation and Pollution Control  
College of Environmental Science and Engineering  
Nankai University  
300071 Tianjin – CHINA

E- mail: zhouqx523@126.com  
563073156@qq.com

# FARMERS' RISK PERCEPTION AND WILLINGNESS TO PAY FOR ENVIRONMENT: CASE STUDY OF GAP-SANLIURFA, TURKEY

Mustafa Hakki Aydogdu\*

Harran University, Agricultural Faculty, Agricultural Economics Department, Osmanbey Campus, 63200 Sanliurfa, Turkey

## ABSTRACT

The aim of this research is to evaluate farmers' risk perception and willingness to pay for sustainable environment at dry farming areas in GAP-Sanliurfa, Turkey and determine the affecting factors that contribute to it. The data used in this study come from a sample of 32,809 farmers at dry farmland in Sanliurfa, 480 of them were chosen via simple random sampling method and interviewed face to face by given questionnaires. Sampling was conducted in all districts of Sanliurfa in 2014. The logistic regression, Odds, Omnibus, Cox and Snell R Square, Nagelkerke R Square, Wald test, Hosmer-Lemeshow fit tests were used for analysis. The results indicate that 39.5% of farmers have risk perception about the environment and 57% of farmers accept to pay for sustainable environment. The average willingness to pay was €55.2 per hectares. Explanatory affecting factors, such as age, education level, land amount, income and commercial livestock were significantly explained risk perceptions and payment acceptance for environment. This study is first of its type in GAP-Sanliurfa, Turkey. Hence, the result of the study can be helpful for decision and policy makers to develop effective environmental strategies for GAP-Sanliurfa, Turkey and other countries with similar technical and socio-cultural characteristics.

## KEYWORDS:

Sustainable environment, risk perception, willingness to pay, GAP-Sanliurfa, Turkey.

## INTRODUCTION

Every society has a natural environment that affects the economy and level of development. Economic activities of human affect environment and also affected from it [1]. Today, natural resources and environmental problems are being experienced in many parts of the world due to different reasons [2] and all the problems arise from human activities. There are a number of duties and responsibilities towards to the natural environment

where human maintains their life and the benefit from it. While, having many important several reasons for humans to protect the environment, and there is no reason for behaving irresponsibly.

One of the most important issues occupying the world's agenda is environmental pollution [3]. This cause to deterioration of ecology that negatively affect water and land resources, production system in agriculture and result to significant yield losses, especially in dry farming areas. Regardless of development levels agriculture has priority in all countries and occupies important place in the economies [4]. There are many environmental problems caused by agricultural activities such as agrochemical and pesticide use, chemical fertilizer, unsuitable soil tillage, animal wastes, the burning of stubble and so on [5]. Natural resources are the main source of life in rural areas and there are a close link between poverty and environmental exhaustion [6] and also vice versa are true.

Perception means receiving sensory information, interpretation, selection and arrangement in psychology and cognitive science and dependent on many factors. Attitude is the individual's perception about a topic that affects his/her behavior [7] and formed based on perception. In this research, it is intended to identify the farmers' risk perception for environment in dry farming areas of Sanliurfa and willingness to pay (WTP) for environment for sustainable agriculture and affecting factors that contribute to it.

## MATERIALS AND METHODS

**Study Area.** Southeastern Anatolian Project (GAP, in its Turkish acronym) is a multi-sectorial regional sustainable development projects that is mainly based on soil and water resources at south eastern part of Turkey. Agriculture is the leading sector with a 3.13 million ha of land in the GAP Region, Within the GAP's scope; there are 22 dams, 19 hydroelectric power plants and irrigation of 1.822 million ha of agricultural land [8] and 424,710 ha of land was been irrigated. There are nine provinces in GAP region that is almost 10% of

Turkey in terms of area and population. Sanliurfa is the second crowded city of GAP with 13 districts, covers 22.3% of region's populations, 37.7% of agricultural land and 24.1% of livestock [9].

**Materials.** There are 54,976 farmers in Sanliurfa according to the farmer registration system in 2014 and 32,809 of them are located in dry farmland. The main material of this research comes from a sample of 480 farmers among 32,809 in Sanliurfa who were chosen via a simple random sampling method. Sample volume was determined by formula [10] with 95% confidence interval that conducting 380 questionnaires would be appropriate, but to be on the safe side, 480 were conducted. Sampling was conducted in 2014 and interviewed face to face by given questionnaires. Within this scope, all the districts were visited in Sanliurfa and local interviewers were used in order to maximize the reliability of the results.

**Methods.** Logistic regression, Odds, Omnibus, Cox and Snell R Square, Nagelkerke R Square, Wald test, Hosmer-Lemeshow fit tests were conducted in SPSS. Logistic regression uses maximum likelihood (ML) estimation in multiple regressions. ML approaches try to find estimates of parameters that make the data actually most likely observed. Odds ratios in logistic regression can be interpreted as the effect of a one unit of change in the predicted odds ratio with the other variables in the model held constant. An important property of odds ratios is that they are constant. It does not matter what values the other independent variables take on [11]. It is defined as division of the probability of an event to the probability of not being event. A Wald test can be used in a great variety of different models including models for dichotomous variables and models for continuous variables [12]. The Wald test in the context of logistic regression is used to determine whether a certain predictor variable is significant or not. Omnibus test is a general name refers to an

overall test and in most cases it is called as: F-test or Chi-squared test. Omnibus test is implemented on an overall hypothesis that tends to find general significance between parameters' variance, while examining parameters of the same type. They test whether the explained variance in a set of data is significantly greater than the unexplained variance, overall [13].

There is not R-squared statistics in logistic regressions that is similar to the regression analysis. In SPSS, there are two modified R-squared value; one developed by Cox and Snell that is never reaches to 1 and the other developed by Nagelkerke. The correction increases the Cox and Snell version to make 1.0 a possible value for R-squared by modified it by Nagelkerke. These values indicate the amount of variance explained by the model. The Hosmer-Lemeshow fit test is designed to correct and use when there are discontinuous and continuous predictors, at the same time and not recommend the use of this test when there is a small n less than 400 [14]. Here is sample size was 480. This test is performed by dividing the predicted probabilities into deciles and then computing a Pearson chi-square that compares the predicted to the observed frequencies. Lower values and insignificances indicate a good fit to the data and, therefore, good overall model fit [15].

## RESULTS AND DISCUSSIONS

All survey respondents were male due to the rural patriarchal family structure. The total amount of cultivated land was 10,099 ha in the surveyed area, 41.7% of the farms are 10 ha or smaller. Wheat was the main crop, and then followed by barley and red lentil. The average income from agricultural activities was calculated as 20,779 TL/year and 988 TL/ha. (TL=Turkish Lira, 1€=2.91 TL at surveyed time, [16]). The descriptive statistics of the model is given in Table 1.

**TABLE 1**  
**Descriptive statistics of the research**

Variables	Definition	Mean	Std. Deviation
Age	Age of the farmer (year)	43,75	11,788
Education	If the farmer: literacy 1, graduated primary school 2, graduated secondary school 3, graduated high school 4, graduated university 5	2,45	1,163
Marital	If the farmer: married 1, if not 0	0,93	0,326
Household	The number of dependent person	7,54	4,052
Experience	Farming experience (year)	22,43	11,844
Land Amount	The amount of cultivated land size (hectare)	21,04	393,196
Income	Income of the farmer from farming (TL/year)	20778,54	28746,541
Livestock	If the farmer does commercial livestock 1, if not 0	0,28	0,649
Risk	If the farmer has environment risk perception 1, if not 0	0,40	0,524
Payment (PES)	If the farmer accept payment for environment 1, if not 0	0,57	0,496

**TABLE 2**  
**Classification table of step 0**

Observed			Predicted		
			Risk Perception		Percentage Correct
			NO	YES	
Step 0	Risk Perception	NO	290	0	100,0
		YES	190	0	0,0
Overall Percentage					60,5

**TABLE 3**  
**Coefficients of variables in the equation**

		B	S.E.(Standard Error)	Wald	df	Significance	Exp(B)
Step 0	Constant	-0,428	0,094	20,777	1	0,000*	0,652

**TABLE 4**  
**Omnibus tests of model coefficients**

		Chi-square	df	Significance
Step 1	Step	247,667	21	0,000*
	Block	247,667	21	0,000*
	Model	247,667	21	0,000*

**TABLE 5**  
**Model summary**

Step	-2 Log likelihood	Cox & Snell R Square	Nagelkerke R Square
1	388,180	0,407	0,551

**TABLE 6**  
**Hosmer and Lemeshow test results**

Step	Chi-square	df	Significance
1	10,961	8	0,204

The rate of farmers, who perceived the risk to the environment that is dependent variable, is 39.5%. The proportion of those with the WTP for a sustainable environment is 57%. These results show that; although there is no risk perception, but 17.5% more of farmers tend to pay. According to the first classification table all the respondents were classified in no by the model and percentage of verification in this case was 60.5%. The classification table based on step 0 is given in Table 2.

The statistics of the variables are located in the initial model, step 0, and is given in Table 3.

According to significance level in Table 3,  $p < 1\%$ , all of the independent variables were making meaningful contribution. The Omnibus tests of model coefficients are given Table 4.

Chi-square test showed that it's statistically significant,  $p < 1\%$ . This significance shows that existing of a relationship between dependent variable that is risk perception to the environment,

and combination of independent variables in the model. The model summary is given in Table 5.

Cox & Snell and Nagelkerke R square values indicate the amount of variance explained by the model. The variance of risk perception to the environment was explained 40.7% by Cox & Snell and 55.1% by Nagelkerke R square. The test result of Hosmer and Lemeshow is located in Table 6.

The test was assessed the compliance of the logistic regression model as a whole and result indicated that it was insignificant ( $p > 0.10$ ) means that existing of an adequate level of model-data fit. The classification table that was obtained from logistic regression result is given in Table 7.

The percentage of verification was increased from 60.5% to 82.5% that indicates that variables make meaningful contribution to the model. Initially more variables were used in the model, given in descriptive statistics, and significant ones were selected after the first run in terms of contribution to the model. The most appropriate multivariable that are age, income, land amount,

commercial livestock, education and PES were selected as variables in logistic regression model. The model was run for the second time and results are given in Table 8.

The results are based on odds ratios; it has been done by logistic regression analysis. Odds ratios presented for dummy variables are interpretable in relation to their respective reference

group and less than one unit change indicate that existing of negative relationship that means having less risk perception about environment. More than a unit change shows that existing of positive relationship that means having more risk perception about environment to their respective reference group.

**TABLE 7**  
Classification table at step1

Observed		Predicted		
		Risk Perception NO	YES	Percentage Correct
Step 1	Risk Perception NO	242	48	83,6
	YES	35	155	81,3
Overall Percentage				82,5

**TABLE 8**  
Logistic regression model's variables in the equation

	B	S.E.	Wald	df	Sig.	Exp(B) Odds ratios
Step 1						
<b>Age (years)</b>						
60 and more (Ref. group)			9,090	3	0,028 <sup>b</sup>	
Between 18-29 years (Gr.1)	1,505	0,652	5,333	1	0,021 <sup>b</sup>	4,505
Between 30-45 years (Gr.2)	1,062	0,493	4,646	1	0,031 <sup>b</sup>	2,892
Between 46-59 years (Gr.3)	0,419	0,477	0,771	1	0,380	1,520
<b>Income (\$/year)</b>						
\$12000 and more (Ref. group)			49,773	3	0,000 <sup>c</sup>	
\$2999 and less (Gr.1)	-3,239	0,548	34,907	1	0,000 <sup>c</sup>	0,039
Between \$3000-5999 (Gr.2)	-2,748	0,428	41,279	1	0,000 <sup>c</sup>	0,064
Between \$6000-11999 (Gr.3)	-1,308	0,362	13,020	1	0,000 <sup>c</sup>	0,270
<b>Land (Hectares)</b>						
25 ha and more land (Ref. group)			43,848	3	0,000 <sup>c</sup>	
5.9 ha and less land (Gr.1)	-3,124	0,807	14,995	1	0,000 <sup>c</sup>	0,044
Between 6-11.9 ha land (Gr.2)	1,255	0,381	10,863	1	0,001 <sup>c</sup>	3,508
Between 12-24.9 ha land (Gr.3)	-0,238	0,356	0,446	1	0,504	0,788
<b>Commercial livestock</b>						
Commercial livestock (Yes)	0,772	0,306	6,380	1	0,012 <sup>b</sup>	2,164
<b>Education (Levels)</b>						
University graduated (Ref. group)			33,894	4	0,000 <sup>c</sup>	
Literacy (Gr.1)	-1,019	0,614	2,751	1	0,097 <sup>a</sup>	0,361
Primary school graduated (Gr.2)	0,175	0,560	0,097	1	0,755	1,191
Secondary school graduated (Gr.3)	-1,792	0,625	8,216	1	0,004 <sup>c</sup>	0,167
High school graduated (Gr.4)	-1,504	0,628	5,730	1	0,017 <sup>b</sup>	0,222
<b>Payment for Environment (PES)</b>						
Average PES value per ha.			160,70	7	0,024 <sup>b</sup>	
PES increased by 25% (Gr.1)	-0,934	0,425	4,833	1	0,028 <sup>b</sup>	0,393
PES increased by 50% (Gr.2)	-1,144	0,391	8,566	1	0,003 <sup>c</sup>	0,319
PES increased by 75% (Gr.3)	-1,278	0,533	5,669	1	0,021 <sup>b</sup>	0,290
<b>Constant</b>	1,413	0,717	3,887	1	0,049 <sup>b</sup>	4,108

<sup>a,b,c</sup> orderly indicates the degree of statistical significance of 10%, 5% and 1%.



There is a relationship between age and risk perception to the environment ( $p < 5\%$ ). The youngest ones (Gr.1) has more perception about the environment as compared to the reference group by 4.51 times in a positive way. The middle aged (Gr.2) has 2.89 times and upper middle aged (Gr.3) has 1.52 times more perception in a positive way. Age has an effect on attitudes of citizens about the environment [17]. The preferences and behaviors are related to expectations and experiences that influence the formation of different value priorities. Environmental concerns and value priorities tends to becoming increasingly important at younger generations replace older generations [17]. The economic and social condition of the Sanliurfa is developing more in each year and this result to positively on farmers' perception about the environment. The results are consistent ( $p < 5\%$ ).

There is a relationship between income level and risk perception ( $p < 1\%$ ). Risk perception is increasing with increasing income of the farmers and vice versa is true, too. The lowest income (Gr.1) has 0.04 times of risk perception as compared to reference group (highest income) that means 96.1% less in a negative way. The Gr.2 has 0.06 times that means 93.6% less, and the Gr.3 has 0.27 times that means 73% less risk perception as compared to the reference group in a negative way. Economic theory suggests that if environmental quality is a normal good, all else constant, higher income households will be more WTP for environmental protection than lower income households [17]. The farmers' income mainly depends on agricultural activities that require an appropriate environment. There is a need for a better environment for a higher income. Higher income groups are more sensitive about sustainable environment. It is statistically significant ( $p < 1\%$ ).

There is a relationship between land amount and risk perception ( $p < 1\%$ ). Farmers' income is dependent on the land amount. The greater amount of land means more revenue for farmers. The Gr.1 and Gr.3 have less risk perception as compared to the reference group by 95.6% and 21.2% respectively in a negative way. These results are consistent with expectations. Gr.2 has more perception about the environment as compared to the reference group by 3.51 times in a positive way. This result is unexpected one and to reveal the reasons, they were interviewed again face to face with those involved in this group by simple random sampling method. 31% of farmers are located in this group, 80% of them land owner, 76.1% of them doing commercial livestock and average income was 1380.5 TL/ha that was 39.73% more than the average value. All the values of this group are more than the average values. So, this group obtains more revenue from land, therefore environment, than the other groups. In this respect, the result is significant ( $p < 1\%$ ).

There is a relationship between commercial livestock and risk perception ( $p < 5\%$ ). The farmers engaged in animal husbandry have the risk perception more than 2.16 times according to those who do not, in a positive way. Although existing of limited income effect, this group has 4.4% more average income as compared to the reference group and 1.3% more than the overall average of the participant. The physical properties and degradation characteristics of the environment is important for feedstuffs that might be potentially used to estimate the nutritive values and can also be applied in a ration formulation [18].

There is a relationship between education levels and risk perception ( $p < 1\%$ ). When education levels decreases, there is a decrease in risk perception. The opposite is true, too. Sensitivity to the environment of the educated farmer is high. Education is an important indicator of life quality and attitudes, thus the environment. The literate farmers (Gr.1) have 0.36 times of risk perception as compared to reference group that means 63.9% less in a negative way. The Gr.3 and Gr.4 have less risk perception by 83.3% and 77.8% respectively in a negative way. The Gr.2 has more risk perception about the environment as compared to the reference group by 1.19 times in a positive way. This result was unexpected. This group is the biggest one in this category and 47.5% of farmers are located with 18.6 ha average land size. Their average income is more than 2.9% of the average value. The average house hold number is 8.2 and 3.8 person is dependent to farming activities, more than the overall average values, that means agriculture is the main source of livelihood. In this regards, result is understandable.

The benefits of the environment are located in the two groups that are usage and non-usage benefits [1] and both of them are necessary for sustainable agriculture. Usage benefits are used for agricultural production for today needs and non-usage benefits would be potential benefits of being for future use of next generations [19]. In such a case, possible values are determined for the environmental resources by non-market analysis techniques [20]. The simplest way is "If you want to know the amount they want to pay for a feature related to the environment, you can directly ask him" [21]. The farmers were asked if they were certain that the money would be used for the sustainable usage of environment (PES), do you want to pay for PES and how much want to pay for a hectare of land. Payments for environment, the non-provisioning part of ecosystem services, target alignment of microeconomic incentives for land users with meso- and macroeconomic societal costs and benefits of their choices across stakeholders and scales [22]. The results were indicated that 57% of the farmers have WTP for the environment with an average PES value is 160.7 TL/ha (55.2€/ha).



Both values are unexpected results. First of all, the farmers who have WTP are more than 17.5% of the farmers who have risk perceptions that was 39.5%. In other words, 17.5% more of the farmers have WTP for PES as compared to the risk perception group. This group is visited again in order to understand the reason. This result simply arises from environmental awareness and being affected by the behavior of more educated farmers, who accepted WTP and PES. Humans, being highly social creatures, rely heavily on the ability to perceive what others are doing and to infer from gestures and expressions what others may be intending to do [23]. Secondly, WTP and PES group has an average income of 1017 TL/ha that is more than the average value and WTP amount is 15.7% of their income per ha that is higher than expected. WTP may depend largely on the ability to pay [24] and is positively related to income and also have to be a reasonable proportion of income [25]. Average WTP is found for irrigation water as 10.73% of the farmers' income at Sanliurfa -Harran plain in Turkey [25]. The farmers expressed that being certain about that the money would be used for the environment is an important factor in their expressed amount for PES. In this regards, it is a matter of trust for payment more. A study in Sanliurfa-Harran plain indicated that existence of relationship between farmers' satisfaction and education levels, trust, land area, age, income, and service quality [26].

There is a negative relationship between acceptance and increased PES amount ( $p < 5\%$  and  $p < 1\%$ ). When the average PES amount increases, acceptance of PES decreases. The opposite is true, too. In order to define the affect of more payment, PES amount was increased by multiple of 25% and done 3 groups. Gr.1 (25% increased PES) has 60.7% of less acceptance as compared to the average PES ( $p < 5\%$ ). Gr.2 (50% increased PES) and Gr.3 (75% increased PES) have less acceptance by 68.1% ( $p < 1\%$ ) and 71% ( $p < 5\%$ ), respectively. Increasing the amount of PES affects negatively the welfare of farmers. The results are consistent and statistically significant.

## CONCLUSION

Agriculture is important at least for food safety and employment that requires natural resources and suitable environment which are limited resources. Climate change is predicted to make the existing problems worse in many regions [2] that will change features of the environment and ecology [27]. Soil characteristics and environmental properties, such as climate, topography, and vegetation, are the major factors that control the movement of pollutants in soils [28]. Therefore environment needs protection and conservation for

sustainability; this can only be achieved by acting together with the stakeholders. The awareness, education and training are necessary for good environmental practices. The farmers have risk perception and WTP for sustainable environment. An environmental program can be applicable together with farmers based on cost sharing. In this way, awareness, ownership and protection can be increased. The results of this research are meaningful and could be considered as guidelines for policy and decision makers about sustainable environment. This study is the first of its type in GAP-Sanliurfa, Turkey.

## REFERENCES

- [1] Basol, K. Durman, M. and Onder, H. (2007) Economic Analysis of Natural Resources and Environment. Alfa Aktüel Yayınları, İstanbul. ISBN: 978-975-253-111-6. (In Turkish).
- [2] Farmer, A. Bassi, S. and Fergusson, M. (2008) Water Scarcity and Droughts. EU Policy Department Economic and Scientific Policy, IP/A/ENVI/ST/2007-17, PE 401.002.
- [3] Baykal, T. (2010) Globalization And Major Global Environmental Pollution. *Mevzuat Dergisi*, 148:4-10.
- [4] Aydogdu, M.H. Karli, B. and Aydogdu, M. (2015) Evaluation of attitude of stakeholders to irrigation water management: A case study of Harran Plain, Turkey. *Journal of Environmental & Agricultural Science*. 4:42-47.
- [5] Sayili, M. and Aknaz, Z. (1994) Agricultural practices and their effects on the environment. *Cevre dergisi, Ekoloji*, 12:1-5 (In Turkish).
- [6] Karacan, A.R. (2007) Environmental Economics and Policy. *Ege Universitesi* 6:116-137. İzmir. ISBN: 978-975-483-751-3. (In Turkish).
- [7] Aydogdu, M.H. Mancı, A.R. and Aydogdu, M. (2014) The Overviews and Perceptions of Faculty of Agriculture Students of Harran University to Agricultural Policies of Turkey. *Turkish Studies*. 9(11):63-77. Doi:<http://dx.doi.org/10.7827/TurkishStudies.7348>
- [8] GAP. (2012) GAP Administration, Latest status in GAP-2012, pp.6-55 Sanliurfa, Turkey.
- [9] GAP. (2015) GAP Administration. Sanliurfa province profile. pp.1-3. Sanliurfa, Turkey.
- [10] Yamane, T. (2001) Basic Sampling Methods. Literatur Publication, İstanbul (In Turkish).
- [11] O'Halloran, S. (2015) Sustainable Development U9611 Econometrics II. Lecture 10: Logistical Regression II— Multinomial Data p.5-8. 12 Dec 2015. [http://www.columbia.edu/~so33/SusDev/Lecture\\_10.pdf](http://www.columbia.edu/~so33/SusDev/Lecture_10.pdf)



- [12] Harrell, F. E. Jr. (2001) "Sections 9.2, 10.5". Regression modeling strategies. New York: Springer-Verlag .ISBN 0387952322
- [13] Anonymous. (2015) [https://en.wikipedia.org/wiki/Omnibus\\_test/Wald\\_test](https://en.wikipedia.org/wiki/Omnibus_test/Wald_test). 12 Dec 2015
- [14] Hosmer, D. W. and Lemeshow, S. (2000) Applied logistic regression (2nd Edition). New York: Wiley.
- [15] Kalayci, Ş. (2014) SPSS applied multivariate statistical techniques. Asil Yayın Dağıtım. Ankara (In Turkish).
- [16] Anonymous. (2014) web:[http://www.isyatirim.com.tr/p\\_exchange.aspx](http://www.isyatirim.com.tr/p_exchange.aspx), 31Dec 2014.
- [17] Ivanova, G. and Tranter, B. (2004) Willingness to pay for the environment in cross national perspective. pp.1-27. Australiasian Political Studies Association Conference, University of Adelaide.
- [18] Hao, X.Y. Xin, H.S. Gao, H. Zhang, X.Y. Lin, C. Xu, W.B. Wang, Y.Z. and Zhang, Y.G. (2016) Relationship between the physical parameters, chemical compositions and rumen degradation kinetics parameters of certain feedstuffs for ruminants, *Animal Feed Science and Technology*, 211(1):84-91. <http://dx.doi.org/10.1016/j.anifeedsci.2015.11.009>
- [19] McPherson, G. Simpson, J.R. Peper, P. J. Maco, S. E. and Xiao, Q. (2005) Municipal forest benefits and costs in five US cities, *Journal of Forestry*, 103(8):411-417.
- [20] Prato, T. (1998) *Natural resources and Environmental Economics*, Blackwell Publishing.
- [21] Ozsabuncuoglu, I. H. and Uygur, A. (2005) *Natural Resource Economics, Management and Policy*. İmaj Yayınevi, Ankara, pp.525
- [22] Noordwijk, M. Leimona, B. Jindal, R. Villamor, G.C. Vardhan, M. Namirembe, S. Catacutan, D. Kerr, J. Minang, P.A. and Thomas P.T. (2012) Payments for Environmental Services: Evolution toward Efficient and Fair Incentives for Multifunctional Landscapes, *Annual Review of Environment and Resources*, 37:389-420. DOI: 10.1146/annurev-environ-042511-150526
- [23] Blake, R. and Shiffar, M. (2007) Perception of Human Motion. *Annual Review of Psychology*, 58:47-73. DOI:10.1146/annurev.psych.57.102904.190152
- [24] Perry C.J. Rock M. and Seckler D. (1997) Water as an economic good: A solution, or a problem? Research Report 14. International Irrigation Management Institute, Colombo, Sri Lanka.
- [25] Aydogdu, M.H. (2016) Evaluation of willingness to pay for irrigation water: Harran Plain Sampling in GAP Region-Turkey, *Applied Ecology and Environmental Research* 14(1):349-365. [http://dx.doi.org/10.15666/aer/1401\\_349365](http://dx.doi.org/10.15666/aer/1401_349365).
- [26] Aydogdu, M. H. Yenigun, K. and Aydogdu, M. (2015) Factors Affecting Farmers' Satisfaction from Water Users Association in the Harran Plain-GAP Region, Turkey. *Journal of Agricultural Science and Technology*, 17(Supplementary issue):1669-1684.
- [27] Akbulut, S. (2000) Possible effects of global warming on insect populations. *Ekoloji*, 9(36):25-27 (In Turkish).
- [28] Atasoy, A.D. (2008) Environmental Problems In Vertisol Soils: The Example Of The Harran Plain. *Fresen Environ Bull.* 17(7):837-843

---

**Received: 06.03.2016**  
**Accepted: 16.09.2016**

---

#### **CORRESPONDING AUTHOR**

---

**Aydogdu Mustafa Hakki**  
Harran University  
Agricultural Faculty  
Agricultural Economics Department  
63200, Sanliurfa, Turkey

E-mail: [mhaydogdu@hotmail.com](mailto:mhaydogdu@hotmail.com)  
[mhaydogdu@harran.edu.tr](mailto:mhaydogdu@harran.edu.tr)



# CO-OCCURRENCE AND DIVERSITY OF NITRITE-DEPENDENT ANAEROBIC METHANE OXIDIZING AND ANAEROBIC AMMONIUM OXIDIZING BACTERIA IN THE WATER-LEVEL FLUCTUATION ZONE OF THE THREE GORGES RESERVOIR, CHINA

Ruifei Wang<sup>1,2</sup>, Xinkuan Han<sup>1</sup>, Peili Lu<sup>3</sup>, Qingxiang Yang<sup>1,2,\*</sup>

<sup>1</sup>College of Life Sciences, Henan Normal University, Xinxiang, China

<sup>2</sup>Key Laboratory for Microorganisms and Functional Molecules (Henan Normal University), University of Henan Province, Xinxiang, China

<sup>3</sup>Department of Environmental Science, Chongqing University, Chongqing, China

## ABSTRACT

Nitrite-dependent anaerobic methane oxidation and anaerobic ammonium oxidation, two important processes relating to carbon and nitrogen cycles, have been reported to co-occur in paddy fields. However, their presence and relationship in water-level fluctuation zones (WLFZs) in large reservoirs is unclear. Here, *Methylomirabilis oxyfera*-like and anammox bacteria performing these two processes were detected in WLFZ soils in the Three Gorges Reservoir in China. Our results from real-time PCR indicated that the copies of *M. oxyfera*-like bacteria in WLFZ soils ranged from  $1.15 (\pm 0.2) \times 10^5$  to  $1.48 (\pm 0.16) \times 10^7 \text{ g}^{-1}$ , which were much higher than those in the paddy field. However, the copies of anammox bacteria in WLFZ soils were much lower than those in the paddy field. Analysis of 16S rRNA and *pmoA* gene libraries suggested that the diversity of *M. oxyfera*-like bacteria in WLFZ soils was higher than that in previously reported environments. Analysis of the *hzsB* gene library indicated that the anammox bacteria in WLFZ soils were mainly distributed in *Candidatus 'Brocadia'*, *Candidatus 'Kuenenia'* and another unidentified genus. High abundance and diversity of *M. oxyfera*-like bacteria in WLFZ soils might be one reason of the low methane emission in this area.

## KEYWORDS:

nitrite-dependent anaerobic methane oxidation; anaerobic ammonium oxidation; water-level fluctuating zone; *pmoA* gene; *hzsB* gene

## INTRODUCTION

Nitrite-dependent anaerobic methane ( $\text{CH}_4$ )

oxidation (n-damo), a recently discovered process, couples anaerobic oxidation of  $\text{CH}_4$  (AOM) and denitrification of nitrite, and constitutes a unique link between the two major global nutrient cycles of carbon and nitrogen [1, 2]. Furthermore, it converts  $\text{CH}_4$  to carbon dioxide ( $\text{CO}_2$ ) with conversion of nitrite to dinitrogen gas ( $\text{N}_2$ ), which alleviates the greenhouse effect. *Candidatus 'Methylomirabilis oxyfera'* is the only species that has been isolated and confirmed to perform n-damo and belongs to candidate division NC10 [2]. Although *M. oxyfera*-like bacteria have been enriched from several freshwater sediments [3-5] and proved to be widely present in various freshwater systems [3-9], their distribution and diversity is not well understood.

The other important nitrite-dependent anaerobic process is anaerobic ammonium oxidation, anammox, which directly uses ammonium and nitrite as electronic donor and acceptor to produce  $\text{N}_2$ . Five genera of anammox bacteria (*Candidatus 'Brocadia'*, *Candidatus 'Kuenenia'*, *Candidatus 'Scalindua'*, *Candidatus 'Anammoxoglobus'* and *Candidatus 'Jettenia'*), which form a monophyletic order of bacteria, the Brocadiales, have been enriched and described [10]. Recently, anammox bacteria were detected in many marine ecosystems, freshwater ecosystems and man-made environments [6, 11] and believed to be responsible for 13 and 50 % of  $\text{N}_2$  production in freshwater and marine ecosystems, respectively [10, 12].

In a specific ecosystem, anammox and n-damo bacteria compete for nitrite. Their presence or co-occurrence is related to some important environmental factors such as  $\text{CH}_4$ , nitrite, and ammonia. This phenomenon was confirmed by a recent research of Haroon et al., in which simultaneous AOM, nitrate reduction and anammox were detected in an anaerobic bioreactor after being

pulse-fed with nitrate, ammonium and CH<sub>4</sub>. In this system, anammox bacterium, Candidatus '*Kuenenia stuttgartiensis*' effectively out-competed '*M. oxyfera*' for nitrite [13]. However, information on the relationship or co-occurrence of n-damo and anammox bacteria in other man-made or natural environment ecosystems is very limited.

The Three Gorges Reservoir Dam is the largest hydroelectric dam in China and even in the world. The water-level fluctuation zone (WLFZ) of the Three Gorges Reservoir locates across Hubei Province and Chongqing Municipality along the Yangtze River with an area of over 400 km<sup>2</sup>, and experiences a novel hydrological regime with half a year (May - September) exposed over summer and the other half (October - April) submerged over winter and with water level fluctuating between the elevations of 145 - 175 m. Since it was formed in 2003, the large variation of ecosystems and heavy nitrogen input from industries and agricultures make the WLFZ of the reservoir a favorable habitat for both anammox and n-damo bacteria, forming a very special micro-ecosystem. However, these two important processes that impact the nitrogen sink and CH<sub>4</sub> emission have never been researched in such an environment.

In this study, the co-occurrence of *M. oxyfera*-like and anammox bacteria was detected in paddy fields near the Yangtze River and the WLFZ soil of the Three Gorges Reservoir. Their abundance, compositions and diversity were discussed.

## MATERIALS AND METHODS

**Sample collection and determination of physical and chemical characteristics.** Six sample sites were selected along WLFZ of the Three Gorges Reservoir in March 2014 (Fig. 1): XXH (Xiangxihe, 30°59'07.38" N, 110°45'38.65" E), WS (Wushan, 31°05'22.25" N, 109°54'03.57" E), WJG (Wangjiagou, 29°54'1.08" N, 107°29'38.41" E), XJ (Xiaojiang, 30°57'50.33" N, 108°42'34.53" E), ZXH (Zhuxihe, 30°49'11.92" N, 108°22'01.89" E) and PS (Paddy soil, 29°48'40.94" N, 107°27'21.66" E). The water level in the WLFZ of the Three Georges Reservoir was decreasing during the sampling period, but the sampling sites were still covered by 20 - 30 cm of water. PS samples were collected from a flooded paddy field along the Yangtze River near Fuling during the rice seedling period. Soil samples were collected from the fields using a plexiglass ring sampler (5 cm diameter and 30 cm length). The soil cores were placed in sterile plastic bags, sealed and transported to the laboratory on ice. Then they were

sliced at 10 cm intervals, and slices of the same depth (at least five slices in one field) were mixed to form one composite sample. All samples were sectioned into two subsamples: one frozen at -80 °C for molecular analysis and the other stored at 4 °C for analysis of physical and chemical characteristics.

The physical and chemical characteristics were determined using standard methods. Soil pH was measured by pH S-2F digital acidity meter (Leici, Shanghai, China) at a soil/water ratio of 1:2.5. Total organic carbon (TOC) was determined by the K<sub>2</sub>Cr<sub>2</sub>O<sub>7</sub> oxidation method and ammonium, nitrite and nitrate were extracted from the soil using 2 M KCl according to the previous report [14]. Then, their contents were measured by Dionex DX-120 ion chromatography following EPA Standard Method 4110. The characteristics of the samples are shown in Table 1.

### DNA extraction, quantification of *M. oxyfera*-like, anammox and total bacteria.

Genomic DNA of each sample was extracted from 0.5 g soil (dry weight) sample using a Soil DNA kit (OMEGA BIO-TEK, Norcross, GA, USA) according to the manufacturer's instructions. Extracted DNA was then examined using a NanoDrop 2000 spectrophotometer (Thermo Fisher Scientific, Wilmington, DE).

The copy numbers of *M. oxyfera*-like, anammox and total bacteria were quantified through a real-time PCR technique. The primers and PCR conditions are shown in Table 1s. The standards were prepared using serially diluted plasmid DNA with 10<sup>3</sup> - 10<sup>8</sup> gene copies μl<sup>-1</sup>. Two independent real-time PCR assays were performed on each of the three replicate DNA samples. Standard curves were generated by plotting the threshold cycle values vs. log<sub>10</sub> of the gene copy numbers.

### Phylogenetic analysis of *M. oxyfera*-like and anammox bacteria.

Phylogenetic analysis of *M. oxyfera*-like bacteria was conducted through analyzing 16S rRNA genes and an important functional gene, *pmoA* gene. For 16S rRNA gene amplifications, nested-PCR was performed with a specific forward primer 202F and a universal bacterial reverse primer 1492R in the first round, and a specific PCR primer-pair of qP1F-qP2R in the second round. For *pmoA* gene amplifications, another nested PCR was conducted with forward primer A189-b and reverse primer cmo682 in the first round, and a specific primer pair of cmo182 and cmo568 in the second round. Phylogenetic relationships of anammox bacteria were analyzed through *hzsB* genes using a pair of primers, *hzsB*-

396F and hzsB-742R, which are very specific to anammox bacteria. The detailed information on all the primers and reaction conditions were shown in Table 1s.

The above PCR products were respectively ligated to pMD19-T vector (TaKaRa) according to the manufacturer's instructions and transformed into *E. coli* DH5- $\alpha$  to construct clone libraries. At least 50 positive clones were selected for sequencing from each library (GENEWIZ, Beijing, China). The quality of the recovered sequences was checked using the Chromas Lite (version 2.01) program. Phylogenetic trees were constructed by using the neighbor joining method in MEGA 4.1 software, and the robustness of tree topology was tested by bootstrap analysis (1000 replicates).

**Statistical analysis.** The operational

taxonomic unit (OTU) cut-off values of 3 and 7 % were applied to determine the 16S rRNA gene and *pmoA* gene diversities of *M. oxyfera*-like bacteria, respectively. Meanwhile, the cut-off values of 10 % were used to determine the *hzsB* gene diversity of anammox. OUT, alpha diversity (Chao1 estimator and Shannon index) and Good's coverage in each clone library were generated by Mothur program.

**Nucleotide sequence accession numbers.** The sequences reported in this study were deposited in the GenBank database under accession numbers KP708851-KP708984 (*M. oxyfera*-like 16S rRNA genes), KP743748-KP743872 (*M. oxyfera*-like *pmoA* genes), and KP743873-KP743791 (anammox *hzsB* genes).

TABLE 1

Physical and chemical characteristics of the samples recovered from soils of the WLFZ. TOC-total organic carbon,  $W_{dm}$ -dry matter content on a mass basis, bd-below detection limit.

Sampling site	Depth (cm)	pH	TOC (g / kg)	$W_{dm}$ (%)	$NO_3^-$ -N (g / kg)	$NO_2^-$ -N (g / kg)	$NH_4^+$ -N (g / kg)	Fe (g / kg)
XXH	0~10	7.13	7.39	76.55	0.022	bd	bd	0.37
	10~20	7.02	3.87	74.88	0.016	bd	bd	0.38
	20~30	7.08	6.78	77.62	0.008	bd	bd	0.18
WS	0~10	7.24	8.6	70.48	0.061	bd	bd	0.41
	10~20	6.84	9.89	75.98	0.176	bd	bd	0.15
	20~30	6.86	8.47	78.01	0.050	0.0004	bd	0.23
WJG	0~10	7.5	9.35	66.34	0.017	bd	bd	0.39
	10~20	7.5	13.95	71.43	0.040	bd	bd	0.44
	20~30	7.93	8.13	73.78	0.020	bd	0.0126	0.39
XJ	0~10	7.5	5.02	75.59	0.023	bd	bd	0.33
	10~20	7.63	4.07	79.08	0.023	bd	bd	0.36
	20~30	7.76	6.71	80.91	0.027	bd	bd	0.36
ZXH	0~10	7.37	14.08	70.23	0.027	bd	bd	0.09
	10~20	7.5	13.13	72.64	0.006	bd	bd	0.31
PS	0~10	7.01	9.08	71.1	0.036	bd	bd	0.34
	10~20	7.05	8.47	73.32	0.014	bd	bd	0.29
	20~30	7.8	7.45	74.99	0.030	bd	bd	0.31

Table 1s. Annual average methane emission of sampling sites and some other environments recovered from publications.

Table 2s. The primers and thermal profiles used in the current study.

Table 3s. The  $\alpha$ -diversity of 16S rRNA and *pmoA* gene in *M. oxyfera*-like bacteria and *hzsB* gene in anammox bacteria collected from the WLFZ.

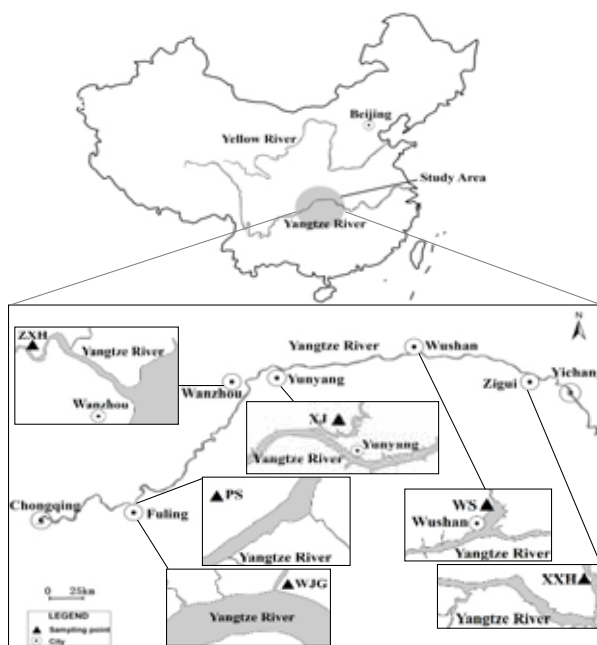


**FIGURE 1**

**The study area and sampling sites in the water-level-fluctuation zone of the Three Gorges Reservoir in China (▲, sampling sites and sampling names; ○ city names).**

Fig. 1s. Relative proportions of the copy numbers of *M. oxyfera*-like and anammox bacteria to total bacteria in different soil samples from WLFZ and the paddy fields. XXH, samples from Xiangxihe, 30°59'07.38" N, 110°45'38.65" E; WS, samples from Wushan, 31°05'22.25" N, 109°54'03.57" E; WJG, samples from Wangjiagou, 29°54'1.08" N, 107°29'38.41" E; XJ, samples from Xiaojiang, 30°57'50.33" N, 108°42'34.53" E; ZXH, samples from Zhuxihe, 30°49'11.92" N, 108°22'01.89" E; PS, samples from Paddy soil, 29°48'40.94" N, 107°27'21.66" E; In each sampling site, three samples were collected from soil core with depth of 0 - 10 cm, 10 - 20 cm and 20 - 30cm, and were assigned the same sampling name.

## RESULTS AND DISCUSSION

**Distribution and abundance of *M. oxyfera*-like and anammox bacteria in the WLFZ of the Three Gorges Reservoir.** Quantitative PCR using primer pairs specific to 16S rRNA genes of total bacteria, *M. oxyfera*-like bacteria and anammox bacteria was conducted across all the samples from six sample sites in Fig. 1. The results reflected relative abundance of these bacteria in different sampling sites (Fig. 2). The copies of total bacteria ranged from  $1.41 \times 10^{12}$  to  $3.73 \times 10^{13} \text{ g}^{-1}$  soil among samples with about one or two orders of magnitude decrease in some deeper samples (20 - 30 cm). The abundance of *M. oxyfera*-like and anammox bacteria clearly varied between different samples, especially in different sites. The copies of *M. oxyfera*-like bacteria in samples of WLFZ ranged from  $1.15 (\pm 0.2) \times 10^5$  to  $1.48 (\pm 0.16) \times 10^7 \text{ g}^{-1}$ , which were much higher than  $1.20 (\pm 0.19) \times 10^4$  to  $2.53 (\pm 0.39)$

$\times 10^4 \text{ g}^{-1}$  in PS samples ( $p < 0.01$ ). However, the copies of anammox bacteria in samples of WLFZ ranged from  $1.07 (\pm 0.42) \times 10^3$  to  $7.77 (\pm 0.87) \times 10^4 \text{ g}^{-1}$ , which were generally much lower than  $9.78 (\pm 0.78) \times 10^3$  to  $3.65 (\pm 0.76) \times 10^6 \text{ g}^{-1}$  in the PS samples ( $p < 0.01$ ).

Fig. 1s shows the trends in the relative proportion of *M. oxyfera*-like or anammox bacteria to total bacteria in different sampling sites, which is consistent with the values of relative abundance.

The abundance of *M. oxyfera*-like bacteria in WLFZ soil cores in this study was similar to the values reported for other freshwater systems, including lake or river sediments, wetland systems and a reported paddy soil ( $10^5 - 10^7$  copies  $\text{g}^{-1}$  sediment or soil) [3, 4, 7, 9, 10]. However, the abundance of anammox bacteria in WLFZ in this study was lower than values reported for the river sediments and paddy fields ( $10^5 - 10^7$  copies  $\text{g}^{-1}$  sediment or soil) [11, 15, 16].

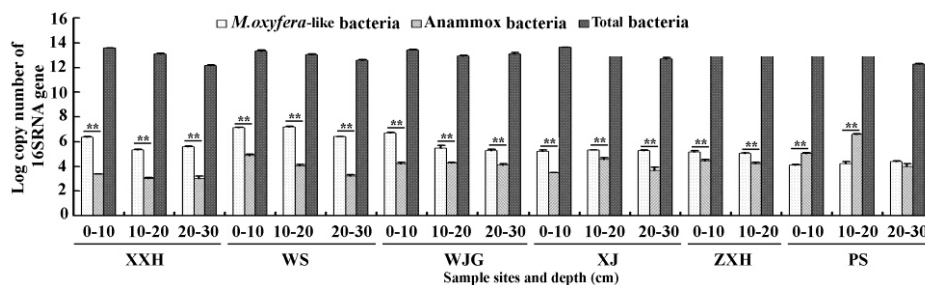


FIGURE 2

Copy numbers of 16S rRNA genes of *M. oxyfera*-like, anammox and total bacteria in different soil samples recovered from WLFZ and the paddy field samples. XXH, samples from Xiangxihe; WS, samples from Wushan; WJG, samples from Wangjiagou; XJ, samples from Xiaojiang; ZXH, samples from Zhuxihe; PS, samples from Paddy soil. Special locations of each sampling site were described in material and methods. In each sampling site, three samples were collected from soil core with depth of 0 - 10 cm, 10 - 20 cm and 20 - 30cm, and were assigned the same sampling name. \*\* $p < 0.01$ . Bars represent means  $\pm$  SD from three independent experiments. Statistical analysis was performed using Student's t-test.

Previous reports showed that *M. oxyfera*-like and anammox bacteria have a competitive relationship in a specific environment and fight for their common nitrogen source, nitrite. Besides the above limited factor, the distribution of these two groups of bacteria also depends on the available electron donors,  $\text{CH}_4$  for *M. oxyfera*-like bacteria and ammonia for anammox bacteria. In conditions of sufficient ammonia, anammox bacteria will out-compete *M. oxyfera*-like bacteria for nitrite [13, 17]. In this study, both groups of bacteria were detected across all samples, suggesting that they co-occurred and were widely distributed in the WLFZ of the Three Gorges Reservoir. However, the contents of nitrite and ammonia were undetectable in most samples (Table 1). One reason might be that nitrite was exhausted by *M. oxyfera*-like and anammox bacteria. Nitrite in nature comes from nitrate reduction mediated by denitrifying bacteria under anaerobic condition, and from ammonia oxidation by ammonia oxidizing bacteria under aerobic conditions. In this case, WLFZ soil was submerged in water for almost six months and formed an absolute anaerobic environment. The emission of  $\text{CH}_4$  in this area has been largely reported (Table 2s). We detected the presence of nitrate across all samples although the values were very low. It is well known that nitrate can be reduced to nitrite in such anaerobic environments. Therefore, the required environmental and nutritional conditions for the co-presence of *M. oxyfera*-like and anammox bacteria were present in WLFZ soil. Because of the co-occurrence of these two groups of bacteria, nitrite might be exhausted to undetectable levels. Similar results were obtained from Qiantang River sediment and an anaerobic bioreactor pulse-fed with nitrate,

ammonium and  $\text{CH}_4$ , in which nitrite was also undetectable [7, 13]. Therefore, nitrite was the limit factor for these two groups of bacteria in WLFZ of the Three Georges Reservoir.

For the above reason, the contents of ammonia and  $\text{CH}_4$  should be the determinative factors for the relative abundance of *M. oxyfera*-like and anammox bacteria in this study. Ammonia was also undetectable in all samples except for WJG in 20-30 cm (Table 1), possibly explaining the relatively low abundance of anammox bacteria.  $\text{CH}_4$  is considered a type of greenhouse gas and its effects were 20 times higher than that of  $\text{CO}_2$  [7]. Some lakes, especially periodically submerged and exposed WLFZs, are believed to be 'hot' sites for producing  $\text{CH}_4$ . However, recent studies reported that the levels of  $\text{CH}_4$  in the WLFZ of the Three Gorges Reservoir in China were not as high as other similar environments such as tropical and some temperate reservoirs as summarized in Table 1s, which might have an intimate relationship with the presence of  $\text{CH}_4$  oxidizing organisms such as *M. oxyfera*-like bacteria or other aerobic  $\text{CH}_4$  oxidizing bacteria. In this study, although *M. oxyfera*-like bacteria usually grow slowly, continuous production of  $\text{CH}_4$  promoted their growth and resulted in much higher abundance of *M. oxyfera*-like than anammox bacteria in WLFZ samples. The high prevalence of *M. oxyfera*-like bacteria greatly decreased the discharge of  $\text{CH}_4$  from sediments and soils in the WLFZ.

Compared to the WLFZ, paddy fields are generally fertilized with nitrogenous fertilizers leading to high nitrate and ammonium input. This would be helpful for the growth of anammox bacteria under anaerobic conditions, although, due to

being largely consumed in the paddy field, the contents of nitrate, nitrite and ammonium in the present study were not raised significantly. Our results from the flooded PS indicated that the anammox bacteria out-competed *M. oxyfera*-like bacteria in such an environment, especially in the top layer of the field (0 - 20 cm). In addition, the prevalence of anammox bacteria in the flooded PS was generally significantly higher than for WLFZ (Fig. 2). The relative abundances of anammox and *M. oxyfera*-like bacteria differed from the values reported by Shen et al (2014c) in which these two groups of bacteria were at levels of the same order [ $10^5$  -  $10^6$  copies  $g^{-1}$  (dry weight)] with slightly higher abundance of *M. oxyfera*-like bacteria in

different layers of a flooded paddy soil. Our sampling rice field has been continuously cropped with rice for many years-no data on  $CH_4$  emission was reported here. However,  $CH_4$  emission from a similar site in Yunyang rice field (also along the Yangtze River near one of our sampling sites, XJ) was  $4.86 \text{ mg m}^{-2} \text{ h}^{-1}$ , which was more than 10 times of the mean  $CH_4$  emission in the WLFZ and the total mean values of the Three Georges Reservoir (Table 2s). Corresponding to this data, the abundance of *M. oxyfera*-like bacteria in the PS was significantly lower than that from the samples in WLFZ, which again suggested that *M. oxyfera*-like bacteria play important roles in lowering  $CH_4$  discharge.

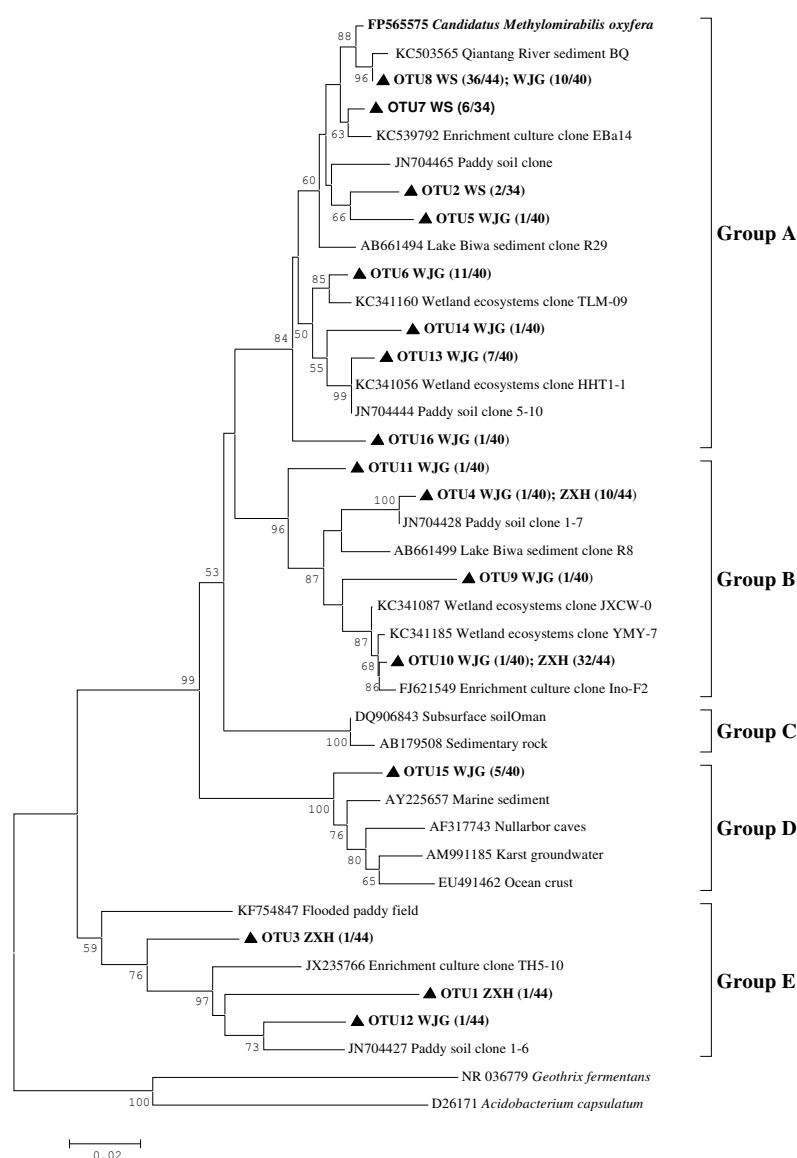


**FIGURE 3**

**Neighbour-joining phylogenetic tree showing the phylogenetic affiliations of *M. oxyfera*-like bacteria based on the 16S rRNA gene sequences recovered from sample WJG, WS and ZXH. Bootstrap values were 1,000 replicates, and the scale bar represents 2 % sequence divergence.**

The difference in abundance of *M. oxyfera*-like or anammox bacteria in samples within sampling sites was not significant ( $p > 0.05$ ), although there was a slight decrease with increasing depth in some sites. This reflected an insufficient sampling depth in this study.

**Compositions and diversity of *M. oxyfera*-like bacteria in WLFZ soils.** Based on the above abundance detection, three sampling sites (WS, WJG and ZXH, respectively) that reflected the highest, middle and lowest abundance of *M. oxyfera*-like and anammox bacteria were selected to research the diversity and compositions of *M. oxyfera*-like and anammox bacteria. The number of sequences, OTUs, Good coverage and  $\alpha$ -diversity were shown in Table 3s.

16S rRNA and *pmoA* genes were used to analyze the diversity and compositions of *M. oxyfera*-like bacteria. A total of 134 positive 16S rRNA gene sequences were obtained from the three samples and 128 of them (i.e. 95.5 %) were identified as related to *M. oxyfera*-like bacteria ( $> 84.38\%$  similarity). These *M. oxyfera*-like bacteria are allocated to the candidate division NC10 (NC10 bacteria). According to Ettwig et al., members of *M. oxyfera*-like bacteria are clustered into four groups, Groups A-D. In this study, the 128 *M. oxyfera*-like 16S rRNA gene sequences were binned into 16 OTUs based on 3 % differences, among which 13 OTUs fell into Groups A, B and D (Fig. 3) [18]. No sequence was found to fall into Group C. In sample WS, all 44 sequences were binned into only three OTUs, among which 81.8 % of them were OTU8. OTU8 was clustered into Group A in the phylogenetic tree and had the highest similarity (98.82 %) with the 16S rRNA gene sequence of *Candidatus 'Methylomirabilis oxyfera'* (FP565575) (Fig. 3) [2]. Sample WJG had much more diversity of *M. oxyfera*-like bacteria, indicated by a total 12 OTUs and distribution in Group A, B, D and E. The most prevalent OTUs (OTU6 and 8) in sample WJG were clustered in Group A together with a wetland ecosystem clone TLM-09 [19] and a Qiantang River sediment clone BQ [7], respectively. The latter was also shared by WS and closely related to the 16S rRNA gene sequence of *Candidatus 'Methylomirabilis oxyfera'* (FP565575) (Fig. 3). Most of sequences in sample ZXH were binned into OTU10 (72.7 %) and OTU4 (22.7 %) which had the most similarity with an enrichment culture clone Ino-F2 and a paddy soil clone, respectively, in Group B [6, 18]. Although Group A was a common group of *M. oxyfera*-like bacteria, no sequence fell into this

group from sample ZXH. Totally, the diversities of *M. oxyfera*-like bacteria were generally higher than other reported environments [3, 5, 9].

Previous studies showed that the *M. oxyfera* bacterial genome contains the complete pathway for aerobic oxidation of  $\text{CH}_4$  [2]. So the *pmoA* gene, which encodes one of the  $\beta$ -subunits of particulate methane monooxygenase, can be used as a functional marker to monitor and identify *M. oxyfera*-like bacteria on a functional level [20]. In this study, a total of 141 positive *pmoA* sequences were obtained from the above three samples and 134 of them were identified as related to *pmoA* of *M. oxyfera* (similarity  $> 84.62\%$ ). They were binned to 10 OTUs based on 7 % differences using Mothur program and fell into the six clusters in the phylogenetic analysis using the phylogenetic tree of Shen et al. [7] as a reference (Fig. 4). In the samples of both WJG and WS, the most abundant *pmoA* genes were represented by OTU8 (in Cluster I) occupying 60 % and 56.2 % of the total *pmoA* sequences for the two samples respectively. Compared to other OTUs, sequences of OTU8 had the highest identities (90.51 - 95.38 %) with the *pmoA* of *M. oxyfera*. This result was consistent with the analysis results of 16S rRNA gene sequences in which the sequences of the most abundant OTUs in the samples of both WJG and WS had the highest identities with *M. oxyfera*. As for the 16S rRNA gene sequence analysis results, *pmoA* gene sequences from ZXH were far from the *pmoA* of the known isolate, *Candidatus 'Methylomirabilis oxyfera'* (FP565575), and no *pmoA* sequence from ZXH was assigned to Clusters I and Cluster II. The most abundant sequences from ZXH were represented by OTU5 occupying 86.8 % of the recovered *pmoA* sequences. They were grouped into Cluster III in the phylogenetic tree and had identities of 88.51 - 88.72 % with the gene from *Candidatus 'Methylomirabilis oxyfera'* (FP565575) (Fig. 4).

Although assigned to 10 OTUs and six clusters, the similarity among the recovered *pmoA* sequences was very high (84.62 - 100 %) in this study. The same phenomena were also found in other environments such as Lake Constance [5], paddy fields [6] and peatlands [4]. This result implied that the evolution of *pmoA* genes was slower than 16S rRNA genes in *M. oxyfera*-like bacteria; however, the *pmoA* were still good biomarkers for *M. oxyfera*-like bacteria in the environment. The diversity of *pmoA* genes in this study was higher compared to previous reports in other paddy soils, a freshwater reservoir, activated sludge [21] and wetlands [9], in which at most seven OTUs were detected.



**FIGURE 4**

**Neighbour-joining phylogenetic tree showing the phylogenetic affiliations of *M. oxyfera*-like bacterial *pmoA* gene sequences recovered from sample WJG, WS and ZXH. Bootstrap values were 1,000 replicates, and the scale bar represents 5 % sequence divergence.**

**Compositions and diversity of anammox *hzsB* genes in WLFZ soils.** Several methods have been used to detect the presence and activity of anammox bacteria in the environment, including 16S rRNA gene-based approaches, among which a *hzsC*, *hzsB* and *hzsA* gene cluster, responsible for the hydrazine synthase protein was confirmed and considered to be very good biomarker due to their absence from other genomes sequenced so far [22]. In this study, we used *hzsB* as the biomarker to investigate the diversity of anammox bacteria in WLFZ soil.

A total of 101 positive *hzsB* sequences were obtained from the three samples (WJG, WS and ZXH) and binned into 11 OTUs based on 10 % differences in the recovered *hzsB* sequences of anammox (Table 3s and Fig. 5). Further phylogenetic analysis showed that all *hzsB* sequences recovered in the three samples were clustered into four groups: Groups A - D (Fig. 5). The sequences in Group A, B and D had identities of 88.02 - 89.06 %, 84.11 - 86.58 % and 89.58 - 98.44 %, respectively, with the *hzsB* from the known anammox species, *Candidatus 'Brocadia fulgida'*, *Candidatus 'Brocadia anammoxdianas'* and

*Candidatus 'Kuenenia'*. The sequences of OTU2 from samples WS and ZXH formed an individual cluster, Group C, displaying 76.82 - 79.43 % identities with *hzsB* from the above described anammox species. Of the 101 *hzsB* sequences, 58.42 % were clustered with *Candidatus 'Brocadia fulgida'* in Group A. These sequences were present in all three samples and thus represented the dominant species of anammox bacteria in WLFZ, especially samples WS and ZXH. The sequences from WJG were mostly distributed in Groups B and D, suggesting that species of *Candidatus 'Kuenenia'* and *Candidatus 'Brocadia anammoxdianas'* were dominant. The phylogenetic tree showed that Groups A and Group B represented different species of genus *Candidatus 'Brocadia'*.

In this study, only two genera, *Candidatus 'Brocadia'* and *Candidatus 'Kuenenia'*, were detected in the samples of WLFZ; and *Candidatus 'Brocadia'* was the most prevalent genus occupying 81.2 % of the total representative sequences (Groups A and B). This result was consistent with previous conclusions that representatives of *Candidatus 'Brocadia'* were the most detected anammox genus in soils [6, 23].



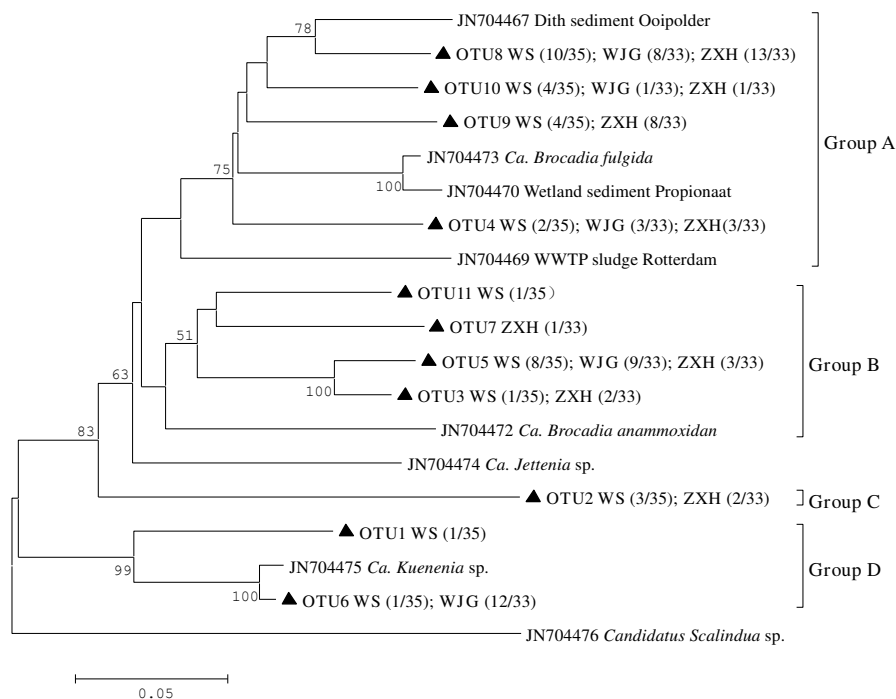


**FIGURE 5**

**Neighbour-joining phylogenetic tree showing the phylogenetic affiliations of anammox *hzsB* gene sequences recovered from sample WJG, WS and ZXH. Bootstrap values were 1,000 replicates, and the scale bar represents 5 % sequence divergence.**

The n-damo process has received much attention in recent years due to its important roles in linking the two major global nutrient cycles of carbon and nitrogen, providing a sink for the greenhouse gas CH<sub>4</sub> and alleviating the greenhouse effects [9]. The presence of *M. oxyfera*-like bacteria that mediated the n-damo process has been confirmed in various environments such as wetlands [9], sediments of lakes [5] and minerotrophic peatland [4], etc. However, the co-occurrence of n-damo and another important nitrogen conversion process, anammox process, has only been reported in paddy fields and saline lakes [6, 10, 24]. This is the first report on co-occurrence of *M. oxyfera*-like and anammox bacteria responsible for these two processes in a WLFZ soil. The special hydrological regime in WLFZs formed a unique soil environment with annual alternating organic matter deposition and anoxic CH<sub>4</sub> emission. Pollution from various sources provides nitrogen nutrients for these two groups of functional bacteria. The results in this study indicated a higher diversity of *M. oxyfera*-like and anammox bacteria in WLFZ soil than other reported environments.

## CONCLUSION

This study includes the first report of the co-occurrence of *M. oxyfera*-like and anammox bacteria in WLFZ soils in the Three Georges Reservoirs in China. The abundance of *M. oxyfera*-like bacteria in all WLFZ soil samples was much higher than in the paddy field in this study. Within WLFZ soil samples, the relative abundance of *M. oxyfera*-like bacteria was significantly higher than that of anammox bacteria, which was contrasted with the case in the paddy field. These phenomena implied that the limited nitrogen source and annual alternating CH<sub>4</sub> emission and organic carbon source deposition in WLFZ environments were the main factors determining the relationship of these two important groups of bacteria in WLFZ, although further confirmation is required. Higher diversities of *M. oxyfera*-like and anammox bacteria were detected in WLFZ soils than in other reported natural environments.

## ACKNOWLEDGEMENTS

The authors would like to acknowledge the financial support from the National Natural Science Foundation of China (NSFC 21477035, NSFC 21277041 and U1504301), Program for Innovative Research Team (in Science and Technology) in University of Henan Province (IRTSTHN, 13IRTSTHN009), The Outstanding Talented Persons Foundation of Henan Province (144200510007), The Specialized Research Fund for the Doctoral Program of Higher Education (20134104110006), Educational Commission of Henan Province of China (15A180016) and Doctor Initiative Foundation of Henan Normal University (qd14166).

## REFERENCES

- [1] Raghoebarsing, A.A., Pol, A., van de Pas-Schoonen, K.T., Smolders, A.J., Ettwig, K.F., Rijpstra, W.I., Schouten, S., Sinninghe Damsté, J.S., den Camp, H.J.O., Jetten M.S.M. and Strous M. (2006) A microbial consortium couples anaerobic methane oxidation to denitrification. *Nature* 440, 918-921.
- [2] Ettwig, K.F., Butler, M.K., Le Paslier, D., Pelletier, E., Mangenot, S., Kuypers, M.M., Schreiber, F., Dutilh, B.E., Zedelius, J., Beer, D., Gloerich, J., Wessels, H.J.C.T., Alen, T.V., Luesken, F., Wu, L.M., Pas-Schoonen, K.T., den Camp, H.J.O., Janssen-Megens, E.M., Francoijs, K.J., Stunnenberg, H., Weissenbach, J., Jetten, M.S.M. and Strous, M. (2010) Nitrite-driven anaerobic methane oxidation by oxygenic bacteria. *Nature* 464, 543-548.
- [3] Kojima, H., Tsutsumi, M., Ishikawa, K., Iwata, T., Mußmann, M. and Fukui, M. (2012) Distribution of putative denitrifying methane oxidizing bacteria in sediment of a freshwater lake, Lake Biwa. *Syst. Appl. Microbiol.* 35, 233-238.
- [4] Zhu, B.L., van Dijk, G., Fritz, C., Smolders, A.J.P., Pol, A., Jetten, M.S.M. and Ettwig, K.F. (2012) Anaerobic oxidation of methane in a minerotrophic peatland: enrichment of nitrite-dependent methane-oxidizing bacteria. *Appl. Environ. Microbiol.* 78, 8657-8665.
- [5] Deutzmann, J.S. and Schink, B. (2011) Anaerobic oxidation of methane in sediments of Lake Constance, an oligotrophic freshwater lake. *Appl. Environ. Microbiol.* 77, 4429-4436.
- [6] Wang, Y., Zhu, G.B., Harhangi, H.R., Zhu, B.L., Jetten, M.S.M., Yin, C.Q. and den Camp, H.J.O. (2012) Co-occurrence and distribution of nitrite-dependent anaerobic ammonium and methane oxidizing bacteria in a paddy soil. *FEMS Microbiol. Lett.* 336, 79-88.
- [7] Shen, L.D., Liu, S., Zhu, Q., Li, X.Y., Cai, C., Cheng, D.Q., Lou, P.L., Xu, X.Y., Zheng, P. and Hu, B.L. (2014) Distribution and diversity of nitrite-dependent anaerobic methane-oxidising bacteria in the sediments of the Qiantang River. *Microbiol. Ecol.* 67, 341-349.
- [8] Shen, L.D., Zhu, Q., Liu, S., Du, P., Zeng, J.N., Cheng, D.Q., Xu, X.Y., Zheng, P. and Hu, B.L. (2014) Molecular evidence for nitrite-dependent anaerobic methane-oxidising bacteria in the Jiaojiang Estuary of the East Sea (China). *Appl. Microbiol. Biotechnol.* 98, 5029-5038.
- [9] Hu, B.L., Shen, L.D., Lian, X., Zhu, Q., Liu, S., Huang, Q., He, Z.F., Geng, S., Cheng, D.Q., Lou, P.L., Xu, X.Y., Zheng, P. and He, Y.F. (2014) Evidence for nitrite-dependent anaerobic methane oxidation as a previously overlooked microbial methane sink in wetlands. *P. Natl. Acad. Sci. U.S.A.* 111, 4495-4500.
- [10] Shen, L.D., Liu, S., Huang, Q., Lian, X., He, Z.F., Geng, S., Jin, R.C., Lou, P.L., Xu, X.Y., Zheng, P. and Hu, B.L. (2014) Evidence for the Co-occurrence of Nitrite-Dependent Anaerobic Ammonium and Methane Oxidation Processes in a Flooded Paddy Field. *Appl. Environ. Microbiol.* 80, 7611-7619.
- [11] Yasunori, K., Koichiro, F., Yuki, T., Kento, Y. and Yanwei, Q. (2012) Temperature effect on nitrogen removal performance and bacterial community in culture of marine anammox bacteria derived from sea-based waste disposal site. *J. Biosci. Bioeng.* 113, 515-520.
- [12] Schubert, C.J., Durisch-Kaiser, E., Wehrli, B., Thamdrup, B., Lam, P. and Kuypers, M.M. (2006) Anaerobic ammonium oxidation in a tropical freshwater system (Lake Tanganyika). *Environ. Microbiol.* 8, 1857-1863.
- [13] Haroon, M.F., Hu, S.X., Shi, Y., Imelfort, M., Keller, J., Hugenholtz, P., Yuan Z.G. and Tyson, G.W. (2013) Anaerobic oxidation of methane coupled to nitrate reduction in a novel archaeal lineage. *Nature* 500, 567-570.
- [14] Shen, L.D., Liu, S., Lou, L.P., Liu, W.P., Xu, X.Y., Zheng, P. and Hu, B.L. (2013) Broad distribution of diverse anaerobic ammonium-oxidizing bacteria in Chinese agricultural soils. *Appl. Environ. Microbiol.* 79, 6167-6172.

- [15] Hu, B.L., Shen, L.D., Zheng, P., Hu, A.H., Chen, T.T., Cai, C., Liu, S. and Lou, P.L. (2012) Distribution and diversity of anaerobic ammonium-oxidizing bacteria in the sediments of the Qiantang River. *Environ. Microbiol. Rep.* 4, 540-547.
- [16] Zhu, G.B., Wang, S.Y., Wang, Y., Wang, C.X., Risgaard-Petersen, N., Jetten, M.S.M. and Yin, C.Q. (2011) Anaerobic ammonia oxidation in a fertilized paddy soil. *ISME J.* 5, 1905-1912.
- [17] Luesken, F.A., Sánchez, J., van Alen, T.A., Sanabria, J., den Camp, H.J.O., Jetten, M.S.M. and Kartal, B. (2011) Simultaneous nitrite-dependent anaerobic methane and ammonium oxidation processes. *Appl. Environ. Microbiol.* 77, 6802-6807.
- [18] Ettwig, K.F., van Alen, T., van de Pas-Schoonen, K.T., Jetten, M.S.M. and Strous, M. (2009) Enrichment and molecular detection of denitrifying methanotrophic bacteria of the NC10 phylum. *Appl. Environ. Microbiol.* 75, 3656-3662.
- [19] Zhu, G.B., Zhou, L.L., Jiang, B., Wang, Y., Wang, S.Y., Jetten, M.S.M. and Yin, C.Q. (2014) Biogeographical distribution of nitrite dependent anaerobic methanotrophic bacteria in wetland ecosystems: from regional scale to global scale. NCBI GenBank web <http://www.ncbi.nlm.nih.gov/nuccore/>. Accessed, 17.
- [20] Luesken, F.A., Zhu, B.L., van Alen, T.A., Butler, M.K., Diaz, M.R., Song, B., den Camp, H.J.O., Jetten, M.S.M. and Ettwig, K.F. (2011) pmoA primers for detection of anaerobic methanotrophs. *Appl. Environ. Microbiol.* 77, 3877-3880.
- [21] Han, P. and Gu, J.D. (2013) A newly designed degenerate PCR primer based on pmoA gene for detection of nitrite-dependent anaerobic methane-oxidizing bacteria from different ecological niches. *Appl. Microbiol. Biotech.* 97, 10155-10162.
- [22] Harhangi, H.R., Le Roy, M., van Alen, T., Hu, B.L., Groen, J., Kartal, B., Tringe, S.G., Quan, Z.X., Jetten, M.S.M. and den Camp, H.J.O. (2012) Hydrazine synthase, a unique phylomarker with which to study the presence and biodiversity of anammox bacteria. *Appl. Environ. Microbiol.* 78, 752-758.
- [23] Humbert, S., Tarnawski, S., Fromin, N., Mallet, M.P., Aragno, M. and Zopfi, J. (2010) Molecular detection of anammox bacteria in terrestrial ecosystems: distribution and diversity. *ISME J.* 4, 450-454.
- [24] Yang, J., Jiang, H.C., Wu, G., Hou, W.G., Sun, Y.J., Lai, Z.P. and Dong, H.L. (2012) Co-occurrence of nitrite-dependent anaerobic methane oxidizing and anaerobic ammonia oxidizing bacteria in two Qinghai-Tibetan saline lakes. *Front. Earth Sci.* 6, 383-391.

---

**Received: 08.03.2016**

**Accepted: 17.08.2016**

---

**CORRESPONDING AUTHOR:**

**Qingxiang Yang**

College of Life Sciences, Henan Normal University,  
Xinxiang 453007 – CHINA

E-mail: yangqx66@163.com

# PHYLOGENETIC RELATIONSHIPS OF *GERANIUM* SPECIES IN DIFFERENT REGIONS OF TURKEY

Onur Koloren\*, Secil Eker

University of Ordu, Faculty of Agriculture, Department of Plant Protection, Ordu, Turkey

## ABSTRACT

Most of the *Geranium* species are cultivated as medical plants and its roots are used in classical medicine, tanning, and staining. In this study, we phylogenetically analysed the 18S-26S rDNA the internal transcribed spacer (ITS) gene of *Geranium* species collected from different regions of Turkey to reveal the genetic diversity of them. Six haplotypes were found within all *Geranium* samples collected from Turkey by creating phylogenetic trees with neighbour-joining (NJ), maximum-parsimony (MP) and maximum-likelihood (ML) algorithms. The relationship between our haplotypes and *Geranium* species was well supported based on nucleotide sequence similarity and the pairwise genetic divergence analyses. Six haplotypes obtained in this study were clearly appeared in the same lineage with *Geranium gracile*, *Geranium ibericum*, *Geranium asphodeloides*, *Geranium microphyllum*, *Geranium* sp., *Geranium dissectum*. In addition, *Geranium microphyllum*, *Geranium* sp. and *Geranium dissectum* are the first reported by molecular phylogenetic analyses based on rDNA-ITS gene within all investigated *Geranium* samples collected from Turkey.

## KEYWORDS:

Geraniaceae, *Geranium*, Internal Transcribed Spacer, phylogeny

## INTRODUCTION

The genus *Geranium* L. (Geraniaceae) covers 400 species which distributed in most of the temperate areas and in tropical mountains of the world [1]. According to the classification reported by Yeo [2], *Geranium* is divided into three subgenera: subgen. *Erodioidea* (Picard) Yeo, subgen. *Robertium* (Picard) Rouy, and subgen *Geranium*. *G.* subgen. *Geranium* is the largest subgenus with more than 370 species classified in ten sections [3,4].

*Geranium dissectum* is a major floras of the Eastern Mediterranean areas and their around. However, *Geranium asphodeloides* (subsp. *asphodeloides* and subsp. *sintenisii*) was accepted as the Turkish taxa by Davis [5]. Davis described subsp.

*sintenisii* as *Geranium asphodeloides* s. str. in that time. *Geranium davisianum* was reported by Pesmen [6] and *Geranium chelikii* as previously described by Kit Tan and Yildiz [7] were new species in Turkey, but their species were included in *Geranium sintenisii*.

*Geranium ibericum* subsp. *jubatum* which is endemic for the Black Sea Region and *Geranium stepporum* were recognized as a distinct species as previously described in the floras of Turkey by Davis [5] and Iranica by Schönbeck-Temesy [8], however more recently, *Geranium stepporum* brought to synonymy of *Geranium tuberosum* [9].

According to our knowledge, several the *Geranium* species in Turkey has been reported with molecular phylogenetic studies providing nucleotide sequence data. *Geranium sintenisii* (AY944417 road Torul to Trabzon and Gumushane, road Yeniyoil to Yagmurdere of Turkey) and *Geranium asphodeloides* (AY944414- Evciler, Kaz Dagi and AY944415- Bandirma, Erdek of Turkey) within the genus *Geranium* L. were reported in Turkey by Aedo et al. [10]. *Geranium gracile* (AJ884925), *Geranium ibericum* (AJ884927), *Geranium kurdicum* (AJ884930), *Geranium libani* (AJ884932), *Geranium platypetalum* (AJ884938), *Geranium tuberosum* (AJ884946) in Turkey were found by Aedo et al. [3].

The phylogenetic relationships of the other native *Geranium* species in Turkey have not been reported, so far. We were performed phylogenetic study to provide more information toward the rDNA-ITS nucleotide sequences of *Geranium* species in Turkey. Thus, the aim of this study was to investigate between phylogenetic relationships of *Geranium* species the different regions of Turkey and the previously reported species from here, using 18S-26S rDNA-ITS nucleotide sequences.

## MATERIALS AND METHODS

**Plant materials.** Fourteen plant samples of the *Geranium* species collected freshly from different geographic locations in Turkey and seven samples from herbarium of Ordu University were used in this study. Table 1 presented the *Geranium* species used in the study with information on locations and origin. The young leaves of *Geranium* plants were taken

**TABLE 1**  
**The *Geranium* species used in the study with information on locations and origin and EMBL accession numbers for the rDNA- ITS nucleotide sequence**

Number of samples	Locations	Origin	EMBL Accession No	Haplotypes
O1	Ordu-Central	Herbarium	KX360638	
O2	Ordu-Central	Fresh young leaves	KX360639	
O3	Ordu-Central	Fresh young leaves	KX360640	
O4	Ordu-Central	Fresh young leaves	KX360641	Haplotype I
O5	Ordu-Fatsa	Fresh young leaves	KX360642	
O6	Ordu-Persembek	Fresh young leaves	KX360643	
O7	Ordu-Gulyalı	Fresh young leaves	KX360644	Haplotype II
O8	Ordu-Ulubey	Fresh young leaves	KX360651	Haplotype III
O9	Ordu-Efirli	Fresh young leaves	KX360652	Haplotype IV
G1	Giresun-Bulancak	Fresh young leaves	KX360649	
G2	Giresun-Piraziz	Fresh young leaves	KX360650	
A1	Adana-Balcalı	Fresh young leaves	KX360645	Haplotype V
A2	Adana-Balcalı	Fresh young leaves	KX360646	
A3	Adana-Catalan	Fresh young leaves	KX360647	
A4	Adana-Catalan	Fresh young leaves	KX360648	
M1	Manisa	Herbarium	KX360653	Haplotype IV
M2	Manisa	Herbarium	KX360654	
M3	Manisa	Herbarium	KX360655	
M4	Manisa	Herbarium	KX360656	
Mu1	Mugla	Herbarium	KX360657	Haplotype VI
Mu2	Mugla	Herbarium	KX360658	

from investigating sites and they were kept in a refrigerator until use for DNA extraction.

#### DNA extraction and PCR amplification.

DNA was extracted from the herbarium and young leaves of the *Geranium* species with CTAB method described by Haymes [11] and this protocol was used with some modifications as described before by Eker and Kolören [12]. Briefly, Starting plant materials (20 mg) were ground using a hand pestle under liquid nitrogen. The extraction buffer, chloroform/isoamylalcohol (24/1), ethanol/acetate (96/4), ethanol (70%) was applied according to Haymes's [11] protocol, respectively. Then, RNase (Qiagen)100 mg/mL) was added to DNA to get rid of RNA contamination. DNA was kept at -20 °C until using for PCR. ITS1 and ITS4 [13] gene fragments were amplified using polymerase chain reaction (PCR). The PCR reaction (25 µL) contained 10 mmol/L dNTPs, 2.5 mmol/L of MgCl<sub>2</sub>, 10 mmol/L of primers, 1 µL of template DNA, 5 U *Taq* polymerase (Thermo Scientific, Maxima Hot Start). The PCR was performed with a thermal cycler (PeqLab), starting at 95 °C for 5 min, followed by 35 cycles of 95 °C for 1 min, 48.7 °C for 2 min and 72 °C for 2 min, and a final extension at 72 °C for 7 min. After staining with ethidium bromide (1 mg/mL), PCR products were appeared under the QUANTUM ST5 (Vilber Lourmat) gel system.

**Phylogenetic analyses.** The PCR products were sequenced commercially by Macrogen Inc. (Amsterdam, the Netherlands) for forward and

reverse with primer set ITS1/ITS4. BioEdit [14] was used for combining the sequenced fragments. BLAST (Basic Local Alignment Search Tool in NCBI) scores for multiple nucleotide alignments between our *Geranium* samples and the other references of *Geranium* from GenBank were applied with ClustalX [15] and set aright with BioEdit [14]. Neighbor-Joining (NJ), Maximum-Parsimony (MP) and Maximum-Likelihood (ML) algorithms were conducted to evaluate the phylogenetic relationships between our samples and references from GenBank. Bootstrap analysis of the MP and ML were performed with 1.000 replications and 10.000 replications for NJ analyses to show satisfied with the trees. Genetic distances for our haplotypes were calculated using MEGA version 5.05. All haplotype sequences obtained in this study were deposited in the European Molecular Biology Laboratory (EMBL) data bank (<https://www.ncbi.nlm.nih.gov/genbank/update/>) under accession numbers KX360638- KX360658 (Table 1).

#### RESULTS AND DISCUSSION

The phylogenetic approaches with ITS and ETS nucleotide sequences are used as an alternative to the systematics of Linnaean system for classification of plant taxa. Thus, more recently, phylogenetically analyses of the rDNA-ITS nucleotide sequences were used to show the genetic diversity among

**TABLE 2**  
**List of reference sequences from EMBL GenBank used for phylogeny analyses with their accession number, origin and references**

Species	EMBL accession No.	Origin	References
<i>Geranium asphodeloides</i>	AY944414	Turkey	[10]
<i>Geranium sintenisii</i>	AY944416	Turkey	[10]
<i>Geranium ibericum</i>	AJ884925	Great Britain	[3]
<i>Geranium pusillum</i>	AF167151	Great Britain	[19]
<i>Geranium tuberosum</i>	AJ884946	Turkey	[3]
<i>Geranium crenophilum</i>	AY944411	Lebanon	[10]
<i>Geranium dissectum</i>	AY944413	Spain	[10]
<i>Geranium gracile</i>	AJ884927	Georgia	[3]
<i>Geranium kurdicum</i>	AJ884930	Turkey	[3]
<i>Geranium libani</i>	AJ884932	Turkey	[3]
<i>Geranium renardii</i>	AJ884938	Georgia	[3]
<i>Geranium sylvaticum</i>	DQ131914	Sweden	[20]
<i>Geranium platypetalum</i>	AJ884938	Georgia	[3]

organisms. ITS and ETS markers have still common phylogenetic signal between datasets, though recombination may have presented among the haplotypes. The similar groups can be appeared in the ITS and ETS networks at the end of branches with multiple paths [16]. The phylogenetic affiliation of the closely related species could be fast evolved by rDNA-ITS regions [17].

There are some researches about rDNA-ITS haplotypes of *Geranium* species were reported in GenBank. For instance, Adeo et al. [10] performed taxonomic revision of *Geranium* sect. *Dissecta* (*Geraniaceae*) and Adeo et al. [3] reported the taxonomic revision of *Geranium* Subsect. *Mediterranean* (*Geraniaceae*) by using plastid *trnL-trnF* spacer and ribosomal nuclear ITS regions with maximum parsimony and bayesian analyses to show phylogenetic relationship of them. Mitchell et al. [16] reported transcribed spacers of nrDNA (ITS1-5.8S-ITS2 and ETS) markers to represent phylogenetic relation of the New Zealand species of *Geranium* and they found that low DNA sequence variation for the indigenous New Zealand species of

*Geranium*. Nishida et al. [18] reported the molecular phylogenetic analyses of *Geranium robertianum* populations recently found in Japan by using the plastid regions of the *trnL* intron, *trnL3'-trnF* and *trnHpsbA* intergenic spacer regions, and the nuclear internal transcribed spacer (ITS).

According to information obtained references, there are limited studies about the *Geranium* species in Turkey, so far. Aedo et al. [3,10] reported the *Geranium* species in Turkey such as *Geranium gracile* (AJ884925), *Geranium ibericum* (AJ884927), *Geranium kurdicum* (AJ884930), *Geranium libani* (AJ884932), *Geranium platypetalum* (AJ884938), *Geranium tuberosum* (AJ884946), *Geranium asphodeloides* (AY944414), *Geranium sintenisii* (AY944416).

In our study, we presented molecular phylogenetic analyses of the *Geranium* species collected from different regions of Turkey by using the 18S-26S (rDNA-ITS) (approximately 695 bp) gene. Thus, we found *Geranium gracile*, *Geranium ibericum*, *Geranium asphodeloides* in investigated area as previously described by Aedo et al. [3,10]. In addition, we found *Geranium microphyllum*, *Geranium* sp., *Geranium dissectum*, besides of previously reported *Geranium* species.

According to BLAST results, we determined our haplotypes are related to *Geranium* species and we set up a data set as shown in Table 2. The list of reference sequences from GenBank used for phylogeny analyses with their accession numbers in this study as presented in Table 2.

Phylogenetic analyses were performed over 648 aligned nucleotides with 372 segregating sites. In our study, we found six haplotypes among analysed plant samples. Haploype-I was presented by six samples (O1, O2, O3, O4, O5, O6). Haplotype-II (O7), Haplotype-III (O8), Haplotype-IV (O9, M1, M2, M3, M4), Haplotype-V (G1, G2, A1, A2, A3, A4) and Haplotype-VI (Mu1, Mu2) were represented in our samples. The phylogenetic trees drawn with NJ, MP and ML algorithms and our haplotypes were placed in the same lineage with *Geranium gracile*, *Geranium ibericum*, *Geranium asphodeloides*, *Geranium microphyllum*, *Geranium* sp. and *Geranium dissectum* as shown in Figure 1.

The nucleotide sequence similarities between our haplotypes and references shared the same lineage as shown in Table 3. Haplotype-I represented as sister to *Geranium gracile* with 100% nucleotide sequence similarity and the pairwise genetic divergence was 0.000. This relation was supported with 97%, 92% bootstrap value in the NJ and ML trees. Haplotype-II appeared as sister to the lineage *Geranium ibericum* and its nucleotide sequence similarity was 100% and the pairwise genetic divergence was 0.000.

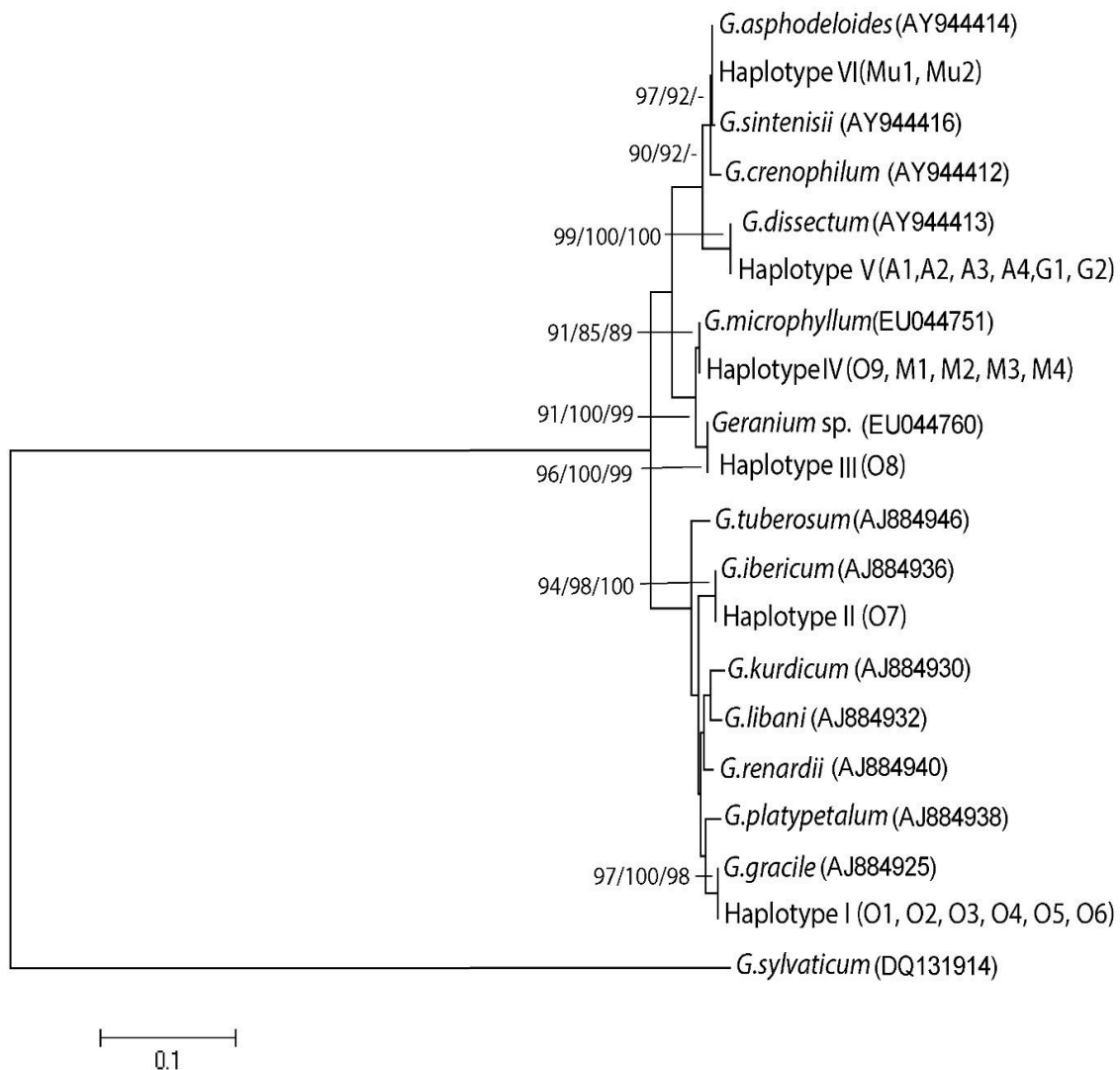


**FIGURE 1**

**Phylogenetic tree with NJ algorithm between *Geranium* haplotypes from this study and references of *Geranium* species obtained from GenBank. Bootstrap values (higher than 70%) from NJ, ML and MP analyses are shown, respectively.**

This node was also approved with 94%, 98% and 100% bootstrap value in the NJ, ML, MP trees. The nucleotide sequence similarity and genetic divergence between Haplotype-III and *Geranium* sp. were 99.8% and 0.001. This relation was supported with 96%, 100% and 99% bootstrap values in the NJ, ML and MP trees. Haplotype-IV represented as sister to *Geranium microphyllum* with 99.2% nucleotide sequence similarity and the pairwise genetic divergence was 0.003. This relation was supported with 91%, 85% and 89% bootstrap values in the NJ, ML and MP trees. The nucleotide sequence similarity and genetic divergence between Haplotype-V and *Geranium dissectum* were 100% and 0.000. This node was also approved with 99%, 100% and 100% bootstrap value in the NJ, ML, MP trees. Haplotype-VI represented as sister to

*Geranium asphodeloides* with 99.6% nucleotide sequence similarity and the pairwise genetic divergence was 0.002. This relation was supported with 97%, and 92% bootstrap values in the NJ, ML trees.

As a result of this study represented that the clade consisting of our six haplotypes in different regions of Turkey are closely related with the clade of *Geranium* subgenus (*Geranium gracile*, *Geranium ibericum*, *Geranium asphodeloides*, *Geranium microphyllum*, *Geranium* sp., *Geranium dissectum*). Whereas, *Geranium gracile*, *Geranium ibericum*, *Geranium asphodeloides* were previously reported in Turkey, *Geranium microphyllum*, *Geranium* sp. and *Geranium dissectum* are the first reported by molecular phylogenetic analyses based on rDNA ITS gene in here.

TABLE 3

The nucleotide sequence percentage similarities and pairwise estimate of evolutionary divergence between *Geranium* haplotypes obtained in this study and related references *Geranium* species from GenBank

	<i>G. microphyllum</i>	<i>G. sylvaticum</i>	<i>G. sintenisii</i>	<i>G. tuberosum</i>	<i>G. dissectum</i>	<i>Geranium sp.</i>	<i>G. asphodeloides</i>	<i>G. kurdicum</i>	<i>G. libani</i>	<i>G. platyepetalum</i>	<i>G. ibericum</i>	<i>G. gracile</i>	<i>G. renardii</i>	<i>G. crenophilum</i>	Haplotype I	Haplotype II	Haplotype III	Haplotype IV	Haplotype V	Haplotype VI
<i>G. microphyllum</i>	ID	0,449	0,925	0,899	0,919	0,989	0,929	0,9	0,904	0,91	0,899	0,908	0,897	0,924	0,908	0,899	0,989	1	0,919	0,929
<i>G. sylvaticum</i>	1,0602	ID	0,446	0,45	0,446	0,451	0,445	0,439	0,444	0,445	0,449	0,447	0,445	0,442	0,447	0,449	0,451	0,449	0,446	0,445
<i>G. sintenisii</i>	0,0570	1,0537	ID	0,376	0,964	0,919	0,992	0,882	0,885	0,887	0,893	0,896	0,888	0,984	0,896	0,893	0,919	0,925	0,964	0,992
<i>G. tuberosum</i>	0,0928	1,0443	0,1111	ID	0,865	0,893	0,878	0,967	0,962	0,953	0,956	0,958	0,958	0,875	0,958	0,956	0,893	0,899	0,865	0,878
<i>G. dissectum</i>	0,0657	1,0700	0,0347	0,1266	ID	0,913	0,97	0,871	0,873	0,882	0,881	0,887	0,876	0,962	0,887	0,881	0,913	0,919	1	0,97
<i>Geranium sp.</i>	0,0114	1,0506	0,0640	0,1004	0,0728	ID	0,922	0,894	0,897	0,904	0,893	0,902	0,891	0,918	0,902	0,893	1	0,989	0,913	0,922
<i>G. asphodeloides</i>	0,0535	1,0666	0,0081	0,1093	0,0280	0,0605	ID	0,884	0,885	0,887	0,891	0,896	0,888	0,99	0,896	0,891	0,922	0,929	0,97	1
<i>G. kurdicum</i>	0,0946	1,0969	0,1110	0,0263	0,1264	0,1021	0,1092	ID	0,978	0,962	0,967	0,968	0,968	0,881	0,968	0,967	0,894	0,9	0,871	0,884
<i>G. libani</i>	0,0930	1,0734	0,1074	0,0297	0,1246	0,1005	0,1075	0,0213	ID	0,959	0,964	0,965	0,968	0,881	0,965	0,964	0,897	0,904	0,873	0,885
<i>G. platyepetalum</i>	0,0855	1,0739	0,1037	0,0434	0,1113	0,0929	0,1037	0,0364	0,0382	ID	0,968	0,976	0,967	0,887	0,976	0,968	0,904	0,91	0,882	0,887
<i>G. ibericum</i>	0,0983	1,0475	0,0981	0,0381	0,1151	0,1058	0,1000	0,0330	0,0347	0,0313	ID	0,975	0,97	0,89	0,975	1	0,893	0,899	0,881	0,891
<i>G. gracile</i>	0,0873	1,0674	0,0944	0,0365	0,1075	0,0947	0,0944	0,0313	0,0330	0,0229	0,0262	ID	0,973	0,893	1	0,975	0,902	0,908	0,887	0,896
<i>G. renardii</i>	0,1003	1,0602	0,1036	0,0365	0,1208	0,1079	0,1036	0,0314	0,0297	0,0331	0,0313	0,0280	ID	0,885	0,973	0,97	0,891	0,897	0,876	0,888
<i>G. crenophilum</i>	0,0587	1,0831	0,0163	0,1130	0,0365	0,0657	0,0097	0,1129	0,1130	0,1037	0,1018	0,0981	0,1074	ID	0,893	0,89	0,918	0,924	0,962	0,99
Haplotype I	0,0873	1,0674	0,0944	0,0365	0,1075	0,0947	0,0944	0,0313	0,0330	0,0229	0,0262	0,0000	0,0280	0,0981	ID	0,975	0,902	0,908	0,887	0,896
Haplotype II	0,0983	1,0475	0,0981	0,0381	0,1151	0,1058	0,1000	0,0330	0,0347	0,0313	0,0000	0,0262	0,0313	0,1018	0,0262	ID	0,893	0,899	0,881	0,891
Haplotype III	0,0114	1,0506	0,0640	0,1004	0,0728	0,0000	0,0605	0,1021	0,1005	0,0929	0,1058	0,0947	0,1079	0,0657	0,0947	0,1058	ID	0,989	0,913	0,922
Haplotype IV	0,0000	1,0602	0,0570	0,0928	0,0657	0,0114	0,0535	0,0946	0,0930	0,0855	0,0983	0,0873	0,1003	0,0587	0,0873	0,0983	0,0114	ID	0,919	0,929
Haplotype V	0,0657	1,0700	0,0347	0,1266	0,0000	0,0728	0,0280	0,1264	0,1246	0,1113	0,1151	0,1075	0,1208	0,0365	0,1075	0,1151	0,0728	0,0657	ID	0,97
Haplotype VI	0,0535	1,0666	0,0081	0,1093	0,0280	0,0605	0,0000	0,1092	0,1075	0,1037	0,1000	0,0944	0,1036	0,0097	0,0944	0,1000	0,0605	0,0535	0,0280	ID

## REFERENCES

- [1] Aedo, C., Garmendia, F.M., and Pando, F., (1998). World checklist of *Geranium* L. (Geraniaceae). *Anales del Jardín Botánico de Madrid*. 56, 211–252.
- [2] Yeo, P.F., (1984). Fruit-discharge-type in *Geranium* (Geraniaceae): its use in classification and its evolutionary implications. *Bot J Lin Soc*. 89, 1–36.
- [3] Aedo, C., Garcia, M.A., Alarcon, M.L., Aldasoro, J.J., and Navarro, C., (2007). Taxonomic revision of *Geranium* Subsect Mediterranea (Geraniaceae). *Syst Bot*. 32(1), 93–128.
- [4] Aedo, C., and Estrella, M.D.L., (2006). Taxonomic revision of *Geranium* subsect. Tuberosa (Boiss.) Yeo. *Isr. J. Plant Sci*. 54, 19–44.
- [5] Davis, P.H., (1967). *Geranium* L. in Flora of Turkey, Eds. P. H. Davis, J. Cullen, and J. E. Coode. Edinburgh: Edinburgh University Press. 2, 451–474.
- [6] Pesmen, H., (1980). Six new species from Anatolia. *Notes from the Royal Botanic Garden, Edinburgh*. 38, 435–441.
- [7] Kit Tan, B., and Yildiz, B., (1989). Thirteen new species from Turkey. *Notes from the Royal Botanic Garden, Edinburgh*. 45, 439–541.
- [8] Schönbeck-Temesy, E., (1970). Geraniaceae. in Flora Iranica, Ed. K. H. Rechinger. Graz: Akademische Druck. 69, 1–67.
- [9] Moghadam, N.S., Mehrvarz, S.S., Namin, A.A., and Shavvon, R.S., (2015). Micromorphology of fruits and seeds of Iranian *Geranium* (Geraniaceae), and its systematic significance. *Nor J of Bot*. 33, 673–683.
- [10] Aedo, C., Fiz, O., Alarcon, M.L., Navarro, C., and Aldasoro, J.J., (2005). Taxonomic revision of *Geranium* section Dissecta (Geraniaceae). *Syst Bot*. 30(3), 533–558.
- [11] Haymes, K.M., (1996). Mini-Prep method suitable for a plant breeding program. *Plant Mol Biol Rep*. 14(3), 280–284.
- [12] Eker, S., and Koloren, O., (2016). Genetic diversity of *Artemisia* species in the Black Sea of Turkey. *Fresen Environ Bull*. 25(8), 3251–3257.
- [13] White, T.J., Burns, T., Lee, S., and Taylor, J., (1990). Amplification and direct sequencing of fungal ribosomal RNA gene for phylogenetics. In: Innis MA et al. editors. *PCR protocols: a guide to methods and applications*, San Diego: Academic Press. p. 315–322.
- [14] Hall, T.A., (1999). BioEdit: a user-friendly biological sequence alignment editor and analysis program for Windows 95/98/NT. *Nucl Acid S*. 41, 95–98.
- [15] Thompson, J.D., Gibson, T.J., Plewniak, F., Jeanmougin, F., and Higgins D.G., (1997). The





ClustalX-Windows interface: Flexible strategies for multiple sequence alignment aided by quality analysis tools. *Nucleic Acids Res.* 25, 4876–4882.

- [16] Mitchell, A.D., Heenan, P.B., and Paterson, A.M., (2009). Phylogenetic relationships of *Geranium* species indigenous to New Zealand. *New Zeal J Bot.* 47, 21–31.
- [17] Schlötterer, C., Hauser, M.T., Von Haeseler, A., and Tautz, D., (1994). Comparative evolutionary analysis of rDNA ITS regions in *Drosophila*. *Mol Biol Evol.* 11(3), 513–522.
- [18] Nishida, S., Azuma, H., Naiki, A., and Ogawa, M., (2012). Molecular phylogenetic analyses of *Geranium robertianum* populations recently found in Japan. *Acta Phytotax Geobot.* 62 (2/3), 79–87.
- [19] Bakker, F.T., Culham, A., Pankhurst, C.E., and Gibby, M., (2000). Mitochondrial and chloroplast DNA-based phylogeny of *Pelargonium* (Geraniaceae). *Am. J. Bot.* 87(5), 727–734.
- [20] Voglmayr, H., Fatehi, J., and Constantinescu, O., (2006). Revision of *Plasmopara* (Chromista, Peronosporales) parasitic on Geraniaceae. *Mycol. Res.* 110(6), 633–645.

---

**Received:** 08.06.2016

**Accepted:** 29.08.2016

---

#### **CORRESPONDING AUTHOR**

---

**Onur Koloren**

University of Ordu, Faculty of Agriculture,  
Department of Plant Protection, Ordu, TURKEY

e-mail: [koloren@yahoo.com](mailto:koloren@yahoo.com)



# OPTIMIZATION OF MICROWAVE INDUCED ELECTRODELESS ULTRAVIOLET DISINFECTION REACTOR USING COMPUTATIONAL FLUID DYNAMICS

Yue Zhang<sup>1,2</sup>, Guangshan Zhang<sup>2</sup>, Peng Wang<sup>1,2,\*</sup>, Qiao Wang<sup>2</sup>

<sup>1</sup> State Key Laboratory of Urban Water Resource and Environment, Harbin Institute of Technology, Harbin 150090, PR China

<sup>2</sup> School of Municipal and Environmental Engineering, Harbin Institute of Technology, Harbin 150090, PR China

## ABSTRACT

This study optimized a microwave induced electrodeless ultraviolet (MW-EUV) disinfection reactor using computational fluid dynamics (CFD). A homemade MV-EUV disinfection reactor was utilized to disinfect artificially contaminated water samples. The reactor models were established using the FLUENT software. The analysis of the flow inside the original reactor showed some vortexes in the main flowing direction ( $z$ -axis), which was disadvantageous to the disinfection. Keeping the shape and size of the reactor unchanged, the layout and the number and length of the folded plates were improved. This improved the flow regime and the water flow could achieve the hydrotechnics conditions of an ideal disinfection reactor. The optimal cylindrical reactor was 160 mm high and 140 mm in diameter. It had four layers of 118-mm-long subtended-opening folded plates, with 32 mm distance between the two plates. The disinfection effects of the optimal and original reactors were compared. The results indicated that the optimized reactor could treat a larger volume of water samples in a shorter hydraulic retention time (HRT). It proved that the bacteria distributed more uniformly in the optimized reactor and received a higher UV dose, so that the disinfection effect improved. Hence, the optimization of the reactor was realized.

## KEYWORDS:

CFD, disinfection, electrodeless ultraviolet, microwave, optimization; reactor.

## INTRODUCTION

Ultraviolet (UV) disinfection is an effective and environmentally friendly technique which is suitable for disinfecting drinking water, wastewater, and reuse water [1-3]. However, UV disinfection may be followed by photoreactivation phenomenon [4]. Microwave induced electrodeless UV (MW-EUV) disinfection is a novel inactivation method. Microwave and UV could function together to kill the bacteria in the water [5]. Microwave disinfection depends on the damage of bacterial cell wall and membrane to cause leakage from the cell. Moreover, microwave can result in the cohesion and denaturation of protein, leading to bacterial death [6], which is an irreversible destruction. Therefore, microwave can offset the photoreactivation of UV. The electrodeless UV (EUV) lamp is used as a UV source that is lighted by microwave. Compared with the traditional UV lamp, the EUV lamp has high lighting efficiency, long service life and flexible design [7-10]. Generally, MW-EUV disinfection is a combined inactivation method of microwave and UV, which can make the full use of energy and is an efficient and energy-saving technique. In a previous work, a MW-EUV disinfection reactor was designed according to the structure and size of the microwave oven, which achieved a good inactivation effect in the municipal secondary effluent disinfection experiments. To improve the sterilization ability of the disinfection reactor, the original one needed to be optimized.

In recent years, advancements in computational fluid dynamics (CFD) have provided a viable alternative approach to the study of gas or water in reactors or specified areas [11]. It has many advantages, such as extensive application range, strong adaptability, no restraint by experimental

models, low cost, and high flexibility. Also, CFD can simulate the conditions that cannot be simulated in the laboratory, such as very complicated multiphase flow, toxicity, high temperature, and flammability [12]. FLUENT is a commonly used commercial CFD software package [13]. It is flow simulation software applicable to each field, which can simulate fluid flow, heat and mass transfer, chemical reactions, and other complex physical phenomena [14]. CFD modeling is a powerful tool for the design of UV disinfection reactors. Flow fields, UV irradiation fields, and microbial inactivation in UV disinfection systems and reactor structures all can be predicted by CFD [15-21]. Based on the aforementioned simulations, the reactor can be designed and optimized.

Aiming at a disinfection reactor with determined dimensions and EUV lamp parameters, CFD was adopted to predict the flow regime inside the disinfection reactor in this study. The layout and the number and length of the folded plates in the reactor were improved. The flow regime was improved, so that the reactor was optimized to achieve the purpose of enhancing sterilization ability. Plus, the simulation results were verified by further experiments.

## MATERIALS AND METHODS

**Preparation of indicator microorganisms and water samples.** *Escherichia coli* ATCC8739 and *Bacillus subtilis* ATCC9327 were supplied by Guangdong Microbiology Culture Center. The bacteria were picked up from the tube with the inoculating loop and grown in the broth medium at 36°C for 24 h. Then, the medium was centrifuged at 4000 rpm for 10 min. The sediment was collected and washed with phosphate-buffered saline solution for two times. The fresh sediment comprised the living bacteria detached from the medium. Then, the bacteria were put into 100 mL of normal saline to make bacterial suspensions. The suspensions should be stored in the refrigerator at 4°C and be used up within two days.

The water samples were prepared with tap water and stored for 2 days to eliminate the effect of residual chlorine. *B. subtilis* and *E. coli* were added to the samples in a proportion of 1:1. The total bacterial counts of the water samples were  $6.3 \times 10^3$  CFU·mL<sup>-1</sup>,  $6.3 \times 10^4$  CFU·mL<sup>-1</sup>, and  $6.3 \times 10^5$  CFU·mL<sup>-1</sup>.

The plate count method was used to measure the total bacterial count, and the multiple-tube fermentation method was adopted to measure the total coliform count. Counting methods and culture medium were based on the contents of the book "Chinese Water and Wastewater Monitoring Analysis Method (Fourth Edition)" [22].

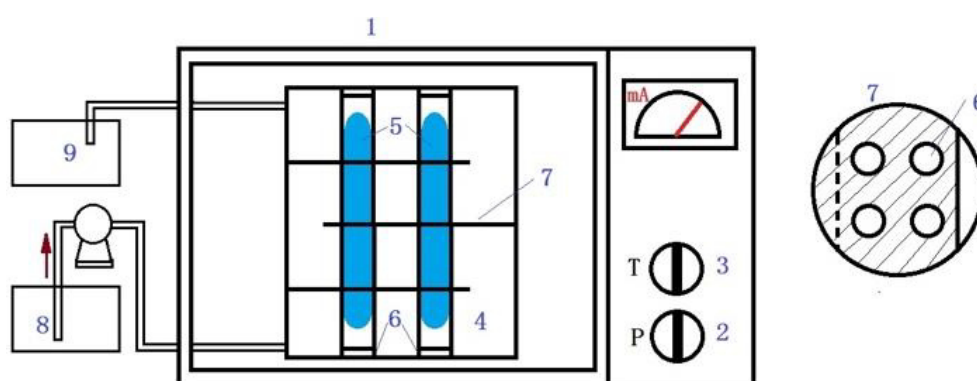


FIGURE 1

The schematic diagram of MW-UV disinfection device:  
 1-microwave oven, 2-power button, 3-time button, 4-disinfection reactor, 5-EUV lamp,  
 6-UV lamp holder, 7-folded plate, 8-water inlet and 9-water outlet.

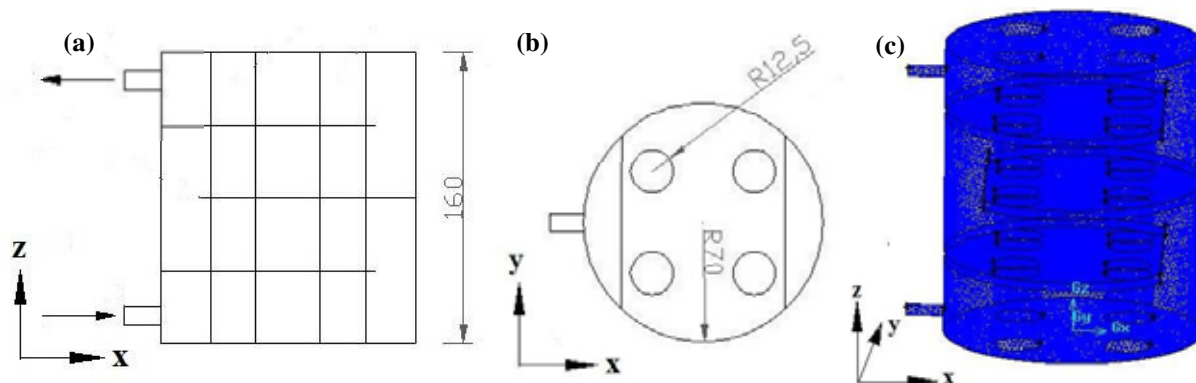


FIGURE 2

**Original reactor configuration and computational mesh used in this work:**  
(a) side view, (b) plan view and (c) computational mesh.

**The original disinfection equipment.** The microwave installation used in this work was a reconstructive domestic microwave oven (EM-202MSI, Sanyo, Nanjing, China). The impulse frequency was 2450 MHz, while the microwave power was continuously output at 0–600 W. As shown in Figure 1, a disinfection reactor was placed in the microwave oven. The reactor had four EUV lamps. The lamps were 16 mm long with an external diameter of 25 mm and had 10 mg Hg and 5 Torr Ar gas inside. After the microwave oven was initiated, the EUV lamps were lighted by microwave. Microwave and UV functioned together to sterilize the water. The light intensity of the EUV lamps improved due to the increase of microwave power. The intensity was  $2.0 \text{ mW} \cdot \text{cm}^{-2}$  when the microwave power was 300 W.

**Modeling approaches. (1) Configuration description.** As shown in Figure 2a, the total height of the reactor was 160 mm. Figure 2b displays the interior of the reactor. The MW–EUV disinfection reactor was cylindrical in shape with a diameter of 140 mm. It had three layers of folded plates with the same size and interval. The pores in every folded

plate were of the same size with a radius of 12.5 mm. The UV lamp holder passed through the pores. The distance between the folded plate opening and the inside wall of the reactor was 22 mm. The water was pumped into the reactor from below by a peristaltic pump. It flowed upward through the EUV lamps. The main flow was plug flow along the  $z$ -axis. Eventually, the water flowed out from the top.

Generation and partitioning of computational grids employed the mixed mesh generation method. The meshes mainly comprised tetrahedral cells, also including some properly positioned hexahedron-, wedge-, and cone-shaped cells. A grid system of 487,976 cells was generated after successive refinement, as shown in Figure 2c. The boundary conditions of the MW–EUV disinfection reactor were defined according to the mesh.

**(2) Flow modeling.** The calculation model needed to be confirmed before CFD software calculation. The water was defaulted to a single-phase flow in the FLUENT software, and the fluid was incompressible viscous fluid. The water had turbulent flow, and the standard  $\kappa$ - $\epsilon$  double equations were used for calculation [23,24]. The governing equations were equation 1 to equation 8:

The continuity equation (mass conservation equation):

$$\frac{\partial u}{\partial x} + \frac{\partial v}{\partial y} + \frac{\partial w}{\partial z} = 0 \quad (1)$$

The momentum conservation equations:

$$\rho \left( \frac{\partial u}{\partial t} + u \frac{\partial u}{\partial x} + v \frac{\partial u}{\partial y} + w \frac{\partial u}{\partial z} \right) = \rho F_x - \frac{\partial p}{\partial x} + \mu \left( \frac{\partial^2 u}{\partial x^2} + \frac{\partial^2 u}{\partial y^2} + \frac{\partial^2 u}{\partial z^2} \right) \quad (2)$$

$$\rho \left( \frac{\partial v}{\partial t} + u \frac{\partial v}{\partial x} + v \frac{\partial v}{\partial y} + w \frac{\partial v}{\partial z} \right) = \rho F_y - \frac{\partial \rho}{\partial y} + \mu \left( \frac{\partial^2 v}{\partial x^2} + \frac{\partial^2 v}{\partial y^2} + \frac{\partial^2 v}{\partial z^2} \right) \quad (3)$$

$$\rho \left( \frac{\partial w}{\partial t} + w \frac{\partial w}{\partial x} + w \frac{\partial w}{\partial y} + w \frac{\partial w}{\partial z} \right) = \rho F_z - \frac{\partial \rho}{\partial z} + \mu \left( \frac{\partial^2 w}{\partial x^2} + \frac{\partial^2 w}{\partial y^2} + \frac{\partial^2 w}{\partial z^2} \right) \quad (4)$$

The standard  $\kappa$ - $\varepsilon$  double equations:

$$v_t = C_\mu k^2 / \varepsilon \quad (5)$$

$$\frac{\partial k}{\partial t} + \overline{U}_j \frac{\partial k}{\partial x_j} = \frac{\partial}{\partial x_j} \left[ \left( \nu + \frac{v_t}{\sigma_k} \right) \frac{\partial k}{\partial x_j} \right] + v_t \left( \frac{\partial \overline{U}_i}{\partial x_j} + \frac{\partial \overline{U}_j}{\partial x_i} \right) \frac{\partial \overline{U}_i}{\partial x_j} - \varepsilon \quad (6)$$

$$\frac{\partial \varepsilon}{\partial t} + \overline{U}_j \frac{\partial \varepsilon}{\partial x_j} = \frac{\partial}{\partial x_j} \left[ \left( \nu + \frac{v_t}{\sigma_\varepsilon} \right) \frac{\partial \varepsilon}{\partial x_j} \right] + C_{1\varepsilon} \frac{\varepsilon}{\kappa} v_t \left( \frac{\partial \overline{U}_i}{\partial x_j} + \frac{\partial \overline{U}_j}{\partial x_i} \right) \frac{\partial \overline{U}_i}{\partial x_j} - C_{2\varepsilon} \frac{\varepsilon^2}{\kappa} \quad (7)$$

$$- \overline{u_i u_j} = v_t \left( \frac{\partial \overline{U}_i}{\partial x_j} + \frac{\partial \overline{U}_j}{\partial x_i} \right) - \frac{2}{3} k \delta_{ij} \quad (8)$$

The empirical constants used in this model were as follows:

$C_\mu = 0.09$ ;  $\hat{\sigma}_k = 1.0$ ;  $\hat{\sigma}_\varepsilon = 1.3$ ;  $C_{1\varepsilon} = 1.44$ ;  $C_{2\varepsilon} = 1.92$ .

**(3) Boundary conditions.** The boundary conditions at the entrance were as follows: velocity inlet was adopted for the water flow inlet, supposing that the water velocity was uniformly distributed at the entrance and perpendicular to the inlet section. The velocity was  $0.39 \text{ m}\cdot\text{s}^{-1}$ . The water flow at the exit was free outflow. The boundary condition on the wall was static with no slip. The inner area was defaulted to the inner area of the MW-EUV disinfection reactor. The cross-section needed in the simulation result analysis was  $y = 0$  section.

**(4) Numerical details.** CFD simulations were performed using commercial GAMBIT 2.2.30 for pretreatment and FLUENT 6.2.16 for post-treatment. The SIMPLE algorithm was applied to address the pressure-velocity coupling. The first-order upwind scheme was employed to discretize convection terms of the transport equations. The convergence of the numerical solution to the exact solution was achieved when the normalized residuals for the continuity, momentum, and turbulence equations were less than  $10^{-4}$ .

## RESULTS AND DISCUSSION

**Flow field result of the original reactor.** The flow field inside the disinfection reactor was reflected by the velocity vector profiles, which showed the magnitude and direction of velocity, short streams, vortex, and back-mixing phenomena. Figure 3 shows the velocity vector chart at  $y = 0$  section simulated by the FLUENT software. The areas marked with circles are existing vortex areas. As shown in Figure 3a, the water flowed into the reactor from the entrance and moved upward across the folded plates after bypassing the lamps. The velocity in the  $z$ -axis was around  $0.02 \text{ m}\cdot\text{s}^{-1}$ , while the one in the  $x$ -axis was about  $2 \times 10^{-6} \text{ m}\cdot\text{s}^{-1}$ . Obviously, the velocity in the  $z$ -axis was larger than the velocity in the  $x$ -axis, so the flow was plug flow in the main orientation ( $z$ -axis). However, if the P point marked in Figure 3a is magnified, an evident vortex could be seen (Fig.3b). There were two to three vortexes around every layer of the folded plate. The vortexes caused the back-mixing of the fluid in the  $z$ -axis. The HRT was different at different places [19], so the UV dose the bacteria received was different, which might have a negative impact on the disinfection effect.

The ideal disinfection reactor needs to ensure that the UV dose the bacteria receive is the same. The

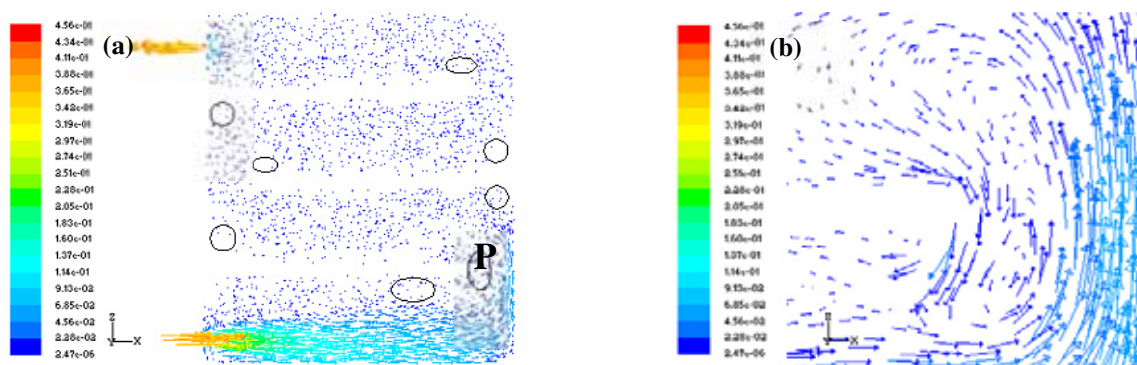


**FIGURE 3**

**The velocity vector profiles of the original reactor: (a) cross-section  $y = 0$  and (b) partial enlarged detail.**

flow inside the disinfection reactor should meet the hydrotechnics conditions as follows [25]: (1) the flow is plug flow in the main orientation without short flow and vortex; and (2) the flow is totally mixed in the direction perpendicular to the main orientation. The first condition makes sure that the HRT of the bacteria inside the disinfection reactor remains the same, while the second condition ensures that the UV dose the water receives in the same cross-section is unchanged. The bacteria can receive the same UV dose by simultaneously meeting the two conditions. Aiming at the first condition, this study optimized the disinfection reactor by changing the conditions of the folded plates to achieve the ideal flow regime [20].

**Optimization of the disinfection reactor. (1) Optimization of the folded plates layout in the disinfection reactor.** According to the simulating results of the flow field inside the original disinfection reactor, the layout of the folded plates was varied to change the flow regime. The disinfection reactor with the variations was drawn into a three-dimensional geometry by the GAMBIT pretreatment software. Figure 4a is the geometry of the original reactor. Based on Figure 4a, the baffles in the  $z$ -axis were added in the middle of every layer of the folded plates. Two same 140-mm-long and 10-

mm-high baffles were put between the two continuous folded plates. The distance of the baffle opening was 20 mm, while the position and size of the entrance and exit remained unchanged (Fig.4b). Also based on Figure 4a, the angle of the folded plates was varied from  $180^\circ$  to  $120^\circ$  (Fig.4c).

Figure 4d and e exhibits the velocity vector chart at  $y = 0$  section after changing the layout of the folded plates. Figure 4d shows that the lengthwise baffles were set in the middle, and the vortices existed around every layer of the baffles. The formation of vortices made the HRT in the  $z$ -axis different, which might have a negative impact on the disinfection effect. The addition of the folded plates increased the head loss and created a dead zone region, resulting in worse hydraulic conditions. Figure 4e shows that the angle was varied to  $120^\circ$ . The fluid flow inside the reactor was a flow-around type, which was a good hydraulic movement form. Nevertheless, this form was more suitable for a higher reactor. However, the number of vortices was the same as the original one, showing no improvement. The layout of the original reactor with subtended-opening folded plates and no baffles in the  $z$ -axis was more advantageous for optimizing the flow regime

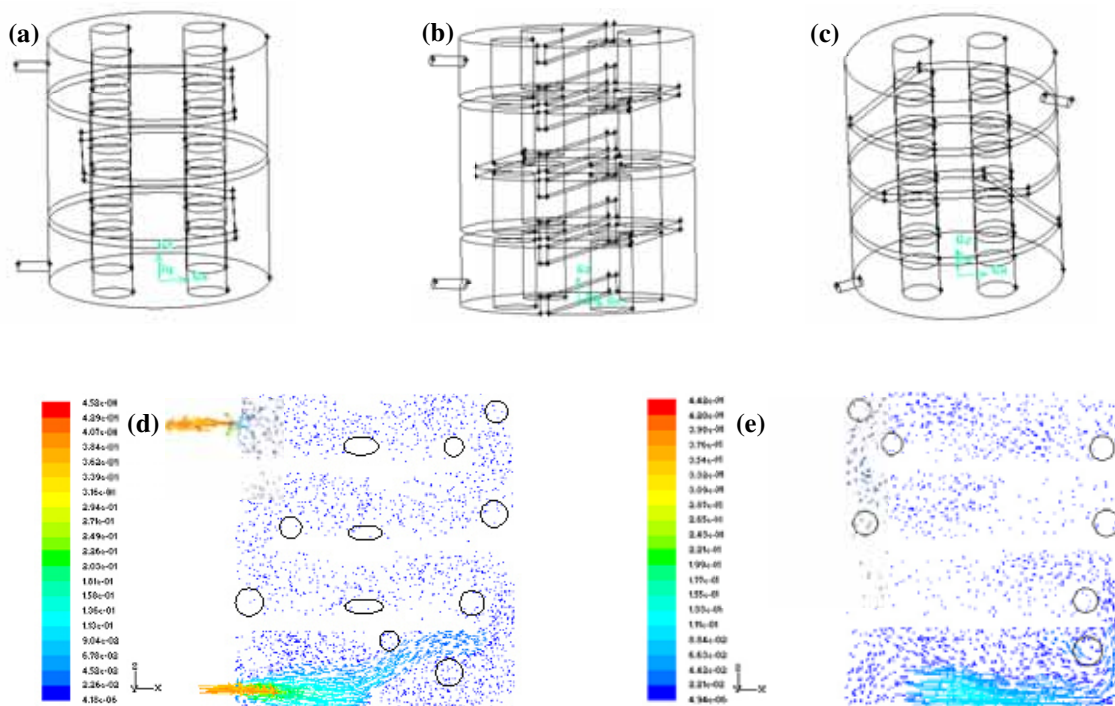


**FIGURE 4**

**Simulation diagram of the disinfection reactors. Three-dimensional geometric model of the disinfection reactors: (a) original, (b) adding lengthwise baffles and (c) changing the angle between the folded plates to 120°. The velocity vector profiles of two reactors: (d) adding lengthways baffles and (e) changing angle between the folded plates to 120°.**

**(2) Optimization of the number and the length of the folded plates in the disinfection reactor.** The number of folded plates was changed from three layers to four, five, and six layers. Figure 5a exhibits the velocity vector chart at  $y = 0$  section for four layers of the folded plates. The distance between the plates was 32 mm. Compared with the original reactor (Fig.3a), the vortices decreased obviously in the new reactor. Also, the flow regime became better. For five and six layers of the folded plates, the distances between the plates were 26 mm and 22 mm, respectively (Fig.5b and c). Compared with the original reactor, the vortices in these two reactors decreased, but still were more than the vortices in the reactor with four layers of the folded plates. The proper area of longitudinal cross-section and the flowing length of the stream could improve

the flow regime inside the reactor. Adding folded plates to some extent could unify the flow regime, while excessive folded plates would increase the head loss, which was disadvantageous to the optimization of the flow regime. After simulation, the optimal proportion of flowing length and longitudinal cross-section height was 4.375 in this reactor, meaning that the proportion of reactor diameter and distance between the two plates was 4.375. In other words, the optimal number of the folded plates was four layers.

The length of the folded plates also affected the flow regime. In this disinfection reactor, changing the length of the folded plates was equivalent to changing the cross-sectional area which the stream passed through the opening of the folded plates. The

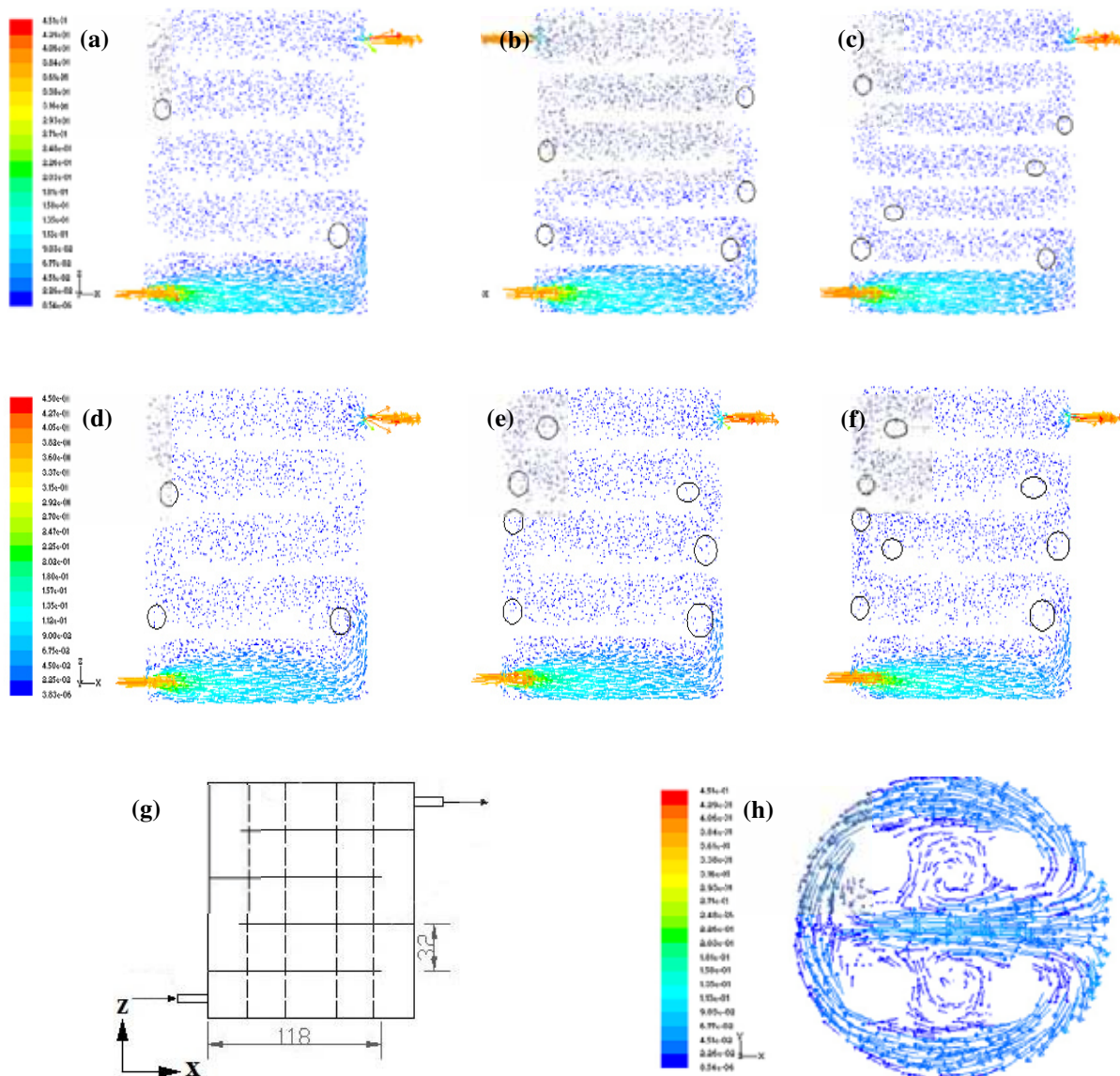


**FIGURE 5**

**Optimization of the disinfection reactor. The velocity vector profiles of the simulated reactors: (a) four layers of the folded plates, (b) five layers of the folded plates, (c) six layers of the folded plates, (d) folded plates with the length 115 mm, (e) Folded plates with the length 122 mm and (f) folded plates with the length 127 mm. The optimal reactor: (g) the reactor configuration and (h) the velocity vector profiles at  $z = 0.2$  section.**

function of the guiding fluid could not be fulfilled if the folded plates were too short, while overlong folded plates would decrease the cross-sectional area and increase the local resistance, which was bad for the flow regime. In the previous simulated reactor with four layers of the folded plates, the length was 118 mm and the distance between the folded plate opening and the inside wall of the reactor was 22 mm. The length of the folded plates was set as 115, 122, and 127 mm in this study, and the flow field inside the reactors was simulated.

Figure 5d shows that fewer zones having vortices inside the reactor with 115-mm-long folded plates, indicating good flow regime. The reactors with 122- and 127-mm-long plates had more zones having vortices, showing worse flow regime (Fig.5e and f). As a result, the length of the folded plates was suggested to be 115–118 mm, meaning that the distance between the plate opening and the inside wall of the reactor was 22–25 mm. The flow regime was better and beneficial to improve the disinfection effect.



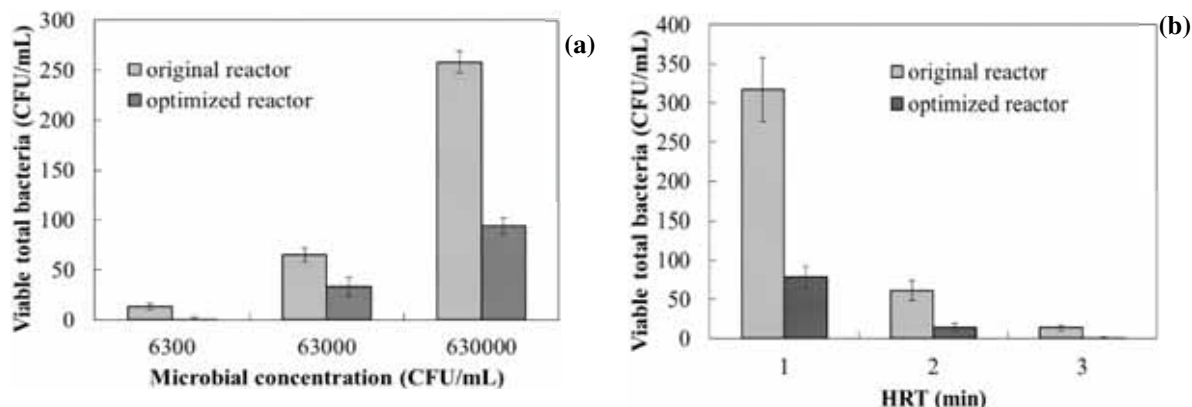


**FIGURE 6**

**Experimental verification of the original and optimized reactors:**

**(a) disinfection effect of different microbial concentrations and (b) disinfection effect of different HRTs.**

Based on the whole flow field predicted results, the four layers of subtended-opening folded plates were laid inside the optimal reactor. The length of the plates was 118 mm with 32 mm distance between the two plates, as shown in Figure 5g. Figure 5h shows the velocity vector chart at the  $z = 0.02$  section (XY section) in the optimized reactor. Owing to the hindrance of the EUV lamps, the vortices were generated around the lamps in the XY section, which well mixed the water flow. It is beneficial for the bacteria to receive the same UV irradiation dose. This phenomenon could meet the second hydrotechnics condition for the ideal reactor: the flow regime is totally mixed in the direction perpendicular to the main orientation.

**Disinfection results of the reactor after optimization.** To validate the simulation results, the inactivation effects of the disinfection reactors before and after optimization were explored (Fig.6). The microwave power was 300 W and the inlet velocity was  $0.39 \text{ m}\cdot\text{s}^{-1}$  (HRT = 3 min). The disinfection effect was studied with different microbial concentrations (Fig.6a). After disinfection, less viable bacteria were present in the optimized reactor than in the original one. With different microbial concentrations, the viable bacterial counts in the optimized reactor were all less than  $100 \text{ CFU}\cdot\text{mL}^{-1}$ . When the microbial concentration remained  $6.3 \times 10^3 \text{ CFU}\cdot\text{mL}^{-1}$ , the disinfection effects of the original and optimized reactors were compared (Fig.6b) with the variation of HRT. Less viable bacteria were present in the optimized reactor than in the original one. The experimental results

indicated that the optimized reactor could treat a greater volume of artificially contaminated water samples in a shorter HRT. The two sets of experiments indicated that the optimized MW–EUV disinfection reactor had a better inactivation effect than the original one, and the experimental results could highly testify the simulating results.

## CONCLUSION

The CFD method was used to optimize MW–EUV disinfection reactor in this study. The flow field in the original reactor was predicted, and some vortices were found in the main flowing direction ( $z$ -axis), which was disadvantageous to the disinfection. The flow regime was improved by the variation of layout, number, and length of the folded plates, so that the flow could achieve the hydraulic conditions of the ideal disinfection reactor. The optimal cylindrical reactor was 160 mm high and 140 mm in diameter. It had four layers of subtended-opening folded plates, which were 118 mm long and 32 mm distance between the two plates. The experimental results indicated that the optimized disinfection reactor could treat a greater volume of the water in a shorter HRT. It was confirmed that the bacteria distributed more uniformly in the optimized reactor and received a higher UV dose, therefore the disinfection effect was enhanced. The experimental results highly testified the simulating results, and the optimization of the reactor was realized.



## ACKNOWLEDGEMENTS

The work was supported by the State Key Laboratory of Urban Water Resource and Environment (Harbin Institute of Technology) (2015DX03), Fundamental Research Funds for the Central Universities (HIT. NSRIF. 201671) and National Science Foundation for Post-doctoral Scientists of China (2014M561356).

## REFERENCES

- [1] Wang, H.B., Hu, C. and Hu, X.X. (2014) Effects of combined UV and chlorine disinfection on corrosion and water quality within reclaimed water distribution systems. *Eng. Fail. Anal.* 39, 12-20.
- [2] Zuo, X., Chu, X. and Hu, J. (2015) Effects of water matrix on virus inactivation using common virucidal techniques for condensate urine disinfection. *Chemosphere* 136, 118-124.
- [3] Guo, M.T., Hu, H.Y., Bolton, J.R. and El-Din, M.G. (2009) Comparison of low- and medium-pressure ultraviolet lamps: Photoreactivation of *Escherichia coli* and total coliforms in secondary effluents of municipal wastewater treatment plants. *Water Res.* 43(3), 815-821.
- [4] Carlson, J.C. (2011) Drinking water treatment using UV/H<sub>2</sub>O<sub>2</sub> an analysis of photochemical properties and efficacy of treatment for removal of microcontaminants, Trent University, Canada.
- [5] Wang, P., Zheng, T. and Zhang, G.S. (2014) Microwave and microwave chemistry. In: *Microwave Chemistry and Technology in Environment*, 1st Ed. Science Press, Beijing, China, 1-37.
- [6] Kim, S.Y., Jo, E.K., Kim, H.J., Bai, K. and Park, J.K. (2008) The effects of high-power microwaves on the ultrastructure of *Bacillus subtilis*. *Lett. Appl. Microbiol.* 47(1), 35-40.
- [7] Barkhudarov, E.M., Christofi, N., Kossyi, I.A., Misakyan, M.A., Sharp, J. and Taktakishvili, I.M. (2007) Killing bacteria present on surfaces in films or in droplets using microwave UV lamps. *World J. Microbiol. Biotechnol.* 24, 761-769.
- [8] Siwaguch, S., Matsumura, K., Tokuoka, Y., Wakui, S. and Kawashima, N. (2002) Sterilization system using microwave and UV light. *Colloids Surf., B* 25, 299-304.
- [9] Barkhudarov, E.M., Kozlov, Y.N., Kossyi, I.A., Malykh, N.I., Misakyan, M.A., Taktakishvili, I.M. and Khomichenko, A.A. (2012) Electrodeless microwave source of UV radiation. *Tech. Phys.* 57(6), 885-887.
- [10] Bergmann, H., Iourtchouk, T., Schops, K. and Bouzek, K. (2002) New UV irradiation and direct electrolysis-promising methods for water disinfection. *Chem. Eng. J.* 85, 111-117.
- [11] Ni, H.Y., Lu, S.J. and Chen, C.X. (2014) Modeling and simulation of silicon epitaxial growth in Siemens CVD reactor. *J. Cryst. Growth* 404, 89-99.
- [12] Julian, I., Herguido, J. and Menendez, M. (2014) CFD model prediction of the Two-Section Two-Zone Fluidized Bed Reactor (TS-TZFBR) hydrodynamics. *Chem. Eng. J.* 248, 352-362.
- [13] Khan, M.J.H., Hussain, M.A., Mansourpour, Z., Mostoufi, N., Ghasem, N.M. and Abdullah, E.C. (2014) CFD simulation of fluidized bed reactors for polyolefin production - A review. *J. Ind. Eng. Chem.* 20(6), 3919-3946.
- [14] Abbasfard, H., Ghanbari, M., Ghasemi, A., Ghahraman, G., Jokar, S.M. and Rahimpour, M.R. (2014) CFD modelling of flow maldistribution in an industrial ammonia oxidation reactor: A case study. *Appl. Therm. Eng.* 67(1-2), 223-229.
- [15] Xu, C., Zhao, X.S. and Rangaiah, G.P. (2013) Performance analysis of ultraviolet water disinfection reactors using computational fluid dynamics simulation. *Chem. Eng. J.* 221, 398-406.
- [16] Bolton, J.R. (2000) Calculation of ultraviolet fluence rate distributions in the annular reactor: significance of refraction and reflection. *Water Res.* 34(13), 3315-3324.
- [17] Lim, S. and Blatchley, E.R. (2009) UV disinfection system for cabin air. *Adv. Space Res.* 44(8), 942-948.
- [18] Li, C., Deng, B.Q. and Kim, C.N. (2010) A numerical prediction on the reduction of microorganisms with UV disinfection. *J. Mech. Sci. Technol.* 24(7), 1465-1473.
- [19] Younis, B.A. and Yang, T.H. (2010) Computational modeling of ultraviolet disinfection. *Water Sci. Technol.* 62(8), 1872-1878.
- [20] Wols, B.A., Uijtewaal, W.S.J., Hofman, J.A.M.H., Rietveld, L.C. and van Dijk, J.C. (2010) The weaknesses of a k-ε model compared to a large-eddy simulation for the



- prediction of UV dose distributions and disinfection. *Chem. Eng. J.* 162(2), 528-536.
- [21] Wols, B.A., Hofman, J.A.M.H., Beerendonk, E.F., Uijttewaal, W.S.J. and van Dijk, J.C. (2011) A systematic approach for the design of UV reactors using computational fluid dynamics. *AICHE J.* 57(1), 193-207.
- [22] (2002) Bacteriological determination of water and wastewater. In: *Water and Wastewater Monitoring Analysis Method*, 4th Ed. Ministry of Environmental Protection of the People's Republic of China, Eds. China Environmental Science Press, Beijing, China, 673-714.
- [23] Liu, D., Wu, C., Linden, K. and Ducoste, J. (2007) Numerical simulation of UV disinfection reactors: Evaluation of alternative turbulence models. *Appl. Math. Model.* 31(9), 1753-1769.
- [24] Chen, J.Y., Deng, B.Q. and Kim, C.N. (2011) Computational fluid dynamics (CFD) modeling of UV disinfection in a closed-conduit reactor. *Chem. Eng. Sci.* 66(21), 4983-4990.
- [25] Kreft, P., Scheible, O.K. and Venosa, A. (1986) Hydraulic studies and cleaning evaluations of ultraviolet disinfection units. *Journal (Water Pollution Control Federation)* 58(12), 1129-1137.

---

**Received:** 12.03.2016

**Accepted:** 20.09.2016

---

#### **CORRESPONDING AUTHOR**

---

**Peng Wang**

School of Municipal and Environmental  
Engineering  
Harbin Institute of Technology  
No.73 Huanghe Road, Nangang District  
Harbin 150090 – CHINA

E-mail: [pwang73@vip.sina.com](mailto:pwang73@vip.sina.com)

# STUDY ON THE IMPACT OF ENVIRONMENTAL REGULATION ON FIRM SIZE DISTRIBUTION: A CASE STUDY OF GUANGDONG PROVINCE

Yang Yuanhua<sup>1,\*</sup>, Niu Guohua<sup>2</sup>, Tang Dengli<sup>3</sup>

<sup>1</sup>Public Management School, Guangdong University of Finance and Economics, Guangzhou 510000, China

<sup>2</sup>Personnel Education Department, Foshan Municipal Local Taxation Bureau, Foshan, 528000, China

<sup>3</sup>Shenzhen Graduate School, Harbin Institute of Technology, Shenzhen 518055, China

## ABSTRACT

We first analyze the mechanism of the influence of environmental regulation on firm size distribution based on literature review. We propose that environmental regulation is an important means of resolving resources and environmental problems. Three pathways of influence of environmental regulation are identified, namely, cost effect, innovative compensation effect and learning effect, and competition effect. Next, an empirical analysis is carried out on 9 major industries in Guangdong Province. It is found that the Pareto index of firm size distribution in Guangdong Province is far below 1. Therefore, the firm size distribution does not conform to Zipf distribution and the balance degree of firm size distribution varies greatly from one industry to another. But as the level of environmental regulation increases, the Pareto index increases as well. This means the environmental regulation has a significant promoting effect on firm size distribution and on the uniformity of firm size distribution.

## KEYWORDS:

environmental regulation; firm size distribution; Zipf distribution

## INTRODUCTION

As the crisis of resources depletion and environmental pollution has been aggravating in recent years, the level of environmental regulation imposed on the firms has also increased [1]. Environmental regulation brings about new constraints on firms' production and policy-making process and compels the firms to adjust their behaviors. But, since the large-sized firms and the mid and small-sized firms are equipped with different capacity to cope with environmental regulation, the same level of environmental regulation may have asymmetrical influence on firms of different sizes. This further affects the firm size distribution. So the question is how environmental regulation affects firm size

distribution and what makes firm size distribution uniform or non-uniform as a result of environmental regulation.

Foreign studies are more concerned about whether firm size distribution conforms to Zipf distribution or not [1-8]. Most studies are confined to the situations in western countries and few address the problems in developing countries. Among Chinese studies, the influence of environmental regulation on firm size distribution within a single industry is investigated, but not across different industries. For example, Sun and Wang only discussed the influence of environmental regulation on firm size distribution in the manufacturing industry [1]. Therefore, more empirical analyzes are needed to elucidate the influence of environmental regulation in other industries. This paper focuses on 9 major industries in Guangdong Province, after a theoretical analysis of the influence of environmental regulation on firm size distribution, we make an assumption and then proceed to test the assumption based on the facts and features of firm size distribution in Guangdong Province. The highlights of the present study are as follows: first, we investigate the influence of environmental regulation on firm size distribution along with the influence mechanism; second, the influence of environmental regulation on firm size distribution is discussed across the industries and therefore the conclusions are more comprehensive; third, the empirical analysis that takes Guangdong Province as an example provides solid references for the making and implementation of environmental policies.

## LITERATURE REVIEW

The existing literature reports in relation to the influence of environmental regulation on firms fall into two categories. The first category is concerned with the influence of environmental regulation on firm productivity, and the second category is related to the influence of environmental regulation on firm export. Both two categories are concerned with the influence of environmental regulation on firm competitiveness. As firm competitiveness changes,

the economic environment will change as well and firm size distribution is an important part of this change. However, the changes of firm size distribution in response to environmental regulation are rarely discussed [9].

Generally Pareto index is used to estimate firm size distribution, whereas the influence of environmental regulation on firm size distribution is much less analyzed. Zipf found that among American firms, the Pareto index of firm size distribution approached 1 and this is known as the Zipf's law [10]. Axtel confirmed that the Zipf's law applied to size distribution of American firms by using large sample size data of American tax-paying firms [2]. Gaffeo *et al.*, Fujiwara *et al.*, Cirillo, Giovanni *et al.*, Garicano *et al.* and Adamopoulos tested whether the Zipf's law applied to firms in G7 countries and other European countries [3-8]. Delli *et al.*, Luttmmer, Cirillo and Hüsler, and Giovanni *et al.* were more concerned with the dynamic trend of firm size and the influence on firm development, but they did not test for the Zipf's law [11-14].

Chinese scholars are not devoted to the issue of firm size distribution until recently. Fang and Nie were the first to conduct an empirical test on the overall size distribution of Chinese firms by using the data of nationwide state-owned industrial enterprises in 1999-2005. They found that the deviations from the Zipf's law were serious in Chinese context [15]. Yang *et al.* estimated Pareto index of size distribution of Chinese industrial firms and found that the Zipf's law was severely disobeyed. Large-sized firms enjoyed advantageous position in all provinces, while the mid and small-sized firms were disadvantaged [16]. Li *et al.* found that Chinese listed enterprises in the manufacturing industry showed age and size dependent effect. The funding constraint has impeded the firm growth and hence the firm size distribution [17]. Sun and Wang took Chinese manufacturing enterprises as samples and found that the Pareto index was less than 1. This means firm size distribution in China disobeys the Zipf's law [1].

We are curious about what influence environmental regulation has generated on firm size distribution in Chinese context. Generally speaking, the firm's control on resources and production elements is decisive to firm size. That is, the larger the size, the stronger the control on resources and production elements. Large-sized firms enjoy more abundant capital and therefore richer resources. In contrast, the mid and small-sized firms may be handicapped by the scarcity of capital and resources. As a result, the mid and small-sized firms are less to expand in scale. Large-sized firms are usually the pillar enterprises and have more access to capital support and favorable tax policies granted by the local government, which may be otherwise denied to mid and small-sized firms. Consequently, large-sized firms are much easier to flourish, while the mid

and small-sized firms may have difficulty surviving. This is an important reason behind the unbalanced size distribution of Chinese firms. Environmental regulation is an important means for solving resources and environmental crisis. The influence on firm size distribution is manifested through cost effect, innovative compensation effect, learning effect and competition effect [1].

(1) Cost effect. Government imposes strict environmental regulation and limits on the emissions of waste gas and wastewater. The enterprises are forced to cut down pollutant emissions either by conforming to the emission standards or by improving the pollution control technology. This will inevitably increase the cost of pollution management [18]. If the enterprises refuse to do this, they will be penalized by administrative measures and fined a large sum. For example, Chapple *et al.* carried out a comparative study on the market value of 58 Canadian sample enterprises belonging to carbon-intensive industry and low-carbon industry. They showed that the carbon-intensive enterprises used 6.57% of their total market value to pay for environmental fines [19]. Large sum of environmental fines will not only increase the cost of enterprises, but also consume the working capital. In some serious cases, the operation of the enterprises may be affected by the lack of capital and the enterprises finally quit the market. Therefore, those who conform to the environmental regulation will enjoy the opportunity to flourish and expand. But the enterprises that are able to bear the environmental cost are usually those with a large size. They proactively adjust the development strategy according to environmental regulation and to keep on expanding and to acquire as much resources as possible. In contrast, the mid and small-sized enterprises may be unable to undertake the environmental cost. Some will seize the chances of technological innovation and process optimization to grow while adapting to environmental regulation. Others may be forced to quit the market due to the burden of environmental cost. Therefore, environmental regulation may fuel the development of large-sized enterprises that can undertake the environmental cost through the cost effect. For mid and small-sized enterprises, those that can achieve technological innovation and process optimize will finally expand and flourish, but those that cannot will quit the market. Consequently, the firm size distribution will become more uniform.

(2) Innovative compensation effect and learning effect. Although environmental regulation will add to the pollutant management cost of the enterprises, to seek the maximum profits, the enterprise will find ways to compensate for the environmental cost paid for emission control. One way of compensation is to optimize the production process and to increase the enterprise productivity. By technological innovation and process

optimization, the enterprises can improve on the pollution control capacity and finally counteract the increment of cost induced by environmental regulation. This is called the innovative compensation effect [18]. According to the Porter hypothesis, innovative compensation effect can promote enterprises' acquisition of advanced process and management and further enhance environmental quality and output. Such output increase brought about by technological advances and higher proficiency is the productivity increase. But how innovative compensation effect affects the firm size? To achieve technological innovation, the enterprises have to invest heavily. Given the total sum of capital, the capital left for production and research and development will be reduced. Enterprises in possession of advanced technology and autonomous innovative capacity usually have a large size and abundant capacity. They also enjoy the policy and innovative capital support from the government. Therefore, they can cope with the temporary lack of innovative capital, develop new products that conform to the environmental regulation, and keep growing [18]. But most mid and small-sized enterprises are faced with the problems of lack of innovative capital and capacity. As the intensity of environmental regulation increases, some enterprises cannot afford to improve the current process and equipments and are forced to shut down. A few mid and small-sized enterprises will learn the new technologies from large-sized enterprises or cooperate with large-sized enterprises to improve the technological level. As a result, they will narrow the gap with the large-sized enterprises, making the firm size distribution more conform to Zipf distribution.

(3) Competition effect. Environmental regulation is the activity that the government formulates policy and measures to standardize the economic behaviors of the enterprises for the purpose of environmental protection and coordinated economic development. As stricter environmental protection standards are formulated, the enterprises have to optimize the production process or pollution control. With the introduction of new environmental standards, the enterprises will compete for market opportunities and gain advantages. Therefore, the stimulus-response pattern will be converted into the virtuous cycle of acquiring green demand information, seeking green business opportunities, innovating products and process, innovating the operation mode and win-win situation of the enterprises and the environment [1]. Amid the fierce competition, large-sized enterprises are more aware of its own reputation and social image and will take efforts to maintain the enterprise image and to seize market opportunities. For mid and small-sized enterprises, some favorable policies such as tax exemption for greenness and green subsidies are implemented, thus providing impetus for environmental protection for these enterprises.

Moreover, Chinese government has launched the campaign focusing on the products and the enterprise image for mid and small-sized enterprises with good social reputation. Building a social image as greenness and environmentally friendly will also bring more funding from various sources. Motivated by these favorable policies, the mid and small-sized enterprises will choose to take actions of environmental protection. This will not only bring in more social capital investment, but also boost enterprise development and scale.

As analyzed above, through cost effect, environmental regulation is not only conducive to the enterprises' pollution control behaviors, but also coerces the enterprises to adopt innovative technologies to optimize process and to increase output and productivity. Through innovative compensation effect and learning effect, the enterprises will seek to compensate for the environmental cost while enhancing enterprise competitiveness. Competition effect urges the enterprises to adopt green behaviors while satisfying the minimal environmental standards. By doing this, the enterprises will gradually flourish. On the whole, in the face of new and stricter environmental regulation, large-sized enterprises enjoy more advantages, stronger adaptability and higher development potentials. Some mid and small-sized enterprises will be eliminated due to lack of capital and necessary technologies. A few mid and small-sized enterprises survive and expand by timely achieving technological innovation and process optimization. In a word, environmental regulation makes large-sized enterprises even larger and some high-potential mid and small-sized enterprises to expand. There are inevitably some enterprises that quit the market because of failure to adapt to environmental regulation. As a result of this, the overall size distribution of the enterprises becomes more uniform. Here we hypothesize that environmental regulation increases Pareto index of firm size distribution, making firm size distribution more balanced.

## **EMPIRICAL ANALYSIS**

**Features and Facts of Firm Size Distribution in China.** Zipf's law originates from Pareto's studying distributions in income. Pareto found that the probability of individual income  $Y$  not below a critical value  $y$  is inversely proportional to the power of  $y$ . This is known as Pareto's law [15]. Zipf distribution reflects optimal allocation of economic resources between enterprises under complete market competition, i.e., an ideal situation of uniform size distribution of the firms [15]. We use Pareto index to depict firm size distribution and test whether firm size distribution in Guangdong province obeys Zipf distribution.

In terms of Pareto index, the function of firm size distribution is expressed as follow:

$$\Pr(F_i > f) = Af^{-\alpha} \quad (1)$$

where  $F_i$  is the size of firm  $i$  (measured by the sales volume);  $\Pr(F_i > f)$  is the probability that the size of firm  $i$  is above the critical value  $f$ ;  $A$  is the estimate parameter;  $\alpha$  is Pareto index. Log linearization of formula (1) is carried out:

$$\ln(\Pr(F_i > f)) = \ln A - \alpha \ln f \quad (2)$$

where the probability  $\Pr(F_i > f)$  of firm  $i$  being above the critical value  $f$  is equivalent to the ratio of rank  $S_i$  to the number of firms  $N$  in the descending order of firm size. Thus, the model for estimating the Pareto index is built as follows:

$$\ln\left(\frac{S_i}{N_i}\right) = \beta - \theta \ln F_i + \varepsilon_{it} \quad (3)$$

where  $\beta = \ln A$  is the constant term, and  $\varepsilon_{it}$  the error term. The economic meaning of estimate parameter  $\theta$  is as follows: the closer the value of  $\theta$  to 1, the better the development of mid and small-sized firms and the more uniform the firm size distribution is; moreover, Zipf distribution is obeyed. If  $\theta < 1$ , it means the large-sized firms have better development, whereas the mid and small-sized firms suffer from poor development, and the firm size distribution is less uniform; the smaller the  $\theta$ , the greater the uniformity is and the more severe the deviations from Zipf distribution.

**Establishment of the Empirical Model.** To estimate the influence of environmental regulation on firm size distribution, the measurement model is built as follows:

$$\text{Distr}_{jt} = \alpha_0 + \alpha_1 \text{ERI}_{jt} + \alpha \text{Controls} + \nu_t + \nu_j + \varepsilon_{jt} \quad (4)$$

The set of control variables Control is:

$$\text{Controls} = \beta_1 \text{herfindhl}_{jt} + \beta_2 \text{pergdp}_t + \beta_3 \text{urban}_t + \beta_4 \text{govern}_t \quad (5)$$

where the subscript  $j$  and  $t$  indicate industry and year, respectively; Distr is the status of firm size distribution, as measured by Pareto index calculated by formula (3). For each industry the Pareto index is calculated separately. Distr is the variable related to the industry; ERI is environmental regulation;  $\nu_t$  and  $\nu_j$  indicate the effect of year and industry, respectively;  $\varepsilon_{jt}$  is random disturbance term.

The following control variables are introduced:

① Market concentration (herfindhl), measured by

Herfindahl-Hirschman Index:

$$\text{herfindhl} = \sum_{i \in I_j} (\text{sale}_{it} / \text{sale}_{jt})^2$$

where sale it is the sales volume of firm  $i$  in year  $t$ , and sale  $jt$  is the total sales volume of industry  $j$  in year  $t$ . The larger the herfindhl, the higher the market concentration is for the industry concerned. By introducing the variable of market concentration, the influence of market competition on firm size distribution is considered; ② Local economic development level (pergdp), measured by per capita GDP. Local market scale is largely influenced by local economic development level. The bigger the local market scale, the more favorable it is to the growth of firms, though the opportunities available for firms of different sizes may vary; ③ Urbanization level (urban), measured by the percentage of non-agricultural population to total population. As the urbanization level increases, the local market structure changes as well. That is why the variable of urbanization level should be taken into account when estimating the firm size distribution; ④ Intensity of local government intervention (govern), measured by the percentage of local government's fiscal expenditure to local GDP. Local government policies can affect firm growth greatly and hence the firm size distribution.

**Measures of Indicators.** (1) Measures of environmental regulation. Comprehensive index method is used to build the comprehensive measurement system of environmental regulation for each industry in Guangdong Province. For indicators are chosen, namely, waste water emission (hundred million ton), sulfur dioxide emission (ten thousand ton), dust and soot emission (ten thousand ton) and solid waste emission (ten thousand ton).

First, each indicator is normalized to eliminate incommensurability:

$$UE_{jg}^s = \frac{UE_{jg} - \min(UE_g)}{\max(UE_g) - \min(UE_g)} \quad (6)$$

where  $UE_{jg}$  is the original value of emission of pollutant  $g$  in industry  $j$ ;  $\max(UE_g)$  and  $\min(UE_g)$  are the maximum and minimum emissions of pollutant  $g$  in all industries, respectively;  $UE_{jg}^s$  is the normalized value of emission of pollutant  $g$  in industry  $j$ .

The adjustment coefficient  $W_g$  of each indicator is calculated, and different weights are assigned to different indicators in the industry.

$$W_g = \frac{E_{jg} / \sum E_{jg}}{Q_j / \sum Q_j} \quad (7)$$

where  $E_{jg}$  is the emission of pollutant  $g$  in industry  $j$ ;  $\sum E_{jg}$  is the total emission of pollutant  $g$  in all industries;  $Q_j$  is gross industrial output in industry  $j$ ;  $\sum Q_j$  is gross industrial output in all industries.

According to the normalized values and weights of each indicator, the comprehensive intensity of environmental regulation in each industry is calculated:

$$S_j = \sum_{g=1}^s W_g \times UE_{jg}^s \quad (8)$$

Through the summation of intensity of environmental regulation for each pollutant in each industry, the average intensity of environmental regulation is obtained.

(2) Data explanations. The data of Pareto index of firm size distribution and the data of control variables related to the industry come from CSMAR Database in 2001-2014. Addressing the problems of missing and abnormal data of indicators, the sample data are processed as follows: ①The observed values with the missing of gross industrial output of the firms and the missing of average annual net balance of firm fixed assets are deleted; ②The samples not conforming to the accounting principles are deleted, that is, the observed values with the total firm assets being smaller than the current assets, the total firm assets being smaller than the average annual net balance of firm fixed assets, and the accumulated depreciation being smaller than the depreciation of the current period. ③Samples of firms not of the specified scale are deleted, that is, the observed values of firms with staff members less than 30 and the revenues from main business less than 5 million RMB. The data on the indicators of environmental regulation and pollutant emission intensity come from Guangdong Statistical Yearbook in the corresponding years. Other missing data are complemented by mean imputation.

## RESULT OF EMPIRICAL ANALYSIS

**Estimate of Pareto Index of Firm Size Distribution.** According to the empirical results, the Pareto index varies between 0.4 and 0.7 and is far below 1. Thus the Zipf distribution is disobeyed. Table 1 shows the estimates of Pareto index among Guangdong's industrial firms in 2000 to 2011. The Pareto index is calculated by WLS regression on the

panel data. As shown in Table 1 and figure 1, the Pareto indices of the sample firms all pass the 1% level of significance test in 2000 to 2011. The average Pareto index is 0.5353, indicating severely unbalanced firm size distribution. There is a large development gap between large-sized firms and mid and small-sized firms. This means the mid and small-sized firms are not fully developed. In contrast, Gaffeo *et al.* showed that economic growth will promote the balanced size distribution of the firms [3]. But our results accord with the findings by Sun and Wang on size distribution of Chinese firms [1]. Specifically, Pareto index is 0.5184 in 2000 and 0.6079 in 2011. The firm size distribution becomes more uniform over time. The market environment is more favorable for the development of mid and small-sized firms along with economic growth.

**TABLE 1**  
Estimates of Pareto index of firm size distribution.

Year	Constant term	Pareto index ( $\theta$ )	Observed value
2000	6.3146	0.5184***	531
2001	6.3146	0.5184***	527
2002	6.1253	0.5020***	531
2003	5.4926	0.4444***	522
2004	6.1005	0.4845***	545
2005	6.6539	0.5129***	553
2006	5.9392	0.5547***	540
2007	6.0602	0.5623***	571
2008	6.0686	0.5576***	567
2009	6.2249	0.5660***	570
2010	6.5967	0.5826***	555
2011	6.4012	0.6079***	565

Note: \*, \*\* and \*\*\* indicate 10%, 5% and 1% significance level, respectively.

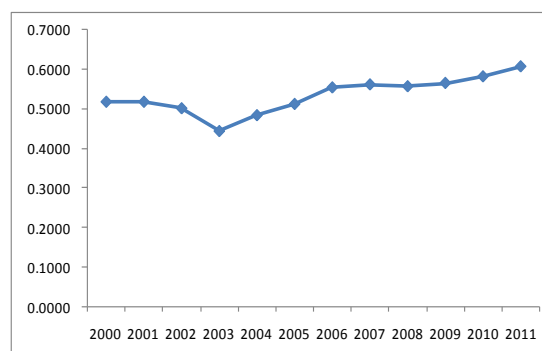


**FIGURE 1**  
Dynamic changes of Pareto index of firm size distribution



**TABLE 2**  
**Estimates of Pareto index of firm size distribution across the industries.**

Year	$\theta_1$	$\theta_2$	$\theta_3$	$\theta_4$	$\theta_5$	$\theta_6$	$\theta_7$	$\theta_8$	$\theta_9$
2000	0.6400	0.5110	0.5700	0.6210	0.4160	0.4750	0.5380	0.5300	0.4990
2001	0.6490	0.5670	0.5430	0.5500	0.4140	0.4830	0.5430	0.4800	0.4900
2002	0.6080	0.5100	0.5150	0.5560	0.4020	0.4880	0.5440	0.4750	0.6030
2003	0.7150	0.3430	0.5180	0.5520	0.3650	0.4630	0.4960	0.4470	0.5060
2004	0.7780	0.3880	0.5500	0.5550	0.3820	0.4640	0.4920	0.4800	0.4980
2005	0.8570	0.3790	0.5480	0.5090	0.3890	0.4530	0.4710	0.4580	0.4500
2006	0.7570	0.3890	0.5860	0.5090	0.4290	0.4930	0.5200	0.5030	0.4950
2007	0.8050	0.3360	0.4770	0.4510	0.3610	0.4610	0.4690	0.4980	0.4680
2008	0.7050	0.3310	0.5070	0.4470	0.3690	0.5150	0.4880	0.5060	0.4910
2009	0.7600	0.3320	0.4920	0.4440	0.3980	0.4670	0.4620	0.5400	0.5000
2010	0.7150	0.3630	0.5540	0.4970	0.4060	0.5150	0.5610	0.5600	0.4790
2011	0.7430	0.3210	0.5690	0.4860	0.3790	0.4630	0.5340	0.5350	0.4770

Note: Pareto index of 9 industries passes 1% level of significance test. Industry 1 represents electronics and information manufacturing industry, industry 2 represents electrical machinery and special equipment manufacturing industry, industry 3 represents petrochemical manufacturing industry, industry 4 represents textiles and apparel industry, industry 5 represents food manufacturing industry, industry 6 represents building materials industry, industry 7 represents papermaking industry, industry 8 represents pharmaceutical manufacturing industry, industry 9 represents automobile industry.

Large differences exist in firm size distribution across the industries. In other words, industry category has a significant impact on firm size distribution. By reference to Guangdong Statistical Yearbook, 9 major industries are included, namely, electronics and information manufacturing industry, electrical machinery and special equipment manufacturing industry, petrochemical manufacturing industry, textiles and apparel industry, food manufacturing industry, building materials industry, papermaking industry, pharmaceutical manufacturing industry and automobile industry. As seen from Table 2, firm size distribution varies greatly from one industry to another. Two industries with smallest average Pareto index are food manufacturing industry and electrical machinery and special equipment manufacturing industry, the values being 0.3925 and 0.3975, respectively. This indicates highly unbalanced size distribution of the firms in the two industries and the phenomenon of monopoly. Electronics and information manufacturing industry has the highest average Pareto index, which is 0.7277. This indicates more balanced size distribution of the firms within the industry and the firms of different sizes all enjoy the chances of development.

Pareto index shows varying trend of changes across the industries. From 2000 to 2011, the electronics and information manufacturing industry, petrochemical manufacturing industry and pharmaceutical manufacturing industry show an increase of Pareto index. In contrast, electrical machinery and special equipment manufacturing

industry, textiles and apparel industry and automobile industry show a decrease of Pareto index. Food manufacturing industry, building materials industry and papermaking industry show a fluctuation of Pareto index.

**TABLE 3**  
**Variable estimate**

Variable	OLS	TSLS
ERI	0.5712*** (4.2935)	0.8125*** (5.0408)
HERFINDHL	1.8149*** (4.8933)	2.3546*** (5.5413)
URBAN	-0.0044** (-1.7670)	-0.0040** (-2.1777)
LNGDP	0.0424* (1.7670)	0.0207 (0.8082)
GOVERN	-0.0288* (-1.7375)	-0.0296* (-1.7565)
C	0.1926 (1.3753)	0.1546 (1.1553)
Year effect	Control	Control
Industry effect	Control	Control
R <sup>2</sup>	0.3790	0.3100
Observed value	108	108

Note: The value in the parentheses is t-statistics; \*, \*\* and \*\*\* indicate 10%, 5% and 1% significance level, respectively.

**Influence of Environmental Regulation on Firm Size Distribution.** OLS regression is

performed on firm size distribution and the estimate result is shown in Table 3. The coefficient of determination of environmental regulation is positive and passes the 1% level of significance test, indicating positive impact of environmental regulation on firm size distribution. That is, the stricter the environmental regulation, the more favorable it is to the development of mid and small-sized firms and the more uniform the firm size distribution will be. This confirms the hypothesis proposed above. Environmental regulation has varying impact on large-sized firms and mid and small-sized firms. The mid and small-sized firms gain more benefits from environmental regulation and the firm size distribution is closer to Zipf distribution.

Among other control variables, market concentration is positively correlated with Pareto index at 1% significance level. That is, the higher the market concentration, the more favorable it is to the development of mid and small-sized firms and the more uniform the firm size distribution will be. Urbanization level is negatively significantly correlated with Pareto index. The higher the urbanization level, the more severe the deviations from Zipf distribution are. The mid and small-sized firms do not reap due benefits from urbanization. The local economic development level is positively correlated with Pareto index at 10% significance level. As local economic development level increases, both large-sized and mid and small-sized

firms are benefited. The coefficient of determination of local government intervention is negative and shows positive correlation with Pareto index at 10% significance level. That means the favorable tax policies are more targeted at large-sized firms, and the mid and small-sized firms are less supported by the local government.

Endogeneity problem in time series may lead to bias and inconsistency of OLS regression. Therefore, regression is performed again using two-stage least squares method on instrumental variables. The selection of instrumental variables of environmental regulation is based on the method by Fu and Li [20]. The standard coal consumption of each industry in Guangdong Province in 2000-2011 is taken as instrumental variable. Standard coal consumption within an industry is closely associated with environmental regulation. The higher the standard coal consumption, the greater the emissions of pollutants and consequently stricter environmental regulation will be imposed. The results of regression using the instrumental variables are shown in Table 3. Except the local economic development level, all other variables show consistent correlations with Pareto index as by OLS regression. The coefficient of determination of environmental regulation is positive and passes 1% level of significance test. Thus environmental regulation has a positive impact on firm size distribution and the hypothesis is confirmed.

**TABLE 4**  
**Robustness test**

Variable	test1	test 2	test 3	test 4
IWW	0.0111* (1.7515)			
IWGE		0.0020* (1.7839)		
ISE			0.0034* (1.8939)	
ISWD				0.0001* (1.8059)
HERFINDHL	0.8028*** (2.8545)	0.8277*** (2.8807)	0.7990*** (2.7675)	0.7490*** (2.7115)
URBAN	-0.0054*** (-2.8112)	-0.0048*** (-2.4382)	-0.0038* (-1.7741)	-0.0061*** (-3.0607)
LNGDP	0.0884*** (3.9295)	0.0822*** (3.5386)	0.0741*** (2.9013)	0.1002*** (4.4020)
GOVERN	-0.0254 (-1.4308)	-0.0220 (-1.2292)	-0.0171 (-0.9087)	-0.0342* (-1.8555)
C	0.1326 (1.2733)	0.1041 (1.0543)	0.0823 (1.5678)	0.1488 (1.3867)
Effect of year	Control	Control	Control	Control
Effect of industry	Control	Control	Control	Control
R <sup>2</sup>	0.24	0.18	0.26	0.21
Observed value	108	108	108	108

Note: IWW represents industrial waste water, IWGE represents industrial waste gas emission, ISE represents industrial soot(dust) emission, ISWD represents industrial solid wastes discharged. The value in the parentheses is t-statistics; \*, \*\* and \*\*\* indicate 10%, 5% and 1% significance level,

respectively.

**Robustness Test.** To test for robustness, the variables of environmental regulation are divided into 4 indicators, namely, wastewater emission, sulfur dioxide emission, dust and soot emission and solid waste emission. Normalized values of the indicators are used as the substitution variables. The regression results are shown in Table 4. The four indicators of pollutant emission show significantly positive correlation with Pareto index of firm size distribution and pass the 10% level of significance test. The significance level of a single indicator decreases somewhat compared with that of the comprehensive variable of environmental regulation. It is indicated that a single indicator can hardly reflect the overall level of environmental regulation. Nevertheless, it is still found that environmental regulation has significantly positive correlation with Pareto index. As the intensity of environmental regulation increases, the firm size distribution is closer to Zipf distribution.

## CONCLUSIONS

We estimate Pareto index of firm size distribution across 9 industries in Guangdong Province from 2000 to 2011. The influence of environmental regulation on firm size distribution is discussed and the following conclusions are drawn.

Pareto index of firm size distribution in Guangdong Province is far less than 1, with deviations from Zipf distribution. But along with economic development, Pareto index increases every year. Thus, not only large-sized firms, but also mid and small-sized firms enjoy the chances of development, leading to more balanced firm size distribution. Moreover, there are large differences in firm size distribution across the industries and industry category has a significant impact on firm size distribution. Electronics and information manufacturing industry has the most balanced firm size distribution, while food manufacturing industry and electrical machinery and special equipment manufacturing industry have the most unbalanced firm size distribution.

In a word, environmental regulation has a positive impact on firm size distribution. As the intensity of environmental regulation increases, the Pareto index of firm size distribution increases gradually. Compared with large-sized firms, mid and small-sized firms gain more benefits from environmental regulation, and consequently firm size distribution becomes more uniform. The above findings provide inspirations for the formulation and implementation of environmental policies.

(1) The intensity of environmental regulation should be raised depending on the pollution status of a specific industry. One major reason for the aggravating environmental crisis in China is

insufficiency of government's environmental regulation and enterprises' efforts in pollution control. The intensity of environmental regulation not only affects the motive of firms' technological innovation, but also determines the comprehensive competitiveness of the firms. To maintain good reputation and stable growth, large-sized firms will proactively adapt to the new environmental regulation by technological innovation and process optimization. However, the mid and small-sized firms lack the motives to adapt to low-intensity environmental regulation by using innovative technologies and optimized process. When environmental regulation becomes stricter, these firms lack the capitals to make adaptations and finally quit the market. There are some mid and small-sized firms that struggle to prosper through technological innovation in the face of new environmental regulation. This is a process of changing and adjustment of firm size distribution within the industry, which results in more balanced firm size distribution. Therefore, properly raising the intensity of environmental regulation is conducive to the balanced size distribution of the firms. The intensity of environmental regulation should vary for different industries considering the variable features of firm size distribution.

(2) The transition from mandatory regulation to incentive-based regulation should be facilitated by using flexible tools of environmental regulation. At present, mandatory environmental regulation still dominates. For example, mandatory limits on the emissions of wastewater, dust and soot and waste solids are laid down by the governments for different industries. The firms must abide by these regulations, otherwise they will be penalized. Such emission control is realized by government's administrative power and by imposing high fines. The firms are compelled to make innovations to adapt to the regulations, and the power of the market is not utilized. Therefore, Chinese government should pay more attention to the use of market-based regulation tools, such as pollution charge system and pollution right trading system. Carbon emission trading market is a sustaining mechanism that enhances the motives of enterprises in adapting to the environmental regulation and reduces the government's cost in environmental regulation. Environmental information publication system should be popularized and the carbon dioxide emission reporting system be encouraged to promote information transparentization between the stakeholders and further development of carbon emissions trading market. Flexible environmental regulation tools can motivate enterprises' adoption of innovative technologies and optimized process. The enterprises can save cost through emissions trading, which is particularly beneficial for mid and small-sized firms lacking in innovation capitals.



Thus the mid and small-sized firms can gain more benefits from environmental regulation and the firm

## ACKNOWLEDGEMENTS

This study was supported by Research Planning Foundation in Humanities and Social Sciences of the Ministry of Education of China(No. 13YJAZH044) and Guangdong Soft Science Item (No. 2016A070706008)

## REFERENCES

- [1] Sun, X.M.; Wang, J. (2014) Effects of environmental regulation on Chinese enterprises size distribution. *China Industrial Economics*. 12, 44-56 [In Chinese].
- [2] Axtell, R.L. (2001) Zipf distribution of US firm sizes. *Science*. 293, 1818-1820.
- [3] Gaffeo, E.; Gallegati, M.; Palestrini, A. (2003) On the size distribution of firms: additional evidence from the G7 countries *Physica A: Statistical Mechanics and its Applications*. 24, 117-123.
- [4] Fujiwara, Y.; Di Guilmi, C.; Aoyama, H.; Gallegati, M.; Souma, W. (2004) Do Pareto-Zipf and Gibrat laws hold true? An analysis with European firms. *Physica A: Statistical Mechanics and its Applications*. 335, 197-216.
- [5] Cirillo, P. (2010) An analysis of the size distribution of Italian firms by age *Physica A: Statistical Mechanics and its Applications*. 389, 459-466.
- [6] Di Giovanni, J.; Levchenko, A.A. (2013) Firm entry, trade, and welfare in Zipf's world. *Journal of International Economics*. 89, 283-296.
- [7] Garicano, L.; Lelarge, C.; Van Reenen, J. (2013) Firm size distortions and the productivity distribution: Evidence from France National Bureau of Economic Research, NBER Working Paper.
- [8] Adamopoulos, T.; Restuccia, D. (2014) The size distribution of farms and international productivity differences. *The American Economic Review*. 104, 1667-1697.
- [9] Song, M.L.; Wang, S.H. (2013) Analysis of environmental regulation, technological progression and economic growth from the perspective of statistical tests. *Economic Research Journal*. 3, 122-134 [In Chinese].
- [10] Zipf, G.K. (1965) Human behavior and the principle of least effort. An introduction to human ecology, etc. New York & London.
- [11] Delli, G.D.; Di Guilmi, C.; Gaffeo, E.; Giulion, G.; Gallegati, M.; Palestrini, A. (2004) Business cycle fluctuations and firms 'size distribution dynamics. *Advances in Complex Systems*. 7, 223-240.

size distribution will be more balanced.

- [12] Luttmer, E.G. (2007) Selection, growth, and the size distribution of firms. *The Quarterly Journal of Economics*. 1103-1144.
- [13] Cirillo, P.; Hübler, J. (2009) On the upper tail of Italian firms' size distribution. *Physica A: Statistical Mechanics and its applications*. 388, 1546-1554.
- [14] Di Giovanni, J.; Levchenko, A.A.; Rancière, R. (2011) Power laws in firm size and openness to trade: Measurement and implications. *Journal of International Economics*. 85, 42-52.
- [15] Fang, Y.M.; Nie, H.H. (2010) The stylized facts of size distribution of China manufacturing industries: a perspective of Zipf's law. *Reviews of Industrial Economics*. 2, 1-17.
- [16] Yang, Q.J.; Li, X.B.; Fang, M.Y. (2010) Market, government and firm size distribution-an empirical research. *World Economic Papers*. 1, 1-15.
- [17] Hongya, L.; Xuegui, S.; Yinjie, Z. (2014) Financial constraints and the size distribution of Chinese enterprises-based on Chinese listed companies manufacturing data. *Modern Economic Science*. 2, 95-109 [In Chinese].
- [18] Jiang, F.X.; Wang, Z.J.; Bai, J.H. (2013) The dual effect of environmental regulations' impact on innovation-an empirical study based on dynamic panel data of Jiangsu manufacturing. *China Industrial Economics*. 7, 44-55 [In Chinese].
- [19] Chapple, L.; Clarkson, P.M.; Gold, D.L. (2013) The cost of carbon: Capital market effects of the proposed emission trading scheme (ETS). *Abacus*. 49, 1-33.
- [20] Fu, J.Y.; Li, L.S. (2010) A case study on the environmental regulation, the factor endowment and the international competitiveness in industries. *Management World*. 10, 87-98 [In Chinese].

**Received: 15.03.2016**

**Accepted: 16.09.2016**

## CORRESPONDING AUTHOR

**Yang Yuanhua**

Public Management School, Guangdong University of Finance and Economics, Guangzhou 510000, China

email: [260782245@qq.com](mailto:260782245@qq.com)

# ENVIRONMENTAL CONTAMINATION OF HEAVY METALS IN THE YAĞLIDERE STREAM (GIRESUN), SOUTHEASTERN BLACK SEA

Arzu Aydin Uncumusaoglu<sup>1,\*</sup>, Umit Sengul<sup>2</sup>, Tamer Akkan<sup>3</sup>

<sup>1</sup> Department of Environmental Engineering, Faculty of Engineering, Giresun University, Turkey

<sup>2</sup> Department of Science Education, Faculty of Education, Giresun University, Turkey

<sup>3</sup> Department of Biology, Faculty of Science and Letters, Giresun University, Turkey

## ABSTRACT

This study was carried out to examine heavy metals concentration in water and sediment samples of Yağlıdere Stream in Giresun, Turkey. Concentrations of Cr, Mn, Fe, Co, Ni, Cu, Cd and Pb were determined by using ICP-MS. The surface water and sediment samples were collected monthly, from at 5 stations between June 2013 and May 2014. Descriptive statistical analysis including One-way ANOVA, significance (0.05) was done. Important differences in the mean values were tested with Duncan's multiple range test. Moreover, with the purpose for determining the level of pollution, the methods of the factor of sediment enrichment factor and the index of geoaccumulation were applied.

Cu, Pb, Ni and Cd concentrations in water samples were very higher than RSWQM standards, Cu, Mn, Fe and Pb concentrations were higher than the EPA standards and also Cu, Mn, Fe, Pb, Cu and Ni concentrations were higher than the WHO guidelines. The result of sediment enrichment factor and geoaccumulation index reveals that surface sediments of the Yağlıdere Stream are unpolluted.

Consequently, it can be concluded that the concentrations of heavy metals in water from Yağlıdere Stream are generally higher than the RSWQM, WHO and EPA standards. It can be concluded that the heavy metal pollution level is high in Yağlıdere Stream and it will be good to adopt protective measures before it's too late.

## KEYWORDS:

Heavy Metal, Water, Sediment, Geoaccumulation, Yağlıdere Stream

## INTRODUCTION

Heavy metals are common pollutants which are distributed in aquatic environment. Pollution of this area with heavy metals has become a serious health concern during recent years. The most

common heavy metal pollutants are arsenic, cadmium, chromium, copper, nickel, lead and mercury. There are different types of sources of pollutants: point sources (localized pollution), and nonpoint sources, where pollutants come from dispersed sources. Although some of these metals are essential for organisms, as micronutrients and their high concentration in the food chain can cause toxicity and environmental impacts and endanger aquatic ecosystems and their users [1, 2]. The natural water bodies and sediments may extensively be contaminated with various heavy metals released from domestic, industrial effluents, draining of sewage, dumping of agricultural activity, hospital sewage and other anthropogenic activities etc. [3-6]. Heavy metals in sediments occur in different geochemical forms, which have distinct mobility, biological toxicity and chemical behaviour. Heavy metal pollution of freshwater ecosystems has been shown to be extensive. High levels of heavy metals have been found in sediment and biota of ponds and lakes, rivers and wetlands. These metals are bioaccumulated by organisms either passively from water or by facilitated uptake. Also sediments play a major role in the determining pollution pattern of aquatic systems. Many studies reported that surface water resources of Turkey have been seriously polluted by heavy metals [1, 2, 7-12]. Moreover, some papers have been published concerning heavy metal levels in sediment [13], biota [14,15] and aquatic organisms [16-19] of the Turkey.

Yağlıdere is a long and highly voluminous stream that flows to northern Black Sea in the west end of the Espiye district in Giresun Province. Yağlıdere stream is a very narrow valley it flows down to Yağlıdere town which is the district center with the same name of the stream, and therefore, it is exposed to domestic waste, petroleum filling facility's waste and agricultural runoff. It has a length of 70 km and originates from the Kurtbeli highlands.

Pollution of the freshwater sources with heavy metals has become a serious health concern during recent years. This area is more susceptible to the harmful effects of pollutant because aquatic

organisms are in close and extended contact with the soluble metals. For this reason, the principal aim of this study, which was done in Yağlıdere Stream (Turkey) was to determine some heavy metals (Cr, Mn, Co, Ni, Cu, Cd, Pb, Fe) in water and sediment.

were collected with an Ekman sampler at the selected stations. After collection the samples were placed in coolers with ice bags while being transported to the laboratory and kept at about 4°C until being analyzed.

## MATERIAL AND METHODS

**Sample location and sampling.** Surface water and sediment samples were collected between June 2013 and May 2014, from 5 stations (Figure 1). Water samples were collected in 1-liter pre cleaned (with 50% HNO<sub>3</sub> and then thrice with deionized water) polyethylene bottles and acidified with 10 ml concentrated HNO<sub>3</sub> per liter of wastewater for the analysis of heavy metals. The sediment samples



**FIGURE 1**  
The Study area and sampling stations

**TABLE 1**  
Heavy Metal Concentrations of surface water samples (ppm)

Heavy Metal	Season n=15	Station					Average Value	US EPA	WHO
		1	2	3	4	5			
Cr	Summer	1.141	1.079	1.530	1.186	0.410	<b>1.069<sup>a</sup></b>		
	Fall	3.500	3.197	3.244	3.020	2.997	<b>3.192<sup>c</sup></b>		
	Winter	2.392	2.485	2.178	2.074	2.323	<b>2.149<sup>b</sup></b>		
	Spring	2.092	1.905	2.401	1.933	1.366	<b>2.081<sup>b</sup></b>		
Mn	Summer	2.660	2.401	8.946	2.462	0.829	<b>3.460</b>	<b>0.16</b>	<b>0.05</b>
	Fall	2.682	2.821	2.709	4.462	4.327	<b>3.400</b>		
	Winter	0.395	0.214	0.255	0.231	0.429	<b>0.305</b>		
	Spring	0.230	0.104	0.459	0.395	0.451	<b>0.328</b>		
Co	Summer	0.296	0.295	0.478	0.249	0.391	<b>0.342<sup>b</sup></b>		
	Fall	0.071	0.043	0.168	0.268	0.079	<b>0.126<sup>a</sup></b>		
	Winter	0.122	0.126	0.137	0.091	0.113	<b>0.118<sup>a</sup></b>		
	Spring	0.176	0.225	0.198	0.309	0.242	<b>0.230<sup>ab</sup></b>		
Ni	Summer	6.286	6.187	7.252	6.239	5.117	<b>6.216<sup>a</sup></b>		
	Fall	19.633	20.242	20.145	19.516	19.132	<b>19.734<sup>b</sup></b>		<b>0.3</b>
	Winter	9.182	9.435	10.909	9.296	1.789	<b>8.122<sup>a</sup></b>		
	Spring	5.859	5.716	6.439	6.518	8.144	<b>6.535<sup>a</sup></b>		
Cu	Summer	2.560	2.312	2.803	2.084	1.426	<b>2.237</b>		
	Fall	1.837	2.191	1.981	4.192	3.941	<b>2.828</b>		<b>0.4</b>
	Winter	0.727	0.861	2.559	1.043	1.935	<b>1.425</b>		
	Spring	38.818	5.599	2.442	3.976	1.388	<b>10.444</b>		
Cd	Summer	1.120	1.120	1.376	1.111	1.107	<b>1.167<sup>b</sup></b>		
	Fall	0.686	0.696	0.708	0.707	0.700	<b>0.700<sup>a</sup></b>	<b>0.145</b>	<b>0.2</b>
	Winter	0.641	0.677	0.752	0.683	0.678	<b>0.686<sup>a</sup></b>		
	Spring	0.862	0.952	0.932	1.032	0.993	<b>0.954<sup>ab</sup></b>		
Pb	Summer	1.691	1.686	2.127	1.668	1.642	<b>1.763</b>		
	Fall	2.390	2.412	2.426	2.362	2.412	<b>2.400</b>	<b>0.004</b>	<b>2</b>
	Winter	1.346	2.242	2.702	1.787	2.135	<b>2.042</b>		
	Spring	1.693	2.449	2.452	3.896	1.647	<b>2.428</b>		
Fe	Summer	6.647	4.621	4.058	12.110	9.861	<b>7.460<sup>ab</sup></b>		
	Fall	10.882	10.417	22.013	6.320	6.313	<b>11.189<sup>b</sup></b>	<b>3.6</b>	<b>3</b>
	Winter	1.228	0.485	1.156	1.282	1.641	<b>1.159<sup>a</sup></b>		
	Spring	0.725	0.683	0.701	0.663	0.642	<b>0.683<sup>a</sup></b>		

Horizontally, letters a and b show statistically significant differences in same group of metals ( $p < 0.05$ )

**TABLE 2**  
**Seasonal changes in Levels of Heavy Metals (ppm)**

		Cr	Mn	Co	Ni	Cu	Cd	Pb	Fe
Summer	Water	1.069±0.273	3.460±1.277	0.342±0.047	6.216±1.635	2.237±0.332	1.167±0.095	1.763±0.254	7.460±1.520
		0.128-3.600	0.014-18.719	0.028-0.600	0.045-14.734	0.316-4.156	0.944-2.224	0.743-4.041	0.026-24.182
	Sediment	2.952±0.085	145.220±8.916	nd	1.888±0.046	15.836±1.978	0.135±0.014	16.726±1.239	1.329±0.677
		2.272-3.447	88.284-215.211	nd	1.658-2.321	9.740-32.991	0.054-0.291	9.817-26.374	0.036-8.000
Fall	Water	3.192±0.181	3.400±1.134	0.126±0.046	19.734±2.752	2.828±0.835	0.700±0.147	2.400±0.090	11.189±4.499
		2.212-4.618	0.127-12.481	0.014-0.680	4.055-27.752	0.246-10.351	0.291-1.492	2.088-2.968	0.875-62.849
	Sediment	3.933±0.157	206.735±5.804	nd	2.525±0.066	31.387±4.337	0.195±0.026	18.638±1.695	1.790±0.524
		2.910-5.136	162.130-250.565	nd	2.067-3.054	15.829-84.006	0.037-0.384	11.945-35.214	0.000-7.000
Winter	Water	2.149±0.185	0.305±0.079	0.118±0.018	8.122±3.046	1.425±0.317	0.686±0.072	2.042±0.268	1.159±0.229
		0.530-2.972	0.050-1.038	0.020-0.219	0.139-27.034	0.127-4.891	0.302-1.077	0.061-4.918	0.033-3.166
	Sediment	4.469±0.113	191.936±8.319	nd	2.840±0.088	24.168±1.856	0.162±0.019	17.185±0.771	0.103±0.012
		3.887-5.545	122.709-243.236	nd	2.432-3.567	13.684-33.506	0.067-0.357	13.558-22.792	0.059-0.222
Spring	Water	2.081±0.231	0.328±0.082	0.230±0.018	6.535±0.863	10.444±7.258	0.954±0.024	2.428 ±0.369	0.683±0.025
		0.842-3.898	0.031-1.072	0.140-0.421	0.292-9.543	0.728-111.461	0.794-1.095	0.434-5.481	0.512-0.817
	Sediment	4.266±0.210	200.718±7.901	nd	2.948±0.176	21.212±1.859	0.130±0.033	14.365±1.266	8.159±0.838
		2.083-5.974	113.492-234.609	nd	1.165-4.178	8.721-39.072	0.010-0.536	6.193-25.521	4.000-15.000

**Heavy metal analysis.** The samples were immediately transported to the laboratory and filtered through acid treated Millipore HA filters (0.45 µm) with vacuum. These samples were stored in darkness at 4 °C up to the analytical treatment [20]. Sediment samples were prepared with a preliminary digesting process via a CEM MARS-5 model microwave instrument. Heavy metal determinations of all samples were carried out with an ICP-MS-Bruker 820-MS [21]. The certified reference materials were used to check the accuracy and reliability of the method. Metal contents were expressed as ppm or µg/g.

**Enrichment factor and index of geoaccumulation.** Enrichment factor (EF) and Geoaccumulation index ( $I_{geo}$ ) are a useful indicator reflecting the status of environmental contamination [22-27]. In calculating the normalized enrichment factors (EF), the original Salomons and Förstner [28] equation was substituted in the present study by Fe because Al data was not available. In order to evaluate a possible anthropogenic origin of the metals, the enrichment factor (EF) and  $I_{geo}$  were calculated for the metal concentration obtained in surface sediments [29].

**Statistically Analysis.** Statistical analysis of data was carried out using SPSS statistical package programs. Descriptive statistical analysis, including One-way ANOVA, significance (0.01 and 0.05) was done. Important differences in the mean values were tested with Duncan's multiple range test.

## RESULTS AND DISCUSSION

Heavy metal analyses of water samples taken periodically from five stations over a period of 4 seasons showed that the levels of Chromium, Manganese, Cobalt, Nickel, Copper, Cadmium, Lead and Iron varied between 0.128-4.618 (2.123±0.145), 0.014-18.719 (1.873±0.464), 0.014-0.680 (0.204±0.021), 0.045-27.752 (10.152±1.315), 0.127-111.461 (4.234±1.844), 0.291-2.224 (0.877±0.053), 0.061-5.481 (2.158±0.134) and 0.026-62.849 (5.122±1.292) ppm, respectively. Moreover, seasonal changes of heavy metal concentrations in surface water are shown in Table 1, 2.

The order of heavy metal concentrations in water samples measured; Fe>Ni>Mn>Cu>Pb>Cd>Cr>Co in summer, Ni>Fe>Mn>Cr>Cu>Pb>Cd>Co in autumn, Ni>Cr>Pb>Cu>Fe>Cd>Mn>Co in winter and Cu>Ni>Pb>Cr>Cd>Fe>Mn>Co in spring.

The sequence of the means of heavy metals in water samples from all seasons were Ni>Fe>Cu>Pb>Cr>Mn>Cd>Co. Fe and Ni were found in higher amounts than other trace microelements. All the 120 surface water and sediment samples of the stream Yağlıdere were analyzed for Cu, Ni, Pb, Cr, Cd, Fe, Mn and Co. The concentrations of these metals exceed the water quality criteria for protection of aquatic life [30].

The mean concentrations of metals detected in the samples were Ni>Cu>Fe>Cr>Mn>Cd>Pb>Co at different locations in present study.

**TABLE 3**  
**Comparative values (ppb) for heavy metals in water from different studies**

Metals	RSWQM, 2015 [30]				References					
	I	II	III	IV	Kizilirmak Stream [7]	Saricay Stream [8]	Kelkit River [9]	Sakarya River [10]	Gediz River, ppm [11]	This Study Mean, ppm (n=60)
<b>Cu</b>	≤20	20-50	50-200	> 200	25-69	310-840	0-120.4	0.24-1.6	5.82-8.43	4.234
<b>Zn</b>	≤200	200-500	500-2000	> 2000	32-1079	nd	0-377.9	0.19-2.9	0.36-0.72	
<b>Mn</b>					35-285	36-168		30-170	14.89-34.46	1.873
<b>Pb</b>	≤10	10-20	20-50	> 50	76-119	20-320	2.28-151.3	0.59-1.5	3.94-5.84	0.204
<b>Ni</b>	≤20	20-50	50-200	> 200	14-114	15.9-21.8		0.39-9		10.152
<b>Cd</b>	≤2	2-5	5-7	> 7	6-14	5-8			1.38-2.85	0.877
<b>Fe</b>						nd-259		1.3-687	37.6-99.16	5.122
<b>Co</b>						13.6-17.6	0-1.789			0.204
<b>Cr</b>					15-511	20.3-241	0.042-20.44			2.123
<b>Hg</b>	< 0.1	0.1-0.5	0.5-2	> 2				0.037-0.81		

The comparison between the present concentrations and those in the literature concluded that generally the concentrations observed in the Yağlıdere Stream were lower than those recorded (Table 3). Pb concentrations had been detected about 100-200 times lower than many studies in Turkey (Table 3). In addition, the concentrations of Cu are lower than found in earlier studies in Turkey (Table 3). However, Ni values were higher than in Sakarya River [10] and in Gediz River [11]. Ayas et al. [31] could not detect the Cd in Göksu Delta in Turkey. However, Cd concentration in Yağlıdere Stream ranged from 0.700-to 1.167 ppm in water.

The seasonal concentrations ( $\mu\text{g/g}$ ) sequence of heavy metals in sediment samples were; Mn>Pb>Cu>Cr>Ni>Fe>Cd>Co in summer, Mn>Cu>Pb>Cr>Ni>Fe>Cd>Co in autumn, Mn>Pb>Cu>Cr>Ni>Cd>Fe>Co in winter and Mn>Cu>Pb> Fe>Cr>Ni> Cd>Co in spring. In sediment; Cr, Mn, Ni, Cu, Cd, Pb and Fe were present in all seasons while Mn was highest. Co was below detection limit in all seasons.

The average metal concentrations ( $\mu\text{g/g}$ ) in the sediment samples from 5 stations varied from 2.952 to 4.469 for Cr, 145.220 to 206.735 for Mn, 1.888 to 2.948 for Ni, 15.836 to 31.387 for Cu, 0.130 to 0.195 for Cd, 14.365 to 18.638 for Pb, 0.103 to 8.159 for Fe (Table 4). The average concentrations of all metals in the sediment were lower than the average shale values [32]. According to Şener and Şener [33], heavy metal concentration levels in the sediment samples Cu: 34.88-336  $\mu\text{g/g}$ , Pb: 12.97-21.12  $\mu\text{g/g}$ , Zn: 55-109.50  $\mu\text{g/g}$ , Ni: 71-139.90  $\mu\text{g/g}$ , Co: 14.30-19  $\mu\text{g/g}$ , Mn: 492-1055  $\mu\text{g/g}$ , As: 6.10-32.10  $\mu\text{g/g}$  and Fe: 2.02-3.11 % were determined and heavy metals were in the sequence as follows: Mn>Ni>Zn>Cu>Pb>As>Co>Fe. Mendil et al. [34] reported that heavy metal accumulations in sediment samples; Cd: 0.55 mg/g, Cu: 38.7 mg/g, Pb: 29.6 mg/g, Ni: 79.2 mg/g and Zn: 126.2 mg/g were determined collected from Yeşilirmak River (Turkey). The average

concentrations of Cu, Pb, Ni and Co obtained in this study was much lower than sediments of Degirmendere River, Yanbolu River and Solaklı River [35] and similar to Klang River except for Co [36].

The influences of anthropogenic metals pollution in surface sediments of Yağlıdere Stream were determined using enrichment factor (SEF-PLI) and geoaccumulation index ( $I_{\text{geo}}$ ) for all metals (Table 5). The  $I_{\text{geo}}$  suggested that individual metal contamination in the sediments could be classified as “practically uncontaminated”. The result from the present investigation showed that  $I_{\text{geo}}$  of Cu: -1.54, Cd: -1.53, Ni: -5.32, Pb: -0.84, Fe: -1.31, Cr: -5.11 and Mn: -2.78, respectively. Also, Enrichment Factor (EF) is a useful indicator reflecting the status of environmental contamination. The results from this study show that enrichment factors of all metals are varied from 0.04 to 0.83 (Table 5) and classified as “no enrichment”. In addition, metal ratios with respect to average shale for the Yağlıdere Stream sediments and SEF values except for Pb, all the ratios are less than 1. Ozseker et al. [35, 37] found evidence of heavy metal pollution on the Trabzon Coast, with SEF and PLI values that were over the pollution limits. Naji and Ismail [36] investigated the accumulation of heavy metals in the surface sediment of the Klang River in Malaysia. Their data were assessed using the EF and  $I_{\text{geo}}$ , indicating that the surface sediment samples were partially contaminated with anthropogenic metals.

According to statistical analysis (one-way ANOVA) Cr, Co, Ni, Cd and Fe in water, Cr, Mn, Ni, Cu, Pb and Fe in sediment concentrations were significantly different between the seasonal changes, with the p-value below 0.05. Furthermore, Table 6 showed the statistical analysis of metal-to-metal correlation matrix in terms of linear correlation coefficient (r) values (significant at 0.05 and 0.01) in water and sediment samples during all seasons, respectively.



**TABLE 4**  
**Heavy Metal Concentrations of sediment samples (µg/g)**

Heavy Metal	Season n=15	Station					Average Value	Average Shale
		1	2	3	4	5		
Cr	Summer	2.94	2.673	3.142	2.906	3.099	2.952 <sup>a</sup>	90
	Fall	4.245	3.926	4.027	3.581	3.886	3.933 <sup>b</sup>	
	Winter	4.573	4.328	4.094	4.298	5.05	4.469 <sup>c</sup>	
	Spring	4.414	4.065	3.523	4.225	5.102	4.266 <sup>bc</sup>	
Mn	Summer	151.319	130.46	159.423	133.465	151.434	145.220 <sup>a</sup>	850
	Fall	219.756	205.973	185.928	194.810	227.207	206.735 <sup>b</sup>	
	Winter	213.047	171.157	203.75	164.568	207.158	191.936 <sup>b</sup>	
	Spring	218.773	207.218	176.071	193.453	208.073	200.718 <sup>b</sup>	
Co	Summer	nd	nd	nd	nd	nd		19
	Fall	nd	nd	nd	nd	nd		
	Winter	nd	nd	nd	nd	nd		
	Spring	nd	nd	nd	nd	nd		
Ni	Summer	1.891	1.806	1.801	1.958	1.983	1.888 <sup>a</sup>	68
	Fall	2.697	2.636	2.334	2.378	2.580	2.525 <sup>b</sup>	
	Winter	2.813	2.602	2.725	2.932	3.128	2.840 <sup>c</sup>	
	Spring	3.078	2.92	2.343	3.316	3.083	2.948 <sup>c</sup>	
Cu	Summer	17.408	11.45	14.091	17.916	18.315	15.836 <sup>a</sup>	45
	Fall	32.118	26.607	17.693	50.711	29.807	31.387 <sup>c</sup>	
	Winter	27.273	21.695	18.722	27.366	25.785	24.168 <sup>bc</sup>	
	Spring	19.826	18.628	15.2	20.33	32.074	21.212 <sup>ab</sup>	
Cd	Summer	0.14	0.129	0.145	0.137	0.121	0.135	0.30
	Fall	0.232	0.210	0.116	0.193	0.225	0.195	
	Winter	0.218	0.152	0.12	0.15	0.171	0.162	
	Spring	0.123	0.225	0.075	0.091	0.134	0.130	
Pb	Summer	19.183	13.529	16.553	16.953	17.41	16.73 <sup>ab</sup>	20
	Fall	18.935	15.056	14.077	24.725	20.395	18.638 <sup>b</sup>	
	Winter	21.495	15.564	14.752	17.052	17.062	17.185 <sup>ab</sup>	
	Spring	14.695	15.006	9.639	12.139	20.345	14.365 <sup>a</sup>	
Fe	Summer	0.078	0.11	2.798	2.423	1.236	1.329 <sup>a</sup>	4.7
	Fall	0.743	2.999	2.554	1.539	1.113	1.790 <sup>a</sup>	
	Winter	0.084	0.133	0.092	0.08	0.124	0.103 <sup>a</sup>	
	Spring	5.758	7.589	7.538	9.699	10.211	8.159 <sup>b</sup>	

Horizontally, letters a and b show statistically significant differences in same group of metals ( $p < 0.05$ )

**TABLE 5**  
**SEF, PLI and Igeo values in surface sediments of Yağlıdere Stream**

Metals	I <sub>geo</sub>	SEF	PLI
Cu	-1.54	0.85	0.50
Cd	-1.53	0.86	0.51
Ni	-5.32	0.06	0.04
Pb	-0.84	1.38	0.83
Fe	-1.31		0.25
Cr	-5.11	0.07	0.04
Mn	-2.78	0.36	0.22

**TABLE 6**  
**Pearson correlation coefficients between heavy metal levels in Yağlıdere Stream**

	Water							
	n=60	Cr	Mn	Ni	Cu	Cd	Pb	Fe
Sediment	Cr	<b>1</b>	-0.171	0.445 <sup>**</sup>	-0.122	-0.279 <sup>*</sup>	0.256 <sup>*</sup>	-0.075
	Mn	<b>0.587<sup>**</sup></b>	<b>1</b>	-0.210	0.001	0.399 <sup>**</sup>	-0.020	0.431 <sup>**</sup>
	Ni	<b>0.794<sup>**</sup></b>	0.674 <sup>**</sup>	<b>1</b>	-0.032	<b>-0.675<sup>**</sup></b>	0.085	-0.183
	Cu	0.260 <sup>*</sup>	0.366 <sup>**</sup>	0.195	<b>1</b>	0.045	-0.018	-0.020
	Cd	0.177	0.269 <sup>*</sup>	0.240	0.408 <sup>**</sup>	<b>1</b>	0.286 <sup>*</sup>	0.465 <sup>**</sup>
	Pb	0.100	0.284 <sup>*</sup>	0.080	<b>0.761<sup>**</sup></b>	<b>0.598<sup>**</sup></b>	<b>1</b>	0.123
	Fe	0.088	0.155	0.175	0.002	-0.238	-0.169	<b>1</b>

\*\*p < 0.01

\*p < 0.05

n = number of samples

## CONCLUSIONS

The results indicate that heavy metal contamination in the water samples of Yağlıdere Stream are higher than reference values. According to the criteria of RSWQM identified for Turkey, the monitoring station of the Yağlıdere Stream has class IV water quality in terms of metal concentrations of Cu, Pb, Ni and Cd. Also Cu, Mn, Fe and Pb concentrations in the water samples are higher than the EPA and WHO standards. Otherwise, the metal concentration levels of surface sediment samples of Yağlıdere Stream are lower than reference values. Seasonal variation of metals from sediment are significant statistically. Moreover, a positive relationship was found. The study revealed that based on computed indexes (SEF, PLI and  $I_{geo}$ ), Yağlıdere Stream is classified as unpolluted.

Based upon result of the present study, heavy metal pollution level is generally high Yağlıdere Stream and it will be good to adopt protective measures before it's too late.

## REFERENCES

- [1] Parlak, H., Çakır, A., Boyacıoğlu, M. and Arslan, Ö.Ç. (2006) Heavy Metal Deposition in Sediments from the Delta of the Gediz River (Western Turkey): A Preliminary Study, *E.U. Journal of Fisheries & Aquatic Sciences*, 23(3-4), 445-448.
- [2] Elmaci, O.L., Delibacak, S., Secer, M. and Bodur, A. (2002) Fertility status, trace elements and heavy metal pollution of agricultural land irrigated from the Gediz River. *Int.J.Wat.* 2, 2/3,184-194.
- [3] Khaled, A., El Nemr, A. and El Sikaily, A. (2006) An assessment of heavy-metal contamination in surface sediments of the Suez Gulf using geoaccumulation indexes and statistical analysis. *Chemistry and Ecology*, 22(3), 239-252.
- [4] Demirak, A., Yılmaz, F., Tuna, A. L. and Ozdemir, N. (2006) Heavy metals in water, sediment and tissues of *Leuciscus cephalus* from a stream in southwestern Turkey. *Chemosphere*, 63, 1451-1458.
- [5] Akkan, T., Kaya, A. and Dinçer, S. (2011) Rate of Cephalosporin Resistance in Gram-Negative Bacteria Isolated from Hospital Sewage Contaminated Seawater. *Türk Mikrobiyoloji Cemiyeti Dergisi*, 41(1), 18-21, doi:10.5222/TMCD.2011.018.
- [6] Akkan, T., Kaya, A. and Dinçer, S. (2013) Antibiotic Levels and heavy metal resistance in gram-negative bacteria isolated from seawater, Iskenderun Organized Industrial Zone. *Journal of Applied Biological Sciences*, 1,10-14.
- [7] Akbulut, A. and Akbulut, N.E. (2010) The study of heavy metal pollution and accumulation in water, sediment, and fish tissue in Kızılırmak River Basin in Turkey. *Environmental Monitoring and Assessment*, 167,521-526.
- [8] Tuna, A.L., Yılmaz, F., Demirak, A. and Ozdemir, N. (2007) Sources and distribution of trace metals in the Saricay stream basin of southwestern Turkey. *Environmental Monitoring and Assessment*, 125,47-57.
- [9] Duran, M., Tüzen, M. and Kayım, M. (2003) Exploration of biological richness and water quality of stream Kelkit, Tokat-Turkey, *Fresen. Environ. Bull.*, 12(4),368-375.
- [10] Dundar, M.S. and Altundag, H. (2007) Investigation of heavy metal contaminations in the lower Sakarya river water and sediments, *Environmental Monitoring and Assessment*, 128,177-181.
- [11] Kucuksezgin, F., Uluturhan, E. and Batki, H. (2008) Distribution of heavy metals in water, particulate matter and sediments of Gediz River (Eastern Aegean), *Environmental Monitoring and Assessment*, 141,213-225.
- [12] Polat, N. and Akkan, T. (2016) Assessment of Heavy Metal and Detergent Pollution in Giresun Coastal Zone, Turkey. *Fresen. Environ. Bull.*, 25(8), 2884-2890.
- [13] Kacar, A., Kocyigit, A. and Uluturhan E. (2016) Concentration of heavy metals and investigation of bacterial toxic metal resistance in costal city sediments (Eastern Aegean Sea), *Fresen. Environ. Bull.*, 25(1), 55-66.
- [14] Tuzen, M., Verep, B., Ogretmen Omur, A. and Soylak, M. (2009) Trace Element Content in Marine Algae Species from the Black Sea, Turkey. *Environ Monit Assess*, 151,363-368.
- [15] Aydın, S. Yagmur, B., Coban, H. and Simsek, H. (2015) The nutritional conditions and some heavy metal contents of the Vineyards in a Semi-Arid Area. *Fresen. Environ. Bull.*, 24(4b), 1573-1578.
- [16] Eroglu, E., Ak, N., Guney, I. and Ersin Sener E. (2016) Component analysis of the different fish samples containing heavy metals in Istanbul Bosphorus, *Fresen. Environ. Bull.*, 25(1), 292-299.
- [17] Uncumusaoğlu, A. A., Gürkan, Ş., Özkan, E. Y. and Büyükişık, H. B. (2012) A preliminary research on heavy metals accumulated in liver and muscle tissue of Seahorse (*Hippocampus hippocampus*) caught from Tirebolu coasts (Giresun, Eastern Black Sea). *Fresen. Environ. Bull.*, 21(11b), 3418-3420.
- [18] Yılmaz, M., Teber, C., Akkan, T., Er, C., Kariptas, E., and Ciftci, H. (2016) Determination of Heavy Metal Levels in Different Tissues of Tench (*Tinca tinca* L.,



- 1758) from Siddikli Kucukbogaz Dam Lake (Kirsehir), Turkey, *Fresen. Environ. Bull.*, 25(6), 1972-1977.
- [19] Verep, B., Akın, Ş., Mutlu, C., Apaydın, G., Ertuğral, B., and Çevik, U. (2007) Assessment of Trace Elements in Rainbow Trout (*Onchorhynchus mykiss*) Cultured in Marine Aquaculture Cages on the Black Sea Coast, *Fresen. Environ. Bull.*, 16(9a), 1005-1011.
- [20] APHA (1998) Standard Methods for the Examination of Water and Wastewater APHA, AWWA, WPCF, WPCF, Washington.
- [21] Alam, M.G.M., Tanaka, A., Stagnitti, F., Allinson, G. and Maekawa T. (2001) Observations on the Effects of Caged Carp Culture on Water and Sediment Metal Concentrations in Lake Kasumigaura, Japan. *Ecotoxicology and Environmental Safety*, 48, 107-115.
- [22] Trefry, J.H. and Presley, B. J. (1976) Heavy metals in sediments from San Antonio Bay and the northwest Gulf of Mexico. *Environ. Geol.* 1, 283-294.
- [23] Sinex, S. A. and Helz, G. R. (1981) Regional geochemistry of trace elements in Chesapeake Bay sediments. *Environmental Geology*, 3 (6), 315-323.
- [24] Helz, G.R., Sinex, S.A., Ferri, K.L. and Nichols, M. (1985) Processes controlling Fe, Mn and Zn in sediments of northern Chesapeake Bay, *Estuarine. Coastal Shelf Sci.* 21, 1-16.
- [25] Windom, H.L., Schropp, S.J., Calder, F.D., Ryan, J.D., Smith, R.G., Burney, L.C., Lewis, F.G. and Rawlinson, C.H. (1989) Natural trace metal concentrations in estuarine and coastal marine sediments of the southeastern United States. *Environmental Science and Technology*, 23, 314-320.
- [26] Lee, C.L., Fang, M.D. and Hsieh M.T. (1998) Characterization and distributing of metals in surficial sediments in southwestern Taiwan, *Mar. Pollut. Bull.*, 36(6), 464-471.
- [27] Woitke, P., Wellmitz, J., Helm, D., Kube, P., Lepom, P. and Litheraty, P. (2003). Analysis and assessment of heavy metal pollution in suspended solids and sediments of the River Danube. *Chemosphere*, 51, 633/42.
- [28] Salomons, W. and Forstner, U. (1984) Metals in Hydrocycle Berlin: Springer.
- [29] Ozseker, K., Eruz, C. and Ciliz, S. (2013) Determination of Copper Pollution and associated Ecological risk in coastal sediment of Southeastern Black Sea Region, Turkey. *Bulletin of Environmental Contamination and Toxicology*, 91(6), 661-666.
- [30] RSWQM, (2015) Regulation on the Surface Water Quality Management, Number of official gazette: 29327.
- [31] Ayaş, Z. and Kolonkaya, D. (1996) Accumulation of some heavy metals in various environments and organisms at Göksu Delta, Türkiye, *Bulletin of Environmental Contamination and Toxicology*, 56, 65-72.
- [32] Turekian, K.K. and Wedepohl, K.H. (1961) Distribution of the elements in some major units of the earth's crust. *Bull. Geo. Soc. Amer.*, 72, 175-192.
- [33] Şener, Ş. and Şener, E., (2015) Assessment of Heavy Metal Distribution and Contamination in the Kovada Lake (Isparta) Bottom Sediments. *Suleyman Demirel University Journal of Natural and Applied Science*, 19(2), 89-96.
- [34] Mendil, D., Ünal, Ö.F., Tüzen, M. and Soylak, M. (2010) Determination of Trace Metals in Different Fish Species and Sediments from the River Yeşilırmak in Tokat Turkey. *Food and Chemical Toxicology*, 48, 1383-1392.
- [35] Ozseker, K., Eruz, C., Ciliz, S. and Mani, F. (2014) Assessment of heavy metal contribution and associated ecological risk in the coastal zone sediments of the black sea: Trabzon. *Clean – Soil, Air, Water*, 42(10), 1477-1482.
- [36] Naji, A. and Ismail A. (2011) Assessment of metals contamination in Klang River surface sediments by using different Indexes. *Environment Asia*, 4(1),30-38.
- [37] Ozseker, K. and Eruz, C. (2011) Heavy Metal (Ni, Cu, Pb, Zn) Distribution in Sediments from the Coast of Trabzon in the Black Sea. *Indian Journal of Marine Sciences*, 40(1), 48-54.

---

**Received:** 15.03.2016

**Accepted:** 19.10.2016

---

#### CORRESPONDING AUTHOR

**Arzu Aydin Uncumusaoglu**

Giresun University, Faculty of Engineering

Environmental Engineering Department

28200 Giresun / Turkey

email: [arzu.a.uncumusaoglu@gmail.com](mailto:arzu.a.uncumusaoglu@gmail.com)



# BIOLOGICAL RISK ANALYSIS OF GREEN LAND IN CHINA

Tang Guimei<sup>1</sup>, Liu Guibin<sup>2</sup>, Huang Yao<sup>2</sup>, Chen Chan<sup>2</sup>, Zheng Huabin<sup>2</sup>,  
Li Jingyi<sup>2</sup>, Long Yuelin<sup>1,\*</sup>, Cheng Tianyin<sup>3</sup>

<sup>1</sup> College of horticulture and landscape architecture, Hunan Agricultural University, Changsha 410128, China

<sup>2</sup> College of Agronomy, Hunan Agricultural University, Changsha 410128, China

<sup>3</sup> College of veterinary medicine, Hunan Agricultural University, Changsha 410128, China

## ABSTRACT

The ecological system of urban green land is a special ecological system which is mainly to the living environment. The denaturalization of urban environment and its environmental stress are becoming more and more serious. The reasons of urban green land producing biological risk are complex, which cause serious threat to the safety of urban landscape and living environment. At the same time, as the mainly collecting and distributing centre of people and logistics, cities are extremely probable to be invaded by harmful biology. This article analyzed the potential biological risks in different types of green land and put forward some measures about reasonable monitoring, preventive treatment, and scientific management to promote the healthy development of ecological green land system in China from the causes of the green land biological risk.

## KEYWORDS:

green land, biological risk, monitoring, early warning, management

## INTRODUCTION

With the speeding of urbanization and the advancement of science and technology, the human capacities to transform the nature are improving. But the process of urbanization also caused a series of ecological environment problems, such as air and water pollution, solid waste, urban heat island effect, noise pollution and so on [1]. As the major body of the urban ecological system, green land bears ecological risk brought by the urbanization, and plays a significant role in improving the environment and reducing ecological risk [2]. According to the definition of green land in "Chinese urban land classification and planning and construction standards (GB50137-2011)", green land must stress the public properties of land, ensure good sanitary conditions, improve the appearance of cities, and build resting places for residents. The range of green land is very wide, including the park green space (park, visiting

garden, street center garden, special garden, and *f* etc), the attached green land (offices, factories and mines, schools, traffic road, residential district green space, and etc), the productive green land (nursery, garden, herb garden, orchard, and etc), the protective green land (windbreaks, isolation belt, high-pressure city greenbelt corridors, and etc), and the other forest area (scenic forest, forest park, wild animals and plants park, wetland, landfill field recovery green land).

Around the construction goal of "ecological civilization" and "beautiful China", Chinese greening construction made exceedingly great achievements. In 2015, China Greening Committee Office published "Bulletin of the state of land greening in China in 2014", which shown that the green coverage area of Chinese urban built-up district is approximately 1.9075 million hectares in 2014, increasing about 95.5 thousand hectares compared to 2013. That accelerated the improvement of the quality of living environment and provided more recreational and active space for people. But the changes of climate and habitat as well as the introduction of new species and varieties of plant material directly provide material conditions for various harmful organisms to parasitism and reproduce, which make pest disasters break out frequently in many areas. According to reports, the total number of trees suffered from termite's disaster (Taiwan milky termites, Black Winged termites, Yellow Winged termites, and etc) is about 828 in Guangzhou Uprising martyrs cemetery garden, accounting for 23% of the total number of the trees in the garden. During 2002 to 2005, termite's disaster has made approximately 60 trees die [3]. Meanwhile, some of organisms living in green land become the medium and carriers of pathogens and the interactions between these organisms and the parasitifer will cause the risk of people and animal infecting diseases. The death events in Henan province in 2010 caused by tick biting disease highlighted that the prevention and control of tick have important public health significances [4]. With the frequent invasion of alien pests, the varieties of invaded alien organisms in China have arrived at 544 types by the end of 2013, quite a part invading into green land. More than 100 kinds of these pests have

already caused large area and serious disasters in China. The International Union for conservation of nature announced 100 kinds of the global most dangerous alien species and more than 50 types have already invaded into China, which cause serious threats to the balance of ecological system [5].

## **THE CAUSING REASONS OF GREEN LAND BIOLOGICAL RISK**

### **Unreasonable allocation of green plants.**

Urban green land system is an artificial open system mainly by artificial regulation and its self-adjustment ability is relatively weak. So the anti-reversion and stability of system are relatively poor and natural enemy resources are relatively scarce, which make it difficult to form a stable natural control mechanism to prevent pests. In addition, the construction of urban green land has some issues. Firstly, garden plants configuration is not reasonable. Secondly, single color plants are secretly planted in large area. Thirdly, the design density of green land is over high or pest heteroecious plants are mixed planting. For example, juniper or *Platycladus* and *Rosaceae* plants are planted together, which creates conditions for the occurrence and prevalence of heteroecious rust of pear, juniper and so on. The planting of a large number of single species directly cause the biological diversity insufficient. For instance, the 35 kinds of landscape tree species surveyed in Guangzhou already account for 70% of the all greening species in the surveyed region [6]. These reasons become an important factor of the instability of Chinese green vegetation community and provide sufficient fodder and spreading environment for certain pests. With the rapid increasing of urban green coverage rate and the continuous introduction of new technologies and varieties of green seedlings, cities are becoming increasingly green. However, urban landscape greening works also exist very large shortages, which mainly reflect that concentrating on construction but ignoring maintenance, fragile artificial environment chain, and difficultly achieving an excellent and balanced ecological environment.

**The impacts of human activities.** The relationship between humans and green land is increasingly close, especially in the urban environment. The limited number of available green land leads to people entering the urban green land systems frequently. Undoubtedly, green land is wildlife habitats as well as recreation ground of people and their pets. Although these urban natural

environment is not suitable for large-scale artificial habitats host, the spreading rate of diseases resulting from pests is exacerbating through smaller mammals (wild host), humans and their pets, especially dogs forced proximity [7]. Take ticks as an example, in the past 10 to 20 years, the increasing of ticks and tick-borne disease cases has been widely reported in Europe. It has been found 192 kinds of infectious organisms (including viruses, spirochetes, rickettsia, bacteria, and etc.), parasites and toxins paralysis ticks that are related to the spreading of ticks bites, particularly a series of tick-borne diseases have been emerged in recent years, which pose threats to human survival and health [8]. The study about ticks and dogs launched in a large suburban park in southwest England showed that the risk of ticks touching dogs is positively correlated to the frequency of its appearing [9].

**The changes in habitat, climate and other conditions.** With the acceleration of Chinese urbanization, a lot of city green lands especially the suburb green land are related to the fields of rural economic crops and grain or connected with them in geography. There are many pests deriving from vegetables and edible crops that become major pests of city landscape plants, except insect diseases of plant itself, and they may cross infect. For example, the meadow moth, *Spodoptera litura*, grasshoppers and underground pests (beetle, cutworm) poured into the city green land and caused great harm. What are the reasons that the main pest species evolving from large to small and from exposing to covering is the impacts of the nutritional factors of city green land (food conditions), cultivation and conservation, as well as the greenhouse effect resulting from abnormal climate [10]. For instance, sucking insects (aphid, *coccoidea*, acarid, thrip, *Aleyrodidae*, *Psyllidae*, plant hopper) are epidemic in the urban green plants, resulting in expanding of the scope of host. Borer pests (*Cerambycidae* *Cossidae*, *Scolytidae* and etc) are continuously spreading, which leads to that the damage rate of some susceptible species is as high as 90%. At the same time the damages of these pests can easily cause a disease called "sooty sick" that does harm to urban green land landscape.

**The unordered transportation of new varieties of green plants.** With the continuous improvement of traffic and the continuous development of the tourism industry, some organisms can be transported to other place and zone that are more suitable for their growth, which results in the spread of pests and cause panic among residents. Although the quarantining of new crop varieties is very strict, the transported management

of new garden plants varieties is not strict and the quarantining department hardly quarantine these transported garden plants, resulting in the phenomena of green plants unordered transporting are very common. A large number of exotic species and seedlings with dangerous pests were introduced through the process of unordered transportation, causing a greater threat to the production of local plants and the greening. Meanwhile, some exotic species can easily be brought through greening projects or other activities, which makes the possibility of the invasion of alien harmful species increase.

**The weak quarantining of import.** There are serious diseases and pest's disasters, as well as the issue of biological invasion in the import quarantining of flowers and seedlings [11]. The weak quarantining of some new garden plants varieties caused some invasive pest disaster, such as *liriomyza sativae*, *opogona sacchari*, *Hyphantria cunea*, *Bursaphelenchus xylophilus*, *Bemisia tabaci*, *Rasbora bankanensis*, *Frankliniella occidentalis*, *Radopholus similis*. *Opogona sacchari* derived from Africa was first found in Beijing in 1997, whose host plants amount to 23 families and 56 species, and it does serious harm to *Dracaena Fragrans*, *Pachira aquatica*, *cycad revoluta*, *Euphorbia pulcherrima* and so on [12]. *Opogona sacchari* has extended all over 22 provinces in China just two years time since it was introduced [13]. After exotic harmful plants invaded into the urban green land system, they can easily occupy the leading position in the food chain, invade ecological niche of native plants, and result in disasters. *Eupatorium adenophorum*, *Eupatorium odoratum*, *Eichhornia crassipes*, *Alternanthera philoxeroides*, *Solidago decurrens* is the first batch of foreign species released by the National Environmental Protection Bureau and their growth regions pose threats to local species survival. More than 30 kinds of native ornamental plants species have disappeared in recent 20 years in Shanghai due to planting *Solidago Canadensis*. Because *Lythrum salicaria* originating in Europe was introduced into North America in more than 100 years ago, the original native plants were died. Many animals migrated due to the change of habitat, and ecological environment and biodiversity were damaged [14].

In addition, low social cognition level, weak foundation of prevention and treatment, insufficient capital investment, single means of prevention and control, and backward technologies are also the significant factors of serious occurrence of organisms' disasters in urban green land system.

## POTENTIAL BIOLOGICAL RISKS OF VARIOUS GREEN LAND IN DIFFERENT REGIONS IN CHINA

**Potential biological risks of various green land in different regions in China.** China is a country with a vast territory and diverse natural landscape. So the biological risks of corresponding diseases and pests' disasters are widely distributed and various. Urban green land is the green space that is closely related to human survival and development. However, based on the current status of research, the survey of potential biological risks in Chinese urban green land systems are not further and systemic, and there are many areas not investigated and studied. The recorded varieties are very limited and the information are scattered. Therefore, it is necessary to summarize and conclude the existing data and find the distributed characteristics of the zones that maybe erupt biological risks in China to provide relevant information for the treatments of harmful organisms and the managements of risks in green land.

According to the characteristics of Chinese geography, climate and administrative region, China is divided into East China, North China, Central China, Southwest China, Southern China, South China, and Northeast China. So the green land in China is also divided into 7 regions, including the North China zone (Beijing, Tianjin, Hebei, Inner Mongolia, Shanxi, Shandong), the East China zone (Shanghai, Zhejiang, Jiangsu, Anhui), the Southern China zone (Fujian, Guangdong, Guangxi, Hainan), the Central China zone (Henan, Hubei, Hunan, Jiangxi), the Southwest China zone (Sichuan, Chongqing, Kunming, Guizhou), the Northeast China zone (Liaoning, Jilin, Heilongjiang), and the Northwest China zone (Shanxi, Ningxia, Qinghai, Gansu, Xinjiang). Combined with the relevant literatures involving biological risks in Chinese green land, the statistics of pests' disasters in various green land systems in the different regions in China was done (Table 1).

**Potential risks of pests' disaster in park green land in Central China.** Take the park green land that can represent typical garden green land in Central China as studied object, including suburban park, visiting garden, street center garden, special garden and so on, we apply two surveyed methods (census and sampling) to experimentize. Because most of insects are in the overwintering state from November to next April, the investigation on the species was performed in April to October and two surveys were separated by 10 days to 15 days every month. Specific processes are that collecting the plants specimens of diseases and pests' disasters in

**TABLE 1**  
**Potential biological risks of various green land in different regions in China [15-23]**

Regions	Major host plant varieties	Potential risks of pests' disaster
Northern China zone	<i>Populus L.</i> , <i>Salix babylonica</i> , <i>Sophora japonica</i> Linn., <i>Robinia pseudoacacia</i> L., <i>Picea asperata</i> Mast., <i>Ailanthus altissima</i> , <i>Pinus armandii</i> Franch., <i>Pinus tabuliformis</i> Carrière, <i>Sabina chinensis</i> (L.) Ant., <i>Platycladus orientalis</i> (L.) Franco, <i>Juglans regia</i> , <i>Ulmus pumila</i> L., <i>Acer mono</i> Maxim., <i>Acer truncatum</i> Bunge, <i>Crataegus pinnatifida</i> Bunge, <i>Acer truncatum</i> Bunge, <i>Paulownia Sieb. et Zucc.</i> , <i>Sophora japonica</i> Linn., <i>Robinia pseudoacacia</i> L., <i>Diospyros kaki</i> Thunb., <i>Salix matsudana</i> Koidz., <i>Lonicera maackii</i> (Rupr.) Maxim., <i>Cercis chinensis</i> , <i>Fraxinus chinensis</i> Roxb., <i>Cerasus ssp.</i> , <i>Nerium indicum</i> Mill., <i>Ailanthus altissima</i> , <i>Euonymus alatus</i> (Thunb.) Sieb., <i>Amygdalus triloba</i> , <i>Osmanthus sp.</i> , <i>Diospyros kaki</i> Thunb., <i>Syringa</i> Linn., <i>Ginkgo biloba</i> L., <i>Pyrus spp</i> , <i>Armeniaca vulgaris</i> Lam., <i>Prunus mume</i> , <i>Cerasus ssp.</i> , <i>Malus spectabilis</i> , <i>Morus alba</i> L., <i>Amygdalus persica</i> var. <i>persica</i> f. <i>duplex</i> , <i>Amygdalus persica</i> L., <i>Malus pumila</i> Mill., <i>Prunus salicina</i> Lindl., <i>Prunus ceraifera</i> cv. <i>Pissardii</i> , <i>Medicago sativa</i> , <i>Rosa chinensis</i> Jacq.	<i>Cinara pinitabulaeformis</i> Zhang et Zhang, <i>Cicadella viridis</i> , <i>Jacobiasca formosana</i> , <i>Hyalopterus arundinis</i> Fabricius, <i>Aphis gossypii</i> Glover, <i>Parathrene tabaniformis</i> Rottenberg, <i>Apriona swainsoni</i> (Hope), <i>Anoplophora glabripennis</i> , <i>Pseudaulacaspis pentagona</i> (Targioni Tozzetti), <i>Phenacoccus fraxinus</i> Tang, <i>Tetranychus cinnabarinus</i> , <i>Macrosiphum rosirvorum</i> Zhang, <i>Semiothisa cmerearia</i> (Bremer et Grey), <i>Stilpnotia salicis</i> (Linnaeus), <i>Parocneria furva</i> (Leech), <i>Cnidocampa flavescens</i> (Walker), <i>Porthesia similis</i> (Fueszly), <i>Cimbex taukushi</i> Marlatt, <i>Serica orientalis</i> Motschulsky, <i>Anomala corpulenta</i> Motschulsky, <i>Prinoxystus robiniae</i> , <i>Dendroctonus valens</i> LeConte, <i>Ips acuminatus</i> , <i>Hyphantria cunea</i> (Drury), <i>Phalera flavescens</i> , <i>Prodenia litura</i> (Fabricius), <i>Celerio hippophaes</i> (Esper), <i>Eucryptorrhynchus brandii</i> (Harold), <i>Chrysobothris succedana</i> , <i>Telphusa chloroderces</i> Meyrich, <i>Lycorma delicatula</i> White, <i>Malacosoma neustria testacea</i> Motschulsky, <i>Boophilus microplus</i>
Eastern China zone	<i>Populus L.</i> , <i>Cinnamomum camphora</i> (L.) presl, <i>Pinus massoniana</i> Lamb., <i>Pinus taeda</i> L., <i>pinus elliottii</i> , <i>Cedrus deodara</i> (Roxb.) G. Don, <i>Sabina chinensis</i> (L.) Ant., <i>Platycladus orientalis</i> (L.), <i>Acer palmatum</i> Thunb., <i>Acer truncatum</i> Bunge, <i>Koelreuteria paniculata</i> , <i>Nerium indicum</i> Mill., <i>Ligustrum sinense</i> Lour, <i>Sapium sebiferum</i> (L.) Roxb., <i>Bischofia polycarpa</i> , <i>Michelia chapensis</i> Dandy, <i>Distylium racemosum</i> Sieb. et Zucc., <i>Aphananthe aspera</i> (Thunb.) Planch., <i>Salix babylonica</i> , <i>Ulmus pumila</i> L., <i>Hibiscus syriacus</i> Linn., <i>Viburnum odoratissimum</i> , <i>Elaeocarpus decipiens</i> Hemsl., <i>Cunninghamia lanceolata</i> (Lamb.) Hook., <i>Sophora japonica</i> Linn., <i>Robinia pseudoacacia</i> L., <i>Myrica rubra</i> (Lour.) S. et Zucc., <i>Cerasus ssp.</i> , <i>Lagerstroemia indica</i> L. <i>Amygdalus persica</i> L., <i>Amygdalus persica</i> var. <i>persica</i> f. <i>duplex</i> , <i>Prunus mume</i> , <i>Malus spectabilis</i> , <i>Rosa chinensis</i> Jacq., <i>Podocarpus macrophyllus</i> , <i>Cycas revoluta</i> Thunb., <i>Pyracantha fortuneana</i> (Maxim.) Li, <i>Gardenia jasminoides</i> , <i>Loropetalum chinense</i> var. <i>rubrum</i> , <i>Spiraea Salicifolia</i> L., <i>Rhododendron simsii</i> Planch., <i>Buxus sinica</i> (Rehder & E. H. Wilson) M. Cheng, <i>Buxus megistophylla</i> Levl., <i>Dichondra repens</i> Forst., <i>Festuca elata</i> Keng ex E. Alexeev, <i>Cynodon dactylon</i> (Linn.) Pers.	<i>Aromia bungii</i> Faldermann, <i>Anoplophora chinensis</i> , <i>Anoplophora glabripennis</i> , <i>Apriona germari</i> (Hope), <i>Hyphantria cunea</i> (Drury), <i>Tinocallis kahawaluokalani</i> Kirkaldy, <i>Periphylus koelreuteria</i> Takahashi, <i>Aphis nerii</i> , <i>Gryllotalpa orientalis</i> Burmeister, <i>Clostera anachoreta</i> , <i>Cnidocampa flavescens</i> , <i>Clania variegata</i> Snellen, <i>Calospilus suspecta</i> Warren, <i>Diaphania perspectalia</i> , <i>Micromelalopha sieversi</i> , <i>Aphis gossypii</i> Glover, <i>Ceroplastes rubens</i> (Maskell), <i>Ceroplastes japonicas</i> Guaind, <i>Trioza camphorae</i> Sasaki, <i>Stephanitis pyriodes</i> , <i>Monochamus alternatus</i> Hope, <i>Hyalomma detritum</i> , <i>Boophilus microplus</i>
Southern China zone	<i>Cinnamomum burmanni</i> (Nees et T.Nees) Blume, <i>Nerium indicum</i> Mill., <i>Murraya exotica</i> , <i>Dendranthema morifolium</i> (Ramat.) Tzvel., <i>Rosa chinensis</i> Jacq., <i>Chorisia speciosa</i> , <i>Bischofia javanica</i> , <i>Mangifera indica</i> L., <i>Hibiscus rosa-sinensis</i> Linn., <i>Osmanthus sp.</i> , <i>Carmona microphylla</i> (Lam.) Don., <i>Ficus microcarpa</i> Linn. f., <i>Pittosporum tobira</i> , <i>Murraya exotica</i> L., <i>Aglaia odorata</i> Lour., <i>Michelia alba</i> DC., <i>Michelia champaca</i> Linn., <i>Michelia figo</i> (Lour.) Spreng, <i>Cycas revoluta</i> Thunb., <i>Ficus altissima</i> , <i>Ficus microcarpa</i> , <i>Ficus benjamina</i> , <i>Lagerstroemia speciosa</i> , <i>Cercis chinensis</i> , <i>Clausena lansium</i> (Lour.) Skeels, <i>Ficus carica</i> Linn., <i>Ligustrum sinense</i> , <i>Syzygium cumini</i> (L.) Skeels., <i>Zoysia tenuifolia</i> Willd. ex Trin.	<i>Brontispa longissima</i> (Gestro), <i>Formosaphis micheliae</i> , <i>Aphis gossypii</i> Glover, <i>Myzus persicae</i> (Sulzer), <i>Jacobiasca formosana</i> , <i>Tetranychus cinnabarinus</i> , <i>Psylla mali</i> , <i>Aleurocanthus spiniferus</i> (Quaintance), <i>Stephanitis pyriodes</i> , <i>Gynaikothrips uzeli</i> Zimm, <i>Ocinara Varians</i> Walker, <i>Sylepta derogata</i> Fabricius, <i>Spodopera pecten</i> , <i>Pericyma cruegri</i> (Butler), <i>Dendrolimus punctatus</i> Walker, <i>Trabala vishnou</i> gigantina (Yang), <i>Psilogamma menephron</i> (Gramer), <i>Chelidonium ar gentatum</i> , <i>Chlumetia transversa</i> , <i>Porthesia scintillans</i> , <i>Pseudaulacaspis pentagona</i> (Targioni Tozzetti), <i>Aglossa caprealis</i> , <i>Holotrichia sauteri</i> Moser, <i>Boophilus microplus</i> , <i>Chilades pandava</i> (Horsfield)
Middle China zone	<i>Cedrus deodara</i> (Roxb.) G. Don, <i>Cinnamomum camphora</i> (L.) Presl., <i>Ligustrum lucidum</i> , <i>Bischofia polycarpa</i> , <i>Metasequoia glyptostroboides</i> Hu & W. C. Cheng, <i>Salix babylonica</i> , <i>Koelreuteria paniculata</i> , <i>Acer palmatum</i> Thunb., <i>Ginkgo biloba</i> L., <i>Punica granatum</i> L., <i>Prunus ceraifera</i> cv. <i>Pissardii</i> , <i>Ailanthus altissima</i> , <i>Fraxinus chinensis</i> Roxb.,	<i>Lycorma delicatula</i> , <i>Aromia bungii</i> , <i>Dictyoploca japonica</i> Butler, <i>Aphis gossypii</i> Glover, <i>Myzus persicae</i> (Sulzer), <i>Tuberocephalus momonis</i> , <i>Ceroplastes japonicas</i> Guaind, <i>Pseudaulacaspis pentagona</i> (Targioni Tozzetti), <i>Drosicha contrahens</i> , <i>Eriococcus legerstroemiae</i> Kuwana, <i>Anoplophora glabripennis</i> , <i>Anoplophora chinensis</i> , <i>Apriona germari</i> (Hope),

	<p><i>Photinia serrulata</i> Lindl., <i>Camptotheca acuminata</i>, <i>Pterocarya stenoptera</i> C. DC, <i>Ulmus pumila</i> L., <i>Sassafras tsumu</i>, <i>Castanopsis sclerophylla</i> (Lindl.) Schott., <i>Ligustrum obtusifolium</i> sieb. Et Zucc., <i>Hibiscus mutabilis</i> Linn., <i>Hibiscus syriacus</i> Linn., <i>Nerium indicum</i> Mill., <i>Cercis chinensis</i>, <i>Amygdalus triloba</i>, <i>Punica granatum</i> L., <i>Magnolia denudata</i> Desr., <i>Amygdalus persica</i> var. <i>persica</i> f. <i>duplex</i>, <i>Malus spectabilis</i>, <i>Amygdalus persica</i> L., <i>Pyrus</i> spp, <i>Cerasus</i> spp., <i>Lagerstroemia indica</i> L., <i>Osmanthus fragrans</i> (Thunb.) Lour., <i>Nandina domestica</i>, <i>Wisteria sinensis</i>, <i>Ligustrum quihoui</i> Carr., <i>Buxus megistophylla</i> Levl., <i>Michelia figo</i> (Lour.) Spreng, <i>Rosa chinensis</i> Jacq., <i>Rhododendron simsii</i> Planch., <i>Gardenia jasminoides</i> Ellis, <i>Cleome spinosa</i> Jacq., <i>Camellia japonica</i> L., <i>Beta vulgaris</i> L. var. <i>ciela</i> L., <i>Oxalis corymbosa</i> DC.</p>	<p><i>Stilpnolia salicis</i> (Linnaeus), <i>Holcocerus insularis</i> Stgr., <i>Dendroctonus valens</i> LeConte, <i>Psilogramma menephron</i>, <i>Clania variegata</i> Snellen, <i>Panonychus citri</i> Mc Gregor, <i>Choristoneura metasequoicola</i>, <i>Dendrolimus punctatus</i> Walker, <i>Odontotermes formosanus</i>, <i>Macrotermes barneyi</i> Light, <i>Synpiezoyrelia lewisi</i>(Roelofs), <i>Dichocrocis punctiferalis</i> Guenée, <i>Cicadella viridis</i>, <i>Jacobiasca formosana</i>, <i>Cryptotympana atrata</i>, <i>Calospilos suspecta</i> Warren, <i>Dictyoploca japonica</i> Butler, <i>Anomala corpulenta</i> Motschulsky, <i>Rhipicephalus haemaphysaloides</i> haemaphysaloides, <i>Boophilus microplus</i>, <i>Trialeurodes vaporariorum</i> (Westwood)</p>
Southwest China zone	<p><i>Bischofia polycarpa</i>, <i>Syringa tomentella</i>, <i>Ulmus pumila</i> L., <i>Fraxinus chinensis</i> Roxb., <i>Ficus concinna</i> (Miq.) Miq., <i>Salix babylonica</i> Phoenix canariensis, <i>Michelia chapensis</i> Dandy, <i>Osmanthus</i> sp., <i>Malus spectabilis</i>, <i>Cerasus</i> spp., <i>Amygdalus persica</i> L., <i>Prunus mume</i>, <i>Prunus ceraifera</i> cv. <i>Pissardii</i>, <i>Amygdalus persica</i> var. <i>persica</i> f. <i>duplex</i>, <i>Ligustrum vicaryi</i>, <i>Cycas revoluta</i> Thunb., <i>Lagerstroemia indica</i> L., <i>Cedrus deodara</i> (Roxb.) G. Don, <i>Cinnamomum camphora</i> (L.) Presl., <i>Camellia japonica</i> L., <i>Schefflera octophylla</i> (Lour.) Harms, <i>Cinnamomum japonicum</i> Sieb., <i>Ligustrum</i> × <i>vicaryi</i> Hort, <i>Rosa chinensis</i> Jacq., <i>Pittosporum tobira</i>, <i>Rosa</i> L., <i>Rhododendron simsii</i> Planch., <i>Fatsia japonica</i> (Thunb.) Decne. et Planch</p>	<p><i>Stephanotis nashi</i> (Esaki et Takeya), <i>Tinocallis Kahawaluokalani</i>(Kirkaldy), <i>Ocinara brunnea</i> Wil., <i>Myzus persicae</i> (Sulzer), <i>Argopistesekooni</i> Chen, <i>Gynaikothrips uzeli</i>(Zimmermann), <i>Aleurocanthus spiniferus</i>(Quaintanca), <i>Chilades pandava</i>, <i>Ericerus pela</i> Chavannes, <i>Ceroplastes rubens</i> (Maskell), <i>Pseudaulacaspis pentagona</i> (Targioni Tozzetti), <i>Eriococcus legerstroemiae</i> Kuwana, <i>Macrohometama gladiatum</i> kuwayama, <i>Liriomyza sativae</i> Blanchard, <i>Rhyncophorus ferrugineus</i>, <i>plagioderia versicolora</i> (Laicharting), <i>Cnidocampa flavescens</i>(Walker), <i>Ceroplastes pseudoceriferus</i> Green, <i>Tetranychus cinnabarinus</i></p>
Northwest China zone	<p><i>Pinus sylvestris</i> var. <i>mongolica</i> Litv., <i>Pinus tabuliformis</i> Carrière, <i>Larix gmelinii</i> (Rupr.) Kuzen., <i>Fraxinus mandshurica</i> Rupr, <i>Betula platyphylla</i> Suk., <i>Betula davurica</i> Pall., <i>Ailanthus altissima</i>, <i>Ligustrum obtusifolium</i> Sieb. et Zucc., <i>Fraxinus chinensis</i> Roxb., <i>Ulmus pumila</i> L., <i>Prunus persica</i> f. <i>rubro-plena</i>, <i>Populus</i> L., <i>Prunus padus</i> L., <i>Crataegus pinnatifida</i> Bunge, <i>Salix babylonica</i>, <i>Amygdalus persica</i> L., <i>Armeniaca vulgaris</i> Lam., <i>Pyrus</i> spp, <i>Gleditsia sinensis</i> Lam., <i>Euonymus maackii</i> Rupr., <i>Lonicera japonica</i> Thunb., <i>Cydonia oblonga</i> Mill, <i>Juglans mandshurica</i> Maxim, <i>Magnolia coco</i> (Lour.) DC., <i>Malus asiatica</i> Nakai, <i>Elaeagnus angustifolia</i> Linn., <i>Sophora japonica</i> Linn., <i>Juglans regia</i>, <i>Acer ginnala</i> Maxim., <i>Platyclusus orientalis</i> (L.) Franco, <i>Ailanthus altissima</i>, <i>Malus pumila</i> Mill., <i>Pinus koraiensis</i> Sieb. et Zucc., <i>Picea asperata</i> Mast., <i>Acer mono</i> Maxim., <i>Celtis bungeana</i> Bl, <i>Abies fabri</i> (Mast.) Craib, <i>Xylosma racemosum</i>(Sieb. et Zucc.)Miq., <i>Lespedeza bicolor</i> Turcz, <i>Syringa</i> Linn., <i>Ligustrum lucidum</i>, <i>Rhododendron simsii</i> Planch., <i>Rosa chinensis</i> Jacq., <i>Spiraea thunbergii</i></p>	<p><i>Hyphantria cunea</i>(Drury), <i>Chrysomela populi</i> Linnaeus, <i>Ambrostoma quadriimpressum</i> Motschulsky, <i>Malacosoma neustria</i> testacea Motschulsky, <i>Tuberocephalusmomonis</i>, <i>Tetranychus cinnabarinus</i>, <i>Anoplophora glabripennis</i>, <i>Cryptorrhynchus lapathi</i> L., <i>Agrotis ypsilon</i> Rottemberg, <i>Semiothisa cmerearia</i> (Bremer et Grey), <i>Agrilus planipennis</i> Fairmaire, <i>Agrilus</i> sp., <i>Chrysobothris succedana</i>, <i>Apriona germari</i>(Hope), <i>Gryllotalpa unispina</i> Saussure, <i>Ericerus pela</i> Chavannes, <i>Holotrichia diomphalia</i> Bates, <i>Trialeurodes vaporariorum</i> (Westwood), <i>Liriomyza sativae</i> Blanchard, <i>Clostera anastomosis</i>, <i>Apocheima cinerarius</i> Erschoff, <i>Stilpnolia salicis</i> (Linnaeus), <i>Aporia crataegi</i>, <i>Papilio xuthus</i>, <i>Yponomeuta evonymallus</i> (Linnaeus), <i>Ips acuminatus</i>, <i>Parathrene tabaniformis</i> (Rottenberg), <i>Cossus cossus</i> Linnaeus, <i>Loxostege sticticalis</i> Linne</p>
Northeast China zone	<p><i>Juglans regia</i>, <i>Quercus aliena</i> Bl., <i>Pinus armandii</i> Franch., <i>Pinus tabuliformis</i> Carrière, <i>Cotinus coggygria</i> Scop., <i>Ulmus pumila</i> L., <i>Salix babylonica</i>, <i>Populus</i> L., <i>Sophora japonica</i> Linn., <i>Robinia pseudoacacia</i> L., <i>Castanea mollissima</i>, <i>Prunus ceraifera</i> cv. <i>Pissardii</i>, <i>Ligustrum lucidum</i>, <i>Buxus sinica</i> (Rehder &amp; E. H. Wilson) M. Cheng, <i>Malus pumila</i> Mill., <i>Pyrus</i> spp, <i>Amygdalus triloba</i>, <i>Armeniaca vulgaris</i> Lam., <i>Amygdalus persica</i> L., <i>Malus prunifolia</i> (Willd.) Borkh., <i>Euonymus alatus</i> (Thunb.) Sieb, <i>Buxus sinica</i> (Rehder &amp; E. H. Wilson) M. Cheng, <i>Amygdalus persica</i> var. <i>persica</i> f. <i>duplex</i>, <i>Elaeagnus angustifolia</i> Linn., <i>Spiraea blumei</i> G. Don, <i>Rosa davurica</i>, <i>Rosa multiflora</i> Thunb., <i>Rhododendron simsii</i> Planch., <i>Calystegia hederacea</i> Wall, <i>Trifolium repens</i> L., <i>Poa annua</i> L., <i>Lolium perenne</i> L, <i>Festuca elata</i> Keng ex E. Alexeev</p>	<p><i>Ericerus pela</i> Chavannes, <i>Pseudaulacaspis pentagona</i> (Targioni Tozzetti), <i>Tetranychus cinnabarinus</i>, <i>Hyalopterus arundinis</i> Fabricius, <i>Tetraneura ulmi</i>(Linnaeus), <i>Aphis ciricola</i> van der Goot, <i>Spilonota lechriaspis</i> Meyrick, <i>Lyonetia clerkella</i> L., <i>Lithocolletis ringoniella</i> Mats., <i>Cnidocampa flavescens</i>(Walker), <i>Pontania bridgmannii</i> Cameron, <i>Diaphania perspectalis</i> (Walker), <i>Atractomorpha sinensis</i> Bolvar, <i>Harmonia axyridis</i> (Pallas), <i>Cicadella viridis</i>, <i>Anoplophora chinensis</i>, <i>Chrysobothris succedana</i>, <i>Anomala corpulenta</i>, <i>Lymantria dispar</i>, <i>Halyomorpha Picus</i> (Fabricius), <i>Sinitinea pyrigalla</i>, <i>Dendroctonus armandi</i>, <i>Plagioderia versicolora</i> (Laicharting), <i>Liriomyza sativae</i> Blanchard, <i>Ixodes persulcatus</i>, <i>Ornithodoros papillipes</i>, <i>Hyphantria cunea</i>(Drury)</p>



**TABLE 2**  
**Potential risks of pests' disaster in park green land in Central China**

No.	Major host plant varieties	Latin name	Classification position	Harmful to people or animals
1.	<i>Pinus massoniana</i> Lamb.	<i>Dendrolimus punctatus</i> Walker	Lepidoptera	Yes
2.	<i>Cerasus</i> ssp., <i>Prunus mume</i> , <i>Osmanthus fragrans</i> (Thunb.) Lour., <i>Amygdalus persica</i> L., <i>Magnolia Grandiflora</i> Linn, <i>Prunus ceraifera</i> cv. <i>Pissardii</i> , <i>Rosa chinensis</i> Jacq., <i>Gardenia jasminoides</i> , <i>Malus spectabilis</i> (Ait.) Borkh., <i>Rosa multiflora</i> , <i>Chimonanthus praecox</i> (Linn.) Link, <i>Spiraea cantoniensis</i> Lour., <i>Pinus massoniana</i> Lamb., <i>Cinnamomum camphora</i> (L.) presl, <i>Pterocarya stenoptera</i> C. DC	<i>Odontotermes formosanus</i>	Isoptera	Yes
3.	<i>Cinnamomum camphora</i> (L.) Presl., <i>Platanus acerifolia</i> Willd., <i>Liquidambar formosana</i> Hance, <i>Ilex cornuta</i> Lindl. et Paxt., <i>Magnolia Grandiflora</i> Linn, <i>Michelia alba</i> DC., <i>Pterocarya stenoptera</i> C. DC, <i>Salix babylonica</i> Linn., <i>Robinia pseudoacacia</i> L., <i>Osmanthus fragrans</i> (Thunb.) Lour.	<i>Macrotermes barneyi</i> Light	Isoptera	Yes
4.	<i>Camellia japonica</i> L., <i>Sophora japonica</i> Linn., <i>Robinia pseudoacacia</i> L., <i>Punica granatum</i> L., <i>Citrus reticulata</i> Blanco, <i>Populus</i> L.	<i>Syynpiezoyrelias lewisi</i> (Roelofs)	Coleoptera	/
5.	<i>Hibiscus syriacus</i> Linn., <i>Punica granatum</i> L., <i>Prunus ceraifera</i> cv. <i>Pissardii</i> , <i>Nerium indicum</i> Mill., <i>Prunus mume</i> , <i>Cercis chinensis</i>	<i>Aphis gossypii</i> Glover	Hemiptera	/
6.	<i>Malus spectabilis</i> (Ait.) Borkh., <i>Cerasus</i> ssp., <i>Nerium indicum</i> Mill., <i>Prunus mume</i> , <i>Amygdalus persica</i> L.	<i>Myzus persicae</i> (Sulzer)	Hemiptera	/
7.	<i>Amygdalus persica</i> var. <i>persica</i> f. <i>duplex</i> , <i>Amygdalus triloba</i> , <i>Cerasus</i> ssp.	<i>Tuberocephalus momonis</i>	Homoptera	/
8.	<i>Robinia pseudoacacia</i> L, <i>Amygdalus persica</i> L., <i>Ligustrum lucidum</i> , <i>Camellia japonica</i> L., <i>Platanus orientalis</i> Linn., <i>Paulownia</i> Sieb. et Zucc., <i>Bambusoideae</i> , <i>Salix babylonica</i> Linn., <i>Populus</i> L., <i>Morus alba</i> L.	<i>Cicadella viridis</i>	Homoptera	Yes
9.	<i>Amygdalus persica</i> L., <i>Ligustrum lucidum</i> , <i>Ilex cornuta</i> Lindl. et Paxt., <i>Buxus megistophylla</i> Levl., <i>Buxus sinica</i> var. <i>parvifolia</i> M. Cheng, <i>Prunus ceraifera</i> cv. <i>Pissardii</i>	<i>Jacobiasca formosana</i>	Homoptera	Yes
10.	<i>Salix babylonica</i> Linn., <i>Amygdalus persica</i> L., <i>Cerasus</i> ssp., <i>Sophora japonica</i> Linn., <i>Robinia pseudoacacia</i> L, <i>Fraxinus chinensis</i> Roxb., <i>Populus</i> L.	<i>Cryptotympana atrata</i>	Homoptera	/
11.	<i>Lagerstroemia indica</i> L., <i>Punica granatum</i> L., <i>Ligustrum lucidum</i> , <i>Ligustrum quihoui</i> Carr., <i>Michelia figo</i> (Lour.)Spreng	<i>Eriococcus legerstroemiae</i> Kuwana	Homoptera	/
12.	<i>Cerasus</i> ssp., <i>Rosa chinensis</i> Jacq., <i>Malus spectabilis</i> (Ait.) Borkh., <i>Prunus ceraifera</i> cv. <i>Pissardii</i> , <i>Ligustrum lucidum</i> , <i>Buxus megistophylla</i> Levl.	<i>Drosicha contrahens</i>	Homoptera	/
13.	<i>Armeniaca mume</i> , <i>Amygdalus persica</i> var. <i>persica</i> f. <i>duplex</i> , <i>Cerasus</i> ssp., <i>Hibiscus syriacus</i> Linn., <i>Cycas revoluta</i> Thunb., <i>Ginkgo biloba</i> L.	<i>Pseudaulacaspis pentagona</i> (Targioni Toz-zetti)	Homoptera	/
14.	<i>Camellia japonica</i> L., <i>Prunus ceraifera</i> cv. <i>Pissardii</i> , <i>Malus spectabilis</i> (Ait.) Borkh., <i>Pinus massoniana</i> Lamb., <i>Cedrus deodara</i> (Roxb.) G. Don, <i>Pinus thunbergii</i> Parl., <i>Albizia julibrissin</i> Durazz., <i>Liquidambar formosana</i> Hance, <i>Robinia pseudoacacia</i> L, <i>Platanus orientalis</i> Linn.	<i>Ceroplastes japonicas</i> Guaind	Homoptera	/
15.	<i>Platanus orientalis</i> Linn., <i>Populus</i> L., <i>Salix babylonica</i> Linn., <i>Ulmus pumila</i> L., <i>Robinia pseudoacacia</i> L, <i>Acer palmatum</i> Thunb.	<i>Anoplophora glabripennis</i>	Coleoptera	Yes
16.	<i>Camellia japonica</i> L., <i>Viburnum odoratissimum</i> Ker-Gawl, <i>Platanus orientalis</i> Linn., <i>Lagerstroemia indica</i> L., <i>Populus</i> L., <i>Salix babylonica</i> Linn., <i>Ulmus pumila</i> L., <i>Robinia pseudoacacia</i> L, <i>Morus alba</i> L., <i>Cerasus</i> ssp., <i>Sophora japonica</i> Linn., <i>Fraxinus chinensis</i> Roxb., <i>Sabina chinensis</i> (L.) Ant. cv. <i>Pyramidalis</i>	<i>Anoplophora chinensis</i>	Coleoptera	Yes
17.	<i>Salix babylonica</i> Linn., <i>Populus</i> L., <i>Robinia pseudoacacia</i> L, <i>Broussonetia papyrifera</i> , <i>Pterocarya stenoptera</i> C. DC, <i>Citrus reticulata</i> Blanco	<i>Apriona germari</i> (Hope)	Coleoptera	/
18.	<i>Populus</i> L., <i>Salix babylonica</i> Linn., <i>Amygdalus persica</i> var. <i>persica</i> f. <i>duplex</i> , <i>Pterocarya stenoptera</i> C. DC	<i>Anomala corpulenta</i> Motschulsky	Coleoptera	Yes
19.	<i>Camellia oleifera</i> Abel., <i>pinus elliottii</i> , <i>Amygdalus persica</i> L.	<i>Dichocrocis punctiferalis</i> Guenée	Lepidoptera	/
20.	<i>Populus</i> L., <i>Salix babylonica</i> Linn., <i>Buxus megistophylla</i> Levl., <i>Buxus sinica</i> var. <i>parvifolia</i> M. Cheng, <i>Buxus bodinieri</i> Levl., <i>Euonymus maackii</i>	<i>Calospilos suspecta</i> Warren	Lepidoptera	/
21.	<i>Cinnamomum camphora</i> (L.) presl, <i>Ginkgo biloba</i> L., <i>Liquidambar formosana</i> Hance, <i>Camptotheca acuminata.</i> , <i>Pterocarya stenoptera</i> C. DC, <i>Diospyros kaki</i> Thunb.	<i>Dictyoploca japonica</i> Butler	Lepidoptera	/
22.	<i>Cinnamomum camphora</i> (L.) presl, <i>Salix babylonica</i> Linn., <i>Populus</i> L.	<i>Holcocerus insularis</i>	Lepidoptera	/



23.	<i>Ligustrum lucidum</i> , <i>Paulownia Sieb. et Zucc.</i> , <i>Fraxinus chinensis</i> Roxb., <i>Gardenia jasminoides</i> , <i>Osmanthus fragrans</i> cv. Tsubergii, <i>Michelia figo</i> (Lour.) Spreng, <i>Cinnamomum camphora</i> (L.) Presl, <i>Catalpa ovata</i> G. Don.	Stgr. <i>Psilogramma menephron</i>	<i>Lepidoptera</i>	/
24.	<i>Pterocarya stenoptera</i> C. DC., <i>Robinia pseudoacacia</i> L., <i>Ginkgo biloba</i> L., <i>Salix babylonica</i> Linn., <i>Platycladus orientalis</i> (L.) Francoptmxijkmsc	<i>Clania variegata</i> Snellen	<i>Lepidoptera</i>	/
25.	<i>Citrus reticulata</i> Blanco, <i>Ailanthus altissima</i> , <i>Osmanthus fragrans</i> (Thunb.) Lour.	<i>Panonychus citri</i> Mc Gregor	<i>Arachnoidea</i>	Yes
26.	Woodland, lawn	<i>Rhipicephalus haemaphysaloides</i>	<i>Arachnoidea</i>	Yes
27.	Woodland, lawn	<i>Boophilus microplus</i>	<i>Arachnoidea</i>	Yes

different vegetation zones in park, luring and killing insects by hanging insecticidal lamps in the appropriate location and identifying species, identifying the collected specimens, analyzing the collected data, and summarizing a directory about green pests (Table 2).

**The monitoring and early warning of green land biological risk.** After many harmful organisms entering the urban green land system, they will undergo an adjustment period, called time delayed period. During this period, taking effective measures basically can achieve the purpose to eradicate or control them. Taking measures to eradicate or control until they widely spreading makes the difficulty and cost very high. Prevention is more important and economic than control. Therefore, in order to forbid the harmful green land organisms from causing serious harm, the establishment of the early warning and monitoring system of harmful urban green land organisms is necessary and imperative [24].

Green biological early warning refers to monitor and predict uncertain events resulting from harmful green land organisms to meet the requirements of treatment and management. Lucas [25] and Zhang [26] put forward the constructing methods of biological early warning and monitoring system about urban garden plants. The early warning system of harmful urban green land organisms is divided into four parts through systematic summary and research, including decision-making and command, technical supporting, risk evaluation, and organization implementing system.

### 1. Decision-making and command.

Decision layer, fully leading the early warning system, is the highest decision-making institution of the early warning system. It is led by the urban branching charge department and aims to establish internet monitoring system, clear responsibilities of each department, examine the early-warning and predicting information, prevent and control decision-making and coordinate other organization.

At the same time, it can also examine the emergency control plan of large emergencies and decide the start and end of the emergency plan.

**2. Technical supporting.** What is the strong technical backing of the construction of early warning system are that making full use of domestic technology, setting up expert database, breeding the professional people in the research field of early warning about harmful organisms, and maintaining relative stability of the team personnel structure and technological superiority. The managing and technical personnel of garden greening should learn the knowledges concerning the identification, monitoring, early-warning and comprehensive treatment of harmful organisms in garden plants through on-site training, special training and interactive communication training to guide the prevention and control of harmful organisms in green land towards the developing direction that people and environment are all safe.

The establishment of the monitoring center, the monitoring station, the risk analysis center and the early-warning information analysis center about harmful organisms in green land is also an important way. Meanwhile, the equipments of specialized instruments as well as researchers and the cooperation of daily monitoring work are indispensable. Researchers should carry out work around the major scientific and technological problems happened in the implementation process of early-warning system and monitoring, and perform extension analysis to monitoring and early-warning information.

**3. Risk evaluation.** Risk assessment of green land organisms, based on the biological data of harmful organisms such as name, classification, host, biological characteristics and harm degree, refers to perform the risk assessment from the aspects of the possibility of introduction, the possibility of diffusion and the impacts to economy, society and environment after they are introduced, and ultimately determine the level of quarantining



and the level of risk. On the other hand, the gradual establishment of the evaluation mechanism of risk analysis of harmful green land organisms' disaster and the classification management of harmful green land organisms on the basis of disaster risk are exceedingly important. Aimed at first class pests who have large disaster risk, the formulation of detailed contingency plans is the efficient measure that can make the disasters immediately eliminate once occurred. Aimed at second and third class pests who have potential disaster risk, establishing strict and systemic monitoring mechanism and reserving the corresponding technologies of prevention and control are effective strategies [27].

#### **4. Organization implementing system.**

Establishing some monitoring points in the range of monitoring is convenient for the fixed-site monitoring of urban harmful green land organisms. The monitoring and early-warning reports of urban harmful green land organisms can regularly update by arranging technical personnel to collect the situation of each monitoring point and relying on the existing database of harmful organisms. The early-warning and monitoring center should further survey the discovered harmful organisms' disasters, and timely make the implementing situation of relative measures feed back to the landscape and Scenic Area Management Office. The monitored objects mainly consist of harmful organisms in urban green land and invaded alien harmful species, including quarantining harmful organisms and harmful garden organisms that may have negative impact on the human body. Meanwhile, it is an advisable measure that monitoring those harmful garden organisms that do not invade, as far as possible to early detect and eliminate, to reduce the possibility of invasion [28].

### **COMPREHENSIVE PREVENTION AND CONTROL OF HARMFUL ORGANISMS IN GREEN LAND**

---

Urban green land system is a complex ecosystem of society, economy and nature. The treatment to harmful organisms in urban green land system is the embodiment of the interaction between human and urban green land environment. The prevention and control of harmful organisms are an important part of the urban green land maintaining and directly affect the sustainable development of the urban ecological environment and ecosystem. However, the phenomenon that emphasizing treatment but ignoring prevention, as well as blind use of chemical pesticides has been widespread up to now in process of the prevention and control of harmful organisms. The abuse of chemical

pesticides, except continuously increase the cost, can also cause the "3R" (Resistance of disease, Resurgence of pests and Residue of pesticides) problem, make the ecological environment worse, and does great harm to the health of human beings.

Human beings continuously explore the new ways of the prevention and control of harmful organisms to forbid biological disasters and maintain ecological balance [29]. Tshernyshev [30] put forward the Ecological Pest Management (referred to as EPM), emphasizing to maintain long-term stability of the system and improve the self-adjustment ability of system. Zhang Zongbing [31] discussed the concept and key points of comprehensive treatment of pests and put forward the tolerant philosophy and treating strategy of comprehensive treatment. According to the specific situation of Chinese green land types, taking the following ecological treatment measures can furthest ensure the stable and healthy development of the green land ecological system of urban landscape.

**Biological prevention and treatment.** The technology of biological prevention and treatment refers to use biological means to intervene harmful urban organisms to achieve the purpose of the prevention and treatment of pest. It is widely used in the prevention and treatment of forest harmful organisms [32]. Its advantages are that it generally does not harm to people, livestock and plants, has great selectivity, does not pollute the air, water and soil, and will not produce resistance. There are some key points about biological prevention and treatment. Firstly, the protection and utilization of natural enemies are important. At the same time, do not use pesticides that have strong lethality on natural enemies to make natural enemy population successfully survive and thrive. Secondly, making full use of biological pesticides is necessary. Biological pesticides include microbial pesticides (such as *Bacillus thuringiensis*, Jinggaangmycin and etc), botanical pesticides (such as pyrethrum pyrethrins) and animal pesticides (such as insect attractants). Compared with chemical pesticides, these biological pesticides have the advantages of no residue, no pollution and no environmental pollution. Meanwhile, they have single-minded effects on relative pest species (called target).

The technology of biological prevention and treatment also has some defects. Biological prevention and treatment in China is mostly confined to prevent and treat harmful organisms through releasing their natural enemies and the release of lots of natural enemies is harmful to system stability. In addition, due to the slow effect, the high technical requirements, and the great restrict from the environmental conditions, this



method cannot achieve the goal to quickly lower the number of harmful organisms in high density environment. Therefore, in order to obtain the best effects, it should cooperate with other methods in most cases in the process of the prevention and treatment of harmful organisms.

**Physical mechanical prevention and treatment.** This technology prevents and treats pests by applying simple instruments or physical factors (light, heat, electricity, wind or radiation, and etc) according to special habits and tropism of pests. For example, ticks can be prevented by the smell of garlic, many moths, mayflies and leafhopper that have phototaxis can be trapped and killed by using black light lamp, lots of adult Coleoptera with the characteristic of feign death can be perished by manual work, and the cutworm with chemotaxis can be trapped and eliminated by sweet and sour liquid [33]. The plants diseases can be prevented and treated through making use of various physical factors, including thermal treatment, mechanical treatment, radiation treatment and surgery. For instance, the use of thermal treatment to seeds, seedlings, scion and soil can eliminate some pathogens, and the use of surgery can scrape the stem disease spot to prevent and treat plant trunk diseases. Physical mechanical prevention and treatment is most simple, economic, efficient and pollution-free compared with other various methods in the prevention and treatment of garden pests.

**Chemical prevention and treatment.** Although chemical prevention and treatment brings a series of negative effects, it is still an irreplaceable preventing and treating method of harmful organisms under special circumstances [34]. In particular, when the sudden or eruptive pests' diseases occur, chemical prevention and treatment is still an emergency measure. Scientific and reasonable application of chemical pesticides can timely and effectively control the pests and diseases. Such as the reasonable mixed or rotational application of pesticides not only can improve the effect of prevention and treatment but also can avoid or delay the pests' resistance to pesticides. The application of specific and highly selective pesticides can reduce the damage to natural enemies. It can reduce the environmental pollution that strictly controlling the use of pesticides types, applying low toxicity, high efficiency and low residue pesticides, and using scientific and proper methods of pesticides application [35].

**Cultivated prevention and treatment.** It is the precondition of guaranteeing the healthy growth of urban greening plants and improving resistance

that basing on the respect to self-adjustment of ecological system in each link of design, planting, construction and maintenance, following the principles of biological symbiosis, biological circulation and biological competition, implementing the reasonable collocation of arbor, bush, vines, flowers and grass, and forming the multi-level plants communities with various species, multilayer, mutual promotion and coexistence. In addition, the choice of the tree species should be based on the distribution regulation of the vegetation and put emphases on native tree species to make trees plant in suitable place [36]. It is an extremely effective strategy that controlling technology after harvest, cooperating with other methods and improving plants vigor through the selection of species and the adjustment of planting period, planting density, reasonable fertilization, as well as irrigation and drainage. At the same time, the mixed planting of the plants that pests are parasitic on and the plants with common pests' disease should be avoided.

**Legal prevention and treatment.** Legal prevention and treatment refers to adopt measures to forbid and restrain the transport of those greening plants and plants products that are infected with particular harmful organisms to prevent the man-made spread of these harmful organisms and ensure the ecological security of urban green land through the establishment of specialized agencies and the legal, administrative and technical means according to laws and rules. Its characteristic is to prevent the introduction, settling and expansion of harmful organisms from the macro overall, especially in the area where harmful organisms are not distributed. With the expansion of the urban construction and the interregional trade, the transport and exchange of seedlings is more frequent, which provides more favorable conditions for the spreading of diseases and pests in green land [37]. The establishment and improvement of the quarantining access rule of garden plants that all seedlings must be examined and only these seedlings that have quarantining certificate can be transported is the effective way to truncate alien invasive pests' propagation.

## **THE MANAGEMENT MEASURES OF BIOLOGICAL RISK IN GREEN LAND**

---

**Emphasizing the early detection of harmful organisms.** Strengthening the monitoring forecast can provide accurate decision-making basis for prevention and treatment of harmful organisms in urban green land. The monitoring forecast is the precondition of performing control work of harmful



organisms. Carrying out the national survey of pest epidemic in green land and performing the aerial surveillance in those provinces with relative conditions can provide experience for large area and regular application. Regularly monitoring harmful organisms in urban green land and publishing predicting information are also necessary [38].

**Strengthening the work of quarantining and anti-disaster.** The quarantining work of preventing the input and export of harmful organisms is an important link to controlling the invasion of harmful organisms into urban green land [39]. Plant quarantining has positive effect on preventing the invasion of harmful species. Some data show that there were 46 ships where darnel, fake sorghum seed, as well as other grass seeds that have about 30 families, 100 genera and 200 species were seized in 349 ships imported from Shanghai port from 1986 to 1990 [40]. The introduction of alien species for landscaping must undergo strict quarantining to prevent the spreading of dangerous diseases, insects and weeds. In addition, these sites, including the seedling and flower production base, the sales and processing establishments of timber, public green land, green land of residential area, station, wharf, port and other places, must carrying out quarantining enforcement. At the same time, quarantining and treating dangerous harmful organisms and controlling the introduction and expansion of dangerous harmful organisms in green land are also significant.

**Emphasizing the kinds of diseases and pests which have caused serious harm in foreign.** Chinese government must pay high attention to the kinds of diseases and pests which have already caused serious harm in foreign at present and should take measures to prevent the spread to China. Such as the disease of *Quercus* sudden death that currently cause Oak Plants suddenly die in the United States. In China, the relevant departments should strengthen cooperation and formulate corresponding measures. At the same time, further strengthening exchange of the epidemic data of information with other countries can make government as soon as possible to understand what the kinds of pests and diseases these countries have. In addition, it is necessary to take measures in advance to prevent those harmful organisms that are likely to endanger the security of urban green land in China.

**Strengthening the management of biological products.** Biological prevention and treatment with the advantages of not polluting environment and not damaging natural enemies and human is an

important measure to control pests and diseases in urban green land in China. The major contents of biological control are that promoting the application of comprehensive prevention and control measures that are mainly based on no-polluted treatment, using biological and microbiological pesticides, fully protecting and utilizing natural resources, and vigorously promoting the technology of insect pheromone to improve the effect of biological prevention and treatment. Nowadays, many countries, such as Russia, Canada, the United States, Japan, Finland and Australia, are actively carrying out the research of biological control and the production and application of biological insecticide. At present, insect virus, bassiana, Bt and natural enemies are large used in the prevention and treatment of pests and diseases in the urban green land in China. Besides Bt, the majority do not have registration certificate. Therefore, producing these biological products with mature technology that are widely used and formulating the technical standards of these products are urgent. Meanwhile, the registration of products and formulating the strict input management procedure of natural enemies are necessary.

**Strengthening the selection and maintenance of plant varieties.** The construction of urban green land should be based on the principle of protecting biological diversity and strengthen the breeding of resistant plant varieties to adapt to the urban ecological environment. The drought resistance, barren resistance, less water consumption, pollution resistance, frost resistance, disease and insect resistance, and extensive management resistance should be the primary standards of the selection of the tree species. The optional introduction of species is inadvisable and planting native garden trees is most suitable. Chen Bo [41] concluded that the blind introduction of species can not only achieve the desired effect of greening, but also cause huge economic losses. Take Kudzu (*Argyrea seguinii* (Levl.) Van. Ex Levl) as an example [42], the United States introduced it from Japan (Japan introduced it from China) in 1930. After 1950s, due to the crazy growth of Kudzu, local animals and plants were perished, resulting in a public nuisance. Therefore, the exotic species introduced for urban greening must undergo strict ecological risk assessment to basically ensure no ecological and economic loss [43]. Meanwhile, strengthening the maintaining management of garden plants and creating the environmental conditions that are conducive to the normal growth of plants and the breeding of natural enemies and are harmful to the production of pest and disaster can effectively control the plant diseases and pests.

## CONCLUSION

With the acceleration of global economic integration, urban construction has entered the sustainable development period in China. What reveal the coming of profound reform of Chinese overall development is that Chinese “thirteen five” plan put forward five developing ideas, called “innovation, harmony, greening, opening and sharing”. The ecological environmental protection already ascended to an unprecedented height in China especially government added the green development concept into plan for the first time. The biological risk analysis and management to green land in China make significantly practical sense of the sustainable development of Chinese urban ecological health. Meanwhile, the biological risk analysis and management to green land in China are the urgent needs to curb the situation that urban green land pest seriously occur, the inevitable choices to maintain public safety and construct ecological civilization, and the strategic measures to safeguard national interests and promote economic development.

## REFERENCES

- [1] Jeger, M., Pautasso, M., & Stack, J. (2011). Climate, globalization and trade: impacts on dispersal and invasion of fungal plant pathogens. *Fungal diseases: an emerging challenge to human, animal and plant health*, 273-296.
- [2] Zhang Yueheng, Huang Ruijian, Chen Bo. (2010). a review of the evaluation of urban green land ecological benefits. *Journal of Hangzhou Normal University: Natural Science Edition*, (4), 268-271.
- [3] Chen Yanfen, Li Haihui. (2007). The Guangzhou uprising martyrs cemetery landscape tree Termite Prevention report. *Guangdong garden*, 29 (1), 64-66.
- [4] Zhang YZ, Zhou DJ, Xiong YW, et al. Hemorrhagic fever caused by a novel tick-borne Bunyavirus in Huaiyangshan, China. *Chin J Epidemiol*. 2011, 32 (3): 209-220.
- [5] Zhu Shuifang, Chen Naizhong, Li Weicai, Zhang Yibing. (2004). The conception of exotic biological invasion and its frontier control system. *Plant quarantine*, 18 (1), 32-36.
- [6] Chen Gang, Hai Xin Liu, Luo Hong, & Tu Xiaoqiang. (2010). The occurrence and control of the urban forest plant diseases and insect pests. *Abstracts of Chinese gardening*, (12): 99-100.
- [7] Schorn, S., Pfister, K., Reulen, H., Mahling, M., & Silaghi, C. (2011). Occurrence of *Babesia* spp., *Rickettsia* spp. and *Bartonella* spp. in *Ixodes ricinus* in Bavarian public parks, Germany. *Parasit Vectors*, 4, 135.
- [8] Smith FD, Ballantane R, Morg ER, et al. (2011). Prevalence distribution and risk associated with tick infestation of dogs in Great Britain. *Medical and Veterinary Entomology*, 25:377-384.
- [9] Jennett, A. L., Smith, F. D., & Wall, R. (2013). Tick infestation risk for dogs in a peri-urban park. *Parasites and Vectors*, 6, 358.
- [10] Logan, J. A., Regniere, J., & Powell, J. A. (2003). Assessing the impacts of global warming on forest pest dynamics. *Frontiers in Ecology and the Environment*, 1(3), 130-137.
- [11] Grousset, F., Petter, F., Suffert, M., & Roy, A. S. (2012). EPPO study on the risk of imports of plants for planting: description and details of the first outcomes. *EPPO bulletin*, 42(2), 185-190.
- [12] Deng Qiming, Zhang Qiufang, & Zhou Shudong. (2006). The risk of invasive alien species and its safety management. *Journal of natural disasters*, 15 (2), 25-31.
- [13] Ju Ruiting, Li Yuezhong, Du Yuzhou, Xu Ying, Yan Wei, Xing Zhenchi. (2005). *Opogona sacchari* in the analysis of the causes of the intrusion of the China. *Plant quarantine*, 19 (3), 129-131.
- [14] Gao Jianliang, Zhao Linyan, Zhao Linfeng. (2006) the harm of alien invasive species in China and the Countermeasures of prevention and cure. *Hunan forestry science and technology*, 32 (6), 72-75.
- [15] Ding Shimin, Zhu Minghui, Jia Hengju. (2010) the main types, characteristics and control of the main pests in the garden green space in Shandong peninsula area, Weifang higher vocational education, 3, 26
- [16] Su Jishen, Zheng Ling, Du Shunbao. (2010). Investigation and analysis of plant diseases and insect pests in Nanjing City Park and its prevention and cure suggestion. *Jiangsu forestry science and technology*, 37 (1), 28-31.
- [17] Wang Zhilong. (2006). Research of flowers and trees species pests investigation and prevention of zhejiang province (Doctoral dissertation, Zhejiang University).
- [18] Jin Hao. (2012) GIS system based on the system of the main green space pest distribution law (Thesis Master's, Shenyang University).
- [19] Jie Yuze, Xu Jinzhu, Qin Changsheng, Zhao Danyang, Yang Hua. (2015). Preliminary investigation of plant diseases and insect pests of important landscape trees in Guangdong province. *Guangdong forestry science and technology*, 31 (2), 130-135.



- [20] Hu Erhong, Chen Wanxing. (2013). Investigation and analysis of plant diseases and insect pests in Taiyuan city. *Shanxi science and technology*, (1), 48-49.
- [21] Cen Bing James, Su Xing. (2003). Landscape plant pest control. Guangzhou: Guangdong science and Technology Press.
- [22] Wu Shiyong. (2005). Forest pest harm of city. Shanghai: Shanghai science and Technology Press.
- [23] Liu Zhenyu, Shao Jinli. (2009). Control of plant diseases and insect pests in garden. Beijing: Chemical Industry Press.
- [24] Cook, R. J., Bruckart, W. L., Coulson, J. R., Goettel, M. S., Humber, R. A., Lumsden, R. D., & Quimby Jr, P. C. (1996). Safety of microorganisms intended for pest and plant disease control: a framework for scientific evaluation. *Biological control*, 7(3), 333-351.
- [25] Lucas, J. A. (2011). Advances in plant disease and pest management. *The Journal of Agricultural Science*, 149(S1), 91-114.
- [26] Zhang le, Ju Ruiting. (2008). Shanghai landscaping forestry harmful biological early warning system. *China's forest diseases and pests*, 27 (3), 42-44.
- [27] Ju Ruiting, Xu Yin, Yi jianping, YanWei, Du Yuzhou. (2005). Building urban green space pest risk analysis system and applications. *Journal of plant protection*, 32 (2), 179-184.
- [28] Andersen, M. C., Adams, H., Hope, B., & Powell, M. (2004). Risk assessment for invasive species. *Risk analysis*, 24(4), 787-793.
- [29] Kogan, M. (1998). Integrated pest management: historical perspectives and contemporary developments. *Annual review of entomology*, 43(1), 243-270.
- [30] Tshernyshev, W. B. (1995). Ecological pest management (EPM): general approaches. *Journal of applied entomology*, 119(1-5), 379-381.
- [31] Zhang Zongbing. (1986). The concept and key points of integrated pest management (one). *Plant protection*, 12 (1), 29-32.
- [32] Jacobsen, B. J. (1997). Role of plant pathology in integrated pest management. *Annual review of phytopathology*, 35(1), 373-391.
- [33] Luo Shijuan, Gao Jiang. (2014). Forest pest control technology of green trees. *Southern agriculture*, 8 (09X), 32-34.
- [34] Waard, M. A., Georgopoulos, S. G., Hollomon, D. W., Ishii, H., Leroux, P., Ragsdale, N. N., & Schwinn, F. J. (1993). Chemical control of plant diseases: problems and prospects. *Annual review of phytopathology*, 31(1), 403-421.
- [35] James, J. R., Tweedy, B. G., & Newby, L. C. (1993). Efforts by industry to improve the environmental safety of pesticides. *Annual Review of Phytopathology*, 31(1), 423-439.
- [36] Hui-ling, P. A. N. (2009). Principles of Landscape Design of Landscape Plants. *Journal of Hebei Agricultural Sciences*, 6, 030.
- [37] Webber, J., Richardson, B., & Hood, I. A. (2010). Pest risk analysis and invasion pathways for plant pathogens. *New Zealand Journal of Forestry Science*, 40, 45-56.
- [38] Mills, P., Dehnen-Schmutz, K., Ilbery, B., Jeger, M., Jones, G., Little, R., & Maye, D. (2011). Integrating natural and social science perspectives on plant disease risk, management and policy formulation. *Philosophical Transactions of the Royal Society B: Biological Sciences*, 366(1573), 2035-2044.
- [39] MacLeod, A., Pautasso, M., Jeger, M. J., & Haines-Young, R. (2010). Evolution of the international regulation of plant pests and challenges for future plant health. *Food Security*, 2(1), 49-70.
- [40] Qiang Sheng, Cao Xuezhong. (2000) investigation and analysis of exotic weeds in China. *Chinese Journal of plant resources and environment*, 9 (4), 34-38. (in Chinese).
- [41] Chen Bo, Bao Zhiyi. (2004). construction of urban forest should be alert to biological invasion. *Urban problems*, (5): 12-16.
- [42] Yao Hejin, Chen Zhijun, Yun Yun, Zhou Weijun. (2009) the harm and prevention of alien invasive species to our country garden green space and its prevention and cure. *World forestry research*, (3), 76-80.
- [43] Stohlgren, T. J., Binkley, D., Chong, G. W., Kalkhan, M. A., Schell, L. D., Bull, K. A., & Son, Y. (1999). Exotic plant species invade hot spots of native plant diversity. *Ecological Monographs*, 69(1), 25-46.

---

**Received: 23.03.2016**

**Accepted: 28.09.2016**

---

**CORRESPONDING AUTHOR**

**Long Yuelin**

College of horticulture and landscape architecture,  
Hunan Agricultural University  
Changsha 410128 – CHINA

E-mail: yuelin62@126.com

# THE RESPONSE OF COTTON (*GOSSYPIUM HIRSUTUM* L.) TO SOIL APPLIED ELEMENTAL SULPHUR UNDER BORON TOXICITY

Firat Kurt<sup>1\*</sup>, Mefhar Gultekin Temiz<sup>2</sup>

<sup>1</sup>MusAlparslan University, Department of Organic Agriculture, Vocational School, Karakopru-Mus, Turkey

<sup>2</sup>Dicle University, Faculty of Agriculture, Department of Field Crops, Diyarbakır, Turkey

## ABSTRACT

This study was conducted between 2013 and 2014 to determine the effect of sulphur fertilization on boron toxicity in cotton. Two sulphur doses (0-1  $\text{tha}^{-1}$ ) as main plots and four boron doses (0, 2.5 ppm, 5 ppm and 15 ppm) as subplots were arranged in randomized complete split block design. According to the results, despite lack of phytotoxic symptoms of B, 5  $\text{mg B kg}^{-1}$ , B treatment showed significant effects on seed cotton yield, gin turnout, fiber maturity, and fiber elongation. However, the influence of B was uneven and inconsistent between years and among B dosages. Therefore, it could be concluded that higher doses of B applications should be avoided for higher lint yield and fiber qualities. In terms of S application, the amount of S dose employed in this study significantly decreased seed cotton yield and gin turnout; however, it had no effect on other lint quality parameters. This result may be of particular importance to the cotton growing soils with higher pH, which is required in applying higher doses of sulphur for optimum yields.

## KEYWORDS:

Cotton; sulphur; boron toxicity; fiber quality properties

## INTRODUCTION

Boron is an essential micro nutrient during cultivation of cotton [1]. Boron (B) toxicity may be observable in plants cultivated in semi-arid and arid regions. The other sources of excessive B are flying ash, mining wastes, irrigation water, and industrial chemicals [2]. Additionally, plants cultivated in saline soils which lack drainage bring about phytotoxicity of B [3]. Excessive B may lead to disruption of cell walls or to plant metabolism binding to ribose moieties of molecules such as nicotinamide adenine dinucleotide (NAD) and nicotinamide adenine dinucleotide phosphate (NADP), which take part in the electron transport system in photosynthesis. Moreover, the fact that B binds to free ribose sugar or ribose sugar in RNA

may cause harm to cell development and division [4].

The B toxicity symptoms in cotton first appear on older leaves as yellowing and chlorosis patches, and in the progressive stage of the toxicity the chlorosis turns into necrotic areas among veins, margins, and tips of leaves [5, 6]. The phytotoxic effects of excessive B in cotton appears at the concentration of 5  $\text{mg B kg}^{-1}$  in soil [5]. Cotton responds better to B fertilizers applied to the soil compared with those applied to the foliage, since mobility of B in phloem is low [7]. The soil properties also may affect the phytotoxicity of B in soils with high pH and high calcareous content [8].

The sulphur (S) requirement of plants is similar to phosphorous [9]. S is an important element of molecules such as RNA, DNA, amino acids, proteins, sulfolipids, flavonoids, lipids, glucosinolates, polysaccharides, and nucleotides. In addition, it is an essential nutrient used in sustaining hormonal activities [10]. Furthermore, the fact is that S has an important role on the mobility of photosynthesis products from source to sink organs, and on carbohydrate metabolism it increases boll weight by increasing the amino acid content of bolls and by decreasing boll shedding [11]. Sulphur application in cotton, either as pesticide or fertilizer, improves cotton lint yield and fiber qualities [11-15]. S can be applied prior to planting; however, applications from pre-plant to the onset of first square did not make any difference on lint yields [16]. The best seed cotton yields were obtained at 30  $\text{kg S}$  and  $\text{gypsum ha}^{-1}$  applied before planting [11]. There are few studies about interaction of S and B in several plants. However, to the best of our knowledge, interaction of boron with Sulphur in cotton was not reported by any authors. Therefore, the objective of this study is to investigate cotton yield and fiber quality properties when these nutrients are applied together.

## MATERIALS AND METHODS

**Soil Sampling and Analyses.** The experiment was carried out at the experimental field of the Faculty of Agriculture, Dicle University,



**TABLE 1**  
**Physio-chemical properties of experimental field.**

Characteristic	Value	Remarks
Textural class	--	Clay
pH	7.68	Moderately alkaline
EC (mScm <sup>-1</sup> )	0.66	Non saline
CaCO <sub>3</sub> (%)	11.70	Moderately calcareous
Organic Matter (%)	0.97	Low
P (mg kg <sup>-1</sup> )-(olsen)	5.18	Low
K (mg kg <sup>-1</sup> ) - (NH <sub>4</sub> -OAcckst.)	723.67	Medium
Ca (mg kg <sup>-1</sup> ) - (NH <sub>4</sub> -OAcckst.)	18517.67	High
Mg (mg kg <sup>-1</sup> ) - (NH <sub>4</sub> -OAcckst.)	1173.67	High
Na (mg kg <sup>-1</sup> ) - (NH <sub>4</sub> -OAcckst.)	423	Medium
Fe (mg kg <sup>-1</sup> ) - (DTPAcckst.)	1.21	Low
Mn (mg kg <sup>-1</sup> ) - (DTPAcckst.)	2.74	Medium
Zn (mg kg <sup>-1</sup> ) - (DTPAcckst.)	0.78	Medium
Cu (mg kg <sup>-1</sup> ) - (DTPAcckst.)	1.30	High
SO <sub>4</sub> -S (mg kg <sup>-1</sup> )	4.89	Medium
Bor (mg kg <sup>-1</sup> )	0.58	Low

Diyarbakir, Turkey between 2013 and 2014. Composite soil samples were taken at 0-30 cm from the field at different locations in October, 2013. The soil samples were analyzed as described by Ryan et al. [17]. The SO<sub>4</sub>-S analysis was made as described Fox et al. [18], while soil boron content was established by hot water method of Dible et al. [19], which is a modified method of Berger and Troug [20]. The soil characteristics of the experiment field were presented in Table 1.

**Experimental Design and Growth Conditions.** Sulphur and boron doses were applied as treatments arranged in split block design with four replications. Main plots were treated with two doses of elemental S (0-1 t S ha<sup>-1</sup>) whereas subplots were applied with four boron levels (0, 2.5, 5 and 15 B ppm) as disodium octaborate tetrahydrate (Na<sub>2</sub>B<sub>8</sub>O<sub>13</sub>·4H<sub>2</sub>O, 20.9 % B). S applications were broadcast and incorporated prior to planting with basal fertilizer as 20-20-0 compound fertilizer (0.35 t ha<sup>-1</sup>). B doses were solved in sufficient water and sprayed on the soil before sowing. After the application of B, the B doses were mechanically incorporated into the soil. The incomplete nitrogen was completed using ammonium nitrate (33%) as 0.30 t ha<sup>-1</sup> prior to the first irrigation. Furrow irrigation was adopted as an irrigation method, and this irrigation was applied when needed. Plots were formed 10 m long and 5.6 m wide consisting of 8 rows with 70 cm spacing. Over-seeded plots were thinned to one plant with 20 cm of spacing. Stoneville 468 (ST 468) was used as the variety of seed cotton. The standard plant protection management practices were used together with

agronomic practices employed for the crop cultivation.

**Cotton Lint Analyses.** At maturity, two middle rows falling into area which is the outer rows of each plot with one meter away from each plot's edge were harvested by hand. Samples taken from each plot's harvest were weighted and seed cotton yields were calculated. The seed cotton yields were ginned in a roller gin and the gin turnout was calculated. Lint quality properties; fiber fineness (mic), fiber length (mm), uniformity index (%), fiber strength (g/tex), maturity (%), elongation (%) and short fiber (%) were measured by HVI (High Volume Instrument).

**Statistical Analysis.** Analysis of variance (ANOVA) was used to analyze the experimental data in Jump software. The means were compared by test of significance, LSD [21].

## RESULTS AND DISCUSSION

The seed cotton yield showed inconsistencies in 2013 and 2014 in terms of B applications (Table 2). The yield significantly differed in 2013 (P<0.01). The highest yield was obtained at 2.5 ppm. Similarly, significant differences were observed in gin turnout (GT) during both years depending on B treatments. The highest GT values were observed from no B application in 2013 and 2014. Our results showed no phytotoxic effect of B observed in cotton at 5 and 15 ppm. Contrary to our findings, Ahmed et al. [22] reported that the highest dry matter yield obtained by application of 3 kg B.

**TABLE 2**  
The effect of B and S applications on seed cotton yield, gin turnout, fiber fineness, fiber length and uniformity index by mean values

Applications/Years	Seed cotton yield (kg ha <sup>-1</sup> )		Gin turnout (%)		Fiber fineness (mic.)		Fiber length (mm)		Uniformity Index (%)	
	2013	2014	2013	2014	2013	2014	2013	2014	2013	2014
B1 (0 ppm)	3855ab	3918.9	43.72a	43.94a	4.80	4.93	27.95	28.43	80.85	81.34
B2 (2.5 ppm)	4007.5a	3902	43.13a	43.75a	4.68	4.74	27.69	28.12	80.09	80.55
B3 (5 ppm)	3790b	3799.5	39.00b	38.63b	4.53	4.74	27.94	28.36	80.63	81.50
B4 (15 ppm)	3556.3c	3988.9	36.97c	38.56b	4.80	4.88	27.72	28.24	81.33	81.21
LSD	19.45**	-	1.04**	1.54**	-	-	-	-	-	-
S1 (1000 kg ha <sup>-1</sup> )	3676.9b	3750.6b	38.13b	38.92b	4.73	4.85	27.62	28.02b	80.94	81.11
S2 (0 kg ha <sup>-1</sup> )	3927.5a	4054.1a	43.28a	43.52a	4.67	4.79	28.03	28.56a	80.50	81.19
LSD	13.75**	28.96*	0.74**	1.09**	-	-	-	-	-	-
<b>General Means</b>	3802.2	3902.3	40.71	41.22	4.70	4.82	27.83	28.29	80.72	81.15

Mean values with different letters in each column represent significant difference at the \*\* P < 0.01 and \*P < 0.05 level based on LSD test.

**TABLE 3**  
The effect of B and S applications on fiber strength, fiber maturity, fiber elongation and short fiber content by mean values

Applications/Years	Fiber Strength (g/tex)		Fiber maturity (%)		Fiber elongation (%)		Short fiber content (%)	
	2013	2014	2013	2014	2013	2014	2013	2014
B1 (0 ppm)	33.49	32.90	0.888a	0.879	6.24a	6.41	8.01	8.45
B2 (2.5 ppm)	33.01	33.35	0.869b	0.876	6.03b	6.01	8.69	8.98
B3 (5 ppm)	33.74	34.15	0.874b	0.876	5.94b	5.91	8.11	8.46
B4 (15 ppm)	33.29	32.75	0.873b	0.878	5.89b	6.08	8.13	8.36
LSD	-	-	0.010**	-	0.18**	-	-	-
S1 (1000 kg ha <sup>-1</sup> )	33.36	33.22	0.875	0.878	5.99	6.13	8.36	8.76
S2 (0 kg ha <sup>-1</sup> )	33.41	33.36	0.876	0.876	6.06	6.08	8.11	8.36
LSD	-	-	-	-	-	-	-	-
<b>General Means</b>	33.38	33.29	0.877	0.877	6.03	6.10	8.24	8.56

Mean values with different letters in each column represent significant difference at the \*\* P < 0.01 and \*P < 0.05 level based on LSD test.

ha<sup>-1</sup> (as Borax 10.8 % B) and application of 5 mg B kg<sup>-1</sup> or higher B doses in soil causes B toxicity symptoms in cotton.

The effect of B treatments on fiber maturity and on fiber elongation significantly differed in 2013 (Table 3). According to the results, increasing doses of B decreased fiber maturity and fiber elongation. The highest values were obtained at 0 ppm level as 0.888 % and 6.24 % for fiber maturity and for fiber elongation, respectively. The effect of B levels on the other parameters such as fiber fineness, fiber length, etc., was found insignificant S application significantly decreased seed cotton yield in 2013 and 2014. The highest seed cotton yields were obtained from the plots without S (0 kg ha<sup>-1</sup>) in both years. Our results cannot be compared to results of previous studies, since applied S doses in this study were different. However, Mullins [16] suggested that higher seed cotton yield was

obtained in the result of 224 kg S ha<sup>-1</sup> in coastal plain soil. Unlike this result, Görmüş [11] reported that 30 kg S ha<sup>-1</sup> application increased number of sympodial branches and boll weight and, therefore, seed cotton yield increased. Correspondingly, Makhdom et al. [23] and Mamatha [26] also suggested that the highest seed cotton yield in sandy soils was obtained with application of 50 kg S ha<sup>-1</sup>. Yin et al. [15] reported that from 8 to 9 % of lint yield increase could be obtained by the application of 22 or 34 kg S ha<sup>-1</sup>.

With regard to gin turnout, S application significantly decreased gin turnout in both years (P<0.01). Our result did not support that of Gobi and Vaiyapuri (2012), who showed that the application of 45 kg S + 10 kg Zn + 1.0 kg B ha<sup>-1</sup> increased gin turnout. Contrary to this, Yin et al. [15], Makhdom et al. [23] and Bukarlı [24] stated that sulphur applications (as elemental or gypsum)

did not change lint quality parameters. Davis [13] also reported that sulphur dioxide fumigation of cotton did not affect GT. The differences among the results can be explained by differences among S doses, along with soil properties.

## CONCLUSIONS

In this study, phytotoxic effects of B treatments were not observed in plots with or without S. This result may be explained by soil properties of the experimental area. Despite lack of phytotoxic symptoms of B, 5 mg B kg<sup>-1</sup>, B treatments showed significant effects on seed cotton yield, gin turnout, fiber maturity, and fiber elongation. However, the influence of B was uneven and inconsistent between years and among B dosages. Based on these results, it could be concluded that higher doses of B applications should be avoided for higher lint yield and fiber qualities. In terms of S application, the amount of S dose employed in this study significantly decreased seed cotton yield and gin turnout; however, it had no effect on other lint quality parameters. This result may be of particular importance to cotton growing soils with higher pH, which is required in applying higher doses of sulphur for optimum yields.

## ACKNOWLEDGEMENTS

The authors would like to express their gratitude to Dicle University Scientific Research Projects Coordination Office (DUBAP) for the dissertation research grant with project number 13-ZF-78. Also, the authors are thankful to the National Boron Research Institute (BOREN) for providing boron fertilizer (Etidot-67) free of charge.

## REFERENCES

- [1] Bogiani, J. C., Sampaio, T. F., Abreu-Junior, C. H. and Rosolem, C. A. (2014) Boron uptake and translocation in some cotton cultivars. *Plant Soil* 375:241–253.
- [2] Nable, R. O., Banuelos, G. S. and Paull, J. G. (1997) Boron toxicity. *Plant and Soil* 193: 181–198.
- [3] Goldberg, S. (1997) Reactions of boron with soils (Chapter 3). *Plant and Soil* 193: 35–48, 1997. 35.
- [4] Cristobal, C. J. J., Rexach, J. and González-Fontes A. (2008) Boron in plants: deficiency and toxicity. *J. Integrative Plant Biol.* 50:1247–1255.
- [5] Ahmed, N., Abid, M. and Ahmad, F. (2008) Boron toxicity in irrigated cotton (*Gossypium hirsutum* L.). *Pak. J. Bot.* 40(6): 2443-2452.
- [6] Rosolem, C. A. and Bogiani, J. C. (2011) Physiology of boron stress in cotton. p. 113-124. In: Oosterhuis, D.M., ed. *Stress physiology in cotton*. The Cotton Foundation, Cordova, TN, USA.
- [7] Rosolem, C. A. and Costa, A. (2000) Cotton growth and boron distribution in the plant as affected by a temporary deficiency of boron. *Journal of Plant Nutrition.* 23:6, 815-825.
- [8] Ahmed, N., Ahmad, W., Zia, M. H. and Malhi, S. S. (2013) Relationship of soil extractable and fertilizer boron to some soil properties, crop yields, and total boron in cotton and wheat plants on selected soils of Punjab, Pakistan. *Journal of Plant Nutrition* 36:3, 343-356.
- [9] Schrer, H. W. (2001) Sulphur in crop production -invited paper. *European Journal of Agronomy.* 14: 81–111.
- [10] Crusciol, C. A. C., Nascente, A. S., Soratto, R. P. and Rosolem C. A. (2012). Upland rice growth and mineral nutrition as affected by cultivars and Sulphur availability. *Soil Sci. Soc. Am. J.* 77:328–335.
- [11] Görmüş, Ö. (2014) Cotton yield response to sulphur as influenced by source and rate in Çukurova region, Turkey. *Süleyman Demirel Üniversitesi Ziraat Fakültesi Dergisi* 9 (1):68-76.
- [12] Ergle, D. R. and Eaton, F. M. (1951) Sulphur nutrition of cotton. *Plant Physiology.* Volume 26:4, 639-654.
- [13] Davis, C. R., Morgan G. W. and Howell, D. R. (1965) Sulphur dioxide fumigation of cotton and its effect on fiber quality. *Agronomy Journal.* 57(3):250-251.
- [14] Nasseem, M. G. and Nasrallah, A. K. (1981) The effect of sulphur on the response of cotton to urea under alkali soil conditions. *Plant and Soil* 62, 255-263.
- [15] Yin, X., Gwatymey, O., Main, C. and Johnson A. (2011). Effects of Sulphur application rates and foliar zinc fertilization on cotton lint yields and quality. *Agronomy Journal.* Volume 103 (6): 1794-1803.
- [16] Mullins, G. L. (1998) Cotton response to the rate and source of sulphur on a sandy coastal plain soil. *J. Prod. Agric.* 11:214–218.
- [17] Ryan, J., Estefan, G. and Rashid, A. (2001) *Soil and Plant Analysis Laboratory Manual*. International Center for Agricultural Research in the Dry Areas (ICARDA), Islamabad, Pakistan. 172p.
- [18] Fox, R. L., Olson, R. A. and Rhoades, H. F. (1964) Evaluating the sulphur status of soils



- by plants and soil tests. *Soil Sci. Soc. Am. Proc.* 28: 243-246.
- [19] Dible, W. T., Truog, E. and Berger, K. C. (1954) Boron determination in soils and plants. *Analytical Chemistry*. 26:2, 418-42.
- [20] Berger, K. C. and Truog E. (1939) Boron determination in soils and plants. *Ind. Eng. Chem. Anal. Ed.* 11:540-545.
- [21] Steel, R. G. D and Torrie J. H. (1980) Principles and procedures of statistics: A biometrical approach. 2nd. (Ed). McGraw Hill, New York, USA.
- [22] Ahmed, N. M., Abid, A., F. Ullah, M. A., Javid, Q. and Ali, M. A. (2011). Impact of boron fertilization on dry matter production and mineral constituent of irrigated cotton. *Pak. J. Bot.* 43(6): 2903-2910.
- [23] Makhdum, M. I., Malik, M. N. A., Chaudhry, F. I. and Din, U.S. (2001) Effects of gypsum as Sulphur fertilizer in cotton. *Int. J. Agri. Biol.*, Vol. 3: No:4, 375-377.
- [24] Bukarlı, M. N. (2007) Diyarbakır koşullarında kükürt uygulanmasının pamuğun verim ve kalite özelliklerine etkisi. Yüksek Lisans Tezi, Çukurova Üniversitesi Fen Bilimleri Enstitüsü, Adana, 79.
- [25] Gobi, R. and Vaiyapuri, V. (2012) Effect of Sulphur and micronutrients (zinc and boron) on growth, yield, attributes and quality of cotton. *International Journal of Current Research*. Vol. 4, Issue, 11, pp. 357-359.
- [26] Mamatha, N. (2007) Effect of sulphur and micronutrients (Iron and Zinc) on yield and quality of cotton in a vertisol, Master of Science (Agriculture), Dharwad University of Agricultural Sciences, College of Agriculture, India.

---

**Received:** 22.03.2016

**Accepted:** 09.09.2016

---

#### **CORRESPONDING AUTHOR**

**Firat Kurt**

MusAlparslan University,  
Department of Organic Agriculture,  
Vocational School,  
Karakopru-Mus, Turkey

e-mail: firat.kurt.usa@gmail.com

# CHARACTERISTICS OF PHOSPHORUS LOSSES DUE TO SURFACE RUNOFF IN A PEACH ORCHARD AND THE EFFECTS OF INTER-PLANTING WHITE CLOVER (*TRIFOLIUM REPENS* L.) ON FRUIT YIELD AND QUALITY

Zhi Guo<sup>1,2</sup>, Hong-jiang Liu<sup>1</sup>, Wei Zhou<sup>1</sup>, Liu-gen Chen<sup>1</sup>, Jian-chu Zheng<sup>1,\*</sup>

<sup>1</sup> Institute of Agricultural Resource and Environment, Jiangsu Academy of Agricultural Sciences, Nanjing 210014, P.R.China;

<sup>2</sup> Key Laboratory for Agricultural Environment, Ministry of Agriculture, Beijing 100081, P.R.China

## ABSTRACT

Within an orchard, in Taihu Lake Basin, China, which contained 12-year-old late-maturing peach trees (cultivar “Hujing”), during 2012–2014, different fertilizer application rates and management practices were applied. The effects of these treatments on soil phosphorus loss due to surface runoff, and peach fruit yield and quality, in the typical peach orchard, were investigated. In T1 (conventional fertilization practice), total phosphorus (TP) losses due to surface runoff were 1.88 and 1.80 kg·hm<sup>-2</sup>, for 2012–2013 and 2013–2014, respectively; these mainly occurred from the peach fruit setting stage to the peach fruit ripening stage. Compared with T1, T2 (reducing fertilization practice to 70% of conventional) significantly reduced the quantity of TP losses, but TP loss coefficients significantly increased by 8.01% and 9.64%. Inter-planting white clover (*Trifolium repens* L.) (T3), not only significantly reduced the TP losses, but also TP loss coefficients by surface runoff (by 23.95% and 29.87%, respectively). And, the peach fruit yield, individual fruit weight, the contents of soluble solids and vitamin C, appeared higher in T3 than T1, but the differences were not significant. Furthermore, T3 fruit had significantly higher reduced sugar content and ratios of soluble solids to titratable acid (9.14% and 7.31%, respectively).

## KEYWORDS:

peach orchard; phosphorus; *Trifolium repens* L.; Surface runoff; peach fruit yield; peach fruit quality

## INTRODUCTION

Phosphorus (P) is an essential macro-element for crop production; it plays an important role in plant physiological and metabolic processes, such as energy metabolism, the synthesis and decomposition

of organic compounds, and signal transduction, among others [1]. However, the amount of phosphorus input into agricultural fields is generally higher than the carrying capacity of the crops produced, which results in a surplus of phosphorus in the farmland ecosystems, leading to a phosphorus-rich soil tillage layer [2-3]. There is an increased risk of soil phosphorus loss from this tillage layer, resulting in agricultural phosphorus emissions; these can become one of the most important non-point pollution sources of phosphorus, and cause water eutrophication, for which phosphorus is often the main limiting factor [4-6]. The contribution of agricultural non-point pollution sources to phosphorus present in the waters of Taihu Lake Basin, China, was estimated to be approximately 15.1% and the rate of phosphorus loss from farmlands in the region was approximately 19.2% [7].

In recent years, a lot of research has focused on reducing the loss of soil nutrients and potential technology to control agricultural non-point source pollution. A “Reduce–Retain–Reuse–Restore” technology system (4R theory) was applied to control the agricultural non-point pollution in countryside at Longyan village, in the watersheds of Zhihugang river, a tributary of Taihu Lake, China [8-9]. Optimum water and soil conservation measures have been defined to control agricultural non-point source pollution in European and American countries [10]. Currently, the most widely used control technologies include the reduction of chemical fertilizer applications [11], balanced fertilization [12], a return to the application of crop straw [13], and the application of new types of fertilizers [14], among others. Previous studies suggest that balanced fertilization and the application of wheat straw can significantly reduce the total phosphorus losses due to surface runoff by 52%–61% and 65%–83%, respectively, from the slopes of maize crops with purple soil, in center of Sichuan Basin, China [12-13]. In addition, the soluble phosphorus concentrations in surface runoff

decreased by 7.1%–94.1% under the controlled application of fertilizers in peanut farmland on sloping fields [14].

Water-saving irrigation [15] and the application of soil amendments [16-17] were also found effective at controlling agricultural non-point source pollution. Qiao et al. [15] found that water-saving irrigation measures and controlled drainage significantly reduced soil nitrogen and phosphorus losses and increase the nutrients utilization efficiency in a paddy field. The application of soil amendments (aluminum hydroxide, limestone, gypsum, fly ash and calcium chloride, among others) significantly reduced available phosphorus and water soluble phosphorus concentrations in the soil, and the concentrations of total phosphorus and dissolved phosphorus in surface runoff, by 13.68%–45.02% and 16.05%–55.38%, respectively, in a phosphorus rich vegetable field [17].

With the development of the economy and society, cropping systems in China have changed and the planting area of fruit trees has gradually expanded. China is one of the largest peach production countries in the world. In 2012, it was estimated that the annual peach and nectarine cultivation area was  $7.72 \times 10^5$  hm<sup>2</sup> and accounted for 51.48% of the worldwide cultivation area [18]. The annual peach and nectarine yield was estimated at  $1.2 \times 10^7$  t in China, accounting for 57.05% of worldwide production [18]. Currently, excessive nutrient (nitrogen and phosphorus) inputs are universal in peach production, which might result in peach gummosis and the symptoms of weakening and aging of tree vitality [19-20]. Kong et al. [21] reported that, during 2006, phosphorus (P<sub>2</sub>O<sub>5</sub>) inputs reached 420.6 kg·hm<sup>-2</sup> in a peach orchard in Pinggu district, Beijing, China. The highest phosphorus inputs reported, of up to 1240.32 kg·hm<sup>-2</sup>, were in mountainous areas in mid-Shandong province (the main peach production regions in China) [22]. In fact, phosphorus inputs in these regions were much higher than the optimal phosphorus inputs for peach orchards (20–100 kg P<sub>2</sub>O<sub>5</sub>·hm<sup>-2</sup>) [23-24].

The high phosphorus inputs have ultimately resulted in widespread phosphorus surpluses, causing an increased risk of soil phosphorus losses directly into surrounding waters, by surface runoff [25]. According to some studies, the contribution rates of phosphorus emissions, caused by the large increase in production of economic crops (fruit trees and vegetables) in southern Jiangsu, within the Taihu Lake Basin, was about 60% [26-27]. Therefore, it is important to systematically study the characteristics of soil phosphorus losses by surface runoff and potential technologies to control runoff in the region.

Ground cover vegetation is an orchard

management pattern in which annual or perennial herbaceous plants are used as covering vegetation on the ground surface of orchards; it has been implemented in orchards across Europe, America, and Japan, and has ecological and economic benefits [28]. Recent studies have demonstrated that ground cover vegetation enhances soil fertility and improves soil structure [29-30], increases the number of soil microbes [31], improves the diversity and stability of the biological communities [29, 32], increases fruit yield, and improves fruit quality [33]. However, due to the potential long-term need for weeding, orchard management using ground cover vegetation has not been adopted widely, and, to date, it has been applied in <20% of the total fruit tree planting area in China [34].

Nevertheless, ground cover vegetation has been gradually applied as a possible approach to control agricultural non-point source pollution in China. Zhang et al. [35] reported that annual phosphorus losses due to surface runoff reached 3.13 kg·hm<sup>-2</sup> under conventional orchard management from a pear orchard in a dense river network plain of Zhejiang province, China. Planting ryegrass in the pear orchard significantly reduced the phosphorus losses, by 38.66% [35]. Yu et al. [36] also found that covering the ground with ryegrass, Chinese milk vetch, and spring vetch in a mountainous peach orchard significantly reduced phosphorus losses due to surface runoff, by 58.5%, 55.6%, and 30.1%, respectively. Further, ground cover with a grass treatment effectively reduced phosphorus concentrations in the surface runoff from a peach orchard in Zhushan bay, in the Taihu Lake watershed [37]. However, to date, limited information is available regarding the effects of inter-planting white clover (*Trifolium repens* L.) on peach fruit yield, fruit quality, and phosphorus losses due to surface runoff, in peach orchards around the Taihu Lake Basin, China.

In the present study, we conducted a two-year field plot experiment (2012–2014) on a typical peach orchard in Taihu Lake Basin, under natural rainfall conditions. The specific objectives of this study were to: (1) systematically investigate the annual inputs of phosphorus, nitrogen, and potassium in the peach orchard, under conventional fertilization practices and peach orchard management; and (2) determine the effects of using different fertilizer application rates and peach orchard management treatments (conventional fertilization practice versus: reducing fertilization application rates and inter-planting with white clover) on soil phosphorus losses due to surface runoff, and peach fruit yield and quality. The results of this study provide a scientific basis and

**TABLE 1**  
**The physical and chemical properties of the yellow soil in the peach orchard**

Soil layers (cm)	pH (H <sub>2</sub> O, 1:5)	Organic matter (g·kg <sup>-1</sup> )	Total nitrogen (g·kg <sup>-1</sup> )	Total phosphorus (g·kg <sup>-1</sup> )	Available nitrogen (mg·kg <sup>-1</sup> )	Available phosphorus (mg·kg <sup>-1</sup> )	Available potassium (mg·kg <sup>-1</sup> )
0~10	4.44	36.78	2.96	0.35	151.95	121.78	739.27
10~20	4.74	24.39	1.89	0.31	125.13	61.38	639.46

**TABLE 2**  
**Nutrient (nitrogen, phosphorus, and potassium) inputs applied to the peach orchard during the experiment (2012–2014)**

Experimental periods	Experimental treatments <sup>^</sup>	Nitrogen (N, kg·hm <sup>-2</sup> )	Phosphorus (P <sub>2</sub> O <sub>5</sub> , kg·hm <sup>-2</sup> )	Potassium (K <sub>2</sub> O, kg·hm <sup>-2</sup> )
2012–2013	T1	838.65	290.70	357.90
	T2	589.05	203.85	264.30
	T3	838.65	290.70	357.90
2013–2014	T1	853.95	213.00	299.40
	T2	610.80	153.45	234.30
	T3	853.95	213.00	299.40

<sup>^</sup>T1, conventional fertilization practice; T2, reduced fertilizer practice; and T3, inter-planting of white clover (*Trifolium repens* L.)

technological support for the source control of agricultural non-point source pollution in Taihu Lake Basin, China.

## MATERIAL AND METHODS

**Site description.** The experiment was conducted in Runyang village, Luoshe Town, Huishan District, Wuxi City, Jiangsu Province, China (31°37'N, 120°07'E) from October 2012 to October 2014. Peach trees are a major crop locally, grown using high fertilizer application rates. Runyang village has a subtropical marine climate with a strong seasonal cycle, in terms of temperature and precipitation. The majority of precipitation occurs from June to October. The average annual air temperature, sunshine hours, and frost-free days at the experimental site were 16°C, 2,000 h, and 230 d, respectively. And, annual precipitation levels were 1,100–1,200 mm during the experimental period. The soils were classified as yellow soil, with a partial sandy texture. The physical and chemical properties of the yellow soil are shown in Table 1. The peach varieties grown in the orchard were late-season maturing “Hujing” honey peach, with 12-year-old trees, arranged in 4 × 4 m grid spacing.

**Experimental design.** The experimental

design was a complete randomized block, with three replicates of three treatments that had different fertilizer application rates and peach orchard management measures: (T1) conventional fertilization practice, in which the standard amounts of organic and inorganic fertilizer used for local peach production were applied (Table 2); (T2) reducing fertilization practice, in which about 70% of the organic and inorganic fertilizers applied in T1 were applied (micro-nutrient fertilizer application rates and peach orchard management measures were the same as T1); and (T3) inter-planting white clover (*Trifolium repens* L.), in which white clover (*Trifolium repens* L.), which was suitable for the local climate conditions, was inter-planted (the fertilization practices and other peach orchard management practices were the same as T1). In T3, the white clover seeds were broadcast sown, at a rate of 120 kg·hm<sup>-2</sup> on 9 November 2012 and 5 November 2013.

From the start of the experiment (October 2012), the annual nutrient (nitrogen, phosphorus, and potassium) inputs to the peach orchard (Table 2) were monitored, including the fertilizer variety, the amount of fertilizer applied, and the fertilization periods. The concentrations of nitrogen, phosphorus and potassium in the fertilizers (mainly organic fertilizers) applied in the peach orchard were measured before fertilization [38]. During the

experimental period, the fertilizers applied in the peach orchard were mainly urea (N, 46%), compound fertilizer (N, 15%; P<sub>2</sub>O<sub>5</sub>, 15%; K<sub>2</sub>O, 15%), compound potassium fertilizer (N, 15%; P<sub>2</sub>O<sub>5</sub>, 7%; K<sub>2</sub>O, 30%), calcium magnesium potassium fertilizer (K<sub>2</sub>O, 2.18%), organic and inorganic compound fertilizer (N, 14%; P<sub>2</sub>O<sub>5</sub>, 3%; K<sub>2</sub>O, 3%), rapeseed cake fertilizer (N, 5.6%; P<sub>2</sub>O<sub>5</sub>, 1.35%; K<sub>2</sub>O, 1.1%), humic acid organic compound fertilizer (N, 120 g·L<sup>-1</sup>; P<sub>2</sub>O<sub>5</sub>, 80 g·L<sup>-1</sup>; K<sub>2</sub>O, 80 g·L<sup>-1</sup>), humic acid fertilizer (N, 10%; P<sub>2</sub>O<sub>5</sub>, 4%; K<sub>2</sub>O, 16%), and a mixture of human excrement and pigeon dung (N, 1.28 g·L<sup>-1</sup>; P<sub>2</sub>O<sub>5</sub>, 0.09 g·L<sup>-1</sup>; K<sub>2</sub>O, 0.38 g·L<sup>-1</sup>), among others.

According to the layout of the peach orchard, each experimental plot consisted of a row of three trees (3 trees, about 48 m<sup>2</sup>) (Figure 1A). To prevent soil moisture and nutrient exchange between the experimental plots, they were separated by 20-cm wide soil ridges, covered by double layers of plastic film, buried into the soil to about 60 cm depth (Figure 1A). A diversion channel (about 30 cm width) on one side of the experimental plot collected surface runoff (via diversion ditches), which flowed into a surface runoff collector and storage tank (30 × 30 × 20 cm; width × length × depth; stainless steel barrel; Figure 1B), installed at the end of each diversion channel. A diversion trough and diversion pipe (PVC pipe) was installed on either side of the surface runoff collector and storage tank. The surface runoff was discharged into a drainage ditch (which collected runoff from other experimental plots) and finally through a flow metering device system (Utility Model Patent, Patent No. ZL201520421554.9; consisted of foundation supports, a cofferdam, an intelligent water flow meter, stainless filter screen, and a cover plate; Figure 1C). The quantities of surface runoff were measured by the differences in the water flow meter dial readings before and after the intensive rainfall and surface runoff events.

**Sampling and analysis. Soil sampling.** Before the experiment, soil samples at different soil layers (0–10 and 10–20 cm) were collected from the peach orchard; the sampling points were randomly selected at a distance of 100–120 cm from the peach tree trunks. The soil pH was measured with an *in situ* pH meter (PHS-3C, Dapu Scientific Instrument Co., Ltd., Shanghai, China) [39]. The organic matter content, total nitrogen, total phosphorus, available phosphorus, and available potassium were measured using the procedures described by Bao [38].

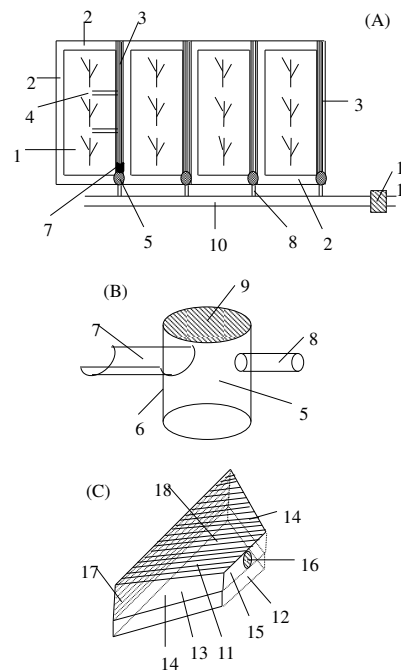


**FIGURE 1**

**The layout of experimental plots in the peach orchard (Panel A); the structure of the surface runoff collector (Panel B); and the structure of the flow metering device system (Panel C). Key: 1, experimental plot; 2, ridges surrounding the experimental plot; 3, diversion channel; 4, diversion ditch; 5, surface runoff collector; 6, surface runoff collector and storage tank; 7, diversion trough; 8, diversion pipe; 9, cover plate of the surface runoff collector and storage tank; 10, drainage ditch; and 11, the flow metering device (including: 12, its foundation supports; 13, a cofferdam; 14, cofferdam side wall; 15, cofferdam front wall; 16, intelligent water flow meter; 17, stainless filter screen; and 18, cover plate)**

**Surface runoff.** The amount of rainfall from each natural rainfall event was recorded. Surface runoff samples were collected in 100 mL polyethylene sampling bottles for chemical analysis. The samples were frozen on collection and then analyzed for total phosphorus (TP), according to standard methods (National Environmental Bureau, 1996); unfiltered samples were digested and analyzed with an automatic continuous flow injection analyzer (SKALAR San<sup>++</sup>, Breda, the Netherlands).

**Peach fruit yield and the main peach fruit quality parameters.** The peaches produced were individually harvested; all the fruit produced in each experimental unit were weighed and their number recorded. The average weight of the peaches was



determined for each experimental unit. A subsample of 15 representative fruit per experimental unit was processed in the laboratory for the following quality parameters: total soluble solids content, reduced sugar content, titratable acid content, vitamin C content, and the ratio of soluble solids to titratable acid. Total soluble solids content of the peach fruit juices (°Brix) was assessed using a digital hand refractometer (PAL-1, ATAGO Co. Ltd., Tokyo, Japan), while vitamin C content ( $\text{mg}\cdot 100\text{g}^{-1}$  FW) and reduced sugar content (%) were measured according to Li [40], using a 2,6-dichloroindophenol titration and 3,5-dinitrosalicylic acid, respectively. The titratable acid content (%) was determined according to Gao [41], using the sodium hydroxide titration method. The ratio of soluble solids to titratable acid was calculated from their respective measurements, as a measure of the peach fruit maturity index. The TP content of the peach fruit was also analyzed; the fruit were cut into slices, dried to a constant weight and then digested with  $\text{H}_2\text{SO}_4\text{-H}_2\text{O}_2$ . The concentration of TP in the digestate was determined using an automatic continuous flow injection analyzer (SKALAR San<sup>++</sup>, Breda, the Netherland).

**Statistical analyzes.** The quantity of TP loss by surface runoff during the peach fruit growth period was calculated as follows:

$$Q = \sum_{i=1}^n C_i \times V_i \times 10^{-3}$$

, where  $Q$  is the quantity of TP loss by surface runoff subjected to different fertilizer application rates and peach orchard management measures during the peach fruit growth period (T1–T3,  $\text{kg}\cdot\text{hm}^{-2}$ );  $C_i$  is the average TP concentration of surface runoff water in each runoff event ( $\text{mg}\cdot\text{L}^{-1}$ );  $V_i$  is the volume of surface runoff water in each runoff event ( $\text{m}^3\cdot\text{hm}^{-2}$ ).

The surface runoff coefficient of phosphorus (%) was calculated as follows:

$$P_i = \frac{Q}{Q_p} \times 100\%$$

, where  $P_i$  is the surface runoff coefficient of phosphorus (%);  $Q$  is the quantity of TP loss by surface runoff subjected to different fertilizer application rates and peach orchard management measures during the peach fruit growth period (T1–T3,  $\text{kg}\cdot\text{hm}^{-2}$ );  $Q_p$  is the quantity of phosphorus fertilizer application under different fertilizer application rates and peach orchard management measures during the peach fruit growth period (T1–T3,  $\text{kg}\cdot\text{hm}^{-2}$ ).

Results are presented as mean  $\pm$  standard error (S.E.), of at least three replicates. Statistical analyses

were performed using SPSS 13.0 and Excel 2010 for Windows. Means were tested by least significant difference, where  $P < 0.05$  was considered significant (LSD 0.05).

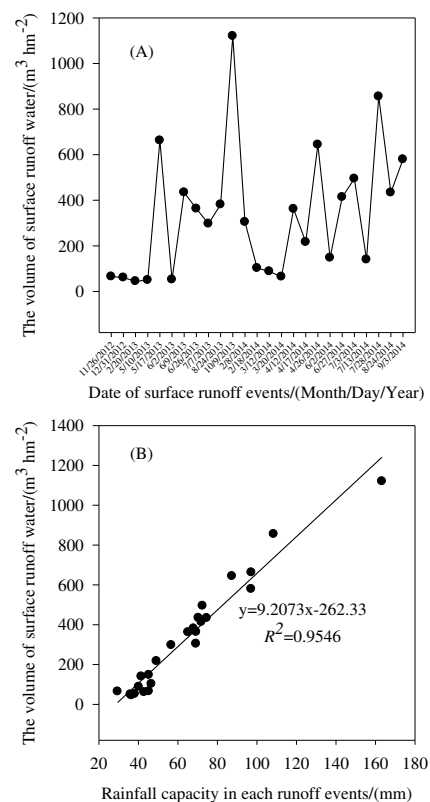


**FIGURE 2**  
Surface runoff from the peach orchard (Panel A); and correlation between surface runoff and rainfall levels (Panel B)

## RESULTS

**Surface runoff and rainfall levels.** Rainfall is the main driver of surface runoff and high levels of surface runoff are one of the most important causes of high soil nutrient losses in farmlands. During the first year of monitoring (2012–2013), there were 11 surface runoff events during the peach fruit growth period, which corresponded to the 11 rainfall events, with rainfall levels of 45.3, 42.9, 36.5, 36.0, 97.2, 38.2, 70.4, 69.3, 56.7, 68.0, and 163.3 mm, respectively. The volumes of surface runoff from these events were 65.55, 61.05, 45.00, 50.10, 662.40, 52.20, 434.40, 363.30, 297.30, 381.45, and 1120.35  $\text{m}^3\cdot\text{hm}^{-2}$  (Figure 2A). The total volume of surface runoff was 3533.10  $\text{m}^3\cdot\text{hm}^{-2}$  during the first year of monitoring (2012–2013).

During the second year of monitoring (2013–2014), there were 14 surface runoff events during the peach fruit growth period, which corresponded to the

14 rainfall events, with rainfall levels of 69.2, 46.6, 40.2, 29.5, 65.2, 49.2, 87.4, 45.3, 71.9, 72.5, 41.5, 108.5, 74.6, and 97.1 mm, respectively. The corresponding volumes of surface runoff were 304.65, 102.45, 88.35, 64.80, 361.95, 216.90, 644.10, 147.75, 413.85, 495.00, 139.80, 855.15, 433.50, and 579.30 m<sup>3</sup>·hm<sup>-2</sup> (Figure 2A). The total volume of surface runoff was 4847.55 m<sup>3</sup>·hm<sup>-2</sup> during the second year of monitoring (2013–2014).

The correlation analysis shows that there was a significant positive linear correlation between the surface runoff and rainfall levels during the peach fruit growth periods ( $R^2 = 0.9546$ ; Figure 2B).

**Soil phosphorus losses.** During the first year of experimental monitoring (2012–2013), total phosphorus (TP) concentrations in surface runoff decreased during the peach growth period (Figure 3A); the peak value occurred during the surface runoff event on 26 December 2012, which was significantly higher than the other surface runoff events. Under conventional fertilization practices (T1), the TP concentrations in the surface runoff peaked at 1.65 mg·L<sup>-1</sup>. The average TP concentrations in the surface runoff, across all events during the first year of experimental monitoring (2012–2013) were significantly higher (by 33.52% and 35.34%, respectively) in T1 than in T2 and T3. Another smaller peak in TP concentrations in the

surface runoff was recorded during the 7 July 2013 event (Figure 3A); this mainly occurred because the rainfall event immediately followed the application of topdressing fertilizer on 5 July 2013.

During the second year of experimental monitoring (2013–2014), TP concentrations in the surface runoff generally also decreased during the peach growth period; peak values were measured during the overwintering and fruit expanding and core-hardening peach stages (Figure 3B). The TP concentration measured in the first peak value (T1; 0.58 mg·L<sup>-1</sup>), during the surface runoff event on 8 February 2014, was significantly higher than the concentrations measured during other surface runoff events across the second year of experimental monitoring (2013–2014). The second peak value mainly occurred as a result of intensive topdressing fertilizer application during the peach fruit expanding and core-hardening stage. TP concentrations (T1; 0.62 mg·L<sup>-1</sup>) in the surface runoff event during 27 June 2014 were significantly higher than those measured in the other surface runoff events during the second year of experimental monitoring (2013–2014). The average TP concentration in the surface runoff for all the surface runoff events during the second year of experimental monitoring (2013–2014) was significantly higher in T1 (by 26.24% and 45.09%, respectively) than in T2 and T3 treatments.

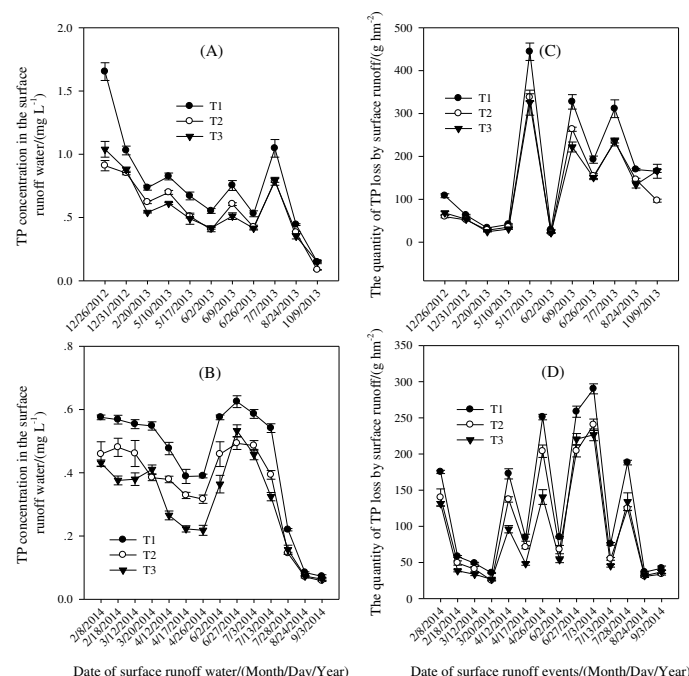


**FIGURE 3**

**Total phosphorus (TP) concentrations in the surface runoff (Panel A, Panel B); and TP losses from the peach orchard due to surface runoff (Panel C, Panel D), for each treatment: T1, conventional fertilization practice; T2, reduced fertilizer practice; and T3, inter-planting of white clover (*Trifolium repens* L.).**

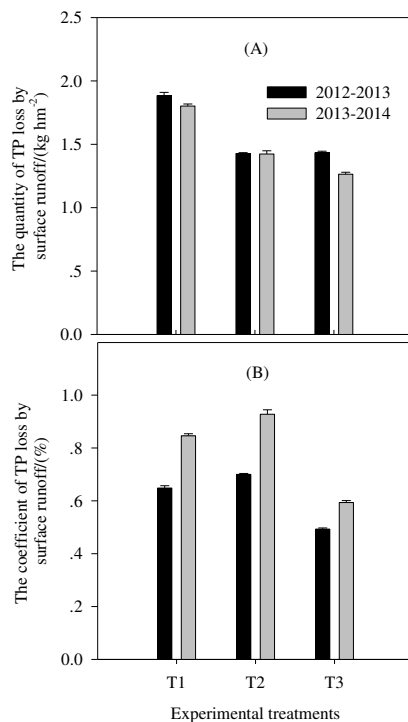


**FIGURE 4**

**Total phosphorus (TP) losses (Panel A) and coefficients of TP losses by surface runoff (Panel B), for each treatment: T1, conventional fertilization practice; T2, reduced fertilizer practice; and T3, inter-planting of white clover (*Trifolium repens* L.)**

The TP losses due to surface runoff mainly occurred from the peach fruit setting stage to the peach fruit ripening stage (Figures 3C, D). In T1, TP losses during the surface runoff events of 17 May 2013, 9 June 2013, 26 June 2013, and 7 July 2013 accounted for 67.67% of that lost during the whole of the first year's peach fruit growth period (2012–2013); and TP losses during the surface runoff events of 26 April 2014, 27 June 2014, 3 July 2014, and 28 July 2014 accounted for 54.83% of that lost during the whole of the second year's peach fruit growth period (2013–2014).

During the first year of experimental monitoring (2012–2013), the TP losses due to surface runoff were 1.88 kg·hm<sup>-2</sup> in T1 (Figure 4A). Compared with T1, T2 and T3 had significantly lower TP losses, by 24.26% and 23.95%, respectively. During the second year of experimental monitoring (2013–2014), the TP losses by surface runoff reached 1.80 kg·hm<sup>-2</sup> in T1 (Figure 4A); in T2 and T3, significantly lower TP losses, by 21.01% and 29.87%, respectively, were recorded.

The coefficients of TP losses by surface runoff from the peach orchard reached 0.65% in T1 during the first year of experimental monitoring (2012–2013). Compared with T1, T3 had a significantly lower correlation coefficient, by 23.95%, but T2 had

significantly higher one, by 8.01%. During the second year of experimental monitoring (2013–2014), the coefficients of TP losses by surface runoff reached 0.85% in T1. Compared with T1, T3 had a significantly lower coefficient, by 29.87%, but T2 was significantly higher, by 9.64%.

**Peach fruit yield.** Peach yield directly affects its economic value. The weights of individual peach fruit are also an important index of peach fruit appearance and quality and size is used to grade them and assess their economic value. Thus weight and size may be better indices to reflect economic value than yield. The average peach fruit yield per tree and weights of individual fruit were 62.38 kg·Plant<sup>-1</sup> and 227.76 g, respectively, in T1. Compared with T1, T2 appeared to have lower individual fruit weights, by 4.13%, but there was no significant difference; however, the yield was significantly lower, by 7.32%. T3 increased the individual fruit weight and the peach fruit yield by 1.54% and 2.04%, respectively, but no significant difference was found between these treatments.

**Peach fruit quality.** The soluble solids and titratable acid contents of peach fruit are important indicators of their intrinsic quality; they are positively and negatively, respectively, correlated with the flavor of the fruit. In T1, the mean soluble solids and titratable acid contents were 14.02% and 0.37%, respectively (Table 3). Compared with T1, T2 fruit had significantly lower soluble solids and reduced sugar contents, by 6.54% and 8.09%, respectively. The fruit in T2 also had slightly (but not significantly) higher titratable acid contents, by 4.81%. The titratable acid content appeared 5.84% lower, and soluble solids content appeared 1.19% higher in T3, compared to T1, but the differences were not significant. T3 fruit did have significantly higher (than T1) reduced sugar contents, by 9.14%. The ratio of soluble solids to titratable acid is the fruit quality parameter most closely related to consumer acceptance of peaches, where an increase in the ratio indicates an improvement in the flavor of the fruit. In T1, the ratio of soluble solids to titratable acid in the fruit was 38.01 (Table 3). Compared with T1, T2 fruit had a significantly lower ratio, by 10.97%, and T3 fruit had a significantly higher ratio, by 7.31%. Vitamin C content is also an important nutritional quality parameter of peach fruit. In T1, the mean vitamin C content of the fruit was 6.47 mg·100 g<sup>-1</sup> FW (Table 3). Compared with T1, T2 fruit had significantly lower vitamin C content, by 9.33%. Although the fruit in T3 appeared to have higher vitamin C content, by 3.17%, compared to T1 fruit, there was no significant difference.

**TABLE 3**  
**Effects of each treatment on the peach fruit quality parameters**

Experimental treatments <sup>^</sup>	Peach fruit quality parameters					Ratio of soluble solid to titrable acid
	Soluble content (%)	solid	Reduced sugar content (%)	Titrable acid content (%)	Vitamin C content (mg·100g <sup>-1</sup> FW)	
T1	14.02±0.19a		1.81±0.04b	0.37±0.01ab	6.47±0.13a	38.01±1.32b
T2	13.10±0.15b		1.67±0.02c	0.39±0.01a	5.87±0.07b	33.84±0.67c
T3	14.18±0.18a		1.98±0.03a	0.35±0.01b	6.68±0.24a	40.79±0.91a

<sup>^</sup>T1, conventional fertilization practice; T2, reduced fertilizer practice; and T3, inter-planting of white clover (*Trifolium repens* L.)

Note: Data are the mean ± standard error from at least three replicates. Different letters in a column indicate significant differences between the treatments at  $P < 0.05$

## DISCUSSION

According to their characteristics of growth, approximately 0.5 kg of nitrogen (N), 0.2 kg of phosphorus (P<sub>2</sub>O<sub>5</sub>), and 0.6–0.7 kg of potassium (K<sub>2</sub>O) are required to produce 100 kg of fresh peach fruit [42–44]. Considering the yields of fruit in this study, the optimized nutrient requirements above represent 193.97–195.94 kg N·hm<sup>-2</sup>, 77.59–78.38 kg P<sub>2</sub>O<sub>5</sub>·hm<sup>-2</sup>, and 232.76–274.31 kg K<sub>2</sub>O·hm<sup>-2</sup> for the peach orchard in Taihu Lake Basin, China. However, the actual annual nutrient inputs to the peach orchard were 838.65–853.95 kg N·hm<sup>-2</sup>, 213.00–290.70 kg P<sub>2</sub>O<sub>5</sub>·hm<sup>-2</sup>, and 299.40–357.90 kg K<sub>2</sub>O·hm<sup>-2</sup>. Thus, the actual nitrogen inputs were over four times higher than the optimized nitrogen requirements, phosphorus inputs were over three times higher than the optimized phosphorus requirements, and the potassium inputs were also excessive. Furthermore, according to the fertilization criteria of peach orchards [21], the nitrogen and phosphorus nutrient inputs were in the ultra-high input category (>400 kg N·hm<sup>-2</sup>, >200 kg P<sub>2</sub>O<sub>5</sub>·hm<sup>-2</sup>), and the potassium inputs were in the high input level category (250–500 kg K<sub>2</sub>O·hm<sup>-2</sup>).

The continuously excessive nutrient inputs could not only have led to a decline in the fertilizer utilization efficiency and decrease in the production efficiency of the peach orchard, but could also have adversely affected the soil quality and surrounding water quality of the peach orchard. A previous study found a significant positive correlation between phosphorus inputs and the soil phosphorus load in a peach orchard, and showed that excessive fertilizer application was the main reason for this [45].

Lu et al. [46] investigated the characteristics of phosphorus fertilizer application rates, surpluses, and phosphorus loads in different regions of China, using a nutrient balance method; the highest soil

phosphorus surplus was found in the peach orchards of Hebei and Shandong provinces, reaching 531.7 and 507.8 kg·hm<sup>-2</sup>, respectively, followed by Beijing city and Henan province, with levels of 359.6 and 327.5 kg·hm<sup>-2</sup>, respectively. They found the soil phosphorus surplus in peach orchards of Jiangsu province to only be 237.2 kg·hm<sup>-2</sup>, lower than the national average phosphorus surplus of peach orchards in China (285.3 kg·hm<sup>-2</sup>) [46]. In our study, the dry and wet deposition of phosphorus and leaching of phosphorus were not considered in our phosphorus balance calculation. In addition, the phosphorus in peach leaves, rotting fruit and thinning fruit from the peach orchard remained in the peach orchard, which was not considered. However, we calculated that phosphorus absorption through the peach fruit harvest was 18.48–18.67 kg P<sub>2</sub>O<sub>5</sub>·hm<sup>-2</sup> (data not shown), and the annual phosphorus surplus in the peach orchard reached about 192.72–270.15 kg P<sub>2</sub>O<sub>5</sub>·hm<sup>-2</sup>.

The soil phosphorus surplus may cause the serious waste of phosphorus resources. It also reduces the potential for the phosphorus to be retained as reactive phosphorus in the solid phase within the soil, directly resulting in an increase in the proportion of reactive phosphorus in the liquid phase; although this may improve (to an extent) the potential soil phosphorus supply, more seriously, it could significantly increase the risk of soil phosphorus losses into the surrounding water; such losses could become one of the most important non-point pollution sources causing eutrophication [47–48]. In fact, soil phosphorus losses mainly occurred due to surface runoff and leaching. As most soils have a strong phosphorus fixation capacity, previously, surface runoff was considered to be the major source of non-point phosphorus pollution into water bodies, with a rare to negligible contribution of soil leaching [25].

Reducing fertilizer application rates was one of

the effective technical approaches to control the loss of soil nutrients from farmland [8]. In this study, although reducing nitrogen, phosphorus, and potassium inputs, by 29.12%, 28.92%, and 23.95%, respectively, significantly reduced the phosphorus emissions (Figure 4), the yield (Figure 5) and quality (Table 3) of the peach fruit also decreased. Yan et al. [49] optimized their fertilization rates by applying a regional fertilization decision-making system, based on GoogleMap and WebGIS for peach orchards; in their study, the chemical fertilizer application rates were significantly decreased, by 45.2% ( $P_2O_5$ ) and 21.0% ( $K_2O$ ), but the organic fertilizer application rates were significantly increased by 34.4% ( $P_2O_5$ ). Considering the total nutrients input, the phosphorus and potassium nutrient inputs from their optimized fertilization rates were 2.7% and 9.6% lower, respectively [49]. Compared with their traditional fertilization practice, applying the optimized fertilization rates increased the peach fruit yield by 27.5%, and significantly improved fruit quality. The main reason for the differences observed between the results of Yan et al. [49] and our study may be that Yan et al. [49] significantly reduced the nitrogen inputs, by adjusting the input structure of the organic and inorganic fertilizers. That is, they did not significantly reduce the phosphorus and potassium inputs in their peach orchard, while the nitrogen, phosphorus, and potassium inputs were decreased synchronously in this study. However, the phosphorus inputs from their optimum fertilization rate were still in the ultra-high input category ( $331 \text{ kg}\cdot\text{hm}^{-2}$ ) [49].

From the perspective of the potential risk to the water environment, phosphorus is generally the main limiting factor for eutrophication [5]. Therefore, the systematic control of phosphorus inputs and phosphorus emissions might have more practical significance for the establishment of a healthy and sustainable production system in the intensively managed peach orchard. Nutrient management in peach orchards, soil nutrients status, the objective yield of peach fruit, and the status of peach tree growth should all be considered [50-51]; within these, the soil nutrients surplus and load, environmental effects of soil nutrients loss, and the economic benefits of peach production are especially important. A balance needs to be found to coordinate high yields and quality of peach fruit, with rational nutrient inputs, and sustainable production in peach orchards.

Previous research has shown that inter-planting grasses could not only improve soil fertility, but also reduce the loss of soil phosphorus in orchards [52]. In this study, inter-planting white clover significantly reduced the phosphorus losses, and the coefficient of soil phosphorus losses by surface runoff, from the peach orchard (Figure 4); these

results were consistent with those of Zhang et al. [35]. Inter-planting white clover may have significantly reduced soil and sediment erosion by surface runoff, which is the main way phosphorus is lost from orchards [35-36]. Meanwhile, vegetation coverage was also identified as an important factor that may reduce the loss of soil nutrients themselves through surface runoff [53-54]; inter-planting white clover likely significantly improved the vegetation cover of the surface soil, which may have contributed to the lower levels of soil phosphorus loss due to surface runoff in the peach orchard. The specific mechanism needs to be explored further.

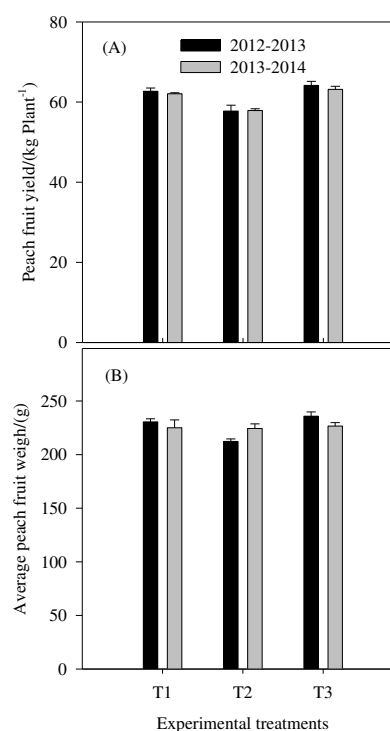


**FIGURE 5**  
**Mean peach fruit yields (Panel A) and weights (Panel B) for each treatment: T1, conventional fertilization practice; T2, reduced fertilizer practice; and T3, inter-planting of white clover (*Trifolium repens* L.)**

Inter-planting white clover not only increased the yield (Figure 5), but also improved the quality of the peach fruit (Table 3) in this study, consistent with previous studies [55-57]. In these, the main reasons for the positive effects of inter-planting grasses, like white clover, in peach orchards, have been considered, including: improvement of the surface microclimate environment [58-60]; promoting the photosynthetic ability of peach leaves [57, 61]; increasing the number of soil microbes [62-65]; improving the diversity and stability of the biological communities [32]; and increasing the activities of soil catalase, urease and alkaline phosphatase [29, 66]. These studies, together with the present

research, indicate that inter-planting white clover in peach orchards not only reduces soil phosphorus emissions, but increases peach fruit yields and quality, providing a sustainable technology for peach fruit production in Taihu Lake Basin.

## ACKNOWLEDGEMENTS

This work was supported by grants from the Jiangsu Agriculture Science and Technology Innovation Fund (JASTIF), P. R. China [CX(12)5053], the Open Fund of Key Laboratory for Agricultural Environment, Ministry of Agriculture, P. R. China [KLAE201307], and the National Key Technology Support Program, P. R. China [2012BAD14B12].

## REFERENCES

- [1] Wu, W. H. (2003) Plant Physiology. Science Press, Beijing, China.
- [2] Lu, R. K. (1998) Principle and Apply Fertilizer of Soil-Plant Nutrition. Chemical Industry Press, Beijing, China.
- [3] Xu, Q., Yang L. Z., and Dong Y. H. (1998) Paddy Soil Ecosystem of China. China Agricultural Press, Beijing, China.
- [4] Boesch, D. F., Brinsfield, R. B., and Magnien, R. E. (2000) Chesapeake bay eutrophication: scientific understanding, ecosystem restoration, and challenges for agriculture. *J. Environ. Qual.*, 30, 303-320.
- [5] Sharpley, A. N., Daniel, T., Sims, T., Lemunyon, J., Stevens, R., and Parry, R. (2003) Agricultural Phosphorus and Eutrophication. Second edition. US Department of Agriculture, Agricultural Research Service, ARS 149.
- [6] Tabuchi, T. (2005) Consideration of Water Quality Conservation of Lakes. Gihodoshuppan Co. Ltd., Tokyo, Japan.
- [7] Jin, X. C., Ye, C., Yan, C. Z., Ren, B. X., Zhang, Y. C., Wang, X. Q., and Wang, Y. B. (1999) Comprehensive treatment plan for key-polluted regions of Taihu Lake. *Res. Environ. Sci.*, 12, 1-5.
- [8] Xue, L. H., Yang, L. Z., Shi, W. M., and Wang, S. Q. (2013) Reduce-retain-reuse-restore technology for controlling the agricultural non-point pollution in countryside in China: source reduction technology. *J. Agro-Environ. Sci.*, 32, 881-888.
- [9] Yang, L. Z., Shi, W. M., Xue, L. H., Song, X. F., Wang, S. Q., and Chang, Z. Z. (2013) Reduce-retain-reuse-restore technology for controlling the agricultural non-point pollution in countryside in China: general countermeasures and technologies. *J. Agro-Environ. Sci.*, 35, 1-8.
- [10] Sharpley, A., and Tunney, H. (2000) Phosphorus research strategies to meet agricultural and environmental challenges of the 21st century. *J. Environ. Qual.*, 29, 176-181.
- [11] Zhang, G., Wang, D. J., and Chen, X. M. (2008) Effects of reduced fertilizer application on environmental quality of paddy field. *Chin. J. Eco-Agri.*, 16, 327-330.
- [12] Xu, T. P., Zhu, B., Kuang, F. H., Wang, T., and Wu, Y. F. (2006a) Effects of balanced fertilization on phosphorus loss by runoff from slope cropland in purple soils. *J. Agro-Environ. Sci.*, 25, 1055-1059.
- [13] Xu, T. P., Zhu, B., Wang, T., and Kuang, F. H. (2006b) Effects of returned straw on nutrient loss from slope cropland of purple soil. *J. Soil Water Conserv.*, 20, 30-36.
- [14] Wang, Y. H., Qiu, X. K., Hu, G. Q., and Dong, Y. J. (2011) Effect of controlled release fertilizer on nitrogen and phosphorus runoff losses from farmland in slope field. *J. Soil Water Conserv.*, 25, 10-14.
- [15] Qiao, X., Shao, D. G., Liu, H. H., and Yuan, J. G. (2011) Study on the moving and transforming law of N and P under water-saving irrigation and controlled drainage. *Shuili Xuebao*, 42, 862-867.
- [16] Brauer, D., Aiken, G. E., Pote, H., Livingston, S. J., Norton, L. D., Way, T. R., and Edwards, J. H. (2005) Amendment effects on soil test phosphorus. *J. Environ. Qual.*, 34, 1682-1686.
- [17] Ma, W. Z., and Zhang, M. K. (2012) Effects of amendments to reduce runoff loss of phosphorus and nitrogen from a vegetable soil with high test phosphorus. *J. Soil Water Conserv.*, 26, 22-27.
- [18] FAOSTAT, <http://faostat.fao.org/default.aspx>.
- [19] Lu, S. C. (2009) Characteristics of Nutrients Input and the Influences on Soil Quality in Intensive Orchards of China. A Doctoral Dissertation, China Agricultural University, Beijing, China.
- [20] Zhang, Y., Li, X. J., Qu, J. L., Li, L. G., and Yang, J. M. (2010) Studies on the pathogen of peach gummosis in Shandong province. *J. Fruit Sci.*, 27, 965-968.
- [21] Kong, X. Y., Li, Y. P., Wang, S. T., Liang, J. F., Jia, X. H., Chen, Q., Zhang, Z. G., He, Y. D., Hao, H. M., Liu, B. Y., and Liu, Y. R. (2010) The effect of nutrient input on the soil nutrient content and peach fruit quality in pinggu peach orchards of beijin suburb. *Chin. J. Soil Sci.*, 41, 355-361.
- [22] Li, G. M. (2011) Evaluation of Soil Nutrient Status in Peach Orchards of Shandong and Studies on Peach Fertilizer Demand

- Characteristics. A Master Dissertation, Shandong Agricultural University, Taian, China.
- [23] Liu, X. S. (2003) Study on the Calculation of Fertilization and Rational Agriculture. Southeast University Press, Nanjing, China.
- [24] Meng, Y. H., Li, F. G., Jia, X. H., He, Y. D., Hao, H. M., Zhang, Z. G., and Chen, Q. (2006) Current situation and problem of conventional nutrient management in peach orchards of Pinggu. *Soil Fert. Sci. China*, 6, 54-56, 61.
- [25] Sharpley, A. N., and Menzer, R. G. (1987) The impact of soil and fertilizer phosphorus on the environment. *Adv. Agron.*, 41, 297-324.
- [26] Zhang, W. L., Wu, S. H., Ji, H. J., and Kolbe, H. (2004a) Estimation of agricultural non-point source pollution in China and the alleviating strategies I. Estimation of agricultural non-point source pollution in China in early 21 century. *Sci. Agri. Sin.*, 37, 1008-1017.
- [27] Zhang, W. L., Xu A. G., Ji, H. J., Kolbe, H. (2004b) Estimation of agricultural non-point source pollution in China and the alleviating strategies III. A review of policies and practices for agricultural non-point source pollution control in China. *Sci. Agri. Sin.*, 37, 1026-1033.
- [28] Greenham, D. W. P. (1995) The environment of the fruit tree managing fruit soils. *HortScience*, 12, 25-31.
- [29] Xi, Z. M., Yue, T. X., Zhang, J., Cheng, J. M., and Li, H. (2011) Relationship between soil biological characteristics and nutrient content under intercropping system of vineyard in northwestern semiarid area. *Sci. Agri. Sin.*, 44, 2310-2317.
- [30] Wang, Y. J., Li, T. C., Zhang, D. Y., Jia, M. L., Li, H. K., and Cao, W. D. (2013) Effects of intercropping white clover on soil aggregates and soil organic carbon of aggregates in apple-white clover intercropping system. *Acta Agrestia Sin.*, 21, 485-493.
- [31] He, L. L., Yang, H. M., Zhong, Z. K., Gong, P. T., Liu, Y. X., Lv, H. H., and Yang, S. M. (2013) Effects of sod culture on soil nutrient characteristics and bacterial community in peach orchard. *Chin. Agri. Sci. Bull.*, 29, 179-183.
- [32] Jiang, J. X., Wan, N. F., Ji, X. Y., and Dan, J. G. (2011) Diversity and stability of arthropod community in peach orchard under effects of ground cover vegetation. *Chin. J. Appl. Ecol.*, 22, 2303-2308.
- [33] Mao, P. C., Meng, L., Zhang, G. F., Hou, F. Q., Zhang, Z. G., and Cui, T. H. (2006) Effect of planting white clover as a cover crop on the microclimate of a peach orchard and the peach quality. *Acta Agrestia Sin.*, 14, 360-364.
- [34] Lv, D. G., Qin, S. J., Du, G. D., Li, F. D., Ma, H. Y., and Liu, G. C. (2012) The research on eco-physiological effects and application of orchard sod culture. *J. Shenyang Agri. Univ.*, 43, 131-136.
- [35] Zhang, H. M., Xu, Q. T., and Zhang, M. K. (2014) Application of different management measures to reduce runoff losses of nitrogen, phosphorus and copper from orchard in dense river network plain. *Transactions of the CSAE*, 30, 132-138.
- [36] Yu, Q. G., Ye, J., Ma, J. W., Sun, W. C., Zou, P., Fu, J. R., Yin, J. Z., and Xu, J. X. (2012) Effects of green manure planting on nitrogen and phosphorus runoff losses in mountainous orchard. *J. Soil Water Conserv.*, 26, 6-10, 20.
- [37] Cheng, Y., Jia, Y. S., Wang, Y., Zhao, X., Yang, L. Z., and Wang, S. Q. (2014) Nutrient inputs and soil fertility status in orchards of Zhushan bay in Taihu Lake watershed. *J. Agro-Environ. Sci.*, 33, 1940-1947.
- [38] Bao, S. D. (2000). Soil and Agricultural Chemistry Analysis (3<sup>rd</sup> ed.) China Agricultural Press, Beijing, China.
- [39] Lu, R. K. (2000) Soil Agricultural Chemical Analysis. China Agricultural Science and Technology Press, Beijing, China.
- [40] Li, H. S. (2000) Principles and Techniques of Plant Physiological Biochemical Experiment. Higher Education Press, Beijing, China.
- [41] Gao, J. F. (2000) Plant Physiology Experimental Technology. Northwest Agricultural and Forestry University Press, Yangling, China.
- [42] Giandon, P., and Consalter, A. (1993) Agrelan: A Software to optimize fertilization. *Acta Hort.*, 383, 499-508.
- [43] Drahorad, W. (1999) Modern Guidelines on Fruit Tree Nutrition. *Compact Fruit Tree*, 32, 91-97.
- [44] Tagliacini, M., and Marangoni, B. (2002) Major nutritional issues in deciduous fruit orchards of northern Italy. *HortTechnology*, 12, 26-31.
- [45] Lu, S. C., Chen, Q., Zhang, F. S., and Jia, W. Z. (2008) Characteristics of soil phosphorus input and phosphorus load risk in major orchards region of Hebei. *Sci. Agri. Sin.*, 41, 3149-3157.
- [46] Lu, S. C. (2013) Soil Quality Status and Improvement in Intensive Orchards of China. Chemical Industry Press, Beijing, China.
- [47] Lu, R. K. (2003) The phosphorus level of soil and environmental protection of water body. *Phosphate Compound Fert.*, 18, 4-7.
- [48] Wang, Y. L., He, Y. Q., Wu, H. S., Li, R. Y., and Jin, F. (2010) Environmental risk analysis of accumulated phosphorus in red soil under long-term fertilization. *Acta Pedologica Sin.*, 47, 880-887.
- [49] Yan, Z. J., Duan, Z. Q., Lu, S. C., and Chen, Q. (2010) Construction and application of regional fertilization decision-making system based on

- GoogleMap and WebGIS for peach orchard. *Transactions of the CSAE*, 26, 207-212.
- [50] Weinbaum, S., Johnson, R., and Dejong, T. (1992) Causes and consequences of over fertilization in orchards. *HortTechnology*, 2, 112-121.
- [51] Hiraoka, K., and Umemiya, Y. (2000) Estimation of balance of nitrogen, phosphorus and potassium in relation to chemical fertilizer application in Japanese orchard fields. *Jap. Agri. Res. Quart.*, 34, 87-92.
- [52] Li, D. R., Dong, W. D., Wang, F. J., Zhang, X. M., and Liu, S. Y. (2004) Influence of different soil and water conservation measurements on phosphorus loss on orchard slope land of red soil. *J. Soil Water Conserv.*, 18, 81-84.
- [53] Nyssen, J., Poesen, J., Moeyersons, J., Haile, M., and Deckers, J. (2008) Dynamics of soil erosion rates and controlling factors in the Northern Ethiopian highlands-towards a sediment budgets. *Earth Surf. Proc. Land.*, 33, 695-711.
- [54] Liu, Y., Tao, Y., Wan, K. Y., Zhang, G. S., Liu, D. B., Xiong, G. Y., and Chen, F. (2012) Runoff and nutrient losses in citrus orchards on sloping land subjected to different surface mulching practices in the Danjiangkou Reservoir area of China. *Agri. Water Manage.*, 110, 34-40.
- [55] Whangchai, K., Gemma, H., Uthaibutra, J., and Iwahori, S. (2001) Post-harvest physiology and microanalysis of mineral elements of Nam Dork Mai mango (*Mangifera indica*) fruit grown under different soil composition. *J. Jap. Soc. Hort. Sci.*, 70, 463-465.
- [56] Deng, F. C., An, G. Y., Yu, J. Y., and Du, Z. H. (2003) Research on growing grass in apple orchard in Weibei upland. *J. Fruit Sci.*, 20, 506-508.
- [57] Tan, B., Cao, X. Y., Liu, H. F., Lu, X. Y., Qin, R., and Ma, B. G. (2011) Effects of planting grass on grape chlorophyll fluorescence characteristics and fruit quality. *J. Shihezi Univ. (Nat. Sci.)*, 29, 683-688.
- [58] Li, Q. S., Wu, J. J., Wang, Z. Q., Yan, L. J., and Ye, X. J. (2000) The effects and simulation of peach orchard intercropped with rye grass on water and heat environments in the near soil surface. *Acta Agri. Zhejiangensis*, 12, 20-24.
- [59] Liu, T. (2007) The effect of the *Chamaecrista rotundifolia* on the growth of the fruit trees and ecology of the red soil region in mountainous orchards. *Chin. Agri. Sci. Bull.*, 23, 322-327.
- [60] Yang, W. Q., Kou, J. C., Han, M. Y., and Wang, A. Z. (2011) Effects of inter-planted *Trifolium repens* on the photosynthetic physiology of peach tree. *Acta Agrestia Sin.*, 19, 771-775.
- [61] Pan, X. J., Zhang, W. E., Fan, W. G., Peng, G. H., and Luo, G. H. (2010) Effects of sod culture and intercropping green manure on the soil nutrient, enzyme activities and microorganisms in bonsai citrus. *Acta Hort. Sin.*, 37, 1235-1240.
- [62] Compant, S., Reiter, B., Sessitsch, A., Nowak, J., Clement, C., and Barka, E. A. (2005) Endophytic colonization of *Vitis vinifera* L. by plant growth-promoting bacterium *Burkholderia* sp. strain PsJN. *Appl. Environ. Microb.*, 71, 1685-1693.
- [63] Ingels, C. A., Scow, K. M., Whisson, D. A., and Drenovsky, R. E. (2005) Effect of cover on grapevines, yield, juice composition, soil microbial ecology, and gopher activity. *Am. J. Enol. Viticult.*, 561, 19-29.
- [64] Whitelaw-Weckert, M. A., Rahman, L., Hutton, R. J., Coombes, N. (2007) Permanent swards increase soil microbial counts in two Australian vineyards. *Appl. Soil Ecol.*, 36, 224-232.
- [65] Xi, Z. M., Li, H., Long, Y., Zhang, J., and Pang, X. L. (2010) Variation of soil microbial populations and relationships between microbial factors and soil nutrients in cover cropping system of vineyard. *Acta Hort. Sin.*, 37, 1395-1402.
- [66] Li, H. K., Zhang, G. J., Zhao, Z. Y., and Li, K. R. (2007) Effects of interplanted herbage on soil properties of non-irrigated apple orchards in the Loess Plateau. *Acta Prataculturae Sin.*, 16, 32-39.

---

**Received:** 22.03.2016

**Accepted:** 19.09.2016

---

**CORRESPONDING AUTHOR**

---

**Jian-chu Zheng**

Institute of Agricultural Resource and Environment,  
Jiangsu Academy of Agricultural Sciences, Nanjing  
210014, P.R. China

email: [zjc@jaas.ac.cn](mailto:zjc@jaas.ac.cn)



# DEVELOPMENT OF FUNGAL BIOFILM ON *LUFFA CYLINDRICA* FOR BIOSORPTION OF ZINC (II) FROM AQUEOUS SOLUTION

Rukhsar Muzaffar<sup>1</sup>, Arifa Tahir<sup>1</sup>, Essam N Sholkamy<sup>2,\*</sup>, Ashraf A Mostafa<sup>2</sup>, Abdullah A Al-arfaj<sup>2</sup>, Tarad Abalkhail<sup>2</sup>, Ahmed Abdel-Megeed<sup>3</sup>

<sup>1</sup>Environmental Science Department, Lahore College for Women University, 54000 Lahore, Pakistan

<sup>2</sup>Botany and Microbiology Department, College of Science, King Saud University, 2455 Riyadh 11145, KSA

<sup>3</sup>Plant Protection Department, Faculty of Agriculture, Alexandria University, 21531 Alexandria, Egypt

## ABSTRACT

Fungal biosorption is relatively effective method that has been shown to have a considerable potential to remove heavy metals from urban waste waters. Given the low cost, high abundance, easy availability, long storage and high biosorption potential of the vegetable sponge *Luffa cylindrica*, this study aimed to immobilize *Aspergillus niger* on vegetable sponge to develop low cost bio-sorbent and optimize the environmental conditions for removal of Zinc (II) from aqueous solutions. The conditions evaluated in this study were pH, incubation temperature, incubation time, heavy metal ion concentration and biosorbent weight. The optimal biosorbent wet weight for maximum biosorption (97.5%) was 0.5 g. The maximum biosorption (97.37%) was observed at pH 2.5. The optimal temperature to give maximum bio-sorption rate (97.12%) was 25°C. The maximum biosorption rate (95.5%) was observed at metal concentration 2 mg/L. Analysis of the Atomic Absorption Spectrophotometer indicated that the biosorbent has a great potential to eliminate Zinc (II) from aqueous solutions contributing to an eco-friendly technology for bioremediation in natural environment.

## KEYWORDS:

*Aspergillus niger*; Biosorption; *Luffa cylindrica*; Eco-friendly technology; Zinc

## INTRODUCTION

Urban ecosystems are filled with the uncontrolled discharge of waste waters containing heavy metals in environment which are hazardous to animals, plants and humans. Due to their high agility and noxiousness, their existence in surface and ground water stances a key inorganic contamination problem [1]. One of the most important priorities of the 21st century is the expansion of technically simple and economically striking techniques of industrial waste purification. [2,3]. Biosorption is the

removal of metals or metalloid species, complexes and particulates from solution by biological material, is a striking technology using indolent and dead biomass to remove heavy metals from aqueous solutions when the metabolic activity for intracellular accumulation is absent [4-6]. Biosorption is influenced by pH [7], Biomass dosage [8] and temperature [9]. For economic reasons, less costly biosorbents are one of kind attention nowadays, such as agricultural wastes including *Luffa cylindrica* [10]. Zinc is of major concern because it is highly used in developing countries for industrial purposes. This metal is used in electroplating, steel industry, paint industry, galvanizing industries, smelting, polymer stabilizer, mining and metallurgical processes [11]. For successful application in detoxifying metal effluents, fungal biomass needs to be immobilized to increase its efficiency, strength, density and resistance to chemical environments. This was achieved in this study by immobilizing the filamentous fungus *Aspergillus niger* on *Luffa cylindrica*. In this study, potential of *Aspergillus niger* for the biosorption of Zn will be evaluated. The aims of this study were biosorption of heavy metal from aqueous solution by fungal immobilization on *Luffa cylindrica*, Utilization of local low cost resources as biosorbent, development of cost effective wastewater treatment technology.

## MATERIAL AND METHODS

The purpose of this experimental work was to understand and analyze the ability of *Aspergillus niger* (RK-54) immobilized on *Luffa cylindrica* to remove Zn<sup>+2</sup> from aqueous solution in different environmental conditions.

### Microorganism & Inoculum preparation.

*Aspergillus niger* (RK-54) previously isolated in Environmental Science lab., was used in all of the experiments. It was isolated from soil in the vicinity of electroplating industry near Lahore Pakistan. Spore suspension of *Aspergillus niger* (RK-54) from

24 hour old PDA slant was used to inoculate Potato dextrose broth (0.6 g in 25ml of distilled water) for solid state inoculum. The pH of media was maintained 5.0 and autoclaved for 20 min. After autoclaving the flask was placed in shaking incubator for 3 days at 25 °C and 150 rpm agitation speed. Then Spores of *Aspergillus niger* were inoculated.

**Biomass production.** Solid state fermentation was used for the production of biomass used in experiments. Trisodic citrate (0.025 g), Ammonium nitrate (0.03 g), Ammonium sulphate (0.04 g), Magnesium sulphate (0.002 g) and Di-hydrogen potassium phosphate (0.05 g) was dissolved in 10ml of distilled water. The solution was autoclaved for 20 min. and then poured onto Wheat bran (10 g) which was inoculated with *Aspergillus niger* inoculum along with the pieces of *Luffa cylindrica* (1×1cm cube) and kept in incubator at 25 °C for 5 days.

**Biosorption technique.** All experimental work was carried out by taking fungal biomass (0.5 g) in ZnSO<sub>4</sub> solution (25 ml) in 250 ml Erlenmeyer flasks. Different environmental conditions (metal concentration, bio sorbent dosage, temperature, incubation time and pH) were optimized. The process was carried out in rotatory shaker (GFL 3033) at 150 rpm for specific time intervals. The influence of initial pH on biosorption rate was investigated at different pH. The incubation temperature was studied in range of 15-30 °C. Biosorbent dosage was varied in range of 0.25-1 g. The effect of incubation time on Zn<sup>2+</sup> removal rate (%) was also assessed. The control flasks were subjected to same conditions but without bio sorbent. To make the process economically feasible the bio sorbent (*Aspergillus niger* immobilized on *Luffa cylindrica*) was reused after each cycle to analyze the bio sorption efficiency of *Aspergillus niger*. After each experiment, the mixture was filtered through whatman filter paper and the residual metal ions concentration was determined by using Atomic Absorption Spectrophotometer.

**Optimization of different environmental conditions for maximum biosorption.** To obtain maximum biosorption, initial pH was varied in range of 2, 2.5, 3 and 3.5 at biosorbent weight 0.5 g, for 10 min at 150 rpm and 25 °C temperature. To obtain maximum bio sorption rate, different heavy metal concentrations were studied in range of 0.5, 1.0, 1.5, 2.0 and 3.0 mg/L under incubation conditions; biosorbent weight 0.5 g, 10 min at 150 rpm and 25 °C. To obtain maximum biosorption rate, biosorbent weight in range of 0.25 g, 0.5 g, 0.75 g, 1.0 g were studied in 25 ml of distilled water in 250 ml of Erlenmeyer flask. Incubation was occurred for 10 min at 150 rpm, pH 2.5 and 25 °C temperature. Incubation time was varied in range of 5, 10, 15 and

20 min to obtain maximum biosorption rate. The incubation was under constant conditions; pH 2.5, weight of biosorbent 0.5 g, at 150 rpm and 25 °C. To obtain maximum biosorption, incubation temperature was varied in range of 15, 20, 25 and 30 °C and the pH was kept constant at 2.5; Biosorbent weight 0.5 g; 10 min at 150 rpm and 25 °C. After each experiment the solution was filtered with Whatman filter paper and the residual metal ions concentration was determined by using Atomic Absorption Spectrophotometer.

**Analysis of results.** Residual metal ion concentration of Zn<sup>2+</sup> in all samples was determined by using Atomic Absorption Spectrophotometer (M Series 08260033, THERMO Electron Corporation, and UK). The percentage removal of metal ions was determined by the following formula:

$$\% \text{ Removal} = \frac{C_e - C_f}{C_e} \times 100$$

Where C<sub>e</sub> is initial metal concentration (mg/L) in ZnSO<sub>4</sub> solution and C<sub>f</sub> is the final metal concentration (mg/L) in ZnSO<sub>4</sub> solution.

## RESULTS

**Effect of initial pH.** The pH of the metal solutions determines the availability of the metal in a soluble form for adsorption, dictates the overall surface change of the adsorbent. The uptake of Zn<sup>2+</sup> by biosorbent (*Aspergillus niger* immobilized on *Luffa cylindrica*) was investigated at different pH levels (2.0, 2.5, 3.0 and 3.5). The pH of the solution was adjusted with NaOH and HCL. The maximum biosorption of Zn<sup>2+</sup> (97.37%) obtained at pH 2.5 (see Figure 1). The removal efficiency of biosorbent increased with decreased pH.

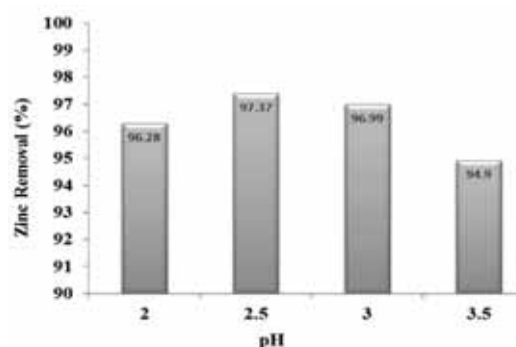


**FIGURE 1**  
Effect of incubation pH on removal (%) of Zinc

**Effect of incubation temperature.** Temperature is the most important factor that has great influence on biosorption of heavy metals. The effect of incubation temperature on biosorption

capacity of bio sorbent (*Aspergillus niger* immobilized on *Luffa cylindrica*) was studied at different temperatures (15, 20, 25, 30 °C). The maximum biosorption rate of  $Zn^{+2}$  (97.12%) was obtained at 25 °C after 10 min of incubation (see Figure 2). Biosorption rate increases with slight increase in temperature. Further increase in temperature decreased the biosorption rate. At higher temperatures, biosorption rate started to decline because fungus started to die.

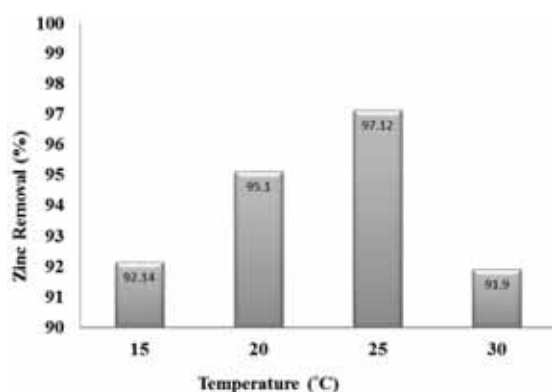


**FIGURE 2**

**Effect of incubation temperature on removal (%) of Zinc**

Environmental conditions: Wet weight of biosorbent 0.5 g, pH 2.5, incubation time 10 min, agitation speed 150 rpm

**Effect of biomass dosage.** Biomass dosage has profound effect on biosorption rate. The effect of biomass on the removal of  $Zn^{+2}$  was studied on different biosorbent weight (0.25 g, 0.5 g, 0.75 g, 1.0 g) at pH 2.5 and 150 rpm agitation speed. The maximum biosorption rate for removal of  $Zn^{+2}$  (97.5%) was observed at 0.5 g dosage of biosorbent (see Figure 3). Further increase in biosorbent dose in limited metal concentration decreases the uptake of  $Zn^{+2}$  because of the saturation of sorption sites on biosorbent.

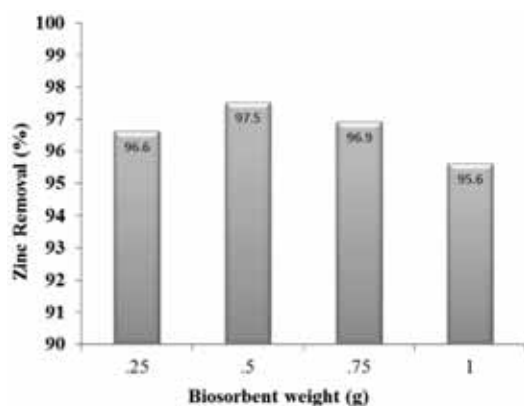


**FIGURE 3**

**Effect of bio sorbent weight (%) on removal of Zinc**

Incubation Conditions: pH 2.5, temperature 25 °C, incubation time 10 min, agitation speed 150 rpm.

**Effect of  $Zn^{+2}$  concentrations and incubation time.** The effect of initial concentration of effluent on biosorption was investigated in the range of 0.5-3 mg/L at pH 2.5 and 150 rpm agitation speed. It was observed that maximum removal was increased with increase in initial concentration of  $Zn^{+2}$ . The maximum biosorption of  $Zn^{+2}$  (95.5%) was observed at 2 mg/L (see Figure 4). After 2 mg/L the biosorption rate started to decline due to saturation of sorption sites on bio sorbent. Maximum biosorption (97.12%) was observed at first 10 min (see Figure 5). Further increase in incubation time decreases the bio sorption rate slightly and then remains almost constant.

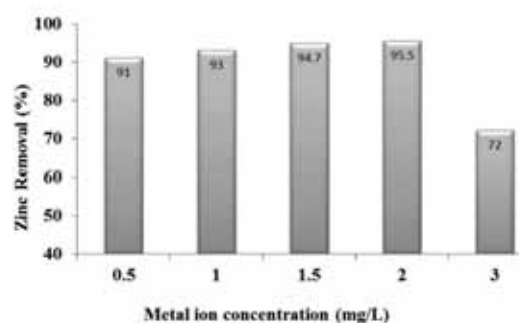


**FIGURE 4**

**Effect of metal ion concentration on removal (%) of Zinc**

Environmental Conditions: Wet weight of biosorbent 0.5 g, pH 2.5 temperature 25 °C, incubation time 10 min, agitation speed 150 rpm.

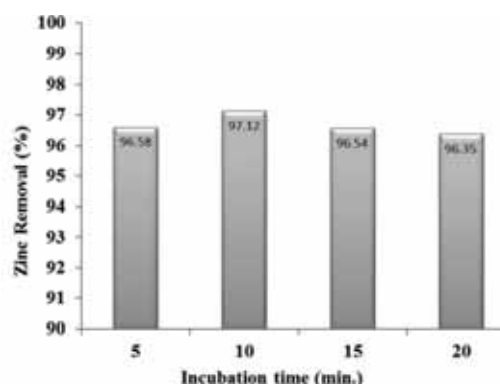


**FIGURE 5**

**Effect of incubation time on removal (%) of Zinc**  
Environmental Conditions: Wet weight of biosorbent 0.5 g, temperature 25 °C, pH 2.5, and agitation speed 150 rpm.

**Reuse of bio sorbent.** To make the process economically feasible the bio sorbent (*Aspergillus niger* immobilized on *Luffa cylindrica*) was reused for up to 15 cycles to analyze the bio sorption efficiency of *A. niger*. The maximum biosorption rate (96%) was observed at first cycle (See Figure 6) which continued to decrease after each cycle and minimum biosorption rate (46%) was observed at 15<sup>th</sup> cycle

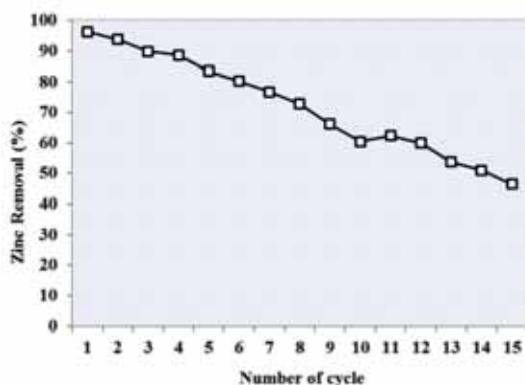


**FIGURE 6**

**Effect of biosorbent recycling on removal (%) of Zinc**

Environmental Conditions: Wet weight of biosorbent 0.5 g, temperature 25 °C, incubation time 10min and agitation speed 150 rpm.

**DISCUSSION**

The present study was aimed for the bio sorption of  $Zn^{+2}$  from aqueous solution of  $ZnSO_4$  by immobilization of *Aspergillus niger* (RK-54) on *Luffa cylindrica* which is widely distributed in tropics and sub-tropics and also in Pakistan. Potato Dextrose Broth (PDB) is most commonly used growth media for fungi [12]. Biosorption is dependent on fungal species, biosorbent size, heavy metal concentration, temperature, incubation time and pH. To achieve the maximum rate of biosorption by fungal immobilization on *Luffa cylindrica*, different environmental conditions were optimized. Factors such as pH, temperature and heavy metal concentration affect biological elimination of pollutants [13, 14]. Biosorption was more effective under agitation conditions than static conditions. The reasons may be that an increased mass and oxygen transfer takes place during continuous agitation [15, 16]. The results indicated that biosorption of  $Zn^{+2}$  by fungal biomass were very effective at moderate agitation speed which was 150 rpm [17]. It was investigated that maximum biosorption of  $Zn^{+2}$  observed at pH 2.5, incubation temperature (25 °C), incubation time (10 min), biosorbent dosage (0.5 g), and heavy metal concentration (2 mg/L).

The pH level is one of the most important parameter for biosorption of metal ions from aqueous solutions. Fungus showed best biosorption at pH 2.5 (97.37%). Insoluble metal ions started precipitating from the solution at higher values of pH, making true biosorption studies impossible. pH has a significant effect on the solubility, speciation of heavy metal, and biosorption capacity of fungi [18]. At very low pH (2.0) fungal surface had a positive charge and prevented contact with metal ions. Similar results were published for  $Pb^{+2}$  removal by using *Penicillium simplicissimum* [19].

It is well documented that solution temperature is an important parameter affecting biosorption of heavy metals [20]. The decrease of biosorption capacity at high temperature may be due to damage of active sites present on biomass [21]. The temperature can affect the stability of cell wall and its configuration [12]. It was found that the metal uptake increased with increase in temperature till 25 °C. The maximum biosorption was obtained at 25 °C (97.18%). While increasing temperature above 25 °C decreased the biosorption capacity [22].

The biosorption capacity increased with increase in time and large number of metal ions (97.12%) was removed till 10 min. This trend for metal ions in binding suggests that the binding may take place through interactions with functional groups on the surface of the biosorbent (Arica *et al.*, 2004). Further increase in time decreases the biosorption rate because less binding sites were available for biosorption. Biosorbent dosage in reaction mixture is equally important factor for biosorption process [23, 24]. It was observed that the biosorption capacity increased with increase in biosorbent dose. Maximum biosorption rate (97.5%) was observed at 0.5 g of biosorbent. But further increase in biosorbent dosage decreases the biosorption capacity of biosorbent to remove  $Zn^{+2}$  from  $ZnSO_4$  solution because of the interference of excess binding sites on biosorbent. Similar trend was observed for removal of  $Zn^{+2}$  using ovulate cones biomass of *Pinus sylvestris* as the biosorbent [25, 26]. It was found that the biosorption of  $Zn^{+2}$  increased with the initial concentration of metal ions. Maximum biosorption (95.5%) was observed at  $Zn^{+2}$  (2 mg/L). The increase could be due to an increase in electrostatic interactions which are relevant to covalent interactions [27].

To make the process economically feasible the bio sorbent (*Aspergillus niger* immobilized on *Luffa cylindrica*) was reused for up to 15 cycles to analyze the bio sorption efficiency of *A. niger*. The maximum biosorption rate (96%) was observed at first cycle which continued to decrease after each cycle and minimum biosorption rate (46%) was observed at 15<sup>th</sup> cycle. The efficiency of biosorbent as a reuse material was investigated and biosorption rate of this reused biomass was half as per previous result. The percentage removal of  $Zn^{+2}$  was 55%. The immobilization of *Aspergillus niger* on *Luffa cylindrica* served as an effective biosorbent for removal of  $Zn^{+2}$ . Biosorption is an important process in the biogeochemical cycling of metals, radio nuclides, and anthropogenic organics should be fully studied in order to understand the source and fates of chemicals. However, research has to be done to highlight these biological methods at national level.

## CONCLUSION

This study gives evidence of benefits using immobilization of *A. niger* on *Luffa cylindrica* as well as optimized environmental conditions for the removal of  $Zn^{+2}$  from the aqueous solution of  $ZnSO_4$ . This study indicated that the various environmental conditions which can affect biosorption process are pH, biomass dosage, temperature, metal ion concentration and incubation time. The maximum biosorption (97.5%) was obtained at biosorbent weight 0.5 g. The maximum biosorption (97.37%) was observed at pH 2.5. The best temperature to give maximum biosorption rate (97.12%) was 25 °C. The maximum biosorption rate (95.5%) was observed at metal concentration 2 mg/L. This study indicated the scope of using low cost biological material for heavy metal uptake to make wastewater treatment an economically feasible method for industries. It is concluded that *Aspergillus niger* immobilized on *Luffa cylindrica* has a great potential for removing  $Zn^{+2}$  from aqueous solutions as an eco-friendly process.

## ACKNOWLEDGEMENTS

The authors extended their appreciation to the Deanship of Scientific Research at King Saud University for their funding the work through the research group project No. RGP-VPP-010.

## REFERENCES

- [1] Pamukoglu, M.Y. and Kargi, F. (2006) Removal of copper (ii) ions from aqueous medium by biosorption onto powdered waste sludge. *Process Biochemistry*, 41, 1047-1054.
- [2] Chubar, N., Carvalho, J.R. and Correia, M.J.N. (2004) Heavy metals biosorption on cork biomass: Effect of the pre-treatment. *Colloids and Surfaces A: Physicochemical and Engineering Aspects*, 238, 51-58.
- [3] Chang, C.-F., Lin, P.-H. and Höll, W. (2006) Aluminum-type superparamagnetic adsorbents: Synthesis and application on fluoride removal. *Colloids and Surfaces A: Physicochemical and Engineering Aspects*, 280, 194-202.
- [4] Esposito, A., Pagnanelli, F. and Veglio, F. (2002) Ph-related equilibria models for biosorption in single metal systems. *Chemical Engineering Science*, 57, 307-313.
- [5] Davis, T.A., Volesky, B. and Mucci, A. (2003) A review of the biochemistry of heavy metal biosorption by brown algae. *Water research*, 37, 4311-4330.
- [6] Soylak, M., Tuzen, M., Mendil, D. and Turkekul, I. (2006) Biosorption of heavy metals on *aspergillus fumigatus* immobilized diaion hp-2mg resin for their atomic absorption spectrometric determinations. *Talanta*, 70, 1129-1135.
- [7] Friis, N. and Myers-Keith, P. (1986) Biosorption of uranium and lead by *streptomyces longwoodensis*. *Biotechnology and Bioengineering*, 28, 21-28.
- [8] Fourest, E. and Roux, J.-C. (1992) Heavy metal biosorption by fungal mycelial by-products: Mechanisms and influence of pH. *Applied Microbiology and Biotechnology*, 37, 399-403.
- [9] Aksu, Z., Sag, Y. and Kutsal, T. (1992) The biosorption of copper by *c. Vulgaris* and *z. Ramigera*. *Environmental Technology*, 13, 579-586.
- [10] Bailey, S.E., Olin, T.J., Bricka, R.M. and Adrian, D.D. (1999) A review of potentially low-cost sorbents for heavy metals. *Water research*, 33, 2469-2479.
- [11] Selatnia, A., Bakhti, M., Madani, A., Kertous, L. and Mansouri, Y. (2004) Biosorption of  $cd^{2+}$  from aqueous solution by a naoh-treated bacterial dead *streptomyces rimosus* biomass. *Hydrometallurgy*, 75, 11-24.
- [12] Congeevaram, S., Dhanarani, S., Park, J., Dexilin, M. and Thamaraiselvi, K. (2007) Biosorption of chromium and nickel by heavy metal resistant fungal and bacterial isolates. *Journal of hazardous materials*, 146, 270-277.
- [13] Whiteley, C. and Lee, D.-J. (2006) Enzyme technology and biological remediation. *Enzyme and Microbial Technology*, 38, 291-316.
- [14] Iqbal, M., Saeed, A. and Edyvean, R. (2008) Biosorption of lead (ii) by free and immobilised fungal biomass of *phanerochaete chrysosporium*: A comparative study. *International Journal of Environment and Pollution*, 34, 353-363.
- [15] Göksungur, Y., Üren, S. and Güvenç, U. (2005) Biosorption of cadmium and lead ions by ethanol treated waste baker's yeast biomass. *Bioresource Technology*, 96, 103-109.
- [16] Bazrafshan, E., Zarei, A.A. and Mostafapour, F.K. (2015) Biosorption of cadmium from aqueous solutions by *trichoderma fungus*: Kinetic, thermodynamic, and equilibrium study. *Desalination and Water Treatment*, 1-11.
- [17] Uçun, H., Bayhana, Y.K., Kaya, Y., Cakici, A. and Algur, O.F. (2003) Biosorption of lead (ii) from aqueous solution by cone biomass of *pinus sylvestris*. *Desalination*, 154, 233-238.
- [18] Vásquez, T.G.P., Botero, A.E.C., De Mesquita, L.M.S. and Torem, M.L. (2007) Biosorptive removal of  $cd$  and  $zn$  from liquid streams with a *rhodococcus opacus* strain. *Minerals engineering*, 20, 939-944.
- [19] Fan, T., Liu, Y., Feng, B., Zeng, G., Yang, C., Zhou, M., Zhou, H., Tan, Z. and Wang, X. (2008) Biosorption of cadmium (ii), zinc (ii) and lead (ii) by *penicillium simplicissimum*:



- Isotherms, kinetics and thermodynamics. *Journal of hazardous materials*, 160, 655-661.
- [20] Wang, J. and Chen, C. (2009) Biosorbents for heavy metals removal and their future. *Biotechnology advances*, 27, 195-226.
- [21] Özer, A. and Özer, D. (2003) Comparative study of the biosorption of pb (ii), ni (ii) and cr (vi) ions onto *S. Cerevisiae*: Determination of biosorption heats. *Journal of hazardous materials*, 100, 219-229.
- [22] Marqués, A.M., Roca, X., Simon-Pujol, M.D., Fuste, M.C. and Congregado, F. (1991) Uranium accumulation by *Pseudomonas* sp. Eps-5028. *Applied Microbiology and Biotechnology*, 35, 406-410.
- [23] Ahalya, N., Kanamadi, R. and Ramachandra, T. (2005) Biosorption of chromium (vi) from aqueous solutions by the husk of bengal gram (*Cicer arietinum*). *Electronic Journal of Biotechnology*, 8(3), 258-264.
- [24] Pan, R., Cao, L., Huang, H., Zhang, R. and Mo, Y. (2010) Biosorption of cd, cu, pb, and zn from aqueous solutions by the fruiting bodies of jelly fungi (*Tremella fuciformis* and *Auricularia polytricha*). *Applied Microbiology and Biotechnology*, 88, 997-1005.
- [25] King, P., Rakesh, N., Lahari, S.B., Kumar, Y.P. and Prasad, V. (2008) Biosorption of zinc onto *Syzygium cumini* L.: Equilibrium and kinetic studies. *Chemical Engineering Journal*, 144, 181-187.
- [26] Kumar, R., Bhatia, D., Singh, R., Rani, S. and Bishnoi, N.R. (2011) Sorption of heavy metals from electroplating effluent using immobilized biomass *Trichoderma viride* in a continuous packed-bed column. *International Biodeterioration & Biodegradation*, 65, 1133-1139.
- [27] Al-Asheh, S. and Duvnjak, Z. (1995) Adsorption of copper and chromium by *Aspergillus carbonarius*. *Biotechnology Progress*, 11, 638-642.

---

**Received: 29.03.2016**

**Accepted: 05.09.2016**

---

#### **CORRESPONDING AUTHOR**

---

**Essam N Sholkamy**

Botany and Microbiology Department, College of Science, King Saud University, 2455 Riyadh 11145, KSA

e-mail: [essam\\_92003@yahoo.com](mailto:essam_92003@yahoo.com)

# DEVELOPMENT OF A MICROBIAL PREPARATION BY USING A CHLORIMURON-ETHYL DEGRADING BACTERIUM, *BACILLUS TEQUILENSIS* JW18

Zhu Jiang-wei<sup>1,\*</sup>, Zhao Yan<sup>2</sup>, Wu Lei<sup>3</sup>, Yang Ying<sup>4</sup>

<sup>1</sup>Collaborative Innovation Center of Sustainable Forestry in Southern China of Jiangsu Province, (Nanjing Forestry University), Nanjing 210037, China

<sup>2</sup>Shanghai Institute of Quality Inspection and Technical Research, Shanghai 200233, China

<sup>3</sup>Department of Medical Examination, Shandong Medical College, Jinan 250002, China

<sup>4</sup>Jinan Landscape Flower and Plantlet Breeding Center, Jinan 250103, China

## ABSTRACT

A strain JW18 capable of highly degrading chlorimuron-ethyl was isolated from soil. JW18 was identified as *Bacillus tequilensis* based on 16S rRNA and analysis of morphology, physiological and biochemical characters. The optimal pH value and temperature were 7.0-7.5 and 37°C. The 96h degradation rate of 50 mg/L chlorimuron-ethyl by JW18 was at about 99% in inorganic salt medium. The strain JW18 could tolerate 800 mg/L of chlorimuron-ethyl and showed a high tolerance to chlorimuron-ethyl. The salt resistance test demonstrated that JW18 grew well at NaCl concentrations ranging from 0.5% to 8.0%. In addition, it was actualized to develop a new microbial preparation for dealing with chlorimuron-ethyl pollution. The commercial preparation (soil conditioner) added by strain JW18 has developed a new function for degrading chlorimuron-ethyl residue in soil, and the negative effect were not detected. Therefore, it was considered that strain JW18 could be applied for bioremediation of chlorimuron-ethyl pollution and development of microbial preparation. This study may provide theoretic basis and reference for prevention and control of pesticides pollution.

## KEYWORDS:

microbial preparation; chlorimuron-ethyl; biodegradation; *Bacillus tequilensis*

## INTRODUCTION

Chlorimuron-ethyl{ethyl 2-[[[(4-chloro-6-methoxypyrimidin-2-yl)aminol] carbonyl] amino] sulfonyl] benzoate} was a broad-spectrum sulfonylurea herbicide[1]. It has been largely used for the control of broadleaf and gramineal weeds[2].

But the chlorimuron-ethyl residue in soil might bring some trouble to sensitive crops, soil microbes and nearby aquatic systems [3-6]. Therefore, Chlorimuron-ethyl degradation and environmental fate in soil were paid close attention. Chemical hydrolysis and microbial degradation were considered the most important pathways of chlorimuron-ethyl degradation in soil, especially microbial degradation[7-9]. Compared with sterilized soil, faster and more effective degradation of some sulfonylurea herbicides in nonsterilized soil revealed that the degradation mainly depended on the soil microbial consortium [10,11].

So far, some studies on the microbial degradation of chlorimuron-ethyl had been reported. Ma et al. isolated a highly efficient chlorimuron-ethyl degrading bacterium *Pseudomonas* sp. LW3, which was capable of using chlorimuron-ethyl as the sole nitrogen source, and degrading some other sulfonylurea herbicides [7]. Yang et al. isolated *Hansschlegelia* sp. CHL1, which could utilize chlorimuron-ethyl as sole carbon and energy source, and could also be used for the bioremediation of chlorimuron-ethyl contaminated soil [12]. Seema Sharma et al. and Zhang et al. obtained chlorimuron-ethyl degrading fungi, *Aspergillus niger* and *Sporobolomyces* sp. LF1, they could degrade chlorimuron-ethyl effectively[13,14]. Besides, the metabolic pathway on biodegradation of chlorimuron-ethyl has been proposed.

But no reports on biodegradation of chlorimuron-ethyl by *Bacillus tequilensis* have been published. In this study, *Bacillus tequilensis* JW18, a strain that could effectively degrade chlorimuron-ethyl was isolated, its degradation potential and the application for agriculture and environment protection were studied. A multifunctional microbial preparation was developed by supplementing strain JW18 into the Haoyang<sup>TM</sup> microbial preparation (it was commercially available). The new preparation had a new function for degrading chlorimuron-ethyl residue besides original function. The successful

experience in this study might be used as reference for prevention and control of herbicides pollution. In addition, it might also provide the foundation for the development of the microbial preparation.

## MATERIALS AND METHODS

**Chemicals and Media.** Chemicals: chlorimuron-ethyl (99.8%) was purchased from Sigma-Aldrich. All other chemicals used were of analytical grade and commercially available.

Culture media: ① Inorganic salt medium:  $MgSO_4 \cdot 7H_2O$  0.2 g,  $K_2HPO_4$  0.1g,  $(NH_4)_2SO_4$  0.1 g,  $CaSO_4$  0.05 g,  $FeSO_4 \cdot 7H_2O$  0.01 g, water 1 L, pH 7.0. ② Isolation medium: inorganic salt medium containing chlorimuron-ethyl (50mg/L) was used to isolate chlorimuron-ethyl degrading bacteria. ③ Enrichment medium: peptone 10 g, yeast extract powder 5 g, beef extract powder 3 g, sodium chloride 5 g, water 1 L, pH7.0.

**Isolation and identification of chlorimuron-ethyl degrading bacteria.** The soil sample was collected from the farmland in Suzhou City, China, in which sulfonylurea herbicide has been used for more than 6 years. 3.0 g soil sample was placed in 100ml inorganic salt culture medium (contained 50 mg/L chlorimuron-ethyl) for shaking culture at 37°C (150 rpm). The degradation effect was measured every 24h (To determine chlorimuron-ethyl concentration according to the determination methods in literatures[15,16]). 5ml culture solution with 3days degradation rate > 50% was switched to enrichment medium with same concentration chlorimuron-ethyl, and continuously switched for more than 5 times. After the degradation effect was verified again, the above enrichment medium was coated on inorganic salt culture plate(contained chlorimuron-ethyl) for inverted culture at 37°C. The eugonic bacterial colonies were selected and repeatedly streaked on the culture plate to obtain the pure culture. The bacterial species were identified using 16SrRNA sequence analysis and Biolog™ microorganism identification system.

**Preparation of chlorimuron-ethyl degrading bacteria inoculum.** The screened chlorimuron-ethyl degrading bacteria were cultured in nutrient broth. The thallus was collected by centrifugation (5000 rpm for 10 min), washed using the sterile saline twice, resuspended with the sterile water until  $OD_{600}=1.5$ . The suspension was taken as the inoculum for subsequent degradation experiments.

**Effect of temperature on degradation of chlorimuron-ethyl by strain JW18.** 3% strain

JW18 inoculum was incubated in inorganic salt culture medium containing 50mg/L chlorimuron-ethyl (pH 7.0). Then the shaking culture was conducted under different temperatures (30°C-45°C). The residual concentration of chlorimuron-ethyl and  $OD_{600}$  value were determined every 12h.

**Effects of pH on degradation of chlorimuron-ethyl by strain JW18.** The pH value of inorganic salt culture medium (containing 50mg/L chlorimuron-ethyl) was adjusted to 6.0, 6.5, 7.0, 7.5 and 8.0. Then 3% inoculum was incubated respectively. The shaking culture was performed at 37°C. The sample was taken regularly for the determination of chlorimuron-ethyl degradation and  $OD_{600}$  value.

**Tolerance of the strain JW18 on chlorimuron-ethyl.** The chlorimuron-ethyl was added in inorganic salt culture medium so that the concentrations reached 50mg/L, 100mg/L, 200mg/L, 400 mg/L and 800 mg/L. The strain JW18 was incubated respectively for shaking cultivation at 37°C.  $OD_{600}$  value was determined regularly, so as to evaluate the tolerance of strain JW18 on chlorimuron-ethyl.

**Tolerance of the strain JW18 on NaCl.** The concentration of NaCl in inorganic salt culture medium (containing 50 mg/L chlorimuron-ethyl) was adjusted, so that the concentrations were 0.5%, 1.0%, 2.0%, 4.0%, 8.0% and 16.0% respectively. Then the isometric strain JW18 was incubated for shaking culture at 37°C. The sample was taken regularly and  $OD_{600}$  value was determined, so as to evaluate the tolerance of the strain JW18 on NaCl.

**Degradation of chlorimuron-ethyl in soil by strain JW18.** The soil samples were derived from the farmland in Suzhou City. These samples were divided into 4 groups: Group A: sterilized soil (The fresh soil was sterilized for 30 min); Group B: fresh soil; Group C: The strain JW18 was added in sterilized soil; Group D: The strain JW18 was added in fresh soil. In addition, the concentration of chlorimuron-ethyl was 50mg/kg in each group. Finally, the sample was cultured at 37°C incubator. The sample was taken every 24h and the concentration of chlorimuron-ethyl was determined.

**Preparation of new microbial preparation by using strain JW18.** The existing microbial preparation was improved by using strain JW18, so that it had the new function of degrading chlorimuron-ethyl. The process of preparing the microbial preparation containing strain JW18 was as follows: The prepared inoculum was mixed with the sterilized nutrient broth medium(1:8, v/v). Then the



shaking culture was performed (120rpm) at 37°C. Finally, the Haoyang™ microbial preparation (a commercial soil conditioner) was taken as the carrier. 30ml prepared mixed liquid and 10g straw powder were added in every 100g carrier. The mixture was cultured in 30°C incubator for 12h, then it was preserved into sterile glass bottle at 0°C.

The microbial preparation containing the strain JW18 was used to degrade chlorimuron-ethyl in soil: The chlorimuron-ethyl was added to fresh soil at first so that the concentration of chlorimuron ethyl was 50mg/kg. Then the soil was subpackaged in a 20 cm\*20 cm box, and the soil depth was 10cm. The weight of each piece of soil was consistent. 15 pieces of soils were divided into 3 groups: Group A, the microbial preparation Haoyang™ was added to the soil (1g microbial preparation was mixed with 30ml sterile water, then they were scattered into a box of soil); Group B, the microbial preparation containing strain JW18 was added to the soil (the method was as same as that of group A); Group C was taken as the control group (30ml sterile water was added in each piece of soil). Finally three groups of soil were cultured in 30°C incubator, stirred every 6 h and supplied water moderately. The concentration of chlorimuron-ethyl in soil was determined every 24 h.

## RESULTS AND DISCUSSION

**Identification and characterization of chlorimuron-ethyl degrading bacteria.** A strain capable of utilizing chlorimuron-ethyl as the sole carbon sources and energy source was isolated from the farmland soil, named JW18. This strain was gram-positive, straight or curvulate bacillus, 1.0×2.5-3.5 um in size. There was oval spores in the middle of thallus. The thallus could move and was aerobic. It forms circular, shaggy and opaque colonies on the nutrient agar plate. It was positive in tests for amylolysis, catalase, gelatin liquefaction, glucose fermentation, indole test and V.P. test. But lactose could not be used for fermentation[17,18]. The strain JW18 was identified as *Bacillus tequilensis* according to 16S analytical method. The identification result was consistent with that of Biolog™ microorganisms identification system (The 16S analysis of strain JW18 was commissioned to Shanghai SANGON company, GenBank accession number KP126484).

### Effects of temperature and pH on the strain JW18 growth and chlorimuron-ethyl degradation.

The strain JW18 could maintain high-level growth at 30-40°C, but the growth status at 37°C was significantly superior to that of other temperature. The growth of the strain JW18 could be inhibited at

45°C, resulting in poor growth (Fig. 1). The degradation efficiency of the strain JW18 would slightly change with temperature at 30-40°C, but the difference was not significant ( $P>0.05$ ). The degradation rate of chlorimuron-ethyl (initial concentration was 50mg/L) was 90% or above after cultured for 3 d, and could reach more than 99% after 4d at 30-40°C. The growth of the strain JW18 would be greatly inhibited if the temperature was 45°C, but it could still effectively degrade chlorimuron-ethyl and the degradation rate still could reach about 80% after 4d (Fig.2). The experimental data showed that the strain JW18 could grow at a wider temperature range and had a strong chlorimuron-ethyl degrading ability. In addition, the result showed that the temperature could affect the growth rate of the strain JW18 and its chlorimuron-ethyl degrading rate. The temperature could not only cause the change of the degrading ability through influencing microbial growth, but also could directly influence the activities of relevant degrading enzymes. Generally, the increase of the temperature would cause the acceleration of enzymatic degradation reaction, but the excessively high temperature would lead to the inactivation of degrading enzymes and other enzymes[9,19]. Based on the above factors, 37°C was considered as the optimum temperature of the strains JW18 for growth and degrading chlorimuron-ethyl.

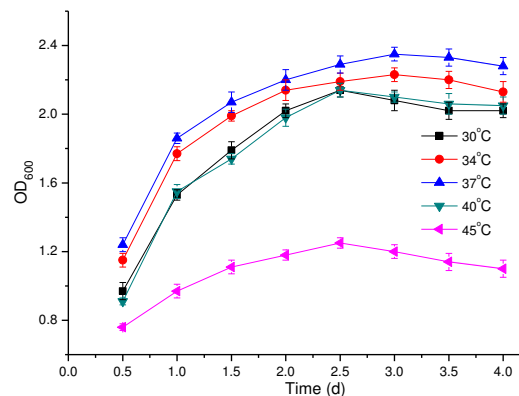


**FIGURE 1**  
Effect of temperature on the growth of strain JW18

The growth status and degradation ability of microorganism were usually affected by pH. Therefore the degradation ability of the strain JW18 to chlorimuron-ethyl in the culture medium with different pH was tested. The results showed that the growth of the strain JW18 at pH 7.5 was more than that of other pH conditions(Fig.3), and the optimum pH of the strain JW18 for degrading chlorimuron-ethyl was pH7.0-7.5 (Fig. 4).

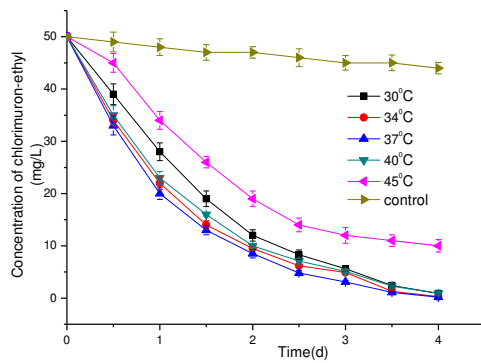


FIGURE 2

Effect of temperature on chlorimuron-ethyl degradation by strain JW18

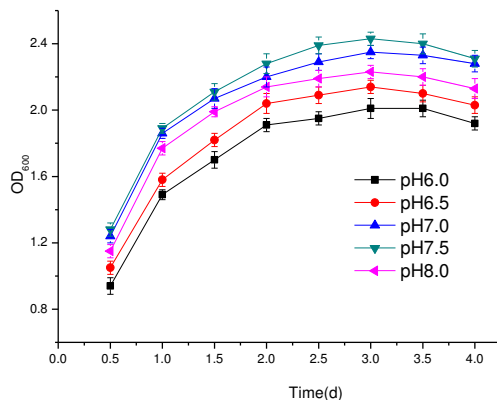


FIGURE 3

Effect of pH on the growth of strain JW18

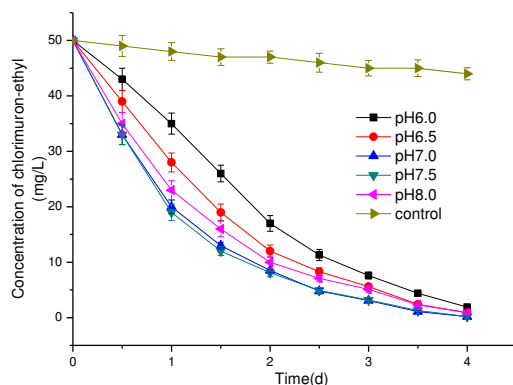


FIGURE 4

Effect of pH on chlorimuron-ethyl degradation by strain JW18

Although the degrading rates of the strain JW18 on chlorimuron-ethyl have changed when the pH value was increased from 6.0 to 8.0, the chlorimuron-ethyl could be efficiently degraded by strain JW18 and the degradation rate could reach above 98% in 4d (Fig. 4). According to Fig.3 and Fig.4, it could be known that pH would affect the strain JW18 growth and chlorimuron-ethyl biodegradation to a certain extent, but the degradation rate after 4d of incubation also showed that the effect of pH on the strain JW18

degrading chlorimuron-ethyl was not significant in later degradation stage. The 4d degradation rate of the strain JW18 on chlorimuron-ethyl could reach above 98% under different pH conditions, it maybe indicate that the strain JW18 had enormous chlorimuron-ethyl degradation ability. The previous research results showed that sulfonylurea herbicides were relatively stable in neutral and alkaline conditions, and they were easy to hydrolyze in acidic conditions[19,20]. But this degradation characteristic was not observed in this experiment. So it could be inferred that the degradation behavior in this experiment was mainly the biodegradation of the strain JW18.

**Tolerance of the strain JW18 on chlorimuron-ethyl.** When the concentration of chlorimuron-ethyl was increased from 50mg/L to 100mg/L,  $OD_{600}$  of strain JW18 would increase slightly (Fig.5), the main reason for this phenomenon might be that 50mg/L chlorimuron-ethyl was not sufficient to meet the strain JW18 demands to carbon source and energy source.  $OD_{600}$  would decrease gradually when chlorimuron-ethyl concentration was increased to 200mg/L, 400mg/L or 800mg/L. These results showed that the growth of the strain JW18 had be inhibited, but it was still growing. Therefore, it was preliminarily considered that the strain JW18 could tolerate at least 800mg/L chlorimuron-ethyl under the experimental conditions. Although the strain JW18 would be significantly inhibited by 800mg/L chlorimuron-ethyl, it still could effectively degrade chlorimuron-ethyl. According to the existing experimental results, it was inferred that: ①the strain JW18 had good tolerance on chlorimuron-ethyl. ②high-concentration chlorimuron-ethyl could influence the growth of the strain JW18. ③the strain JW18 had very strong degradation ability to chlorimuron-ethyl, which could be used in wider chlorimuron-ethyl concentration range. ④it was possible that the strain JW18 was used in the bioremediation of chlorimuron-ethyl pollution. The degradation ability of the strain JW18 might be closely related with the long-term use of chlorimuron-ethyl in farmland soil. According to the record, the application history of chlorimuron-ethyl in the related farmland was more than 6 years. Generally, the edaphon that continuously encounter the artificially synthesized compound might induce the ability to degrade the compound [21,22].

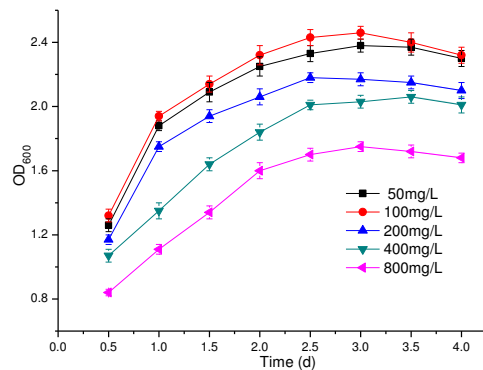


FIGURE 5

Effect of concentration of chlorimuron-ethyl on the growth of strain JW18

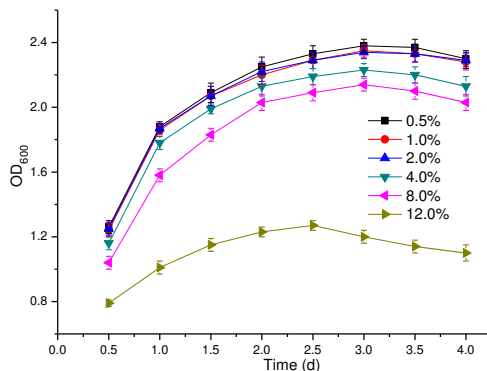


FIGURE 6

Effect of concentration of NaCl on the growth of strain JW18

**Tolerance of the strain JW18 on NaCl.** When the NaCl concentration was increased from 0.5% to 4%, OD<sub>600</sub> of the strain JW18 was not significantly different ( $P > 0.05$ ) (Fig. 6). If the NaCl concentration was further increased to 8.0%, OD<sub>600</sub> would decrease by about 6%, but OD<sub>600</sub> value was still at a higher level, which showed that the strain JW18 could tolerate 8.0% NaCl at least. In addition, there was only chlorimuron-ethyl as carbon source in the culture medium, to degrade chlorimuron-ethyl would be the only means obtained carbon source. Thereby, suggesting that strain JW18 could still maintain chlorimuron-ethyl degrading ability under high salt stress. Moreover, even though NaCl concentration was increased to 16%, the strain JW18 could still maintain growth at low level. So the salt tolerance of strain JW18 was above medium degree. The salt tolerance of strain JW18 might have some relationship with the saline alkali soil of the sampling sites. Generally, microorganisms could be induced to enhance salt tolerance under sustained osmotic pressure stress. The salt tolerance of organism could be enhanced usually by two means: osmotic adjustment and protein adjustment.

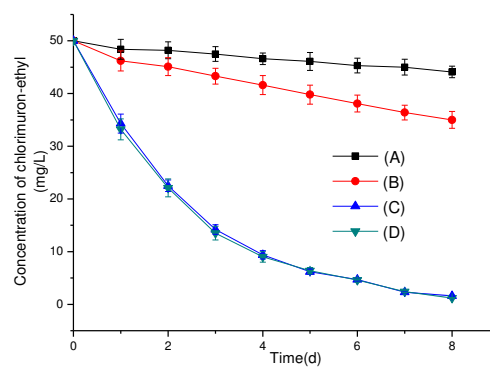


FIGURE 7

The curve on chlorimuron-ethyl degradation in the different treated soils [(A)-Sterilized soil, (B)-Fresh soil, (C)-Sterilized soil + JW18, (D)-Fresh soil + JW18 ]

#### Degradation of chlorimuron-ethyl in soil.

The results in Fig. 7 showed that it was feasible to degrade chlorimuron-ethyl in soil through directly applying the strain JW18. To put the strain JW18 in soil contained chlorimuron-ethyl could significantly improve the degradation rate of chlorimuron-ethyl. The degradation rate of chlorimuron-ethyl (50mg/kg) in soil adding with the strain JW18 could reach about 97.0% in 8d, but the degradation rate were only 30.0% and 11.8% if no strain JW18. So it was considered that the strain JW18 had good survival ability in the tested soil and could efficiently degrade chlorimuron-ethyl. Compared with sterilized soil, faster and more effective degradation of chlorimuron-ethyl in fresh soil revealed that some natural microorganism in fresh soil were involved in biodegradation of chlorimuron-ethyl. In sterilized soil, the chlorimuron-ethyl content was also decreased by 11.8% in 8d (Fig. 7), which might be caused by hydrolysis and photolysis[19,23]. Some studies had showed that degradation of chlorimuron-ethyl or other sulfonylurea herbicides were affected by many factors, such as pH, temperature, light, microorganism, soil type and fertility[12,20,24]. Generally, high temperature and acidic condition would accelerate the decomposition of sulfonylurea herbicides.

**Degradation of chlorimuron-ethyl by the microbial preparation containing strain JW18.** The strain JW18 was added in Haoyang™ microbial preparation so as to develop a multifunctional microbial preparation. The new preparation containing strain JW18 had the original function as well as a new function for degrading chlorimuron-ethyl. (Haoyang™ preparation was a soil conditioner, including *Bacillus licheniformis*, *Bacillus mucilaginosus*, *Rhodopseudomonas*

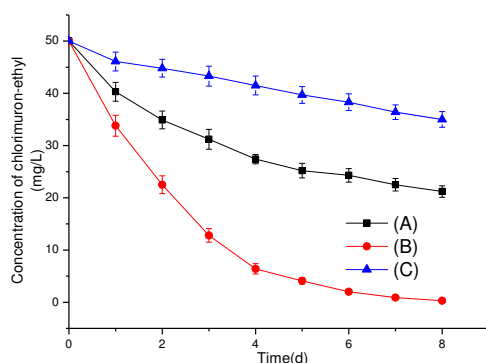


**FIGURE 8**

**Degradation of chlorimuron-ethyl by the microbial preparation. [A-microbial preparation (Haoyang™, no strain JW18), B-microbial preparation containing strain JW18, C-control]**

*palustris*, *Bacillus thuringiensis* and *Lactobacillus plantarum*, etc. Main function were to improve soil properties, control crop diseases and pest, and promote crop growth.) The experimental results (Fig. 8) showed that the microbial preparation could degrade chlorimuron-ethyl in soil, especially new preparation containing strain JW18. The degradation rate of chlorimuron-ethyl (50mg/kg) could reach above 99.0% by the microbial preparation containing strain JW18 in 8d, which should attribute to chlorimuron-ethyl degrading bacteria and related assistant strains in microbial preparation. In addition, it could be considered that some microorganisms in Haoyang™ microbial preparation could degrade chlorimuron-ethyl or assist to degrade chlorimuron-ethyl, but its degrading ability was inferior to the strain JW18. The concentration of chlorimuron-ethyl in control group was also decreased by about 30% in 8d, which might be caused by chlorimuron-ethyl degrading strains in natural soil, and some physical or chemical factors.

The preliminary application result of the microbial preparation containing strain JW18 indicated that it would not bring the adverse influence on the growth of crops, also would not affect the original function of Haoyang™ microbial preparation, which might attribute to edaphology source of the strain JW18. In addition, the mutual effect and proper match between the degradation strains and original strains in microbial preparation need further study, especially the complex mutual effect should be concerned. On the other hand, environmental factors such as physical and chemical properties of matrix, nutrition status, pH, temperature and biotic factors such inoculum density would interfere the accomplishment of any bioremediation process [7,9,24-26]. The existing research results also indicated that pH, temperature, concentration of pesticides and some other factors

would affect the biodegradation of chlorimuron-ethyl to a certain extent. Therefore, the specific environment conditions still need be paid attention in the application research.

## CONCLUSION

In this study, *Bacillus tequilensis* JW18 was isolated from soil, which could effectively degrade chlorimuron-ethyl. In inorganic salt culture medium containing 50mg/L chlorimuron-ethyl, the degradation rate of chlorimuron-ethyl by strain JW18 could reach above 99% in 4d. The appropriate pH of strain JW18 was 7.0-7.5, and the appropriate temperature was 30-40°C (37°C was the optimum temperature). The strain JW18 also had high tolerance to chlorimuron-ethyl and NaCl. It could tolerate at least 800mg/L chlorimuron-ethyl and 8.0% NaCl. The degradation rate of chlorimuron-ethyl (50mg/kg) could reach about 97.0% in 8d through applying the strain JW18 directly in the polluted soil. It was considered that strain JW18 could be applied for bioremediation of chlorimuron-ethyl pollution and development of microbial preparation. The subsequent researches would focus on the degradation mechanism and application of strain JW18. It was expected that strain JW18 could be utilized for developing multifunctional microbial preparation used in pesticides residue degradation, farmland soil improvement and crop disease control, etc.

## ACKNOWLEDGEMENTS

This study was funded by the National Basic Research Program of China (973 Program, No. 2012CB416904), and partially by a post-doctoral program in Nanjing Forestry University and Priority Academic Program Development of Jiangsu Higher Education Institutions.

## REFERENCES

- [1] J. Wang, H. Zhang, X. Zhang.(2013) Effects of long-term chlorimuron-ethyl application on the diversity and antifungal activity of soil *Pseudomonas* spp. in a soybean field in Northeast China. *Ann. Microbiol.*, 63, 335-341.
- [2] M. Xiong, Z. Hu, Y. Zhang. (2013) Survival of GFP-tagged *Rhodococcus* sp. D310-1 in chlorimuron-ethyl-contaminated soil and its effects on the indigenous microbial community. *J. Hazard. Mater.*, 252-253(4), 347-354.

- [3] Wang M.E., Zhou Q.X. (2006) Effects of herbicide chlorimuron-ethyl on physiological mechanisms in wheat (*Triticum aestivum*). *Ecotox. Environ. Safe*, 64(2), 190-197.
- [4] Zawoznik M.S., Tomaro M.L. (2005) Effect of chlorimuron-ethyl on *Bradyrhizobium japonicum* and its symbiosis with soybean. *Pest Manag. Sci.*, 61(10), 1003-1008.
- [5] Zhang X., Li X., Zhang C. (2011) Ecological risk of long-term chlorimuron-ethyl application to soil microbial community: an in situ investigation in a continuously cropped soybean field in Northeast China. *Environ. Sci. Pollut. Res. Int.*, 18(3), 407-415.
- [6] Nader Soltani, Peter H. Sikkema, Darren E. Robinson. (2005) Vegetable crop responses to chlorimuron-ethyl applied in the previous year. *Crop Protection*, 24, 685-688.
- [7] Ji-Ping Ma, Zhe Wang, Peng Lu. (2009) Biodegradation of the sulfonylurea herbicide chlorimuron-ethyl by the strain *Pseudomonas sp.* LW3. *FEMS Microbiol. Lett.*, 296(2), 203-209.
- [8] C.H. Xu, C.Y. Li, M.H. Xiong. (2012) Study on combination and bioremediation of chlorimuronethyl-degrading strains. *Adv. Mater. Res.*, 340, 215-221.
- [9] A.K. Sarmah, J. Sabadie. (2002) Hydrolysis of sulfonylurea herbicides in soils and aqueous solutions: a review. *J. Agric. Food. Chem.*, 50, 6253-6265.
- [10] Yutai Li, WT Zimmerman, MK Gorman. (1999) Aerobic soil metabolism of metsulfuron-methyl. *Pestic. Sci.*, 55(4), 434-445.
- [11] Andersen S.M., Hertz P.B., Holst T. (2001) Mineralisation studies of <sup>14</sup>C-labelled metsulfuron-methyl, tribenuron-methyl, chlorsulfuron and thifensulfuron-methyl in one danish soil and groundwater sediment profile. *Chesphere*, 45, 775-782.
- [12] Yang Liqiang, Li Xinyu, Li Xu. (2014) Bioremediation of chlorimuron-ethyl contaminated soil by *Hansschlegelia sp.* strain CHL1 and the changes of indigenous microbial population and N-cycling function genes during the bioremediation process. *J. Hazard. Mater.*, 274, 314-321.
- [13] Sharma S., Banerjee K., Choudhury P.P. (2012) Degradation of chlorimuron-ethyl by *Aspergillus niger* isolated from agricultural soil. *FEMS Microbiol. Lett.*, 337, 18-24.
- [14] Zhang Xiaoli, Zhang Huiwen, Li Xu. (2009) Isolation and characterization of *Sporobolomyces sp.* LF1 capable of degrading chlorimuron-ethyl. *J. Environ. Sci.*, 21, 1253-1260.
- [15] Partha P. Choudhury and P. Dureja. (1998) Simultaneous determination of chlorimuron-ethyl and its major metabolites in soil and water by reversed phase liquid chromatography. *Biomed. Chromatog.*, 12, 94-96.
- [16] Ye G.B., Zhang W., Cui X. (2006) Determination of ten sulfonylurea herbicides in soil samples by liquid chromatography with electrospray ionization mass spectrometric detection. *Chin. J. Anal. Chem.*, 34(9), 1207-1212.
- [17] Kaynar, P. and Beyatli, Y. (2008) Protein profiles and biochemical characterizations of *Bacillus spp.* strains isolated from fishes. *Fresen. Environ. Bull.*, 17, 1316-1321.
- [18] Ersoy Omeroglu E., Karaboz I., Sukatar A., Uzel A., Sayan M. and Sanlidag T. (2008) Phenotypic and molecular characterization of luminous bacteria isolated from Izmir Gulf in Turkey: *Vibrio harveyi* TEM O5 and TEM S1 strains. *Fresen. Environ. Bull.*, 17, 506-510.
- [19] Dinelli G., Vicari A., Bonetti A. (1997) Hydrolytic dissipation of four sulfonylurea herbicides. *J. Agric. Food. Chem.*, 4(45), 1940-1945.
- [20] W.J. Ren, M.E. Wang, Q.X. Zhou. (2011) Effect of soil pH and organic matter on desorption hysteresis of chlorimuron-ethyl in two typical Chinese soils. *J. Soils Sediments.*, 11, 552-561.
- [21] Petric I., Karpouzas D.G., Bru D. (2016) Nicosulfuron application in agricultural soils drives the selection towards NS-tolerant microorganisms harboring various levels of sensitivity to nicosulfuron. *Environmental Science and Pollution Research*, 23(5), 1-14.
- [22] Felsot A., Maddox J.V. and Bruce W. (1989) Enhanced microbial degradation of carbofuran in soils with histories of carbofuran use. *Bull. Environ. Contam. Toxicol.*, 26, 781-788.
- [23] Partha P. Choudhury and P. Dureja. (1997) Studies on photodegradation of chlorimuron-ethyl in soil. *Pestic. Sci.*, 51, 201-205.
- [24] Menne H.J., Berger B.M. (2001) Influence of straw management, nitrogen fertilization and dosage rates on the dissipation of five sulfonylureas in soil. *Weed Res.*, 41, 229-244.
- [25] Lakshmi C.V., Kumar M. and Khanna, S. (2008) Biotransformation of chlorpyrifos and bioremediation of contaminated soil. *Int. Biodeterior. Biodegrad.*, 62, 204-209.
- [26] Comeau, Y., Greer, C.W. and Samson, R. (1993) Role of inoculums preparation and density on the bioremediation of 2,4-D contaminated soil by bioaugmentation. *Appl. Microb. Technol.*, 38, 681-687.



---

**Received: 30.03.2016**

**Accepted: 18.10.2016**

**CORRESPONDING AUTHOR**

---

**Zhu Jiang-wei**

Collaborative Innovation Center of Sustainable  
Forestry in Southern China of Jiangsu Province,  
(Nanjing Forestry University), Nanjing 210037,  
China

Email: [jw\\_zhu2016@qq.com](mailto:jw_zhu2016@qq.com)

# MULCHING AND ORGANIC-INORGANIC FERTILIZER APPLICATION REDUCE RUNOFF LOSSES OF NITROGEN FROM TOBACCO FIELDS

Hou Maomao <sup>1,\*</sup>, Chen Danyan <sup>2</sup>, Shao Xiaohou <sup>3,4</sup>, Zhai Yaming <sup>3,4</sup>

<sup>1</sup> Postdoctoral research center, College of Horticulture, Fujian Agriculture and Forestry University, Fuzhou 350002, China

<sup>2</sup> Nanjing Yuangu Ecological Agriculture Co. Ltd, Nanjing 210098, China

<sup>3</sup> Key Laboratory of Efficient Irrigation-Drainage and Agricultural Soil-Water Environment in Southern China, Hohai University, Nanjing 210098, China

<sup>4</sup> College of Water Conservancy and Hydropower, Hohai University, Nanjing 210098, China

## ABSTRACT

Nitrogen loss has limited the sustainable development of tobacco agriculture and led to serious non-point pollution in China, especially those areas suffered from excessive rainfalls. A study on the characters of nitrogen loss under different cultural practices was conducted in eastern China. The cultural practices were distinguished by different nitrogen application methods and different cultivated conditions, including CK (no fertilizer with no mulching), IF-NM (inorganic fertilizer with no mulching), IF-M (inorganic fertilizer with mulching), OIF-NM (60% organic+40% inorganic fertilizer with no mulching) and OIF-M (60% organic+40% inorganic fertilizer with mulching). Results showed that the main nitrogen form in the runoff waters was  $\text{NH}_3\text{-N}$ . The concentration of  $\text{NH}_3\text{-N}$  in runoff waters correlated closely to the time of both basal and additional fertilizer application. Mulching increased runoff volume by 12.5% while decreased the  $\text{NH}_3\text{-N}$  concentration, overall reduced the accumulative amount of  $\text{NH}_3\text{-N}$  and significantly ( $p<0.05$ ) decreased the amount of total N in runoff waters. Combined application of organic and inorganic nitrogen fertilizer also reduced the concentration of  $\text{NH}_3\text{-N}$  and the amount of  $\text{NH}_3\text{-N}$  and total N, but the effectiveness was not as good as that of mulching. Mulching combined with the organic-inorganic fertilizer application (OIF-M) reduced the runoff losses of total N by 50.4%,  $\text{NH}_3\text{-N}$  by 52.5%,  $\text{NH}_4^+\text{-N}$  by 52.9% and the N in other forms by 35.9%, and was proved to be optimal in decreasing the runoff losses of nitrogen among the different treatments. This mainly because that OIF-M was more conducive to reserve the  $\text{NH}_3\text{-N}$  in plough layer and enhance the nitrogen mineralization, thus increase the crop nitrogen use

efficiency. Therefore, we highlight the importance of mulching in reducing the nitrogen loss in runoffs and recommend similar areas to use organic-inorganic compound fertilizer under a mulch-cultivated condition.

## KEYWORDS:

Mulch, Organic fertilizer, Runoff, Nitrogen loss, Nitrate nitrogen

## INTRODUCTION

Non-point pollution caused by nitrogen loss has become a worldwide environmental problem, and has influenced many areas and countries including USA [1], Europe[2,3], central Africa[4], east and south Asia [5,6,7]. In China, 50% of the nitrogen leaching to ground water stems from agricultural soils [8]. Therefore, how to decrease the nitrogen loss is an urgent issue that must be addressed during agricultural production.

Nitrogen fertilizer is the major cause for the loss of large amounts of nitrogen in water [9]. The non-point pollution is more serious after nitrogen fertilizer application particularly when the precipitation occurs [10]. Usually, the non-point pollution caused by one time nitrogen fertilizer application is long-lasting [11]. Runoff loss is one of the major pathways for the loss of fertilizer nitrogen [12]. And among the different forms of nitrogen in the runoff waters,  $\text{NH}_3\text{-N}$  is the one needs to get enough attention [13]. The amount of  $\text{NH}_3\text{-N}$  occupied a proportion of more than 30% for the total N loss in runoffs [14].

Flue-cured tobacco is an important cash crop and is significant to the national economy in China

[15]. Nitrogen fertilizer is a key factor to regulate the quality and yield of the tobaccos [16]. However, many tobacco-cultivated areas in China serve the yield and economic benefit as the first object, large quantities of nitrogen fertilizer had been applied during last decades [17]. Excessive nitrogen fertilization results in low nitrogen use efficiency, increases production costs for farmers, and unnecessary large losses of nitrogen causing serious environmental problems such as  $\text{NH}_3\text{-N}$  contamination in groundwater [18]. In tobacco cultivated area of southern China, nitrogen losses accounted for 25.1% of the applied fertilizer nitrogen, reaching  $33.9 \text{ kg ha}^{-1}$ , and the amount of  $\text{NH}_3\text{-N}$  loss accounted a high proportion of 72.8% for the total nitrogen losses [19].

In order to control the runoff losses of nitrogen from agricultural fields, many methods have been applied, including the straw mulching [20], the application of slow release fertilizer [21] and organic fertilizer [22], the shelter cultivation [23] and so on. Although some studies investigate the runoff losses of nitrogen under mulching condition or inorganic-organic fertilizer application, few studies have looked into their combined effects in reducing nitrogen losses by runoff. In this study, flue-cured tobacco K326 was chosen as the plant material, and the tobaccos were cultivated under five cultural practices which distinguished by different nitrogen application methods (inorganic fertilizer and organic-inorganic fertilizer) and cultivated conditions (mulching and no mulching). The objective is to evaluate the effects of mulching, organic-inorganic fertilizer application and their combination on reducing runoff losses of nitrogen.

## MATERIAL AND METHOD

**Experimental condition.** The experiments were carried out at the Vegetables (Flowers) Scientific Institute (latitude  $32^\circ 13' \text{N}$ , longitude  $119^\circ 04' \text{E}$ ) in Hengxi town, Nanjing, Jiangsu province, China during the growing season of flue-cured tobacco from April to August 2014.

The experimental site belongs to a subtropical humid region, with an average annual rainfall of approximately 1,107 mm in the rainy season, starting from the end of June and continuing until the middle of September. However, the average yearly evaporation was approximately 1,473 mm. The experimental sites also has an annual sunshine duration of 2017 hours, an average annual

temperature of  $15.7^\circ\text{C}$ , a maximum average humidity of 81% and a wind speed of  $19.8 \text{ m s}^{-1}$ .

The soil type of the experimental fields was Alfisols, with a pH of 6.10, bulk density of  $1.36 \text{ g cm}^{-3}$ , organic matter of 1.212%, available nitrogen of  $116.72 \text{ mg kg}^{-1}$ , available phosphorus of  $22.10 \text{ mg kg}^{-1}$  and available potassium of  $158.76 \text{ mg kg}^{-1}$  at 0-40 cm soil depth. The soils were mixed uniformly before the experiment.

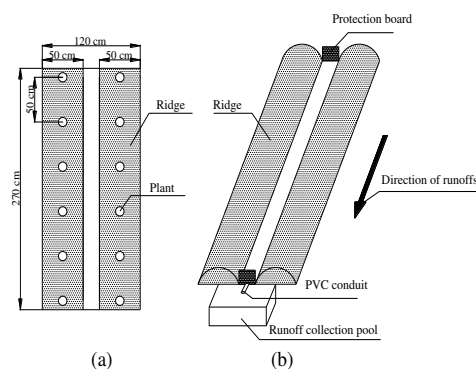


**FIGURE 1**

**The experimental plot (one treatment)**  
**(a) The arrangement of flue-cured tobacco plant, (b) The collections of runoffs**

**Treatments and experimental design.** The total area of the experimental field was  $90 \text{ m}^2$ . The experimental fields were slightly leaned in order to collect the runoffs more efficiently. Single experimental plot for one treatment was shown in Fig 1, each plot occupied an area of  $2.7 \times 1.2 = 3.24 \text{ m}^2$  (except for the area of runoff collection pool). Soil ridges were established before the experiment, with each ridge planting only one line of flue-cured tobaccos. The gap between two ridges was 20 cm, and the plant-to-plant space of tobaccos was 50 cm. Totally two lines of twelve tobaccos were included in a single plot as one treatment. At the front of each plot, a 60 L runoff collection pool was installed. The pools were prefabricated cubic tanks that made of plastic, they were buried into the fields prior to the experiment. The upside of the pools was in an even height with the fields. A PVC conduit with 5 cm diameter was employed to induce the runoff waters into the collection pools. The water-inlet of the conduit was covered with gauze in order to prevent the sediments from sneaking into the pools. When collecting the runoffs, the upside of the pools was covered with plastic board to make them



hermetically closed. The covering board only reserved a hole that was the same size as the outlet of PVC conduit, and the crevice between the hole and the conduit was filled by soft rubbers. Moreover, at both front and end of the plot, protection boards were installed to keep the purity of the runoffs inside the treatment (Fig 1). For cutting off the lateral seepages, different plots were separated by 80 cm depth plastic films.

The experiment contained five treatments: CK (control), IF-NM (inorganic fertilizer with no mulching), IF-M (inorganic fertilizer with mulching), OIF-NM (organic-inorganic fertilizer with no mulching) and OIF-M (organic-inorganic fertilizer with mulching), each treatment repeated three times. CK was applied with no nitrogen fertilizer, IF-NM, IF-M, OIF-NM and OIF-M were all applied with a 120 kg ha<sup>-1</sup> of pure nitrogen. In OIF-NM and OIF-M treatment, the proportion of inorganic fertilizer and organic fertilizer was 6:4. The inorganic fertilizer was consisted of 80% tobacco dedicated inorganic fertilizer (produced by Guizhou Institute of Tobacco Science, made of urea, potassium phosphate and ammonium phosphate, N:P<sub>2</sub>O<sub>5</sub>:K<sub>2</sub>O=1:1:3) and 20% sodium nitrate. The type of organic fertilizer (produced by Guizhou Institute of Tobacco Science) was bio-organic fertilizer with nitrogen content of 1.5% and organic matter content of 30%. The pure nitrogen application amount of IF-NM, IF-M, OIF-NM and OIF-M were kept the same (Table 1), while other fertilizer elements such as phosphorus and potassium were not considered.

Tobacco cultivar K326 was adopted as plant material, tobacco seedlings with around six expanded leaves were transplanted into the fields at April 16. The date of final harvest was August 5. Before transplanting, 70% of the fertilizers were applied as basal fertilizer, and the remaining 30% were applied at 29 DAT (days after transplanted) as additional fertilizer. The tobaccos were top pruned

timely when they entered into the flowering stage. Weed control and field management were conducted corresponding to the local practice. During the growth period of tobaccos, no additional light, heat and CO<sub>2</sub> were provided.

**Soil and plant measurements.** The runoff waters were collected each time when the runoffs generated. The volume of runoff waters were measured. Meanwhile, the content of total N, NH<sub>3</sub><sup>-</sup>-N and NH<sub>4</sub><sup>+</sup>-N in the waters were determined. After the final harvest of tobaccos, the soil samples at 0-20, 20-40 and 40-60 cm depth were collected to determine NH<sub>3</sub><sup>-</sup>-N and NH<sub>4</sub><sup>+</sup>-N content. Also the total N content in the tobacco plants was determined.

The total N content in runoff waters was measured after potassium sulfate oxidation using the indophenol blue colorimetry method [24], and the total N content in the soil and plant samples were measured using the kjeldahl method [25]. The NH<sub>3</sub><sup>-</sup>-N content was measured using the ultraviolet spectrophotometry method [26], and the NH<sub>4</sub><sup>+</sup>-N content was measured using the indophenol blue colorimetry method [24].

The nitrogen amount in other forms (kg ha<sup>-1</sup>) in runoff waters was the total N amount that minus the sum of NH<sub>3</sub><sup>-</sup>-N and NH<sub>4</sub><sup>+</sup>-N amount.

The nitrogen amount in the tobacco plants (N<sub>tobacco</sub>, kg ha<sup>-1</sup>) that sourced from the applied fertilizer was calculated as [27,28]:

$$N_{\text{tobacco}} = N_{\text{tobacco+N}} - N_{\text{tobacco+0}}$$

Where, N<sub>tobacco+N</sub> represented the nitrogen amount in the tobacco plants with nitrogen fertilizer application, N<sub>tobacco+0</sub> represented the nitrogen amount in the tobacco plants with no nitrogen fertilizer application (CK).

**Data analysis.** The data were compared statistically in SPSS software Version 17.0 [29].

**TABLE 1**  
**Design of the planting methods and nitrogen application**

Treatment	Planting methods	Nitrogen application amount (kg ha <sup>-1</sup> )	Nitrogen formation
IF-NM	No mulching	120	100% Inorganic fertilizer
IF-M	Mulching	120	100% Inorganic fertilizer
OIF-NM	No mulching	120	60% Inorganic fertilizer -40% Organic fertilizer
OIF-M	Mulching	120	60% Inorganic fertilizer -40% Organic fertilizer
CK	No mulching	0	---

**RESULT**

**Precipitation.** Fig 2 displays the precipitation during the whole growth period of flue-cured tobaccos. In this study, the root-extending, vigorous and maturity stage approximately correspond to 1-30, 30-60 and 60-110 DAT. The precipitation amount was relatively small but stable in the root-extending and vigorous stage, no precipitation more than 20

mm was appeared during this period. However, the precipitation amount increased dramatically in the maturity stage, particularly during 68 DAT to 91 DAT, which reached a high level of 298 mm, accounting for 44.0% of the total precipitation amount (678 mm). The cause of this phenomenon is that Nanjing enters into the plum rain season each year beginning from late June, it rains constantly until the end of the rain season.

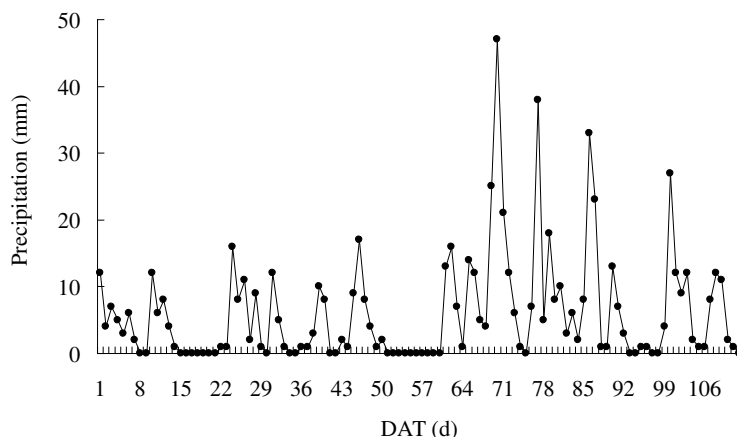


**FIGURE 2**

**The precipitation during the growth period of flue-cured tobaccos**  
 DAT represented the days after transplanted

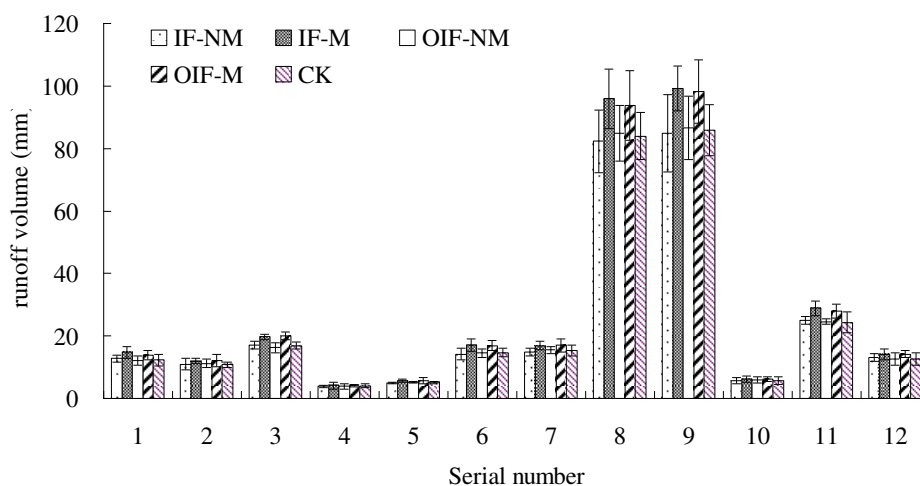


**FIGURE 3**

**The volume of runoff during precipitation period**

IF-NM, IF-M, OIF-NM, OIF-M and CK represented the five treatments of inorganic fertilizer with no mulching, inorganic fertilizer with mulching, organic-inorganic fertilizer with no mulching, organic-inorganic fertilizer with mulching and control, respectively. Runoff waters were collected twelve times in total, as reflected in the serial number.

**TABLE 2**  
**Runoff coefficient during the precipitation periods**

Serial number	Precipitation duration (DAT)	Precipitation (mm)	Runoff coefficient (%)				
			IF-NM	IF-M	OIF-NM	OIF-M	CK
1	1-5	37	34.5	39.8	32.8	37.6	33.2
2	9-12	30	36.6	39.9	37.4	40.7	36.1
3	23-27	46	37.1	42.8	35.3	43.4	36.8
4	30-31	17	22.6	24.2	22.9	24.1	23.5
5	37-39	21	23.7	26.8	24.9	27.1	24.3
6	44-47	38	37.4	44.9	38.3	44.6	38.7
7	60-62	36	41.3	46.8	43.0	47.2	42.5
8	64-72	146	56.4	65.7	58.1	64.3	57.5
9	75-86	161	52.7	61.6	53.8	61.0	53.3
10	89-91	23	24.7	27.1	25.9	26.6	24.6
11	98-103	66	37.9	43.7	37.2	42.5	36.8
12	106-109	33	39.9	42.6	37.9	43.1	38.4

DAT represented the days after transplanted. IF-NM, IF-M, OIF-NM, OIF-M and CK represented the five treatments of inorganic fertilizer with no mulching, inorganic fertilizer with mulching, organic-inorganic fertilizer with no mulching, organic-inorganic fertilizer with mulching and control, respectively.

**Runoff volume and coefficient.** The observed results of runoff volume for the twelve collection times are shown in Fig 3. The detailed duration of runoff collection and the coefficient of runoff generation are shown in Table 2. The precipitation amount for the twelve collection times ranged from 17-161 mm. For each time of collection, the runoff volume correlated closely to the precipitation amount, this regularity was particularly evident in 8th and 9th collections. The precipitation amount for 8th and 9th collection reached 146 mm and 161 mm respectively, and the runoff volume of these two times were in a significantly higher level of 82.3-95.9 mm and 84.9-99.2 mm correspondingly. Moreover, the different cultural practices also influenced the volume of runoff, the primary impact factor was the cultivated condition, while different nitrogen fertilizer application methods had no clear effects on the runoff volume and coefficient. In the mulching treatments, the runoff volume under treatments of inorganic and organic-inorganic nitrogen application were increased respectively by 6.8-20.1% and 2.7-22.9%, and by 13.2% and 11.8% in average.

**The accumulative amount of  $\text{NH}_3\text{-N}$  and the  $\text{NH}_3\text{-N}$  concentration in runoff waters.** The  $\text{NH}_3\text{-N}$  concentration in runoff waters is shown in Fig 4. The  $\text{NH}_3\text{-N}$  concentration by the 1st collection was the highest, reaching 11.7-28.3 mg L<sup>-1</sup> under the different cultural practices. Between the 1st and 3rd

collection, the  $\text{NH}_3\text{-N}$  concentration overall presented a decline trend, while it increased in the 4th collection, which were increased to a range of 12.6-23.2 mg L<sup>-1</sup> under different treatments (except CK). After that, the  $\text{NH}_3\text{-N}$  concentration decreased irregularly and obtained the lowest values of 1.2-4.2 mg L<sup>-1</sup> with different treatments in the 12th collection. In general,  $\text{NH}_3\text{-N}$  concentration in runoff waters of different treatments were in descending order as IF-NM > OIF-NM > IF-M > OIF-M > CK, this regularity was reflected clearly in the 1st, 2nd, 3rd, 4th, 6th, 8th, 9th, 11th and 12th collections. Under the condition of no-mulching and mulching, the application of organic-inorganic nitrogen fertilizer decreased the  $\text{NH}_3\text{-N}$  concentration by 16.6% and 31.3% respectively when compared to only inorganic nitrogen fertilizer application. Under the application of inorganic and organic-inorganic nitrogen fertilizer, mulching decreased the  $\text{NH}_3\text{-N}$  concentration by 35.8% and 46.7% respectively when compared to no-mulching.

The accumulative amount of  $\text{NH}_3\text{-N}$  in runoff waters increased slowly during the previous seven collection times (Fig 5), and the increase extent were similar among the different cultural practices. However, in 8th collection, the accumulative amount of  $\text{NH}_3\text{-N}$  increased noticeably, and the differences among the treatments became manifest. After the 9th collection, the increase of accumulative amount of  $\text{NH}_3\text{-N}$  tended to be stably. The accumulative amount of  $\text{NH}_3\text{-N}$  in the runoff waters were 4.9-29.7

kg ha<sup>-1</sup> with different treatments in the 12th collection. Among the treatments of cultural practices, the no-mulching treatments of IF-NM and OIF-NM detected an obvious higher accumulative amount of NH<sub>3</sub><sup>-</sup>-N in comparison with the mulching treatments of IF-M and OIF-M. Besides, under the same cultivated condition, accumulative amount of NH<sub>3</sub><sup>-</sup>-N with the organic-inorganic nitrogen fertilizer application were found lower when compared to the only application of inorganic nitrogen fertilizer.

**Amount of nitrogen loss with different forms in the runoff waters.** The total N loss along with the runoff waters were 16.8-33.9 kg ha<sup>-1</sup> under different cultural practices (Table 3), and the total N loss originating from fertilizers were approximately 10.1-27.2 kg ha<sup>-1</sup>. This meant that 8.4-22.7% of the applied nitrogen was lost along with the runoffs. Among the total lost nitrogen, NH<sub>3</sub><sup>-</sup>-N occupied a maximum proportion of 73.1-87.6%, N in other forms occupied a proportion of 11.5-23.9%, while NH<sub>4</sub><sup>+</sup>-N occupied the lowest proportion of 0.9-2.7%.

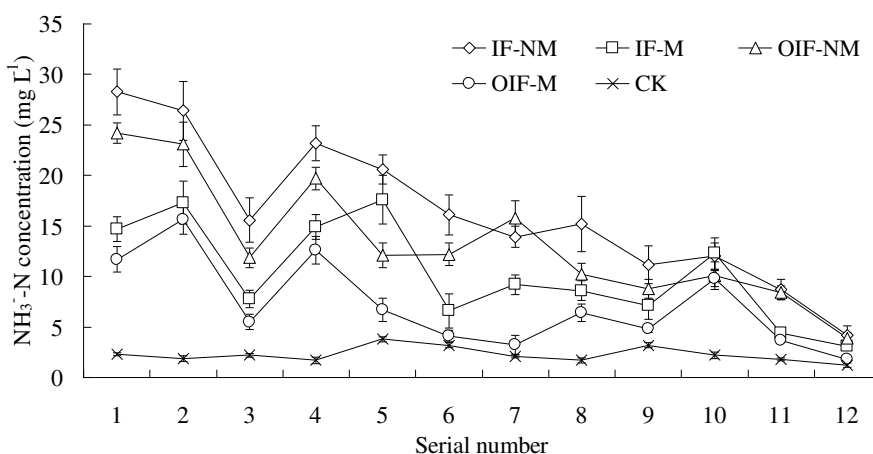


FIGURE 4

**The NH<sub>3</sub><sup>-</sup>-N concentration in runoff waters**

IF-NM, IF-M, OIF-NM, OIF-M and CK represented the five treatments of inorganic fertilizer with no mulching, inorganic fertilizer with mulching, organic-inorganic fertilizer with no mulching, organic-inorganic fertilizer with mulching and control, respectively. Runoff waters were collected twelve times in total, as reflected in the serial number.

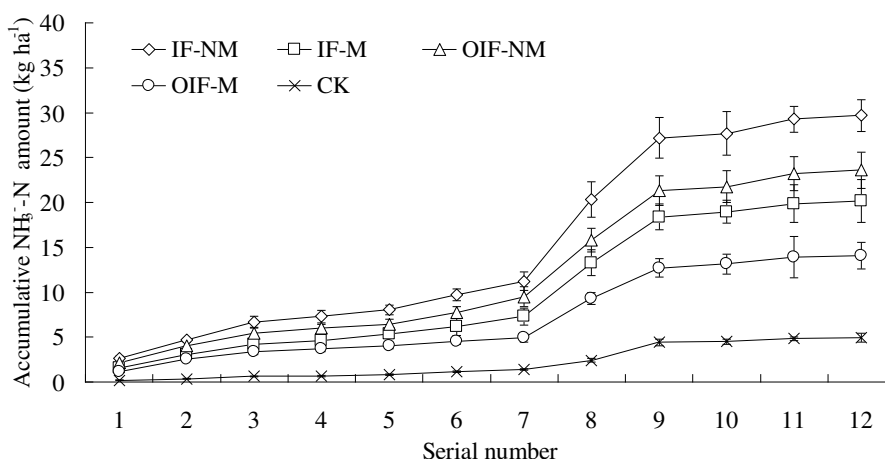


FIGURE 5

**The accumulative amount of NH<sub>3</sub><sup>-</sup>-N in runoff waters**

IF-NM, IF-M, OIF-NM, OIF-M and CK represented the five treatments of inorganic fertilizer with no mulching, inorganic fertilizer with mulching, organic-inorganic fertilizer with no mulching, organic-inorganic fertilizer with mulching and control, respectively. Runoff waters were collected twelve times in total, as reflected in the serial number.

**TABLE 3**  
**The amount of nitrogen loss in runoff waters with different forms**

Treatment	Total N (kg ha <sup>-1</sup> )	NH <sub>3</sub> <sup>-</sup> -N (kg ha <sup>-1</sup> )	NH <sub>4</sub> <sup>+</sup> -N (kg ha <sup>-1</sup> )	Mineral N (kg ha <sup>-1</sup> )	N in other forms (kg ha <sup>-1</sup> )
IF-NM	33.9±3.9a	29.7±1.8a	0.34±0.09a	30.0±1.4a	3.9±0.7a
IF-M	23.5±3.4b	20.2±2.4b	0.21±0.06ab	20.4±2.6b	3.1±0.4ab
OIF-NM	27.3±3.1b	23.6±2.0b	0.29±0.05ab	23.9±2.2b	3.4±1.1ab
OIF-M	16.8±2.0c	14.1±1.5c	0.16±0.04b	14.3±1.7c	2.5±0.3b
CK	6.7±0.6d	4.9±0.5d	0.18±0.04b	5.1±0.6d	1.6±0.3c

IF-NM, IF-M, OIF-NM, OIF-M and CK represented the five treatments of inorganic fertilizer with no mulching, inorganic fertilizer with mulching, organic-inorganic fertilizer with no mulching, organic-inorganic fertilizer with mulching and control, respectively. Each value is the mean ± SD (n = 3). Means followed by the same letter (a, b, c) do not differ significantly at the 0.05 level, according to Duncan's multiple range test.

Both the mulching and the application of organic-inorganic nitrogen fertilizer significantly ( $p < 0.05$ ) decreased the loss of total N and NH<sub>3</sub><sup>-</sup>-N in runoff waters. Compared to IF-NM, OIF-M decreased the loss of total N and NH<sub>3</sub><sup>-</sup>-N by 50.4% and 52.5% respectively. However, the loss of NH<sub>4</sub><sup>+</sup>-N and N in other forms were not significantly ( $p > 0.05$ ) influenced by the single use of the mulching or the organic-inorganic nitrogen fertilizer application, but were significantly ( $p < 0.05$ ) by the combined use of them. OIF-M decreased the loss of NH<sub>4</sub><sup>+</sup>-N and N in other forms by 52.9% and 35.9% respectively, when compared to IF-NM.

**Content of NH<sub>3</sub><sup>-</sup>-N and NH<sub>4</sub><sup>+</sup>-N in different soil layers.** Fig 6-a shows the NH<sub>3</sub><sup>-</sup>-N content in different soil layers. The NH<sub>3</sub><sup>-</sup>-N content in soils applied with nitrogen fertilizer was significantly ( $p < 0.05$ ) higher than that with no nitrogen fertilizer (CK). Under the same fertilizer application method, mulching significantly ( $p < 0.05$ ) increased NH<sub>3</sub><sup>-</sup>-N content in the plough layer (0-20 cm), and by 33.8% and 39.1% with the application of inorganic and organic-inorganic nitrogen fertilizer, respectively. Under the same cultivated condition, the application of organic-inorganic nitrogen fertilizer also significantly ( $p < 0.05$ ) increased NH<sub>3</sub><sup>-</sup>-N content in the plough layer, and was by 13.2% and 20.1% under the condition of no-mulching and mulching. The soil NH<sub>3</sub><sup>-</sup>-N content in the mulching treatments of IF-M and OIF-M decreased with the depth of soil layer. However, soil NH<sub>3</sub><sup>-</sup>-N content in IF-NM treatment presented an increasing trend, reaching maximum in the 40-60 cm soil layer. Besides, the soil NH<sub>3</sub><sup>-</sup>-N content in OIF-NM treatment increased first then decreased, which reached highest value in the 20-40 cm. Overall, the different cultural practices mainly affected NH<sub>3</sub><sup>-</sup>-N content in the relatively shallower

soil layer.

Fig 6-b shows the NH<sub>4</sub><sup>+</sup>-N content in different soil layers. Although the NH<sub>4</sub><sup>+</sup>-N content in the plough layer increased slightly under those treatments with mulching and organic-inorganic nitrogen fertilizer application, but the differences among different treatments were not significant ( $p > 0.05$ ). Similarly, the treatments also had no significant ( $p > 0.05$ ) effects on the NH<sub>4</sub><sup>+</sup>-N content in the 20-40 cm soil layer. Moreover, it could be found that the NH<sub>4</sub><sup>+</sup>-N content distributed evenly in different soil layers.

## DISCUSSION

In our study, precipitation amount was the primary impact factor of the runoff generation, a significant correlation between precipitation amount and runoff amount was detected (Fig 7). This agrees with Huang's [30] findings that rainfall regimes which have such features as high intensity, short duration and high frequency produce more runoff. Different methods of nitrogen fertilizer application had no clear effects on the runoff volume. However, mulching obviously increased the runoff volume under both the inorganic and the organic-inorganic fertilizer treatments (by 13.2% and 11.8%, respectively), which confirmed the results of the earlier studies [31,32,33]. Moreover, the observed results (Table 2) also proved that mulching could increase the runoff coefficient and accelerate the runoff generation, particularly during the high-intensity precipitation process. The study carried out by Zhang [34] indicated that the wide-plastic-mulch treatment significantly ( $P < 0.05$ ) reduced runoff compared to the narrow-plastic-mulch treatment.

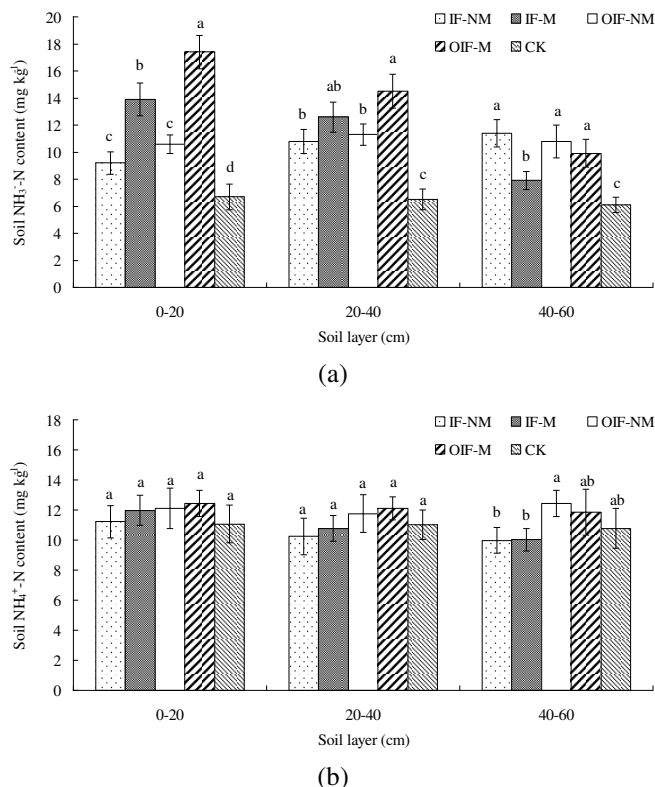


**FIGURE 6**  
**The content of NH<sub>3</sub><sup>-</sup>-N and NH<sub>4</sub><sup>+</sup>-N in different soil layers**

IF-NM, IF-M, OIF-NM, OIF-M and CK represented the five treatments of inorganic fertilizer with no mulching, inorganic fertilizer with mulching, organic-inorganic fertilizer with no mulching, organic-inorganic fertilizer with mulching and control, respectively. Each value is the mean ± SD (n =3). Means followed by the same letter (a, b, c) do not differ significantly at the 0.05 level, according to Duncan’s multiple range test.

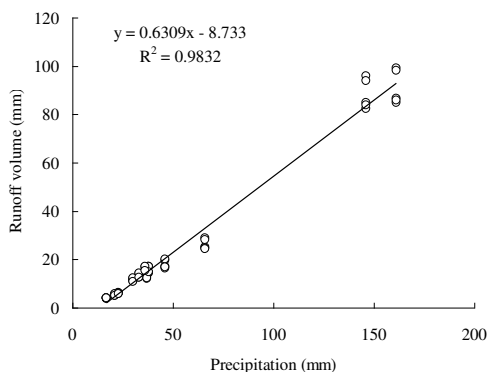


**FIGURE 7**  
**Relationship between the volume of precipitation and runoff**

The high concentration of NH<sub>3</sub><sup>-</sup>-N in runoff waters that observed at the 1st collection mainly caused by the applied basal fertilizer. And at the 4th collection, NH<sub>3</sub><sup>-</sup>-N concentration was detected to present an obvious rising trend. It should be noticed that the 4th collection was carried out from 30 to 31

DAT, which was the closest to the date of additional fertilizer application (29 DAT). This information suggested that the NH<sub>3</sub><sup>-</sup>-N concentration in our study mainly decided by the time of both basal and additional fertilizer application. Similar study by Moriasi [35] pointed out that the reduction in nitrogen application rate yielded great reduction in NO<sub>3</sub><sup>-</sup>-N losses. Also the study by Davis [36] indicated that runoff soon after fertilizer application resulted in highest losses of the soluble nitrogen. However, no obvious relationship was found between precipitation amount and the NH<sub>3</sub><sup>-</sup>-N concentration.

Our study found a satisfactory decreasing-effect of NH<sub>3</sub><sup>-</sup>-N concentration under the mulching condition, this agrees with the findings of Yagioka [37]. Although the organic-inorganic nitrogen fertilizer application also decreased the concentration of NH<sub>3</sub><sup>-</sup>-N in runoff waters, the effectiveness was not better than that of mulching. Coupling effects of mulching and organic-inorganic nitrogen fertilizer application (OIF-M) was the optimal in decreasing NH<sub>3</sub><sup>-</sup>-N concentration

compared to other cultural practices. These regularities indicated that mulching was the first choice to control  $\text{NH}_3\text{-N}$  concentration, where possible, organic-inorganic compound fertilizer should be adopted to reach a better decreasing effect. The accumulative amount of  $\text{NH}_3\text{-N}$  at 8th collection increased dramatically, indicating that a higher volume of runoff water resulted in higher  $\text{NH}_3\text{-N}$  loss. The 9th observation on the runoff losses of  $\text{NH}_3\text{-N}$  also supported this conclusion.

Judging by the comparative results on the amount of nitrogen in the different forms (Table 3),  $\text{NH}_3\text{-N}$  occupied a maximum proportion of more than 70% for the total loss of nitrogen, which highlight the importance of nitrate nitrogen fertilizer application and management. Differences of the amount of  $\text{NH}_4^+\text{-N}$  in runoff waters under different cultural practices were not as significant as that of  $\text{NH}_3\text{-N}$ , while the  $\text{NH}_4^+\text{-N}$  was also significantly ( $p < 0.05$ ) decreased by OIF-M (compared to IF-NM), as well as the N in other forms. This reflected that OIF-M had advantages in reducing runoff losses of nitrogen for the different forms.

Precipitation in our study distributed unevenly during the whole growth period. The amount of precipitation during maturity stage accounted for nearly half of the total amount. Although this was unfavorable for the growth, development and maturation of the tobaccos, it was beneficial for reducing runoff losses of nitrogen since fertilizations were conducted in the early growth period which dodged the heavy precipitation in maturity stage. Our study found that 8.4-22.7% of the applied nitrogen was lost along with the runoffs, the proportion was less than that in the similar study conducted by Wang [38], mainly because that high-intensity precipitation occurred during the period of fertilization in Wang's experiment. Our study revealed that mulching could decrease the runoff losses of nitrogen, which could be explained by two reasons: firstly, mulching reduced the opportunity of the fertilizer nitrogen that exposed to runoffs; secondly, mulching increased the nitrogen amount that absorbed by tobaccos (Fig 8), indirectly reducing the nitrogen loss. Previous studies showed that mulching could improve the micro-environment of root zone thus provide a favorable condition for crop [39]. Meanwhile, mulching also resulted in higher mineralization of nitrogen [40] and less leaching of mineral nitrogen [41], consequently increased the nitrogen use efficiency of crops. Besides, in our study, application of inorganic-organic fertilizer also increased the absorbed amount

of fertilizer nitrogen by crops (Fig 8) and reduced total nitrogen loss (Table 3), similar results were also obtained by the experiment conducted in the tobacco-cultivated area of southern China [42]. Possibly, the organic-inorganic compound fertilizer application promoted soil biological activity, enhanced the soil microbial biomass [43], thus increased nitrogen amount that immobilized by microorganisms [44]. The study in Taihu Lake basin of China showed that the application of organic fertilizer reduced the nitrogen runoff loss by 15.70–18.14% compared to conventional fertilizer application, and organic-inorganic compound fertilizer reduced nitrogen runoff loss by 27.37–36.27% compared with conventional fertilizer [45]. Zhang [46] reported that the combined application of arbuscular mycorrhizal fungi and normal fertilizer was observed to reduce nitrogen runoff by 27.2%.

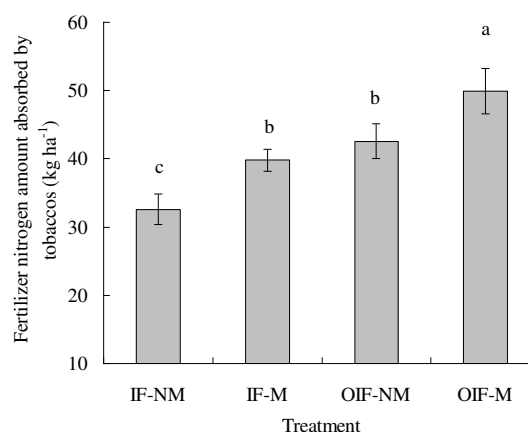


**FIGURE 8**  
**Fertilizer nitrogen amount that absorbed by tobacco plants with different treatments**

IF-NM, IF-M, OIF-NM, OIF-M and CK represented the five treatments of inorganic fertilizer with no mulching, inorganic fertilizer with mulching, organic-inorganic fertilizer with no mulching, organic-inorganic fertilizer with mulching and control, respectively. Each value is the mean  $\pm$  SD ( $n = 3$ ). Means followed by the same letter (a, b, c) do not differ significantly at the 0.05 level, according to Duncan's multiple range test.

Mulching increased  $\text{NH}_3\text{-N}$  content (Fig 6) in plough layer, and effectively prevent  $\text{NH}_3\text{-N}$  from moving into the deeper soil layer, while which had no clear effects on the  $\text{NH}_4^+\text{-N}$  content. The application of organic-inorganic nitrogen fertilizer



could also increased the  $\text{NH}_3\text{-N}$  content in plough layer, but it had little influences on the profile distribution of both  $\text{NH}_3\text{-N}$  and  $\text{NH}_4^+\text{-N}$ . Demurtas [47] noted that the  $\text{NH}_3\text{-N}$  leaching in autumn–winter could not be easily controlled by nitrogen fertilizer management because it was mainly associated to the natural water surplus and the low nitrogen uptake from the winter crop.

In the tobacco-cultivated areas of eastern and southern China, ridge planting was a common cultivation method for the flue-cured tobaccos. However, large quantities of fertilizer nitrogen that leached into the ditch were lost with the runoff waters, resulting in a low nitrogen use efficiency and serious environmental problems [48]. Our study proved that single application of mulching or organic-inorganic fertilizer could effectively reduce the runoff losses of nitrogen, while combined use of mulching and organic-inorganic nitrogen fertilizer application obtained the optimal effects. Our experiment was carried out in eastern China, where has a subtropical climate. Similar studies related to the climate factors needs to be conducted in the future.

## CONCLUSION

The main nitrogen form in runoff waters was  $\text{NH}_3\text{-N}$ . The concentration of  $\text{NH}_3\text{-N}$  in runoff waters correlated closely to the time of both basal and additional fertilizer application. Mulching increased the runoff volume by 12.5% while decreased the  $\text{NH}_3\text{-N}$  concentration, overall reduced the accumulative amount of  $\text{NH}_3\text{-N}$  and significantly ( $p < 0.05$ ) decreased the amount of total N in runoff waters. The combined application of organic and inorganic nitrogen fertilizer also reduced the concentration of  $\text{NH}_3\text{-N}$  and the amount of  $\text{NH}_3\text{-N}$  and total N, but the effectiveness was not as good as that of mulching. Mulching combined with the organic-inorganic fertilizer application (OIF-M) reduced the runoff losses of total N by 50.4%,  $\text{NH}_3\text{-N}$  by 52.5%,  $\text{NH}_4^+\text{-N}$  by 52.9% and the N in other forms by 35.9%, and was proved to be optimal in decreasing the runoff losses of nitrogen among the different treatments. This mainly because that OIF-M was more conducive to reserve the  $\text{NH}_3\text{-N}$  in soils and increase crop nitrogen use efficiency. Therefore, we highlight the importance of mulching in reducing the nitrogen loss in runoffs and recommend similar areas to use organic-inorganic compound fertilizer under a mulch-cultivated

condition.

## ACKNOWLEDGEMENTS

This work was financed by the Young Talent Project of Horticultural College of Fujian A&F University (received by Hou Maomao), the Natural Science Foundation of Fujian Province (2016J05069), the Natural Science Foundation of China (20145039011), the Postdoctoral Funds of Fujian A&F University (received by Hou Maomao) and the Open Foundation of Key Laboratory of Efficient Irrigation-Drainage and Agricultural Soil-Water Environment in Southern China (E2015002).

## REFERENCES

- [1] Sharratt B, Strom L, Pressley S. (2015) Nitrogen loss from windblown agricultural soils in the Columbia Plateau. *Aeolian Research* 18, 47-53.
- [2] Oygarden L, Deelstra J, Lagzdins A, Bechmann M, Greipsland I, et al. (2014) Climate change and the potential effects on runoff and nitrogen losses in the Nordic–Baltic region. *Agriculture, Ecosystems & Environment* 198, 114-126.
- [3] Povilaitis A, Sileika A, Deelstra J, Gaigalis K, Baigys G. (2014) Nitrogen losses from small agricultural catchments in Lithuania. *Agriculture, Ecosystems & Environment* 198, 54-64.
- [4] Kringel R, Rechenburg A, Kuitcha D, Fouepe A, Bellenberg S, et al. (2016) Mass balance of nitrogen and potassium in urban groundwater in Central Africa, Yaounde/Cameroon. *Science of the Total Environment* 547, 382-395.
- [5] Iqbal S, Guber AK, Khan HZ. (2016) Estimating nitrogen leaching losses after compost application in furrow irrigated soils of Pakistan using HYDRUS-2D software. *Agricultural Water Management* 168, 85-95.
- [6] Cao D, Cao W, Fang J, Cai L. (2014) Nitrogen and phosphorus losses from agricultural systems in China: A meta-analysis. *Marine Pollution Bulletin* 85, 727-732.
- [7] Wang G, Chen X, Cui Z, Yue S, Zhang F. (2014) Estimated reactive nitrogen losses for intensive maize production in China. *Agriculture, Ecosystems & Environment* 197, 293-300.
- [8] Gao S, Xu P, Zhou F, Yang H, Zheng C, et al. (2016) Quantifying nitrogen leaching response to fertilizer additions in China's cropland.



- Environmental Pollution 211, 241-251.
- [9] Xiong-hui JI, Sheng-xian Z, Yan-hong LU, Yulin L. (2007) Study of Dynamics of Floodwater Nitrogen and Regulation of Its Runoff Loss in Paddy Field-Based Two-Cropping Rice with Urea and Controlled Release Nitrogen Fertilizer Application. *Agricultural Sciences in China* 6, 189-199.
- [10] Southwick LM, Willis GH, Bengtson RL. (1993) Runoff Losses Of Norflurazon - Effect Of Runoff Timing. *Journal of Agricultural and Food Chemistry* 41, 1503-1506.
- [11] Choudri BS, Baawain M. (2014) Effects of Pollution on Freshwater Organisms. *Water Environment Research* 86, 1832-1868.
- [12] Xi-Yuan W, Zhang L-P, Fu X-T, Wang X-Y, Zhang H-S. (2011) Nitrogen loss in surface runoff from Chinese cabbage fields. *Physics and Chemistry of the Earth, Parts A/B/C* 36, 401-406.
- [13] Gafur A, Jensen JR, Borggaard OK, Petersen L. (2003) Runoff and losses of soil and nutrients from small watersheds under shifting cultivation (Jhum) in the Chittagong Hill Tracts of Bangladesh. *Journal of Hydrology* 274, 30-46.
- [14] Ramos MC, Martínez-Casasnovas JA. (2006) Nutrient losses by runoff in vineyards of the Mediterranean Alt Penedès region (NE Spain). *Agriculture, Ecosystems & Environment* 113, 356-363.
- [15] Wu W, Tang X-P, Yang C, Liu H-B, Guo N-J. (2013) Investigation of ecological factors controlling quality of flue-cured tobacco (*Nicotiana tabacum* L.) using classification methods. *Ecological Informatics* 16, 53-61.
- [16] Karaivazoglou NA, Tsotsolis NC, Tsadilas CD. (2007) Influence of liming and form of nitrogen fertilizer on nutrient uptake, growth, yield, and quality of Virginia (flue-cured) tobacco. *Field Crops Research* 100, 52-60.
- [17] Yunju L, Kahr F, Jianjun P, Roland-Holst D, Yufang S, et al. (2012) Fertilizer use patterns in Yunnan Province, China: Implications for agricultural and environmental policy. *Agricultural Systems* 110, 78-89.
- [18] Zhang S, Gao P, Tong Y, Norse D, Lu Y, et al. (2015) Overcoming nitrogen fertilizer over-use through technical and advisory approaches: A case study from Shaanxi Province, northwest China. *Agriculture, Ecosystems & Environment* 209, 89-99.
- [19] Gong Y (2008) Nitrogen loss in tobacco areas of southern China that suffered from excessive rainfall: Beijing.
- [20] Xia L-Z, Liu G-H, Wu Y-H, Ma L, Li Y-D. (2015) Protection Methods to Reduce Nitrogen and Phosphorus Losses from Sloping Citrus Land in the Three Gorges Area of China. *Pedosphere* 25, 478-488.
- [21] Chilundo M, Joel A, Westrom I, Brito R, Messing I. (2016) Effects of reduced irrigation dose and slow release fertiliser on nitrogen use efficiency and crop yield in a semi-arid loamy sand. *Agricultural Water Management* 168, 68-77.
- [22] Cavalli D, Cabassi G, Borrelli L, Geromel G, Bechini L, et al. (2016) Nitrogen fertilizer replacement value of undigested liquid cattle manure and digestates. *European Journal of Agronomy* 73, 34-41.
- [23] Gu L, Liu P, Shao L, Wang J, Dong S, et al. (2014) A lysimeters study of Chinese wheat and maize varieties: I. The lysimeters-rain shelter facility and the growth and water use of wheat. *Soil and Tillage Research* 144, 133-140.
- [24] Peyton DP, Healy MG, Fleming GTA, Grant J, Wall D, et al. (2016) Nutrient, metal and microbial loss in surface runoff following treated sludge and dairy cattle slurry application to an Irish grassland soil. *Science of The Total Environment* 541, 218-229.
- [25] Hou MM, Shao XH, Chen LH, Chang TT, Wang WN, et al. (2012) Study on fertilizer N leaching, accumulation, and balance in tobacco fields with N-15 tracing technique. *Journal of Food Agriculture & Environment* 10, 1284-1289.
- [26] Ojeda G, Tarrason D, Ortiz O, Alcaniz JM. (2006) Nitrogen losses in runoff waters from a loamy soil treated with sewage sludge. *Agriculture, Ecosystems & Environment* 117, 49-56.
- [27] Hou MM, Shao XH, Li YY. (2013) Effects of water and N-15-labelled fertilizer coupling on the growth, N uptake, quality and yield, of flue-cured tobaccos : A two-year lysimeter experiment. *Research on Crops* 14, 950-959.
- [28] Hou M, Shao X, Jin Q, Gao X. (2016) A 15N tracing technique-based analysis of the fate of fertilizer N: a 4-year case study in eastern China. *Archives of Agronomy and Soil Science* 1-10.
- [29] Hou M, Shao X, Zhai Y, Yuan Y, Ding F. (2016) Analysis on reutilization characters of fertilizer N in tobacco field with 15N tracing technique. *Nongye Gongcheng Xuebao/Transactions of the Chinese Society of Agricultural Engineering* 32, 118-123.

- [30] Huang ZG, Ouyang ZY, Li FR, Zheng H, Wang XK. (2010) Response of runoff and soil loss to reforestation and rainfall type in red soil region of southern China. *Journal of Environmental Sciences* 22, 1765-1773.
- [31] Tesfahuney WA, Van Rensburg LD, Walker S. (2013) In-field runoff as affected by runoff strip length and mulch cover. *Soil and Tillage Research* 131, 47-54.
- [32] Prats SA, MacDonald LH, Monteiro M, Ferreira AJD, Coelho COA, et al. (2012) Effectiveness of forest residue mulching in reducing post-fire runoff and erosion in a pine and a eucalypt plantation in north-central Portugal. *Geoderma* 191, 115-124.
- [33] Prosdocimi M, Jordan A, Tarolli P, Keesstra S, Novara A, et al. (2016) The immediate effectiveness of barley straw mulch in reducing soil erodibility and surface runoff generation in Mediterranean vineyards. *Science of the Total Environment* 547, 323-330.
- [34] Zhang G, Zhang X, Hu X. (2013) Runoff and soil erosion as affected by plastic mulch patterns in vegetable field at Dianchi lake's catchment, China. *Agricultural Water Management* 122, 20-27.
- [35] Moriasi DN, Gowda PH, Arnold JG, Mulla DJ, Ale S, et al. (2013) Modeling the impact of nitrogen fertilizer application and tile drain configuration on nitrate leaching using SWAT. *Agricultural Water Management* 130, 36-43.
- [36] Davis AM, Tink M, Rohde K, Brodie JE. (2016) Urea contributions to dissolved 'organic' nitrogen losses from intensive, fertilised agriculture. *Agriculture, Ecosystems & Environment* 223, 190-196.
- [37] Yagioka A, Komatsuzaki M, Kaneko N, Ueno H. (2015) Effect of no-tillage with weed cover mulching versus conventional tillage on global warming potential and nitrate leaching. *Agriculture, Ecosystems & Environment* 200, 42-53.
- [38] Wang J. (2010) Influence of different planting methods on runoff losses of nitrogen in tobacco field soils *Journal of soil and water conservation* 24, 68-73.
- [39] Liu Q, Chen Y, Liu Y, Wen X, Liao Y. (2016) Coupling effects of plastic film mulching and urea types on water use efficiency and grain yield of maize in the Loess Plateau, China. *Soil and Tillage Research* 157, 1-10.
- [40] Mohanty S, Nayak AK, Kumar A, Tripathi R, Shahid M, et al. (2013) Carbon and nitrogen mineralization kinetics in soil of rice-rice system under long term application of chemical fertilizers and farmyard manure. *European Journal of Soil Biology* 58, 113-121.
- [41] Zhang H, Liu Q, Yu X, Lü G, Wu Y. (2012) Effects of plastic mulch duration on nitrogen mineralization and leaching in peanut (*Arachis hypogaea*) cultivated land in the Yimeng Mountainous Area, China. *Agriculture, Ecosystems & Environment* 158, 164-171.
- [42] Li Y. (2009) Effects of Different Fertilizer Ratio on Nutrient Leaching in Tobacco Fields of South China. *Chinese Tobacco Science* 30, 47-52.
- [43] Zhao J, Ni T, Li J, Lu Q, Fang Z, et al. (2016) Effects of organic-inorganic compound fertilizer with reduced chemical fertilizer application on crop yields, soil biological activity and bacterial community structure in a rice-wheat cropping system. *Applied Soil Ecology* 99, 1-12.
- [44] Liang B, Zhao W, Yang X, Zhou J. (2013) Fate of nitrogen-15 as influenced by soil and nutrient management history in a 19-year wheat-maize experiment. *Field Crops Research* 144, 126-134.
- [45] Shan L, He Y, Chen J, Huang Q, Lian X, et al. (2015) Nitrogen surface runoff losses from a Chinese cabbage field under different nitrogen treatments in the Taihu Lake Basin, China. *Agricultural Water Management* 159, 255-263.
- [46] Zhang S, Wang L, Ma F, Zhang X, Fu D. (2016) Reducing nitrogen runoff from paddy fields with arbuscular mycorrhizal fungi under different fertilizer regimes. *Journal of Environmental Sciences* 3, 11-19.
- [47] Demurtas CE, Seddaiu G, Ledda L, Cappai C, Doro L, et al. (2016) Replacing organic with mineral N fertilization does not reduce nitrate leaching in double crop forage systems under Mediterranean conditions. *Agriculture Ecosystems & Environment* 219, 83-92.
- [48] Tian Y-H, Yin B, Yang L-Z, Yin S-X, Zhu Z-L. (2007) Nitrogen Runoff and Leaching Losses During Rice-Wheat Rotations in Taihu Lake Region, China\*. *Pedosphere* 17, 445-456.



---

**Received:** 30.03.2016

**Accepted:** 18.10.2016

---

**CORRESPONDING AUTHOR**

---

**Hou Maomao**

Postdoctoral Research Center

College of Horticulture

Fujian Agriculture and Forestry University

Fuzhou 350002 – CHINA

E-mail: njhoumaomao@126.com



# CHANGE IN ECOSYSTEM CARBON STORAGE OF THE MANGROVE FOREST ALONG THE CHINESE COAST BETWEEN 1990 AND 2010

Gang Wang<sup>1, 2, 3</sup>, Dongsheng Guan<sup>2, 3\*</sup>, Mervyn R Peart<sup>4</sup>, Rongbo Xiao<sup>1</sup>, Qiuping Zhang<sup>5</sup>

<sup>1</sup>Guangdong Provincial Academy of Environment Science, Guangzhou 510045, China

<sup>2</sup>School of Environmental Science and Engineering, Sun Yat-sen University, Guangzhou 510275, China

<sup>3</sup>Guangdong Provincial Key Laboratory of Environmental Pollution Control and Remediation Technology, Guangzhou 510275, China

<sup>4</sup>Department of Geography, University of Hong Kong, Hong Kong

<sup>5</sup>School of Life Science, Sun Yat-sen University, Guangzhou 510275, China

## ABSTRACT

Mangrove forests provide important ecological services, and play a critical role in global carbon cycling. Although temporal changes in ecosystem carbon storage have been assessed in upland forests, there has been a lack of scientific evaluation of such change in mangrove forests. In this study, in order to overcome the shortage of soil organic carbon (SOC) data for estimating SOC storage, a simple linear regression equation between vegetation biomass and SOC density ( $R = 0.697$ ,  $P < 0.01$ ,  $N = 39$ ) was derived to quantify the change of ecosystem carbon storage by combining field measurements with data from the published literature. Significant correlation was found between vegetation biomass and SOC concentration of the surface soil layer in the mangrove forests. Ecosystem carbon storage increased from 1037.55 Gg in 1990 to 1449.96 Gg in 2010, with an average carbon accumulation of 111.53 Gg/year in the mangrove forests along the Chinese coast. Ecosystem carbon density increased from 280.56 t/ha in 1990 to 299.14 t/ha in 2010, with an average carbon uptake of 0.93 t/(ha·year). Average carbon accumulation rate in the soil accounted for more than 80% of the total carbon accumulation rate. Mangrove forests accumulate more ecosystem carbon in comparison with other types of forests located at the same latitudes. Our results suggest that afforestation and reforestation will increase carbon sequestration in the mangrove forests along the Chinese coast, as both vegetation carbon and SOC storage increased in association with biomass growth.

## KEYWORDS:

mangrove forest, ecosystem carbon storage, soil organic carbon (SOC), carbon accumulation, Chinese coast

## INTRODUCTION

Carbon storage and fluxes of mangrove forests have attracted worldwide attention because of their potential to act as “blue carbon” sinks in the global carbon cycle [1, 2]. This reflects the fact that mangrove forests are responsible for about 10% of the global organic carbon burial and export [3] whilst only accounting for less than 0.1% of the earth’s continental surface [4]. Moreover, their ecosystem carbon stocks (both accumulated in vegetation biomass and soil) are among the highest of any forest type [5]. Since mangrove forests exchange large amounts of CO<sub>2</sub> with the atmosphere through respiration and photosynthesis, they have a large potential to sequester significant amounts of CO<sub>2</sub> in both vegetation biomass and soil [6-8]. Obviously, estimates of temporal changes in ecosystem carbon storage are useful for understanding carbon dynamics associated with forest changes or land-use conversion [9, 10]. However, most of the studies on ecosystem carbon storage have been targeted at terrestrial forest ecosystems [11, 12], rather than mangrove forests. This is because current approaches to quantifying the temporal changes in ecosystem carbon storage through field survey are very laborious, time-consuming and destructive [13].

Mangrove forests are mainly located along tropical and subtropical coastlines. As a result of conversion to other uses around the world, mangrove forests have been dramatically degraded and their area has been substantially reduced [14]. The annual areal loss rate of mangrove forests is estimated at around 1%~2%, and this rate exceeds the deforestation rates of inland tropical forests [2]. In China, mangrove forest area decreased from 50, 000 ha to 17, 874 ha as a result of long-term land reclamation, aquaculture, and port and wharf construction in the last century [15]. Since the important ecological and economic values of mangrove forests were recognized by the Chinese government in the early 1990s, China’s Biodiversity

Conservation Action Plan has increased mangrove conservation areas [16]. It is expected that protection of the mangrove forests over last two decades will have positive effects on the biological environment (e.g. increasing of ecosystem carbon storage). Quantification of these impacts will provide important guidelines for designing future protection strategies to increase ecosystem carbon storage [6].

Temporal changes in forest ecosystem carbon storage have usually been studied using data from the national forest and soil surveys in China, based on the continuous biomass expansion factor (BEF) method in association with the Geographic Information System (GIS) [17-19]. Ironically, both BEF and GIS methods cannot be used to identify the carbon dynamics of mangrove forests because mangrove forests were excluded from national forest and soil survey in China [4]. Consequently, little is known about carbon storage in the mangrove forests of South China, which has limited our capacity for evaluating the carbon budget at the national scale [19]. Fortunately, analysis of published data combined with additional field-sampling data can be considered an effective method for estimating the carbon storage or carbon dynamics in mangrove forests at the global or regional scale [4, 14].

Previous studies have shown that soil organic carbon (SOC) content was positively correlated with vegetation biomass in both upland forests and mangrove forests [7, 20]. It was also noted that there was insufficient SOC data to estimate SOC storage and dynamics in China for mangrove forests. Consequently, in this study, a linear regression equation was built using data from direct field measurement of vegetation biomass and SOC density in mangroves along the Chinese coastline. This linear regression equation was used to overcome the shortage of SOC data for estimating SOC storage in mangroves. Thus, national ecosystem carbon storage (vegetation biomass carbon plus SOC) and its dynamic changes in mangrove forests in China could be estimated using the empirical regression equation. This would be helpful for evaluating the effectiveness of the Governments afforestation efforts and designing future management policy for mangrove forests in China.

## MATERIALS AND METHODS

**Description of mangroves along Chinese coast.** The area of interest includes the mangrove forests of Taiwan and Zhejiang, Fujian, Guangxi,

Guangdong and Hainan provinces along the Chinese coast (extending from 18°N to 30°N, as shown in Fig. 1). There are thirty-eighth mangrove species documented, representing 20 families and 25 genera with thermophile eurytopic species being the dominant components [15]. Species richness is higher in the lower-latitude provinces than in the higher-latitude provinces (Table 1). Since the 1990s, the Chinese government has made a huge effort to restore mangrove forest in order to construct a green screen along the coastline [7], and thus the area of mangrove forest has been increased from 17874 ha in 1990 to 23413 ha in 2010. According to the National Mangrove Resource Inventory Report in 2002 [21], the main mangrove species are *Avicennia marina*, *Aegiceras corniculatum*, *Kandelia obovata*, *Rhizophora stylosa*, *Bruguiera gymnorrhiza*, *Bruguiera sexangula*, *Sonneratia caseolares*, *Sonneratia apetala*, respectively. These mangrove species accounted for more than 80% of mangrove area. Most of the mangrove forests are monospecific communities [4] and the proportion of different mangrove communities is shown in Fig 2.

**Data source.** Data with lower-case letters a, b and c were collected from [15], [22] and [23], respectively; Data with lower-case letters d and e give the number of field sampling sites in 1990 and 2010, respectively.

Data on the various mangrove forest communities were collected from four sources, namely: 1) published vegetation biomass and SOC data in the literature, 2) data collected and measured by ourselves for this study in both 1990 and 2010, 3) SOC data estimated using the regression equation between SOC density and vegetation biomass, and 4) the National Mangrove Resources Inventory Report of 2002. The National Mangrove Resources Inventory Report of 2002 was used to estimate the proportion of the dominant community types, as mentioned above. Ecosystem carbon storage includes carbon accumulated in both the vegetation biomass and soil. The first source on ecosystem carbon storage of mangrove forests in China was collected from “Google Scholar Database” and “China Knowledge Resource Integrated Database”. The second source, a direct forest inventory was carried out by this study. Using either previously published data or measured data from the forest inventory for the different mangrove communities, a regression equation was built to estimate the SOC density according to vegetation biomass and which will be discussed in more detail in section 2.4. The number of field sampling sites for 1990 and 2010 respectively, are given in Table 1.

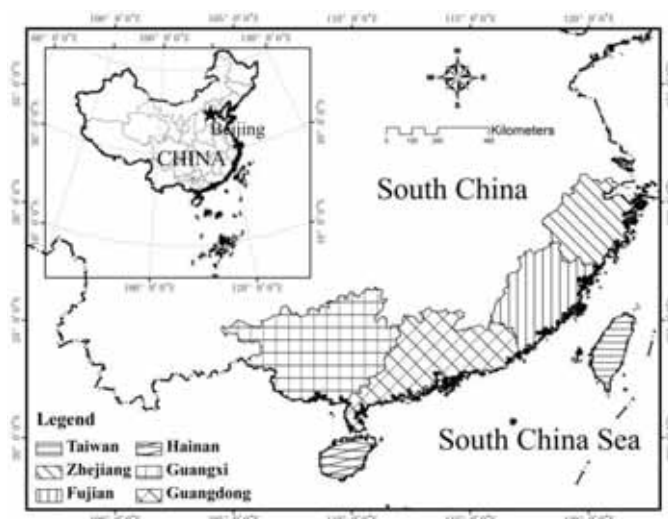


**FIGURE 1**  
Mangrove distribution in six provinces (Taiwan, Zhejiang, Fujian, Guangxi, Guangdong and Hainan) along the Chinese coast

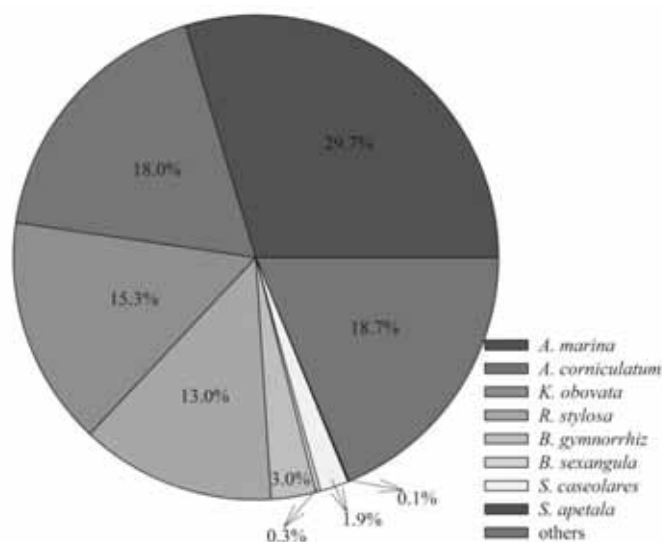


**FIGURE 2**  
The proportion of different mangrove communities along the Chinese coast

#### Field investigation and laboratory analysis.

Similar to the assessment of upland forest ecosystem carbon dynamics, both geographical and species factors were taken into consideration in the sampling design for fieldwork [4]. In April of 2012 and 2013, at least three quadrats were established at each sampling site. Both aboveground and belowground biomass and SOC density were measured in each quadrat. The final data base include 291 sites for biomass measurement (147 sites were sampled in this study, and the others were reported, and derived from, the literature), and 96 sites for SOC measurement (30 sites were sampled in this study, and the others were reported in the literature).

At the 147 sites sampled for biomass in this study, 10 m×10 m quadrats were established to determine the structures and standing biomass of the different mangrove communities. Within each quadrat, all trees were identified and the number of trees of each species and tree height were recorded. Tree diameter of *S. apetala* and *S. caseolaris* was measured at the breast height 1.3m (DBH). Stem basal diameter ( $D_0$ ) of *A. marina*, *A. corniculatum*, *K. obovata* and *B. gymnorrhiz* was measured. DBH of *R. stylosa* was measured above the highest prop-root when this grew from the stem at a height over 1.3 m [7]. Species-specific allometric equations as shown in [4] were used to determine the aboveground and belowground biomass of different

**TABLE 1**  
**Mangrove species, area and number of field sampling sites used for the determination of vegetation biomass and SOC.**

Location	Area (ha)		Number of species	Number of sites from which biomass and soil organic carbon data were obtained	
	1990 <sup>a</sup>	2010 <sup>b</sup>		Biomass	SOC
Hainan Province	4836	3930	38	16 <sup>d</sup> +6 <sup>e</sup>	15 <sup>e</sup>
Guangdong Province	7787	9414	23	32 <sup>d</sup> +150 <sup>e</sup>	49 <sup>e</sup>
Guangxi Province	4523	8375	19	21 <sup>d</sup>	7 <sup>d</sup> +5 <sup>e</sup>
Fujian Province	260	912	18	11 <sup>d</sup> +34 <sup>e</sup>	4 <sup>d</sup> +2 <sup>e</sup>
Zhejiang Province	8.4	22	19	3 <sup>e</sup>	—
Hong Kong	276	380	16	—	1 <sup>e</sup>
Macau	64	60	8	—	—
Taiwan Province	120	320 <sup>c</sup>	19	4 <sup>d</sup>	—
Total	17874	23413	38	277	83

mangrove species. Different mangrove forest types have differing conversion rates between biomass and carbon density because of various factors such as community composition, age structure, stand origins, and so on. These conversion rates usually range from 0.41 to 0.48 [24, 25] and this study calculated a conversion rate of 0.45.

At the same time as the biomass survey, soil samples were collected to determine SOC concentration and SOC density using a stainless steel corer of 5 cm diameter. Within each plant quadrat, three soil samples were collected from each 10-cm layer for the top 50 cm (five layers), while 50-70 cm and 70-100 cm soil layers were also sampled. For each soil sample, soil bulk density was calculated as the ratio of soil dry weight to the soil cutting ring's volume. The soil samples were air dried and then three soil samples collected from the same quadrat, were mixed and sieved to 0.15 mm after plant residues, including roots, were sorted out. SOC concentration was determined by wet combustion with  $K_2Cr_2O_7$  [26]. Average density of soil organic carbon (SOCD) for the top 100 cm of the soil profile was estimated using the following formula:

$$SOCD = \sum_{i=1}^n T_i \times \theta_i \times C_i \times (1 - \delta_i\%) / 10 \quad (1)$$

Where  $n$  denotes the number of soil layers involved,  $\delta_i\%$  is the gravel content (>2mm) in the soil layer  $i$ ,  $\theta_i$  signifies the bulk density of the soil layer  $i$  ( $g \cdot cm^{-3}$ ),  $C_i$  represents the organic carbon concentration in the soil layer  $i$  ( $g \cdot kg^{-1}$ ), and  $T_i$  stands for the thickness of the soil layer  $i$  (cm).

**Building a regression equation between vegetation biomass and SOC.** The aforementioned data on vegetation biomass, SOC concentration and SOC density were statistically analyzed by the software SPSS 19.0. Regression equations and their coefficients of correlation between SOC density and

vegetation biomass were used to determine the SOC density where only vegetation biomass was measured in this and previous studies. Coefficients of correlation between SOC concentration and changes of vegetation biomass and latitude were also determined. Other statistical characteristics of the collected data base, such as the mean and standard deviation, were also analyzed using SPSS 19.0 software.

**Estimated ecosystem carbon density and ecosystem carbon storage for China.** Biomass carbon density (BCD) plus SOC density (SOCD) was used to determine the ecosystem carbon density (ECD) of each mangrove community. Thus, ecosystem carbon storage (ECS) was estimated using the following formula:

$$ECS = \sum (SOCD + BCD) \times S \quad (2)$$

Where  $S$  signifies the area of different forest communities. Although ecosystem carbon density may be affected by both the geographical location and community types [7], only the effect of different community types was taken into consideration in this study.

## RESULTS

**Regression equation between vegetation biomass and SOC.** As vegetation biomass experiences growth, both SOC concentration and SOC density also increase (Fig. 3 and Fig. 4). It is shown in Fig. 3, that the SOC concentration of the surface soil layer was positively correlated with aboveground biomass, belowground biomass and total vegetation biomass. Their Pearson Correlation Coefficients were close to or more than 0.7 ( $P < 0.01$ ,  $N = 116$ ). A similar result was also found between total vegetation biomass and SOC density of the 0-

100 cm soil layer (Fig. 4). The derived linear regression relating SOC density (Y) to vegetation biomass (X) was  $Y = 0.565X + 143.185$  ( $R = 0.697$ ,  $P < 0.01$ ,  $N = 39$ ). These results confirm that increasing vegetation biomass by reforestation and protection is an important way to increase ecosystem carbon sequestration along Chinese coastal areas.

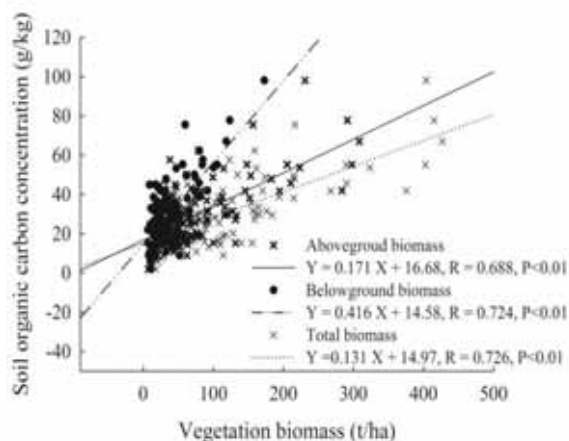


**FIGURE 3**

**Relationships between vegetation biomass (total biomass, belowground and aboveground biomass) and SOC concentration of the surface soil layer**

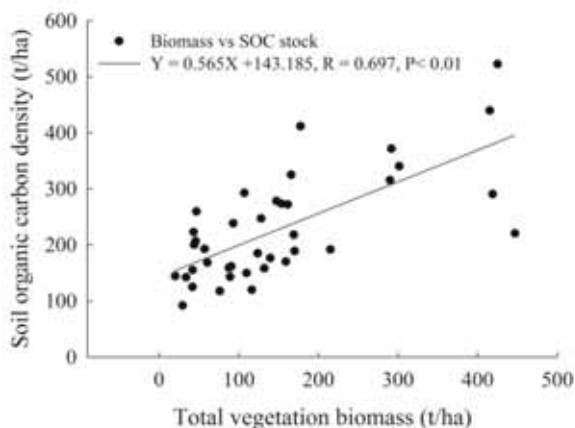


**FIGURE 4**

**Relationship between total vegetation biomass and SOC density of the 0-100 cm soil layer**

**Change of vegetation carbon.** As shown in Table 2, biomass carbon density varied among the different mangrove communities. The *B. sexangula* community had the highest mean biomass carbon density followed by the *R. stylosa* community, whilst the lowest mean carbon biomass density occurred in the *S. caseolares* community. To some degree, average biomass carbon density of the different

mangrove communities increased with time, which is to say from 1990 to 2010 (Table 2). The *R. stylosa* and *B. gymnorhiz* communities had relatively higher rates of increase in biomass carbon density than did the other mangrove communities, and their biomass carbon density increased from 99.15 t/ha and 40.84 t/ha in 1990 to 124.35 t/ha and 71.40 t/ha in 2010, respectively. Table 2 shows that carbon storage accumulated in biomass, increased from 1037.55 Gg in 1990 to 1449.96 Gg in 2010, while forest area increased from 17874 ha to 23413 ha (Table 1). The biomass carbon storage of the *A. marina*, *A. corniculatum*, *K. obovata* and *R. stylosa* communities accounted for almost 70% of the whole vegetation biomass carbon storage during the study period. The average biomass carbon accumulation rate was 20.62 Gg/year. Average vegetation carbon density of all communities increased from 61.78 t/ha in 1990 to 65.32 t/ha in 2010, with an average carbon uptake of 0.18 t/(ha•year).

**Change of SOC.** Generally, SOC density varied among the different mangrove communities and also, in general, increased with time (Table 3). More specifically in 2010, the *B. sexangula* community had the highest mean SOC density, followed by the *R. stylosa* and *S. caseolares* communities. The *S. caseolares* community had the highest increase rate of SOC density for the period 1990 to 2010 compared to the other mangrove communities, followed by the *B. gymnorhiz* and *A. corniculatum* communities (see Table 3 for the data). In comparison with vegetation biomass carbon, SOC density had a relatively higher accumulation rate. It is shown in Table 3 that carbon accumulated in the soil, increased from 3710.46 Gg in 1990 to 5528.61 Gg in 2010. The SOC storage of the *A. marina*, *A. corniculatum*, *K. obovata* and *R. stylosa* communities accounted for more than 70% of all SOC storage during this study period. The average accumulation rate reached 90.91 Gg/year whilst the average SOC density of all communities increased from 218.48 t/ha in 1990 to 233.82 t/ha in 2010, with an average carbon uptake of 0.77 t/(ha•year).

**Change of ecosystem carbon.** According to the formula (2), ecosystem carbon storage in the mangrove forest along the coast of China increased greatly from 4748.01 Gg in 1990 to 6978.57 Gg in 2010. Vegetation biomass carbon storage accounted for 21.85% and 20.78 % of ecosystem carbon storage in 1990 and 2010, respectively. Average accumulation rate of ecosystem carbon was 111.53 Gg/year and SOC accounted for 81.51% of the carbon accumulation in these Chinese mangrove forests. During the study period, ecosystem carbon density increased from 280.56 t/ha in 1990 to 299.14 t/ha in 2010, with an average carbon uptake of 0.93 t/(ha•year).



**TABLE 2**  
**Change of vegetation biomass carbon storage between 1990 and 2010 for the different mangrove ecosystems along the Chinese coast (mean  $\pm$  standard deviation)**

Forest type	number of data		Biomass carbon density (t/ha)		Carbon storage of different years in biomass (Gg)	
	1990	2010	1990	2010	1990	2010
<i>A. marina</i>	14	58	27.17 $\pm$ 24.88	35.12 $\pm$ 14.96	144.23 $\pm$ 132.08	244.21 $\pm$ 104.03
<i>A. corniculatum</i>	10	17	39.14 $\pm$ 20.93	42.54 $\pm$ 20.64	125.93 $\pm$ 67.34	179.28 $\pm$ 86.98
<i>K. obovata</i>	34	47	79.33 $\pm$ 37.82	57.86 $\pm$ 30.28	216.95 $\pm$ 103.43	207.27 $\pm$ 108.47
<i>R. stylosa</i>	6	18	99.15 $\pm$ 59.37	124.35 $\pm$ 52.17	230.39 $\pm$ 137.95	378.48 $\pm$ 158.79
<i>B. gymnorrhiz</i>	6	20	40.84 $\pm$ 12.74	71.40 $\pm$ 35.10	21.90 $\pm$ 6.83	50.15 $\pm$ 24.65
<i>B. sexangula</i>	2	3	187.99 $\pm$ 1.62	187.61 $\pm$ 1.33	10.08 $\pm$ 0.09	13.18 $\pm$ 0.09
<i>S. caseolares</i>	5	5	19.84 $\pm$ 4.40	19.51 $\pm$ 4.34	6.74 $\pm$ 1.49	8.68 $\pm$ 1.93
<i>S. apetala</i>	2	21	71.17 $\pm$ 58.84	79.40 $\pm$ 37.85	1.27 $\pm$ 1.05	1.86 $\pm$ 0.89
others	5	5	83.79 $\pm$ 30.99	83.79 $\pm$ 30.99	280.06 $\pm$ 103.58	366.85 $\pm$ 135.68
Total	84	194	61.78 $\pm$ 45.75	65.32 $\pm$ 41.26	1037.55 $\pm$ 142.00	1449.96 $\pm$ 141.54

**TABLE 3**  
**Change of SOC density and storage between 1990 and 2010 for mangrove ecosystems along the Chinese coast (mean  $\pm$  standard deviation)**

Forest type	number of data		SOC density (t/ha)		Carbon storage of different years in soil (Gg)	
	1990	2010	1990	2010	1990	2010
<i>A. marina</i>	14	65	166.13 $\pm$ 39.37	195.93 $\pm$ 49.79	881.91 $\pm$ 209.00	1362.43 $\pm$ 346.22
<i>A. corniculatum</i>	12	28	187.89 $\pm$ 30.62	235.76 $\pm$ 40.67	604.50 $\pm$ 98.51	993.57 $\pm$ 171.40
<i>K. obovata</i>	34	63	239.42 $\pm$ 51.54	206.61 $\pm$ 50.52	654.75 $\pm$ 140.95	740.12 $\pm$ 180.97
<i>R. stylosa</i>	6	27	293.18 $\pm$ 76.97	289.03 $\pm$ 103.91	681.24 $\pm$ 178.85	879.72 $\pm$ 316.27
<i>B. gymnorrhiz</i>	6	23	199.80 $\pm$ 26.38	247.96 $\pm$ 57.18	107.14 $\pm$ 14.15	174.16 $\pm$ 40.16
<i>B. sexangula</i>	2	3	379.21 $\pm$ 2.04	399.48 $\pm$ 35.12	20.33 $\pm$ 0.11	28.06 $\pm$ 2.47
<i>S. caseolares</i>	5	4	168.10 $\pm$ 5.52	401.19 $\pm$ 94.06	57.09 $\pm$ 1.87	178.47 $\pm$ 41.84
<i>S. apetala</i>	2	26	232.54 $\pm$ 73.88	229.42 $\pm$ 63.76	4.16 $\pm$ 1.32	5.37 $\pm$ 1.49
others	5	5	209.23 $\pm$ 63.32	266.48 $\pm$ 52.28	699.34 $\pm$ 211.64	1166.71 $\pm$ 228.89
Total	86	225	218.48 $\pm$ 63.07	233.82 $\pm$ 89.72	3710.46 $\pm$ 214.84	5528.61 $\pm$ 290.85

## DISCUSSION AND CONCLUSIONS

**Relationship between biomass and SOC.** It has been reported that the ratio between soil- and vegetation- carbon density increases with increasing latitude and that ecosystem carbon density also increases with increased latitude for upland forest ecosystems [27]. However, ecosystem carbon density in mangrove forests has been reported to decrease with increased latitude while vegetation carbon density decreased [28]. For example, it was reported that ecosystem carbon densities were 466.3 t/ha in Micronesian mangrove forests (N 7°) and 119.3 t/ha (N 26°) in Japanese mangrove forests, while their biomass carbon densities were 151.4 t/ha and 62.0 t/ha, respectively. As mangrove forests experience growth, the carbon accumulated in both plant and soil also increase [7, 8]. As shown in Fig.

3 and 4, this study found that vegetation biomass was positively correlated with SOC (including both SOC density and SOC concentration of the surface soil layer) and the Pearson Correlation Coefficients were close to, or more than, 0.7. These results are in agreement with the previous reports of Gleason and Ewel [29] and Donato et al. [10] in mangrove forests. Donato et al. found that there were positive correlations between belowground and aboveground carbon density ( $R^2 = 0.21$  and  $0.50$  in estuarine and ocean sites, respectively) [10]. Jones et al. also found that SOC density of the 0-100 cm layer increased along with vegetation biomass growth in the tropical mangrove forests of Northwest Madagascar [2]. Similar results also exists for upland forest ecosystems. For example, Zhang [30] found that linear relationships occurred between SOC density (0-100 cm) and vegetation biomass in both *Eucalyptus* and *Acacia* forests of the Pearl River

Delta, South China and their coefficients of determination were 0.37 and 0.64, respectively. A much stronger correlation ( $R^2 = 0.79$ ) has been reported in some other *Eucalypt-Acacia* forest and monocultures [20]. The results of this study, along with those reported in the literature, indicate that increasing vegetation biomass through both afforestation and protection strategies, would increase the carbon accumulation rate. This is because biomass growth can increase the net primary production, which results in a higher input of dead roots and root exudates as well as increased litter fall [25].

**Carbon accumulation rate.** Mangrove forests absorbed carbon at a rate of 111.53 Gg/year during the study period from 1990 to 2010 along the Chinese coast. This result suggests that mangroves can be considered as an important carbon sink to mitigate the greenhouse effect. On an area basis, the carbon accumulation rate was 0.18 t/(ha•year) in vegetation biomass along the Chinese coast and this value was considerably lower than those reported for upland forest ecosystems of the USA (0.52-0.71 t/(ha•year)) and Europe (0.60-1.50 t/(ha•year)) [31]. Moreover, the carbon accumulation rate of the mangrove biomass in this study was only 49% of the carbon accumulation rate observed in bamboos [32]. The carbon accumulation rate of mangrove biomass is at the lower limit of values reported for planted forest ecosystems in Guangdong, South China [6]. Zhou et al. (2008) found that between 1994 and 2003 the planted forest vegetation stored up to 0.27-1.19 t/(ha•year), whilst this study on mangroves derived a value of 0.18 t/(ha•year). In addition, the SOC accumulation rate was 0.77 t/(ha•year) in the mangrove forest ecosystem along the Chinese coast which is more than 4 times the biomass carbon accumulation rate in the same mangrove forest. This SOC accumulation rate for this study is also close to the reported values of biomass carbon accumulation rates in USA and Europe cited previously. This observed SOC accumulation rate is 67% of the global value of 1.15 t/(ha•year) estimated for mangrove forests by Bouillon et al. (2008) [3]. Ecosystem carbon storage of mangrove forest along the Chinese coast increased remarkably with an average carbon uptake of 0.93 t/(ha•year) during the study period. This ecosystem carbon accumulation rate was relatively higher in the mangrove forests in comparison to those reported in the upland forests of Southwest and Southeast of China [17]. Ecosystem carbon accumulation rates of these upland forests ranged from 0.43 to 0.67 t/(ha•year). The carbon accumulation rate of mangrove forest ecosystem was at a relatively high level for the study period, indicating that mangrove forests could be considered as a state carbon sink consequent upon mangrove afforestation and forest protection strategies [33].

**Carbon density in comparison with other forest ecosystems.** During the study period, ecosystem carbon density of mangrove forests maintained a high level ranging from 280.56 to 299.14 t/ha. This carbon density in the Chinese mangrove forests was relatively higher than in upland forests of the same latitude, but it was relatively lower than in mangrove forests at lower latitudes [5, 7, 10]. In the upland forests of South China, Zheng et al. found that ecosystem carbon density ranged from 102.95 to 141.99 t/ha for different tree species used for reforestation [34]. It was reported that ecosystem carbon density of evergreen forests in the Pearl River Delta varied from 127.54 to 288.88 t/ha [35]. Vegetation carbon density of upland forests accounted for almost 50% of the ecosystem carbon density, while in comparison, vegetation carbon density of mangrove forests accounted for only about 20% of ecosystem carbon density. The relatively higher SOC density resulted in the presence of large ecosystem carbon stocks in the mangrove forest and this occurs because mangrove soils are usually anaerobic with lower decomposition rates which is favorable to the accumulation of organic carbon in the soil in comparison with upland forests [36]. The ecosystem carbon density for mangrove forests reported by Kauffman et al. in Micronesia [5] and Adame et al. in Mexico [37], are considerably higher than the values of this study. The ecosystem carbon density of these tropical mangrove forests ranged from 381 to 798 t/ha [5, 37]. This is attributed to the lower latitude of the tropical mangrove forests investigated by Kauffman et al. and Adame et al. compared to those of the China coast, and which result in a higher vegetation biomass and more carbon-rich soil [7].

**Uncertainties of ecosystem carbon storage.** In order to fill in research gaps and add more evidence about the potential of mangrove forests to act as carbon sinks, more information about mangrove's carbon dynamics is needed [13]. Unfortunately, current research approaches via field survey is often expensive, time-consuming, laborious and destructive. This study collected both biomass carbon density and SOC density data, and subsequently found that a good linear regression equation between biomass carbon density and SOC density could be established and which was used to quantify carbon dynamics in mangrove forests along the Chinese coast. Despite the fact that relatively high Pearson Correlation Coefficients existed for the linear regression equations established in this study, vegetation biomass only accounted for 48.58% of the variance of SOC density and thus some uncertainties remain with respect to carbon dynamics in mangrove forests of the Chinese coast. This is because variations in ecosystem carbon density (especially vegetation biomass carbon) are related to changes in geographical locations and forest communities,

which are in turn driven by both physical (e.g. soil types and nutrient) and biological (e.g. bioturbation, vegetation structure, primary productivity and decomposition) factors [38]. It is not possible to provide any estimate of the contribution associated with the field measurement (sampling error) and those attributed to error in the regression equations [18]. However, Phillips *et al.* have suggested that sampling error accounted for more than 90% of the total error in forest carbon budgets [39]. If Phillips *et al.* are correct, then the error could be substantially minimized in the future studies by increasing the number of sites sampled for the different mangrove communities at different locations and which should result in much better regression equations between SOC density and vegetation biomass that can be used to estimate ecosystem carbon storage. However, this study is, to-date, the most comprehensive analysis of change of ecosystem carbon storage in mangrove ecosystems along the Chinese coast. If only the effects of geographical locations were considered, ecosystem carbon storage was estimated according to the result of the average ecosystem carbon density multiplied the area of each province in 2010. This gives an estimated carbon storage value of 6.85 Tg and which is similar to our estimated carbon storage of 6.98 Tg. Our estimated ecosystem carbon storage is also close to a reported value of 6.90 Tg in Liu *et al.* for mangroves in China [4]. These similarities suggest that our estimation method can be used to study the change of ecosystem carbon storage along the Chinese coast. Also, the estimates of carbon dynamics presented here will be helpful for estimating carbon sink if mangrove forests are planted or protected.

Combining field measurements with data from the literature, a linear regression equation was established to quantify the change of ecosystem carbon storage in mangrove forests along the Chinese coast. Significant correlations were found between vegetation biomass and both SOC density and SOC concentration of the surface soil layer. China's mangrove forests increased ecosystem carbon storage by 111.53 Gg/year and ecosystem carbon density by 0.93 t/(ha·year) from 1990 to 2010. Our results further support the conclusion from other research that reforestation increases carbon sequestration in mangrove forests. Mangrove forests accumulate more ecosystem carbon in comparison to upland forests located in the same latitudes. Ecosystem carbon density of mangrove forests is affected by the species composition and biomass differences. More sampling and long-term monitoring are needed to increase our understanding of ecosystem carbon dynamics in the various mangrove communities at different geographical locations.

## ACKNOWLEDGEMENTS

This work was funded by the Research Fund for the National Natural Science Foundation of China (No. 41371109, No. 51039007 and NO.31470703) and the Doctoral Program of Higher Education (NO.20110171110019). Moreover, this work was also supported by the Fundamental Research Funds for the Central Universities of China. We would also like to thank the members of the team.

## REFERENCES

- [1] Kauffman, J.B. and Donato, D.C. (2012) Protocols for the measurement, monitoring and reporting of structure, biomass and carbon stocks in mangrove forests. *Bogor, Indonesia: Center for International Forestry Research (CIFOR)*.
- [2] Jones, T.G., Ratsimba, H.R., Ravaoarinorotsihoarana L., Cripps G. and Bey A. (2014) Ecological Variability and Carbon Stock Estimates of Mangrove Ecosystems in Northwestern Madagascar. *Forests* 5: 177-205.
- [3] Bouillon, S., Borges, A.V., Castañeda Moya, E., Diele, K., Dittmar, T., Duke, N.C., et al. (2008) Mangrove production and carbon sinks: a revision of global budget estimates. *Global Biogeochem Cy* 22: 1-12.
- [4] Liu, H., Ren, H., Hui, D., Wang, W., Liao, B. and Cao, Q. (2014) Carbon stocks and potential carbon storage in the mangrove forests of China. *J Environ Manage* 133: 86-93.
- [5] Kauffman, J.B., Heider, C., Cole, T.G., Dwire, K.A. and Donato, D.C. (2011) Ecosystem carbon stocks of Micronesian mangrove forests. *Wetlands* 31: 343-52.
- [6] Zhou, C., Wei, X., Zhou, G., Yan, J., Wang, X., Wang, C., et al. (2008) Impacts of a large-scale reforestation program on carbon storage dynamics in Guangdong, China. *Forest Ecol Manag.* 255: 847-54.
- [7] Wang, G., Guan, D., Peart, M.R., Chen, Y. and Peng, Y. (2013) Ecosystem carbon stocks of mangrove forest in Yingluo Bay, Guangdong Province of South China. *Forest Ecol Manag.* 2013: 539-46.
- [8] Jana, B.K., Biswas, S., Majumder, M., Roy, P.K. and Mazumdar, A. (2009) Carbon sequestration rate and aboveground biomass carbon potential of four young species. *Journal of Ecology and Natural Environment* 1: 15-24.
- [9] Dixon, R.K., Solomon, A.M., Brown, S., Houghton, R.A., Trexler, M.C. and Wisniewski, J. (1994) Carbon pools and flux of

- global forest ecosystems. *Science* 263: 185-90.
- [10] Donato, D.C., Kauffman, J.B., Murdiyarso, D., Kurnianto, S., Stidham, M. and Kanninen, M. (2011) Mangroves among the most carbon-rich forests in the tropics. *Nat Geosci* 4: 293-7.
- [11] Harmon, M.E., Ferrell, W.K. and Franklin, J.F. (1990) Effects on carbon storage of conversion of old-growth forests to young forests. *Science* 247: 699-702.
- [12] Fang, J., Chen, A., Peng, C., Zhao, S. and Ci, L. (2001) Changes in forest biomass carbon storage in China between 1949 and 1998. *Science* 292: 2320-2.
- [13] Wicaksono, P., Danoedoro, P., Hartono, H., Nehren, U. and Ribbe, L. (2011) Preliminary work of mangrove ecosystem carbon stock mapping in small island using remote sensing: above and below ground carbon stock mapping on medium resolution satellite image. *SPIE Remote Sensing: International Society for Optics and Photonics* p. 81741B.
- [14] Siikamäki, J., Sanchirico, J.N. and Jardine, S.L. (2009) Global economic potential for reducing carbon dioxide emissions from mangrove loss. *Proceedings of the National Academy of Sciences* 109: 14369-74.
- [15] Li, M.S. and Lee, S.Y. (1997) Mangroves of China: a brief review. *Forest Ecol Manag* 96: 241-59.
- [16] Chen, L., Wang, W., Zhang, Y. and Lin, G. (2009) Recent progresses in mangrove conservation, restoration and research in China. *J Plant Ecol* 2: 45-54.
- [17] Piao, S., Fang, J., Ciais, P., Peylin, P., Huang, Y., Sitch, S., et al. (2009) The carbon balance of terrestrial ecosystems in China. *Nature* 458: 1009-13.
- [18] Zhang, H., Guan, D. and Song, M. (2012) Biomass and carbon storage of Eucalyptus and Acacia plantations in the Pearl River Delta, South China. *Forest Ecol Manag* 277: 90-7.
- [19] Wang, S., Zhou, C., Liu, J., Tian, H., Li, K. and Yang, X. (2002) Carbon storage in northeast China as estimated from vegetation and soil inventories. *Environ Pollut* 116: S157-65.
- [20] Forrester, D.I., Pares, A., O Hara, C., Khanna, P.K. and Bauhus, J. (2013) Soil organic carbon is increased in mixed-species plantations of Eucalyptus and nitrogen-fixing Acacia. *Ecosystems* 16: 123-32.
- [21] Ministry of Forestry. (2002) National Mangrove Resource Inventory Report: Ministry of Forestry of China.
- [22] Lv, J. (2008) Studies on distribution and management of Chinese mangrove forests: Beijing Forestry University.
- [23] Shih, S., Yang, S., Lee, H., Hwang, G. and Hsu, Y. (2011) Development of a salinity-secondary flow-approach model to predict mangrove spreading. *Ecol Eng* 37: 1174-83.
- [24] Cao, Q. (2010) The Estimation of Mangrove Biomass and Carbon Storage Using Remote Sensing Data in Beibu Gulf Coast. Chinese Academy of Forestry.
- [25] Ren, H., Chen, H., Li, Z.A. and Han, W. (2010) Biomass accumulation and carbon storage of four different aged *Sonneratia apetala* plantations in Southern China. *Plant Soil* 327 : 279-91.
- [26] Jiang, P. and Xu, Q. (2006) Abundance and dynamics of soil labile carbon pools under different types of forest vegetation. *Pedosphere* 16: 505-11.
- [27] Lal, R. (2005) Forest soils and carbon sequestration. *Forest Ecol Manag* 220: 242-58.
- [28] Saenger, P. and Snedaker, S.C. (1993) Pantropical trends in mangrove above-ground biomass and annual litterfall. *Oecologia* 96: 293-9.
- [29] Gleason, S.M. and Ewel, K.C. (2002) Organic Matter Dynamics on the Forest Floor of a Micronesian Mangrove Forest: An Investigation of Species Composition Shifts. *Biotropica* 34: 190-8.
- [30] Zhang H. (2012) Biomass and Carbon Storage of *Eucalyptus* and *Acacia* Plantations in the Pearl River Delta, South China. Sun Yat-Sen University.
- [31] Janssens, I.A., Freibauer, A., Ciais, P., Smith, P., Nabuurs, G., Folberth, G., et al. (2003) Europe's terrestrial biosphere absorbs 7 to 12% of European anthropogenic CO<sub>2</sub> emissions. *Science* 300: 1538-42.
- [32] Pan, Y., Luo, T., Birdsey, R., Hom, J. and Melillo, J. (2004) New estimates of carbon storage and sequestration in China's forests: effects of age-class and method on inventory-based carbon estimation. *Climatic Change* 67 : 211-36.
- [33] Zhang, J., Shen, C., Ren, H., Wang, J. and Han, W. (2012) Estimating change in sedimentary organic carbon content during mangrove restoration in southern China using carbon isotopic measurements. *Pedosphere* 22: 58-66.
- [34] Zheng, H., Ouyang, Z., Xu, W., Wang, X., Miao, H., Li, X., et al. (2008) Variation of carbon storage by different reforestation types in the hilly red soil region of southern China. *Forest Ecol Manag* 255: 1113-21.
- [35] Sun, L. (2011) Study on Carbon Storage of Subtropical Broad-leaved Forest Ecosystem in the Pearl River Delta. Sun Yat-Sen University.
- [36] Matsui, N. (1998) Estimated stocks of organic carbon in mangrove roots and sediments in



- Hinchinbrook Channel, Australia. *Mangroves and Salt Marshes 2*: 199-204.
- [37] Adame, M.F., Kauffman, J.B., Medina, I., Gamboa, J.N., Torres, O., Caamal, J.P., et al. (2013) Carbon stocks of tropical coastal wetlands within the karstic landscape of the Mexican Caribbean. *Plos One* 8: e56569.
- [38] Mcleod, E., Chmura, G.L., Bouillon, S., Salm, R., Björk, M., Duarte, C.M., et al. (2011) A blueprint for blue carbon: toward an improved understanding of the role of vegetated coastal habitats in sequestering CO<sub>2</sub>. *Frontiers in Ecology and the Environment*. 9: 552-60.
- [39] Phillips, D.L., Brown, S.L., Schroeder, P.E. and Birdsey, R.A. (2002) Toward error analysis of large-scale forest carbon budgets. *Global Ecol Biogeogr* 9: 305-13

---

**Received:** 11.04.2016

**Accepted:** 08.09.2016

---

#### **CORRESPONDING AUTHOR**

---

**Dongsheng Guan**

135 Xingang West

School of Environmental Science and Engineering

Sun Yat-sen University

P.R. CHINA

e-mail: eesgds@mail.sysu.edu.cn

# USING NTA AND EDTA TO ENHANCE Cd PHYTOEXTRACTION BY *AMARANTHUS HYBRIDUS* L.

Zhangwei Li\*, Boling Xu and Huimin Zhang

<sup>1</sup>College of Chemistry and Environment Engineering, Hanshan Normal University, Chaozhou 521041, P. R. China

## ABSTRACT

Applying chemical enhancements may improve the phytoremediation of soils contaminated with heavy metals. This pot experiment study assessed the ability of *Amaranthus hybridus* L. to bioaccumulate Cd, both alone and with the addition of chelators. Ethylenediamine triacetic acid (EDTA) was added at concentrations of 1.5 and 3.0 mmol·kg<sup>-1</sup>; and nitrilotriacetic acid (NTA) was added at concentrations of 2.5 and 5.0 mmol·kg<sup>-1</sup> to assess the plant's ability to uptake Cd when the soil was contaminated at concentrations of 5 to 40 mg kg<sup>-1</sup> Cd. Adding EDTA and NTA enhanced the accumulation capacity of Cd in the plant shoots. Cd concentrations in the plant shoots were higher with the EDTA treatment than with the NTA treatment. This indicates that EDTA treatments enhanced Cd phytoremediation in this species more than NTA. Applying 1.5 and 3.0 mmol·kg<sup>-1</sup> EDTA for the soil contaminated with 40 mg kg<sup>-1</sup> Cd resulted in up to 100 mg·kg<sup>-1</sup> Cd in the plant shoots, exceeding the critical content (100 mg·kg<sup>-1</sup>) for Cd-hyperaccumulators. The total Cd uptake in plants was higher in EDTA treatment than in NTA treatment, suggesting that EDTA more effectively enhanced Cd accumulation in *A. hybridus*. The most Cd accumulation in shoots, 1181.57 µg·pot<sup>-1</sup>, was seen when 1.5 mmol·kg<sup>-1</sup> EDTA was used with soils contaminated with 40 mg Cd kg<sup>-1</sup>. In conclusion, *A. hybridus* may be an attractive candidate for phytoremediation through Cd-hyperaccumulation, with the application of EDTA.

## KEYWORDS:

*Amaranthus hybridus* L., Hyperaccumulator, Chelator, EDTA, NTA, Cadmium

## INTRODUCTION

Rapid industrial development has increased the presence of soils polluted with heavy metals. For example, cadmium (Cd) is a non-essential heavy metal that is toxic to living cells at a very low concentration. Additionally, Cd can accumulate to toxic levels in organisms and persist indefinitely

in the environment [1,2]. The presence of Cd in soils has greatly increased because of industrial inputs, such as smelters, industrial sewage, sludge, and agricultural fertilizer applications [3,4]. The resulting environmental problems heighten the importance of exploring effective remediation methods to clean-up Cd-contaminated soil, while not adversely impacting soil biological and ecological health.

Phytoremediation, the application of green plants to remove pollutants from soils, has received increased attention in recent years, and may be better than conventional technologies for remediating contaminated soil [5]. This plant-based technique has shown significant economic, aesthetic, and technical advantages compared with traditional techniques, which include immobilization, mechanical separation, electrokinetic remediation, and chemical washing [6]. To date, over 400 plants have been identified to be hyperaccumulators. Many of these are Ni-hyperaccumulators; there are also a few hyperaccumulators of Cd, copper (Cu), lead (Pb), and zinc (Zn) [7]. *Solanum nigrum* [8], *Thlaspi caerulescens* [9], and *Viola baoshanensis* [10] have been identified as Cd hyperaccumulators. However, because of their small biomass and slow growth, these hyperaccumulators may not be suitable for larger scale phytoextraction efforts.

Plants in the *Amaranthus* genus are widely distributed worldwide. Plant species in this genus include *Amaranthus dubius* L. [11], *Amaranthus hybridus* L. [12], and *Amaranthus hypochondriacus* L. [13], and reports indicate the potential for these plants to be Cd hyperaccumulators. Additionally, these plants are fast growing, have a high biomass, and are easily cultivated, facilitating this species' ability to efficiently extract Cd from contaminated soils [14].

To increase the efficiency of plant remediation, it is possible to increase the solubility of soil-bound heavy metals, using chemical approaches. This includes adding chelators that are associated with phytoremediation [15,16]. For instance, ethylenediamine triacetic acid (EDTA) is a synthetic chelating agent that efficiently mobilizes Pb, Cd, and Zn from soil contaminated with heavy metals [17,18]. Unfortunately, EDTA is often reported to be toxic to the plants and restricts plant

**TABLE 1**  
**Basic soil properties**

pH	Organic matter (g·kg <sup>-1</sup> )	Available (mg·kg <sup>-1</sup> )			Total (mg·kg <sup>-1</sup> )		
		N	P	K	Pb	Cd	Zn
6.74	38.7	51.2	40.8	65.1	20.3	0.17	35.0

growth [19]. Nitrilotriacetic acid (NTA) is another chelating agent; it is less toxic to the plants and biodegrades more easily in soils. As such, is often used in enhance phytoextraction [20,21]. A number of studies have demonstrated the ability of chelators to promote metal uptake by plants; however, few investigations have explored chelator-assisted phytoextraction by *Amaranthus* species in soils contaminated with heavy metals. One study, using *Amaranthus hybridus* L., demonstrated this species' potential for reducing Cd pollution in soil [12]. However, few reports have explored how Cd accumulation by *A. hybridus* might be enhanced by applying chelators, such as EDTA or NTA.

Given this background, this study used pot experiments to identify the capacity of *Amaranthus* to support Cd remediation in soil, using a concentration gradient experiment; and identify any improvement in remediation capacity created by applying chelators.

## MATERIALS AND METHODS

**Soil sample properties.** The soil samples used for this experiment were collected from vegetable gardens not contaminated by heavy metals. After being air-dried, the soil samples were grounded to a particle size that passed through a 4.0 mm sieve. The soil was then used for the pot experiments. The soil organic matter was measured using a wet digestion process with K<sub>2</sub>Cr<sub>2</sub>O<sub>7</sub> and H<sub>2</sub>SO<sub>4</sub>. Available N, P, and K were measured using standard methods recommended by Lu [22]. Soil pH was measured in a 1:2.5 soil to water suspension with a combination pH electrode. Total Pb, Cd, and Zn in the soil was determined using atomic absorption spectrophotometer (AAS), following HF-HNO<sub>3</sub>-HClO<sub>4</sub> digestion procedures [22]. Table 1 provides the soil's basic physiochemical properties and the Cd background level.

**Pot culture experiment design.** According to the National Soil-Environmental Quality Standard of China (GB15618 1995), the concentration gradient experiment with single Cd and two kinds of chelators: NTA and EDTA were selected and designed for the pot culture experiment. Table 2 lists the treatments conducted for the experiments.

There were five separate treatments with Cd concentrations of 5, 10, 20, 30, and 40 mg·kg<sup>-1</sup>. Cd was spiked as 3CdSO<sub>4</sub>·8H<sub>2</sub>O.

First, 3.0 kg of the sieved soil was placed into each plastic pot. Samples were then mixed with the different concentrations of 3CdSO<sub>4</sub>·8H<sub>2</sub>O and left alone for one month to equilibrate. Eight pre-germinated *A. hybridus* seeds were then sown in each pot, which was fertilized with P 100 mg·kg<sup>-1</sup> (calcium phosphate), K 40 mg·kg<sup>-1</sup> (potassium chloride) and N 50 mg·kg<sup>-1</sup> (ammonium sulfate). This fertilization provided adequate nutrition for plant growth. Seven days after plant emergence, seedlings were thinned to four per pot.

The *A. hybridus* was grown in a greenhouse maintained at a temperature of 26-30°C. After four weeks of growth, EDTA and NTA were added to the pots, which were prepared with pure salts as Na<sub>2</sub>-EDTA and Na<sub>3</sub>NTA. EDTA concentrations were set at 1.5 and 3.0 mmol·kg<sup>-1</sup> and the NTA concentrations were 2.5 and 5.0 mmol·kg<sup>-1</sup>. These levels align with the thresholds proposed by Nowack [23] and Hseu [21] for chelator enhanced phytoextraction. Three replicates of pot soil were tested, during incubation and following plant growth. All plants were harvested one week after applying the chelator.

**Metal analysis.** Once the plant samples were removed from the pots, they were divided into two parts: shoots and roots. The roots were washed with tap water to remove soil particles, and immersed in 20 mM Na<sub>2</sub>-EDTA for 1 hour to remove exchangeable Cd. The shoots and roots were further washed three times with deionized water, then placed in an oven at 105°C for 20 minutes, and then heated further at 70°C until a constant weight was reached. The dry weights were measured, and the dried plant tissues were then ground to powder and passed through a 2 mm sieve.

Soil samples were collected from the pots after the plants were harvested. The soil was air-dried at room temperature, and then passed through a 0.149 mm sieve. The Cd in plants was extracted using acid digestion mixture (HNO<sub>3</sub> and HClO<sub>4</sub>). The plant samples were heated with the HNO<sub>3</sub> and HClO<sub>4</sub> mixture until the color became clear; they were then filtered, reconstituted to the desired volume, and measured using the AAS for Cd. For soil extractable Cd, 20 ml of 0.01 mol·L<sup>-1</sup> CaCl<sub>2</sub> was added to 2 g of soil sample in a 50 ml

polypropylene centrifuge tube. The tube was shaken for 16 h at 25°C, and then centrifuged at 4000 rpm for 15 min. After being filtered, AAS was used to measure the extractable Cd concentrations in the samples.

**TABLE 2**  
**Summary of pot treatments with different Cd, NTA, and EDTA concentrations**

Treatment	Cd (mg·kg <sup>-1</sup> )	NTA (mmol·kg <sup>-1</sup> )	EDTA (mmol·kg <sup>-1</sup> )
1	5	0	0
2	5	2.5	0
3	5	5.0	0
4	5	0	1.5
5	5	0	3.0
6	10	0	0
7	10	2.5	0
8	10	5.0	0
9	10	0	1.5
10	10	0	3.0
11	20	0	0
12	20	2.5	0
13	20	5.0	0
14	20	0	1.5
15	20	0	3.0
16	30	0	0
17	30	2.5	0
18	30	5.0	0
19	30	0	1.5
20	30	0	3.0
21	40	0	0
22	40	2.5	0
23	40	5.0	0
24	40	0	1.5
25	40	0	3.0

**Translocation factor and bioconcentration factor.** The bioconcentration factor (BCF) is defined as the ratio of the metal concentration in plant shoots to the concentration in the soil. The translocation factor (TF) is the ratio of metal concentration in plant shoots to the concentration in plant roots. BCF and TF are important indexes that indicate the plant's ability to accumulate a particular metal from the soil [21].

**Statistical methods .** The means and standard deviations (SD) were calculated using Microsoft Excel 2003. The statistical tests, including analysis of variance (ANOVA), were conducted using SPSS version 17.0 (SPSS Inc., USA). Differences between means were measured using the Duncan test, with a significance level of  $P < 0.05$ . Figures were plotted using Origin 7.5.

## RESULTS

**Effect of EDTA and NTA on *A. hybridus* height and biomass production.** None of the plants wilted as a result of the study treatments. However, the plants treated with 3.0 mmol·kg<sup>-1</sup> EDTA and 5.0 mmol·kg<sup>-1</sup> NTA growing in soil with 40 mg·kg<sup>-1</sup> Cd, developed dark green leaves and necrotic spots. The treatment with 3.0 mmol·kg<sup>-1</sup> EDTA in the soil with 40 mg·kg<sup>-1</sup> Cd resulted in lower plant heights than with other treatments. The samples with 1.5 mmol·kg<sup>-1</sup> EDTA and 2.5 mmol·kg<sup>-1</sup> NTA did not exhibit significant differences in plant height compared to the control (Table 3).

Fig.1 shows *A. hybridus* biomass after being grown in soils with different Cd, NTA, and EDTA concentrations. In the treatment without the NTA and EDTA chelators, plant biomass decreased as Cd concentration increased when adding with 10, 20, 30 and 40 mg·kg<sup>-1</sup> Cd in soil. When the Cd concentration in the soil increased to 30 and 40 mg·kg<sup>-1</sup>, the plant clearly suffered from phytotoxicity. Adding 2.5 mmol·kg<sup>-1</sup> NTA and 1.5 mmol·kg<sup>-1</sup> EDTA did not stunt plant growth. However, the shoot biomass markedly decreased when NTA and EDTA concentrations increased to 5.0 mmol·kg<sup>-1</sup> and 3.0 mmol·kg<sup>-1</sup>, respectively. Similar to the shoot biomass, the root biomass decreased while increasing the soil Cd concentration by 10 to 40 mg·kg<sup>-1</sup>. The addition of 2.5 mmol·kg<sup>-1</sup> NTA did not significantly reduce the root biomass production compared to control except treating with 10 mg·kg<sup>-1</sup> Cd in soil. However, the dry root weight of the plant markedly decreased in the treatment of 5.0 mmol·kg<sup>-1</sup> NTA and 3.0 mmol·kg<sup>-1</sup> EDTA. This suggests that applying high levels of NTA and EDTA was toxic to *A. hybridus*.

### Effect of EDTA and NTA on Cd concentration in *A. hybridus* shoots and roots.

The Cd concentration in plant shoots increased as the Cd concentration in soil increased (Fig.2). In the control treatments (no EDTA or NTA), the Cd concentrations in plant shoots were 23.35, 25.69, 29.41, 38.32, and 59.34 mg·kg<sup>-1</sup> when Cd concentrations in soil were 5, 10, 20, 30, and 40 mg·kg<sup>-1</sup>, respectively. Adding the chelators facilitated Cd accumulation in plant shoots, with Cd concentrations in the shoots increasing 1.5 to 3.0-fold compared to the treatment without chelators. Cd concentrations were higher in the shoots treated with EDTA than NTA. For example, after applying 3.0 mmol·kg<sup>-1</sup> EDTA to the soil sample with 40 mg·kg<sup>-1</sup> Cd, the Cd concentration in the shoots peaked at 124.24 mg·kg<sup>-1</sup>. In contrast, applying 5.0 mmol·kg<sup>-1</sup> NTA resulted in a Cd concentration in the shoots of 95.69 mg·kg<sup>-1</sup>.

However, the increase in the dosage of EDTA and NTA increased the Cd concentration in the



**TABLE 3**  
Shoot height per plant of *A. hybridus* on the soils exposed to different concentrations of Cd treated with chelators.

Treatment	Cd concentration(mg·kg <sup>-1</sup> ) in the soil				
	5.0	10.0	20.0	30.0	40.0
Shoot					
Control	29.11±1.19 a	27.47±1.38 a	24.86±1.65 a	22.80±2.76 a	21.27±1.51 a
2.5 mmol·kg <sup>-1</sup> NTA	28.23±2.04 a	27.21±2.33 a	23.10±2.10abc	20.31±1.05 ab	18.57±2.11 a
5.0 mmol·kg <sup>-1</sup> NTA	25.15±2.78 bc	21.56±1.42 b	19.95±1.42 c	18.19±1.12 b	17.71±1.41 ab
1.5 mmol·kg <sup>-1</sup> EDTA	27.39±1.41 ab	25.93±2.92 a	23.63±1.52 ab	19.36±2.91 ab	19.14±2.34 a
3.0 mmol·kg <sup>-1</sup> EDTA	24.26±2.57 c	19.43±1.70 b	20.83±1.41 bc	17.21±1.59 b	14.73±1.39 b

Data with a different letter in the same column indicate a statistically significant difference, according to the Duncan test.  $P < 0.05$

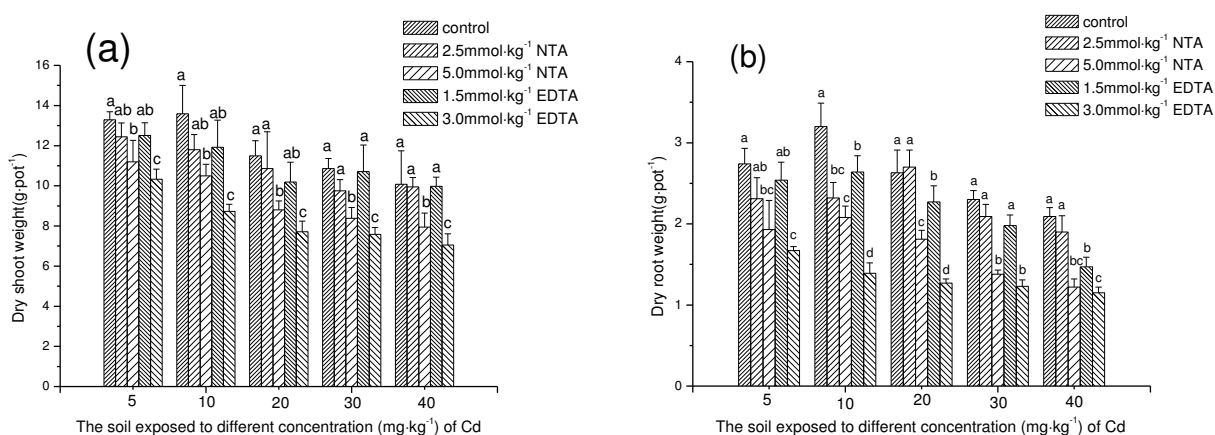


**FIGURE 1**

**Dry material weight(g·pot<sup>-1</sup>) of the shoot (a) and root (b) of *A. hybridus* on the soil exposed to different concentrations of Cd treated with NTA and EDTA. Different letters following the vertical bars are different significantly between treatments at  $P < 0.05$  level according to Duncan's multiple range test.**

shoots. In soil samples with Cd concentrations ranging from 5 to 40 mg·kg<sup>-1</sup>, the Cd concentrations in the shoots ranged from 48.94 to 118.51 mg·kg<sup>-1</sup> with the addition of 1.5 mmol·kg<sup>-1</sup> EDTA, and ranged from 28.10 to 79.22 mg·kg<sup>-1</sup> with the addition of 2.5 mmol·kg<sup>-1</sup> NTA. Applying 3.0 mmol·kg<sup>-1</sup> EDTA and 5.0 mmol·kg<sup>-1</sup> NTA resulted in Cd concentrations in shoots ranging from 49.59 to 124.24 mg·kg<sup>-1</sup> and 32.08-95.69 mg·kg<sup>-1</sup>, respectively. This confirms that higher levels of EDTA and NTA enhanced Cd accumulation. Similar to the results seen with the plant shoots, without chelators, the Cd concentrations in *A. hybridus* roots increased as the Cd concentration in the soil increased. However, adding chelators resulted in a decrease in Cd concentration in the roots except in the 5 mg·kg<sup>-1</sup> Cd treatment level; the reduction was greater with the EDTA treatment than with the NTA treatment. Without EDTA or NTA, the Cd concentration in the roots was 74.10 mg·kg<sup>-1</sup> in the soil

contaminated with 30 mg·kg<sup>-1</sup> Cd. When treated with 5.0 mmol·kg<sup>-1</sup> NTA and 3.0 mmol·kg<sup>-1</sup> EDTA, the Cd concentrations in the roots decreased to 69.54 and 58.36 mg·kg<sup>-1</sup>, respectively. At a Cd contamination level of 40 mg·kg<sup>-1</sup> in the soil, without chelators, the Cd concentration in the roots was 105.19 mg·kg<sup>-1</sup>. This level decreased to 90.05 mg·kg<sup>-1</sup> after treatment with 5.0 mmol·kg<sup>-1</sup> NTA and 76.86 mg·kg<sup>-1</sup> after treatment with 3.0 mmol·kg<sup>-1</sup> EDTA. This results were similar to Liu[6], who found that the Cd concentration in the roots of *Althaea rosea cav.* decreased after treatment with SDS, EDTA, and EGTA in 100 mg·kg<sup>-1</sup> Cd contaminated soil, compared to the control. These results suggest that more Cd was translocated to shoots when NTA and EDTA were added.

After applying EDTA and NTA, the Cd concentration was higher in plant shoots than roots. This is an important characteristic of this hyperaccumulator. When concentrations of 1.5 and

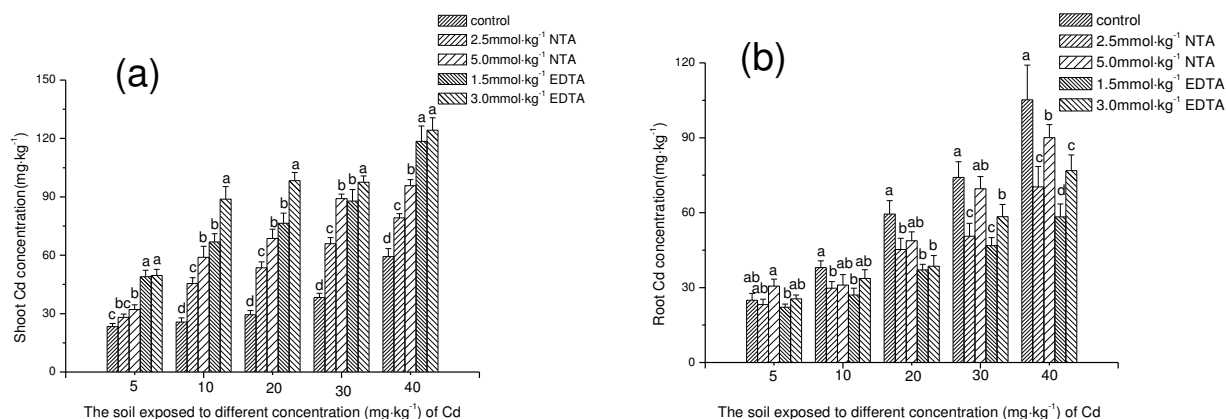


FIGURE 2

Cadmium concentration ( $\text{mg}\cdot\text{kg}^{-1}$ ) of the shoot (a) and root (b) of *A. hybridus* on the soil exposed to different concentrations of Cd treated with NTA and EDTA. Different letters following the vertical bars are different significantly between treatments at  $p<0.05$  level according to Duncan's multiple range test.

3.0  $\text{mmol}\cdot\text{kg}^{-1}$  EDTA were added to the soil contaminated with 40  $\text{mg}\cdot\text{kg}^{-1}$  Cd, the Cd concentration in the shoot reached 118.51 and 124.24  $\text{mg}\cdot\text{kg}^{-1}$ , respectively. This is higher than when the Cd concentration was 100  $\text{mg}\cdot\text{kg}^{-1}$ , the critical concentration of a Cd hyperaccumulator [24].

**Effect of EDTA and NTA on total Cd uptake by *A. hybridus*.** Adding chelators increased the total Cd uptake in the shoots compared with the control (Fig.3). Without adding chelators, the Cd accumulation in *A. hybridus* shoots ranged from 310.35 to 598.19  $\mu\text{g}\cdot\text{pot}^{-1}$ . After the NTA and EDTA treatment, the Cd uptake in plant shoots ranged from 349.45 to 788.21  $\mu\text{g}\cdot\text{pot}^{-1}$  (NTA) and 512.29 to 1181.57  $\mu\text{g}\cdot\text{pot}^{-1}$  (EDTA). As noted above, the Cd accumulation was higher with the addition of EDTA. The maximum Cd uptake in the shoots occurred with the addition of 1.5  $\text{mmol}\cdot\text{kg}^{-1}$  EDTA in the 40  $\text{mg}\cdot\text{kg}^{-1}$  Cd contaminated soil; this resulted in the plant's uptake of 1181.57  $\mu\text{g}\cdot\text{pot}^{-1}$  Cd. The accumulation of Cd in the plant was higher with EDTA than with NTA. This suggests that adding EDTA was more effective in enhancing Cd accumulation in the *A. hybridus* plant.

**Effect of EDTA and NTA on BCF and TF of Cd in *A. hybridus*.** All BCFs of shoots were higher than 1.0; most BCFs were higher than 3.0 in the soils exposed to different Cd levels. Levels were higher with the added chelators than with the control. This result indicates that the translocation ability of *A. hybridus* was somewhat strengthened by adding EDTA and NTA. Adding 3.0  $\text{mmol}\cdot\text{kg}^{-1}$  EDTA resulted in the highest BCFs in plant shoots, across all levels of Cd contamination.

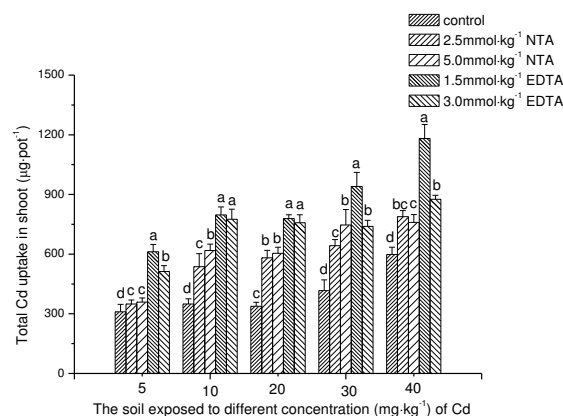


FIGURE 3

Total cadmium ( $\mu\text{g}\cdot\text{pot}^{-1}$ ) of *A. hybridus* in shoot on the soil exposed to different concentrations of Cd treated with NTA and EDTA. Different letters following the vertical bars are different significantly between treatments at  $p<0.05$  level according to Duncan's multiple range test.

The BCFs in all samples (control and with chelator treatment) decreased compared to the increase in Cd contamination levels in soil. The TFs ranged from 0.49 to 2.65 in all samples (control and with chelator treatment). Similar to the BCFs, the TFs were higher in the soil treated with chelators than in the controls samples. Applying 3.0  $\text{mmol}\cdot\text{kg}^{-1}$  EDTA resulted in the highest TFs across all the treatment levels, except for the soil sample with 30  $\text{mg}\cdot\text{kg}^{-1}$  Cd. Applying EDTA resulted in higher values than when applying NTA in both BCFs and TFs. This further demonstrates that the

**TABLE 4**  
**The average values of BCF and TF of *A. hybridus* on the soils exposed to different concentrations of Cd treated with NTA and EDTA.**

Treatment	Cd concentration(mg·kg <sup>-1</sup> ) in the soil				
	5.0	10.0	20.0	30.0	40.0
<b>BCF</b>					
Control	4.67±0.59 c	2.57±0.31 d	1.47±0.22 c	1.28±0.04 c	1.48±0.05 d
2.5 mmol·kg <sup>-1</sup> NTA	5.62±0.38 bc	4.55±0.50 c	3.30±0.19 b	1.78±0.25 bc	1.98±0.13 cd
5.0 mmol·kg <sup>-1</sup> NTA	6.42±0.52 b	5.89±0.87 b	4.46±0.20 a	2.29±0.06 b	2.39±0.27 bc
1.5 mmol·kg <sup>-1</sup> EDTA	9.79±0.82 a	6.69±0.49 b	3.82±0.39 b	2.93±0.34 a	2.96±0.25 ab
3.0 mmol·kg <sup>-1</sup> EDTA	9.92±0.53 a	8.88±0.70 a	4.91±0.32 a	3.25±0.21 a	3.11±0.42 a
<b>TF</b>					
Control	0.94±0.06 c	0.68±0.02 c	0.49±0.03 d	0.52±0.05 c	0.56±0.03 c
2.5 mmol·kg <sup>-1</sup> NTA	0.92±0.05 c	1.53±0.05 b	1.30±0.22 c	1.10±0.09 b	0.88±0.01 c
5.0 mmol·kg <sup>-1</sup> NTA	1.38±0.04 b	1.90±0.06 b	1.28±0.07 c	1.52±0.20 ab	1.36±0.04 b
1.5 mmol·kg <sup>-1</sup> EDTA	1.92±0.20 a	2.47±0.13 a	1.98±0.14 b	1.88±0.03 a	1.54±0.16 b
3.0 mmol·kg <sup>-1</sup> EDTA	2.24±0.21 a	2.64±0.02 a	2.65±0.21 a	1.67±0.22 a	2.13±0.28 a

EDTA supplement was more effective than NTA in enhancing Cd accumulation by the plants.

transforming Cd from the insoluble to the soluble fraction

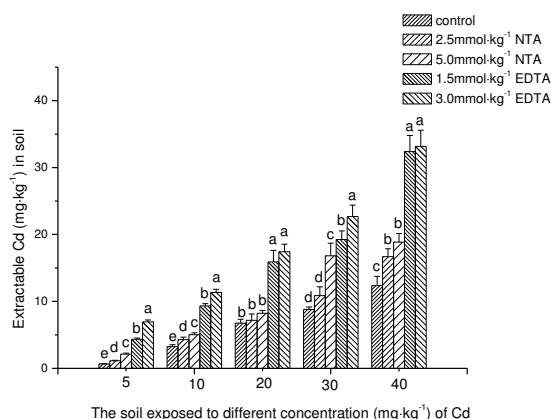


**FIGURE 4**  
**Extractable Cd (mg·kg<sup>-1</sup>) on the soil exposed to different concentrations of Cd treated with NTA and EDTA. Different letters following the vertical bars are different significantly between treatments at  $p < 0.05$  level according to Duncan's multiple range test.**

**Effect of EDTA and NTA on available Cd of soil.** Fig.4 shows the CaCl<sub>2</sub> extractable Cd concentration in the soil after applying different NTA and EDTA doses. In all treatments without chelators, the CaCl<sub>2</sub> extractable Cd concentration increased as the incremental level of Cd in soil increased. NTA and EDTA treatments increased the concentration of CaCl<sub>2</sub> extractable Cd in soil; the degree of increase related to the relative levels of NTA and EDTA. When the NTA and EDTA doses were at the same level, there were higher concentrations of CaCl<sub>2</sub> extractable Cd in the EDTA treated soil than the NTA treated soil. This indicates that EDTA is more effective in

## DISCUSSION AND CONCLUSIONS

Plant selection is an important factor in phytoremediation; further, environmental and economic concerns require minimal chelator use. As such, selecting the plant and selecting the chelators are best done simultaneously [25,26]. In this experiment, *A. hybridus* thrived in soil exposed to Cd concentration up to 40 mg·kg<sup>-1</sup>, despite the addition of NTA and EDTA. This indicates that this plant tolerates high levels of Cd contamination. Plant height decreased as the Cd in soil increased. Adding 5.0 mmol·kg<sup>-1</sup> NTA and 3.0 mmol·kg<sup>-1</sup> EDTA resulted in significant decreases in plant height compared to the control. The reduction ranged from 13.6% to 21.5% and 16.2% to 30.7%. No significant reduction of plant height was observed when adding 1.5 mmol·kg<sup>-1</sup> EDTA and 2.5 mmol·kg<sup>-1</sup> NTA, suggesting that low levels of EDTA and NTA did not inhibit *A. hybridus* growth.

Other studies also found that applying synthetic chelators, such as EDTA, NTA, EDD, SDS, and EGTA, negatively impacted plant growth [27,19,6,28]. Liu [6] reported that the *Althaea rosea* cav. shoot biomass decreased by 60% after soil contaminated with 30 mg·kg<sup>-1</sup> Cd was treated with 1.0 mmol·kg<sup>-1</sup> EDTA. Munn[28] found that adding 0.1 g·kg<sup>-1</sup> EDTA to soil contaminated with 30 mg·kg<sup>-1</sup> Cd, resulted in a 22.6% and 56.6% reduction of *Thlaspi caerulescens* and *Helianthus annuus* biomass, respectively. Quartacci [27] found that applying 5 mmol·kg<sup>-1</sup> NTA reduced *Brassica carinata* biomass by 16.7% in soils contaminated with 61 mg·kg<sup>-1</sup> Cd. This stunted plant growth can be attributed to the combination of high heavy metal concentrations and chelator application that



exceeded the plants' capacity to activate a defense system [29]. In this study, *A. hybridus* biomass was reduced when treated with 3.0 mmol·kg<sup>-1</sup> of EDTA and 5.0 mmol·kg<sup>-1</sup> of NTA. Biomass did not decrease when the soil was treated with 1.5 mmol·kg<sup>-1</sup> EDTA and 2.5 mmol·kg<sup>-1</sup> NTA. However, the average biomass of *A. hybridus* in this experiment was higher than the biomass seen in other Cd hyperaccumulators, such as *Bidens pilosa* L. [30], *Sedum alfredii* [31], and *Thlaspi caerulescens* L. [32]. Sun planted the hyperaccumulator *Bidens pilosa* L. in soils contaminated with 8 to 100 mg·kg<sup>-1</sup> Cd for 120 d and found that the shoot biomass was only 0.8 to 1.2 g per plant [30]. Wang [31] used *Sedum alfredii* to remediate Cd contaminated soil, finding that after growing for 60 days, the shoot biomass was only 0.3 to 0.8 g per plant. The Cd hyperaccumulator *Thlaspi caerulescens* L. accumulated more than 600 mg kg<sup>-1</sup> Cd in its shoots, but its biomass was only 0.3 g per plant [32]. These hyperaccumulators are characterized by slow growth and low biomass, making phytoremediation in the field impractical. In this experiment, most of the plant biomass exceeded 2 g per plant in the control and in the soil treated with chelators. This biomass was higher than was seen with many other Cd-hyperaccumulators. Another study [14] found that in farmland, *A. hybridus* could achieve a fresh shoot biomass of 25-30 t·ha<sup>-2</sup>. Moreover, this plant grows very quickly and the plant's cultivation systems are well established and highly mechanized. These factors suggest that *A. hybridus* is a candidate to effectively remediate Cd contaminated soil.

As many studies have reported, chelators are able to increase the concentration of bioavailable metals in the soil. First, the chelator combines soluble metals in the soil solution. As the concentration of free metals in the soils decrease, bound metal ions begin to dissolve to compensate for the equilibrium shift. As a result, metals are freed from the soil bound matrix. This process enhances heavy metal bioavailability, and increases phytoremediation effectiveness [33,34]. Adding NTA and EDTA to soils enhanced Cd solubility in this experiment. In this study, the soluble Cd in the tested soil correlated well ( $r^2=0.81$ ,  $P<0.05$ ) with the Cd concentration in plant shoots. The correlation is described by the following linear model:  $Y=3.06X+29.7$ , where X is the content of soluble Cd in soil and Y is Cd concentration in plant shoots. The Cd concentration in the plant shoots and roots were higher with the EDTA treatment than with the NTA treatment, indicating that EDTA enhanced Cd uptake in *A. hybridus* more than NTA. This result may be explained by the fact that the stability constant value was higher for the EDTA-Cd complex (LogK 16.5) than for the NTA-Cd complex (LogK 10.5). The higher stability

constant value of the EDTA-Cd complex means that EDTA induced higher Cd solubility. This allowed more bioavailable forms of Cd in soil to be taken up by plants, enhancing the plant's ability to translocate the Cd from roots to shoots [27].

Successful phytoextraction requires high heavy metal concentrations in above-ground tissue. Chelating agents have successfully increased metal accumulation in plant shoots. Many researchers have focused on improving EDTA effectiveness in enhancing heavy metal uptake by hyperaccumulators [28,35,26]. Munn [28] tested the ability of EDTA at two concentrations (0.1 and 0.3 g·kg<sup>-1</sup>) to enhance the phytoremediation of Cd, Cr, and Ni in *helianthus annuus* and *thlaspi caerulescens* at two different metal concentrations (24.75 mg·kg<sup>-1</sup> and 90 mg·kg<sup>-1</sup>). The EDTA increased the total metal uptake of Cd, Cr, and Ni by 10 - 25%. Marques[35] assessed the effect of EDTA on Zn tissue accumulation in *solanum nigrum* L. grown in naturally contaminated soil. Adding EDTA increased *S. nigrum* accumulation of Zn by up to 231% in the leaves, 93% in the stems, and 81% in the roots. In this study, the Cd concentration in the shoots of *A. hybridus* in the control samples ranged from 23.35 to 59.34 mg·kg<sup>-1</sup>. Adding EDTA and NTA increased the Cd accumulation in plant shoots. Treatments of 1.5 and 3.0 mmol·kg<sup>-1</sup> EDTA in soil contaminated with 40 mg·kg<sup>-1</sup> Cd resulted in higher Cd concentrations in plant shoots (118.51 and 124.24 mg·kg<sup>-1</sup>) than with the other treatment. This is higher than the critical concentration (100 mg·kg<sup>-1</sup>) of a hyperaccumulator.

BCF is an important factor in phytoremediation; it describes metal uptake, metal transfer from root to shoot, and metal accumulation in the aerial plant biomass. TF is another important value, and indicates the plant's ability to transfer metal from roots to shoots. A TF greater than 1.0 indicates that heavy metal concentrations in the shoots are higher than the roots. BCF and TF are used to evaluate a plant's phytoremediation efficiency [21]. The BCF values in the plant shoots for Cd ranged from 1.28 to 9.92, higher than the critical level (1.0) for metal accumulators. Adding the chelator increased the BCF values in all the treatment levels compared to the control. This suggests that the accumulation ability of *A. hybridus* was strengthened by the chemically enhanced treatment. Furthermore, TF values increased when NTA and EDTA were added, with most TF values exceeding 1.0. The high BCF and TF values indicated that *A. hybridus* has a significant ability to take up and transport Cd.

Some studies have reported high BCF and TF values associated with *Amaranthus*. Li [13] investigated the bioconcentration factor (BCF) and transfer factor (TF) of Cd for three *Amaranthus Hypochondriacus* cultivars growing for 60 days in



soil contaminated with 5 mg·kg<sup>-1</sup> Cd. The study found that the BCF of three amaranth plants ranged from 17.7 to 29.7, with a TF between 1.0 to 2.0. This is higher than Cd accumulators used in other studies, such as *viola baoshanensis* [10], *arabidopsis halleri* [36], *solanum nigrum* [8], and *rorippa globosa* [37]. In this study, the increased BCF and TF when chelators were added suggest that *A. hybridus* could serve as a Cd hyperaccumulator.

There are two equally important factors for a plant to be a successful metal accumulator: metal concentration in biomass and total plant biomass [38]. Amendments can improve metal uptake and plant growth. In this study, the total Cd accumulated by the plant shoot with no chelator treatment ranged from 310.35 to 598.19 µg·pot<sup>-1</sup>. The total shoot uptake of Cd suggests that NTA and EDTA are needed for *A. hybridus* to increase the Cd uptake from soils.

The test plant's accumulation Cd in this study allows an estimate of the amount of Cd that can be removed from contaminated soil, and supports the selection of chelators for phytoextraction remediation. The results show that treatment with EDTA and NTA resulted in a total Cd uptake from Cd contaminated soil that was higher than the control. However, doses of 3.0 mmol·kg<sup>-1</sup> EDTA and 5.0 mmol·kg<sup>-1</sup> NTA were too high to improve phytoextraction, because the high EDTA and NTA levels impeded *A. hybridus* growth. Therefore, adding EDTA and NTA at levels of 1.5 and 2.5 mmol·kg<sup>-1</sup> levels were suitable for soils contaminated with a range of Cd levels.

Based on the observed plant height and biomass, Cd concentration, accumulation, and BCF and TF values of *A. hybridus* in this experiment, it can be concluded that EDTA and NTA significantly increased Cd uptake and accumulation in *A. hybridus*. This demonstrates the plant's ability to be an effective Cd-accumulator, resulting in Cd removal through phytoremediation.

This is the first study examining *A. hybridus* as a Cd-hyperaccumulator using EDTA and NTA. *A. hybridus* showed a strong tolerance to Cd-driven soil toxicity, and was able to accumulate Cd when grown in soil contaminated with up to 40 mg·kg<sup>-1</sup> Cd with added doses of 1.5 and 3.0 mmol·kg<sup>-1</sup> of EDTA and 2.5 and 5.0 mmol·kg<sup>-1</sup> of NTA. Consistent with the increase of soluble Cd amounts in the soils, applying with EDTA and NTA enhanced the capacity of *A. hybridus* shoots to take up Cd. However, EDTA was more effective in enhancing phytoextraction by *A. hybridus* than NTA. When treated with 1.5 and 3.0 mmol·kg<sup>-1</sup> EDTA in 40 mg·kg<sup>-1</sup> Cd contaminated soil, the Cd in the shoots of *A. hybridus* reached 118.51 and 124.24 mg·kg<sup>-1</sup>. These levels meet the critical concentrations of Cd for a hyperaccumulator,

resulting in its ability to be classified as a Cd-hyperaccumulator.

Furthermore, after adding EDTA, the TF values of *A. hybridus* exceeded 1.0 in all the treatments, which higher than the critical level (1.0) for the metal accumulator in this study. Applying EDTA at rates of 1.5 mmol·kg<sup>-1</sup> in 40 mg·kg<sup>-1</sup> Cd contaminated soil resulted in the highest total amount of Cd accumulated in all the treatments: 1181.57 µg·pot<sup>-1</sup>. Study results demonstrated that applying EDTA effectively improves Cd accumulation by *A. hybridus* and could serve as a new chelator-assisted tool for the phytoextraction treatment of Cd metal contaminated soils.

## ACKNOWLEDGEMENTS

This work was supported by the Funding of Hanshan Normal University (No.LF201402) and the Funding of Characteristics and Innovation Projects in the Field of Education and Research of Guangdong Education Department (No.2014GXJK124).

## REFERENCES

- [1] Wan Y., Luo S.L., Chen J.L., Xiao X., Chen L., Zeng G.M., Liu C.B., He Y.J., (2012). Effect of endophyte-infection on growth parameters and Cd-induced phytotoxicity of Cd-hyperaccumulator *Solanum nigrum* L., *Chemosphere* 89,743-750.
- [2] Chen Z.J., Sheng X.F., He L.Y., (2013). Effects of root inoculation with bacteria on the growth, Cd uptake and bacterial communities associated with rape grown in Cd-contaminated soil. *Journal of Hazardous Materials*, 244,709-717.
- [3] Li Z.W., Liao W.M., Zhong Z.R., (2015). Co-remediation of the lead, cadmium, and zinc contaminated soil using exogenous hydroxyapatite, zeolite, limestone and humic acids., *Fresen. Environ. Bull.*, 24:1425-1433
- [4] Cui H.B., Zhou J. Zhao Q.G., Si Y.B., Mao J.D., Fang G.D., and Liang J.N., (2013). Fractions of Cu, Cd and enzyme activities in a contaminated soil as affected by applications of micro- and nanohydroxyapatite. *Journal of Soils and Sediments*, 13(4):742-752.
- [5] Ma Y., Rajkumar M., Luo Y.M., Freitas H., (2011). Inoculation of endophytic bacteria on host and non-host plants-effects on plant growth and Ni uptake. *Journal of Hazardous Materials* 195. 230-237.
- [6] Liu J.N., Zhou Q.X., Wang S., Sun T., (2009). Cadmium tolerance and accumulation of *Althaea rosea* Cav. and its potential as a hyperaccumulator under chemical

- enhancement. *Environmental monitoring and assessment*, 149:419-427.
- [7] Brooks R.R.(1998).Geobotany and hyperaccumulator. In:Brooks, R.R.,editors. Plants that hyperaccumulate heavy metals, their role in phytoremediation, microbiology,archaeology,mineral exploration andphytomining.Wallingford,UK:CAB,International.p.55-94.
- [8] Chen L.,Luo S.L.,Li X.J.,Wan Y.,Chen J.L.,Liu C.B.,(2014). Interaction of Cd-hyperaccumulator *Solanum nigrum* L. and functional endophyte *Pseudomonas* sp.Lk9 on soil heavy metals uptake. *Soil biology and biochemistry*,68:300-308.
- [9] Martínez-Alcalá I., Bernal M., Fuente C., Gondar D., Clemente R.,(2016), Changes in the heavy metal solubility of two contaminated soils after heavy metals phytoextraction with *Noccaea caerulea*.*Ecological Engineering*, 89:56-63.
- [10] Zhong W.L.,Li J.T.,Chen Y.T.,Shu W.S.,Liao B.,(2012).A study on the effects of lead, Cadmium and phosphorus on the lead and cadmium uptake efficacy of *Viola baoshanensis* inoculated with arbuscular mycorrhizal fungi. *Journal of environmental monitoring*, 14(9): 2497-2504.
- [11] Chunilall V.,Kindness A.,Jonnalagadda S.B.,(2005).Heavy metal uptake by two edible *Amaranthus* herbs grown on soils contaminated with lead, mercury,cadmium and nickel. *Journal of Environmental Science and Health*, Part B40.375-384.
- [12] Zhang X.C.,Zhang S.R.,Xu X.X.,Li T.,Gong G.S.,Jia Y.X.,Li Y.,Deng L.J.,(2010).Tolerance and accumulation characteristics of cadmium in *Amaranthus hybridus* L. *Journal of Hazardous Materials*.180,303-308.
- [13] Li N.Y.,Fu Q.L.,Zhuang P.,Guo B.,Zou B.,Li Z.A.,(2012a).Effect of fertilizers on Cd uptake of *Amaranthus hypochondriacus*, a high biomass, fast growing and easily cultivated potential Cd hyperaccumulator.*International journal of phytoremediation*,14.162-173.
- [14] Li N. Y., Li Z. A., Zhuang P., Fu Q. L., Guo B., (2012b). Effect of fertilizers on Cd uptake of two edible *amaranthus* herbs. *Acta Ecologica Sinica*, 32(18):5937-5942. (In Chinese)
- [15] Jagetiya B.,Sharma A.,(2013).Optimization of chelators to enhance uranium uptake from tailings for phytoremediation.*Chemosphere*, 91(5):692-696.
- [16] Wang S.,Liu J.N.,(2014).The effectiveness and risk comparison of EDTA with EGTA in enhancing Cd phytoextraction by *Mirabilis jalapa* L..*Environmental monitoring and assessment*, 186(2):751-759.
- [17] Clabeaux B.L.,Navarro D.A.,Aga D.S., Bisson M.A., (2013), Combined effects of cadmium and zinc on growth, tolerance, and metal accumulation in *Chara australis* and enhanced phytoextraction using EDTA, *Ecotoxicology and environmental safety*, 98:236-243.
- [18] Eissa M.A.,(2016).Effect of sugarcane vinasse and EDTA on cadmium phytoextraction by two saltbush plants, *Environmental science and pollution research*, 23:1-8.
- [19] Liu J.N.,Zhou Q.X., Sun T.,Ma L.Q.,Wang S., (2008a), Identification and Chemical enhancement of two ornamental plants for phytoremediation. *Bull Environ Contaminated Toxicology*, 80:260-265.
- [20] Lan J.C.,Zhang S.r.,Lin H.C.,Li T.,Xu X.X.,Li Y.,Jia Y.X.,Gong G.S.,(2013), Efficiency of biodegradable EDDS, NTA and APAM on enhancing the phytoextraction of cadmium by *Siegesbeckia orientalis* L. grown in Cd-contaminated soils, *Chemosphere* ,91(9):1362-1367.
- [21] Hseu Z.Y.,Jien S.H.,Wang S.H.,Deng H.W.,(2013). Using EDDS and NTA for enhanced phytoextraction of Cd by water spinach. *Journal of Environmental Management*, 117, 58-64.
- [22] Lu,R.K., (1999) .Analytical methods for soils and agricultural chemistry, China Agricultural Science and Technology Press, Beijing, China.
- [23] Nowack B.,Schulin R., Robinson B.H.,(2006).Critical assessment of chelant-enhanced metal phytoextraction. *Environment Science Technology*. 40,5225-5232.
- [24] Baker A.J.M.,Brooks R.R., (1989). Terrestrial higher plants which hyperaccumulate metallic elements- a review of their distribution, ecology and photochemistry. *Biorecovery*, 1:81-126.
- [25] Baker A.J.M.,McGrath S.P.,Reeves R.S.,Smith J.A.C.,(2000).Metal hyperaccumulator plant:a review of the ecology and physiology of a biological resource for phytoremediation of metal-polluted soils. In:Terry,N.,Banelos G.N.(EDs.), phytoremediation of contaminated soil and water.Lewis Publishers, New York, pp:85-107.
- [26] Leštan D., Luo C.L.,Li X.D., (2008), The use of chelating agents in the remediation of metal-contaminated soils: A review, *Environmental pollution*, 153,3-13.
- [27] Quartacci M.F.,Irtelli B., Baker A.J.M.,Navari-Izzo, F., (2007).The use of NTA and EDDS for enhanced phytoextraction of metals from a multiply contaminated soil by *Brassica Carinata*, *Chemosphere*, 68,1920-1928.



- [28] Munn J., January M. Cutright T.J.,(2008).Greenhouse evaluation of EDTA effectiveness at enhancing Cd,Cr and Ni uptake in *Helianthus annuus* and *Thlaspi caerulescens*. *Journal of soils sediments*, 8,(2),116-122.
- [29] Luo C.L.,Shen Z.G.,Li X.D.,Lou L.Q.,(2006).EDDS and EDTA-enhanced phytoextraction of metals from artificially contaminated soil and residual effects of chelant compounds. *Envrionmental pollution*,144, 862-871.
- [30] Sun Y.B., Zhou Q.X., Liu W.T.,An J.,Xu Z.Q.,Wang L., (2009). Joint effects of arsenic and cadmium on plant growth and metal bioaccumulation: a potential Cd-hyperaccumulator and As-excluder *Bidens pilosa* L. *Journal of Hazardous Materials*, 165:1023-1028.
- [31] Wang K., Zhang J.,Zhu Z.Q.,Huang H.G.,Li T.Q.,He Z.L.,Yang X.E.,Alva A., (2012).Pig manure vermicompost(PMVC) can improve phytoremediation of Cd and PAHs co-contaminated soil by *Sedum alfredii*, *Journal of soils and sediments*, 12:1089-1099.
- [32] Liu M.Q.,Yanai J.,Jiang R.F.,Zhang F.,Mcgrath S.P.,Zhao F.J.,(2008b).Does cadmium play a physiological role in the hyperaccumulator *Thlaspi caerulescens*? *Chemosphere*, 71,1276-1283.
- [33] Huang J.W., Berti W.R., Cunningham S.D.,(1997).Phytoremediation of lead-contaminated soils:role of synthetic chelates in lead phytoextraction. *Environmental Science and Technology*, 31,800-805.
- [34] Schmidt U., (2003), Enhancing phytoextraction:the effect of chemical soil manipulation on mobility,plant accumulation, and leaching of heavy metals.*Journal of envrionmetal quality*, 32,1939-1954.
- [35] Marques A.P.G.C., Oliveira R.S., Samardjieva K.A., Pissarra J.,Rangel A.O.S.S., Castro P.M.L.,(2008), EDDS and EDTA-enhanced zinc accumulation by *solanum nigrum* inoculated with arbuscular mycorrhizal fungi grown in contaminated soil, *Chemosphere*, 70,1002-1014.
- [36] Huguet S.,Isaure M.P.,Bert V.,Laboudigue A., Proux O.,Flank A.M.,Vantelon D.,Sarret G.,(2015), Fate of cadmium in the rhizosphere of *Arabidopsis halleri* grown in a contaminated dredged sediment, *Science of the total environment*, 536:468-480.
- [37] Wei S.H., Ji D., Twardowska I., Li Y., Zhu J., (2014), Effect of different nitrogenous nutrients on the cadmium hyperaccumulation efficiency of *Rorippa globosa* (Turcz.) Thell, *Environmental Science Pollution research*,22(3):1999-2007.
- [38] Lin W.J., Xiao Y.Y., Wu Y.Y., Ao Z.Q.,Ning Z.P.,(2012), Hyperaccumulation of zinc by *Corydalis davidii* in Zn-polluted soils, *Chemosphere*, 86(8):837-842.

---

**Received:** 15.04.2016

**Accepted:** 09.09.2016

---

#### CORRESPONDING AUTHOR

---

**Zhangwei Li**

College of Chemistry  
and Environment Engineering,  
Hanshan Normal University,  
Chaozhou 521041, P. R. China

e-mail: 99094001@163.com

# ORNITOFAUNA OF KORFEZ WETLANDS (KOCAELİ, TURKEY)

Bilgenur Yasa<sup>1</sup>, Ali Uzun<sup>2\*</sup>

<sup>1</sup>Sakarya University, Institute of Science and Technology, Esentepe Campus, Sakarya-Turkey,

<sup>2</sup>Sakarya University, Arts and Science Faculty, Department of Biology, Esentepe Campus, Sakarya-Turkey,

## ABSTRACT

Körfez Wetland is located in Kocaeli Province in the northwest of Turkey. It is situated on the migration route of birds flying from Europe to Africa and Asia. The area is an important shelter, feeding and breeding field for the migratory and resident birds. Körfez Wetland with freshwater and saltwater ecosystems has an important bioecological sanctuary in terms of Ornithofauna of Turkey. Ninety-three different bird species were identified in the area as a result of a year-long analysis. Among these species, 42 were resident, 22 were winter migrants, 8 were transit migrants and 21 were summer migrants.

## KEYWORDS

Turkey, Ornithofauna, Körfez Wetland, Bioecology

## INTRODUCTION

The aim of this study is to define the ornithofaunistic properties of the Körfez Wetland by identifying various species and numbers of individuals, immigration status of the species, and the factors that pose a threat to the area. It has also been targeted to compare with other ecologically similar areas in Turkey.

Wetland ecosystems, form a wide range of habitats including floodplains, swamps, rivers, estuaries and near-shore coastal areas, and constitute approximately 6% of the Earth's land surface. Wetlands provide a variety of critical ecosystem services such as supporting wildlife habitat, filtering air and water, and reducing flooding and drought. Despite their importance, wetlands are under threat due to climate change and human encroachment [1]. Large wetlands are generally protected. However, the medium and small ones cannot be controlled and both are very crucial for local and migratory birds. Avifauna is an important component of aquatic ecosystems worldwide. It can be considered as an indicator of water bodies due to its quality, efficiency and function. Birds favor this type of ecosystem. They play an important role in transporting energy from water to the terrestrial system. Birds may obtain their food from different environment peripherals in

the aquatic system through the use of spatial separator of the environment or atmosphere [2]. Birds use wetlands for many purposes including breeding, feeding and resting needs owing to minimal predation [3].

Körfez wetland is an important shelter, feeding and breeding area for the native species and the migratory waterfowls that depend on the wetlands. In particular, holding a place on international migration chain path increases the importance of the area. The most significant threat of the area is its location in close proximity to intensive residential and industrial regions.

**Study Area.** Körfez Wetland is located in Kocaeli Province and borders on northwestern Turkey. The boundaries of the area were declared and designated by National Wetlands Commission in 2009. The area consists of 4 regions each according to its ecological characteristics: Absolute protection area (51.45 ha), ecological effected zone (3.79 ha), special provisions zone (39.15 ha) and buffer zone (7.299 ha) (Figure 1). Densely populated residential and industrial areas surround Körfez wetland. The area includes freshwater and saltwater ecosystems on the coast of the Körfez Region of the Marmara Sea. The two channels of the Kilez stream flowing to the sea creates the fresh water potential of the area in the northern and southern ends and these two channels carry fresh water to the area throughout the year. Extensive reed beds cover the coastline area. The southern protection region is bordered by highway and recreation areas. There are new recreation studies on the northern part of the area where the majority of the species exist and the studies are about to be concluded. This is especially significant as, this section was recently reforested.

## MATERIALS AND METHODS

This study was conducted between June 2014 and May 2015. During this time, one year period was completed by field study in 10 different months.



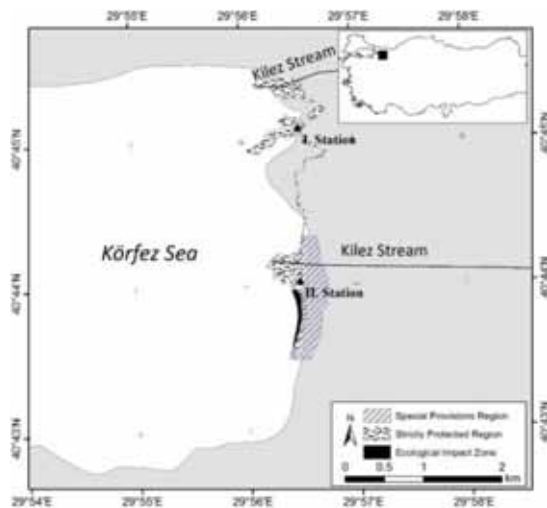


**FIGURE 1**

**Körfez Wetland (Kocaeli) and Stations Location.**

Observations were conducted during the day from 10:00 to 17:00 by using point and line length counting methods. The book of Hayman and Hume [4] was used for identification of the species. The observations in the field studies were done with the naked eye and by using binoculars (Nikon 10x40). Moreover, the field and the species were photographed by Canon 550D Camera and Sigma 150-500 mm tele objective lens. The working area was divided into two stations for convenience in determining of the species type and individual numbers. During observations, attention was paid to each station at different times of the day and recorded. The 1<sup>st</sup> station covered the northern part of the wetlands while the 2<sup>nd</sup> station covered the southern part. There was a bird observation tower at the 2<sup>nd</sup> station. The tower was used continuously during the field studies. On the basis of determined species, formulas to calculate the incidence of the species and the dominance of the species in the field, was taken from Kocatas [5].

*Frequency Analysis.*  $F\% = \frac{Na}{Nn} \times 100$  (Na = observed number of a species, Nn= total number of all observations).

F% of observed species is classified in five categories;

1–20%: rarely, 21–40%: seldom, 41–60%: generally, 61–80%: frequently, and 81–100%: commonly observed species.

*Dominance Analysis*  $.D\% = \frac{Na}{Nn} \times 100$  (D= Dominancy, Na= individual number of only species, Nn= total individual number of all observed species).

D% of observed species is classified in five categories;

0= not, += rare or the most rare, 1= population

size of species smaller than 5%, 2= population size of species between 5–25%, 3= population size of species between 25–50%, 4= population size of species between 50-75% and 5= population size of species greater than 75%.

*Margalef Diversity Index.*  $D = \frac{S-1}{\log_e N}$  (D = Diversity Index, S = species number in total species, N = number of total individuals).

*Sorensen Similarity Index.*  $Q = \frac{2c}{a+b}$  (Q=Similarity Index, a = species number in the 1<sup>st</sup> station, b= species number in the 2<sup>nd</sup> station, c = common species on both stations).

## RESULTS

Ninety-three bird species belonging to 31 families of 11 suborders have been identified in Körfez Wetland and around it. Among the identified species, the distribution was as follows; 42 native, 21 summer migrants, 22 winter migrants, and 8 transit migrants. The observed orders of the identified species were: 38 Passeriformes, 24 Charadriiformes, 10 Anseriformes, 4 Ciconiiformes, 4 Pelecaniformes, 4 Falconiiformes, 3 Columbiformes, 2 Podicipediformes, 2 Gruiformes, 1 Phoenicopteriformes, and 1 Coraciiformes. The majority of the species (38) were from Passeriformes order and Coraciiformes and Phoenicopteriformes orders were represented with one species in the field. The highest number of species (10) recorded was from Scolopacidae and Anatidae families. One species was identified from the Pelecanidae, Threskiornithidae, Phoenicopteridae, Falconidae, Haematopodidae, Glareolidae, Alcedinidae, Troglodytidae, Turdidae, Remizidae, Laniidae, and Sturnidae families.

According to IUCN [6], among the identified species, *Pelecanus crispus* VU (Vulnerable), *Gallinago media* and *Numenius arquata* were in NT (Near Threatened) and *Phalacrocorax pygmeus* was in DD (Data Deficient) categories. Other species were in LC (Least Concern) status (*Podiceps cristatus*, *Tachybaptus ruficollis*, *Phalacrocorax aristotelis*, *Phalacrocorax carbo*, *Ardea cinerea*, *Casmerodius albus*, *Egretta garzetta*, *Platalea leucorodia*, *Phoenicopus roseus*, *Cygnus olor*, *Tadorna tadorna*, *Anas platyrhynchos*, *Anas crecca*, *Anas acuta*, *Anas clypeata*, *Anas strepera*, *Netta rufina*, *Aythya ferina*, *Mergus merganser*, *Circus aeruginosus*, *Circus cyaneus*, *Buteo buteo*, *Falco naumanni*, *Gallinula chloropus*, *Fulica atra*, *Haematopus ostralegus*, *Charadrius dubius*, *Charadrius alexandrinus*, *Pluvialis squatarola*, *Tringa hypoleucos*, *Calidris minuta*, *Calidris canutus*, *Calidris alba*, *Tringa totanus*, *Tringa nebularia*, *Philomachus pugnax*, *Gallinago*

*gallinago, Glareola, ratincola, Larus melanocephalus, Larus minutus, Larus ridibundus, Larus genei, Larus canus, Larus, arinus, Larus ichthyaeus, Larus cachinnans, Sterna hirundo, Columba livia, Streptopelia decaocto, Streptopelia senegalensis, Alcedo atthis, Galerida cristata, Alauda arvensis, Hirundo rustica, Hirundo, aurica, Motacilla flava, Motacilla alba, Troglodytes troglodytes, Turdus merula, Locustella naevia, Acrocephalus scirpaceus, Acrocephalus arundinaceus, Hippolais icterina, Sylvia atricapilla, Phylloscopus trochiloides, Phylloscopus sibilatrix, Phylloscopus collybita, Phylloscopus trochilus, Muscicapa striata, Ficedula parva, Erithacus rubecula, Cercotrichas galactotes, Parus major, Saxicola, ubetra, Saxicola torquatus, Remiz pendulinus, Lanius collurio, Pica pica, Corvus corone corone, Corvus monedula, Corvus frugilegus, Corvus corone cornix, Sturnus vulgaris, Passer domesticus, Passer hispaniolensis, Fringilla coelebs, Carduelis Carduelis, Emberiza hortulana, Emberiza melanocephala*). According to Kiziroğlu [7] the distribution of the species in the protected categories was as follows: 4 A.1.2 (Critically Endangered), 7 A.2 (Endangered), 25 A.3 (Vulnerable), 15 A.3.1 (Declining), 9 A.4 (Near Threatened), 18 A.5 (Least Concern), 1 B.1.2 (Critically Endangered), 2 B.2 (Endangered), 8 B.3 (Vulnerable), 2 B.3.1 (Declining), and 2 B.4 (Near Threatened). According to Kiziroğlu [8], the number of strictly protected species in Annex I was 22. The number of species in Annex II that stand for the warrantable species in geographical seas and land was 9. The number of warrantable species determined by the member countries in Annex-II-B category was 20. The number of species in Annex-III-A category that can be warranted in a controlled manner was 1. And finally the number of species belongs to Annex-III-B category that the member

countries can practice according to their own laws was 5. According to CITES [10] the distribution of the categories of the identified species was: 1 Annex-I-B (trade is banned), 6 Annex-II-B (trade is partially allowed), and 7 Annex-III-B (trade is allowed partially). Other species were not included in any of the protected status. According to BERN Convention [9], out of 93 species, 51 were from Annex-II (strictly protected species), and 42 were from Annex-III (protected species) categories. Only *Pelecanus crispus, Casmerodius albus, Egretta garzetta, Platalea leucorodia, Anas crecca, Anas acuta, Anas clypeata, Circus aeruginosus, Circus cyaneus* and *Falco naumanni* were in protected status in five evaluations [6,8,9,10].

The number of species-individuals identified in the field studies varied in different stations and months. During the studies, the highest number of species was recorded in September (57), and the lowest was in May (30) (Figure 2). The highest number of individuals was counted in January (11010) and the smallest was in May (854). The total number of the recorded individuals during the study for 93 species was 38,360 (Figure 3).

The number of the species at the 1<sup>st</sup> station was 74 and the total number of individuals was 33,857. For the 1<sup>st</sup> station, the highest number of species was recorded in January (39), and the lowest was recorded in May (24) (Figure 2). Majority of the individuals was counted in January (9,975) and the smallest was counted in May (634). In the second station total of 68 species were identified and the total number of individuals was 4,503. Among the recorded species, the majority was from June (39), and the least were from May (20). The highest number of the individuals was recorded in January (1,035), and the smallest number of individuals was in June

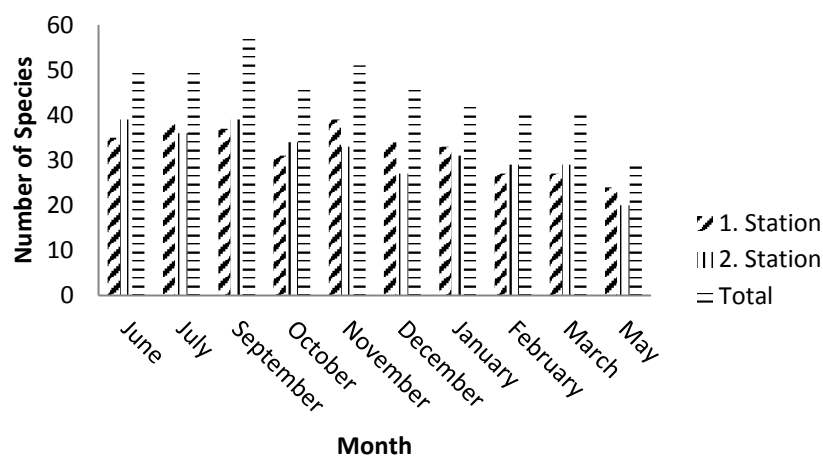


**FIGURE 2**  
The number of the species by months.

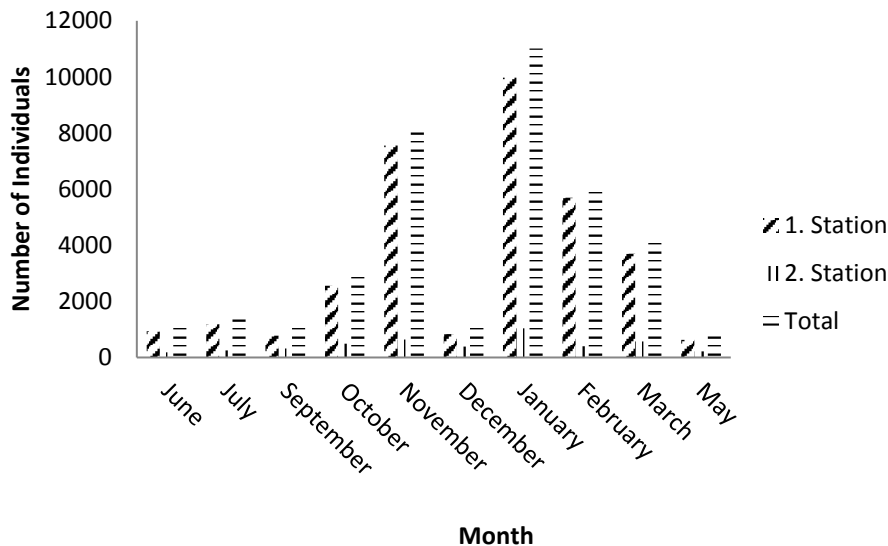


**FIGURE 3**  
The number of the species by months.

**TABLE 1**  
Number of Species by Frequency and Dominance Value

Frequency		Dominance	
Value	Number of Species	Value	Number of Species
% 1-20	18	< % 5	88
% 21-40	32	% 5-25	4
% 41-60	18	% 25-50	1
% 61-80	10	% 50-75	–
% 81-100	15	% 75 >	–

(186) (Figure 3). Among the 93 identified species in Körfez Wetland, 25 species were observed only at the 1<sup>st</sup> station and 19 were observed only at the 2<sup>nd</sup> station. Forty-nine species were observed at both stations.

Most of the species (32) were in the “rarely observed” category according to frequency values. Ten species were in “frequently observed” category and 15 species were recorded in every field study. According to dominance value, the population size of 93 species was as follows: 88 species were less than 5%, 4 species were between 5 - 25%, and 1 species (*Larus genei*) was between 25 - 50% (Table 1).

## DISCUSSION

According to the literature, there was no comprehensive ornitofaunistic study for the Körfez Wetland. However, the T.C. Ministry of Water Affairs and Forestry [11] published a report on the field and 101 bird species were observed and recorded at İzmir Körfez Wetland. In the same report, the number of species in Bird Bank database was expressed as 165 according to records of the last

seven years. The number of identified species in our species was 93 in June 2014-May 2015 period. Although long-term observation may seem an advantage to fully reveal the diversity of species in the area, as many of those who contributed data to Bird Bank were amateur bird watcher and photographers, makes the identified 165 species controversial. It is because these amateur observers may record the individuals at adult, young and nestling stages and the male and female individuals of the same species as different species. However, the location and the bioecological properties of the area make continuous monitoring of bird species necessary. The most significant disadvantage of the area is its location in a densely populated and industrial area resulting in intense pressure. This pressure may lead the birds to abandon the area if necessary protection and usage policy are not put in place immediately.

Kiziroğlu [7] contains a list of Turkey bird species and their immigration status. The immigration status of some bird species in the Marmara Region varies with our study when compared to this source. According to Kiziroglu [8], while *Pelecanus crispus*, *Platalea leucorodia*, *Anas strepera*, *Netta rufina*, and *Saxicola rubetra* were listed as N, for the Körfez Wetland, the immigration

status of these species were identified as TM. Similarly, *Mergus merganser* was recorded as WV in his study while in this study it was recorded as TM, *Casmerodius albus*, *Streptopelia decaocto*, *Streptopelia senegalensis*, *Alauda arvensis*, *Motacilla alba*, and *Remiz pendulinus* were recorded as N and in this study they were identified as SM. *Phoenicopiterus roseus*, *Cygnus olor*, *Tadorna tadorna*, *Anas platyrhynchos*, *Anas crecca*, *Anas acuta*, *Anas clypeata*, *Aythya ferina*, *Charadrius dubius*, *Charadrius alexandrinus*, *Tringa hypoleucos*, and *Tringa totanus* were recorded as N and in this study they were recorded as WV. *Glareola pratincola* was SM and N and in this study it was WV. Moreover, while *Larus minutus*, *Larus genei*, *Larus canus*, *Larus ichthyaetus* were recorded as WV in Kiziroglu's [6] study, they were recorded as N, N, SM and N in this study, respectively. *Phylloscopus trochilus* and *Ficedula parva* were identified as TM in his study and they were identified as N and SM in this study, respectively. Finally, *Gallinago media*, *Phylloscopus trochiloides*, *Phylloscopus sibilatrix* were recorded as SM and in this study they were identified as WV, N, and N in this study, respectively. The difference in the immigration status of these species was thought to be resultant of the data that covers all the Marmara Region in the study of Kiziroglu [7]. The data in this study, however, only includes the Körfez Wetland. Thus, the difference is natural when compared to the data obtained from a wider geographical sample of the Marmara Region.

There is no scientific study about the Körfez Wetland outside the report prepared in 2015. For this reason, the ornitofaunistic features of the area were compared with important bird areas at various distances and areas in the Marmara Region (Table 2). Although Körfez Wetland is quite small (absolute protection zone) compared to other areas, it has a

significant number of different bird species.

Although the fact that the Körfez Wetland is located in an intensely populated, industrial and transport (sea, land and air) region and these pressures will increase over time, the area comes after Acarlar Lake when the diversity indexes of the areas were compared (Table 3). Moreover, there is a larger area of reed beds that was separated by a road (habitat fragmentation) from the absolute protection area where the bird species were recorded. This part is identified as the edge of the Kilez Stream. However, because of the reasons arising from industrial organizations, birds cannot use this part and the area gradually loses its protective properties. The area that birds use is a narrow coastal strip where marine and recreation activities are carried out. The diversity indexes of the species in Büyükçekmece Lake, Ulubat Lake, and Sarıçay Delta cannot be calculated since the total individual numbers could not be accurately obtained. Thus, a comparison with other areas in terms of diversity indexes could not be carried out.

Among the areas compared in this study, Acarlar Lake, Sapanca Lake, İznik Lake and Ulubat Lake contains only freshwater ecosystem. Büyükçekmece Lake, Sarıçay Lake and Körfez Wetland contain both freshwater and saltwater ecosystems and together and they are coastal wetlands. They have more in common and are similar ecologically with Körfez Wetland. According to Sorenson Similarity Index results, Körfez Wetland matches 87% with Büyükçekmece Lake (Table 3). This result supports the ecological similarities. Although Sapanca Lake is the closest area to Körfez Wetland, increased similarity with Büyükçekmece Lake shows that ecological match is more important than distance. However, despite the area's ecologically similarity with Sarıçay Delta

**TABLE 2**  
**Ornitofaunistic Properties of Wetlands**

City	Name	Size (ha)	Number of Ordo	Number of Familia	Number of Species	Number of Individuals	Literature
Bursa	İznik Lake	29800	11	29	58	31337	[12]
Sakarya	Sapanca Lake	4500	12	28	69	117413	[13]
İstanbul	Büyükçekmece Lake	2850	14	42	170	-	[14]
Çanakkale	Sarıçay Delta	39378	15	34	90	-	[15]
Sakarya	Acarlar Lake	7200	17	39	178	73632	[16]
Bursa	Uluabat Lake	13600	-	-	33	-	[17]
Kocaeli	Körfez Wetlands	51,45	11	31	93	38360	This Study

**TABLE 3**  
**Number of Species by Frequency and Dominance Value**

Margalef Index (D)		Sorenson Index (S)	
Wetlands	Value	Compared Wetlands	Value
Acalar Lake	36,41	Körfez Wetlands-Büyükçekmece Lake	% 87
Körfez Wetlands	20,08	Körfez Wetlands-Sapanca Lake	% 56
Sapanca Lake	13,43	Körfez Wetlands-İznik Lake	% 50
İznik Lake	12,69	Körfez Wetlands-Acarlar Lake	% 47
		Körfez Wetlands-Sarıçay Delta	% 43
		Körfez Wetlands-Uluabat Lake	% 34

and host close number of individuals, the similarity index was calculated at 43% due to the fact that they are on different migration routes. The aviary immigrants entering Turkey from Balkans continue their migration by separating into two as Çanakkale and İstanbul lines [6]. This has differentiated observed species in the area.

As a result, Körfez Wetland has a significant importance for bird species and their life cycles in terms of both its location and ecological features. The area is increasingly under pressure and stands to lose its natural structure due to growing anthropogenic encroachment. Protection of such areas is extremely important for the continuation of the diversity of flora and fauna, especially for bird species.

## REFERENCES

- [1] Chui, T.F.M., Low, S.Y., Liong, S. (2011), An ecohydrological model for studying groundwater-vegetation interactions in wetlands. *Journal of Hydrology*, 409, 291–304.
- [2] Quiroga, M., Leon, E., Beltzer, A., Olgun, P. (2013), Diet of Black-crowned Night-herons (*Nycticorax nycticorax*) in a Wetland of the Parana River's Alluvial Valley. *Ekoloji*, 22, (88), 43–50.
- [3] Newbrey, J.L., Paszkowski, C.A., Dumenko, E.D. (2013), A Comparison of Natural and Restored Wetlands as Breeding Bird Habitat Using a Novel Yolk Carotenoid Approach. *Wetlands*, 33:471–482.
- [4] Hayman P., Hume R. (2005), Kuş Gözlemcisinin Cep Kitabı-Avrupa'nın Kuşları, Kuş Araştırmaları Derneği Yayınları. (1st ed.) Ankara, Turkey.
- [5] Kocataş, A. (1997), Ekoloji ve Çevre Biyolojisi. Ege Üniv. Basımevi, İzmir, Turkey.
- [6] IUCN, International Union for Conservation of Nature and Natural Resources. (2014), www.iucnredlist.org, 01.03.2016
- [7] Kızıroğlu İ., Turan L., Erdoğan A. (1992), Sultansazlığı'nın Eko-Ornitolojisi ve Son Durumu, *H.Ü. Eğitim Fakültesi Dergisi*, C.7, 217-227.
- [8] Kızıroğlu İ. (2008), Red Data Book for Birds of Turkey, Center for Environmental Education,

Avian Studies and Bird Ringing, Hacettepe University.

- [9] Convention on the Conservation of European Wildlife and Natural Habitats (1979) [http://www.persona.uk.com/a21Ton/Core\\_dox/J/J2.pdf](http://www.persona.uk.com/a21Ton/Core_dox/J/J2.pdf) 01.03.2016
- [10] CITES, Convention on International Trade in Endangered Species of Wild Fauna and Flora, <https://www.cites.org/> 01.03.2016
- [11] T.C. Ministry of Water Affairs and Forestry (2015) Gulf Wetland Region Avian Species Report.
- [12] Irmak Türkmen E.N., Uzun A. (2010), İznik Gölü (Bursa) Ornitofaunasının Biyoekolojisi, *SAÜ Fen Edebiyat Dergisi*. 12 (1) 77-89
- [13] Uzun A. (2010-I), Sapanca Gölü (Sakarya) Ornitofaunasının Biyoekolojisi, *SAÜ Fen Edebiyat Dergisi*. 12 (1) 1-14.
- [14] Bacak E. (2012), İstanbul Büyükçekmece Gölü Avifaunası Üzerine Araştırmalar (Master Thesis), İstanbul Üni., Fen Bil. Enst., Yük. Lis. Tezi, İstanbul, Turkey.
- [15] Gürkan M. (2005), Çanakkale Sarıçay Deltası'nın Ornitofaunası, (Master Thesis) *Çanakkale Üni. Fen Bil. Enst., Yük. Lis. Tezi*, Çanakkale, Turkey.
- [16] Uzun A., Tabur M.A., Ayvaz Y. (2008), Birds of Lake Acarlar and Environmental Problems, *Çev. Kor. Ekoloji*, 17, (66), 1-14.
- [17] Mutlu S. (2005), Uluabat Gölü'nde 2003 Yılında Üreyen Kuş Türleri Üzerine Araştırmalar, (Master Thesis) *Uludağ Üni. Fen Bil. Enst. Yük. Lis. Tezi*, Bursa, Turkey.

**Received: 12.04.2016**

**Accepted: 22.07.2016**

## CORRESPONDING AUTHOR

**Ali Uzun**

Sakarya University, Arts and Science Faculty,  
Department of Biology, Esentepe Campus, Sakarya-  
Turkey

e-mail: [aliuzun@sakarya.edu.tr](mailto:aliuzun@sakarya.edu.tr)

# A STUDY ON THE DEVELOPMENT PERFORMANCES OF GOJI BERRY (*LYCIUM BARBARUM* L.) VARIETIES

H Ibrahim Oguz\*, Oktay Erdogan

The University of Nevşehir Hacı Bektaş Veli, Engineering-Architecture Faculty, Department of Biosystem Engineering, Nevşehir, Turkey

## ABSTRACT

This study was conducted in Adıyaman's Tut district during the 2012-2013 period, with the aim of determining the morphologic development of Damaye and NQ1 Goji Berry varieties, as well as the physical quality criteria and phytochemical rates of change of their fruits under the ecologic conditions of South-eastern Anatolia Project (GAP) upper region. In this context, in 2012 Damaye and NQ1 Goji Berry varieties were planted as tube seedling in randomized blocks experimental design, with three replications and 10 plants in each replicate, with an interval of 3 x 2 meters, starting from the second half of July in both years, some morphologic (plant height, shoot size, stem diameter, fruit width, fruit length, fruit weight, yield) measurements were made on varieties in each parcel, fruit samples were taken from the same parcel and certain physical and chemical (water soluble dry matter-WSDM, pH, ash, raw oil, protein,  $\beta$ -carotene quantity, total phenol, flavonoid, malic acid, ascorbic acid) analyses were also been conducted. According to the variance analysis results; the variety x year interaction was significant at ( $P \leq 0.05$ ) in terms of plant height, shoot size, yield and ascorbic acid characteristics, while in stem diameter, fruit size, fruit weight, WSDM, ash, raw oil, protein,  $\beta$ -carotene, total phenol and flavonoid characteristics, only the variety was significant at ( $P \leq 0.05$ ). Of the characteristics analysed during 2012, plant height (71.35 cm), shoot size (7.91 cm), yield (0.33 kg/tree) were observed to be higher in Damaye variety than in NQ1 variety, while in 2013, plant height (67.02 cm), shoot size (7.91 cm), yield (0.33 kg/tree) values were in contrast, where these values were higher in NQ1 variety when compared to Damaye variety. Ascorbic acid values were observed to be (10.78-12.29 mg/100 g) higher in NQ1 variety in both years. Values related to characteristics to such as fruit size (15.78 mm), fruit weight (4.13 g), protein rate, (11.68%), raw oil rate (8.12%),  $\beta$ -carotene quantity (8.83  $\mu\text{g/l}$ ), total phenol (351.35 mgGAE/100 g) and flavonoids (51.09 mgQE/g) were higher in NQ1 variety than in Damaye variety, while characteristics such as stem diameter (6.55 mm) and WSDM (27.49%) were higher in Damaye variety than in NQ1.

## KEYWORDS:

Goji berry, morphologic characteristics, physical analysis, chemical analysis, yield

## INTRODUCTION

Known as Goji Berry (*Lycium barbarum* L.) or "Wolfberry" in the world, "Kurt Üzüümü (Wolf Grape)" is not so popular in Turkey; however it has made its mark as the "Super Fruit" of the 21<sup>st</sup> century. Goji Berry is mostly being grown in south-western parts of China, and it is also being widely grown and used in south-eastern Asian countries and many European countries, particularly for medical aromatic plant purposes [1]. The origin of Goji Berry is rooted back to Asia and mostly it is being grown in the Himalayas, the highest mountains in the world, placed in Tibet and Mongolia [2]. Botanically, it is a member of the Solanaceae family, and the most common types are *Lycium barbarum* and *Lycium sinensis*. Goji Berry is a deciduous plant in bush form, grown in China. It has a red coloured, bright, ellipsoid and 1-2 cm long grape-like fruit. It is also being consumed with light or alcoholic drinks with its concentrated extracts and brewed juices [3]. Goji Berry fruit growing and studies on using it in other areas as a medical plant increasingly continues. It has the highest nutritional value in the world and is also a powerful antioxidant, and this fruit is being used for 2000 years in China for medical purposes. In addition, it is also one of the most important fruits of Chinese cuisine. It is being widely used along with meat and vegetables, in soups, rice porridge etc. The fruit harvested from August to October is generally dried, while it is consumed fresh in May. In addition, its fresh leaves are consumed as vegetable. Because of all these characteristics, Goji Berry plant is rapidly increasing its popularity among the grape-like fruits [4, 5]. Many scientific studies were conducted on this issue. Researchers were reported that Goji Berry plant is particularly rich in polysaccharides, a renowned antioxidant, and its fruit contains 52 different flavonoid and phenolic acids, again in antioxidant compositions [6]. In a previously conducted study, the water distillable essential basic oils in *L. barbarum* and *L. ruthenicum* fruits were analysed by the use of

GC-MS, and as basic compositions in the oils, hexadecanoic acid (47.5%), linoleic acid (9.1%),  $\beta$ -Elemene (5.4%), myristic acid (4.2%), ethyl hexadecanoate (4.0%) rates were determined. In *L. ruthennium* fruits on the other hand, the basic oil compositions were defined as heptacosane (14.3%), ethyl linoleate (10.0%), hexacosane (7.0%), nonacosane (6.2%), and ethyl hexadecanoate (5.8%) [7].

The amount of studies conducted in relation to Goji Berry variety is not sufficient in Turkey. In this sense; it was aimed to determine the development performances of Damaye and NQ1 Goji Berry varieties in upper GAP Region and the phytochemical characteristics of its fruit.

## MATERIALS AND METHODS

**Material.** In the study, plant material were one year old tube seedling of *L. barbarum* L. crossbreed, self-yielding, fresh fruit diameter 1.25 cm - 2.80 cm, fresh fruit yield 8 - 8.4 ton/acre NQ1 variety and Ningxiya variety crossbreed, with oval fruits and a bit smaller than NQ-1, self-yielding, fresh fruit diameter of 1.25 cm - 2.80 cm, fresh fruit yield of 7.5 - 8 ton/acre Damaye Goji Berry varieties obtained from Yaban Company [8, 9].

**Methods. 1. Experimental site and experimental design.** The Province of Adiyaman was chosen as our study area. It is located in Turkey's South-eastern Anatolia Region with a 7.644 km<sup>2</sup> land area and geographic coordinates of 38° 11' N and 37° 25' N latitude and 39° 14' E and 37° 31' E longitude. The study area consists of Tut districts of Adiyaman. The experiment was carried out using three replications in a randomized blocked design and to be 10 plants in each replicate with one-year of Goji Berry (tube seedlings) at distances 3 x 2 meters.

**2. Morphologic measurements.** Starting from the second half of July in both years, measurements were made on 60 pieces of tube seedlings in each parcel 60 by considering the below issues [10].

**Plant height:** 30 plants in each parcel were measured from 15 cm above the main stem of the plant.

**Shoot size:** Shoot sizes of 30 plants in each parcel were measured.

**Stem diameter, fruit width, fruit length:** these were measured in 30 plants in each parcel by using a digital calliper with a sensitivity of 0.01mm.

**Fruit weights:** 20 fruit samples from each parcel were weighed by using a precision balance with a sensitivity of 0.01.

## 3. Physical and chemical analysis.

During the month of August in both years, 1.5 kg of fruit samples were taken from the varieties in each parcel, and until the execution of the analyses, these samples were kept at -80°C in a deep-freezer. Then the following physical and chemical analysis method was applied.

**Water soluble dry matter (WSDM):** This was obtained by directly measuring the fruit juice in an ATAGO made refractometer [11].

**pH value:** Obtained by the use of a digital pH-metre (SCHOTT G6 840) [12].

**Ash determination:** Obtained by burning the samples in an ash furnace at 550°C until they became white ash [13].

**Raw oil analysis:** Determined by the use of soxhlet extraction mechanism [14].

**Protein analysis:** The protein quantities of the fruits were obtained through Kjeldal method [15].

**$\beta$ -carotene quantity:**  $\beta$ -carotene quantity was obtained in accordance with AOAC (1980) [16].

**Phenolic compounds:** The phenolic matter quantity in fruit juice was determined in accordance with Folin-Ciocalteu method [17].

**Flavonoid analysis:** The total flavonoid contents in fruit samples were defined by using spectrophotometric analysis method based on 430 nm maximum absorbance complex flavonoid-aluminium formation [18].

**Ascorbic acid content:** Ascorbic acid value in fruits was analysed by using a reverse phased HPLC with quad automatic sampling, diode array sensor and Hewlett-Packard 1100 system [19].

**Data analysis.** Data collected on different parameters were analysed statistically by using JMP statistical software program (5.0.1, SAS Institute, Cary, NC) for analysis of variance and means were compared using Fisher's protected least significance difference (LSD) test at 5 % probability level [20].

## RESULTS AND DISCUSSION

The variance analysis table related to all the characteristics analysed in NQ1 and Damaye varieties were provided in Table 1. According to Table 1, variety x year interaction was significant at ( $P \leq 0.05$ ) in terms of plant height, shoot size, yield and ascorbic acid, while in terms of stem diameter, fruit length, fruit weight, WSDM, ash, raw oil, protein,  $\beta$ -carotene, total phenol and flavonoid characteristics, only the variety was significant at ( $P \leq 0.05$ ). Then in terms of fruit width, pH and malic acid characteristics, both the variety and variety x year interaction were not significant at ( $P \leq 0.05$ ).

**TABLE 1**  
Results of variance analysis for the investigated characters and mean of sum of squares

Source of Variance	Df	PH (cm)	PSD (mm)	SL (cm)	FW (mm)	FL (mm)	FW (g)	Y (kg/tree)
Rep.	2	40.671	0.235515	0.04017	1.3858643	20.111529	0.00732052	0.0005142
Year (Y)	1	14754.272	66.513341	135.78144	0.3057133	5.675125	0.00799112	2.4329600
Variety (V)	1	37.737ns	0.514903*	3.47382*	0.0834976ns	53.013969*	0.22954112*	0.000943ns
V x Y	1	186.020*	0.046094ns	13.61825*	0.3089139ns	6.450934ns	0.0029349ns	0.2794679*
Error	6	65.574	0.111046	1.01487	0.4138681	36.48554	0.0063824	0.0680807
Total	11	15084.275	67.420899	153.92855	2.4978572	121.73710	0.25417010	2.7819659

Df: degrees of freedom; \* Significant at the 0.05 probability level; ns= not significant.

PH= Plant Height; PSD=Plant Stem Diameter; SL= Shoot Length; FW= Fruit Width; FL= Fruit Length; FW= Fruit Weight; Y= Yield

**TABLE 1**  
Results of variance analysis for the investigated characters and mean of sum of squares

Source of Variance	Df	WSDM (%)	Ash (g/100)	pH	CO (%)	Protein (%)
Rep.	2	5.856906	0.00034739	0.01393206	0.0097778	0.1711491
Year (Y)	1	0.005072	0.00095362	0.00044464	0.0010721	0.1075069
Variety (V)	1	55.494174*	0.00180094*	0.01920364ns	7.4280882*	7.4227010*
V x Y	1	0.033000ns	0.00145584ns	0.00011436ns	0.0070773ns	0.1671309ns
Error	6	7.211556	0.00148266	0.04327227	0.0512352	0.3845333
Total	11	68.600708	0.00604044	0.07696696	7.4972507	8.2530213

Df: degrees of freedom; \* Significant at the 0.05 probability level; ns= not significant.

WSDM= Water Soluble Dry matter; CO= Crude Oil

**TABLE 1**  
Results of variance analysis for the investigated characters and mean of sum of squares

Source of Variance	Df	AA (mg/100 g)	BC (µg/l)	MA (mg/100)	Total phenol (mgGAE/100 g)	Flavonoids (mg QE/g)
Rep.	2	0.0160707	0.13373648	19.313253	0.34320	0.512404
Year (Y)	1	0.0024884	0.03783932	9.367162	0.10166	0.576787
Variety (V)	1	7.4773068*	0.87020786*	38.098566ns	436.76025*	14.489893*
V x Y	1	0.0172371*	0.01641679ns	8.676518ns	0.47025ns	0.720530ns
Error	6	0.0119295	0.0610762	47.35055	3.85170	3.942948
Total	11	7.5250326	1.1192766	122.80605	441.52706	20.242562

Df= degrees of freedom; \* Significant at the 0.05 probability level; ns= not significant.

AA= Ascorbic Acid; BC= β-Carotene Quantity; MA= Malic Acid

The average values of plant height, shoot size, yield and ascorbic acid characteristics in NQ1 and Damaye varieties were provided in Table 2. In terms of plant height, shoot size, yield and ascorbic acid characteristics, variety x year interaction was significant at ( $P \leq 0.05$ ). In 2012, plant height in Damaye variety was 71.35 cm, and in NQ1 variety, it was 67.02 cm; shoot size in Damaye variety was 7.91 cm, while in NQ1 variety it was 6.86 cm; yield in Damaye variety was 0.33 kg/tree, and in NQ1 variety it was 0.22 kg/tree. Then in 2013, in contrast to 2012 and in terms of analysed characteristics, plant height in NQ1 variety was 143.03 cm, and in Damaye variety it was 133.61 cm; shoot size in NQ1 was 15.72 cm, and in Damaye it was 12.51 cm; yield in NQ1 variety was 0.75 kg/tree, and in Damaye variety it was 0.58 kg/tree. In 2012 and 2013 the NQ1 variety ascorbic acid values (12.39 mg/100 g – 12.29 mg/100 g)

were higher than the Damaye variety ascorbic acid values (10.74 mg/100 g – 10.78 mg/100 g) (Table 2). During the first year, Damaye variety had a better performance in terms of plant height, shoot size and yield per tree, compared to NQ1, but in the second year, NQ1 variety displayed a better performance than Damaye variety in terms of plant height, shoot size and yield per tree. In both years, ascorbic acid values were higher in NQ1 variety than Damaye variety. In a study conducted in Bulgaria on JB 1 and JB 2 Goji Berry varieties, it was reported that the varieties reached a length of 40 cm in a year and in JB 1 variety, yield was 0.56 kg/tree [21]. In a study conducted on the fruits of two Goji Berry varieties, *L. barbarum* and *L. chenensis*, it was observed that the ascorbic acid content was 36.24 mg/100 g – 68.26 mg/100 g in both [22].



**TABLE 2**  
The average values of plant height, shoot length, yield, ascorbic acid for Goji Berry varieties

Varieties	2012				2013			
	PH (cm)	SL (cm)	Y (kg/tree)	AA (mg/100 g)	PH (cm)	SL (cm)	Y (kg/tree)	AA (mg/100 g)
NQ1	67.02 b	6.86 b	0.22 b	12.39 a	145.03 a	15.72 a	0.75 a	12.29 a
DAMAYE	71.35 a	7.91 a	0.33 a	10.74 b	133.61 b	12.51 b	0.58 b	10.78 b
LSD	14.982*	1.448*	0.494*	0.223*	12.162*	1.490*	0.405*	0.114*

\*Different letters between genotypes denote significant differences at 5% probability level

PH= Plant Height; SL= Shoot Length; Y= Yield; AA= Ascorbic Acid

**TABLE 3**  
The average values of plant stem diameter, fruit length, fruit weight, water soluble dry matter, ash for Goji Berry varieties

Varieties	PSD (mm)	FL (mm)	FW (g)	WDM (%)	Ash (%)
NQ1	6.14 b	15.78 a	0.70 a	23.19 b	0.08 a
DAMAYE	6.55 a	11.57 b	0.43 b	27.49 a	0.05 b
LSD	0.192*	3.483*	0.676*	1.548*	0.022*

\*Different letters between genotypes denote significant differences at 5% probability level

PSD=Plant Stem Diameter; FL= Fruit Length; FW= Fruit Weight; WDM= Water Soluble Dry Matter

**TABLE 4**  
The average values of protein, crude oil,  $\beta$ -carotene quantity, total phenol, flavonoids for Goji Berry varieties

Varieties	Protein (%)	Crude oil (%)	BC ( $\mu$ g/l)	Total phenol (mgGAE/100 g)	Flavonoids (mg QE/g)
NQ1	11.68 a	8.12 a	8.83 a	351.33 a	51.09 a
DAMAYE	10.11 b	6.55 b	8.29 b	339.26 b	48.89 b
LSD	0.357*	0.130*	0.142*	0.212*	1.145*

\*Different letters between genotypes denote significant differences at 5% probability level.

BC=  $\beta$ -Carotene Quantity

The average values of stem diameter, fruit size, fruit weight, WSDM and ash contents in NQ1 and Damaye varieties were provided in Table 3. According to Table 3, the varieties were significant at ( $P \leq 0.05$ ) in terms of stem diameter, fruit size, fruit weight, WSDM and ash contents. In Damaye variety the stem diameter was 6.55 cm, and in NQ1 variety it was 6.14 cm; fruit size in NQ1 variety was 15.78 mm, and in Damaye variety it was 11.57 mm; fruit weight in NQ1 variety was 0.70 g, and in Damaye variety it was 0.43 g; WSDM in Damaye was 27.49%, and in NQ1 it was 23.19% and ash content in NQ1 variety was 0.08 %, and in Damaye variety it was 0.05%. In terms of stem diameter and WSDM characteristics, Damaye variety ranked first, while in terms of fruit size, fruit weight and ash content characteristics, NQ1 variety was ranked first. The data gathered in the study was in parallel to the findings of other studies on the same subject. In a study conducted on Ningxia Goji Berry variety, an ash content of  $0.95\% \pm 0.11$  was reported in fruits [23]. In another study conducted on the physical

quality criteria of Goji Berry fruit, fruit size was reported as 11.50 mm and water soluble dry matter was reported as 11.63% [22]. In another study on Goji Berry fruit, water soluble dry matter was reported as 59.16 % and ash content was reported as 0.063% [18].

The average values of protein, raw oil,  $\beta$ -carotene, total phenol and flavonoids in NQ1 and Damaye varieties were provided in Table 4. The varieties were significant at ( $P \leq 0.05$ ) in terms of protein, raw oil,  $\beta$ -carotene, total phenol and flavonoids. Protein content in NQ1 variety was 11.68%, and in Damaye variety it was 10.11%; raw oil content in NQ1 variety was 8.12%, and in Damaye variety it was 6.55%;  $\beta$ -carotene content in NQ1 variety was 8.83  $\mu$ g/l, and in Damaye variety it was 8.29  $\mu$ g/l; total phenol in NQ1 variety was 351.33 mg GAE/100 g, and in Damaye variety they were 339.26 mg GAE/100 g and flavonoid in NQ1 variety was 51.09 mg QE/g, and in Damaye variety it was 48.89 mg QE/g. Protein, raw oil,  $\beta$ -carotene, total phenol and flavonoid characteristics in NQ1

variety were higher than Damaye variety (Chart 4). The data gathered in the study was similar to the findings of other studies on the same subject. In a study conducted on Goji Berry fruit, it was reported that this fruit contains 268.35 mg GAE/100 g of total phenol and 116.27 mg/100 g of flavonoid [22]. The researchers were reported 12.20± 1.38% raw protein in Ningxia variety Goji Berry fruit [23]. In a study conducted on Goji Berry (*L. barbarum* L.) fruit, 4.11% raw oil, 3.44 mg GAE/ 100 ml total phenol and 8.9% protein were reported [24]. In another study conducted on the fruits of two different Goji Berry varieties; it was reported that *L. barbarum* samples contained 61.59 ± 1.68 mg GAE/100g total phenol, 43.73 ± 1.3 mg RE/g phenoloid, while in *L. chinensis* variety, 80.64 ± 2.02 mg GAE/100g total phenol and 61.65 ± 0.95 mg RE/g phenoloid were measured [25].

## CONCLUSION

Considering the two year morphologic and phytochemical characteristics of NQ1 and Damaye Goji Berry varieties; it was concluded that in 2012, Damaye variety was displayed a better performance than NQ1 variety in terms of plant height, shoot size and yield. However, in 2013, plant height, NQ1 variety was displayed a better performance than Damaye variety in terms of shoot size and yield. The reasons for NQ-1 variety exhibiting a slower development than Damaye variety during the first year can be associated with a longer duration of completing the vegetative development due to variety characteristics, when compared to Damaye variety, and also with the fact that in the following years, after completing its vegetative development, there is a difference in terms of efficient yield, again when compared to the Damaye variety. In terms of ascorbic acid, the highest ascorbic acid content was again observed in NQ1 variety fruit. In terms of phytochemical characteristics such as protein, raw oil, β-carotene quantity, total phenols and flavonoids, higher values were obtained in NQ1 variety than in Damaye variety. In terms of all morphologic and phytochemical characteristics analysed in upper GAP Region in 2013, NQ1 variety was ranked first. However, to be able to recommend NQ1 variety, more detailed studies need to be conducted on this variety, in different locations, and by including varieties with different characteristics.

## ACKNOWLEDGEMENTS

We would like to express our gratitude to Yaban Company and Mr. Atilla SEVILMIS for their assistance in field use and plant material supply.

## REFERENCES

- [1] Amagase, H. and Nance, D.M. (2008). A randomized, double-blind, placebo controlled, clinical study of the general effects of a standardized *Lycium barbarum* (goji) juice, GoChi. *Journal of Alternative and Complementary Medicine*, 14:403-12.
- [2] Song M.K., Salam N.K., Roufogalis B.D. and Huang T.H. (2011). *Lycium barbarum* (Goji berry) extracts and its taurine component inhibit PRAR-γ-dependent gene transcription in human retinal pigment epithelial cells: Possible implications for diabetic retinopathy treatment, *Biochemical Pharmacology*, 82(9):1209-1218.
- [3] Amagase, H. and Farnsworth, N.R. (2011). A review of botanical characteristics, phytochemistry, clinical relevance in efficacy and safety of *Lycium barbarum* fruit (Goji), *Food Research International*, 44: 1702–1717.
- [4] Potterat, O. and Hamburger M. (2008). Goji juice: a novel miraculous cure for longevity and well being? A review of composition, pharmacology, health-related claims and benefits. *Schweiz Zschr Ganzheitsmedizin*, 20: 399–405.
- [5] Potterat, O. (2010). Goji (*Lycium barbarum* and *L. chinense*): Phytochemistry, Pharmacology and Safety in the perspective of traditional uses and recent popularity, *Planta Med.*, 76: 7-19.
- [6] Anonymous (2010). Environmental Nutrition. “Are Goji Berries Really the Healthiest Food on the Planet?” [http://www.environmentalnutrition.com/issues/3\\_1\\_6/features/151700-1.html](http://www.environmentalnutrition.com/issues/3_1_6/features/151700-1.html)
- [7] Altintas, A., Kosar, M., Kirimer, N., Baser, K. H. C. and Demirci, B. (2006). Composition of The Essential Oils of *Lycium barbarum* and *L. ruthenicum* Fruits. *Chemistry of Natural Compounds*, 42 (1): 24-25.
- [8] Anonymous, 2016 a. <http://pegasus-bio.gr/en/cultivations/goji-berries>
- [9] Anonymous, 2016 b. <http://www.tanaduk.com/contact.html>
- [10] Bostan, S. Z. and Islam A. (1998). Kayısıda Bir ve İki Yaşlı Çöğür Anaçlarının Fidan Gelişimine Olan Etkileri. *Turkish Journal of Agriculture and Forestry*, 22:291-293. (in Turkish)
- [11] Cemeroglu, B. 1992 Meyve Sebze İşleme Endüstrisinde Temel Analiz Metotları. Biltav Yayınları, Ankara. (in Turkish)
- [12] Anonymous (1983). Gıda Maddeleri Muayene ve Analiz Yöntemleri. T.C. Tarım Orman ve Köyşleri Bakanlığı, Gıda İşleri Genel Müdürlüğü, Ankara, Özel Yayın No: 62-105: 72-73. (in Turkish)
- [13] Yamankaradeniz, R. (1983). Farklı Olum Asamalarındaki Kuşburnu (*Rosa spp.*)'nun



- Fiziksel ve Kimyasal Nitelikleri. Gıda, 8(4):151-156. (in Turkish)
- [14] Regnell, C.J. (1976). İşlenmiş Sebze Meyve Kalite Kontrolü ile ilgili Analitik Metotlar. Bursa Gıda Kontrol Eğt. Arş. Enst. Yayın No:2. (in Turkish)
- [15] Anonymous (1982). Analysis. IFFJP.Int'l Fedn. Of Fruit Juice Producers, Paris.
- [16] Çetin, E.S., Babalık, Z., Göktürk Baydar, N., 2012. Bazı Sofralık Üzüm Çeşitlerinde Tanelerdeki Toplam Karbonhidrat, Fenolik Madde, Antosiyanin, B-Karoten ve C Vitamini İçeriklerinin Belirlenmesi. IV. Ulusal Üzümsü Meyveler Sempozyumu, 151-159, Antalya. (in Turkish)
- [17] France Singleton, V.L. and Esau, P. (1969). Phenolic Substances in Grapes and Wine and Their Significance. Advance in Food Research, 282 p. Academic Pres. New York.
- [18] Cordenunsi, B.R., Oliveira Do Nascimento, J.R., Genovese, M.I. and Lajolo, F.M. (2002). Influence of Cultivar on Quality Parameters and Chemical Composition of Strawberry Fruits Grown in Brazil. J. Agric. Food Chem., 50:2581-2586.
- [19] Istrati, D., Vizireanu, C., Iordachescu, G., Dima, F. and Garnai, M. (2013). Physico-Chemical Characteristics and Antioxidant Activity Of GojiFruits Jam and Jelly During Storage. The Annals of the University Dunarea de Jos of Galati. Fascicle VI – Food Technology, 37(2):100-110.
- [20] Steel, R.G.D., Torrie, J.H. and Dickey, D.A. (1997). Principles and procedures of statistics: A biometrical approach. 3rd edition, McGraw Hill Book Co. Inc. 400-428.
- [21] Dzhugalov, H., Lichev, V., Yordanov, A., Kaymakanov, P., Dimitrova, V. and Kutoranov, G. (2015). First Results Of Testing Goji Berry (*Lycium barbarum* L.) In Plovdiv Region, Bulgaria. Scientific Papers. Series B, Horticulture, 47-50, ISSN 2285-5653.
- [22] Yan, Y., Ran, L., Cao, Y., Qin, K., Zhang, X., Luo, Q., Jabbar, S., Abid M. and Zeng, X. (2014). Nutritional, Phytochemical Characterization and Antioxidant Capacity of Ningxia Wolfberry (*Lycium barbarum* L.). J.Chem.Soc.Pak., 36(6):1079-1087.
- [23] Donno, D., Beccaro, G.L., Mellano, M.G., Cerutti, A.K. and Bounous, G. (2015). Goji berry fruit (*Lycium* spp.): antioxidant compound fingerprint and bioactivity evaluation. Journal of Functional Foods, 18:1070-1085.
- [24] Endes, Z., Uslu, N., Özcan, M.M. and Er, F. (2015). Physico-chemical properties, fatty acid composition and mineral contents of goji berry (*Lycium barbarum* L.) fruit. Journal of Agroalimentary Processes and Technologies, 21(1):36-40.
- [25] Mocan, A., Vlase, L., Vodnar, D. C., Bischin, C., Hanganu, D., Gheldiu, A.-M., Oprean, R., Silaghi-Dumitrescu, R. and Crişan, G. (2014). Polyphenolic Content, Antioxidant and Antimicrobial Activities of *Lycium barbarum* L. and *Lycium chinense* Mill. Leaves. Molecules, 19:10056-10073.

---

**Received:** 18.04.2016

**Accepted:** 05.08.2016

---

**CORRESPONDING AUTHOR**

**H. Ibrahim Oguz**

Nevşehir Hacı Bektaş Veli University  
Department of Biosystem Engineering  
50300 Nevşehir-TURKEY

e-mail: hioguz64@gmail.com

# COMPARISON OF HEAVY METALS AND BENEFICIAL ELEMENTS IN NORTHEASTERN AND SOUTHERN RICE OF CHINA BY ICP-MS

Zhang Hongxing<sup>1,2,\*</sup>, Liu Hui<sup>1,2</sup>, Xie Yuanhong<sup>1,2</sup>

<sup>1</sup> Beijing University of Agriculture, Beijing Laboratory of Food Quality and Safety, Beijing Key Laboratory of Agricultural Product Detection and Control for Spoilage Organisms and Pesticide, Beijing, 102206, China

<sup>2</sup> Beijing Engineering Technology Research Center of Food Safety immune rapid detection, Beijing, 102206, China

## ABSTRACT

Northeastern rice is one of the best rice brand in China, which has good taste and rich in nutrition. But the difference of heavy metals and healthy trace elements in northeastern and southern rice were few reported. Nineteen northeastern rice and seventeen southern rice samples were investigated. Northeastern rice contained more Ca, Mn, Fe, Zn, and Cu, but less Se and Mo as compared to southern rice. But southern rice contained more Cd and Cr; especially Cd often exceeded than national standard. All these data should be related to the content of these elements in soil. In summary, we can conclude that northern rice is more nutritional and safer than southern rice in China.

## KEYWORDS:

Northeastern rice of China, Heavy metals, Healthy trace elements, Cadmium, Food safety, ICP-MS

## INTRODUCTION

Northeastern rice is one of the best rice brand in China, which is mainly grown in northeast China including Heilongjiang, Liaoning and Jilin provinces, has good taste and rich in nutrition [1]. Rice quality is significantly related to the local climate [2] and the environment of the soil [3], and the quality of northeastern rice is better than southern rice, including protein content, lower amylase content and higher phospholipids content [4].

Except nutrition content, heavy metals have also become an important index to evaluate rice quality especially after “CADMIUM RICE EVENT” in 2013 [5]. The cadmium (Cd) contamination of rice and its potential health risk of 484 rice samples. The mean Cd content ranged

from 0.149 to 0.189 mg·kg<sup>-1</sup> and Cd concentration in more than 18% of rice samples exceeded the maximum allowable Cd concentration, and the highest level of 41.1 % was observed in samples from Hezhang, Guizhou, south of China [6]. So it is very meaningful to compare the content of heavy metals and healthy trace elements in northeastern and southern rice.

## MATERIALS AND METHODS

**Materials.** Total Nineteen samples of northeastern rice were selected, ten samples from Heilongjiang province, four from Liaoning province and five samples from Jilin province. Seventeen samples from the harder-hit area of Cadmium rice which is located in the south of China, eleven samples from Hunan province and six samples from Guangdong province were selected.

**Methods.** The ICP-MS PQ Excel instrument (ELAN DRCII, PE Company, USA) from Central Laboratory, School of Public Health, Peking University was used for analysis. Sample preparation and Instrument parameters were referred to Zhang and Rui's research [7-8].

## RESULTS AND DISCUSSIONS

**Content of beneficial elements.** Rice contained many kinds of trace elements, such as Ca, Mn, Zn, Fe, Cu, Mo, and Se (Table 1), which are essential for human health. As compared to southern rice, northeastern rice contained more Ca, Mn, Fe, Zn, and Cu, but less Se and Mo. All these data is related to the content of these elements in soil. So, we can conclude northern rice is more nutritional than southern rice.

**TABLE 1**  
**Content of beneficial elements in Northeastern rice**

Elements	Northeastern rice	Southern rice
Ca	97.6-120.7 $\mu\text{g}\cdot\text{g}^{-1}$	81.7-100.5 $\mu\text{g}\cdot\text{g}^{-1}$
Mn	61.5-80.0 $\mu\text{g}\cdot\text{g}^{-1}$	44.8-71.3 $\mu\text{g}\cdot\text{g}^{-1}$
Fe	12.3-15.7 $\mu\text{g}\cdot\text{g}^{-1}$	11.5-13.8 $\mu\text{g}\cdot\text{g}^{-1}$
Zn	34.9-43.2 $\mu\text{g}\cdot\text{g}^{-1}$	27.4-36.4 $\mu\text{g}\cdot\text{g}^{-1}$
Cu	5.3-8.1 $\mu\text{g}\cdot\text{g}^{-1}$	3.7-6.7 $\mu\text{g}\cdot\text{g}^{-1}$
Se	15.5-18.3 $\text{ng}\cdot\text{g}^{-1}$	33.7-42.6 $\text{ng}\cdot\text{g}^{-1}$
Mo	200.5-277.6 $\text{ng}\cdot\text{g}^{-1}$	253.8-377.6 $\text{ng}\cdot\text{g}^{-1}$

**TABLE 2**  
**Content of heavy metals in Northeastern rice ( $\mu\text{g}\cdot\text{kg}^{-1}$ )**

Elements	Northeastern rice	Southern rice
Cr	2.3-6.8	8.7-10.7
As	130.5-161.7	80.8-151.3
Cd	52.5-80.9	145.8-211.3
Pb	9.9-19.6	2.7-10.5

**Content of heavy metals.** The results of heavy metals Cr, As, Cd, and Pb are shown in Table 2. Northern rice contained more As and Pb than southern rice, which is mainly dependent on As and Pb content in soil. However, southern rice contained more heavy metals Cd and Cr, especially Cd often exceeded than national standard (0.2 $\mu\text{g}/\text{kg}$ ). All these data mainly depend on the heavy metals content in soils, because the Cadmium pollution in southern soil is very severe.

#### ACKNOWLEDGEMENTS

The authors acknowledge the support by the Importation and Development of High-Caliber Talents Project of Beijing Municipal Institutions (CIT&TCD20140315). We also appreciate Mrs. Li Ouyang from Peiking University for detecting.

#### REFERENCES

- [1] Zhang Hongxing, Rui Yukui and Li Yaxiong (2013) Determination of Beneficial Elements, Heavy Metals and Rare Earth Elements in Northeastern Rice Brand of China by ICP-MS, *Asian J Chem* 25(4): 2315-2316
- [2] Xia Liya, Li Xiaoting, Hu Xiaoling, Wang Yanfeng (2009) Analysis on the Relationship between Quality of Panjin Rice and Environment of Producing Area. *J Anhui Agr Sci* 37(31):15186-15188
- [3] Zhou Chongsong, Liu Wenhong, Fan Biwei, et al (2003) Study on Correlation between Trace Elements and Quality and Output of Rice in Sichuan. *Trace Elem Sci* 10:56-59
- [4] Chi Mingmei (2005) Investigation and Analysis on edible quality of rice in Northeast China. *Mach Cereal oil Food Proc* 2: 61-63
- [5] Li Guoqing (2013) On Chinese Supervision of Grain Quality Safety from “Cadmium Rice” Event in Guangdong. *J Henan Univ Tech* 9(3): 20-23
- [6] Ke Shen, Cheng Xi-Yu, Zhang Ni (2015) Cadmium contamination of rice from various polluted areas of China and its potential risks to human health. *Environ Monit Assess* 187(7):408
- [7] Zhang Hongxing, Rui Yukui (2011) Determination of Trace Elements, Heavy Metals and Rare Earth Elements in Corn Seeds from Beijing by ICP-MS Simultaneously. *E-j chem* 8(2):782-786
- [8] Rui Yukui, Guo Jing, Huang KunLun (2007) Application of ICP-MS to the detection of heavy metals in transgenic corn. *Spectrosc Spect Anal* 27(4): 796-798

**Received: 25.04.2016**

**Accepted: 13.09.2016**



## **CORRESPONDENCE AUTHOR**

---

### **Zhang Hongxing**

Beijing Key Laboratory of Agricultural Product  
Safety Detection and Control  
Department of Food Science  
Beijing University of Agriculture  
102206 Beijing– CHINA

e-mail: zhanghx511@126.com

# AN EXPERIMENTAL STUDY INTO HYDRAULIC COEFFICIENT IN TRAPEZOIDAL LABYRINTH WEIR AND PIANO KEY WEIR

Ramin Gharibvand<sup>1</sup>, Mohammad Heidarnejad<sup>2,\*</sup>, HeidarAli Kashkouli<sup>2</sup>, Houshang Hasoonizadeh<sup>3</sup>, Amir Abbas Kamanbedast<sup>2</sup>

<sup>1</sup> Department of Water Science Engineering, Khuzestan Science and Research Branch, Islamic Azad University, Ahvaz, Iran

<sup>2</sup> Department of Water Science Engineering, Ahvaz Branch, Islamic Azad University, Ahvaz, Iran

<sup>3</sup>Iran's Khuzestan Water and Power Authority

## ABSTRACT

Due to significant cost reduction, simpler implementation procedure, and capability in managing large flows, the application of labyrinth weir has attracted the designers of such structures. This is because of elongation of effective length of weir within a limited width of excavated area in the outlet channel of the spillway. Among the advantages of labyrinth weirs are high capacity, simple aeration, and low water flow surface over the weir. The piano key weirs (PKW) are a new type of high discharge capacity spillways. This study investigated the discharge coefficient of a PK weir and a trapezoidal labyrinth weir. Results showed that the discharge coefficient in the PK weir increased by about 30%, relative to trapezoidal labyrinth weir. The difference in flow coefficient decreases with increasing hydraulic load. This factor is equal in both weirs at the submerged and post-submerged discharge rates

## KEYWORDS:

Labyrinth Weir, Trapezoidal Weir, Piano Key Weir, Discharge Coefficient

## INTRODUCTION

Weirs have a significant role in the safety of dams, and are responsible for a large portion of dam construction costs. They are among structures used for the measurement and management of water flow. One of the main reasons for dam failure is insufficient discharge capacity of weirs. Therefore, designing weirs with high discharge rate is very important. The labyrinth weirs are recognized with their indirect axis in plan that is repeated periodically. Relative to the weirs with linear crests, these types of spillways have longer linear crest, within a certain width, and greater discharge capacity at an equivalent hydraulic load. The

efficacy of such weirs at low hydraulic load is significant, as an increase in nappe width will lead to interference of flow layers and decreased discharge coefficient. At the flood peak, the overflow discharge usually reaches a maximum value in a short time which necessitates a weir with high discharge capacity. To this end, labyrinth weirs, which have a greater discharge capacity than linear weirs, are used [1]. The PK weirs are a new type of economically very efficient spillways with a very high discharge capacity.

Similar to labyrinth weirs, PKWs are curved in plan. This characteristic allows them to increase the discharge rate within a certain width of weir channel. In a similar vein to labyrinth weirs, PK weirs are a good solution to meet such needs of dam projects as higher discharge capacity or smaller cross-section devoted for flood discharge. At present, there is limited knowledge about the effect of different geometric parameters of PKWs on their hydraulic performance (Figure 1).

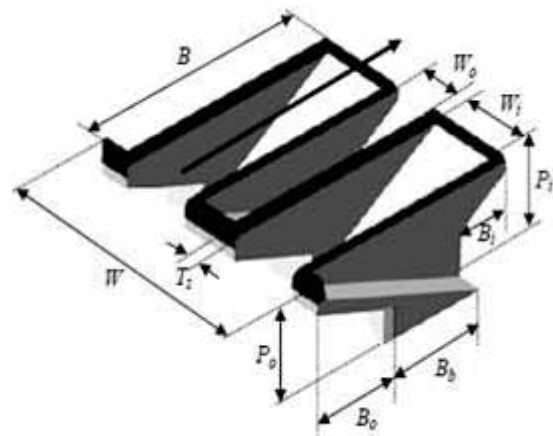


FIGURE 1  
Piano Key Weir [2].

As a result, the construction of such weirs increases discharge rate and lowers free upstream head, relative to linear spillways. This is very

important when it functions as a flood discharge control structure by facilitating the flood routing [3].

The early studies by Hay and Taylor (1970) showed that the performance of Labyrinth weirs is independent of W/P ratio, where W and P stand for cycle width and weir height respectively. Complementary studies by Falvey (2003) have revealed that if w/P ratio is below a certain level, it will have a significant effect on the reduction of weir's efficacy.

The first PKW was installed in 2006 at the Goulours dam in France [5]. During 2008-2010, PK weirs were used to improve flood discharge at different dams such as Mark Saint, Etroit, and Goulours. Laboratory studies by Ouamane and Lempérière (2006) showed two dominant flow types in PKWs, as follows: The inlet key attracts the approach flows, and similar to sharp-crested weirs with sloped sidewall, nappe flow discharges into downstream over the inlet crest. The second pattern is formed on the outlet keys in that the outlet crest jet flow discharges into the downstream of the sloped discharge key.

Leite Riberio et al. (2012) used the results of existing physical models to develop a general equation for PKW's discharge-stage relationship. According to their findings, the capacity of such weirs is mainly a function of over the weir water height, overall length, the inlet key height, and the transverse width.

Machiels (2012) reported the positive effect of parapet wall on hydraulic performance of such weirs by increasing weir height to reach the optimal height.

Crookston and Tullis (2012c, 2012d) investigated the characteristics of nappe interference and local submergence in triangular labyrinth side weirs with two and four cycles and different apex angles in a laboratory. Results showed that in low discharge rates, the discharge coefficient is larger in triangular labyrinth side weirs than the linear weir due to the small nappe interference, and the interference intensity gradually increases with increasing discharge. This leads to the reduction of discharge coefficient to an amount similar to discharge coefficient in a broad-crested weir.

Anderson and Tullis (2012) compared the hydraulic performance of Labyrinth weirs and rectangular PKWs. Results indicated better performance of PKWs because of the loss reduction in inlet keys.

Ouamane and Lempérière (2006) concluded that the application of PK weirs as common free-flow spillways is a simple, safe, and efficient solution. The PK weirs can increase the discharge rate by four times, significantly decrease the costs in new dams and ensure their safety, and improve current flood control mechanisms in many existing dams.

To have a better understanding of the shape of a piano key weir and its characteristics, it should be said that a change in standard design parameters such as upstream flow conditions, a slight crest-shape modification, or structural change can alter flow properties.

Crookston et al. (2012) performed some studies into two- and four-cycle trapezoidal labyrinth weirs with the sidewall angles of 15°. Their results are presented in Figure 2.

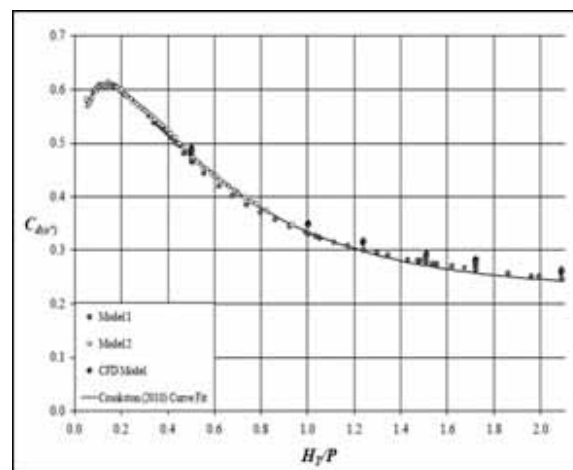


**FIGURE 2**

**Discharge ratio to  $H_t/p$  for trapezoidal labyrinth weir with sidewall angle of 15° [12].**

In addition, Anderson and Tullis (2013) compared the performance of PK weirs in the inlet-outlet key ratios of 0.67-1.5, and concluded that increased  $W_i/W_o$  (the inlet key width to the outlet key width) increases flow coefficient. In this figure,  $C_d$  is the flow coefficient,  $H_t$  is the head over a weir, and  $P$  stands for weir height (Fig. 3). They also studied the flow coefficient in trapezoidal labyrinth weirs with different sidewall angles, and observed maximum flow coefficient at the sidewall angle of 35° (Fig. 4).

Javaheri and Kabirisamani (2011) performed several studies on 20 geometrically different laboratory models to determine the effect of geometric and hydraulic parameters on PKW discharge. They investigated the impact of effective geometric parameters including weir length, weir height, and inlet and outlet widths on PKW's discharge coefficient. Finally, an equation with the least error rate was proposed as the best equation for determination of weir discharge coefficient at free flow condition, using general equation of weirs.



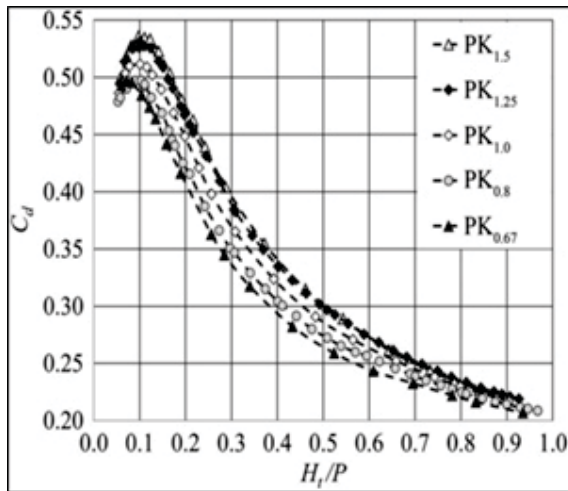


**FIGURE 3**

Discharge coefficient relative to  $H_t/p$  for five types of inlet key to outlet key ratios in PKW [13].

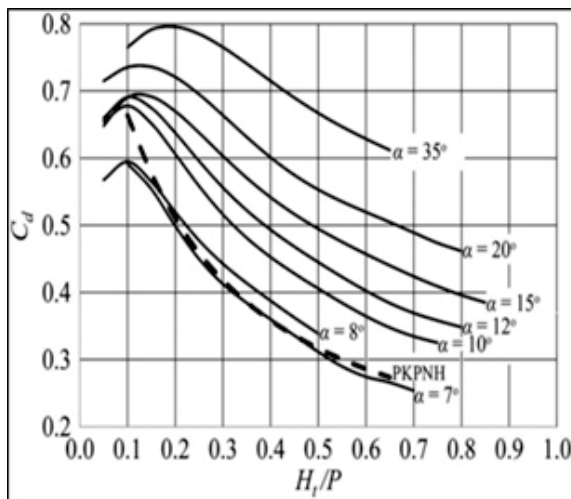


**FIGURE 4**

Discharge coefficient to  $H_t/p$  for trapezoidal labyrinth weir with different sidewall angles[13].

Karimi-Chahartaghi et al. (2014) studied the effect of varying crests at the angles of  $0^\circ$  and  $10^\circ$  on the discharge coefficient and discharge-stage curve of PKW physical model. They finally estimated the discharge coefficient values as about 1.76 at the crest angle of  $0^\circ$  and almost 6.13 at the crest angle of  $10^\circ$ , using general equation of weirs. These results indicate that a slight change in weir crest increases the discharge coefficient by 3.5 times, which is economically efficient.

In a laboratory study, Heidarpour et al. (2006) investigated the condition of one-cycle Labyrinth weirs with rectangular and U-shaped plans. Results from the experiments suggested that the discharge coefficient within a certain  $H_t/P$  (the ratio of overall upstream energy to weir height) increases with

increasing weir height (Fig. 3). In addition, comparisons illustrated that elongation across flow direction in Labyrinth weirs reduced discharge coefficient, whereas an elongation perpendicular to flow direction increased discharge coefficient.

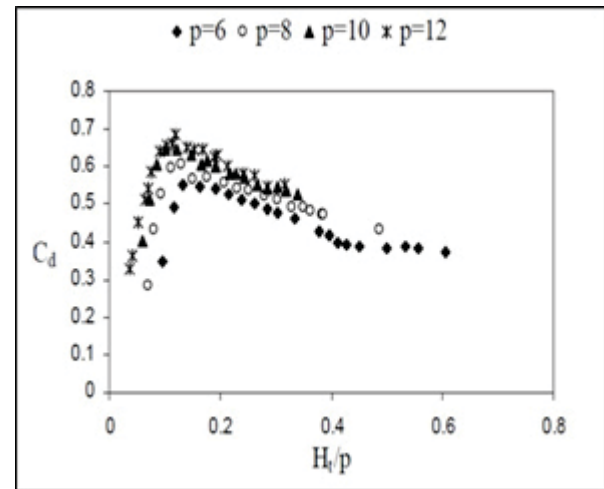


**FIGURE 5**

Discharge changes in rectangular Labyrinth Weir at different elevations[16].

Few people have performed hydraulic research into PK weirs. Ouamane and Lempérière (2006) believe that the discharge rate in PK weirs is at least by 4-time larger than conventional weirs, which increases the capacity of reservoir. Barcodá et al. (2006), Hien et al. (2006), Lempérière and Ouamane (2003), Lempérière and Ouamane (2006), Anderson and Tullis (2011), Laugier et al. (2011), Machiels et al., (2011), Pralong et al. (2011), and Lempérière and Ouamane (2006) concluded that adding to the number openings in low heads improves the efficacy of the weir. Lempérière and Ouamane (2006), Hien et al. (2006), and Barcodá et al. (2006) showed that if the inlet opening was considered bigger than the outlet opening, the discharge rate in the weir would be increased.

Despite some previously conducted studies into the performance of PK weirs, this research performed some experiments to determine the discharge coefficient in a PK weir and a two-cycle trapezoidal Labyrinth weir.

## **DIMENSIONAL ANALYSIS**

According to Fig. 6, the important geometric parameters in a PKW design are as follows: weir height ( $P$ ), height of crest to center of sloped floor ( $P_m$ ), crest centerline length ( $L$ ), slope of the inlet key ( $S_i$ ) and outlet key ( $S_o$ ) floors, spillway width ( $W$ ), spillway length ( $B$ ), outlet key length ( $B_o$ ), inlet

key length ( $B_i$ ), inlet key width ( $W_i$ ), outlet key width ( $W_o$ ), wall thickness ( $T_s$ ), overall key width ( $w$ ; where  $w = W_i + W_o - T_s$ ), and number of keys ( $N$ ).

Important geometric ratios in a PKW design include: weir crest length over spillway width ( $n=L/W$ ), inlet-outlet weir lengths ratio ( $B_i/B_o$ ), inlet-outlet key widths ratio ( $W_i/W_o$ ), and finally wall thickness to weir height ( $T_s/P$ ).

According to previous studies and observations, there are six factors affecting discharge capacity of PK weirs: Crest shape and thickness, submergence of crest, mutual impacts of nappe over the weir, approach flow conditions, critical cross-section along the inlet key, and head loss in the entrance of the inlet key[8].

According to previous studies, factors affecting the performance of trapezoidal Labyrinth weirs are as follows: Geometric parameters including weir width, crest length, height of crest above the upstream floor, length of apex's inner face, and angle of weir wall to main flow direction; structural configurations including crest shape, presence of aprons, and wall thickness; exploitation conditions including overall hydraulic load, and different stages of weir submergence and de-aeration; downstream conditions including crest height, water depth, sloped or non-sloped downstream, etc.; upstream conditions including inlet conditions, shape of guide wall, sloped and non-sloped upstream, etc. [23].

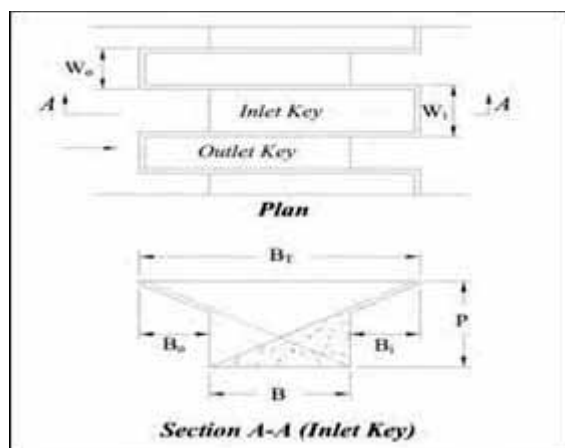


**FIGURE 6**

**Important geometric parameters in PKW design [12].**

The exact description of a three dimensional flow in Labyrinth weirs is very difficult. This is because a mathematical equation is needed in which energy, momentum, and continuity equations, along with such parameters as weir geometry, crest shape, local submergence, interference of flow layers over a weir, non-parallel flow lines, pressure under nappe, presence or absence of an air pocket behind nappe,

effects of surface tension and viscosity, etc. are considered.

Anderson and Tullis (2011) developed several laboratory prototypes to study the geometry of PK weirs, and developed coefficient of discharge ( $C_d$ ) for the assumed discharge ( $Q$ ), using Equation 1.

$$Q = \frac{2}{3} C_d L \sqrt{2g} H_0^{1.5} \quad (1)$$

In Equation 1,  $Q$  = weir discharge,  $L$  = length (like length of weir),  $g$  = acceleration of gravity,  $H_0$ =overall hydraulic load, and  $C_d$ =dimensionless discharge coefficient, which are determined through experiments.

In general, effective hydraulic quantities in PK weirs can be presented as follows

$$\eta = f(Q, B_i, B_o, S_i, S_o, t, p, D, W, n, H_0, H_d, S_e, S, Y, V, g, \mu, \rho, \nu, \sigma) \quad (2)$$

where,  $Q$ =channel discharge,  $B_i$ =inlet key width,  $B_o$ =outlet key width,  $Y$ =depth of flow in channel,  $V$ =velocity of flow in channel,  $g$ =acceleration of gravity,  $\mu$ =dynamic viscosity=fluid density,  $t$ =thickness of weir wall,  $U$ =cinematic viscosity,  $S_i$ =inlet key slope,  $S_o$ =outlet key slope,  $D$ =weir height in downstream,  $p$ =weir height in upstream,  $W$ =cycle width,  $n$ =cycle number,  $\sigma$ =surface tension,  $H_0$ =overall hydraulic load on upstream,  $H_d$ =overall hydraulic load in downstream,  $S$ =channel slope,  $B$ =channel width,  $S_e$ =factor determining the shape of crest cross-section.

Regarding the fixed values of  $\nu$ ,  $t$ ,  $\rho$ ,  $\mu$ ,  $g$ ,  $B_o$ ,  $B_i$ ,  $B$ ,  $S$ ,  $\sigma$ ,  $n$ ,  $W$ , and  $S_e$ , and  $P=D$  in this study, the effect of hydraulic head on hydraulic conductivity in trapezoidal Labyrinth and PK weirs were investigated at three different weir elevations:

$$C_d = F(H_0/P, P) \quad (3)$$

## MATERIALS AND METHODS

This study investigated and compared PK and trapezoidal Labyrinth weirs from a hydraulic perspective. This was conducted by recording the flow depth and velocity at upstream and downstream, and calculating the discharge rate.

Laboratory experiments in this study on a laboratory flume were carried out in the Hydraulic Laboratory of the Water and Electricity Organization of Khuzestan-Iran. In this study, laboratory prototypes of the weirs were examined in a rectangular free-flow flume with the length, width, and depth of 10m, 0.3m, and 0.6m respectively. The flume walls were made of transparent glass, and thus the water surface profile and flow conditions were observable. To ensure the accuracy of the tests results, the flume was checked in terms of sealing and any probable cracks in its edges. Specifications

of different parts of the flume and laboratory equipment used in this study are as follows (Fig. 7):

Groundwater storage tank, digital flow meter for the measurement of discharge with an accuracy of 0.2 L/s, stilling tank (head tank), 3-inch electric submersible pump with maximum discharge of 120m<sup>3</sup>/h

The flume bottom was kept fixed and horizontal (the bed slope was almost zero). First, the pump discharged the flow from the storage tank to the head tank at flume inlet (flume upstream). The low volume of flow slowly discharged in the channel and smoothly flowed over the spillway installed on the flume bed. Then, discharge rate was changed to study and record the hydraulic conditions of weir discharge. Finally, water flow entered the pump tank through downstream channel and returned to the cycle.

In this study, the trapezoidal Labyrinth and PK weirs were tested with different discharge rates and heights. The weirs used in this research were made of Plexiglas (Fig. 8). After the models dimensions were obtained, the required cuts were made with a laser cutting machine.

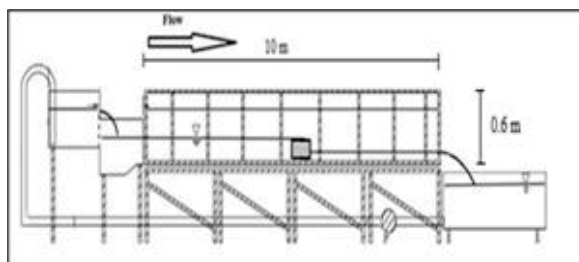


**FIGURE 7**  
General scheme of laboratory flume

Then, different pieces of weir were connected with a specific adhesive. Installation of the laboratory prototypes of weirs was carefully done by balancing and waterproofing them with adhesive (Fig. 8). In all experiments, upstream and downstream beds were equally balanced. In addition, the width of discharge channel was considered as 30cm, and w/p ratios were considered as 2, 2.5, and 3. The thickness (t) and apex diameter (A) of the trapezoidal Labyrinth weir were considered as 5mm and 3.5cm, respectively. For highly accurate determination of H<sub>0</sub>/p effect on the performance of investigated weirs, 12 flows (from 5 to 100m<sup>3</sup>/h) (before submergence to submergence and after submergence) with different hydraulic loads were applied to each weir. Submergence refers to the situation in which the downstream flow depth exceeds crest elevation [24]. According to the studies, the effect of submerged Labyrinth weirs is similar to that of linear weirs, in that if the downstream water depth does not exceed the crest

elevation, it will have no impact on the performance of the weir. In other words, the discharge rate starts decreasing only if the tailwater depth exceeds the crest elevation. It is worth noting that the use of Labyrinth weirs is not recommended under extreme submergence [25]. In studies into fuse gates, Falvey and Trielle (1995) reported similar results. In addition, Hay and Taylor (1970) disapproved the use of Labyrinth weirs in extreme submergence conditions.



**FIGURE 8**  
Installation of trapezoidal & PK weir in laboratory flume

The complexity of flow pattern and the effect of different and uncertain factors on the hydraulic characteristics of Labyrinth weirs have caused the extended use of physical models in studying, designing, and using such weirs. In Labyrinth weirs, it is expected to see changes in the discharge capacity efficacy with geometric fluctuations in their length. However, due to the flow interference, the flow coefficient is smaller in Labyrinth than linear weirs within the same length[4].

The geometric and hydraulic specifications of the examined weirs are presented in Tables 1 and 2.

**TABLE 1**  
Geometric and hydraulic specification of PK weirs

Model	W(cm)	w/p	L (mm)	T(mm)	N	Wi/Wo	No. of tests
PKW	15	2, 2.5, and 3	135	5	2	1.25	36

**TABLE 2**  
Geometric and hydraulic specifications of 2-cycle trapezoidal weir

Model	W(cm)	w/p	L (mm)	T(mm)	Trapezoidal Sidewall Angle	N	No. of tests
Trapezoidal	15	2, 2.5, 3	136	5	7	2	36

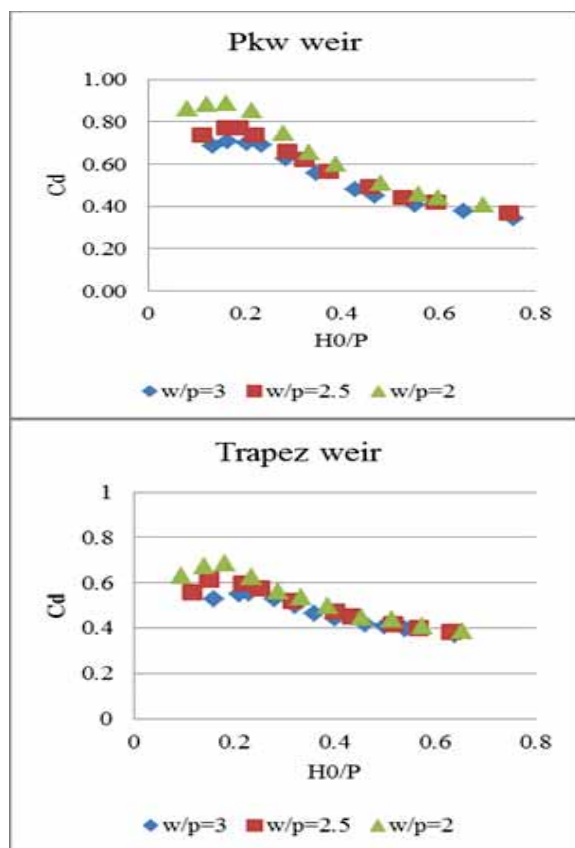


**FIGURE 9**  
Effect of flow on discharge coefficient in trapezoidal plan-form and PK weirs

## FINDINGS AND DISCUSSION

Flow coefficient in trapezoidal plan-form and PK weirs under the influence of weir height

In this study, hydraulic performance of a trapezoidal plan-form Labyrinth weir was compared with that of a PK weir in laboratory. It is worth noting that both of the investigated PK and trapezoidal plan-form weirs had two cycles. The comparisons suggested that in both investigated weirs, the flow coefficient first raised to its maximum level with increasing hydraulic load ratio to almost 0.2 ( $H_0/P=2.0$ ), and then started decreasing. According to the research findings, both

weirs showed the maximum flow coefficient in small hydraulic load ratios. ( $H_0$ =hydraulic load over the weir,  $P$ =weir height)

According to Fig. 9, with a 50% increase in weir height ( $p$ ) from 5cm to 7.5cm ( $w/p=3$  to  $w/p=2$ ) in the PKW, the flow coefficient rises by about 26%. In the trapezoidal plan-form weir, 50% increase in weir height from 5cm to 7.5cm ( $w/p=3$  to  $w/p=2$ ) increases the flow coefficient by about 24%.

The obtained results are consistent with the findings of Heidarpoor et al. (2006) in their laboratory study into the condition of discharge coefficient in one-cycle Labyrinth weirs with rectangular and U-shape plan-forms. Tests results suggested that the discharge coefficient in a certain  $H_t/P$  (overall upstream energy to weir height) increases with increasing weir height.

In both trapezoidal plan-form and PK weirs, the flow coefficient increased with increasing weir height at low hydraulic load ( $H_0/P < 0.4$ ), whereas the flow coefficient did not significantly increase with increasing weir height at higher hydraulic load ( $H_0/P > 0.4$ ). In general, the effect of weir height on flow coefficient decreases with approaching the submerged discharge (which occurs when the water head in downstream is equal to weir head), in that in post-submerged discharge, weir height increase does not have any impact on flow coefficient.

Tullis et al. (2007) showed that the submergence effect of Labyrinth weirs is similar to that of linear weirs, insofar as if the water depth in downstream does not exceed the crest head (submerged discharge), it will have no impact on the weir performance. In other words, the discharge rate decreases only when the tailwater depth exceeds the crest head. It is noteworthy that the use of Labyrinth weirs is not recommended in extreme submergence conditions. Moreover, Hay and Taylor (1970) disapproved the application of such weirs in extreme submergence conditions.

The submergence thresholds in PK and trapezoidal plan-form weirs occurred in the  $H_0/P > 0.54$  and  $H_0/P > 0.51$  respectively ( $H_0$ = head over the weir and  $P$ =weir head).

According to Figure 9, the maximum flow coefficient (almost 0.88) occurred in PK weir in the

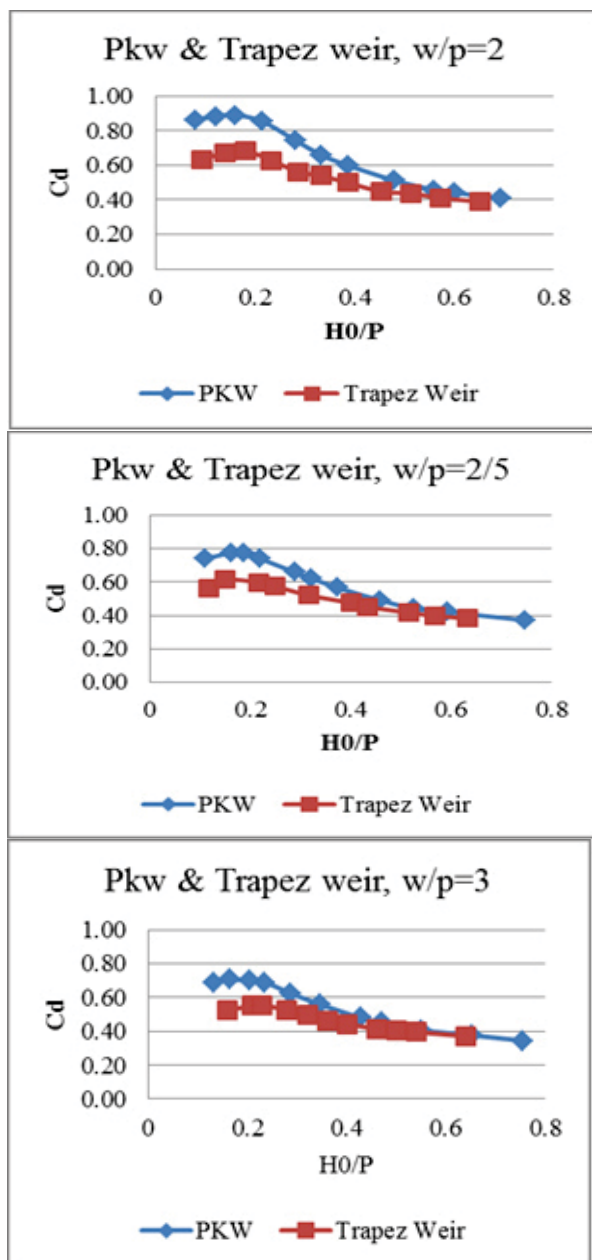


**FIGURE 10**

**Flow coefficient in trapezoidal plan-form and PK weirs in different height ratios**

$H_0/p=0.17$  (hydraulic load ratio) and  $w/p=2$  (cycle width to weir height). In addition, the maximum flow coefficient in trapezoidal Labyrinth weir (almost 0.68) occurred in  $H_0/P=0.18$  and  $w/p=2$ . In both weirs, the flow coefficient increased with increasing weir height ratio. In addition, in both weir types, with increasing the hydraulic load, the flow coefficient first increased and then decreased, and reached to its minimum value in the submerged discharge. In that, the flow coefficient had ascending trend in PK weir in hydraulic load ratios  $<0.17$  and reached its maximum amount, after which it started

decreasing. In the trapezoidal plan-form weir, the flow coefficient was increasing in hydraulic load ratios  $<0.2$ , after which it followed a descending trend.

The results obtained in this part are consistent with the findings of Crookston and Tullis, maintaining that in low discharge rates, discharge coefficient is larger than linear weir due to the small nappe interference, which gradually becomes more extreme with increasing discharge. This leads to a discharge coefficient reduction to an amount similar to discharge coefficient in broad-crested weir (Crookston and Tullis, 2012c, 2012d).

Comparison of the coefficient of discharge ( $C_d$ ) in trapezoidal plan-form and PK weirs under the influence of different hydraulic conditions

To study the flow coefficient in both PK and trapezoidal plan-form weirs, three prototypes of each weir type were first built with different heights and then compared in equal elevation ratios. It is worth mentioning that the cycle width ( $w$ ), cycle number ( $N$ ), and weir heights in them were considered as 15cm, 2, and 6-6-7.5cm ( $w/p=2, 2.5, \text{ and } 3$ ) respectively. Figure 10 shows the comparison of flow coefficient in the trapezoidal plan-form and PK weirs in different height conditions.

According to Fig. 10, the flow coefficient is significantly greater in PK weir than the trapezoidal plan-form weir insofar as this difference is big in low hydraulic load. However, it gradually reduces with increasing hydraulic load and approaching the submerged discharge, which is a value where the water depth in weir downstream and weir head are equal. It should be said that in submerged discharges, and post-submerged discharges, both weirs function as a barrier to the flow; therefore, the flow coefficients would be equal in them.

It is seen at  $w/p=3$  (weir height of 5cm) that the maximum flow coefficient in PK weir is by 26% greater than the maximum flow coefficient in trapezoidal plan-form weir. This difference became smaller with increasing hydraulic load. In addition, the flow coefficients in both weirs became almost equal in submerged and post-submerged discharges.

The same is true at  $w/p=2.5$ , in that the maximum flow coefficient in PK weir is by 26% greater than the maximum flow coefficient in trapezoidal plan-form weir. This difference became smaller with increasing hydraulic load ratio. In addition, the flow coefficients in both weirs became almost equal in submerged and post-submerged discharges.

The same is true at  $w/p=2$ , in that the maximum flow coefficient in the PK weir was by 30% greater than the maximum flow coefficient in trapezoidal plan-form weir. This difference became smaller with increasing hydraulic load ratio. In addition, the flow

coefficients in both weirs became almost equal in submerged and post-submerged discharges.

## CONCLUSION

Comparison of PK and trapezoidal plan-form weirs suggests that the flow coefficient is bigger in all pre-submerged discharge conditions in PK weir than trapezoidal plan-form weir in that the biggest difference was observed in  $w/p=2$  (the greatest weir height), in which the flow coefficient was 30% bigger in PKW than trapezoidal plan-form weir. The difference in flow coefficient decreased in both weirs with increasing  $w/p$  ratio (weir height reduction). This increase was greater in lower hydraulic loads, but decreased with approaching submerged discharge value. In addition, the flow coefficients of both weirs became almost equal in submerged and post-submerged discharge values. This was because both weirs acted as a barrier against the flow. Moreover, a 50% increase in PKW height (from 5 to 7.5cm) increased flow coefficient by 26%. With respect to the trapezoidal plan-form weir, a 50% increase in weir height increased the flow coefficient by 24%.

## ACKNOWLEDGEMENTS

The writers of this article, hereby, express their sincere gratitude to the Educational Complex of Water and Electricity Organization of Khuzestan for providing us with the laboratory flume and equipment. In addition, the provided guidance by Mr. Moradi and Mr. Amiri is also appreciated.

## REFERENCES

- [1] Falvey, H. T. (2003) Hydraulic Design of Labyrinth Weirs. ASCE press, USA.
- [2] Pralong, J., Vermeulen, J., Blancher, B., Laugier, F., Ercicum, S., Machiels, O., Piroton, M., Boillat, J.L., Leite Ribeiro, M., Schleiss, A.J. (2011) A naming convention for the Piano Key weirs geometrical parameters. Proc. Intl. Conf. Labyrinth and Piano Key Weirs Liège B, , 271–278. CRC Press, Boca Raton, FL.
- [3] Crookston B.M. and Tullis B.P. (2012) Discharge efficiency of reservoir application specific labyrinth weirs. J.Irrig. Drain. Engr. ASCE. b, 138(6) 773-776.
- [4] Hay N., and Taylor G. (1970) Performance and design of labyrinth weirs. J. Hyd. Div., ASCE 96 (2), ,: 2337-2357.
- [5] Laugier, F. Design and construction of the first Piano Key Weir (PKW) spillway at the Goulours dam, Hydropower and Dams, 2007, 13(5), 94-101.
- [6] Ouamane, A. and Lempérière, F. (2006) Design of a new economic shape of weir, in proc.of International Symposium on Dams in the Societies of the 21st Century. Barcelona, Spain, 463-470.
- [7] Leite Ribeiro, M., Pfister, M., Boillat, J.-L., Schleiss, A.J. and Laugier, F., (2012) “Piano key weirs as efficient spillway structure”, 24th ICOLD Congress on Large Dams, Kyoto (J), Q.94 – R.13.
- [8] Machiels, O., (2012) “Experimental study of the hydraulic behaviour of Piano Key Weirs”, PhD Thesis ULgetd-09252012-224610, University of Liège (B).
- [9] Crookston B.M., and Tullis B.P. (2012) Arced labyrinth weirs. J. of Hydraul. Eng. ASCE, c, 138(6): 555-562.
- [10] Crookston B.M., and Tullis B.P. (2012) Labyrinth weirs: nappe interference and local submergence. J. Irrig. Drain Eng. ASCE, d, 138(8): 757-765.
- [11] Anderson, R.M. and Tullis, B., (2012 ) “Comparison of Piano Key and Rectangular Labyrinth Weir hydraulics”, Journal of Hydraulic Engineering, Volume 138, Issue 4, pp. 358-361,.
- [12] Crookston, B. M., Paxson, G. S., and Savage, B. M. (2012). “It can be done! Labyrinth weir design guidance for high headwater and low cycle width ratios.” Proc., Dam Safety 2012, ASDSO, Denver, CO.
- [13] Anderson, R.M. and Tullis, B., (2013) “Piano Key Weir Hydraulics and Labyrinth Weir Comparison” Journal of Irrigation And Drainage Engineering . ASCE., 246-253.
- [14] Javaheri A. and Kabirisamani, A. (2011) Determination of PKW discharge coefficient in free flow condition. The first International Conference and the Third National Conference on Dam and Hydroelectric Plants, Tehran, pp. 1-8.
- [15] Karimi-Chahartaghi M, Nazari, S., & Karimi-Chahartaghi M. (2014). Laboratory study into discharge coefficient in PKW with variable crest. Eighth National Congress of Civil Engineering, Babol, Noshirvani University of Technology, pp.1-7.
- [16] Heidarpoor, M., Mousavi, F., & Roshani-Zarmehri A.R. (2006). Labyrinth weirs with rectangular and U-shape plan-forms. Journal of Agricultural Sciences and Natural Resources,



- Isfahan University of Technology, 10(3A), pp.1-11
- [17] Barcouda M., Cazaillet O., Cochet P., Jones B.A., Lacroix S., Laugier F., Odeyer C. and Vigny J.P. (2006), Cost effective increase in storage and safety of most dams using fusegates or P. K. Weirs, in proceedings of 22ème congrès des grands barrages, CIGB/ICOLD, Barcelona.
- [18] Hien, T.C., Son, H.T., & Khanh, M.H.T. (2006). "Results of some piano keys weir hydraulic model tests in Vietnam." Proc. of the 22nd Congress of ICOLD., Barcelona, Spain.
- [19] Lempérière, F. and Ouamane, A., (2003) "The Piano Keys weir: a new cost-effective solution for spillways", International Journal of Hydropower and Dams, Volume 10, Issue 5, pp. 144-149.
- [20] Anderson, Ricky M. and Tullis, B., (2011) "Piano Key Weir Head Discharge Relationships". All Graduate Theses and Dissertations (Utah State University), Paper 880.
- [21] Laugier F., Pralong J. and Blancher B. (2011), Influence of structural thickness of sidewalls on PKW spillway discharge capacity, in proceedings of Labyrinth and piano key weirs-PKW, CRC Press, London, 159-165.
- [22] Machiels O., Epicum S., Archambeau P., Dewals B.J. and Piroton M. (2011), Piano Key Weir preliminary design method - Application to a new dam project, Labyrinth and piano key weirs-PKW 2011, CRC Press, London, 199-206.
- [23] Crookston B.M. Labyrinth weirs. Ph.D. thesis, Utah State Univ., Logan, UT. 2010
- [24] Villemonte J. R; (1947) "Submerged weir discharge studies" Engineering News Record, Vol. 139, No. 26, pp: 54-56.
- [25] Tullis B., Young J., and Chandler M. Head- (2007) Discharge Relationships for Submerged Labyrinth Weirs. J. Hydraul. Eng., 133(3), 248–254.
- [26] Falvey, H. & Trielle . (1995) "Hydraulics and design of fusegates." J. of Hydr. Engrg., ASCE, 121(7), 512–518.

---

**Received: 07.05.2016**

**Accepted: 07.09.2016**

---

#### **CORRESPONDING AUTHOR**

**Mohammad Heidarnejad**

Department of Water Science Engineering, Ahvaz Branch, Islamic Azad University, Ahvaz, Iran

e-mail: mo\_he3197@yahoo.com

# EFFECT OF WATER FLOODING AND PLANTING DENSITY ON THE CHLOROPHYLL FLUORESCENCE RESPONSE IN COCULTIVATED *CYNODON DACTYLON* AND *HEMARTHRIA ALTISSIMA*

Wenchao Ma, Hong Wei\*, Yuan Liu, Ting Wang, Cui Zhou, Zhenxia Wang, Yeyi Zhang

Key Laboratory of Eco-environments in Three Gorges Reservoir Region (Ministry of Education),  
Chongqing Key Laboratory of Plant Ecology and Resources Research in Three Gorges Reservoir Region,  
School of Life Sciences, Southwest University, Chongqing 400715, PR China

## ABSTRACT

*Cynodon dactylon* and *Hemarthria altissima* are plants that grow in the water-level fluctuation zone (WLFZ) of the Three Gorges Reservoir (TGR). This study investigated the effects of different water levels and mixed-plant densities on the fluorescence characteristics of *C. dactylon* and *H. altissima* and explored the optimal mixed-plant mode in the WLFZ. We established four types of water treatments: a control group, a light flooding-light drought group, a light flooding group, and a flooded group. We also established four planting densities: 1 strain/pot, 2 strains/pot, 4 strains/pot, and 12 strains/pot. The photosynthetic pigments and chlorophyll fluorescence characteristics of *C. dactylon* and *H. altissima* were measured, and the water levels and planting densities had different effects on the photosynthetic pigments of *C. dactylon* and *H. altissima*. The photosynthetic pigment content of *C. dactylon* was lowered, whereas that of *H. altissima* was maintained at a higher level. Both non-flooded *C. dactylon* and *H. altissima* plants maintained a stable photochemical reaction. Obvious differences in the photosynthetic reaction parameters were not observed among the different density treatments. Under the flooded treatment, the leaves of *C. dactylon* withered and fell and then experienced rapid re-growth after the removal of the stress, whereas the maximum photochemical efficiency and potential activity of photosystem II (PSII) of *H. altissima* were both inhibited. In the mixed-planting mode, *H. altissima* displayed a growth advantage over *C. dactylon*. During the vegetation recovery period, the mixed-planting density of *C. dactylon* and *H. altissima* should be adjusted according to the actual water conditions.

## KEYWORDS:

*Cynodon dactylon*; *Hemarthria altissima*; flooding; planting density; fluorescence characteristics

## INTRODUCTION

Artificial dams are constructed to develop and utilize river resources; however, these structures cause periodic fluctuations of reservoir water levels and form water-level fluctuation zones (WLFZs) characterized by repeated “flooding-drought-flooding” patterns [1]. Flooding has a negative effect on photosynthesis and related plant traits, especially for species that are not resistant to flooding [2]. Flooding results in reductions of photosynthetic pigment content [3], photosystem II (PSII) photochemical efficiency [3], Rubisco activity [4], electron transport rates [5] and photosynthetic product transport rates [6]. Therefore, the net photosynthetic rate decreases, which in turn influences the survival of plants and causes vegetation degradation and ecological function deterioration in WLFZs. The artificial construction of vegetation is an important measure for improving the ecological environment in WLFZs [7-11]. According to the hydrological regime of a WLFZ, artificial communities are constructed at different altitudes by selecting flood-resistant species to restore and improve the structure and function of the ecological system in the WLFZ.

The Three Gorges project is the largest hydropower project in the world, and it exerts a negative impact on the environment as it improves power and navigation. According to its operation scheduling scheme, the reservoir water level of the Three Gorges Dam falls to 145 m from June to September and peaks at 175 m as impoundment begins in October, which generates approximately 350 km<sup>2</sup> of a seasonally submerged riparian zone with a maximum water level difference of 30 m [12]. Flooding is one of the greatest disturbances to vegetation in the Three Gorges Reservoir (TGR) area and represents an important influence on vegetation composition, species diversity and plant growth [13]. Perennial anti-seasonal flooding is detrimental to the original plant species in the WLFZ and even leads to the death of species with



a poor submergence tolerance, thereby posing a serious threat to the ecological welfare of the WLFZ and the reservoir area [7,14,15]. *Cynodon dactylon* and *Hemarthria altissima* are highly adaptable riparian plants that are widely distributed in the Yangtze River Basin. Thus, they are common herbaceous plants used in the construction of vegetation communities in the TGR WLFZ [11,16,17]. The stability of the plant community is closely related to the species composition and species interactions, and the interplay between specific species has been successfully promoted in ecological restoration practice [18,19]. Under the natural growth conditions of the WLFZ plant community, *C. dactylon* and *H. altissima* often grow together; thus, during vegetation restoration, a hybrid planting scheme should be considered. Studies have shown that planting density is an important factor in determining plant growth because changes in planting density can directly affect the light, nutrition, ventilation and microenvironment conditions; impact physiological and ecological characteristics; affect plant growth; and further influence the plant's capacity to manage environmental stress [20]. In addition, because the reservoir water level fluctuates periodically, plants in the WLFZ will encounter water stress in the form of waterlogging, flooding, drought, and flooding and drought alternation. Different water stress levels have different effects on the plant density [21,22].

Researchers have studied the growth and physiological and ecological characteristics of *C. dactylon* and *H. altissima* under water stress. Flooding causes a decline in plant coverage by *C. dactylon*, and increased flooding depths result in a more significant decrease in plant coverage. *C. dactylon* is suitable for growth at an altitude range of 175-150 m in the TGR WLFZ [23], maintains a 100% survival rate after it is submerged to depth of 25 m, and has a high capacity for growth restoration [24]. *C. dactylon* displays sensitivity and plasticity in response to water stress and planting density treatments, and it exhibits a positive response to water stress through biomass allocation, leaf and shoot reductions, and internode elongation. Under increasing stress conditions, a high-density planting can facilitate the growth of *C. dactylon* [25]. Although the water and planting density treatments appeared to exert a negative effect on *C. dactylon* growth, the performance of its "intrinsic" photosynthetic characteristics remained rather stable [20]. Previous studies have shown that water and density treatments significantly influence the growth and morphological characteristics of *H. altissima*. Under flooding treatments, its root, stem, and leaves grow slowly to reduce energy consumption and achieve survival. In an environment

characterized by wet and dry alternating conditions and soil water saturation, higher biomass can be achieved by stem elongation and an increase in leaf area [26]. Compared with the non-flooded group, the  $Fv/Fm$  and  $Fv/Fo$  ratios of *H. altissima* did not show significant difference after a 2-month period of flooding at 20 cm above ground, and its PSII was not obviously damaged [27]. However, the response of *C. dactylon* and *H. altissima* to water stress in a hybrid planting mode has not been examined. To further improve the bio-diversity and stability of the artificially recovered community of the TGR, it is important to optimal methods of combining the communities of *C. dactylon* and *H. altissima* under water-level fluctuations to determine their capacity for vegetation recovery in the WLFZ of the reservoir.

Photosynthesis is an important metabolic process in plants that can be used as an indicator to assess plant growth and resistance [28]. Photosynthetic pigments are the material basis of plant photosynthesis, and the levels of these pigments are closely associated with the amount of photosynthesis in plants [29]. Chlorophyll fluorescence kinetic characteristics can directly reflect the photosynthetic characteristics of plants and may be used to sensitively and non-destructively analyze the potential mechanisms influenced by external factors [30,31]; thus, by measuring a plant's fluorescence characteristics during photosynthesis, the growth, disease, stress and other physiological conditions can be understood [32,33]. By simulating 4 water conditions in the TGR areas, we explored the photosynthetic fluorescence adaptation strategy in *C. dactylon* and *H. altissima* under different mixed-planting densities to provide a reference for the construction of vegetation restoration plant communities in the WLFZ.

## MATERIALS AND METHODS

**Experimental materials.** This experiment utilized cutting seedlings of *C. dactylon* and *H. altissima* collected in the same year as the samples. The branches of *C. dactylon* and *H. altissima* were obtained in the Beibei section (29° 41' 2" N, 106° 26' 56" E; Fig 1) of the Jialing River, and they were cut into small segments of 7-10 cm and 15-18 cm in length, respectively, for cultivation. The cutting seedlings of *C. dactylon* and *H. altissima* grew similarly well and were transplanted into pots according to the experimental design; the pots were 17 cm in height, the pot mouth was 22 in diameter, and the bottom was 15 cm in diameter. Each pot was filled with 2 kg of sundried purple soil with the impurities removed. All of the potted seedlings were placed under a canopy with a transparent roof and open sides in the Ecological



FIGURE 1

Sampling sites for the *C. dactylon* and *H. altissima* seedlings used in the experiments.

Experimental Garden of Southwest University (249 meters above the sea level) for cultivation under uniform conditions. Prior to treatment, only the main stems of each plant were reserved.

Approval for this study was obtained from the Department of Technology and Environmental Protection of the Three Gorges Group, China.

**Experimental design.** The experiment treatments began on May 15, 2012. The cutting seedlings of *C. dactylon* with an average length of 32 cm and of *H. altissima* with an average length of 35 cm were divided into 4 groups at random. The water levels and planting densities were set as the independent variables in the experiment. There were 4 types of water treatments: (1) normal water supply (control (CK): the field moisture capacity was maintained at 70-80% and the soil moisture was measured using the ring sampling method [34]); (2) light flooding-light drought group (FD): 10 d soil water saturation with waterlogging 5 cm above the soil and 10 d mild drought at a field moisture capacity of 50-55%; (3) light flooding group (LF): water logging 5 cm above the soil surface; and (4) flooded group (FL): tops of the plants submerged 5 cm beneath water. During the experiment, periodic inspections were performed every day. The weighing method was used to supplement any water loss to ensure that the water conditions were fixed. The mixed-planting density treatments were divided into four levels: (1) a control group with a density of 1 strain/pot (i.e., without the influence of other strains; the control group included the two species); (2) a low-density group with a density of 2 strains/pot (planting proportion of *C. dactylon* and *H. altissima* was 1:1); (3) a medium-density group with a density of 4 strains/pot; and (4) a high-density group with a density of 12 strains/pot. The four density groups were approximately equivalent to 29 strains/m<sup>2</sup>, 58 strains/m<sup>2</sup>, 116 strains/m<sup>2</sup>, and 348 strains/m<sup>2</sup> (calculated according to a soil surface diameter of 21 cm).

This study adopted a completely randomized experimental design with 16 treatments in total. Each treatment was designated by the four water treatments plus a subscript number. For example, for the CK water treatments, the groups CK<sub>1</sub>, CK<sub>2</sub>, CK<sub>3</sub>, and CK<sub>4</sub> were included, and the subscript “1” represented 1 strain/pot, etc. Each treatment had four replicates. The experimental sampling and measurements concluded on August 4, 2012. The average value for all of the strains in each pot was used as the value for that pot.

**Measurement of photosynthetic pigments.** Photosynthetic pigments were measured according to the extraction method [35]. Healthy and mature leaves were selected, and 0.1 g of fresh leaf was accurately weighed and cut into pieces. A Shimadzu UV-2550 spectrophotometer (Shimadzu, Suzhou, China) was used to measure the light absorption values of the chlorophyll a, chlorophyll b, and carotenoids (A663, A645 and A470, respectively). The measured contents were then calculated and converted into the unit fresh weight content. The total chlorophyll content was calculated as follows: total chlorophyll content = chlorophyll a content + chlorophyll b content.

**Measurement of chlorophyll fluorescence parameters.** The chlorophyll fluorescence parameters were measured using a PAM-2100 portable chlorophyll fluorometer (Walz Company, Effeltrich, Germany) according to the manufacturer's instructions. The samples were subjected to a 3 h dark adaptation period and then measured. First, a 600 Hz detection light (photon flux density (PFD) <0.1 mol·m<sup>-2</sup>·s<sup>-1</sup>) was switched on to measure the *F<sub>o</sub>*, and a one-time saturated pulse light (PFD of 8000 μmol·m<sup>-2</sup>·s<sup>-1</sup> and frequency of 20 KHz for 0.8 s) was switched on to measure the *F<sub>m</sub>* and *F<sub>v</sub>/F<sub>m</sub>*. After the pulse, the actinic light (PFD of 336 μmol·m<sup>-2</sup>·s<sup>-1</sup>) was turned on. When the fluorescence was stable, the *F<sub>s</sub>* was measured.

**TABLE 1**  
**Effects of the water treatments and plant densities on the photosynthetic pigment content of *C. dactylon* and *H. altissima* plants.**

Species	Photosynthetic pigments	Water treatment		Plant density		Interaction	
		<i>F</i>	<i>P</i>	<i>F</i>	<i>P</i>	<i>F</i>	<i>P</i>
<b><i>C. dactylon</i></b>							
	Chls/mg·gFW <sup>-1</sup>	863.3	<0.001	607.5	<0.001	225.5	<0.001
	Car/mg·gFW <sup>-1</sup>	928.3	<0.001	814.1	<0.001	273.1	<0.001
	Chla/Chlb	53.2	<0.001	48.3	0.011	32.8	<0.001
	Chls/Car	224.3	<0.001	86.0	<0.001	55.6	<0.001
<b><i>H. altissima</i></b>							
	Chls/mg·gFW <sup>-1</sup>	64.6	<0.001	63.0	<0.001	44.4	<0.001
	Car/mg·gFW <sup>-1</sup>	9.3	<0.001	33.5	<0.001	30.1	<0.001
	Chla/Chlb	317.1	<0.001	7.4	<0.001	11.3	<0.001
	Chls/Car	449.1	<0.001	23.5	<0.001	6.6	<0.001

Then, the saturated light was turned on again to measure the  $F_m'$ . The actinic light was turned off for dark adaptation, and then the far-red light (PFD of approximately  $5 \text{ mol} \cdot \text{m}^{-2} \cdot \text{s}^{-1}$  for 3 s) was turned on to measure the  $F_o'$ . The formulae for calculating the PSII maximal photochemical efficiency ( $F_v/F_m$ ), PSII potential activity ( $F_v/F_o$ ), actual photochemical quantum yield of PSII ( $Yield$ ), electron transport efficiency ( $ETR$ ), photochemical quenching coefficient  $qP$ , and non-photochemical quenching coefficient  $qN$  are as follows:

$$F_v/F_m = (F_m - F_o)/F_m;$$

$$F_v/F_o = (F_m - F_o)/F_o;$$

$$Yield = (F_m' - F_s)/F_m';$$

$$ETR = Yield \times PDE \times 0.5 \times 0.84;$$

$$qP = (F_m' - F_s)/(F_m' - F_o');$$

$$qN = (F_m - F_m')/F_m'.$$

where  $F_o$  is the initial fluorescence,  $F_m$  is the maximal fluorescence,  $F_v$  is the maximal variable fluorescence under the dark adaptation state when all non-photochemical processes are at their minimum,  $F_m'$  is the fluorescence yield when the reaction centers of PSII are in an off state under light adaptation and all non-photochemical processes are in their optimal state,  $F_s$  is the fluorescence yield in the stable state, and  $PFD$  is the photon flux density.

**Statistical analysis.** In this experiment, the water levels and planting density were considered factors that influenced the measured indicators, and the two-factor variance analysis method (SPSS 22.0) was adopted to reveal the influence of the water level and mixed-planting density on the photosynthetic pigments and chlorophyll fluorescence of *C. dactylon* and *H. altissima*. Duncan's method was used to test for significant differences between indicators in the plants grown under the different water treatments and planting density treatments ( $P < 0.05$ ).

## RESULTS

**Photosynthetic pigment contents.** The water level, planting density and their interactions all significantly influenced the total chlorophyll, carotenoid, chlorophyll a/chlorophyll b and total chlorophyll/carotenoid ( $P < 0.05$ ) (Table 1) contents of *C. dactylon*. The leaves of *C. dactylon* in the FL treatment turned yellow and withered one week after flooding. Throughout the experiment, newly germinated leaves were not observed. At 3 to 5 d after the removal of the flooding stress, new leaves were observed to germinate from the flooded plants. Under the different water treatments, the planting density had different effects on the photosynthetic pigments of *C. dactylon*. For the LF group, increased planting density caused a gradual decrease in the photosynthetic pigment content. For the FD group, each density treatment significantly decreased the photosynthetic pigment content of *C. dactylon* compared with that of the CK. The photosynthetic pigment content of the FD<sub>12</sub> group was higher than that of the FD<sub>2</sub> and FD<sub>4</sub> groups. At the same planting density, the water treatments significantly decreased the photosynthetic pigment content of *C. dactylon* compared with the CK (except for the FD<sub>12</sub> group) (Fig 2). For each treatment group, the ratios of chlorophyll a to chlorophyll b and total chlorophyll to carotenoids were greater than 3:1 and essentially stable.

The effects of the water levels, planting densities, and their interactions on the photosynthetic pigments of *H. altissima* were significant ( $P < 0.05$ ) (Table 1). For the CK group, the photosynthetic pigment content decreased with increases in planting density. Planting density had a negative effect on *H. altissima*, and for the other three water treatments (except for the LF<sub>4</sub> and LF<sub>12</sub> group), the photosynthetic pigment contents of *H. altissima* were higher than that of the CK (Fig 3).

At the same planting density, the water treatments significantly influenced the ratio of chlorophyll a to chlorophyll b and of total chlorophyll to carotenoids (Fig 3), and these ratios under the FL treatment were significantly lower than those of the other water treatments. For all of the treatments, the ratios of chlorophyll a to chlorophyll b and of total chlorophyll to carotenoids were greater than 3:1.

Our results demonstrate that the photosynthetic pigment contents of *C. dactylon* and *H. altissima* were significantly influenced by the water levels, planting densities, and the interactions between these variables. However, the photosynthetic pigment response differed. Under

the same conditions, the photosynthetic pigment of the mixed-planted *C. dactylon* was lower than that of the CK under the same water treatment, and in the FL treatment, the leaves of *C. dactylon* withered and fell, whereas *H. altissima* maintained a satisfactory state and its photosynthetic pigments increased (except for in the CK). However, an obvious difference was observed between the chlorophyll contents of the plants because under the same conditions, the photosynthetic pigment content of *C. dactylon* was far higher than that of *H. altissima*.

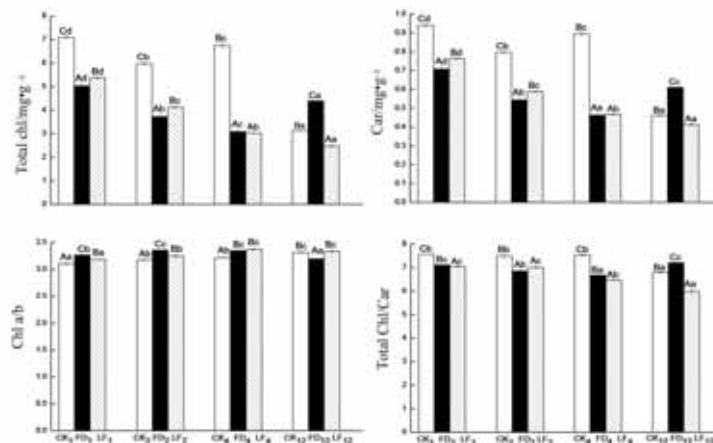


FIGURE 2

Effects of the water treatments and plant densities on the photosynthetic pigment content of *Cynodon dactylon* plants. The values in the figure are the average value  $\pm$  standard error ( $n = 3$ ). Different capital letters indicate a significant difference between the water treatments under the same density conditions ( $P < 0.05$ ), whereas different small letters indicate a significant difference between the density groups under the same water conditions ( $P < 0.05$ ). CK: control group; FD: light flooding-light drought group; LF: light flooding group; and FL: flooded group.

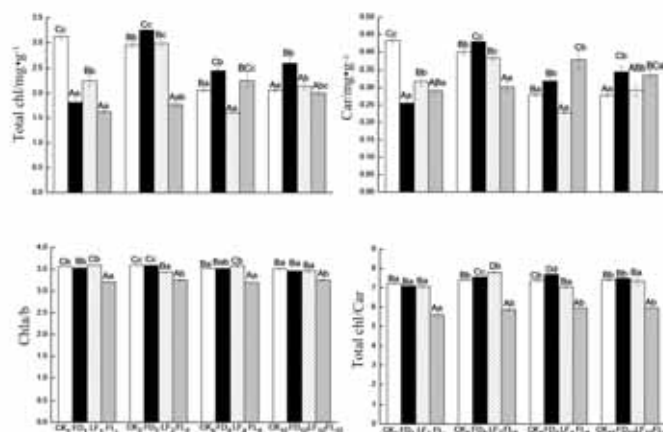
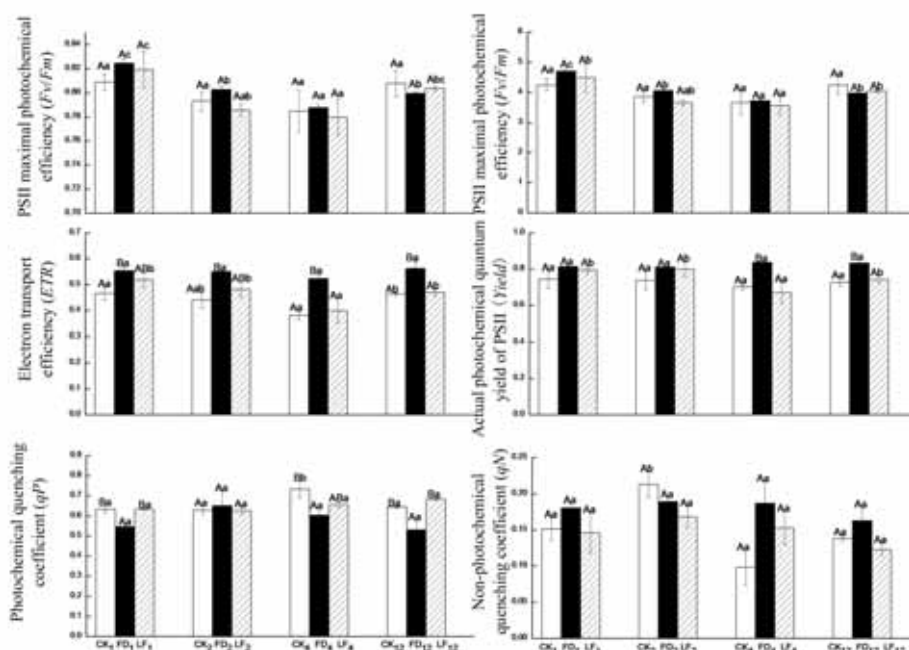


FIGURE 3

Effects of the water treatments and plant densities on the photosynthetic pigments of *H. altissima* plants. The values presented in the figure are the average value  $\pm$  standard error ( $n = 3$ ). Different capital letters indicate a significant difference between the water treatments under the same density conditions ( $P < 0.05$ ), whereas different small letters indicate a significant difference between density groups under the same water conditions ( $P < 0.05$ ). CK: control group; FD: light flooding-light drought group; LF: light flooding group; and FL: flooded group.

**TABLE 2**  
**The effects of water treatments and plant density on Chlorophyll fluorescence in *Cynodon dactylon* and *Hemarthria altissima* plants.**

Species	Chlorophyll fluorescence	Water treatment		Plant density		Interaction	
		F	P	F	P	F	P
<i>C. dactylon</i>	<i>Fv / Fm</i>	2.0	0.157	11.6	<0.001	1.3	0.312
	<i>Fv/Fo</i>	1.8	0.191	10.4	<0.001	0.937	0.487
	<i>ETR</i>	34.4	<0.001	12.7	<0.001	2.025	0.102
	<i>Yield</i>	13.6	<0.001	2.7	0.066	2.3	0.059
	<i>qP</i>	7.1	0.004	2.3	0.108	1.9	0.122
	<i>qN</i>	3.8	0.038	4.5	0.013	2.7	0.040
<i>H. altissima</i>	<i>Fv / Fm</i>	178.6	<0.001	1.7	0.180	1.7	0.139
	<i>Fv/Fo</i>	278.3	<0.001	2.7	0.063	2.5	0.028
	<i>ETR</i>	3.1	0.040	19.4	<0.001	6.2	<0.001
	<i>Yield</i>	31.1	<0.001	9.8	<0.001	5.7	<0.001
	<i>qP</i>	24.9	<0.001	58.7	<0.001	14.2	<0.001
	<i>qN</i>	9.6	<0.001	12.4	<0.001	17.5	<0.001



**FIGURE 4**

The effects of water treatments and plant density on Chlorophyll fluorescence in *Cynodon dactylon* plants. The values in the figure are the average  $\pm$  standard error ( $n = 3$ ). Different capital letters indicate a significant difference between water treatments under the same density condition ( $P < 0.05$ ), whereas different small letters indicate a significant difference between density groups under the same water condition ( $P < 0.05$ ). CK: control group; FD: light flooding-light drought group; LF: light flooding group; FL: flooded group.

**Chlorophyll fluorescence characteristics.** The water treatments significantly influenced the *ETR*, *Yield*, *qP* and *qN*, whereas density treatments significantly influenced *Fv/Fm*, *Fv/Fo*, *ETR*, and *qN* of *C. dactylon* ( $P < 0.05$ ). Their interaction had a significant influence over *qN* alone ( $P < 0.05$ ) (Table 2). For the non-flooded group, under the same planting density, there was no significant difference between *Fv/Fm* and *Fv/Fo* for each

water treatment. At different planting densities, *Fv/Fm* and *Fv/Fo* of *C. dactylon* were all maintained a high level (Fig 4). The *ETR* of FD was significantly higher than that of CK and LF. Compared with CK, *Yield*, *qP* and *ETR* of *C. dactylon* at different planting densities were all maintained at the same level. Under the same conditions, *qN* of *C. dactylon* under different water treatments did not differ significantly.

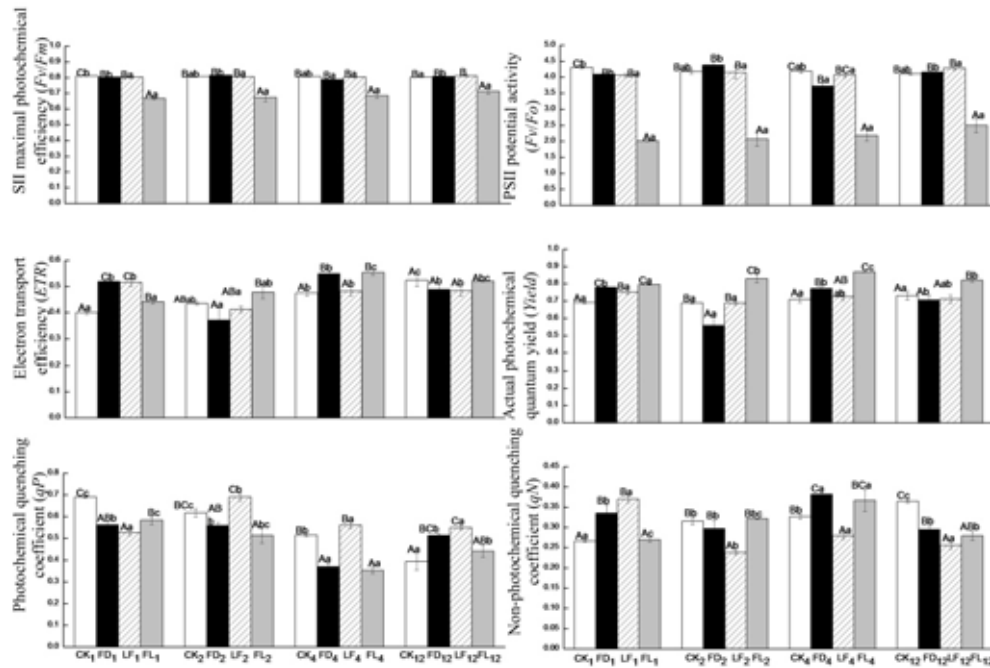


FIGURE 5

Effects of the water treatments and plant densities on the chlorophyll fluorescence of *H. altissima* plants. The values in the figure are the average  $\pm$  standard error ( $n = 3$ ). Different capital letters indicate a significant difference between the water treatments under the same density conditions ( $P < 0.05$ ), whereas different small letters indicate a significant difference between density groups under the same water conditions ( $P < 0.05$ ). CK: control group; FD: light flooding-light drought group; LF: light flooding group; and FL: flooded group.

Water level and planting density and their interaction had different effects on the chlorophyll fluorescence of *H. altissima* (Table 2). Water treatments all had significant effects on the fluorescence characteristics of *H. altissima* ( $P < 0.05$ ). The density treatments significantly influenced the *ETR*, *Yield*, *qP*, and *qN* of *H. altissima* ( $P < 0.05$ ). The interactions between the parameters significantly influenced the *Fv/Fo*, *ETR*, *Yield*, *qP*, and *qN* of *H. altissima* ( $P < 0.05$ ). The *Fv/Fm* and *Fv/Fo* of *H. altissima* in the non-flooded groups were all maintained at a relatively high level (Fig 5). The *Fv/Fm* and *Fv/Fo* of the FL treatment were lower than those of the non-flooded treatments. Compared with the CK, the *ETR* and *Yield* of *H. altissima* at different planting densities were maintained at a relatively high level, and the water treatment had a facilitative role on the *ETR* and *Yield* of *H. altissima* plants in certain treatments (Fig 5). The *Yield* of the FL group was markedly higher than that of the other water treatment groups. Compared with *C. dactylon*, the *qP* and *qN* of *H. altissima* were more sensitive to the water and density treatments. Significant differences were observed in the *qP* and *qN* among the *H. altissima* treatments. Under the same treatment conditions, the *qP* and *qN* of *H. altissima* exhibited opposite trends.

The photochemical reaction system of *C. dactylon* and *H. altissima* in the non-flooded groups did not sustain obvious damage, whereas a marked negative effect was observed in the flooding treatment. Compared with the obvious differences exhibited by their photosynthetic pigments, the *Fv/Fm* and *Fv/Fo* parameters were generally equivalent and decreased within the normal scope. The water treatments played a facilitative role for *C. dactylon* and *H. altissima* plants in certain treatments. Compared with the CK group under the same water treatment regimen, the *Yield*, *ETR*, *qP* and *qN* of *C. dactylon* were relatively stable under increasing planting densities, whereas those of *H. altissima* exhibited a higher sensitivity.

## DISCUSSION

The periodic “flooding-drought-flooding” environment in the TGR WLFZ leads to a severe degeneration of vegetation. The key to vegetation recovery is to increase the vegetation biodiversity and community stability. The interactions between different plants within the community, which vary according to the external environment, can directly influence the growth characteristics, morphological characteristics, development and

life history of individual plants, and as a result, these interactions can influence the distribution of plants, co-occurrence and diversity of species, as well as the structure and function of the ecological system [36-38]. Whether the mixed community consisting of *C. dactylon* and *H. altissima* will remain stable is dependent on interactions between the plants. In this experiment, the photosynthetic pigments and chlorophyll fluorescence of *C. dactylon* and *H. altissima* exhibited different response characteristics under different water stresses and planting densities.

Photosynthetic pigments trap light energy during photosynthesis, and the pigment content of a plant can directly affect its ability to trap light energy and subsequently affect the accumulation of photosynthetic products and growth of the plant [39]. Photosynthetic pigments can be directly involved in light absorption, transfer, distribution and transformation. The photosynthetic pigment content of a plant can reflect its photosynthetic capacity, growth, development, physiological metabolism, and nutrient levels; therefore, this parameter can be used as an indicator of environmental physiology [40]. When plants grow under stress, their physiological processes are disrupted, which results in negative effects, such as damage to the membrane structure, reduced synthesis of proteins, and an accumulation of harmful metabolites, and all of these effects influence the plant's photosynthetic pigment content and further alter the photosynthetic performance [41]. Thus, the photosynthetic pigment content of plants can be used to determine their growth status.

Because of structural and physiological differences, plants present different response strategies to stress. In this experiment, different mixed-planting densities resulted in different responses in the photosynthetic pigments of *C. dactylon* and *H. altissima*. With an increase in planting density, the photosynthetic pigment content of *C. dactylon* significantly decreased compared with that of the CK under the same water treatment, which might be have been related to *C. dactylon*'s ability to respond to competition for nutrition and light between plants. Increases in planting density caused a gradual reduction in the photosynthetic pigment content compared with that of the *H. altissima* CK group. However, with an increase in water stress, the density treatment had a facilitative role with regards to the photosynthetic pigment content of *H. altissima*. The photosynthetic pigment content of most of mixed-planted *H. altissima* plants was higher than that of the CK under the same water treatment, indicating that the presence of certain neighbors can improve the microenvironment between plants and help plants to adapt to stressful environments [42,43]. The water treatments led to the decline in

the photosynthetic pigment content of *C. dactylon*, and the leaves of *C. dactylon* in the FL group turned yellow and fell one week after the experiment because of the damage sustained by the plant's leaf membrane caused by flooding and electrolyte leakage, which led to further withering and leaf fall [44,45]. Research has shown that a reduction in biomass is an adaptive strategy employed by plants under flooding conditions [46], and the *C. dactylon* leaf fall in the FL group might be a coping strategy in response to an extreme adverse environment. In addition, under water logging conditions, anaerobic respiration is the main respiration form available to the roots. However, the insufficient nutrition supply accessible to the roots under these conditions decreases the ability of the plant to effectively absorb mineral elements, thereby inhibiting photosynthetic pigment synthesis [47]. In this experiment, the *C. dactylon* in FL were able to germinate new leaves 3 to 5 days after the removal of water stress; thus, these plants exhibited an excellent ability to recover growth, which is consistent with the results of Zeng et al. [20]. Compared with *C. dactylon*, certain water treatments improved the photosynthetic pigment content of *H. altissima*, which increased under the FD treatment compared with that of the CK. Obvious leaf withering and fall did not occur for *H. altissima* in the FL group. Research has shown that wet-dry alternations play a certain role in the promotion of photosynthetic pigment synthesis in plants [48], which is favorable for the maintenance of photosynthetic capacity and the anti-stress functions of plants.

The main function of chlorophyll a is the conversion of gathered light energy into chemical energy for photosynthetic reactions, whereas that of chlorophyll b is the collection of light energy [49]. The ratio of chlorophyll a to chlorophyll b in the normal leaf is 3:1, and changes in the chlorophyll a/chlorophyll b ratio in the leaf may reflect the intensity of leaf photosynthetic activity. In this experiment, with the exception of *C. dactylon* plants in the FL group, the ratio of chlorophyll a to chlorophyll b was consistently greater than 3:1. This ratio can reflect the degree of thylakoid stacking in the chloroplast, and a higher ratio indicates a higher degree of stacking in the thylakoid and a complete photosynthetic system for photosynthesis [50]. Mixed planting did not have an obvious effect on the photosynthetic system. A decline in the chlorophyll a/b ratio can improve the trapping efficiency of blue-violet light in the blade and enhance the leaf's ability to utilize low light [49]. Under flooding conditions, the chlorophyll a/b ratio of *H. altissima* decreased significantly, which may represent an adaptation to the dim underwater environment. In this experiment, the total chlorophyll/carotenoid

contents of *C. dactylon* and *H. altissima* in the mixed-planting group were greater than 3:1, which was higher than that in the CK group and ensured a sufficient amount of reaction center pigments [51]. Overall, the photosynthetic pigment content of *C. dactylon* and *H. altissima* was affected to a certain degree. However, the proportion was maintained at a normal level, thereby ensuring photosynthesis and *C. dactylon* and *H. altissima* survival in an adverse environment.

Chlorophyll fluorescence technology is considered a rapid and non-destructive method of assessing a plant's photosynthetic function [52], and chlorophyll fluorescence signals emitted by plants are rich in information regarding photosynthesis and closely associated with the plant's nutrition and stress levels [53]. The chlorophyll fluorescence parameter  $F_v/F_m$  reflects the intrinsic light energy conversion efficiency of the PSII center and represents the ability of PSII to utilize light energy [48]. Under normal conditions, the  $F_v/F_m$  value generally falls between 0.75 and 0.85, and decreases markedly when damaged or in an adverse environment, and a smaller decline in its magnitude indicates lower photoinhibition [54]. The  $F_v/F_o$  value reflects the potential activity of PSII. When pressure from the external environment increases, this parameter always decreases [55]. In this experiment, both the  $F_v/F_m$  and  $F_v/F_o$  values were maintained at a relatively high level. Significant differences did not occur between the CK and the mixed-planting group, which indicated that the intrinsic light energy conversion efficiency of the PSII reaction centers was stable. Li et al. [27] submerged *H. altissima* 20 cm aboveground for 2 months and found that its  $F_v/F_m$  and  $F_v/F_o$  values were not significantly different from the control group, which is consistent with the results of our experiment. Previous research has shown that *H. altissima* adopts a 'silent' strategy for managing extreme environmental stress in which its growth nearly stops [56]. The  $F_v/F_m$  and  $F_v/F_o$  values of *H. altissima* in the FL group significantly decreased, demonstrating this "silent" strategy. The  $ETR$  value indicates the electron transport rate of PSII and can represent the plant's photosynthetic capacity. The  $Yield$  value refers to the actual photochemical quantum yield of PSII and can act as an indicator of the plant's  $ETR$ . In a stressful environment, a higher  $Yield$  value is indicative of a lower influence of stress [52, 57]. In this experiment, the  $ETR$  and  $Yield$  values of *C. dactylon* (except FL) and *H. altissima* were maintained at a relatively high level, indicating that the water and mixed-planting density did not result in obvious damage to their photosynthetic systems.

The photochemical quenching coefficient  $qP$  reflects the light energy share that the antenna pigment of PSII absorbs and uses for

photochemical electron transport as well as the openness of the PSII reaction centers. A greater  $qP$  value indicates higher electron transport activity. The non-photochemical quenching value  $qN$  reflects the light energy that is absorbed by the antenna pigment of PSII and dissipated as heat and cannot be used for photosynthetic electron transport. Heat dissipation can be used to evaluate the plant's ability to dissipate excess activation energy [33, 52]. The results of this experiment show that the  $qP$  and  $qN$  values of *C. dactylon* did not change significantly, which indicates that the electron transport of PSII was not impeded and the light energy used for other forms of dissipation did not change significantly. However, the  $qP$  value of *H. altissima* changed significantly, and the fluctuations between treatments were substantial. It is worth noting that the  $qN$  of *H. altissima* could promote changes within the plant that led to the dissipation of surplus energy in a timely manner.

The different water levels and mixed-planting densities influenced the photosynthetic pigment content and chlorophyll fluorescence characteristics of *C. dactylon* and *H. altissima*. Under the water stress conditions, the photosynthetic pigment content of *C. dactylon* was inhibited, and its leaves fell under the FL treatment. Mixed planting had a negative effect on the photosynthetic pigment content of *C. dactylon*. Notably, under the same water conditions, the mixed-planting densities had different effects on the photosynthetic pigments. Under the same treatment conditions, *H. altissima* maintained a higher level of photosynthetic pigment content. Certain water treatments facilitated the synthesis of photosynthetic pigments by *H. altissima*. Compared with the CK group under the same water treatment, the mixed-planting groups promoted an increased synthesis of photosynthetic pigments in *H. altissima*. In terms of the chlorophyll fluorescence characteristics, the photochemical reaction systems of *C. dactylon* and *H. altissima* in the non-flooded groups did not sustain apparent damage and maintained a stable photochemical reaction. Significant differences were not observed in the photosynthetic reaction parameters among the different density treatments, whereas an obvious inhibition of these parameters was observed in the flooding treatments. However, we did not examine the fluorescence characteristics during the late recovery stage, and the photosynthetic pigment and fluorescence characteristics of these two plants over time during growth recovery should be investigated. In addition, differences were observed between the experimental treatment and natural growth that might cause the results to deviate to a certain extent; thus, an *in situ* experimental study should be conducted.

Based on the results of this experiment, *H.*



*altissima* in a mixed-planting environment has an obvious competitive advantage. Planting density is not a limiting factor for the growth of *H. altissima*; however, increased density exerts a negative effect on *C. dactylon*. Under different water conditions, the planting mode should be selected according to the characteristics of *C. dactylon*. A low planting density and high planting density are recommended for the waterlogging zone and the wet-dry alternating zone, respectively. However, based on actual field observations of the WLFZ of the TGR, *C. dactylon* enjoys a competitive advantage over *H. altissima*, which might be related to the high photosynthetic pigment content of *C. dactylon* and the more vigorous re-growth ability after the withdrawal of water stress in *C. dactylon* compared with *H. altissima*. Thus, during vegetation recovery, the mixed-planting density of *C. dactylon* and *H. altissima* should be adjusted according to the actual water conditions.

#### ACKNOWLEDGEMENTS

The authors have declared that no competing conflicts of interest exist. This study was supported by the National and International Scientific and Technological Cooperation Project (2015DFA90900); Follow-up Work of Ecological Biodiversity Conservation Project in the Three Gorges Reservoir Area (5000002013BB5200002); the Forestry Science and Technology Key Project in Chongqing Municipality (2015-6); and the Forestry Science and Technology Demonstration Project by Central Finance (2014-10).

#### REFERENCES

- [1] Tan, S. D., Zhu, M. Y., Dang, H. S., Wang, Y. and Zhang, Q. F. (2009) Physiological responses of Bermudagrass (*Cynodon dactylon* (L.) Pers.) to deep submergence stress in the Three Gorges Reservoir Area. *Acta Ecologica Sinica* 29, 3685-3691.
- [2] Luo, F. L., Wang, L., Zeng, B., Ye, X. Q., Chen, T., Liu, D., Zhang, Y. H. and Arnd, K. (2006) Photosynthetic responses of the riparian plant *Arundinella anomala* Steud. in Three Gorges reservoir region as affected by simulated flooding. *Acta Ecologica Sinica* 11, 3602-3609.
- [3] Mauchamp, A. and Methy, M. (2004) Submergence induced damage of photosynthetic apparatus in *Phragmites australis*. *Environ Exp Bot* 51, 227-235.
- [4] Liao, C. T. and Lin, C. H. (1996) Photosynthetic response of grafted bitter melon seedlings to flood stress. *Environ Exp Bot* 36, 167-172.
- [5] Waldhoff, D., Furch, B. and Junk, W. J. (2002) Fluorescence parameter, chlorophyll concentration, and anatomical features as indicators for flood adaptation of an abundant tree species in Central Amazonia: *Symmeria paniculata*. *Environ Exp Bot* 48, 225-235.
- [6] Sij, J. W. and Swanson, C. A. (1973) Effect of petiole anoxia on phloem transport in squash. *Plant Physiol* 51, 368-371.
- [7] Liu, Y. F. and Liu, Z. X. (2006) Primary Study on Vegetation Regeneration Modes along the Eat and Flow Zone of the Three Gorges Reservoir. *Journal of Chongqing Three Gorges University* 22, 4-7.
- [8] Fan, D. Y., Xiong, G. M., Zhang, A. Y., Liu, X., Xie, Z. Q. and Li, Z. J. (2015) Effect of water-level regulation on species selection for ecological restoration practice in the water-level fluctuation zone of Three Gorges Reservoir. *Chinese Journal of Plant Ecology* 39, 416-432.
- [9] Huang, S. Y., Ma, L. H., Fang, W., Liu, Y. and Chen, X. Y. (2013) Study on the Reconstruction and Ecological Restoration Techniques of Vegetation in Hydro-Fluctuation Belt of the Three Gorge Reservoir. *Journal of Southwest Forestry University* 33, 74-78.
- [10] Wang, Y., Liu, Y. F., Liu, S. B. and Huang, H. W. (2005) Vegetation Reconstruction in the Water-level-fluctuation Zone of the Three Gorges Reservoir. *Chinese Bulletin of Botany* 22, 513-522.
- [11] Bao, Y. H., He, X. B., Zhong, R. H., Gao, J. C. and Tang, Q. (2014) Revegetation and Its Effects on Soil Reinforcement in the Riparian Zone of Three-Gorge Reservoir. *Research of Soil and Water Conservation* 21, 171-174.
- [12] Lv, M. Q., Wu, S. J., Chen, C. D., Jiang, Y., Wen, Z. F., Chen, J. L., Wang, Y., Wang, X. X., Huang, P. (2015) A review of studies on water level fluctuating zone (WLFZ) of the Three Gorges Reservoir (TGR) based on bibliometric perspective. *Acta Ecologica Sinica* 35, 3504-3518.
- [13] Nilsson, C. and Svedmark, M. (2002) Basic principles and ecological consequences of changing water regimes: Riparian plant communities. *Environ Manage* 30, 468-480.
- [14] Dai, F. X., Xu, W. N. and Chen, F. Q. (2006) Reflection on the Ecological System in Three Gorges Water Level Fluctuating Zone and Its Ecological Restoration. *Soil and Water Conservation in China* 12, 6-8. (in Chinese)
- [15] Yuan, H., Wang, S. A., Zhan, Y. H., Huang, C. and Hu, G. (2006) Health Evaluation System on the Water-Level-Fluctuation Zone in the Three Gorges Area. *Resources and Environment in the Yangtze Basin* 15, 249-253.

- [16] Hong, M., Guo, Q. S., Nie, B. H., Kang, Y., Pei, S. X. and Jin, J. Q. (2011) Responses of *Cynodon dactylon* population in hydro-fluctuation belt of Three Gorges Reservoir area to flooding –drying habitat change. *Chinese Journal of Applied Ecology* 22, 2829-2835.
- [17] Wang, H. F., Zeng, B., Li, Y., Qiao, P., Ye, X. Q. and Luo, F. L. (2008) Effects of Long-term Submergence on Survival and Recovery Growth of Four Riparian Plant Species in Three Gorges Reservoir Region, China. *Journal of Plant Ecology (Chinese Version)* 32, 977-984.
- [18] Merinmartín, L. (2004) Applying plant facilitation to forest restoration: A meta-analysis of the use of shrubs as nurse plants. *Ecol Appl* 14, 1128-1138.
- [19] King, E. G. (2008) Facilitative effects of *Aloe secundiflora* shrubs in degraded semi-arid rangelands in Kenya. *J Arid Environ* 72, 358-369.
- [20] Zeng, C. C., Chen, J. P., Wang, Z. X., Jia, Z. M. and Wei, H. (2015) Response of growth and chlorophyll fluorescence characteristics of *Cynodon dactylon* seedlings to water treatment and planting densities. *Practacultural Science* 32, 1107-1115.
- [21] Fogliatto, S., Vidotto, F. and Ferrero, A. (2010) Effects of winter flooding on weedy rice (*Oryza sativa* L.). *Crop Prot* 29, 1232-1240.
- [22] Atik, A. (2013) Effects of Planting Density and Treatment with Vermicompost on the Morphological Characteristics of Oriental Beech (*Fagus orientalis Lipsky.*). *Compost Sci Util* 21, 87-98.
- [23] Qin, H. W., Liu, Y. F., Liu, Z. X., Zhou, D. X., Li, Y. J., Liu, R. H., Yang, J. N., Shi, R. J., Gan, L. P., Hu, L., Wan, C. Y. and Wang, J. (2012) The effects of simulate submerged test in three gorges reservoir hydro-fluctuation area on growth of 4 species of herbs. *J Biol* 29, 52-55.
- [24] Tan, S. D., Zhang, S. J., Zhang, K. R., Dang, H. S., Li, M. and Zhang, Q. F. (2009) Effect of Long-term and Deep Submergence on Recovery Growth and Photosynthesis of Three Grass Species in Three Gorges Reservoir Area. *Journal of Wuhan Botanical Research* 27, 391-396.
- [25] Zeng, C. C., Wang, Z. X., Chen, J. P., Gu, Y. W., Jia, Z. M. and Wei, H. (2016) The Effects of Different Water Treatments on Intraspecific Interactions of *Cynodon dactylon*. *Acta Ecologica Sinica* 5, 36.
- [26] Chen, J. P., Wang, Z. X., Zeng, C. C., Li, S. and Wei, H. (2015) Effects of different water levels and planting densities on the growth and morphology of *Hemarthria altissima*. *Acta practacultural Sinica* 24, 39-46.
- [27] Li, M., Yang, D. and Li, W. (2007) Leaf gas exchange characteristics and chlorophyll fluorescence of three wetland plants in response to long-term soil flooding. *Photosynthetica* 45, 222-228.
- [28] Xu, D. Q. (1988) Photosynthetic Efficiency. *Plant Physiology Communications* 5, 1-7.
- [29] Zhang, X., Huang, G., Bian, X. and Zhao, Q. (2013) Effects of root interaction and nitrogen fertilization on the chlorophyll content, root activity, photosynthetic characteristics of intercropped soybean and microbial quantity in the rhizosphere. *Plant Soil Environ* 368, 407-417.
- [30] Tung, J., Goodwin, P. H. and Hsiang, T. (2013) Chlorophyll fluorescence for quantification of fungal foliar infection and assessment of the effectiveness of an induced systemic resistance activator. *Eur J Plant Pathol* 136, 301-315.
- [31] Ye, Z. P., Yu, Q. and Kang, H. J. (2012) Evaluation of photosynthetic electron flow using simultaneous measurements of gas exchange and chlorophyll fluorescence under photorespiratory conditions. *Photosynthetica* 50, 472-476.
- [32] Briantais, J., Vernotte, C., Picaud, M. and Krause, G. H. (1980) Chlorophyll fluorescence as a probe for the determination of the photo-induced proton gradient in isolated chloroplasts. *Biochimica et Biophysica Acta (BBA) – Bioenergetic* 591, 198-202.
- [33] Van, K. O. and Snel, J. F. (1990) The use of chlorophyll fluorescence nomenclature in plant stress physiology. *Photosynth Res* 25, 147-150.
- [34] Chen, L. X. and Guan, J. Y. (2005) *A Course on Soil Experiment and Practice*. Northeast Forestry University Press, Harbin, China.
- [35] Hao, J. J., Kang, Z. L. and Yu, Y. (2006) *Experiment Technology of Plant Physiology*. Chemical Industry Press, Beijing, China.
- [36] Brooker, R. W., Maestre, F. T., Callaway, R. M., Lortie, C. L., Cavieres, L. A. and Kunstler, G. (2008) Facilitation in plant communities: the past, the present, and the future. *J Ecol* 96, 18-34.
- [37] Yu, F., Li, P., Li, S. and He, W. (2010) *Kobresia tibetica* tussocks facilitate plant species inside them and increase diversity and reproduction. *Basic Appl Ecol* 11, 743-751.
- [38] Li, P. X., Kruesi, B. O., Li, S. L., Cai, X. H. and Yu, F. H. (2011) Facilitation associated with three contrasting shrub species in heavily grazed pastures on the eastern Tibetan Plateau. *Community Ecol* 12, 1-8.
- [39] Pan, R. C. (2004) *Plant Physiology*. High Education Press, Beijing, China.
- [40] Hoertensteiner, S. and Kraeutler, B. (2011)

- Chlorophyll breakdown in higher plants. *Biochimica et Biophysica Acta (BBA) - Bioenergetics* 1807, 977-988.
- [41] Wang, T., Wang, S. P., Guo, S. Y. and Sun, Y. J. (2006) Research Advance about Hypoxia-stress Damage and Hypoxia-stress-adapting Mechanism in Plants. *Acta Botanica Boreali-Occidentalia Sinica* 26, 847-853.
- [42] Choler, P., Michalet, R. and Callaway, R. M. (2001) Facilitation and competition on gradients in alpine plant communities. *Ecology* 82, 3295-3308.
- [43] Yu, G. L. (2011) Effects of waterlogging on intraspecific interactions of the clonal herb *Alternanthera philoxeroides*. *Chinese Journal of Plant Ecology* 35, 973-980.
- [44] Smethurst, C. F. and Shabala, S. (2003) Screening methods for waterlogging tolerance in lucerne: comparative analysis of waterlogging effects on chlorophyll fluorescence, photosynthesis, biomass and chlorophyll content. *Funct Plant Biol* 30, 335-343.
- [45] Islam, M. A. and Macdonald, S. E. (2004) Ecophysiological adaptations of black spruce (*Picea mariana*) and tamarack (*Larix laricina*) seedlings to flooding. *Trees-Struct Funct* 18, 35-42.
- [46] Chen, F. and Xie, Z. (2009) Survival and growth responses of *Myricaria laxiflora* seedlings to summer flooding. *Aquat Bot* 90, 333-338.
- [47] Wang, J. L., Long, Q. Y., Wang, L. P., Luo, H. B., Lv, H. F. and Xu, C. R. (2013) Effects of Flood Stress and Stress Relieve on Melon Photosynthetic Pigments and Synthesis Character. *China Vegetables* 8, 50-55.
- [48] Wang, Z. X., Wei, H., Lv, Q., Li, C. X., Zhou, J., Gao, W. and Chen, W. (2013) Response of photosynthesis and chlorophyll fluorescence characteristics of *Pterocarya stenoptera* seedlings to submergence and drought alternation. *Acta Ecologica Sinica* 33, 888-897.
- [49] Yi, Y. J., Li, F. B. and Liu, J. Y. (2008) Physiological response of chlorophyll fluorescence in moss *Plagiomnium cuspidatum* to mixture heavy metal solution. *Acta Ecologica Sinica* 28, 5437-5444.
- [50] Dong, C. W. H., Chen, Z. Y., Ji, P. and Zhong, C. (2009) Effects of Attenuated UV-B Radiation on Dynamic Changes of Photosynthetic Pigment Contents in Flue-cured Tobacco under Natural Conditions. *Journal of Wuhan Botanical Research* 27, 637-642.
- [51] Li, C. X. and Zhong, Z. C. (2005) Simulative Study on Photosynthetic Physio-response of *Taxodium Ascendens* Seedlings to Soil Water Change in the Hydro-fluctuation Belt of Three Gorges Reservoir Area. *Acta Hydrobiologica Sinica* 29, 712-716.
- [52] Li, X., Feng, W. and Zeng, X. C. (2006) Advances in Chlorophyll Fluorescence Analysis and Its Uses. *Acta Botanica Boreali-Occidentalia Sinica* 26, 2186-2196.
- [53] Krause, G. H. and Weis, E. (1991) Chlorophyll fluorescence and photosynthesis: The basics. *Ann Rev Plant Physiol* 42, 313-349.
- [54] Maxwell, K. and Johnson, G. N. (2000) Chlorophyll fluorescence-a practical guide. *J Exper Bot* 51, 659-668.
- [55] Force, L., Critchley, C., Rensen, J. J. S. V. (2003) New fluorescence parameters for monitoring photosynthesis in plants. *Photosynth Res* 78, 17-33.
- [56] Luo, F., Nagel, K. A., Scharr, H., Zeng, B., Schurr, U., Matsubara, S. (2011) Recovery dynamics of growth, photosynthesis and carbohydrate accumulation after de-submergence: a comparison between two wetland plants showing escape and quiescence strategies. *Ann Bot* 107, 49-63.
- [57] Chen, S. R., Yu, L. Q., Yi, J., Wu, R. N., Ji, R. H. and Liu, S. N. (2011) Influence of Chlorophyll Fluorescence Characteristics on Alfalfa Seedlings under Cryogenic Stress. *Acta Agrestia Sinica* 19, 596-600.

---

**Received: 04.05.2016**

**Accepted: 15.09.2016**

---

#### **CORRESPONDING AUTHOR**

---

##### **Hong Wei**

Key Laboratory of Eco-environments in Three Gorges Reservoir Region (Ministry of Education), Chongqing Key Laboratory of Plant Ecology and Resources Research in Three Gorges Reservoir Region, School of Life Sciences, Southwest University, Chongqing 400715, PR China

e-mail: [weihong@swu.edu.cn](mailto:weihong@swu.edu.cn),  
[weihong\\_se@163.com](mailto:weihong_se@163.com)



# GENETIC IDENTIFICATION FOR SOME *FUSARIUM* SPP. USING RANDOM AMPLIFIED POLYMORPHIC DNA POLYMERASE CHAIN REACTION (RAPD-PCR) TECHNIQUE

Ayten Celebi Keskin<sup>1\*</sup>, Leyla Acik<sup>2</sup>, Aydan Araz<sup>3</sup>, Perihan Guler<sup>4</sup>

<sup>1</sup>Kirikkale University, Faculty of Engineering, Department of Bioengineering, Kirikkale, Turkey

<sup>2</sup>Gazi University, Faculty of Science, Department of Biology, Ankara, Turkey

<sup>3</sup>Plant Protection Central Research Institute, Ankara, Turkey

<sup>4</sup>Kirikkale University, Faculty of Science and Arts, Department of Biology, Kirikkale, Turkey

## ABSTRACT

The *Fusarium* species that is the cause of the disease that we used in our study takes an important place among microfungi that cause disease in agricultural plant species and economic loss. The subgroups and races of this species especially cause diseases with various symptoms on cereals such as wheat, barley, corn and clover, on fruit trees, and garden and ornamental plants. The definition of these microfungi that are pathogens at the genetic material level is important in terms of determining the disease they cause. The aim of the present study was to determine the genetic relationship among twenty isolates of *Fusarium* spp. (18 *Fusarium* species) isolated from wheat, maize and clover in Turkey using RAPD technique. In the present study, Random Amplified Polymorphic DNA (RAPD) markers were used to assess the genetic diversity within 20 isolates of *Fusarium*. RAPD analysis was performed with 16 decamer primers selected from a total of 30 primers. A total of 408 reproducible fragments were amplified by 16 RAPD primers. All the fragments were polymorphic (100%). The size of these fragments ranged from 100 to 3000 bp. The number of bands per primer varied between 14 and 39. Similarity indexes were calculated to determine the genetic relationships among these populations and subsequently dendograms based on Unweighted Pair-Group Method using Arithmetic Averages (UPGMA) was derived. Based on DNA finger prints, all isolates of *Fusarium* were categorized into three major clusters. The results demonstrated that RAPD analysis can be used for assessing the genetic diversity and the relationships among the *Fusarium* species.

## KEYWORDS

DNA finger prints; *Fusarium*; Genetic identification; RAPD-PCR

## INTRODUCTION

The genus *Fusarium* is one of the most economically important genera. It contains many pathogenic species that infect in plants, animals and humans and produce secondary metabolites named mycotoxins. The consumption of mycotoxin-contaminated food and feed products pose an acute risk to human and animal health [1, 2]. Therefore the accurate classification of the *Fusarium* genus is very important. The differentiation of *Fusarium* spp. is based on physiological and morphological characteristics such as the shape and size of macroconidia, the presence or absence of microconidia and chlamydospores and colony morphology [3]. These observations need some practice and are difficult for a non-specialist [4, 5]. Therefore a rapid and reliable assay is needed for the routine identification of pathogenic *Fusarium* spp. the agricultural industry, and the control measure of diseases caused by these fungi.

In recent year, molecular approaches for genetic analysis have led to a great increase in our knowledge of fungal systematic studies [6]. Random amplified polymorphic DNA (RAPD) is one of the PCR-based techniques that is rapid, inexpensive, and conservative in use of genomic DNA [7]. RAPD has provided information on genetic variability among strains [8-10]. Therefore RAPD technique has been used since a long time for fungal and *Fusarium* populations [11-13] at species, intraspecific, race and strain levels [14, 15]. There are many reports on differentiation of *Fusarium* species using RAPD markers. Bonde et al [15] studied genetic diversity among fourteen different *Fusarium* species by using RAPD markers. They obtained 180 polymorphic bands from four RAPD markers and reported UPGMA analysis of the RAPD data separated the *Fusarium* species in two clusters. Similarly, a genetic diversity of *Fusarium* spp. associated with sugarcane wilt were characterized using seven RAPD markers by Poonkothai [16].

The aim of the present study was to determine the genetic relationship among twenty isolates of *Fusarium* spp. isolated from wheat, maize and clover in Turkey using RAPD technique.

## MATERIALS AND METHODS

**Fungal Species.** Twenty *Fusarium* isolates used in this study were procured from Department of Cereal Disease of Plant Protection Central Research Institute. These isolates were previously isolated from wheat, maize and clover in different geographic regions of Turkey (Table 1).

**DNA extraction.** The *Fusarium* isolates were grown on Potato Dextrose Agar (PDA) at 28°C for 6 days and mycelia were transferred to flask of potato-dextrose broth (PDB) an incubated on a rotary shaker at 150 rpm for 5 days at 28°C. For DNA extraction of fungal cultures, the mycelium were harvested and ground to fine powder in liquid nitrogen. Total genomic DNA was extracted using the CTAB method [9].

**Primers and RAPD analysis.** PCR reactions were conducted according to Williams et al [17] using 10-mer random primers (Operon Technologies, Alameda, CA, USA) (Table 2). The reaction mixture contained: 50 mM KCl; 25 mM MgCl<sub>2</sub>; 50 mM Tris HCl (pH 9.0); 1 U of Taq DNA polymerase (Promega, GoTaq Flexi DNA Polymerase); 10 mM of each dNTP; 0.2 mM of primer, and about 20 ng of DNA. Amplification of genomic DNA was made on a Biometra

thermocycler, using the arbitrary decamers.

The 30 primers were tested from Operon Technologies (Alameda CA, USA). Sixteen primers were selected from the initial screening, because they produced consistent polymorphisms. The PCR program consisted of the following steps: first cycle at 94°C for 4 min, followed by 45 cycles at 94°C for 40 sec./ 30°C for 40 sec./ 72°C for 40 sec. and a final extension step at 72°C for 7 min. All applications were done in duplicate and on different days. PCR products generated by amplification were separated on %2 (w/v) agarose gel in TAE buffer at 90 V. A 100 bp Plus DNA ladder was used as molecular weight markers (Thermo Scientific GeneRuler 100 bp, SM0321). The gels were stained with ethidium bromide. The DNA fragments were visualized under UV light, and photographed using a BioDocAnalyze UV Transilluminator (Biometra).

**Data analysis.** Photographs from ethidium bromide stained agarose gels were used to score the RAPD data for analysis. The presence of the product was scored as 1 and the absence as 0. Bands with the same mobility were treated as identical fragments. The positions of the PCR bands obtained were compared with the molecular weight standards (Thermo Scientific GeneRuler 100 bp, SM0321). To determine the genetic variability, the data of the primers was used to construct a matrix, which was analyzed through Vilber Lourmat Bio1D++ Software computer program. Genetic similarities were calculated using Nei's similarity coefficients and the dendrograms were built by the Unweighted Pair Group Method using the Arithmetic Average (UPGMA) [18].

**TABLE 1**  
Geographical origin and sources of isolation of *Fusarium* species used in this study

Species	Sources of isolation	Origin
<i>F.avenaceum</i>	wheat	Konya
<i>F.acuminatum</i>	wheat	Sakarya
<i>F.equisetii</i>	wheat	Sakarya
<i>F.semitectum</i>	wheat	Eskişehir
<i>F.culmorum</i>	wheat	Sakarya
<i>F.crookwellense</i>	wheat	Sakarya
<i>F.solani</i>	wheat	Ankara
<i>F.solani</i>	clover	Ankara
<i>F.oxysporum</i>	wheat	Sakarya
<i>F.oxysporum</i>	maize	Ankara
<i>F.subglutinans</i>	wheat	Sakarya
<i>F.maniforme</i>	wheat	Sakarya
<i>F.maniforme</i>	maize	Ankara
<i>F.verticillioides</i>	wheat	Eskişehir
<i>F.proliferatum</i>	wheat	Sakarya
<i>F.graminearum</i>	wheat	Sakarya
<i>F.heterosporium</i>	wheat	Konya
<i>F.inflexum</i>	wheat	Konya
<i>F.poeae</i>	wheat	Ankara
<i>F.dimerum</i>	wheat	Sakarya

**TABLE 2**  
Primers used for RAPD-PCR amplification

Primer	Sequence (5'.....3')	Primer	Sequence (5'.....3')
A1	CAGGCCCTTC	OPB05	TGCGCCCTTC
A2	TGCCGAGCTG	OPB08	GTCCACACGG
A7	GAAACGGGTG	OPC02	GGTCTACACC
B18	CCACAGCAGT	OPI18	TGCCCAGCCT
OPA04	AATCGGGCTG	OPO04	AAGTCCGCTC
OPA11	CAATCGCCGT	OPU16	CTGCGCTGGA
OPA14	TCTGTGCTGG	OPW06	AGGCCCGATG
OPA17	GACCGCTTGT	M13	GAGGGTGGCGTTCT

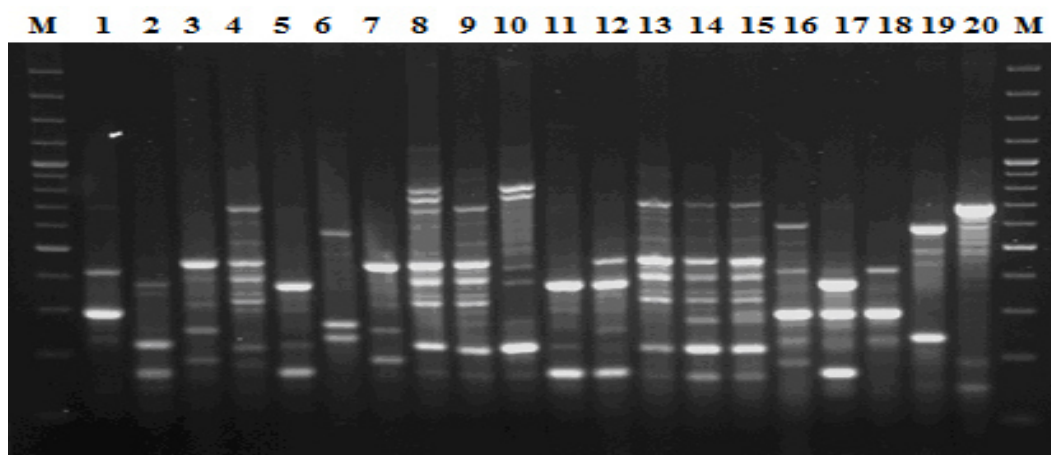


**FIGURE 1**  
RAPD profiles generated with the primer M13

**M:** Marker (Thermo Scientific SM0321), 1- *F.avenaceum* (wheat), 2- *F.acuminatum* (wheat), 3- *F.equisetii* (wheat), 4- *F.semitectum* (wheat), 5- *F.culmorum* (wheat), 6- *F.crookwellense* (wheat), 7- *F.solani* (wheat), 8- *F.solani* (clover), 9- *F.oxysporum* (wheat), 10- *F.oxysporum* (maize), 11- *F.subglutinans* (wheat), 12- *F.maniliforme* (wheat), 13- *F.maniliforme* (maize), 14- *F.verticillioides* (wheat), 15- *F.proliferaum* (wheat), 16- *F.graminearum* (wheat), 17- *F.heterosporium* (wheat), 18- *F.inflexum* (wheat), 19- *F.poa* (wheat), 20- *F.dimerum* (wheat), **M:** Marker (Thermo Scientific SM0321)

**TABLE 3**  
Genetic similarity matrix of *Fusarium* species based on RAPD profiles

	<i>F.avenaceum</i> (wheat)	<i>F.acuminatum</i> (wheat)	<i>F.equisetii</i> (wheat)	<i>F.semitectum</i> (wheat)	<i>F.culmorum</i> (wheat)	<i>F.crookwellense</i> (wheat)	<i>F.solani</i> (wheat)	<i>F.solani</i> (clover)	<i>F.oxysporum</i> (wheat)	<i>F.oxysporum</i> (maize)	<i>F.subglutinans</i> (wheat)	<i>F.maniliforme</i> (wheat)	<i>F.maniliforme</i> (maize)	<i>F.verticillioides</i> (wheat)	<i>F.proliferaum</i> (wheat)	<i>F.graminearum</i> (wheat)	<i>F.heterosporium</i> (wheat)	<i>F.inflexum</i> (wheat)	<i>F.poa</i> (wheat)	<i>F.dimerum</i> (wheat)
<i>F.avenaceum</i> (wheat)	1.00																			
<i>F.acuminatum</i> (wheat)	0.11	1.00																		
<i>F.equisetii</i> (wheat)	0.23	0.25	1.00																	
<i>F.semitectum</i> (wheat)	0.14	0.19	0.37	1.00																
<i>F.culmorum</i> (wheat)	0.09	0.44	0.15	0.16	1.00															
<i>F.crookwellense</i> (wheat)	0.13	0.16	0.08	0.09	0.11	1.00														
<i>F.solani</i> (wheat)	0.24	0.15	0.54	0.30	0.14	0.12	1.00													
<i>F.solani</i> (clover)	0.15	0.16	0.30	0.59	0.15	0.13	0.39	1.00												
<i>F.oxysporum</i> (wheat)	0.14	0.17	0.34	0.69	0.14	0.09	0.36	0.75	1.00											
<i>F.oxysporum</i> (maize)	0.08	0.10	0.10	0.18	0.13	0.10	0.16	0.39	0.20	1.00										
<i>F.subglutinans</i> (wheat)	0.12	0.27	0.18	0.06	0.51	0.11	0.09	0.07	0.08	0.09	1.00									
<i>F.maniliforme</i> (wheat)	0.09	0.22	0.22	0.12	0.31	0.11	0.28	0.13	0.13	0.15	0.45	1.00								
<i>F.maniliforme</i> (maize)	0.12	0.16	0.30	0.60	0.17	0.10	0.34	0.59	0.65	0.17	0.13	0.14	1.00							
<i>F.verticillioides</i> (wheat)	0.14	0.13	0.25	0.54	0.12	0.07	0.26	0.52	0.58	0.15	0.08	0.10	0.71	1.00						
<i>F.proliferaum</i> (wheat)	0.14	0.09	0.28	0.52	0.10	0.09	0.30	0.50	0.58	0.17	0.11	0.08	0.64	0.69	1.00					
<i>F.graminearum</i> (wheat)	0.31	0.14	0.19	0.11	0.05	0.16	0.13	0.15	0.14	0.14	0.06	0.11	0.14	0.16	0.16	1.00				
<i>F.heterosporium</i> (wheat)	0.25	0.11	0.15	0.10	0.18	0.17	0.16	0.17	0.15	0.13	0.28	0.27	0.09	0.16	0.13	0.45	1.00			
<i>F.inflexum</i> (wheat)	0.21	0.07	0.09	0.06	0.04	0.07	0.08	0.09	0.14	0.04	0.12	0.10	0.09	0.12	0.14	0.47	0.29	1.00		
<i>F.poa</i> (wheat)	0.18	0.05	0.10	0.11	0.06	0.35	0.08	0.13	0.13	0.11	0.11	0.13	0.09	0.09	0.08	0.20	0.20	0.11	1.00	
<i>F.dimerum</i> (wheat)	0.13	0.10	0.11	0.12	0.08	0.19	0.03	0.08	0.11	0.06	0.11	0.04	0.09	0.11	0.09	0.24	0.20	0.19	0.30	1.00

## RESULTS AND DISCUSSION

In this study, a total of 20 *Fusarium* isolates (18 *Fusarium* species) isolated from wheat (17 isolates), corn (two isolates) and clover (one isolate) were used. The genomic DNA obtained from 20 *Fusarium* isolates was examined for RAPD-PCR analysis. Of the 30 RAPD primers used, only 16 RAPD primers resulted in reproducible banding pattern. A total of 408 reproducible fragments were amplified by 16 RAPD primers. It was observed that they were all of polymorphic (100%) with an average of 25.50 bands per primer. The size of fragments ranged from 100 to 3000 bp. When evaluation was made from the primers point of view, the highest number of bands was provided by OPB08 primary (39 bands) while the lowest number of bands was provided by OPA14 and OPC02 primaries (14 bands). Sample gel images of the amplified products obtained using the M13 primer are shown in Fig. 1.

The pair-wise distances were computed from the RAPD band data. These values are given in Table

3. The remaining values, displaying different intermediate levels of similarity, are grouped with the others. It is graphically represented as a dendrogram using the UPGMA method, as shown in Fig. 2. Twenty isolations of *Fusarium* were clustered into three main groups (Cluster I, II and III). Cluster I was further divided into three subgroups. The first subgroup included *F. avenaceum*, *F. graminearum*, *F. inflexum*, *F. heterosporium*. The second subgroup included *F. equisetii* and *F. solani* (wheat). The third subgroup included *F. semitectum*, *F. solani* (clover), *F. oxysporum* (wheat), *F. maniliforme* (maize), *F. verticillioides*, *F. proliferatum*. Cluster II included *F. crookwellense*, *F. poae*, *F. dimerum* and cluster III included *F. acuminatum*, *F. culmorum*, *F. subglutinans*, *F. maniliforme* (wheat), *F. oxysporum* (maize). The minimum similarity value of 0.03 was observed between *F. solani* (wheat) and *F. dimerum* and the maximum similarity value of 0.75 was observed between *F. solani* (clover) and *F. oxysporum* (wheat). Accordingly it was observed that there is a high genetic difference between *Fusarium* species.

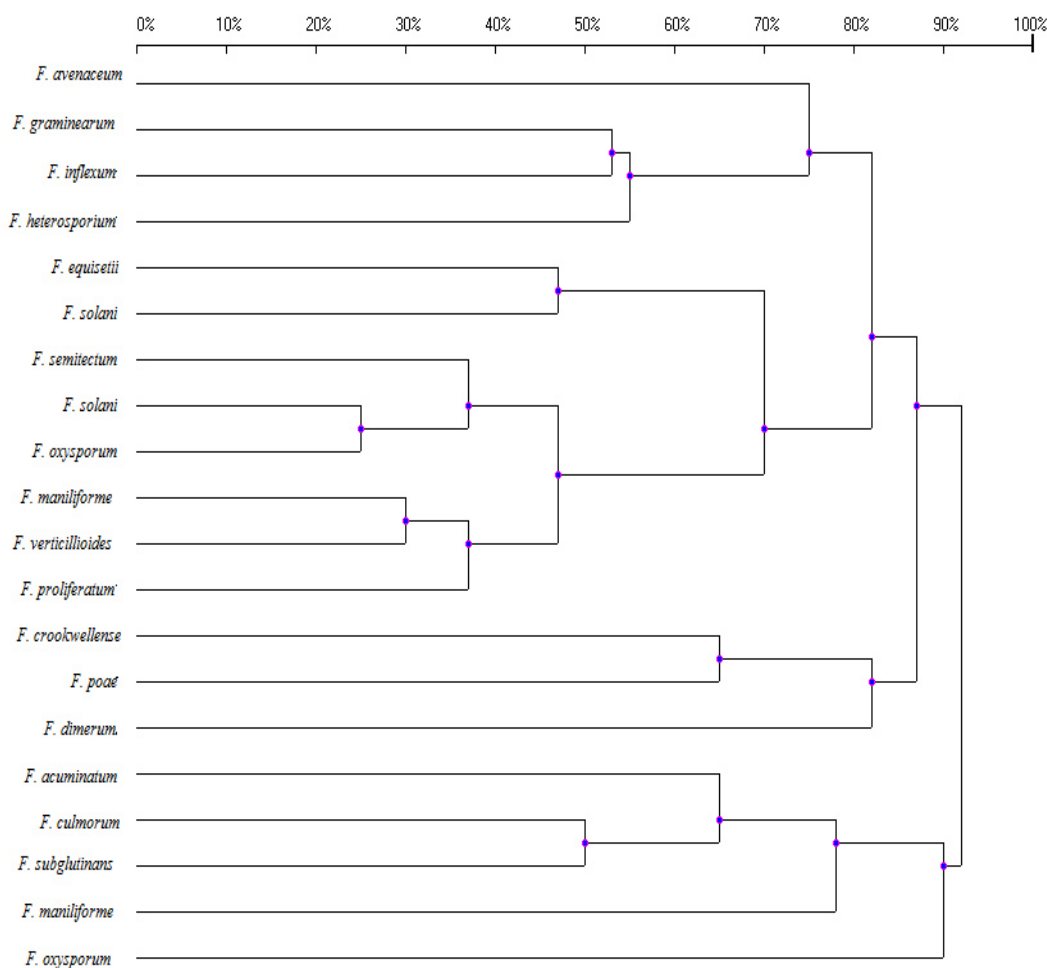


**FIGURE 2**  
Dendrogram displaying the genetic distances among *Fusarium* species obtained from cluster analysis of RAPD data

In studies with similar results to our study, Abd-Elsalam et al [19] determined by using 20 random RAPD primaries on 12 *Fusarium* species that genetic differences between species vary between 28-62%, while Maina et al [20] determined by using six random RAPD primaries on 26 *Fusarium* isolates that genetic differences between species vary between 25-58% and Arif et al [21] determined by using 18 random RAPD primaries on 25 *Fusarium* isolates that genetic differences between species vary between 17.4-94.5%. In a classification made by Nirenberg and Mitteilungen [22] it was stated that *F. proliferatum* and *F. verticilloides* are synonyms of *F. moniliforme*. However, the differentiation of *F. proliferatum* from *F. moniliforme* is made according to morphology of their spore structures. In some Australian isolates it was stated that the microconidia chains of *F. proliferatum* composed of polyphialides are generally shorter compared to chains formed by *F. moniliforme* [23]. According to the dendrogram we obtained in our study, although these three species are lined on top of one another in the same group, there are significant genetic differences between them. The genetic difference between *F. proliferatum* and *F. maniliforme* is 0.36 while the genetic difference between *F. verticilloides* and *F. maniliforme* is found to be 0.29. In addition, in a study performed by Zakaria et al [24] they characterized *F. oxysporum*, *F. solani* and *F. proliferatum* species which they isolated from *Dendrobium* in Malaysia by the RAPD-PCR method and also determined that they are consistent with morphological characters and that these species are in different groups as a result of cluster analysis and are significantly different from each other. In our study, although these three species are in the same group similar to this study, significant genetic differences were determined between them. The genetic difference between *F. solani* and *F. oxysporum* was determined to be 25%, between *F. solani* and *F. proliferatum* 50% and between *F. oxysporum* and *F. proliferatum* 42%. Also, *F. oxysporum* and *F. solani* are species that are *Fusarium* species that are mostly mistaken for each other. From the long monophialids of *F. solani*, microconidia are formed. On the other hand in *F. oxysporum*, microconidia are formed from relatively shorter monophialids [23]. In another study, Khokhar et al. [25] studied the molecular characterization of 10 *Fusarium* isolates they obtained from maize samples in various regions of India [*F. proliferatum* (four isolates), *F. verticilloides* (five isolates) and *F. pallidoroseum* (one isolate)] by the RAPD-PCR technique and according to cultural and morphological characters they stated that these 10 isolates demonstrate differences and that these isolates are divided into two main clusters according to RAPD analysis and that this technique revealed the differences between

*Fusarium* species obtained from maize. According to the obtained results they stressed that the RAPD-PCR technique completed the morphological characters in determination of genetic relations between different *Fusarium* species. They stated that the RAPD technique is cheap, quick, reliable and useful in the determination of genetic variations both within *Fusarium* species and between different *Fusarium* species in different studies. [15, 26, 27].

## CONCLUSION

---

According to the results of this study RAPD-PCR was a cheap, quick, reliable and useful method in determination of the genetic variations between 18 *Fusarium* species that we used in our study after isolating from wheat, maize and clover in various regions of Turkey. However, it should be emphasized that epidemiology and taxonomic relations within the species and between the species of *Fusarium* that cause disease in cereal products should be better understood. In addition, quick and accurate diagnosis is important especially in the diagnosis of pathogen species, in case of infections, for selecting effective treatment, in case of epidemics, in cases when new species appear and in determination of incidence rates. For this reason in order to obtain preeminently reliable and accurate results it is suggested that the number of isolates representing the species should be increased and that different molecular markers such as ITS, IGS, ISSR and DNA sequence analysis be used.

## ACKNOWLEDGEMENTS

---

This financial support by Kırıkkale University Scientific Research Projects (SRP) Coordination Unit via grant numbered BAP-2008/26 is acknowledged gratefully.

## REFERENCES

---

- [1] Withanage, G.S., Murata, H., Koyama, T. and Ishiwata, I. (2001) Agonistic and antagonistic effects of zearalenone, an estrogenic mycotoxin, on SKN, HHUA, and HepG2 human cancer cell lines. *Veterinary and Human Toxicology* 43, 6-10.
- [2] Faria, C.B., Lumi Abe, C.A., Novais da Silva, C., Tessmann, D.J. and Barbosa-Tessmann, I.P. (2012) New PCR assays for the identification of *Fusarium verticilloides*, *Fusarium subglutinans*, and other species of the Gibberella fujikuroi complex. *International Journal of Molecular Sciences* 13(1): 115-132.





- [3] Llorens, A., Hinojo, M.J., Mateo, R., González Jaén, M., Valle-Algarra, F.M., Logrieco, A. and Jiménez, M. (2006) Characterization of *Fusarium* spp. isolates by PCR-RFLP analysis of the intergenic spacer region of the rRNA gene (rDNA). *International Journal of Food Microbiology* 106, 297-306.
- [4] Bluhm, B.H., Flaherty, J.E., Cousin, M.A. and Woloshuk, C.P. (2002) Multiplex polymerase chain reaction assay for the differential detection of trichothecene- and fumonisin-producing and trichothecene-producing groups of *Fusarium* species. *Journal of Food Protection* 67, 536-543.
- [5] Abedi-Tizaki, M. and Sabbagh, S.K. (2012) Morphological and molecular identification of *Fusarium* head blight isolates from wheat in north of Iran. *Australian Journal of Crop Science* 6(9): 1356-1361.
- [6] Nayaka, S.C., Wulff, E.G., Udayashankar, A.C., Nandini, B.P., Niranjana, S.R., Mortensen, C.N. and Prakash, H.S. (2011) Prospects of molecular markers in *Fusarium* species diversity. *Applied Microbiology and Biotechnology* 90(5): 1625-1639.
- [7] Amoah, B.K., McDonald, M.V., Rezanoor, H.N. and Nicholsan, P. (1996) The use of random amplified polymorphic DNA technique to identify mating groups in the *Fusarium* section *Liseola*. *Plant Pathology* 45, 115-125.
- [8] Keressies, A., Bosker-van Zessen, A.I., Wagemakers, C.A.M. and Van Kan, J.A.L. (1997) Variation in pathogenicity and DNA polymorphism among *Botrytis cinerea* isolates sampled inside and outside a glasshouse. *Plant Disease* 81(7): 781-786.
- [9] Sabir, J.S.M. (2006) Genotypic identification for some *Fusarium sambucinum* strains isolated from wheat in Upper Egypt. *World Journal of Agricultural Sciences* 2(1): 6-10.
- [10] Ingle, A.P., Karwa, A., Rai, M.K. and Gherbawy, Y. (2009) *Fusarium*: Molecular detection, mycotoxins and biocontrol. In: Gherbawy, Y., Mach, R., Rai, M. (Eds.). *Current Advance in Molecular Mycology*. Science Publishers Inc., Enfield, New Hampshire.
- [11] Kini, K.R., Leth, V. and Mathur, S.B. (2002) Genetic variation in *Fusarium moniliforme* isolated from seeds of different host species from Burkina Faso based on random amplified polymorphic DNA analysis. *Journal of Phytopathology* 150, 209-212.
- [12] Liu Weicheng, X., Jingtliu, L., Hong Yu, P.H., Yu, H.H., Qiao Lai, G.Y. and Ronglin, B. (2002) RAPD analysis of isolates from *Fusarium* spp. causing wheat head blight in Northeast China. *Mycosystem* 21(1): 63-70.
- [13] Bayraktar, H. (2010) Genetic diversity and population structure of *Fusarium oxysporum* f. sp. *cepae*, the causal agent of *Fusarium* basal plate rot on onion, using RAPD markers. *Journal of Agricultural Sciences* 16, 139-149.
- [14] Gupta, V.K., Misra, A.K., Gaur, R., Pandey, R. and Chauhan, U.K. (2009) Studies of genetic polymorphism in the isolates of *Fusarium solani*. *Australian Journal of Crop Science* 3, 101-106.
- [15] Bonde, S.R., Gade, A.K. and Rai, M.K. (2013) Genetic diversity among fourteen different *Fusarium* spp. using RAPD marker. *Biodiversitas* 14(2): 55-60.
- [16] Poonkothai, M. (2015) Diversity of *Fusarium* spp. associated with sugarcane wilt. *Indian Journal of Science* 15(47): 149-163.
- [17] Williams, J.G.K., Kubelik, A.R., Livak, R.J., Rafalski, J.A. and Tingey, S.V. (1990) DNA polymorphisms amplified by arbitrary primers are useful as genetic markers. *Nucleic Acids Research* 18, 6531-6535.
- [18] Nei, M. (1978) Estimation of average heterozygosity and genetic distances from a small number of individuals. *Genetics* 89, 583-590.
- [19] Abd-Elsalam, K.A., Khalil, M.S., Aly, A.A. and Asran-Amal, A. (2002) Genetic diversity among *Fusarium oxysporum* f. sp. *vasinfectum* isolates revealed by UP-PCR and AFLP markers. *Phytopathologia Mediterranea* 41, 1-7.
- [20] Maina, P.K., Okoth, S., Njoroge, C.N. and Monda, E. (2009) Genetic relatedness among *Fusarium* species isolated from Taita Taveta region. *Kenya Tropical and Subtropical Agroecosystems* 11, 337-345.
- [21] Arif, M., Pani, D.R., Zaidi, N.W. and Singh, U.S. (2011) PCR-Based identification and characterization of *Fusarium* sp. associated with mango malformation. *Biotechnology Research International* 2011, 1-6.
- [22] Nirenberg, G.W. and Mittelellungen, H. (1982) The genus *Fusarium*- a Pictorial Atlas, Aus der Biologischen Bundesanstalt für Land- und Forstwirtschaft Berlin-Dahlem pp. 406.
- [23] Burgess, L., Summerell, A.B., Bullock, S., Gott, P.K. and Backhouse, D. (1994) *Laboratory Manual for Fusarium Research* 3rd Edition, *Fusarium Research Laboratory Department of Crop Sciences University of Sydney and Royal Botanic Gardens, Sydney* pp. 133.
- [24] Zakaria, L., Zain, N.H., Salleh, B. and Zakaria, M. (2009) Morphological and RAPD analysis of *Fusarium* species associated with root and stem rot of *Dendrobium* orchid in Northern Peninsula Malaysia. *HAYATI Journal of Bioscience* 16 (2): 64-68.
- [25] Khokhar, M.K., Sharma, S.S., Hooda, K.S. and Roat, B.L. (2015) Morphological and molecular characterization of *Fusarium* spp. causing post flowering stalk rot of maize. *International Journal of Plant Research* 28(1): 113-121.



- [26] Gupta, V.K. (2012) PCR-RAPD profiling of *Fusarium* spp. causing guava wilt disease in India. *Journal of Environmental Science and Health, Part B* 47(4): 315-325.
- [27] Mukhtar, I., Bajwa, R., Nasim, G. and Hafeez, F.Y. (2014) Evaluation of genetic diversity among phytopathogenic isolates of *Fusarium solani* complex causing shisham dieback disease in Pakistan. *The Journal of Animal and Plant Science* 24 (6): 1724-1728.

---

**Received: 11.05.2016**

**Accepted: 19.09.2016**

---

#### **CORRESPONDING AUTHOR**

---

**Ayten Celebi Keskin**

Kirikkale University, Faculty of Engineering,  
Department of Bioengineering,  
71450 Yahsihan, Kirikkale – TURKEY

e-mail: [aytencelebi@gmail.com](mailto:aytencelebi@gmail.com)

# WATER AND SEDIMENT QUALITY IN THE NATIONAL MARINE PARK OF ALONISSOS AEGEAN SEA

Paraskevi Ovezikoglou, Manos Ladakis, Manos Dassenakis\*

National and Kapodistrian University of Athens,  
Dept of Chemistry, Lab of Environmental Chemistry, Athens, Greece

## ABSTRACT

The aim of this work is to assess the quality of the marine environment in the Greek National Marine Park of Alonissos which has been established more than 30 years ago. The Marine Park's main mission is the protection of the Mediterranean monk seal *Monachus monachus*.

Sampling cruises were carried out in the area during the summer of 2011; sediment and seawater samples were collected and in situ measurements were performed.

Low values were determined for the phosphates, silicates and nitrites while quite elevated values were determined for the nitrates. Concerning the dissolved and particulate forms of the metals, low values were determined for the majority of them. The studied sediments were not rich in metals as almost none exceeded the respective Probable Effect Level (PEL), above which adverse effects on benthic biota are frequently observed. In conclusion, the under study marine park is from the chemical point of view in a fair environmental condition.

## KEYWORDS :

Alonissos, Metals, Nutrients, Sediment, Marine Park

## INTRODUCTION

The National Marine Park of Alonissos in the archipelagos of North Sporades (Figure 1) was established in 1983 as a contribution to the protection of the threatened by extinction Mediterranean monk seal *Monachus monachus*. Alonissos is the largest and the only inhabited island of the park's area. The area also encompasses six smaller islands and a number of islets.

The Marine Park consists of two zones: Zone A, (1,587 km<sup>2</sup>) is the zone of strict protection while Zone B (678 Km<sup>2</sup>) includes the inhabited island Alonissos and is open to visitors.

Although the success of the marine park is depended on the good environmental status in the area, there are not any official procedures for the

monitoring of the marine environment. The aim of this study is to assess the quality of the marine environment in the Marine Park of Alonissos. For this purpose, we attempted:

a) To assess the pollution level of seawater by determining the concentration of some main chemical parameters such as the micronutrients and the heavy metals.

b) To assess the pollution of the marine sediments by determining their content in heavy metals.

## MATERIALS AND METHODS

A sampling cruise was carried out during the summer of 2011.

Surface seawater and sediment samples were collected from 17 sampling stations in the area of the marine park (Figure 1). This sampling network is as representative as possible of this extended marine area. 8 sampling points are located along the coastline of the Alonissos island, 3 in the marine area between Alonissos and Peristera, 4 close to the coastline of uninhabited islets, one near Piperi island, which is the most significant island for the seals while the last one (SA16) lies the middle of the marine protected area.

Seawater samples were collected at a depth of 1 meter by Hydro-Bios polypropylene bottles and were filtered through pre-weighed 0.45 μm Millipore membrane filters. The dissolved trace metals were pre-concentrated on Chelex-100 resin in NH<sub>4</sub><sup>+</sup> form [1] and then eluted with a mixture of 2N:1N HNO<sub>3</sub>:HCl after the removal of Ca and Mg with ammonium acetate solution [2].

Sediments were collected with the use of a grab sampler and were treated with a mixture of strong acids [3] in PTFE bakerys at a temperature of 200 °C to complete dissolution.

The trace metals were determined by the use of flame or furnace atomic absorption spectroscopy using a VARIAN SpectrAA 200 instrument (Flame AAS) and a VARIAN SpectrAA 640Z instrument (Graphite Furnace AAS) with Zeeman background correction.

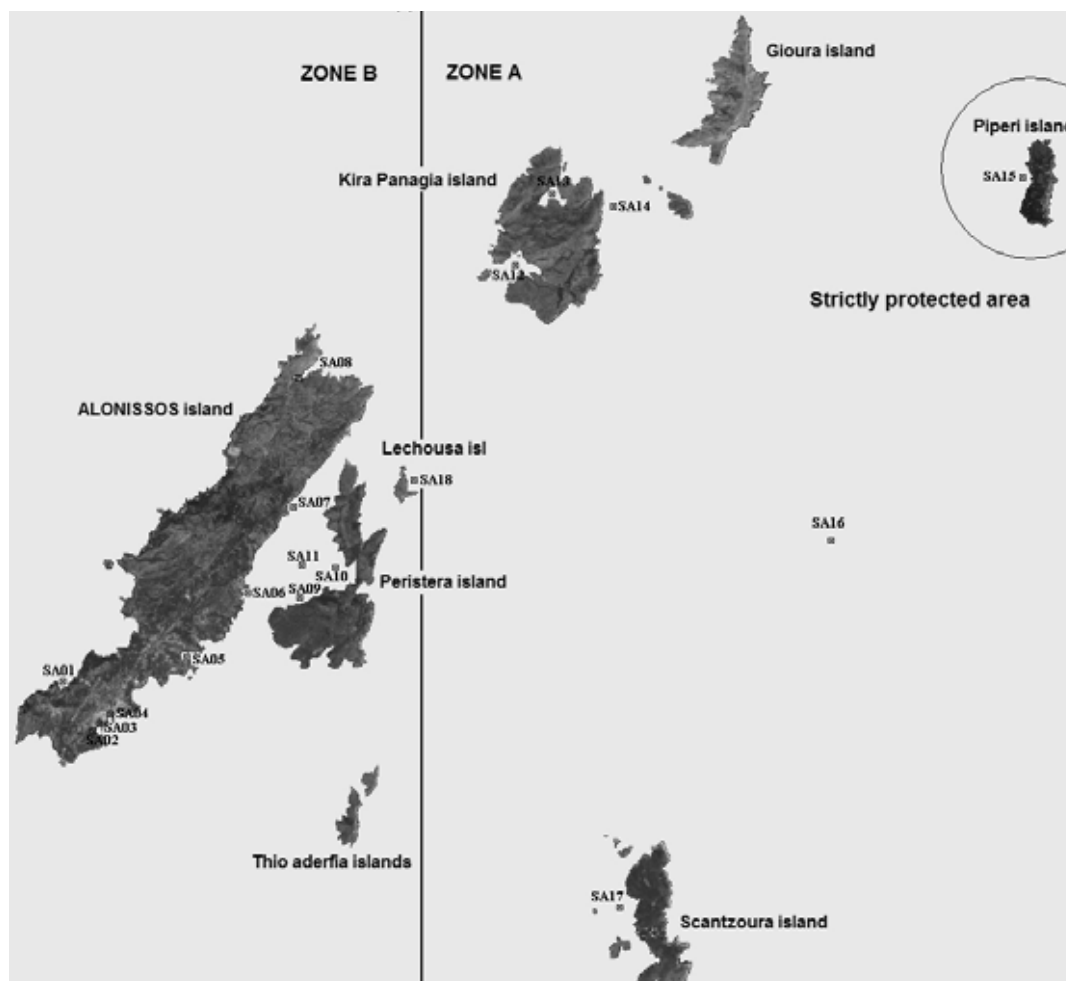


FIGURE 1

The map of the area of the Marine Park of Alonissos

**TABLE 1**  
Range and mean values of nutrients in the water column of the Marine Park (All values in  $\mu\text{M}$ ,  $\text{SiO}_4^{4-}$  in  $\mu\text{g/l}$ , BDL = Below Detection Limit).

Parameter	Min – Max	Mean
$\text{NO}_3^-$	BDL-4.35	0.87
$\text{NO}_2^-$	0.01-0.09	0.03
$\text{NH}_4^+$	BDL-3.00	0.80
totN	5.60-11.5	7.84
DON	2.25-10.2	6.14
$\text{PO}_4^{3-}$	BDL-0.08	0.04
totP	BDL -0.20	0.05
DOP	BDL-0.17	0.02
$\text{SiO}_4^{4-}$	0.83-11.30	2.54

Spectrophotometric methods were used for the determination of inorganic nutrients ( $\text{NO}_2^-$ ,  $\text{NO}_3^-$ ,  $\text{NH}_4^+$ ,  $\text{PO}_4^{3-}$ ,  $\text{SiO}_4^{4-}$ ) [4]. A UV-Vis spectrophotometer VARIAN Cary 1E was used for this purpose. The organic N and P were determined by the Valderama method [5]. In situ measurements

of some main physicochemical parameters were carried out by portable equipments.

All methods have been tested in the laboratory for their accuracy and reproducibility, using reference materials and replicate samples. All determinations were repeated three times and the average value was calculated.

## RESULTS AND DISCUSSION

The under study marine area was saturated in dissolved oxygen, the temperature was approximately  $25^\circ\text{C}$  and the salinity was about 38‰.

**Nutrients.** The range and mean concentrations of the nitrogen and phosphorus compounds, as well as the silicates, are presented in Table 1.

The highest values for  $\text{NO}_3^-$ ,  $\text{NO}_2^-$  and  $\text{SiO}_4^{4-}$  were determined in the enclosed bay of Gerakas (sampling station 8), a small port for fishing boats. On the other hand, the highest values for  $\text{NH}_4^+$ , DON and totN were determined in the marine area between Alonissos and Peristera islands (Sampling

Stations 6, 7, 9, 10 and 11). Considerable values were also recorded in the sampling stations 2, 3 and 4), all of them lying around the harbour of the island. Remarkably low values for  $\text{PO}_4^{3-}$  and  $\text{NO}_2^-$  were as well recorded in the marine area; the percentage of the dissolved organic nitrogen (DON) as a rate of the total nitrogen was rather high (30-99%) [6], whereas the dissolved organic phosphorus (DOP) was very low, with the exception of the coastal station of Gerakas (SA08), where the determined value was  $0.17 \mu\text{M/l}$ .

The concentration of silicates was also low; it didn't exceed the value of  $2 \mu\text{g/l}$ , with the exception of Gerakas (SA08) and Gialia (SA01), where the values were 11.3 and  $6.00 \mu\text{g/l}$  respectively. According to Table 2, the concentrations of  $\text{NO}_2^-$ ,  $\text{NO}_3^-$  and  $\text{PO}_4^{3-}$  in the Marine Park do not differ significantly from the prevailing values in the North Aegean Sea. On the other hand, there was a relative increase in  $\text{NH}_4^+$ . The values for the 2011 period were lower than the corresponding values for 1998 [7]. In any case, the concentrations of nutrients do not exceed the limits for Good Environmental Status

(GES) recommended by the EU Marine Strategy Framework Directive 2008/56/EC.

As extracted from Figure 2 the marine area around the harbour, as well as between Alonissos and Peristera islands are rich in nitrogen compounds.

**Metals in the water-column.** The range and mean values of some heavy metals in the water column are presented in Table 3 while the surface distribution of the dissolved Pb, Cd and Zn are presented in Figure 3.

The highest values for the dissolved Cu and Pb were determined at the bay of Gerakas (Station 8); on the other hand the highest values for the dissolved Fe, Mn and Ni were located at the sampling station of Gialia (Station 1) while those for the dissolved Cd were located at Patitiri (Station 2). Increased values of the most of the dissolved metals were determined in the area between Alonissos and Peristera. The marine area near the urban areas of Alonissos is rich in Cd and Cu.

The concentration of the dissolved metals in some areas of the Aegean Sea as well as the quality thresholds defined by the US Environmental

**TABLE 2**  
Mean concentration of nutrients in some areas of the Aegean (values in  $\mu\text{M}$ ,  $\text{SiO}_4^{4-}$  in  $\mu\text{g/l}$ )

Area	$\text{NO}_2^-$	$\text{NO}_3^-$	$\text{NH}_4^+$	$\text{PO}_4^{3-}$	$\text{SiO}_4^{4-}$	TIN	N/P
Marine Park of N. Sporades 1998 [7]	0.03	1.25	1.11	0.12	0.90	2.39	20
Open Saronikos gulf (2000-2002) [8]	0.12	1.18	0.24	0.11	1.97	1.54	14
Inner Saronikos gulf (2000-2002) [8]	0.14	0.96	0.40	0.24	1.81	1.50	6
Central Evoikos gulf 1998 [9]	0.18	5.81	2.71	0.22	8.14	8.70	40
Northern Aegean Sea 1994 [10]	0.04	0.84	0.34	0.07	1.65	1.22	17
Southern Aegean Sea 1994 [10]	0.03	0.78	0.28	0.06	1.83	1.09	18
Marine Park of N. Sporades 2011 (present work)	0.03	0.87	0.80	0.04	2.54	1.70	64
EU Marine Strategy [11] (a)	0.01	0.6 (< 1.0)	(< 0.55)	0.2 (< 0.5)	(< 3.0)	(< 2.0)	

(a): proposed upper limits in brackets

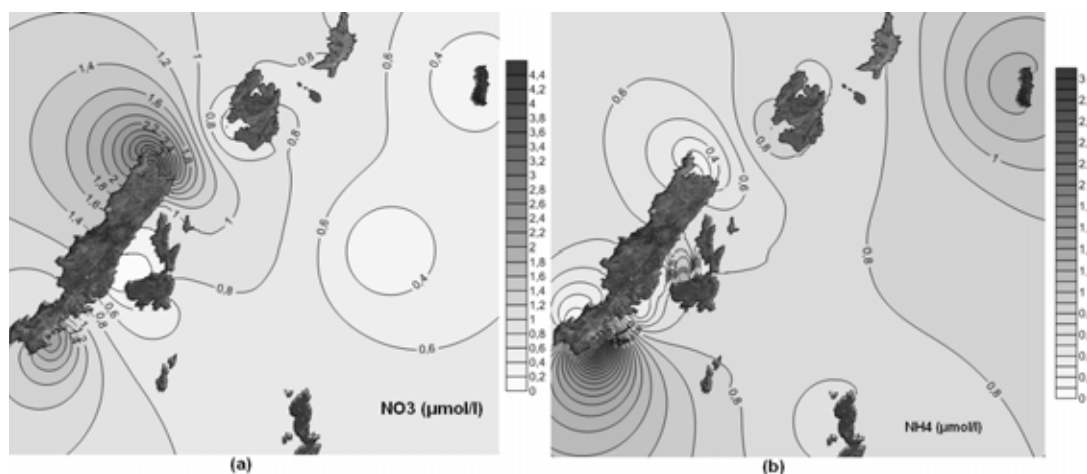


**FIGURE 2**  
The distributions of  $\text{NO}_3^-$  (a) and  $\text{NH}_4^+$  (b) in the surface seawater of the area of the Marine Park of Alonissos

**TABLE 3**  
Range and mean values of the dissolved and particulate forms of metals in the water column of the Marine Park of Alonissos (values in  $\mu\text{g/l}$ )

Metal	Dissolved		Particulate	
	Range	Mean	Range	Mean
Zn	0.67 – 10.9	3.83	0.01 – 1.86	0.43
Fe	0.42 – 6.44	1.52	0.28 – 493	53.2
Cu	0.16 – 0.65	0.32	0.01 – 1.45	0.15
Pb	0.04 – 0.34	0.15	BDL – 3.46	0.30
Cd	0.04 – 0.07	0.04	BDL – 0.002	0.001
Ni	0.37 – 0.72	0.51	0.00 – 2.10	0.26
Mn	0.28 – 1.79	0.65	0.18 – 4.59	1.15

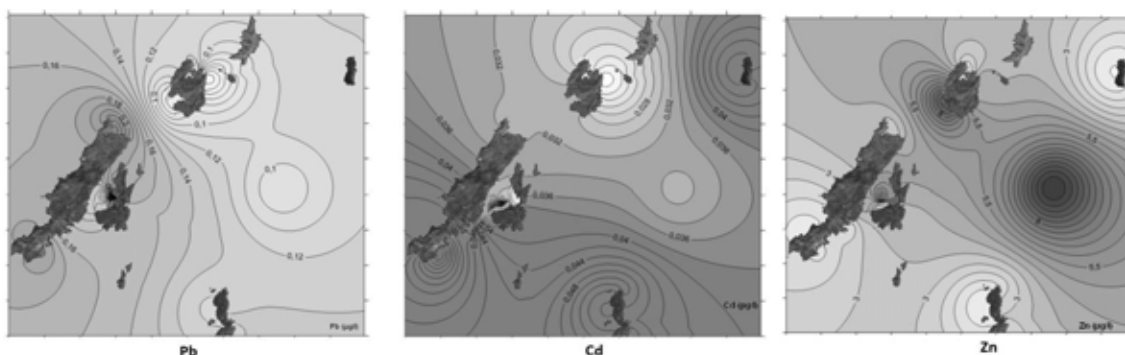


**FIGURE 3**  
Surface distribution of the dissolved Pb, Cd and Zn in the Marine Park of Alonissos.

**TABLE 4**  
Concentration of dissolved metals in some areas of the Aegean Sea (values in  $\mu\text{g/l}$ )

	Zn	Cu	Pb	Cd	Ni	Mn
Marine Park of N. Sporades 1998 [7]	9.19	1.03	0.58	0.82	3.06	1.38
North Aegean [22]	1.72-71	0.4-9.2	0.04-19.7	0.00-0.80		
Central Aegean [22]	0.75-9.51	0.04-4.57	0.02-4.80	0.00-0.25		
Kaloni-Lesvos island [12]	1.05-2.66	0.22-0.37			0.70-2.11	1.87-4.09
Outer Saronikos [13]	2.88		0.14	0.02		0.32
MPA Alonissos 2011 - this study	0.67-10.90	0.16-0.65	0.04-0.38	0.02-0.07	0.37-0.72	0.28-1.79
(d)	(3.83)	(0.32)	(0.15)	(0.04)	(0.51)	(0.65)
EPA Acute (a) [14]	90	4.8	210	40	74	
EPA Chronic (b) [14]	81	3.1	8.1	8.8	8.2	
EU Marine Strategy [11] (c)	1 (100)	0.5 (10)	0.5 (10)	0.1 (1)		

(a): adverse effects for short term exposition; (b): adverse effects for long term exposition;

(c): reference values -proposed threshold for GES in brackets; (d): mean values in brackets



**FIGURE 4**  
Surface distribution of the particulate Pb, Cu and Zn in the Marine Park of Alonissos.

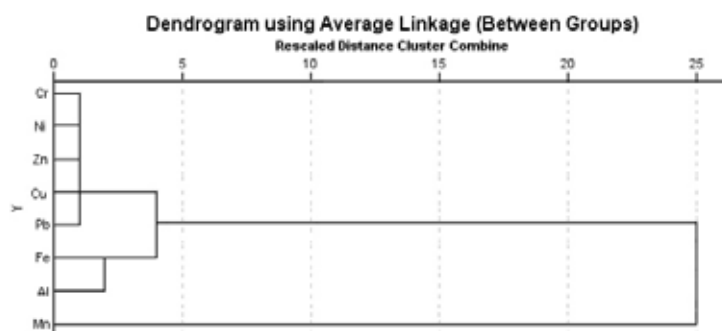


**FIGURE 5**  
Correlation dendrogram between the metals in marine sediments.

The concentrations of the under study metals during 2011 were remarkably lower than the determined ones in the previous study in 1998 at the same area [7] as well as than the ones prevailing in other areas of the north and central Aegean Sea. They were also lower than the recommended by the EPA and the EU ones.

Remarkably low values were also determined as it concerns the particulate form of the metals (Table 3). The distribution plots for Pb, Cu and Zn, presented in Figure 4, indicate that the area between Alonissos and Patitiri is the richest in particulate metals. As expected, open sea has the lowest values concerning the particulate form of metals.

**TABLE 5**  
Total sediments content in heavy metals (grain size fraction <1mm; values in mg/Kg)

metal	range	mean
Zn	7.72-135	32.4
Fe	253-51,300	12,000
Cu	7.62-89.4	20.0
Cd	0.06-0.07	0.06
Cr	3.23-214	34.8
Ni	5.38-157	33.4
Pb	3.91-181	34.0
Mn	32.7-351	167
Al	932-53,600	14,200

The results of this study indicate that the seawater of the Marine Park of Alonissos is not polluted with heavy metals neither in their dissolved nor in their particulate form.

**Metals in the sediment.** The ranges and mean values of the total content of the marine sediments in heavy metals are presented in Table 5.

The highest values for all the studied metals, except Mn, were determined in the area between of Alonissos and Peristera islands. On the other hand the sediments in the centre of the marine park (the marine area around the island of Piperi) were found to be the least rich in metals. The application of the Pearson correlation in combination with the “nearest neighbour” method using the SPSS-software, indicate that all the metals with the exception of Mn, were strongly correlated between each other ( $r > 0.90$  for  $p < 0.01$ ) probably because of their common origin. Mn displayed a different behaviour as it did not correlate with any of the studied metals. A correlation dendrogram between all the studied metals in sediments is presented in Figure 5.

The values of the total metal content of the sediments for various marine areas of the East Mediterranean are presented in Table 6:

**TABLE 6**  
heavy metal content of marine sediments (values in mg/Kg, Fe in g/Kg) in various areas of the East Mediterranean

Location	Zn	Cu	Cd	Cr	Ni	Pb	Mn
Ismir Gulf inner 2009 [15]	79.0	22.0	0.07	122	82.0	18.0	493
Ismir Gulf middle 2009 [15]	112	34.0	0.09	156	119	24.0	556
Ismir Gulf offshore 2009 [15]	209		0.33	166	103	51.0	551
Mediterranean background [16]	50.0	15.0	0.1-2.3	15		25.0	
Gulf of Souda (2007) [17]	54.4	23.9	0.07		55.0	28.4	176
MPA Alonissos 1998 [18]	45.3	15.5			22.7	24.1	172
MPA Alonissos 2011 (this study)	32.4	20.0	0.06	39.8	33.4	34.0	167
EU Marine Strategy [11] (a)	40 (150)	10 (40)	0.1 (1.2)			10 (50)	

(a): reference values -proposed threshold for GES in brackets;

According to this table, the total content of the area's sediments in Zn, Cu, Cd, Mn and Ni is lower than the respective ones of other coastal areas. Concerning Zn Cu and Cd, the values found are close to East Mediterranean reference values included at the Technical Report of the Framework Directive 2008/56/EU and also similar to the Mediterranean background. Although the concentration of Cr was elevated in comparison to the Mediterranean background, it was lower than the ones of other areas.

Two factors are commonly used in order to assess the enrichment of the sediments in metals:

a) The Enrichment Factor (EF) which is used to evaluate the anthropogenic inputs of heavy metals in marine sediments and is expressed by the equation:  $EF = ([Me]_s/[Al]_s) / ([Me]_b/[Al]_b)$

$[Me]_s$ ,  $[Al]_s$  are the concentrations of the metal and the Al respectively in the surface sediment and  $[Me]_b$ ,  $[Al]_b$  are the concentrations of these elements in the background, namely the average composition of the Upper Continental Crust (UCC). Sediments with  $EF > 1.5$  are considered as enriched in metals due to anthropogenic inputs. The calculated values of EF for the under study metals were 11.01 for Pb, 7.06 for Ni, 3.41 for Cd, 3.18 for Cr, 2.82 for Cu, 2.66 for Zn, 1.58 for Fe and 1.19 for Mn. These values indicate that the area's marine sediments are remarkably enriched in Pb, Ni, Cd, Cr and moderately enriched in Cu and Zn.

b) The geoaccumulation index (iGeo). It is calculated by the equation:  $iGeo = \log_2(Cn/1.5Bn)$  where Cn is the content of the sediment in the metal and Bn is the content of the background (the average argillaceous shale) in the same metal. Although the iGeo is applied in clays (the fraction of the sediment with grain size  $< 2 \mu m$ ) several researchers [19, 20] have used it in mud (grain size  $< 63 \mu m$ ), using as background values the regional ones. The iGeo values of the under study sediments were 2.85 and 1.13 for Pb and Ni respectively, indicating that the sediments of the area are classified as moderate to strongly polluted in Pb and moderate polluted in Ni. Concerning the rest of studied metals, the sediments are characterized as not polluted.

The TEL/PEL Sediment Quality Guideline [21] is applied to marine sediments in order to characterize their capability to cause adverse effects to benthic biota. The 'rarely' qualification indicates that there is a small probability for the benthic organisms to be severely effected whereas the 'occasionally' and 'frequently' qualifications indicate a fair and obvious probability respectively. The sediments of the Marine Park can rarely harm the benthic biota, with the exception of the sampling station SA10 which is seriously enriched with the most of the studied metals. Among all the studied metals, nickel has the greatest capability to cause adverse effects to the benthic organisms, as its content in the sediments is elevated.

## CONCLUSIONS

According to our measurements, the concentrations of nutrients and heavy metals in the studied area do not differ significantly to those prevailing in the open sea or to the ones determined in the previous study of 1998 and there is not any indication for significant marine pollution.

According to the TEL/PEL Sediment Quality Guideline, the content of the sediments in metals for the most sampling stations is not dangerous for benthic organisms. The increased values in sediments and seawater at the station SA10 indicates a trend that must be taken in account. The marine sediments of the area are also enriched in Ni, as values exceeded PEL in 3 out of 9 sampling points. This finding in combination with the values of EF and iGeo indicates that the content of the sediments in Ni is elevated and have to be studied further.

According to our opinion, a more efficient system or procedure should be applied in order to adequately monitor the marine area. In order to enrich our Database as well as to create a reliable time-series, the determination of the environmental parameters in this marine area must become a routine.

## REFERENCES

- [1] Riley, J.P. and Taylor, D. Chelating resins for the concentration of trace elements from seawater and their analytical use in conjunction with A.A.S. Analytical Chemical Acta. 1968;40:479–484
- [2] Kingston, H.M, Barness, I.L., Brady, T.J, Rains, T.C, and Champ, M.A. Separation of eight transition elements from alkali and alkaline earth metals in estuarine and seawater with chelating resin and their determination by graphite furnace atomic absorption spectrophotometry. Analytical Chemistry. 1978; 50: 2064 – 2070
- [3] UNEP. Reference Methods for Marine Pollution Studies, Report no 31 – 39, 1985.
- [4] Grasshof K. and Kremling, K. Methods of Seawater Analysis. III Edition –WILEY-VCH. 1997; 159-209
- [5] Valderama J. The simultaneous analysis of total N and total P in natural waters. Marine Chemistry, 10: 109-122.
- [6] Berman T. and Bronk D. Dissolved Organic Nitrogen: a dynamic participant in aquatic ecosystems. Aquat Microb Ecol, 2003, 31, 279-305
- [7] Ladakis E., Skoullou M. and Dassenakis E. Water Quality in a Mediterranean Marine Protected Area (North Sporades Islands – Greece). Chemistry and Ecology. 2003; 19(1): 47 – 57.





- [8] Pavlidou A., Kontoyannis H. and Psyllidou-Giouranovits R. Trophic conditions and stoichiometric nutrient balance in the inner Saronikos Gulf (Central Aegean Sea) affected by Psittalia Sewage outfall. *Fresen. Environ. Bull.*, 2004; 13 No 12b: 1509-1514.
- [9] Dassenakis M., Arsenikos S., Botsou F., Depiazi, G., Adrianos H., Zaloumis P. and Drossis G. General Trends in Marine Pollution of the Central Part of Euvoikos Gulf. *Proceedings of the 6th International Conference on Environmental Science and Technology - Samos, Greece; 1999.*
- [10] Kukuksegin F., Balci a., Kontas A. and Altay O. Distribution of nutrients and chlorophyll-a in the Aegean Sea. *Oceanologica Acta* 1995, 18, 3, 343 – 352.
- [11] The accompanying technical report of the European Union's Frame-Directive 2008/56/EC for the Marine Strategy: The action plan of the marine strategies in Greece (369 pp) – proposed thresholds are included. Web page: [marinestrategy.opengov.gr](http://marinestrategy.opengov.gr) (last accessed: 27/08/2014).
- [12] Gavriil A.M and Angelidis M.O. Metal and organic carbon distribution in water column of a shallow enclosed bay at the Aegean Sea Archipelago: Kalloni bay, island of Lesbos. *Estuarine, Coastal and Shelf Science* 644 (2005) 200 – 210.
- [13] V., Paraskevopoulou, V., Zeri, C., Kaberi, H., Chalkiadaki, O., Krasakopoulou, E., Dassenakis, M., Scoullou, M. Trace metal variability, background levels and pollution status assessment in line with the water framework and Marine Strategy Framework EU Directives in the waters of a heavily impacted Mediterranean Gulf. *Marine Pollution Bulletin* 2014; 87: 323 - 337.
- [14] United States Env Protection Agency. National recommended water quality criteria: web page: <http://www.water.epa.gov/scitech/swguidance/standards/current/> (last accessed: 10/08/2014).
- [15] Kucuksegin F., Kontas A., and Uluturhan E.: Evaluations of heavy metal pollution in sediment and *Mullus barbatus* from the Izmir Bay (Eastern Aegean) during 1997 – 2009. *Marine Pollution Bulletin*. 2011: 62 (2011), 1562 – 1571
- [16] UNEP: Report on the state of pollution in the Mediterranean Sea. In governmental review Meeting of Mediterranean Coastal States on the Mediterranean Action Plan. UNEP/IG.11/INF 4. 1978
- [17] Dassenakis M., Thessalou-Legaki M., Katsanevakis S., Ladakis M., Mpotsou F., Rousselaki E., Petrochilou M., and Dassenaki M. The existing environmental situation of the gulf of Souda – Crete. Technical report ordered by the municipality of Souda, 2008.
- [18] Ladakis M., Sakelariadou F., Megalofonou P., Dasenakis M. and Roussis B. Metal content in sediments and benthic organisms from the National Marine Park of N. Sporades in Aegean Sea. 38<sup>th</sup> European Marine Biology Symposium (EMBS), 8 – 12 September 2003, Aveiro Portugal, Book of Abstracts No 245, p 184.
- [19] Subramanian V. and Mohanachandram G. Heavy metals distribution and enrichment in the sediments of the Southern – East Coast of India. *Marine Pollution Bulletin* 2 (1990) 324 – 330.
- [20] Sahu K. C. and Bhosale U. Heavy metal pollution around the island city of Bombay, India. Part 1: Quantification of heavy metal pollution of aquatic sediments and recognition of environmental discriminants. *Chemical Geology* 91 (1991), 263 – 283.
- [21] MacDonald D. D., Carr S.R., Calder F.D., Long E.R. and Ingersoll C.G. Development and evaluation of sediment quality guidelines for Florida coastal waters. *Ecotox.* 1996; 5: 253 – 278.
- [22] Lab Network for the Environmental Quality Monitoring of the Hellenic Seas. Technical Report, pp 212-213, Athens 2006.

---

**Received:** 12.05.2016  
**Accepted:** 21.09.2016

---

#### **CORRESPONDING AUTHOR**

---

**Manos Dassenakis**  
National and Kapodistrian University of Athens  
Department of Chemistry,  
Laboratory of Environmental Chemistry  
Panepistimioupolis 157-84  
Athens –GREECE

e-mail: [edassenak@chem.uoa.gr](mailto:edassenak@chem.uoa.gr)  
[eladakis@chem.uoa.gr](mailto:eladakis@chem.uoa.gr)

## AUTHOR INDEX

**A**

Aasim, M.	5113	Alkan, A.	5245
Abaci Gunyar, O.	5180	Al-Najjar, T.	5253
Abalkhail, T.	5528	Al-Tawaha, M.	5347
Abdel-Megeed, A.	5528	Altundas, A.	5411
Abu Khadra, K.	5253	Anil, S.	5419
Acik, L.	5611	Anlas, C.	5358
Adomas, B.	5096	Araz, A.	5611
Agar, G.	5411	Artun, F.T.	5419
Akkan, T.	5492	Aydin Uncumusaoglu, A.	5492
Aktas, B.	5297	Aydin, C.	5305
Al-Arfaj, A. A.	5528	Aydogdu, M.H.	5449
Al-Jawasreh, R.	5347		

**B**

Baciak, M.	5096	Bayindir, A.	5365
Bai, Y.	5394	Bini, C.	5347
Baranowska, A.	5381	Biyik, H.	5297
Basti, S.	5432	Bizhu, H.	5555
Bati, B.	5245	Bordbr, A.	5138

**C**

Cao, X.	5120	Chen, L.	5326, 5516
Celebi Keskin, A.	5611	Chen, X.	5145, 5261
Celik, M.	5287	Chengjie, S.	5371
Chan, C.	5499	Copty, N.K.	5217

**D**

Dai, Y.	5394	Diao, J.	5226
Danyan, C.	5542	Dogan, M.	5113
Dassenakis, M.	5618	Doygun, H.	5202
Dayioglu, H.	5237	Doygun, N.	5202
Dengli, T.	5483		

**E**

Eker, S.	5467	Erdogan, Y.	5411
Erdogan, O.	5581	Eslem Kadak, A.	5287

**F**

Fan, C.	5326	Feng, L.	5261
Fang, G.	5208		

**G**

Gassaymah, R.	5253	Guibin, L.	5499
Gelibolu, S.	5287	Guimei, T.	5499
Gercek, G.	5287	Guler, P.	5611
Gharibvand, R.	5590	GültekinTemiz, M.	5511
Gozcu, M.	5202	Guo, Y.	5208
Gu, J.	5406	Guo, Z.	5516
Guan, D.	5555	Guohua, N.	5483
Gugala, M.	5381		

**H**

Haliki Uztan, A.	5180	Hekimhan, H.	5388
Han, X.	5261, 5456	Hongxing, Z.	5587
Han, Y.	5145	Hou, H.	5080
Han, Z.	5280	Hsieh, Y.	5336, 5341
Hasoonizadeh, H.	5590	Hu, S.	5326

He, Z.	5186	Huabin, Z.	5499
Heidarnejad, M.	5138, 5590	Hui, L.	5587
<b>J</b>			
Jelonkiewicz, E.	5271	Jiang, P.	5406
Jelonkiewicz, L.	5271	Jiao, L.	5080
Ji, Y.	5394	Jingjing, L.	5371
Jiang, H.	5261	Jingyi, L.	5499
Jiang-Wei, Z.	5534		
<b>K</b>			
Kalyoncu, H.	5237	Kilcik, F.	5237
Kamanbedast, A.A.	5138, 5590	Kizil, H.E.	5411
Kang, H.	5291	Koloren, O.	5467
Kapela, K.	5381	Komendova, R.	5172
Karaca, I.	5365	Krasnodebska, E.	5381
Karagoz, A.	5419	Krzesiwo, K.	5271
Karatas, M.	5113	Kucukgulmez, A.	5287
Kashkouli, H.	5590	Kultur, S.	5419
Keskin, N.	5180	Kumar Sahu, S.	5432
Khalaf, M.	5253	Kurt, F.	5511
Khalaf, N.	5253	Kuta, J.	5172
<b>L</b>			
Ladakis, M.	5618	Lippi, M.	5347
Lei, W.	5534	Liu, H.	5151, 5516
Lenart-Boron, A.	5271	Liu, J.	5186
Li, H.	5145	Liu, M.	5186
Li, Q.	5130	Liu, W.	5145
Li, X.	5394	Liu, Y.	5120, 5261, 5599
Li, Z.	5313, 5565	Lu, P.	5456
Lian, J.-Z.	5336, 5341	Luo, S.	5326
Liang, S.-K.	5424	Luo, Z.	5326
Liao, X.	5145	Lv, D.	
Liping, W.	5371	Lv, Y.	5394, 5399
<b>M</b>			
Ma, F.	5226	Melikoglu, G.	5419
Ma, S.	5162, 5313	Meng, C.	5162
Ma, W.	5599	Miao, X.	5440
Maomao, H.	5542	Mostafa, A.A.	5528
Maric, I.	5105	Muzaffar, R.	5528
<b>N</b>			
Nenkovic-Riznic, M.	5105	Niu, C.	5326
Nevrla, J.	5172		
<b>O</b>			
Ogutcu, H.	5411	Ovezikoglou, P.	5618
Oguz, I.H.	5581	Ozger, S.	5365
Onucyildiz, M.	5217		
<b>P</b>			
Peart, M.R.	5555	Prajsnar, J.	5271
Piotrowicz-Cieslak, A.I.	5096	Pucar, M.	5105
Poyrazoglu Coban, E.	5297	Purmohammadi, M.H.	5138
<b>Q</b>			
Qi, W.	5186	Qiao, X.	5145
Qiao, H.	5226		

**R**

Rostami, H. 5138

**S**

Sabancı, K.	5305	Sikorska, A.	5381
Sahu, C.	5432	Sipahi, H.	5388
Sedat Sevinc, M.	5365	Sommer, L.	5172
Sengul, U.	5492	Song, C.	5120
Senol, N.	5354	Song, Q.	5406
Shaomang, W.	5371	Su, R.	5186
Sholkamy, E.N.	5528		

**T**

Tahir, A.	5528	Tsai, C.T.	5336, 5341
Tianyin, C.	5499		

**U**

Ustuner, O.	5358	Uzun, A.	5575
Ustunturk-Onan, M.	5419		

**W**

Wahsha, M.	5253, 5347	Wang, T.	5599
Wang, C.	5424	Wang, X.	5424
Wang, G.	5555	Wang, Y.	5130
Wang, L.	5162, 5186, 5194	Wang, Z.	5599
Wang, M.	5145	Wei, C.	5130
Wang, N.	5280	Wei, H.	5599
Wang, P.	5473	Wei, Z.	5162
Wang, Q.	5473	Wen, X.	5208
Wang, R.	5456	Wolanin, A.	5271
Wang, S.	5120, 5399	Wu, H.	5130

**X**

Xia, X.	5371	Xu, B.	5565
Xiao, R.	5555	Xu-xiang, L.	5291
Xiaohou, S.	5542		

**Y**

Yagan Asci, M.	5245	Yarar, A.	5217
Yaming, Z.	5542	Yasa, B.	5575
Yan, Z.	5534	Ying, Y.	5534
Yanar, Y.	5287	Yoltas, A.	5180
Yang, J.	5162	Yu, Y.	5186
Yang, Q.	5456	Yuanhong, X.	5587
Yang, T.	5080	Yuanhua, Y.	5483
Yang, X.	5280	Yuelin, L.	5499
Yao, H.	5499	Yumurtaci, A.	5388
Yao, Y.	5194		

**Z**

Zarzecka, K.	5381	Zhao, J.	5145
Zelazny, M.	5271	Zhao, S.	5080
Zeybek, Z.	5419	Zheng, J.	5516
Zhang, B.	5394	Zhong, J.	5226
Zhang, F.	5162	Zhou, C.	5599
Zhang, G.	5473	Zhou, L.	5130, 5208
Zhang, H.	5399, 5565	Zhou, P.	5186
Zhang, J.	5406	Zhou, Q.	5440
Zhang, L.	5151, 5313	Zhou, R.	5280

Zhang, P.	5424	Zhou, W.	5516
Zhang, Q.	5555	Zhou, Y.	5120, 5145
Zhang, S.	5194	Zhou, Z.	5120
Zhang, X.	5151	Zhu, S.	5130
Zhang, Y.	5120, 5473, 5599	Zhu, W.	5399
Zhao, B.	5226		

## SUBJECT INDEX

### A

Adsorption	5151, 5326, 5371	Andik Stream	5237
Aflatoxine B <sub>1</sub>	5411	Antibacterial activity	5419
age dependent life table	5365	Antimicrobial Activity	5411
Air quality grades	5162	Antimutagenic effect	5411
Algae-laden water	5406	Aqaba	5253
Alonnisos	5618	AR27	5341
alternative stable state	5120	Archaeology	5347
Amaranthus hybridus L.	5565	artificial neural network	5217
Amberlite XAD-4	5245	Aspergillus niger	5528
Amoxicillin	5358	Aspidiotus nerii	5365
anaerobic ammonium oxidation	5456		

### B

Bacillus subtilis strain	5394	Bibliometric	5080
Bacillus tequilensis	5534	biochar	5226
Bacteria	5130, 5297	biodegradation	5534
Barley	5388	Bioecology	5575
BDE-209	5280	biological risk	5499
Beauveria bassiana	5180	Biosorption	5528
Białka river	5271	boron toxicity	5511

### C

Cadmium	5565, 5587	chlorimuron-ethyl	5394, 5534
carbon accumulation	5555	chlortetracycline	5096
carbon dioxide evolution	5432	Clean Development Mechanism	5313
Carbon nanotubes	5151	Climate change	5208
Carbonaceous components	5162	Coking wastewater	5130
cationic surfactant	5172	comet assay	5358
cattle manure	5226	Concentrations	5253
Cd	5280	constant darkness	5096
CFD	5473	Contaminated site	5145
characteristic	5406	Correlation analysis	5208
chelating material	5326	Cotton	5511
Chelator	5565	cycle	5138
chemical analysis	5581	Cycloalkylaminocyanothiophenes	5411
Chinese coast	5555	Cynodon dactylon	5599
Chitosan	5287		

### D

data	5180	discharge-scale curve	5138
decolorization	5336, 5341	disinfection	5473
Degradation	5394	Disk diffusion assay	5419
denitrification	5120	distribution	5145, 5424,
Diatom Indices	5237	dithiocarbamate	5245
diatomite	5371	DNA finger prints	5611
discharge coefficient	5138, 5590	dredged sediments	5399

### E

early warning	5499	Environmental benefits	5313
Eco-friendly technology	5528	environmental regulation	5483
ecological risk assessment	5424	enzyme activities	5432
ecosystem carbon storage	5555	Escherichia coli	5271
EDTA	5565	EST	5388
Eisenia foetida	5354	European eel	5287
electroless ultraviolet	5473	Extraction	5297
entomopathogenic fungus	5180		

**F**

Fatty acids	5287	Fluorescence characteristics	5599
fiber quality properties	5511	Food safety	5587
firm size distribution	5483	forms	5399
Fishes	5253	Functionalization	5151
flame atomic absorption spectroscopy	5245	furnace iron waste	5336
flooding	5599	Fusarium	5388, 5611

**G**

Galleria bait method	5180	Geranium	5467
GAP-Sanlıurfa	5449	GF-1	5261
Genetic identification	5611	GIS modeling	5105
genotoxicity	5358	Goji berry	5581
Geoaccumulation	5492	green land	5499
Geographic information systems (GIS)	5291	Green space	5202
Geraniaceae	5467		

**H**

Habitat environmental quality index	5291	Hemarthria altissima	5599
hand-warmer	5341	herbicides	5381
Healthy trace elements	5587	Histopathological	5354
heavy metal	5226, 5354, 5440, 5492	Hyperaccumulator	5565
heavy metals	5113, 5253, 5326, 5587	hzbB gene	5456

**I**

ICP-MS	5172, 5587	Inorganic elements	5162
Image processing	5305	Internal Transcribed Spacer	5467
Imines	5411	isolation	5180, 5297
In vitro	5113	Isolation and screening	5394
industrial park	5440		

**J**

Jiaozhou Bay	5424	joint exposure	5280
--------------	------	----------------	------

**K**

Kahramanmaraş	5202	Körfez Wetland	5575
kinetic	5371		

**L**

Labyrinth weir	5138, 5590	Lead	5354
land surface temperature	5194	Leaf area index (LAI)	5261
Land use	5432	Levels	5253
landfill site selection	5105	lichens	5172
LDA	5186	Luffa cylindrica	5528
leaching	5399	Lupinus luteus L.	5096

**M**

Macroelements	5381	micronucleus	5358
management	5499	microsatellites	5388
mangrove forest	5555	microwave	5473
Marine Park	5618	modified cellulose of cassava	5326
maternal age effect	5365	Molecular diversity	5130
mesophilic bacteria	5271	monitoring	5499
Metals	5618	morphologic characteristics	5581
Methanolich extracts	5419	MTT method	5419
Methylene blue	5336	Mulch	5542
microbial preparation	5280, 5534	multi regression	5217

<b>N</b>			
Near infrared spectroscopy	5186	Nonylphenol	5424
nirS	5120	Northeastern rice of China	5587
Nitrate nitrogen	5542	NTA	5565
nitrite-dependent anaerobic methane oxidation	5456	Numerical Simulation	5313
Nitrogen loss	5542	nutrients	5271, 5618
Noise pollution	5202		
<b>O</b>			
O <sub>2</sub>	5406	optimization	5297, 5473
OCPs	5145	Organic compounds	5186
OMNIDIA	5237	Organic fertilizer	5542
Oncorhynchus mykiss	5358	Ornitofauna	5575
<b>P</b>			
patch	5194	Piano Key Weir	5590
Pattern recognition	5186	planting density	5599
PCA	5186	Platinum group metals	5172
peach fruit quality	5516	PM <sub>2.5</sub>	5080, 5162
peach fruit yield	5516	pmoA gene	5456
peach orchard	5516	Pollutants emission reductions	5313
Pedostratigraphy	5347	pollution trends	5440
Petra	5347	Poly-β-Hydroxybutyrate	5297
phosphorus	5399, 5516	potato	5365, 5381
photochemical formation	5406	Poyang Lake	5261
photoperiod	5096	precision agriculture	5305
phylogeny	5467	preconcentration	5172
physical analysis	5581	Principal component analysis	5291
<b>Q</b>			
Quantitative evaluation system	5291		
<b>R</b>			
RAPD-PCR	5611	Research orientation	5080
reactor	5473	Research performance	5080
Red Sea	5253	risk perception	5449
regeneration	5326	robotic weeding	5305
Remote Sensing	5261	Runoff	5542
<b>S</b>			
sediment	5120, 5492, 5618	soil organic carbon (SOC)	5555
separation	5172	Solid phase extraction	5151
sewage treatment plant	5271	solidification	5399
shallow lakes	5120	sorption	5226
Shellfish waste	5287	spatial analysis of GIS	5194
Shrimp	5287	Spatial-temporal responses	5208
Skin	5354	Stem node explants	5113
Snow cover	5208	Streamflow modeling	5217
social criteria	5105	sulphur	5511
Soil	5145	Surface runoff	5516
Soil ecosystem functioning	5432	Sustainable environment	5449
Soil erosion levels			
<b>T</b>			
Taihu Lake	5399	Trapezoidal Weir	5590
thermodynamics	5371	Trace metals	5245
Tibetan Plateau	5208	Trifolium repens L.	5516
TOC removal	5341	Turkey	5237, 5449, 5575
topsoil	5440		



<b>U</b>			
urban environmental protection	5202		
<b>V</b>			
Vegetation indexes	5261	villages in Serbia	5105
<b>W</b>			
WAsP Climate Analyst	5313	wavelet transform	5217
Water	5492	weed control	5305
Water landscape	5194	weed control methods	5381
Water quality	5113, 5237	weir with rectangular-shaped plan	5138
water-level fluctuating zone	5138, 5456	willingness to pay	5449
Water-soluble inorganic ions	5162	Wind Energy Resources	5313
<b>Y</b>			
Yağlıdere Stream	5492	yield	5581
<b>Z</b>			
zero-valent iron	5336	Zipf distribution	5483
Zinc	5528		

## FEB – GUIDE FOR AUTHORS

### General

FEB accepts original papers, review articles, short communications, research abstracts from the entire sphere of environmental-chemistry,-biology,-microbiology,- technology, -biotechnology and-management, furthermore, about residue analysis/ and ecotoxicology of contaminants.

Acceptance or no acceptance of a contribution will be decided, as in the case of other scientific journals, by a board of reviewers. Papers are processed with the understanding that they have not been published before (except in form of an abstract or as a part of a published lecture, review or thesis); that they are not under consideration for publication elsewhere; that their publication has been approved by all co-authors, if any, as well as tacitly or explicitly- by the responsible authorities at the institute where the work has been carried out and that, if accepted, it will not be published elsewhere in the same form, in either the same or another language, without the consent of the copyright holders.

### Language

Papers must be written in English. Spelling may either follow American (Webster) or British (Oxford) usage but must be consistent. Authors who are less familiar with the English language should seek assistance from proficient colleagues in order to produce manuscripts that are grammatically and linguistically correct.

### Size of manuscript

Review articles should not exceed 30 typewritten pages. In addition up to 5 figures may be included. Original papers must not exceed 14 typewritten pages. In addition up to 5 figures may be included. Short-Communications should be limited to 4 typewritten pages plus not more than 1 illustration. Short descriptions of the authors, presentation of their groups and their research activities (with photo) should together not exceed 1 typewritten page. Short research abstracts should report in a

few brief sentences (one-fourth to one page) particularly significant findings. Short articles by relative newcomers to the chemical innovation arena highlight the key elements of their Master and PhD-works in about 1 page.

Book Reviews are normally written in-house, but suggestions for books to review are welcome.

### Preparation of manuscript

Dear authors,

FEB is available both as printed journal and as online journal on the web. You can now e-mail your manuscripts with an attached file. Save both time and money. To avoid any problems handling your text please follow the instructions given below:

When preparing your manuscripts have the formula K/SS (Keep It Simple and Stupid) in mind. Most word processing programs such as MS-Word offer a lot of features. Some of them can do serious harm to our layout. So please do not insert hyperlinks and/or automatic cross-references, tables of contents, references, footnotes, etc.

1. Please use the standard format features of your word processor (such as standard.dot for MS Word).
2. Please do not insert automatisms or secret link-ups between your text and your figures or tables. These features will drive our graphic department sometimes mad.
3. Please only use two fonts for text or tables "Times New Roman" and for graphical presentations "Arial".
4. Stylesheets, text, tables and graphics in shade of grey
5. Turn on the automatic language detection in English (American or British)
6. Please - check your files for viruses before you send them to us!!

**Manuscripts should send to: [parlar@wzw.tum.de](mailto:parlar@wzw.tum.de)  
or: [parlar@prt-parlar.de](mailto:parlar@prt-parlar.de)**

Thank you very much!

## STRUCTURE OF THE MANUSCRIPT

**Title page:** The first page of the manuscript should contain the following items in the sequence given: A concise title of the paper (no abbreviations). The names of all authors with at least one first name spelled out for every author. The names of Universities with Faculty, City and Country of all authors.

**Abstracts:** The second page of the manuscript should start with an abstract that summarizes briefly the contents of the paper (except short communications). Its length should not exceed 150-200 words. The abstract should be as informative as possible. An extended repetition of the paper's title is not considered to be an abstract.

**Keywords:** Below the Summary up to 6 key words have to be provided which will assist indexers in cross-indexing your article.

**Introduction:** This should define the problem and, if possible, the frame of existing knowledge. Please ensure that people not working in that particular field will be able to understand the intention. The word length of the introduction should be 150 to 300 words.

### Materials and methods:

Please be as precise as possible to enable other scientists to repeat the work.

**Results:** Only material pertinent to the subject must be included. Data must not be repeated in figures and tables.

**Acknowledgements:** Acknowledgements of financial support, advice or other kind of assistance should be given at the end of the text under the heading "Acknowledgements". The names of funding organisations should be written in full.

**References:** Responsibility for the accuracy of references rests with the authors. References are to be limited in number to those absolutely necessary. References should appear in numerical order in brackets and in order of their citation in the text. They should be grouped at the end of the paper in numerical order of appearance. Abbreviated titles of periodicals are to be used according to Chemical or Biological Abstracts, but names of lesser known journals should be typed in full. References should be styled and punctuated according to the following examples:

### ORIGINAL PAPERS:

1. Author, N.N. and Author, N.N. (Year) Full title of the article. Journal and Volume, first and last page.

### BOOK OR PROCEEDING:

2. Author, N.N. and Author, N.N. (Year) Title of the contribution.

In: Title of the book or proceeding. Volume (Edition of klitor-s, ed-s) Publisher, City, first and last page

### DOCTORAL THESIS:

3. Author, N.N. (Year) Title of the thesis, University and Faculty, City

### UNPUBLISHED WORK:

Papers that are unpublished but have been submitted to a journal may be cited with the journal's name followed by "in press". However, this practice is acceptable only if the author has at least received galley proofs of his paper. In all other cases reference must be made to "unpublished work" or "personal communication".

**Discussion and Conclusion:** This part should interpret the results in reference to the problem outlined in the introduction and of related observations by the author/s or others. Implications for further studies or application may be discussed. A conclusion should be added if results and discussion are combined.

**Corresponding author:** The name of the corresponding author with complete postal address

### Precondition for publishing:

**A minimum number of 25 reprints must be ordered and prepaid.**

**1 - 4 pp.: 200,- EURO + postage/handling**

**5 - 8 pp.: 250,- EURO + postage/ handling**

**More than 8pp: 1.50 EURO/page x number of reprints +postage/ handling.**

**The prices are based upon the number of pages in our journal layout (not on the page numbers of the submitted manuscript).**

**Postage/ Handling: The current freight rate is Germany 10 €, Europe 18,00 €, International 30 €.**

**VAT: In certain circumstances (if no VAT registration number exists) we may be obliged to charge 7% VAT on sales to other EU member countries. MESAEP and SECOTOX members get a further discount of 20% (postage/ handling full).**